Australian Government
Geoscience Australia

Professional Opinion

No. 2010/01

Ord Valley AEM Interpretation Project

Final Report: Using The SkyTEM Time Domain Airborne Electromagnetics (AEM) System to Map Aquifer Systems & Salinity Hazard in the Ord Valley, Western Australia

Lawrie, K.C., Tan, K.P., Clarke, J.C., Munday, T.J., Fitzpatrick, A., Brodie, R.S., Apps, H., Halas, L., Cullen, K., Pain, C.F., Kuske, T.J. ,Cahill, K. & Davis, A.

PREPARED FOR:

Ord Irrigation Cooperative & Rangelands NRM Group

February 2010

Ord Valley AEM Interpretation Project

FINAL REPORT: USING THE SkyTEM TIME DOMAIN AIRBORNE ELECTROMAGNETICS (AEM) SYSTEM TO MAP AQUIFER SYSTEMS & SALINITY HAZARD IN THE ORD VALLEY, WESTERN AUSTRALIA

GEOSCIENCE AUSTRALIA PROFESSIONAL OPINION 2010/01

PREPARED FOR

ORD IRRIGATION COOPERATIVE & RANGELANDS NRM GROUP

FEBRUARY 2010

Rangelands NRM Western Australia

rd Irrigation Cooperative Ltd

National Research FLAGSHIPS Water for a Healthy Country

CSIRO

Australian Government
Department of the Environment, Water, Heritage and the Arts

GOVERNMENT OF WESTERN AUSTRALIA

Australian Government
Geoscience Australia

Department of Resources, Energy and Tourism
Minister for Resources, Energy and Tourism: The Hon. Martin Ferguson, AM MP
Secretary: Mr John Pierce

Geoscience Australia
Acting Chief Executive Officer: Dr Chris Pigram

GeoCat Number: 69583

Bibliographic reference: Lawrie, K.C.[1], Tan, K.P.[1], Clarke, J.C.[1], Munday, T.J.[2], Fitzpatrick, A.[2], Brodie, R.S.[1], Apps, H.[1], Halas, L.[1], Cullen, K.[1], Pain, C.F.[1], Kuske, T.J.[1] ,Cahill, K.[2] & Davis, A.[3*], 2010. Using the SkyTEM Time Domain Airborne Electromagnetics (AEM) System to Map Aquifer Systems and Salinity Hazard in the Ord Valley, Western Australia. Geoscience Australia Professional Opinion 2010/01, 500p.

[1] Geoscience Australia
[2] CSIRO, Water for a Healthy Country Flagship Project
[3*] Formerly RMIT University, currently Geoscience Australia

Cover Images: From top left to right: Diversion Dam (Ken Lawrie); Boab trees on margins of ORIA Stage 1 (Ken Lawrie); SkyTEM survey over M1 supply channel (Anna Price); Image below: crops in Ivanhoe Plain (Geoff Strickland).

Executive Summary

This report documents the findings of the Ord Valley Airborne Electromagnetics (AEM) Interpretation Project. Co-funded by the Australian Government in partnership with the Western Australian Government, this project provides information relating to salinity and groundwater management in the Ord River Irrigation Area (ORIA), in the north of Western Australia through the acquisition, analysis and interpretation of airborne electromagnetic (AEM) and Light Ranging and Detection (LiDAR) surveys, and complementary hydrogeological data. The project was undertaken under the auspices of the National Action Plan for Salinity and Water Quality, and managed by Ord Irrigation Cooperative (OIC) for the WA Rangelands NRM Group.

A total of 5,936 line km of AEM data were acquired in July and August 2008, using the SkyTEM time domain AEM system. The project area covered the existing Ord Irrigation Area (ORIA) Stage 1, and the ORIA Stage 2 areas earmarked for irrigation expansion. The AEM survey was configured to map regional scale variations in ground conductivity that might be associated with broad scale changes in the character of the alluvial aquifer, ground water conductivity and salinity. It was not designed for detailed "within – paddock" investigations.

Data obtained from the employment of an advanced drilling technology in conjunction with existing hydrogeological information provided the basis for the validation and interpretation of the SkyTEM AEM dataset, and the production of a suite of derived products including maps of salinity hazard, salt stores and groundwater salinity. The study also generated revised maps of key elements of the alluvial aquifer system, specifically the 3D distribution of sands, gravels, and silts and clays, that are critical to understanding the behaviour of the aquifer when subject to irrigation development.

The principal findings of the study with respect to the ORIA are:

1. Key elements of the alluvial aquifer system were mapped in three dimensions over most of the project area with the aid of AEM data. Key general points to note include:
    - A smooth model 1D layered earth inversion, applied from a regional perspective (i.e. without local constraint), effectively mapped variations in ground conductivity at scales relevant to the regional characterisation of the alluvial aquifer and groundwater system.
    - In general terms, the modelled conductivity structure defined from the SkyTEM smooth model Layered Constrained Inversion (LCI) matches that defined from available bore data exceptionally well, with an adjusted $r^2 = 0.84$ determined. It is therefore reasonable to assume that the modelled ground response from the inverted SkyTEM data provides a good approximation of 'true' ground conductivity as defined by the borehole conductivity tool, and is a reliable base from which to derive a suite of interpretation products including salt store and lithology maps.
    - Modelling and associated ground investigations confirmed that the SkyTEM system's depth of investigation was not limited by the thickness or conductivity of the alluvial aquifer and that conductivity variations in the underlying basement were resolved.
    - Overall, the hydrogeological framework documented in earlier investigations, has been confirmed. However, this study provided greater spatial detail on critical elements of the hydrostratigraphy in the alluvial aquifer, including palaeochannel delineation, and the mapping of the extent and thickness of gravel, sand, silt, clay units in 3D, as well as the mapping in 3D of salt stores and groundwater quality.
    - The SkyTEM AEM system mapped conductivity variations within and beneath relatively thin deposits of the Cockatoo Sands, although it is likely that differentiation of sands with and without high salt content is difficult in the unsaturated zone.
2. Salinity hazard maps for the ORIA have been produced using an informed GIS-based approach. Salinity is a hazard when it has the potential to be moved to where it can threaten assets such as agriculture, infrastructure, water resources and biodiversity (Spies & Woodgate, 2005). In this study, the salinity hazard maps combine AEM-derived maps of salt stored in the unsaturated zone with maps of depth to the watertable. These maps have been designed to predict groundwater-driven salinity hazard. The salinity hazard is assessed as high when there are significant quantities of salt stored in the alluvium or

soils in areas of shallow groundwater, and lowest where there is little or no salt stored in the alluvium and groundwater tables are deep. Assumptions are made that water levels will rise after land clearing and the onset of irrigation, and that shallow watertables may lead over time to salt accumulation through capillary rise (if within 2-3m of the surface). Prior modelling suggests that relatively modest salinity levels (>750 mg/l TDS) may become a significant salinity hazard to irrigated agriculture through evapotranspiration in the shallow sub-surface.

3. Salinity risk is a measure of the chance that a salt hazard will cause harm to an asset at some time in the future. The project has produced a number of other AEM-derived products, including maps of sand, gravel, silt and clay distribution, and groundwater salinity that are designed for input into groundwater models that can be used to produce maps of salinity risk of the area. Generation of groundwater models and salinity risk maps should be used to underpin development decisions in the ORIA including design of Stage 2 irrigation infrastructure and sustainable cropping strategies.

4. The interpreted salinity hazard in each of the ORIA sub-areas is summarised below:
   - Mantinea Plain and Carlton Hill: very high salinity hazard in the western half of the areas earmarked for potential irrigation development. High salt stores (>100t/ha/m) in the unsaturated zones, saline groundwater (1,000 to 10,000 mg/l TDS) in a shallow sand aquifer, coupled with an inherently shallow watertable (<5 to 10m), contribute to this assessment. Recharge potential is higher in Carlton Hill than in Mantinea Plain. The potential for soil waterlogging is also likely to be high in this area.
   - The Parry's Lagoon wetland and lower Ord Floodplain have very high salt stores (>500 t/ha/m), very shallow water tables (<2m) and extremely high salinity hazard. There are no discernible freshwater lenses beneath the Parry's Lagoon wetlands, although there is some evidence of mixing (of fresh surface water and saline groundwater) in the top 6m. In essence, the wetlands appear to be perched on saline clays and a sand aquifer with very high groundwater salinities (>46,000 mg/l TDS). Salinity is a natural part of this landscape, however it remains unclear to what extent the hydrological balance has been altered post-Ord River regulation. The salinity hazard in this area lies not in the threat to irrigation assets, but to the freshwater environmental assets (and tourism assets indirectly) in the lagoons.
   - Weaber Plain: the salinity hazard is highly variable across the area earmarked for development, ranging from very high to very low, but with >50% of the area ranked at least moderate. The very high salinity hazard areas occur in the western Weaber Plain where there are areas of high salt store in the unsaturated zone (<68/t/ha/m) and saturated zone (< 131 t/ha/m), relatively high groundwater salinities (< 5,000 mg/l TDS), and a very shallow (<5m) groundwater table. The soil waterlogging potential is also likely to be high in this area. Elsewhere in the area earmarked for development, the lower salinity hazard coincides with the palaeochannels, while the flanking clay-rich areas have a moderate to high salinity hazard.
   - Knox Creek and Keep River Plains: very low to low salinity hazard in the north of the area, but with a moderate to high salinity hazard in the southern-central area of Knox Creek Plain, coincident with a thick sequence of clays with subsidiary silts and gravels. The southern half of Knox Creek Plain has an area with very high salt stores in the unsaturated zone (30-70 t/ha/m) and saturated zones (60- 130 t/ha/m), as well as high groundwater salinities (>5,000 mg/l TDS).
   - ORIA Stage 1 Ivanhoe Plain: highly variable salinity hazard across this area, ranging from very low to very high. The northern part of the area has areas of high to very high salinity hazard, as does Cave Springs Gap. Very shallow water tables (<5m) combined with moderately high salt stores in the unsaturated (< 30t/ha/m) and saturated zones (<130 t/ha/m).
   - In ORIA Stage 1 Packsaddle Plain: the salt stored in the unsaturated and saturated zones is between 10 and 40t/ha/m, which is considerably lower than Ivanhoe Plain. There is a low to moderate potential risk of soil salinisation in this area.

The salinity hazard by hectare and percentage overall for the ORIA Stage 1 + Stage 2 areas, is summarised in Table A below. The areas not assessed include areas outside the AEM survey, as well as areas of bedrock within the survey area.

Table A: *Predicted salinity hazard (based on AEM-derived unsaturated zone salt store and depth to water table) for individual sub-areas. Note: these figures have been rounded to the nearest whole number.*

Area Name	Hazard Class	Hectares	Percent
Mantinea Plain, Carlton Hill and Parry's Lagoon	1-3.Very Low to Moderately Low	2574	50
	4. Moderate	434	9
	5. High	371	7
	6. Very High	559	11
	7. Extremely High	1170	23
Mantinea Plain, Carlton Hill and Parry's Lagoon Total		5110	100
ORIA Stage 1	1.Very Low	2436	16
	2. Low	3195	21
	3. Moderately Low	4470	30
	4. Moderate	2729	18
	5. High	1156	8
	6. Very High	500	3
	Area not assessed	547	4
ORIA Stage 1 Total		15032	100
ORIA west bank	1.Very Low	2706	98
	2. Low	49	2
	3. Moderately Low	14	0
	Area not assessed	4	0
ORIA West Bank Total		2772	100
Packsaddle Stage 1 and 2	1.Very Low	29	1
	2. Low	2138	41
	3. Moderately Low	1767	34
	4. Moderate	884	17
	5. High	86	2
	Area not assessed	358	7
Packsaddle Total		5263	100
Weaber Plain	1.Very Low	4822	33
	2. Low	1505	10
	3. Moderately Low	2031	14
	4. Moderate	1610	11
	5. High	493	3
	6. Very High	267	2
	Area not assessed	3937	27
Weaber Total		14665	100
Keep River (WA) and Knox Creek Plain	1.Very Low	6832	81
	2. Low	709	8
	3. Moderately Low	139	2
	4. Moderate	433	5
	5. High	177	2
	6. Very High	1	0
	Area not assessed	118	1
Knox Plain Total		8409	100
Grand Total		**51250**	**100**

A more detailed breakdown of salinity hazard by hectare and percentage for the Weaber Plain area is shown in Table B below.

Table B: *Predicted salinity hazard (based on AEM-derived unsaturated zone salt store and depth to water table) for the Weaber Plain Development area and the Buffer Zone. Areas not assessed include areas that lie outside the AEM area and areas of bedrock outcrop within the project area. Note: these figures have been rounded to the nearest whole number.*

Area Name	Hazard Class	Hectares	Percent
Weaber Plain Buffer Zone	1.Very Low	2834	19
	2. Low	817	6
	3. Moderately Low	513	3
	4. Moderate	306	2
	5. High	56	1
	6. Very High	0	0
	Area not assessed	1898	13
Weaber Plain Buffer Zone Total		6423	44
Weaber Plain Development Area	1.Very Low	1988	13
	2. Low	688	5
	3. Moderately Low	1519	10
	4. Moderate	1305	9
	5. High	437	3
	6. Very High	267	2
	Area not assessed	2039	14
Weaber Plain Development Area Total		8242	56
Grand Total		**14665**	**100**

5. Potential surface (soil) salinity maps produced in this study are based on classification of Landsat 5 TM data integrated with geomorphic maps using an informed GIS-approach. They successfully identify most of the known surface salt scalds in the area. However, these maps are more powerful when used in conjunction with maps of shallow conductivity (0-2m) that are integrated with maps of moisture persistence (produced by temporal analysis of Landsat data). The latter identify areas of surface moisture persistence and high conductivity where salts are thought to accumulate at surface (in areas of deeper water tables). Examples include internal drainage basins where there is perching and/or low rates of deep drainage (e.g. northern Weaber Plain). In these locations, salt is likely to be concentrated in soils and sub-soils by evapotranspiration of infiltrated rainwater and/or spring-derived water. Salt concentration in Green's Location and Martin's Swamp in the Stage 1 area may have originated in this way.
6. The AEM survey, validated by drilling data, has been used to map key elements of the hydrogeological system associated with the alluvial aquifer. Some key findings are summarised below:
   - In the ORIA Stage 1 area:
     i. The presence and orientation of three discrete palaeochannels, interpreted as elements of the palaeo-Ord drainage system have been mapped beneath Ivanhoe and Packsaddle Plains.
     ii. Overall, the amount and extent of gravel present in the Stage 1 areas appears to be significantly less than previously thought, with gravel aquifers present in laterally confined palaeochannel systems. Sand aquifers also appear to be more laterally restricted than previously mapped.
     iii. Buried bedrock ridges and areas of thick clays may retard groundwater flow westward towards the Ord River in the Ivanhoe Plain.
   - In the Weaber Plain:
     i. One discrete palaeochannel system can be mapped in the AEM data. This palaeochannel is the main Ord Palaeochannel that enters Weaber Plain through Caves Springs Gap, and exits though the present Keep River Plain is narrower than previously mapped, and appears to have a very low thalweg gradient (to the NE).
     ii. An older, smaller, discontinuous palaeochannel system occurs in the north of the Weaber Plain. This is heavily weathered, consists of interbedded gravels and clays, and is associated with tufa deposits. This unit does not have a distinct AEM signature. The

hydraulic conductivities of the gravels in this palaeochannel are interpreted to be significantly reduced.

iii. The area of gravel aquifer storage in the Weaber Plain appears to be considerably less than previously considered. Sand aquifers are also more confined, with an abundance of fine-grained silts interpreted to be present higher in the alluvial sequence and laterally connected to the interpreted gravel-rich palaeochannels.

iv. There are several buried bedrock ridges and shallow pediments that are interpreted to reduce aquifer storage within the alluvium.

- In the Keep River and Knox Creek Plains, a higher percentage of clay is interpreted to be present in the alluvium than previously mapped, with gravels, where present, mainly occurring as thin lenses in silts and clay units. The limited lateral extent and thickness of the coarser textured units prevents their detailed mapping.
- In the Mantinea Plain-Carlton Hill-Parry's Lagoon area, the presence of a marine sand aquifer containing very saline groundwater is confirmed beneath much of the area.

7. In the Weaber, Keep River and Knox Creek Plains, analysis of bore hydrographs has revealed periods of significant watertable rise in areas that have yet to be cleared but which are earmarked for irrigation development. A number of important findings have been made:
   - There have been relatively rapid watertable rises across the Weaber, Keep River and Knox Creek Plains (with some local variability). These were initiated in the early 1990's, and water table rises of 10m have been recorded in some bores (southern Weaber Plain near Cave Springs Gap) in this period. This recharge is related to rainfall events. It is notable that this recharge has occurred prior to land clearing, and the recharge rates are much higher than predicted in previous reports.
   - An earlier, but less dramatic rise in the watertable is specifically observed in bores located in the southern half of the Weaber Plain near Cave Springs Gap. This rise of 3-6m, occurred over a 30 year time period, and commenced shortly after irrigation. This is inferred to relate to recharge associated with irrigation drainage via Cave Spring Gap, either as lateral flow through the Ord palaeochannel, and/or through recharge of excess surface waters at the termination of the M1 water supply channel.
   - The hydrograph responses are contrary to most previous predictions, but are consistent with recent observations about the links between recharge and rainfall in the ORIA Stage 1 areas (Smith, 2008). The hydrograph results point to a need for a fundamental reassessment of the methods of recharge estimation in areas of cracking clay soils in the tropics, where macropore bypass flow may be the key recharge mechanism.

8. An interpretation of the AEM dataset coupled with complementary drilling and other surface mapping data have been used to address specific salinity and groundwater management questions identified by the Project Steering Committee. Potential management implications that can be drawn from the analysis of these data and derived products are summarised below. It is emphasised that further groundwater modelling is essential to provide enhanced spatial and temporal predictions of groundwater movement and salinity risk as a consequence of irrigation development, landuse and /or climate change:
   - The salinity hazard in many of the Stage 2 areas earmarked for irrigation development is high, with salt stores and groundwater salinity often much higher than in the Stage 1 areas, and pre-clearing water tables relatively shallow. Management of deep drainage to control water and salt balance will be essential, and may be particularly challenging in some areas. Cropping strategies will also have to make allowance for the potential for higher root zone salinities than encountered in the Stage 1 areas.
   - In the Weaber-Keep River-Knox Creek Plains, the rapid rise in the groundwater tables over the past decade in response to increased rainfall is of concern, as it demonstrates that the aquifer storage is filling up more rapidly than groundwater flow can drain the system naturally (to the Keep River). This is consistent with the AEM mapping that shows the confined nature of the palaeochannel system, the lack of apparent lateral connectivity across the area, and the low gradient observed at the base of the palaeochannel. Climate modelling suggests this increased rainfall trend is unlikely to reverse in the short to medium term, hence recharge control is likely to be a major factor in determining the sustainability of irrigation in this area (particularly given the need to manage water balance on-farm).

- The pre-1990s rise in the Weaber Plain hydrographs near Cave Springs Gap suggests the probability of groundwater flow between the ORIA Stage 1 area and the Weaber Plain. This is supported by the AEM mapping of the palaeochannel that connects these two areas. Other possible contributions to watertable rise come from leakage from the D8 drain and the D8 swamp. It is suggested that this possible groundwater connection needs to be factored in to any groundwater modelling and management, including potential 'back-flow' to ORIA Stage 1.
- In the ORIA Stage 1 area, recent watertable decline beneath a stand of unirrigated Sandalwood and African mahogany in Martins Location on Ivanhoe Plain has suggested that tree plantations can significantly influence groundwater levels by decreasing local groundwater replenishment and increasing transpiration. Observations also suggest that dissolved salt moves downwards through the profile as groundwater levels drop, indicating it is relatively mobile even in the fine-grained sediments found around Martins location.
- The AEM-derived products provide a basis for assessing the potential for leakage from water supply and drainage infrastructure. In the Stage 1 area, there are several locations where irrigation infrastructure transects areas of high potential salinity hazard, as well as areas of higher potential deep drainage.
- In two of the workshops held with local stakeholders, feedback from individual irrigators was that there is an apparent correlation between areas of high conductivity (mapped using both ground and airborne EM systems) in the top few metres of the landscape and reduced crop productivity (for some crops). While no detailed analysis of land use, crop yield and EM data was carried out in this project, it is a potentially valuable observation that requires follow-up investigation.

Overall, the products and accompanying analysis and interpretation detailed in this report should provide a useful framework for planning irrigation development in the ORIA Stage 2 areas, as well as providing an important environmental baseline dataset for Stage 2 development. The utility of the derived datasets will be maximised if they are incorporated in future groundwater modelling and planning processes.

The broader implications from this work include:

1. The project has demonstrated the potential for 'calibrated' AEM systems and Fast Approximate Inversion software to shorten AEM project timelines significantly. More specifically:
    - Survey acquisition times were reduced through not having to fly as many repeat calibration tests or tie lines.
    - Although reducing the time employed to check and assess the quality of the AEM dataset acquired, it did not eliminate this requirement. Nonetheless, fewer 'corrections' were required in the finalisation of data.
    - AEM data inverted using the fast approximate inversion (iTEM) were obtained within 24 hrs of data acquisition. The early availability of high quality estimates of ground conductivity facilitated the early design of a drilling program, the extension of the survey whilst it was in progress, and the initiation of data interpretation immediately.
    - The initial multi-layer iTEM inversions had high correlation coefficients (>0.8) when comparing FID points to adjacent borehole induction logs, and the inversions have proven to be very robust.

2. This project has demonstrated the benefits of a phased or staged approach to assessing the methods and technologies used as part of a 'hydrogeological systems' approach when developing the framework for salinity and groundwater management.

The main recommendations arising from this study for the ORIA are:

1. A program of groundwater and land use modelling in the Stage 2 areas is recommended to produce refined salinity hazard and risk maps building on the framework of information provided as part of this study.
2. The modelling should also use the data and information contained within this report to assist with assessing the likely impacts of land clearing and irrigation (as currently planned) on the groundwater system, and the long-term sustainability of the proposed irrigation developments. It is recommended that

the resulting model be used further to develop strategies to minimise groundwater recharge and to develop sustainable cropping strategies.

3. Groundwater and land use modelling is also recommended to assess the potential impacts of irrigation development on high value environmental assets adjacent to and/or downstream of the Ord Stage 2 areas (Keep and Ord Rivers). In particular:
   - The potential impacts on perched freshwater lagoons and groundwater dependent ecosystems (GDEs) in the adjacent Ramsar wetlands in Parry's Lagoon should be studied.
   - Modelling is also required to investigate the potential impacts on freshwater flush zones that support riparian vegetation along the Ord River upstream of the estuarine limit in the Stage 2 areas.
   - Given the high potential surface salt hazard in the northern Weaber Plain, consideration needs to be given to revising surface flow modelling to assess the potential downstream salinity impacts via modified Border Creek flows.
   - Hydrograph data from Smith (2008) and others, when linked to the new water table surface generated in this study suggest that as the groundwater mound in the Western Weaber Plain rises further, there is potential for groundwater to flow back towards ORIA Stage 1 (this may already be occurring- Tony Smith, pers. comm, 2009).
4. There remain important knowledge and data gaps in the Stage 2 areas. These may be addressed by implementing:
   - A targeted program of additional shallow drilling to remove ambiguities in the interpretation of the AEM dataset and parameterise future groundwater models is required within the Stage 2 areas.
   - A limited hydrogeochemical study to assess the relative contributions of groundwater recharge in the Stage 2 areas, and to understand surface water – groundwater interactions and processes more generally.
   - A program of soil mapping at an appropriate scale to provide sufficient detail to assist with planning of irrigation infrastructure.
5. Testament from growers combined with some limited scientific studies suggest there is some evidence of a relationship between high electrical conductivities in the shallow sub-surface and poor crop productivity in ORIA Stage 1. The issue is complicated by other possible causes of poor crop productivity including sodicity, alkalinity and waterlogging (Richards, 2002). It is recommended that a focussed study involving the assessment of soils, sub-soils and available EM datasets (ground and airborne) be undertaken to clarify this relationship. The results of such an investigation are required to help understand salinity and groundwater processes, and translate the salinity hazard maps into salinity risk maps that will help identify specific areas of potential damage to crops. These investigations would also assist with determining crop suitability in both ORIA Stage 1 and Stage 2.
6. In support of the recommendations of Smith & Price (2008), it is recommended that long-term annual monitoring of soil salinity and groundwater conditions (water levels and salinity) be established at strategic locations within the ORIA in Stage 1 where secondary salinisation has been identified and a high salinity hazard and risk is assessed. Similar monitoring should be undertaken to provide baseline data in areas assessed to have high salinity hazard and risk in the Stage 2 areas. The objective of the monitoring should be to measure the degree, extent and trend of soil salinity at each location and across the irrigation area.
7. Hydrograph assessment in the Weaber, Keep River and Knox Creek Plains, highlights the need for robust baseline monitoring of groundwater conditions in the area. An improved understanding of groundwater dynamics and underlying mechanisms could be achieved by:
   - The ongoing maintenance and monitoring of bores that already have a long-term data record (such as Bore 8365 in the southern Weaber Plain).
   - Installation, regular downloading, and maintenance of data loggers in key bores, to provide a more detailed time series of groundwater levels. The time period between measurements in the existing data record is in the order of months or years. Loggers, calibrated with regular (typically 3-monthly) on-site measurements, would enable the (sub) hourly collection of groundwater level data. This greater frequency is critical for observing groundwater response to rainfall events, and

to identify seasonal fluctuations in water levels. It is currently difficult to distinguish seasonal variability from any underlying longer-term watertable trends.

- Collection of supporting data to help interpret recharge mechanisms. This includes groundwater sampling and hydrochemical analysis, such as age dating using isotopes or atmospheric tracers (e.g. CFCs). Time series monitoring of both groundwater level and electrical conductivity (salinity) using combined data loggers at specific bores, and/or the routine measurement of the stable isotope composition of aggregated monthly rainfall samples would be useful for understanding both recharge processes and groundwater dynamics.
- For monitoring and evaluation purposes, it is recommended that additional shallow piezometers and automated borehole loggers be sited in strategic locations using the AEM data and derived products.
- It is further recommended that groundwater modelling should incorporate different climate scenarios including the 'average' CSIRO climate model prediction, as well as drier and wetter scenarios using local longer-term records.

8. There remain specific knowledge gaps in our understanding of the hydrogeochemistry and dynamics of groundwater and surface-groundwater interactions across the ORIA. To assist with refining salinity hazard and risk, it is recommended that:
    - Pore fluid analyses from this study should be combined with historic groundwater sampling to better characterise hydrogeochemical domains.
    - Hydrochemistry of source waters (such as rainfall, irrigation supply and drainage, river and estuarine water) be better characterised, both by analysis of existing water quality data, or by additional data acquisition through specific water sampling programs. This is important to define end-members and to assess groundwater chemistry variations on the basis of mixing ratios.
    - Incorporating other hydrochemical analyses of groundwater samples such as age dating techniques (e.g. tracers such as chlorofluorocarbons) should be undertaken to obtain a better understanding of groundwater dynamics and processes.
    - Time series monitoring of hydrochemistry will provide insights into groundwater dynamics, in particular the understanding of recharge processes.
9. It is recommended that further analysis of the AEM data should be undertaken to assist with identifying leakage zones from irrigation infrastructure, and optimising drainage effectiveness in the existing irrigation areas. Specifically:
    - Further analysis should be undertaken of the AEM data along the M1 supply channel to identify potential leakage zones. This would require some ground validation to validate the interpretation.
    - Synthetic AEM sections (i.e. not sections along original flight lines) should be constructed for the other supply channels and drains in the existing ORIA Stage 1 area to assist with identifying leakage zones and areas of ineffective drainage. A program of targeted ground validation would be required to validate the interpretation and calibrate the groundwater responses.
    - Synthetic AEM sections should be constructed for the M2 and M2N supply channels and proposed drains in the Weaber Plain. This study should incorporate available geotechnical analysis of pits along these routes, as well as further targeted drilling to validate the interpretation and obtain groundwater data, and establish monitoring and evaluation boreholes.
10. From a salinity management and salt balance perspective, tree plantations such as found at Martins location may locally keep water tables well below the surface in areas where the aquifer has a relatively low transmissivity, and they may also encourage salt to move down and accumulate beneath the rooting zone. It is recommended that deep-rooting plantations such as mahogany be considered for water table and salinity management as buffers in areas of finer-grained silt and clay lithologies.
11. The probable connection, through Cave Springs Gap, of the groundwater systems between ORIA Stage 1 and the Weaber Plain suggests that there is a need to consider groundwater management in the Stage 1 and Stage 2 (Weaber) developments as one management system. Groundwater models should certainly consider this connection.
12. It is also recommended that OIC and the relevant State agencies consider an approach to the wider communication of this report and associated data, thereby enabling further consultation and analysis of

its content to the wider benefit of the community. At present only a few of the community and growers have had the chance to look at the data and fewer have been able to take the data away to interpret in their own farms or circumstances. A process to do this should be considered with the OIC, involving both industry, and its representatives, such as the Department of Agriculture and Food, Water and Environment and Conservation.

13. It is recommended that a scoping and technical risk evaluation study be carried out to assess the suitability of AEM methods for mapping salinity hazard and key elements of the hydrostratigraphy in the Keep River Plain in the Northern Territory. Based on the results in this report, an AEM survey may provide valuable information on salinity hazard and environmental baseline conditions, although it is noted that ground conductivities are likely to be much higher in this area, with a higher technical risk likely.

More general recommendations include:

1. It is recommended that integrated hydrogeological assessments be carried out in advance of proposed irrigation development in northern Australia. Integrated assessments should be phased, and include:
    (i) Collation and review of existing information for the purpose of identifying critical knowledge gaps;
    (ii) Scoping and technical risk evaluation to assess the methods and technologies best suited to addressing identified knowledge gaps;
    (iii) Integrated geoscientific studies to enable key elements of the hydrogeological system to be mapped, and groundwater flow and hydrogeochemical processes to be understood;
    (iv) Data synthesis and interpretation using contemporary 'systems' approaches, with an emphasis on delivering products that address specific issues and assist with the improved parameterisation of hydrogeological models;
    (v) Groundwater, surface-groundwater modelling and land use modelling to ascertain the sustainability of proposed developments. Modelling should utilise the best available climate data and modelling scenarios.
2. The acquisition of ground and airborne geophysical data for salinity hazard mapping should only be considered within the context of the broader, integrated, hydrogeological assessment of an area. Technical risk evaluation is required to gauge the merits of employing different geophysical approaches and technologies.
    - Acquisition of AEM data should only proceed after completion of scoping studies to assess the likelihood of success arising from their acquisition.
    - Scoping studies are required to identify target aquifers and groundwater systems, and the scale, depth and orientation of target objectives (where possible). This should then be followed by completion of a technology suitability assessment exercise in each area. Technology selection should include forward modelling of system responses, and should follow the best practice procedures developed by the Commonwealth, taking particular note of the ability of AEM system to map key elements of relevant elements of the hydrogeological system.
    - AEM data analysis and interpretation should follow a 'hydrogeological systems' approach based on the methodology recommended by the Joint Academies of Science Review of Salinity Mapping Methods in the Australian Landscape Context (Spies & Woodgate, 2005). Based on these recommendations, AEM-based projects need to incorporate a drilling program, complementary ground investigations and hydrogeochemical studies to ensure appropriate survey calibration, validation and interpretation.
3. A similar, phased approach is recommended for the assessment of groundwater resource and Managed Aquifer Recharge opportunities in priority catchments in northern Australia.
4. Future AEM surveys should carefully consider the merits of using calibrated AEM systems and inversion software that can significantly shorten data acquisition and delivery timeframes. These technologies and methods can significantly shorten overall project timeframes and potential costs.

5. The use of sonic drilling technology was an unqualified success in this project with nearly 100% core recovery in wide range of unconsolidated and consolidated geological materials, and delivery of uncontaminated core for hydrogeochemical investigation. The use of this technology in similar studies is strongly commended.
6. Within the context of broader, integrated, hydrogeological assessments, and following on from previous AEM-based studies in the Murray-Darling Basin, it is also recommended that acquisition of AEM data be considered more broadly in Australia to:
    - Assist with the reconfiguration of existing irrigation assets and map potential links to environmental flows.
    - Provide environmental baseline data for proposed and planned future irrigation districts elsewhere in Australia (e.g. in Tasmania).

The knowledge and products generated as part of this study provide a framework for the ongoing assessment of salinity and groundwater management options in the ORIA. More specifically, through their incorporation in further groundwater and land use modelling and the construction of new salinity risk maps, they will provide a firm basis to assist with salinity mitigation, improved groundwater management, enhanced water use efficiency, improved crop production (and crop suitability), and protection of environmental assets. The methodology developed and applied in this project, have the potential to be applied to a range of projects in northern Australia, and elsewhere.

Contents

List of Figures

List of Tables

1 Introduction

1.1 PROJECT BACKGROUND

The Ord Valley Airborne Electromagnetic (AEM) Interpretation Project (AEM Interpretation Project) was established to provide information relating to salinity and groundwater management in the Ord River Irrigation Area (ORIA), near Kununurra in the north of Western Australia (Figure 1). The Ord was recognised as a priority catchment under the National Action Plan for Salinity and Water Quality (NAPSWQ). The location of the project area with respect to the major drainage sub-catchments and RAMSAR-listed wetlands is shown in Figure 2. The project was designed to fill hydrogeological knowledge and data gaps in the existing ORIA Stage 1 irrigation area, as well as provide baseline hydrogeological data for the planning of future (Stage 2) irrigation areas (Figure 3). The project was co-funded by the Australian and Western Australian Governments under the auspices of the NAPSWQ, and managed by Ord Irrigation Cooperative (OIC) for the Rangelands NRM Group.

The AEM Interpretation Project originated in 2005 when OIC contracted the Cooperative Research Centre for Landscape, Environments and Mineral Exploration (CRC LEME) to assess gaps in hydrogeological data and knowledge, and to explore the appropriateness of ground and airborne electromagnetic (EM) techniques to delineate aquifer systems, and to map water quality variations, recharge and infrastructure leakage. A number of studies had previously examined the hydrogeology and salinity of the region (O'Boy *et al*., 2001; Salama & Pollock, 2003; Pollock *et al*., 2003, Barr *et al*., 2003; and Smith *et al*., 2005). However, the more recent of these studies had concluded that the existing hydrogeological models of aquifer systems in the ORIA Stage 1 area were inadequate to explain observed groundwater flows between individual aquifers, and between the aquifers and the deeply incised river system and drainage works (Smith *et al*., 2005). Post-1965 development has seen a substantial rise in groundwater to within a few meters of the surface in much of the Stage 1 irrigation area, posing a salinity risk in the district (Salama *et al*., 2001).

The CRC LEME study involved a re-assessment of aquifer stratigraphy and connectivity based on a contemporary approach to the analysis of sedimentary facies architecture from borehole data (Lawrie *et al*., 2006a, b). The study proposed a new model to explain the evolution of the Ord Floodplain and the depositional environment and inter-connectivity of the sand and gravel aquifers. Ground and borehole geophysical surveys were also carried out and integrated with soil and aquifer textural data to assess the suitability of electromagnetic (EM) techniques for mapping key elements of the hydrostratigraphy. The study concluded that *some* AEM methods should be able to map the sand and gravel aquifers, clay-rich layers, and the regolith-basement interface in places (Lawrie *et al*., 2006a). However, the study also concluded that there was insufficient contrast in water quality (and hence electrical conductivity) between surface and groundwater for EM techniques to map recharge and leakage from irrigation infrastructure directly. Rather, an indirect, surrogate approach based on mapping sand/gravel and clay lithologies was recommended as a way of predicting zones of preferential recharge, deep drainage and maps of groundwater flow (Lawrie *et al*., 2006a).

Upon consideration of the findings of the initial study, CRC LEME was asked by OIC to scope a follow-on project using AEM methods and complementary drilling data. This project was required to map the aquifer systems and salinity in both the ORIA Stage 1 and Stage 2 areas (including the Weaber, Keep River and Knox Creek Plains, and the Mantinea-Carlton Hill-Parry's Lagoon area, as well as the Northern Territory component of the Stage 2 development). A proposal involving CRC LEME was submitted to obtain NAPSWQ funds in 2007, however with delays in funding approval, and the cessation of CRC LEME in June 2008, the individual parties involved in the original CRC LEME project proposal were contracted to carry out the work. Geoscience Australia (GA) was contracted to develop customised map products designed to map key elements of the hydrogeological system and salinity hazard using the AEM and complementary datasets. Curtin University managed the acquisition of the LiDAR dataset, while the Commonwealth Scientific and Industrial Research Organisation (CSIRO), through the Water for a Healthy Country Flagship (WfHC), were contracted to manage the AEM acquisition. CSIRO were also sub-contracted to GA for specialised AEM processing and inversion services, and to assist with data interpretation and modelling.

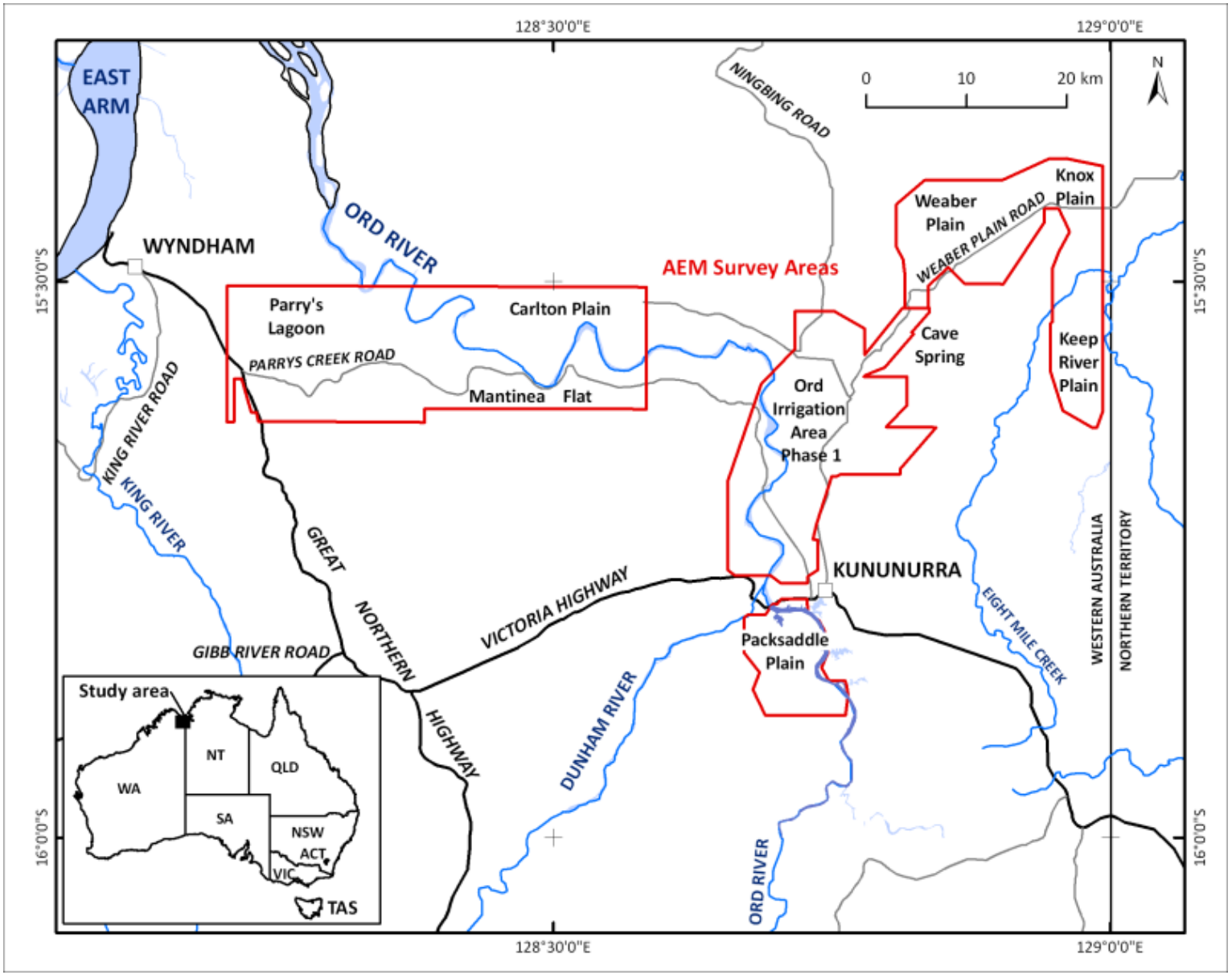

Figure 1: *Study area location map showing the location of the study area and project area boundaries.*

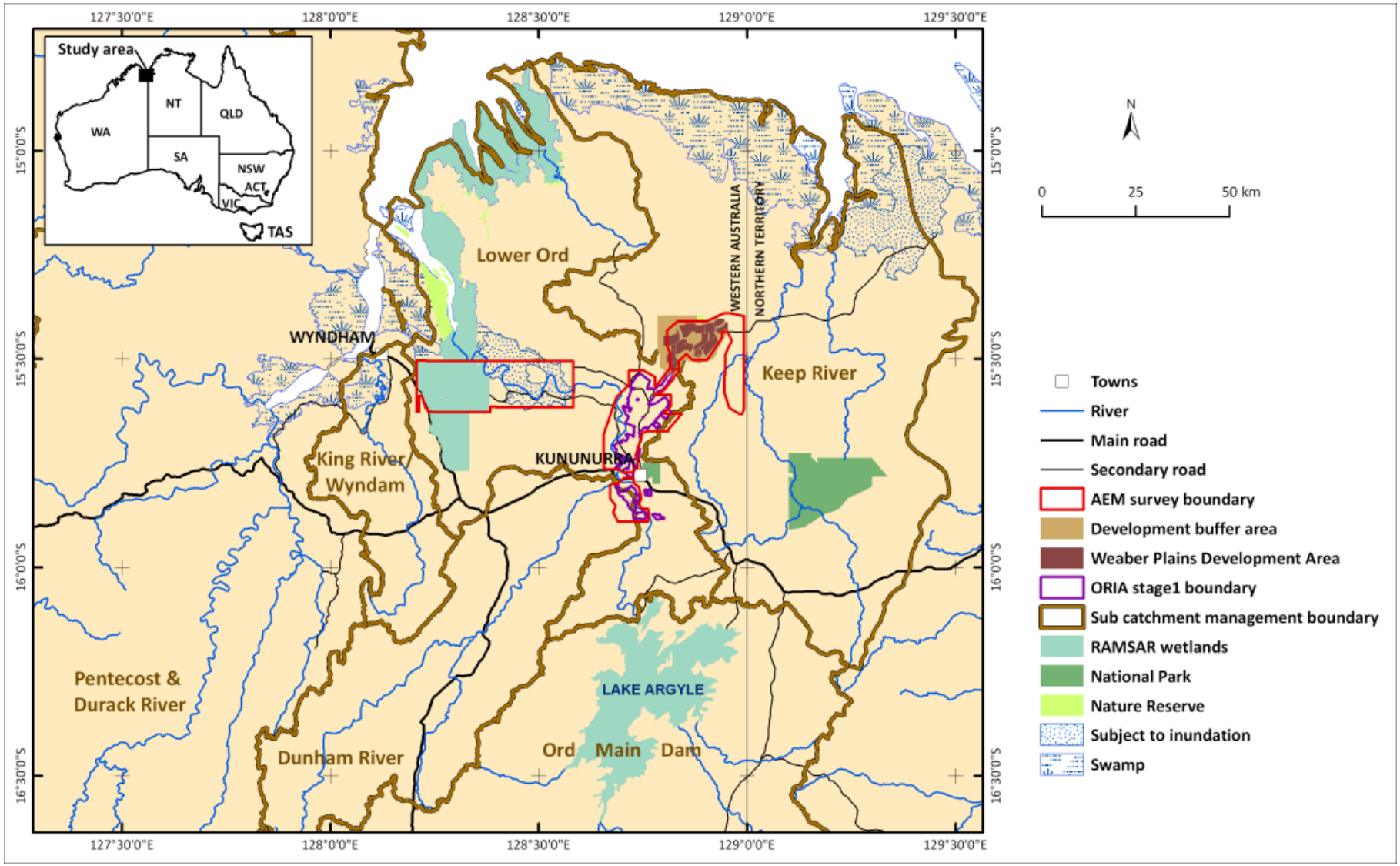

Figure 2: *Map showing the location of the Ord Valley AEM project relative to the major surface drainage sub-catchments (boundaries sourced from DoW) in the project area. The ORIA Stage 1 area lies within the Lower Ord sub-catchment. The Weaber Plain, which is earmarked as the first Stage 2 area to be developed, lies in the Keep River sub-catchment. Ramsar-listed areas are also shown.*

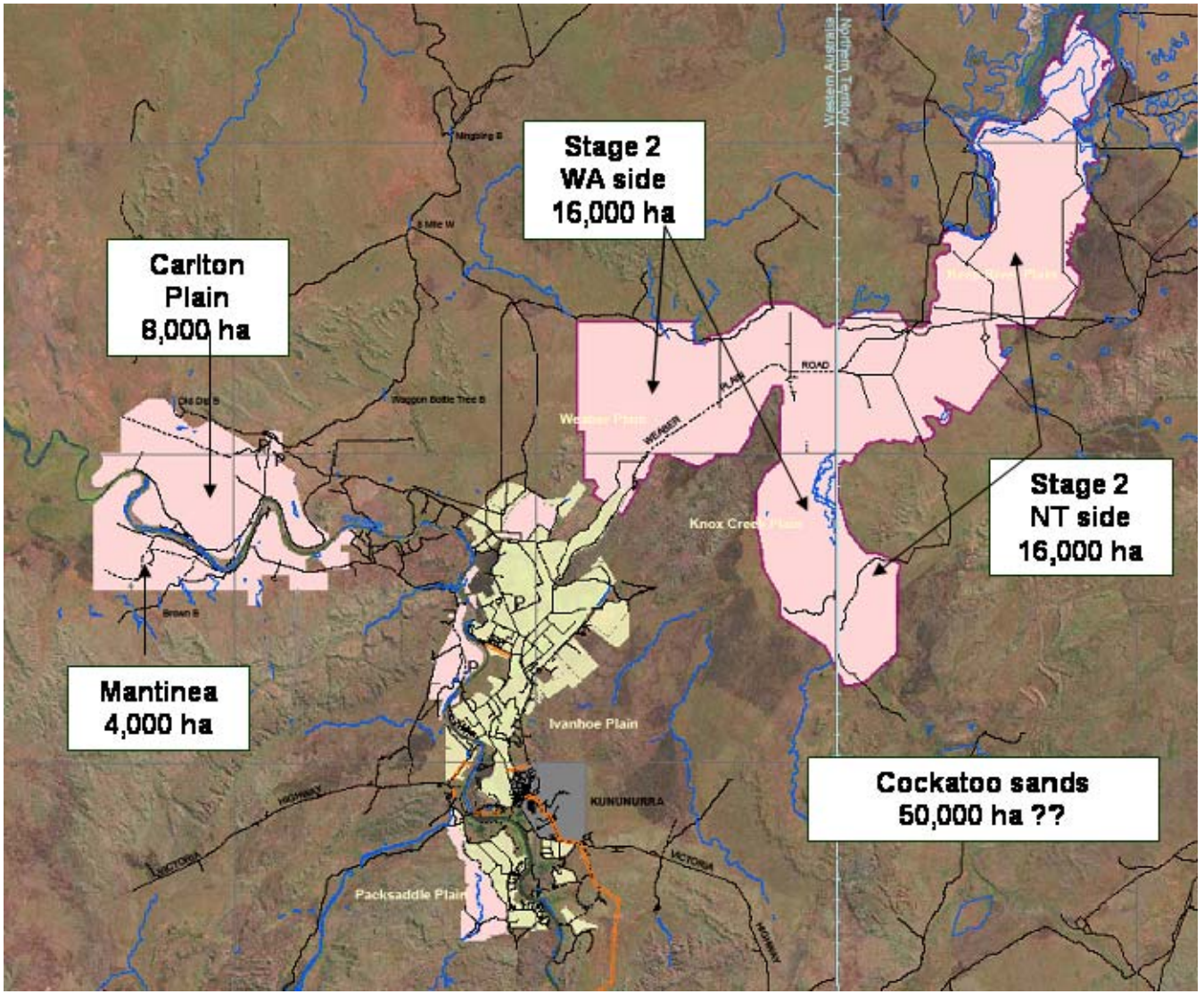

Figure 3: *Map showing proposed Stage 2 irrigation areas (pink), relative to the existing Stage 1 area (beige).Image supplied by Geoff Strickland, OIC.*

.

A Project Steering Committee provided general oversight of the project and helped establish the key salinity and groundwater management outcomes and outputs for the project, in addition to providing an important link with stakeholders and the broader community. The steering committee was chaired by the CEO of OIC (initially Tony Chafer, and then Geoff Strickland), coordinated by Anna Price from OIC (subsequently Brolgas Environment), and comprised representatives from the WA Departments of Water (DoW), and Agriculture (DAFWA), the Ord Catchment Reference Group and the Rangelands NRM Group, as well as local irrigators, CSIRO and GA. The work of the steering committee enabled the science team to scope the project appropriately, and to design a suite of interpretation products to answer the key management questions and provide the appropriate products to help achieve the desired management goals. The Steering Committee also played an important role in organising stakeholder knowledge exchange workshops, coordinating local feedback and comment on products and reports, the organisation of knowledge transfer workshops, and in the peer review process generally.

Phase 2a of the project commenced in mid-2008, with an AEM forward modelling and technology selection study carried out to assess the most suitable AEM system for the project objectives (Fitzpatrick *et al*., 2008). Phase 2b of the project involved the acquisition of airborne electromagnetic (AEM) and Light Ranging and Detection (LiDAR) surveys, and complementary drilling, borehole geophysics, laboratory analysis and interpretation services. Scientific and technical standards for the project followed the guidelines established by the Joint Academies of Science Review of Salinity Mapping in the Australian Landscape Context (Spies & Woodgate, 2005).

Due to difficulties encountered using conventional drilling techniques, supplementary NAPSWQ funds ($126k) were sought to fund a drilling program using advanced Sonic drilling technology. The drilling program was successfully carried out upon receipt of the funds in May 2009. Integration of the laboratory data derived from the drilling campaign to produce customised AEM interpretation products delayed the completion of the project until end September 2009. The total cost of Phase 2 of the project was approximately $2m. The cost of individual activities is summarised in Table 1.

Table 1: *Project Costing and Responsibility.*

Project Phase	**Project Activity**	**Organisation(s)**	**Cost**
Phase 1	Ground geophysics and borehole analysis and AEM suitability assessment	CRC LEME (Geoscience Australia, Curtin University & Adelaide University)	$168k
Phase 2a	Forward modelling and technology selection	CRC LEME (Geoscience Australia and CSIRO)	$15k
Phase 2b	Salinity Mapping project		
	LiDAR data acquisition, processing and product generation, Qa/Qc and project management	Fugro Spatial Solutions Pty Ltd (with Qa/Qc by Curtin University)	$200k
	AEM data acquisition & Qa/Qc	Geoforce Pty Ltd (with Qa/Qc by CSIRO)	$0.92m
	Drilling permits and community liaison	Brolgas Environment	$15k
	Initial aircore drilling and sonic drilling program	Boart-Longyear Pty Ltd (sonic drillcore)	$110k
	Project management, borehole and ground geophysics, surface mapping, data analysis and integration, interpretation and final product and report generation, peer review and publication	Geoscience Australia in partnership with CSIRO's Water for a Healthy Country Flagship	$580k*
		TOTAL	**$1.994m (ex GST)**

* Note this does not include ~$600k in matching co-investment from CSIRO and Geoscience Australia for overheads and on-costs.

1.2 THE ORD RIVER IRRIGATION AREA (ORIA)

The ORIA Stage 1 irrigation area comprises 14,000 ha developed largely on the black soil plains of the Ord River Floodplain (Figure 1; Figure 4). Irrigation in the Stage 1 area commenced upon completion of the Kununurra Diversion Dam (Figure 5; Figure 6) and the M1 supply channel on the Ivanhoe Plain in 1963 (Figure 7).

Figure 4: *Photograph of a new sandalwood plantation in the southern Ivanhoe Plain, ORIA Stage 1. Sandalwood was introduced to the area in the late 1990's.*

Figure 5: *Photographs show the Ord Dam (top left), Kununurra Diversion Dam (top centre) and Lake Kununurra (top right).*

The Kununurra Diversion Dam (Figure 5) is a 20m high structure that dams the Ord River for ~50km upstream, forming Lake Kununurra with a storage capacity of 101GL (Figure 5; Figure 6; Figure 7). Upstream, the larger Ord River Dam (Figure 5), which was completed in the early 1970s, provides much larger storage (10,700GL) in the Lake Argyle Reservoir. This large surface water resource provides water security for the region, including the planned expansion of irrigation in the East Kimberly. Irrigation water for the ORIA is sourced from Lake Argyle, conveyed via the Ord River to Lake Kununurra, where it is stored locally behind the Diversion Dam, prior to release through a system of largely gravity-fed supply

channels (Figure 7). The existing Stage 1 area is a through-flow system, with excess irrigation waters draining back to the Ord River downstream of the development, and excess water from the main M1 supply channel discharging in the Weaber Plain.

Figure 6: *Photograph of the Kununurra Diversion Dam, taken when the Ord River is in flood. Lake Kununurra lies behind the structure.*

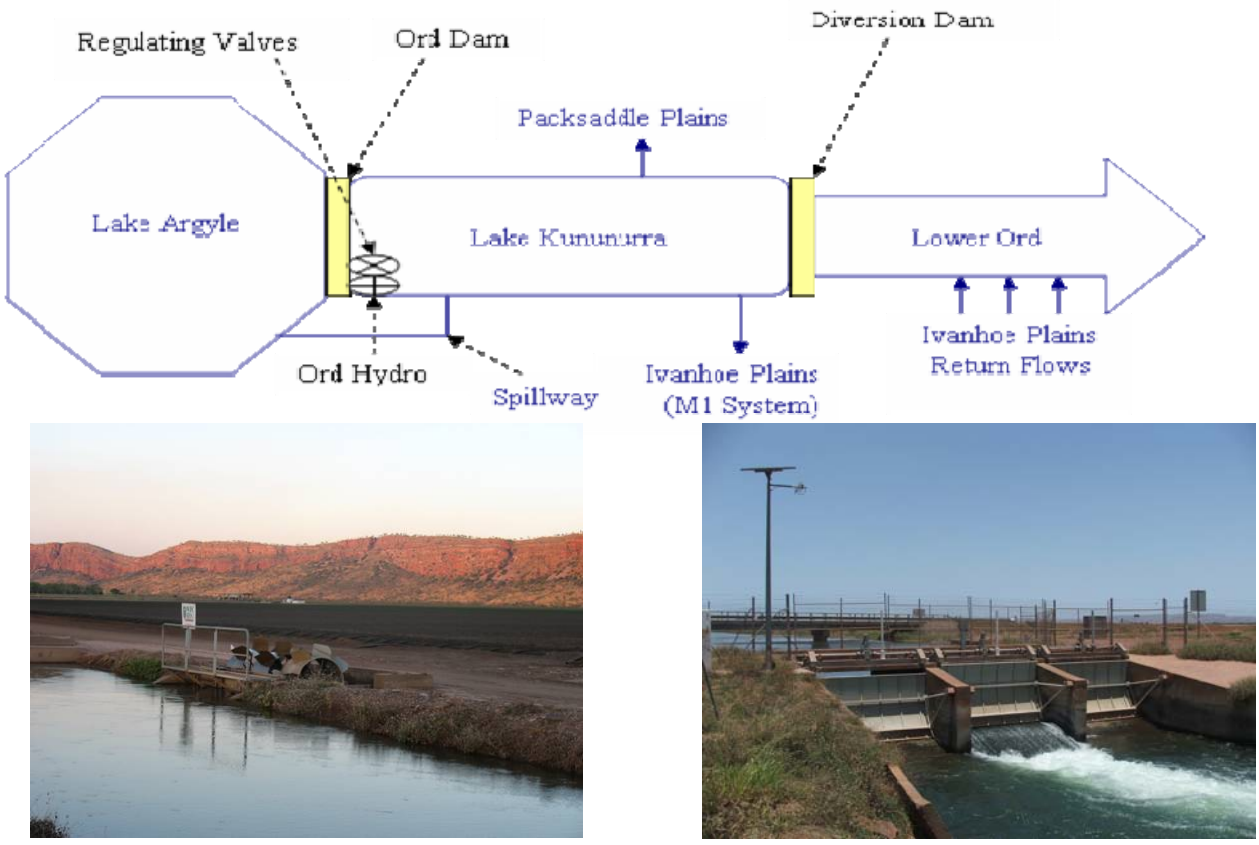

Figure 7: *Diagrammatic representation of the surface water supply for the ORIA Stage 1 irrigation district. Photographs the M1 supply channel in Cave Springs Gap (bottom left) and a control gate on the M1 channel in Ivanhoe Plain (bottom right).*

Recently, the West Australian Government earmarked $220m for the Ord-East Kimberley Expansion Project (Figure 8; www.water.wa.gov.au/ordexpansion), with $195m from the Australian Government funds to support social infrastructure development in the area. It is planned to release 8,000 ha of land in the Weaber Plain for irrigation in 2011 as the first phase in the ORIA Stage 2 development (Figure 1, Figure 2 and Figure ***3***). The Weaber Plain area will be serviced by a new (M2) irrigation supply channel that is an extension of the M1 channel. Importantly, the new development is not planned as a flow-through scheme, but rather will have to manage water on-farm. Over a longer period of time, it is planned to increase the size

of the irrigated area around Kununurra to about 28,000ha. In the longer term, development is also being considered in the adjacent areas of sandy soils (Cockatoo Sands).

Figure 8: *A hoarding placed outside Kununurra announcing the Ord Expansion. It is planned to release 8,000 ha of land in the Weaber Plain for irrigation in 2011 as the first phase in the ORIA Stage 2 development.*

1.3 SALINITY AND GROUNDWATER MANAGEMENT ISSUES, SPECIFIC QUESTIONS, AND DESIRED MANAGEMENT OUTCOMES

Background

Salt occurs naturally and extensively in Australian landscapes (NLWRA, 2001). Much of the salt is derived from aerosols brought in by rainfall and concentrated in the sub-surface over tens or hundreds of thousands of years, with virtually no area of the country free from salt accession and/or storage in the sub-surface (Herczeg *et al.,* 2001; NLWRA, 2001). While there are vast quantities of salt stored in the landscape, the presence of saline soil or salt stored deeper in the ground does not necessarily imply that the surface extent of primary salinity will expand, or that additional salt will rise to the surface and develop new areas of 'secondary' or dryland salinity (Spies & Woodgate, 2005).

The general consensus is that the increase in salinity extent in Australia over the past few decades is due to excess land clearing and changed land use (NLWRA, 2001). This has resulted in increased recharge to groundwater and rising watertables over the past 100-150 years, with significant salinity discharge at the surface in many landscapes (MDBC, 1999; NLWRA, 2001). Land clearing and development of irrigated agriculture in the tropics is generally less extensive than in the south, with a shorter development history, and consequently less time for secondary salinity to develop. Importantly, as the potential expansion of irrigated agriculture in tropical areas is considered, such as in Ord Stage 2, it is important to understand baseline salinity and hydrogeological processes in order to inform development and minimise the potential for secondary salinisation to develop. This study aims to provide key baseline hydrogeological data on which to base sustainable irrigation practices.

Salinity occurrences and processes in general have not been well documented or studied in Australia's dry and wet tropical landscapes, although a similar story of salt accession and accumulation appears to be operating in many tropical landscapes, including the Ord (Tickell *et al.*, 2007; O'Boy *et al.*, 2001; Ali *et al.*, 2002; Ali & Salama, 2003; Smith & Price, 2008). In addition to aerosol-related salinity accumulation, salt is also a feature of many coastal landscapes, although the relative contributions from present day and palaeo-seawater intrusion are not well understood. Present day and palaeo-seawater intrusion may reach tens of kilometres inland in many flat-lying coastal landscapes in northern Australia, including the lower Ord and Keep River estuaries (O'Boy *et al.,* 2001). While some hydrological processes may differ from those in sub-tropical zones, the potential threat of salinity developing in these landscapes cannot be ignored (O'Boy *et al*., 2001, Smith & Price, 2008).

This study was limited to the production of salinity hazard maps and products that will provide a firm basis for further groundwater modelling and generation of salinity risk maps. Salinity is a *hazard* when it has the potential to be moved to where it can threaten assets such as agriculture, infrastructure, water resources and biodiversity (Spies & Woodgate, 2005). *Salinity risk* is a measure of the chance that a salt hazard will cause harm to an asset at some time in the future. Risk should be assessed in the context of the assets to be protected, including agriculture, water quality, infrastructure and the environment (Spies & Woodgate, 2005).

To begin to address these issues, it was recognised as essential to have knowledge of the distribution of salinity and other key elements of the hydrogeology that control groundwater flow and salinisation processes. A review facilitated by the Australian Academy of Sciences and the Australian Academy of Technological Sciences and Engineering for the Australian Federal Government's Natural Resource Management Ministerial Council in 2004-2005 found that the only broadacre, remote sensing technique that can detect and resolve salinity in the sub-surface deeper than the root zone is airborne electromagnetics (AEM; Spies & Woodgate, 2005).

Over the past 6 years, AEM surveys have been shown to be cost-effective in addressing salinity and land management issues when appropriately scoped and planned (Walker *et al.,* 2004; Lawrie *et al.,* 2008, 2009a). These surveys have been particularly successful where they have been designed to address specific land and water management questions within the context of broader natural resource management strategies (Walker *et al*., 2004). Essential to the success of using these technologies has been the development of a multi-disciplinary, systems-based 4-D landscape analysis approach to the interpretation of the AEM datasets (Lawrie *et al.*, 2000, 2008, 2009a, b). This approach incorporates an understanding of landscape evolution and scale, utilises modern investigative approaches to the conceptualisation of aquifer systems, and incorporates data on water, salinity and vegetation dynamics to provide key constraints on aquifer systems. This approach has been greatly facilitated by development of rapid inversion methods (Brodie & Sambridge, 2006; Auken *et al*., 2007, 2009; Christensen, *et al.*, 2009) that facilitate more rapid-turn around in developing interpretation products (Lawrie, 2008, 2009b).

Issues in the ORIA

The principle concerns in the ORIA revolve around salinity and groundwater management and the sustainability of irrigation in the district, as well as the potential impacts on adjacent and/or downstream high value environmental assets. This study was commissioned in an environment where there was still uncertainty over whether groundwater levels in ORIA Stage 1 had stabilised after rising for 40 years, and in the knowledge that some salinity discharge sites had developed in areas marginal to the ORIA Stage 1 (Smith, 2008; Smith & Price, 2008). There was also concern over the long-term salinity hazard and risk in the Stage 2 areas earmarked for development, given higher background groundwater salinity levels (O'Boy *et al.,* 2001), and the need for different drainage strategies in Stage 2, including the need to contain excess irrigation water on-farm.

The high level questions being asked by stakeholders, and summarised in the Ord Land and Water Management Plans (2000, 2006), included:

- Will Ord Stage 1 have a salinity risk in future? If so, where?
- What is the lifetime of ORIA Stage 1 area if salinity is present?
- Will Ord Stage 2 have a salinity risk? If so, where?
- What is the lifetime of ORIA Stage 2 if salinity is present?
- What are effective management strategies to mitigate the threat of salinity?
- Are the high value environmental assets adjacent to and/or downstream of the irrigation areas at risk of salinity as a consequence of irrigation?

The desired management outcomes in the ORIA are essentially:

- Salinity mitigation
- Improved groundwater management
- Enhanced water use efficiency

- Improved crop production (and crop suitability)
- Protection of environmental assets

Using the experience built up in previous AEM salinity projects, the Project Steering Committee worked with local stakeholders to link the desired management outcomes and the practical on-ground management options available to farmers and catchment managers, to the physical attributes of the landscape and groundwater system that could potentially be mapped by the AEM system. These are summarised below:

- Salinity risk mitigation. To be achieved through improved cropping and drainage strategies, and informed by development of maps of salt store, clay and sand distribution, and salinity hazard
- Improved groundwater management. To be achieved through:
  - Development of groundwater management options and plans. These could include guidelines for infrastructure, horticultural and/or tree precincts, and to guide improvements in irrigation field layout and bed and furrow configuration for optimising water use.
  - Adjusting cropping and drainage strategies. This requires quantification of the level of accessions to groundwater, identifying high recharge zones.
  - Identification of leaky parts of the channel, drainage and water storage infrastructure to enable remedial sealing and lining or relocation of this infrastructure.
  - Identification of areas where trees can be planted strategically to control groundwater levels (e.g. clay pans may prevent optimal rooting depth for crops/trees).
  - Identification of areas where sub-surface drainage can be installed to control groundwater levels (e.g. identification of where to deepen surface drains, install vertical sub-surface drainage, tile/horizontal drains).
  - Development of groundwater pumping strategies. This requires a knowledge of water tables, and knowledge of the 3D distribution, hydraulic conductivity and connectivity of sand and gravel aquifers.
- Enhanced water use efficiency and cropping. To be achieved through:
  - Matching crops to sub-soil conditions/barriers water quality. This requires the mapping of sub-soil conditions (e.g. clays vs. sands, mapping of the water table, salt stores and groundwater quality variability).
  - Adjusting land use (e.g. irrigation bay layout) and irrigation methods (i.e. flood, spray or drip irrigation) to prevent leakage to the groundwater system from the application of water within paddocks. Requires identification of high recharge areas, and maps of aquifer systems.
- Protection of environmental assets. To be achieved through:
  - Establishment of buffer zones to protect high value environmental assets. The success of this strategy requires baseline hydrogeological data and maps to understand the groundwater systems and processes that operate and may link the existing and proposed irrigation areas to the environmental assets. These data are required to adjust drainage and cropping strategies appropriately.
  - Establishment of appropriate groundwater monitoring regimes. This requires an understanding of the groundwater systems and aquifers to site monitoring boreholes appropriately.

The Project Steering Committee translated these desired management outcomes, practical management actions and physical attributes into a number of specific priority questions for the AEM Project Interpretation team to focus on. These are listed below:

- Where is salt stored in the landscape (in the saturated and unsaturated zones)?
- What is the distribution of groundwater quality?
- Where are the areas of highest salinity hazard across the ORIA, and what is the regional salt balance?
- What are the extent (in 3D), storativity, and hydraulic conductivity of the sand and gravel aquifers, and how are they connected?

- What is the extent and thickness of clays in the sub-surface?
- What are the spatial and temporal trends in groundwater salinity?
- Are there different groundwater and salinity processes across the ORIA?
- Is it possible to identify areas where salt is at higher risk of being mobilised?
- What are the drivers of recharge across the ORIA, and where are the high recharge zones?
- Where does leakage occur from the water supply infrastructure?
- What processes are driving groundwater rise?
- How do the surface and groundwater systems interact across the ORIA?
- What is the nature of surface-groundwater interaction within the Lower Ord Floodplain (Parry's Lagoon)?
- What is the nature of the freshwater-saltwater interface in the Lower Ord Floodplain?
- What is the salinity and waterlogging risk to native vegetation and wetlands in the proposed buffer zones around the Stage 2 areas?
- How useful are AEM systems in mapping salinity and regolith in areas away from the floodplain (e.g. where much of the development of the Cockatoo systems is proposed)?
- What science data and knowledge gaps remain after the AEM study?

The Project Steering Committee recognised that the AEM and complementary data could fill key knowledge and data gaps, but that not all of the questions listed above could be answered without further investigation and groundwater modelling. In particular, it was recognised that additional hydrogeochemical studies would be required to improve the understanding of groundwater processes in the ORIA, while hydrodynamic modelling utilising the datasets and knowledge gained in this project would also be required to provide temporal and spatial predictions of groundwater movements and salinity risk.

1.4 PROJECT AIMS AND OUTPUTS

This project was commissioned primarily to fill hydrogeological knowledge and data gaps in the existing ORIA Stage 1 area, and to provide baseline hydrogeological data for the planning of future (Stage 2) irrigation areas. Shortly prior to AEM data acquisition, the project boundary was extended to cover the Ramsar-listed Parry's Lagoon wetlands (Figure 1; Figure 2), for which baseline hydrogeological data was also sought. While the primary focus of the project was to deliver on outcomes within the ORIA, the project was also used as a vehicle to test the broader applications of the approach used in this project for mapping groundwater and salinity in similar landscapes in northern Australia.

The specific aims of the project relevant directly to the ORIA, were to:

- Map key elements of the hydrogeological system to inform drainage and cropping strategies and enhance groundwater management within the ORIA Stage 1 irrigation area.
- Identify, quantify and understand the salinity hazard in the ORIA Stage 1 and Stage 2 irrigation areas.
- Provide baseline hydrogeological and salinity data for the planning of future (Stage 2) irrigation developments.
- Address specific salinity and groundwater management questions identified by the Project Steering Committee, in the Stage 1 and Stage 2 irrigation areas.
- Produce baseline data for environmental assessments and the design of groundwater monitoring programs in the Stage 1 and Stage 2 irrigation areas.
- Provide baseline data on the Parry's Lagoon wetlands to assist with understanding surface – groundwater interactions and future potential impacts of land clearing and irrigation in adjacent Stage 2 areas.
- Assess the applicability of AEM methods for salinity and groundwater studies in areas of the Cockatoo Sands.

- Provide recommendations on further hydrogeological investigations where these would assist irrigation management and further development in the ORIA.

Broader aims of the project included making assessments and recommendations on:

- The role of AEM methods as part of a 'hydrogeological systems' approach to the management of groundwater and existing and future irrigation developments in Northern Australia.
- The potential for 'calibrated' AEM systems and Fast Approximate Inversion software to shorten AEM project timelines.
- The applicability of the sonic drilling technique for recovery of core materials and pore fluid analysis in a range of geological materials.

To address (as far as possible) the specific salinity, groundwater and irrigation management questions identified by the Project Steering Committee, it was planned to produce a suite of customised AEM-based interpretation products. These are listed below:

- AEM conductivity depth slices.
- AEM floodplain elevation slices.
- AEM conductivity depth sections.
- Geomorphology / Landforms.
- Vegetation Health (NDVI Differences).
- Surface Salinity.
- Extent and thickness of clays.
- Extent and thickness of sands and gravels.
- Extent, and depth to top of bedrock geology.
- River flush zone extent and thickness.
- Soil Permeability.
- Recharge Potential.
- Surface moisture retention.
- Groundwater Quality.
- Salt Store in the unsaturated zone (above the regional watertable).
- Salt Store in the saturated zone.
- Salinity Hazard.

Many of the AEM-derived products listed above require porosity, grain size and pore fluid data from drillcore. To accomplish this, a drilling program acquired 12 new holes using the advanced Sonic drilling technique. Cores were retrieved from alluvium in the Ivanhoe, Packsaddle, Weaber, Keep River and Knox Creek Plains, and Mantinea-Parry's Lagoon areas. Collection of lithological, hydrogeochemical and hydrogeophysical data from these cores enabled the customised interpretation products listed above to be produced. These provide a sound foundation for addressing the specific salinity and groundwater management questions, including the assessment of salinity hazard.

1.5 SCOPE OF THIS REPORT

The main purpose of this report is to document the use of AEM and complementary borehole and field data in addressing salinity and groundwater management issues in the ORIA Stage 1 and Stage 2 areas. The report incorporates the results from the AEM and LiDAR surveys, geomorphic mapping program, and the drilling and laboratory analysis. The report contains analysis and interpretation of AEM data and AEM-derived customised interpretation products, and seeks to address, as far as possible, the Project Steering Committee's specific salinity and groundwater management questions. The report makes recommendations on the relevance and value that may lie in using AEM-derived map products within hydrodynamic and broader land use modelling frameworks. Overall, this report aims to provide an opportunity for project stakeholders to evaluate the effectiveness of AEM data in assisting with addressing salinity, groundwater and irrigation management issues.

Complementary outputs include reports on the aquifer systems and AEM suitability (Lawrie *et al*., 2006a); forward modelling and AEM technology selection (Fitzpatrick *et al*., 2008); acquisition of the AEM data (Reid *et al*., 2008); and LiDAR data acquisition (Wilkes, 2008; Fugro, 2008). A preliminary overview atlas of AEM products (Fitzpatrick *et al.*, 2008) and overview and sub-area atlases containing final data and products have also been produced (Apps *et al*., 2009a-d). An Appendix volume containing a collection of data that stakeholders may find useful in hard copy form has also been produced (Cullen *et al*., 2010).

In addition, a comprehensive project GIS has been produced (Apps *et al*., 2009e). This 3-volume DVD set contains all data acquired by Geoscience Australia, CSIRO and Curtin University, and all products generated in the course of the project. The GIS was compiled using ESRI ArcGIS Version 9.3 software. The ArcMap projects have also been saved in Versions 9.2 and 8.3. The data are structured in directories for easy viewing and interrogation in ArcGIS. A user guide has been provided to explain firstly the data directory structure and secondly the data structure in the GIS.

2 Land Use, Vegetation and Climate

2.1 LAND USE

The ORIA Stage 1 irrigation area is developed largely on the black soil plains of the Ord River Floodplain, and comprises 14,000 ha of irrigated land, growing a wide diversity of crops (Figure 9 to Figure 12). After a chequered history, the ORIA has been profitable in recent years, with farm gate exports worth about $100m in 2008 (OIC data, 2009; Figure 10).

Irrigation in the Stage 1 area commenced upon completion of the Kununurra Diversion Dam and the M1 supply channel on the Ivanhoe Plain in 1963. Land use in the Ord Stage 1 area has varied greatly over time, from previous emphases on cotton and sugar cane to more recent crops such as sandalwood. The most recent data used in the compilation of this report show that the largest single land use by area is forest, especially sandalwood (Figure 9 to Figure 12). Other crops include pumpkins, melons and mangos. The annual cropping patterns for most of the non-forest areas (with the exception of mango orchards) allows for rapid adaptation to changing economic and environmental conditions.

Recently, the West Australian Government earmarked $195m for the Ord-East Kimberley Expansion Project (with matching Australian Government funds to support infrastructure development in the area). It is planned to release 8,000 ha of land in the Weaber Plain for irrigation in 2011 as the first phase in the ORIA Stage 2 development (Figure ***3***; Figure 11). The Weaber Plain area will be serviced by a new (M2) irrigation supply channel that is an extension of the M1 channel. Importantly, the new development is not planned as a flow-through scheme, but rather will have to manage water on-farm. Over a longer period of time, it is planned to increase the size of the irrigated area around Kununurra to about 28,000ha. In addition to the planned expansion in the Weaber Plains, 4,000ha are earmarked for expansion in the black soil plains in the Mantinea area, 1,300ha in the Ord West Bank, and 1,400ha in Packsaddle Plain, with an additional 8,000ha in Carlton Plain, and 8,000ha in the Keep River-Knox Creek Plain area (Figure ***3***; Figure 11).

In the longer term, development is also being considered in the adjacent areas of sandy soils (Cockatoo Sands). Presently, only limited used had been made in the ORIA of the Cockatoo sands for spray or trickle irrigation to grow peanuts and other annual and perennial horticultural crops. Because they are well drained, access is possible in the wet season. The well-drained nature is confirmed by observations during this study, with the caveat that waterlogging can occur at the base of the sands because of the marked permeability contrast with underlying bedrock.

The Ord Land and Water web page (http://www.olw.com.au/land.htm) indicates that at present sandy soils are used mainly for tree crops (bananas, mangoes, pawpaw and other tropical tree fruits) and annual horticultural crop production (cucurbits, onions, tomatoes and other small crops) using either under tree micro sprinklers or trickle irrigation. Grundon (2000) reported some success for cashews grown on the

Cockatoo soils. Given his observation of the poor results for Cashews grown in areas prone to waterlogging means that our observation of seasonal saturation in the profile at depth may need further investigation.

2.2 VEGETATION

The study area lies within the Ord-Victoria Plains bioregion. Within this area, the native vegetation consists of two main components largely determined by the underlying geology: (i) the Proterozoic and Phanerozoic ranges and scattered hills and mesas are mantled by shallow sand and loam soils which support hummock grasslands with sparse low trees; and (ii) extensive plains underlain by the Cambrian volcanic and limestone lithologies have two main communities, with short grass on dry calcareous soils and medium-height grassland communities on cracking clays (CSIRO, 2009).

Field surveys of the vegetation in the study area have been summarised by O'Boy *et al*. (2001). These reported the presence of 682 plant taxa from 87 families. The dominant families are grasses (Poaceae), eucalyptus and paperbarks (Myrtaceae), sedges and rushes (Cyperaceae), wattles (Mimosaceae), daises (Asteraceae), peas (Fabaceae) and Combretacea. The vegetation is noteworthy because of the presence of Indo-Malayan elements because of its proximity to Asia, and Gondwanan elements, most obviously the boab.

Vegetation on the uncleared alluvial plains is predominantly savannah grassland while that in the riparian zone is savannah woodland. Hill areas have a stunted vegetation of trees and Spinifex. Deeper sandy soils of pediments are also dominated by Spinifex with some trees. Coolabahs occur in areas of seasonal flooding and Pandanus zones of groundwater seepage at the foot of slopes and along bedrock fractures. Both fires and floods cause significant short-term changes to the vegetation structure (Storey & Marshall, 2008).

A somewhat different classification from DEWHA is shown in Figure 13. In this classification, the uncleared alluvial plains are predominantly grassland with scattered clumps of trees. Terrace areas and some pediments in the lower Ord River in the region of Carlton and Mantinea Plains are characterised by open woodlands to woodlands. Hills are dominated by shrub land to grassland vegetation. The coastal plain consists of swamps passing into saline flats. The map is based on the NVIS classification where descriptions were attributed to Level 4 standardised structural names (see NVIS metadata). Classification was then further enhanced by incorporating the ORD GIS Geomorphology layer where areas of irrigation were combined for one class (irrigated areas) regardless of the NVIS classification. This was also done for swamp and stream channel areas.

Within the study area, the lower Ord River Floodplain and Lake Kununurra are listed as Ramsar Wetlands of International Importance. The lower Ord River Floodplain is a large system of river, tidal mudflat and floodplain wetlands that supports mangroves, and a large numbers of waterbirds and Saltwater Crocodiles. The Lake Kununurra Ramsar site is large system of human-made reservoirs and associated wetlands used extensively by waterbirds, particularly during the dry season (CSIRO, 2009).

The construction of the Ord River Dam has caused major changes to the flow regime of the Ord River. Prior to its construction, the Ord River flooded regularly, inundating large areas of its floodplain once in every two to three wet seasons. Most floods were sufficiently powerful to scour the riparian vegetation from banks of the river downstream of the Kununurra Diversion Dam. Flows receded rapidly following the wet season, ceasing by June in most dry seasons, with the river reducing to a series of unconnected pools. After construction of the Ord River Dam, wet season floods have been reduced by a factor of about ten and the river has continued to flow strongly throughout the dry season. Typical flow rates have increased from about zero to 50 m3/second over the driest five months of the dry season. These changes have altered the ecology of the lower Ord River, making it more like a river from the wet tropics, rather than the dry tropics of the Kimberley region. Reductions in the size and erosive power of floods has resulted in a more stable, dense band of riparian vegetation approximately 15 m wide along the water's edge within the main river channel. The permanent dry season flows have increased aquatic habitat and encouraged larger sized fish to develop in the lower Ord River than in nearby unregulated rivers, although the range of fish species found has remained very similar.

Parry's Lagoon (or Floodplain) is a good example of a tropical floodplain with permanent billabongs, seasonal marshes and wooded swamp. It is one of the few such floodplains of substantial area in Western Australia. It is listed jointly with the Ord Estuary System as a Wetland of International Importance under the Ramsar Convention (Government of Western Australia, 1990, 2000).The site has an area of 9000 ha and an elevation ranging between 5 and 10 m above sea level (Environment Australia, 2001). Since the construction of the Ord River Dam in 1972, the lower Ord River floods onto the Parry Floodplain much less frequently and most of the wet season runoff is generated from local creeks (e.g. Wild Goose Creek, Parry Creek) which generate most flows and local flooding in this Ramsar wetland (Rodgers & Ruprecht, 2001). Overbank flows on the lower Ord River are now mainly a result of runoff from the catchment below the Ord River Dam (~10 percent of the previous total catchment); therefore, the Parry Floodplain is now mainly fed by local inflow and local flooding, with much less frequent flooding from the lower Ord River (CSIRO, 2009).

The floodplain's herb land/grassland communities are the most extensive in Western Australia (Burbidge *et al*., 1991; WADCALM, 1990). Seventy-seven waterbird species have been recorded at the site (one of the highest totals in the Kimberley). The permanent freshwater and food resources of the site were valuable to Indigenous people. Areas of this site are popular picnic and bird-watching areas and the site in general is popular with tourists. The Cockatoo sands support open woodland vegetation with *Eucalyptus tectifica, Eucalyptus confertiflora* and *Adansonia gregorii.* Understorey grasses include *Themeda triandra* and *Sorghum* sp (Schoknecht & Grove 1996).

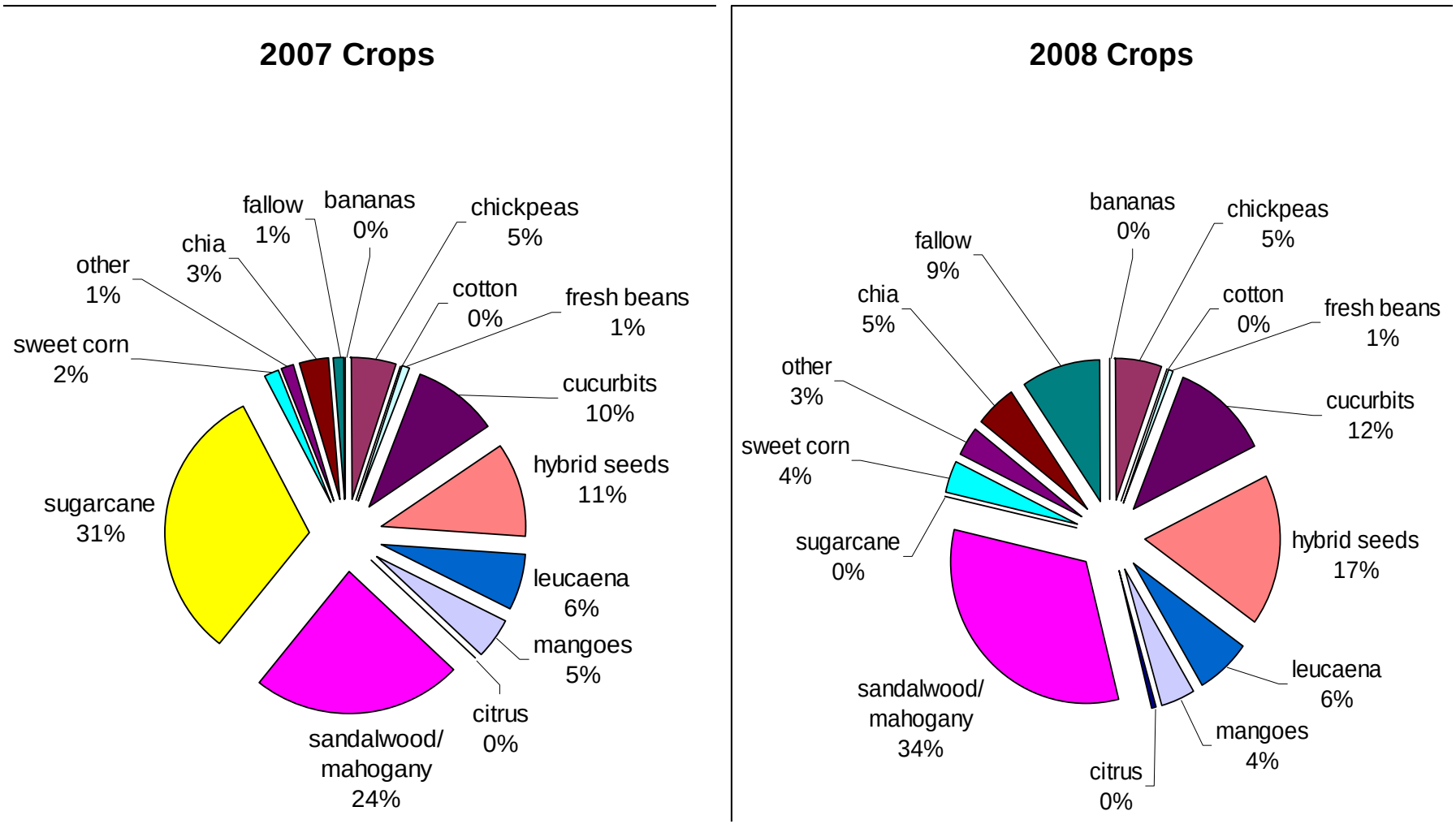

Figure 9: *Annual crop production in ORIA Stage 1 for 2007 and 2008. Note that there is a significant shift in crops grown, with a loss of sugar cane commensurate with closure of the local sugar mill. The diversity of crops grown is one of the strengths of the district. The changes in cropping strategies poses an issue for land use modelling, with significant knowledge gaps in understanding the rooting depths and water quality tolerances and watering regimes required to optimise sandalwood growth and host species.*

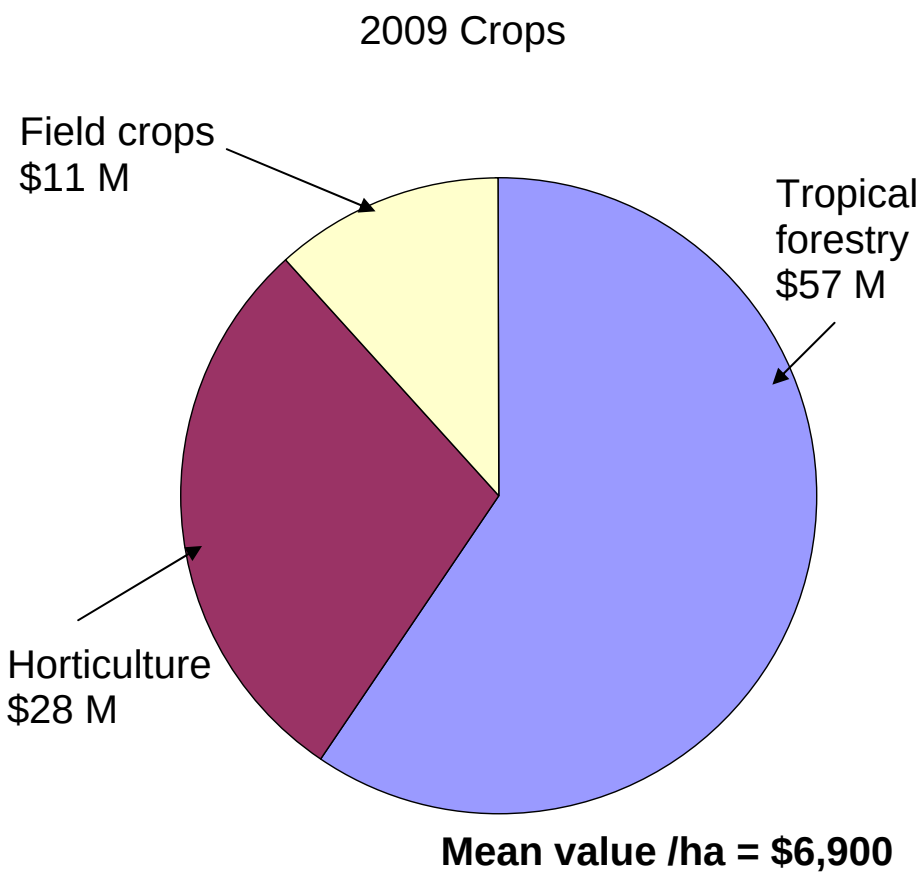

Figure 10: *Annual crops grown in 2009. Note that the dominant crop by value is now tropical forestry (primarily sandalwood). Photographs above show the diversity of crops grown in the area.*

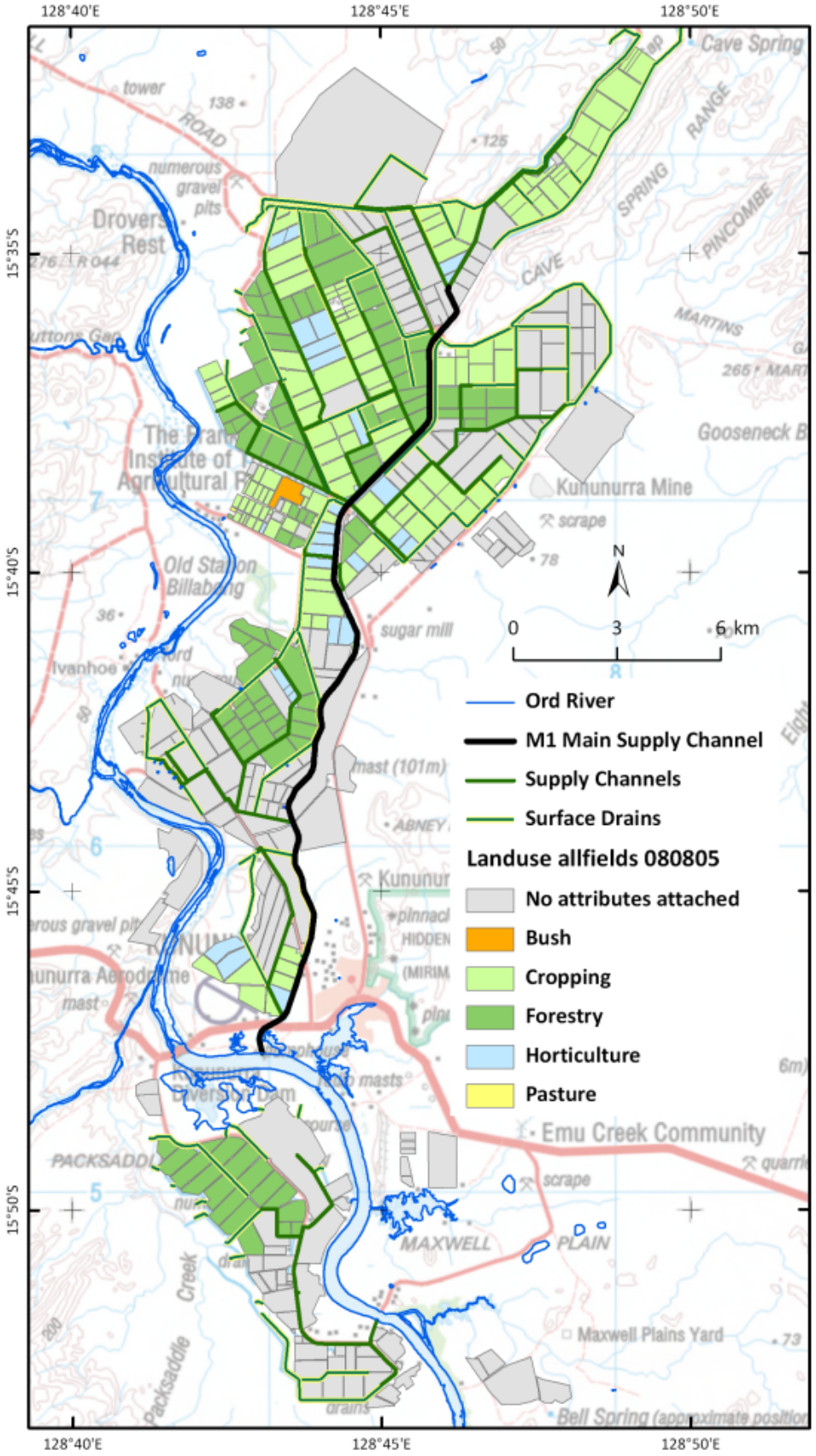

Figure 11: *Overall land use patterns as of May 2008. Data received from OIC.*

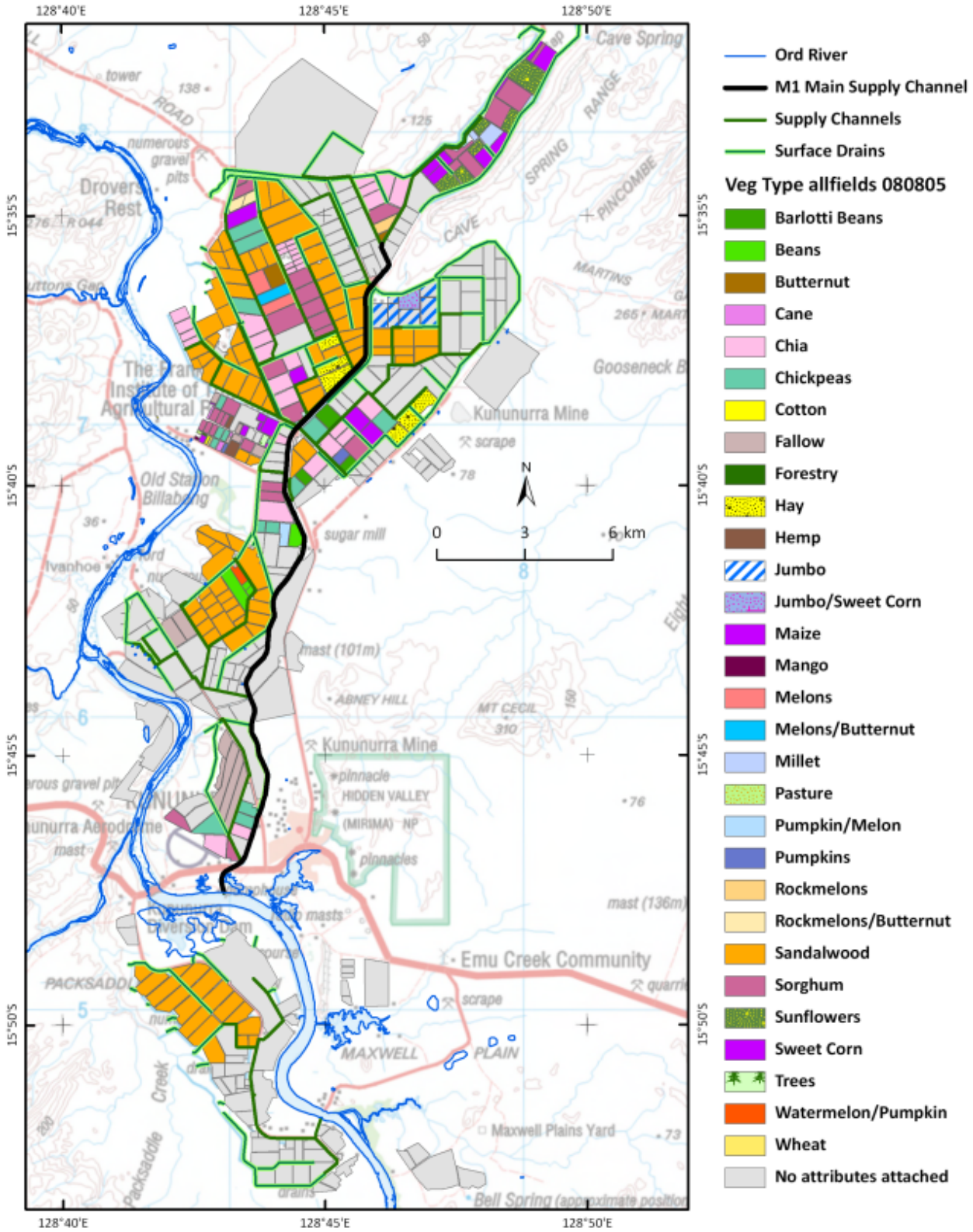

Figure 12: *Cropping distribution in the Ord Stage 1 area as of May 2008. Data received from OIC.*

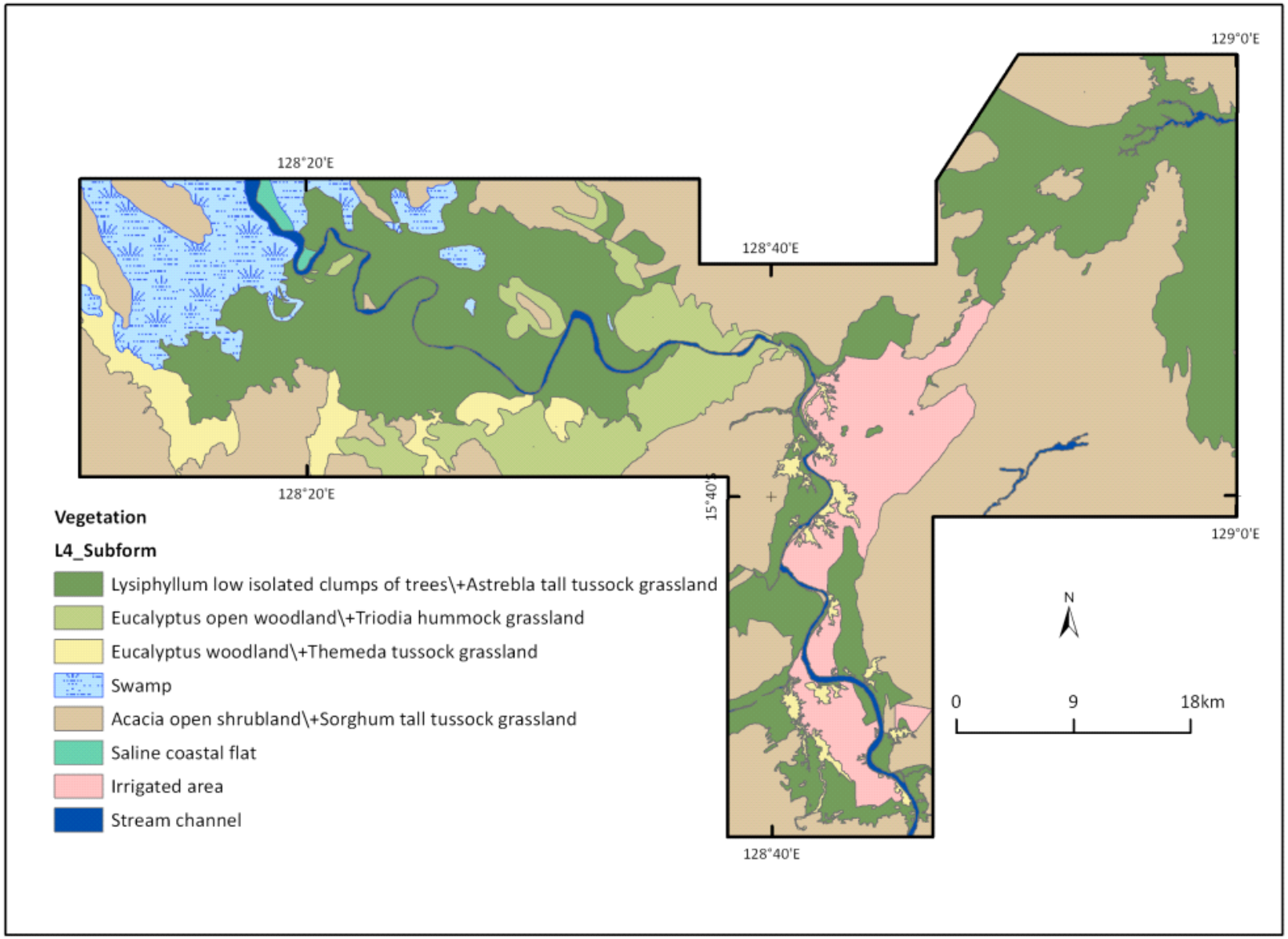

Figure 13: *Map of vegetation communities in project area. Data from DEWHA (2008).*

2.3 CLIMATE

2.3.1 Present Climate

The climate of the ORIA is typical of the monsoonal tropics (O'Boy *et al*., 2001). Settler terminology divides the annual climate into two seasons, "wet" and "dry". The wet season runs from November to April and the dry season lasts the rest of the year. The ORIA receives 90% of its rainfall during the wet season from cyclonic and convective systems. Average annual rainfall at the Kimberley Research Station was 833 mm (BoM, 2009), although there is significant variation. Average annual wet-season rainfall (July to June) from 1962 to 2005 was 0.8 m/year but significant variation between years is common (Figure 14). The maximum wet-season rainfall during the same period was 1.63m in 1982–83 and the minimum was only 0.37m in 1969–70.

Average annual pan evaporation is around 2.8m/year and mean monthly pan evaporation exceeds rainfall in all months except February. Air temperatures are generally high to very high throughout the year. Mean daily maxima and minima temperatures are 39 and 25°C during November, the hottest month, and 31 and 14°C during July, the coolest month. During the wet seasons, winds are predominantly north-westerly. In the dry season, they are mostly from the southeast.

2.3.2 Analysis of Historical Rainfall Data

Studies of the climate record in Northern Australia have interpreted a trend of increasing rainfall in recent years. In a study of the water resources of the Ord-Bonaparte region, CSIRO (2009) noted that rainfall during the 1996-2007 period was statistically significantly higher than the historical average. At the continental scale, northwest Australia recorded the largest rainfall increases over the past 50 years (Suppiah *et al*., 2001; Shi *et al*., 2008; Figure 14). Suppiah & Hennessy (1996) noted that increasing trends in summer rainfall for the 1910-1990 record at many Northern Australia stations were associated with increased frequency of large rainfall events (exceeding the long-term 90th percentile).

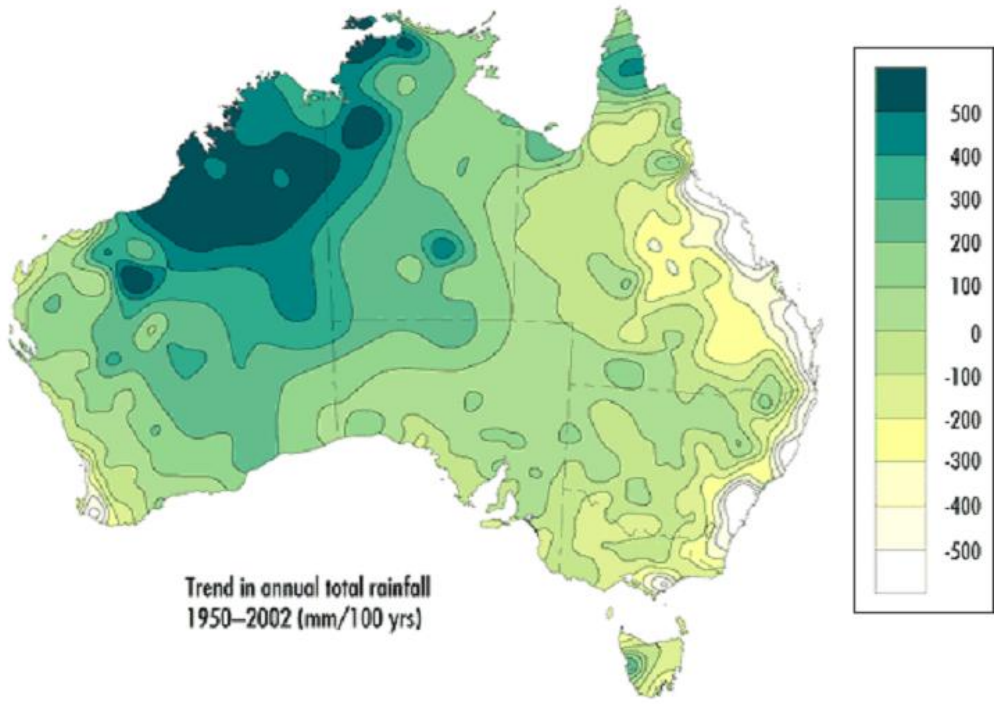

Figure 14: *Trend in annual total rainfall 1950-2002. Source: http://www.bom.gov.au.info/climate/change/gallery/45.shtml*

These regional rainfall trends can have a significant impact on the groundwater systems in the study area. Higher rainfall, particularly associated with increased frequency of large events, can increase episodic recharge and be reflected in rising watertable trends. With this in mind, the available long-term rainfall

record was analysed, focussing on the Kununurra station data. With respect to data collected from 1976 to 2009, the residual mass curve shows the cumulative deviation of the monthly rainfall from the long term mean (Figure 15). Decreasing trends in the residual mass curve indicate conditions below the long-term average, static trends means average rainfall conditions and rising trends mean above average conditions. Over this time period, the first half (1976-1991) is relatively dry compared to the second half (which shows a stepped pattern of a combination of 'average' years and some very wet years).

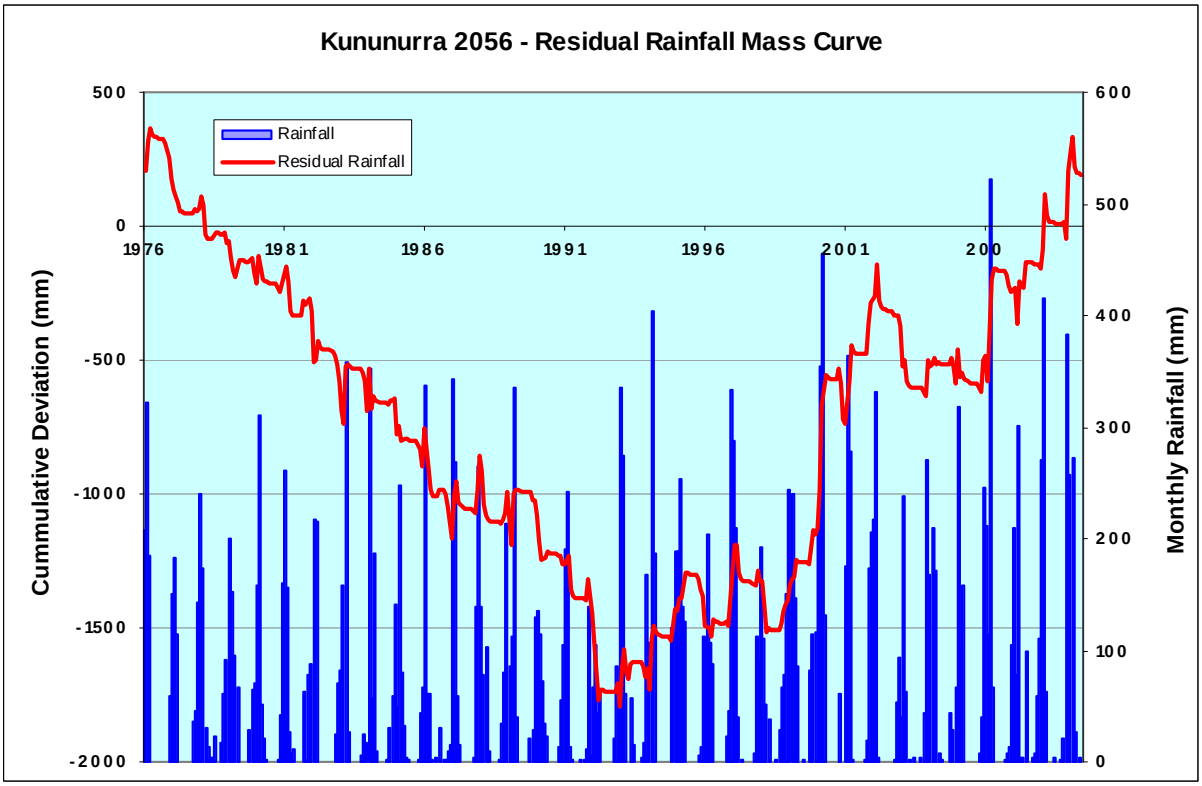

Figure 15: *Residual rainfall mass curve for Kununurra rainfall station (2056).*

The monthly rainfall for the Kununurra station is also plotted in Figure 15. It is evident that it is the very large events that have occurred post-1991 that control the significant positive shifts in the residual mass curve. If the Kununurra 1976-2009 monthly rainfall data are ordered (Table 2), the top five monthly rainfalls which exceed the 99th percentile are all post-1991 (with 3 of the 5 since 2005).

As rainfall is extremely seasonal, aggregating the monthly data based on the calendar year is of limited value. Hence, annual statistics are based on the water year from July to June to capture the rainfall data for a complete wet season which typically is between October and March. The resulting water year rainfall totals (Figure 16) reinforces the apparent transition in 1991 evident in the residual mass curve of Figure 15. Prior to 1991, the water year totals are relatively consistent (with a drying trend during 1988-1991). Post-1991, the water year totals are more variable, but show an underlying increasing trend. Figure 17 plots the maximum monthly rainfall for each of the water years spanning the 1976-2009 record. This shows a similar pattern of a more variable but increasing trend after 1991.

Table 2: *Kununurra monthly rainfall data ranked in descending order.*

Rank	Year	Month	Monthly Precipitation Total (mm)	Post 1991
1	2006	3	522.4	Y
2	2000	3	455.8	Y
3	2008	2	414.8	Y
4	1994	2	404.2	Y
5	2008	12	382	Y
6	2001	2	364	Y
7	1983	3	358.5	N
8	2000	2	354.6	Y
9	1984	1	352.2	N
10	1987	1	343.4	N
11	1986	1	337.6	N
12	1989	3	335.8	N
13	1993	1	334.4	Y
14	1996	12	333.2	Y
15	2002	2	330.8	Y
16	1976	2	322.8	N
17	2005	1	318.2	Y
18	1980	2	311.2	N
19	2007	3	300.4	Y
20	1997	1	288	Y

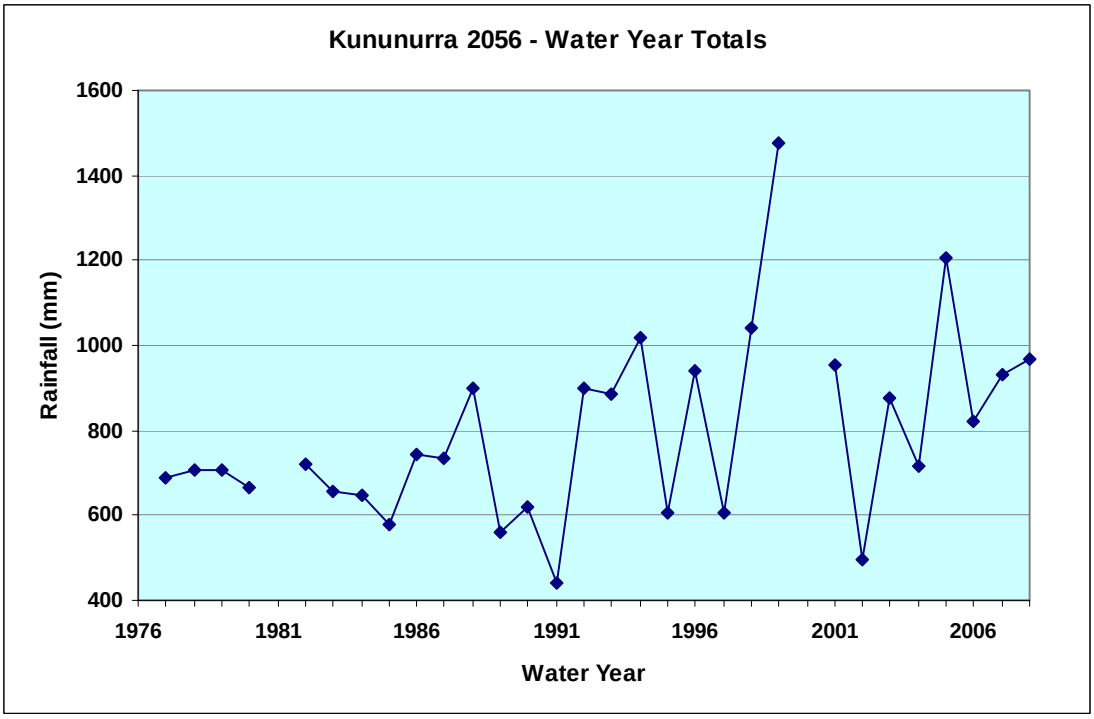

Figure 16: *Water year rainfall totals for Kununurra station 2056.*

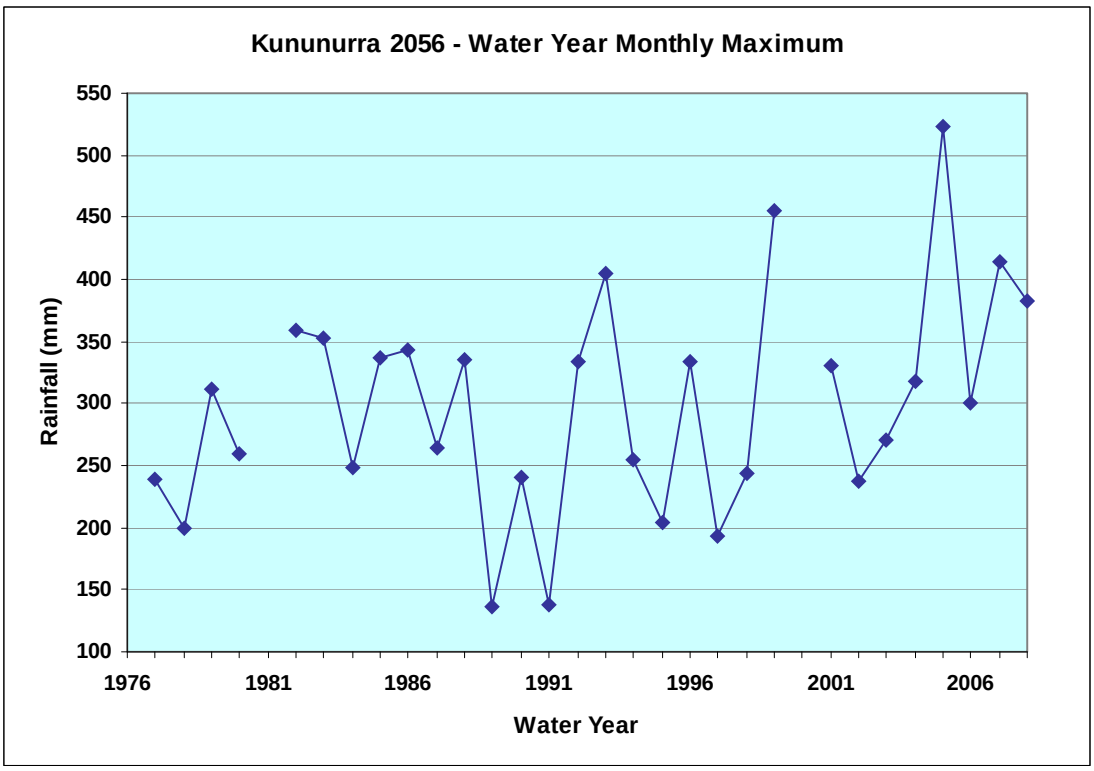

Figure 17: *Water year monthly maxima for Kununurra rainfall station.*

Table 3 compares the statistics for the two periods in question (1976-1991 and 1992-2008). This shows the magnitude of the difference between the two periods, with post-1991 more variable but generally wetter. AMRR based on monthly means from 1946 to 2008 show that Kununurra is currently experiencing an increase in rainfall and rainfall intensity, which commenced in the early 1990s, with a similar 'wet' climate experienced in the late 1930s and 1940s (Figure 18). Even longer-term records from Argyle Downs Station are shown in Figure 19. These data show several wetter and drier cycles, while the AMRR shows an almost 80 year cycle of decline in rainfall-low rainfall from 1918 to 1998.

Table 3: *Kununurra station water year rainfall summary statistics for 1976-1991 and 1992-2008.*

Water Year Statistic (mm/year)	1976-1991	1992-2008
Average	669	903
Standard Deviation	106	237
Minimum	441	497
Maximum	901	1476
Median	677	915
10^{th} Percentile	564	606
90^{th} Percentile	743	1124

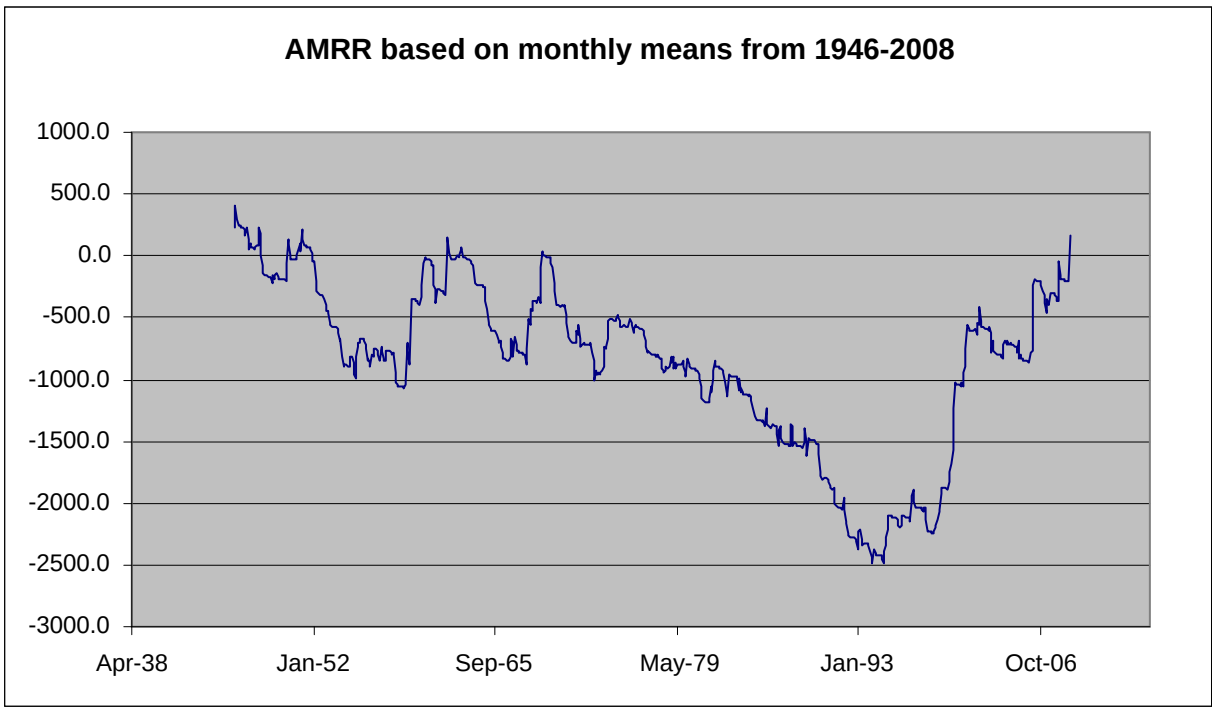

Figure 18: *AMRR based on monthly means from 1946 to 2008.*

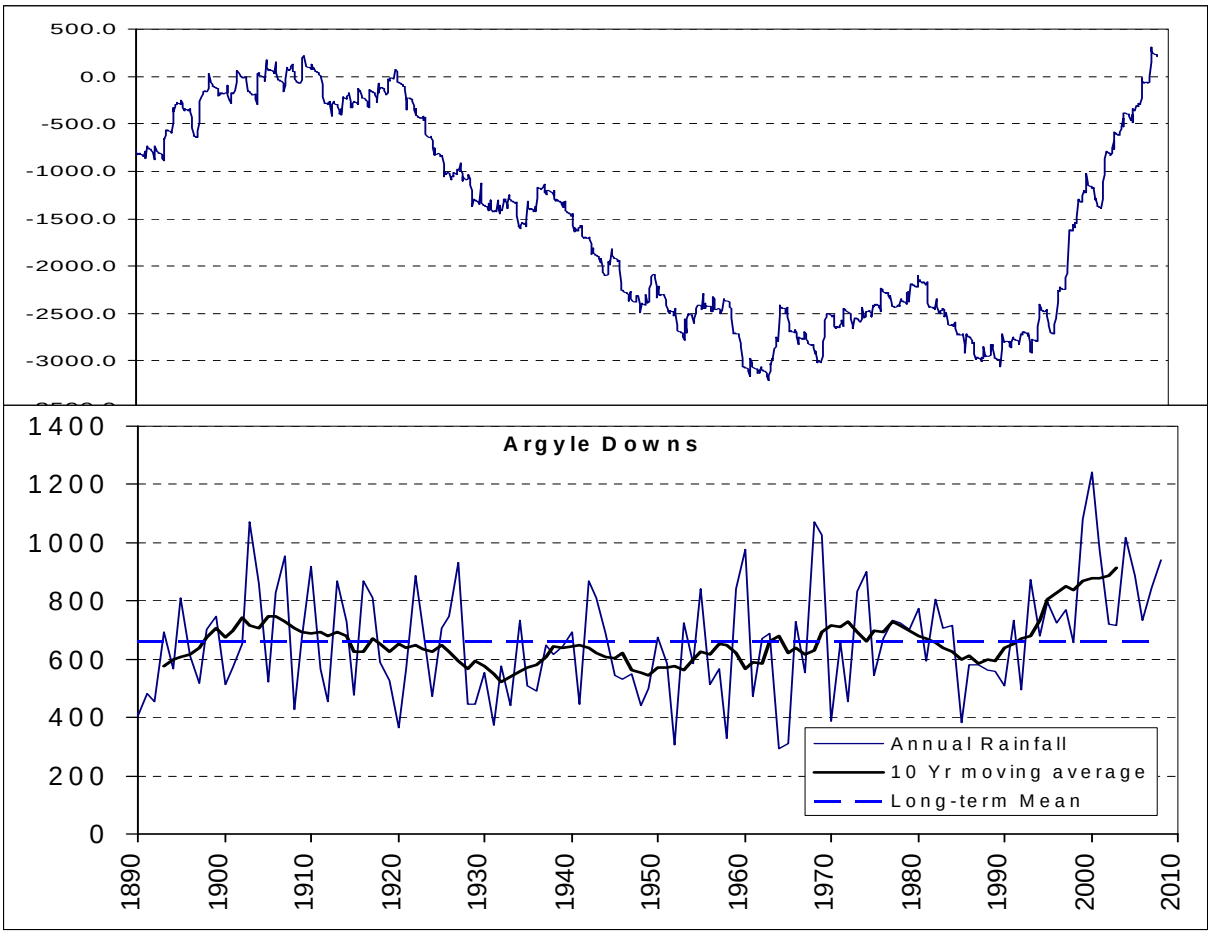

Figure 19: *AMRR (top) and annual rainfall showing moving averages and long term means (bottom) for the Argyle Downs Station from 1890 to present day. Data from Richard George.*

2.3.3 Predicted Climate Change

CSIRO (2009) summarised the results of climate change models for the region. These show a great deal of disagreement in predicting the future climate of the Kimberley. Rainfall-runoff modelling with climate change projections from seven of the GCMs shows an increase in mean annual runoff, while rainfall-runoff modelling with climate change projections from six of the GCMs shows a decrease in mean annual runoff. Two of the GCMs show neither an increase nor decrease in mean annual runoff. For the high global warming scenario rainfall-runoff modelling with climate change projections from three of the GCMs indicates a decrease in mean annual runoff greater than 10 percent while rainfall-runoff modelling with climate change projections from three of the GCMs indicates an increase in mean annual runoff greater than 10 percent.

For the Ord catchment, under the median future climate there would be a 3 percent increase in water availability and no change to diversions for irrigation. Mean annual diffuse groundwater recharge is likely to be slightly higher than the historical average across most of the region. Considering all water products the average annual controlled release would increase by 1 percent (CSIRO, 2009).

For the Ord catchment the CSIRO (2009), study of climate extremes for 2030 indicate:

- under the wet extreme future climate, water availability increases 20 percent and there is no change to the diversions for irrigation. Average controlled releases increase 5 percent.
- under the dry extreme future climate, water availability decreases 21 percent and total diversions decrease 7 percent. Average controlled releases decrease 9 percent (CSIRO, 2009).

In summary, the CSIRO (2009) study showed that for the Ord catchment, the climate modelling for 2030 and future development indicate:

- under the median future climate and future development there would be a 3 percent increase in water availability and a 113 percent increase to diversions for irrigation. Considering all water products the average annual controlled releases decreases by 4 percent
- under the wet extreme future climate and future development, water availability increases 20 percent and there is a 114 percent increase to the diversions for irrigation. Average controlled releases decrease 1 percent.
- under the dry extreme future climate, water availability decreases 21 percent and there is a 92 percent increase to the diversions for irrigation. Average controlled releases decrease 14 percent.

Overall, there is great uncertainty in the climate modelling, however under the wet extreme scenarios, any further increase in rainfall in this area will provide additional challenges for recharge management, given the links between water table rise and increased rainfall (Smith, 2008).

2.3.4 Links between Climate and Salinity

In considering the hydrologic regime and possible salinisation scenarios in the study area, the impact of the tropical climate and more recent climate variability stand out as issue to be considered. Even in southern climates, as drought conditions in southern Australia have recently demonstrated, it is also possible for relatively rapid changes in water tables to result from changes in rainfall (Littleboy, 2008; Reid, 2008). This has highlighted the fact that the more general contribution of climate variability to water table change appears to have largely been discounted in analysis of secondary salinity in Australia, despite significant variability in rainfall over the past 150 years (CSIRO, 2009).

In ORIA Stage 1 there is clear evidence that the rainfall contribution to rising water tables is important (Smith, 2009). With significant changes in rainfall observed throughout the Kimberley over the past decade, as noted above, increased recharge is likely to provide additional impetus to rising water tables, and provide an additional potential salinity hazard. The salinity risk in the Stage 2 areas can only be quantified through appropriate hydrodynamic and land use modelling. Presently, with rising trends in water tables observed, it is unclear when a new equilibrium in the water tables in the Stage 2 areas will be reached, and at what levels this will occur. The dynamics of water table change in these areas will most likely change yet again as a consequence of land clearing, land modification, and the introduction of irrigation.

3 Data Acquisition and Processing

This section details the new datasets that were commissioned as part of this study, and other datasets that were customized for the project. Principally, the new datasets funded and acquired as part of this project included a LiDAR or ALS (Airborne Laser Scanner) survey that was required to produce a new Digital Elevation Model (DEM), Orthophotograph Imagery; an Airborne Electromagnetics (AEM) survey, 12 new drillholes cored using sonic technology, borehole conductivity logs and water quality (salinity) data from exiting and the new boreholes. Existing Shuttle Radar Terrain Mission (SRTM) data, Satellite Imagery (Landsat and SPOT), and older QUESTEM AEM data were processed for specific analysis as part of this study. Further information on each of these datasets is provided below.

3.1 DIGITAL ELEVATION MODELS AND ORTHOPHOTOGRAPH IMAGERY

Two main Digital Elevation Model (DEM) datasets were used for the Ord AEM Interpretation Project. These were the Shuttle Radar Terrain Mission (SRTM) and a high resolution Light Detection and Ranging (LiDAR) survey, acquired specifically for the study.

3.1.1 Shuttle Radar Terrain Mission (SRTM) DEM

The version 1.0 DEM (90m resolution), which was used initially as the base for fieldwork where higher resolution DEM data were not available. The SRTM DEM was used as supplementary data only, as the spatial and vertical resolution are too low and the noise level too high at a scale of 1:25,000. An example of this product is shown in Figure 20.

After fieldwork was completed, a new 30m resolution version of the SRTM DEM became available for use by government agencies, and this was utilised in final products where there was no higher resolution coverage. The high-resolution LiDAR dataset was stitched to the lower resolution 1 second SRTM DEM (~30m horizontal resolution). This stitched dataset provided a basis for spatial analysis of the broader project area and surrounds.

3.1.2 Light Detecting and Ranging (LiDAR) Survey

The LiDAR or ALS (Airborne Laser Scanner) survey was commissioned from Fugro Spatial Solutions Pty. Ltd. (FSS) to provide Digital Elevation Model (DEM) and Orthoimagery for the study area (Figure 21 and Figure 22). The total area covered in the survey was 939sq km. The main products acquired were:

- A bare earth DEM at +/- 30cm vertical and a horizontal accuracy of +/- 5m, at a nominal 1.9m^2 per point (Figure 23 and Figure 24).
- Digital orthoimagery at 0.35m resolution (Figure 25).
- 1m contour data.

Product specifications and formats are listed in Table 4.

Table 4: *LiDAR and orthoimagery products and formats.*

Product	Item	Format	Media	Projection
ALS				
Digital Elevation Model	Bare Earth, all points, 5m by 5m, Key point filtered and 10m by 10m	(ASCII) XYZ or Geodatabase or SQL Server	DVD	MGA94/52+AHD
Contours	1m interval	SHP or MAP	DVD	MGA94/52+AHD
Orthoimagery				
0.35m GSD Resolution	3km x 3km tiles	ECW Tiles	DVD	MGA94/52

3.1.3 Digital Elevation Model (DEM)

FSS acquired the LiDAR survey using an airborne Leica ALS50 LiDAR unit and used the ALS observations to generate a ground model (DEM) over the site with the vertical accuracy outlined above. FSS captured the project with a nominal average point density per flight line. This value is an average density based upon the resultant "zigzag" scan pattern of the ALS system. Figures can only be quoted as nominal due to variations of the aircraft's altitude above the terrain, and variations in aircraft speed and heading. It was not possible to penetrate either water bodies or sugar cane encountered in the area.

ALS data were Georeferenced to GDA94, MGA Zone 52 and elevations reduced to the Australian Height Datum (AHD) via the Ausgeoid98 geoid model. The accuracy of ALS observed elevations is a function of the accuracy of the geodetic network within the area and the accuracy of the Ausgeiod98 model throughout the region. FSS utilised existing high accuracy survey marks for GPS base station locations for the ALS survey. New control points acquired for the survey were connected to the local geodetic network via static GPS observations and geodetic network adjustment. These points formed the primary geodetic network for the survey. FSS also established perimeter control points and internal elevation checkpoints, via static survey observations and connections to the primary geodetic network.

Acquired point cloud data were processed using appropriate software. Each laser 'range' was georeferenced upon acquisition and recorded in up to 4 returns. The point cloud was then processed to the two different coverage classes, being ground and non-ground. Only the ground elevations are used to determine the ground surface model. Processing was aided by the digital imagery. The ground surface model was tiled under supervision of P. Wilkes from Curtin University. A 1km x 1km regular grid was selected, as file sizes can be handled by many GIS applications. Data were gridded at Curtin University into a raster DEM model. The ground surface model was output as ASCII X Y Z space delimited files.

In order to provide coverage for the entire project area, the DEMs produced from the LiDAR survey and the SRTM dataset were spliced together for analysis in some areas (e.g. Mantinea Plain-Carlton Hill-Parry's Lagoon). The SRTM dataset is of lower resolution than the LiDAR dataset, and hence surface modelling in areas covered by the SRTM dataset has lower confidence levels.

3.1.4 Orthophoto Imagery

During the acquisition of the ALS data, Fugro Spatial Solutions Pty. Ltd. acquired RGB imagery using a medium format digital camera. Since the prime deliverable of the project was the ALS dataset, and insufficient funds were available to acquire orhtophotos in a separate survey, the survey was executed to achieve the optimal requirements for ALS collection. This resulted in collection of the orthoimagery in non-ideal conditions, including data collection early morning and at dusk where long shadows were sometimes present, an when some cloud cover was present. The Orthoimagery was supplied as georeferenced ECW tiles. The orthophotos have a resolution of 35cm, and the imagery was projected to the MGA94/52 datum.

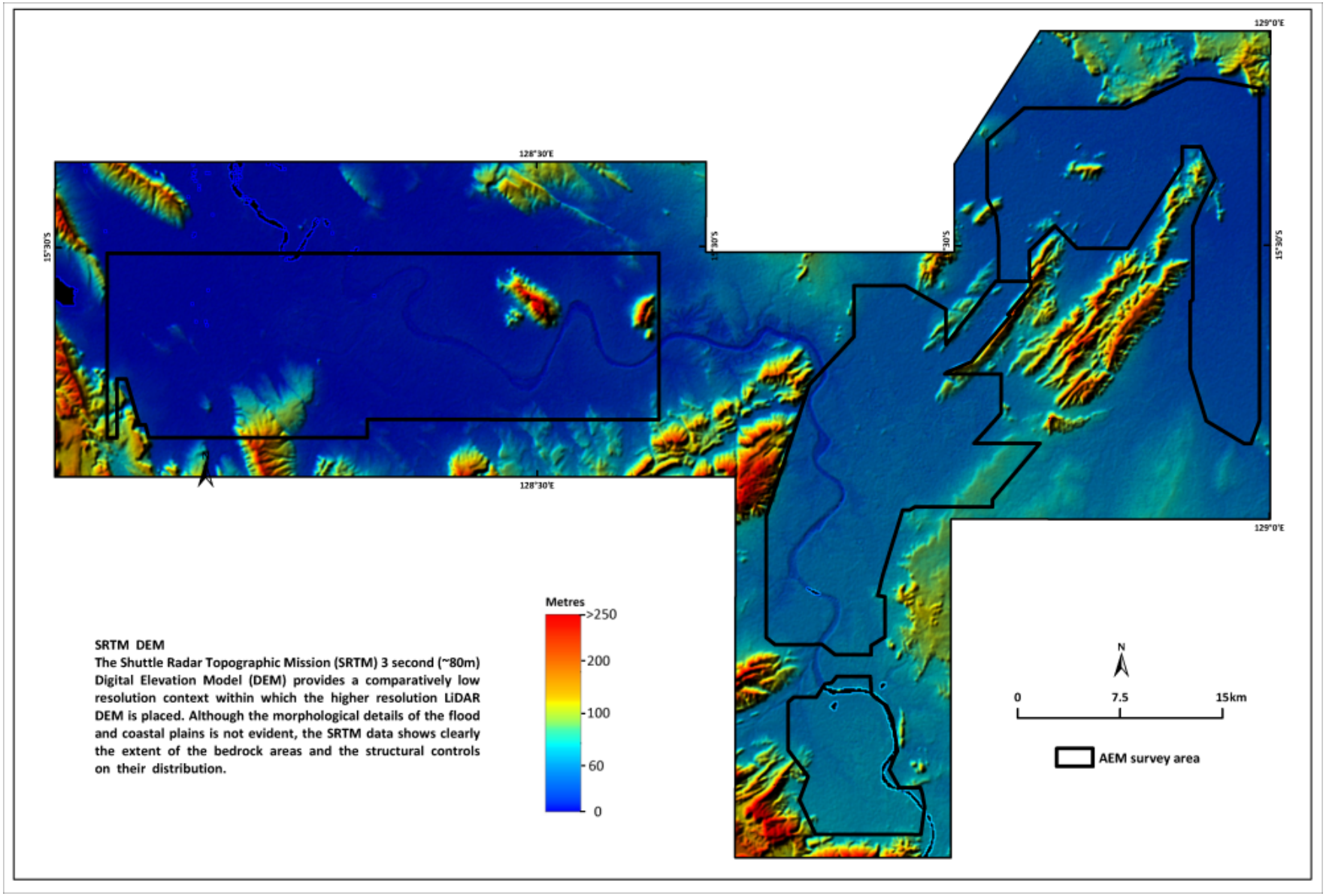

Figure 20: *SRTM 3-second digital elevation model.*

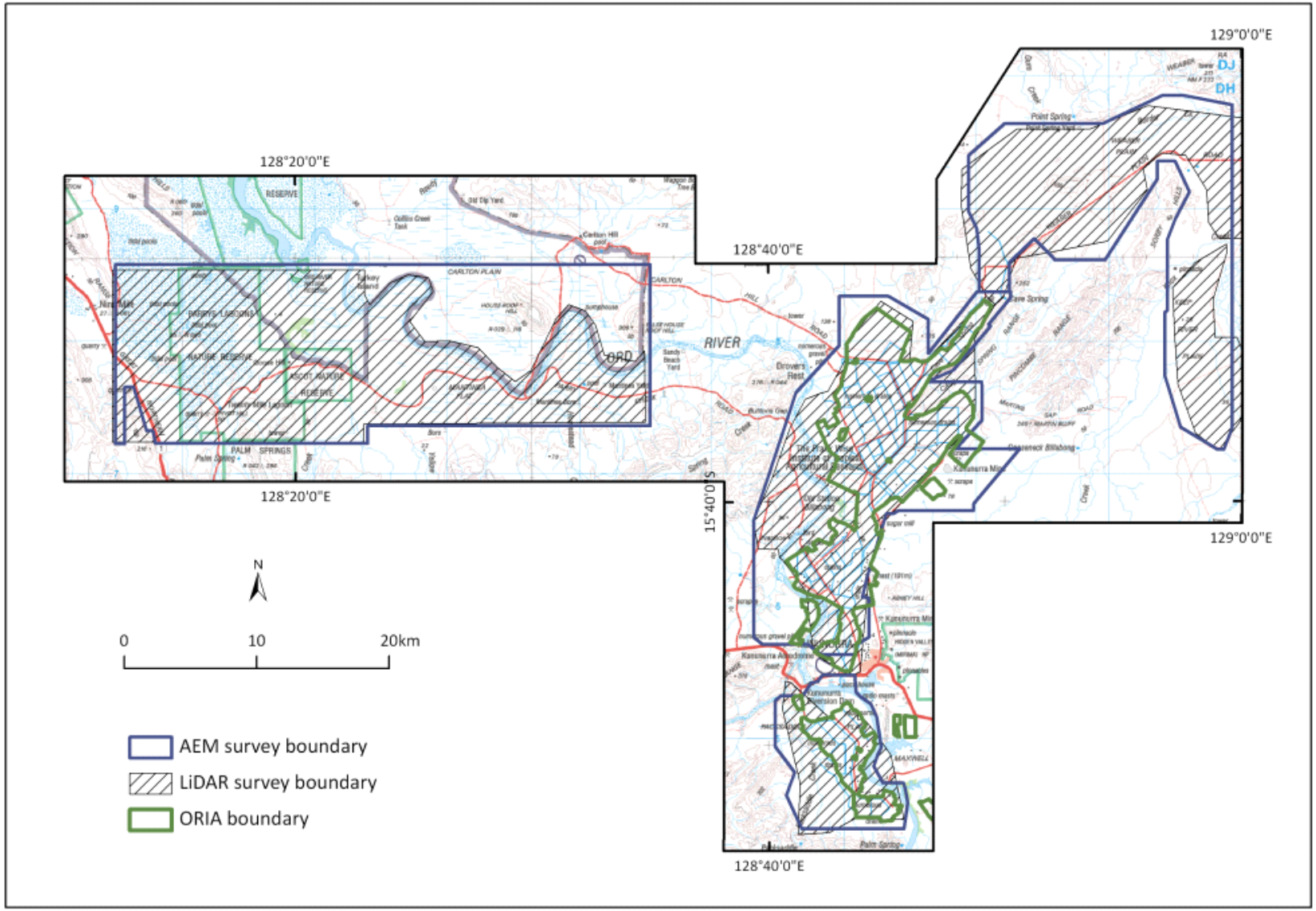

Figure 21: *Extent of LiDAR and orthoimagery survey and AEM survey boundary (which defines the project boundary).*

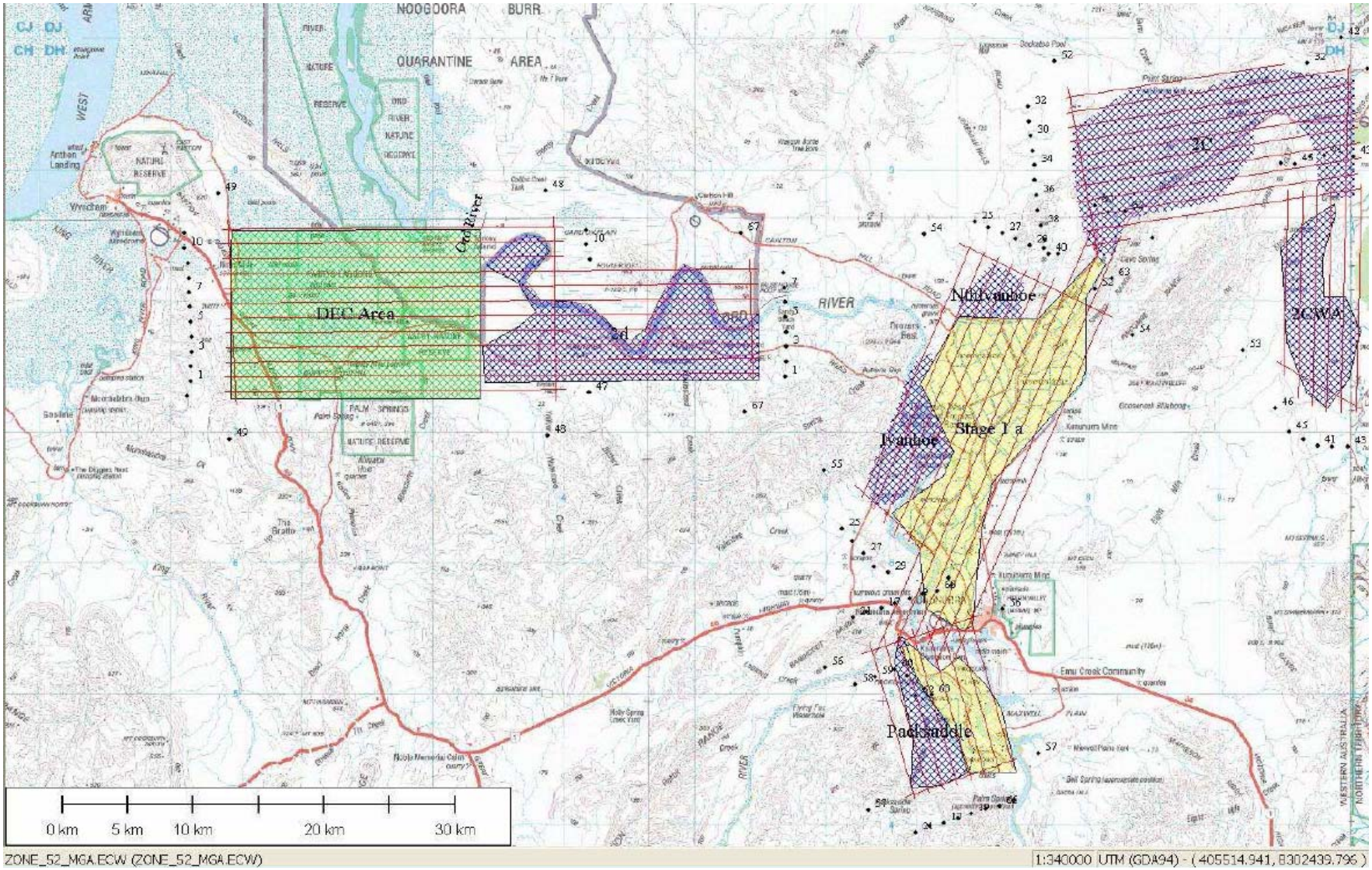

Figure 22: *Area of coverage of LiDAR and orthoimagery imagery including acquisition flight lines. The colour shading of the areas reflects the potential Stage 2 irrigation areas (purple), the Stage 1 area (yellow) and the Parry's Lagoon nature reserve area funded by DEC (green).*

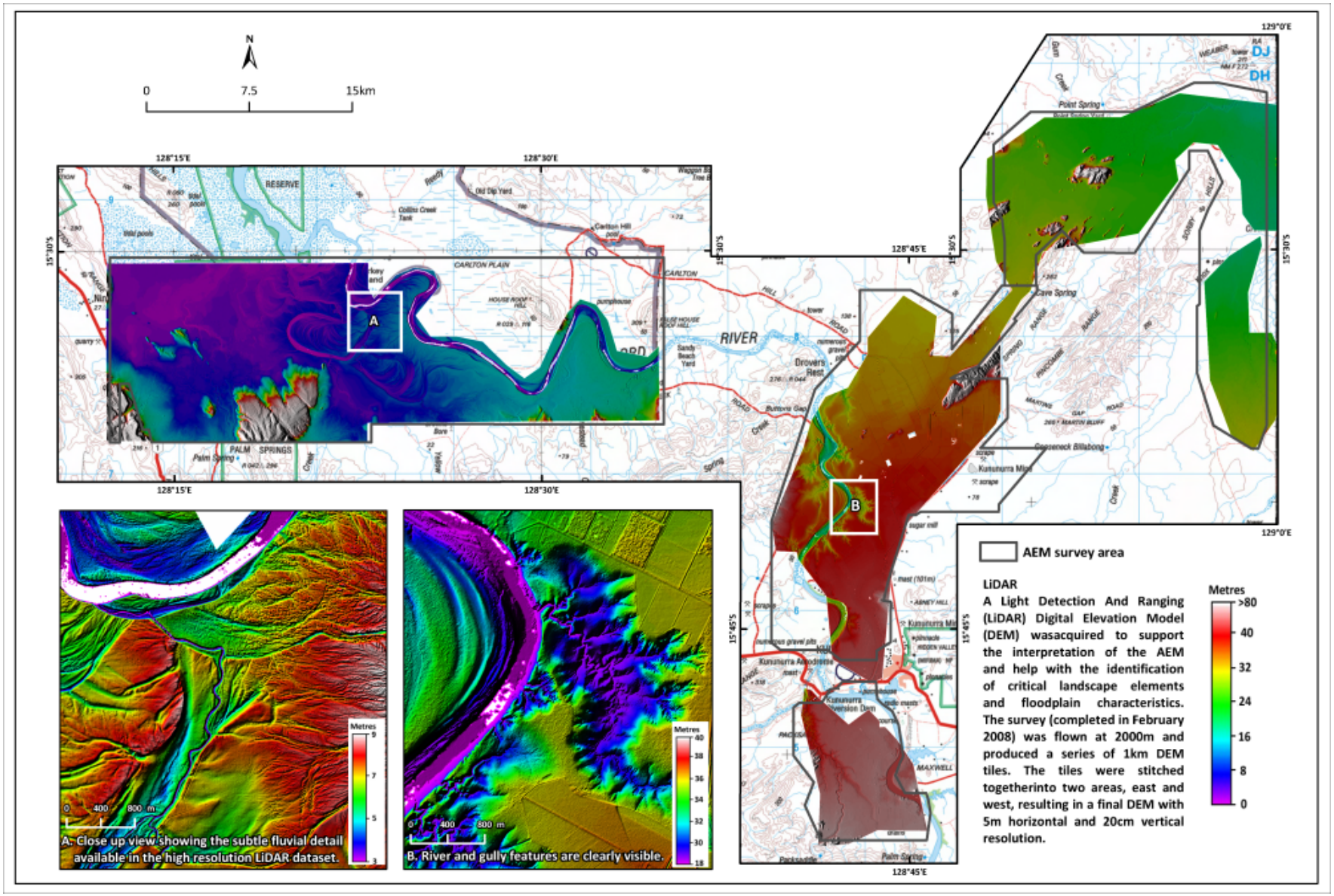

Figure 23: *LiDAR bare earth image.*

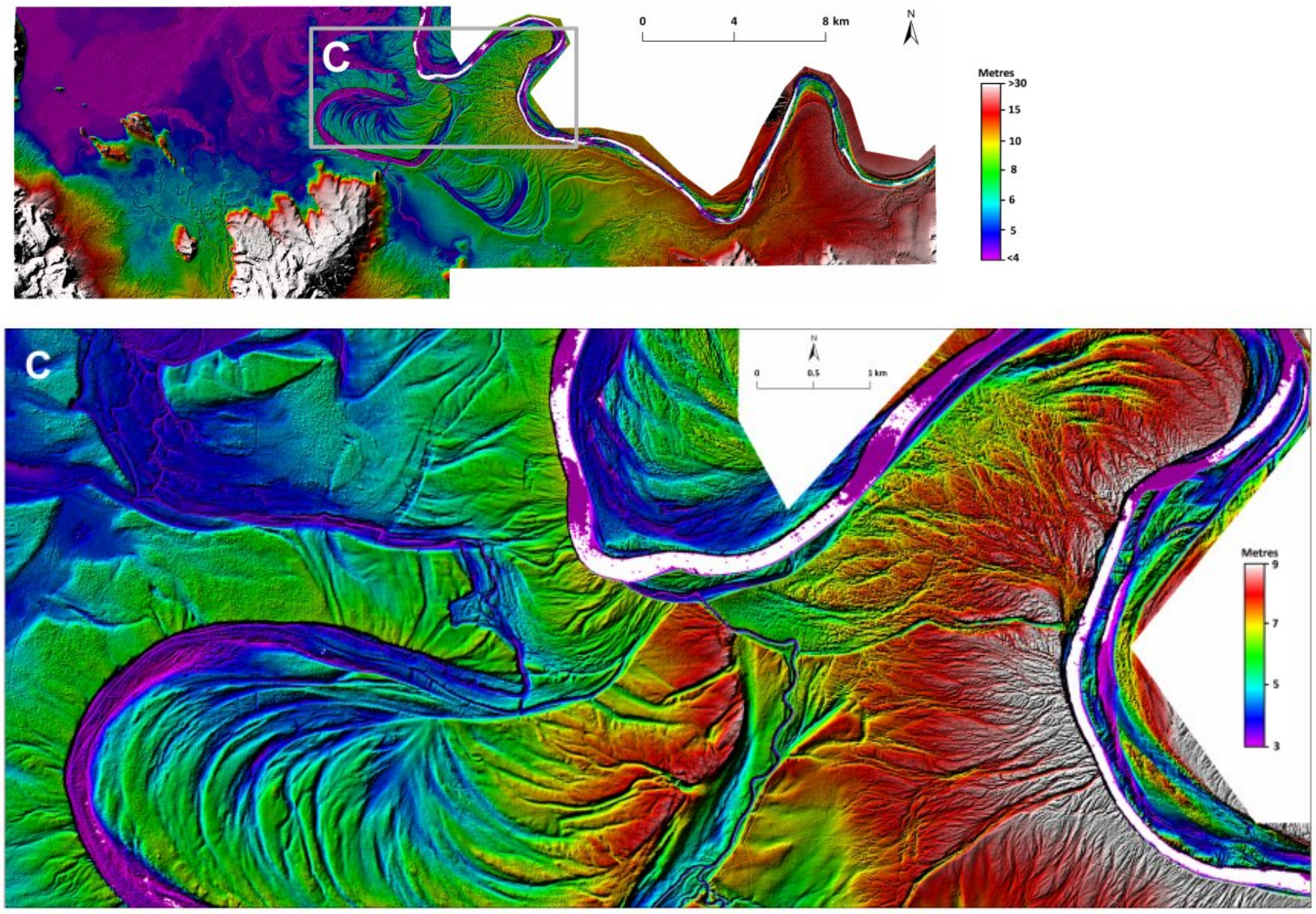

Figure 24: *LiDAR bare earth image shown at high resolution. The image shows the active meander belt and scroll bars in the Mantinea Plain-Parry's Lagoon area.*

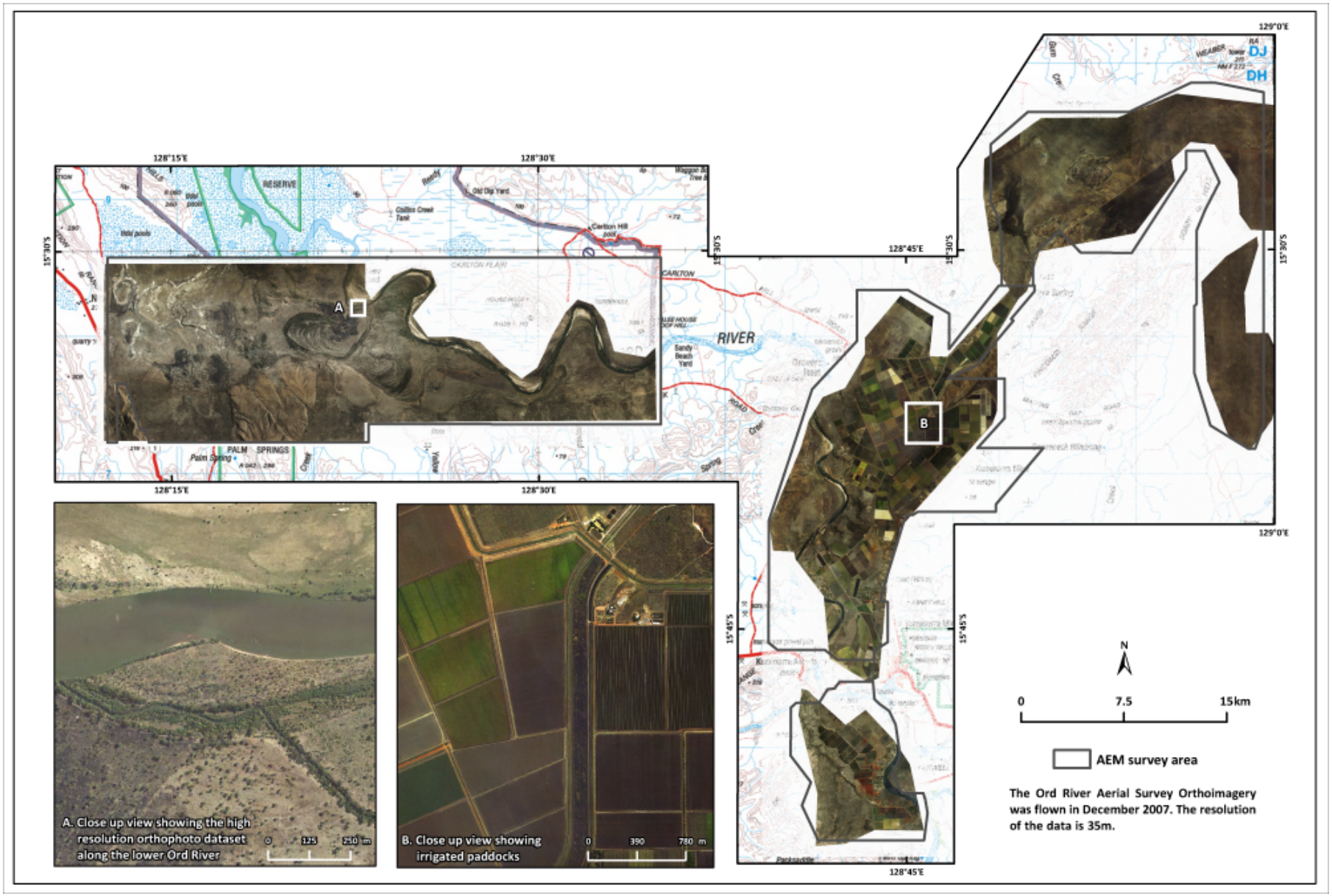

Figure 25: *Orthoimagery for the Ord River survey area.*

3.2 SATELLITE DATA

Remotely sensed images, especially Landsat 5 TM, and Satellite Pour l'Observation de la Terre (SPOT), were used for assessing surface features such as surface salinity, surface materials and vegetation. SPOT scenes for the Ord Valley project area, obtained with 2.5 m resolution, were also acquired from GA. These covered most of the project area, with LANDSAT data to infill data gaps. The SPOT imagery was also re-sampled to 10m resolution for modelling purposes. Bands 3, 2 and 1 were displayed in a composite RGB image. This imagery was used mainly to help constrain the vegetation health mapping, as well as assist with construction of the surface (soil) salinity maps and the geomorphology mapping.

In addition, four LANDSAT 5 Thematic Mapper images were selected for the project to assess moisture persistence, particularly in the Weaber Plain. These images are shown in Figure 26.

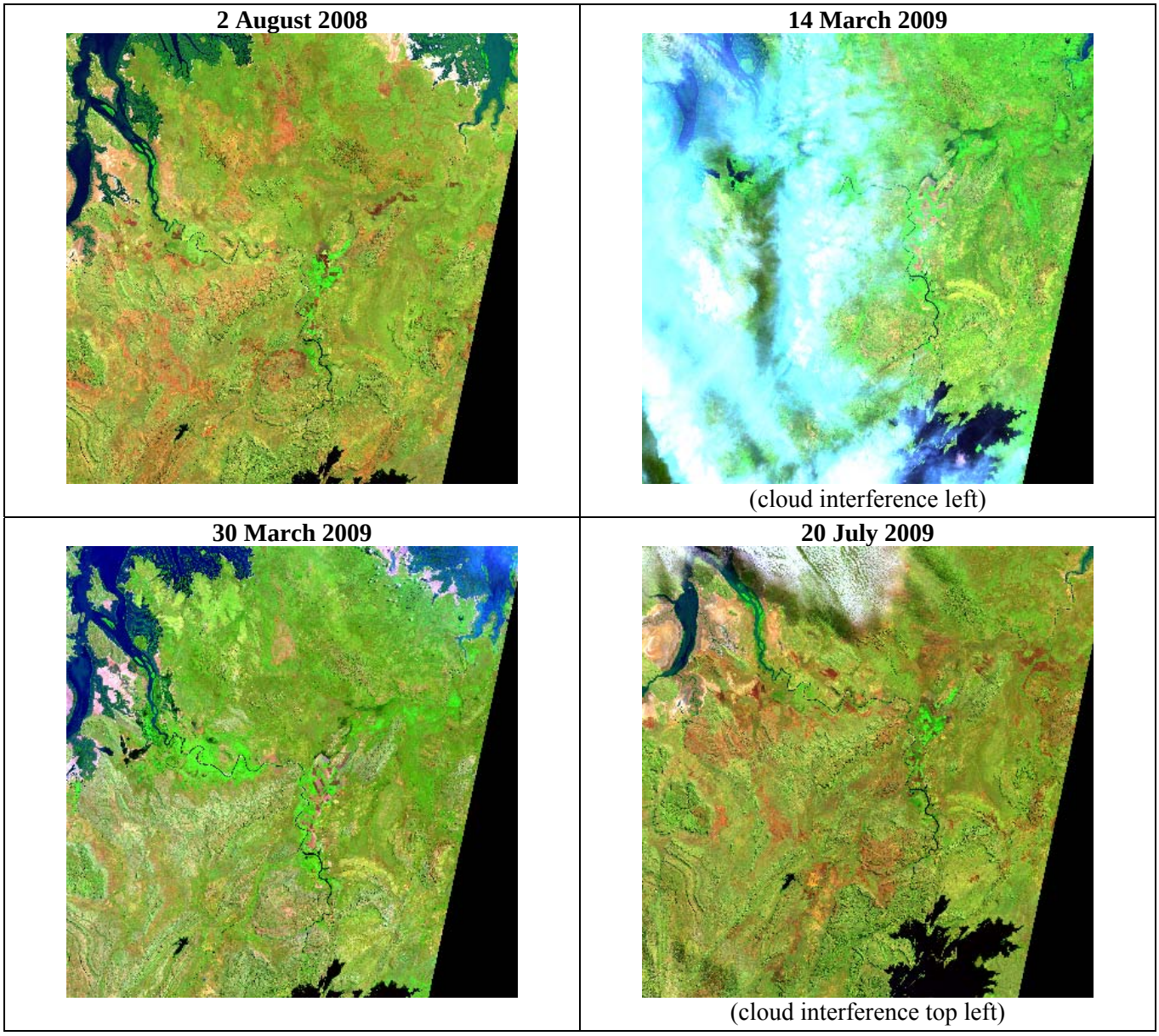

Figure 26: *The four Landsat images of the Ord River area acquired for the project.*

The imaging dates were:

1. **2 August 2008** which was considered as a 'dry' image because it occurred 5 months after any significant rainfall and 4 months before the next rain season.
2. **14 March 2009** which was considered as a 'wet' image because it occurred 1-2 weeks after significant rainfall (cloud cover left of image).

3. **30 March 2009** which was considered as a 'wet' image because it occurred about 1 month after significant rainfall.
4. **20 July 2009** which was considered as a 'dry' image because it occurred nearly 5 months after significant rainfall (some cloud in top left of image).

These imaging dates were selected to minimise cloud cover, and as representative of surface conditions during the later dry season and at the end of the wet in the same cycle. Two supplementary images were also selected for persistence of moisture investigations, (March 14th and July 20th July 2009). The initial images were centred on 15 degrees, 44 minutes and 59 seconds South and 128 degrees 35 minutes East, and were ortho corrected. The images are 130km x 130km in size. The latter two images were centred on 15 degrees 35 minutes South and 128 degrees 40 minutes East.

Atmospheric Corrections
A dark pixel correction was applied to each image to account for atmospheric scattering of light according to ERMapper recommendations. The formula: "INPUT1 – RMIN(,R1,I1)" was applied to correct the atmospheric effects by subtracting the darkest pixel value from each pixel of each band in every image. The resulting images were then used for processing.

3.3 BOREHOLE INFORMATION

3.3.1 Existing Bore Holes

The project area contains a high number of pre-existing boreholes due to active diamond, gold and base metal exploration over the last 50 years (O'Boy *et al.,* 2001). In addition to the mineral exploration holes, a number of drilling programs have been undertaken to provide baseline hydrogeological data and groundwater monitoring sites (Nixon, 1995, 1996, 1997a-h). Many of the original geological logs for the mineral exploration holes appear to have been lost, however summary logs were used to construct new hydrogeological maps and cross-sections of the area (O'Boy *et al*., 2001).

For this study, approximately 750 borehole lithological logs of variable quality were available for use in validating and interpreting the AEM data. The wide distribution of the drill sites and the geological descriptions for each hole made these an invaluable resource for validation of the AEM data and the mapping of sedimentary textures and bedrock in particular. Of the 750 bores, 719 bores are located in Ord, Weaber, Keep and Knox Creek Plains, with only 31 bores in the Parry's Lagoon-Mantinea Plain-Carlton Hill area. The location of the pre-existing boreholes used in this study is shown in Figure 27.

The borehole data were retrieved from a variety of sources and databases, and came in a range of formats. The highly variable nature of the lithological descriptions necessitated a labour-intensive exercise in standardisation and summation. The summary descriptions are contained in Appendix 1 (Cullen *et al.,* 2010). Very few of these bores had useful geophysical logs, and all the holes drilled by the Minerals Exploration industry had been filled in. Previous induction and gamma logging of representative holes in the Stage 1 area (Lawrie *et al*., 2006a) was augmented by a further program throughout the ORIA at the time of survey.

3.3.2 New Bore Holes

Rationale
Lithological and geophysical data from boreholes are essential for the calibration and validation of AEM datasets (Lawrie *et al*., 2000; Spies & Woodgate, 2005). Data from pre-existing boreholes can be invaluable, while the recovery of drill chip materials and the sampling of groundwater from new bores can also provide useful information and sites for geophysical logging and hydrogeochemical sampling if the holes are still open (and not cased using metal). However, in the past decade, the demand for AEM surveys to address more specific salinity and groundwater management questions and produce more quantifiable products, has led to the development of more sophisticated interpretation products. The latter, such as 3D maps of regolith and alluvial materials, groundwater salinity, salt store and salinity hazard, require accurate grain size and compositional data, as well as data on porosity and pore fluid chemistry (Lawrie, 2008; Tan *et al.,* 2009). This invariably requires the recovery of samples from new drillcore located using the AEM data.

In this study, budget limitations initially restricted drilling to use of air core rigs that were in the area. This failed due to limitations in the capacity of the air compressors, the loss of air in high hydraulic conductivity material, and lack of sample return generally. Additional funds were successfully sought, and twelve new boreholes were drilled using the advanced sonic drilling technique. These were sited using the AEM data, and were selected to recover samples from a range of materials throughout the ORIA. The location of the new bores is shown in Figure 28. GPS coordinates for all the drillholes are given in Table 5.

Table 5: *Location and attributes of new holes drilled for this project.*

Hole ID	Easting	Northing	Depth (m)	EC (μS/cm)*	SWL (below ground)	Temp (C)
O1*	469494	8259587	29.9	189	4.45	27.9
O2*	468097	8263573	26	256	6.55	29
O4*	477331	8278799	38	342	1.47	30.7
O7*	475310	8271510	19.9	312	4.71	37.5
O11*	469049	8251702	20	309	1.84	29.5
KS1	488588	8290313	24	188	8.79	30.2
KP1	497886	8293663	26	189	2.37	30.9
KP2	498645	8293676	35	216	11.54	33
KP3	497442	8286200	23	232	12	39.5
PL1	434810	8275719	17	5504	2.57	38.7
PL2	439381	8278373	16.2	3648	5.59	34.7
PL3	417509	8281371	17	24200	0.24	30.5

**Note: boreholes in the ORIA Stage 1 area are designated either ORD or O (short form).*

A more complete description of drilling sites is given in Appendix 2 (Cullen *et al.,* 2010). Drilling licences for specific sites were obtained on behalf of the project by Brolgas Environments. This was a difficult task, with a number of restrictions which limited site choice.
In summary, the specific aims of the drilling program were:

- Geophysical and hydrogeological validation of specific anomalies and patterns in the AEM data.
- Provision of boreholes for induction logging in areas with no prior borehole geophysical data.
- Recovery of drillcore for lithological characterisation, facies analysis and detailed grain size and compositional analysis.
- Petrophysical characterisation of aquifers and aquitards.
- Hydrogeochemical analysis of pore fluids.

Technology
After quotes were received from a number of contractors, a sonic drilling rig (Figure 29 and Figure 30) supplied by Boart-Longyear Pty Ltd., was chosen to drill 12 boreholes. Although slightly more expensive than more traditional techniques, this advanced technology has a short but successful track record in recovering core from a wide variety of geological materials and difficult drilling environments. The core recovery method has a number of advantages over more conventional drilling methods including:

- A very high success rate in the recovery of samples from all types of rock and sediments including those that are almost impossible to recover by more conventional means, including flowing sands and coarse gravels.
- The ability to be drilled almost dry, with limited use of water during drilling, and consequently only minor disturbance of the aquifer sediments and fluids. Combined with almost full core recovery, this allows accurate mapping of geological contacts, identification of many sedimentary features, and facilitation of textural, compositional and petrophysical analysis.
- Recovery of uncontaminated pore fluids.
- Greatly reduced environmental impact because of the reduced use of water for drilling. As noted, the holes in this area were drilled dry, and only comparatively small quantities of water are used to flush out the space between the core barrel and the casing.

The drilling locations were targeted to validate specific conductivity anomalies (Figure 31). Summary data for the 12 holes drilled are contained in (Table 5, Table 6 and Figure 28). The diameter of the core (PQ) is 85 mm (internal). The core was discharged from the core barrel into clear plastic sleeving in lengths of 1 m or less (Figure 30). These were labelled and placed in labelled core trays. As only the ends of each length could be easily examined, only summary logging was conducted in the field, with more detailed logging carried out in the laboratory in Geoscience Australia. Once drilling was complete and a temporary piezometer installed for down-hole geophysical logging, the standing water level, water temperature, and water table conductivity were measured.

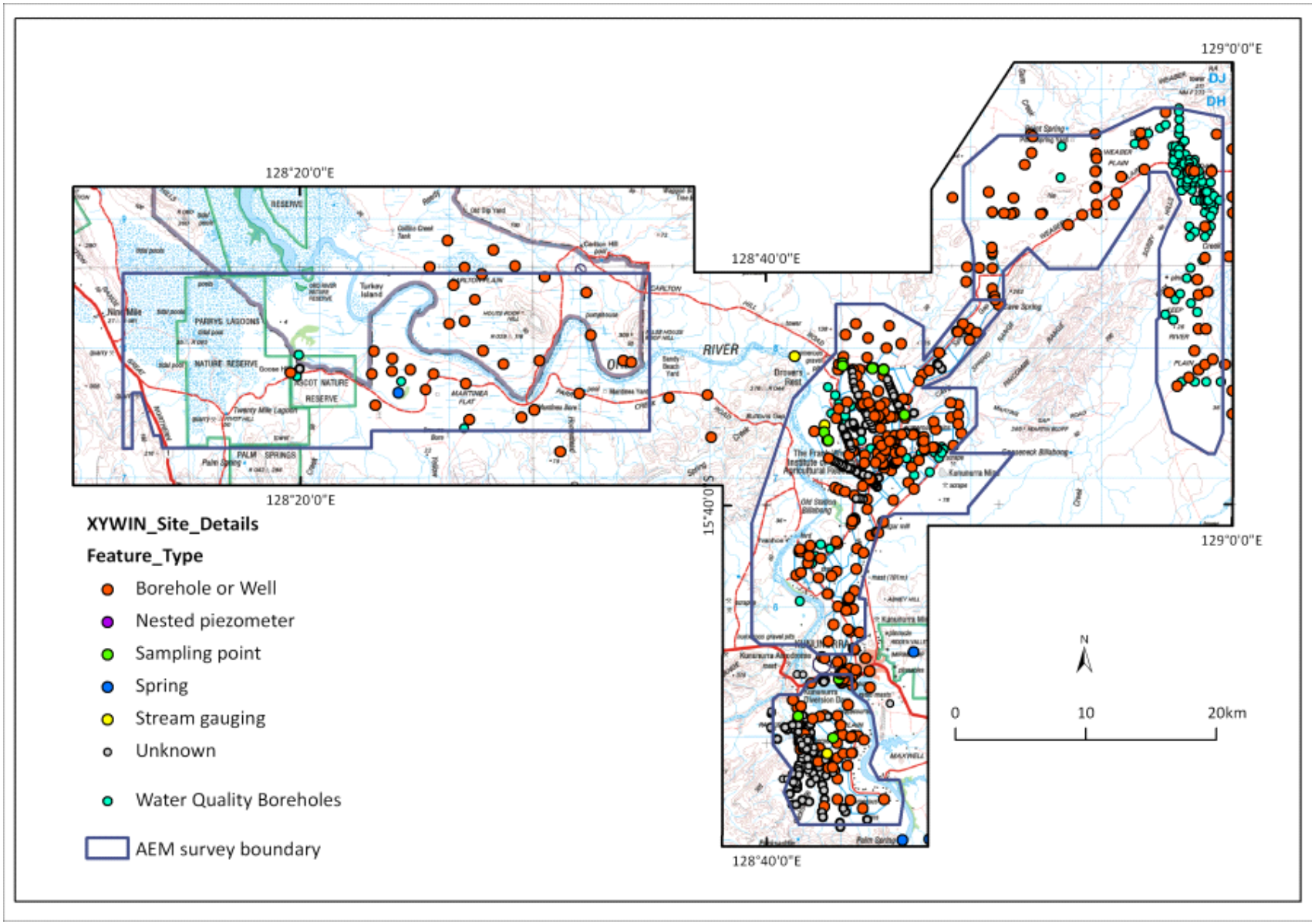

Figure 27: *Distribution of existing borehole and water sampling points. The data are contained in Appendix 3.*

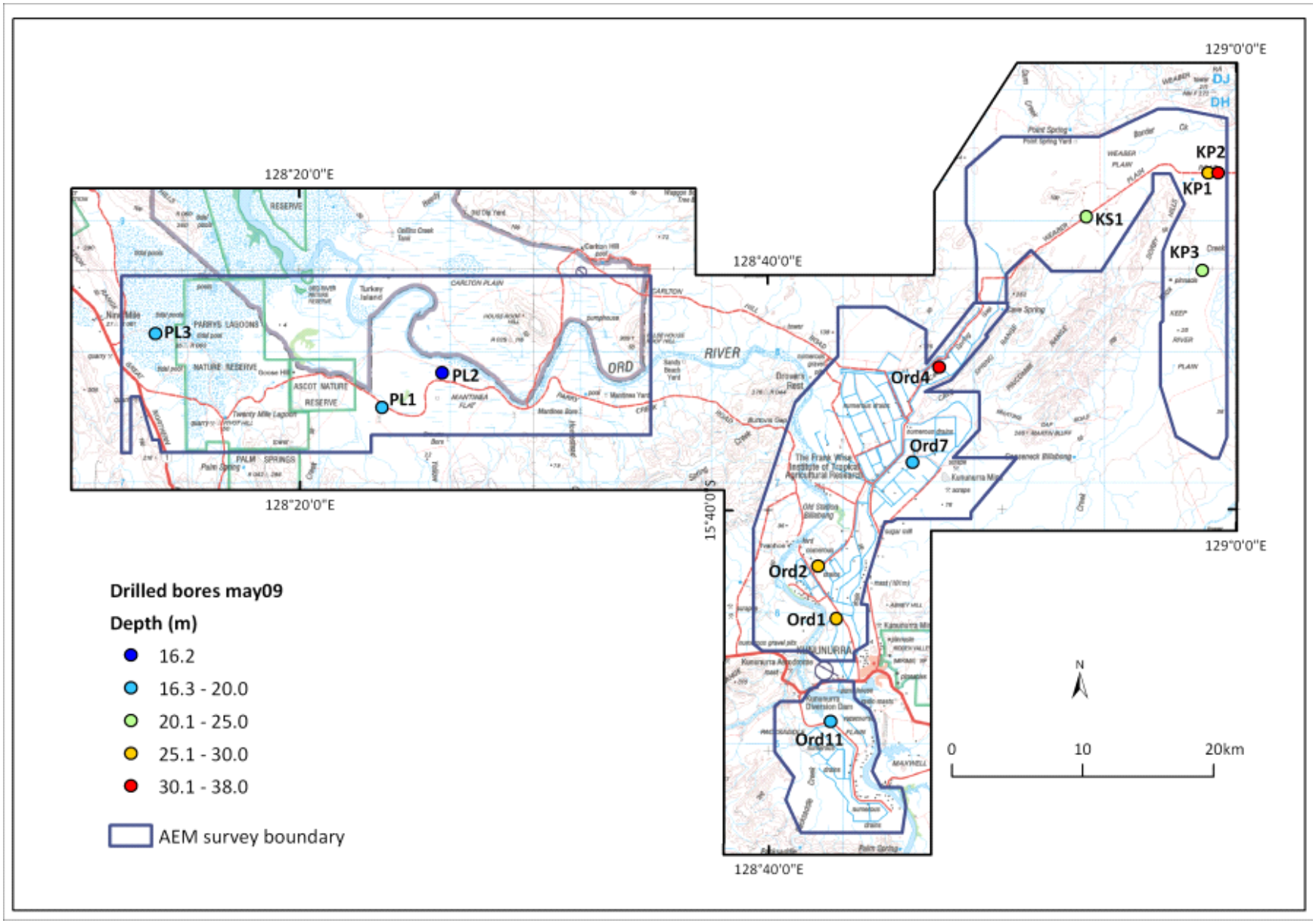

Figure 28: *Location of new boreholes in project area.*

Figure 29: *The sonic rig on site at hole O4.*

Figure 30: *Sonic rig samples being laid out and labelled prior to stacking in core trays. Hole O11.*

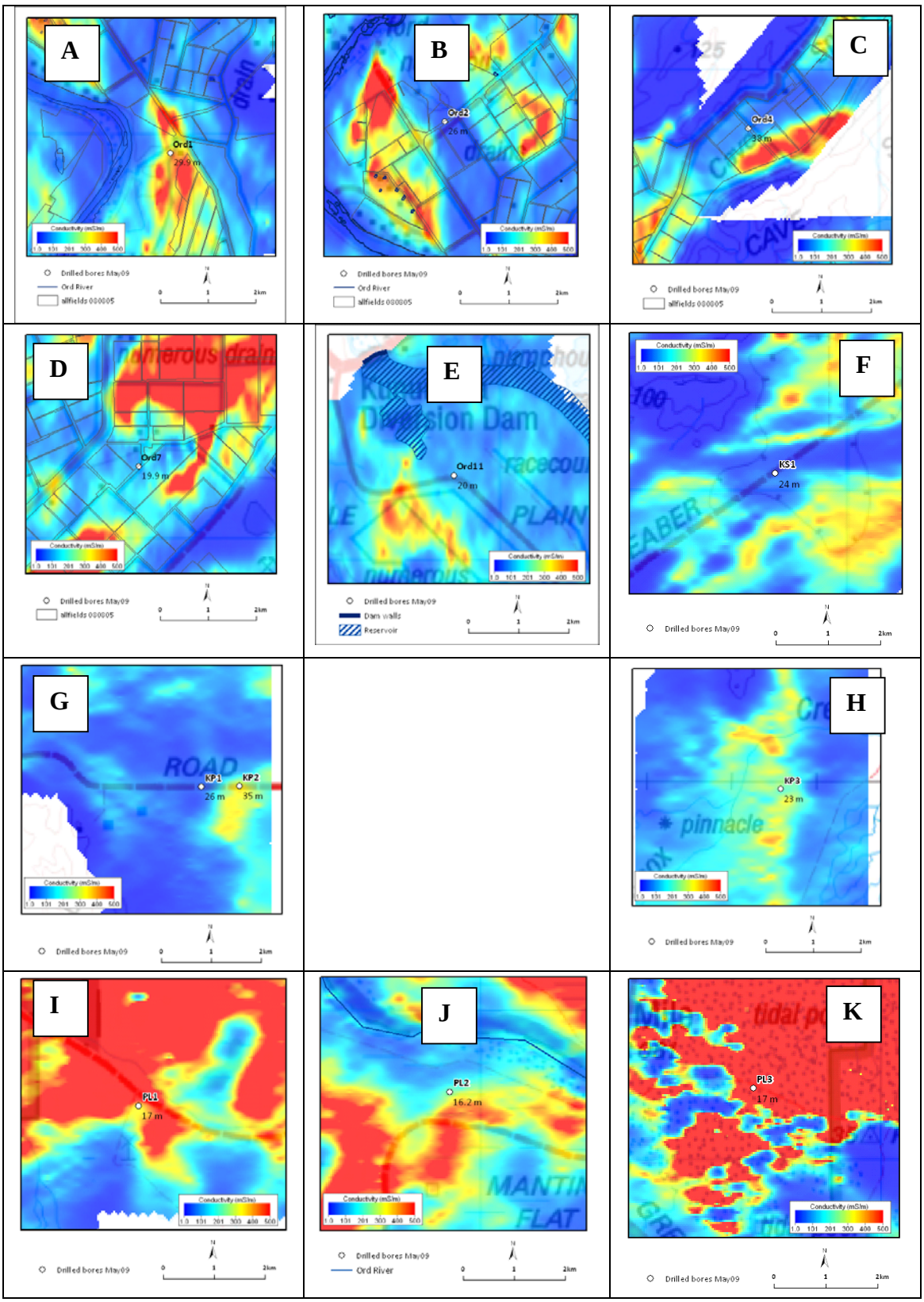

Figure 31: *Locations of all new boreholes superimposed on representative conductivity depth slices from the AEM data. A shows borehole O1; B shows borehole O2; C shows borehole O4; D shows borehole O7; E shows borehole O11; F shows borehole KS1; G shows boreholes KP1 and KP2; H shows borehole KP3; I shows borehole PL1; J shows borehole PL2; K shows borehole PL3.*

Table 6: *Location and purpose of boreholes drilled for this project.*

Hole	Purpose
O1	Targeted on a moderately resistive succession beneath Ivanhoe Plains. These were inferred to represent a thicker succession of floodplain sediments and a thinner succession of channel sands and gravels than in 02. The hole was sited on a farm access track.
O2	Targeted in a north-south highly resistive unit connecting two bends of the Ord River channel. This was interpreted as being a palaeochannel with thick sands and gravels, the drill hole was intended to test this hypothesis. The hole was sited beside Research Road
O4	Targeted on the inferred thick coarse gravel sequence through Cave Springs Gap. A secondary target was a surface conductivity anomaly. This however could not be adequately tested because farm logistic requirements meant that the final drill position was offset from the original site.
O7	Targeted to intersect the resistive anomaly beneath the mahogany forest, as near as practically possible to its centre. Access issues controlled the precise location of the borehole.
O11	Targeted on the edge of a conductive unit beneath packsaddle plains. Access was provided on an easement beside Packsaddle Road.
KS 1	Targeted on a resistive unit inferred to represent the palaeochannel of the Ord River where it formerly flowed east towards the Keep River. The hole was sited on the side of the Keep River Road.
KP1	Targeted to intersect a resistive unit that might represent a sand and gravel palaeochannel fill replated to the former coarse of the Ord River when it flown east to what is now the Keep River estuary. Access was provided by the keep River Road, beside which the hole was drilled.
KP2	The target of hole was to test a deep conductive unit and determine whether it was due to conductive bedrock or clay rich and water saturated palaeovalley sediments.
KP3	The target was a shallow resistive unit between the Keep River to the east and Knox Creek to the west. Access was provided by a north-south farm track.
PL1	Targeted on the floodplain succession of the lower Ord River away from the scroll plain and to intersect the conductive layer beneath the surface. The hole was intended to be sited on an existing track. This could not be located on the ground so the hole was drilled at the approximate position.
PL2	Targeted to intersect the scroll bars and underlying sediments of the Ord meander plain. Also targeted was the interpreted freshwater flush zone adjacent to the river. The hole was sited along a fence line to use the track for access.
PL3	Drilled to intersect the shallow, highly conductive layer visible in the AEM data and to provide information on the stratigraphy at the extreme west of the survey area. Evidence for marine or marginal marine sediments was expected. The exact location was chosen to be on an existing track at a reasonable distance from any outcropping bedrock as rises or hills.

3.3.3 Laboratory Analysis of Drill Core Materials

The samples were transported by road to Geoscience Australia in Canberra where the plastic sleeving was cut open and the core described in detail (Appendix 4; Cullen *et al*., 2010), photographed and sampled. Samples were analysed for grainsize (using sieving for the gravel fraction and laser granulometry for the sand and finer fractions), bulk density, pore fluid extraction, XRD mineralogy and PIMA analysis of clay types (Appendix 5, Cullen *et al*., 2010), moisture content and, where not suitable for pore fluid extraction for laboratory measurements of EC 1:5 (Appendix 6; Cullen *et al*., 2010).

3.4 BOREHOLE GEOPHYSICAL DATA

A geophysical borehole logging program was completed for 45 piezometers located within the AEM flight area, prior to and during the airborne survey. Their locations are plotted in Figure 32. The primary purpose of this program was to help validate the derived conductivity model from the AEM data set. This was then followed up with a second logging campaign to log the 12 holes drilled in mid 2009 as part of the follow-up sonic drilling program. Due to a number of historic problems with borehole logging tools and methods (Davis & Ley-Cooper, 2010), historic borehole logging data were not used for comparison with the AEM data. In total, induction and gamma logs were obtained for 57 holes in the project area (Appendix 7; Cullen *et al.,* 2010).

3.4.1 Conductivity Logging

Conductivity logging is an electromagnetic technique measuring the electrical conductivity of rocks around the borehole. The electrical conductivity of a rock is a complex function of a number of factors. These listed in order of decreasing importance are (Hallenberg, 1984; Lane, 2002):

- Porosity and water content
- Water chemistry (i.e. salinity)
- Rock chemistry and mineralogy
- Degree of rock alteration and mineralisation
- Amount of evaporates
- Amount of humic acids and
- Temperature

Although there are a number of geophysical tools which measure electrical conductivity or its reciprocal, resistivity, electromagnetic logging can be used in wet or dry holes and cased or uncased (if PVC cased, not if steel cased) boreholes. Resistivity techniques require the probe to be in direct contact with the formation and require saturated conditions. Conductivity logging, also referred to as induction logging, is a non-contact method, by which a current is induced into the formation and the secondary magnetic response is measured by a receiver coil. The measurements are converted to apparent conductivity using a simple half space approximation (Hallenberg, 1984). All conductivity and gamma logs are reproduced in Appendix 7 (Cullen *et al*., 2010).

3.4.2 Geophysical Equipment

Borehole geophysical logging was undertaken with two AUSLOG tools, specifically inductive conductivity and natural gamma tools. The specifications of these tools are listed below (Table 7, Table 8).

Table 7: *Specifications of the AUSLOG Natural Gamma Tool.*

Model	**A031 High Sensitivity**
	Natural Gamma Tool
Diameter	43 mm
Length	1130 mm
Weight	4.0 kg
Pressure Rating	21000 kPa
Temp Rating	0 - 70°C
Power	30 VDC
Detector Type	Scintillation Crystal
Crystal	NaI(Ti)
Size	25.4 mm x 76.2 mm

Table 8: *Specifications of the AUSLOG A034E Inductive Conductivity Tool.*

Model	**A034E**
Diameter	38 mm
Length	140 cm
Weight	5 kg
Max Working Temperature	0 - 70°C
Max Working Pressure	10 000 kPa
Min No. of Cable Conductors	1 or 4
Supply Voltage Range	30 VDC
Nominal Current Consumption	80 mA
Supply Voltage Polarity	+ on central conductor - on probe shell
Measuring Parameters	
Conductivity Range	0 mS/m - 1000 S/m
Noise Level	<0.5 mS/m
Accuracy	3% over most of range
Sensor	two coil system
Intercoil Spacing	300 mm
Operating Frequency	~900 Hz

3.4.3 Calibration of Geophysical Tools

Laboratory calibration of the gamma tool and conductivity tools were conducted at CSIRO's Perth office, prior to the tools being shipped to the study area. The gamma tool was calibrated to API standard values using two gamma radiation sources. The conductivity tool was placed in a Faraday cage to reduce external electrical interference and calibrated using a zero free-air measurement and 1000 mS/m calibration disc. Both logging tools are expected to stay calibrated for periods between 1 to 3 months.

The calibration procedure adopted for the field program is summarised as follows: each tool was calibrated via AUSLOG supplied software used to record logged measurements. A lookup table is developed for each tool type and is then used to convert measured tool units (counts) to a unit commensurate with the measured quantity, e.g. mS/m for conductivity. More specifically the field procedure used for calibration is:

Conductivity Tool

1. At the start of the survey, locate an area away from cultural noise and from metal objects. Record field measurement with the 100mS/m 300mS/m, 1000mS/m and 3000 mS/m calibration discs (and free air measurement). Reset the calibration numbers (the actual calibration file in the AUSLOG software) to the calibration values. Repeat free air measurements and calibration discs measurements ensure stability of the tool in the middle and end of the day. Repeat this procedure at the start of each day, and note any variations in the calibration.
2. Note any anomalous values/readings during measurement. For each borehole measurement, complete a free air measurement, before and after logging.
3. Re-log a "base station" borehole in the survey area each day and monitor. If possible, log this hole 2-3 times a day. This hole is re-logged at the start and end of each day, for the first few days to check the system stability and performance. If all data look consistent, re-log the hole once a day or at the least once every two days.

Natural Gamma

Natural gamma measurements were calibrated using a lookup table created with a known 'total count' source placed near the scintillation detector within the tool.

Logging Settings
Down-hole logging was completed at 12-15 metres/min, up-hole logging was completed at 6metres/min. Both logs were simultaneously plotted to ensure repeatability, and the up-hole logs were kept as the final measurement for each borehole.

3.5 IRRIGATION SCHEDULING DATA (AT TIME OF AEM SURVEY)

To provide baseline data on soil moisture levels in the irrigation areas at the time of the AEM survey, and as a check on the drivers of the AEM response in the top few metres, data on irrigation scheduling were gathered by staff from Brolgas Environment. Data collation was a significant undertaking, and despite a significant effort, it was only possible to gather information on the irrigation dates at the time of survey for only half of the ORIA Stage 1 (Figure 33). The irrigation scheduling data were added into the theme 'allfields' in the GIS (to augment data supplied by OIC for May 2008), where it is available for further analysis.

Attributes added to the theme in the GIS were the date the AEM survey was flown, the date the crop was irrigated plus the difference between these two dates. Where irrigation was carried out over several days, the day closest to the survey date was used and if the AEM survey was flown prior to irrigation, days received a negative value. It was intended that these data would provide a useful contextual dataset for more detailed analysis of the AEM data at a paddock scale (at the time of survey).

The data complement 'persistence of moisture' data for non-irrigated areas obtained from analysis of remote sensing data (see Section 4.4).

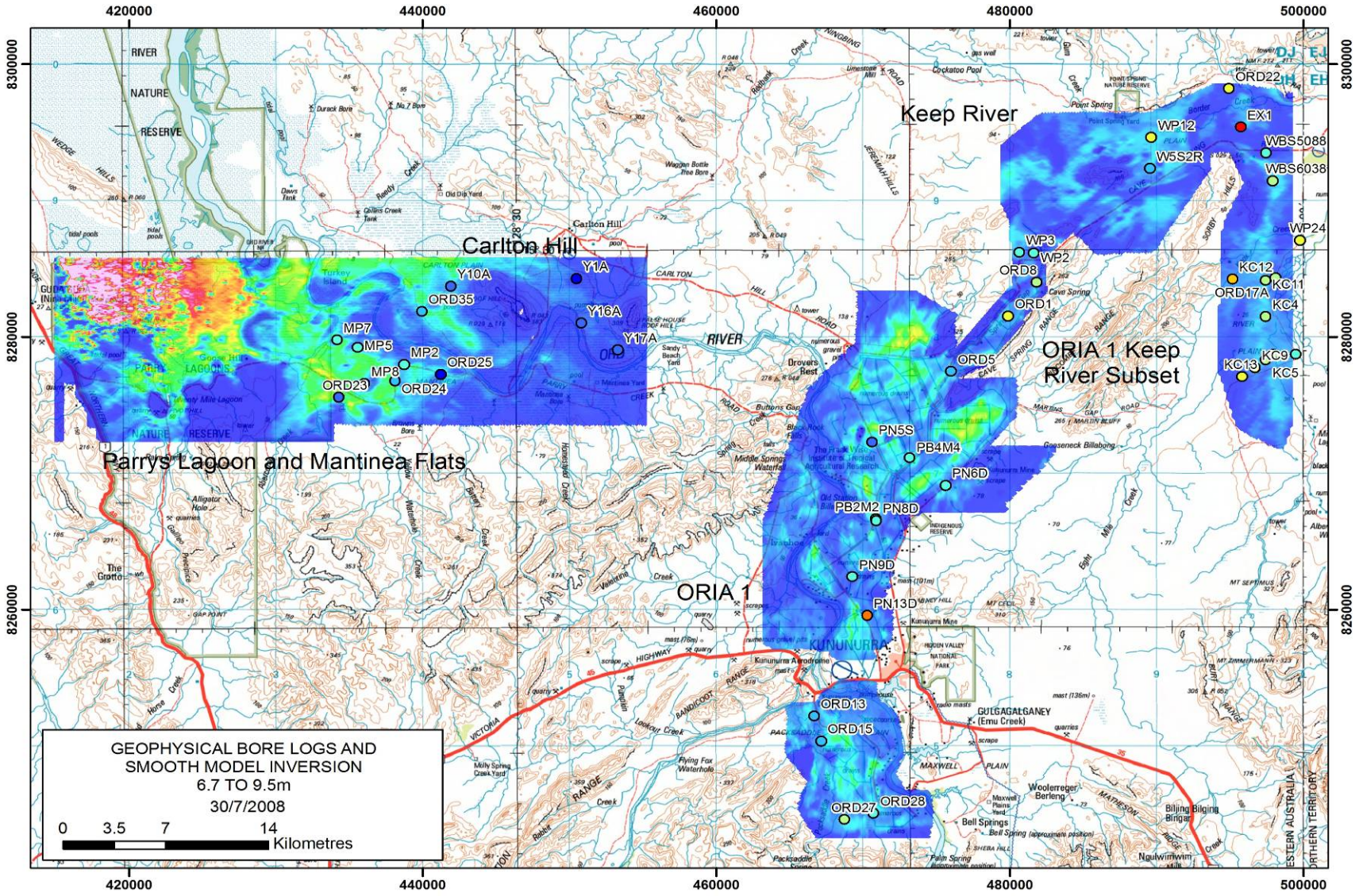

Figure 32: *Location of piezometers that were geophysically logged in the study area.*

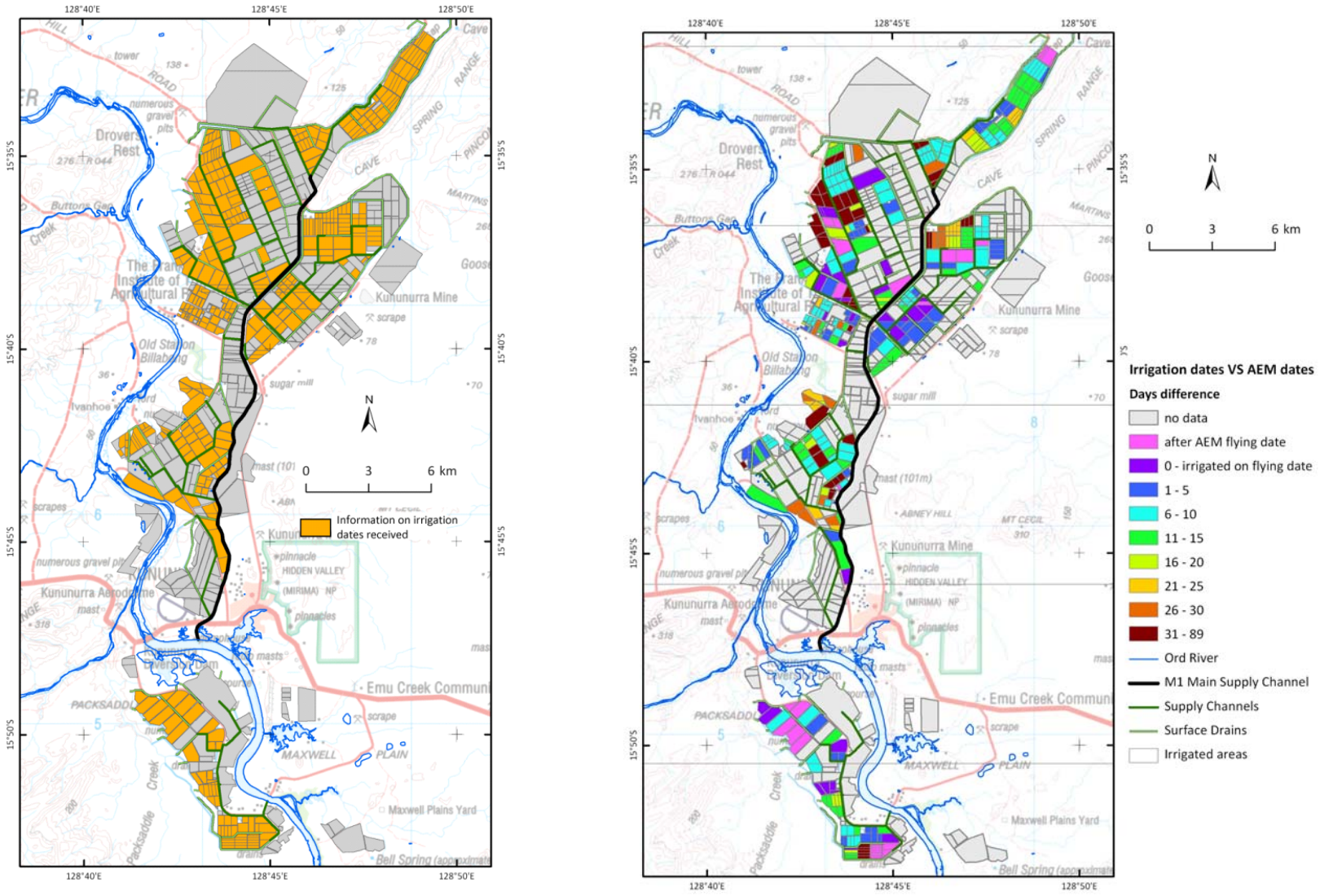

Figure 33: *Properties where irrigation data were supplied (left) and time between AEM survey and previous watering (right*).

3.6 AEM DATA

3.6.1 Previous AEM Surveys in the ORIA

The ORIA, including the Stage 1 and proposed Stage 2 areas, have been the focus for previous hydrogeophysical investigations using airborne electromagnetic (AEM) technologies. Their application was primarily intended to provide further insight into the hydrogeology of the proposed Stage 2 areas, particularly in the Weaber Plains and Keep River areas. In August 1994, a QUESTEM AEM survey was commissioned, covering the Stage 2 areas proposed for WA and the NT, with a full interpretation described by Humphreys *et al*., 1995, 2002; and O'Boy *et al*. (2001). QUESTEM was an uncalibrated fixed-wing time domain EM system primarily designed for minerals exploration, with only a limited capability for resolving near surface variations in conductivity or variations of conductivity with depth.

Recent developments in AEM system technologies (see Thompson *et al*., 2007; Macnae, 2007) with the better definition of system geometry and the greater attention to calibration, have contributed to substantial improvements in the definition of conductivity both near surface (less than 5m) and at depth (greater than 100m). These trends coupled with our ability to better process, image and display AEM data, have made these newer systems a more relevant geophysical technology for the systematic characterisation of the groundwater quality and salt stores in alluvial aquifer systems such as those found in the Ord region.

3.6.2 Forward Modelling and AEM Technology Selection

To ensure that the most appropriate AEM system was selected to map key elements of the aquifer systems and salinity, a full AEM system review was carried out against a set of desired targets (Fitzpatrick *et al*., 2007). Specifically, this study was initiated to:

1. Conduct a geophysical forward modelling study to ascertain whether commercially available helicopter airborne electromagnetic (HEM) systems can assist in defining variations in near surface soils, aquifer characteristics and groundwater quality in the Ord Irrigation Area , Stage 1 and Stage 2, Western Australia.
2. Define the most effective airborne geophysical system to employ and appropriate survey parameters, based upon the forward modelling study outcomes.
3. Provide some indicative costing on the acquisition of HEM data for the proposed survey areas.

After initial consideration of the likely hydrogeological targets, a forward modelling study encompassing the likely variability in the ORIA Stage 1 and 2 areas was conducted for the RESOLVE FDHEM and SkyTEM TDHEM systems. 26 scenarios describing variability in the conductivity and thickness of sedimentary units found in these areas (Lawrie *et al*., 2007; Fitzpatrick *et al*., 2007) were defined from a combination of field investigation, borehole logs and interpretation of prior AEM data sets. Results from the modelling suggested that SkyTEM would outperform RESOLVE in defining the variability expected across the Stage 1 and 2 areas. However, an iteration on the modelling using (improved) survey noise estimates for SkyTEM suggested that although SkyTEM might still outperform RESOLVE the differences would be less pronounced. Both systems were found to satisfy the criteria of mapping the sand and gravel aquifers in 3D, mapping near-surface salinity and shallow saline groundwater, and defining the aquifer boundaries.

Indicative data acquisition costs suggested that Stage 1 and 2 areas could be covered with a line spacing of 200m for less that $1m, with similar resources required to drillholes to calibrate and validate the survey and invert and interpret the acquired data. After a targeted tender process, the SkyTEM helicopter EM system was selected for the Ord Survey.

3.6.3 SkyTEM TDHEM System and Operating Principle

The Ord survey was undertaken by Geoforce Pty Ltd with the SkyTEM Time Domain helicopter EM (TDHEM) system. This system has been successfully applied to the mapping of palaeochannel systems in south-western Australia (see, for example Reid *et al*., 2007) and has a demonstrated ability to define both a near-surface and deep conductivity structure in these environments.

The SkyTEM time domain EM system is carried as a sling load towed beneath the helicopter (Figure 34). A full technical description of the SkyTEM is given by Sorensen & Auken (2004) and Halkjaer *et al*., (2006). The nominal survey altitude of the transmitter for SkyTEM surveys is 30m, with variations largely determined by the presence of trees, hills or other cultural features. The transmitter, mounted on a lightweight wooden lattice frame, is a four-turn, 16 x 16m^2 eight-sided loop divided into segments for transmitting a low moment in one turn and a high moment in all four turns. The transmitter loop area is 311m^2 (Reid *et al*., 2008).

SkyTEM is capable of operating in a dual transmitter mode as detailed in Sorensen & Auken (2004). In the Low Moment mode, a low current, high base frequency and fast switch off provides early time data for shallow imaging. In contrast, when in High Moment mode, a higher current and a lower base frequency provide late time data for deeper imaging. The two modes can be run sequentially during a survey, as was done in the Ord survey. In low moment mode, the transmitter base frequency is 222.22 Hz and in High Moment mode base frequency is 25 Hz. Nominal peak current in the low moment is 39 A with a typical turn-off (ramp) time of about 8μs; while the high moment transmits approximately 95 A and has a typical turn-off time of about 39μs. The receiver loop is rigidly mounted at the rear and slightly above the transmitter loop in a near-null position relative to the primary field, thereby minimizing distortions from the transmitter (see Figure 34). X and Z components are recorded.

3.6.4 Principles of AEM Data Acquisition

EM surveying techniques involve the measurement of the varying response of the ground due to the propagation of electromagnetic fields. Primary fields are generated by passing a current through a loop or coil positioned in the air, referred to as the transmitter loop (see Figure 35). A secondary field is induced in the ground and these fields are detected by the alternating currents that are induced to flow in a receiver coil, positioned at the rear, and offset from the transmitter loop in the SkyTEM system (see Figure 34), by a process known as electromagnetic induction. As the induction of current flow results from the magnetic component of the electromagnetic field, there is no need to have physical contact between transmitter or receiver and the ground. Consequently, EM surveys can proceed effectively both on the ground and in the air.

The primary field travels from the transmitter to the receiver via paths above and below the ground surface (Figure 35). In the presence of a conducting body (for example a conductive soils), the magnetic component of the electromagnetic field penetrating the ground induces eddy or alternating currents to flow in the conductor. These eddy currents generate the secondary electromagnetic field which is measured by the receiver (Peters, 2001). The receiver coils record the response of a decaying signal in the ground at various times after the transmitter pulse has been switched off.

The difference between the transmitted (primary) and received (secondary) electromagnetic fields will be determined by the geometry and electrical properties of conductors in the ground. Materials that are highly conductive produce strong secondary electromagnetic fields. Sediments, soils or other regolith materials that contain saline pore water generate such fields. The shape of the decaying signal provides information about the conductivity structure of the ground.

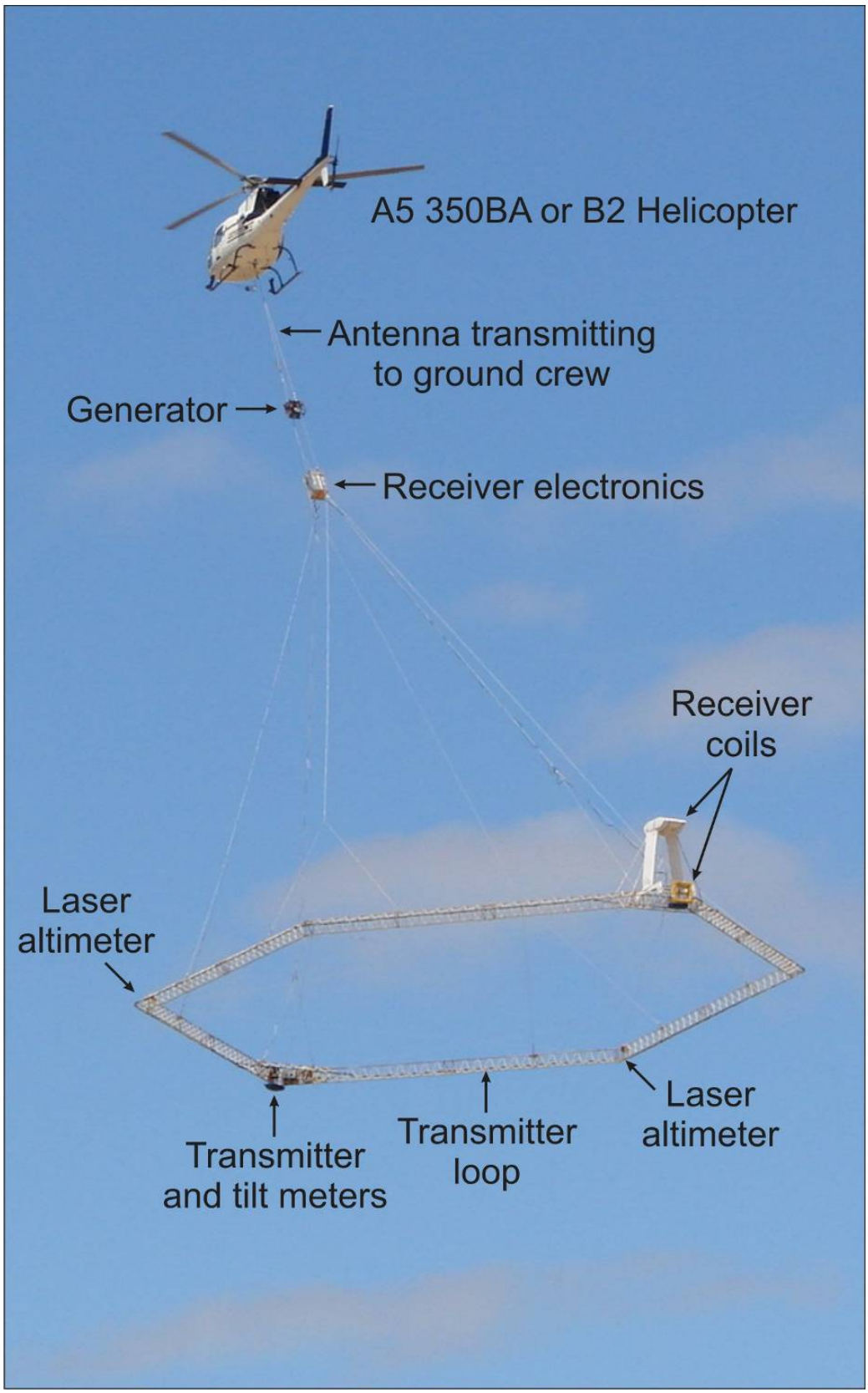

Figure 34: *The SkyTEM airborne electromagnetic system in flight mode.*

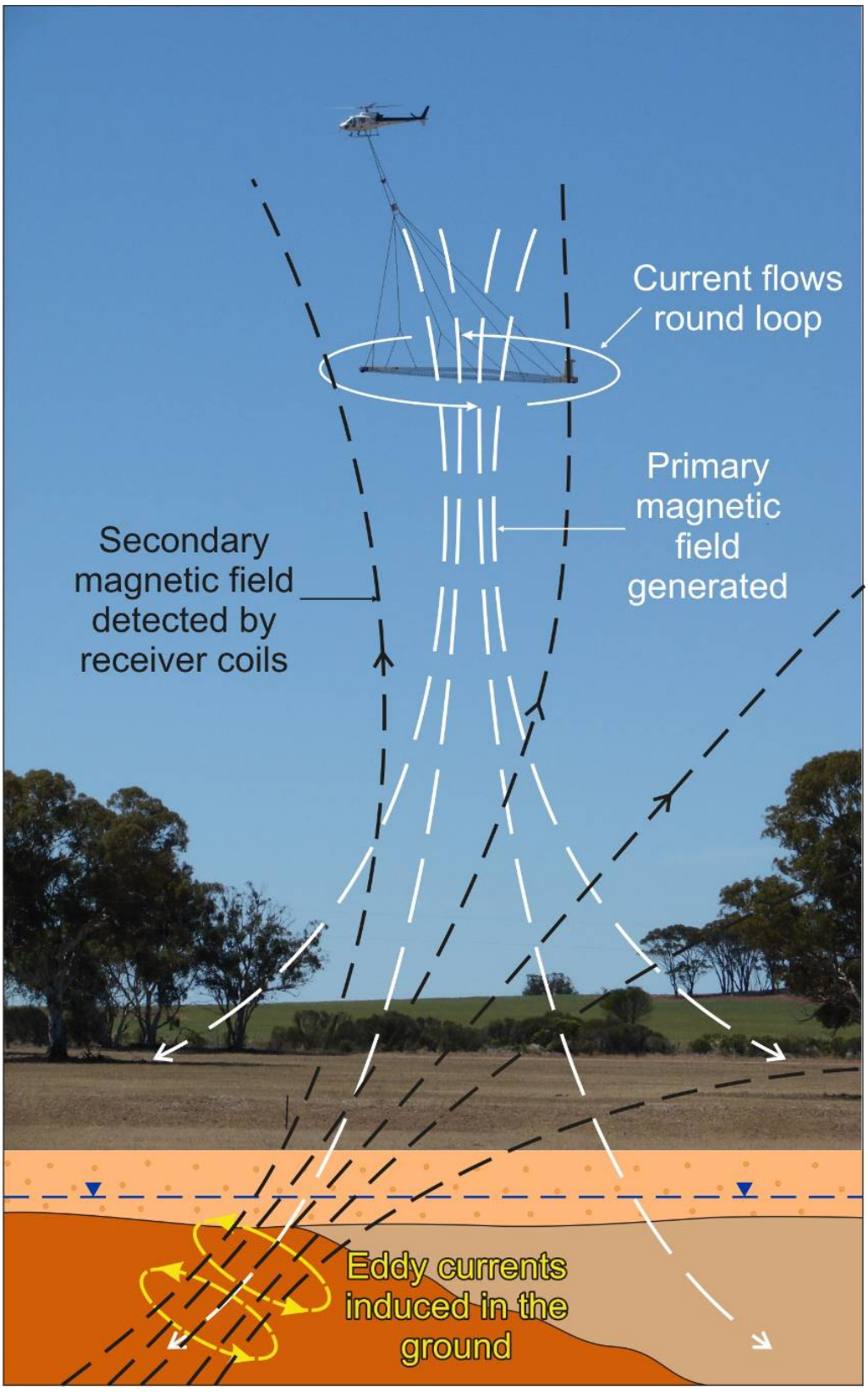

Figure 35: *Operating principles of the SkyTEM AEM system.*

3.6.5 Ord SkyTEM Survey Logistics

The Ord survey was undertaken between the 23rd July and the 26th August 2008. A photograph of the helicopter-towed frame in acquisition mode is shown in Figure 36. Full logistical details are provided in Reid *et al*. (2008). Summary details are presented in Table 9. Details of the survey extent and the flight line orientations are shown in Figure 37. For air safety reasons, the original survey boundary close to Kununurra Airport was adjusted, and supplementary acquisition occurred over the Cockatoo Sands area and along the M1 Canal. The total number of line kilometres flown was 5936 line km (Table 9).

Figure 36: *The SkyTEM AEM system in acquisition mode in ORIA Stage 1.*

Table 9: *System and survey specifications for the Ord SkyTEM survey.*

Specifications	System and Survey Parameters
Line Spacing:	200m (Keep River, ORIA1, Keep River/ORIA1 subset, Parry's Lagoon); 300m (Carlton Hill); 400m (Cockatoo Sands)
Line Orientation:	000-180 (Parry's Lagoon, Carlton Hill, Keep River); 090-270 (ORIA1); 39-210 (Keep river/ORIA1),
Tie Line Orientation:	None flown
Sensor Height:	Nominally 30m
Survey Flown:	July-August 2008
Total Line kilometres flown	5936
Aircraft Type:	Squirrel AS350B2 VH-NRW
AEM System:	SkyTEM
Navigation	DGPS
Data Positioning:	Real Time Kinematic GPS
GPS System:	Novatel DLV-3, 12 Channel
Laser Altimeter:	LaserAce IMHR 300

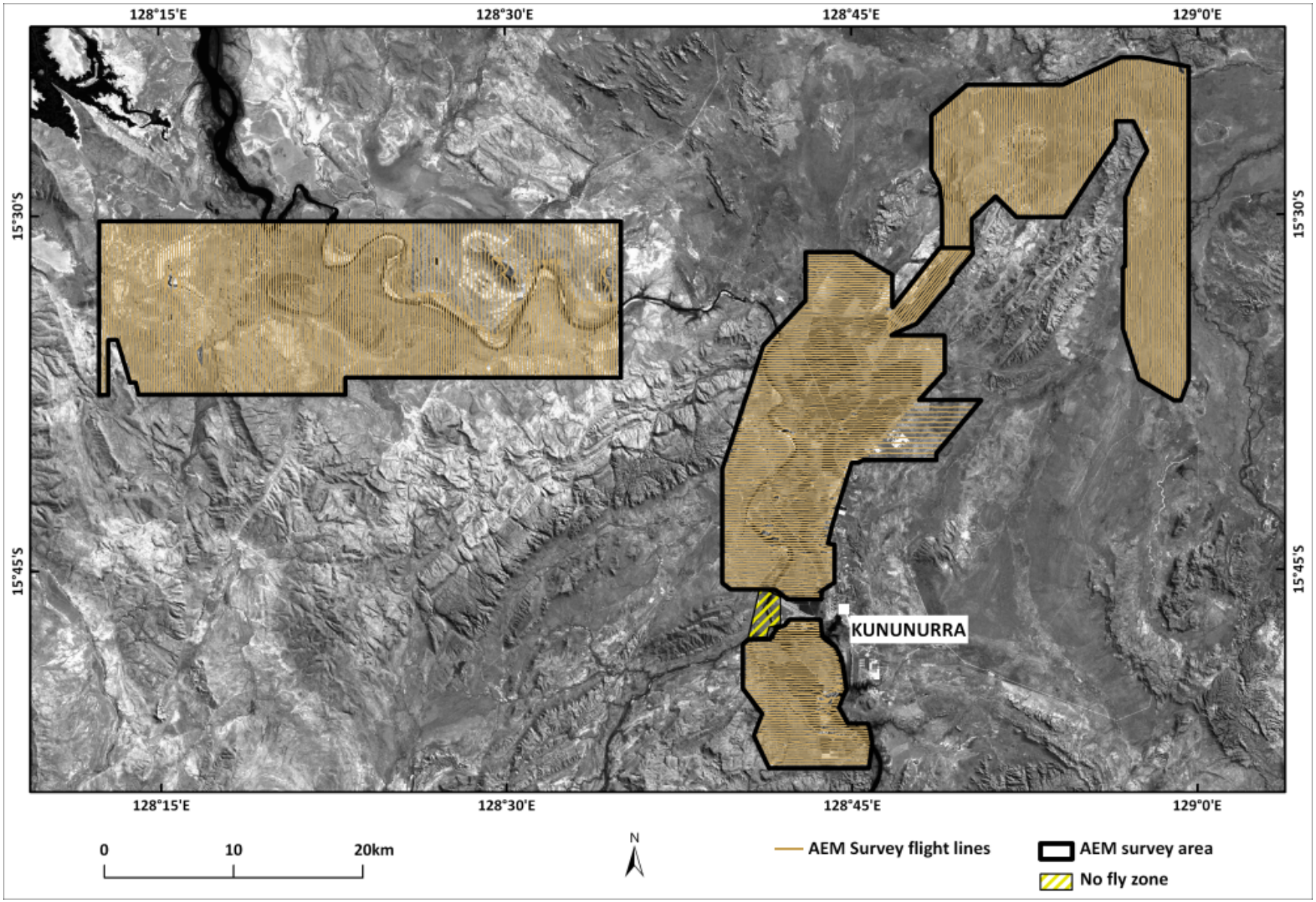

Figure 37: *Flight line diagram for the Ord SkyTEM survey.*

3.6.6 AEM System Spatial Resolution

The spatial resolution of an AEM system varies with the system type, sample time or frequency, and with ground conductivity (see Spies & Woodgate, 2005). It is different in the horizontal and vertical direction. Commonly resolution is considered in terms of the volume of the ground that contributes most of the response for each measurement. Helicopter systems such as SkyTEM return a weighted average response over lateral distances of several tens of metres. The smallest lateral features that can be resolved near surface are around 30-60m for helicopter systems where good conductivity contrasts are present. These figures increase with depth. Normally the highest resolution is measured along a flight line, with the perpendicular resolution being determined by line spacing. Wide line spacing (>200m) will limit the definition of conductivity variations both at surface and at depth. These issues should be borne in mind when comparing models of ground conductivity or other products derived from the AEM data to information collected from bore data, or individual soil pits.

3.6.7 SkyTEM System Calibration

SkyTEM is referred to as a calibrated AEM system (Sorensen & Auken, 2004; Halkjaer & Reid, 2008). This is calibrated in the laboratory, and verified at the Danish National Reference site. However, in this study we sought to verify it's claimed performance and to determine whether further system adjustments were required. The methodology used was based on a procedure described by Davis & Macnae (2007a, b). This uses flying the system over a ground loop located on electrically resistive terrain. This procedure permits the extraction of airborne waveforms by deconvolution of ground-loop data and the calibration of the system (if required) within limitations of the AEM system transmitter/receiver amplitude (gain), and system geometry/altitude.

The experiment used a ground loop to obtain the transmitter current waveform of the SkyTEM airborne electromagnetic system (AEM). The experiment was undertaken by CSIRO, with the assistance of RMIT, in August 2008. It involved laying out a 150m × 50m loop on a resistive ridge in the NE portion of the ORIA survey area, and then overflying the loop several times using the SkyTEM system flying in an operational mode. Currents induced in the ground loop were recorded by an NI 9233 24-bit data acquisition system (DAS) connected across a 1Ω bridging resistor. In all, 4 lines were flown over the ground loop (Figure 38).

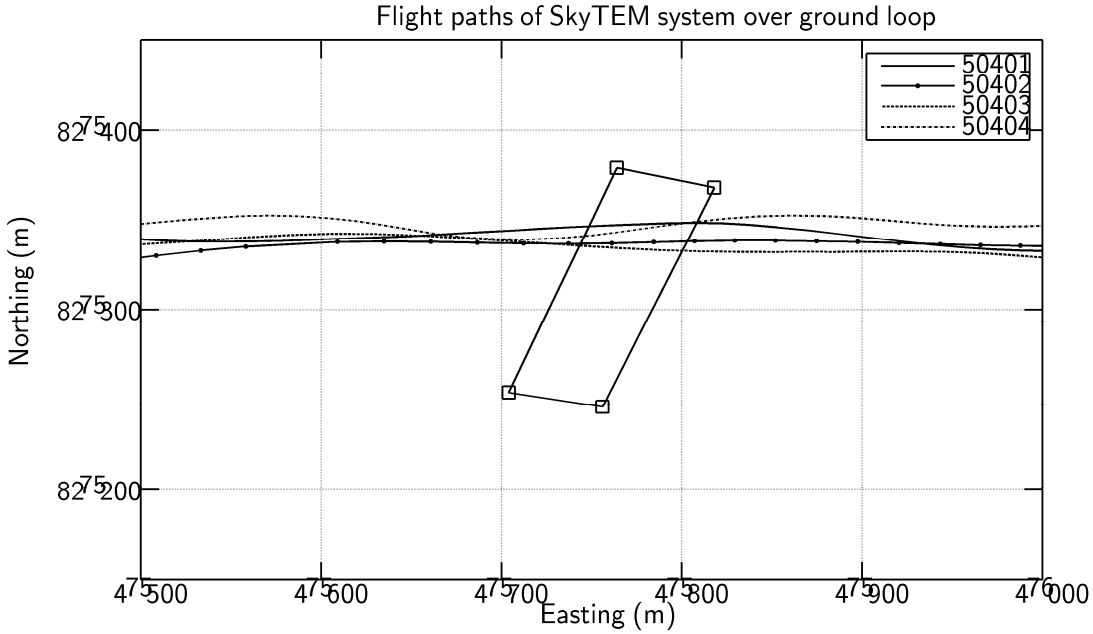

Figure 38: *SkyTEM flight paths over ground loop.*

The ground loop used was a 4-turn loop of wire laid out on a resistive ridge. The loop was insulated from the ground to limit the amount of electric field leakage/coupling to the earth beneath. Resistance of the ground loop was 22.6Ω.

3.6.8 Deconvolution of Waveforms

The SkyTEM transmitter (Tx) waveforms were obtained from the current induced in the ground loop. The current induced as the SkyTEM system was flown over the loop was measured and an example of the current envelope produced is shown in Figure 39.

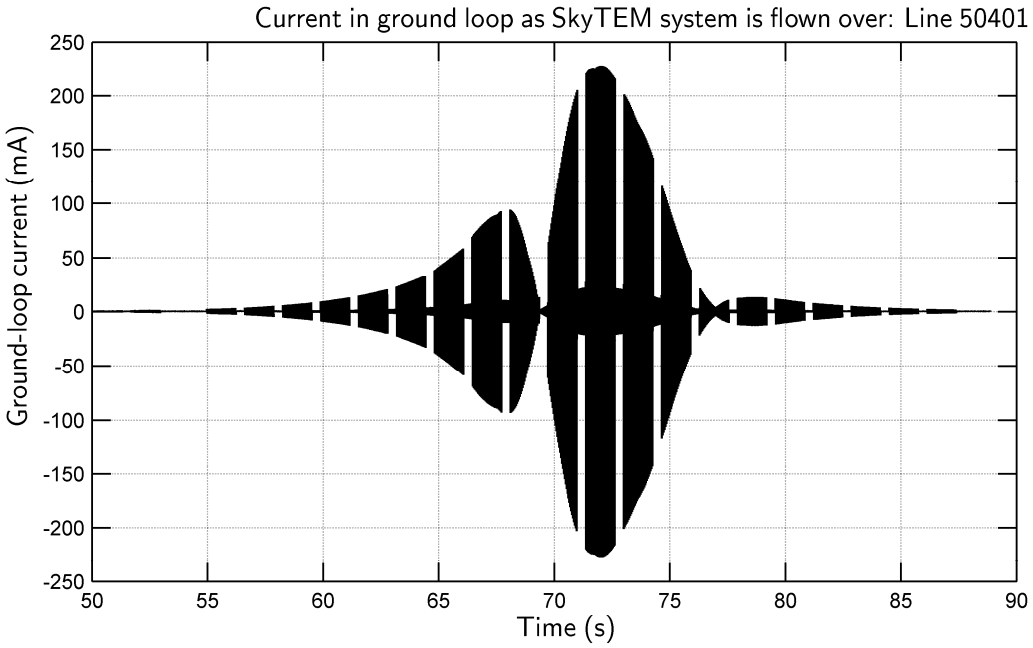

Figure 39: *Current measured in the ground loop as the SkyTEM is flown over, Line 50401.*

The ground loop current for both high- and low-moment Tx waveforms was stacked, using a procedure that went through the streamed data to find the maximum peak value of the ground-loop current at the moment of Tx shut-off. Once a peak was found for one repetition of the waveform, a value of the maximum slope both before and after the peak value was then defined. This represented a time zero. A time zero was then defined for every waveform in the data to be stacked. An interpolation of each waveform from its zero-time to the zero-time in the next waveform defined the mean of the resulting stack, which was then used as the ground-loop response of a nominal SkyTEM Tx measurement.

Using the exponential decay in the ground loop following the Tx shut-off, a decay constant τ was calculated for the ground loop. Using a modelled response of the DAS to a 25Hz square wave determined in the lab, a Tx current waveform was then deconvolved from the (stacked) ground-loop response using the method described by Davis & Macnae (2007b). This was done for both high and low moments.

High Moment

Figure 40 shows the ground-loop deconvolved Tx current waveform compared to the linear approximation of the current waveform provided by Geoforce. There is excellent agreement between all 3 waveforms; however, a zoom of the Tx shut-off shows slight variations. Figure 41 appears to show that the deconvolved ground-loop waveform has a shut-off slightly longer in duration than the linear approximations. This difference (an apparent spreading of turn-off) is attributed to the bandwidth limitations of the DAS system monitoring current in the ground loop during overflight. Sampling frequency of the DAS used was 50000Hz, which limits the data sampling to 20μs. This time scale is on the same order as the nominal Tx current shut-off described in the survey report (see Reid *et al*., 2008).

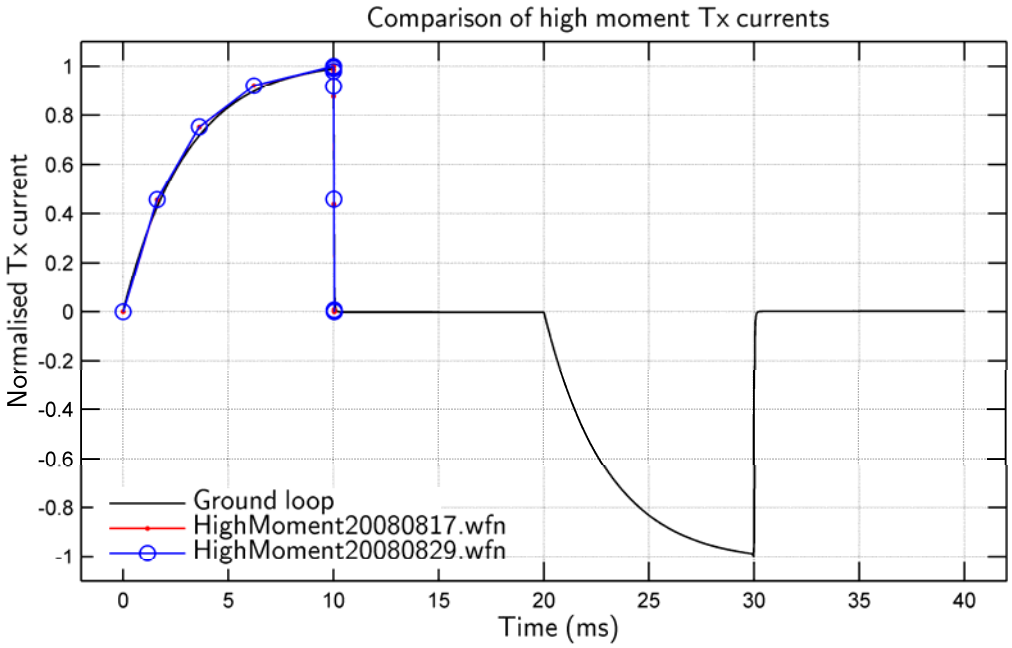

Figure 40: *Comparison of Tx current waveform obtained from ground-loop deconvolution to the linear approximations provided by Geoforce. Linear approximations are dated from 17 August 2008 (red curve) and 29 August 2008 (blue curve).*

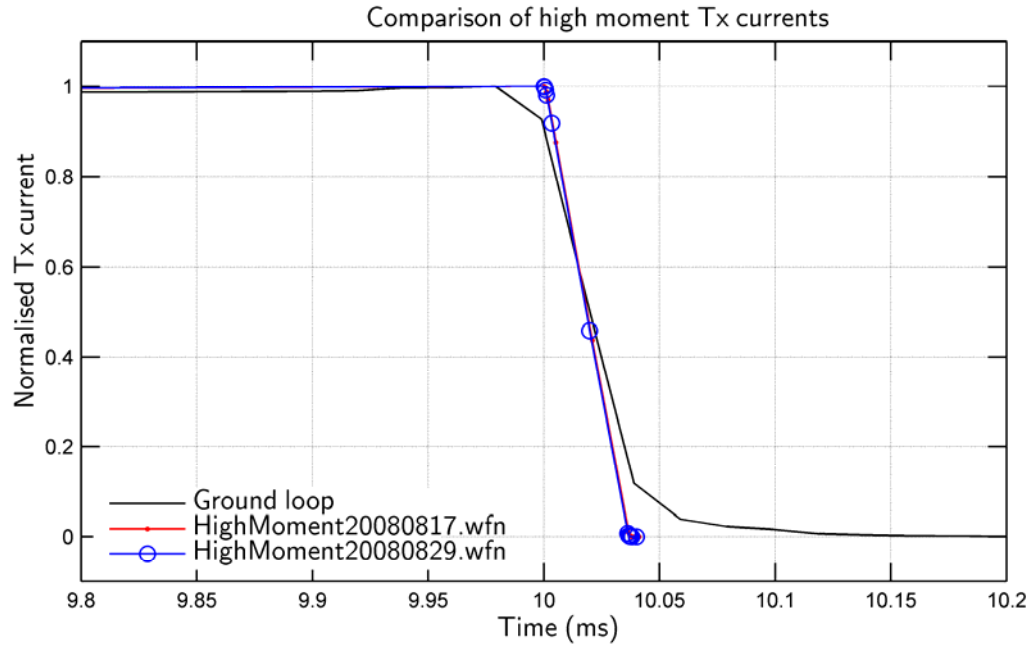

Figure 41: *Close-up of the Tx current shut-off (cf. Figure 40), showing slight variation between the ground-loop deconvolved waveform and the linear approximations.*

Figure 42 shows a comparison between the ground-loop Tx current waveform and streamed waveforms obtained by Geoforce when the system was energised on the ground prior to flying. Again, excellent agreement is seen between the 3 waveforms, with the exception that the ground-loop waveform has a slightly slower rise-time. Figure 43 shows a zoom on the Tx shut-off. The ground-loop waveform agrees with the streamed data waveforms within the limitations due to the sampling period of the DAS, although it appears that the Geoforce waveforms have a slightly faster shut-off than the one obtained from the ground loop.

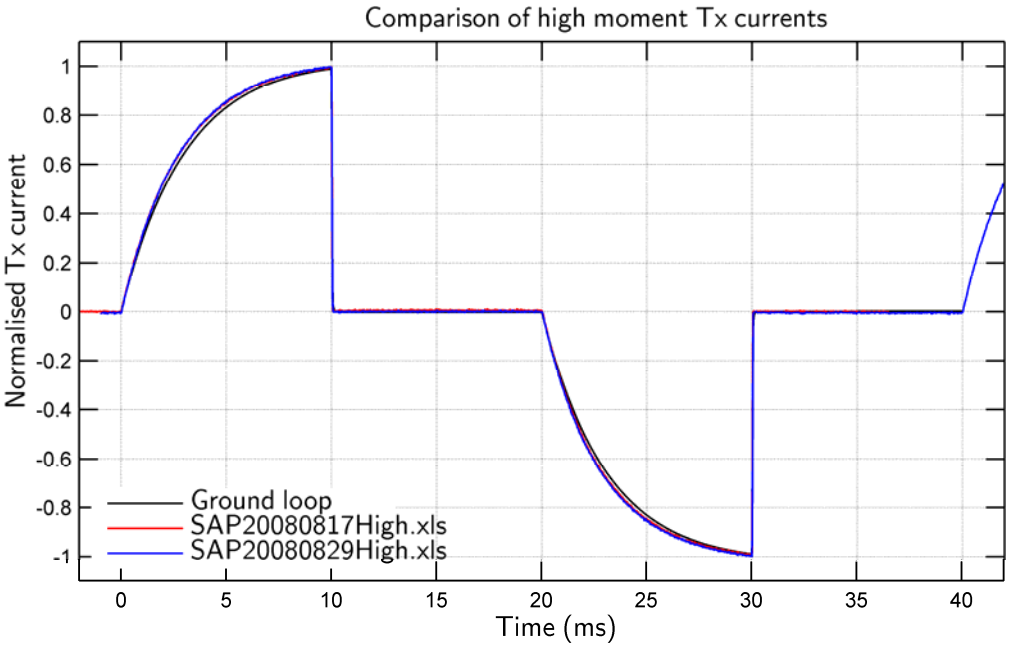

Figure 42: *Comparison of ground loop deconvolved Tx current waveform to the streamed Tx* current *obtained by Geoforce on 17 August 2008 (red curve) and 29 August 2008 (blue curve).*

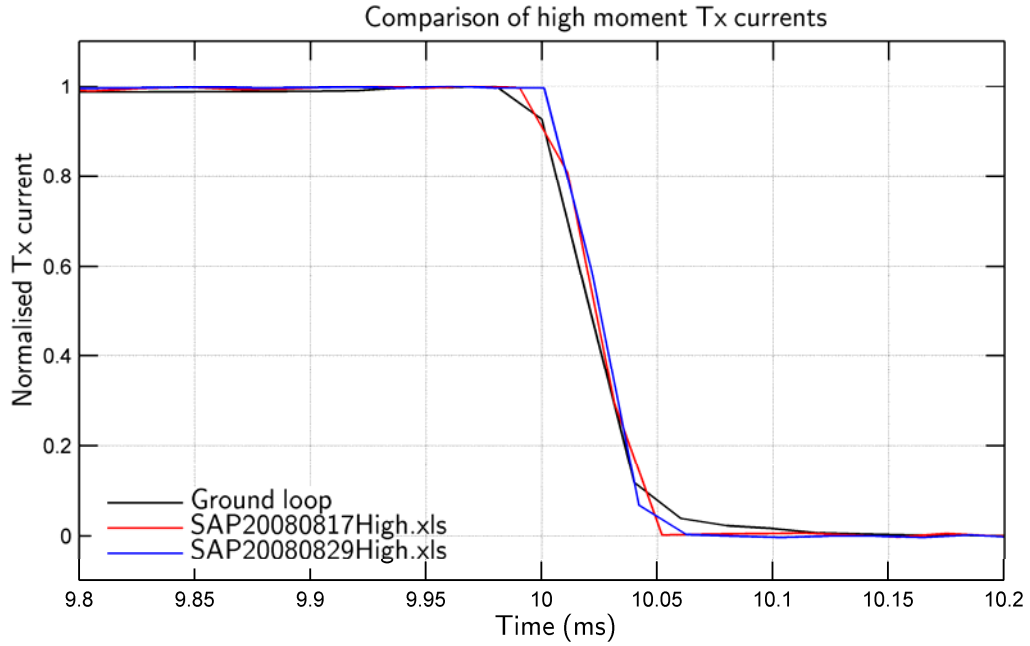

Figure 43: *Close-up of the Tx current shut-off (cf. Figure 42) showing bandwidth limitations in all measurements. Shut-off times all agree within the band limits.*

Low Moment

Ground-loop currents for the low-moment Tx current were defined using the same procedure stacking and processing method described previously. In the low moment case, the nominal shut-off time for the Tx waveform is about 8μs, which is much less than the minimum sampling period of the NI 9233 used. Figure 44 shows the deconvolved Tx current waveform obtained from the ground loop as well as the linear approximations used by Geoforce to approximate their streamed data. On-ramp shape is very similar; however Figure 45 shows that the Tx current shut-off from the ground-loop waveform is much longer than the linear approximations. This is due to the band-limited sampling of 50kHz, which tends to act as a filter to the data. It was not possible to resolve such a fast shut-off with the ground monitoring equipment used in this study.

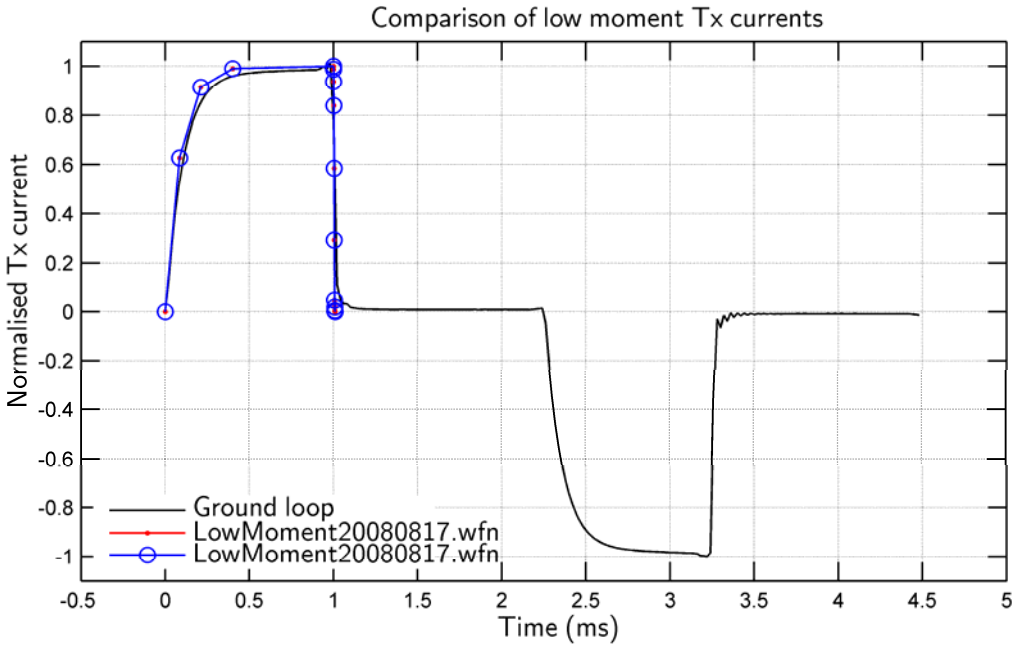

Figure 44: *Comparison of the low-moment SkyTEM Tx current waveforms. Ground-loop rise-time is slightly lower than the linear approximation, but overall shapes agree well.*

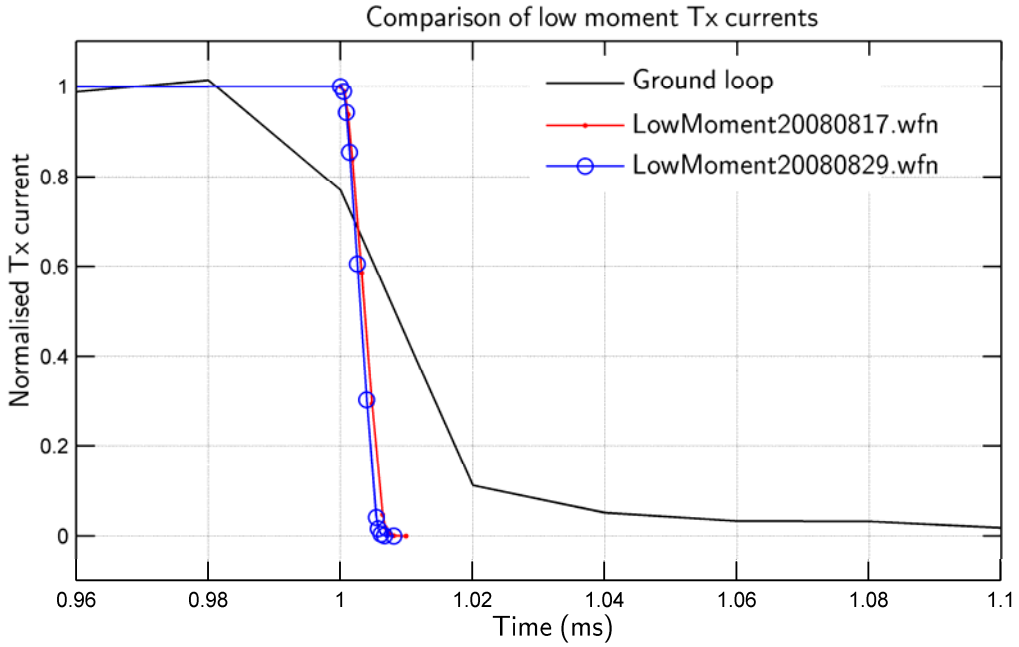

Figure 45: *A close-up of the Tx current shut-off (cf. Figure 44). Ground loop deconvolved shut-off is much longer than the approximations provided by Geoforce.*

3.6.9 Calibration of SkyTEM Receiver

In the previous section it was determined that the Tx current waveforms, deconvolved from the ground-loop responses, agreed well with the streamed and approximated waveforms provided by Geoforce to within the timing errors that are a consequence to the finite sampling by the NI 9233 DAS. Since the ground-loop deconvolved Tx current waveforms agreed with the linearly approximated data waveforms given by Geoforce, the latter were used to predict the ground-loop response of the SkyTEM receiver during flyover, details of which are presented in the following section. In the high-moment case, the linear approximation to the Tx current waveform from 17 August 2008 was used. For the low-moment case, the linear approximation obtained on 30 August 2008 was employed, following discussions with Geoforce who indicated that the

August 17 2008 waveform prediction suffered form from noise contamination. The shut-off was approximated with a straight line.

Data Assumptions

In assessing the calibration of the SkyTEM survey data the information detailed in Table 10 and Table 11, relating to the ground loop and the airborne EM system respectively, were assumed to be valid at the time of survey:

Table 10: *List of loop data variables used in calibration calculations.*

Parameter	Value
Resistance, R	22.6Ω
Positions of loop corners (UTM coordinates, Zone 52)	475704E 8275254N 475764E 8275379N 475818E 8275368N 475756E 8275246N
Time constant, τ	446.33μs
Self inductance, L	10.09mH
Number of turns, n	4

Table 11: *List of SkyTEM system data variables used.*

Parameter	Value
SkyTEM Tx size and positions	SkyTEM Ord River Final Report*
SkyTEM Rx_Z and Rx_X positions	SkyTEM Ord River Final Report*
High-moment Tx current waveform	HighMoment20080817.wfn
Low-moment Tx current waveform	LowMoment20080829.wfn
Laser altimetry; pitch; roll; peak current; Rx_Z responses; Rx_X responses;	From datasets: 20080822_2_high_csirotest 20080822_2_low_csirotest
Number of Tx turns, High/Low	4/1
Tx area	311m^2
Rx area	34.1m^2
Receiver window start, end and centre times	SkyTEM Ord River Final Report*

* *SkyTEM Ord Survey Final Report (Reid et al., 2008)*

Induced ground-loop currents

For the purposes of this study, only lines 50401 and 50404 were used since they were both closed with the 1Ω bridging resistor. Lines 50402 and 50403 were closed with the 1000Ω resistor, lowering the time constant by a factor of 1000. This essentially meant that there was no recordable signal at the SkyTEM receivers. From Figure 46, it is observed that the peak induced ground-loop currents follow the general shape of the measured ground-loop currents, although the amplitudes do not match. There are several possible explanations for this behaviour, specifically:

1) the absolute geometry of the ground loop is not well known;
2) there is an error in the value of the bridging resistor closing the ground loop (i.e., the resistor value is <1Ω);
3) there is an altitude error in the measured altimeter values or
4) the assumption that the system has a laser-defined altitude over a "flat earth" is incorrect.

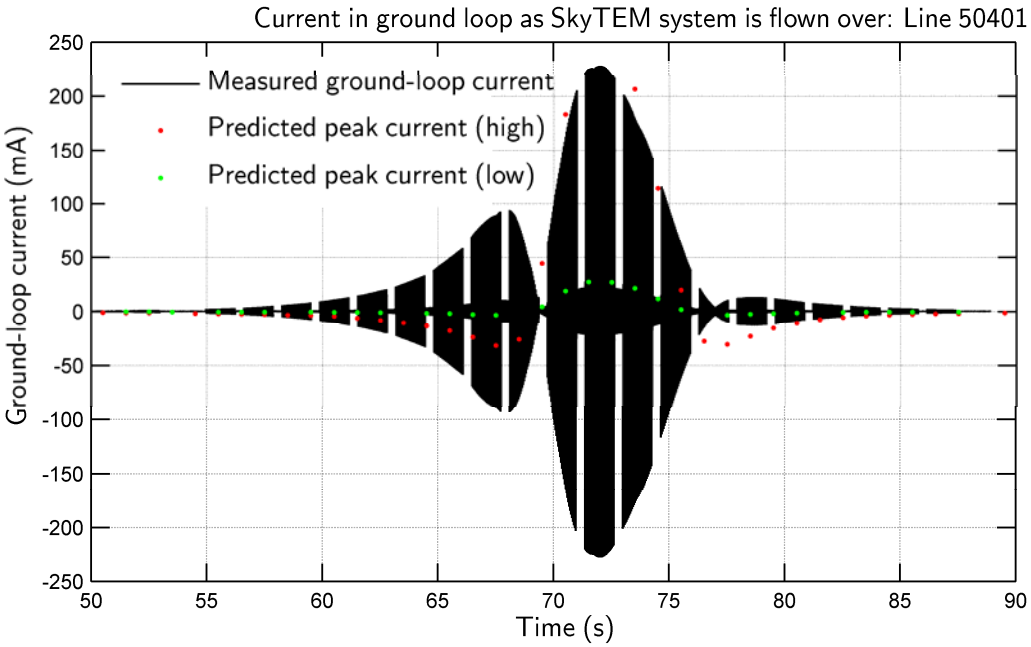

Figure 46: *Induced ground-loop current, line 50401. Red dots are predicted peak current values for high moment current, while green dots show peak currents for low moment. The shoulders do not fit well since topography has not been accounted for.*

We believe points 1) and 4) are the most likely. The ground loops are typically draped over the topography in a roughly rectangular shape. However, their sides are rarely parallel and horizontal. More often, they are laid out on rough ground that has a slight slope that raises one side or one 'shoulder' of the loop above the others. Moreover, the corners of the ground loop are estimated from handheld-GPS position solutions, which have dubious positions particularly with respect to the altitude. In this case, the true altitude of the loop corners was unknown; and the assumption of a flat earth was used in all calculations. Whilst this is a normal approach, it was further complicated by the ground loop being laid out on a ridge that had a sharp side. We believe that the large induced current shoulder in the envelope (prior to 70s) is underestimated based on the system geometry measurements and the effects of topography (Figure 47).

For the low moment case, it appears that the predicted and measured peak current values are more closely matched. This is attributed o the smaller dipole moment of the low-moment transmitter current, i.e. the relative difference is still the same despite the smaller amplitudes.

Unfortunately, the loop corner altitudes were not measured and we can say nothing more concrete about this phase of the error determination process. With GPS altitudes on the loop corners, we could have used the flight survey GPS altitudes for the Tx geometry and then calculated mutual inductance couplings that way.

Measured Responses: High moment

Figure 48 shows the measured and predicted ground-loop responses for the Z-component of the SkyTEM receivers as a result of flying over the ground loop, line 50401. The predicted response (red) is overpowered by the near-surface response of the earth in the early channels. Assuming that the ridge test-site was sited over resistive bedrock, we can predict that the late-time decay channels in the measured response should not be greatly affected by the earth response. With this in mind, a background response was stripped form the measured response over the times from 71s to 77s. Although the early channels in the measured response will not match the loop response, we can expect a reasonable agreement between measured and predicted channels in the late time, with measured responses decaying at the same rate as the predicted responses, regardless of early-time amplitudes.

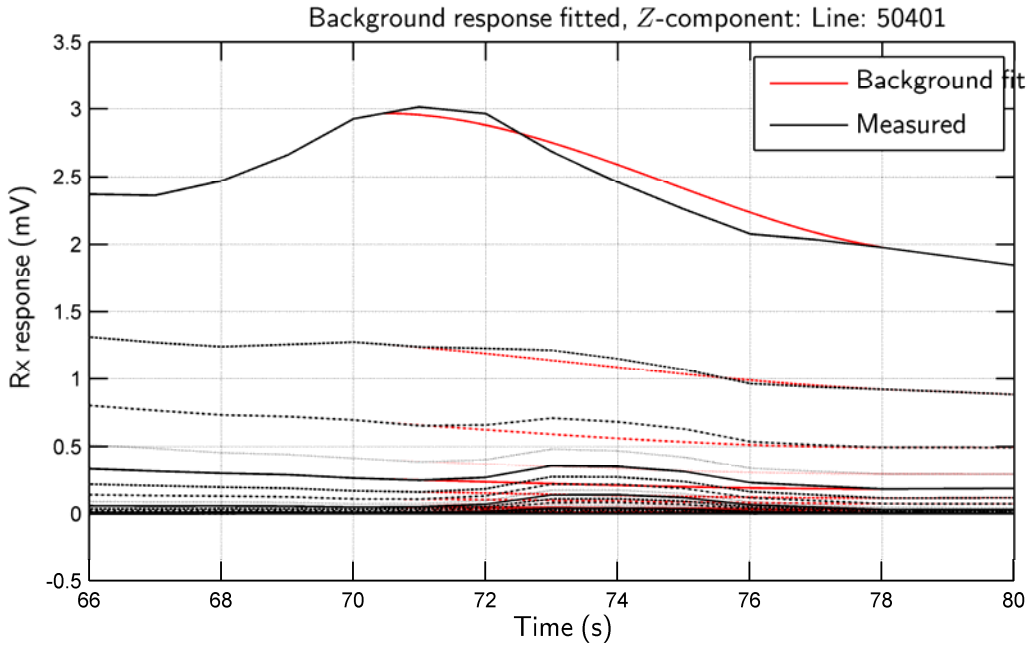

Figure 47: *Cubic interpolations of the background responses (red) shown superimposed on the measured SkyTEM responses (black), line 50401.*

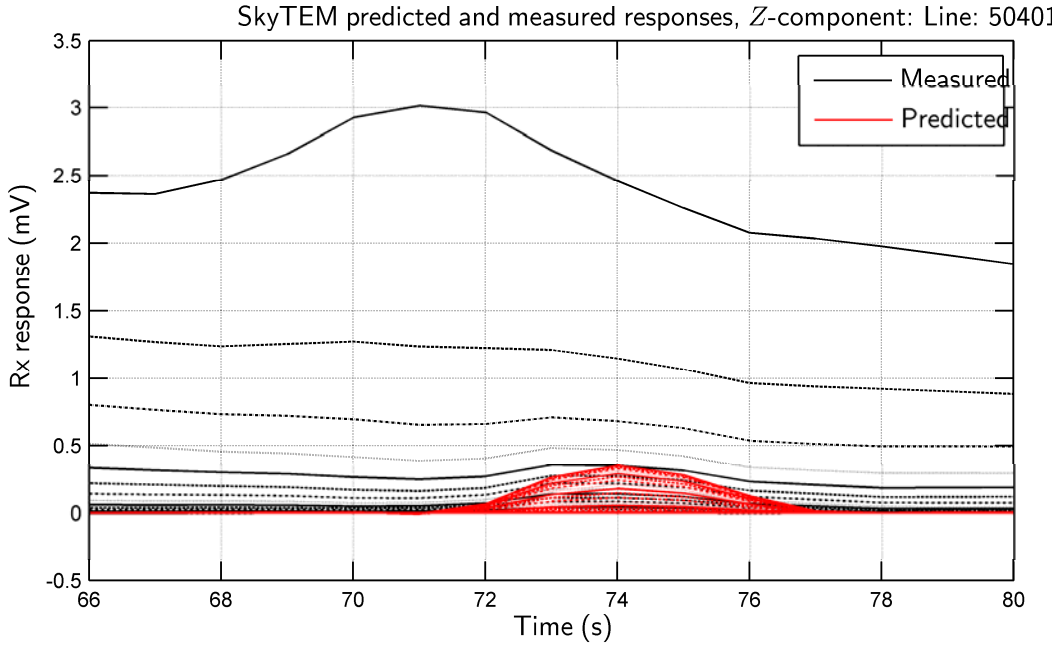

Figure 48: *Measured (black) and predicted (red) SkyTEM responses as a result of ground loop overflight.*

Figure 47 shows the measured responses and the cubic interpolation used to represent the background response of the earth, neglecting the presence of the ground loop. This method of background subtraction is an arbitrary way of removing the near-surface response of the earth, thereby altering the quantitative comparison of measured and predicted responses. For early time, this degrades any possible quantitative comparison, but inspection of Figure 47 shows that the background response stripped from late-time channels is very small. Once we do subtract the background response from the measured signal, the ground loop response measured by the SkyTEM Z-direction receiver is much more apparent, Figure 49. Clearly, the early-time channels do not match the predicted responses, but we would expect good agreement between the measured and predicted late-time channels. The green lines shown in Figure 49 mark the time values used to calculate an average above-loop response. The background-stripped measured and predicted ground-loop responses for the X-direction receiver coil, are shown in Figure 50.

As with Figure 49, Figure 50 shows that the early time measured and predicted responses do not match due to the method used to strip the background response from the measured data. However, the green vertical line in the figure shows the decay response measured at the fiducial at 73s. The results of the averaged response calculated from Figure 49, and the decay response in Figure 50, are shown in Figure 51.

This figure shows the average Z-direction over-loop measured and predicted responses in the top panel and the measured and predicted over-loop response for the X-direction receiver in the bottom panel. Both time and amplitude are on a logarithmic scale, with negative data shown with circles and positive data shown with solid dots. The top panel shows that the average measured over-loop decay follows the predicted decay within an amplitude scale of about 30% for late-time channels, where we would expect the best fit. However, the measured response is consistently lower than the predicted response for even the mid-range to late-time channels until the measured response reaches the noise-level of about 1μV around 2ms after current shut-off. Therefore, we can say that the measured amplitudes are consistently lower then those we might expect for the ground-loop response.

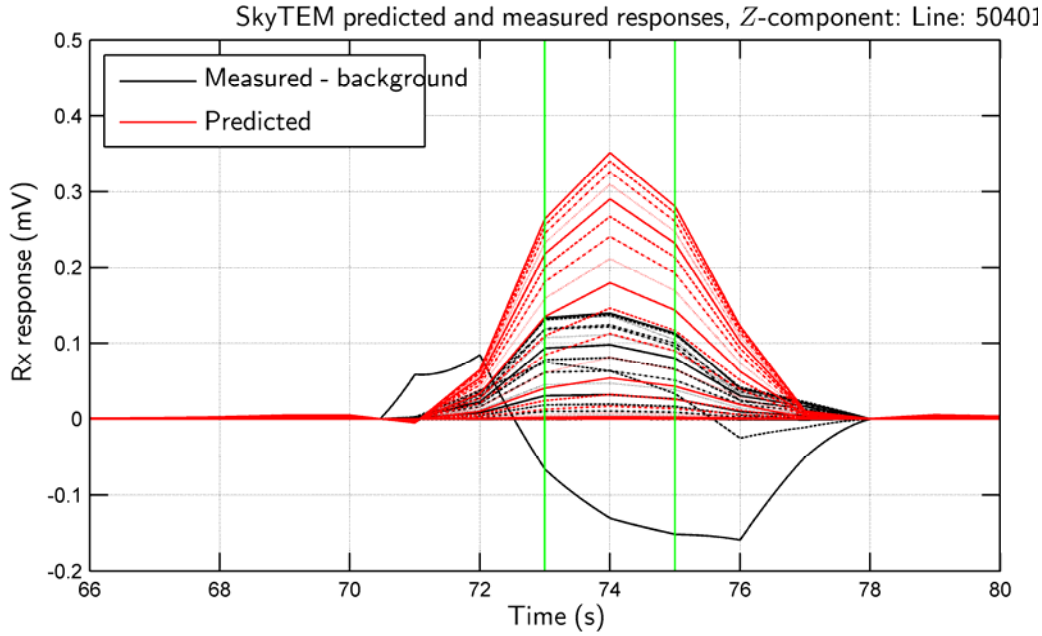

Figure 49: *Stripped measured SkyTEM response (black) and predicted Z-direction responses (red) based on flight geometry. Green lines mark the region used to calculate an average background response.*

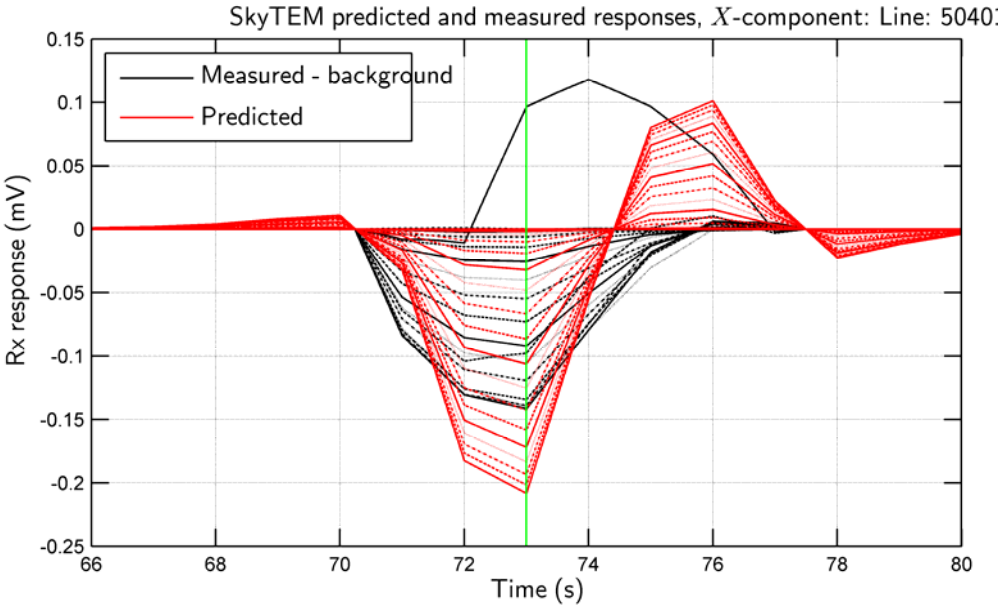

Figure 50: *Stripped measured SkyTEM response (black) and predicted Z-direction responses (red) based on flight geometry. Green line marks the fiducial used to calculate an average background response.*

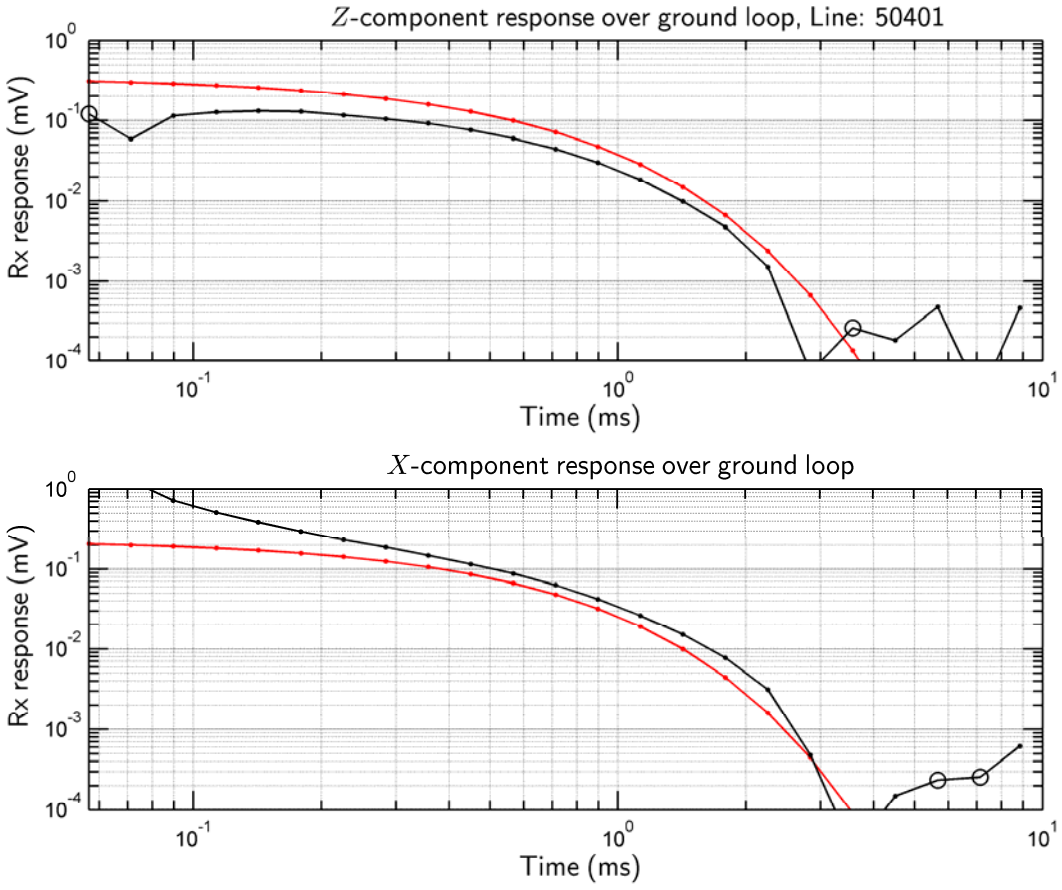

Figure 51: *Top panel: average over-loop response for the Z-direction receiver coil response calculated between the vertical green lines shown in Figure 49 (black) and the predicted over-loop response (red). Bottom panel: fiducial 73 s measured response for the X-direction receiver (black) and the predicted ground-loop decay (red).*

The most likely reason for this discrepancy is related to altitude errors in estimating the geometry of the loop, although we would expect good altimeter readings for when the Tx is directly above the centre of the ground loop. Other possible reasons for the difference is that there could be an error in the timing gates reported in the Ord River Final report, or an error in the linear approximation to the SkyTEM Tx current waveform,

particularly marking the beginning of the current shut-off (the actual shut-off starts earlier or is longer than reported), or it could be a combination of all 3 factors. Early-time response is impossible to fit due to the background stripping method used, but this is a less likely reason for the late-time channels where we would not expect background response.

The bottom panel of Figure 51 shows the measured and expected decay curve for the X-direction receiver response over the loop. In this case, the measured amplitude is consistently higher than the predicted response for the entire decay (until noise takes over the recorded signal). These observed differences may be linked to the reasons given above for the Z-direction response, but they could also be due to pitching and tilting of the Tx during this fiducial. The X-direction field sensors in all airborne systems are typically very sensitive to geometry changes such as pitch and roll.

As a test for line-to-line consistency, the measured and predicted responses for line 50404 were also defined in the same manner as described above for line 50401. After looking at the data and choosing valid regions to strip the background response from the measured data, removing background and averaging the Z-direction data over a suitable range to ensure a strong response from the ground loop, and similarly for the X-direction data, we see that the Z-component data are again consistently lower than expected over the ground loop and the X-direction response is consistently larger. This is shown in Figure 52.

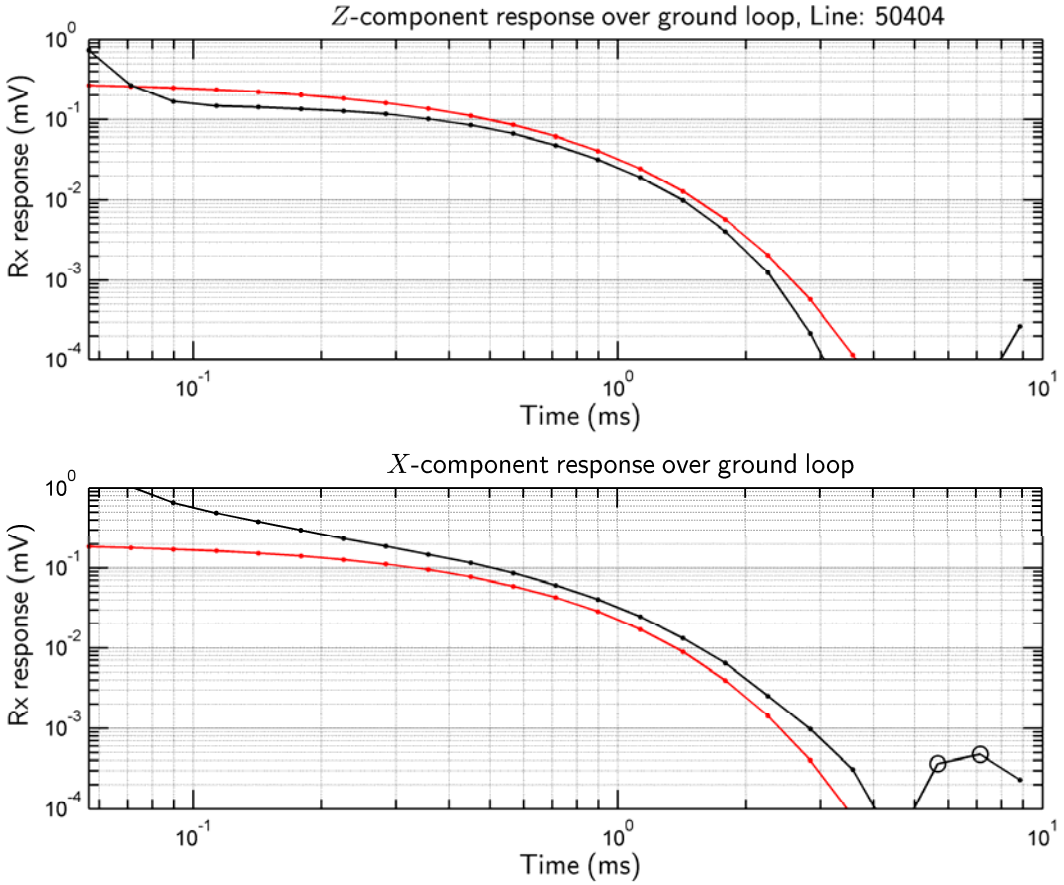

Figure 52: *Top panel: average over-loop response for the Z-direction receiver (black) compared to the expected over-loop response (red) for line 50404. Bottom panel: measured (black) and predicted (red) response for the X-direction receiver over the ground loop.*

In the top panel of Figure 52, the measured response is again larger than the expected response, although by a smaller factor. This provides further evidence to support the notion that altimetry is a large factor in determining the amplitude differences. One of the assumptions made here is that the altitude measured by the twin laser altimeters has been corrected for slant range errors and also corrected for the centre of the Tx loop, thereby representing an average Tx altitude. As before, the X-direction SkyTEM response is generally larger than the expected response.

Measured Responses: Low Moment

As similar approach to that described above was taken to the low moment data, and results are presented for the over-loop responses for lines 50401 and 50404. Figure 53 shows the measured and predicted over-loop responses for the low-moment Tx signal recorded for line 50401, while Figure 54 shows the responses for line 50404. In these cases, the mismatch between measured and expected responses is attributed to the background subtraction method used. Given that the Tx magnetic moment is much lower and the repetition rate of the Tx waveform is significantly faster than for the high-moment case, the observed ground response is much more apparent in the measured signal. That said however, it is apparent that in every case, the data recorded by the SkyTEM receivers matches, in rate of decay, the decay rate of the ground loop.

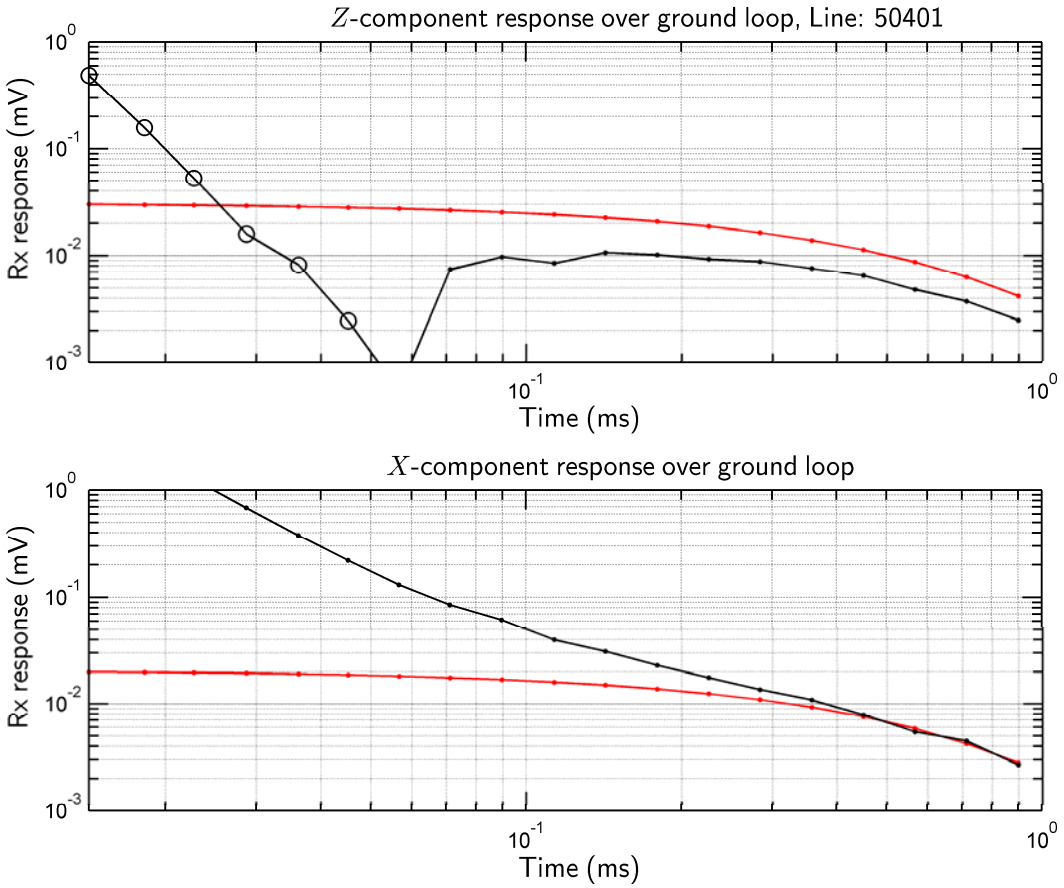

Figure 53: *Top panel: average over-loop response for the Z-direction receiver coil response (black) and the predicted over-loop response (red), line 50401, low Tx moment. Bottom panel: measured response for the X-direction receiver (black) and the predicted ground-loop decay (red).*

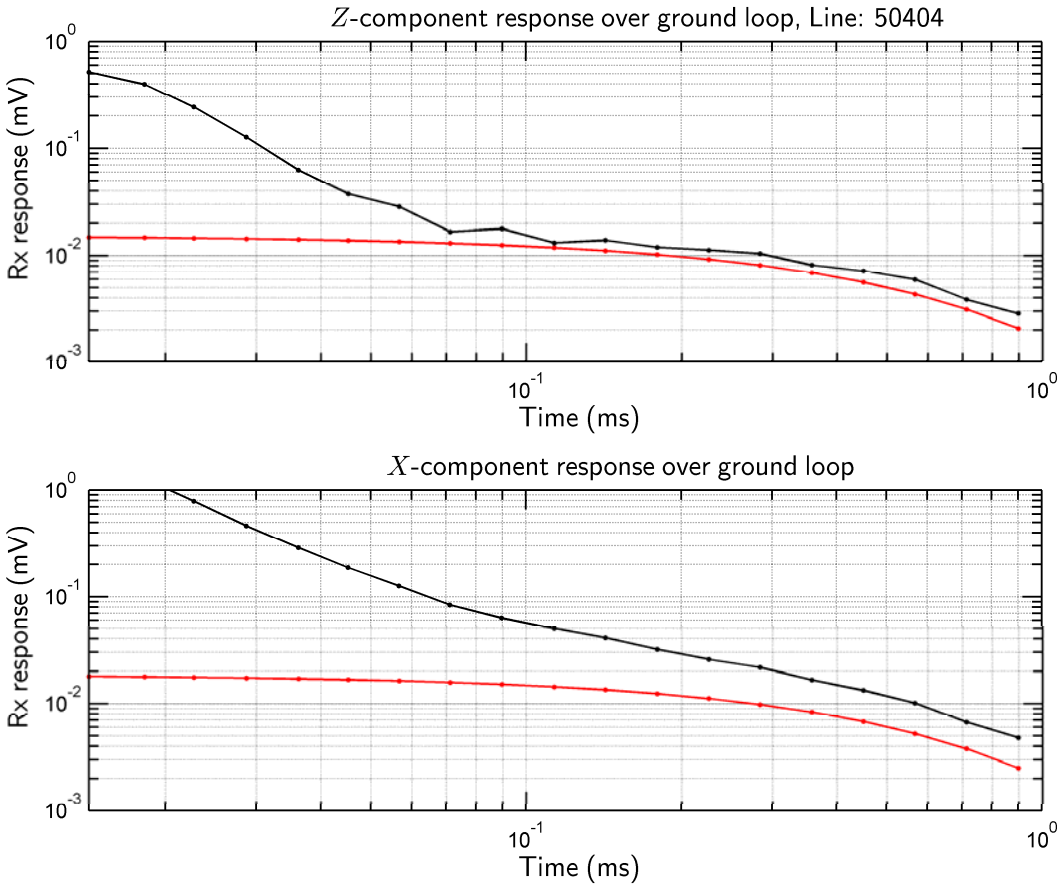

Figure 54: *Top panel: average over-loop response for the Z-direction receiver coil response (black) and the predicted over-loop response (red), line 50404, low Tx moment. Bottom panel: measured response for the X-direction receiver (black) and the predicted ground-loop decay (red).*

Conclusions

Ground-loop recorded data have been processed to provide a robustly stacked ground-loop induced current response for the 1Ω and 1000Ω bridging resistor cases. Applying established methods, the SkyTEM transmitter waveform has been deconvolved from the ground-loop response using the measured resistance of the loop and the loop's intrinsic decay constant measured from the ground loop currents induced well after the SkyTEM Tx current shut-off. The deconvolved waveforms for the SkyTEM transmitter current operating at high-moment matched the streamed-data Tx current waveforms as measured independently by Geoforce during their field operations. The differences between the two are attributed to the finite sampling time used by the different approaches and more particularly systems. In both cases, the Tx current shut-off were closely matched to each other. Both methods gave a longer Tx current shut-off than the linear approximations obtained using inversion.

For the low-moment case, the sampling period of the ground-loop deconvolution method is too long to achieve an accurate sampling of the Tx current waveform, particularly during its shut-off or off-ramp. Overall, the ground-loop Tx current waveform deconvolution method faithfully reproduced both the streamed and linearly approximated waveforms provided by Geoforce. One item to consider, however, is that the streamed waveforms were recorded with the SkyTEM system on the ground. The proximity of the system to the ground creates a capacitive and inductive coupling between the Tx loop and the ground which may influence the recorded signal.

For the ground loop testing of the SkyTEM system, the near-surface earth-response dominated the ground-loop signal at early times. Removing a background response from the measured data permitted the ground-loop response to be observed in both the Z- and X-direction receivers at both high- and low-moment. Overall, for the high-moment operation, the decay curves of both receivers closely matched the predicted curves. However, the Z-direction amplitudes are consistently lower than the predicted curves. This may be in part due to the background subtraction, although for the late time channels, this is less likely. It is more

probable that the differences are due to altitude; particularly an altitude ambiguity in the ground loop coordinates. By comparison, the X-direction responses are consistently higher than the predicted responses. For the high moment data, this is a consistent observation for two of the calibration lines. For the low-moment operation, it is more difficult to arrive at a quantitative assessment of the SkyTEM receivers, principally due to the large response from the overburden dominating the signal during flyover. However, as both sensors follow the predicted decay curve over the loop, it suggests that the timing of the receiver windows is correct.

It is clear that the amplitudes of the high-moment receivers follow the ground-loop responses predicted by existing theory. That said we have some limited concerns about the waveforms used for the predictive model. The low amplitudes of the Z-receivers indicate that the nominal linear approximation waveform used, begins its shut-off earlier than is reported, or that the shut-off is longer than reported. There may be, however, an issue with the amplifier gains used in the receivers. SkyTEM is typically calibrated over a layered earth at the test-site in Denmark. The gains of the receivers are adjusted so that an inversion of the data calculates resistances consistent with the test-site which itself is calibrated using a commercially available ground-based TEM system. For the purposes of this study, it has been assumed these are correctly calibrated devices.

Given the various assumptions, it is reasonable to assume that the waveforms agree within the sampling frequency used for the experiment (20μs) and the amplitudes agree with the predicted amplitudes to within 30%. Without accurately measuring the altitude profile of the ground loop and processing with the GPS recordings taken on the loop, it is not possible to say more. Overall, it is reasonable to assume that the SkyTEM system was operating within specifications during the Ord survey and that the measured ground response provides the basis for calculating a mean ground conductivity as it varies with depth.

3.6.10 AEM Data Processing and Interpretation

Given that one of the primary objectives of the Ord AEM survey was to map ground conductivity it was necessary to convert measurements of the ground electromagnetic response, through a process of inversion, into an estimate of this parameter. Through the application of approximate transforms or layered inversions, conductivity-depth values can be calculated for each observation or sounding made by the AEM system, and then stitched together into sections to provide a representation of the 2D variation of conductivity. This is sometimes referred to as a ‘parasection’. Further, the conductivity depth profiles can be combined into a 3D gridded volume from which arbitrary sections, horizontal depth slices (or interval conductivity images) and isosurfaces can be derived. The schematic in Figure 55 summarises the process of acquiring AEM data, inverting the resulting data, and presenting the results as conductivity images.

The representation of essentially continuous and gradational conductivity distributions as discrete conductive ‘units’ or bounding layers is an effective way summarising information from large AEM surveys. This is particularly so when the application calls for mapping the conductivity, depth to top and or the thickness of a semi-continuous layer of sediments or in situ regolith. The processing and presentation of AEM data as maps or sections is now recognised as an effective way of displaying conductivity data.

AEM data acquired for exploration or environmental applications are commonly modelled using algorithms such as conductivity depth transforms (CDT’s) or Layered Earth Inversions (LEI’s) that assume a 1D earth (Sattel, 2005). To date, full 2.5 or 3D inversion of AEM data remains limited , and in many respects unrealistic and unnecessary particularly for hydrogeological investigations in many Australian basins where the assumption that the sub-surface can be represented as a series of horizontal layers holds reasonably well, particularly at the scale of the footprint of most AEM systems (Lane, 2000; Sattel, 1998). The 1D model assumption is also legitimate in sub-horizontal, layered sedimentary areas where it produces results that are only slightly distorted by 2D or 3D effects such as might be induced by faults, fractures, or other geological phenomena (Auken *et al*., 2005; Newman *et al.,* 1987; Sengpiel & Siemon, 2000).

3.6.11 AEM Inversion Procedures

Data processing procedures applied to the SkyTEM data collected over the Ord Survey area are summarised elsewhere (e.g. Reid *et al*., 2008), and follow those described by Auken *et al*., (2007). SkyTEM data are intended to be comparable to that measured with similar ground-based TEM system (e.g., a Geonics PROTEM), with the data not significantly distorted by drift or bias and ready to be inverted and interpreted without further data processing, such as levelling.

Fast Approximate Inversion
Initial field/lab processing of the SkyTEM data involved the use of a fast approximate inversion procedure (iTEM) developed by Christensen (2008).

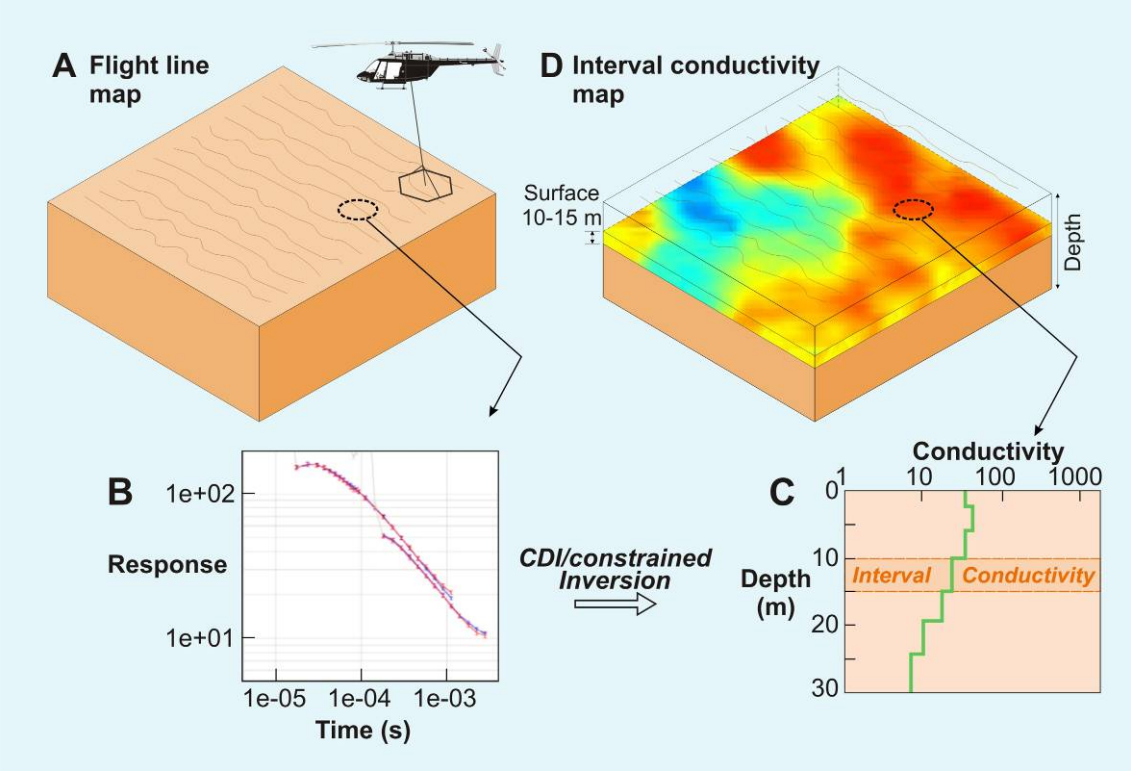

Figure 55: *Schematic representation of helicopter time domain EM data acquisition and interpretation. A) Data are acquired along parallel flight lines, with high and low moment data recorded at varying intervals along each flight line; B) The EM receiver located behind and offset from the transmitter towed beneath the helicopter measures the secondary high and low moment responses; C) The measured response is used to determine the conductivity-depth function by transformation or inversion. D) Conductivity-depth values can be calculated for each observation and then stitched together into sections to provide a representation of the 2D variation of conductivity, sometimes referred to as a "parasection". Conductivity depth profiles can be combined into a 3D gridded volume from which arbitrary sections, horizontal depth slices (or interval conductivity images) and isosurfaces can be derived showing the spatial distribution of conductivity as it varies with depth.*

The method is based on fast approximate forward computation of transient electromagnetic step responses and their derivatives with respect to the model parameters of a 1D model. The inversion is carried out with multi-layer models in a state-of-the-art formulation of a least-squares iterative inversion scheme including explicit formulation of the model regularization through a model covariance matrix. The method is 50 times faster than conventional inversion for a layered earth model and produces model sections of concatenated 1D models and contoured maps of mean conductivity in elevation intervals. To ensure lateral smoothness of the model sections and to avoid spurious artefacts in the mean conductivity maps, the Lateral Parameter Correlation method is applied to the results of the individual inversion models (Christensen *et al*., 2009). In this way, well-determined parameters are allowed to influence the more poorly determined parameters in the survey area.

Applied to the Ord SkyTEM dataset, this approximate inversion procedure allowed the production of produces model sections and conductivity maps that revealed the distribution of conductivity in the area on the same day as data acquisition. The procedure was employed to determine whether it was worthwhile extending survey coverage over the Cockatoo Sands area, immediately after the data had been acquired by Geoforce.

Full Non-Linear Inversion

The high and low moment SkyTEM data for the Ord survey were fully inverted using a non-linear smooth model 1-D Laterally Constrained Inversion (LCI) developed for inversion of CVES and PACES ground data (Auken *et al*., 2005). The inversion was undertaken using the Aarhus Geophysics Workbench software package (Auken *et al*., 2009). In this inversion scheme the model parameters are tied together laterally with a spatially dependent covariance, as represented schematically in Figure 56.

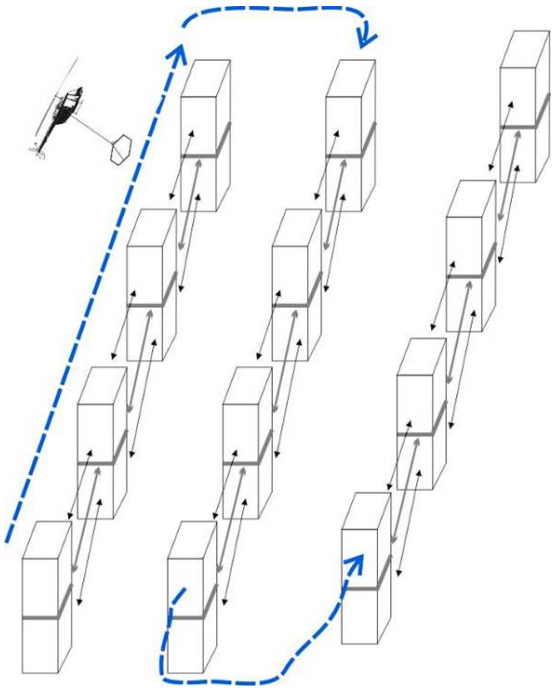

Figure 56: *Schematic representation of how model parameters from individual soundings along flight lines in a survey are linked together laterally in the LCI procedure.*

Constraining the model parameters tends to enhance the resolution of layer conductivities and layer boundaries which may not be so well resolved in an independent inversion of each sounding. The LCI inversion scheme was originally developed for parameterized inversion with normally 4 or 5 layers. More recently, the algorithm has been further developed to include smooth inversion with e.g. 15 or more layers each having a fixed thickness but a free resistivity. Both schemes have advantages. Layer interfaces and conductivities are best determined from the parameterized blocky inversion. Also, the depth of penetration is better estimated. On the other hand the smooth inversion is more independent of the starting model and gradual transitions in ground conductivities, that might be present in a complex alluvial aquifer such as that present in the Ord valley, are more easily recognizable. Both inversion types were calculated but the bulk of the data interpretation for this study was undertaken with an 18 layer smooth model down to a depth of 100m below ground surface.

Figure 57 shows examples of the blocky and smooth model results for a particular interval conductivity. It also shows these results against a comparable interval conductivity determined by the fast approximate inversion discussed in the previous section. It is interesting to note that the apparent success of the approximate method in defining the conductivity structure of the alluvium can, in part, be attributed to the sediments behaving essentially as a 1D body to an AEM system, and that errors arising from that assumption coupled with calibration and altitude/geometrical uncertainties, are larger than the approximations made to speed up the conversion of data to conductivity-depth (Macnae, 2007). Results from the inversion are presented in the accompanying GIS (Apps *et al.,* 2009e) and atlas products (Apps *et al.*, 2009a-d).

A comparison of the SkyTEM data set with the previously acquired QUESTEM data provides some indication of the relative merits that have accompanied the more recent advances in hardware and software (See Figure 58, Figure 59 and Figure 60). Although not directly comparable, as two different approximate inversion algorithms were used (EMFlow for QUESTEM and iTEM for SkyTEM), the results indicate that more subtle conductivity variations are apparent in the SkyTEM data compared with the QUESTEM data, both laterally and vertically.

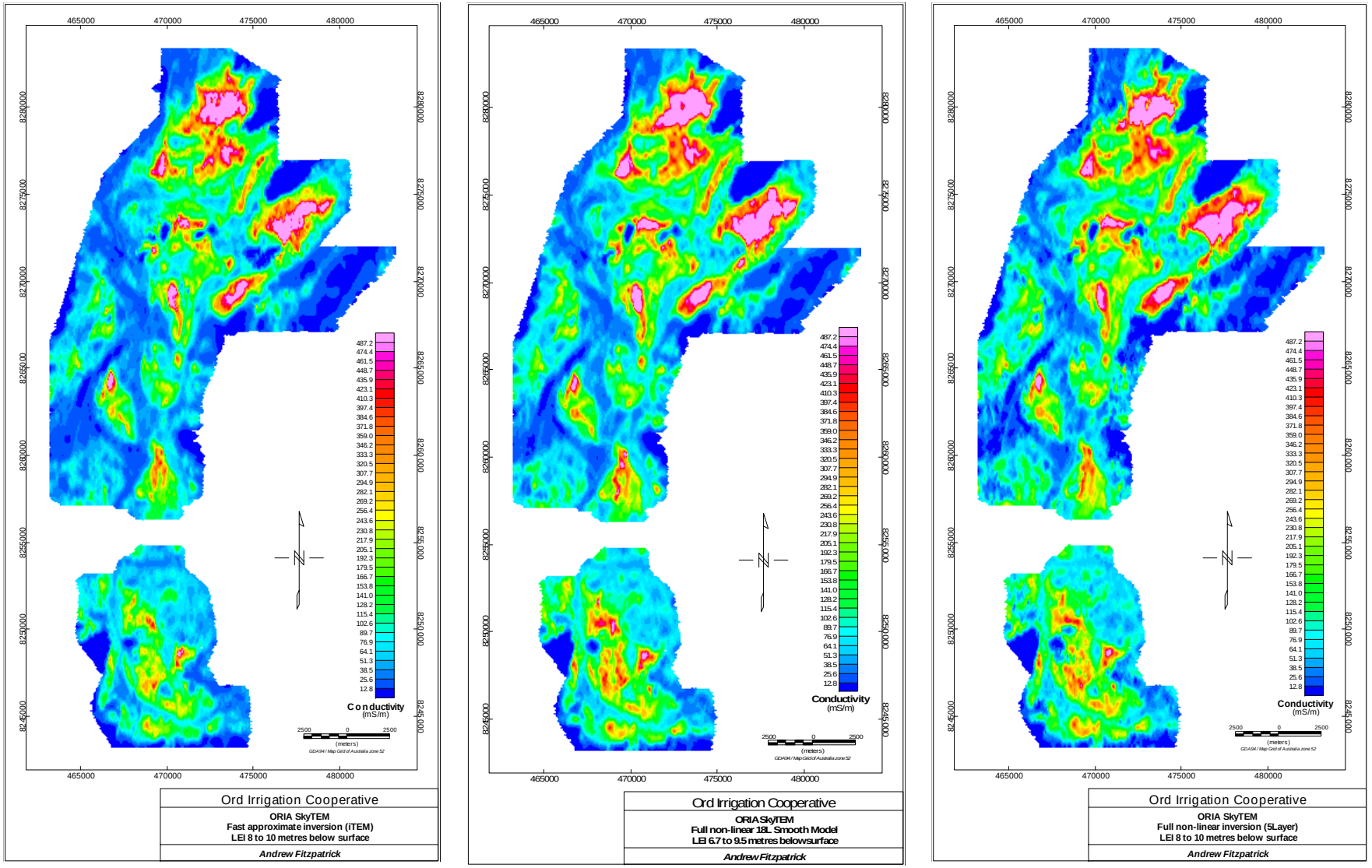

Figure 57: *Comparable interval conductivity images derived form a fast approximate inversion and full non-linear inversions (smooth and blocky models) of SkyTEM data for the ORIA 1 area.*

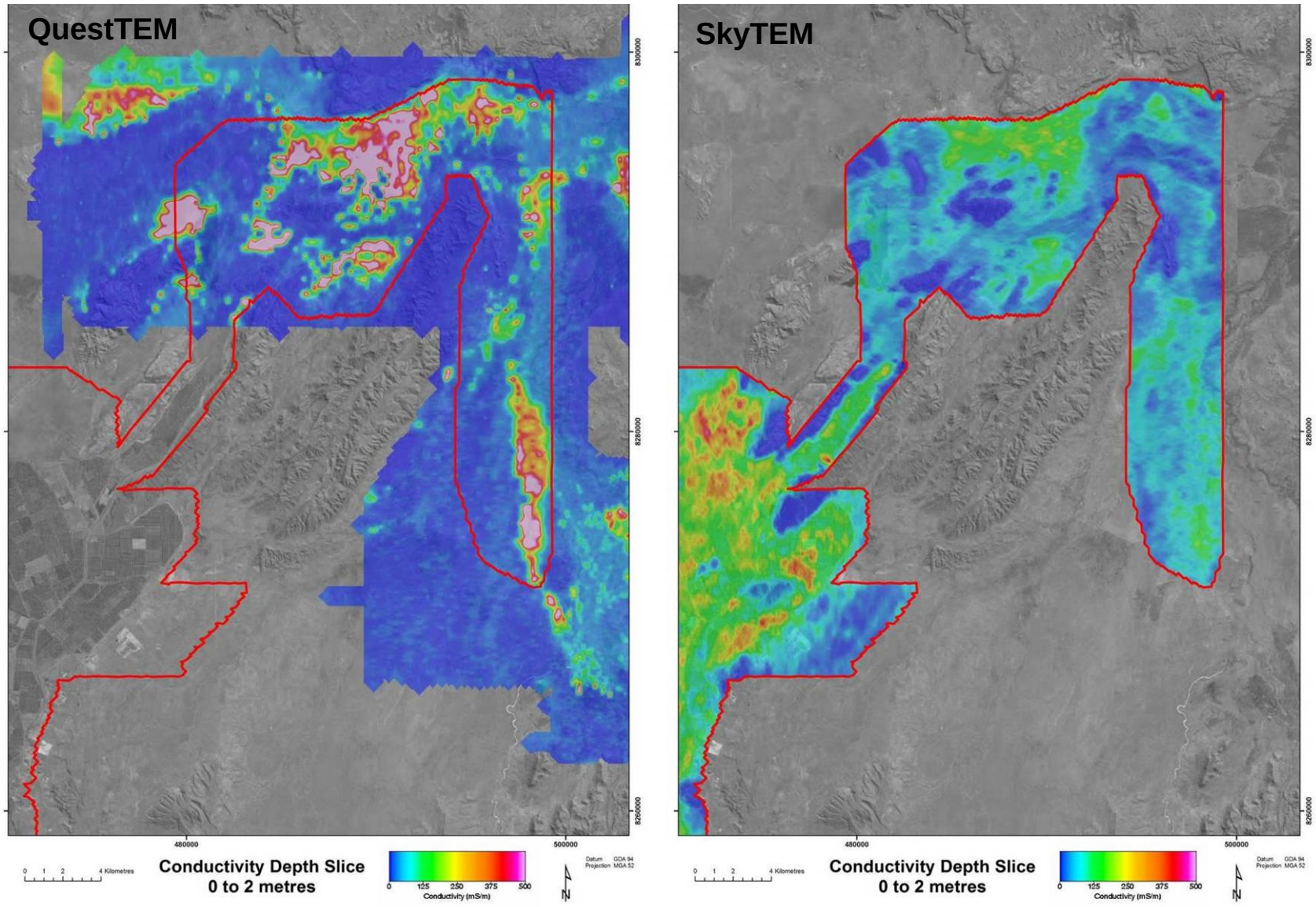

Figure 58: *Comparison between a 0-2m interval conductivity defined for QUESTEM and SkyTEM.*

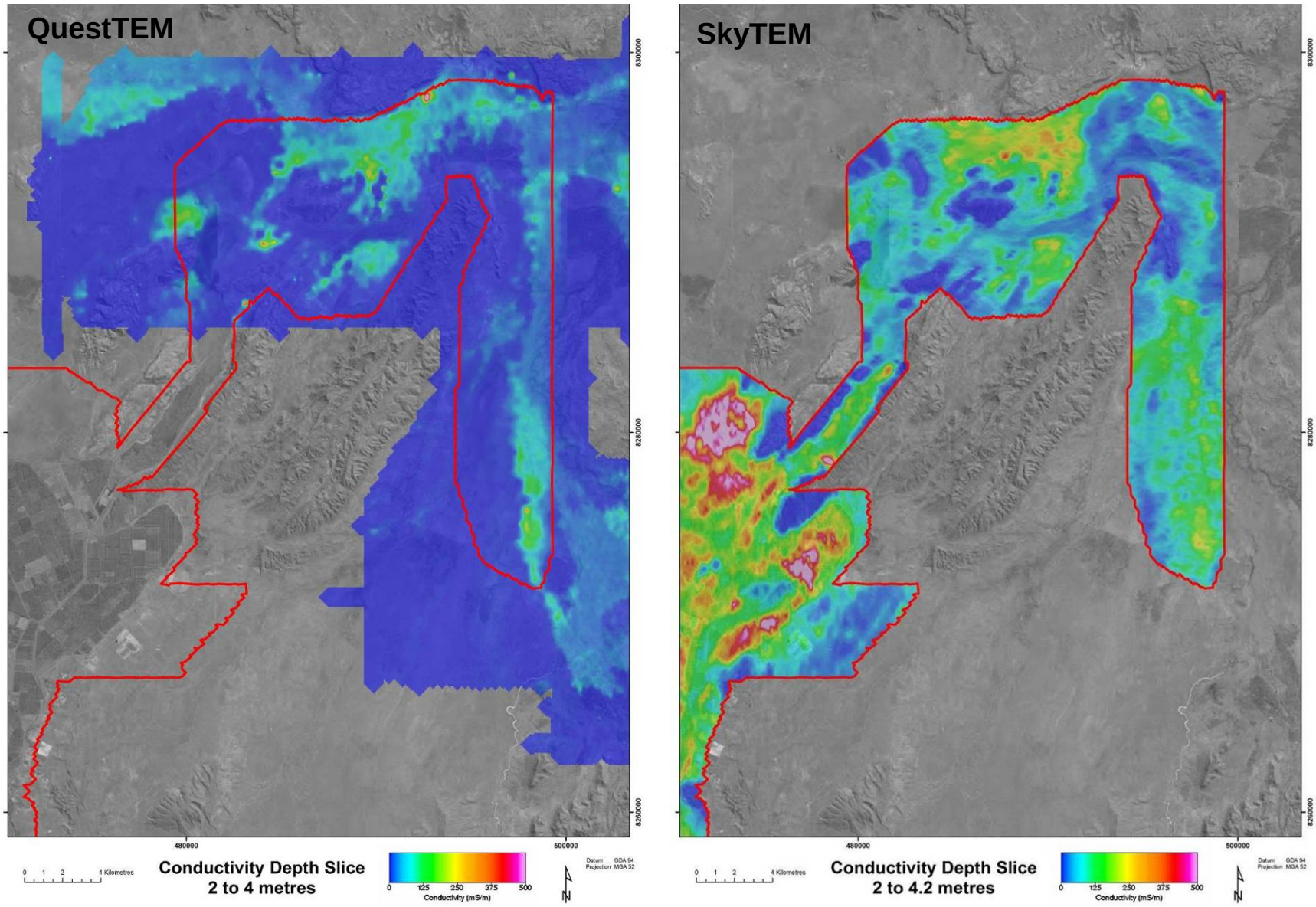

Figure 59: *Comparison between a 2-4m interval conductivity defined for QUESTEM and SkyTEM.*

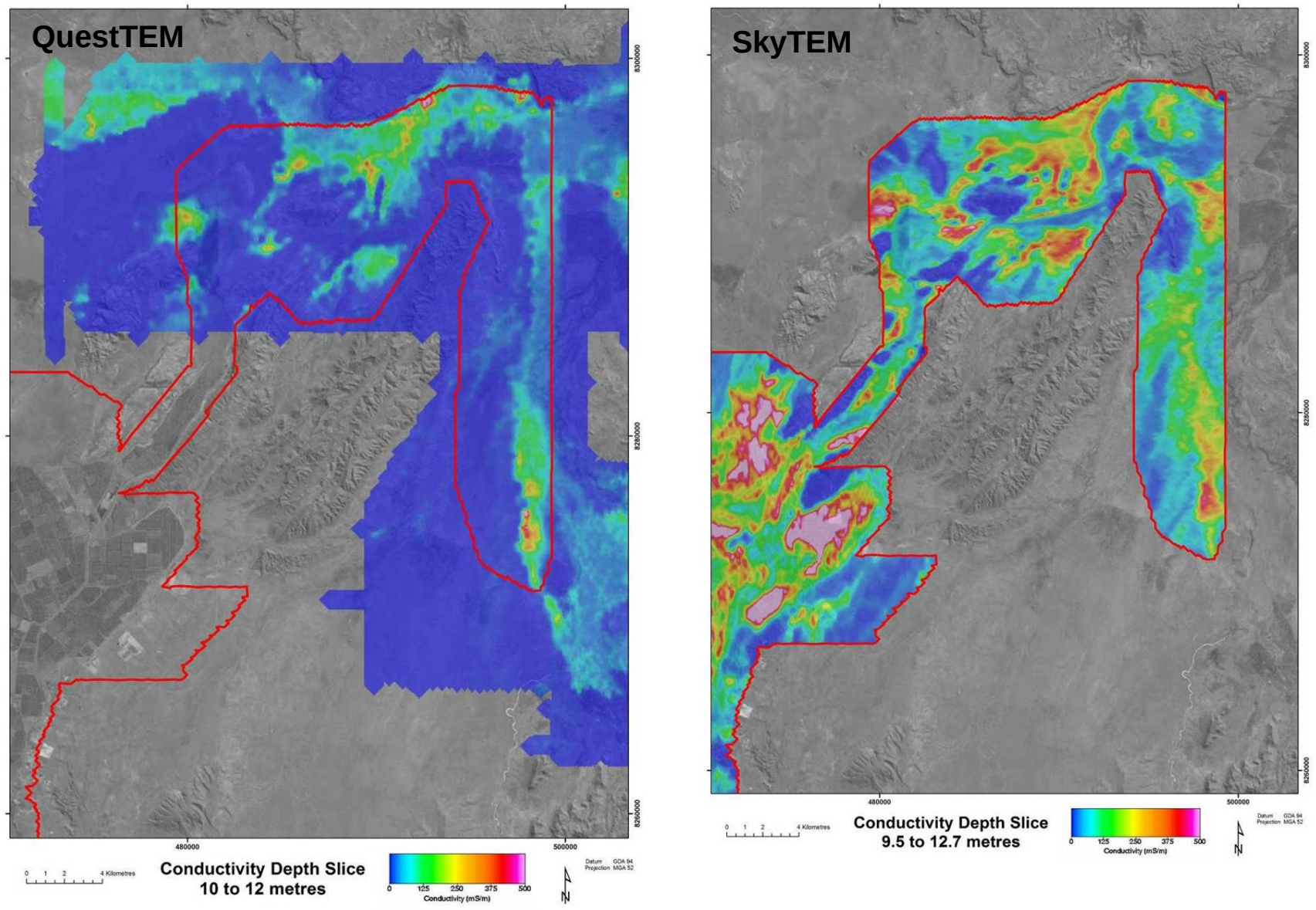

Figure 60: *Comparison between a 10-12m interval conductivity defined for QUESTEM and SkyTEM.*

Given the system characteristics of the QUESTEM (Humphreys *et al*., 1995, 2002), little confidence can be given to the modelled conductivities in the near surface (top 20+ metres), with the patterns reflecting artefacts from the approximate inversion procedure. Further evidence for problems associated with mapping detailed variations in ground conductivity with the QUESTEM data is provided in Figure 61 which shows a conductivity depth image (CDI) for a near coincident flight line for both the QUESTEM and SkyTEM datasets for the Keep River area. The detailed vertical conductivity structure defined in the SkyTEM data is not apparent in the QUESTEM data.

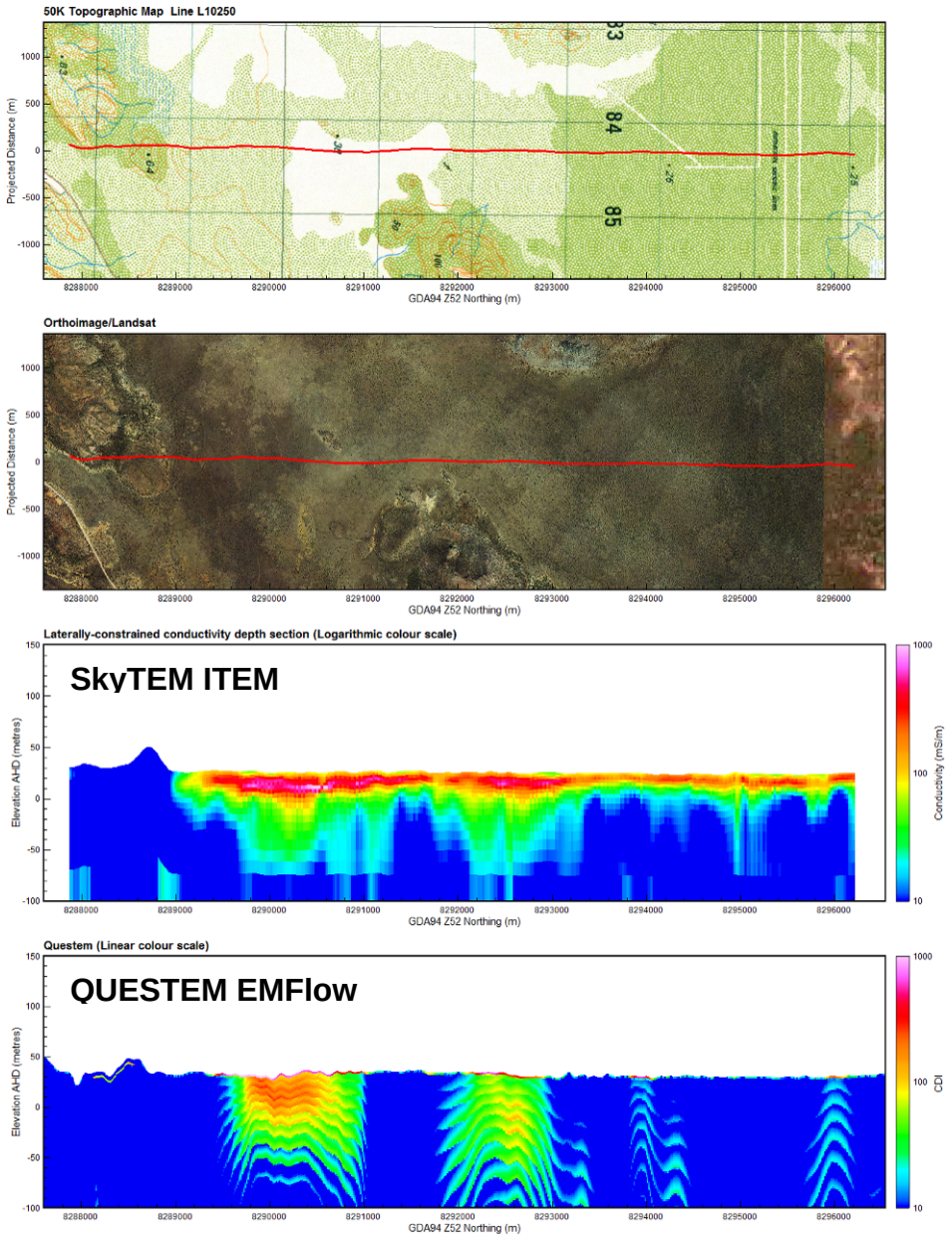

Figure 61: *Vertical conductivity depth sections for a near coincident QUESTEM and SkyTEM flight line over the Keep River area.*

3.6.12 Comparison Borehole and SkyTEM Conductivity Data

Whilst borehole data are often cited as 'truth' when it comes to validating the response of an airborne EM system, considerable caution should be exercised when interpreting a comparison of conductivity measurements made with a borehole inductive conductivity tool, against those derived from an AEM system (see Lane *et al*., 2001). Whilst both systems measure an inductive response from the ground, the system and data characteristics and sampling volumes are markedly different.

The vertical resolution does not vary with depth when making borehole conductivity measurements, as both the transmitter loop and receiver coil are present in the tool. The borehole conductivity tool samples a cylinder with extent parallel to the hole of less than a metre, and radius less than ~0.5m. Given the small sampling volume, measurements can be subject to the effects of sediment formation changes that arise during and subsequent to drilling. The consequences of groundwater of varying quality entering the hole from different levels in the hole are unknown (Lane *et al*., 2001). Added to these issues, is the matter relating to the calibration accuracy of the logging tool which is also generally unknown, contrary to a commonly held understanding.

SkyTEM measurements are made with a transmitter loop and receiver coils positioned about 30m above the ground. As a consequence, the vertical resolution of conductivity diminishes with depth. Ground response is measured as a function of delay time with the sampling volume increasing in lateral and vertical extent with increasing delay time (Lane *et al*., 2001). If we take a simplification of the near-surface footprint (indicative of the resolution of an AEM system), a definition provided by Liu & Becker (1990), the footprint of the SkyTEM system could be estimated as a multiple of the "scale" of the system, where scale is the function of the transmitter loop ground clearance (~30m). The multiple would be between 1 and 4 depending on the receiver coil component and the amount of the ground response that originates from within the footprint. For SkyTEM this would be between ~30m and 120m.

In an ideal situation ground conductivity from a series of closely spaced bores sampling the entire footprint of the SkyTEM system would be combined, prior to a comparison with the modelled conductivity from the airborne dataset. This would ensure that local variations in conductivity defined in the borehole logs could be incorporated into a weighted or average ground response, thereby forming a more valid basis for comparison with the airborne data. Realistically these data are rarely available, and therefore a comparison between the two is, at best, indicative rather than definitive.

An added issue to consider is that the inversion procedure used to derive a model of ground conductivity from the SkyTEM dataset assumes that the conductivity is horizontally layered within the ground, and that the conductivity value defined for each discrete depth layer accounts for the average ground conductivity defined for that depth interval. With SkyTEM, the along line sampling intervals differ for the high and low moments respectively, and although the sampling interval along flight lines is relatively close (<20m), this adds an additional limit to the spatial resolution of the system.

To provide some indication as to whether the modelled conductivity from the SkyTEM data was similar to that measured in the boreholes, average conductivities for the FID's (fiducials, or soundings) closest to the logged bores were extracted and plotted against the average bore conductivity. The results are shown in Figure 62. An adjusted $r^2 = 0.843$ was determined suggesting that SkyTEM ground conductivity model provided a reasonable estimate of average ground conductivities as defined at scales measured by the borehole geophysical tool. The result suggests that for the most part, ground conductivity varies slowly in the spatial sense and that the ground is acting like a horizontally layered earth. However, the scatter can be attributed to sampling issues mentioned previously.

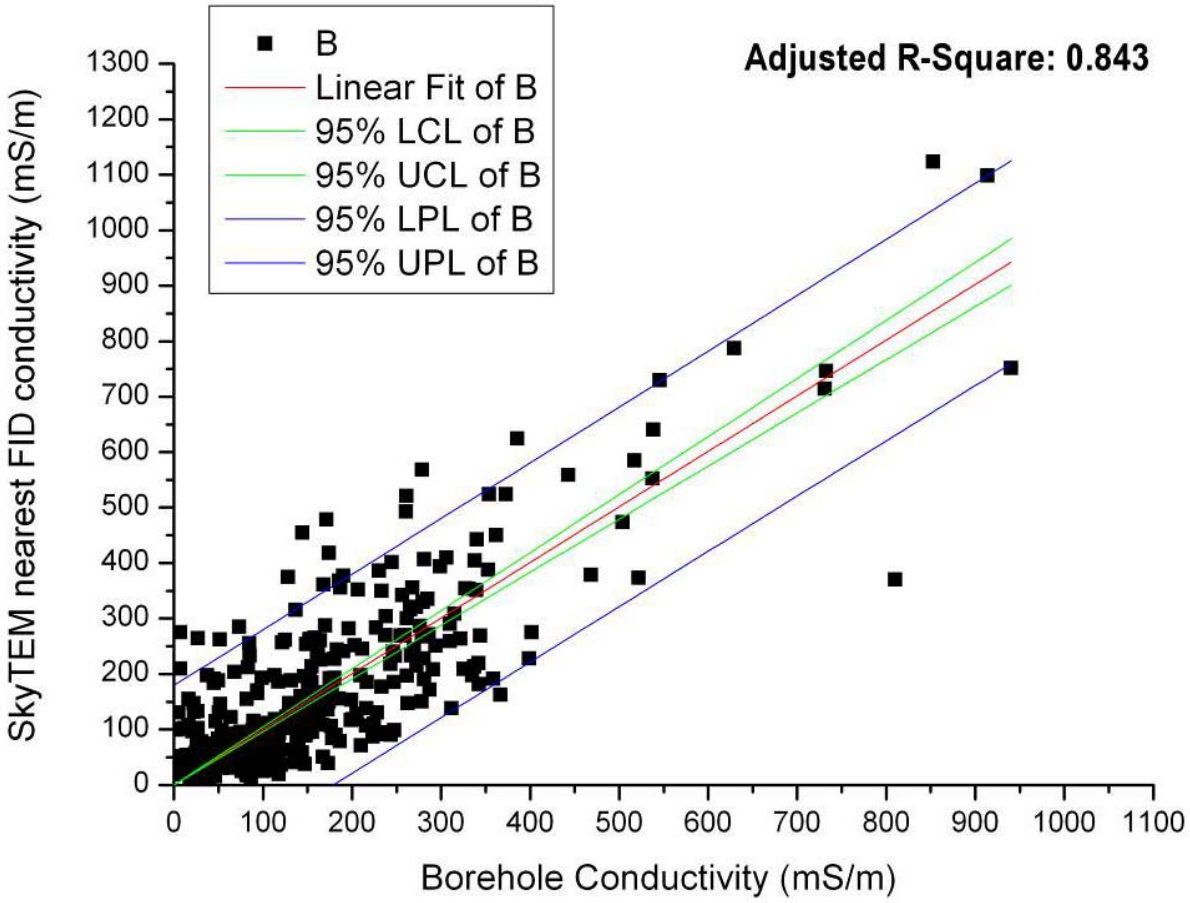

Figure 62: *Plot of average borehole conductivities against average ground conductivity defined from the nearest SkyTEM fiducial (or sounding). (UCL= upper confidence limit; LCL= lower confidence limit, LPL = lower prediction limit, UPL = upper prediction limit).*

A comparison of individual logs against data from the smooth model LCI for the closest SkyTEM fiducials is presented in Figure 63 to Figure 69, and in Appendix 8 (Cullen *et al*., 2010). In general terms, the modelled conductivity structure defined from the SkyTEM smooth model LCI matches that defined from the bore data, except in the detail. It is therefore reasonable to assume that the modelled ground response from the inverted SkyTEM data provides a reasonable approximation of to "true" ground conductivity, if we accept the latter as being defined by the borehole conductivity tool.

Predicting the ground response as would be observed from the SkyTEM system using the bore data should consider the possibility of local heterogeneity in ground conductivity. Simply using the relationship shown in Figure 62, suggests that for a given bore conductivity response, it is possible to predict a range of likely AEM responses (+/- 150mS/m). Therefore, we caution against the simple application of this relationship, without consideration of local conditions and subsurface variability in soil/geology.

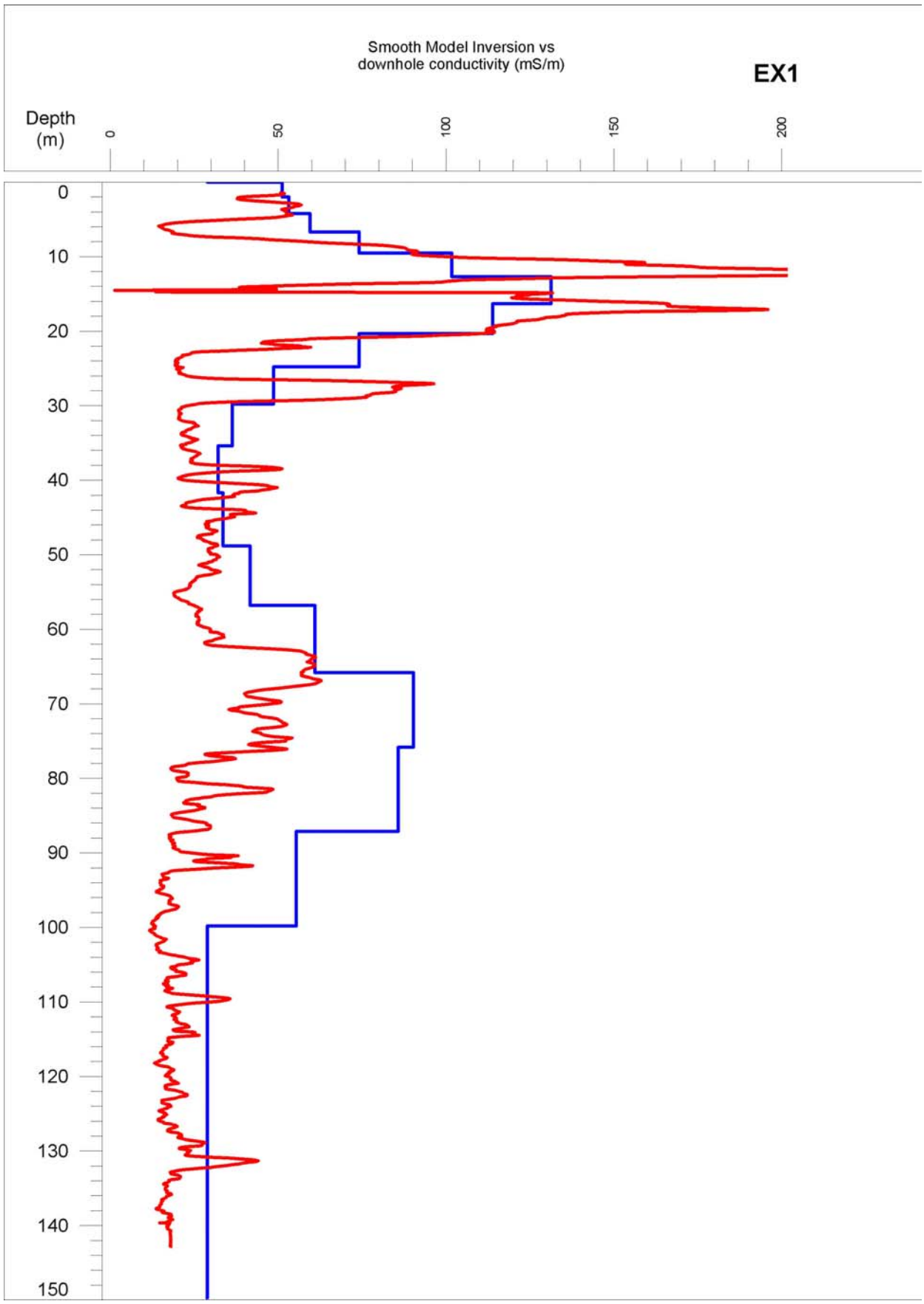

Figure 63: *FID point comparison of borehole conductivity data against SkyTEM smooth model LEI for bore EX1. The AEM response from the FID point nearest the EX1 borehole is in blue, while the induction log response is in red.*

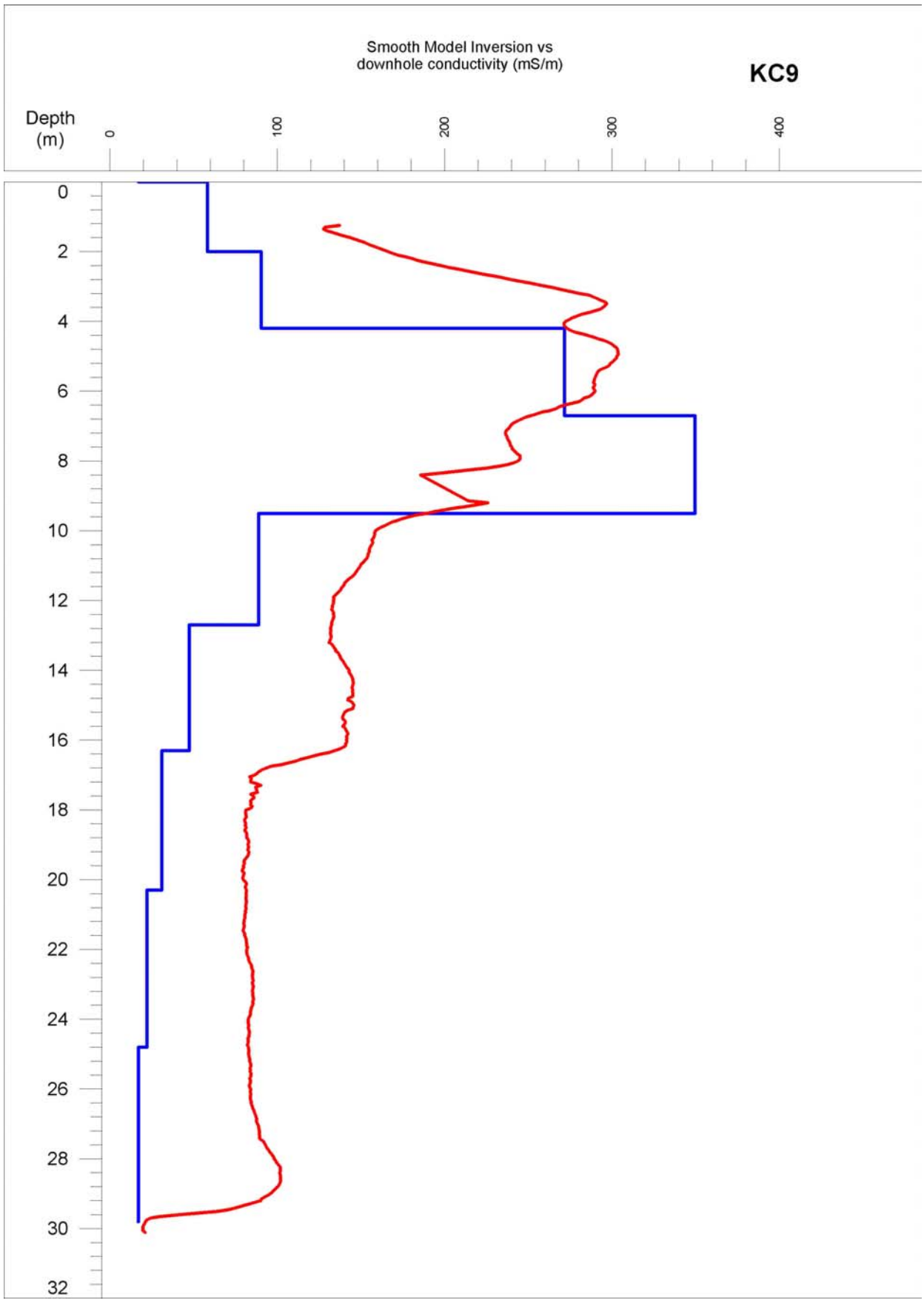

Figure 64: *FID point comparison of borehole conductivity data against SkyTEM smooth model LEI for bore KC9. The AEM response from the FID point nearest the KC9 borehole is in blue, while the induction log response is in red.*

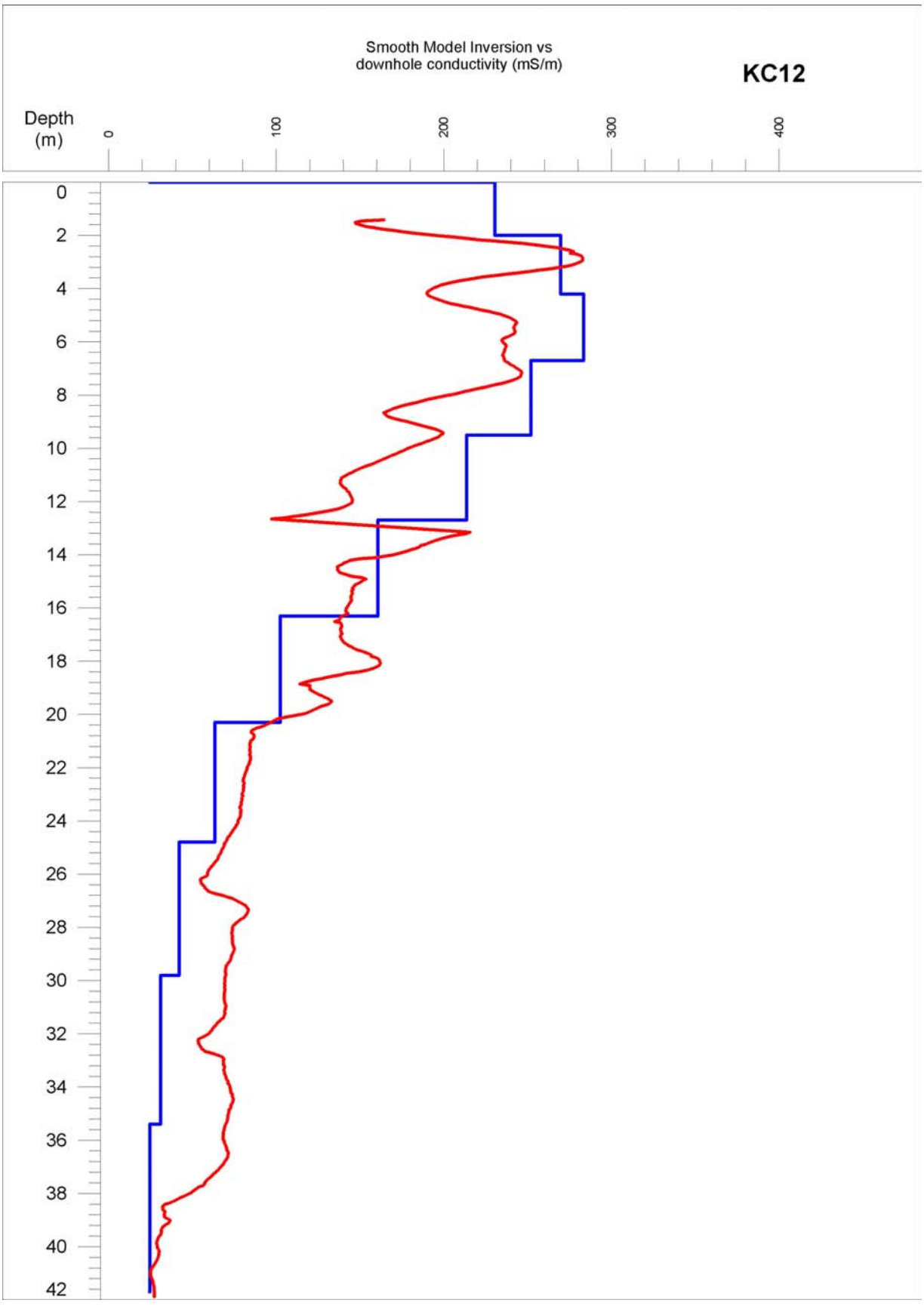

Figure 65: *FID point comparison of borehole conductivity data against SkyTEM smooth model LEI for bore KC12. The AEM response from the FID point nearest the KC12 borehole is in blue, while the induction log response is in red.*

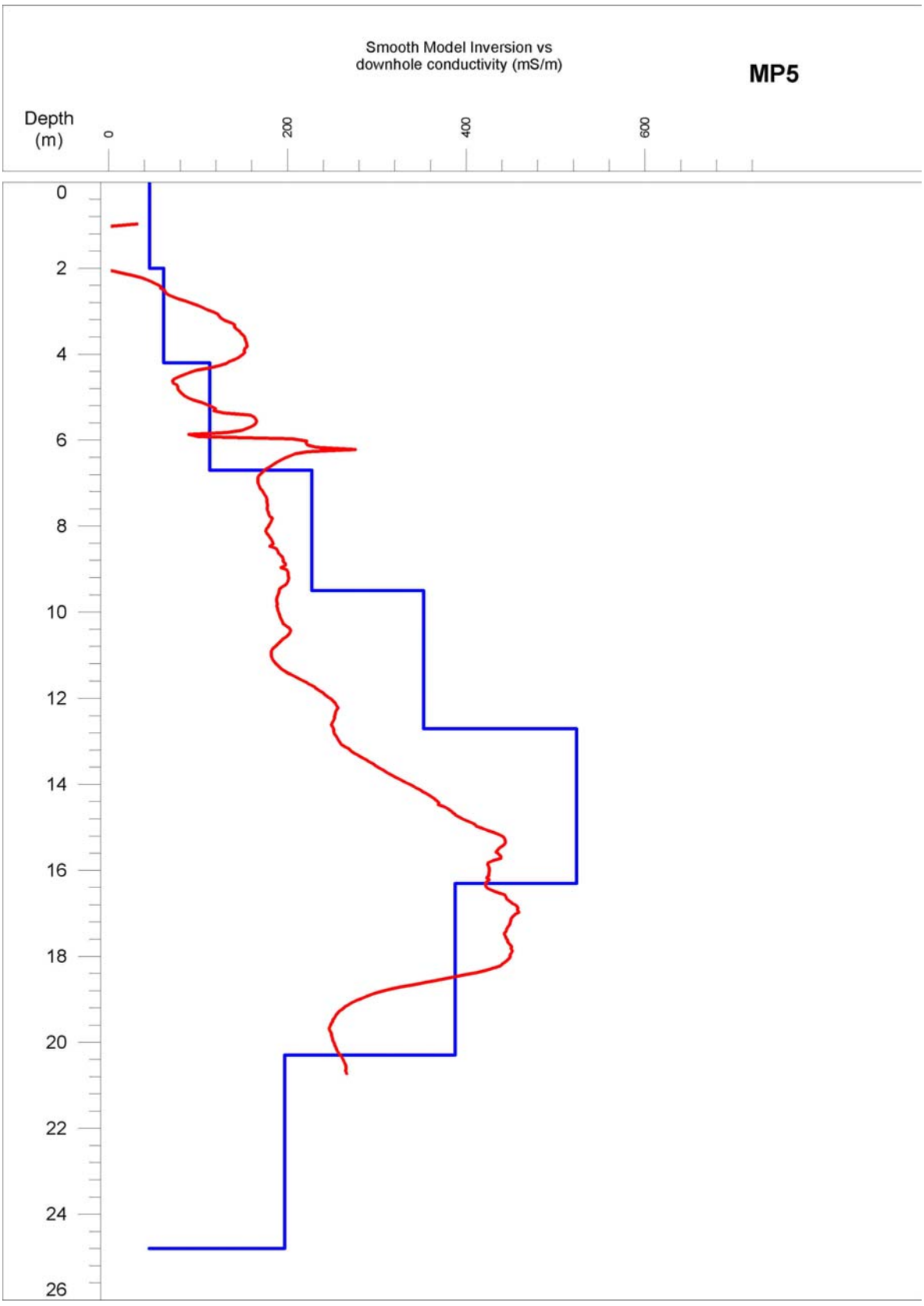

Figure 66: *FID point comparison of borehole conductivity data against SkyTEM smooth model LEI for bore MP5. The AEM response from the FID point nearest the MP5 borehole is in blue, while the induction log response is in red.*

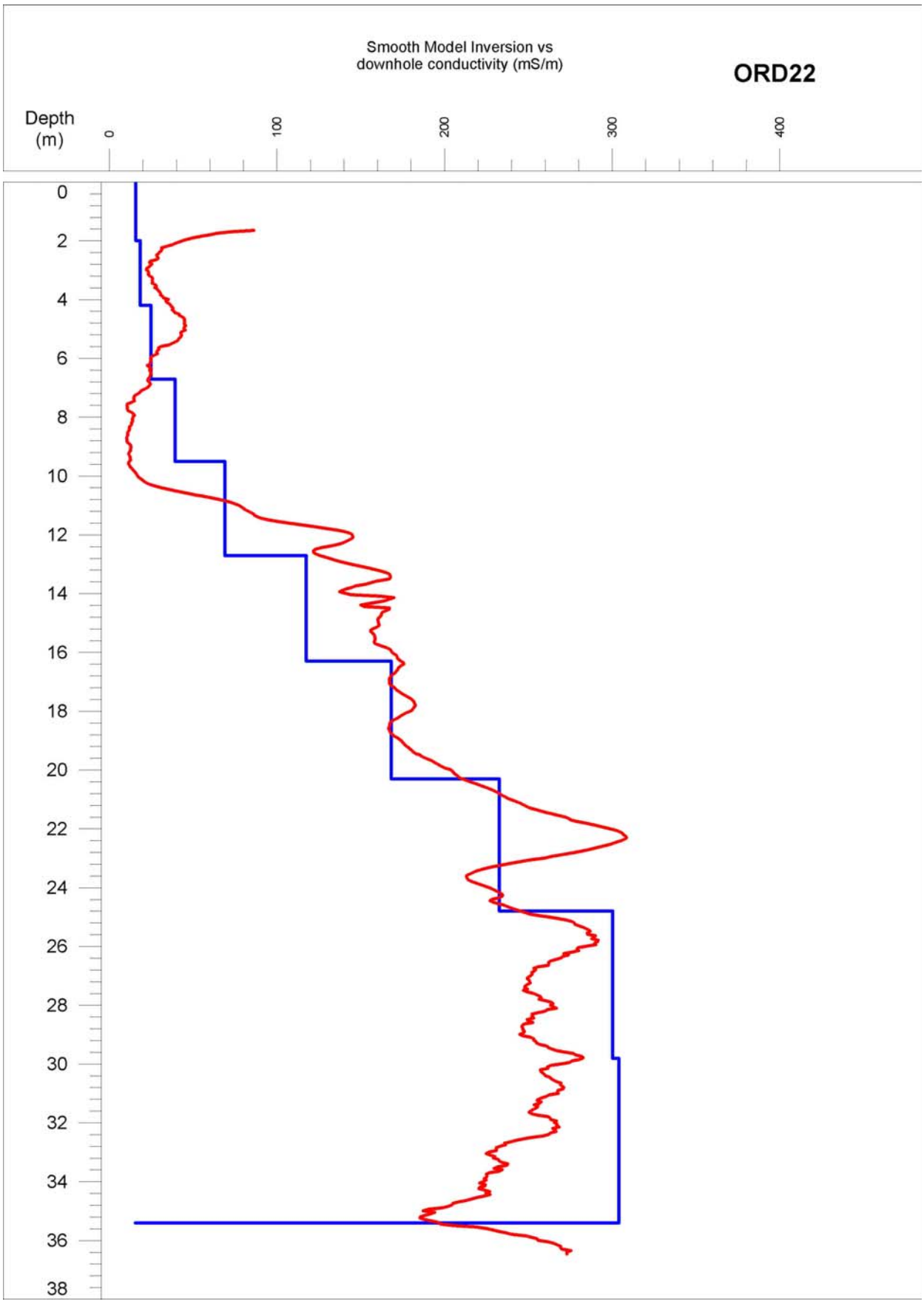

Figure 67: *FID point comparison of borehole conductivity data against SkyTEM smooth model LEI for bore ORD22. The AEM response from the FID point nearest the ORD22 borehole is in blue, while the induction log response is in red.*

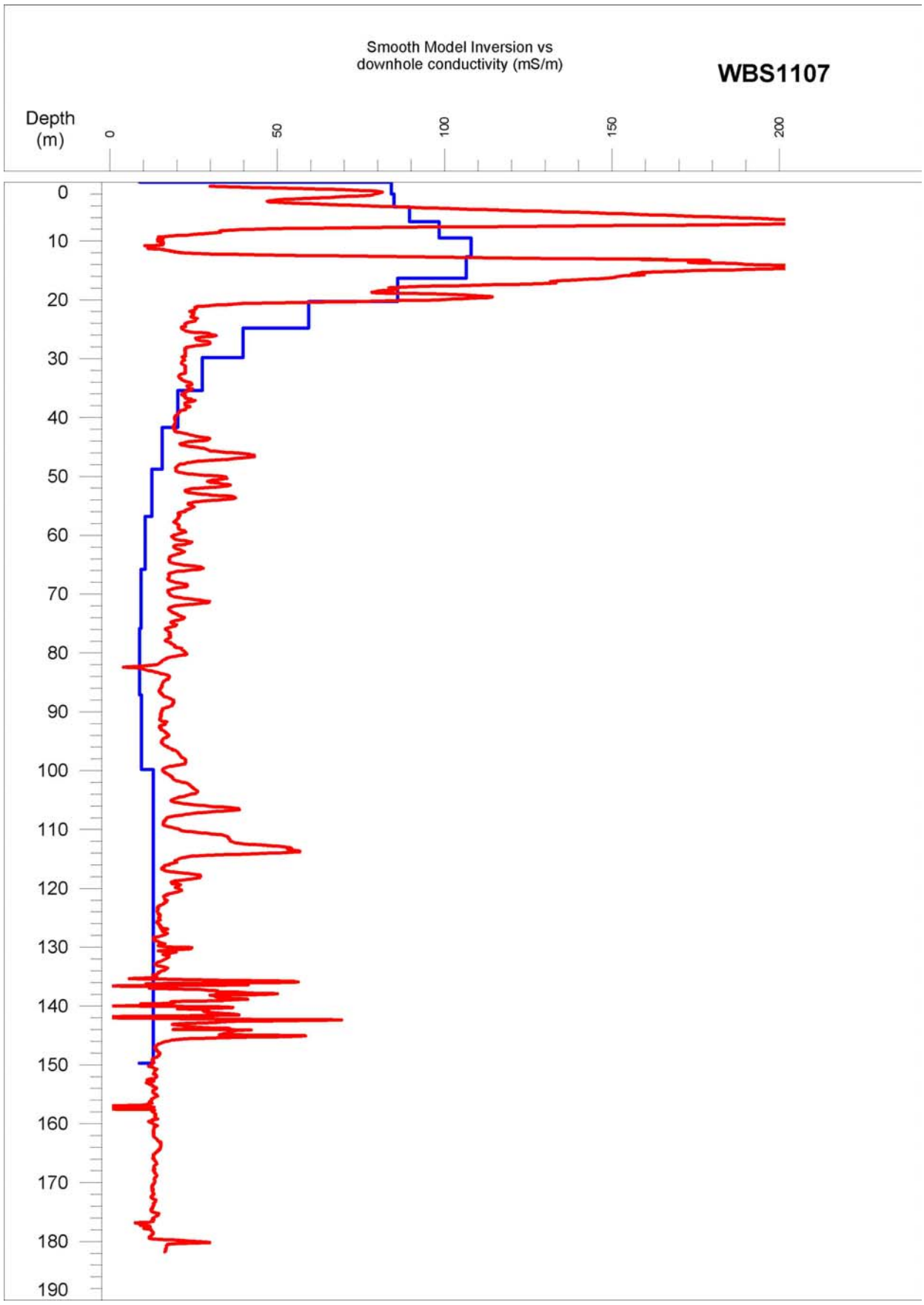

Figure 68: *FID point comparison of borehole conductivity data against SkyTEM smooth model LEI for bore WBS1107. The AEM response from the FID point nearest the WBS1107 borehole is in blue, while the induction log response is in red.*

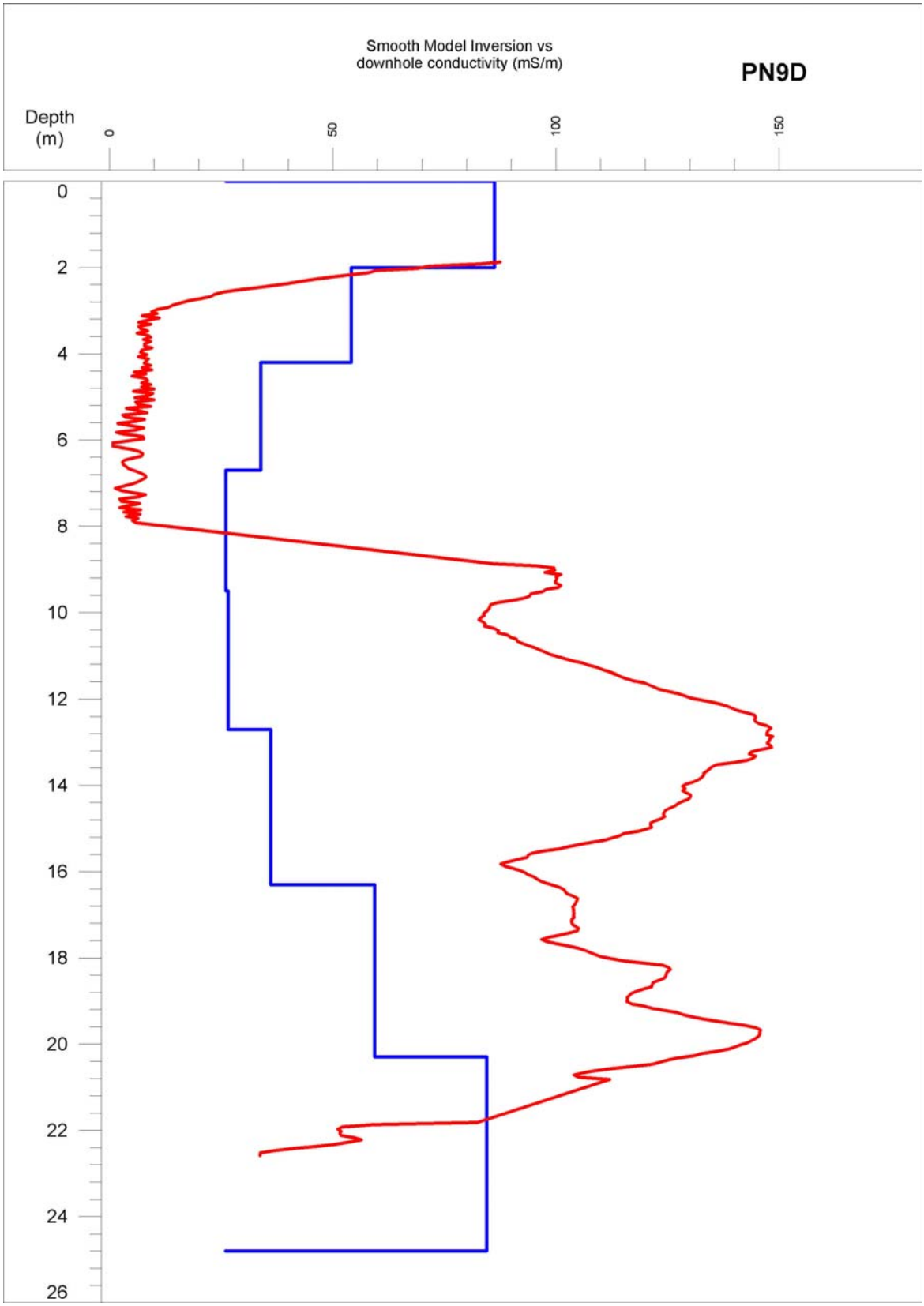

Figure 69: *FID point comparison of borehole conductivity data against SkyTEM smooth model LEI for bore PN9D. The AEM response from the FID point nearest the PN9D borehole is in blue, while the induction log response is in red.*

3.6.13 Comparison of Airborne and Ground EM Responses

Examination of the interval conductivity data for the survey areas indicates a complex and spatially varying vertical conductivity structure, in both the alluvial cover and in the underlying bedrock. The varying ground conductivity for the ORIA and Keep River areas are shown in Appendix 9 (Cullen *et al.,* 2010). The interval conductivities defining ground conductivity variations in the Parry's Lagoon and Carlton Hill area are shown in Appendix 10 (Cullen *et al.,* 2010).

Previous Ground EM surveys
Quite a substantial amount of the ORIA has been surveyed using ground EM techniques, although these data are generally commercial-in-confidence or unpublished (Richards, 2002). Lawrie *et al*. (2006a) carried out a comparative analysis of NanoTEM and pre-existing EM data (from Richards, 2002). The latter was acquired by Terrabyte Services Pty. Ltd. using Geonics EM 31 and EM 38 induction devices mounted in the horizontal modes on a four-wheeled motor bike. A total of 8 agricultural blocks were surveyed (Table 12). Apparent conductivity readings were collected with transect spacing of 18m at all sites except for block 26 which was surveyed at 30m spacing.

The EM31 instrument measures the apparent conductivity of the soil to a depth of 6 metres but with the majority of the response generated from an area between 2 and 4m below the soil surface. The EM38 measures the apparent conductivity of the soil to a depth of 1.5m with the majority of the response generated from a soil volume between 0.2 and 0.6m below the soil surface (Richards, 2002).

Table 12: *EM Surveyed sites and sites selected for validation sampling (from Richards, 2002).*

Block ID	Cropping status	Validation sampling
68	Harvested cane	No
69	Fallow cane	No
56	Rock melons - harvest	Yes-
45	Fallow	No
59	Fallow sugar cane	Yes
26 a	Cane harvested	No
26 b	Cane harvested	No
76	Perimeter	No
22-10	Harvested cane	Yes

Richards (2002) found that soil and sub-soil types, textures and soil salinity profiles vary significantly over distances of 10's -100's of metres in the top 0-6m of the EM31 surveys. These surveys demonstrated that similar electrical conductivity responses in different areas were due to variations in texture *and* soil moisture (and pore fluid salinities) due to perched water table effects. The EM surveys also mapped a scale of variability not recorded in existing soil maps. A similar scale of variability was evident in ground NanoTEM data (Lawrie *et al.,* 2006a).

In this study, a comparison was made between the SkyTEM data and pre-existing EM31 data from the Richards (2002) survey. Figure 70 shows the near-surface SkyTEM data for the 2-4.2m depth interval gridded with a 40m cell size, and scaled from 0-200mS/m. For comparative purposes, the EM31 data were sampled along the SkyTEM flight lines and gridded with a 40m cell size (Figure 71). Overall, the spatial patterns for the observed conductivity are similar, demonstrating that the two techniques give a similar response at a regional scale. Only a slight improvement in spatial resolution of the ground system is evident when the EM31 data are gridded with a 4m cell size and the same conductivity range (Figure 72). However, the contrasts are more evident when the EM31 is scaled (50-350mS/m) to maximise the spatial detail (Figure 73), and compared with similarly scaled SkyTEM data gridded with a 40m cell size (Figure 74). These comparisons clearly show the advantages of using EM31 for mapping paddock-scale conductivity variations in the shallow sub-surface, although much of the conductivity structure is discernable in the SkyTEM data.

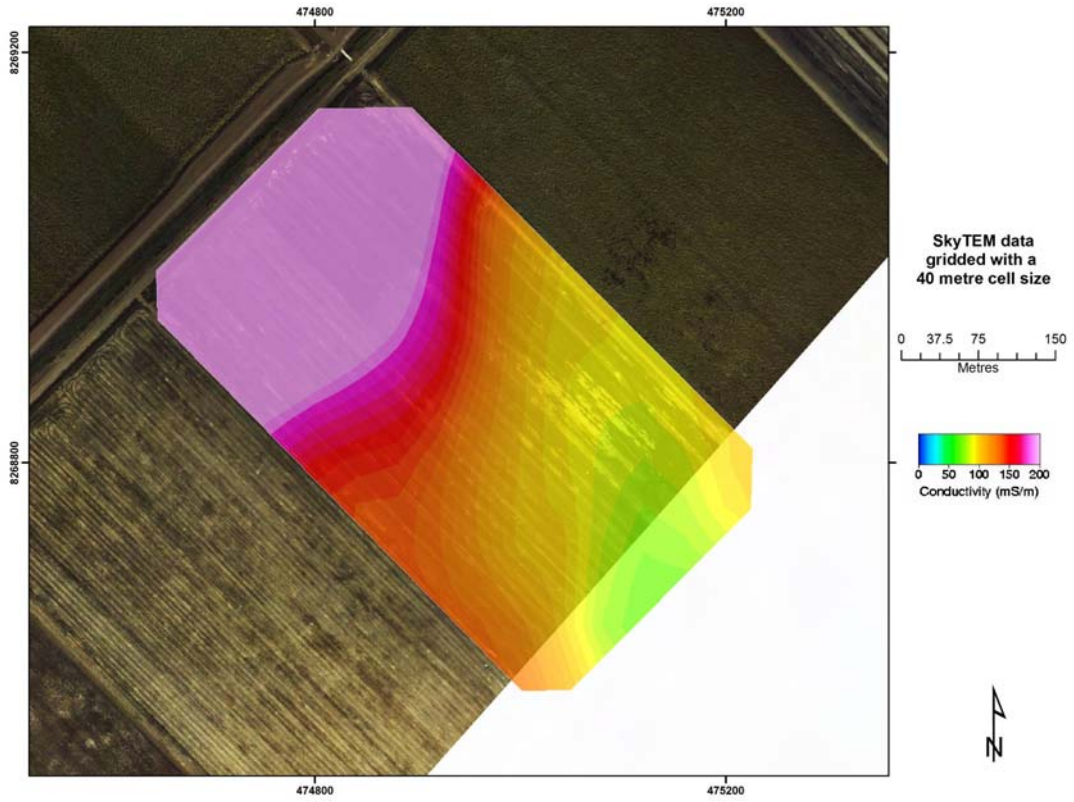

Figure 70: *SkyTEM data for 2-4.2m depth interval gridded with a 40m cell size.*

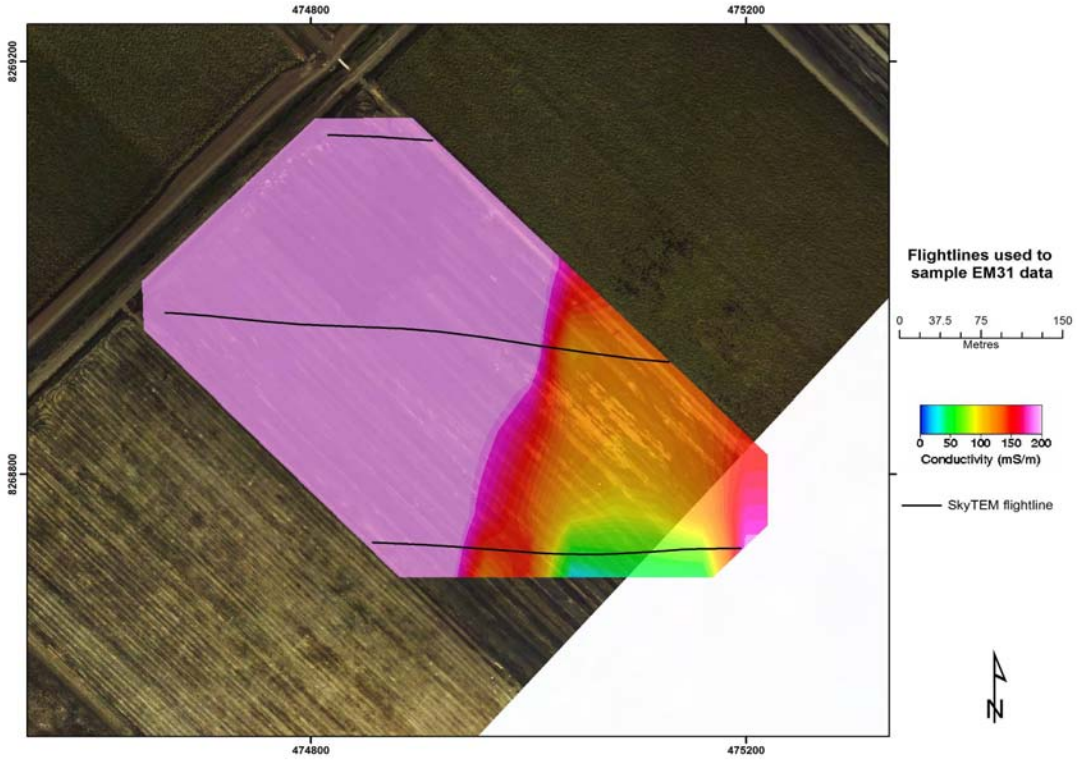

Figure 71: *EM31 data sampled along SkyTEM flight lines and gridded with a 40m cell size.*

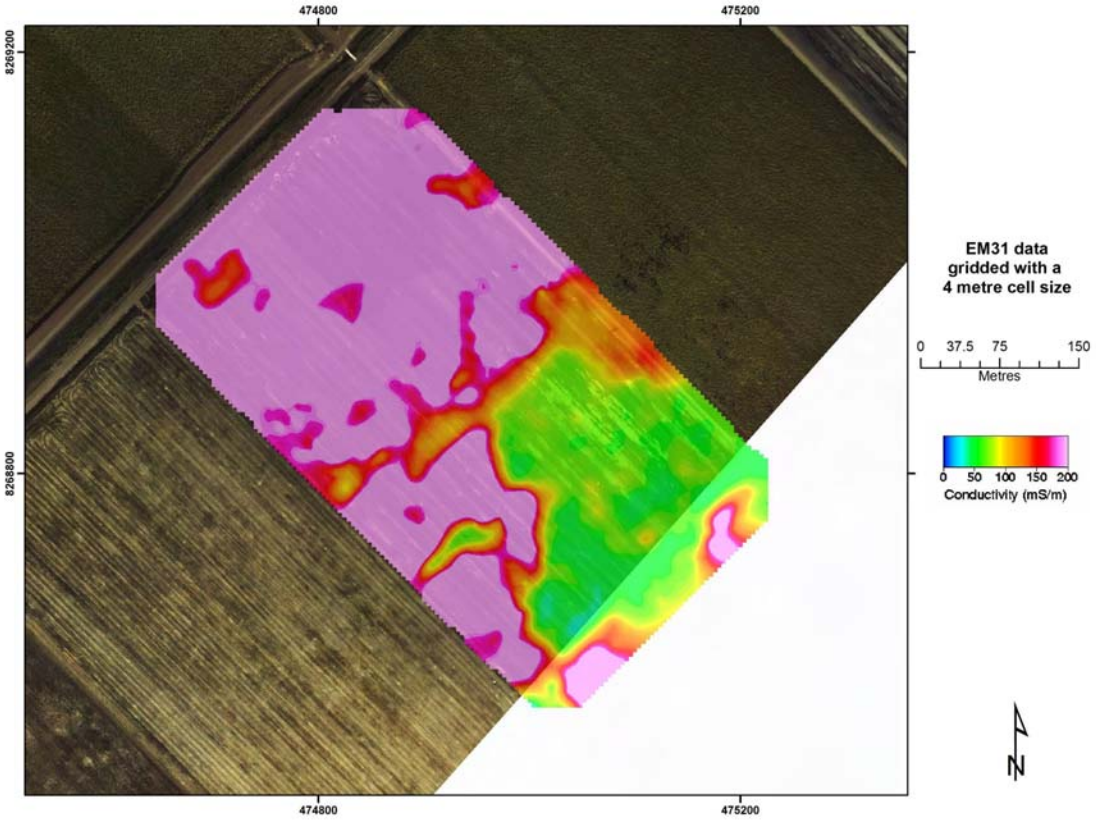

Figure 72: *EM31 data sampled along SkyTEM flight lines and gridded with a 4m cell size.*

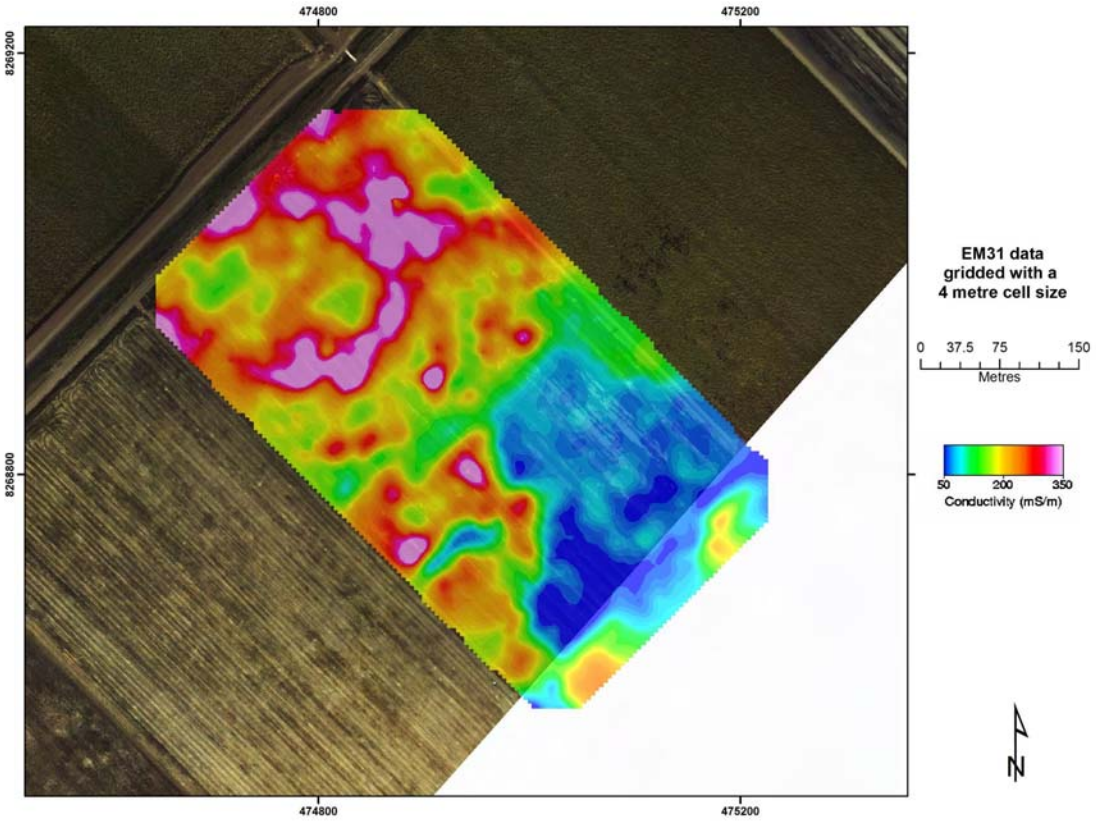

Figure 73: *EM31 data gridded with a 4m cell size, and scaled from 50-350mS/m/.*

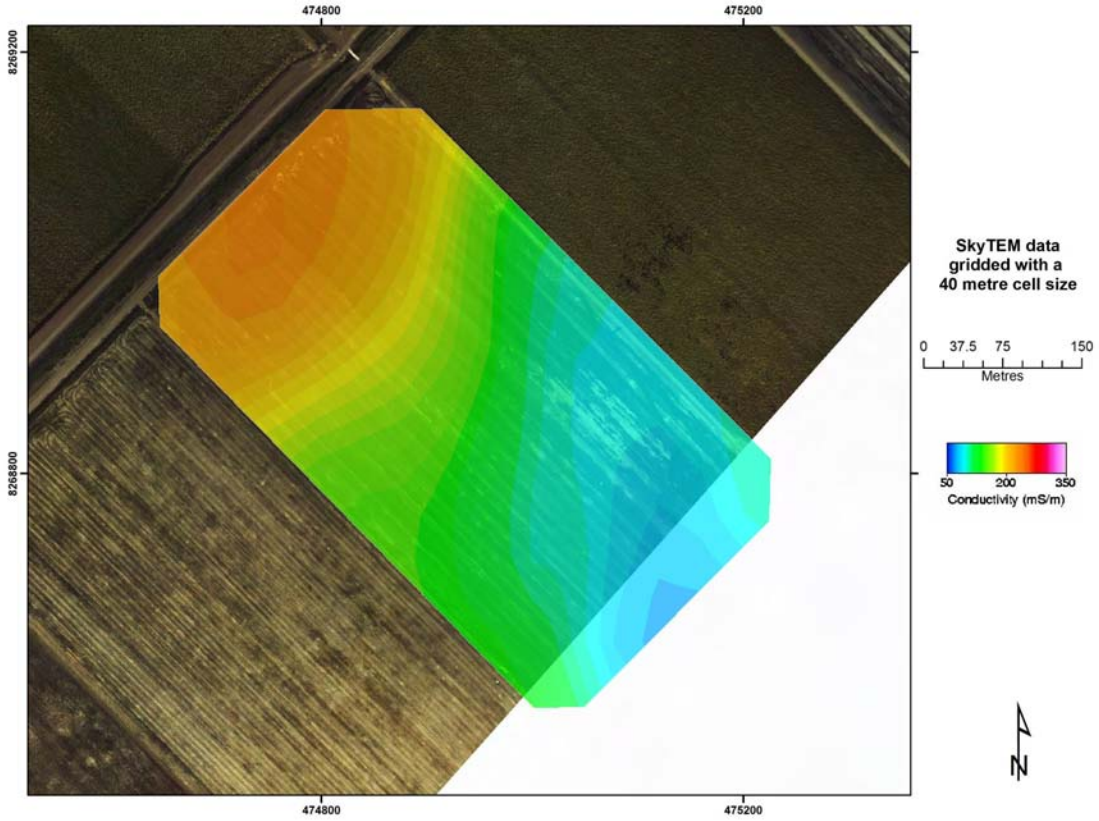

Figure 74: *SkyTEM data for the 2-4.2m depth interval gridded with a 40m cell size, and scaled from 50-350mS/m/.*

A similar comparison of EM31 and SkyTEM data was carried out at a recently cleared area at Green's Location at the northern end of Ivanhoe Plain. At Green's, the modelled conductivity structure from the inverted SkyTEM data in the near surface compares very well with the EM31 data (Figure 75 to Figure 78). Overall, the spatial patterns for the observed conductivity are similar, and although the high resolution of the ground system permits the resolution of additional spatial detail, much of the conductivity structure is discernable in the SkyTEM data.

However, unlike the AEM system, the EM31 cannot resolve variations in ground conductivity at greater depths. Also, some caution should be exercised in interpreting the conductivity from the latter, particularly in areas of higher ground conductivity, for reasons discussed by Lane *et al*. (2004). The SkyTEM data suggest that there may be significant salt stored at below 6m (Figure 77), salt that could be mobilised were water levels to rise in the area. However, there was no ground data available to the project team in this area to validate the interpretation, nor was any temporal groundwater data available to the project team.

SkyTEM Interval Conductivity	EM31 Apparent Conductivity

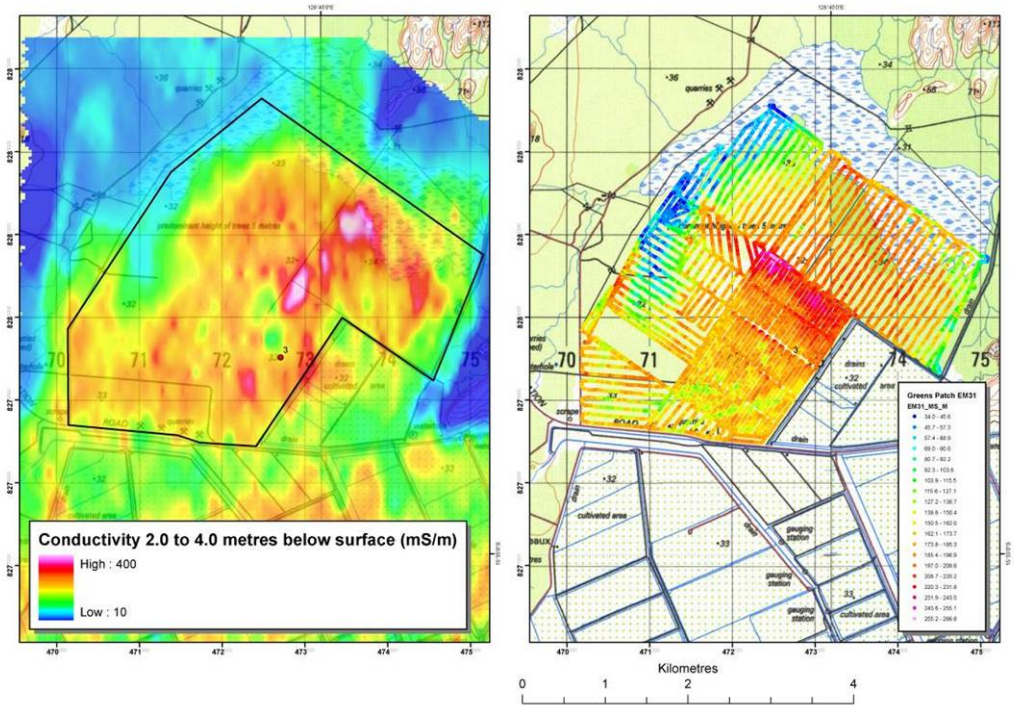

Figure 75: *Comparison between SkyTEM interval conductivity (2-4m) and Geonics EM 31 apparent conductivity data for Greens Location. The interval conductivity for SkyTEM approximately matches the depth beneath the ground surface that would be resolved by a Geonics EM31 (a single frequency ground EM system).*

SkyTEM Interval Conductivity	EM31 Apparent Conductivity

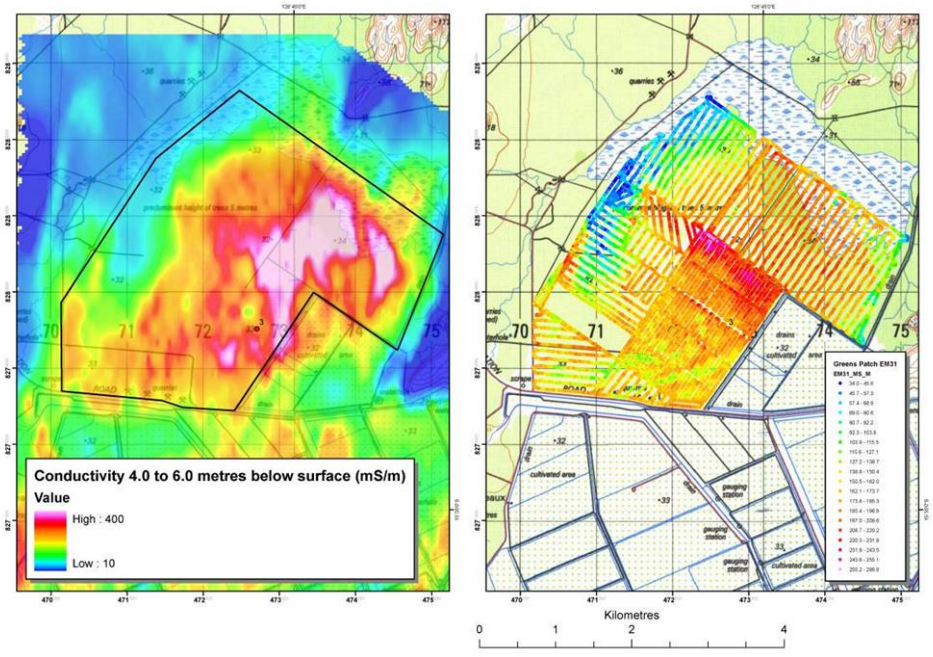

Figure 76: *SkyTEM interval conductivity (4-6m) and Geonics EM 31 apparent conductivity.*

SkyTEM Interval Conductivity	EM31 Apparent Conductivity

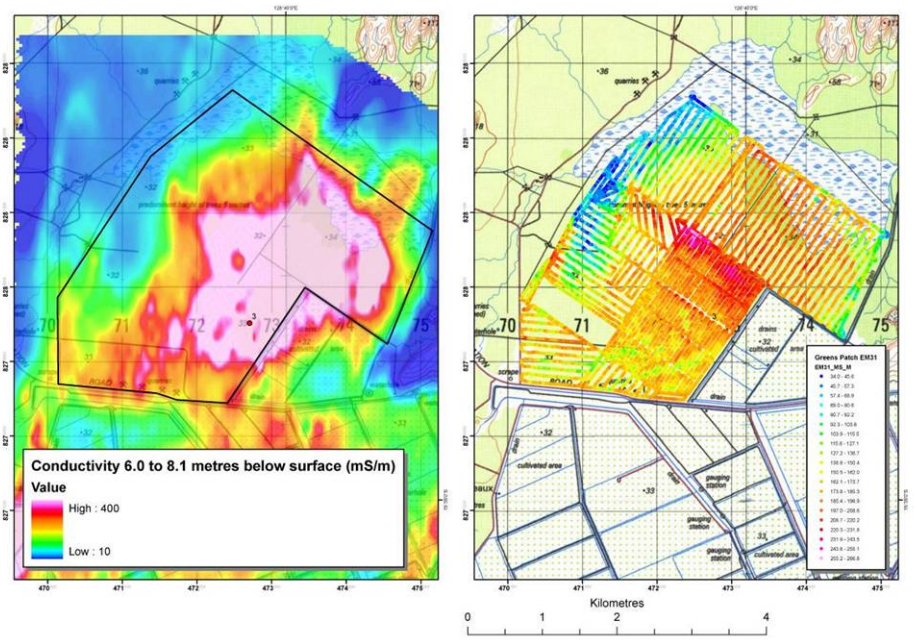

Figure 77: *SkyTEM interval conductivity (6-8.1m) and Geonics EM 31 apparent conductivity.*

SkyTEM Interval Conductivity	EM31 Apparent Conductivity

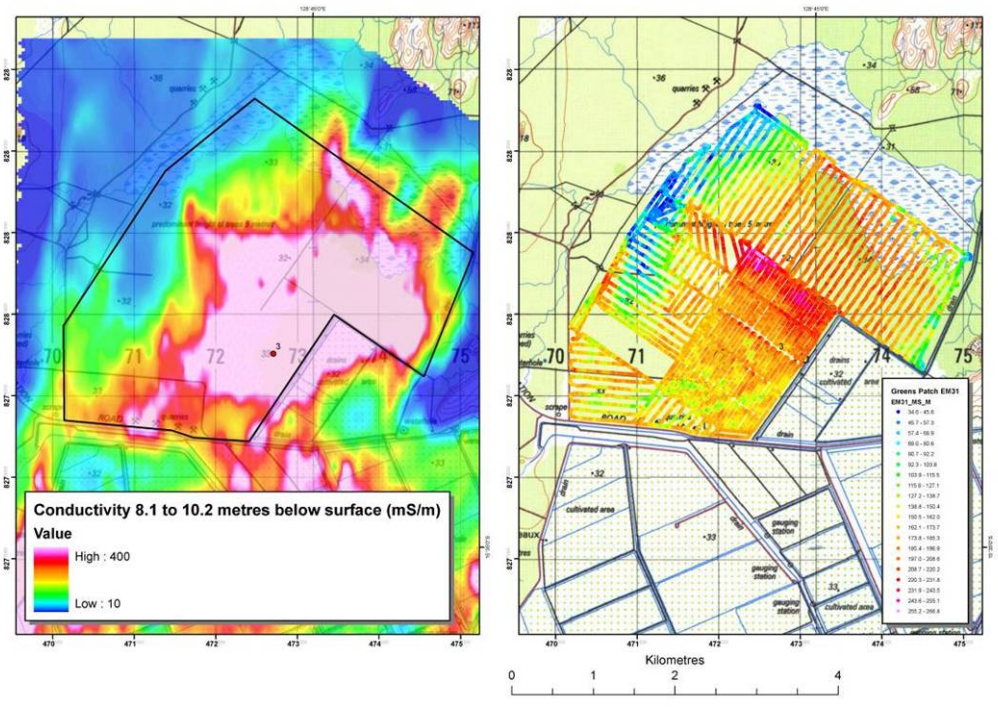

Figure 78: *SkyTEM interval conductivity (8.1- 10.2m) and Geonics EM 31 apparent conductivity.*

3.6.14 Comparison of AEM Data with NanoTEM Ground EM

In addition to a comparative study of the SkyTEM data against conductivity information acquired by the ground EM31 instrument we also reviewed the former against some ground TEM data collected as part of an earlier investigation in the ORIA Stage 1 area (see Lawrie *et al.,* 2006a). These ground TEM data were acquired to assess the ability of ground and airborne EM techniques to delineate aquifer systems, map water quality variations, and recharge and infrastructure leakage, and provided conductivity information to depths of 40m to 50m below the ground surface. Several traverses were collected in the original study, but we limit the comparison of the SkyTEM data to two of the ground traverses.

A Zonge multipurpose NT-32 II (NanoTEM) receiver was used to acquire the ground TEM data. This receiver is backpack-portable, microprocessor-controlled and capable of simultaneously gathering data in up to three channels. Source fields for all the surveys catalogued in this report were generated with the internal transmitter built into the NT-32II receiver. It was set to transmit at 2.0 amps and was powered by a 12-volt battery pack. The receiver provided control of the square-wave transmitter waveform.

The transmitter loop was made up of a single turn of standard 2.5mm^2 copper wire, and was 20 by 20m square. The receiving antenna was made up of a single turn of standard 2.5mm^2 copper wire and was 5 by 5m square and was placed in the centre of the transmitter loop (additional details are provided in Lawrie *et al.* (2006a). Data were acquired using a repetition rate of 32Hz and a sampling rate of 1.6ms.

Following acquisition, the TEM dataset was inverted using a 1D smooth model layered earth inversion – STEMINV (Zonge Engineering, 2009). The results were then stitched and presented as a conductivity-depth section. The 1D model assumption used for this inversion is valid in sub-horizontal, layered sedimentary settings that are encountered in the study area, where it produces results that are only slightly distorted by 2D or 3D effects that could be induced by marked changes in substrate topography, faults, fractures, or other short wavelength geological phenomena.

Overall, the results from both systems are directly comparable with the scale of the observed conductivity structure and variability being similar, particularly in the near surface. Figure 79 shows a conductivity depth section for an east west traverse located near Martins Location in the northern Ivanhoe Plain. Figure 80 shows a section located in the southern part of the Ivanhoe Plain. Both sections (systems) identify a variably conductive near surface layer, representing conductive clay-rich soils and sub-soils, underlain by a resistive zone where sand and gravel-filled elements of the alluvial aquifer are present.

3.6.15 Comparison of Irrigation Scheduling Data with AEM Data

A preliminary analysis of the irrigation scheduling data was carried out for the northern Ivanhoe Plain. In brief, a comparison of AEM data (0-2m conductivity depth slice) with irrigation water scheduling data, shows that a few paddocks appear to show some correlation between watering schedule and conductivity (Figure 81). However, most conductivity patterns follow broader, larger scale patterning (Figure 81) that most likely represents underlying soil textures (and salt stores) modified to varying degrees by soil moisture. At an irrigation district scale, the irrigation scheduling data is too incomplete for a more rigorous geostatistical comparison, although the data may have some benefit in analysing the response in individual paddocks. Such an analysis was beyond the scope of this current project.

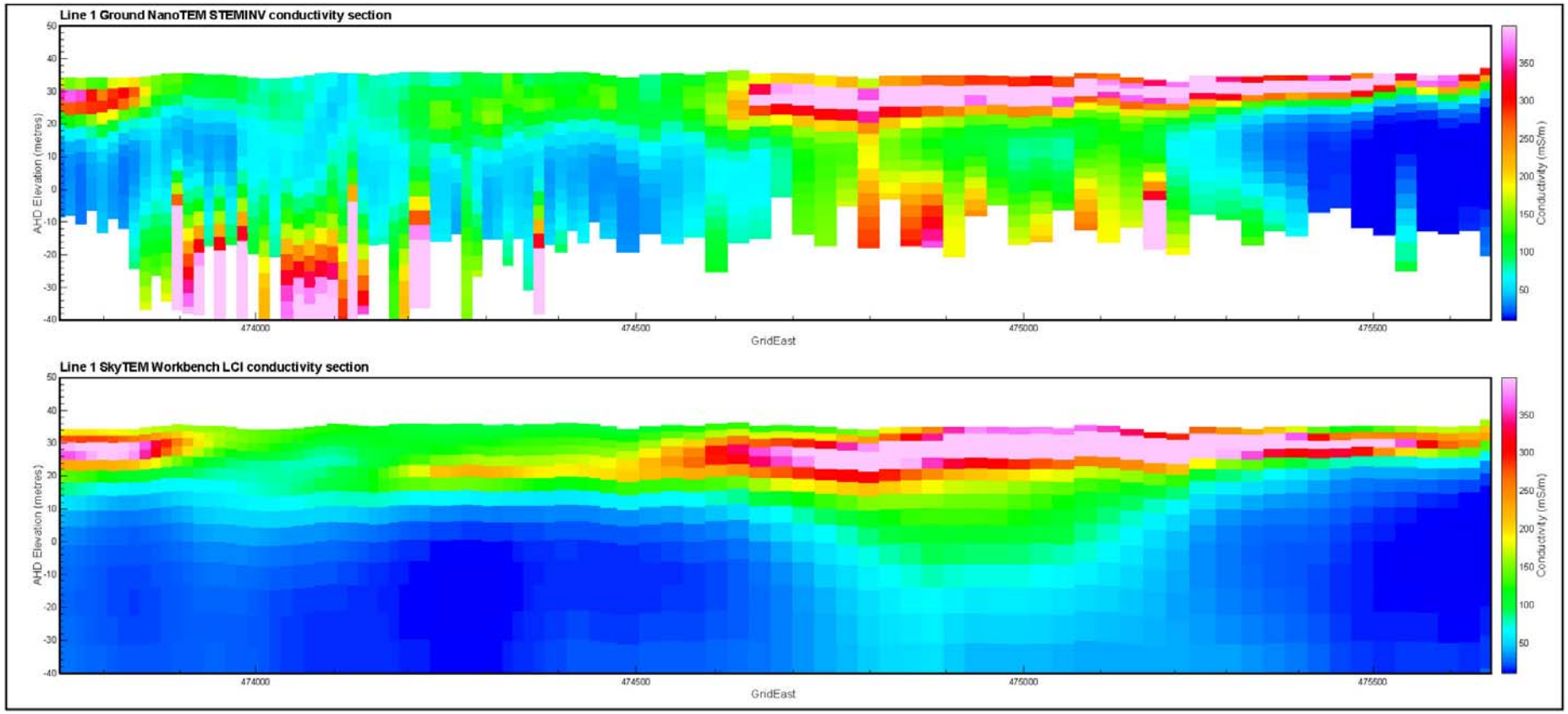

Figure 79: *Conductivity depth section for NanoTEM ground TEM data (top) vs. SkyTEM data (bottom). More conductive layers are shown in reds and pinks, resistive layers in blue. Conductive clay-rich soils and sub-soils, are underlain by a layer of silty sands and sands. The basement interface is difficult to define in this section with confidence.*

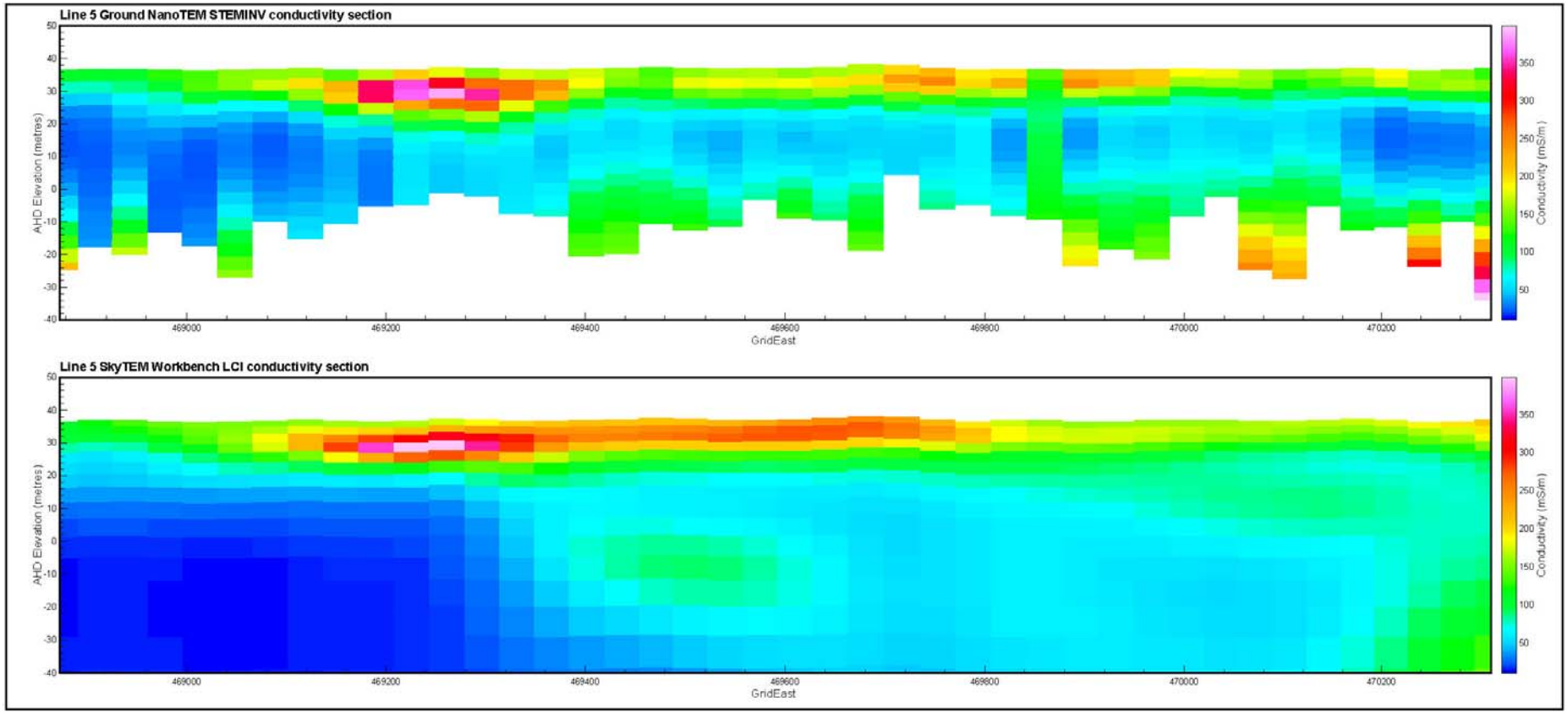

Figure 80: *Conductivity depth section for NanoTEM ground TEM data (top) vs. SkyTEM data (bottom) for the southern Ivanhoe Plain. More conductive layers are shown in reds and pinks, resistive layers in blue. Conductive clay-rich soils and sub-soils, are underlain by a layer of silty sands and sands. The basement interface is difficult to define in this section with confidence.*

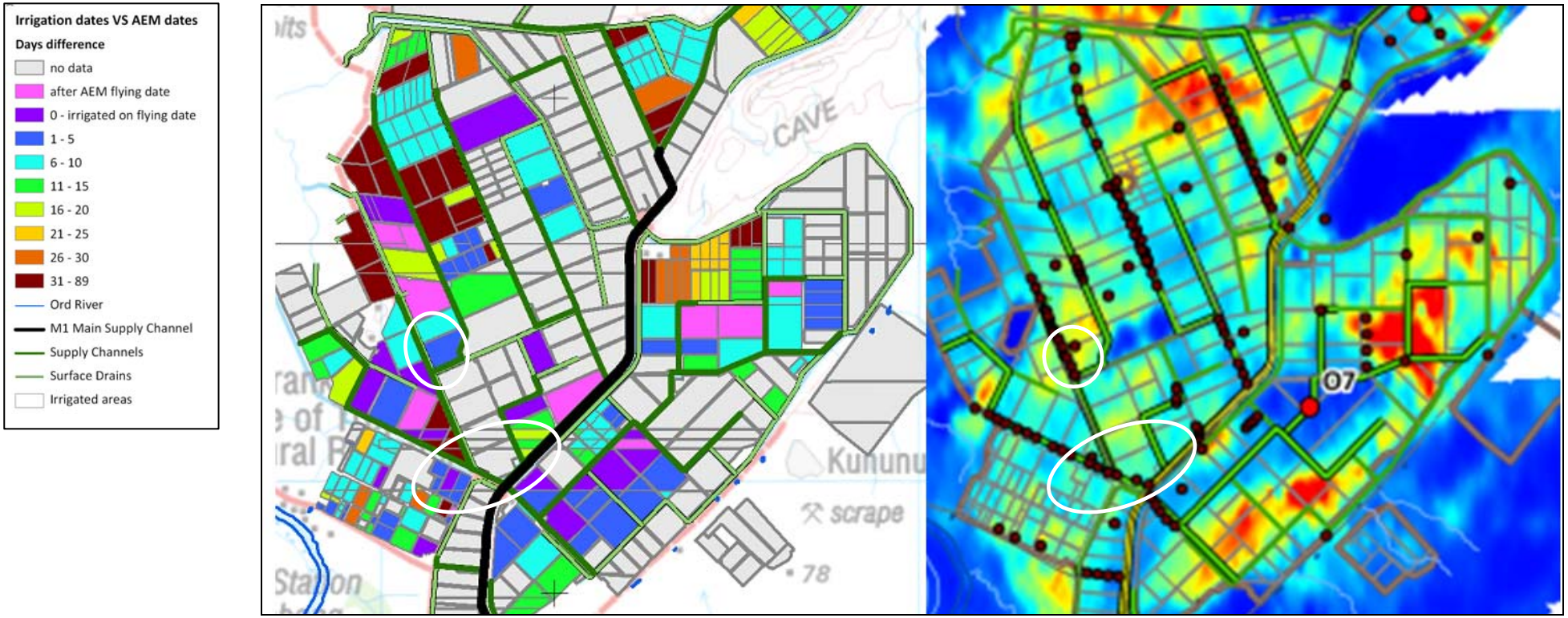

Figure 81: *Comparison of AEM data (0-2m conductivity depth slice) with irrigation water scheduling data. While a few paddocks appear to show some correlation between watering schedule and conductivity, most conductivity patterns follow broader, larger scale patterning that most likely represents underlying soil textures modified to varying degrees by soil moisture.*

3.6.16 AEM Survey Summary

With regard to the SkyTEM survey, key general points to note include:

- A smooth model 1D layered earth inversion, applied from a regional perspective (i.e. without local constraint), effectively mapped variations in ground conductivity at scales relevant to the regional characterisation of the alluvial aquifer and groundwater system.
- In general terms, the modelled conductivity structure defined from the SkyTEM smooth model Layered Constrained Inversion (LCI) matches that defined from available bore data exceptionally well, with an adjusted $r^2 = 0.84$ determined. It is therefore reasonable to assume that the modelled ground response from the inverted SkyTEM data provides a good approximation of 'true' ground conductivity as defined by the borehole conductivity tool, and is a reliable base from which to derive a suite of interpretation products including salt store and lithology maps.
- Modelling and associated ground investigations confirmed that the SkyTEM system's depth of investigation was not limited by the thickness or conductivity of the alluvial aquifer and that conductivity variations in the underlying basement were resolved.
- The SkyTEM AEM system mapped conductivity variations within and beneath relatively thin deposits of the Cockatoo Sands, although it is likely that differentiation of sands with and without high salt content is difficult in the unsaturated zone.

The project has demonstrated the potential for 'calibrated' AEM systems and Fast Approximate Inversion software to shorten AEM project timelines significantly. More specifically:

- Survey acquisition times were reduced through not having to fly as many repeat calibration tests or tie lines.
- Although reducing the time employed to check and assess the quality of the AEM dataset acquired, it did not eliminate this requirement. Nonetheless, fewer 'corrections' were required in the finalisation of data.
- AEM data inverted using the fast approximate inversion (iTEM) were obtained within 24 hrs of data acquisition. The early availability of high quality estimates of ground conductivity facilitated the early design of a drilling program, the extension of the survey whilst it was in progress, and the initiation of data interpretation immediately.
- The initial multi-layer iTEM inversions had high correlation coefficients (>0.8) when comparing FID points to adjacent borehole induction logs, and the inversions have proven to be very robust.

4 Methodology for Producing Map Products

This chapter aims to explain the methodologies that were used to create the map-based products from the datasets described in the previous chapter. More specifically, this section covers how the landform/geomorphic maps were produced, and how the lithology maps of the alluvium and depth to bedrock interface were derived from combining the AEM and drilling data. The methods used to produce vegetation vigour, persistence of surface moisture, watertable maps and 'surrogate' approaches for mapping recharge are also explained. There are also detailed explanations of how the AEM data have been used to generate salt store, groundwater salinity, river flush zone and salinity hazard maps.

The products described in this chapter are incorporated in the accompanying atlas (Apps *et al*., 2009a-d), and GIS products (Apps *et al*., 2009e), and are analysed and discussed later in this report. Table 13 lists the data and information layers produced in this study. The products are utilised as the basis for analysis, interpretation and discussion in Sections 6-9.

Table 13: *List of data and products for the Ord AEM Project.*

1.	Project Area	24.	Recharge Potential (from 0-2m soil data)
2.	Satellite Imagery	25.	Soil permeability (0-20cm from soil data)
3.	Topographic Information	26.	Surface wetness index maps
4.	Pre-existing Hydrogeology	27.	Deep Drainage (from AEM map of clay thickness)
5.	Borehole Locations	28.	Lithology interpretations of each conductivity depth slice through the alluvium
6.	Pre-existing Geology	29.	Lithology interpretation of depth to bedrock in AEM/O'Boy cross-section transects
7.	Geomorphology	30.	Depth to bedrock
8.	Vegetation Structure	31.	Extent of gravels
9.	NDVI Difference	32.	Thickness of gravels
10.	Watertable at time of AEM survey	33.	Extent of sands
11.	Gamma Ray Spectrometry	34.	Thickness of sands
12.	Aeromagnetics	35.	Extent of silts
13.	SRTM Digital Elevation Model	36.	Thickness of silts
14.	Digital Elevation Model (10m)	37.	Extent of clays
15.	AEM Flight Survey Lines	38.	Thickness of clays
16.	AEM Cross Sections	39.	Salt Store in the unsaturated zone
17.	AEM Conductivity Depth Slices	40.	Salt Store in the saturated zone)
18.	AEM cross-sections along O'Boy transects	41.	Salinity Hazard
19.	3D AEM model	42.	Images to address specific Salinity management Questions (with water infrastructure overlays)
20.	Flush zone Extent (3 depth intervals)	43.	Drilling data logs
21.	Flush Zone Thickness	44.	Sonic coring program textural and hydrogeochemical data
22.	Flush Zone Conductivities (-5 to -10 & -10 to -15m)	45.	Irrigation scheduling data for AEM survey
23.	Surface Salinity		

4.1 LANDFORM AND GEOMORPHOLOGY MAPS

Landforms are the basis of the science of geomorphology. Because landforms are the result of the interaction of the geological fabric of the landscape, the processes acting on it, and time, they can be used to infer surface processes and materials. Geomorphic maps thus assist in the interpretation of soils data, AEM information, and vegetation maps. The geomorphology map was complied from two main data sources. These were the DEMs and the surface imagery. Polygons of landform units were derived from interpretation of DEM images, supplemented by gamma ray radiometric data and satellite imagery. The mapping was based on interpretation of variations in elevation, surface texture and patterns in the data that reflect fundamental processes operating in fluvial landscapes (see Friend, 1983, Gibling *et al*. 1998; Makaske, 2001; Miall 1992; Reineck & Singh 1980; Schumm & Etheridge, 1994 for examples). Mapping was carried out in ArcGIS and the polygons were field checked where possible against the available access roads in the project area.

Two different DEMs were stitched together for the purposes of mapping. These were the One Second SRTM data, which has an approximate 30 m horizontal resolution, and the Ord LiDAR Survey, which has an approximate 2 m horizontal resolution. The LiDAR DEM showed much more detail but was available only over the immediate project area, except for the Carlton Plains. The SRTM DEM was used to connect the separate project areas, supply coverage over Carlton Plains, and to provide a regional context.

Likewise, two different image datasets were used. These consisted of the high resolution Orthophotos, which covered most of the project area except Carlton Plain, and a LANDSAT 5 TM image. The LANDSAT 5 TM image was used to provide coverage of Carlton Plain, between the project areas, and to supply the regional context.

Polygon boundaries were drawn using geomorphic features visible in the DEMs. These boundaries were then cross-checked again boundaries visible in the imagery. Where DEM resolution was low, some boundaries were only visible in that imagery. Polygons were attributed using the categories in RTMAP (Pain *et al*., 2007). Twenty-two different units were mapped (Figure 82, Table 14), with the greatest subdivision occurring on the units in the plains. Only limited subdivision was applied to the hills because most of these fell outside the project area and were of lesser importance to the project than the plains.

Samples collected in the field for validation purposes were transported in sealed polyethylene bags. In the laboratory samples they were weighed, oven-dried at 105^{o}C for 24 hours and re-weighed to determine moisture content. The oven-dried samples were then analysed for electrical conductivity (EC), pH, and mineralogy by X-Ray Diffraction (XRD), chemistry by X-Ray Fluorescence (XRF) and grainsize by laser diffraction.

Table 14: *Landforms mapped in the ORIA.*

Unit	Map Code	Description
Alluvial plain	**ap**	A level, or gently sloping, or slightly undulating land surface produced by extensive deposition of alluvium, generally adjacent to a river that periodically overflows its banks; it may be situated on a flood plain, a delta, or an alluvial fan.
Flood plain	**af**	Alluvial plain characterised by frequently active aggradation by over-bank stream flow (i.e. by flooding more often than every 50 years) and erosion by channelled stream flow.
Meander plain	**am**	Flood plain aggraded and eroded by meandering streams. Flood plain with widely spaced, rapidly migrating, moderately deep alluvial stream channels that form a unidirectional integrated non-tributary network. There is frequently active aggradation and erosion by channelled stream flow with subordinate aggradation by over-bank stream flow.
Stream channel	**ar**	Linear, generally sinuous open depression, in parts eroded, excavated, built up and aggraded by channelled stream flow. This element comprises streambed and banks.

Alluvial terrace	**at**	Former flood plain on which erosion and aggradation by channelled and over-bank stream flow is slightly active or inactive because of deepening or enlargement of the stream channel has lowered the level of flooding. A pattern that includes a significant active flood plain, or former flood plains at more than one level, becomes terraced land.
Alluvial swamp	**aw**	Almost level, closed or almost closed depression with a seasonal or permanent water table at or above the surface, commonly aggraded by overbank stream flow and sometimes biological (peat) accumulation.
Tidal flat	**ct**	Level landform pattern with extremely low relief and slowly migrating deep alluvial stream channels which form dendritic tributary patterns; it is aggraded by frequently active tides.
Coastal plain	**cp**	Level landform pattern with extremely low relief either with or without stream channels, built up by coastal, usually tidal, processes.
Pediment	**ei**	Gently inclined to level (< 1% slope) landform pattern of extremely low relief, typically with numerous rapidly migrating, very shallow incipient stream channels that form a centrifugal to diverging integrated reticulated pattern. It is eroded, and locally aggraded, by frequently active channelled stream flow or sheet flow, with subordinate wind erosion. Pediments characteristically lie down-slope from adjacent hills with markedly steeper slopes.
Rises	**er**	Landform pattern of very low relief (9 - 30 m) and very gentle to steep slopes. The fixed erosional stream channels are closely to very widely spaced and form a dendritic to convergent, integrated or interrupted tributary pattern. The pattern is eroded by continuously active to slightly active creep and sheet flow.
Hills	**eh**	Landform pattern of high relief (90 - 300 m) with gently sloping to precipitous slopes. Fixed, shallow erosional stream channels, closely to very widely spaced, form a dendritic or convergent integrated tributary network. There is continuously active erosion by wash and creep and, in some cases, rarely active erosion by landslides.
Alluvial fan	**fa**	Level (< 1% slope) to very gently inclined complex landform pattern of extremely low relief with a generally fan-shaped plan form. The rapidly migrating alluvial stream channels are shallow to moderately deep, locally numerous, but elsewhere widely spaced. The channels form a centrifugal to divergent, integrated, reticulated distributary pattern. The landform pattern includes areas that are bar plains, being aggraded or eroded by frequently active channelled stream flow, and other areas comprising terraces or stagnant alluvial plains with slopes that are greater than usual, formed by channelled stream flow but now relict. Incision in the up-slope area may give rise to an erosional streambed between scarps.
Colluvial fan	**fc**	Very gently to moderately inclined complex landform pattern of extremely low relief with a generally fan-shaped plan form. Divergent stream channels are commonly present, but the dominant process is colluvial deposition of materials. The pattern is usually steeper than an alluvial fan.
Levee	**rl**	Very long, very narrow, nearly level sinuous ridge immediately adjacent to a stream channel, built up by over-bank flow. Levees are built, usually in pairs bounding the two sides of a stream channel, at the level reached by frequent floods. This element is part of a covered plain landform pattern. For an artificial levee, use Embankment. See also Prior stream.
Channel bench	**fb**	Flat at the margin of a stream channel aggraded and in part eroded by over-bank and channelled stream flow; an incipient flood plain. Channel benches have been referred to as 'low terraces', but the term terrace should be restricted to landform patterns above the influence of active stream flow.

Prior stream	**rp**	Long, generally sinuous low ridge built up from materials originally deposited by stream flow along the line of a former stream channel. The landform element may include a depression marking the old streambed, and relict levees.
Gully	**vg**	Open depression with short, precipitous walls and moderately inclined to very gently inclined floor or small stream channel, eroded by channelled stream flow and consequent collapse and water-aided mass movement. Sapping may also play a role.
Tidal creek	**vt**	Intermittently water-filled open depression in parts eroded, excavated, built up and aggraded by channelled tidewater flow; type of stream channel (qv) characterised by a rapid increase in width downstream.
Swamp	**vw**	Almost level closed, or almost closed, depression with a seasonal or permanent water table at or above the surface, commonly aggraded by over-bank stream flow and sometimes biological (peat) accumulation.
Ox-bow	**dx**	Long, curved, commonly water-filled closed depression eroded by channelled stream flow but closed as a result of aggradation by channelled or over-bank stream flow, during the formation of a meander plain landform pattern. The floor of an ox-bow may be more or less aggraded by over-bank stream flow, wind, and biological (peat) accumulation.

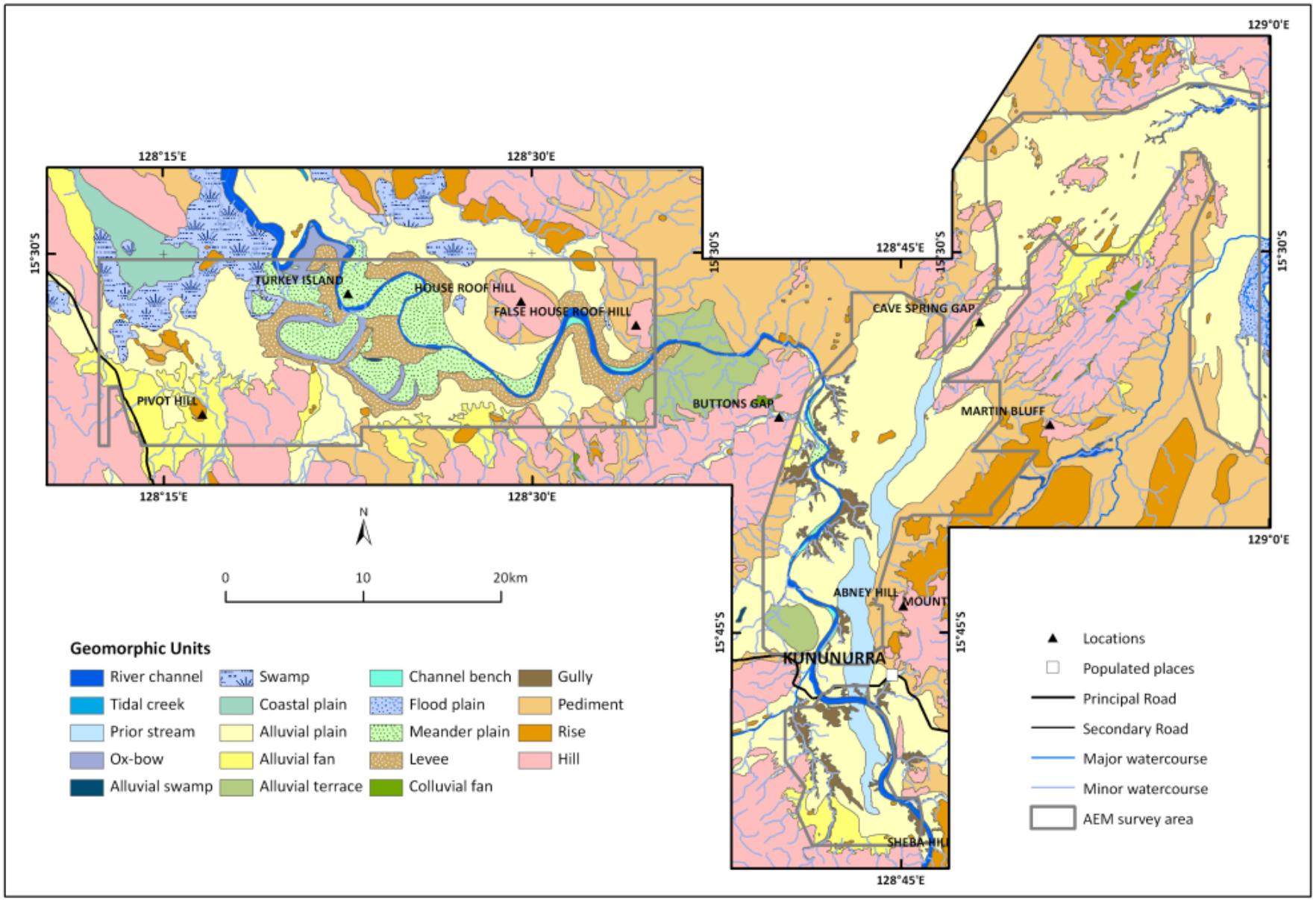

Figure 82: *Geomorphology of the project area.*

4.2 MAPPING DEPTH TO BEDROCK AND STRATIGRAPHY WITHIN THE ALLUVIUM

4.2.1 Lithology Maps of the Ord Valley and Ord Palaeo-Valley Alluvium (using AEM Depth Slice Interpretation)

Previous studies have developed multi-disciplinary, multi-scale 4D system approaches to the integration, analysis of interpretation of complex hydrogeological, hydrogeophysical and hydrogeochemical datasets such as those in the Ord Valley Interpretation Project (Lawrie *et al.,* 2000; Lawrie, 2008; Lawrie *et al.,* 2009a). These approaches incorporate an understanding of landscape evolution and scale, utilise modern investigative approaches to the conceptualisation and mapping of aquifer systems and aquitards, and combine state of the art hydrogeochemical and hydrogeophysical techniques to assess hydrogeological processes.

In this study, the specific approach used to produce maps of key elements of the hydrostratigraphy, including lithology maps, is described in detail below. In essence, the approach relies primarily on the use of all available borehole data to interpret individual conductivity depth slices. The depth slices for each area were interpreted systematically, starting from the surface, and going progressively deeper. These interpretations were checked using conductivity flight line sections and interpretation of synthetic AEM sections (i.e. not sections along original flight lines) generated along the 30 cross-sections previously constructed by O'Boy *et al.,* (2001). Due to unavoidable resourcing issues, interpretation of the depth slices and cross-sections was carried out separately by two teams. After completion of preliminary interpretations, these were reconciled to produce a consistent interpretation in 3D.

The interpretation of the depth slices was challenging in this landscape, particularly towards the basement-alluvium interface where units with similar resistivity were encountered, and in the Parry's Lagoon area where highly saline groundwater tended to mask lithology responses (described later). However, the interpretation of the depth slices was aided by the spatial patterning evident in the conductivity data. Borehole data appear to confirm that in many places the observed conductivity patterning reflects variations in sedimentary textures. Modern conceptual approaches to facies analysis facilitate interpretation in these instances (Lawrie *et al.,* 2000; Lawrie *et al*., 2009a, b). However, by contrast, analysis and interpretation of the depth sections with limited recourse to looking at adjacent sections and depth slices, proved to be more challenging. This is due in large measure to the fact that facies variability tends to be easier to discern in the horizontal dimension than in the vertical plane.

Detailed methodology used in this study

In this study, a total of 561 bores with lithological descriptions were used in the analysis and interpretation of the hydrostratigraphy. Of these, 549 bores were part of the pre-existing WA Water Departments Water Quality Database information, while 12 new sites were cored in 2009 as part of this project. The available borehole data are not distributed evenly across the area, with data from only 31 bores available from the Parry's Lagoon - Mantinea Plain - Carlton Hill area.

Conductivity responses are driven by several factors including texture, porosity, moisture content and water quality. To resolve the dominant drivers in the ORIA, an initial assessment was made to determine how unique the conductivity responses were for each lithological unit in the project area. The approach used is based on that developed in other studies (Tan *et al.,* 2005, 2009). Laser grain size and sieve analysis of samples taken from the 12 new project cores were used to identify 4 main sedimentary texture classes, i.e. sand, silt, clay and gravel. Descriptions for each textural class may contain a variety of textural subdivisions (e.g. gravely sand, silty sand, muddy sand, and a variety of fine to very coarse sand with varying degree of sorting). Bedrock present in the drill cores includes basalt, shale and sandstone.

Grain size data were then compared with EC_a data from borehole conductivity logs. Downhole conductivity values were collated at 5cm intervals within the lithological units mapped in 9 of the project drill holes from the ORIA and Weaber Plains. These data are summarised in Table 15. Comparative analysis of these data found that high EC_a values equate well with clay units in these areas. As such, high EC_a values appear to be a useful indicator of clay distribution rather than water quality in these areas. However, water quality variations do appear to contribute more to EC_a responses in cores from Parry's Lagoon. In the latter, very

high salinity values are obtained from pore fluids in marine sands, thus resulting in high EC_a, making it more difficult to differentiate sands and clays in this area using conductivity responses alone.

In the ORIA and Weaber Plains core, sand, basalt and sandstones have similar low EC_a values, e.g. mean EC_a values are 87, 88 and 92mS/m respectively. While interpretation of coarser-grained lithological units within the alluvial sequence is relatively straightforward, it is not so easy to differentiate sands and gravels (and textural variants) based on conductivity response alone. Similarly, the overlapping EC values of gravels, sands and bedrock lithologies makes interpretation of the base of the alluvium quite difficult using conductivity values alone. As found in other studies (Lawrie *et al.,* 2000; Lawrie *et al*., 2009a), additional information, such as borehole lithological logs and recognisable geomorphic, sedimentological and structural patterns in the conductivity depth slices, are required to interpret the AEM depth slices. Correlation with cross-sections is also important, although interpretation of the latter is made more difficult by the difficulty in observing depositional patterns in cross-section.

Table 15: *Statistical summary of apparent conductivity (downhole logs) and the lithological classes.*

EC_a mS/m	Sand	Silt	Clay	Gravel	Basalt	Shale	Sand-stone
maximum	245	569	655	61	203	39	131
75th percentile	143	251	520	25	122	35	99
mean	87	189	334	16	88	30	92
median	47	178	335	11	89	32	93
25th percentile	22	115	146	4	23	26	89
minimum	1	6	12	0	2	12	6
N	*212*	*461*	*405*	*91*	*213*	*62*	*121*

Up to 9 AEM depth slices (Table 16) were used to map the lithological units within each sub-area. The surface 0-2m was not mapped using AEM as the later was found to be insensitive to materials (cracking clays appear highly resistive). The soil-landform map of 2009 best depicts texture variation to 2m depth.

Table 16: *Depth Slices used in mapping the lithological units*.

Ord, Weaber and Knox Plains	Parry's Lagoon, Carlton Hill
2 – 4.2 m	2 – 4.2 m
4.2 – 6.7 m	4.2 – 6.7 m
6.7 – 9.5 m	6.7 – 9.5 m
9.5 – 12.7 m	9.5 – 12.7 m
12.7 – 16.3 m	12.7 – 16.3 m
16.3 – 20.3 m	16.3 – 20.3 m
20.3 – 24.8 m	20.3 – 24.8 m
24.8 – 29.8 m	24.8 – 29.8 m
29.8 – 35.4 m	

To aid interpretation of the AEM data, the EC_a values of each depth slice at Ord, Weaber and Knox plains were organised and displayed in 9 classes (Table 17). To interpret the more resistive bedrock at depth (>20.3m), 11 classes are used. Due to the highly conductive values at Parry's Lagoon – Carlton Hill, a separate demarcation of 10 threshold values are used (Table 17).

Table 17: *Apparent conductivity (ECa) classes.*

Ord, Weaber and Knox Plains, < 20.3m depth (EC_a mS/m)	Ord, Weaber and Knox Plains, > 20.3m depth (EC_a mS/m)	Parry's Lagoon, Carlton Hill (EC_a mS/m)
0 - 25	0 - 20	0 - 50
25 - 50	20 - 40	50 - 100
50 - 75	40 - 60	100 - 150
75 - 100	60 - 80	150 - 200
100 - 125	80 - 100	200 - 250
125 - 150	100 - 125	250 - 300
150 - 200	125 - 150	300 - 500
200 - 300	150 - 200	500 - 800
>300	200 - 250	800 - 1000
	250 - 300	>1000
	>300	

To facilitate the calculation of attributes such as 'depth to bedrock' and 'thickness of gravel', 3 types of information were recorded in the GIS attribute tables. Firstly, the mapped units were differentiated based on their designation as alluvium or bedrock. These were then further subdivided into various sedimentary textures and/or bedrock types (e.g. limestone, siltstone, sandstone or basalt etc.). Finally, lithologies were further subdivided based on the dominant sedimentary texture (e.g. gravel, sand, silt and clay). No further subdivision of the bedrock units was undertaken.

To gauge the reliability of the pre-existing lithological data, pre-existing borehole lithological descriptions from 518 pre-existing boreholes across the project area were grouped into 8 simplified textural classes: i.e. clay, sand, silt, gravel, pebble, boulder, bedrock and others. Textural classes of the 9 interpreted lithological depth slices were compared to these simplified bore textural information across the specific depth intervals. Selection of depth intervals and the respective lithological description was carried out using ArcGIS. The matching and non-matching results with each texture across the depth intervals were tabulated (Table 18).

Overall, there are some relatively good correlations, despite the reliance on pre-existing descriptions of lithology from drill chips. The best matches between the borehole textural information and the interpreted lithological units attained scores of at least 80%, and included the two near surface depth slices from 2m to 4.2m and 4.2m to 6.7m. The lowest matches (50%) occur in the depth slice from 12.7m to 16.3m.

Table 18: *Percentages of matched and non-match between borehole texture and interpreted lithological units based on AEM depth slices.*

Depth slices m	Matched count	Total count	Matched %	Non Matching %
2 – 4.2	194	235	82	18
4.2 – 6.7	187	233	80	20
6.7 – 9.5	113	181	62	38
9.5 – 12.7	93	160	58	42
12.7 – 16.3	78	157	50	50
16.3 – 20.3	112	174	64	36
20.3 – 24.8	104	192	54	46
24.8 – 29.8	87	139	63	37
29.8 – 35.4	48	68	71	29

Factors that contribute to the poorer correlations between borehole lithological logs and interpreted units in some intervals include incomplete and/or biased sample returns from aircore drilling, and reliance on visual descriptions of chip materials only. Similarly, lithological descriptions from pre-existing drilling are of highly variable quality. The quality of this pre-existing information has compounded uncertainty in classifying textures in the alluvium. In particular, the interpretation of 'mixed' materials (e.g. silty sands) is often very subjective.

Scale is another key issue. For example, the SkyTEM system was deployed to map regional variations in conductivity, and the 200m+ line spacing will not map all local variability (see Section 3.6.13). Likewise, AEM systems in general are generally quite poor at resolving multiple thin layers. Moreover, it needs to be recognised that while borehole lithological logs represent a point of truth, the mapping scale used (1:100,000) has been tailored to map regional variations in conductivity. This makes it nearly impossible to incorporate all textural heterogeneity observed in closely spaced boreholes, with the result that variations within a local scale may not be incorporated in the mapped units. Furthermore, the thickness of the conductivity depth slices varies with depth, ranging from 2m near the surface to 5m at depth. The mapped textures are averaged across these depth intervals. Thus, a bed 1m thick, may be omitted from the mapping of a 5m thick conductivity depth slice at depth as it is too thin. For example, in the Knox Creek Plain there are thin gravel lenses up to 1m thick interlayered with thicker beds (2m to 3m thick) of silt and sand. In this case, the lithology has been mapped (grouped) as 'sand'. Taking another example, near the base of the alluvium, borehole data may indicate 1m of bedrock at the base of the 4m conductivity depth interval. However, in this case, the bedrock is unlikely to be identified in that layer, and has been mapped in the following depth slices instead. In summary, it is important to recognise that the lithology maps are generalised constructs, and thin interbeds or lenses in the alluvium are not necessarily mapped.

It is worth noting that due to time and resource limitations, the interpretation methods used in this study were more limited than in some previous studies (e.g. Lawrie *et al*., 2009a). For example, interpretation of the AEM dataset could have been improved through the interpretation of individual AEM flight lines using all available borehole data, in the same way that each conductivity depth section has been interpreted. Also, interpretation of elevation slices (relative to AHD) is generally preferred to the use of conductivity depth sections for interpreting hydrostratigraphy and groundwater salinity >5m below the land surface, (or below the water table). Such an approach is much more labour- and time- intensive, but could potentially resolve some of the more complex patterning that is observed in the AEM data with greater confidence. Such an approach is recommended in future studies (time and resources permitting).

4.2.2 Thicknesses of Lithological Units

Attributed lithological polygons were converted into grids using ArcGIS. The thicknesses were assigned according to the depth slice thickness, and range from 2.2m to 5.6m (Table 19). The lithological units were mainly mapped as full thickness, except at the base where sediment and bedrock constitute similar vertical proportions of the depth slice. In these instances, these sediment grids were assigned half the thickness of the depth slice.

Table 19: *Thickness of the depth slices used to attribute the lithological grids*.

Depth Slice	Thickness (m)
2 – 4.2 m	2.2
4.2 – 6.7 m	2.5
6.7 – 9.5 m	2.8
9.5 – 12.7 m	3.2
12.7 – 16.3 m	3.6
16.3 – 20.3 m	4
20.3 – 24.8 m	4.5
24.8 – 29.8 m	5
29.8 – 35.4 m	5.6

Clay and gravel units were individually extracted from attributed lithological polygons for each depth slice. Extracted polygons were converted into grids using ArcGIS. Thicknesses were assigned to each grid according to the depth slice thickness, ranging from 2.2m to 5.6m (Table 19). The lithological units were primarily mapped as full thickness, except those where sediment and bedrock were mapped as one class in the same polygon. In this instance, the sediment grids were assigned as half the thickness of the depth slice, and an average taken from borehole lithological descriptions. For example, when a polygon was mapped as gravel/bedrock with a thickness of 5.6m, the total thickness of the gravel was taken as 2.8m. To determine the total thickness of clays and gravels, the thickness grids of each texture unit from each depth interval were summed.

4.2.3 Depth to Bedrock

Where bedrock was identified in the depth slice, the top depth was assigned to the bedrock units (Table 20). The lithological units were primarily mapped as full thickness, except where sediment and bedrock were mapped as one class in the same polygon. In this instance, the sediment grids were assigned as half the thickness of the depth slice. For example, depth to bedrock was assigned at 32.6m in the depth slice 29.8m to 35.4m where sediment (e.g. gravel) is underlain by bedrock.

To obtain the depth to bedrock, the bedrock units were extracted from each lithological extent map. Each layer was attributed with its depth, and all layers were combined such that the shallowest depth to bedrock appeared on top. The final polygon shape file was gridded in ArcGIS.

Table 20: *Attributed depth to bedrock for each depth slice.*

Depth Slice	Attributed depth to Bedrock (m)
2 – 4.2 m	2
4.2 – 6.7 m	4.2
6.7 – 9.5 m	6.7
9.5 – 12.7 m	9.5
12.7 – 16.3 m	12.7
16.3 – 20.3 m	16.3
20.3 – 24.8 m	20.3
24.8 – 29.8 m	24.8
29.8 – 35.4 m	29.8

4.2.4 Interpretation of Depth to Bedrock on Conductivity Cross-sections

The first step carried out was the production of synthetic profiles along the 30 O'Boy *et al*. (2001) cross sections. These were generated from the AEM data using the Aarhus Workbench package. Because the areal extent of this project is more limited that that of the previous study, AEM data on some of these lines are more restricted. Cross-sections in the NT were also excluded from this study (specifically sections R-R', S-S', T-T' and a-a').

The surface profile was generated using the SRTM data. The vertical data were plotted at a vertical exaggeration of 1:100 (the same that was used by O'Boy *et al*. (2001), with a horizontal scale of 1:100,000 used. A fixed conductivity stretch was applied to the AEM data (i.e. from 0-300mS/m). Subsequently, bores on or near these lines were plotted from the WINSITE (WA borehole) database. Not all the borehole data used by O'Boy *et al*. (2001) were available in the WINSITE database, so the borehole control in this study is more limited. However, a thorough assessment of the pre-exiting lithology has resulted in simplified textural classification that has assisted in map interpretations.

To interpret the cross-sections, individual borehole interpretations were compared with the conductivity data. Interpreting AEM cross-sections is inherently more difficult than using conductivity depth slices, as there is no unique signature for each lithology, and the interpreter does not have the benefit of the spatial 'geomorphic' or 'sedimentary facies' patterns often evident in conductivity depth slices. To ensure consistency in interpretation, the interpreted depth was cross-checked against the AEM depth slices for obvious contradictions. These results are shown on a section-by-section basis in Section 6, and compared directly with the sections in O'Boy *et al*. (2001). The depth to bedrock was interpreted from each section, on the basis of the best fit of borehole and AEM data.

4.3 VEGETATION VIGOUR (NDVI) MAPS

Vegetation indices are effective measures of vegetation features on the Earth's surface through the use of different band combinations. Vegetation's response to the electromagnetic spectrum is influenced by factors

such as difference in chlorophyll content, nutrient levels, water content and underlying soil characteristics (Zhao *et al.,* 2009). The Normalised Difference Vegetation Index (NDVI) is an image transform that uses the reflective signature contrast between the near infrared (NIR) and visible red (VIS) wavelengths (Elmore *et al.,* 2000). In the case of Landsat 5 Thematic Mapper (TM) imagery, the respective wavelengths occur at Band 4 (0.76-0.90μm) and Band 3 (0.63 – 0.69μm). The NDVI is given by Equation 1. Values range from -1 to 1; NDVI values are close to zero in the absence of green leaves.

$$NDVI = \frac{NIR - VIS}{NIR + VIS} \qquad \text{Equation 1}$$

NDVI is widely accepted as an indicator of vegetation health and vigour. The advantage of NDVI is that it can partly eliminate some effects of the solar zenith angle, sensor's observing angle, and atmospheric conditions (Kaufman & Tanre, 1992). However, NDVI has the limitation that the index is sensitive to both atmospheric aerosols (Holben, 1986) and soil background (Lillesaeter, 1982). Also, when vegetation cover is more than 80% NDVI will saturate (Huete, 1985).

In this study, cloud-free Landsat 5 TM imagery for the 30th March 2009 was acquired from the ACRES database which was used for the resultant NDVI grid. All QA/QC measures were carried out by the ACRES staff to ensure a quality image.

An NDVI algorithm was used to transform the Landsat imagery into a grey scale image. The brightest pixels indicate high vigour and the darkest low vigour. The image was then brought into ArcGIS and a grid was created whereby values of the resultant grid were then divided into 7 classes (legend), based on differentiation of known features such as bedrock, water and bare ground (from irrigated areas).

The resultant image (Figure 83) was visually assessed against the original Landsat imagery, SPOT imagery, geomorphology and vegetation layers via the use of the vegetation signatures, assumed vegetation density and structure for better accuracy and consistency.

Data have been checked visually on plots and for consistency using in-house routines and Arc/Info GIS software. As much as possible, every effort has been made to ensure that the accuracy and standards have been maintained.

4.4 PERSISTENCE OF SURFACE MOISTURE MAPS

Four LANDSAT images of the Ord River area were acquired:

1. 2nd August 2008 which was considered as a 'dry' image because it occurred 5 months after any significant rainfall and 4 months before the next rain season.
2. 14th March 2009 which was considered as a 'wet' image because it occurred 1-2 weeks after significant rainfall (cloud cover left of image).
3. 30th March 2009 which was considered as a 'wet' image because it occurred about 1 month after significant rainfall.
4. 20th July 2009 which was considered as a 'dry' image because it occurred nearly 5 months after significant rainfall (some cloud in top left of image).

Wetness Index

A wetness detection wizard (Tasselled cap RGB) using ERMapper was used to define three bands (from images containing 7 bands): brightness, greenness (vegetation), and wetness (moisture). The wetness index calculation from the RGB wizard is based on the normalised difference moisture index (NDMI) but modified where the tasselled cap uses the sum of SWIR. The NDMI uses the near infrared (NIR) (band 4) and the shortwave infrared bands (SWIR) (or just band 5) (Jin & Sader, 2005):

$$\text{NDMI} = \frac{\text{NIR}(4) - \text{SWIR}(5)}{\text{NIR}(4) + \text{SWIR}(5)}$$

The tasselled cap RGB wizard applies the following equation to generate a wetness index (WI) from an image:

$$WI = Band1 \times 0.1509 + Band2 \times 0.1973 + Band3 \times 0.3279 + Band4 \times 0.3406 + Band5 \times -0.7112 + Band6 \times -0.4572$$

A mask was applied to the wetness image within ArcMap using the DEM for the Ord area. Any data values that were at 30m elevation or higher were excluded from the map. The reason for this exclusion was due to errors arising from aspect shadows being identified as wetness. The resulting wetness image was then used to display areas of more or less wetness.

Thresholds were applied to show areas of differing wetness. Typically a value of zero or greater was used to indicate that an area was fully saturated, i.e. extremely wet. Areas with a wetness value of below zero (negative values) were interpreted either as damp soils, or due to vegetation in standing water. Decreasing values indicate drier soil and/or vegetation conditions.

Thresholds were chosen according specifically to the site where irrigation dates and water bodies were known so the values of wetness could be determined accordingly.

From this, the following classification was derived:

>-5	Ponded water or open water body (extremely wet).
-5 – -15	Very wet vegetation or soil (or vegetation in standing water).
-15 – -25	Moist vegetation or soil.
-25 – -40	Drying vegetation or soil.
>-40	Dry vegetation or soil.

Wetness indices were not calculated for Parry's Lagoon for the date 14th March 2009 due to the interference of cloud in that area of the image.

ArcMap was used to create a map showing all four areas of wetness on one map as well as 'common wet areas' between all combinations of dates (Figure 84). This helped to identify areas of similar wetness at different dates. The same was done a second time, with the exception of the 14th March 2009 dataset which was excluded due to the cloud interference in part of the image.

4.5 WATERTABLE LEVEL MAP

The watertable image was generated from water level data collected from piezometers across the entire project area at the time of survey (Figure 85). A smaller sub-set of the bores than was used for the lithological analysis was accessible (as most exploration holes have been filled in). The borehole data used to construct the watertable map are contained in Appendix 10 (Cullen *et al.,* 2010).

The watertable data were converted to a Reduced Standing Water Level (RSWL) relative to Australian Height Datum (AHD) (Figure 85). The RSWL data were gridded using a minimum curvature algorithm with 200m cell size and extrapolated to the extent of the airborne geophysical survey area. Areas of outcrop identified on the geomorphological map were excised from the modelled surface, so the watertable was representative of that in the alluvial aquifer. The modelled surface was then subtracted from the SRTM DEM data to produce the regional depth to water table image (Figure 86).

The resulting watertable map was then compared with the water level surfaces generated for 2005-06 (the most recent dataset available) for the ORIA Stage 1 area (Smith, 2008). As can be seen from comparison of the two maps (Figure 87), there is generally a very good comparison between these products. The Smith (2008) study only includes data with a long record of observations to enable temporal comparisons to be made, whereas the surface generated in this study included measurements in bores from the recent drilling campaign as well as bores without such a long record of measurements. As such, the watertable level map produced in this study is simply a snapshot in time (at the time of AEM survey).

Using these data linked to a map of basement elevation, the conductivity model can then be sliced to yield maps of the average conductivity from surface to the watertable (the unsaturated zone conductivity) (Figure 88). The same approach can be used to produce maps of conductivity below the water level at various intervals, including maps of the average conductivity for the full extent of the saturated alluvium (see Figure 89 to Figure 97).

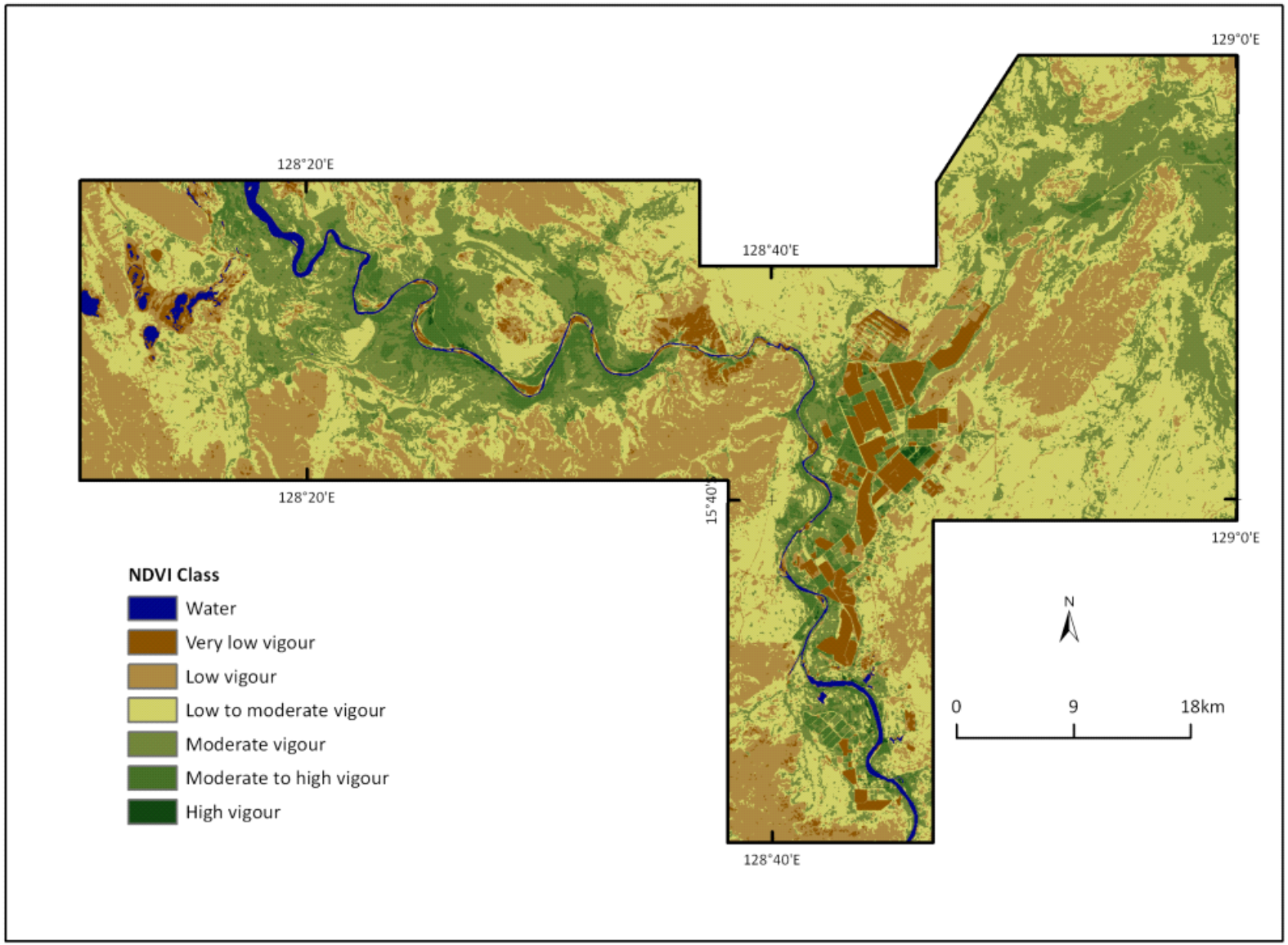

Figure 83: *NDVI for the project area. The image shows moderate to good vegetation vigour in most of the Stage 2 areas, in accordance with increased rainfall over the past decade.*

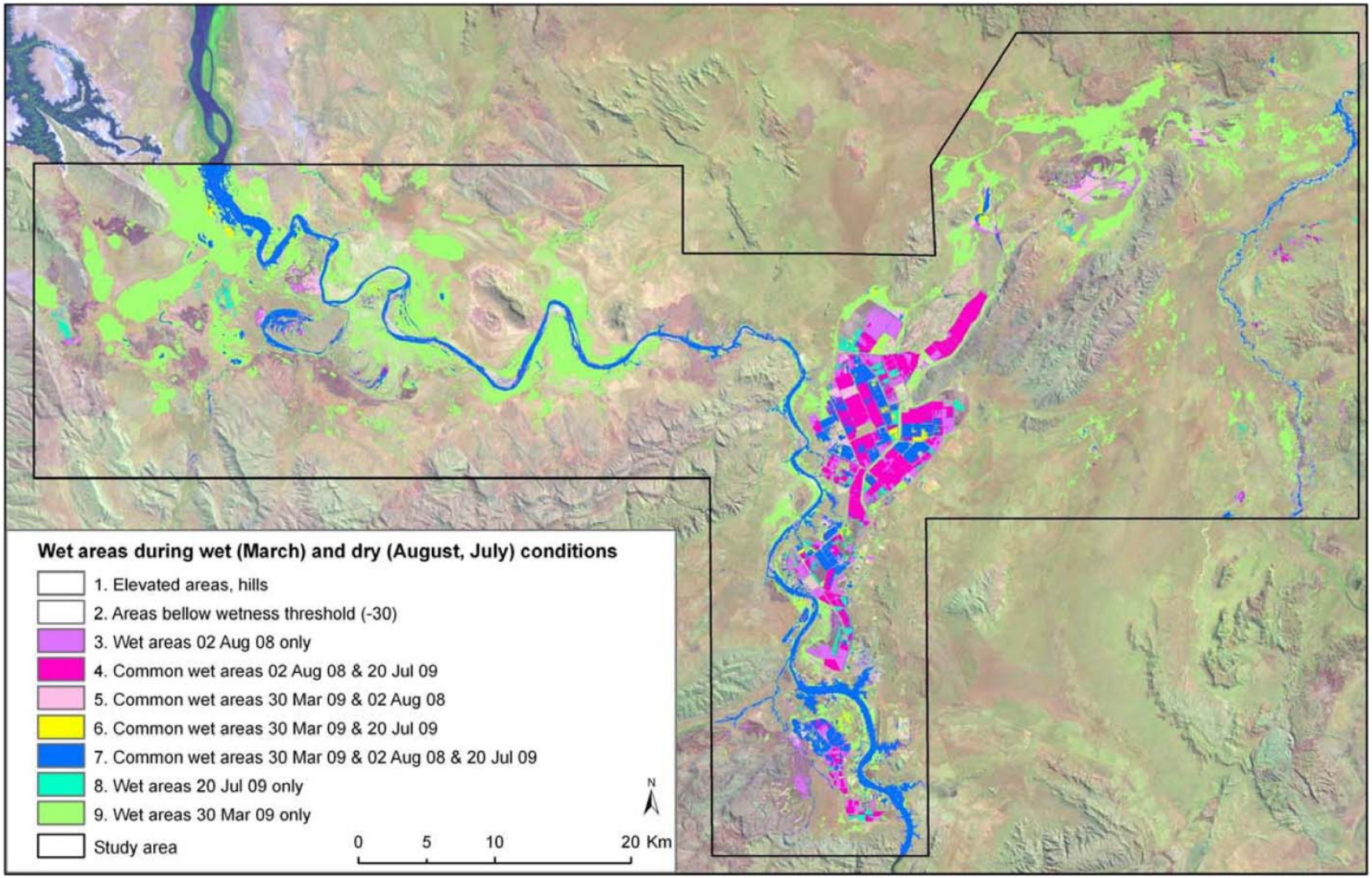

Figure 84: *Wet areas during wet and dry seasons (from Landsat 5TM). Note that, apart from irrigated areas, the lower parts of the alluvial plains remain wetter for longer than higher parts.*

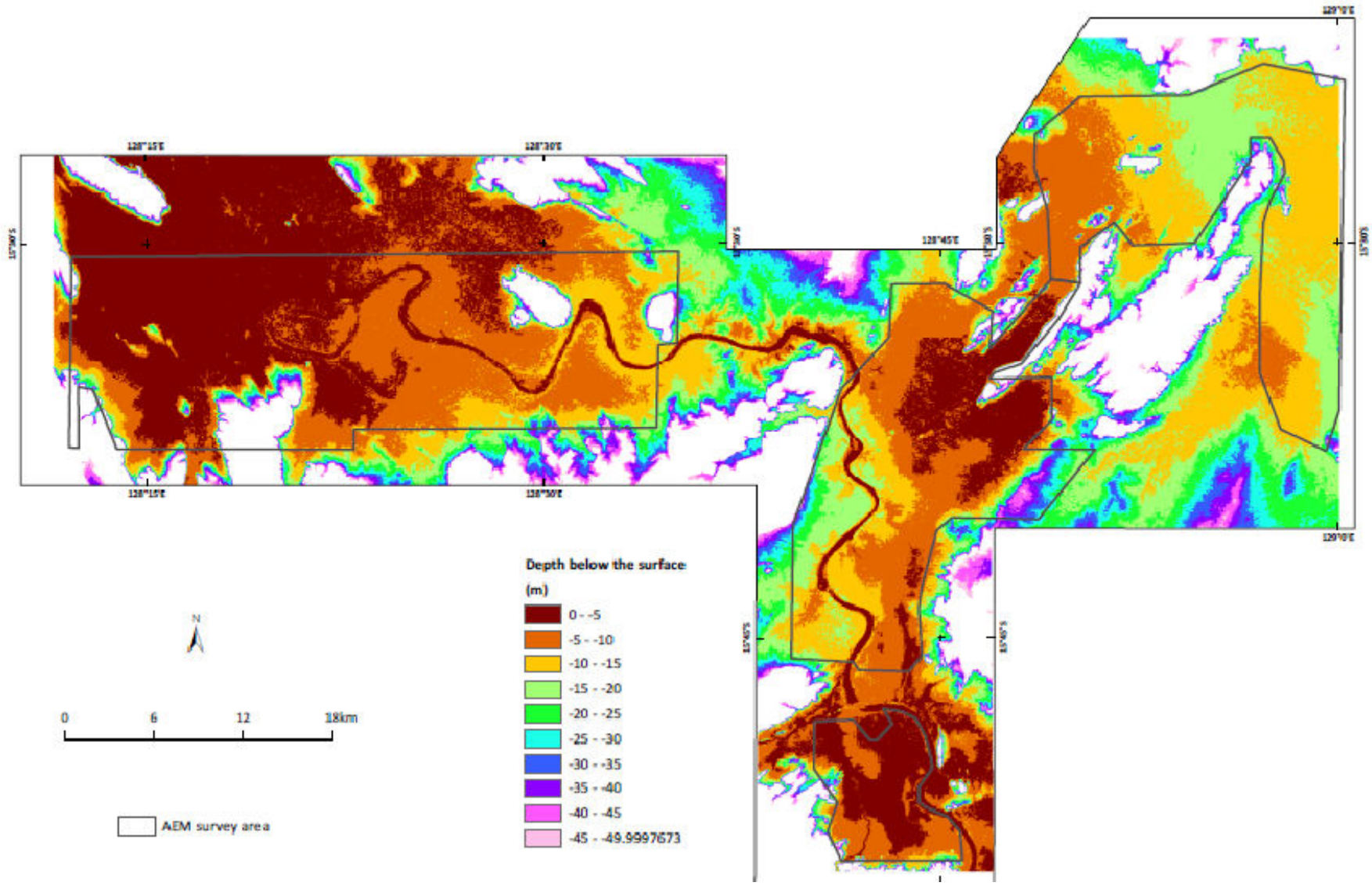

Figure 85: *Depth to groundwater in the alluvial aquifer at the time of the survey. The distribution of borehole and water sampling points used to construct the watertable map are shown in Figure 16*

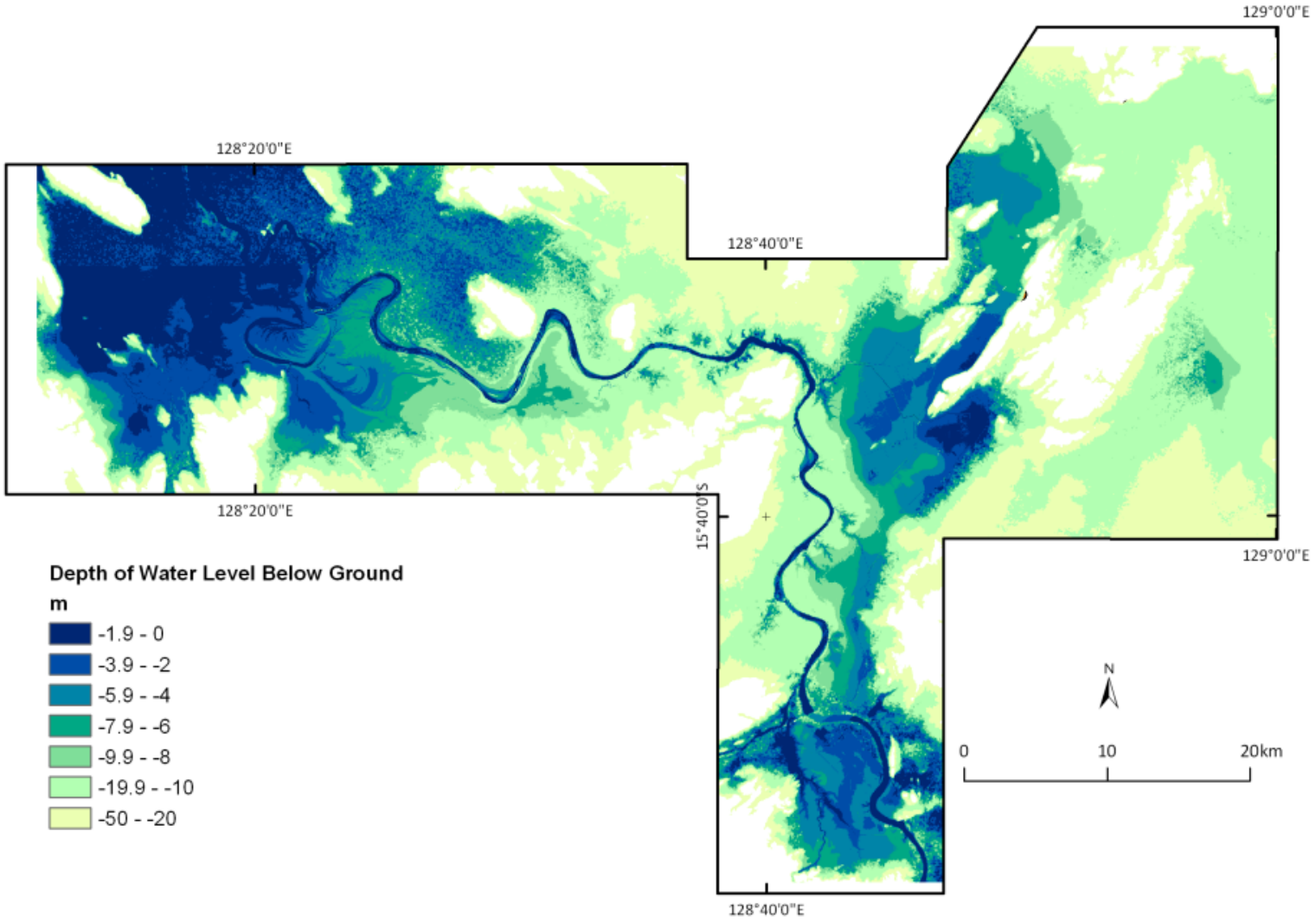

Figure 86: *Depth of watertable below surface in the alluvial aquifers, derived by adjusting the regional water table to take account of surface elevation. The distribution of borehole and water sampling points used to construct the watertable map are shown in Figure 16. This map is a smoothed version of the previous figure.*

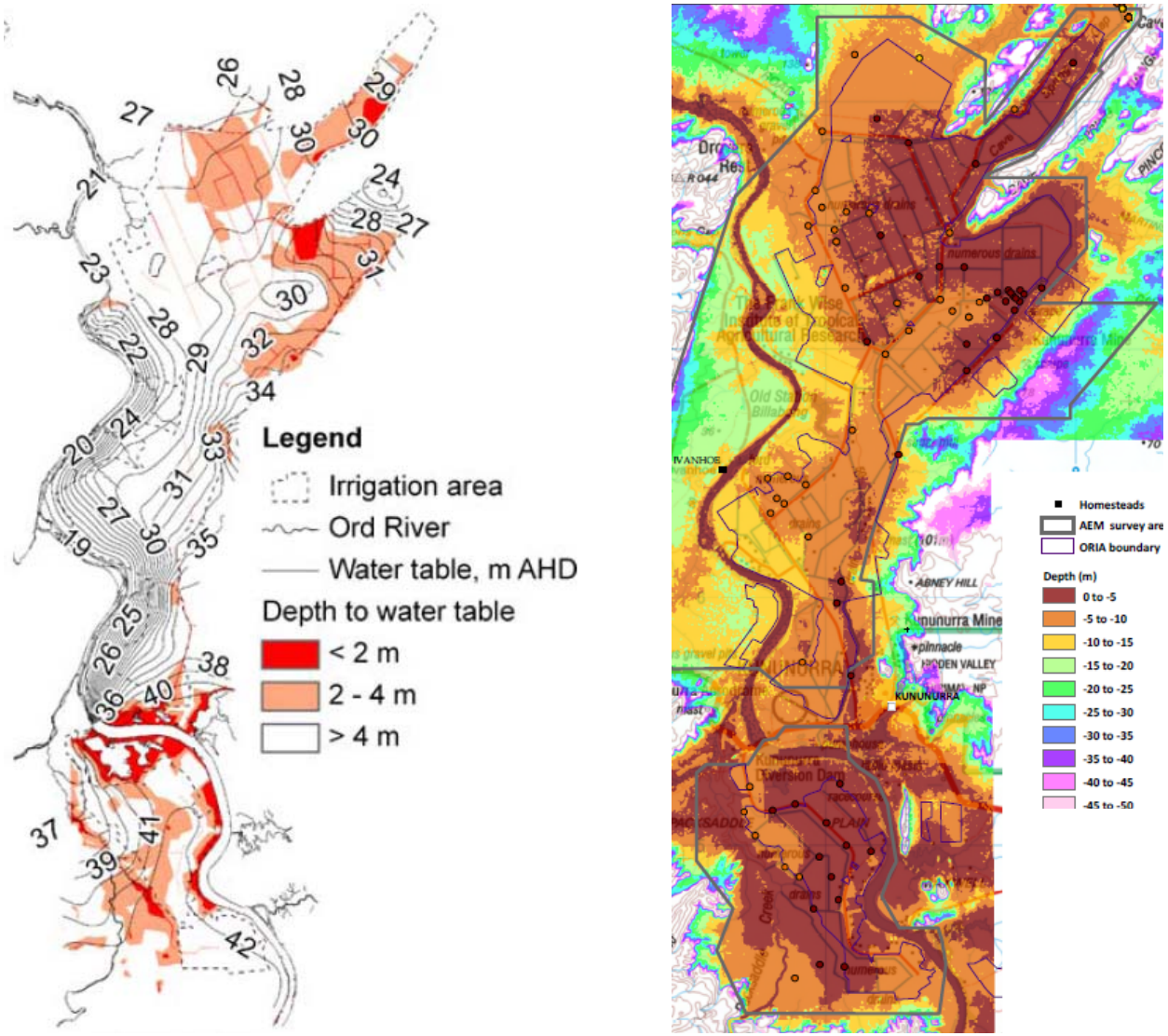

Figure 87: *The figure on the left is the mean annual watertable interpolated below ground for July 2005 to June 2006 for ORIA Stage 1. Contours are based on water level measurements from 65 monitoring sites (from Smith, 2008). The image on the right is the regional water table produced in this study for August 2008. Comparisons show good correlations, although the regional watertable map (on right) does not have the same depth resolution, and there is a 2-3 year time difference in the data used to draw the surfaces.*

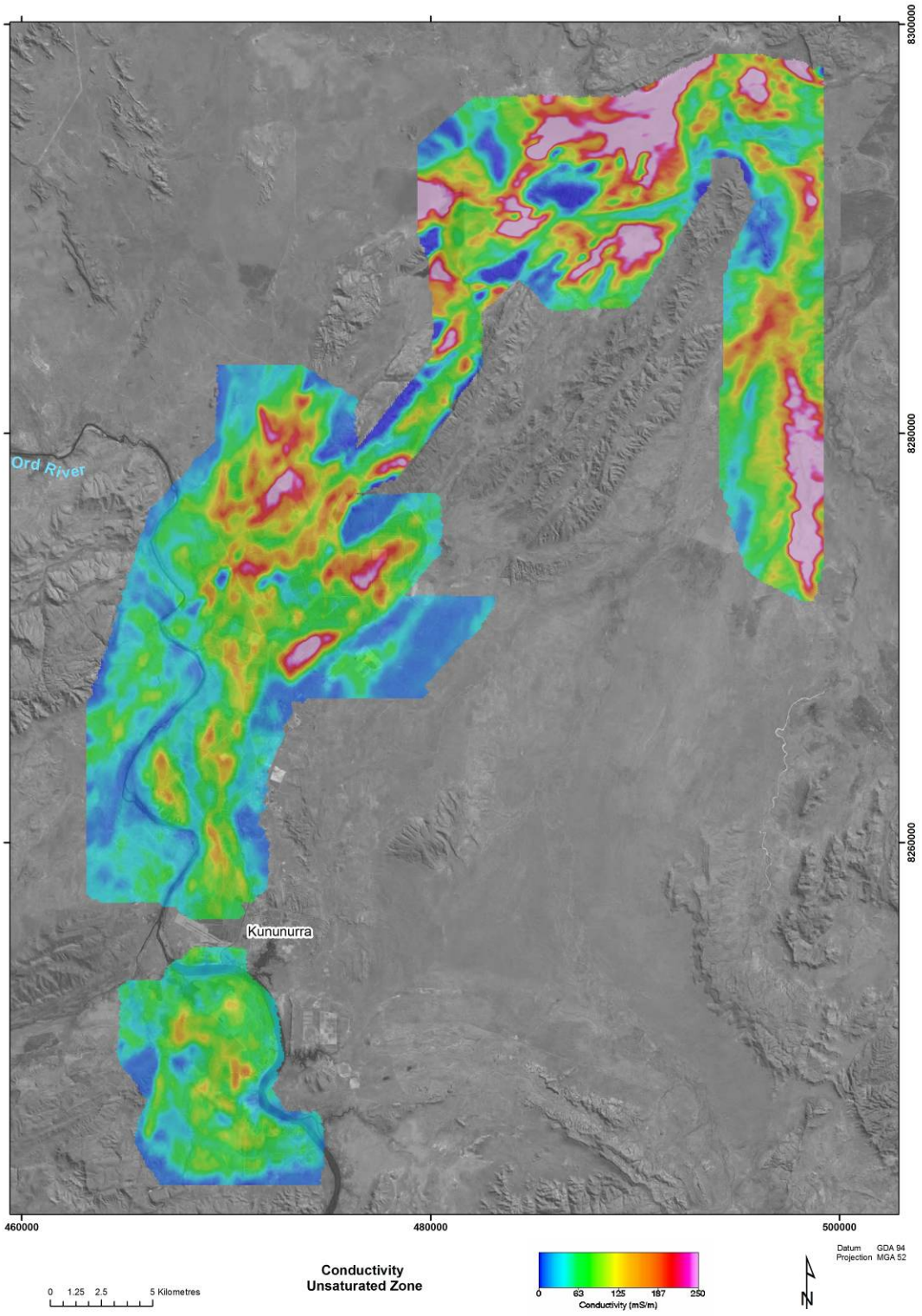

Figure 88: *Average conductivity of the unsaturated part of the alluvial aquifer – ORIA and Keep River areas.*

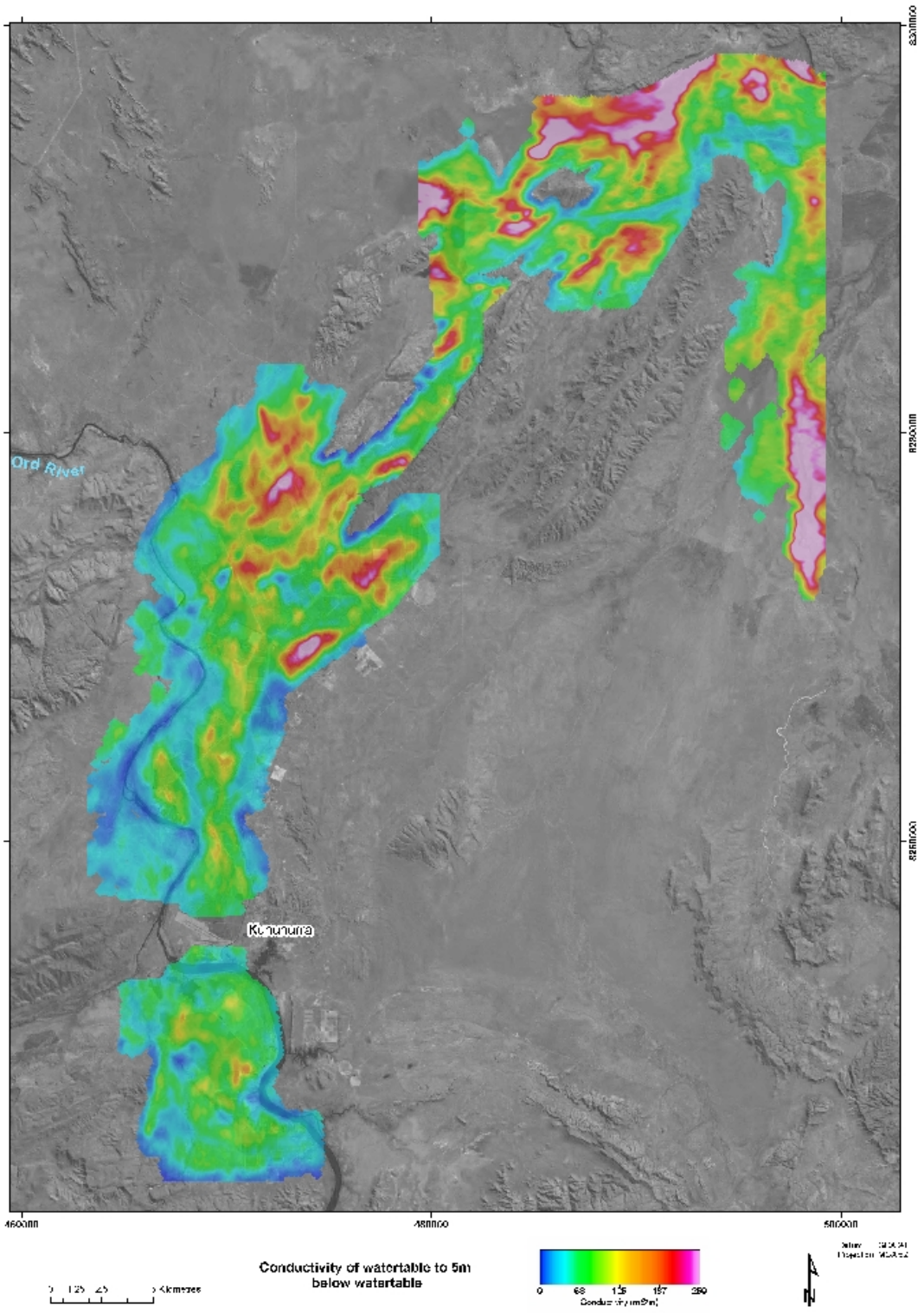

Figure 89: *Average conductivity for a 5m slice beneath the watertable in the alluvial aquifer – ORIA and Keep River areas. Extent has been clipped to exclude areas of basement.*

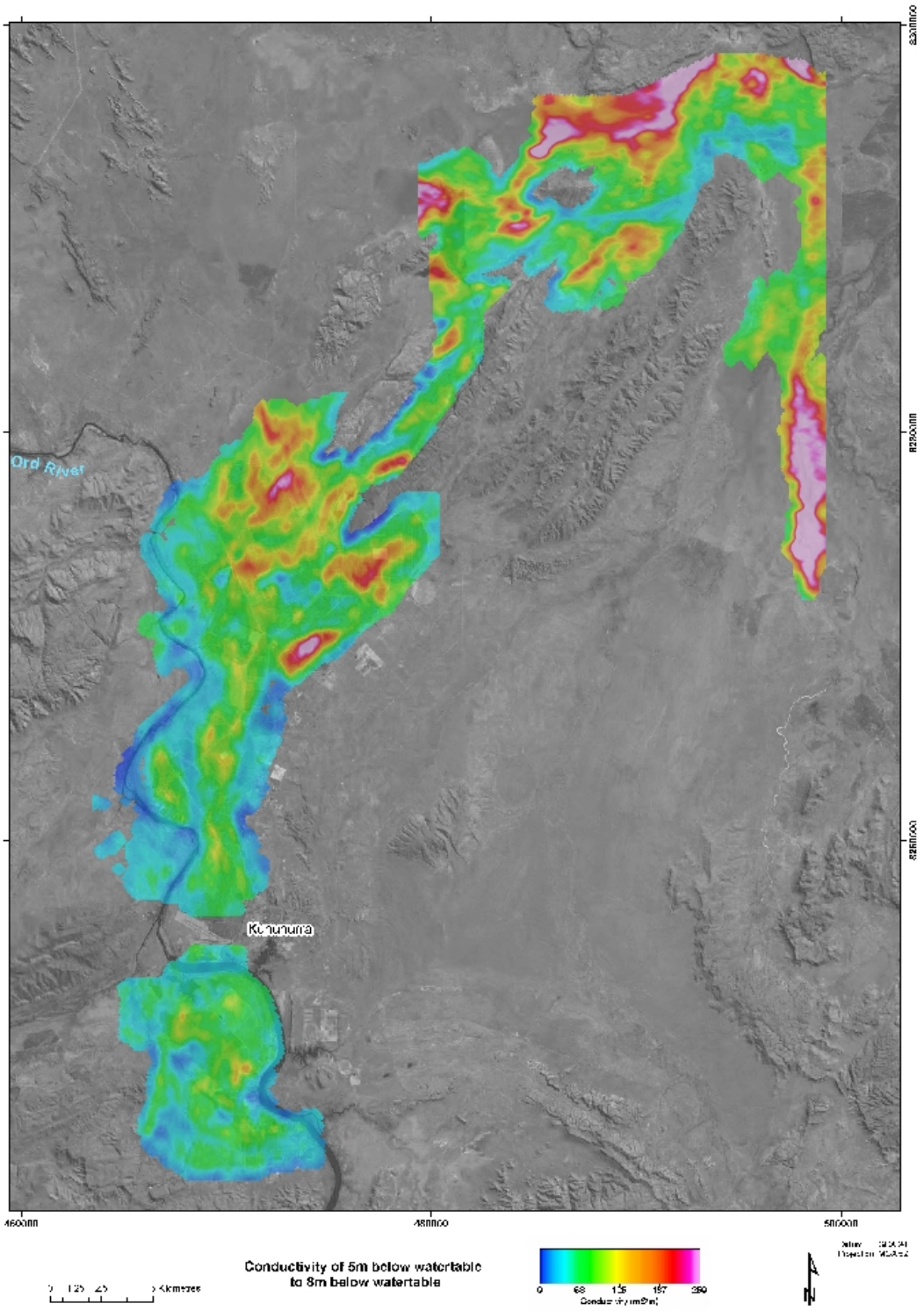

Figure 90: *Average conductivity for a depth interval 5-8 m beneath the watertable in the alluvial aquifer – ORIA and Keep River areas. Extent has been clipped to exclude areas of basement.*

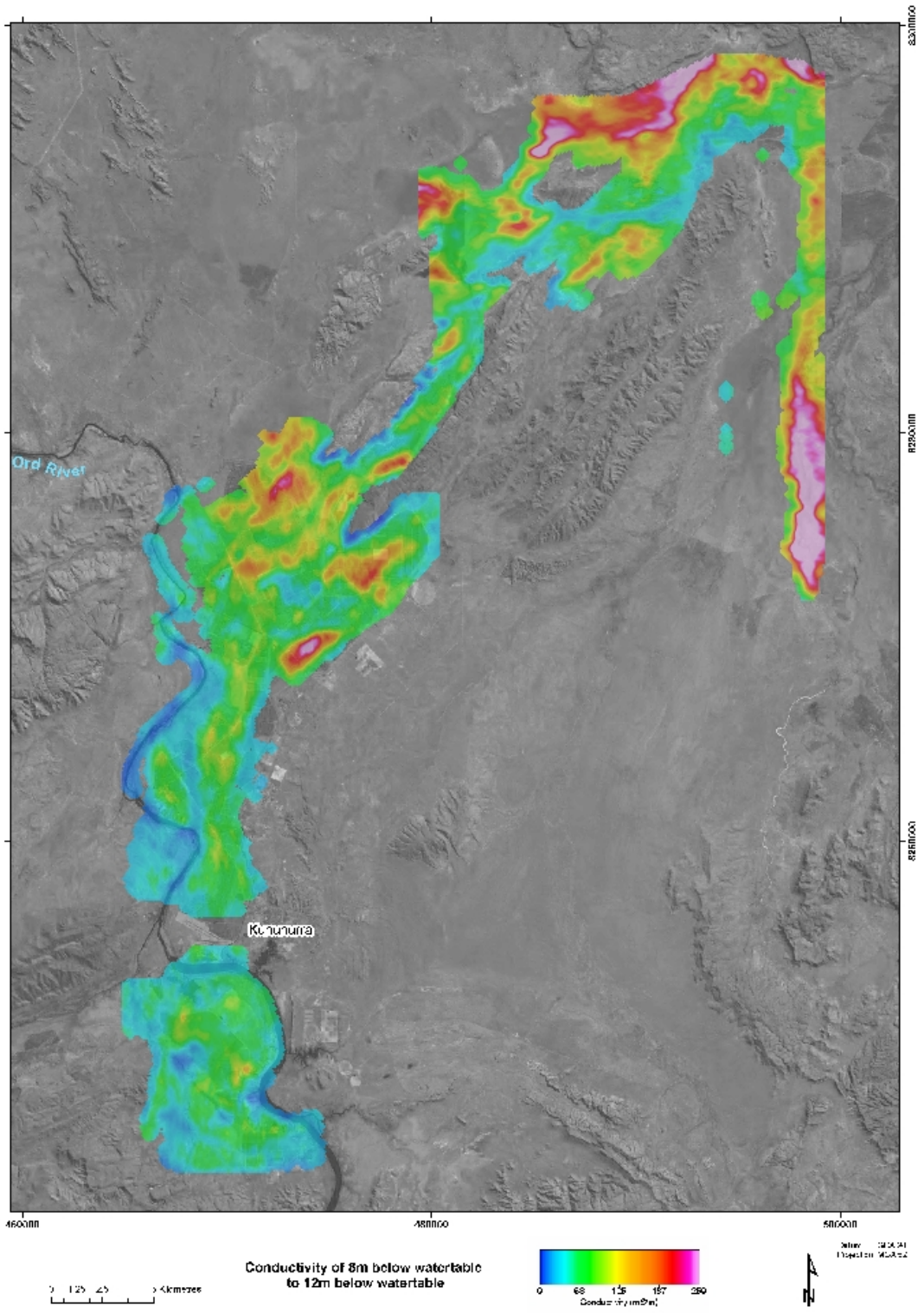

Figure 91: *Average conductivity for a depth interval 8-12m beneath the watertable in the alluvial aquifer – ORIA and Keep River areas. Extent has been clipped to exclude areas of basement.*

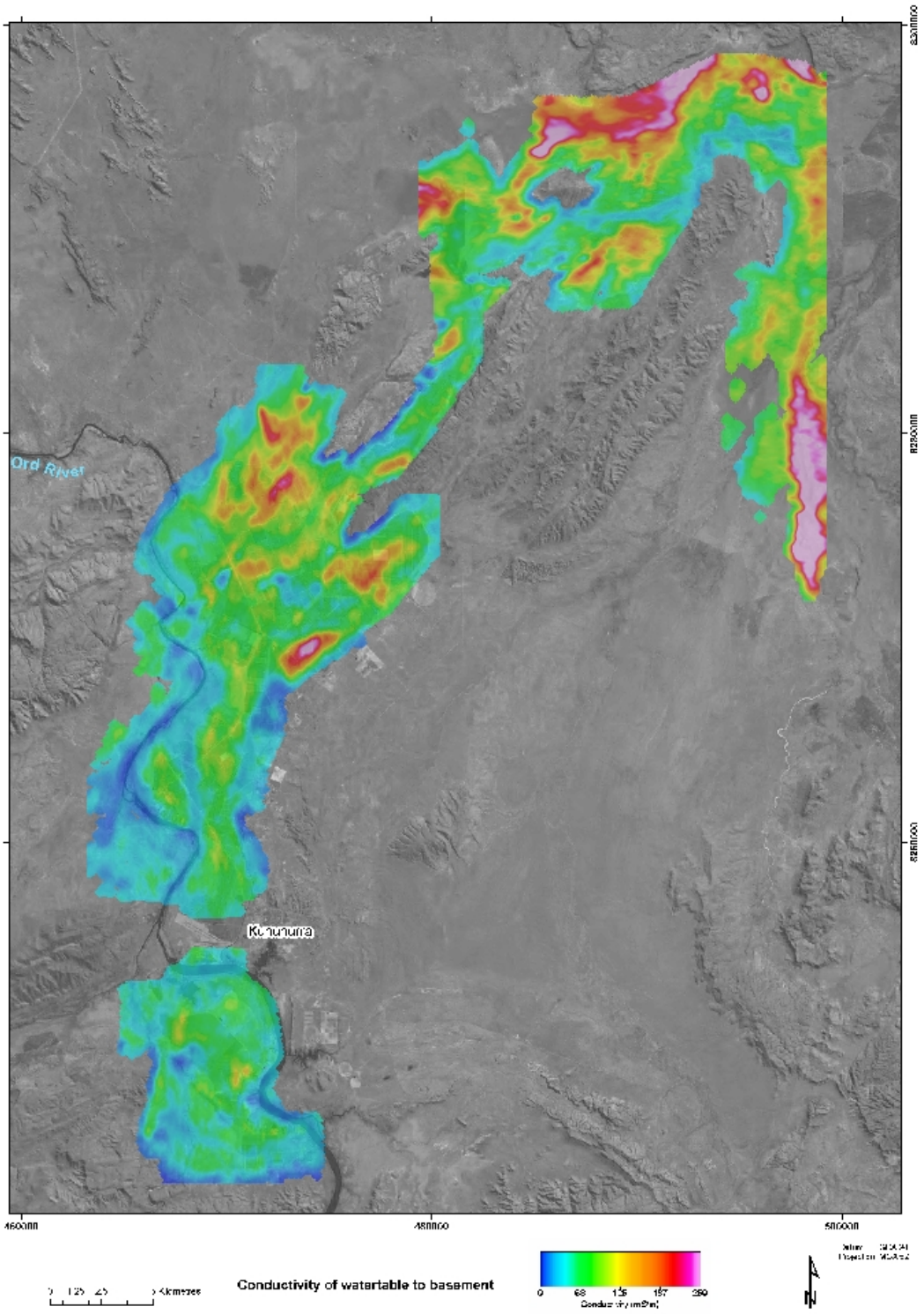

Figure 92: *Average conductivity for a depth interval from the watertable in the alluvial aquifer to basement – ORIA and Keep River areas. Extent has been clipped to exclude areas of basement.*

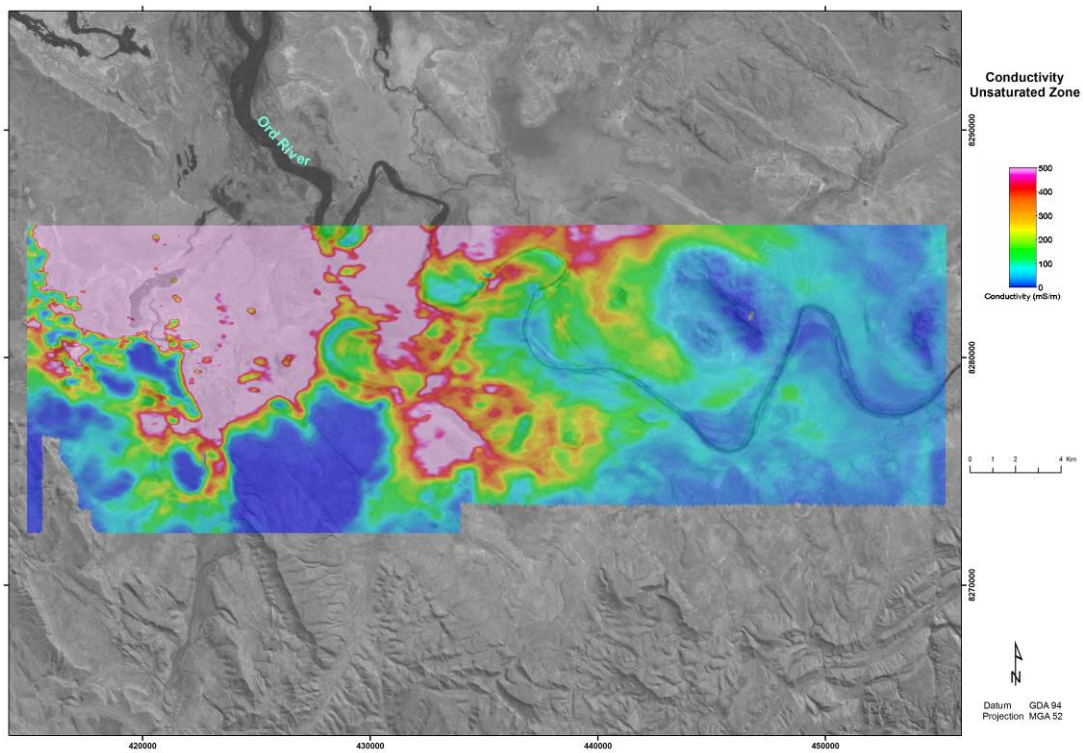

Figure 93: *Average conductivity of the unsaturated part of the alluvial aquifer – Parry's Lagoon.*

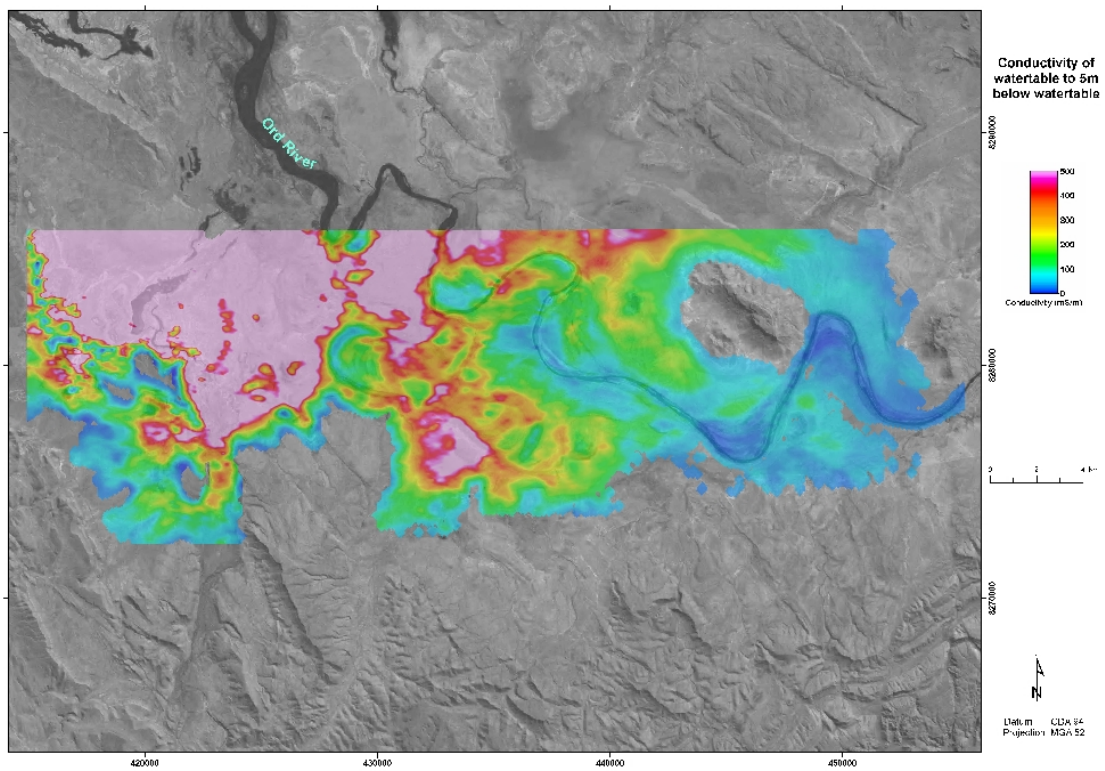

Figure 94: *Average conductivity for a 5m slice beneath the watertable in the alluvial aquifer – Parry's Lagoon. Extent has been clipped to exclude areas of basement.*

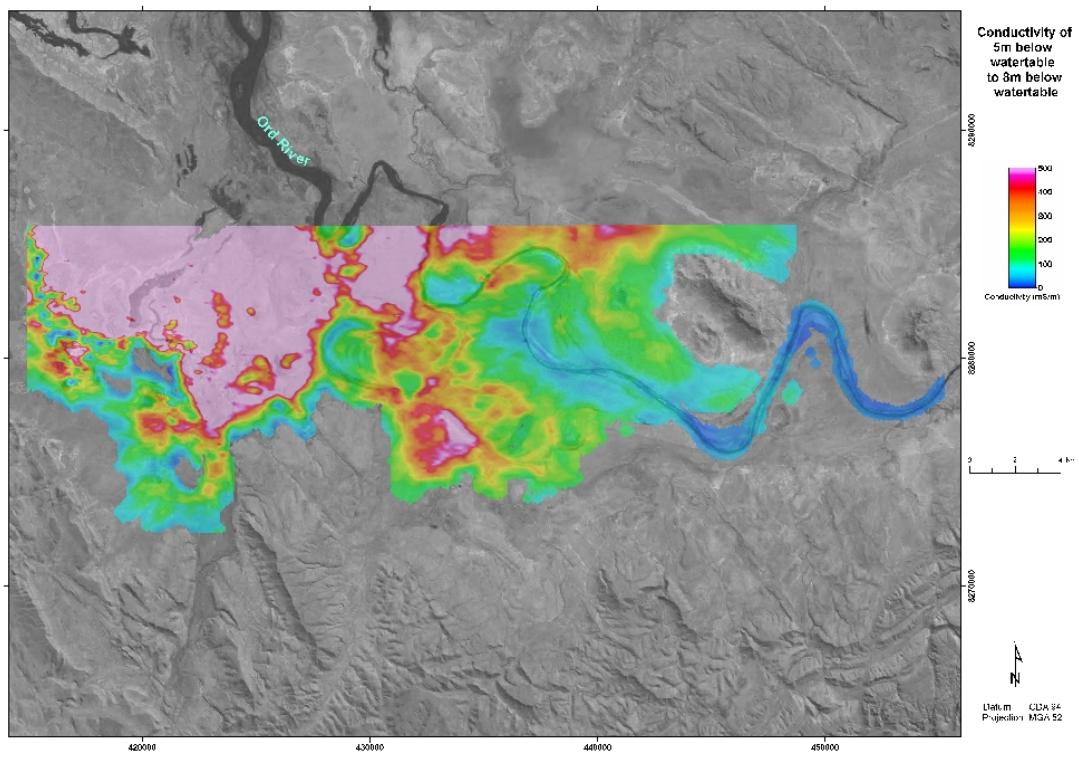

Figure 95: *Average conductivity for a depth slice 5-8m beneath the watertable in the alluvial aquifer – Parry's Lagoon. Extent has been clipped to exclude areas of basement.*

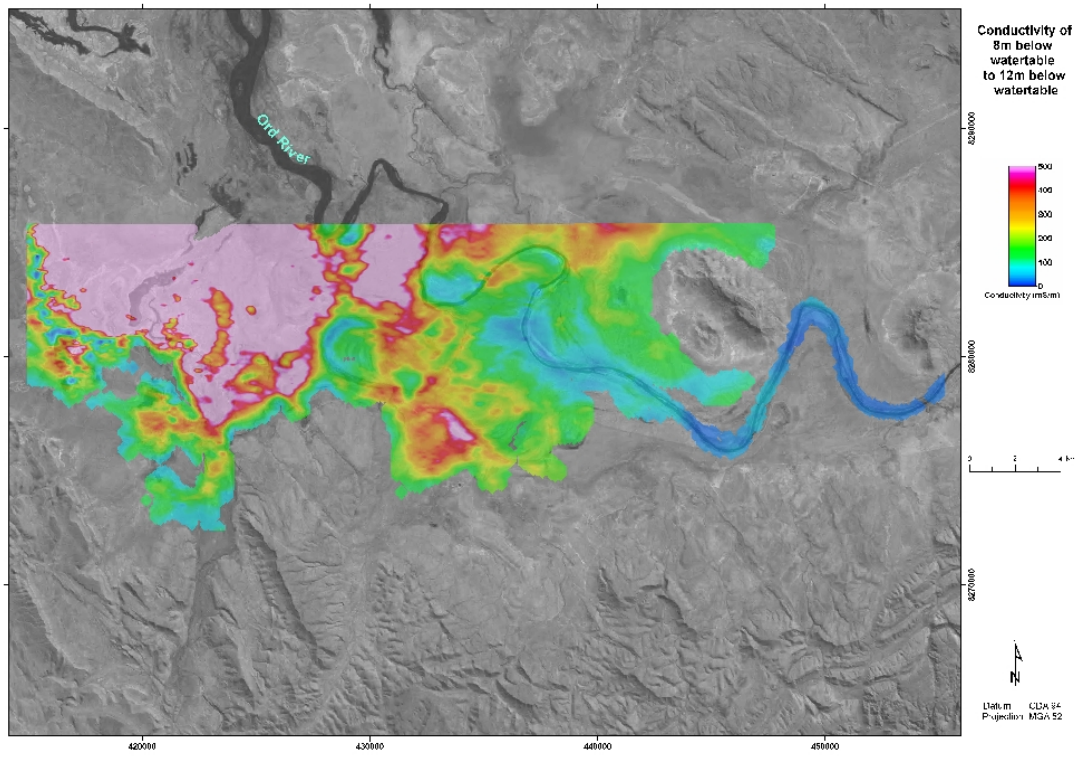

Figure 96: *Average conductivity for a depth slice 8-12m beneath the watertable in the alluvial aquifer – Parry's Lagoon. Extent has been clipped to exclude areas of basement.*

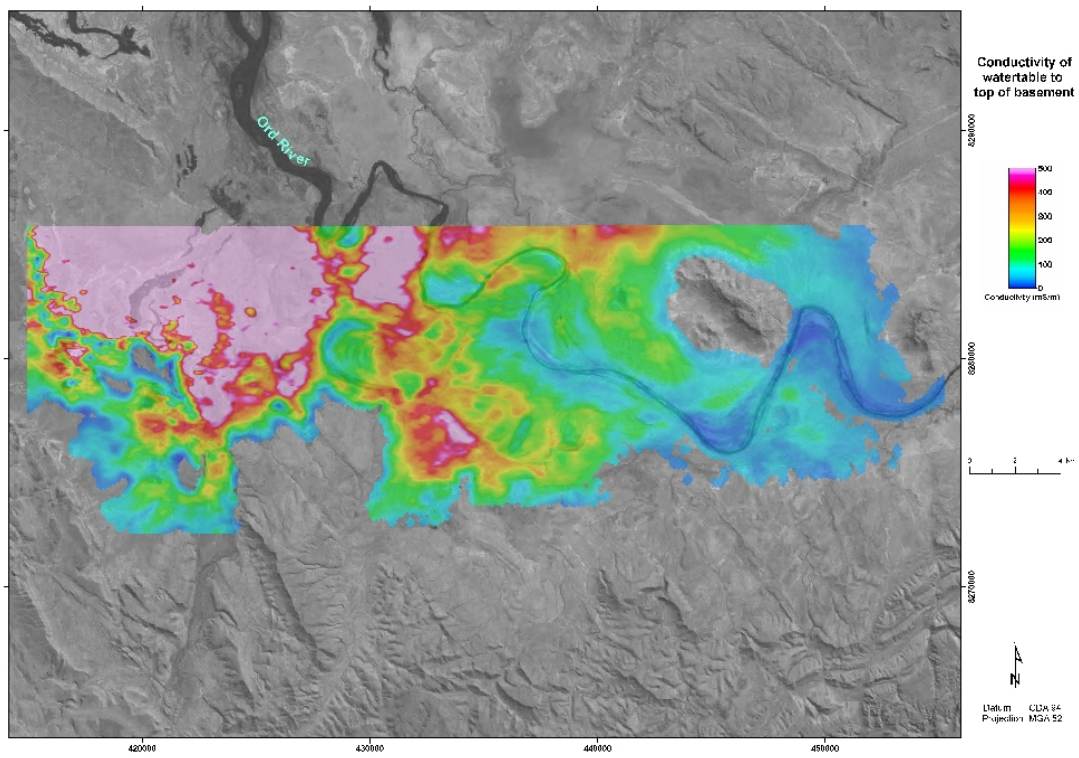

Figure 97: *Average conductivity for a depth interval from the watertable in the alluvial aquifer to basement – Parry's Lagoon. Extent has been clipped to exclude areas of basement.*

4.6 SURROGATE MAPPING APPROACHES FOR DETERMINING RECHARGE

A recent review of global groundwater recharge (Scanlon *et al.,* 2006) found that average recharge rates estimated over large areas (10s to 100s of km^2) range from 0.2 to 35mm per year, representing 0.1–5% of long-term average annual precipitation. They also noted that local variability in recharge, with rates up to 720m per year, results from focussed recharge beneath ephemeral streams and lakes and preferential flow mostly in fractured systems. These observations apply to the Ord study area, where rates may be highly variable, especially laterally along palaeochannels and other places where permeability is high.

When discussing recharge estimation, it is important to ensure consistent and correct terminology is used (see Sophocleous, 2004; Pain *et al*., 2010). In the past, the term 'recharge' and other terms such as 'deep drainage', have often been interchanged and used incorrectly. Walker *et al.* (2002) used the terms 'deep drainage', 'recharge' and 'potential recharge' to clarify this. De Vries & Simmers (2002) and Scanlon *et al.* (2002) also defined terms that describe types of recharge. For the purpose of this work, we adopt their definitions:

Recharge is the amount of infiltrated water that reaches a specific groundwater system.
Deep Drainage is the flux of water that moves past the root zone of vegetation. Deep drainage becomes recharge only when no impeding layers exist that would prevent water from moving down to the groundwater system.
Potential Recharge (Deep Drainage) becomes future recharge. Where a change of land use occurs, a time delay occurs for the recharge associated with the new land use to reach the water table.
Diffuse (Direct) Recharge is water added to the groundwater system in excess of soil-moisture deficits and evapotranspiration by direct vertical percolation through the vadose zone.
Indirect Recharge is percolation to the water table through the beds of surface-water courses.
Localized (Focussed) Recharge is an intermediate form of groundwater recharge resulting from the horizontal (near-) surface concentration of water in the absence of well-defined channels.

The absence of key input data at appropriate scales, notably soils, sub-soil, land use and vegetation data at appropriate scales, meant that it was not possible to produce groundwater recharge maps using recognised

approaches. Instead, surrogate approaches, described below, have been used to produce a suite of derived products.

Various mechanisms contribute to recharge (Figure 98). The floodplains in the Stage 1 and Stage 2 areas earmarked for development are dominantly cracking clay soils (Figure 99 to Figure 101). Crack depths appear to vary significantly, with ranges of up to 1.5m recorded previously (Kinhill, 1999), although cracks of 2-3m depths and up to 20cm wide were observed in this study in the Weaber Plain.

Analysis in other studies (Pain *et al.,* 2009) suggests that recharge will continue through filled cracks at reduced rates even when the cracks are filled. It is important to differentiate between cracks that are closed through swelling (low recharge potential), and those that are closed through infilling by other materials (higher recharge potential). The nature, intensity and duration of flow and/or rainfall events may be important in determining recharge through these crack networks, even in more natural landscapes. In high intensity rainfall events, cracks may not have time to seal, and significant flow may bypass soils and subsoils. This is particularly important where cracks extend through clay units to underlying sand units, and may in part account for the correlation between increased intensity and amounts of rainfall and rising water tables in some Stage 2 areas.

Smith *et al*. (2005) and Smith (2008) recognised the links between rainfall fluctuations, recharge and hydrograph response in the ORIA Stage 1. Smith (2008) found that rapid infiltration and groundwater accession following individual irrigation events occurs predominantly through the soil macropore system, and that contemporary wet-season accession in the ORIA is equally, if not more, important than dry-season accession (Figure 102).
Analysis in this study of hydrographs in the Weaber and Knox Creek Plains (Section 8.4) suggests that much higher pre-clearing recharge rates are possible in similar soils, and is dependent on the intensity and magnitude of rainfall events in the wet season.

There are very few data on infiltration rates or saturated hydraulic conductivity for the ORIA. Experiments carried out in the 1940s show that the rate of infiltration varies considerably between different soils (Figure 103). The permeability maps are based on soils data provided by the Department of Agriculture and Food, WA. Each soil map unit was attributed with saturated hydraulic conductivity (Ksat; Table 22) and clay percent values (Table 23) for each horizon. These values are estimated from the field texture of the soil horizons, as shown in Table 22 and Figure 104.

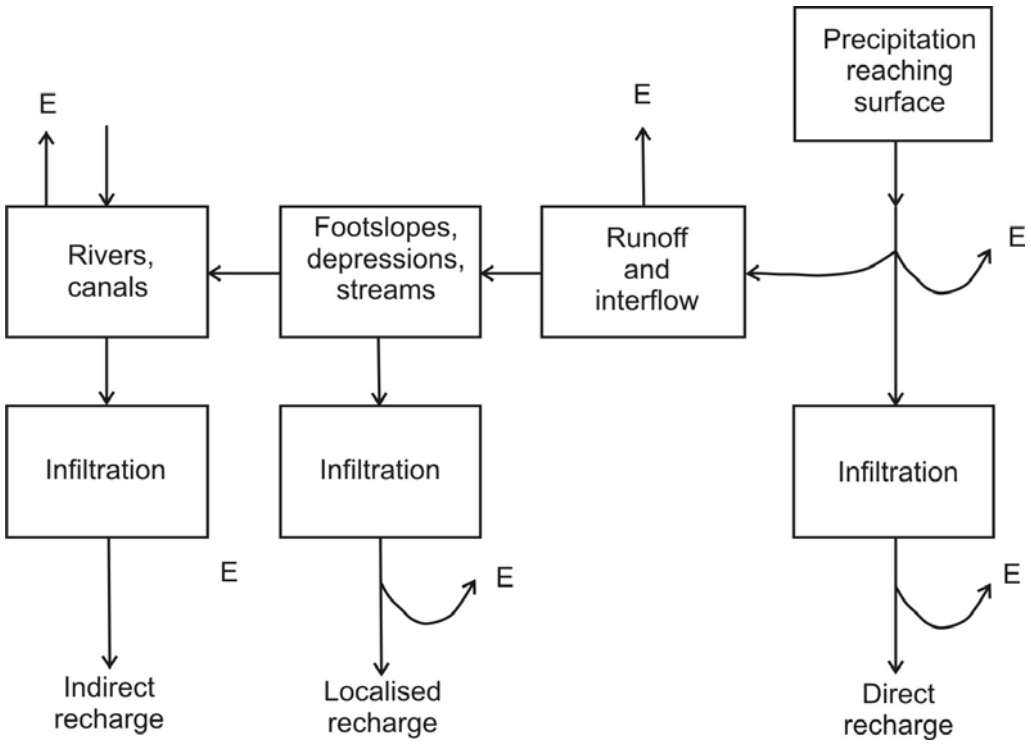

Figure 98: *The various mechanisms of recharge (Lerner, 1997).*

CSIRO (2009, p 237), in a summary of the hydrogeology of palaeochannel sediments in the Ord River Irrigation Area, note that under natural conditions, high rainfall and river flooding in the wet season recharges the alluvial aquifer directly through the more permeable floodplain sediments (Salama *et al.*, 2002; CSIRO, 2009). This would happens particularly through sandy levee deposits, and importantly for the ORIA, through subsurface palaeochannels. Significant river recharge can also occur through the incised banks during high river flows, particularly where the basal sands and gravels, and palaeochannel deposits, are incised by the river. Some of this bank storage and groundwater returns to the river as the floodwaters recede and the dry season progresses.

Currently, the influence of the permanent surface water feature in Lake Kununurra in addition to recharge from irrigation activities across the floodplain, has resulted in rising groundwater trends in the palaeochannel sediments (CSIRO, 2009). It was thought that the rate of subsurface drainage to the Ord River from the existing irrigation area would increase in response to the mounting hydraulic gradient in the aquifer, and the watertable would re-stabilise at a safe distance below ground surface. However, Smith *et al.* (2006) pointed out that the degree of connectivity between the aquifer system beneath the irrigation area and the Ord River is much less than previously thought. Groundwater beneath a large part of Ivanhoe Plain does not drain effectively to the river and the aquifer has filled to form a groundwater mound (Salama *et al.,* 2002). The watertable beneath Ivanhoe Plain has risen steadily by around 0.3 to 0.5 m/year (15 to 20m in total) during the past 40 years and has now risen to within several metres of ground surface. This impact may extend to the Weaber Plain.

The Ord River and the various irrigation canals contribute water to recharge, especially when they are full, during the wet season (Kinhill Pty Ltd., 2000). These provide a linear source of recharge. The same applies to depressions, palaeochannels and footslopes, which are areas with faster infiltration rates. Footslope locations, or more specifically the boundary between footslopes and pediments, and the floodplain or alluvial plain, are potentially important because these areas have rapid runoff or interflow during rainfall events.

Recharge rates vary over the Ord project area. These rates vary spatially as a result of soil type and underlying regolith, and landscape position. They also vary temporally depending on the cycle of wet and dry seasons, and in irrigated areas with cycles of water application. There can be significant recharge from channels, both natural and artificial irrigation canals.

For example Kinhill Pty Ltd (2000) reported, with reference to the Stage 1 irrigation area, that:

- The M1 Channel has a significant influence on the groundwater levels in its vicinity, but the contribution to groundwater recharge by the channel has decreased slightly in absolute terms in recent years (up to 2000).
- The volume of recharge from irrigated farmland has increased since 1970, and especially since 1990.
- Groundwater accession from 1966 to 1990 averaged approximately 5% of the applied irrigation water volume, and since 1990 has been approximately 10%.
- The proportion and volume of recharge from the M1 Channel versus recharge from the irrigated farmland has changed considerably over time, ranging from an estimated 69% contribution from the M1 Channel and 31% accession from farmland in 1970; through to an estimated 19% recharge from the M1 Channel and 81% accession from farmland in 1996.

Kinhill Pty Ltd (2000) consider there to be very little recharge through the black clay soils because of their low hydraulic conductivity, and because most of the water added to these soils from rainfall evaporates before it can infiltrate to become recharge. However, they also note that recharge is more important in creeks and in sandy soils. They use values of 2mm/day for channels and 100mm/year for cropped areas in their groundwater model. Estimating recharge from the permeability of soils and underlying materials assumes that water movement is dominantly vertical.

In other studies, surface recharge maps based on materials have been produced mainly by using soil texture as a surrogate (Cook *et al.,* 2004). However the available soils maps and related point data made this method unsuited to this study. Munday *et al*., (2004) advocated use of clay thicknesses and drainage units as an alternative approach. However, although clay thickness maps have been derived from the AEM data, the

relatively resistive near surface and AEM system characteristics employed for the Ord survey meant that this was not considered a reliable strategy for the purposes of recharge mapping in this study. Overton and Jolly (2004) combined a methodology similar to Munday *et al*. (2004) with information from subsurface flushing from geophysics and vegetation mapping. Again, there was insufficient vegetation data to permit the reliable application of their approach in this study.

Three different surrogate approaches were taken to estimate different aspects of 'recharge'. These map products are designed primarily as data layers for input into a groundwater model. The approaches and products are described below.

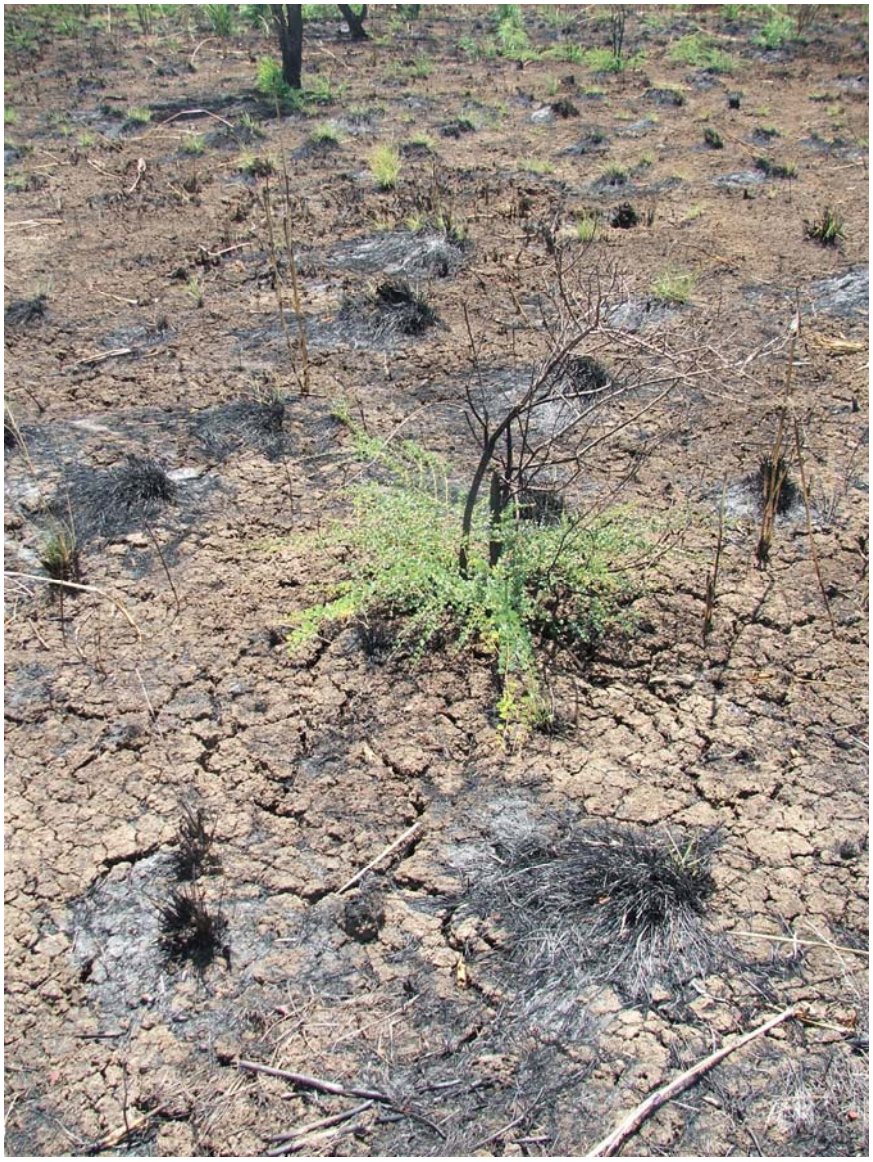

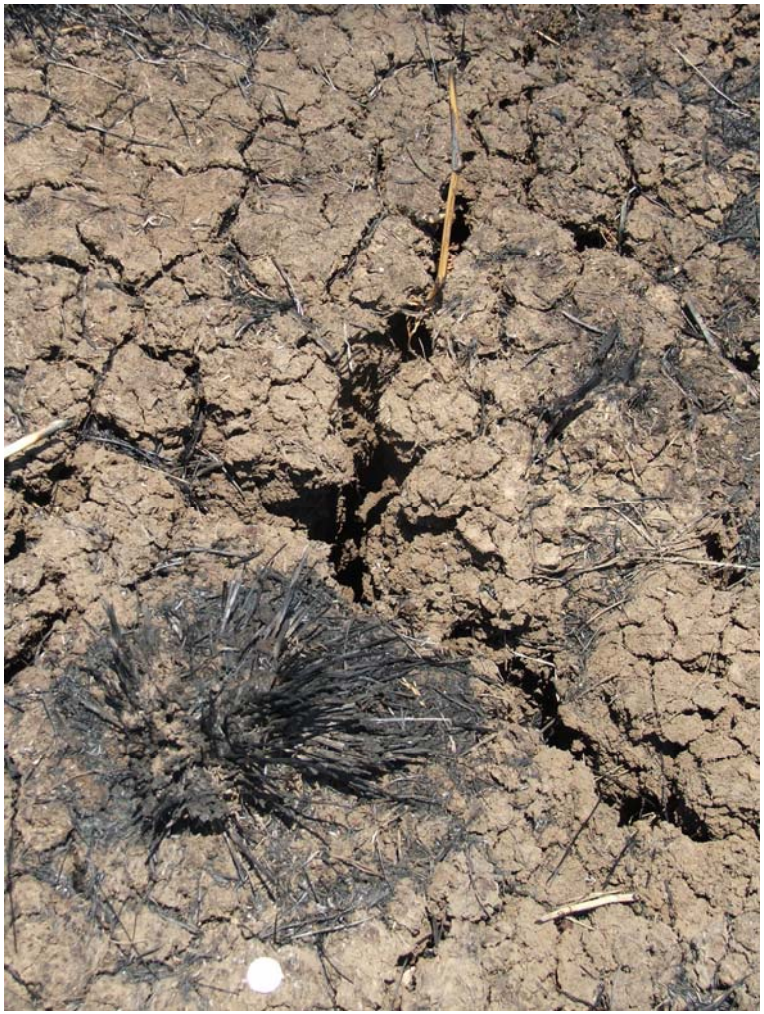

Figure 99: *Cracking clay soils revealed after a bushfire. Even in the undeveloped Stage 2 areas, the scale density and extent of cracks varies significantly across the study area depending on a range of factors including landscape/soil/vegetation/hydrology associations.*

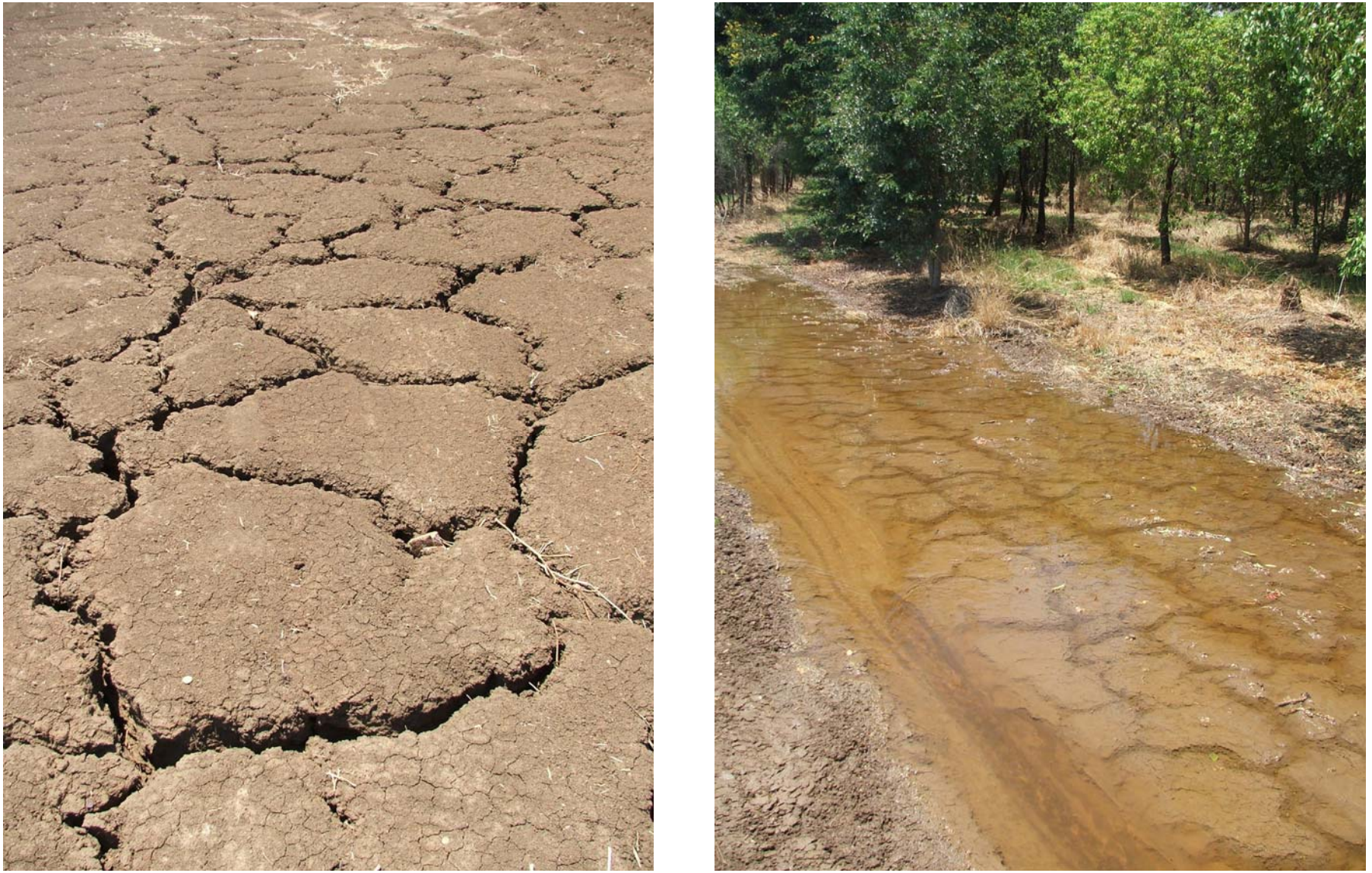

Figure 100: *Cracking clay soils at Packsaddle. Cracks vary up to 15cm in width and up to 2m in depth. Irrigation waters in channels fill the cracks with fine silt, preserving the cracking patterns in low flow parts of the channels.*

Figure 101: *Prior crack networks preserved in low flow sections of irrigation channels, but are filled and/or covered with fine silts and/or clays in higher flow parts of the channels. Cracks are not preserved or are covered with fine silts and sands in higher flow parts of channels.*

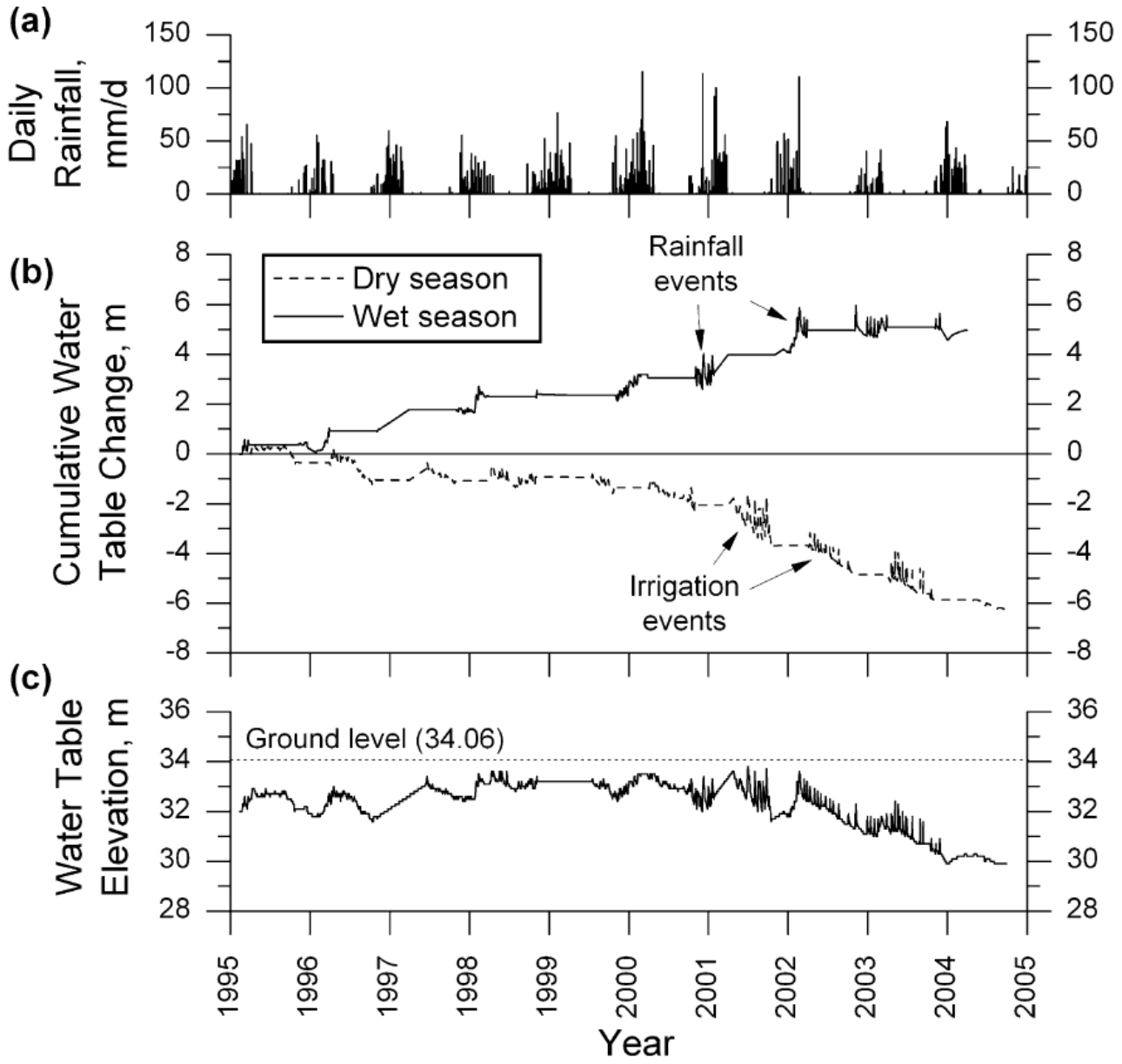

Figure 102: *a Daily rainfall, b cumulative wet season and cumulative dry season water-table responses and c water-table elevation in piezometer 94–29. Figure from Smith (2008).*

Figure 103 shows that the amount of infiltration varies considerably between different soils. The surface hydraulic conductivity maps are based on soils data provided by the Department of Agriculture and Food, WA. Landscape position was used because it has some control over materials at the surface and at depth, so reflects potential recharge (Figure 105). Each soil map unit (Figure 106) was attributed with permeability and clay content values for each horizon.

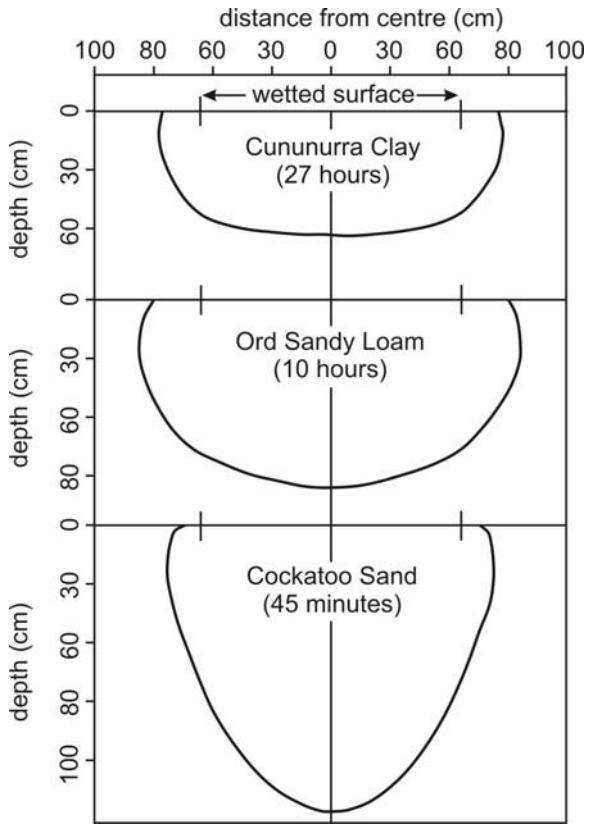

Figure 103: *Variations in amount of infiltration of water added to the surface of different soil types (redrawn from Burvill, 1991).*

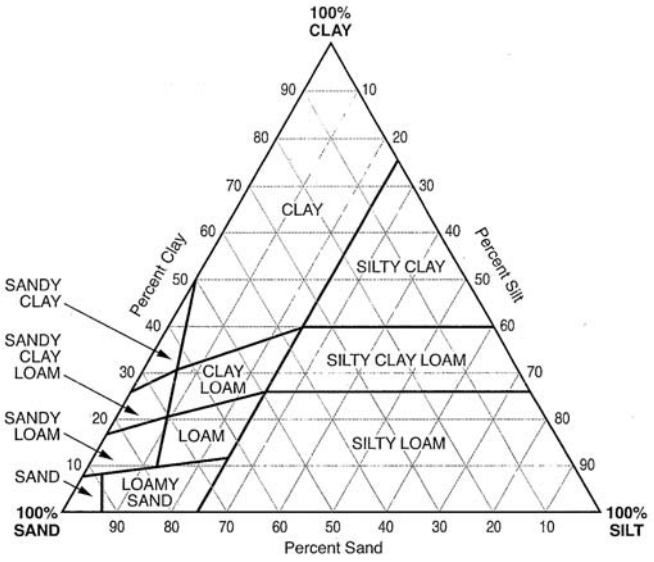

Figure 104: *Triangular texture diagram used to estimate clay % for soil polygons (From McDonald & Isbell, 2008).*

A few soils polygons in the project area were not fully attributed in the soils data provided. A geomorphology map prepared for the project (Figure 82) was used to infill some gaps, with areas of bedrock landforms labelled as very slow recharge but high runoff. The resulting map shows surface hydraulic conductivity classes (Table 21).

Table 21: *Attributes to assign hydraulic conductivity classes to soil polygons.*

Hydraulic Conductivity Class	Landscape Position	Saturated Hydraulic Conductivity (mm/hr)	Clay Content
Rapid	High Runoff Areas (hill slopes, pediments, alluvial fans)	160 to 300	< 5%
Moderately Rapid	Levees, other sandy alluvium	120 to 230	5-10%
Moderate	Scroll bars, prior streams, higher floodplain levels	50 to 145	10-20%
Moderately Slow	Higher floodplain levels, eroded floodplains	45 to 100	20-30%
Slow	Higher floodplain levels	10 to 100	20-36%
Very Slow	Lower floodplain levels	10 to 19	>36%

Vegetation information was not incorporated into these products because there are very few data on recharge as it is affected by vegetation under the climatic environment of northern Australia, and there is only coarse-scale vegetation data for the project area. The maps provide a spatial framework, but do not provide a recharge estimate because other factors such as evaporation and permeability of materials between the base of the soil and the watertable are also involved. Nor does it take into account lateral recharge from the high runoff areas, or lateral movement along buried channels from within or outside the area.

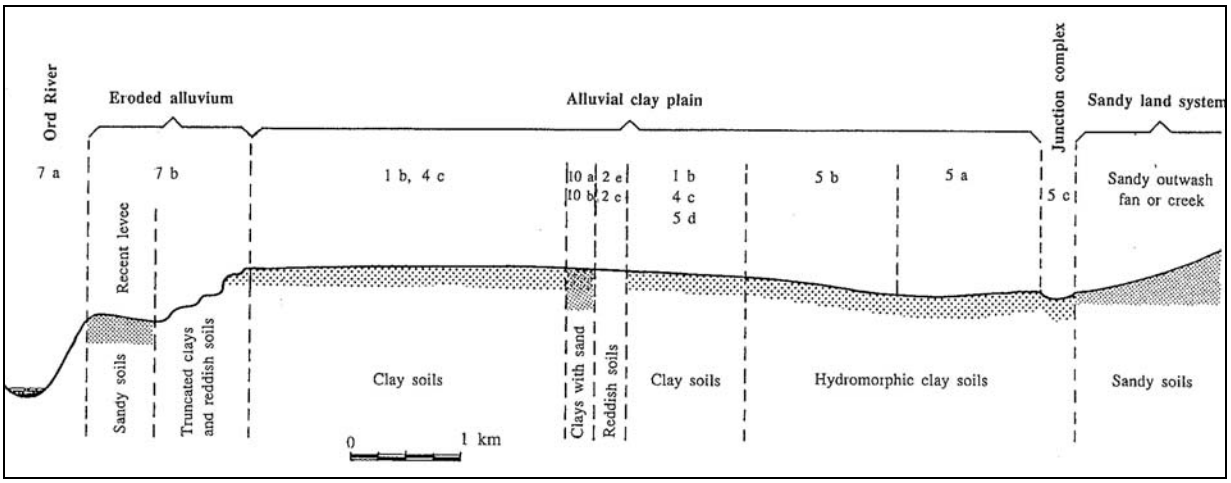

Figure 105: *Soil types and landscape position in the ORIA stage 1 (from Aldrick et al., 1990).*

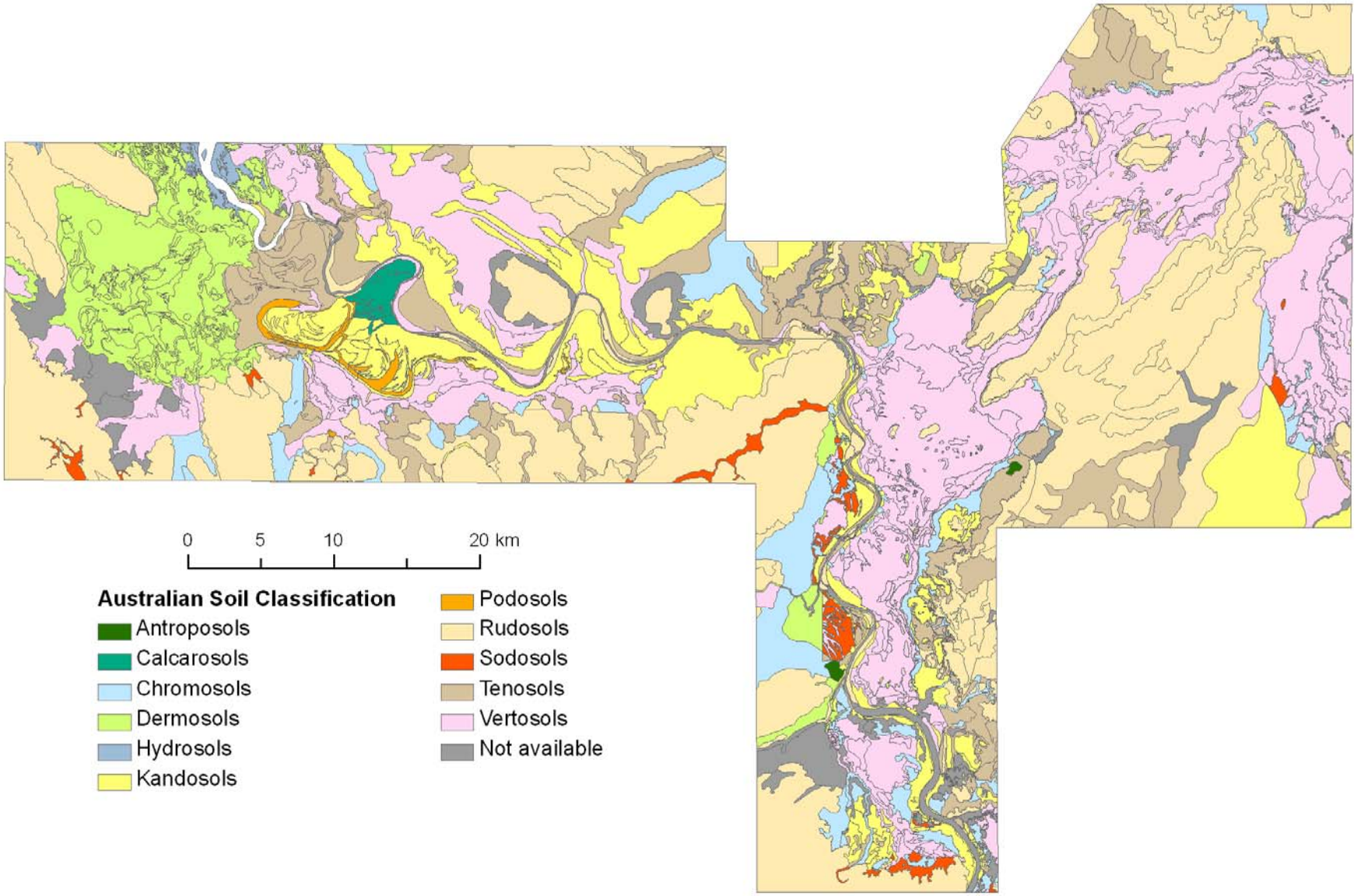

Figure 106: *Soils of the ORIA classified according to the Australian Soil Classification (Isbell, 1996). This map was generated from data supplied by DAFWA (2009).*

Table 22: *Estimates of saturated hydraulic conductivity (mm/hr) for combinations of different soil attributes.*

Soil texture	Loose (G)	Earthy or porous (E)	Poorly structured (P)	Moderately structured (M)	Strongly structured (S)	Shrink-swell (SW)	Fractured rock, or pan, weathered pan (PF, RF, PW)*	Weathered rock (RW)*	Hard rock or pan (PH,RH)*	No data (XX)
Medium to coarse sand	400	300	280							
Medium sand	240	160	120							
Coarse sand	400	300	280							
Very weak clayey coarse sand	235	155	110							
Very weak clayey sand	235	155	110							
Sand	230	150	110							
Fine sand	220	140	100							
Weak clayey coarse sand	220	140	100							
Weak clayey sand	220	140	100							
Loamy sand	220	140	100					80		
Loamy coarse sand	220	140	100					80		
Clayey sand	210	135	90					70		
Heavy clayey sand	170	125	80					65		
Sandy loam	120	110	70	90	110			55		
Loam	110	100	70	90	100			55		
Light sandy clay loam	80	75	50	65	80			40		
Sandy clay loam		60	40	50	70			30		
Clayey sandy loam		55	35	45	65					
Clay loam		50	30	40	60					
Sandy clay		30	14	26	40	10				
Light clay		25	10	25	35	10				
Clay		15	3	15	25	2				
Light medium clay		12	2.5	12	20	2				
Medium clay		11	2	10	17	2				
Medium heavy clay		10	1.5	8	15	2				
Heavy clay		6	0.5	3	6	2				
No data							15	300	0.2	0

Table 23: *Estimates of clay % for different textures (see Figure 104).*

Texture	Estimated Clay Content
Medium to coarse sand	<2% clay. Assume 1%
Medium sand	<2% clay. Assume 1%
Coarse sand	<8% clay. Normally 2-5% clay. Assume 4%
Very weak clayey coarse sand	2-4% clay. Assume 3%
Very weak clayey sand	2-4% clay. Assume 3%
Sand	<8% clay. Normally 2-5% clay. Assume 4%
Fine sand	<8% clay. Normally 2-5% clay. Assume 4%
Weak clayey coarse sand	4-8% clay. Assume 5%
Weak clayey sand	4-8% clay. Assume 5%
Loamy sand	<12% clay. Assume 6%
Loamy coarse sand	<12% clay. Assume 6%
Clayey sand	<12% clay. Assume 8%
Heavy clayey sand	<12% clay. Assume 11%
Sandy loam	8-21% clay. Assume 14%
Loam	10-26% clay. Assume 18%
Light sandy clay loam	18-31% clay. Assume 21%
Sandy clay loam	18-31% clay. Assume 24%
Clayey sandy loam	21-35% clay. Assume 28%
Clay loam	23-40% clay. Assume 31%
Sandy clay	25-50% clay. Assume 37%
Light clay	31-45% clay. Assume 38%
Clay	35-50% clay. Assume 40%
Light medium clay	45-50% clay. Assume 47%
Medium clay	50-55% clay. Assume 52%
Medium heavy clay	55-60% clay. Assume 57%
Heavy clay	>60% clay. Assume 67%
No data	not applicable Assume 0%

Three different derived recharge map products were produced using a surrogate approach. These are described below.

4.6.1 Subsurface Permeability

Sub-surface permeability maps show classes for the uppermost soil horizon, and are based on clay content and saturated hydraulic conductivity (KS). Permeability values for subsoil materials were obtained from various sources (e.g. Kinhill Pty Ltd, 2000). These values were extrapolated to other parts of the study area using lithologies mapped by the AEM where no permeability measurements have been made. AEM data were used to estimate the lithology of materials below the soils and provide the spatial context for extrapolation. A map of sub-surface permeability for the whole project area is shown in Figure 107.

4.6.2 Recharge Potential Maps (Subsurface Permeability)

The second map uses a surrogate approach to map recharge potential, and emphasises the horizon with the lowest permeability value and highest clay content for each unit. This contrasts with the subsurface permeability maps which use classified values at different depth intervals. The recharge potential maps assume that the layer with the lowest permeability and highest clay unit will be rate determining- i.e. this layer will control the potential rate of downward water movement. Permeability values for subsoil materials were obtained from various sources (e.g. Kinhill Pty Ltd., 2000). These values were used to extrapolate to

other parts of the study area where no permeability measurements have been made. AEM data were used to estimate the lithology of materials below the soils and provide the spatial context for extrapolation.

The surface permeability and soil recharge properties maps are based on available soils data only, and the products do not take into considerate macropore bypass flow (Smith, 2008). The hydrograph analysis of bores in pre-cleared and irrigation areas shows that recharge to the groundwater table can be significant and rapid, and this is not necessarily predicted by the soil-based products described above. However, there was insufficient soils data describing the macropore behaviour and distribution to evolve the products further. A recharge potential map of the top 2m for the whole project area is shown in Figure 108.

4.6.3 Deep Drainage (based on clay thickness above the water table)

An additional suite of surrogate recharge maps that attempt to show ***potential deep drainage*** (or recharge to the groundwater table). These maps were produced by integrating the surface soils data with the AEM-based mapping of clay thickness validated by pore fluid and textural analysis, and overlying these elements over the regional watertable map (Figure 109). This provides a qualitative guide to deep drainage rates, as recharge is likely to be much slower in general through a thick sequence of clays than a similar thickness of sands.

Importantly, the groundwater recharge figures for sub-areas within the study area can best be obtained from hydrograph response data summarised in Smith (2009) for ORIA Stage 1, and from the more limited data for Stage 2 areas, notably the Weaber Plain (Appendix 11, Cullen *et al.,* 2010). In particular, the water table maps produced by Smith (2008) for the period 1995-2008 provide a reliable guide to recharge to the water table as seen in annual variations in water table level in ORIA Stage 1. The data for the Stage 2 areas are too sparse to produce water table recharge maps, but the hydrograph response data should provide a useful constraint in future groundwater modelling.

4.6.4 Summary

The maps provide a spatial framework, but do not provide a recharge estimate because other factors such as evaporation and permeability of materials between the base of the soil and the watertable are also involved. Nor do they take into account lateral recharge from the high runoff areas, or lateral movement along buried channels from within or outside the area. The actual recharge can be obtained from the rise in water table levels that are shown by the hydrographs.

Surface soil hydraulic conductivity, or permeability, varies considerably over the study area. Areas shown as having high runoff occur on bedrock slopes where soils are very thin. Most of the areas with rapid permeability are on hills and rises on bedrock. Soils are thin, and water that does not runoff immediately infiltrates rapidly and then moves laterally downslope as interflow. There are also areas of rapid infiltration along levees adjacent to the Ord River and along the river channel where it flows on sediments. Moderate and moderately rapid infiltration also occurs in bedrock areas where soils are thicker, and also on levees. Moderate infiltration occurs in some bedrock areas, and also on levees and in places where coarser alluvium is exposed on the surface of alluvial plains. Moderate infiltration is also mapped along some levees and scroll bars, especially in the Parry's Lagoon area.

Moderately slow infiltration is found on pediments and in areas where fine alluvial sediments are eroded, exposing sandy material deeper in the profile. Finally, slow and very slow rates of infiltration are confined mainly to areas of alluvial plains covered with alluvial clay and cracking clay soils. Higher parts of the alluvial plains tend to have slow rates, while the lower parts have very slow rates. The latter reflect the presence of hydromorphic cracking clay soils in places where water persists for longer after rainfall and flood events (Figure 109).

Surface infiltration rates are thus controlled to a large extent by the landforms and geomorphic history of the area, and for that reason exhibit a complex pattern of potential infiltration into the upper layers of the regolith. These classes (Figure 107) are thus important for assessing the potential for water to enter the regolith, although there are many other factors that determine whether it becomes recharge to the water table.

The distribution of permeability classes in the upper 2 m of the regolith (Figure 108) shows a much simpler distribution, and in places seems to contradict the surface permeability classes (Figure 107). First, all areas having landforms that fall into the groups hills and rises, pediments, upland valleys, alluvial fans and channels on bedrock are grouped into an area of high runoff and high subsurface interflow. These areas consist either of bedrock or of thin and coarse material over bedrock. Rain either runs off directly, or infiltrates into the over lying materials and then moves as interflow downslope to the edges of the alluvial valley floors. It is unlikely that any of this water contributes directly to diffuse recharge.

On the alluvial plains there are areas of moderate to rapid permeability associated with coarser soils, and eroded areas that expose coarser materials. However, over much of the alluvial plains area there is very little variation, most of the plains being slow or very slow. In particular the Weaber Plains are more-or-less uniform in their very slow permeability. This is because all horizons are considered in this map, and this has smoothed out the predictions, there being at least one layer with high clay content and low KS. It is thus not surprising that Figure 108 shows less variability than Figure 107.

There do not appear to be any areas where high recharge sandy units may lead to perched water tables. There are, however, some units where prior streams, meander scrolls, or levees have soils with a lower clay content and correspondingly higher sand content. These areas may contribute more infiltration and therefore potentially more recharge than other parts of the alluvial plains where clay content is much higher. There are also areas with strongly cracking vertosols that have higher infiltration rates than there clay content would suggest. This is because the cracks remain transmissive even when the soils expand and the cracks close (Smith, 2008).

Also, Figure 109 shows that there is very little relationship between depth of the water table below the surface and permeability of the surface soils. This suggests that the water table level is controlled by factors other than surface permeability.

Other influences on drainage include factors such as peak wet-season drain flows, which can be a factor 10 greater than mean dry season flows (Viney, 2003). High water levels and elevated hydraulic head in drains that occur during large wet season flow events are likely to cause significant leakage to groundwater on those occasions.

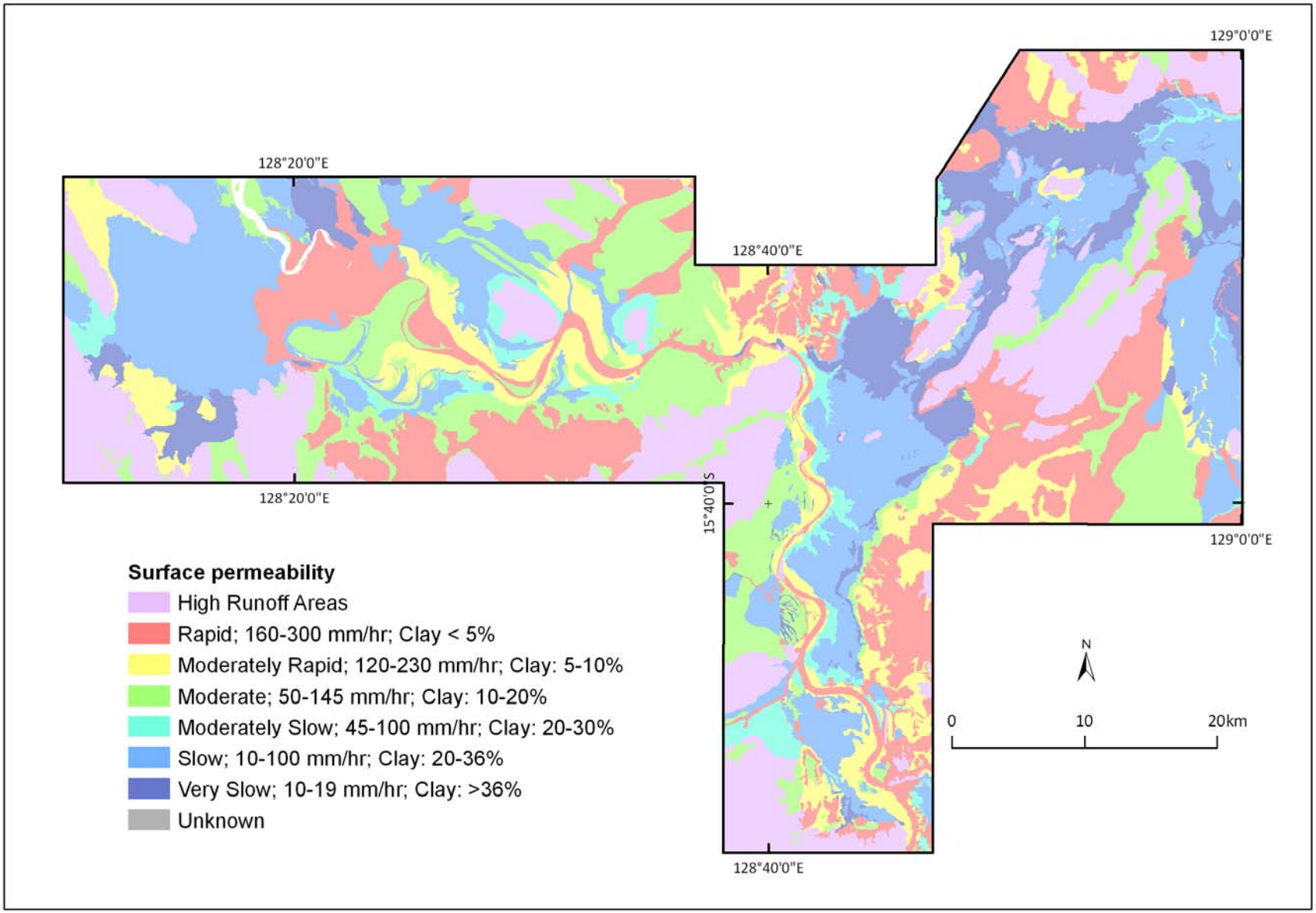

Figure 107: *Surface soil hydraulic conductivity.*

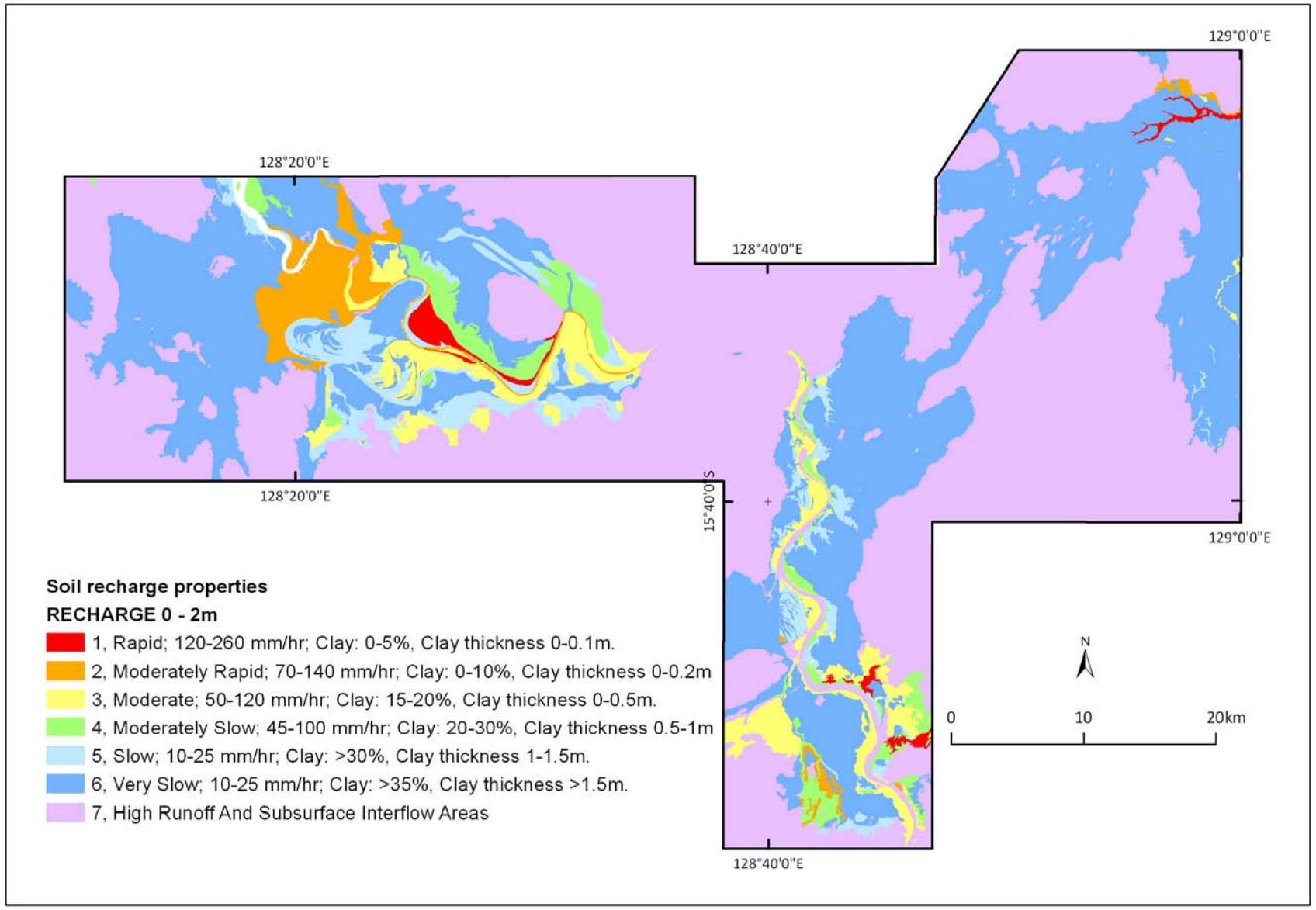

Figure 108: *Recharge potential of the upper 2 m.*

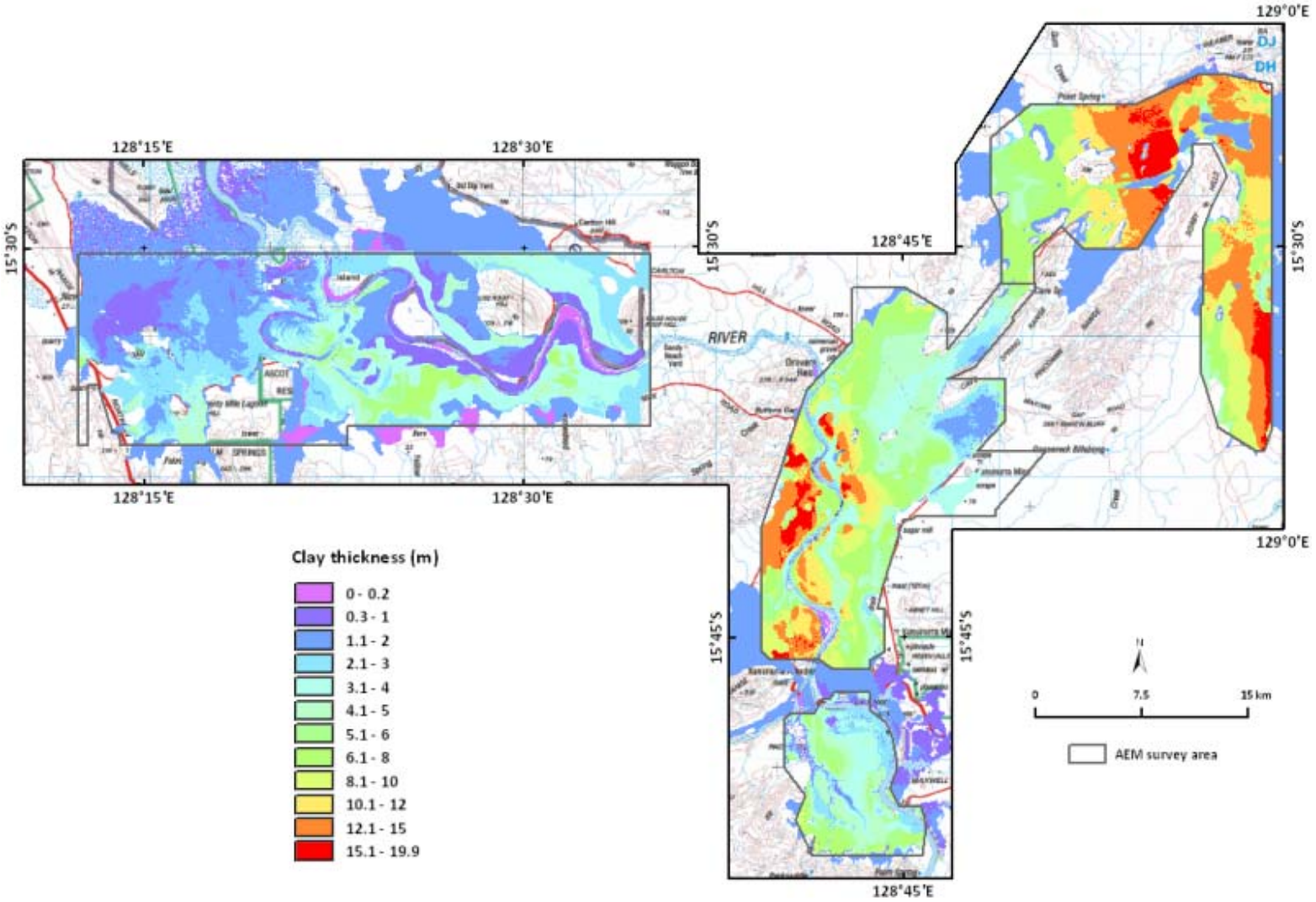

Figure 109: *Map of potential deep drainage (or recharge to the groundwater table). This map was produced by integrating the surface soils data with the AEM-based mapping of clay thickness, and validated using pore fluid and textural analysis. These elements were then overlain over the regional watertable map.*

4.7 SALT STORE MAPS

The apparent conductivity of a material is the weighted summation of the electrical conductivity of liquid and solid phases (Equation 1; Rhoades *et al*., 1976; Mullen *et al.*, 2007).

$$EC_a = EC_w\theta\tau + EC_s \qquad \text{Equation 1}$$

where EC_a is the apparent conductivity, EC_w is the pore water conductivity, θ is the volumetric water content, τ is the tortuosity and EC_s is the solid phase conductivity.

Mullen *et al.,* (2007) noted that there is a nearly linear relationship between Average Salt Load and AEM conductivity. This relationship can be expressed as linear functions (Equation 2):

$$EC_a = y \times \text{Total-Salt mS/m} \qquad \text{Equation 2}$$

where y = derived regression slope of the graphs as shown below.

Variations in apparent conductivity are a function of a range of factors, including salinity and moisture content (and bulk conductivity), so the value for y has to be re-calculated for each area. Where there is a strongly resistive and dry unsaturated zone, separate calculations need to be made for both saturated and unsaturated materials. Pore fluid salinities from borehole materials in the ORIA were plotted against apparent conductivity (EC_a), with linear relationships observed for both the unsaturated (Figure 110) and saturated zones (Figure 111).

Using the relationships between texture, moisture content and apparent conductivity, it has become common practice to derive salt store maps from AEM data (Tan *et al.,* 2005; Mullen *et al.*, 2007; Tan *et al.,* 2008, 2009). To produce these map products, it is necessary to obtain pore fluid data for aquitards and aquifers. In this study, a lack of pre-existing data meant that data for the salt store determinations relied primarily on analysis of data derived from the project drilling campaign.

Plots generated using data from the laboratory analysis of drill core materials for Knox Creek and Weaber Plains and the Stage 1 areas (Packsaddle and Ivanhoe Plains), are shown for the unsaturated (Figure 110) and saturated zones (Figure 111). For Parry's Lagoon, only the plot for the saturated zone (Figure 112) is shown because of the shallow watertable near the drill sites (< 2m depth).

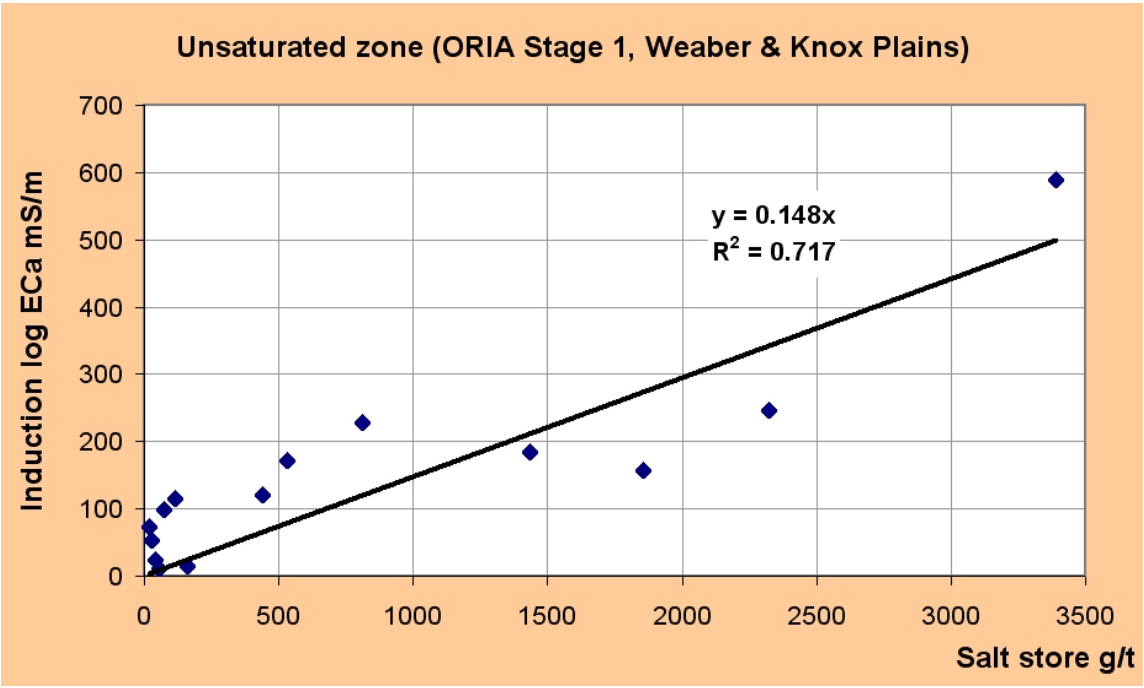

Figure 110: *Salt store calculation for the unsaturated zone beneath the ORIA Stage 1 (Packsaddle and Ivanhoe Plains), Weaber and Knox Creek Plains.*

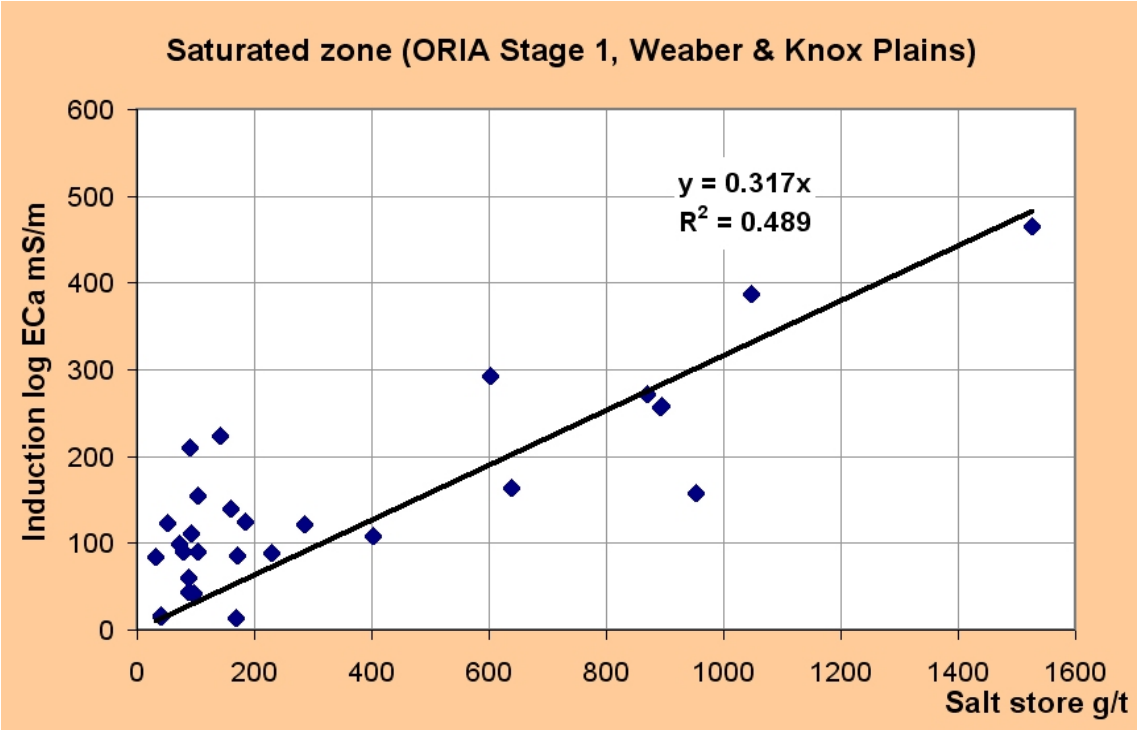

Figure 111: *Salt store calculation for the saturated zone ORIA Stage 1 (Packsaddle and Ivanhoe Plains), Weaber and Knox Creek Plains.*

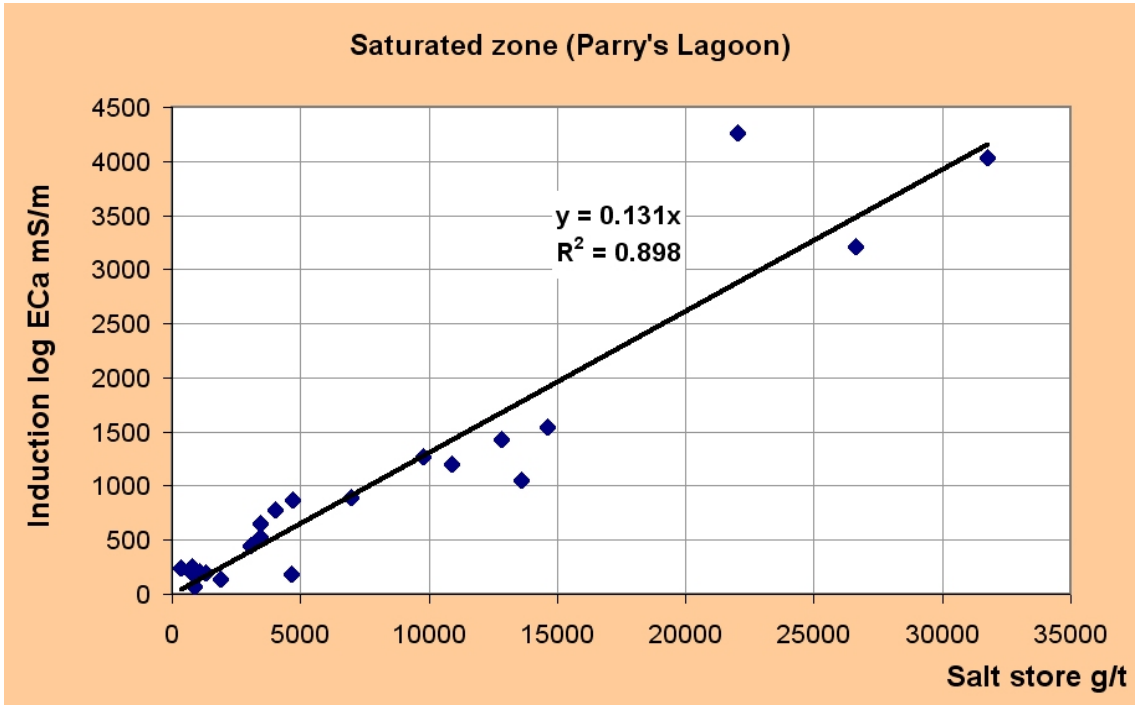

Figure 112: *Salt store calculation for the saturated zone at Parry's Lagoon.*

To convert salt store from grams per tonne to tonnes per hectare, the following calculations are carried out. Taking bulk density of sediment as 1.7g/cm^3:

$$\frac{tonne\ salt}{hectare \times metre} = \frac{tonne\ salt}{tonne\ alluvium} \times \frac{tonne\ alluvium}{hectare \times metre}$$

$$\frac{tonne\ salt}{hectare\ metre} = \frac{gram\ salt}{tonne\ alluvium}\frac{t}{g} \times \frac{tonne\ alluvium}{m^3}\frac{m^2}{ha}$$

$$\frac{tonne\ salt}{hectare \times metre} = \frac{EC_a\ (mS/m)}{y} \times 10^{-6} \times 1.7 \times 10^4 \qquad \text{Equation 3}$$

where y = derived regression slope of the graphs

Applying the regression slope y from the graphs (Figure 110, Figure 111 and Figure 112) into equation 3 results in the conversion factors (Table 24) from g/t to t/ha. The resulting equation is shown below.

Salt Store (t/ha/m) = EC_a (mS/m) x Conversion factor Equation 4

where EC_a is derived from the AEM conductivity depth slices.

Maps of unsaturated zone and saturated zone salt store for the project area are shown in Figure 113 and Figure 114 respectively.

Table 24: *Salt store calculations.*

Location		Regression slope	t/ha/m	mS/m	Conversion factor g/t to t/ha
ORIA Stage 1, Knox Ck., & Weaber Plains	**Unsaturated**	0.148	Total salt	= ECa x	0.1081
ORIA Stage 1, Knox Ck., & Weaber Plains	**Saturated**	0.317	Total salt	= ECa x	0.0505
Parry's Lagoon	**Saturated**	0.131	Total salt	= ECa x	0.1221

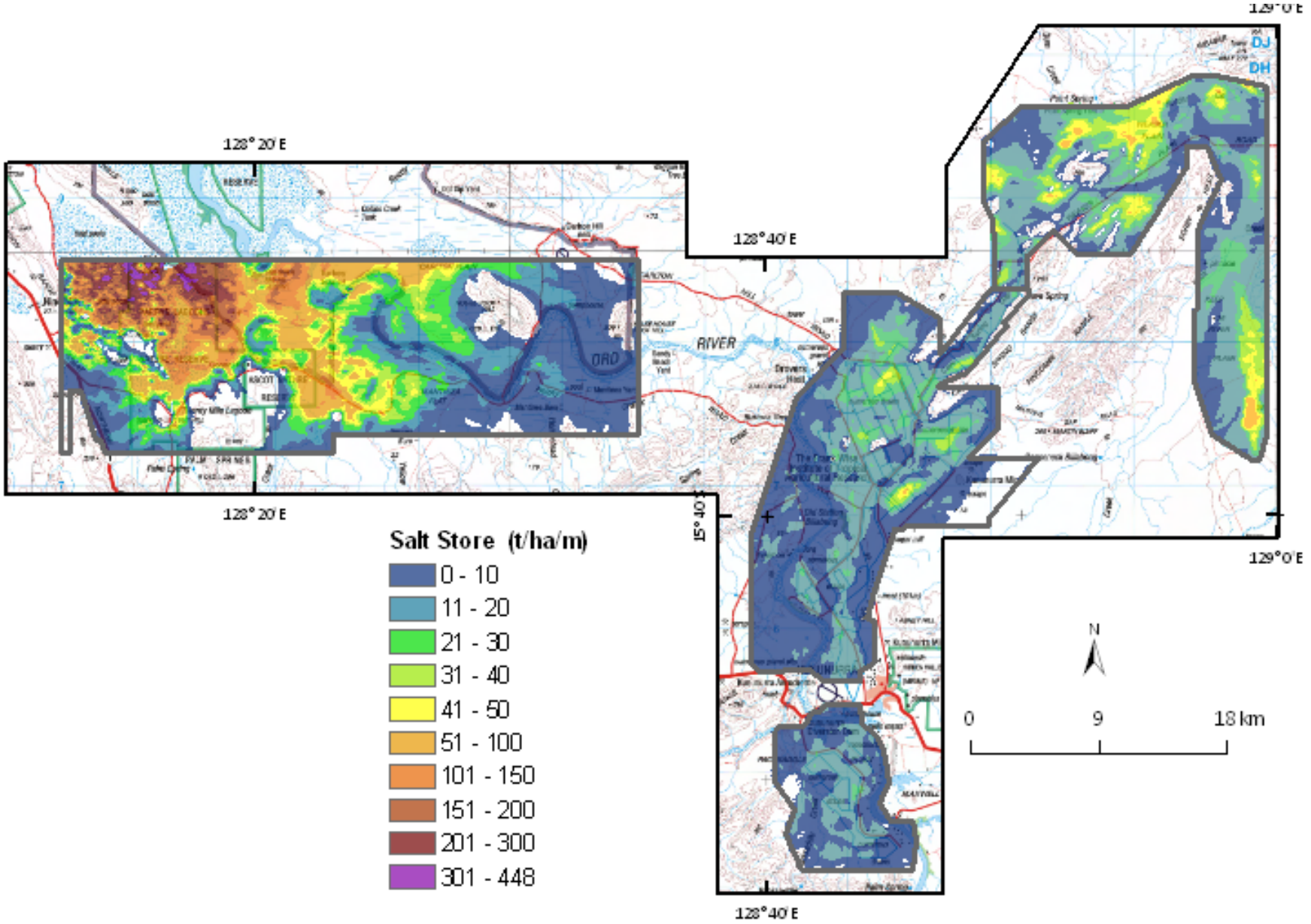

Figure 113: *Map of unsaturated zone salt store (all areas).*

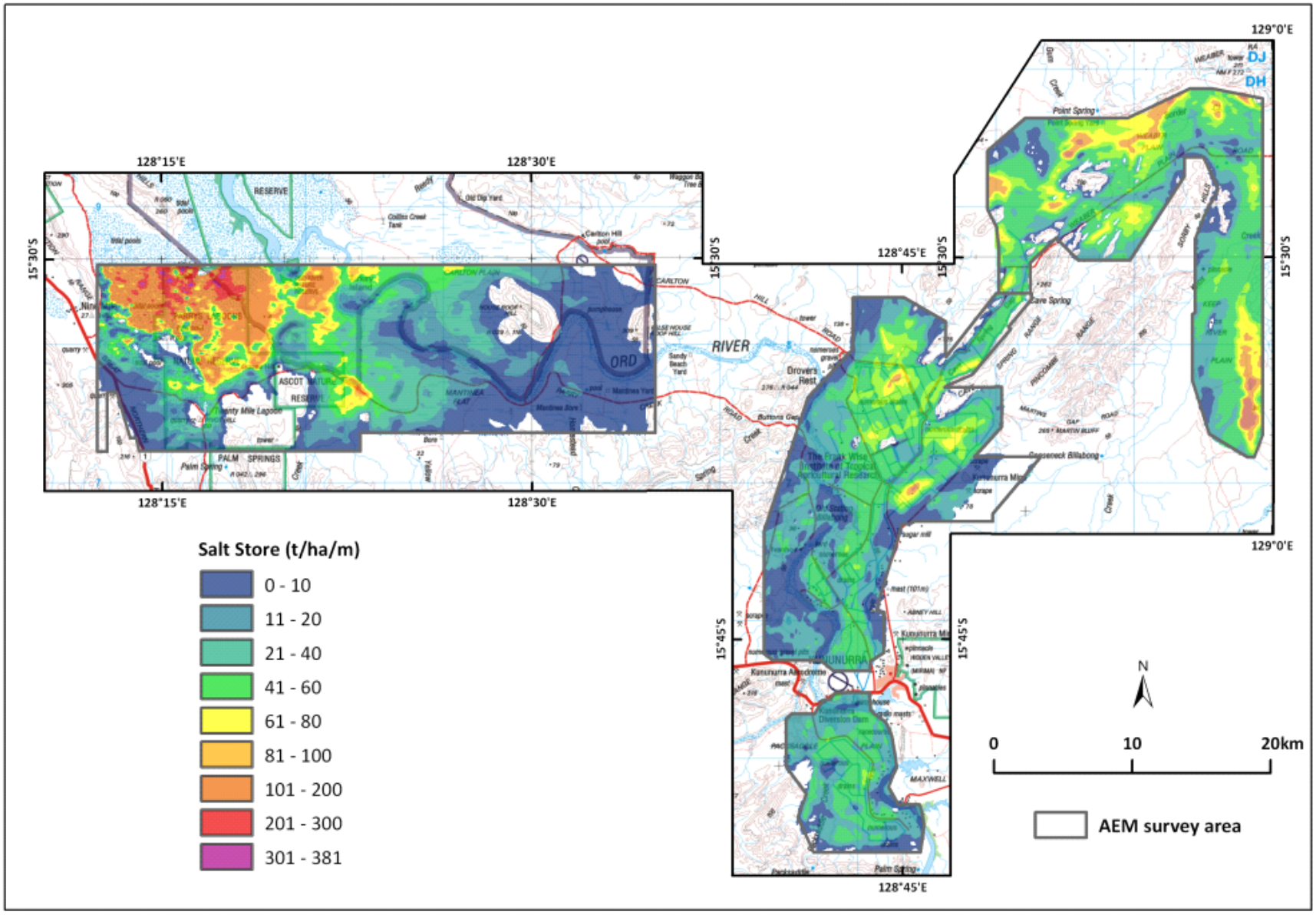

Figure 114: *Map of salt store below water table (all areas).*

4.8 GROUNDWATER QUALITY (SALINITY) MAPS

Previous studies have demonstrated that it is possible to produce maps of groundwater salinity by using pore fluid chemistry and apparent conductivity data from down-hole induction logs to calibrate and validate AEM data (Lawrie *et al*., 2008, 2009a; Tan *et al.,* 2009). This method requires access to uncontaminated drillcore materials.

In this study, pore fluids were extracted from drillcore samples collected from bores drilled specifically for validation and calibration of the AEM data. Pore fluid samples were recovered from different sediment types using a hydraulic pressing method. The fluids were analysed for major cations and anions. Cations include calcium, potassium, magnesium, sodium and silica. Anions analysed includes fluoride, chloride, bromide, nitrate, phosphate and sulphate. The cations were measured using inductively coupled plasma – optical emission spectrometry (ICP-OES) and the anions were analysed using ion chromatography (IC). The alkalinity was measured using titration technique. The summation of these ions gives the total dissolve solutes (TDS).

Laboratory analysis has shown that the pore fluids from ORIA Stage 1, Weaber and Knox Plains are mainly fresh to brackish, whereas pore fluids from the Parry's Lagoon – Mantinea Plain areas display a wide range of salinity values, ranging from slightly brackish to highly saline (~90,000mg/l TDS). Due to the large range of salinities, data from the two sub-areas were treated separately. Graphs of salinity versus apparent conductivity data (Figure 115) from both areas show positive relationships (Figure 115 and Figure 116). In the Parry's Lagoon – Mantinea Plain area (Figure 116), two sample populations were identified. Pore fluids analysed from the top 6m of core (pink squares in Figure 116), have lower TDS and EC_a overall, and are interpreted as a mixing zone between more saline groundwater below and freshwater that inundates the floodplain in the wet season, and infiltrates through the floodplain surface.

The regression equations from the graphs were used to derive the salinities of the groundwater, and these relationships were used to transform the apparent conductivity values in the AEM dataset to maps of groundwater salinity from the regional standing watertable to the bedrock). The calculations of salinity are only applicable to sedimentary systems, and areas occupied by rises and hills (fractured bedrock rock aquifer) are masked.

Due to the presence of an upper mixing zone in the Parry's Lagoon-Mantinea Plain area, pore fluid values for this area were bulked (Figure 117) to provide a single regression equation (with a much lower $r^2 = 0.259$). This regression equation was used to produce a map of average values for the saturated zone in Parry's Lagoon-Mantinea Plain-Carlton Hill. In maps derived from this equation, the upper mixing zone is not evident, while salinities of groundwater at depth will appear lower than actual.

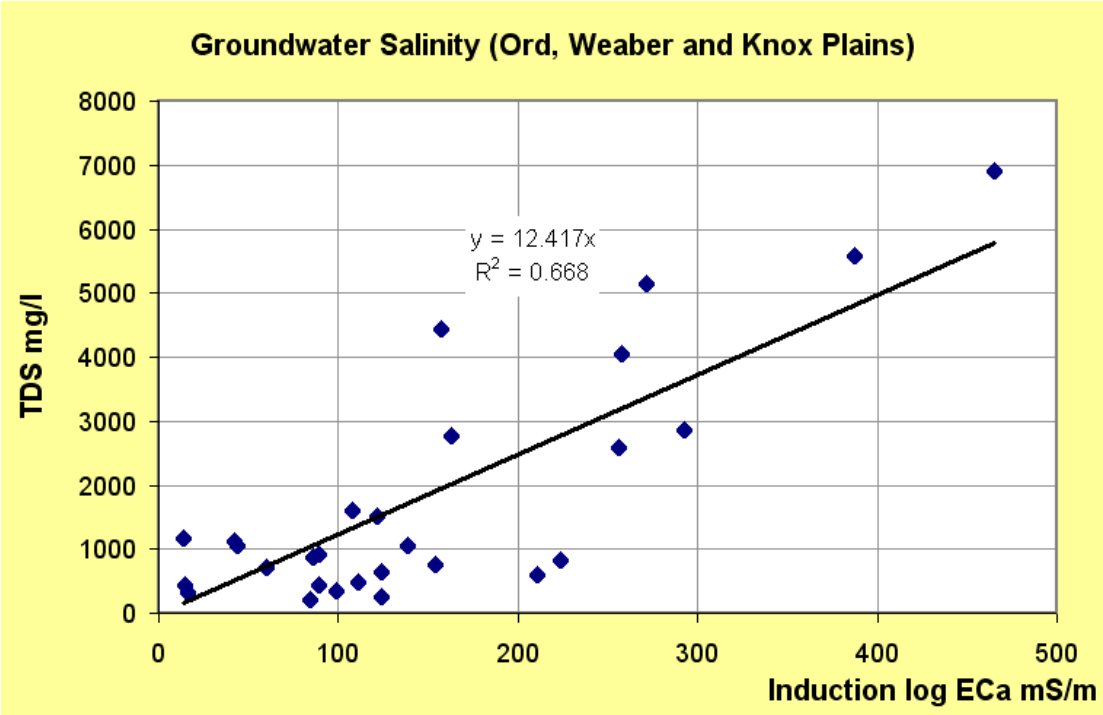

Figure 115: *Graph of pore fluid salinity and apparent conductivity (Data obtained from ORIA Stage 1, Weaber and Knox Creek Plains).*

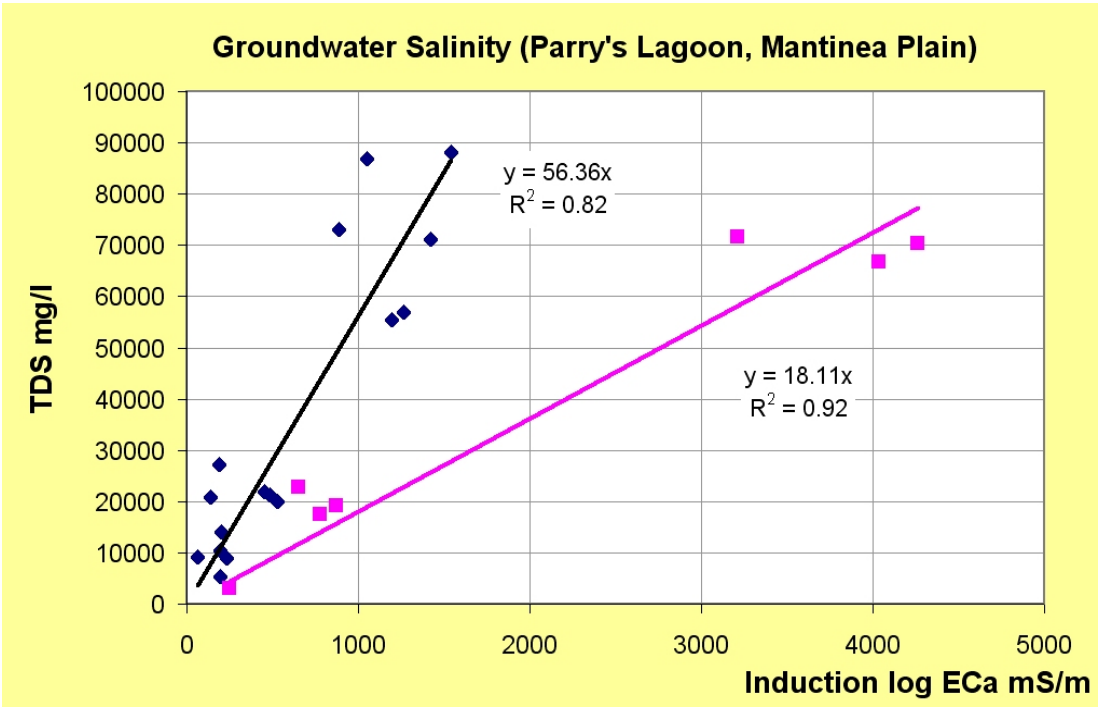

Figure 116: *Graph of pore fluid salinity and apparent conductivity (Data obtained from Parry's Lagoon – Mantinea Plain). Two populations are evident, from the top 6m (pink squares and regression line), and those sampled from greater depth.*

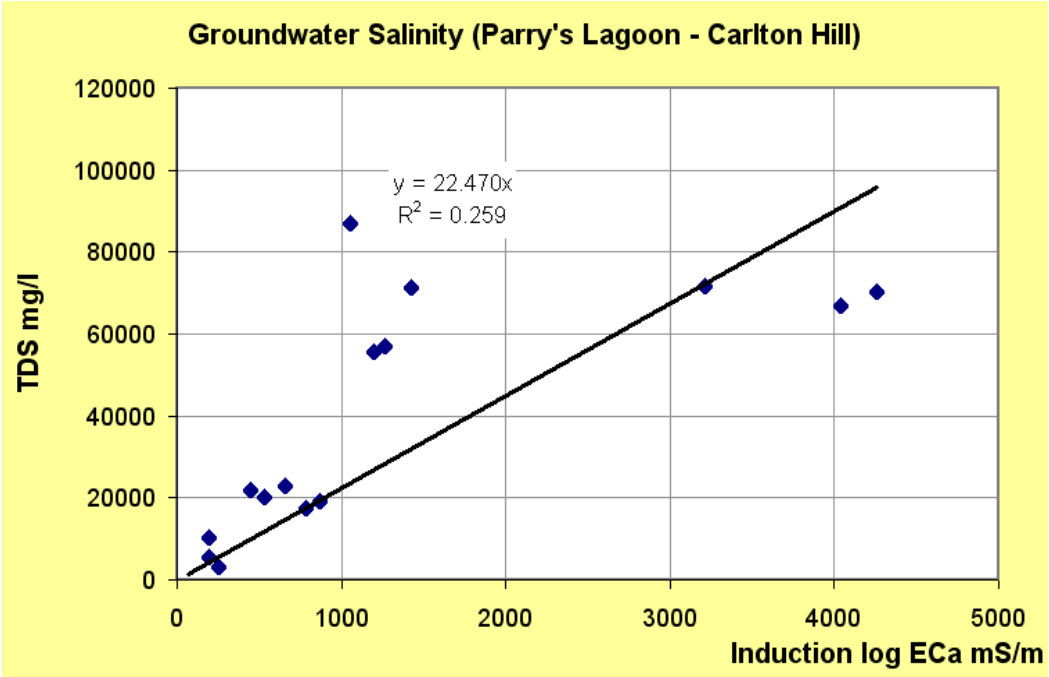

Figure 117: *Graph of pore fluid salinity and apparent conductivity (Data obtained from Parry's Lagoon – Mantinea Plain). Data populations have been merged to produce a 'bulk' map of groundwater salinity for the area. In maps derived from this equation, the upper mixing zone is not evident, while salinities of groundwater at depth will appear lower than actual.*

An additional reliability check on the predicted groundwater salinity was carried out using TDS values from 30 bores across the Weaber Plain. These bores have varying screen depth intervals and most have been sampled throughout various months over a few years. To match the dry seasons when the AEM survey was conducted, salinity results from July to October were selected for the validation. To compare the salinity between the wells, which were screened from 10m to 35m depths, the AEM conductivity values from the corresponding depth slices were used. These include 6 depth slices within the depths of 9.5m and 35.4m.

Since the data used to derive the regression equations (Figure 115) for calculating the groundwater salinity have a maximum of 7000 mg/l TDS, saline groundwater (> 10,000 mg/l TDS) from 3 bores were omitted from this validation exercise. The resulting 27 TDS values were plotted against the predicted salinity (Figure 118). The results show a positive correlation with r^2 of 0.54. The data appear to comprise 2 populations, one that falls close to the regression line and the other that lies closer towards the x-axis. Close examination on the spatial locations of the latter shows that the values belong to 3 closely spaced sites located on the south-eastern part of Weaber Plain. A map of groundwater salinity calculated using these data and approach is shown in Figure 119.

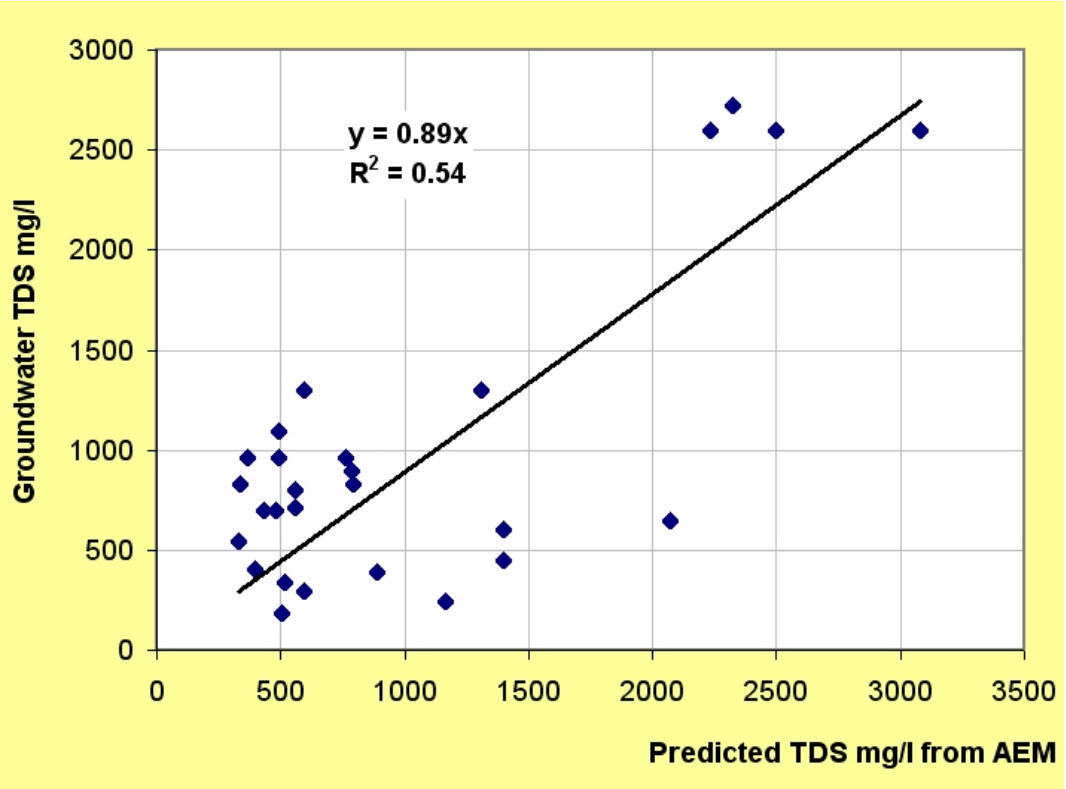

Figure 118: *Graph of groundwater salinity against predicted groundwater salinity based on AEM data and pore fluids from the Weaber Plain.*

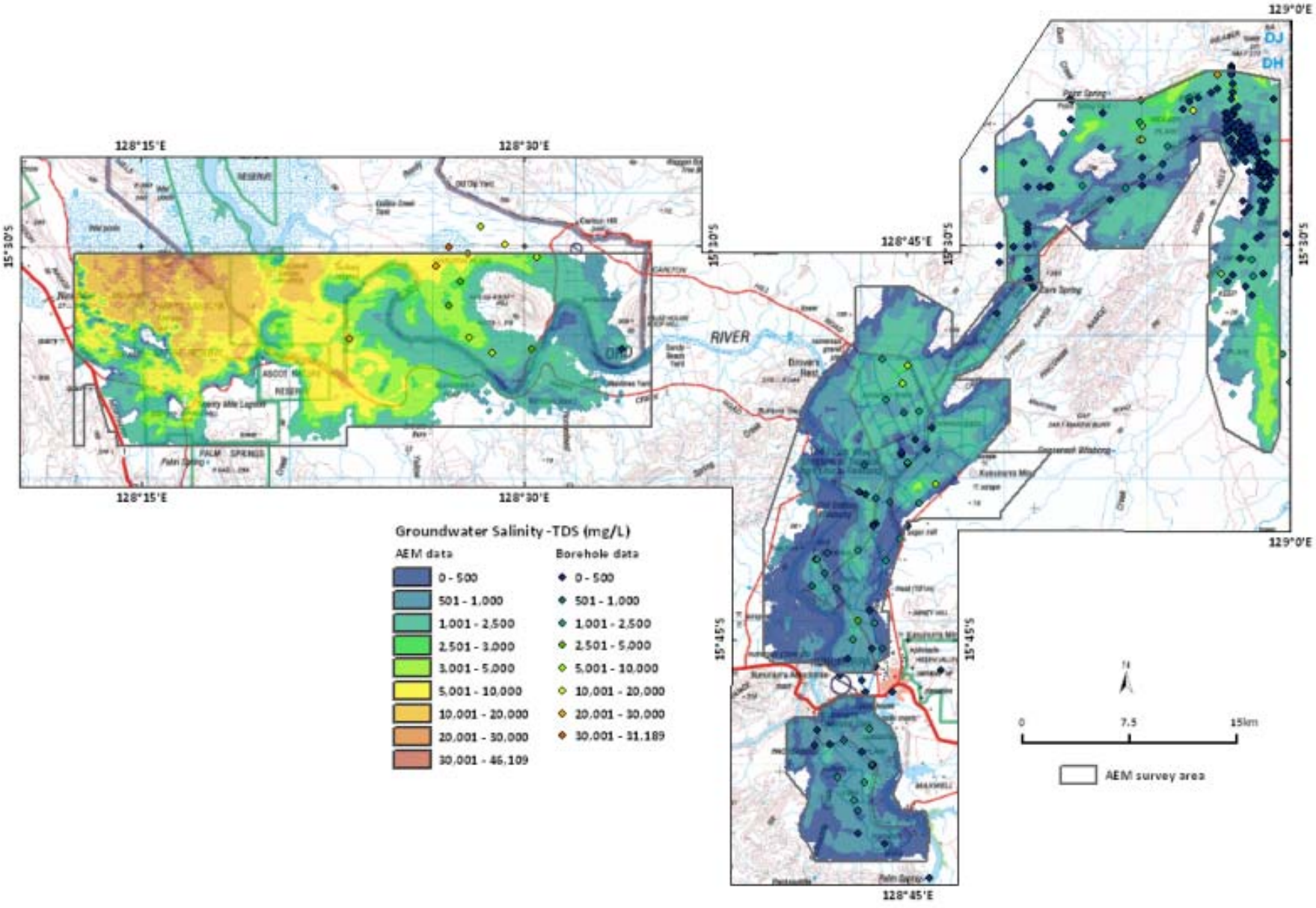

Figure 119: *Map of groundwater salinity (all areas).*

4.9 RIVER FLUSH ZONE MAPS (THICKNESS, EXTENT AND WATER QUALITY)

4.9.1 Flush Zone Water Quality (Salinity) Maps

River flush zones are defined as areas where low salinity waters from streams have flushed out more conductive, saline water from marginal sediments beside or beneath the channel. River flush zones include fresh water (up to 1000 µS/cm) and slightly brackish water (1000 to 3000 µS/cm). Previous experiments have demonstrated a positive relationship between NaCl and EC (Tan *et al.,* 2009; Figure 120). According to the regression equation shown in Figure 120, at 1000 µS/cm and 3000 µS/cm, the TDS (in a pure NaCl system) is equivalent to 496 mg/l and 1524 mg/l NaCl respectively. For the areas where groundwater salinity (TDS) is dominated by NaCl, this relationship is used to relate EC values to groundwater salinity (NaCl). NaCl-dominated groundwater is encountered in the Parry's Lagoon- Mantinea Plain area.

Statistical result of pore fluid salinities obtained from sediment cores in the ORIA Stage 1 (Ivanhoe & Packsaddle Plains), Weaber and Knox Creek Plains and apparent conductivity of induction logs suggest a positive correlation, with the regression equation shown in Figure 121. At 496mg/l and 1524mg/l TDS, the apparent conductivities are equivalent to 33mS/m and 102mS/m respectively (Table 25).

At Parry's Lagoon – Mantinea Plain, another regression equation is obtained from the salinity results (Figure 121). Using this equation, the apparent conductivities of 17mS/m and 51mS/m are equivalent to 496mg/l and 1524mg/l TDS respectively (Table 25).

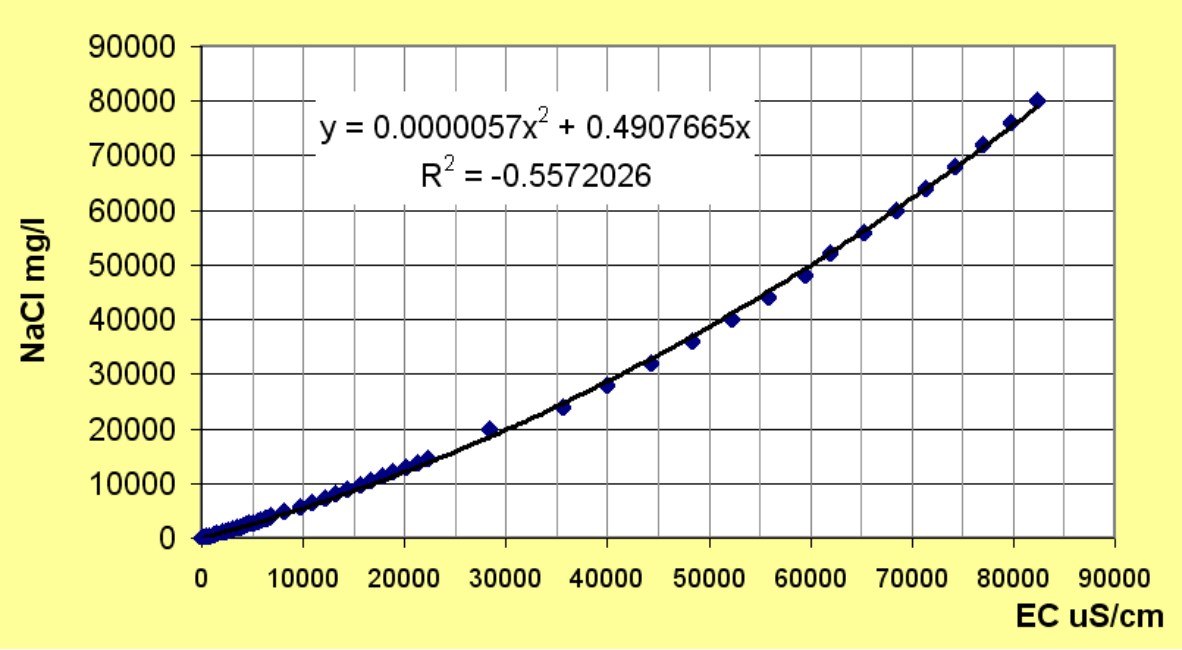

Figure 120: *Scatter plot between dissolved salt (TDS of NaCl) and electrical conductivity (EC).*

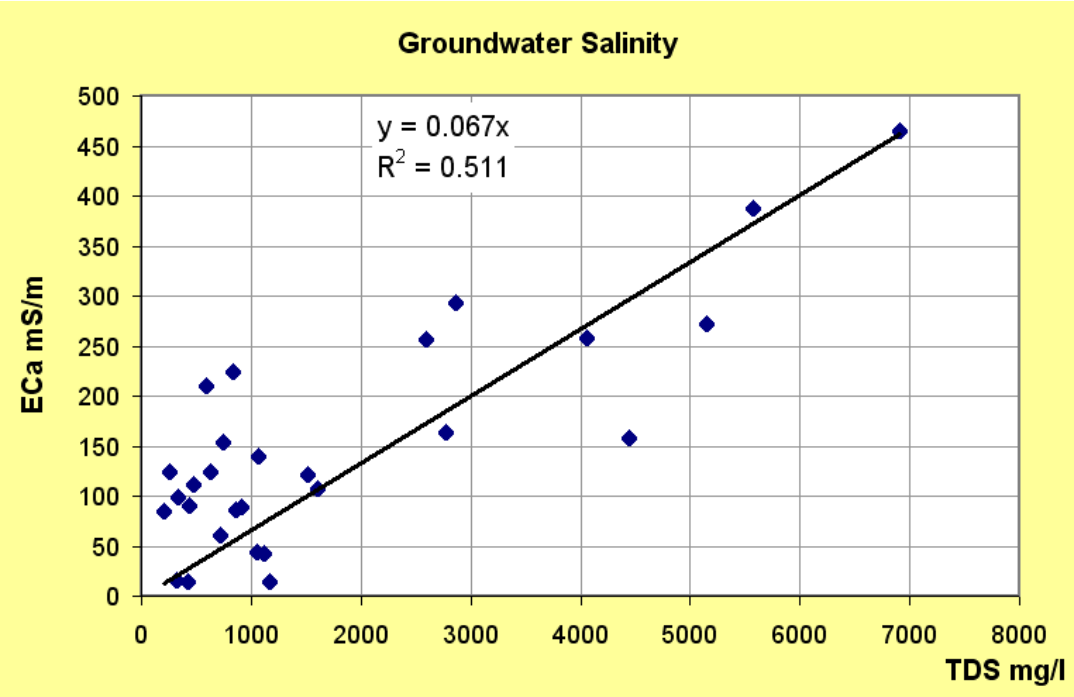

Figure 121: *Scatter plot between apparent conductivity (ECa) and pore fluid salinity (TDS) obtained from the sediment cores.*

Table 25: *Classification of water quality and apparent conductivity of sediment.*

Water quality	Fresh	Slightly Brackish
Water EC	< 1000 µS/cm	1000 – 3000 µS/cm
Apparent Conductivity at Ord, Weaber and Knox Creek Plains	< 33 mS/m	33 – 102 mS/m
Apparent Conductivity at Parry's Lagoon – Mantinea Plain	< 17 mS/m	17 – 51 mS/m

Since the regional groundwater table and the AEM depth slices have different gradients, customized AEM depth slices using the regional standing water level as the datum were produced to facilitate the mapping of the flush zone extent and thickness. This customized depth slices aims to overcome 2 issues. The first is to minimize the occurrence of both unsaturated and saturated zones occurring within each AEM depth slice. This allows the differentiation between resistive flush zone and unsaturated materials (e.g. sand). The second is to distinguish between flush zone and resistive bedrock. This is achieved by masking out the areas occupied by bedrock across specific depth intervals, calculated from the 'Depth to Bedrock' grids. Taking the apparent conductivity values and the depth of extent into consideration, three customized AEM depth slices, i.e. 0 – 5m, 5 – 8m and 8 – 12m below the regional water table were generated. The threshold values shown in Table 25 were used to generate the flush zone extent for each customized depth slice. The relatively weak r^2 values obtained in this analysis reflects the low number of drillhole samples relative to a much greater lithological heterogeneity evident in the study area. The flush zone maps for the Parry's Lagoon-Mantinea Plain-Carlton Hill area are displayed and discussed in Section 8.5.

4.9.2 Flush Zone Thickness

This product complements the 'River Flush Zones' and shows areas and thickness where fresh or slightly brackish water are potentially present. Three customized AEM depth slices, i.e. 0 – 5m, 5 – 8m, and 8 – 12m below the water table, were used to generate the flush zone thickness. These depth slices are converted to grids and assigned with the full thickness. For Parry's Lagoon – Mantinea Plain, areas less or equal than 51mS/m from the three grids were summed. The resulting grid depicts the flush zone thickness. For ORIA Stage 1, Weaber and Knox Creek Plains, areas less or equal than 102mS/m from the three grids were summed and the resulting grid depicts the flush zone thickness.

4.9.3 Flush Zone Extent Maps

Three customized AEM depth slices, 0 – 5m, 5 – 8m and 8 – 12m from the regional water table to bedrock, were used to generate the flush zone extent. In the Parry's Lagoon –Mantinea Plain area, each depth slice was divided into 6 classes (Table 26), with the first 2 classes depicting the fresh and slightly brackish flush zone. For the ORIA Stage 1 (Ivanhoe & Packsaddle), Weaber and Knox Creek Plains, no flush zone was derived as the river is incised into crystalline bedrock.

Table 26: *AEM values and water quality at Parry's Lagoon – Carlton Hill area.*

AEM EC_a mS/m	Water Quality
0 – 17	Fresh
17 – 51	Slight brackish
51 – 102	Moderately brackish
102 – 340	Brackish
340 – 1000	Saline
> 1000	Very Saline

4.9.4 3D AEM Model

The 3D AEM model was generated using Encom's Profile Analyst v9.0. The 3D conductivity voxel was gridded with a 50m cell size for the 18 layers from the laterally constrained inversion conductivity data. The gridding process used by this utility (EM Voxel), creates a 3D voxel model output, but its internal operation is in reality only a 2.5 dimensional gridding process. Each layer of data for the input multi-banded data fields was horizontally gridded using a spline method. Once the grids for each available depth are gridded, they are then combined and output to form the voxel model. The 3D conductivity voxel is in UBC format and consists of two files (a header and data file (.DAT)). The resultant voxel is then offset with the combined LiDAR - SRTM DEM in order to add topography to the 3D model. A separate topography surface was added as a second layer to the 3D model with a 50K topography map overlaid to provide a geographic reference. This layer was duplicated and made semi-transparent. The 3D model also incorporates the flight line sections which consist of PNG's for each flight line which are georeferenced internally within Profile Analyst.

The 3D model (which has been broken up into two, the eastern and western areas) can be viewed using Encom's PA Viewer (included on the DVD in the 3D_viewer_software folder or by downloading free from http://www.encom.com.au/template3.asp?pageid=78). The model can also be viewed using Profile Analyst Explorer or Profile Analyst Professional. The 3D conductivity voxel is in UBC format and consists of two files (a header and data file (.DAT)). A screenshot example of the model is shown in Figure 122.

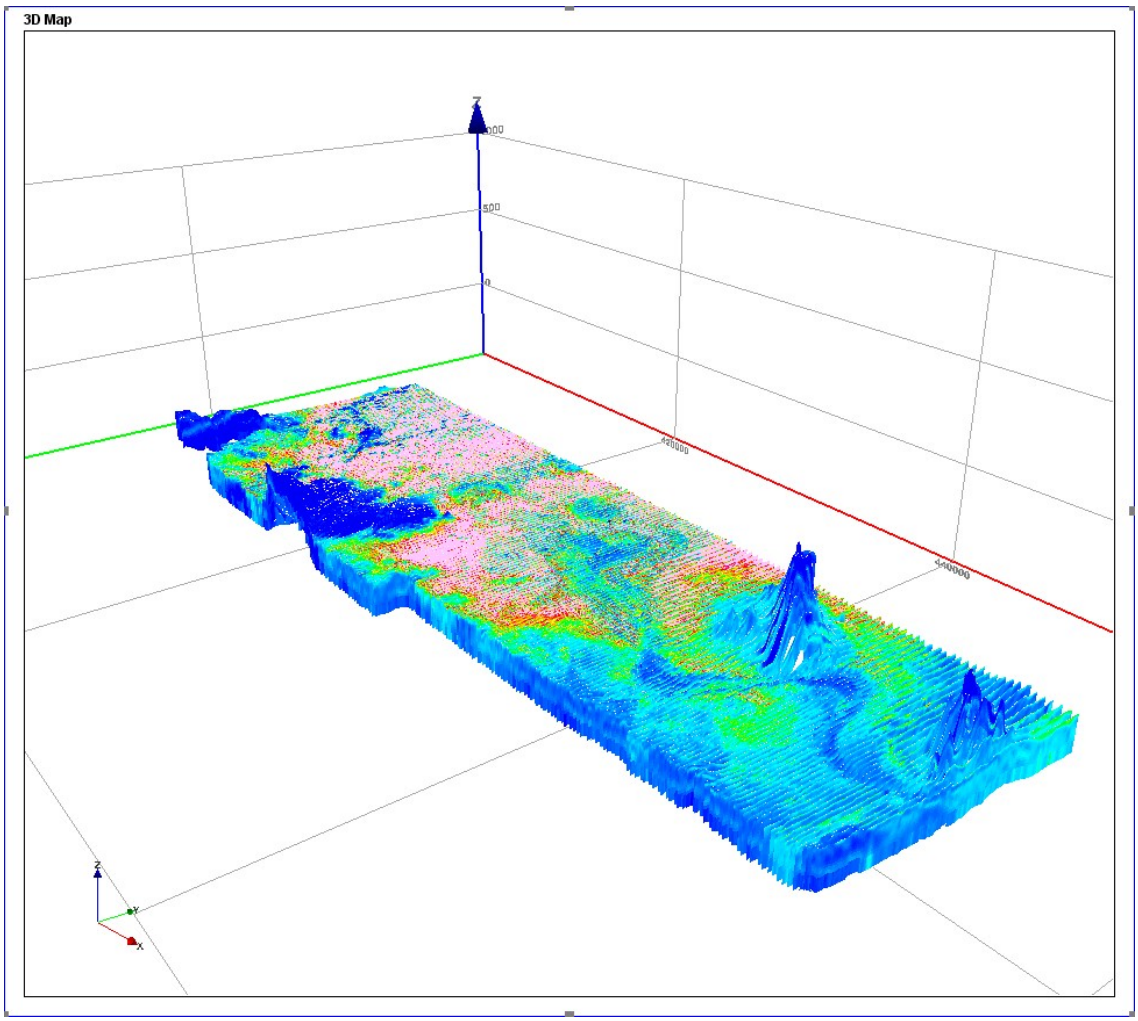

Figure 122: *A low-resolution screenshot example of the 3D model.*

4.10 SALINITY HAZARD MAPS AND INPUTS TO RISK MAPPING AND MODELLING

Salinity is a *hazard* when it has the potential to be moved to where it can threaten assets such as agriculture, infrastructure, water resources and biodiversity (Spies & Woodgate, 2005). *Salinity risk* is a measure of the chance that a salt hazard will cause harm to an asset at some time in the future. Risk should be assessed in the context of the assets to be protected, including agriculture, water quality, infrastructure and the environment. Cost–benefit analyses in salinity management should take into consideration total cost and total benefit in context with the value of all assets.

In their national review of salinity mapping, Spies & Woodgate (2005) concluded that Australia's growing problem of landscape salinisation could not be reliably assessed without a thorough three-dimensional understanding of the landscape and the hydrological processes that operate within it. Mapping salinity hazard involves describing the current extent, depth and concentration of the salt store and salt expression in the landscape (Spies & Woodgate, 2005). Some mapping systems can directly detect salt in the landscape (e.g. soil or borehole sampling) and some can indirectly infer its presence (e.g. through its effect on vegetation or by observing changes to electromagnetic conductivity signals). However, the only broadacre, remote sensing technique that can detect and resolve salinity in the sub-surface deeper than the root zone is electromagnetics (EM) (Spies & Woodgate, 2005).

There are several fundamental questions that land managers and scientists must ask and address to establish whether they are likely to have a salinity problem in the future (George *et al.*, 2003; Spies & Woodgate, 2005). In areas where salinity has yet to express itself at the surface to any significant extent, one of the most basic questions asked by farmers and other land managers is:

Is there salt in the landscape somewhere on or under the land area that I manage that has the potential of being mobilised by water to cause problems for me (or for others)?

To address this question it is important to recognise that not all salt stored in the ground has the potential to be mobilised and transported. Salts may effectively be 'locked up' within clay aquitards, and not available to be mobilised except in geological timescales. However, in tropical climates, extremely high evapotranspiration of relatively fresh to slightly brackish groundwater in shallow floodplain clays can lead to landscape salinisation over time (Ali & Salama, 2003). Hence, while a knowledge of the materials that salt is stored within is important, the depth to groundwater is perhaps more important in these situations.

Challenges for scientists using AEM methods to map and assess the salinity hazard include:

- discriminating the response of different soil and regolith materials from groundwater of different water quality;
- discriminating between electrically conductive salts and clays;
- discriminating between electrically resistive sands/gravels containing fresh groundwater and dry salt-bearing lithologies in the unsaturated zone (Lawrie *et al.,* 2009a);
- establishing where the salt is stored in the landscape;
- mapping watertables;
- determining how much of that salt is stored in aquitards, and as such is unlikely to be mobile;
- quantifying how much of the salt is likely to be mobile;
- establishing the hydrogeological processes that may transport the salt vertically and horizontally.

Managing salinity more strategically is hampered by a lack of knowledge about the location of concentrations of salt in the subsurface and whether they are likely to be mobilised by groundwater and pose a risk to assets. Mapping key elements of the hydrogeology, and determining hydrogeological processes, are the keys to understanding how salt stores are mobilised through the earth, both vertically and horizontally (Spies & Woodgate, 2005).

Are the land area that I manage and the assets that I value at risk of being adversely affected by salinity at some time in the future?

This assessment of risk is far more complicated than salt 'hazard' because it requires an understanding of the factors that operate to govern the movement of salt through time in such a way that the salt is likely to end up damaging the value of assets, either locally or some distance away, at some time in the future. Risk implies a prediction about the severity of the damage that is likely to occur and a prediction about when the damage will occur, and the range of assets likely to be affected (Spies & Woodgate, 2005).

Many factors affect the movement of surface water and groundwater. The following factors define the hydrogeological framework (Spies & Woodgate, 2005).

- Climate: the long-term cycle of droughts and rains, evaporation and precipitation. Climate modifies the water cycle over time.
- Weather: the local affect of rain and sunshine. Weather determines the water cycle over shorter periods.
- Land use and management: the effect of tree clearing, farming, borehole water use and drains. Land use and management practices are the most powerful human-induced activities affecting dryland salinity.
- Terrain: steepness, the location of streams and rivers and break of slope. The combination of terrain and gravity drags water through the landscape.
- Regolith: the unconsolidated material between the surface and fresh bedrock, including soil and weathered rock. The regolith varies in its ability to allow water to permeate and be transmitted elsewhere (hydraulic permeability and transmissivity) and may contain preferential pathways for water movement.
- Soils: the varied composition and structure of different soils affect their susceptibility to the development of salinity.
- Ancestral or prior river and stream systems known as palaeochannels: occur within the regolith. The old stream or river systems that are buried and difficult to detect by the naked eye can preferentially permit the passage of groundwater.
- Bedrock structural highs and buried rock masses: can act as barriers to the passage of water.
- Geological faults and dykes: may act either as underground channels that encourage the movement of water or as barriers to the passage of water.
- Vegetation: is most important because the roots of vegetation take up water through a process known as transpiration. Different vegetation types of varying ages and densities transpire different amounts of water. Moreover, different vegetation types have differing abilities to tolerate salt when it comes in contact with their roots.
- Groundwater itself: its present location, depth, extent, rate of lateral movement and salt content.

These factors govern the rate, location and destination of groundwater. In order to predict salinity risks the behaviour of each of these factors needs to be understood and described. Ultimately the combined interpretation of the role of these factors can be used to prepare maps of salinity risk that show the extent, severity and timing of the threat of dryland salinity in relation to the class of assets being considered. A 'risk map' has higher inherent value (and is more likely to be acted on) if it is targeted at the particular asset for which management decisions need to be made. Modelling techniques are normally used to forecast risk.

This study was limited to the production of salinity hazard maps, and the generation of maps of key elements of the hydrogeological system that will provide a firm basis for further groundwater modelling and generation of salinity risk maps. In this project, two different approaches and products were developed to assess the salinity threat:

- ***Salinity hazard maps***. These combine AEM-derived maps of salt stored in the unsaturated zone with maps of depth to the water table. These data layers are integrated using an informed GIS-based approach that applies variable weighting to these factors. Consequently, the salinity hazard is assessed as high when there are significant quantities of salt stored in the alluvium or soils in areas of shallow groundwater, and lowest where there is little or no salt stored in the alluvium and groundwater tables are deep.
- ***Potential surface (soil) salinity maps***. These maps are based on the analysis and classification of Landsat 5 TM data. These are combined with geomorphic maps using an informed GIS-

approach, and validated using a combination of pre-existing and new data on soil salinity. They are scaled to reflect the potential for salinity to develop in susceptible soils with stored salts, and are ranked from very low potential to extreme.

4.10.1 Sub-Surface Salinity Hazard Maps from AEM data

The 'salinity hazard maps' *sensu stricto* were developed to assess the salinity threat posed by the rise of groundwater to shallow levels, primarily as a consequence of land clearing and irrigation development. The key data layers in this AEM-based suite of maps reflect the key elements of the hydrogeology (watertable depth, salt store in the unsaturated zone and alluvium texture) considered most likely to predict areas of groundwater-driven salinity in soils and sub-soils.

The main drivers for sub-surface salinity hazard are depth to water table and salt store in the unsaturated zone. Of these, the depth to water table has more influence than salt store, as evapo-transpiration will take place readily when the water table is within 2m from surface. Previous studies suggest that the soil will become salinized through repeated cycles of wetting and drying even when the initial groundwater is fresh to brackish (Ali & Salama, 2003).

The depths to standing water level (SWL) across the study area range from 0 to 50m and the calculated salt store in the unsaturated zone range from 0 to > 50t/ha/m (Table 27). Seven subsurface salt hazard classes were assigned using a combination of depth to SWL and unsaturated zone salt stores (Table 28). These classes include very low; low; moderately low; moderate; high; very high and extreme. Extreme salt hazard class is only present in Parry's Lagoon – Carlton plain due to the presence of very shallow and saline groundwater.

Table 27: *Range and classes of standing water level (SWL) and calculated salt store in the unsaturated zone*.

SWL Depth below Surface (m)	Unsaturated zone Salt Store (t/ha/m)
0 – 2	0 to 10
2 – 4	10 to 20
4 – 6	20 to 30
6 – 8	30 to 40
8 – 10	40 to 50
10 – 20	> 50
20 – 50	

Table 28: *Sub-surface salt hazard classes and the combination of depth to SWL and salt store.*

Salt Hazard Class	SWL Depth below surface (m)	Unsaturated zone Salt Store (t/ha/m)
Extreme	0 – 2	30 – 40
	2 – 4	40 – 50
	4 – 8	50 – 100
	8 – 10	> 100
Very High	0 – 2	20 – 30
	2 – 4	30 – 40
	4 – 8	> 40
	8 – 10	> 50
High	0 – 2	10 – 20
	2 – 4	20 – 30
	4 – 8	30 – 40
	8 – 10	40 – 50
	10 – 20	> 50
Moderate	0 – 2	0 – 10
	2 – 4	10 – 20
	4 – 8	20 – 30
	8 – 10	30 – 40
	10 – 20	40 – 50
	20 – 50	> 50
Moderately Low	2 – 4	0 – 10
	4 – 8	10 – 20
	8 – 10	20 – 30
	10 – 20	30 – 40
	20 – 50	40 – 50
Low	4 – 8	0 – 10
	8 – 10	10 – 20
	10 – 20	20 – 30
	20 – 50	30 – 40
Very Low	8 – 10	0 – 10
	10 – 20	0 – 20
	20 – 50	0 – 30

The approach used in this project to produce the salinity hazard maps makes a number of assumptions, specifically:

- The new watertable map is an accurate reflection of the current situation;
- Watertable levels will rise after land clearing and the onset of irrigation;
- Watertable rise is vertical, with no lateral component to flow;
- Watertable rise is a greater hazard where it is already at shallow depths beneath the surface;
- Evapotranspiration of shallow water tables may lead over time to salt accumulation through capillary rise and evapotranspiration, if the watertable rises to within 2-3m of the surface (and either continue to rise and discharge to the surface, or equilibrate at these depths);
- AEM-derived salt store maps accurately quantify the amount of salt stored in the landscape;
- Salt stored in the landscape is available to be mobilised.

These assumptions and their implications are discussed later in this report.

4.10.2 Surface (Soil) Salinity Potential Map

'Potential surface (soil) salinity maps' were developed mainly in recognition that in some Stage 2 areas there are areas of moisture persistence that remain at or near the land surface for much of the dry season in areas where watertables are currently at significant depths below the surface. The water in these latter areas comes primarily from wet season run-off that is localised in internal drainage basins where there is perching and/or

low rates of deep drainage. There are also occurrences fed by groundwater-driven springs and by overflow from the D8 swamp (in the northern Weaber Plain). In these locations, salt is concentrated in soils and sub-soils by evapotranspiration of infiltrated rainwater and/or spring-derived water.

AEM data were not used in the construction of the 'potential surface (soil) salinity maps', due to the desiccation of many of the soil profiles in much of the Stage 2 areas at the time of survey, and lack of soils data at appropriate scales to validate this layer. However, it should be noted that there is a close correlation between areas of high conductivity in the 0-2m depth slice and some of these moisture persistence areas (e.g. northern Weaber Plain). This is taken as further evidence that these are sites of salt accumulation in the landscape, although further ground validation is required.

Previous investigations have used satellite remote sensing imagery validated by field investigations to produce maps of surface (soil) salinity potential (Metternicht & Zinck, 2003; Lawrie *et al*., 2009a). In this study, a Landsat-5 TM scene acquired on 30 March 2009. Image enhancement was carried out on 6 bands (except band 7) using principal component analysis (PCA). The 1st component was divided into 15 land-cover classes based on reflectance values. The 1st component was divided into 15 land-cover classes based on reflectance values. These classes were then combined with geomorphic units ranked according to susceptibility of geomorphic units to surface salinity.

The LANDSAT classes were combined with the irrigation layer to separate cleared ground within irrigation areas, bare eroded ground and surface salinity scalding. These classes were then combined with geomorphic units ranked according to susceptibility to salinisation. Classes were assessed against soil salinity data and grouped, and assigned to respective surface salinity class. The geomorphic map was produced as part of this project, and the methodology used is described earlier.

To validate these data, 12 soil samples were collected by GA staff in May 2009 and used to supplement the 53 EC 1:5 data points from 7 transects and 76 EC 1:5 data points from 22 locations (Smith & Price, 2008). This approach has produced a map of potential surface (soil) salinity, ranked from very low potential to extreme, reflecting the potential for salinity to develop in susceptible soils with stored salts (Figure 123).

Using this approach has enabled excellent correlations to be obtained between the GIS-modelled predictions of higher salinity and field data. Over 90% of the salt scalds validated by field mapping were identified using this modelling approach. However, it was recognised that this approach by itself was not able to identify areas in Stage 2 where the salt store in the sub-soil layers may be high.

Rather, these maps are more powerful when used in conjunction with maps of shallow conductivity (0-2m) that are integrated with maps of moisture persistence (produced by temporal analysis of Landsat data). The latter identify areas of surface moisture persistence and high conductivity where salts are thought to accumulate at surface (in areas of deeper water tables). Significant areas of moisture persistence, where water and/or high soil moisture levels remain at or near the land surface for much of the dry season, were mapped in areas where watertables are currently at significant depths below the surface.

Given adequate resources, there are a number of additional ways in which these maps could be improved significantly. For example, integration of the two products and longer term temporal analysis of the Landsat data (back to 1978) could be undertaken to provide a picture of annual and seasonal fluctuations of surface water body and vegetation vigour. This could be used to build an understanding of the links between rainfall and surface moisture. Integration with hydrogeochemical studies could help to determine if any of the shallow salt stores have a (palaeo-) groundwater component, while the products could be improved through additional ground validation. Integration with soils data at appropriate scales would also be extremely valuable, while the use of the soils maps to validate the AEM data which could be used to map sub-soils in the deeper part of the soil profile and top layer in the sub-soils (1-4m).

Overall, the existing potential surface (soil) salinity maps have limited use, but used in conjunction with maps of shallow conductivity (0-2m) integrated with maps of moisture persistence, may provide valuable baseline data on potential surface and near-surface soil salinity hazard in areas that have yet to be developed.

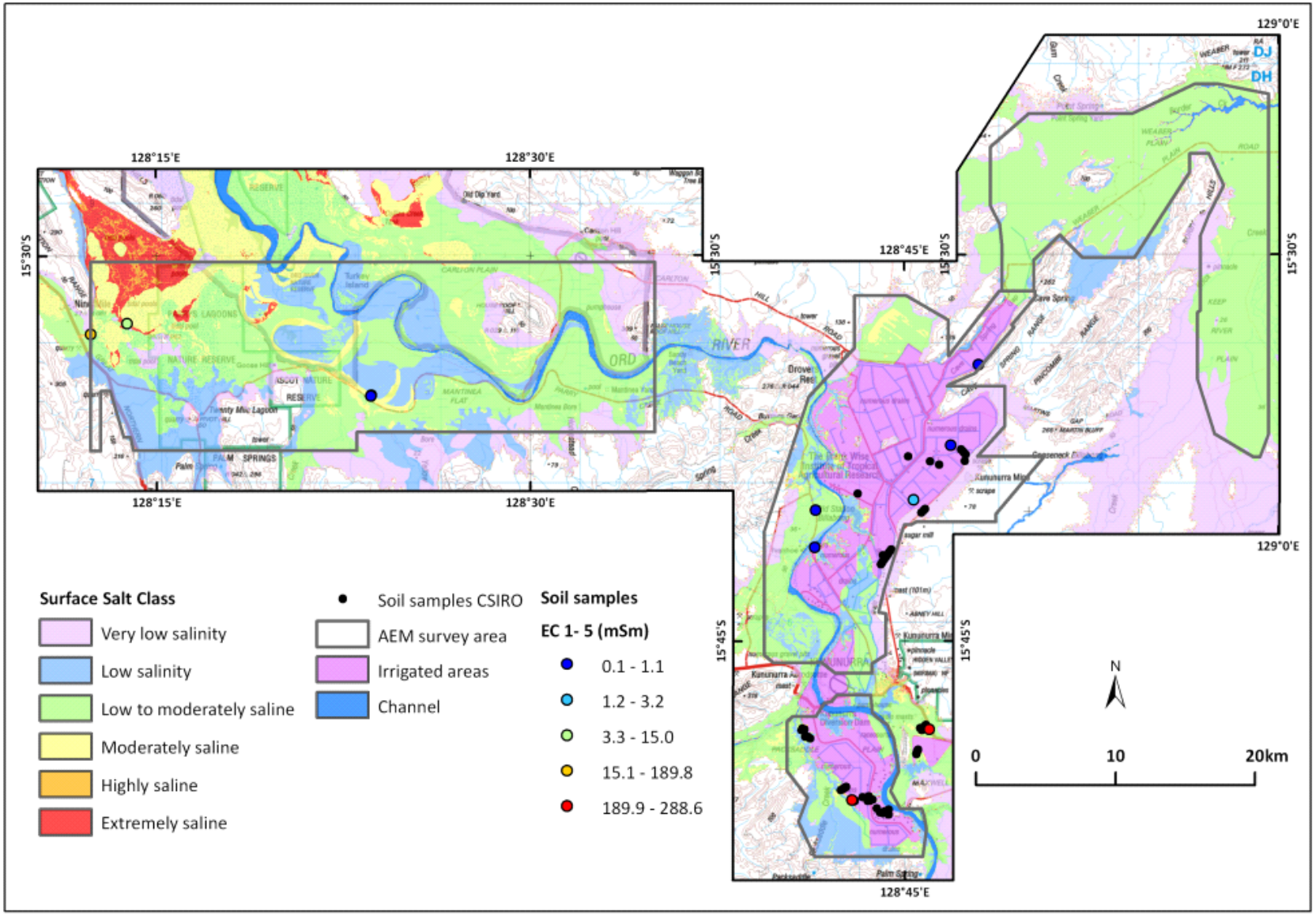

Figure 123: *Potential surface salinity mapped from classification of LANDSAT imagery.*

5 Landscape Setting, Geomorphology, Regolith, Landscape Evolution, and Soils

5.1 LANDSCAPE SETTING, GEOMORPHOLOGY AND REGOLITH

The land systems, geology, landforms, soils, vegetation and land use of the Ord – Victoria area, of which the ORIA is a component, are described by Stewart *et al*. (1970). The latter study was based on fieldwork carried out in the early 1950s, and is the first comprehensive report on the physical geography of the area. Most of the Ord Irrigation Area falls within the Ivanhoe Land System, the details of which are summarised in Figure 124. Five of these landform units (Units 1, 3, 4, 6 and 7) are mapped on the landform/geomorphology map prepared for this project.

Very little geomorphological research has been carried out in the basin of the Ord River. Coleman and Wright (1978) described the estuarine and deltaic sediments of the Ord and Pentecost rivers in Cambridge Gulf. Cluett (2005) described the changes in channel morphology and riparian vegetation below the diversion dam since the onset of flow regulation. There have been no published studies on the sedimentology the flood plains in the ORIA (the Packsaddle, Weber, and Ivanhoe Plains) or of the surrounding landscape.

The ORIA Stage 1 and Stage 2 areas straddle the Ord and Keep River sub-catchments (Figure 2). The floodplains of the Ord River downstream of Lake Argyle have been compartmentalised into several distinct zones. These consist of the Packsaddle, Ivanhoe, and the Mantinea and Carlton Hill Plains. The plains are bounded by hills of Proterozoic sediments, mostly quartzites with some siltstones and shales, and of Palaeozoic sediments, in particular Devonian sandstone and Carboniferous limestone, with minor volcanic lithologies.

The landscape in the study consists of two main elements: alluvial plains and low hills rising steeply out of them (Figure 82, Figure 125 and Figure 126). The hills fall largely outside the study area (Figure 23). Larger bedrock features were classified as hills (Figure 126), smaller ones as rises (Figure 127) or towers (Figure 128). There are also extensive areas of pediments where low angle slopes with shallow bedrock occur marginal to the main valley floors. The pediments are typically mantled by colluvial to residual gravel between one and two metres thick (Figure 129).

The plains themselves (Figure 4, Figure 36 and) can be subdivided into geomorphically distinct features, the relict floodplains of the Stage 1 ORIA (Packsaddle and Ivanhoe Plains; e.g. Figure 4), the relict to active transitional floodplains of the Knox Creek and Weaber Plains (e.g. Figure 130), and the active floodplain of the lower Ord (Figure 82, Figure 24 and Figure 131).

The topography of the Packsaddle and Ivanhoe Plains has been extensively modified by laser levelling in the course of the development of irrigation works. However, analysis of pre-clearing aerial photographs suggests that the landscape was very flat initially (D. Gibson, pers. com.). Comparison with uncleared areas and the morphology of the Weaber Plain immediately adjacent to Ivanhoe Plains in Cave Springs Gap also indicates that the original surface of these plains was very flat.

Geomorphically significant deviations from this extremely flat surface include: the meandering channel of the Ord River itself (Figure 125), now incised into the alluvial section (Figure 132); gullies which occur along the edge of the incised channel (Figure 23 and Figure 125); a prior stream on Ivanhoe Plain represented by a low sinuous rise that is partly exploited by the M1 supply channel (Figure 23); and Packsaddle Creek which runs along the western side of Packsaddle Plains at a lower elevation than the rest of the Plain (Figure 23). The Ord River is cut down to bedrock for most of its reach through the Packsaddle and Ivanhoe Plains (Figure 125, Figure 133 and Figure 134).

(47) Ivanhoe Land System (2200 sq miles)

Many small to medium areas of gently sloping alluvial "black soil" plains with some timbered "red" soil in the central and northern parts of the area.

Climate.—Wettest locality: mean annual rainfall 35 in.; mean agricultural growing season 18 wk; mean pasture growing season 22 wk. Driest locality: mean annual rainfall 22 in.; mean agricultural growing season 10 wk; mean pasture growing season 14 wk.

Geology.—Quaternary alluvia.

Geomorphology.—Fine-textured fluvial plain.

Drainage.—The flood-plains of the Ord and Victoria Rivers are characterized by deep broadly meandering channels, and the flood-plains of the upper Baines and Armstrong Rivers have an intense pattern of braided stream channels.

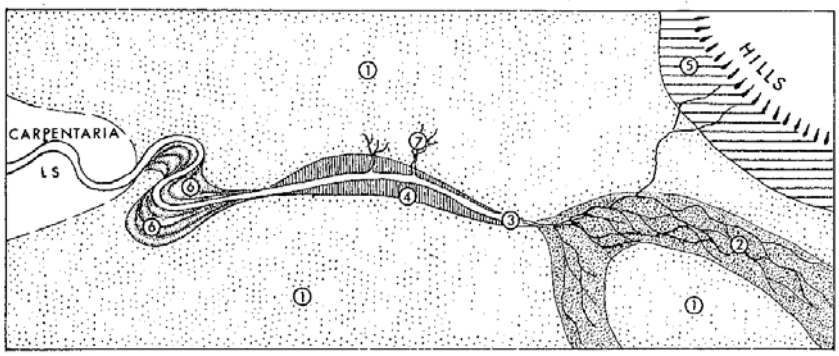

Unit	Area	Land Forms	Soils	Vegetation
1	Large	Nearly flat plains	Cununurra—grey cracking clays with small areas of Argyle—brown cracking clays	Blue grass tall grass (*Dichanthium* spp., *Astrebla squarrosa*, *Sorghum stipoideum*, *Ophiuros exaltatus*, *Aristida latifolia*) with fringing forest and fringing tall grasses near stream lines
2	Small	Valley floors up to 2 miles with intense braided pattern of small channels		
3	Very small	Major stream channel, ¼–¾ mile wide and up to 60 ft deep		Fringing communities
4	Very small	Levees associated with major stream channels	Mostly Manbulloo and Katherine—brown sand or sandy loam over permeable reddish brown subsoil; Ord along Ord River and its major tributaries	Frontage woodland (*E. papuana*, *E. tectifica*, *E. terminalis*) with frontage tall grass (*Sorghum stipoideum*, *Chrysopogon latifolius*, *Panicum* sp., *Aristida* spp.)
5	Very small	Plains adjacent to sandstone hills, in upper part of West Baines River valley	Manbulloo and Katherine	Northern box–bloodwood woodland (*E. grandifolia*, *E. latifolia*) or silver-leaved box sparse low woodland (*E. pruinosa*) with three-awn mid-height grass (*Aristida* spp., *Chrysopogon fallax*)
6	Very small	Scroll plains with alternating low levee ridges and swales; adjacent to and inland from Carpentaria land system	Brown alluvial soils with stratified sediments at shallow depth	Frontage woodland (*E. papuana*, *E. tectifica*, *E. terminalis*) with frontage tall grass (*Sorghum stipoideum*, *Chrysopogon latifolius*, *Panicum* sp., *Aristida* spp.)
7	Very small	Moderately to steeply sloping gully systems up to 60 ft deep	Various undefined loamy and clayey soils, commonly with carbonate concretions at the surface	Scattered trees and sparse grass

Figure 124: *The Ivanhoe Land System, from Stewart et al. (1970). Units 1, 3, 4, 6 and 7 occur in the Ord Irrigation Area.*

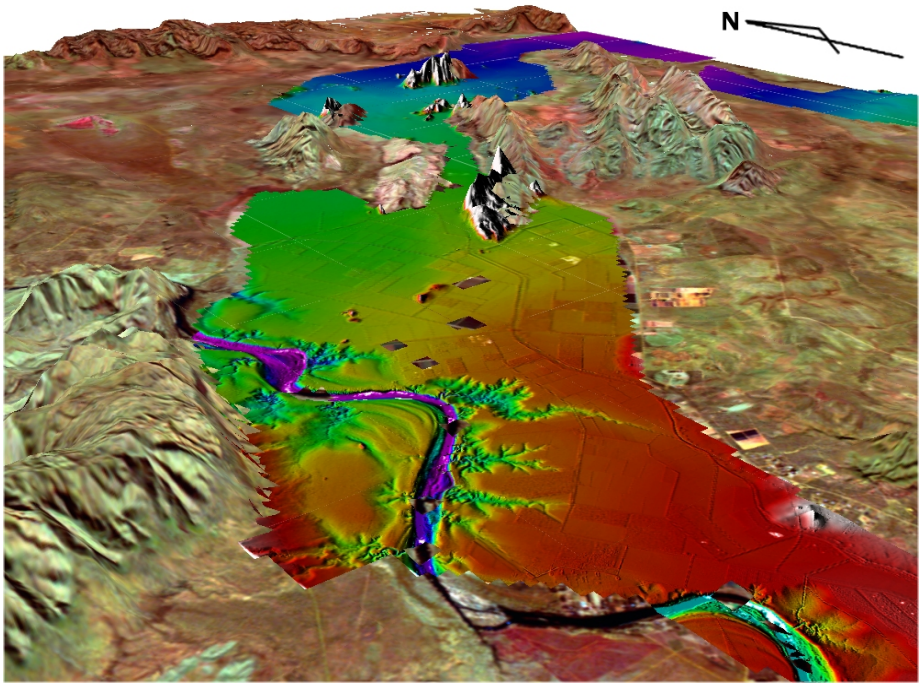

Figure 125: *Perspective view of the LiDAR DEM draped over an Orthophotograph of the eastern half of the project area, (vertical exaggeration). This image shows the flat alluvial plains of the Ivanhoe Plain in the foreground and the Weaber Plain in the distance, visible through Cave Springs Gap. The sinuous Ord River is visible in the foreground. Very small, low hills are evident in the Ivanhoe Plain.*

Figure 126: *Hill along Keep River Road (part of Cave Springs Range).*

Figure 127: *Dumas Lookout, in Ivanhoe Plain. This low rise in the foreground comprises almost unweathered Proterozoic basalts, while the hills in the background comprise Devonian sandstones*.

Figure 128: *Towers of Devonian sandstone near Kununurra.*

Figure 129: *Pediment-mantling gravels over Wyndham Shale along old Wyndham Road.*

Figure 130: *Northern Weaber Plain looking northward towards scarp of Weaber Range.*

Figure 131: *View looking northwards from the old telegraph station looking over Parry's Lagoon and the active lower Ord floodplain.*

Figure 132: *The Ord River at Ivanhoe Crossing, looking west. The River is incised into 15-20m of alluvium at this location, and is floored by Cambrian basalt bedrock.*

Figure 133: *Photograph showing Bandicoot Bar (silicified Proterozoic sandstone) on which the Ord Diversion Dam is built.*

Figure 134: *Photograph showing K.P. Tan standing on Cambrian basalt bedrock along the banks of the Ord River at Tarrara bar.*

5.1.1 Packsaddle and Ivanhoe Plains, and Tarrara Bar

The present landscape surface of the Ivanhoe and Packsaddle Plains is composed almost exclusively of clay and clay-derived soils. Silts are present to the north of Greens Location and northeast of Martins Location. These silts are mostly likely associated with sheet wash and pediment cover. Sands are restricted mainly to marginal areas of the floodplains in relatively minor colluvial and alluvial fans. Packsaddle Plain occurs upstream of Bandicoot Bar on which the Ord Diversion Dam is built (Figure 133), and the confluence of the Dunham and Ord Rivers (Figure 82). Areas of colluvial and alluvial fans at the base of the hills and rises are especially well developed along the southern margin of Packsaddle Plain (Figure 82). Elsewhere they are a minor feature of the landscape. The fan deposits are likely to be poorly sorted, and contain both coarse and fine-grained material fixed together and poorly differentiated. The present-day surfaces of both Packsaddle and Ivanhoe Plains have been strongly modified by laser levelling.

Bedrock occurs as hills and rises emerging from this fluvial landscape. These are largely composed of Devonian and Proterozoic sandstones (Figure 4 and Figure 36). The Devonian sandstones in particular are developed into joint controlled sandstone towers (Figure 128), surrounded by pediments of slightly weathered bedrock. Other low hills were composed of Cambrian basalts (the Antrim Plateau Volcanics; Figure 127).

The moderately sinuous channel of the present-day Ord River has been incised into the Packsaddle and Ivanhoe alluvial plains through its entire length north to Tarrara Bar (Figure 134). The bedrock surface exposed by the channel is stepped, with a narrower incised channel occupied by the dry season river and a broader bedrock surface that forms the bed during wet reason flow (Figure 132). This upper surface is being exposed by lateral erosion of the alluvium. The incision of the Ivanhoe and Packsaddle Plains may be related to the river finding a new outlet to the west through the Tarrara Bar. This would have resulted in a new, steeper downstream gradient profile and down and back cutting as the river established a few equilibrium profile. At Tarrara Bar the Ord abruptly swings to the west and runs through a narrow valley (Figure 135) cut through the Deception Range until it reaches the Ord Estuary. At Tarrara Bar, coarse sand anti-dunes (up to 5m high) occur on the banks. These were deposited during peak flood flow when Tarrara Bar is under water and current velocity exceeds ~2m per second (Figure 136).

Figure 135: *The Ord River at Tarrara bar as it cuts through the Deception Ranges. Photograph taken looking downstream.*

Figure 136: *View across Tarrara Bar from north to south, upstream is on the left side. Coarse sand anti-dunes (up to 5m high) deposited during peak flood flow when bar is under water and current velocity exceeds ~2 m per second.*

5.1.2 Cave Springs Gap, Weaber, Knox Creek and Keep River Plains

The Ord River is inferred as having formerly flowed through Cave Springs Gap (Figure 137) to form the Weaber Plains (Gunn, 1968). These plains maintain their gradient to sea level though continuity with the Keep River Plains and the Victoria River estuary. The Weaber Plain (Figure 130) is relatively flat and geomorphically inactive, although large parts are subject to inundation during the wet season. It is bounded by hills that rise abruptly at its margins (Figure 130 and Figure 138). Alluvial and colluvial fans (Figure 138 and Figure 139), some with coarse debris flows (Figure 140), are present along its margins. The fans do not appear to extend any significant difference onto (or under) the Plain, with sharp boundaries observed (Figure 140).

Figure 137: *The M1 supply channel as it heads through Caves Springs Gap. Photograph taken looking east.*

Figure 138: *Hills rise abruptly along the eastern side of Cave Springs Gap. Alluvial and/or colluvial fans are developed along some of these margins.*

Figure 139: *Close-up of an alluvial/colluvial fan on the southern margin of the Weaber Plain.*

Figure 140: *Abrupt terminus of a coarse debris flow at the southern margin of the Weaber Plain.*

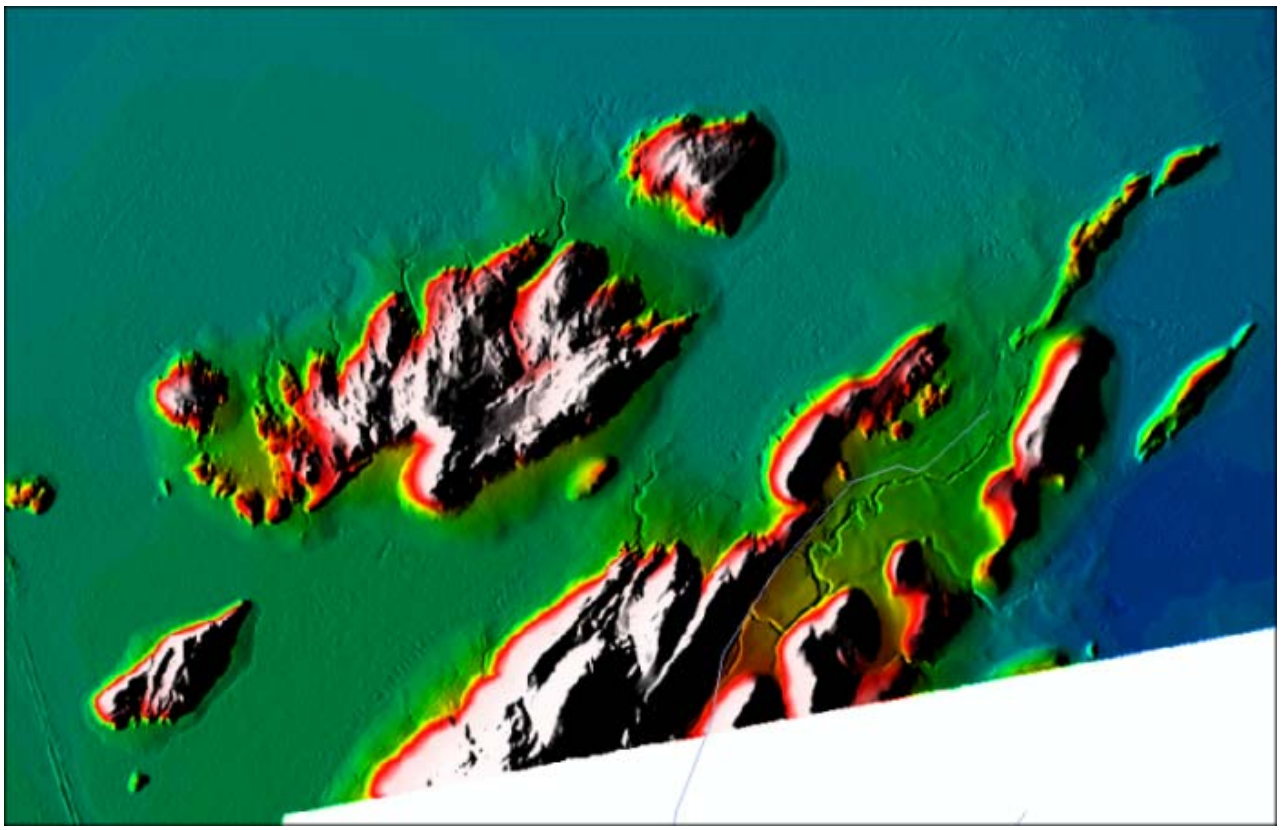

Figure 141: *Close up of the LiDAR DEM of the southern Weaber Plain showing bedrock hills (white) mantled by colluvial fans which are abruptly truncated on the plains.*

A number of intermittent watercourses from the surrounding hills discharge on to the plain. This water spreads out as sheet flow as the greater part of the plain has no incised channel. Only at the northern extremity of the plain is there defined drainage, where Border Creek carries water eastwards into the Keep River, although only in exceptionally wet periods. The course of Border Creek is fixed, narrow, and highly sinuous.

Point Spring and Cave Spring are two small but permanent water bodies that occur at the foot of the Weaber Range and the Cave Spring Range respectively (O'Boy *et al*., 2001). Both are interpreted to have formed by discharge of groundwater derived through fracture flow from the adjacent ranges. More recently, a shallow surface water body (the D8 swamp) has formed on the western portion of the Weaber Plain as a consequence of drainage releases from ORIA Stage 1 (Figure 142). The D8 swamp varies in size with climatic conditions and volume of discharge; however, at times it is about 5km long and 2km wide (Figure 142). At times of heavier rainfall, this water body appears to overflow, with water observed in satellite imagery to flow to Point Spring.

Figure 142: *Google earth image showing the location of the D8 swamp (wetland) formed from discharge from the D8 drain.*

The Knox Creek Plains are of composite derivation, consisting of the aggraded floodplains of both Knox Creek to the west and the Keep River to the east (Figure 143). Knox Creek also is appears to have a fixed, narrow, and highly sinuous morphology. By Contrast, satellite and aerial imagery shows that the Keep River consists of a sandy meander plain between 0.8 and 1.5km wide, composed of channels ~20m wide, slightly inset into the clay-rich floodplain. The Knox Creek and Keep River Plains are mostly well drained due to their relatively uniform gradients.

Figure 143: *Alluvial plain at Knox Creek, typical also of Weaber Plains and probably packsaddle and Ivanhoe Plains prior to development.*

5.1.3 Lower Ord Plains (including Mantinea Plain, Parry's Lagoon and Carlton Plains/Hill)

The lower reaches of the Ord are composed of an active depositional plain with a strong estuarine influence, which increases as it nears Cambridge Gulf (Coleman & Wright, 1978; Thom *et al*., 1975; Wright *et al*., 1973). The lower Ord Plains, consisting of the Carlton and Mantinea Plains to the north and south of the river respectively, and the coastal plain to the north-west, are much more complex geomorphologically than the other areas.

This reach of the Ord River is characterised a very large scale and actively migrating meander plain (Figure 23 and Figure 82). Although only eight or nine meanders bends are developed before the estuarine funnel is

reached, the meanders have a wavelength of 5-9km, an amplitude of 3-6km, and the channel varies from 200-300m wide (Figure 23).

Mantinea Plain and Carlton Hill are the actively aggrading floodplains lying south and north of the Ord River respectively (Figure 82). Colluvial and alluvial fans occur at the base of the hills and rises along the southern edge of Mantinea Plain (Figure 82). The fan deposits are likely to be poorly sorted and contain both coarse- and fine-grained material that is poorly differentiated. Run-off from the adjacent hills appears to contribute significantly to replenishment of freshwater bodies in Parry's Lagoon (Figure 131 and Figure 144). Prominent hills with a distinctive harder capping, rise from the centre of the plains and dominate the landscape (Figure 145; Figure 146).

An unexpected discovery of this study, albeit one hinted at by the report of Nixon (1996, 1997c, d) of shelly material in some bores, is the discovery of extensive coastal plain sediments formed by the infill of a former embayment in the area. Much of the Carlton and Mantinea Plains are composed of this material and the Ord River floodplain is inset slightly into it.

The Ord eventually enters the sea via Cambridge Gulf. Wolanski *et al*. (2001) showed how reduced coarse bedload transport by the Ord as a result of river regulation. They noted increased saltation and predicted reductions in channel depth and width, reduced length of saltwater wedge, and much stronger tidal asymmetry. Cluett (2005) investigated the changes in channel morphology and riparian vegetation below the diversion dam since the onset of flow regulation and noted that increased bank stability and more dense vegetation (Figure 147) were likely.

Figure 144: *Marlgu Billabong.*

Figure 145: *House Roof Hill viewed from Mantinea Plain. These distinctive hills are Proterozoic in age, with shales in the lower half and a thin sandstone capping.*

Figure 146: *False House Roof Hill, Carlton Station. Photograph looking south, shows alluvial fans along the margins.*

Figure 147: *The Ord River as it cuts through Mantinea Plain. Photograph shows members of the project team and Richard George (far right). The photograph shows dense vegetation along the riverbanks and exposed bed, which have stabilised since river regulation.*

Three different alluvial surfaces are evident in new geomorphic mapping. The first is associated with the actively migrating channel of the Ord River and consists of a meander plain (Figure 148), oxbows, and levee banks. The second is a smooth plain that is of slightly higher elevation than the meander plain, which appears to be inset into it. The third is a higher-level terrace whose margins are being actively gullies. This lies in the extreme east of the project area and much of the unit lies outside it.

Figure 148: *Undulations representing scroll bars and swales on meander plain of lower Ord River at site PL2. Truck is parked on top of scroll bar with a swale between it and the camera.*

To the west and north there is a coastal plain (Figure 131 and Figure 149). This consists of an extremely flat, moderately saline surface with numerous shallow, freshwater seasonal swamps and permanent billabongs (Figure 131; Figure 144). The coastal plain passes laterally to the north and west into tidal flats, and is interpreted to be the result of seaward progradation of freshwater deposits over the tidal flats. These tidal flats all occur outside the project area, but where mapped as part of the broader context. The tidal flats are drained by tidal creeks, but again, none occur in the project area.

Figure 149: *Coastal plain west of Parry's Lagoon, near drill site PL3. Plain is seasonally inundated and saline groundwater occurs within a few cm of the surface.*

5.1.4 Regolith Weathering

Bedrock weathering

Weathering is almost completely absent in the bedrock beneath the alluvial successions in all boreholes where it was encountered. At most, 1-2m of slightly weathered material was present, regardless of whether this was Proterozoic sandstone or shale, Cambrian basalt, or Carboniferous shale and limestone. Otherwise, weathering of bedrock is limited to development of thin rinds and varnishes. Varnishes of iron and manganese are also locally common, especially on sandstones.

The lack of weathering profiles can be interpreted in one of two ways: either weathering rates are very slow, or erosion exceeds weathering. Given that weathering rates should be high in a tropical, sub-humid

environment such as occurs today at Kununurra, the second possibility seems more likely (Lawrie *et al*., 2006a). The sandstone towers developed on the Palaeozoic sandstones to the east of Kununurra (for example in the Hidden Valley NP) suggest that solution is plays an important or dominant role in erosion (c.f. Bungle Bungles, Young, 1986).

The lack of saprolith development may be important hydrogeologically, as there is a low probability of there being a low permeability aquifer or potential salt store at depth beneath the alluvial fill, and volcanic and sandstone basement lithologies beneath the valley fill will most likely act as a fractured rock aquifers. There is therefore likely to be good hydraulic connectivity between underlying bedrock and the alluvial aquifers. This factor may have to be considered within any future groundwater modelling.

Weathering of the Ord valley alluvial sediments

Weathering overprints are commonly observed within the Ord alluvium. Most commonly, weathering is noted as silicification and ferruginisation of the alluvial fill. This is present as duricrusts in some outcrops, and recorded as significant cementation of sands and gravels in mineral exploration drillhole reports (Lawrie *et al.,* 2006a). Tufa formation is also recorded, particularly in Weaber Plain (Nixon, 1997a-h). These zones of intense weathering most likely reduce the hydraulic conductivity of basal sands and gravels, however mineral exploration reports suggest these indurated zones have a patchy distribution, but can still form laterally extensive areas with individual drillholes intercepting zones 5- 12m in vertical extent (e.g. in the vicinity of Ivanhoe Crossing).

These zones most probably originally marked zones of higher groundwater flow, but now most likely form localised barriers to groundwater flow in the alluvial aquifers. Zones of silicified alluvium are noted particularly in the banks of the present day Ord River. These indurated zones are formed from interaction of surface water with groundwater, and may be localised around areas of preferential recharge and/or basement faulting. Hardened crusts developed within the regolith profile are very important features for understanding the groundwater migration paths through the landscape. Some duricrusts are highly permeable, and act as groundwater conduits. Other duricrusts can act as aquitards.

In the ORIA, the main duricrust commonly observed was a widespread but patchy ferricrete composed of haematite, goethite and silica meniscus-cemented granules and pebbles of regolith-derived goethitic and haematite clasts was observed in many locations resting on bedrock of both Proterozoic and Palaeozoic age (Figure 150). This unit varies across the area from 30cm to 2m in thickness, and has locally been quarried for road base. The ferricrete is highly porous and is predicted to be a major groundwater flow zone in the area, especially where it occurs at the base of the alluvial succession overlying shallow (<5m) less permeable bedrock. In several locations these processes have resulted in silicification and ferruginisation of basal breccias and conglomerates, and/or silicification and ferruginisation of brecciated bedrock, to form conglomeratic ferricrete (Figure 151). The latter form semicontinuous zones 1-2m zone thick, and are common at the top of shallowly buried Devonian Sandstones (Figure 150).

These indurated zones appear to be highly porous and permeable at their base, and form laterally extensive (>100's of metres) layers that focus groundwater flow, and are common in the Junction soil complex (Burvill 1990). These units appear to localise the lateral seepage of groundwater into the D1 drain (Figure 152). At Mulligan's Lagoon, presence of this conglomeratic ferricretes is coincident with salinity discharge, and the management action taken was to rip the material to attempt to improve drainage (Smith & Price, 2008).

Earlier observations (Lawrie *et al.,* 2006a) provided significant insight into the genesis of duricrusts and ferricretes in the project area. Exposures of the ferricrete in the drains along the eastern margin of the ORIA show visible seepage from within the ferricrete and along its base. Other exposures of the basal alluvium near the diversion dam, where there is patchy ferricrete, and in a quarry to the northwest of the irrigation area, also show significant lateral flow along the base of the alluvial succession. Furthermore, at both localities, there are visible rafts of ferrihydrite on the surface of the discharging waters (Figure 153), indicating significant lateral transport and precipitation of iron within the ferricrete horizon during the wet season (Lawrie *et al.,* 2006a).

Other features of note include pedogenic carbonate exposures within older red-brown alluvial silts and sandy silts in the banks of the Ord River (Lawrie *et al*., 2006a). The pervasiveness of the carbonate cements points

to predominantly alkaline groundwater conditions during the diagenesis of the flood plain sediments. In addition, there is a widespread iron and silica cemented horizon along the basal unconformity.

Other cements observed within outcrops of alluvium include:

1. Carbonate cements surrounding former roots (rhizomorphs) in silty deposits exposed in the eroded flood plain (e.g. at Ivanhoe Crossing).
2. Pervasive intergranular carbonate cements in moist gravels exposed in the river bank at various locations along the Ord River.
3. Incipient clay and haematite cementation of old floodplain sediments at Packsaddle Plain.

Figure 150: *Photograph showing ferricrete breccia forming on top of sandstone bedrock on the east bank of the D4 drain near Milligan's Lagoon Road. The breccia is between 1.5m and 2m thick. Seepage at the bedrock-ferricrete interface is still evident at the end of the dry season.*

Figure 151: *Close up of conglomeratic ferricrete developed on slightly weathered sandstone.*

Figure 152: *Seepage at the interface of ferricrete breccias and sandstone bedrock along the eastern bank of the D4 drain.*

Figure 153: *Visible rafts of ferrihydrite and iron chellates forming on the surface of discharging waters at the site of iron ferricrete formation.*

5.2 GEOCHRONOLOGICAL CONSTRAINTS ON LANDSCAPE EVOLUTION

As a consequence of its avulsion, the Ord River Floodplain is now a relict feature, with the river once again having incised it way to bedrock. This incision may be related to the river finding a new outlet to the west. This would have resulted in a new, steeper downstream gradient profile and down and back cutting as the river established a new equilibrium profile.

Optically Stimulated Luminescence (OSL) dating was carried out on three sub-soil samples from the Ord floodplain (Figure 154 to Figure 156). The samples were collected to provide some reconnaissance age dating on the age of the alluvial sequence in the Ivanhoe Plain. The samples were collected in 2006 and were dated in 2007 by Dr Ed. Rhodes at the Australian National University, Canberra.

The OSL results were from two sites, samples 1/1 and 1/2 were from Ivanhoe crossing while the Diversion Dam was the site for sample 2/3 (Table 29).

Table 29: *OSL site locations, descriptions and dates.*

Sample Site	Site Coordinates	Sample Number	Description of sampling site	Age Date (BP)
Site 1: eastern river bank of Ord River at Ivanhoe Crossing	15° 47' 24.62"S and 128° 41' 51.96"E.	Sample A	Silty sands ~2 metre below the top of the bank	1,800 +/0.2
Site 1: eastern river bank of Ord River at Ivanhoe Crossing	15° 47' 24.62"S and 128° 41' 51.96"E.	Sample B	Silty sands with abundant carbonate root casts, approx. 5 m below the top of the bank	1,880 +/0.7
Site 2; ~1 m above bedrock on the eastern bank of the Ord River, just downstream of the Diversion dam	15° 41' 25.92"S and 128° 41' 21.43"E.	Sample C	Sandy sediment	12,000 +/0.9

The sub-soil OSL dates suggest that the deposition of the Ivanhoe Plains commenced at least 12,000 years before present and ceased at ~1,800 years ago. Sample C is from near the base of the alluvium exposed near the present Ord River at Ivanhoe Crossing, however this point is on the flank of the older palaeovalley, and there is a thicker depositional sequence along the course of the palaeochannel. It is likely that there are older sediments at the base of the palaeochannel. It is also considered likely that the cause of the cessation of deposition was the change in course of the Ord River from a north-easterly direction though Cave Springs Gap to the Keep River to the present course across Tarrara Bar to Cambridge Gulf.

The architecture of this flood plain shares common features with other non-marine flood plain systems of northern Australia. One example is the lower reaches of much-studied Magela Creek system, in Kakadu National Park (Nanson *et al*., 1993), where the anastomosing channel and upstream sand-rich, bedrock-confined reaches resembles aspects of the subsurface architecture of the Ord.

As noted in the previous section, at some time in the past the Ord changed its course to the present position to the west, where its estuary has joined that of the Pentecost River to form Cambridge Gulf. Previously, the Ord formerly flowed to the north east through Cave Springs Gap across the Weaber Plain to join the Keep River and enter the sea in the Victoria River estuary (Gunn, 1969). The Weaber Plain is topographically continuous with the Ivanhoe Plain through Cave Springs Gap, with a slope gently down to the northeast and up to the south along the upper reaches of the Keep River. These are interpreted as the aggregational surface of the former Ord River floodplain and its tributaries prior to its diversion to the west though Tarrara Bar.

While new age dating of the sediments of the Ivanhoe Plain suggests a relatively recent avulsion and re-incision of the Ord River in the Holocene, further work is required to better constrain floodplain evolution. However, the change in sedimentary environments in the western Joseph Bonaparte Gulf from clear-water carbonate deposits between 120,000 to muddy sediments from 7,000 years ago (Clarke & Ringis, 2000) is consistent with the proposed time frame.

In 2009, further sampling was undertaken to attempt to constrain further the landscape evolution in the area. Samples of bedrock exposed at the river base were collected from Tarrara Bar and Ivanhoe Crossing for cosmogenic isotope dating of exposure surfaces. At the time of report writing, the results of this work were not complete. Photographs of sample locations and materials are shown for Tarrara Bar (Figure 157) and Ivanhoe Crossing (Figure 158).

Figure 154: *OSL sampling. Site 1, Sample B.*

Figure 155: *OSL sampling. Site 1, Sample A.*

Figure 156: *OSL sampling. Site 2.*

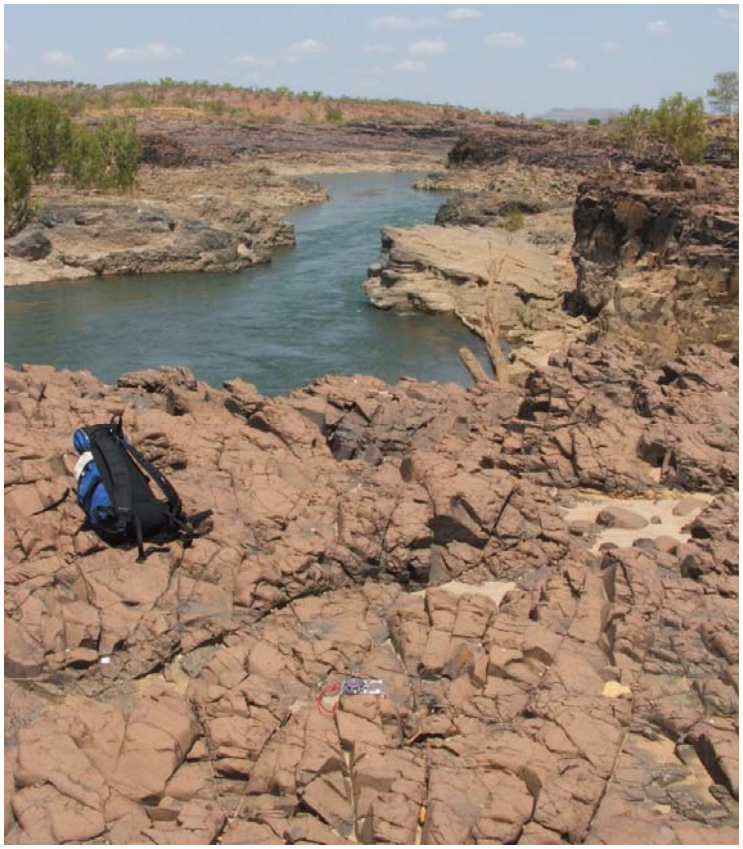

Figure 157: *Sample sites for cosmogenic isotope dating of exposure surfaces at Tarrara Bar. The image on the left shows the location of the sample site close to the Ord River, while the image on the right shows a close-up of the sample site and material (basalt). At the time of report writing, the results of this work were not complete*.

Figure 158: *Sample sites for cosmogenic isotope dating of exposure surfaces at Ivanhoe Crossing. The image above shows the location of the sample site on the east bank of the Ord River, while the image below shows a close-up of the sample site and material (basalt). At the time of report writing, the results of this work were not complete.*

5.3 SOILS

There are a number of reports on the soils of the ORIA, carried out mainly by the Western Australian Department of Agriculture (Aldrick *et al*., 1990; Burvill 1991; Dixon, 1996; Schoknecht, 1996, 1998; Schoknecht & Grose, 1996a, 1996b, 1996c; and Stoneman, 1972, 2001). These studies are summarised by O'Boy *et al*. (2001). The resulting soil maps (Figure 106) reflect a wide range of subtle variations in the soil cover.

Preliminary soil survey work, reported by Burvill (1991), was carried out in 1944, during an arduous field campaign that included non-arrival of stores and equipment because of Japanese air raids. The survey focussed on two areas, what was called the Carlton Reach Plain (now included in the Ivanhoe Plains), and Mantinea Flats area to the northwest of what is now the ORIA. This study identified many of the basic soil types now known to be widespread across the ORIA. The main soils recognised were the Ord sandy loam, Cununurra clay, Meruin sandy loam, and the Cockatoo sand. The Ord and Meruin sandy loams are a brown alluvial soils, locally referred to as 'red' soil. The Cununurra Clay is dark grey clay commonly known locally as a 'black' soil. The Cockatoo sand is a deep sandy soil that occurs on the pediments between the alluvial plains and the sandstone hills. The contact between the sandy pediment and alluvial soil is a belt of different units including ferruginous gravels and boulders known as the Junction soil complex. Predicted recharge data have been collected on all these soil types.

Stewart *et al*. (1970) provided an early summary description of soils in the Ord – Victoria area. Two soil families are prominent in the Ivanhoe Land System. Cracking clay soils of the Cununurra family dominate. These are heavy clay soils that develop a deep network of polygonal cracks when they dry out during the dry season (Figure 159). These cracks vary enormously in width but 10-20cm cracks being quite common. When dry a granular or blocky surface horizon sits on a lower horizon with large blocks and cracks. They are typically a metre or more in depth, and contain small manganiferous and carbonate concretions.

Fieldwork by the project team in 2009 measured many of the larger crack networks on the Weaber Plain to extend greater than 1-5-2m depth. Similarly, cracks on heavily modified soils on Packsaddle Plain were found to extend to greater than 1.5m (Figure 159). They are formed on fine textured alluvium derived from calcareous rocks, or intermediate to basic igneous rocks. Ord family soils occur on levees and on sandy scroll

plains. They have a grey-brown or dull brown sandy loam surface horizon merging into brown micaceous sandy clay loam.

The soils of the area mapped according to the Australian Soil Classification (Isbell, 1996; Isbell *et al*., 1997). The dominant soils are Vertosols (VE on legend in Figure 106), Kandosols (KA) and Tenosols (TE) (Figure 106). Vertosols are clay soils with shrink-swell properties that show strong cracking with dry, and at depth have slickensides. In places, they form gilgai micro relief. In the ORIA, they are the dominant soil on the clay plains.

Kandosols lack strong texture contrast, have weak or no structure in their B horizons and have less clay than vertosols. In the ORIA they occur on the plains, where they occupy areas dominated by levees or by abandoned channels.

Tenosols are soils with only weak pedogenic organisation apart from a distinct A horizon. In the ORIA they may have strongly developed organic-rich horizons, and tend to occur in areas adjacent to streams or rivers, in the lower parts of floodplains.

The Mantinea area has a small area of Calcarosols (CA), soils that are calcareous through out. Here they appear to be calcareous alluvium, and may have formed through the weathering of marine sands. In the same area, there are small areas of Podosols (PO) which are strongly leached and have B horizons rich in organic matter and iron.

Figure 159: *Extensive polygonal cracking network developed in black clay soils in Packsaddle Plain.*

Cockatoo Sands

The Cockatoo Sands are a soil type developed the Cockatoo Land System (Schoknecht and Grove 1996). The land system comprises low slopes below hills of Devonian and Proterozoic ferruginous sandstone (see O'Boy *et al.* 2001) in the Ord, Keep, and Victoria River region. Schoknecht and Grove (1996) describe the slopes as consisting of colluvial and alluvial outwash deposited in low relief fans. In this study, field observations indicate active transport across these surfaces during heavy rainfall events and the presence of low relief braided channels.

The soils themselves are somewhat variable in character, but is typically an apedal reddish brown loamy sand grading to red clayey sand at depth (Schoknecht & Grove 1996). In this study, observations indicate an iron and silica-cemented ferruginous conglomerate is present almost everywhere at the base of the sands and immediately overlying bedrock. This becomes water logged after heavy rain with migration of dissolved Fe^{2+} and its precipitation as Fe^{3+} as ferrihydrite in seeps and in the capillary fringe of the water table when oxidised. Pre-irrigation data for the Cockatoo sands (Ali *et al.* 2002) indicate soil depth of 0–3.50m and pH ranges of 6.3–6.7. A typical profile (Schoknecht and Grove 1996) consists of:

> A1 0-10 Reddish brown (2.5YR 5/4) loamy sand, apedal and massive, pH 7.6, clear boundary.
>
> C 10-100 Red (10R 4/8) clayey sand, apedal and massive, pH 8.0.

Note that the pH ranges of Ali *et al.* (2002) are weakly acidic compared to those of Schoknecht & Grove (1996) which are weakly basic. It may be that the pH values of Schoknecht and Grove (1996) represent post rather than pre-irrigated values, but this remains to be confirmed. The water holding capacity has been measured at 182mm (Cobiac, 2006). This is the highest value for any of the measured soils in the Victoria River region. Schoknecht & Grove (1996) note that the variable soil types, variable infiltration rates and sloping relief make the Cockatoo sands unsuitable for flood irrigation.

6 Geology and Hydrostratigraphy

6.1 BEDROCK GEOLOGY

The bedrock geology of the area consists of flat lying to moderately dipping Proterozoic and Palaeozoic sediments (Plumb & McGovern, 1968). The Proterozoic sediments comprise part of the King Leopold & Halls Creek Orogens (Griffin & Grey, 1990a), the Kimberley Basin (Griffin & Grey, 1990b) and the Palaeozoic sediments part of the Bonaparte Basin (Mory, 1990a). South of Kununurra, similar rocks make up the Ord Basin (Mory, 1990b). Structural and stratigraphic boundaries between these different elements are shown in Figure 160.

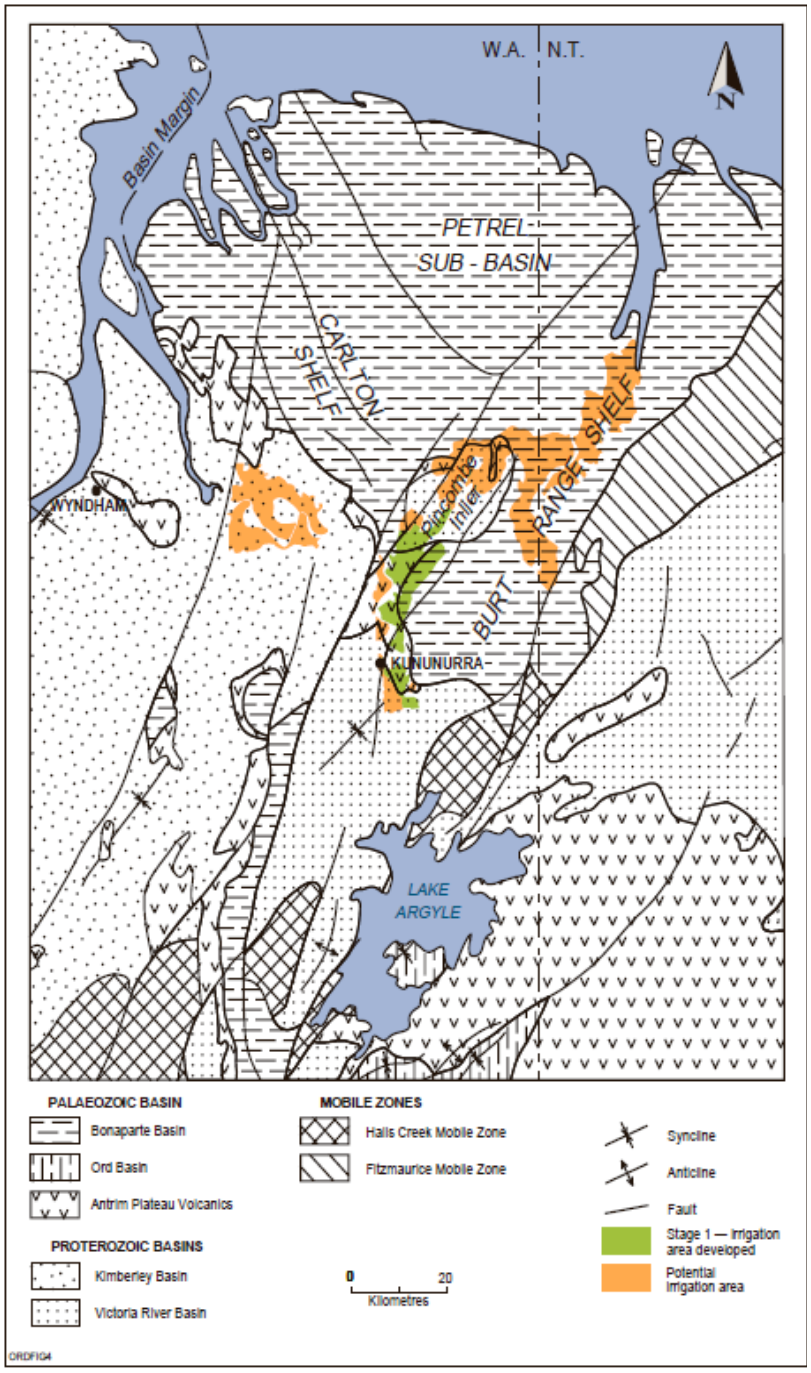

Figure 160: *Structural elements of the bedrock geology of the project area and its surrounds. Taken from O'Boy et al. (2001), which was based on data in Mory & Beere (1988).*

The distribution and thickness of Proterozoic rocks is shown in Table 30. These lithologies are all very well indurated and locally silicified along fault zones.

Table 30: *Proterozoic stratigraphy of the ORIA.*

Age	Basin or Orogen	Group	Unit & dominant lithology	Thickness	Occurrence
Late Proterozoic	King Leopold	Carr Boyd	Bandicoot Range Beds (sandstone)	1035m	Bandicoot Range
			Pincombe Formation (siltstone)	Up to 2500m	Carr Boyd Range (S) Pincombe & Cave Ranges (E)
			Stonewall Sandstone	300-450m	Carr Boyd Range (S) Pincombe & Cave Ranges (E)
Middle Proterozoic	Kimberley	Baston	Cockburn Sandstone	>500m	House Roof & False House Roof Hill and S of Ord
			Wyndham Shale	700m	House Roof & False House Roof Hill and S of Ord
			Medena Fm (sandstone, siltstone, dolostone)	110-150m	Ranges S of Ord
		Kimberley	Pentecost Sandstone	420-1350m	Ranges S of Ord
			Elgee Siltstone	40-480m	Ranges S of Ord
			Warton Sandstone	60-600m	Ranges S of Ord
			Carson Volcanics (basalt)	60-1140m	Ranges S of Ord
			King Leopold Sandstone	Up to 1340m	Ranges S of Ord
		Speewah	Luman Siltstone	Up to 95m	Dunham R & Valentine Ck valleys
			Landsdowne Arkose	30-500m	Dunham R & Valentine Ck valleys
		Ungrouped	Hart Dolerite	Up to 3000m	Dunham R & Valentine Ck valleys

The Palaeozoic sediments of the Bonaparte Basin occur in the eastern part of the project area. Their nature and occurrence is summarised in Table 31. Some minor units are omitted. Compared with the Proterozoic sandstones, the Palaeozoic sandstones are less well indurated. In the project area, the bedrock geology is complex (Figure 161).

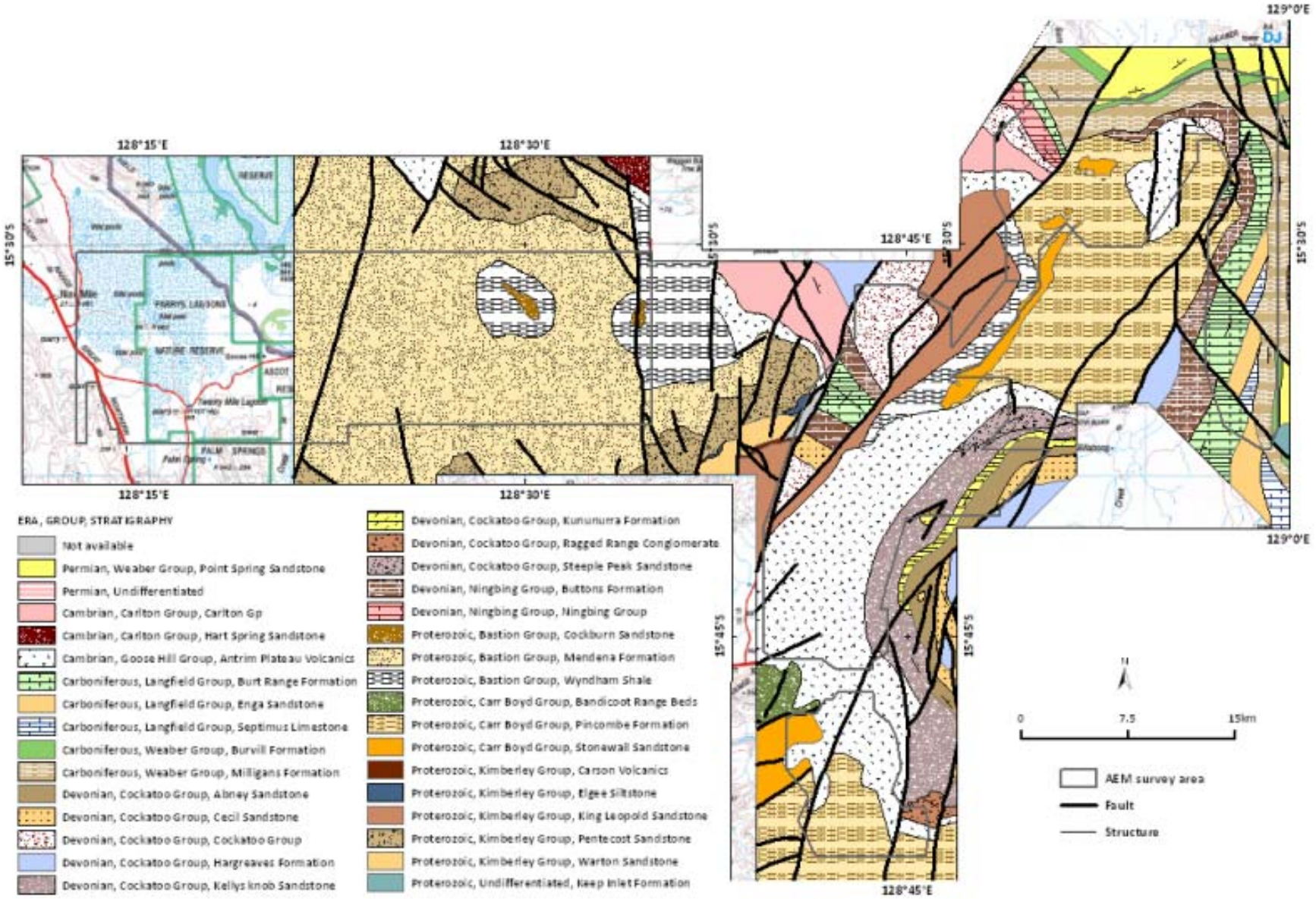

Figure 161: *Solid geology of the ORIA.*

Table 31: *Nature and occurrence of Palaeozoic sediments of the Bonaparte Basin*.

Age	Unit & dominant lithology	Thickness	Occurrence
Carboniferous	Point Spring Sandstone	130-380 m	Weaber Range
	Burvill Formation	50-90 m	Weaber Range
	Milligans Formation (shale)	300-2142	Beneath Knox Ck Plain
	Septimus Limestone	25-300 m	Beneath Weaber and Knox Ck Plains
	Enga Sandstone	160-320 m	Western side of and beneath Knox Ck Plain
	Burt Range Formation	220-460 m	Western side of and beneath Knox Ck Plain
Devonian	Hargreaves Formation (dolomitic sandstone)	230-1300 m	Hills along eastern side of Ivanhoe Plains and beneath the Weaber Plains
	Cecil Sandstone		Hills along eastern side of Ivanhoe Plains
	Abney Sandstone		Hills along eastern side of Ivanhoe Plains
	Kununurra Fm (sandstone)		Hills along eastern side of Ivanhoe Plains
	Kellys Knob/Steeple Peak Sandstone	0-260 m	Hills along eastern side of Ivanhoe Plains
Cambrian	Antrim Plateau Volcanics (basalt)	0-155 m	Mostly subsurface beneath ORIA stage 1, crops out at Kellys Knob, southern edge of Pincombe Range, and a few other areas.

Due to the relatively resistive nature of the alluvial sequence, and the nature of the AEM system, conductivity patterns are observed in the bedrock to some considerable depths (at least 100m). The AEM datasets reveal complex conductivity patterns in the bedrock. From drilling, it is known that there is little to no weathering of bedrock in this area, even under the alluvial fill, so the conductivity patterns observed are not due to variations in weathering patterns. In general, the more conductive units are shales, while limestones and dolostones as well as some sandstones, are mostly resistive (Figure 162). However, a lot of variability is observed even in the more resistive units such as the dolostones, where conductivity variations may reflect variations in porosity and salinity in larger fissures.

The AEM data also reveal a considerable amount of detail in structural geology, however analysis of bedrock geology was beyond the scope of this project. For future studies however, it is noted that while many buried structures in this area have previously been mapped largely using aeromagnetic data, the AEM data assist with the mapping of individual faults by revealing offsets in lithologies that are non-magnetic. The structural control on conductivity patterns in both the basement and in structures that propagate to the near surface is particularly evident in areas such as Parry's Lagoon (Figure 163 and Figure 164).

Prior to the commencement of this study, the hydrogeology of the ORIA had been summarised in some detail by the work of O'Boy *et al*. (2001). Bedrock hydrogeology in the ORIA is highly variable, and includes largely impermeable, moderately permeable, and permeable units. The impermeable unit are the Proterozoic sandstones (quartzites) and shales, as well as the Antrim Plateau volcanic lithologies where flow is almost entirely fracture controlled. Permeable units consist of the Palaeozoic sandstones, especially of the Devonian. The moderately permeable units are the Palaeozoic limestones and dolostones where flow is controlled by solution enlarged (cavernous) flow systems.

All of these units are, however mostly of low permeability compared to the alluvial aquifers. Yields are typically <5l/s. Compared to the alluvial aquifers these units act effectively as aquitards. Exceptions occur in karst zones, where discharge rates can be as high as 25l/s, and along faults (O'Boy *et al*., 2001). It has also

been shown that there is good hydraulic connection between the palaeochannels sands and gravels and the dolomitic limestone aquifer in the Sorby Hills area (Dudgeon & Cox, 1981).

The AEM data show considerable variability in conductivity within the limestones and dolostones, and this may relate either to variations in lithology, water quality and /or porosity. Salinities of up to 10,000mg/l TDS have previously been reported from the dolostones (O'Boy *et al*., 2001). Drilling is required to validate the conductivity patterns. Examples of fault-controlled discharge occur along the foot of fault-controlled scarps where the seepage supports distinctive Pandanus vegetation communities (Figure 165).

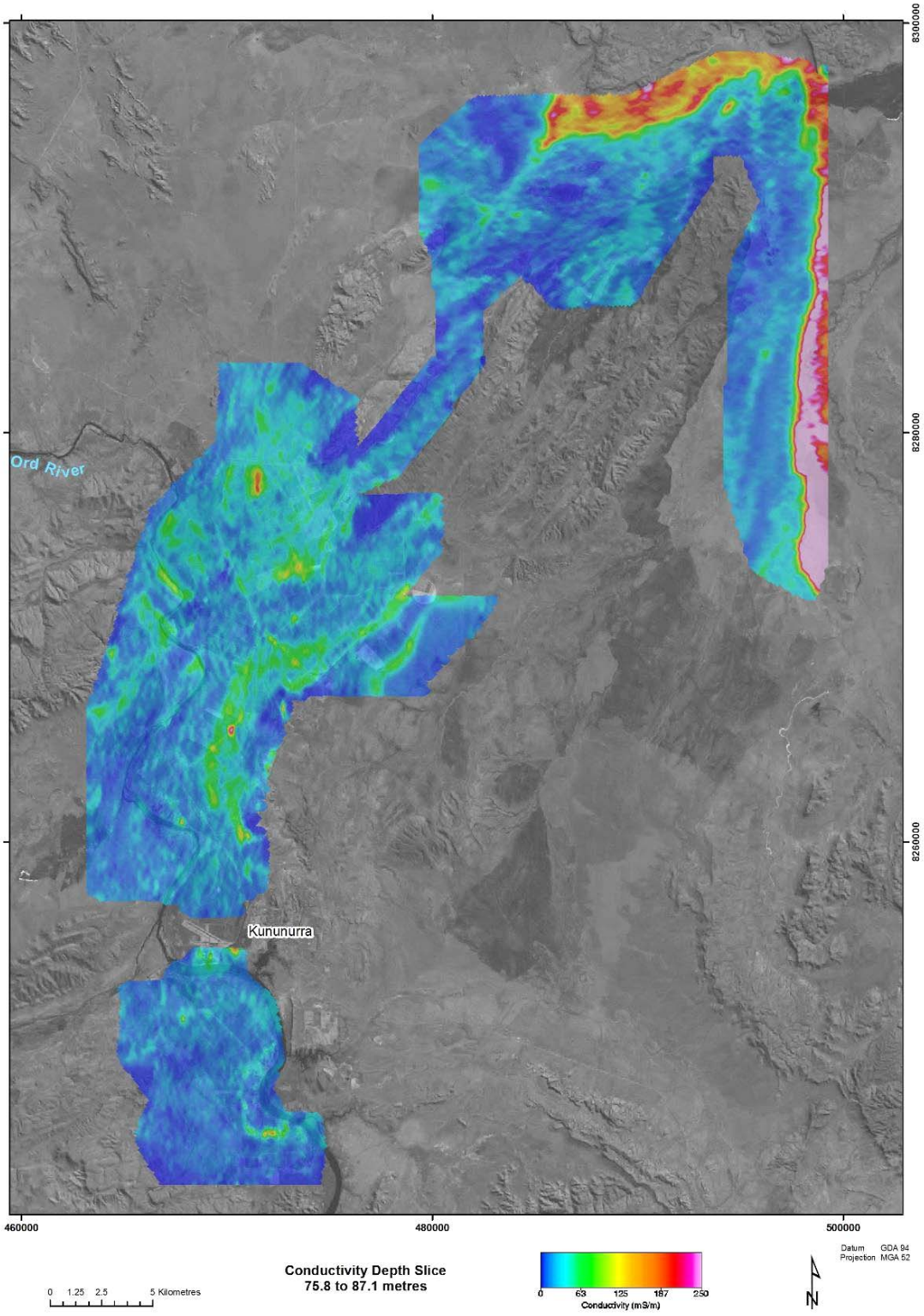

Figure 162: *Spatial variations in conductivity from depths of 75-87m reflect variability in bedrock geology.*

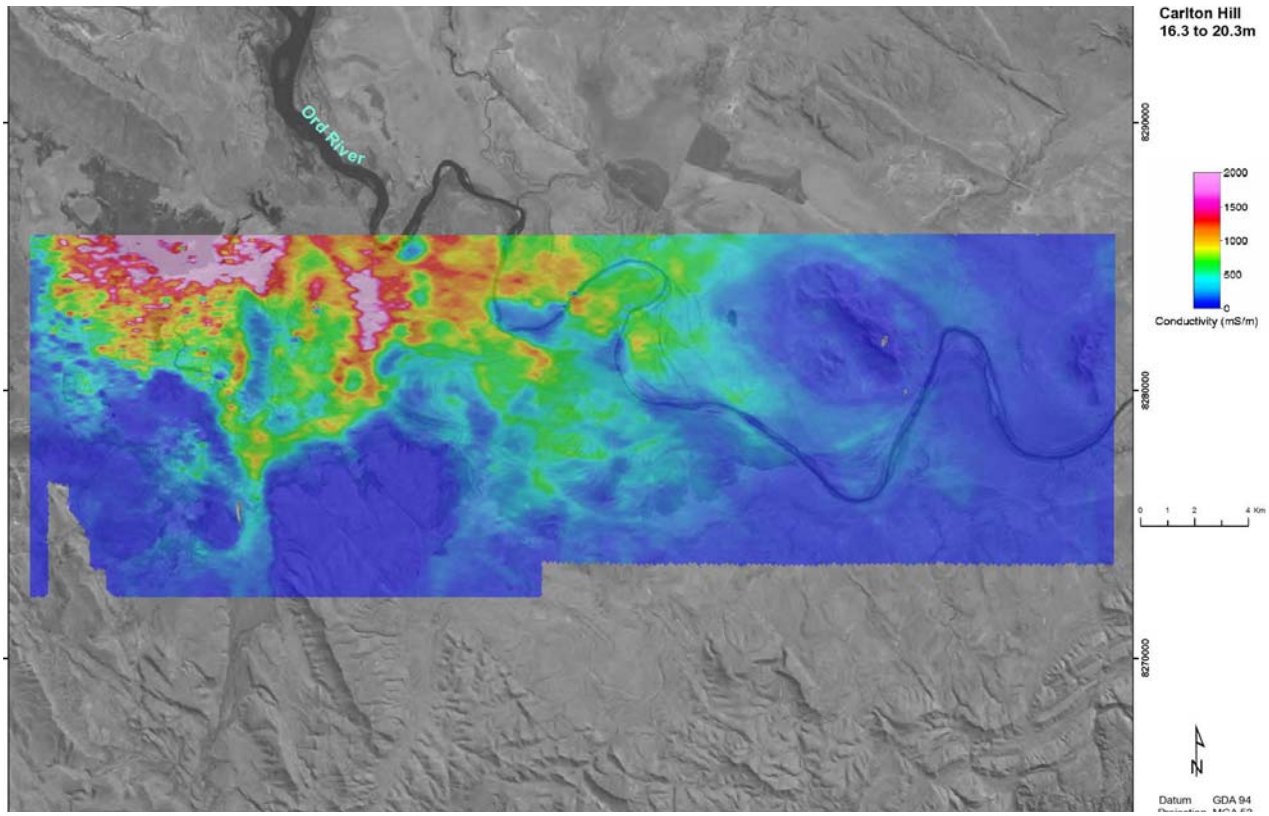

Figure 163: *Structural control on conductivity patterns in the near surface.*

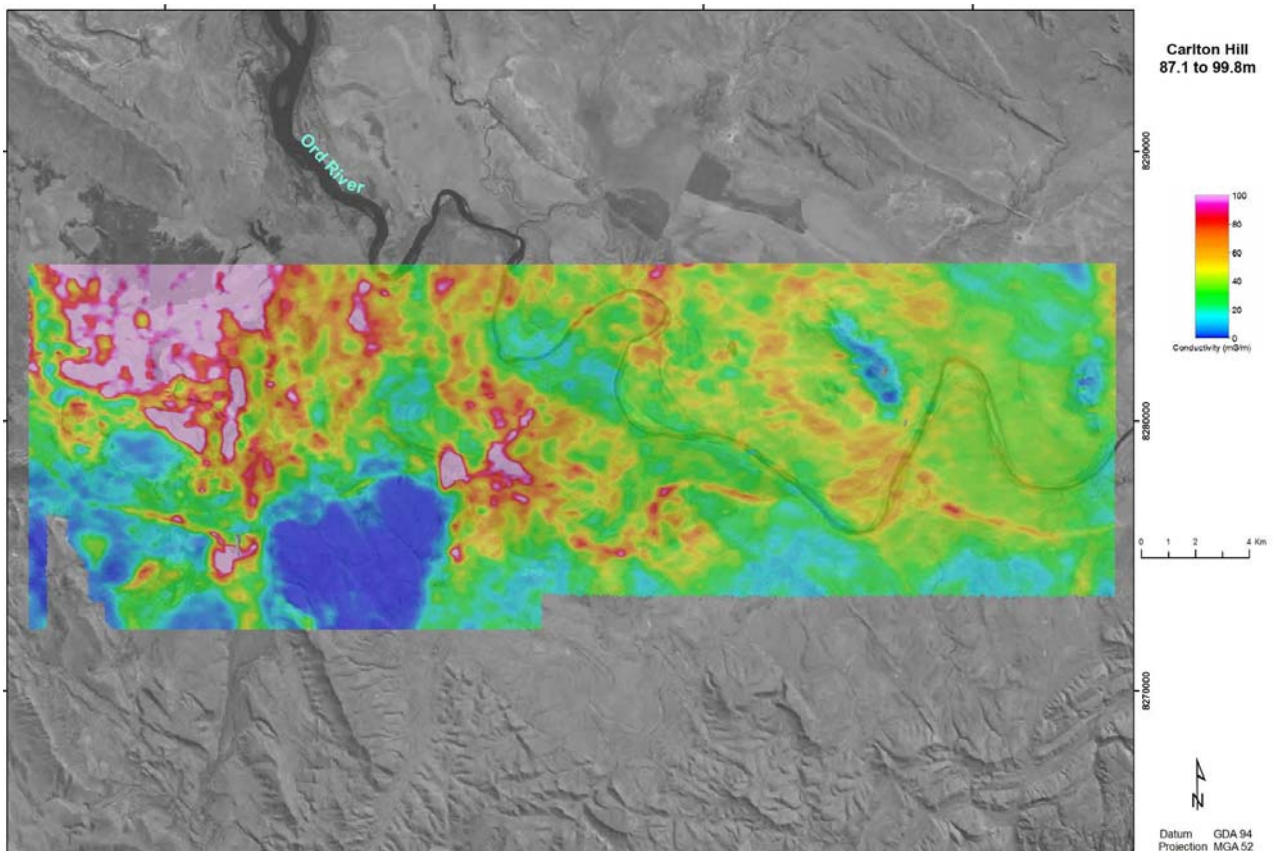

Figure 164: *NW-SE trending faults play a role in controlling the conductivity patterns at depth (as well as near surface).*

Figure 165: *Dark green* Pandanus *communities marking the position of spring discharge at foot of fault-controlled slope (to left), northwest of Ivanhoe Crossing.*

6.2 HYDROSTRATIGRAPHY OF THE ORD VALLEY ALLUVIAL FILL AND ORD PALAEO-VALLEY SEDIMENTS

The hydrostratigraphy of the Ord Valley alluvial fill has previously been described in some detail by O'Boy *et al*., (2001). The latter study was based on a comprehensive review of extensive mineral exploration drilling and targeted drilling for hydrogeological investigations (Nixon, 1996a-h), and provides an excellent starting point for further hydrogeological studies. The hydrogeological map produced in the latter study is displayed in Figure 166.

The general features of the hydrostratigraphy recognised by O'Boy *et al*., (2001) are confirmed in this study. However, the 3D AEM data, aided by core recovery from 12 new boreholes, assisted with the generation of more detailed maps of key elements of the hydrostratigraphy, including the extent and thickness of sands, gravels, silts and clays. The location of these new bores is shown in Figure 28.

Three separate sedimentary successions were identified in the core. These are provisionally named the Ord, Parry's Lagoon, and Knox Creek successions. The Ord succession consists of the gravels, sands, silts and clays deposited by the Ord River, both in its current course out to Cambridge Gulf across Mantinea and Carlton Plains, and the course taken in the past to the Keep River. En route, it deposited the Packsaddle, Ivanhoe, and Weaber Plains.

The Knox Creek succession consists of upward fining gravels, sands, silts and clays. Deposition is inferred to have occurred in an aggrading fluvial plain similar to environments interpreted for the Ord succession. Sediments of the Knox Creek succession can be distinguished from by the presence of indurated bands. The induration takes the form of clay and iron oxide-cemented sandstones, often stained by manganese. The induration suggests that the Knox Creek succession represents deposition over a longer timeframe, even though its surface is continuous with the Ord succession. It is also characterised by the presence of tufa

deposits of carbonate rich clays and silts, and carbonate cemented sands. These are inferred to be from the discharge of carbonate-saturated waters from the limestone karst aquifers along the margins of the Knox Creek Plains. Modern counterparts of these have been reported from creeks and rivers elsewhere in the Kimberley (Wright, 2000).

The Parry's Lagoon succession consists of marine and/or estuarine basal sands that fine rapidly upwards into non-marine fluvial silts and clay. These are capped by mangrove muds and /or lagoonal deposits. This sequence has been incised by the fluvial sediments of the Ord River when it shifted position to its current course, leading to the deposition of fluvial gravels on top of a thin succession of marine or marginal marine sediments.

The main aquifer units in the alluvial successions are the basal gravels and sands. Secondary aquifers occur in shallower sand and gravels units. The aquifers are separated and overlain by silts and clays. Hydraulic properties of these units were compiled by O'Boy *et al*. (2001), and are shown in Table 32.

Table 32: *Hydraulic properties of aquifer units in the ORIA. Units are arranged in stratigraphic order. Modified from Smith et al., (2007).*

Unit	Value	Units
Upper clays and silts in low permeability aquifer	0.05-0.5	litres /second
Silt-sandy-silt and silty sand low permeability aquifer	0.5-5	litres /second
Sand aquifer (in palaeochannels)	>5	litres /second
Basal gravel and sand aquifer (in palaeochannels)	5- >25	litres /second

While hydraulic gradients are largely down valley and towards the Ord River (Smith, 2008), groundwater flow is likely to be disrupted by local bedrock barriers. Examples include the ridge formed by Bandicoot Bar and the hills at Dumas Lookout, and the bedrock ridges in the west of Ivanhoe Plain. Upstream of the Ord Diversion Dam, water was predicted to enter the basal aquifer.

Lithological maps and cross-sections derived from AEM data

In this study, the specific approach used to produce maps of key elements of the hydrostratigraphy, including lithology maps, was described in Section 4.2. Essentially, the approach relied primarily on the use of all available borehole data to interpret individual conductivity depth slices. The depth slices for each area were interpreted systematically, starting from the surface, and going progressively deeper. These interpretations were checked using conductivity flight line sections and interpretation of synthetic AEM sections generated along the 30 cross-sections previously constructed by O'Boy *et al.,* (2001). The location of the 30 synthetic AEM cross-sections is shown in Figure 167.

In a systems analysis approach, a range of datasets and knowledge were drawn together to inform the interpretation of the AEM dataset. Importantly, the sediments in the valley were found not to have unique conductivity signatures due to a combination of textural and water quality variations (Section 4.2). However, in many areas, the conductivity patterning in the depth slices was found to reflect variations in sedimentary texture and facies. Interpretation was guided primarily by the observed patterning in the AEM data, validated using borehole data and AEM cross-sections. Interpretation of the extent of aquifer units (sand and gravel bodies) was also supported by recent research into the extent to which sand bodies can be laterally extrapolated from borehole data Miall (1996), Makaske (2001), Payenberg & Reilly (2003), and Gibling (2006). These studies provide practical constraints on the extrapolation and correlation process, and serve as a check on interpretations (Lawrie *et al.,* 2006a, b).

These authors demonstrated that the extent to which sand bodies can be extrapolated across a fluvial section is generally much more limited than generally shown on most cross-sections interpreters have a tendency to 'join the dots' across far greater distances than is actually justified by facies architecture. For example, in this study, findings that the basal gravels cannot be correlated across distances of more than 300 times their thickness across the width of the unit are entirely consistent with these previous studies. Likewise, findings that sand bodies in the upper part of the alluvial sequence appear to be correlated for distances of less than 100 times their thickness across the width of the unit are again consistent with findings elsewhere. Apparent width of units, where the sections cut through sand and gravel units at low angle may, of course, be much

greater. These factors have been taken into account when checking the validity of AEM interpretations in this study.

Interpretation of the AEM depth sections utilised all available boreholes in the WINSITE database that fall on or close to the line of section. For clarity, some shallow or extremely closely spaced holes were omitted. Unfortunately, not all the boreholes used by O'Boy *et al.* (2001) appear to have been captured by the WINSITE database. As a result, the number of boreholes that could be used for correlation is smaller than in that earlier study. These were augmented by the additional 12 holes drilled through the alluvial sequence, in Packsaddle, Ivanhoe, Weaber, Keep River, Knox Creek and Mantinea Plains, as well as in Caves Springs Gap and Parry's Lagoon (Figure 29). Preliminary conclusions from analysis of new drilling data collected in May 2009 are consistent with the general findings of O'Boy *et al*. (2001).

Soil, recharge and salinity products based on the AEM 0-2m depth slices

A lack of available soils maps and ancillary supporting data *at appropriate scales* made it impossible to produce a reliable soils map from the AEM data with available project resources. Moreover, it should be noted that in the Stage 2 areas in particular that the modelled AEM response in the top 2m is quite good when compared with borehole data and available ground EM data in the ORIA Stage 1 area. However, soil profiles in the 0-2m depth slice were very dry over much of the ORIA Stage 2 areas at the time of survey, as well as in some Stage 1 areas. Further analysis in these dry soil areas may not be able to discriminate dry sands and dry clays with a high degree of confidence. The interpretation of the 0-2m depth slice has had to rely on the available (regional) soils data. There is also an issue of scale to consider, as the AEM survey was not designed to underpin detailed paddock scale interpretations or comparisons. Ground EM is more suited to these tasks.

Furthermore, a ground calibration study of the SkyTEM system conducted at the time of the survey, revealed several small inconsistencies between the modelled and observed responses of the SkyTEM system in operation. Whilst they were judged not to significantly affect the definition of ground conductivity, particularly at depth (>4m), caution needs to be exercised in using the SkyTEM data for defining conductivities in the near surface (0-2m). The targeted use of ground EM methods is recommended to define the conductivity structure in this depth interval, although it is suggested that such surveys be conducted while soil moistures are likely to be relatively high.

The utility of the 0-2m AEM depth slice is an important issue, as testament from growers combined with some limited scientific studies (e.g. Richards, 2002; Medway, pers. comm., 2006, 2009), suggest there is some evidence of a relationship between high electrical conductivities in the shallow sub-surface and poor crop productivity in ORIA Stage 1. The issue is complicated by other possible causes of poor crop productivity including sodicity, alkalinity and waterlogging (Richards, 2002).

Despite some doubts on the utility of the 0-2m AEM depth slice, feedback from individual irrigators in two workshops is that there is quite a significant correlation between areas of high conductivity mapped using the SkyTEM system and reduced crop productivity (for some crops). To assess the utility of the 0-2m depth slice further, it is therefore recommended that a focussed study involving the assessment of soils, sub-soils and available EM datasets (ground and airborne) be undertaken to clarify this relationship. The results of such an investigation are required to help understand salinity and groundwater processes, and translate the salinity hazard maps into salinity risk maps that will help identify specific areas of potential damage to crops. Interpretation of this dataset should also assist with recharge studies and would also assist with determining crop suitability in both ORIA Stage 1 and Stage 2.

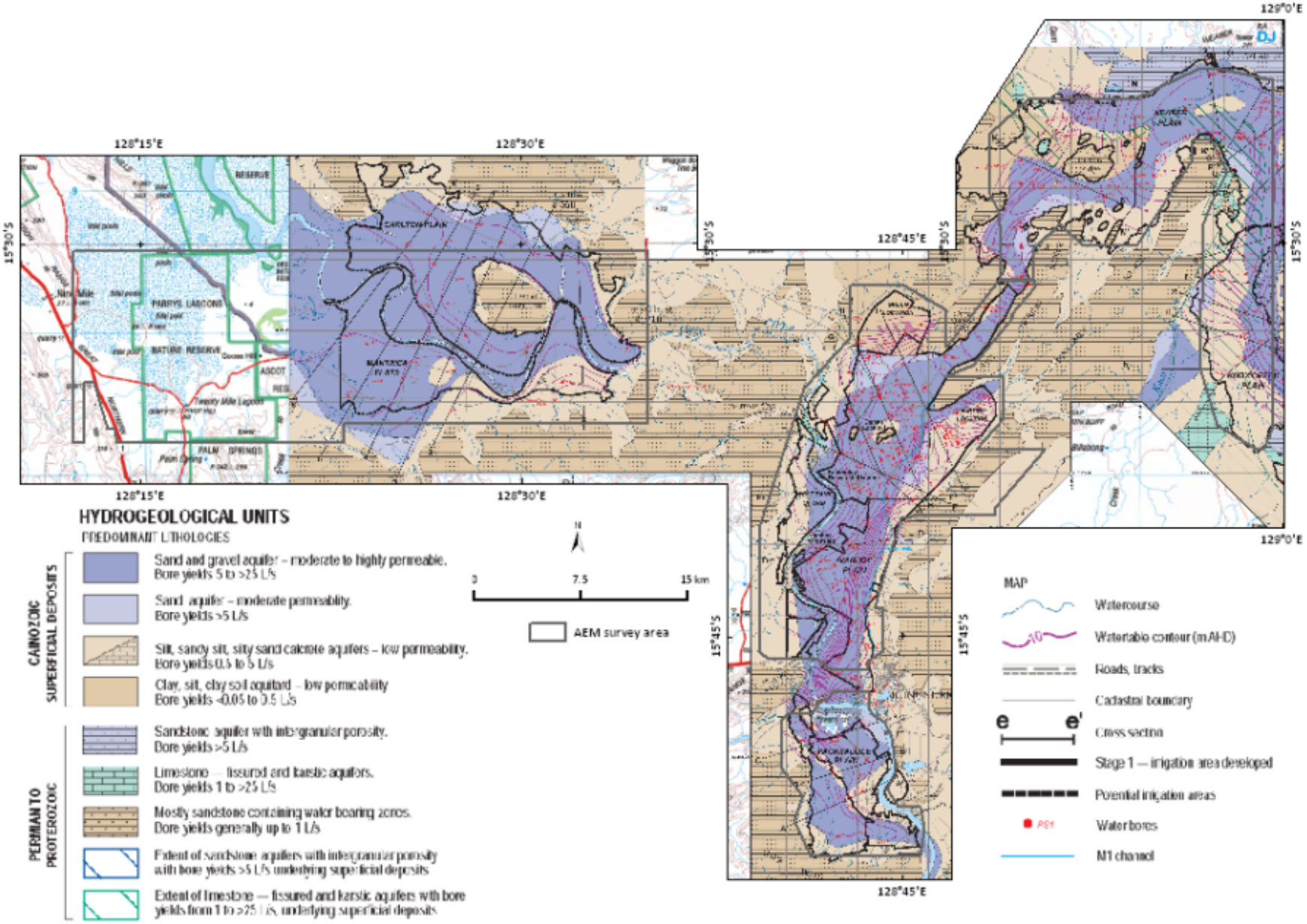

Figure 166: *Pre-existing hydrogeological knowledge of the ORIA.*

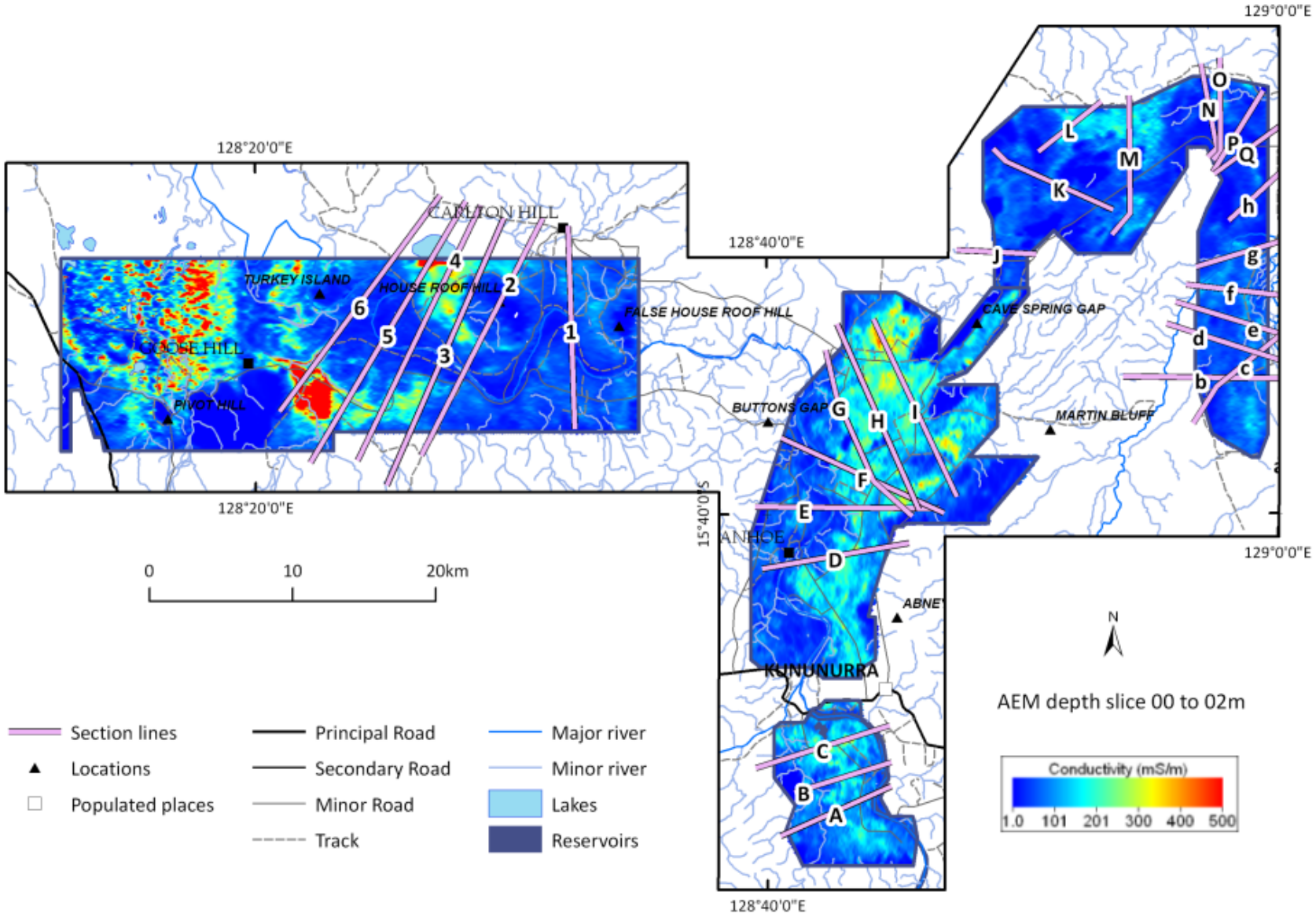

Figure 167: *Map showing location of AEM and geological cross-sections used in this study. The initial section lines were drawn by O'Boy et al., 2001.*

6.3 HYDROSTRATIGRAPHY OF THE ORIA STAGE 1 ALLUVIUM (PACKSADDLE AND IVANHOE PLAINS AND ORD WEST BANK)

Interpretation of the hydrostratigraphy from the AEM and drilling data

The Ord Succession sediments are essentially bimodal, dominated by either coarse sands and gravels, or fine silts and clays (Lawrie *et al.,* 2006a). The sediments were deposited as incised valley-fill within a basin confined on all sides by bedrock hills. The alluvial fill rest unconformably on a range of older bedrock lithologies. The lower half of the fill typically consists of sands and gravels, and the upper half is divided between silts and clays. These gravels are very coarse, with cobbles up to 70 mm in diameter, and are composed of the lithologies found in the catchment areas.

Four major facies are recognised in the drillcore: channel gravels and pebbly sands, channel-filling sands, channel margin sands and silts, floodplain silts and clays. Channel gravels and pebbly sands form the basal part of the channel sequence and, in the main course of the Ord River, form thick stacked deposits that can exceed 10 m in thickness. They are best developed in holes O2 and O4. When encountered in drilling they indicate that a major palaeochannel has been intersected. The gravels have erosional basal contacts with the underlying basement rocks.

Channel filling sands consists of thick, coarse gravelly sands, sometimes pebbly, with minor gravel lenses, especially at the base. They are best developed in O2 where they fill the channel on top of the basal channel gravels. Channel margin sands and silts are well developed in holes O7 and O11. These sediments are deposited in environments immediately flanking the main channel and often form levee banks.

Floodplain silts and clays are present in all holes. They fine upwards and become darker, indicating the presence (ore preservation) or more organic material. Holes O2 and O11 contain palaeosols, indicating episodic interruption to deposition on the floodplain. These fine-grained sediments are the main aquitards impeding the rate of vertical recharge from surface water to the aquifer units, and lateral flow between laterally confined aquifer units and other aquifer units and the Ord River.

The alluvial fill rest unconformably on a range of older bedrock lithologies. Weathering is almost completely absent in the bedrock beneath the alluvial successions in all boreholes where it was encountered. At most, 1-2 m of slightly weathered material was present, regardless of whether this was Proterozoic sandstone or shale, Cambrian basalt, or Carboniferous shale and limestone.

The interpretation of the AEM data followed previous methods where a systems-based approach that brings together all relevant geomorphic, sedimentological, stratigraphic, hydrogeological, hydrogeophysical and hydrogeochemical data and knowledge (See Section 4.2). This approach assists with analysis of the AEM data using all available borehole data, and uses these data to interpret both conductivity depth slices and depth sections.

Five new bores were drilled in the ORIA Stage 1 during this project: O1, O2, O4, O7 and O11. The locations of these holes are shown in Figure 28. Detailed logs of boreholes O1, O2, O4, O7 and O11 are presented in Figure 168 to Figure 172. The locations and depths of pre-existing holes used in this study for validation of the AEM dataset in this area are shown in Figure 173.

The 0-2m conductivity depth slice (Figure 174), and nine conductivity depth slice maps with corresponding maps of interpreted lithology for Packsaddle Plain are shown in Figure 175 to Figure 183. Similarly, the 0-2m conductivity depth slice (Figure 184) and nine conductivity depth slice maps and corresponding maps of interpreted lithology for Ivanhoe Plain are shown in Figure 185 to Figure 193. Cross-sections through the ORIA Stage 1 areas are shown in Figure 194 to Figure 202. These are synthetic AEM sections (i.e. not sections along original flight lines), and follow the sections originally constructed by O'Boy *et al.,* (2001). For each cross-section, the figures show the original interpretation from O'Boy *et al*., (2001) in the top panel, the new synthetic AEM sections in the centre panel, and the new interpretation in the bottom panel.

Analysis of the depth slices and the cross-sections reveals that clays dominate in the upper part of the valley. With increasing depth, the amount of clay decreases and the proportion of sand and silt generally increase. At a depth of 6.7-9.5m, a distinct pattern emerges in the conductivity data, indicating the presence of coarser-

grained (electrically resistive) palaeochannel-fill materials. This has been validated by drilling data. Gravel becomes more common with increasing depth. However, it is not until the 12.7-16.3m conductivity depth slice that gravels coincide with resistive features that can be mapped as coherent features.

The sand and gravels are interpreted to lie within three major palaeochannels (Figure 203). These have been numbered 1-3 from oldest to youngest based on the depth that these occur at in the palaeovalley.

Palaeochannel 1 infills the deepest part of the palaeovalley below 16.3m and runs roughly south to north through Packsaddle and Ivanhoe Plains before swinging northeast to pass through Cave Springs Gap (Figure 203).

Palaeochannel 2 is mostly oriented north south and is inferred to have followed the approximate course of the current Ord River before cutting off several major bends in the river north of the turnoff of Research Station Road from Ivanhoe cross road (Figure 203). At the northern end, it turns east to Cave Springs Gap before merging with Palaeochannel 1 as it passes through. Its presence was confirmed by drill hole O2 which intersected a thick succession of sand and gravel in this location.

Palaeochannel 3 extends both from the approximate position of the pump house and flows north along the eastern side of Ivanhoe Plains (Figure 203). The M1 supply channel is approximately coincident with this feature. There is a low rise in the landscape coincident with this feature, which is mapped as a prior stream on the geomorphology map. This palaeo-channel terminates near the southern entrance to Cave Springs Gap.

Validation of the 12.7-16.3m depth slice confirms that abundant gravels occur coincidently with the feature identified as Palaeochannel 2 and the downstream end of Palaeochannel 1 (Figure 203). Sands and gravels also appear to confirm the presence of Palaeochannel 1 where it connects the current course of the Ord River to Cave Springs Gap (continuing through to the northeast). There is no evidence for Palaeochannel 3 at these depths. The extent of bedrock at these depths is similar to that at surface.

However, there is a significant reorganisation of the alluvial architecture below a depth of 16.3m. The width of the bedrock valley narrows considerably from the southern end of the area to as far north as the research station. This abrupt change in width indicates that the buried valley beneath these plains has a ‘steer’s head’ cross-section. Within the (higher energy) keel of this palaeovalley, the alluvial sediments are composedly largely of gravels. Only north of here as far as Cave Springs Gap does the alluvium retain anything like its former width. The alluvium comprises relatively narrow sand and gravel palaeochannels within flanking floodplain sediments of silt and clay. Some gravel occurs as isolated bodies on the eastern side of the palaeovalley, however these gravels in section are quite conductive and may present and older alluvial unit elsewhere removed. By the time a depth of 24.8m is reached, even the northern end has narrowed to form a gravel-filled valley (Palaeochannel 1).

The bedrock valley continues to narrow and the extent of the fine-grained facies decreases until at a depth of 24.8-29.9m the alluvium consists entirely of gravel flowing in a bedrock-confined valley with numerous rocky rises. The valley is between 1000 and 4000m in width, with its narrowest portion in the centre of northern Ivanhoe Plain near Dumas Lookout. Below this depth, the alluvial trace along the thalweg of the palaeo-valley becomes discontinuous, reflecting differential erosion prior to the earliest phase of deposition. At depths greater than 35.4m, any residual alluvial material becomes indistinguishable from bedrock in the AEM slice.

Palaeochannels 2 and 3 occur in the upper part of the steer’s head fill. Palaeochannel 2 is probably the main former course of the Ord River prior to its evulsion through Buttons Gap. The narrow channel defined by sands and wide fine-grained floodplain indicate that the channel was mostly fixed. Palaeochannel 3 may present an anabranch channel occupied only during high flow and filled by sands and silts.

Comparisons with previous studies

For each of the nine cross-sections, a comparison between the original cross-sections and the new interpretations, based on the AEM data, has been made. Similarly, comparisons with the original sand and gravel extent maps (O’Boy *et al.*, 2001), are also made. These comparisons are documented below.

Section A-A'
There is good correspondence in the position of the bedrock surface between the original section and the new data (Figure 194). The main differences are that the western margin of the valley fill is much steeper than original shown, and that there is a tributary valley to the east of the main one originally shown. This palaeovalley also appears on the next section to the north (Figure 195). Especially noteworthy is the correspondence between the gravels interpreted from AEM data and the boreholes on the original section. These correspond to Palaeochannel 1.

Section B-B'
There is reasonable correspondence between the original section and the position of the bedrock surface in the new data (Figure 195). Gravels and other channel units of the western side of the section correspond to Palaeochannel 1, as discussed previously. The main differences are the western palaeovalley does not appear to be as pronounced as originally shown and the bedrock high dividing the two does not reach as close to the surface.

The western boundary of the alluvial sediments in original section correctly identifies the steep nature of the contact evident in the AEM data. The AEM suggests that amount of gravel is probably less than in the original section, confirming the interpretation in Lawrie *et al*. (2006a). Lastly, there is a buried bedrock pinnacle that was not intersected in drilling but is visible in the AEM in the western part of the section.

Section C-C'
The correspondence between the position of the bedrock surface in the original section and the new data is only moderate (Figure 196). This may be due to the fact that the new data cover only a fraction of the original line. The bedrock surface appears to be more complex than the single valley shown on the original surface, and the bedrock also appears to be deeper on the eastern end that likewise originally interpreted. The AEM indicates that amount of gravel is likely to be somewhat less than in the original sections and in the reinterpretation in Lawrie *et al*. (2006a). This is shown on the reinterpreted section with limited gravel lenses in bores and near the modern river. Gravels and other channel units of the western side of the section correspond to Palaeochannel 1.

Section D-D'
There appears to be a good correlation between the position of the bedrock surface in original section and the new data (Figure 197). The main differences are that the alluvium appears deeper on the western side of the river than originally shown, however the original data were unconstrained by boreholes west of the river and the bedrock profile was therefore speculative. Noteworthy is the present of a shallow resistive unit between WINSITE boreholes 8320 and 23022795 that marks the presence of a thick gravel palaeochannel shown on the original section.

This palaeochannel was intersected in borehole O2 (off-section, and so not shown) which confirmed the presence of thick sand and gravels, and is interpreted as being Palaeochannel 2 overlying Palaeochannel 1. However, gravels noted in drill logs in the eastern side of the palaeovalley do not show up on AEM. There appear to be several reasons for this: the gravels are described as being interbedded with silts and clays, overprinted in places by tufa, and may contain more saline water (1000-2500 mg/l). Even allowing for this, the extent of gravel is less than in previous interpretations. The sands in WINSITE bore 20082900 are associated with Palaeochannel 3.

Section E-E'
Correspondence between the position of the bedrock surface in the original section and the new data is at best moderate (Figure 198). The main differences are, however, on the western side of the Ord River where the borehole data is limited. Noteworthy features here are the apparently over steepened contact between the bedrock and the alluvium, suggesting the presence of a reverse fault, and the presence of a resistive unit that extends from bedrock to the surface, corresponding with a set of scroll bars on the western river bank. This is the only section that shows this part of the western margin of the Ivanhoe Plain and therefore is the only one that shows the reverse faulted nature of this margin at depth.

The eastern margin appears to be composed more of mantled pediments rather than exposed bedrock, as originally interpreted. Gravel units appear less extensive than originally interpreted. The nature of the

strongly conductive unit on the western end is not clear, but it may be composed of more clay-rich materials by comparison with other sections. There is no bore data to constrain interpretation, only the geomorphic mapping, but it is possibly an older floodplain or scarp foot unit.

Section F-F'

The correlation in the position of the bedrock surface appears reasonable between the new data and the original section (Figure 199). The main differences are again on the eastern margin where the bedrock surface appears to be a mantled pediment rather than bare rock. Also, a bedrock pinnacle appears to be present just east of the river (visible in the DEM data). However, previous interpretations appear to have over-estimated the amount of gravel in the section. The accretionary point sands and gravels of the Ord River within its incised valley are again visible as strongly resistive units. The silt-filled palaeochannel 3 is visible as a moderately conductive ridge. Palaeochannel 2 is not evident, having been re-excavated by the incision of the Ord River.

Section G-G'

This cross-section cuts across the northern part of the Ivanhoe Plains and no longer intersects the current course of the Ord River. The correlation in the position of the bedrock surface between the original section and the new data is moderate (Figure 200). The main differences are along the western side, again where there was little data in the original section, and the large buried hill of Cambrian basalt that was interpreted, but does not appear in the AEM data. The nature of the four highly conductive units is not clear, but may be clay-rich lithologies. The gravels in the eastern side palaeovalley appear to contain more saline than those associated with the main palaeochannel of the Ord and, by analogy with those below the Weaber and Knox Creek Plains, may represent an earlier depositional cycle.

The higher conductivity is interpreted to be due to higher salinity groundwater, some bores in the area have salinities in the 5000-10000mg/l range. Even allowing for this, the extent of gravel appears considerably less than originally interpreted. The channel features in the central part of the cross-section are those associated with Palaeochannel 1. Palaeochannel 2 inferred as an intermediately resistive unit in the mid-western part of the section, but not tested by drilling. The silt-filled Palaeochannel 3 is again visible as a moderately conductive ridge.

Section H-H'

The correlation in the position of the bedrock surface between the new data and the original section appears very good (Figure 201). There is good correspondence between the buried bedrock highs and basal gravel units interpreted on the section and the AEM patterning. Some of the highly conductive areas in the AEM data also appear to correspond with thicker clay units as well. The amount of gravel is perhaps a quarter of that shown in earlier interpretations. The basal gravels of Palaeochannel 1 occur in the central part of the section, and are overlain by the sandier unit of Palaeochannel 2. Palaeochannel 3 is present in the western end of the section as a feature of moderate to low conductivity separating two conductivity highs.

Section I-I'

The AEM section shows a good correlation with the original cross-section in the position of the bedrock surface (Figure 202). The only major divergence is the presence of a small bedrock high, visible in the AEM and DEM data that was not on the original cross-section. Noteworthy correlations include the resistive gravels in the central part of the palaeovalley and the close association of conductive units with thick clays. The basal gravels comprise Palaeochannel 1, while Palaeochannel 2 is defined by the narrow resistive unit extending from the basal gravels up to the near surface between WINSITE bores 20092476 and 20092478. This was the main course of the main Ord palaeovalley before it entered Cave Springs Gap. Despite the presence of this palaeochannel, the AEM data indicate that amount of gravel aquifer is much less in this section than previously inferred. Palaeochannel 3 is more obscure and occurs adjacent to the northern side of the bedrock high.

Summary

Comparing the distribution of lithologies mapped using the new AEM-based interpretation with earlier studies (O'Boy *et al*., 2001; Smith, 2008) reveals important differences in the distribution of sand and gravel aquifers. This serves to highlight the difficulty in mapping lithologies and parameterising hydrogeological

models using drilling data alone. Figure 204 shows a comparison of sand and gravel aquifers using data from this study, and from O'Boy *et al*. (2001) and Smith (2008). The sand and gravel aquifers are not differentiated on the O'Boy *et al*. (2001) maps, while the map of Smith (2008) is the interpreted maximum extent of gravels in the subsurface, although no depth is given. By contrast, the 24.8-29.9m depth slice in the interpreted AEM data from this study, which is the shallowest depth at which continuous gravels occur, shows that gravels are much more restricted, occurring only in the deepest part of the steer's head cross-section.

Similarly, Figure 205 compares the distribution of sand aquifers with the mapped extents of sand aquifers from O'Boy *et al*. (2001) and Smith (2008). The O'Boy *et al*. (2001) map is the same as for the gravels, as the sands and gravels are not differentiated, however the sand extent from Smith (2008) is mapped (again with no depth mentioned). These maps are compared with the interpreted 9.5-12.7m conductivity depth slice from this study. Again, this study concludes that the extent of sand is much less extensive than previously interpreted. Rather than being a major palaeochannel-filling unit, the sand aquifers occur at shallower depths, with deposition restricted within palaeochannels.

Lastly, we compare the interpreted silt and clay map in Figure 7c of Smith (2008) with the most silt and clay rich unit conductivity depth slice mapped in this study, which is at 4.2- to 7.7m (Figure 206). In the new interpretation while silt and clay dominate the conductivity depth slice, thin sand-containing palaeochannels are still present, and some of the silt also occurs as palaeochannels fill within more clay-rich overbank materials. This fine-grained unit still contains locally significant sandy units associated with palaeochannels that could act a significant pathway for recharge of the aquifers from the surface.

Overall, this study confirms the broad stratigraphy demonstrated in earlier studies (O'Boy *et al.,* 2001). However, the AEM data provide additional volumetric data which enables a clearer picture of the 3D distribution of the alluvial materials to be constructed. In particular, this provides improved constraints on the distribution of sand and gravel aquifers.

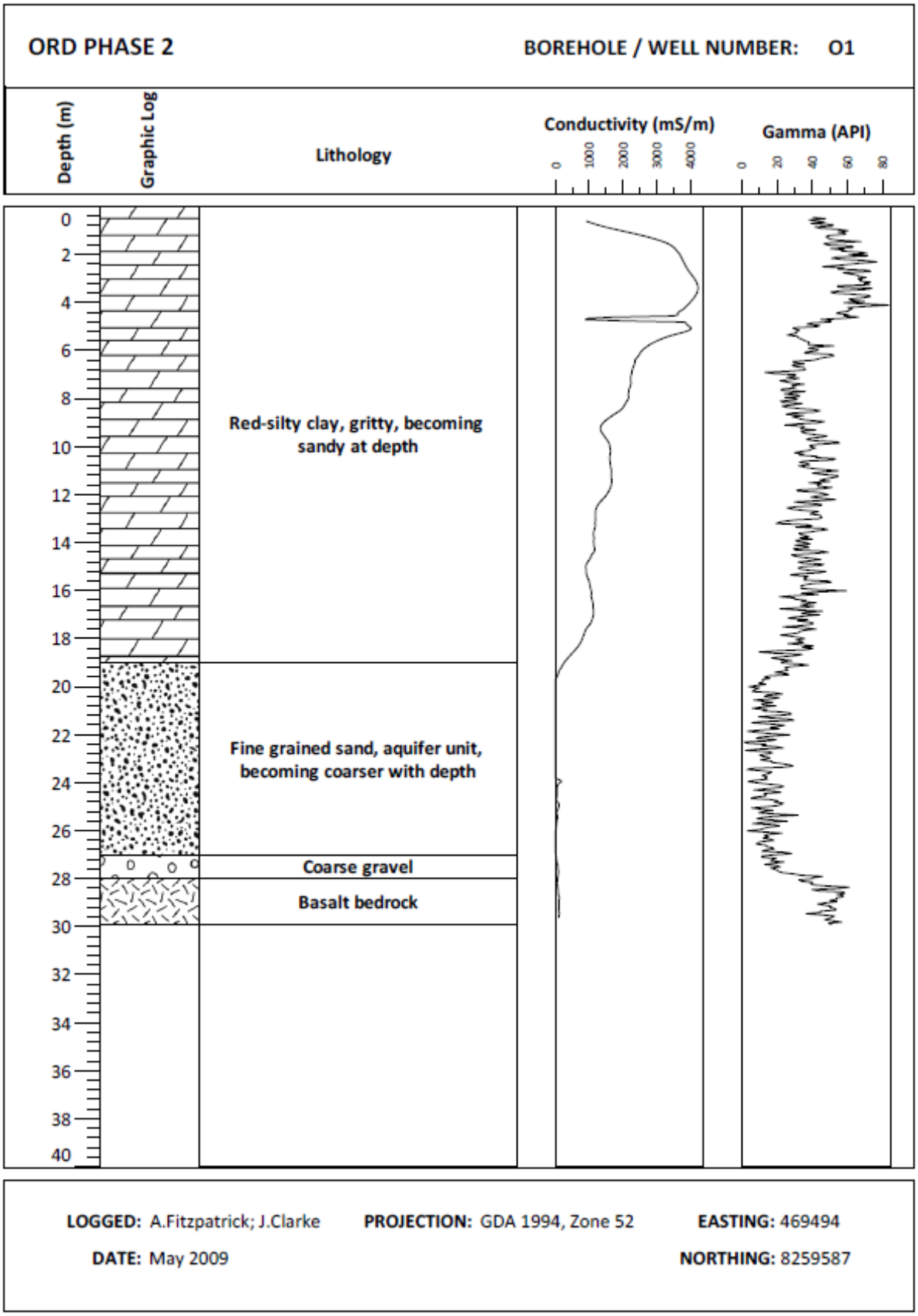

Figure 168: *Ord Phase 2 borehole number O1.*

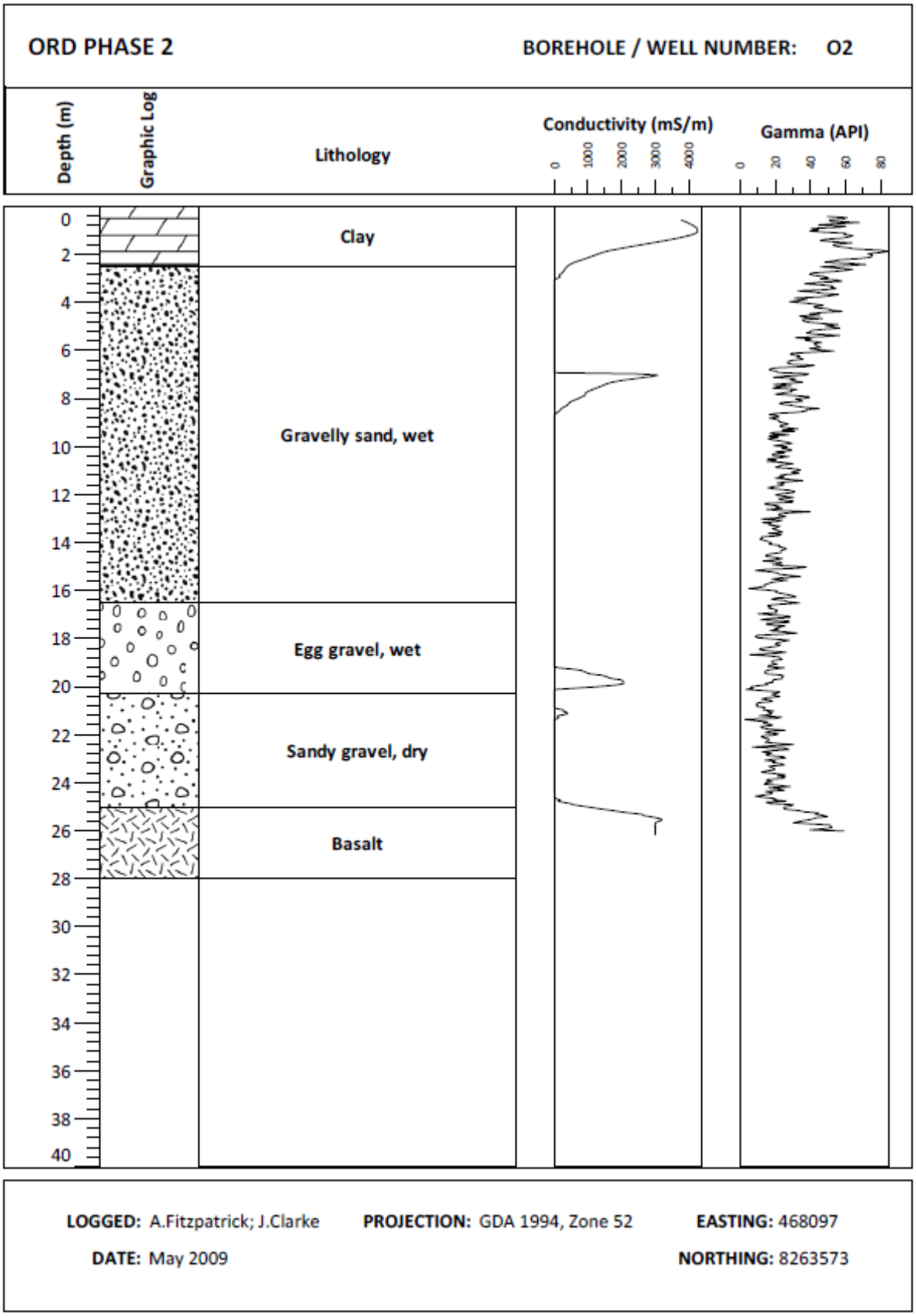

Figure 169: *Ord Phase 2 borehole number O2.*

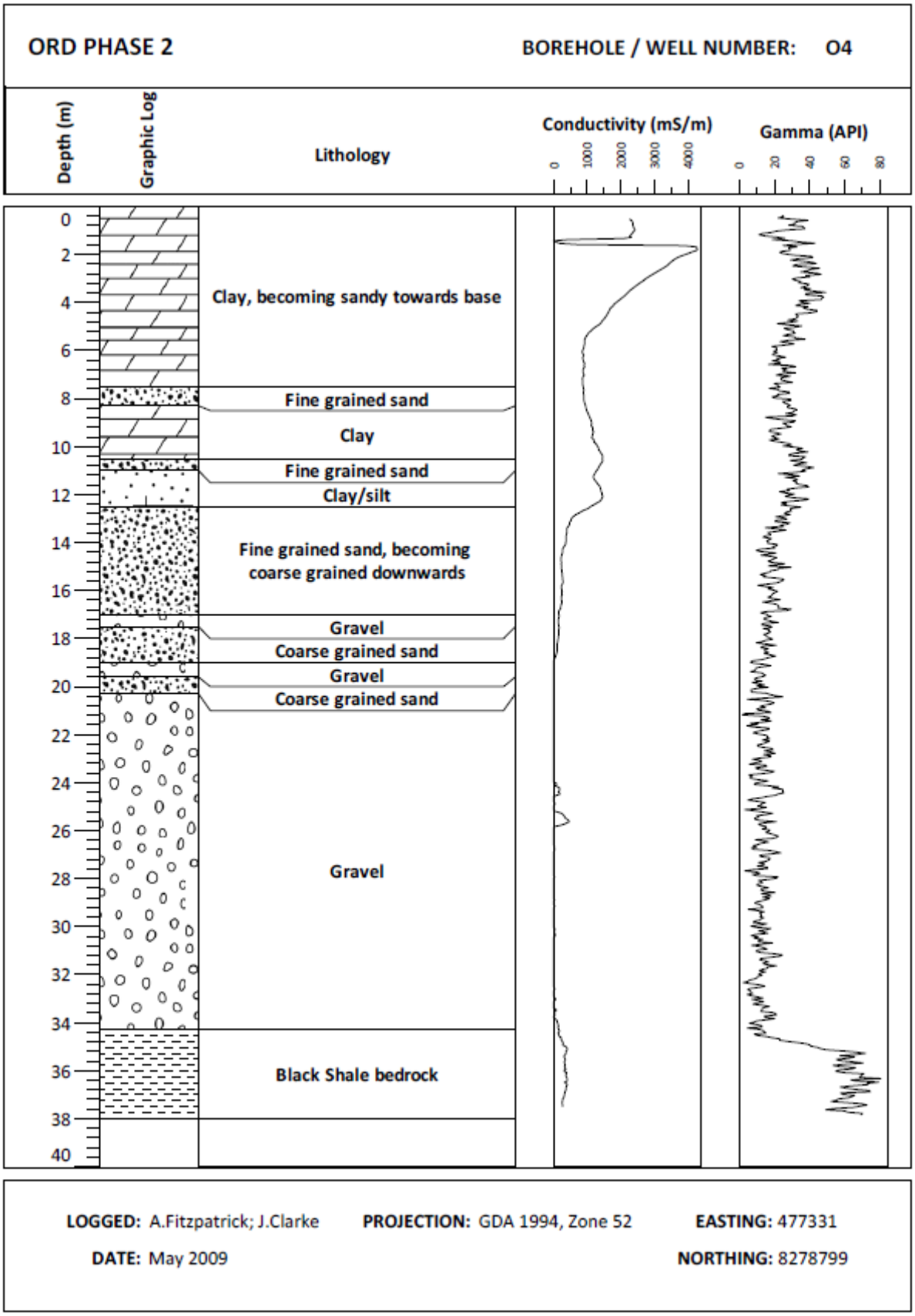

Figure 170: *Ord Phase 2 borehole number 4.*

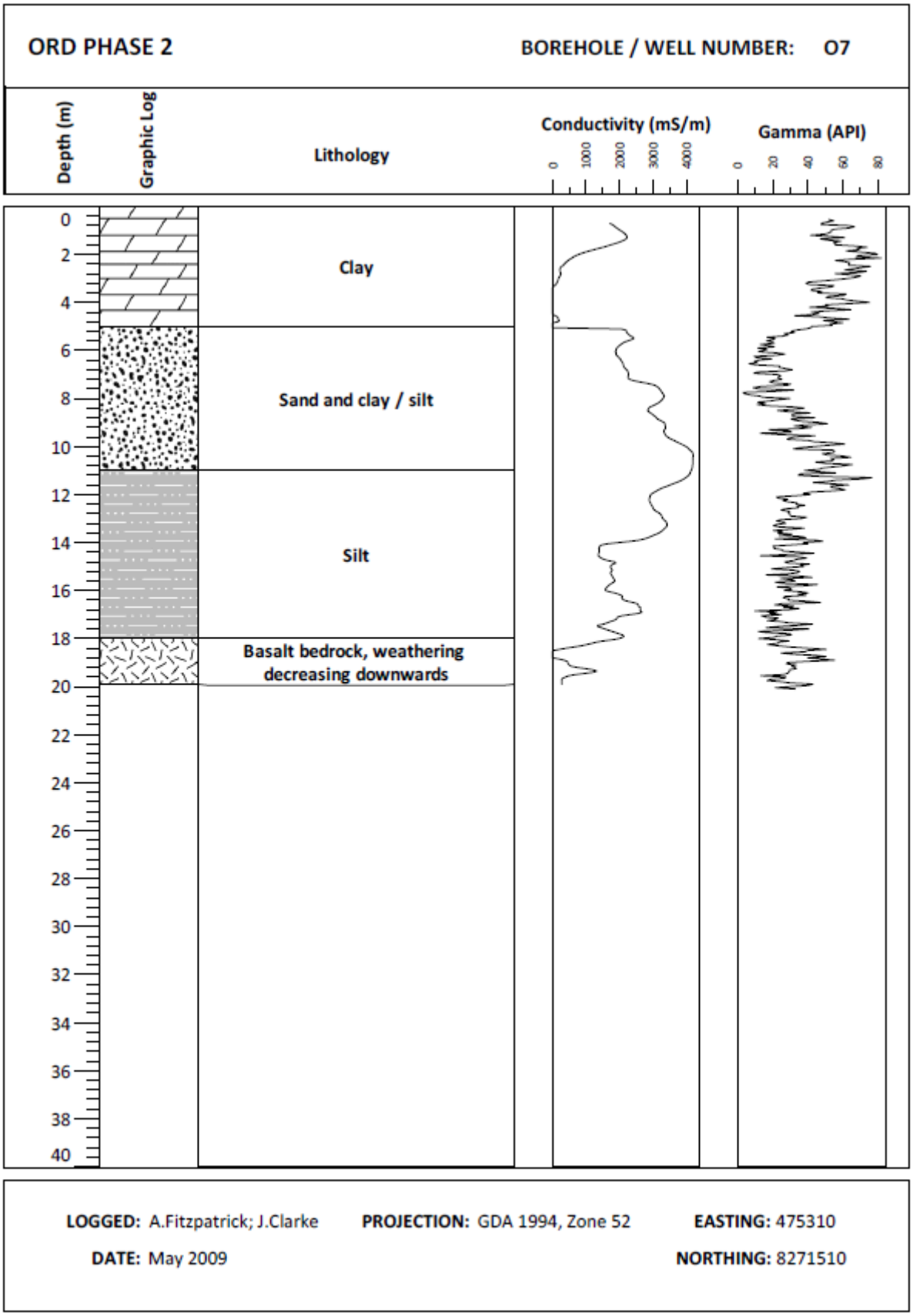

Figure 171: *Ord Phase 2 borehole number 7.*

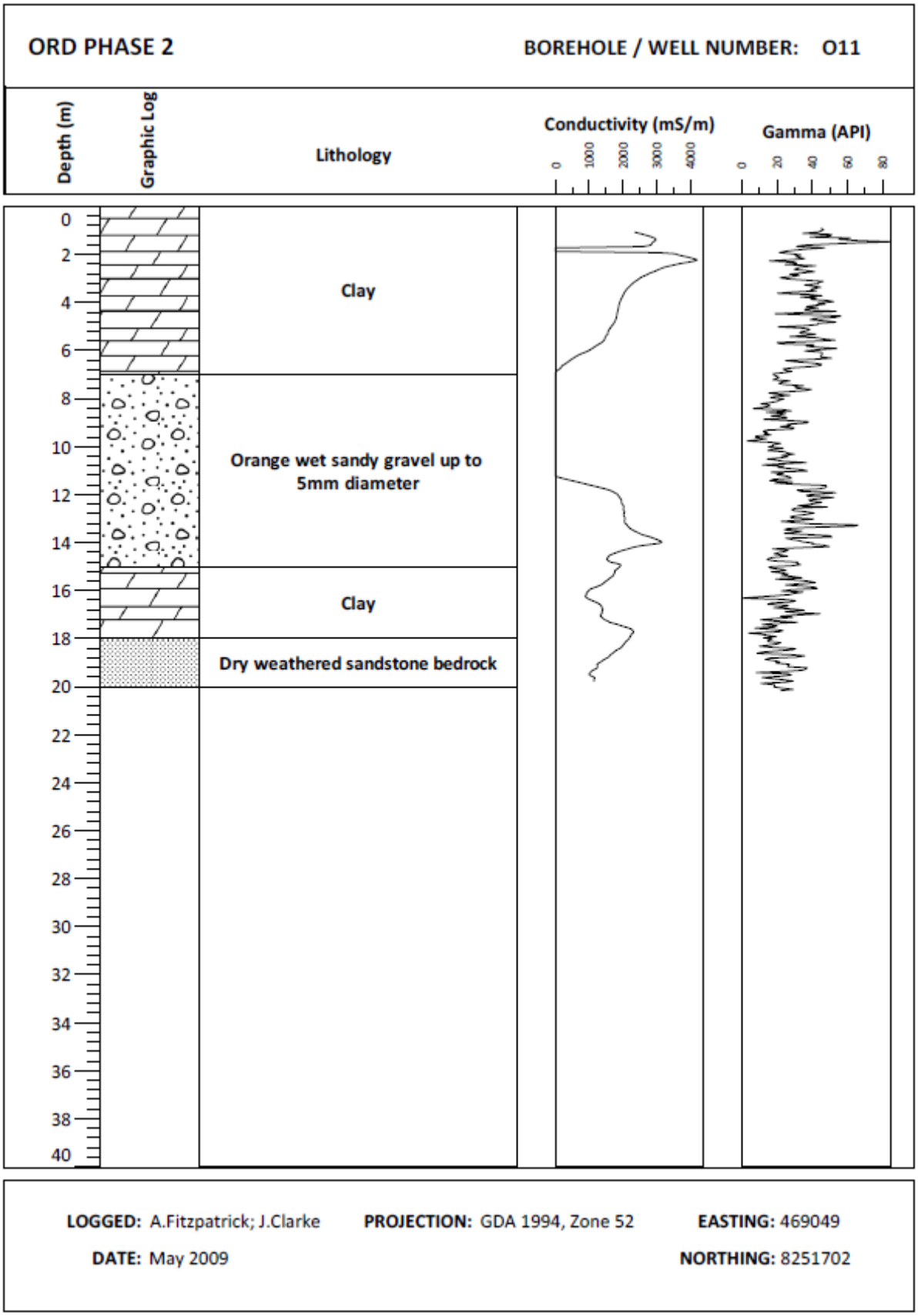

Figure 172: *Ord Phase 2 borehole number 11.*

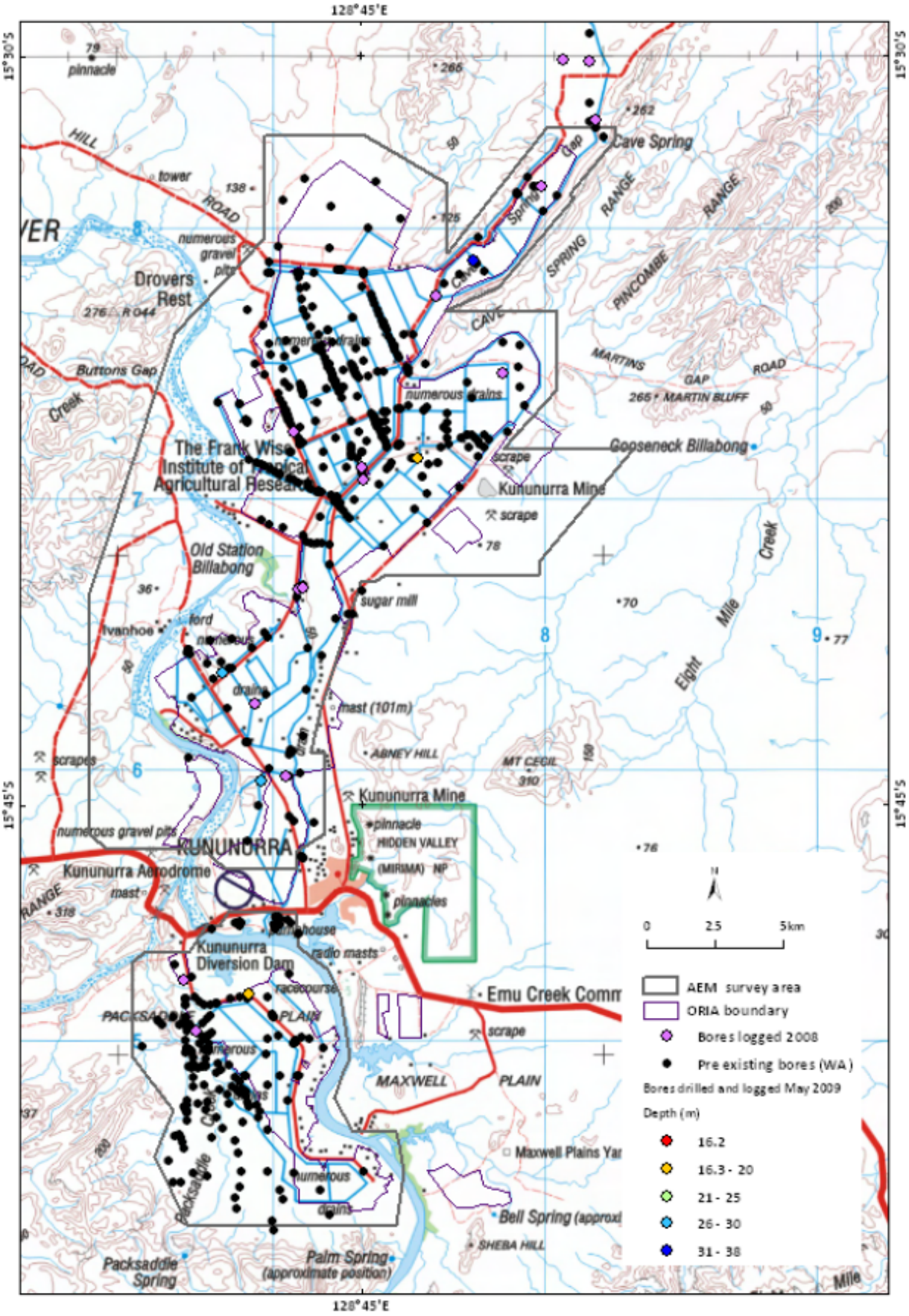

Figure 173: *Borehole locations in the ORIA Stage 1 area.*

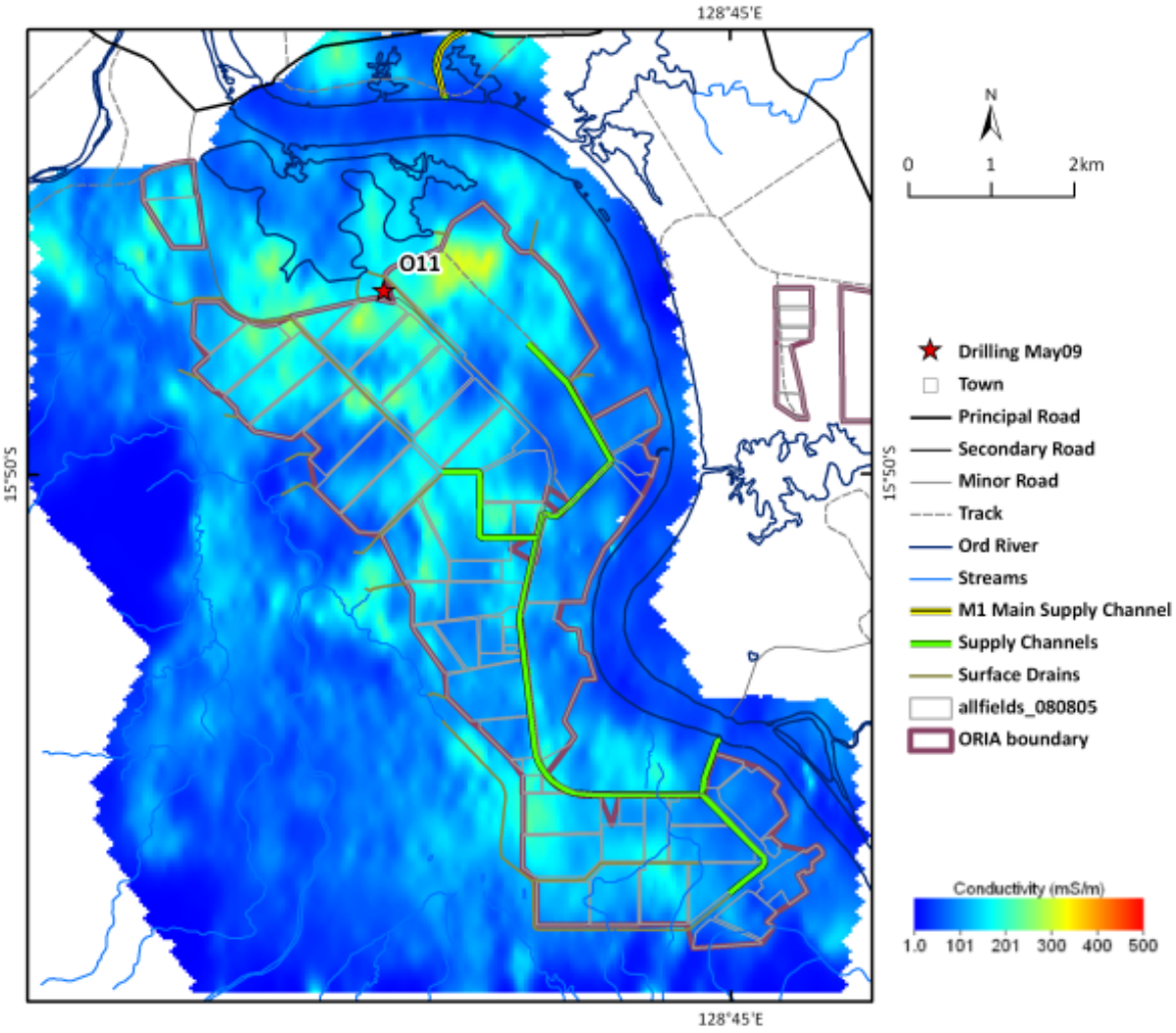

Figure 174: *AEM 0-2m conductivity depth slice for Packsaddle Plain.*

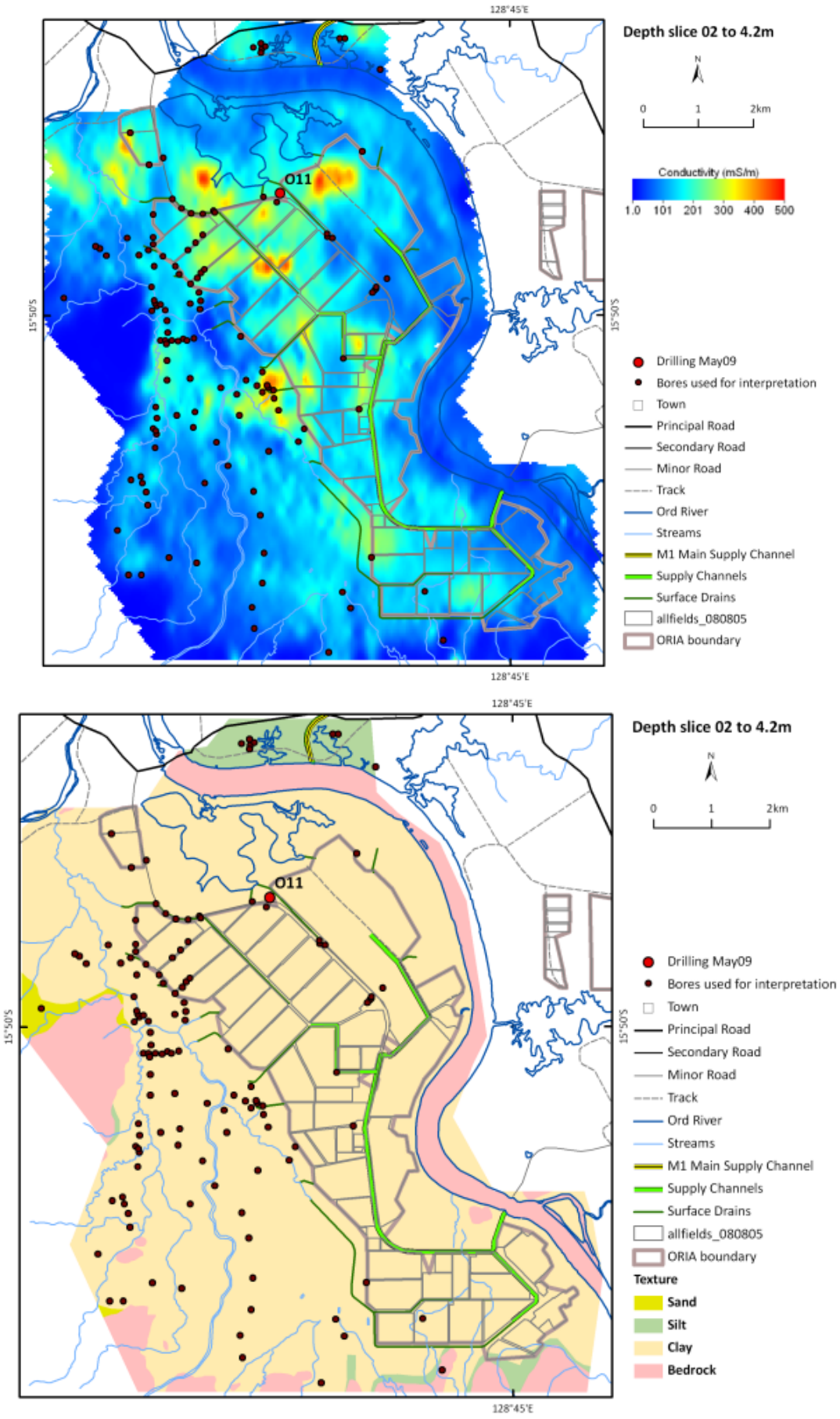

Figure 175: *Packsaddle Plain. Top: conductivity depth slice 2 – 4.2m. Bottom: interpreted lithology.*

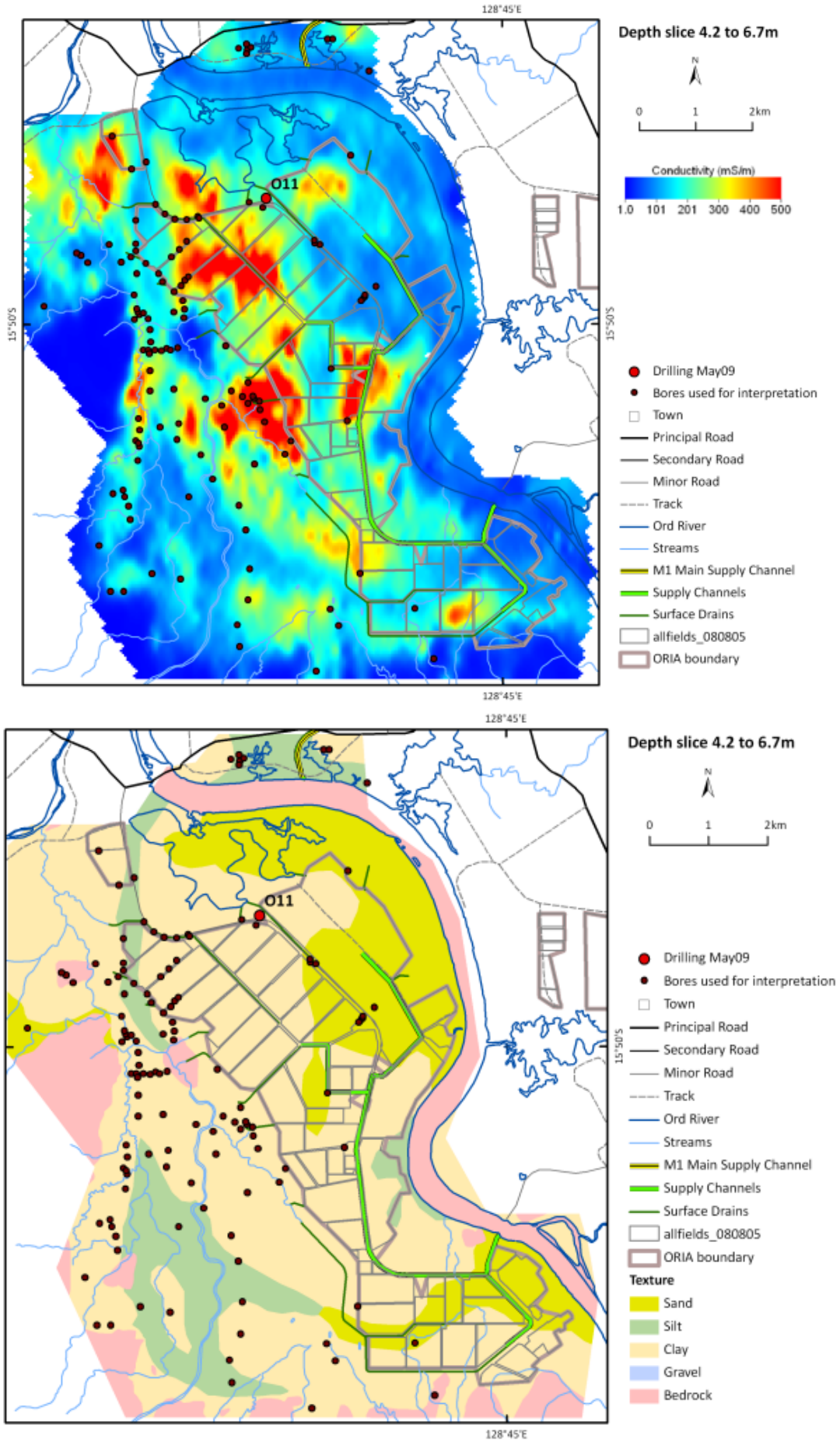

Figure 176: *Packsaddle Plain. Top: conductivity depth slice 4.2 – 6.7m.* ***Bottom:*** *interpreted lithology.*

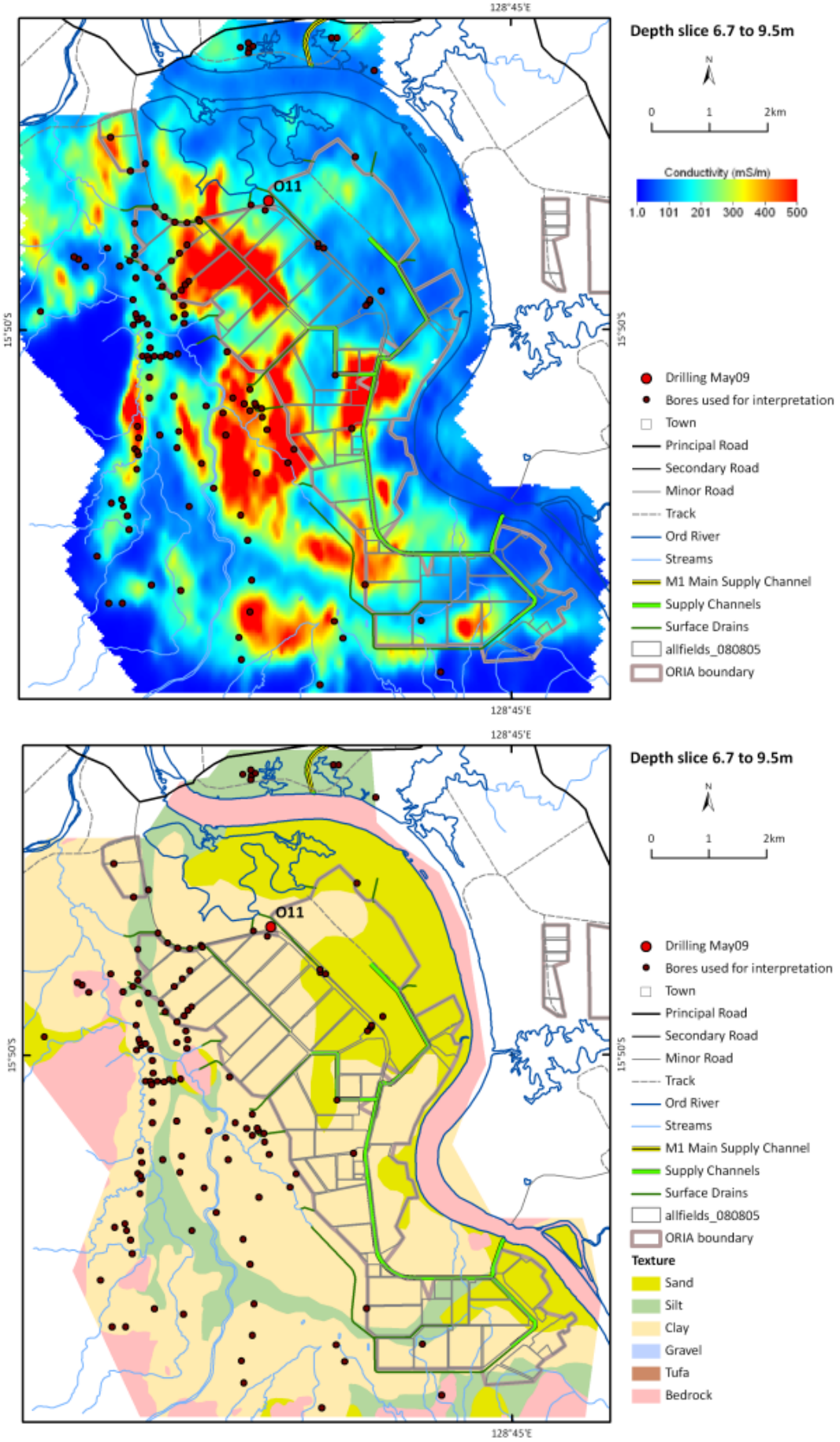

Figure 177: *Packsaddle Plain.Top: conductivity depth slice 6.7 – 9.5m.* ***Bottom:*** *interpreted lithology.*

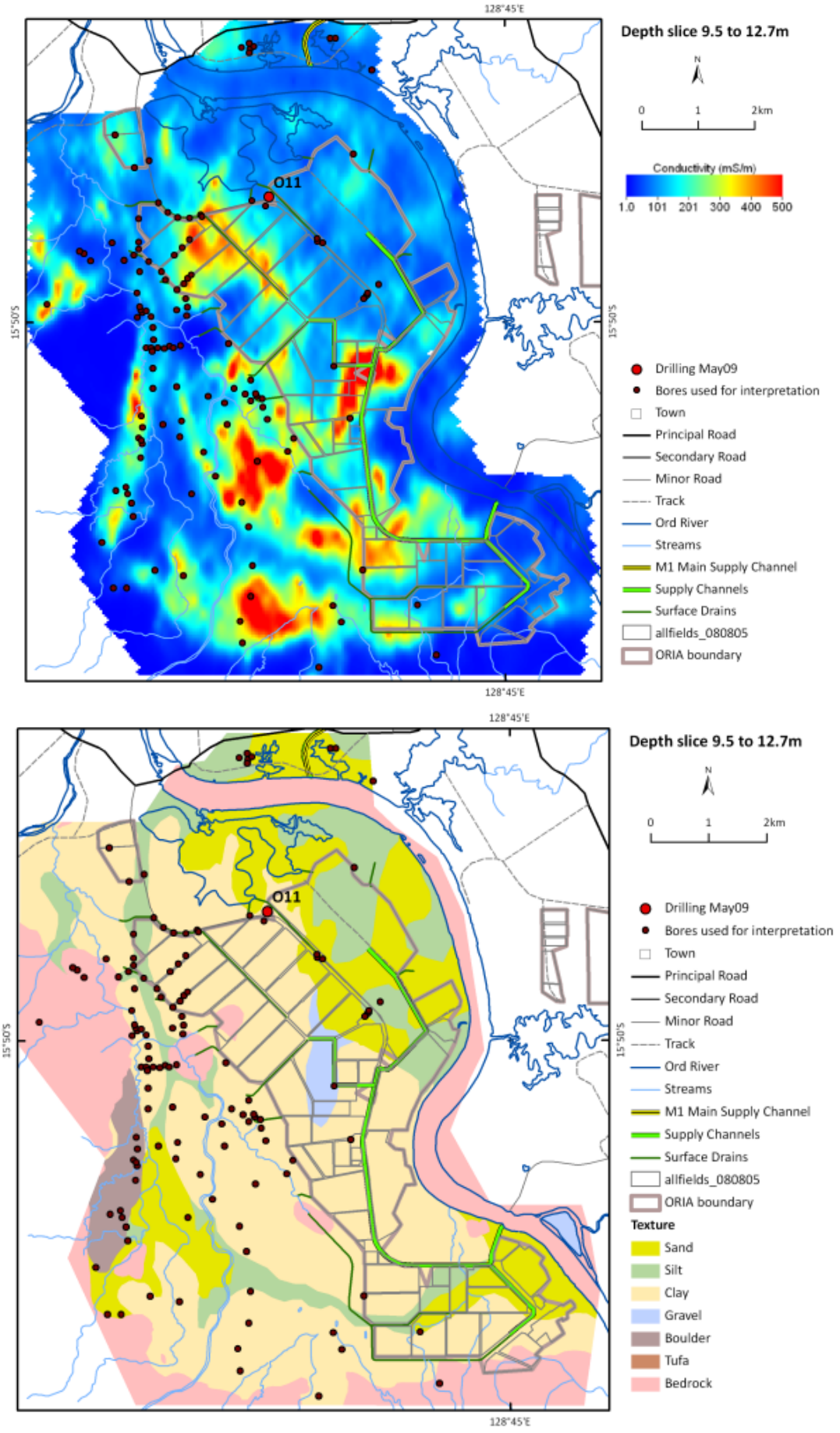

Figure 178: *Packsaddle Plain. Top: conductivity depth slice 9.5 – 12.7m. Bottom: interpreted lithology.*

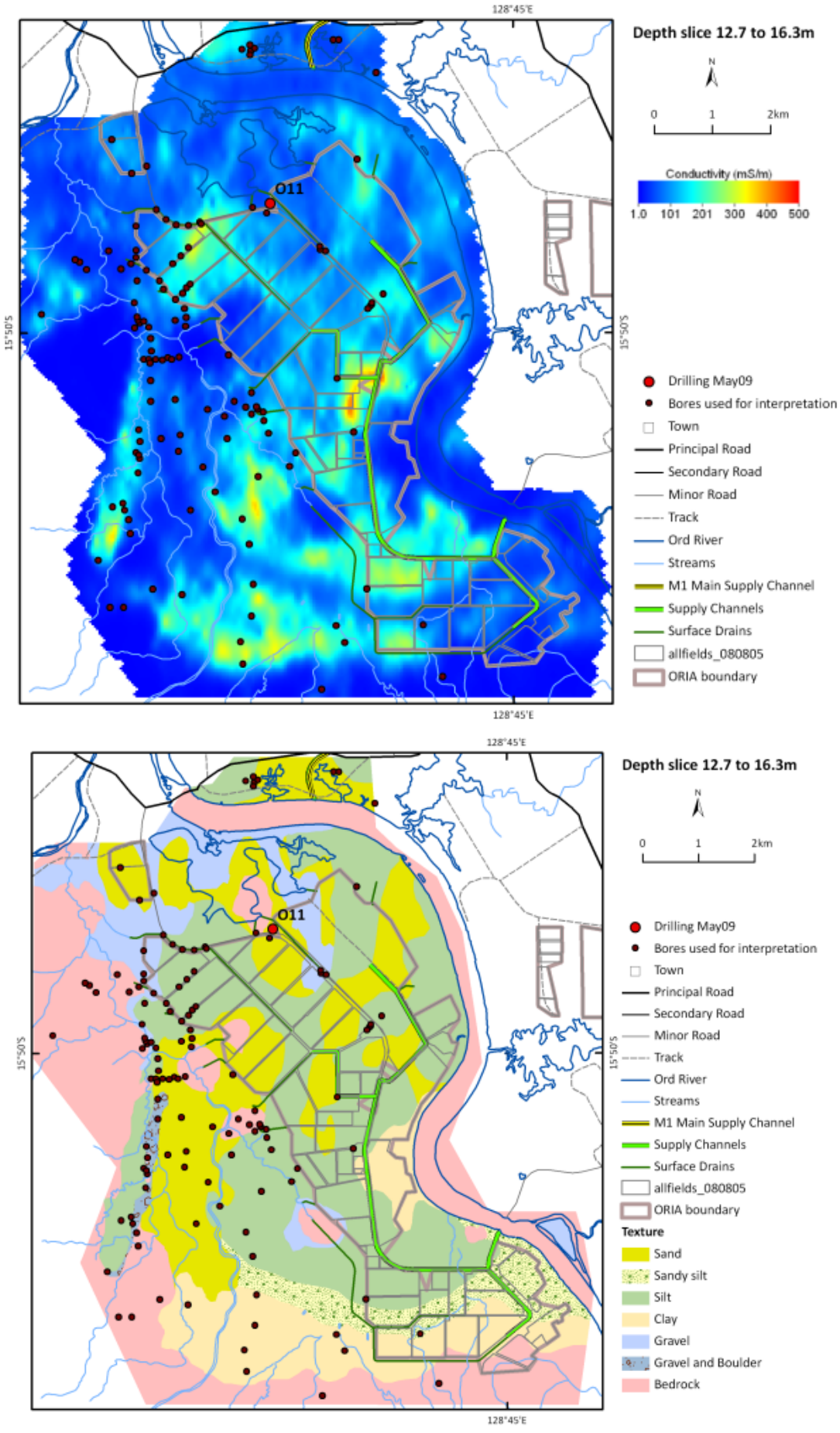

Figure 179: *Packsaddle Plain. Top: conductivity depth slice 12.7 – 16.3m.* ***Bottom:*** *interpreted lithology*

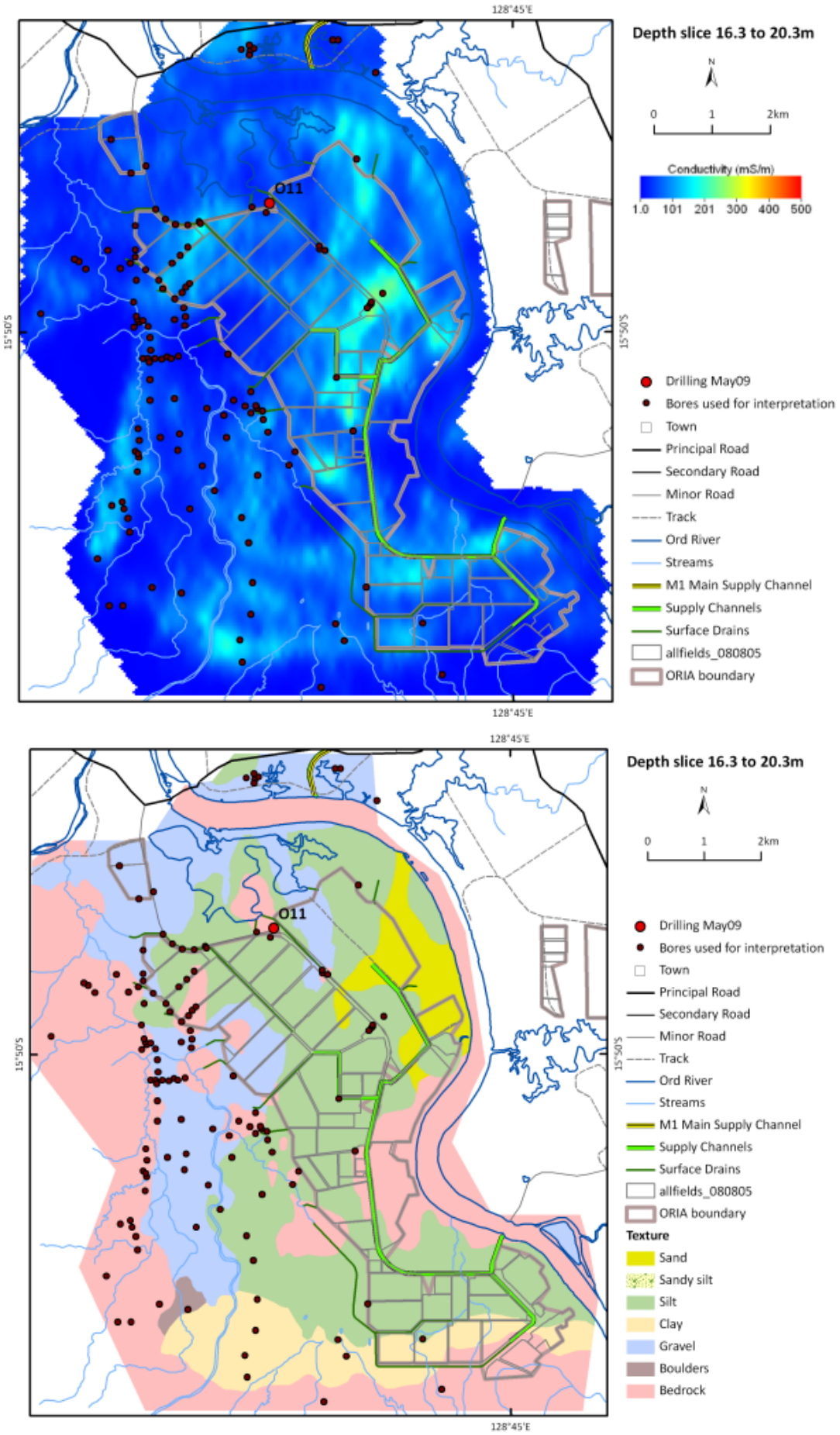

Figure 180: *Packsaddle Plain. Top: conductivity depth slice 16.3 – 20.3m.* ***Bottom:*** *interpreted lithology.*

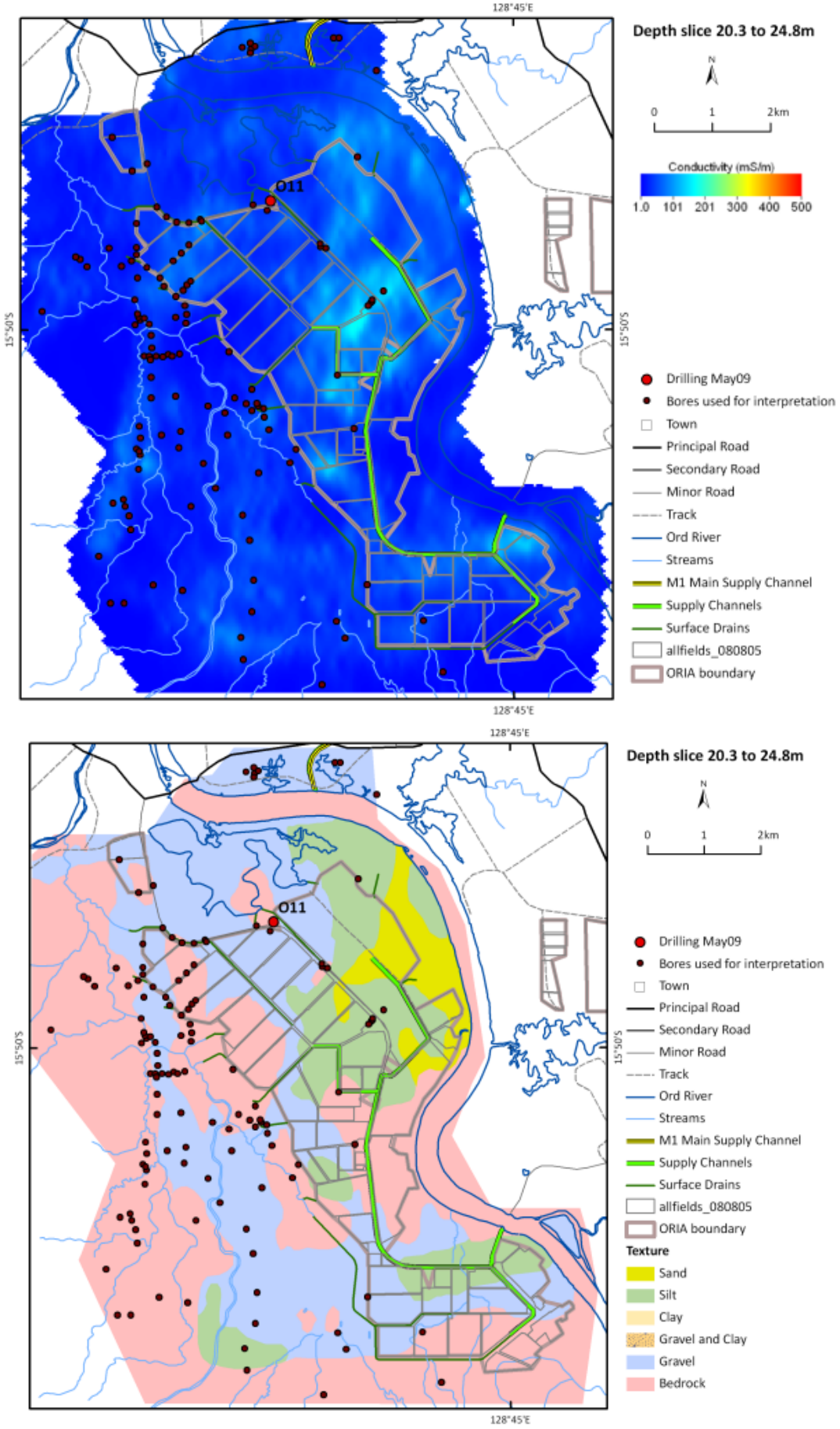

Figure 181: *Packsaddle Plain. Top: conductivity depth slice 20.3 – 24.8m. Bottom: interpreted lithology.*

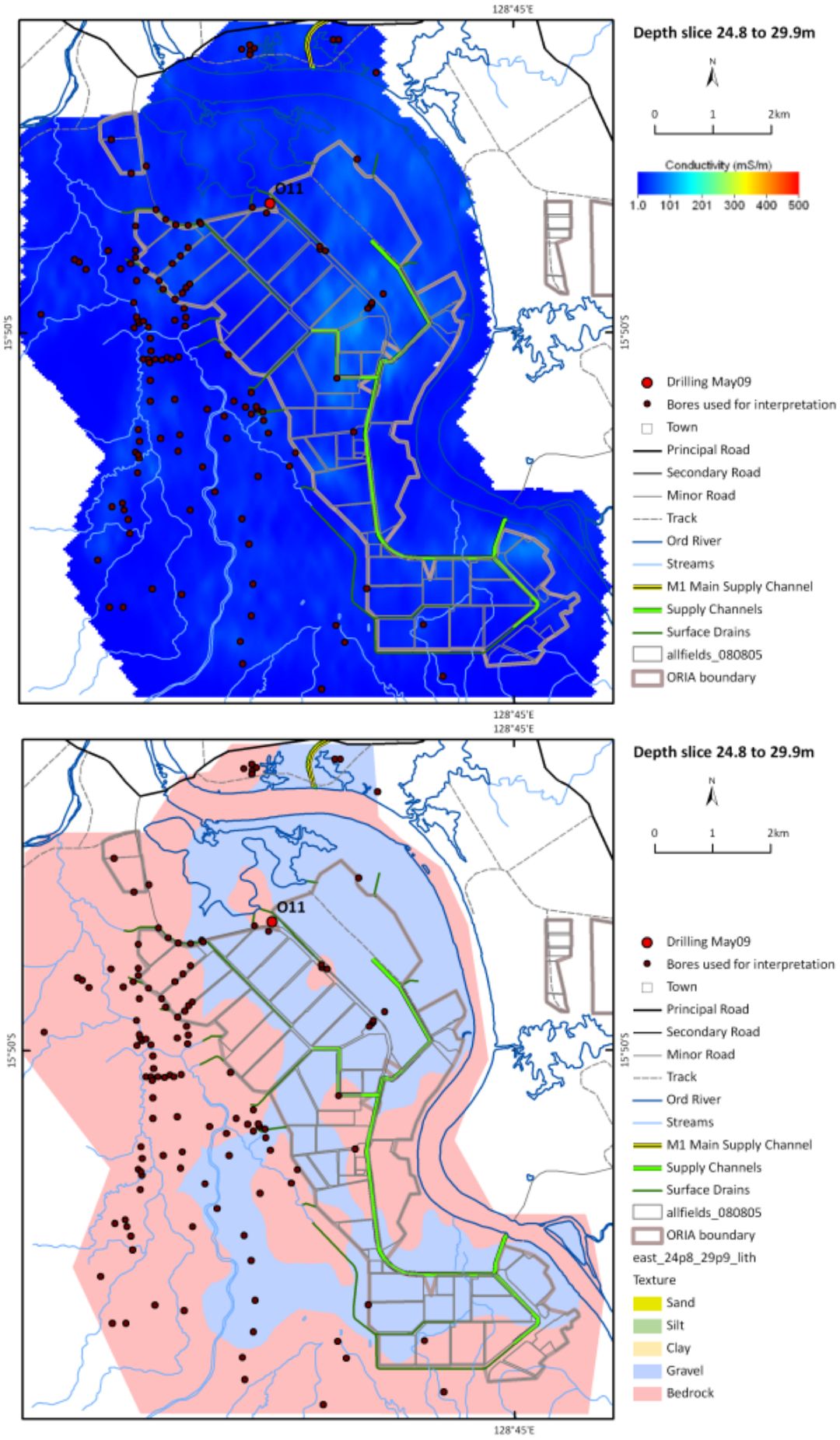

Figure 182: *Packsaddle Plain. Top: conductivity depth slice 24.8 – 29.9m.* ***Bottom:*** *interpreted lithology.*

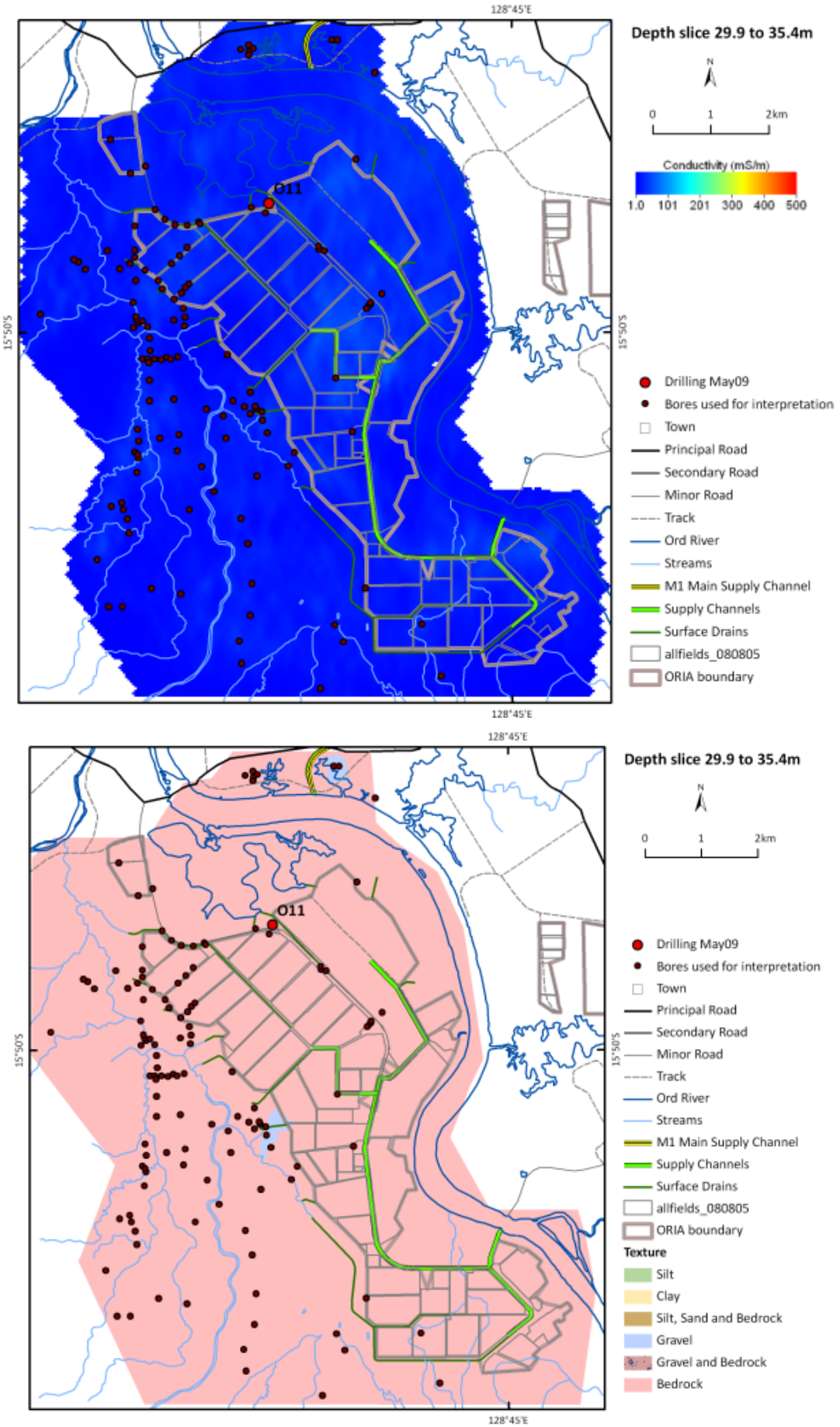

Figure 183: *Packsaddle Plain. Top: conductivity depth slice 29.9 – 35.4m.* ***Bottom:*** *interpreted lithology.*

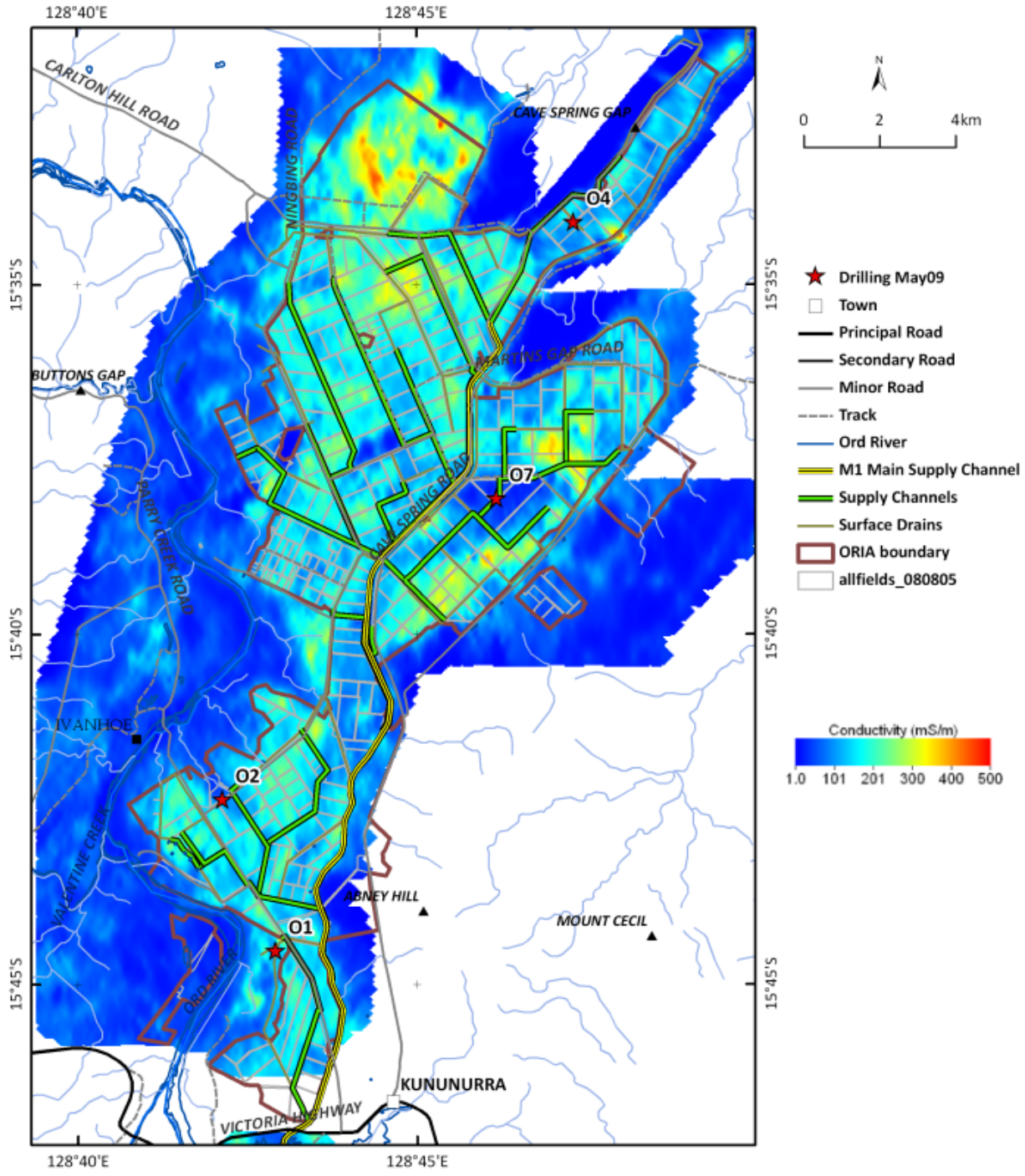

Figure 184: *ORIA Phase 1 Ivanhoe Plain and Ord West Bank conductivity depth slice 0 – 2m* **.**

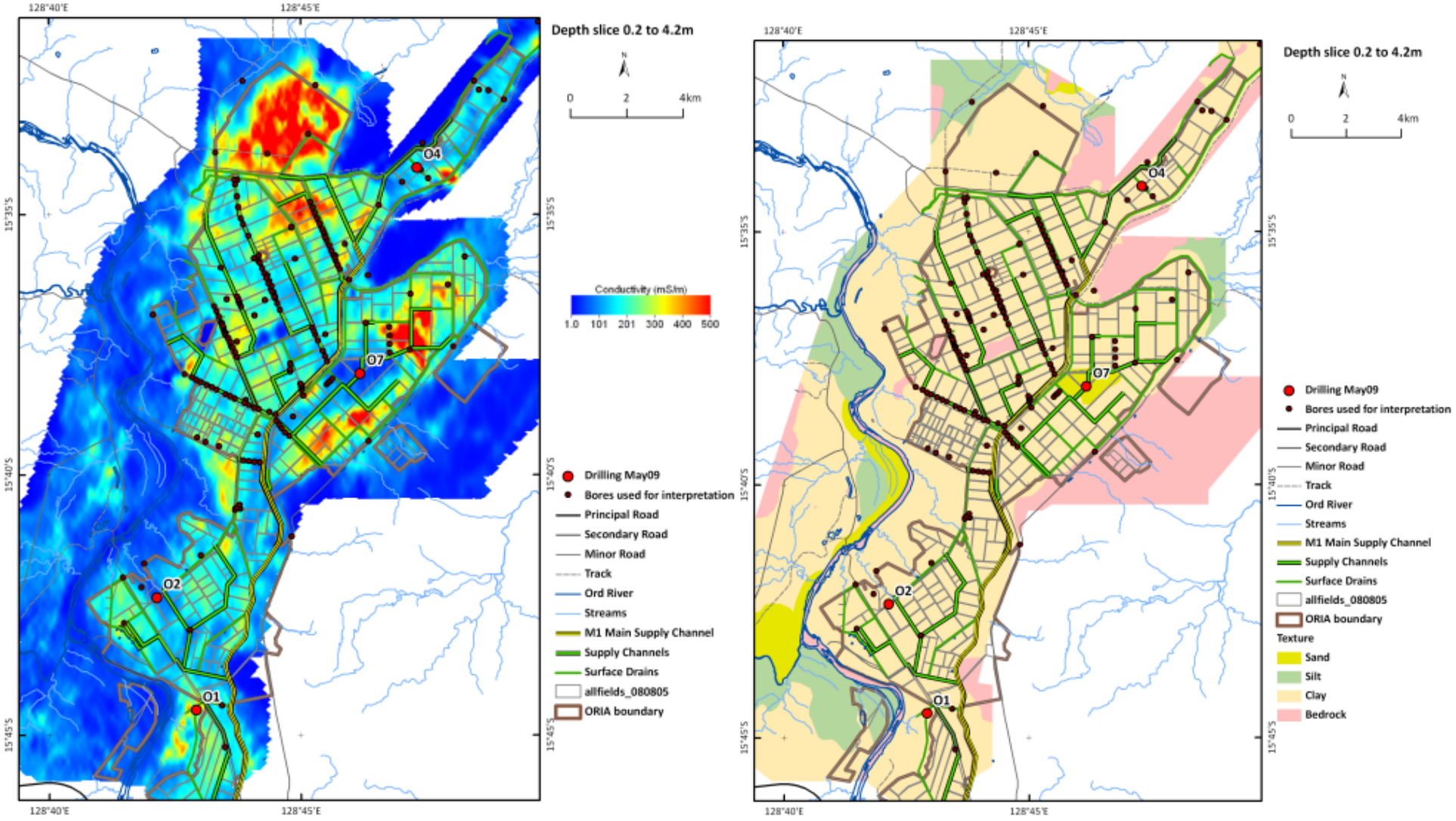

Figure 185: *ORIA Phase 1 Ivanhoe Plain and Ord West Bank. Left: conductivity depth slice 2 – 4.2m.* ***Right:*** *interpreted lithology.*

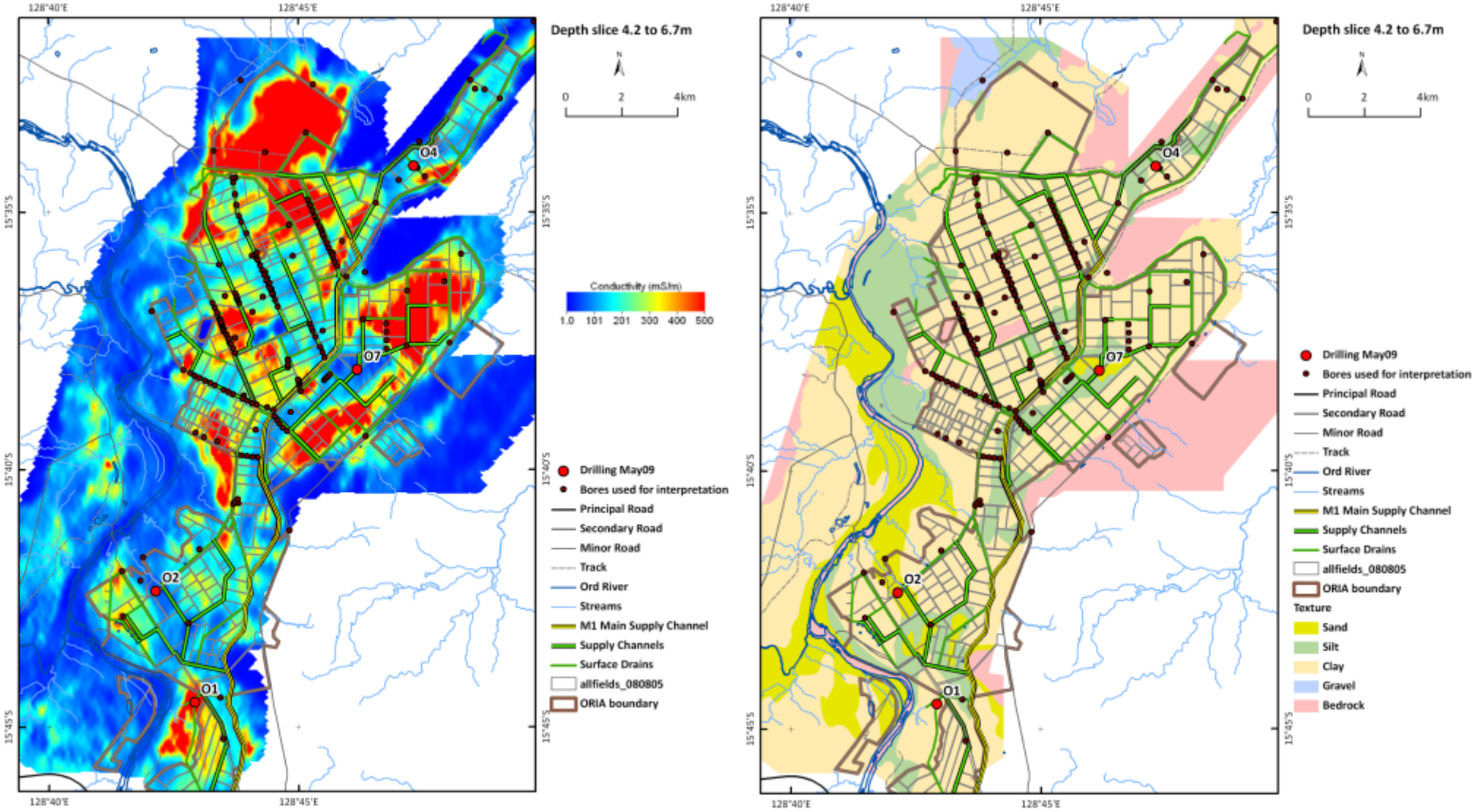

Figure 186: *ORIA Phase 1 Ivanhoe Plain and Ord West Bank. Left: conductivity depth slice 4.2 – 6.7m. Right: interpreted lithology.*

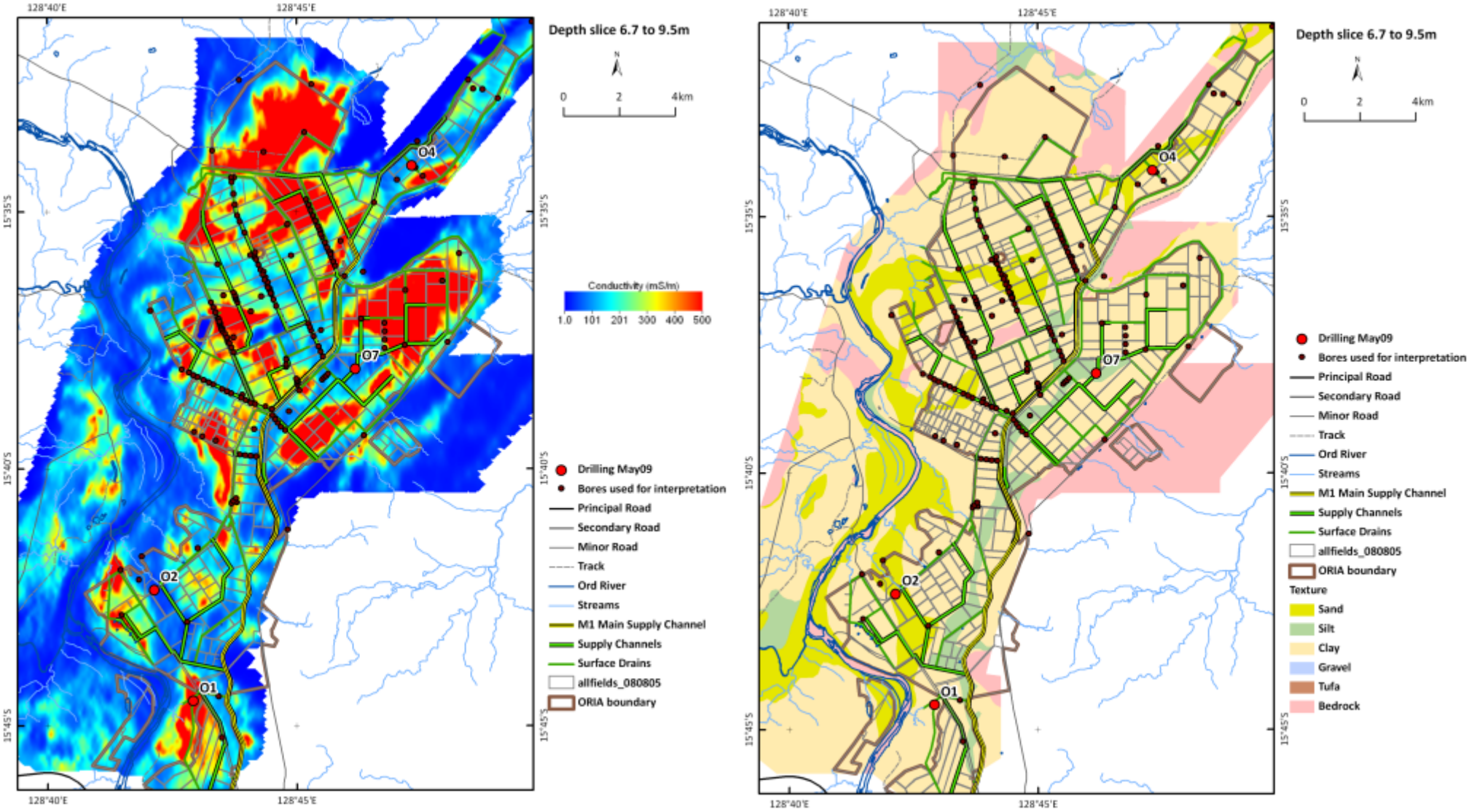

Figure 187: *ORIA Phase 1 Ivanhoe Plain and Ord West Bank. Left: conductivity depth slice 6.7 – 9.5m.* ***Right:*** *interpreted lithology.*

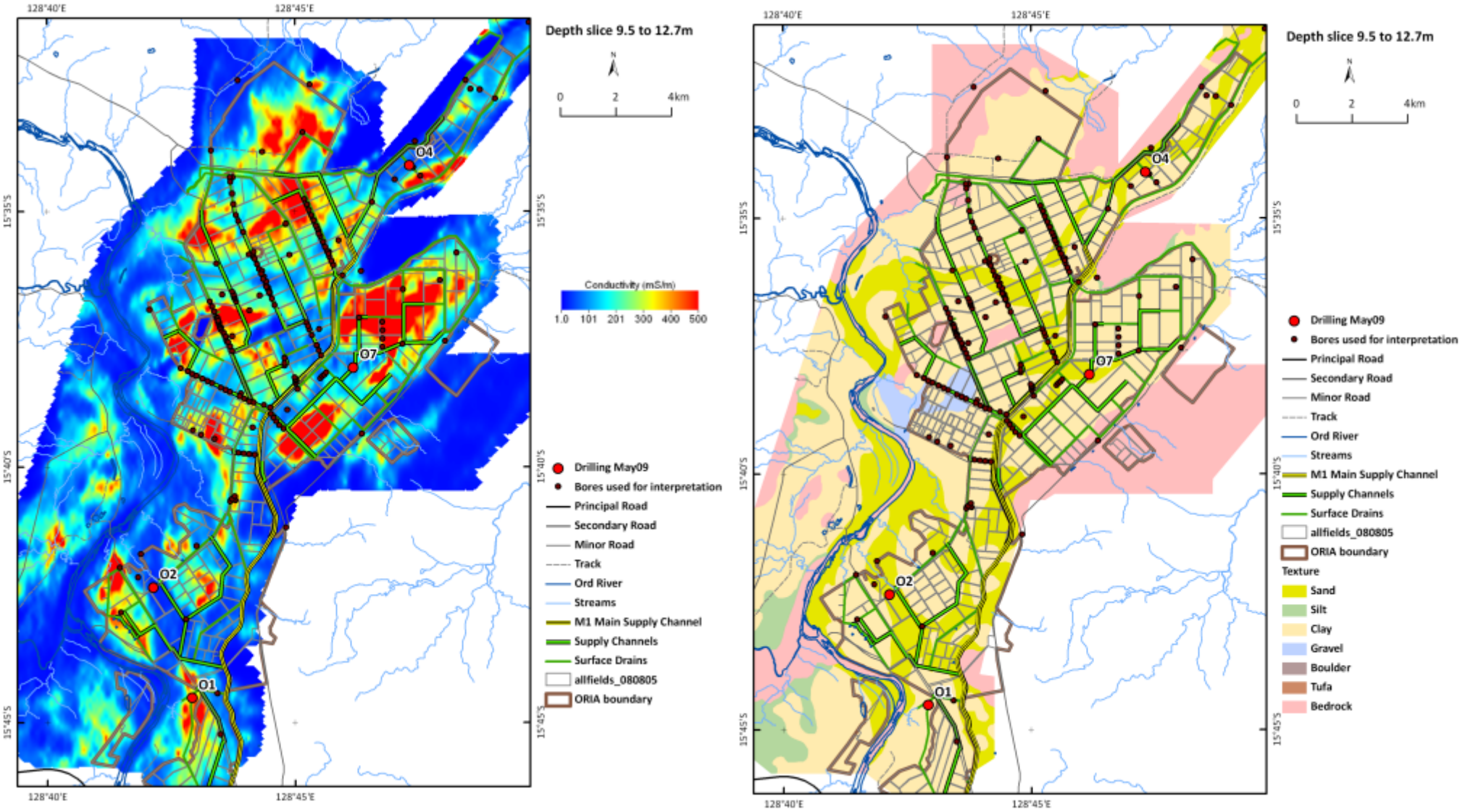

Figure 188: *ORIA Phase 1 Ivanhoe Plain and Ord West Bank. Left: conductivity depth slice 9.5 – 12.7m.* ***Right:*** *interpreted lithology.*

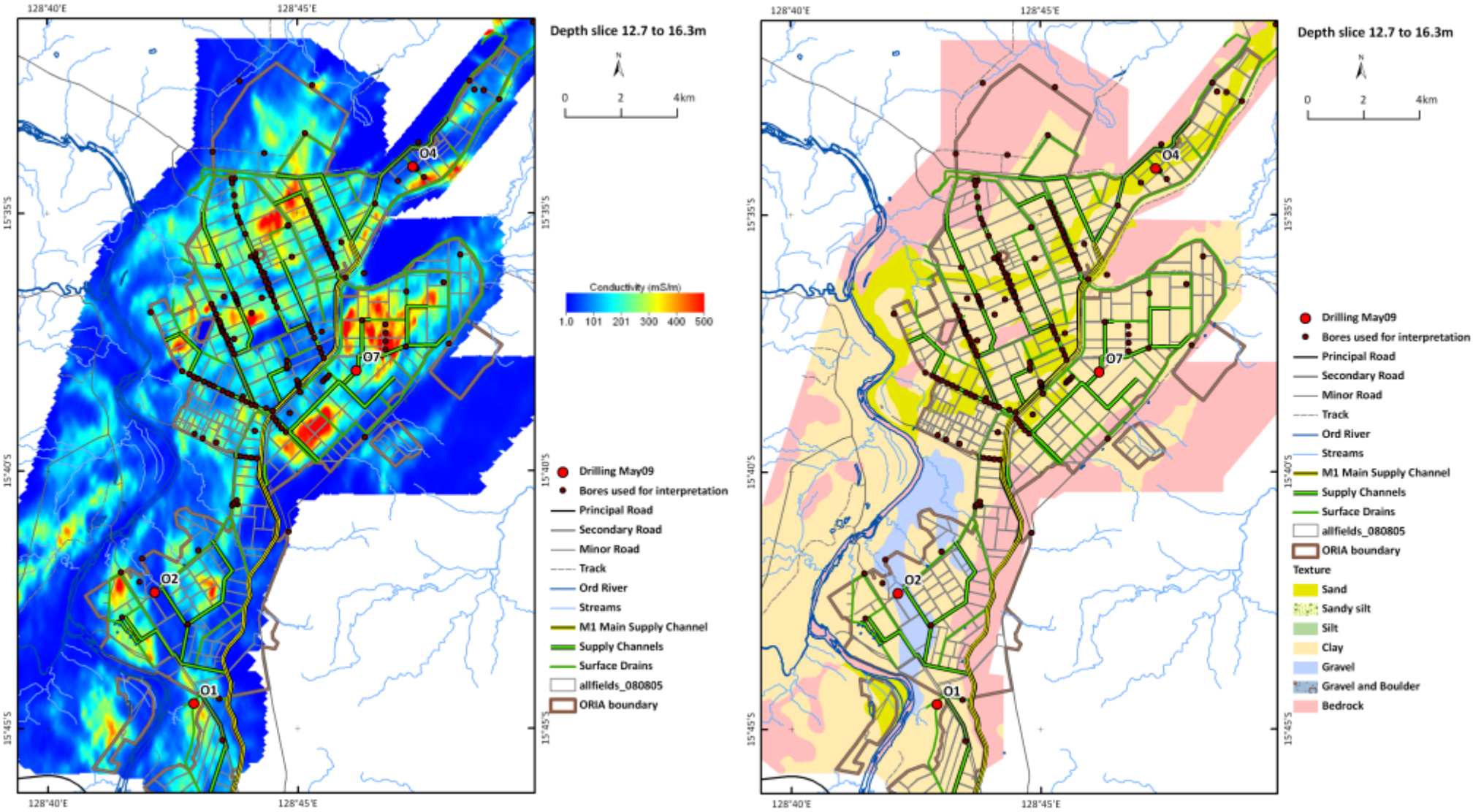

Figure 189: *ORIA Phase 1 Ivanhoe Plain and Ord West Bank. Left: conductivity depth slice 12.7 – 16.3m.* ***Right:*** *interpreted lithology.*

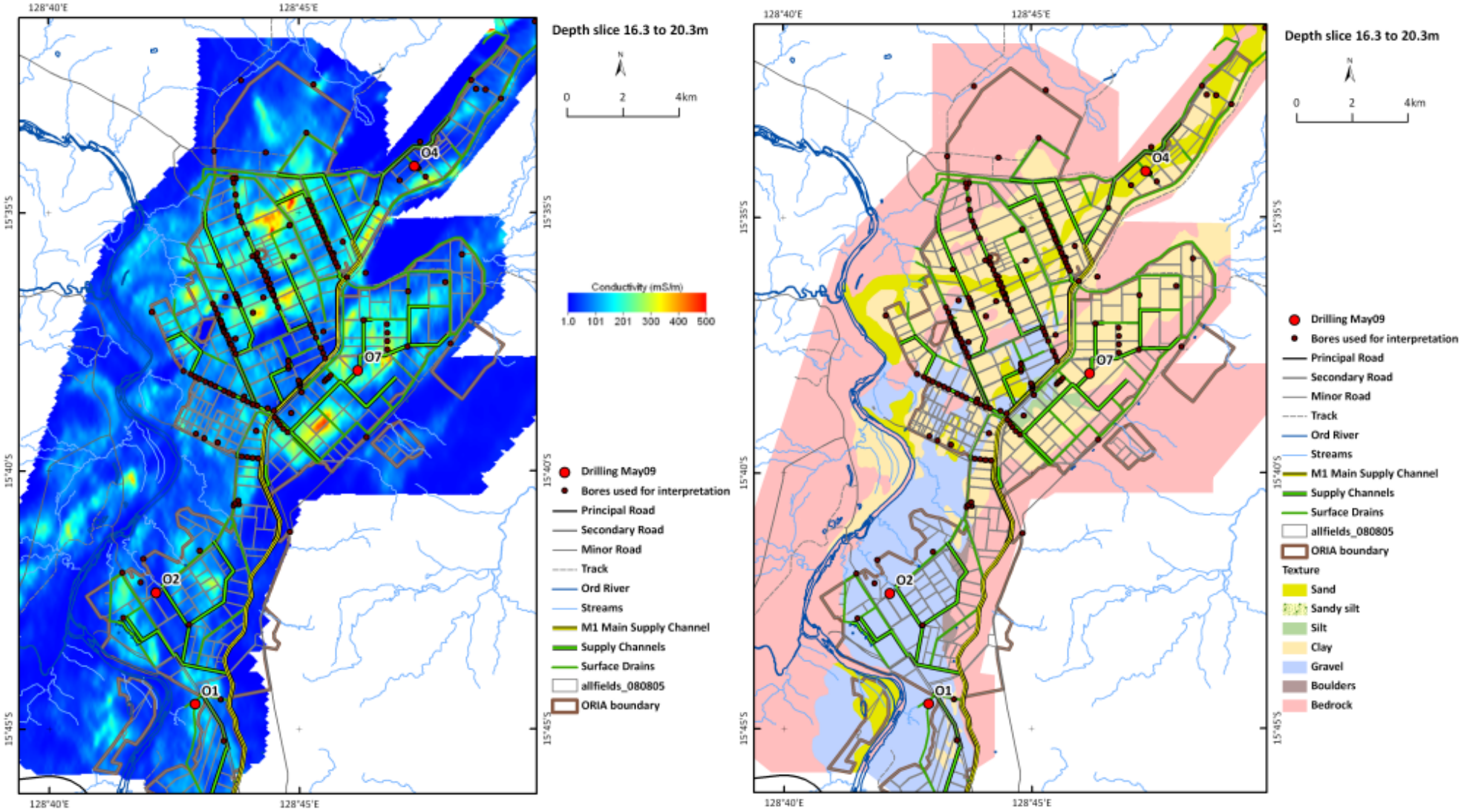

Figure 190: *ORIA Phase 1 Ivanhoe Plain and Ord West Bank. Left: conductivity depth slice 16.3 – 20.3m.* ***Right:*** *interpreted lithology.*

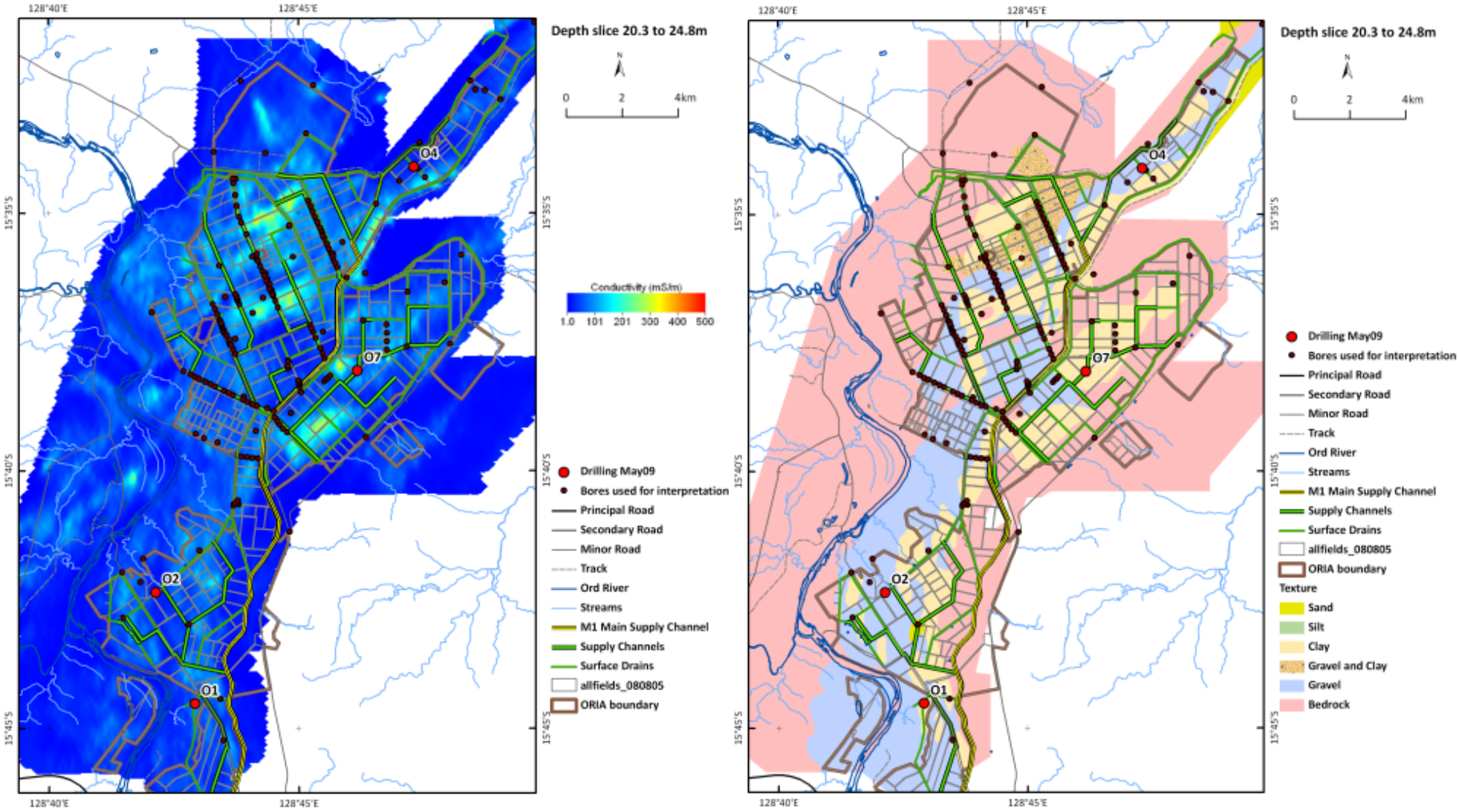

Figure 191: *ORIA Phase 1 Ivanhoe Plain and Ord West Bank. Left: conductivity depth slice 20.3 – 24.8m. Right: interpreted lithology.*

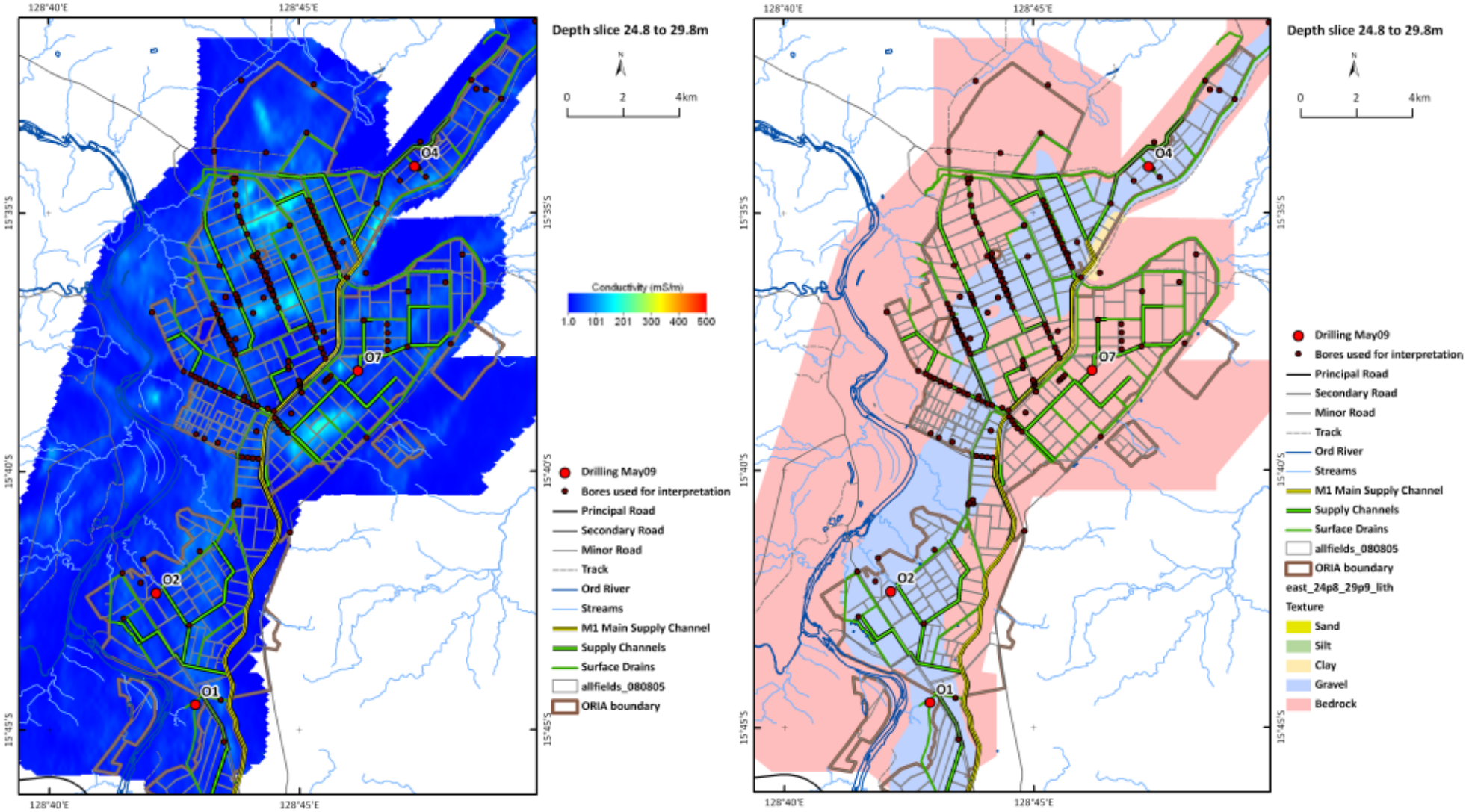

Figure 192: *ORIA Phase 1 Ivanhoe Plain and Ord West Bank. Left: conductivity depth slice 24.8 – 29.8m.* ***Right:*** *interpreted lithology.*

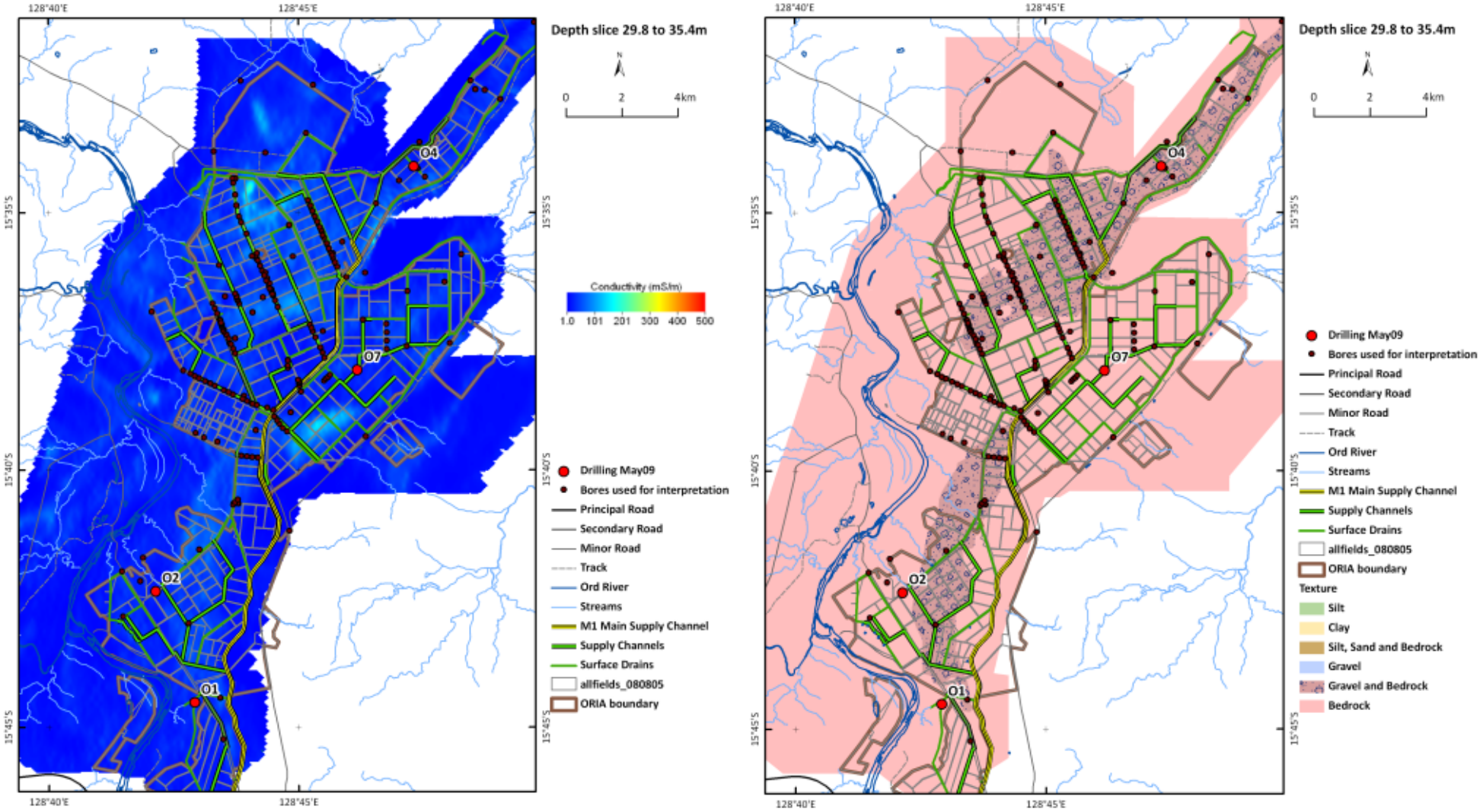

Figure 193: *ORIA Phase 1 Ivanhoe Plain and Ord West Bank. Left: conductivity depth slice 29.8 – 35.4m. Right: interpreted lithology.*

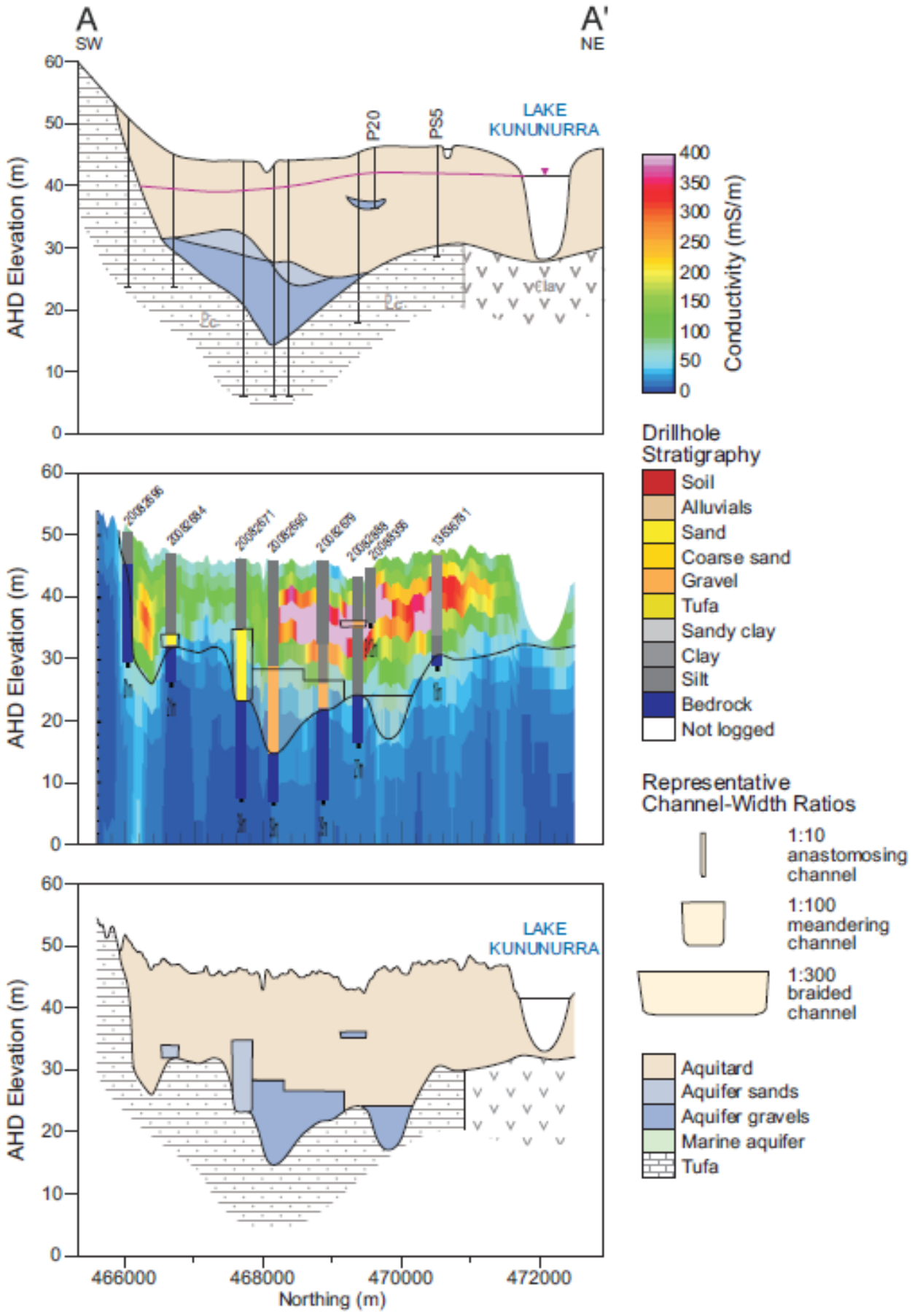

Figure 194: *Packsaddle Plain cross-section A-A'. Top panel is cross-section from O'Boy et al., (2001); middle panel is synthetic AEM section showing drillholes colour coded for lithology and with lithology extent interpretation line work displayed; bottom panel is revised lithology interpretation produced in this study.*

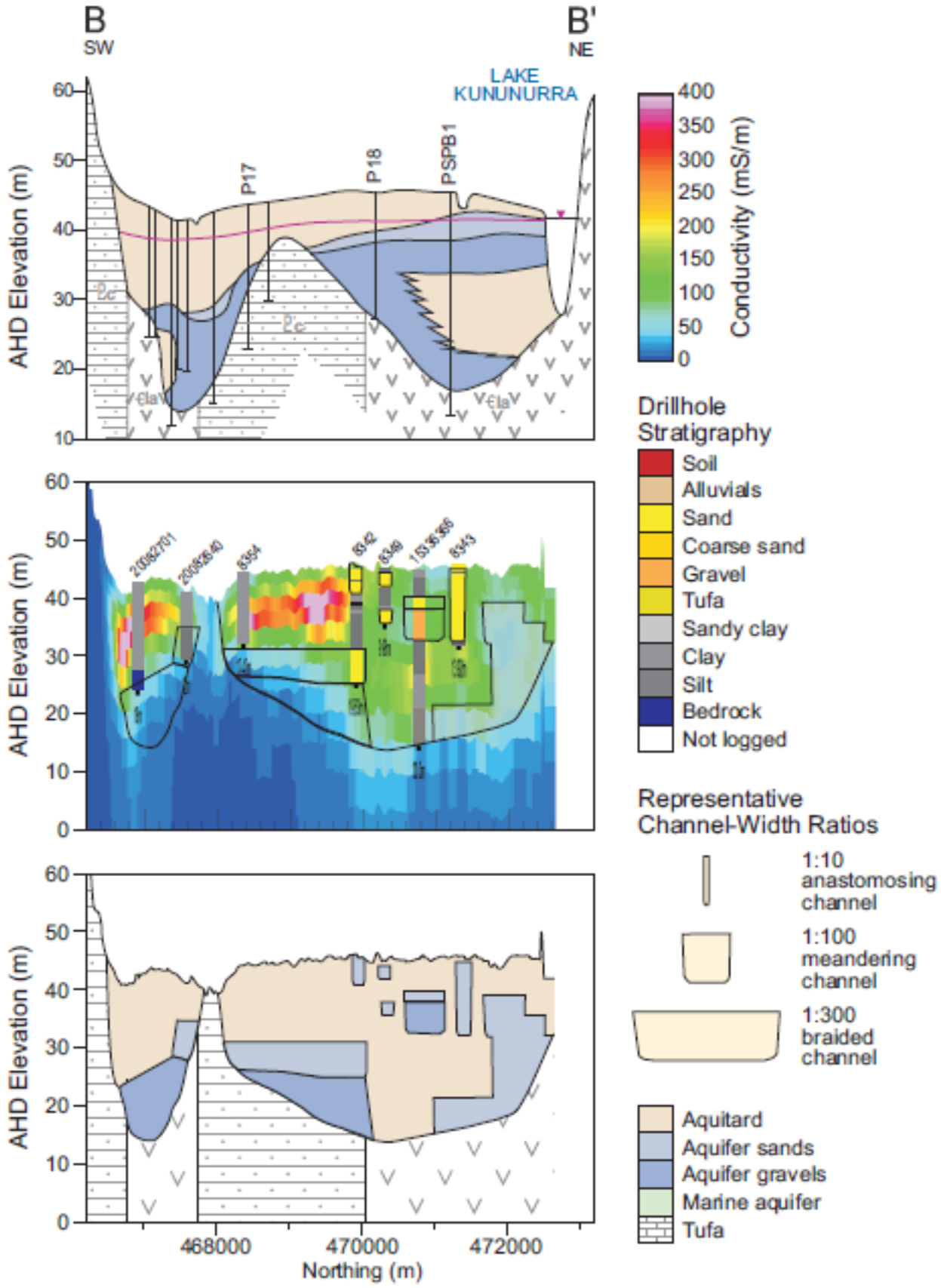

Figure 195: *Packsaddle Plain cross-section B-B'. Top panel is cross-section from O'Boy et al., (2001); middle panel is synthetic AEM section showing drillholes colour coded for lithology and with lithology extent interpretation line work displayed; bottom panel is revised lithology interpretation produced in this study.*

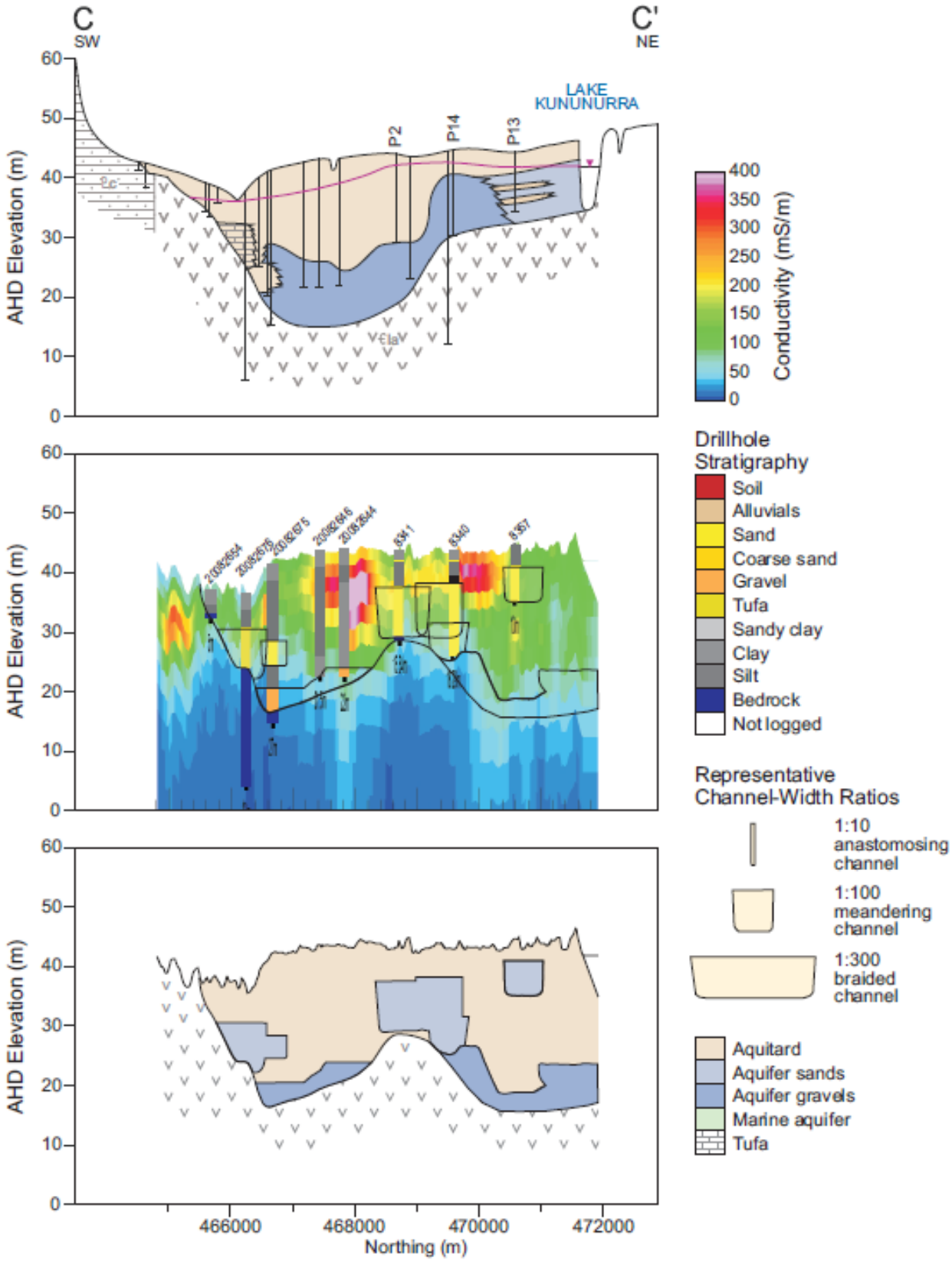

Figure 196: *Packsaddle Plain cross-section C-C'. Top panel is cross-section from O'Boy et al., (2001); middle panel is synthetic AEM section showing drillholes colour coded for lithology and with lithology extent interpretation line work displayed; bottom panel is revised lithology interpretation produced in this study.*

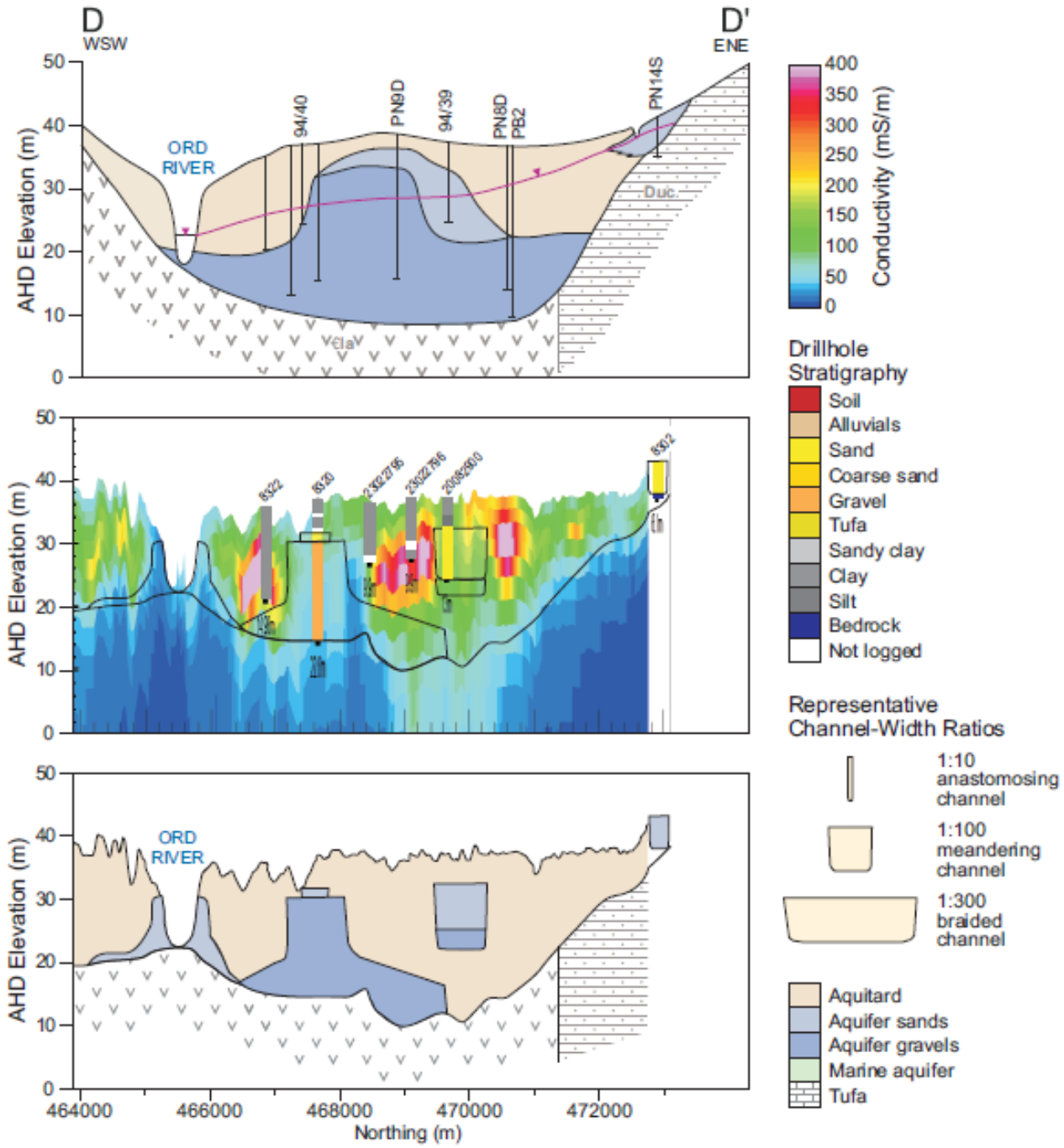

Figure 197: *Ivanhoe Plain cross-section D-D'. Top panel is cross-section from O'Boy et al., (2001); middle panel is synthetic AEM section showing drillholes colour coded for lithology and with lithology extent interpretation line work displayed; bottom panel is revised lithology interpretation produced in this study*

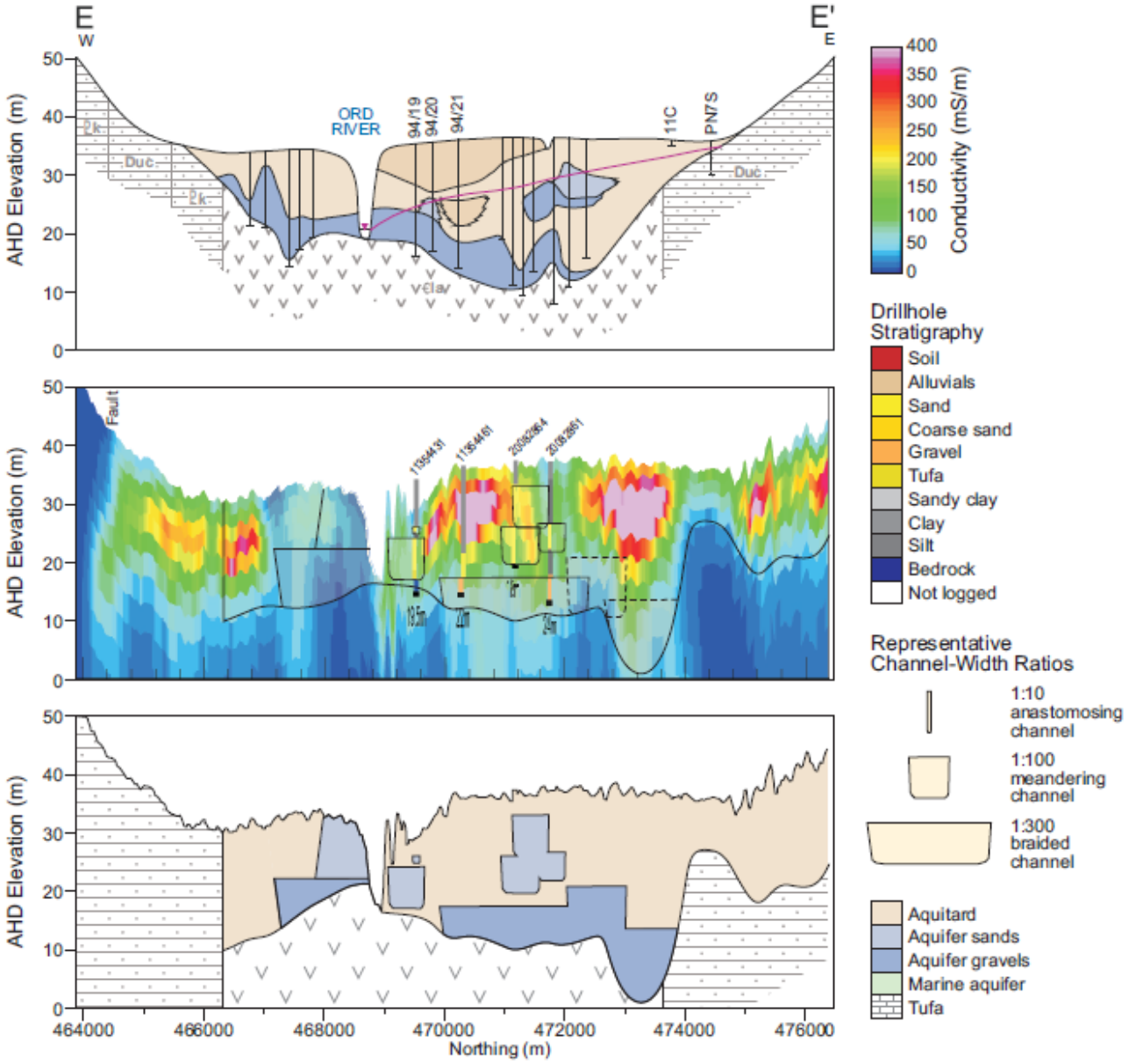

Figure 198: *Ivanhoe Plain cross-section E-E'. Top panel is cross-section from O'Boy et al., (2001); middle panel is synthetic AEM section showing drillholes colour coded for lithology and with lithology extent interpretation line work displayed; bottom panel is revised lithology interpretation produced in this study*

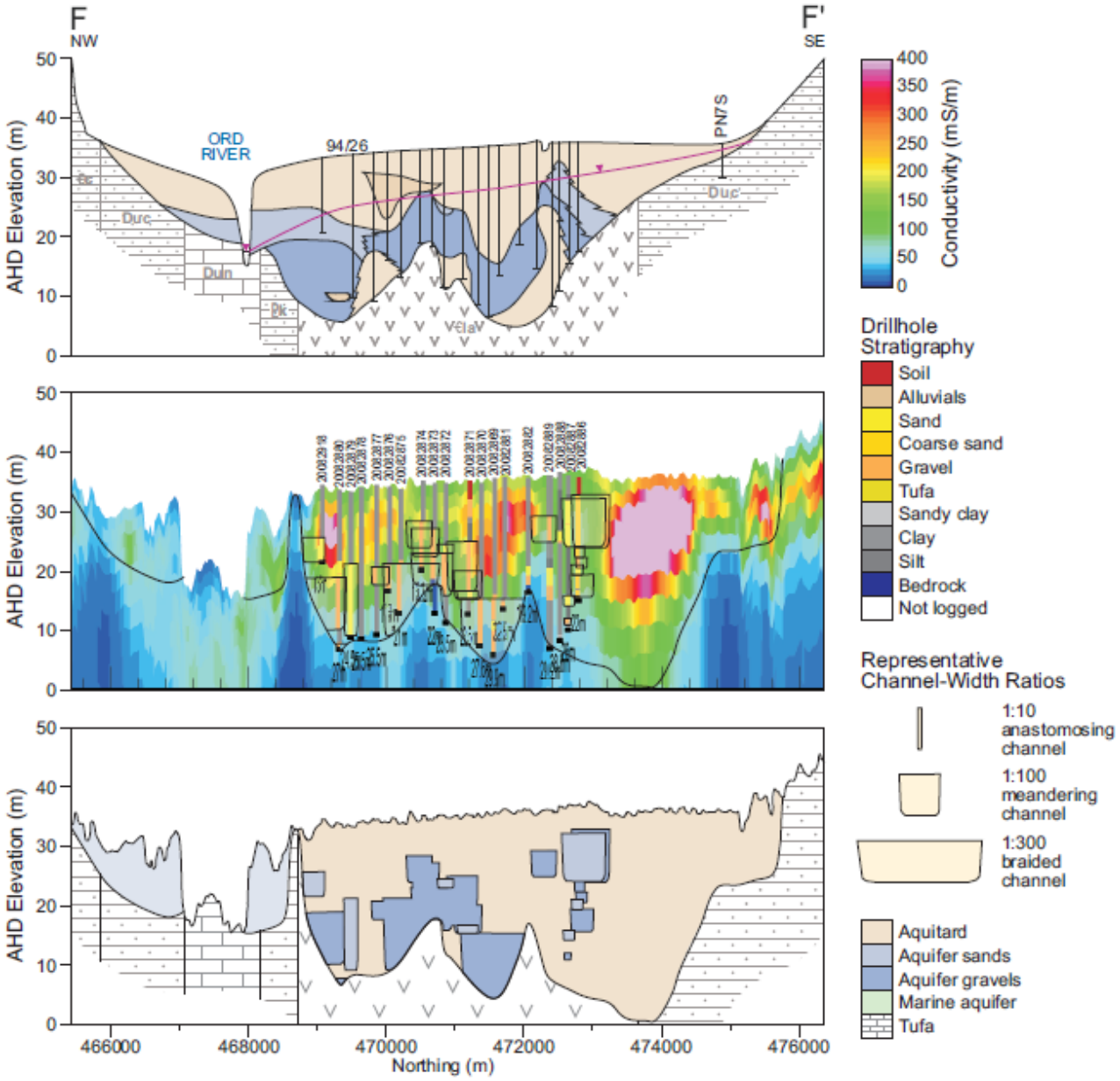

Figure 199: *Ivanhoe Plain cross-section F-F'. Top panel is cross-section from O'Boy et al., (2001); middle panel is synthetic AEM section showing drillholes colour coded for lithology and with lithology extent interpretation line work displayed; bottom panel is revised lithology interpretation produced in this study*

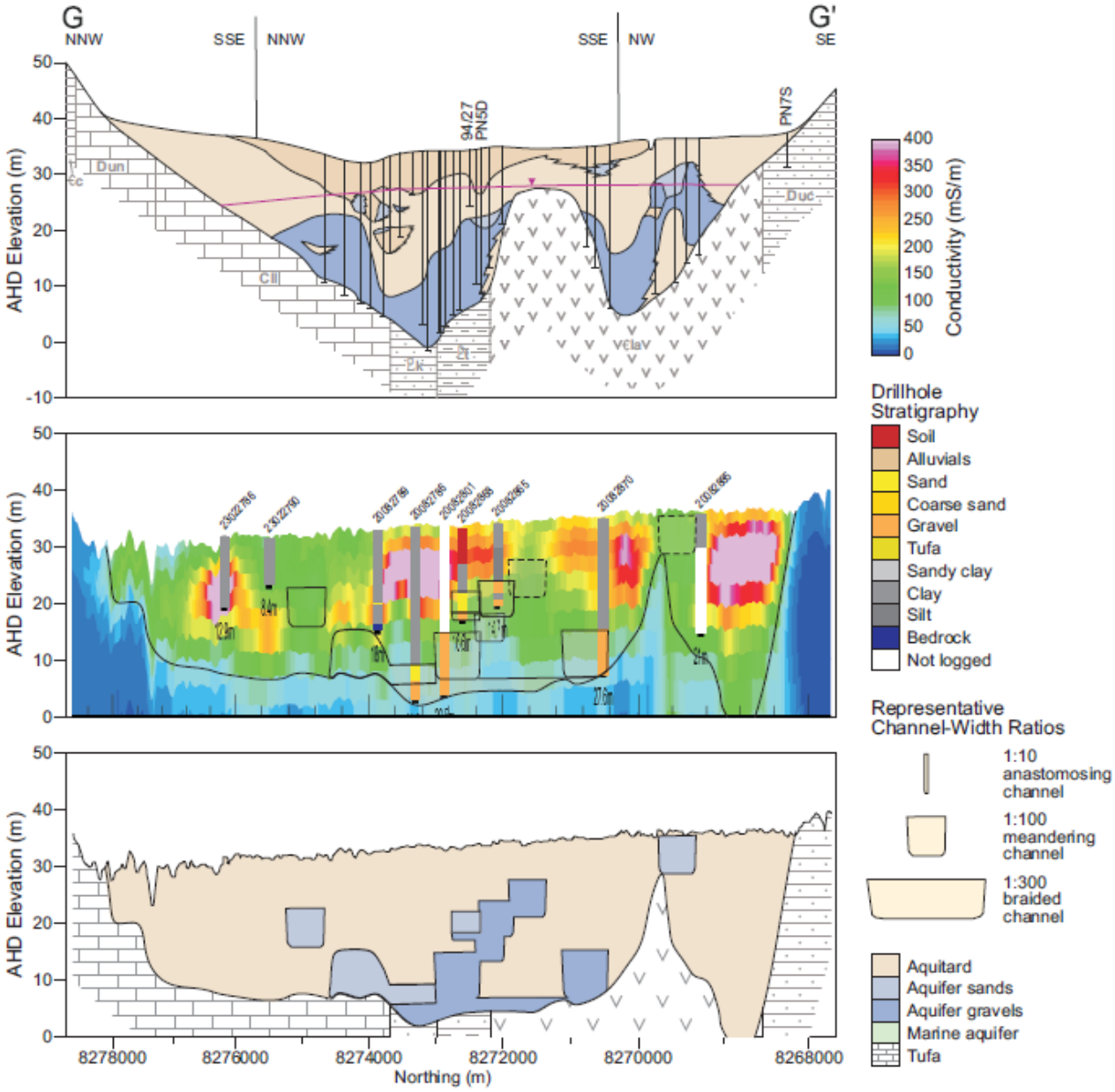

Figure 200: *Ivanhoe Plain cross-section G-G'. Top panel is cross-section from O'Boy et al., (2001); middle panel is synthetic AEM section showing drillholes colour coded for lithology and with lithology extent interpretation line work displayed; bottom panel is revised lithology interpretation produced in this study*

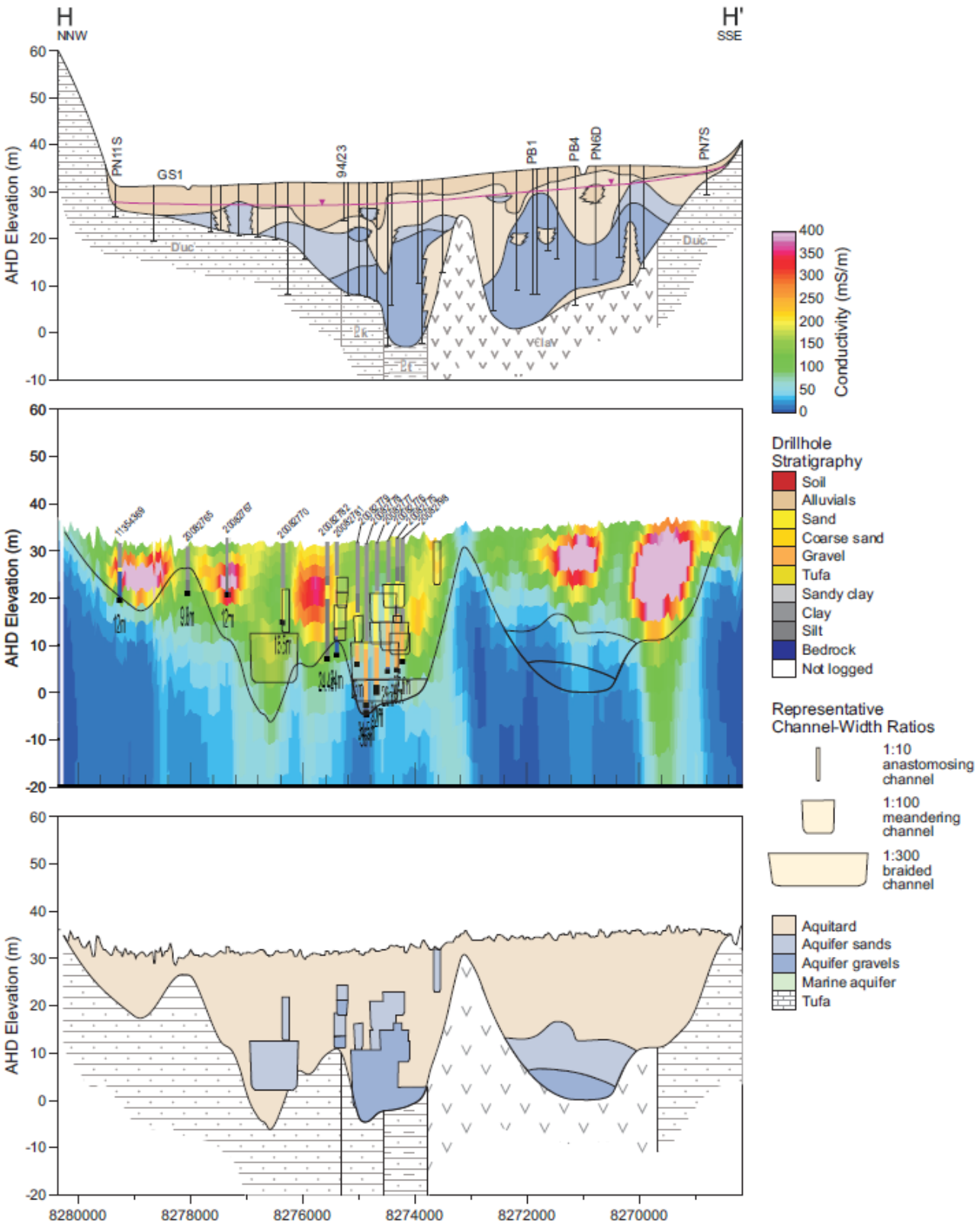

Figure 201: *Ivanhoe Plain cross-section H-H'. Top panel is cross-section from O'Boy et al., (2001); middle panel is synthetic AEM section showing drillholes colour coded for lithology and with lithology extent interpretation line work displayed; bottom panel is revised lithology interpretation produced in this study*

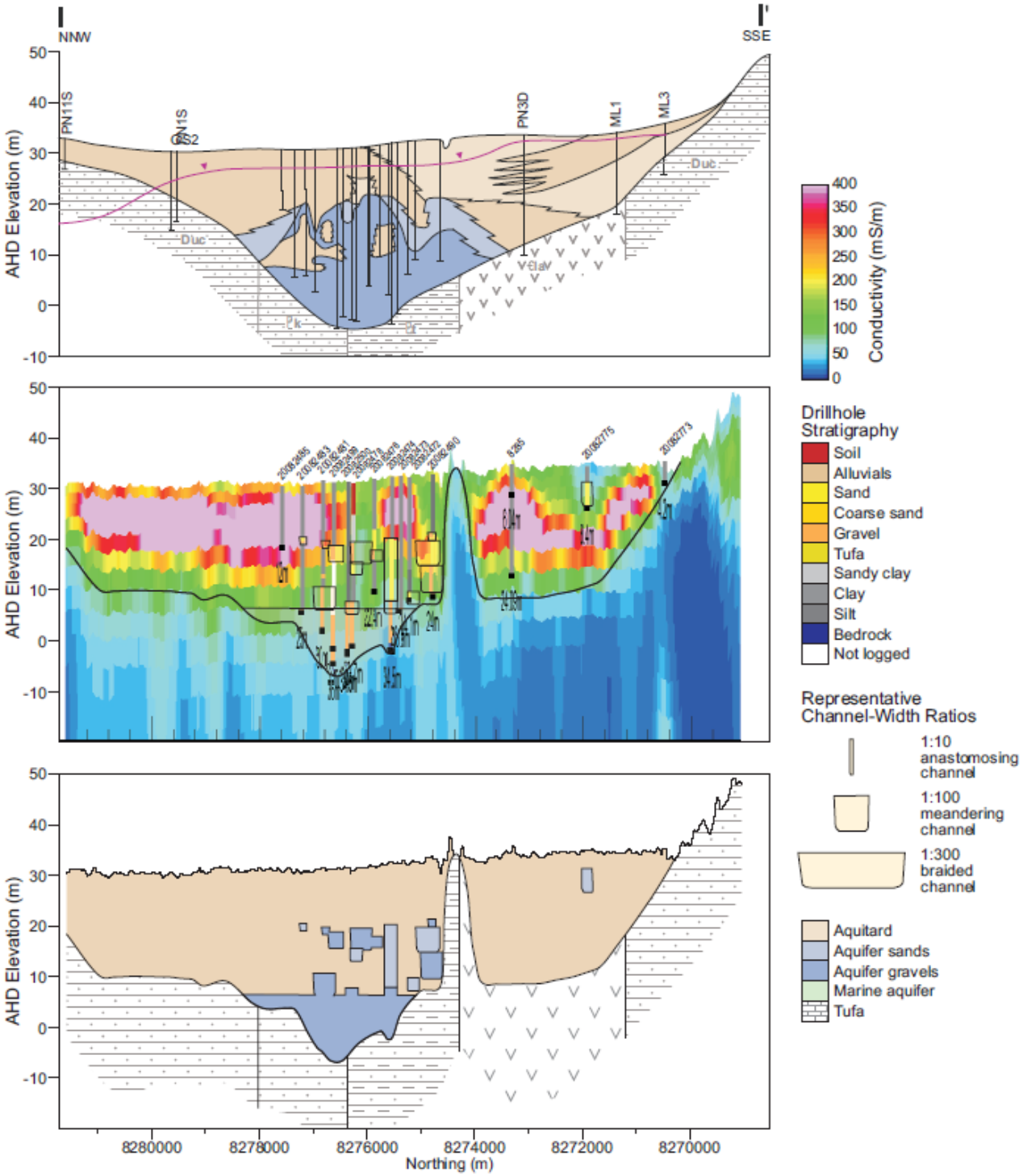

Figure 202: *Ivanhoe Plain cross-section I-I'. Top panel is cross-section from O'Boy et al., (2001); middle panel is synthetic AEM section showing drillholes colour coded for lithology and with lithology extent interpretation line work displayed; bottom panel is revised lithology interpretation produced in this study.*

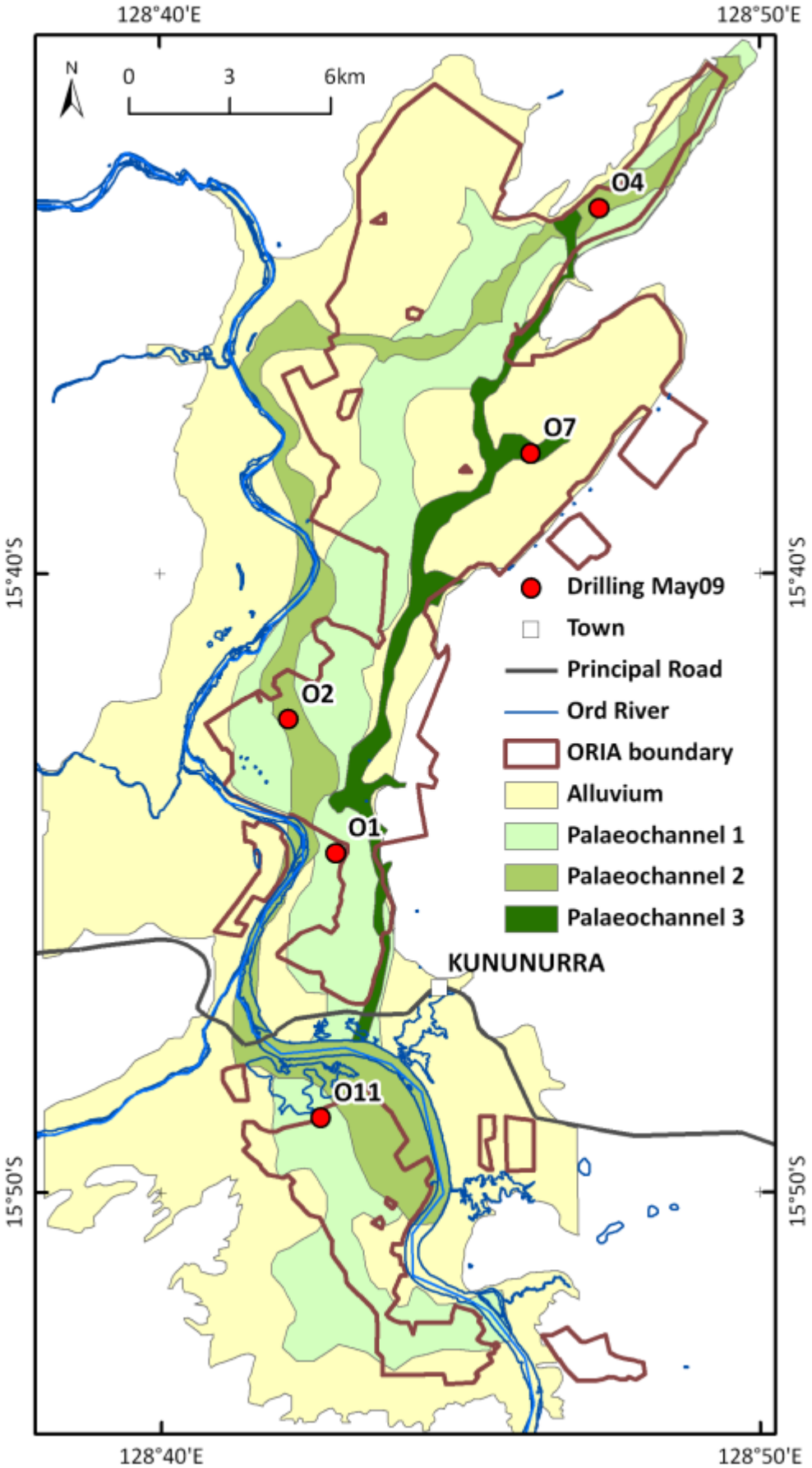

Figure 203: *Summary diagram showing the location of the main palaeochannels identified in the ORIA Stage 1.*

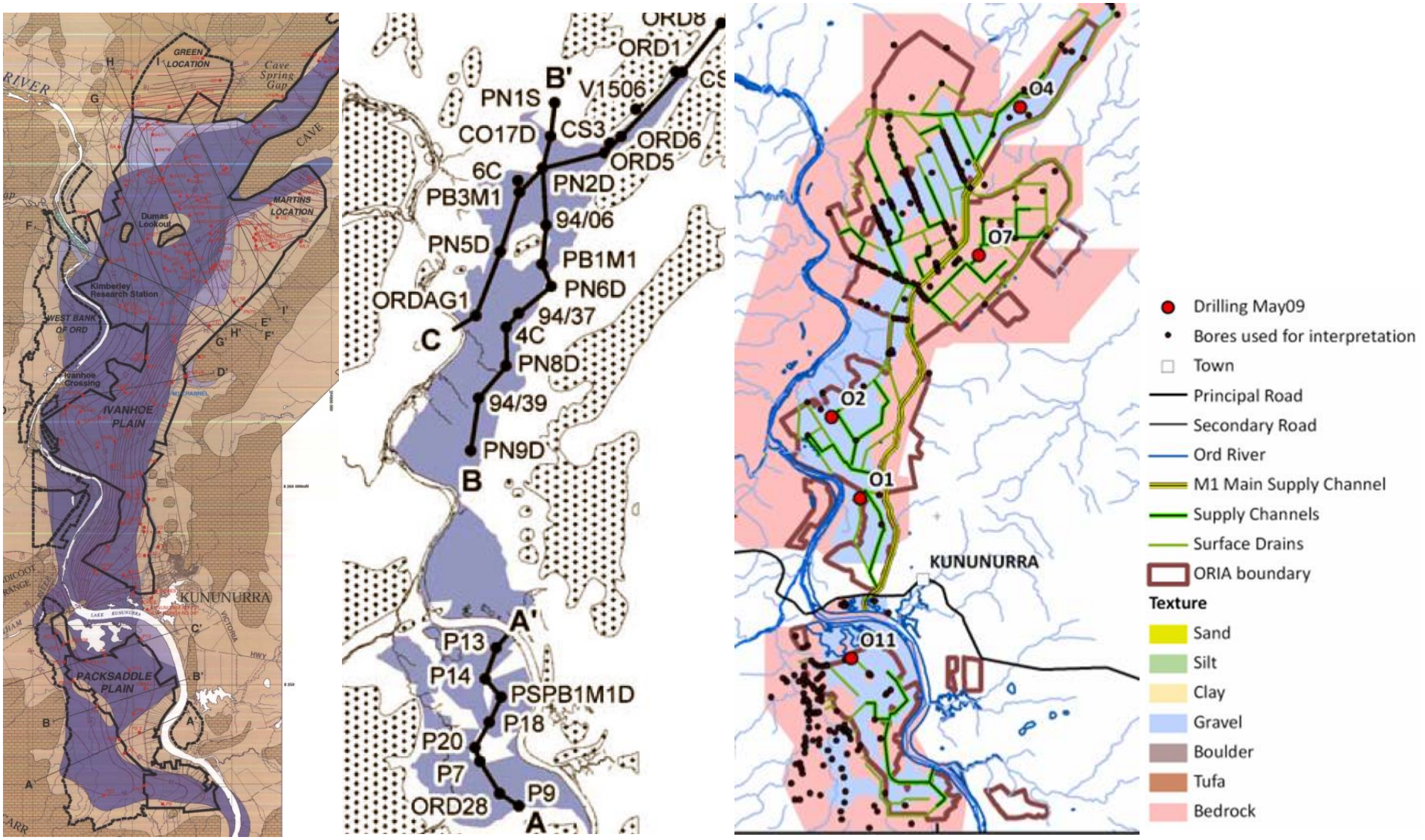

Figure 204: *Comparison between the extent of gravels with maps from O'Boy et al., 2001 (left), Smith, 2008 (centre) and this study (right). Depth section included here in from 24.8-29.9 m.*

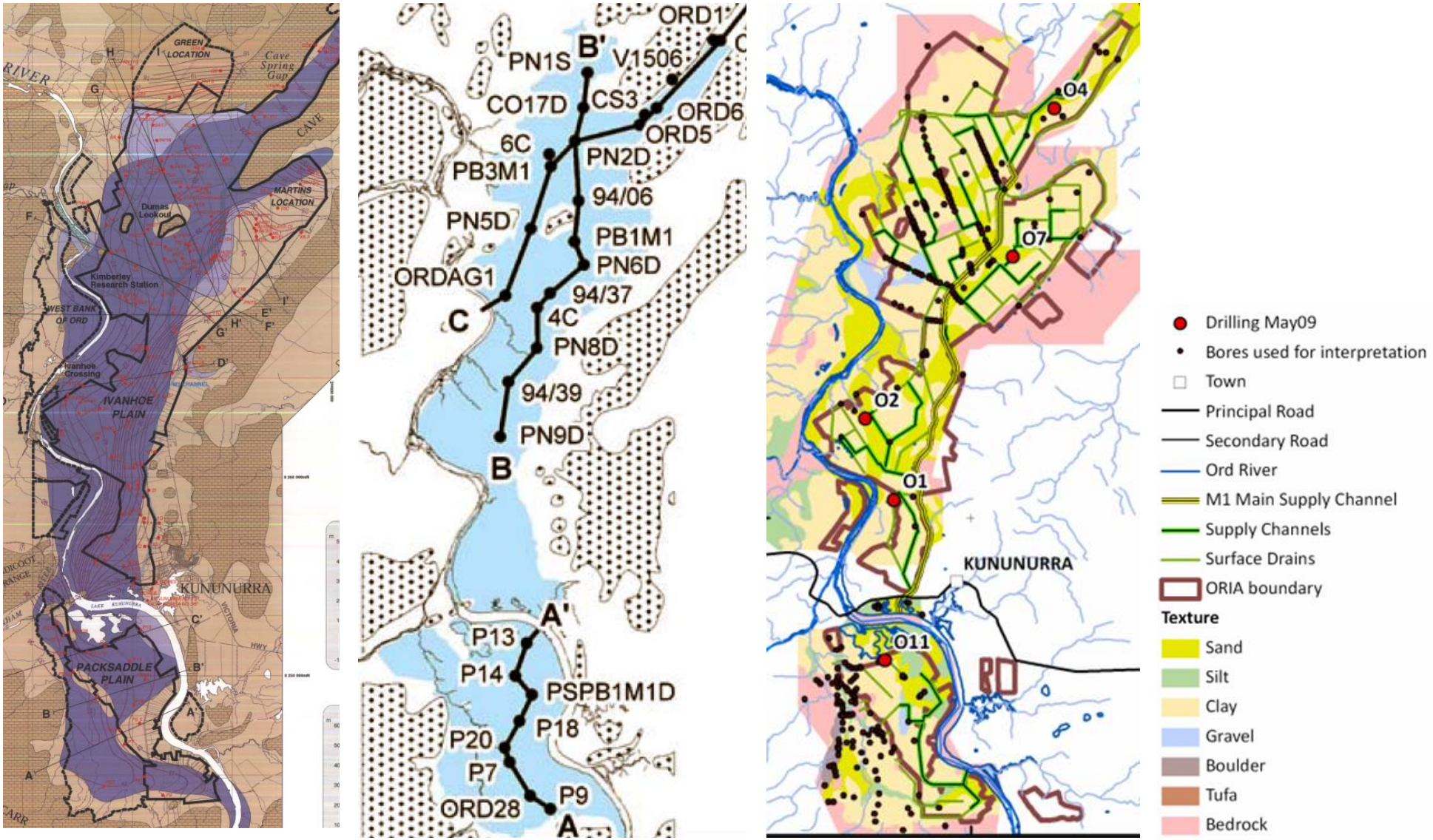

Figure 205: *Comparison between the extent of sands with maps from O'Boy et al., 2001 (left), Smith, 2008 (centre) and this study (right). Depth section included here in from 9.5-12.7m.*

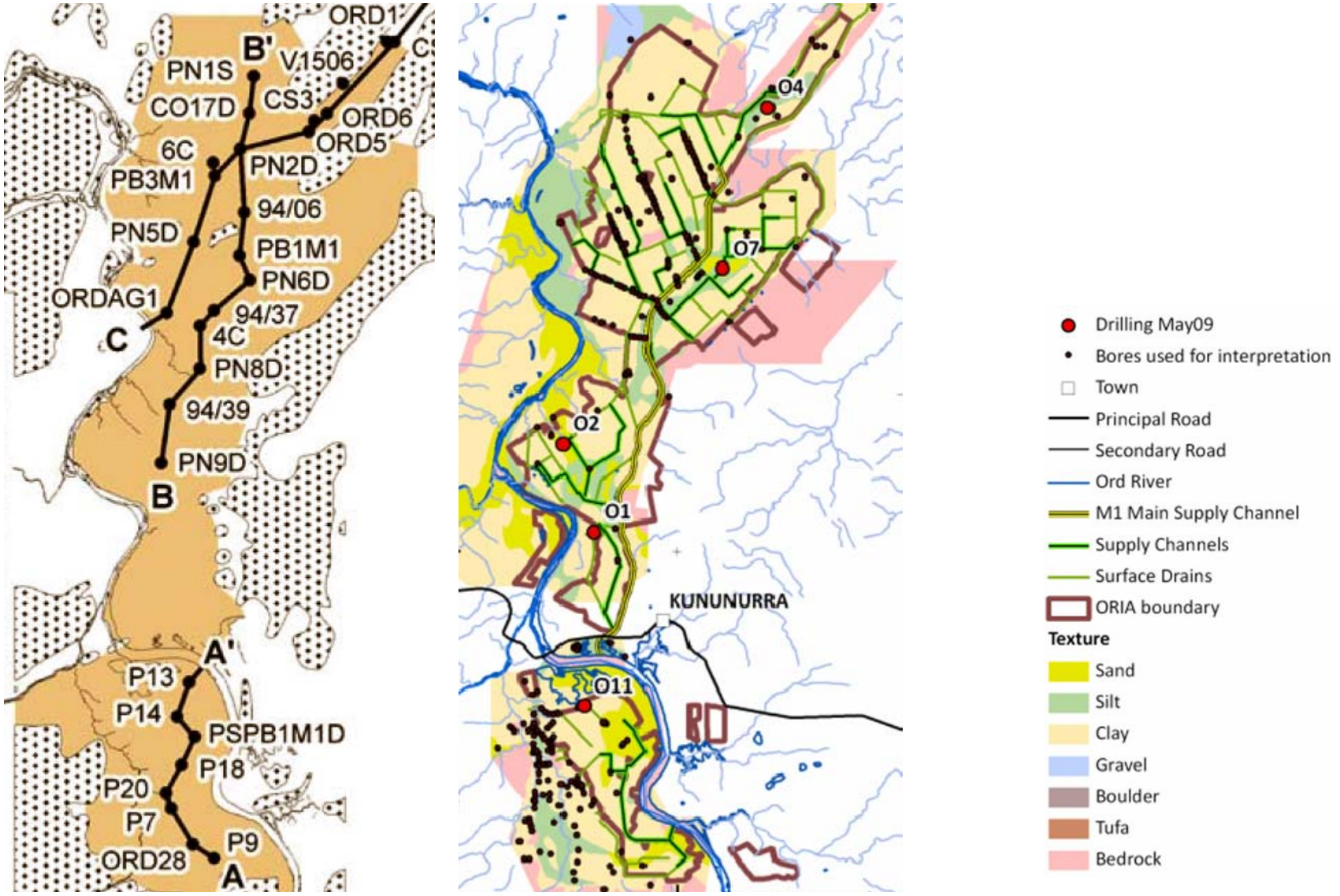

Figure 206: *Comparison between the extent of sands with maps from Smith, 2008 (centre) and this study (right). Depth section included here in from 4.2-6.7m.*

6.4 HYDROSTRATIGRAPHY OF THE WEABER PLAINS

The alluvium of the Weaber Plains is part of the Ord Succession, deposited by the Ord River, en route to the Keep River. The Ord Succession in this area comprises gravels, sands, silts and clays (O'Boy *et al.,* 2001). As in the case of the ORIA Stage 1 areas, the general features of the hydrostratigraphy recognised by O'Boy *et al*., (2001) are confirmed in this area. Four major facies, deposited in a fining-upwards sequence, are recognised in the drillcore: channel gravels and pebbly sands, channel-filling sands, channel margin sands and silts, floodplain silts and clays.

Three new bores were drilled in the ORIA Stage 2 areas of the Weaber Plain. One borehole (KS1) was drilled in the central Weaber Plain, while two further holes (KP1 and KP2) were drilled in the far east of the Weaber Plain, immediately north of the Knox Creek Plain. The latter two holes were targeted to intercept the Ord palaeochannel. The locations of these holes are shown in Figure 28. Detailed logs of boreholes KS1, KP1 and KP2 are presented in Figure 207 to Figure 209. The locations and depths of pre-existing holes used in this study for validation of the AEM dataset are shown in Figure 210. A soils map for the area is displayed in Figure 211.

Interpretation of the hydrostratigraphy from the AEM data

The 0-2m conductivity depth slice (Figure 212), and nine conductivity depth slice maps with corresponding maps of interpreted lithology for Weaber Plain are shown in Figure 213 to Figure 221. Cross-sections through the Weaber Plain are shown in Figure 222 to Figure 229. These are synthetic AEM sections (i.e. not sections along original flight lines), and follow the sections originally constructed by O'Boy *et al.,* (2001). For each cross-section, the figures show the original interpretation from O'Boy *et al*., (2001) in the top panel, the new synthetic AEM sections in the centre panel, and the new interpretation in the bottom panel.

Analysis of the conductivity depth slices and cross-sections reveals that the near- surface alluvium in the Weaber Plains is composed almost entirely of clay-rich sediments. The main except to this consists of sandy foot slope deposits at the base of the Sorby Hills. With increasing depth, a discontinuous stringer of silts and sands marks the position of the palaeochannel that emerged from the north-eastern end of Cave Springs Gap. The length of these stringers increases until at a depth of 6.7m they connect to form a single palaeochannel. This feature is interpreted to be the palaeochannel of the Ord River formed when it previously flowed out to the sea in what is now the Keep River estuary. This palaeochannel we consider to be the continuation of the merged Palaeochannel 1 and 2 which entered the southern end of Cave Springs Gap.

In the 6.7 to 9.5m conductivity depth slice, the palaeochannel of the Ord is clearly evident from the north-eastern end of Cave Springs Gap to the NT border. Once the palaeochannel clears Cave Springs Gap it trends east south of Folly Rock until it is deflected north by the Sorby Hills. From there it trends north to north east and bifurcates, one branch trending directly east while the other continues north-east until deflected east by the Weaber Range. The bifurcation is inherited from the palaeogeography of greater depths where the palaeochannel passes on either side of a buried hill. The palaeochannel is filled mostly by sand except at the end north and east of Sorby Hills where gravels are present at a depth of between 9.5 and 12.7m. Areas of sediment north of this palaeochannel may consist of older sand, gravel and silt sequences that are partially indurated

At a depth of 20.3m a marked architectural reorganisation occurs. The palaeovalley narrows abruptly and gravels replace sands along its entire length. Areas of sediment north of this palaeochannel are again likely to consist of older sand, gravel and silt sequences that are partially indurated. At depths of greater than 35.4m any palaeovalley sediments can no longer be distinguished. In the case of hole KS1, the abundance of sand suggests that the hole has penetrated very close to the channel but the absence of gravels means that it has no encountered the channel itself.

Also of note in the western Weaber Plain in particular, and around Sorby Hills, is the presence from shallow depths of extensive bedrock pediments. These show up as resistive features in the conductivity depth slices. In the western Weaber Plain these appear within a few metres (<5m) of the surface, forming a 'fringe' around the valley, particularly along the southern margin and in the north-west. In several places, these pediments extend over 2km from the valley edge at surface. These bedrock pediments, and some additional

bedrock ridges, significantly reduce the volume of alluvial aquifer storage in the western Weaber Plain, and constrict the location of the Ord palaeochannel. Constriction is particularly marked below 16m depths.

Comparisons with previous studies

For each of the cross-sections, a comparison between the original cross sections and the new interpretations, based on the AEM data, has been made. Similarly, comparisons with the original sand and gravel extent maps (O'Boy *et al*., 2001), are also made (Figure 230). Overall, the AEM data provide a greater clarity on the 3D thickness of the gravels, while there is also a significant difference in interpretation of gravel extent in the northern Weaber Plain. These comparisons are documented below.

Section J-J'

Due to the limited AEM coverage in this section, it is not possible to assess whether the amount of gravel is consistent with the original work of O'Boy *et al*. (2001). The degree of correlation in the position of the bedrock surface between the original section and the new data is also difficult to determine as the AEM data were collected over only a fraction of the original area considered in the O'Boy *et al*. (2001) report. However, the presence of thick alluvium and basal gravels is at least consistent with the original interpreted section (Figure 222). There is a resistive unit, interpreted as a palaeochannel ~400m wide across the section. This palaeochannel extends all the way from the basal gravels to the surface.

Section K-K'

A comparison of the sections generated in this study using a combination of AEM and borehole data, and the original sections interpreted from borehole data alone (O'Boy *et al.,* 2001) shows significant differences (Figure 223). The AEM and DEM data reveal a difference in the bedrock-alluvium interface at the western end of Weaber Plain, including the presence of several small bedrock rises that were not intersected by drilling and consequently not identified in the original interpretation. However, the presence of the main palaeochannel of the Ord in the south-western end of the section is confirmed. The AEM data also show a narrow (~400m wide) resistive unit extending to the surface that, by extrapolation from the data in section I-I', probably represents the final phase of deposits of channel sands by the Ord River before it ceased flowing out of Cave Springs Gap. Overall, the AEM data indicate that there is much less gravel than originally interpreted by O'Boy *et al.,* (2001).

Section L-L'

This section represents the stratigraphy on the north-western side of Weaber Plains. There is a reasonable correlation in the position of the bedrock surface between the original interpretation and the new AEM data (Figure 224). The AEM data also show the contrast between the highly resistive Ninbing group limestones and the more conductive shales of the Milligans Formation on the north-eastern end of the line.

The gravels in the deepest part of the palaeovalley at the south-western end do not show up as resistive units in the AEM data, however, bores in the area commonly contain water with salinities in the 1000-2500 mg/l range, and occasionally in the 10000-20000 range. These gravels are part of the older or more slowly deposited units of the Weaber Plains succession described earlier.

Section M-M'

The correlation in the position of the bedrock surface between the original interpreted section and the AEM data appears reasonable (Figure 225). The main differences are that the palaeochannels appear more flat floored than originally shown. As in the previous section, the palaeochannel of the Ord can be seen as a 200-400m wide resistive unit extending from the basal gravels to near the surface. The gravels in the northern area appear to be relatively conductive and are once again interpreted as being the moderately indurated iron oxide rich and relatively saline sediments of the Weaber Plains succession. The most conductive materials in the AEM data correlate reasonably well with clays in drilling. The carbonate unit in the valley filling sediments in the original section probably represents tufa deposited from springs in the underlying limestone. Compared with the original cross-section, the AEM indicates that there is less gravel overall.

Section N-N'

Generally, there is excellent correlation in the position of the bedrock surface between the original interpreted section and the AEM data (Figure 226). The main differences is the presence of a resistive zone up to 1km wide in the AEM that may present the Ord palaeochannel that is not evident in the drilling of the

original section. Its presence is confirmed however by the log of WINSITE 20083080 which shows a thick sand and gravel section. This width is apparent rather than real because of the section cutting the palaeochannel at an oblique angle. The gravels in the northern part are relatively conductive and are once again interpreted as being the moderately indurated iron oxide rich and relatively saline sediments of the Weaber Plains succession. As before, there is no clear conductive response for the tufa units. While the amount of gravel in the northern section is similar to that in the original interpretation, there is less in the basal part of the section in the southern palaeovalley. However resistive (and inferred thus coarse-grained units) units extend almost to the surface along the narrow palaeochannel. An excessively thick section of sandy material was recovered from WINSITE bore 20083060. This is far deeper than is common in most over boreholes in the area and may represent the infill of a doline (collapsed cave) in the limestone bedrock.

Section O-O'

A reasonable correlation exists between the original interpreted section and the AEM data in the position of the bedrock surface (Figure 227). The main difference is once again the presence of a resistive zone up to 1km wide in the AEM that represents the Ord palaeochannel. The presence of this is confirmed by the existence of shallow sandy and gravely sediments in WINSITE bore 20083079. It is not clear why this was not detected in the drilling used in the compilation of the original section. Apart from this palaeochannel, however, the amount of gravel associated with the section appears much less than original interpreted. As with other sections in Weaber Plains (L-L', M-M', and N-N'), the gravels in the northern area are relatively conductive probably have been moderately indurated iron oxide rich and are relatively saline sediments of the Weaber Plains succession. Comparison with the original interpreted section shows the presence of some very thick alluvial sections in some of the bores. No evidence for this was found, but given the limestone substrate, it is possible that these may have filled dolines in the underlying bedrock.

Section P-P'

The amount of gravel aquifer in this section is much less, and confined largely to the position of the Ord Palaeochannel, although there is good correspondence between the AEM data and original interpretation of the bedrock interface (Figure 228). The Ord palaeochannel appears to have shifted during deposition from the deepest parts of the southern valley to a more central position once the ridge dividing the two palaeovalleys had been filled in. The apparently great width of the palaeochannel in this section (>1km) is due to it being cut obliquely by the section. The gravels in the northern part are once more relatively conductive.

Section Q-Q'

Although only the south-western portion of the original interpreted section is covered by AEM data, the section which exists shows a reasonable correspondence with respect to the position of the bedrock surface (Figure 229). There is no evidence for the resistive gravels represent the Ord palaeochannel, and we infer from this that the palaeochannel is probably located on the northern limits of the AEM survey. The gravels that do exist are conductive. The amount appears similar to that originally interpreted.

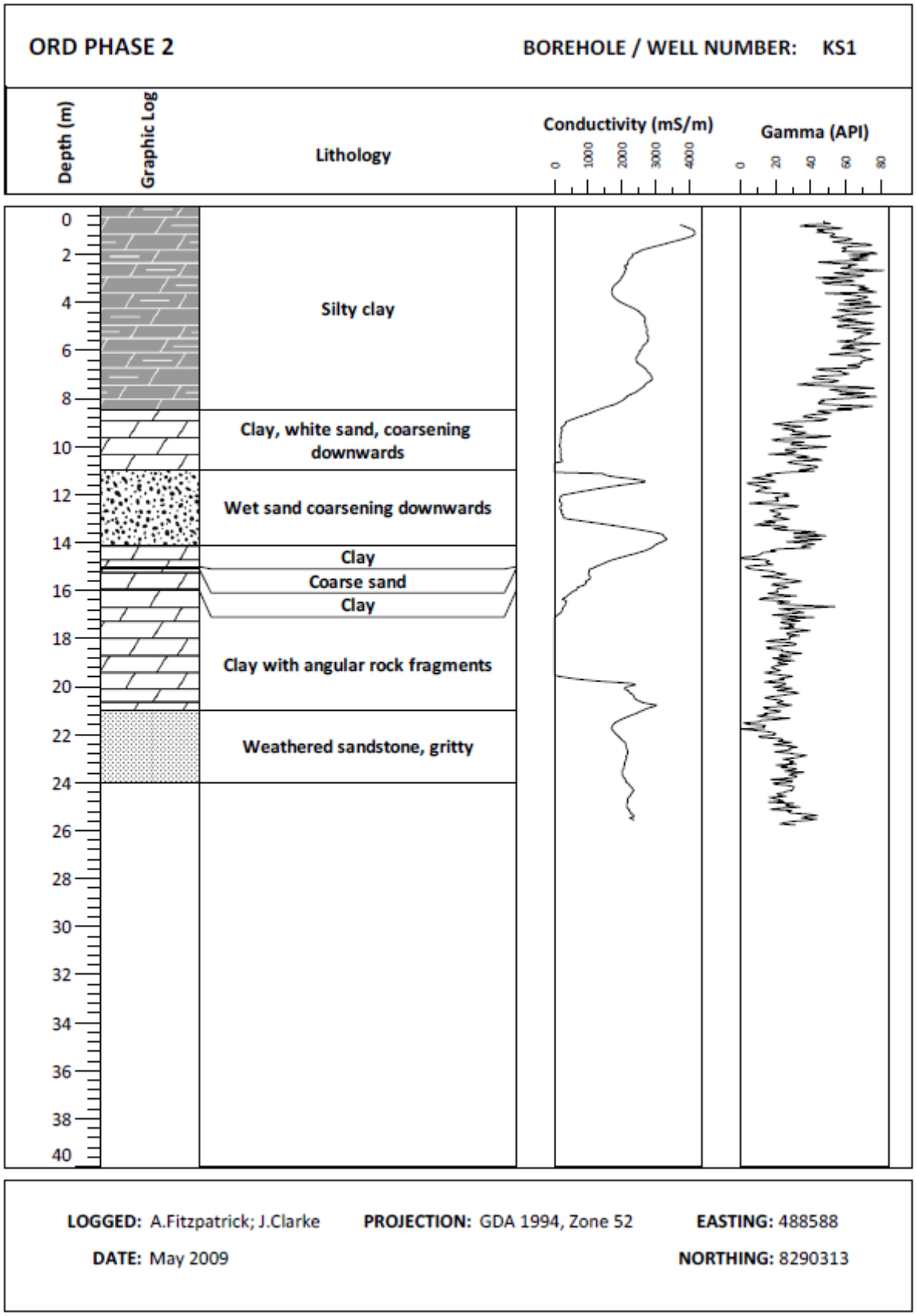

Figure 207: *Ord Phase 2 borehole number KS1.*

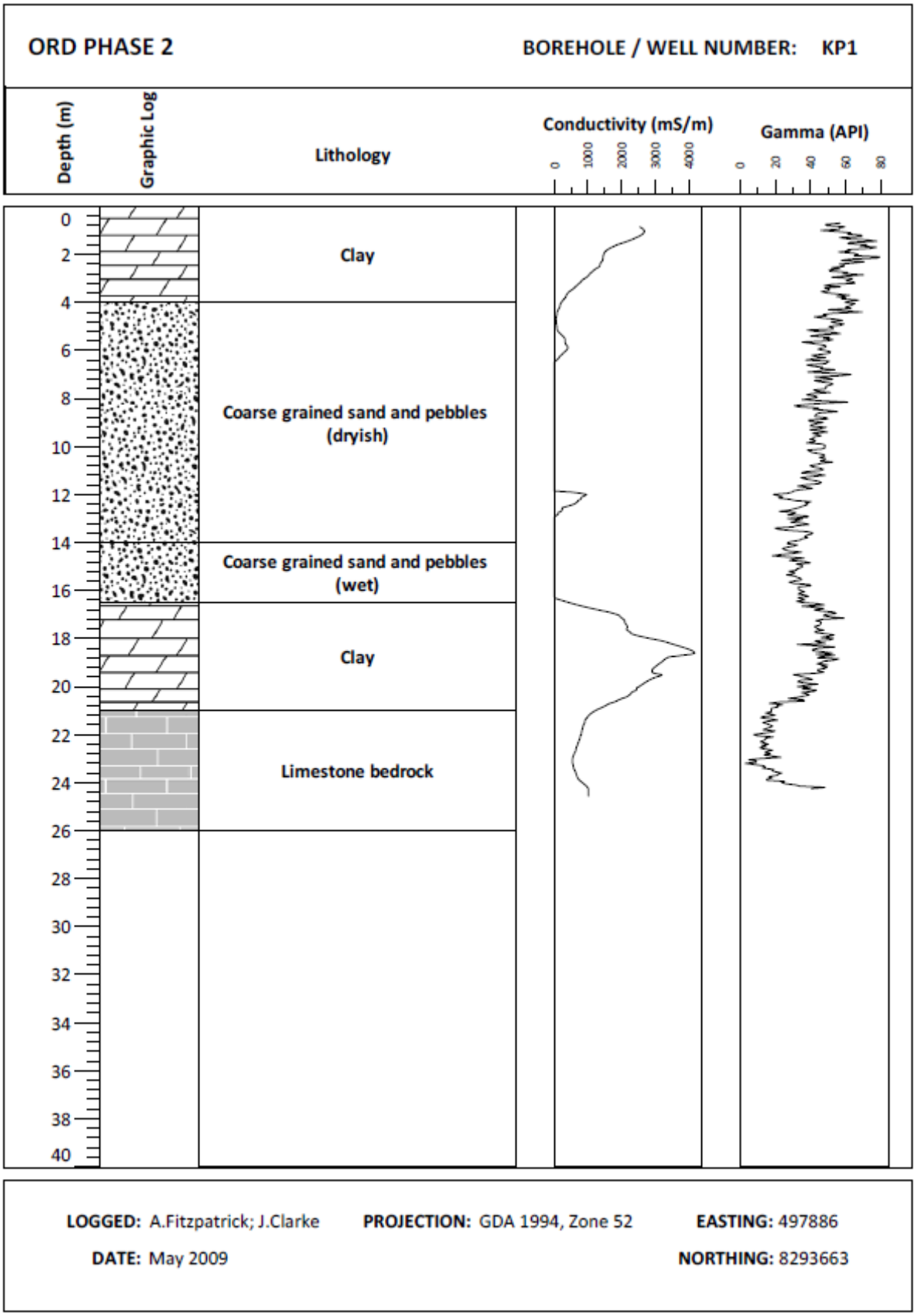

Figure 208: *Ord Phase 2 borehole number KP1.*

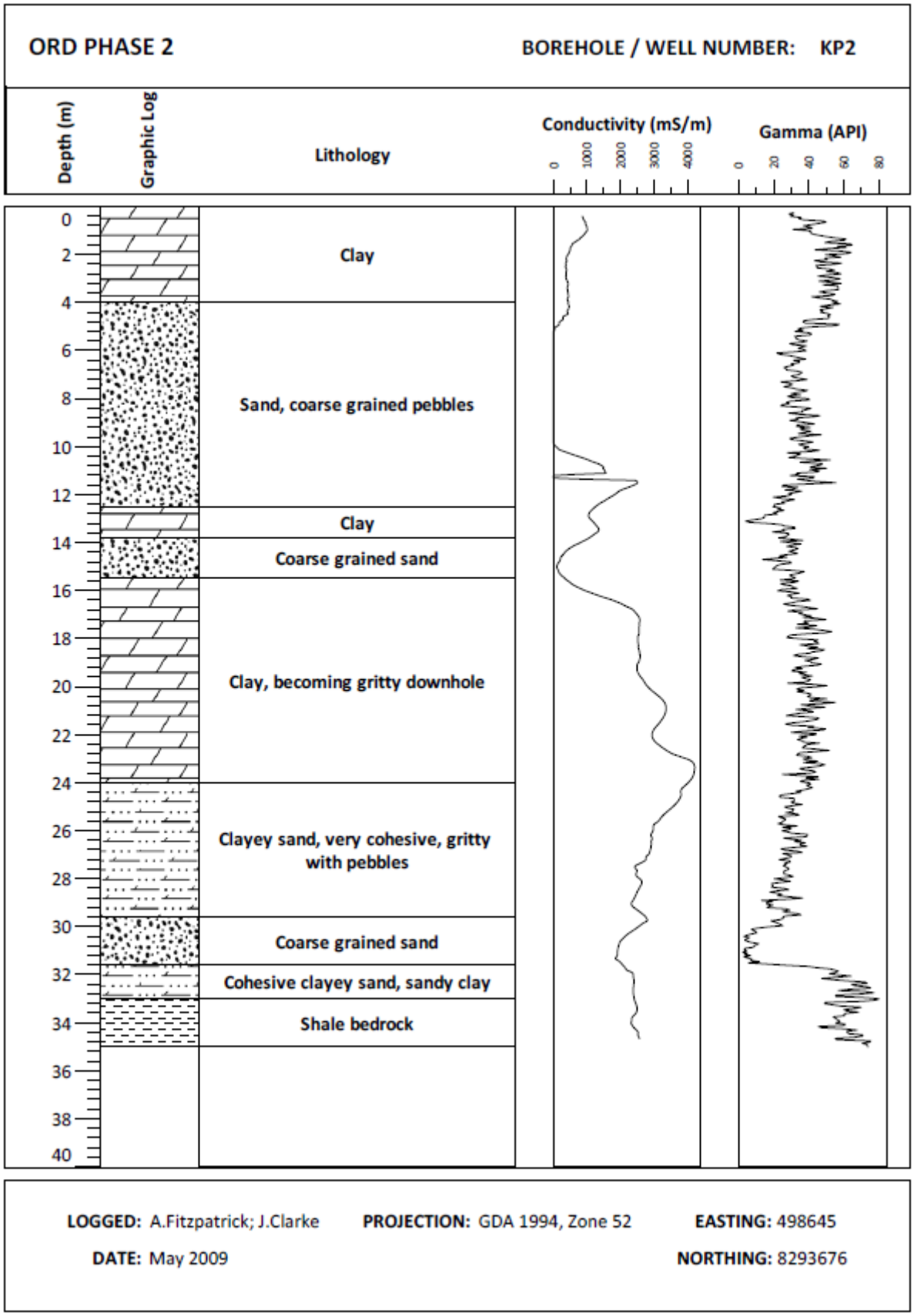

Figure 209: *Ord Phase 2 borehole number KP2.*

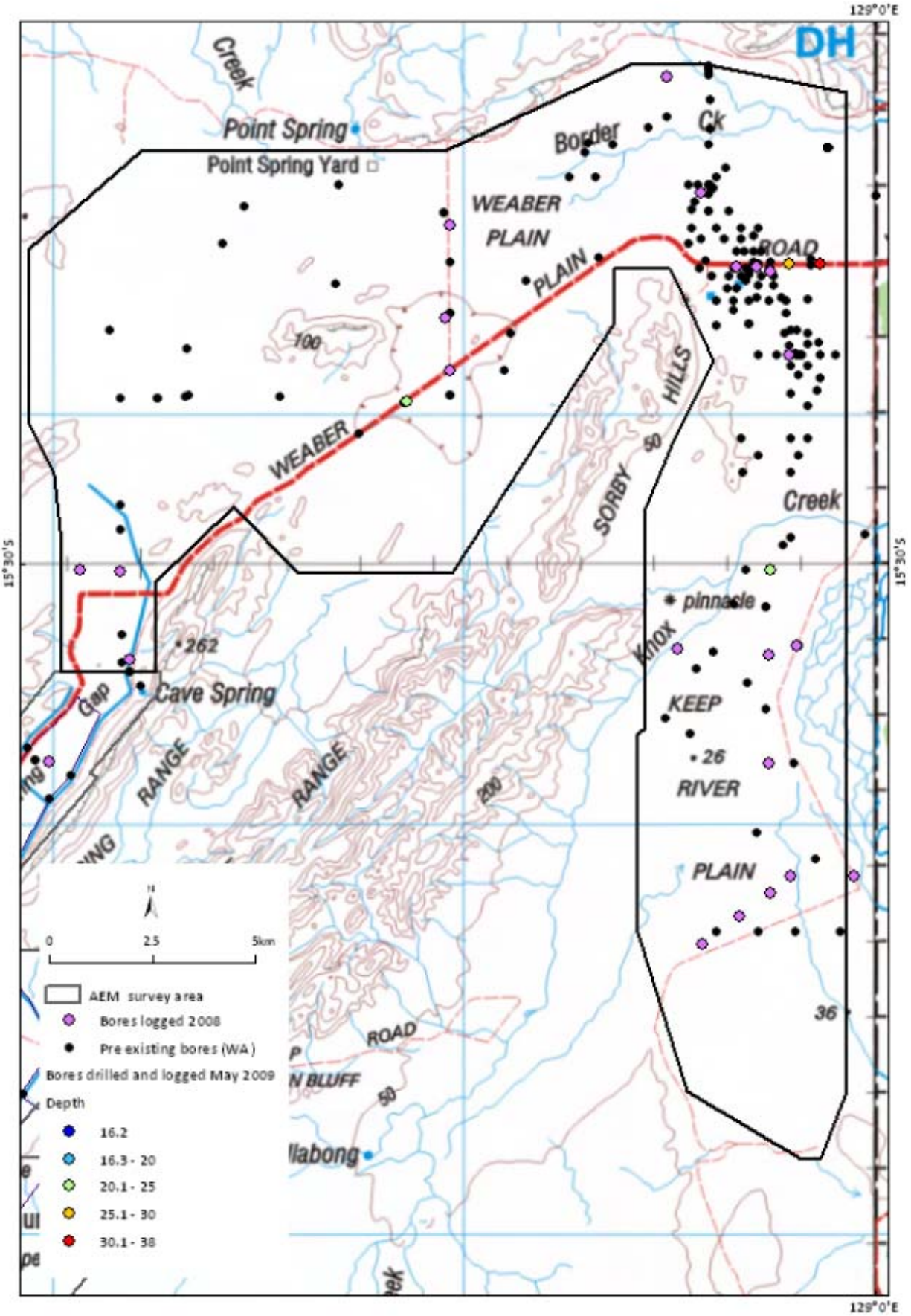

Figure 210: *Borehole locations for Weaber Plain, Knox Plain and Keep River Plain.*

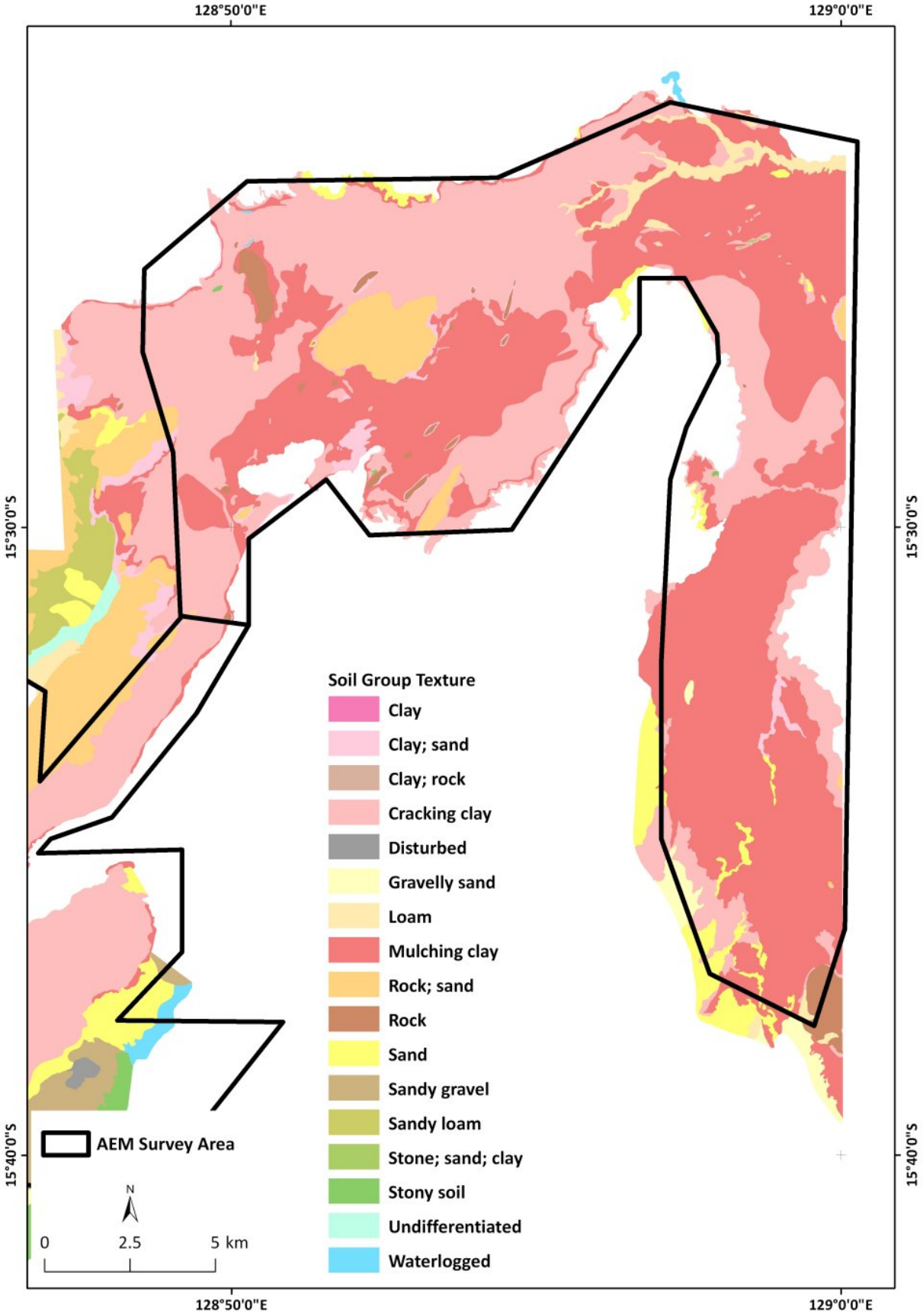

Figure 211: *Soils map of the Weaber Plain (and the Knox Creek-Keep River Plains). Digital data supplied by Schoknecht (2009) and compiled from various sources (e.g. Dixon, 1996).*

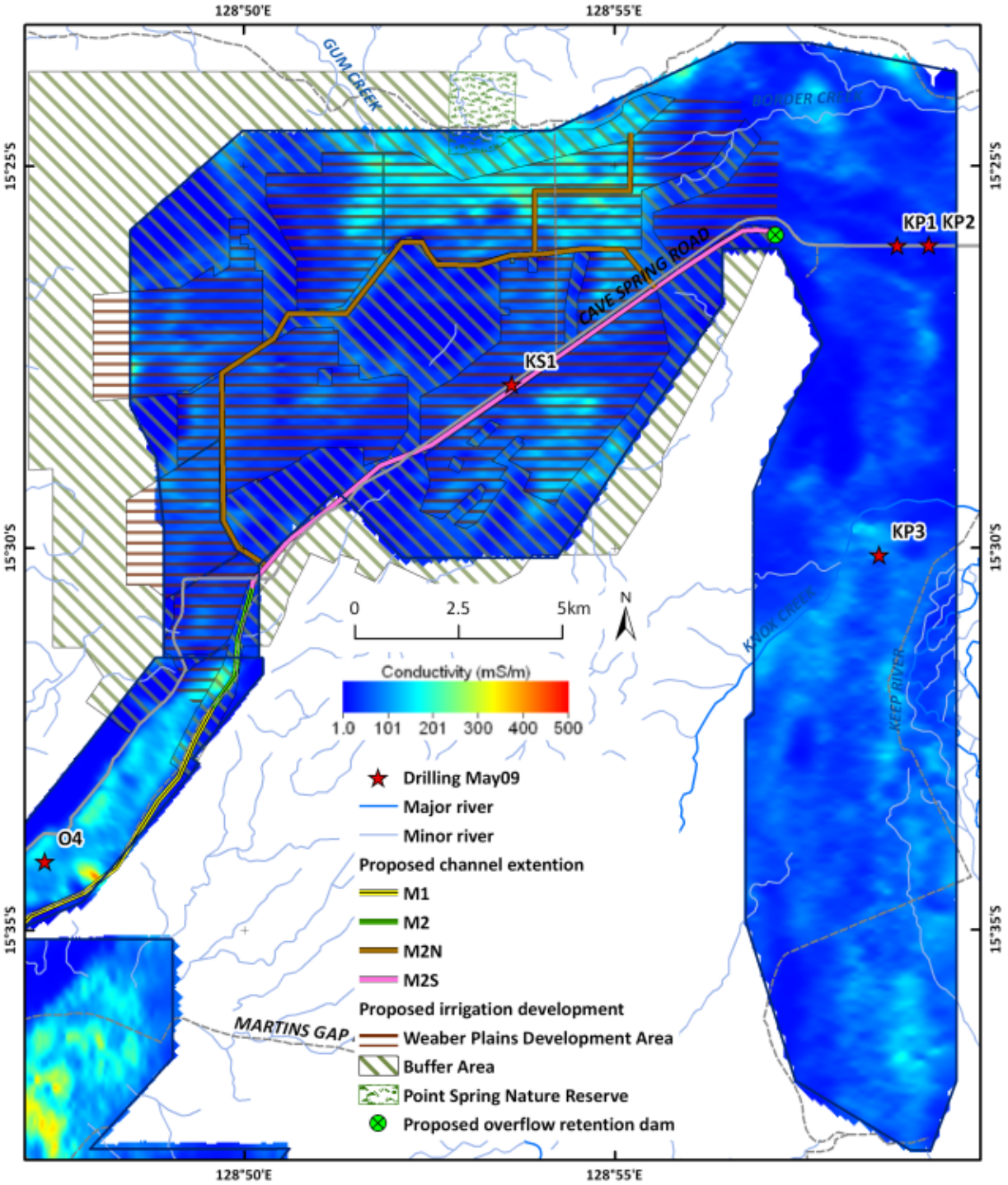

Figure 212: *0-2m conductivity depth slice for the Weaber, Knox Creek and Keep River Plains.*

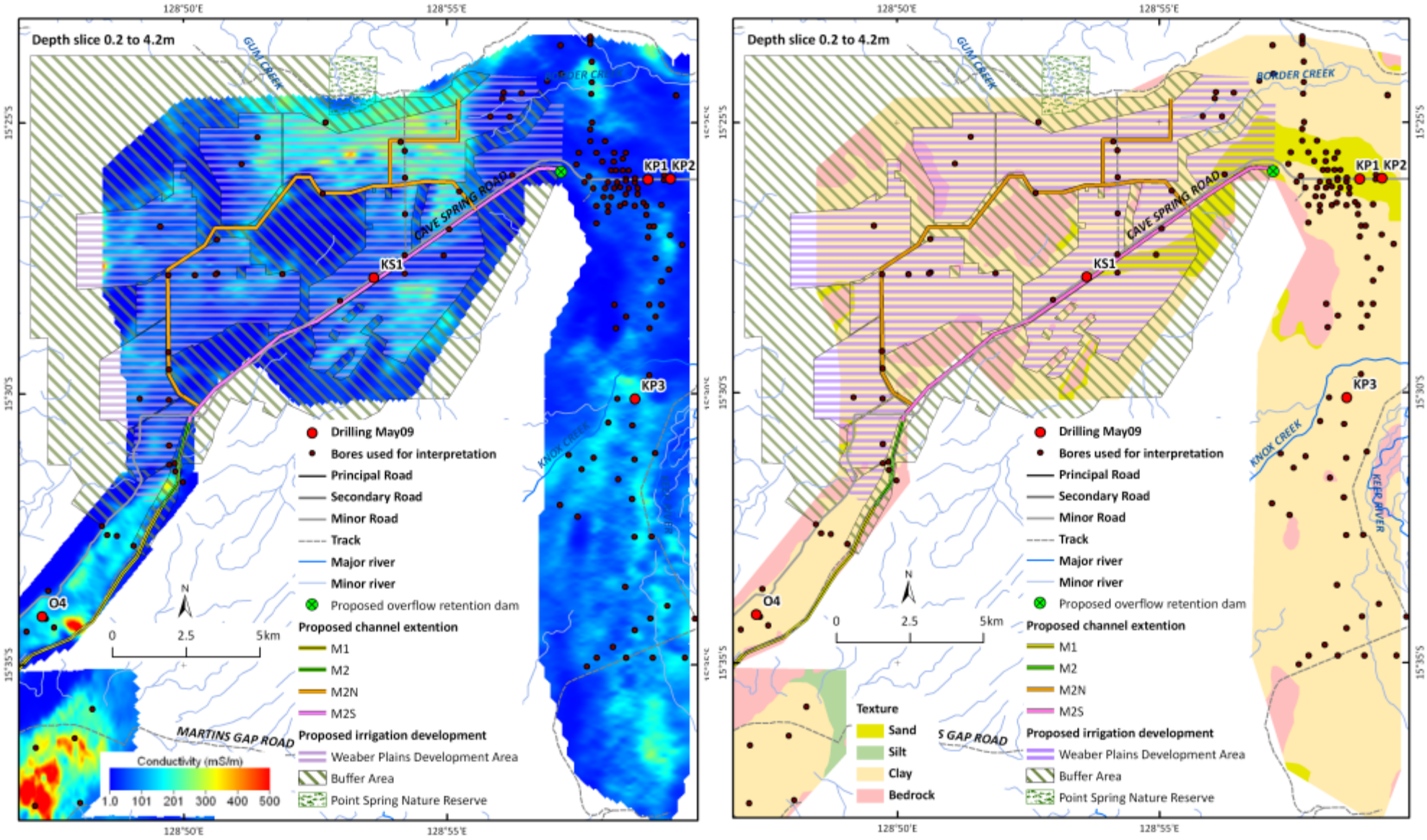

Figure 213: *Weaber, Knox Creek and Keep River Plains. Left: conductivity depth slice 2 – 4.2m.* ***Right:*** *interpreted lithology.*

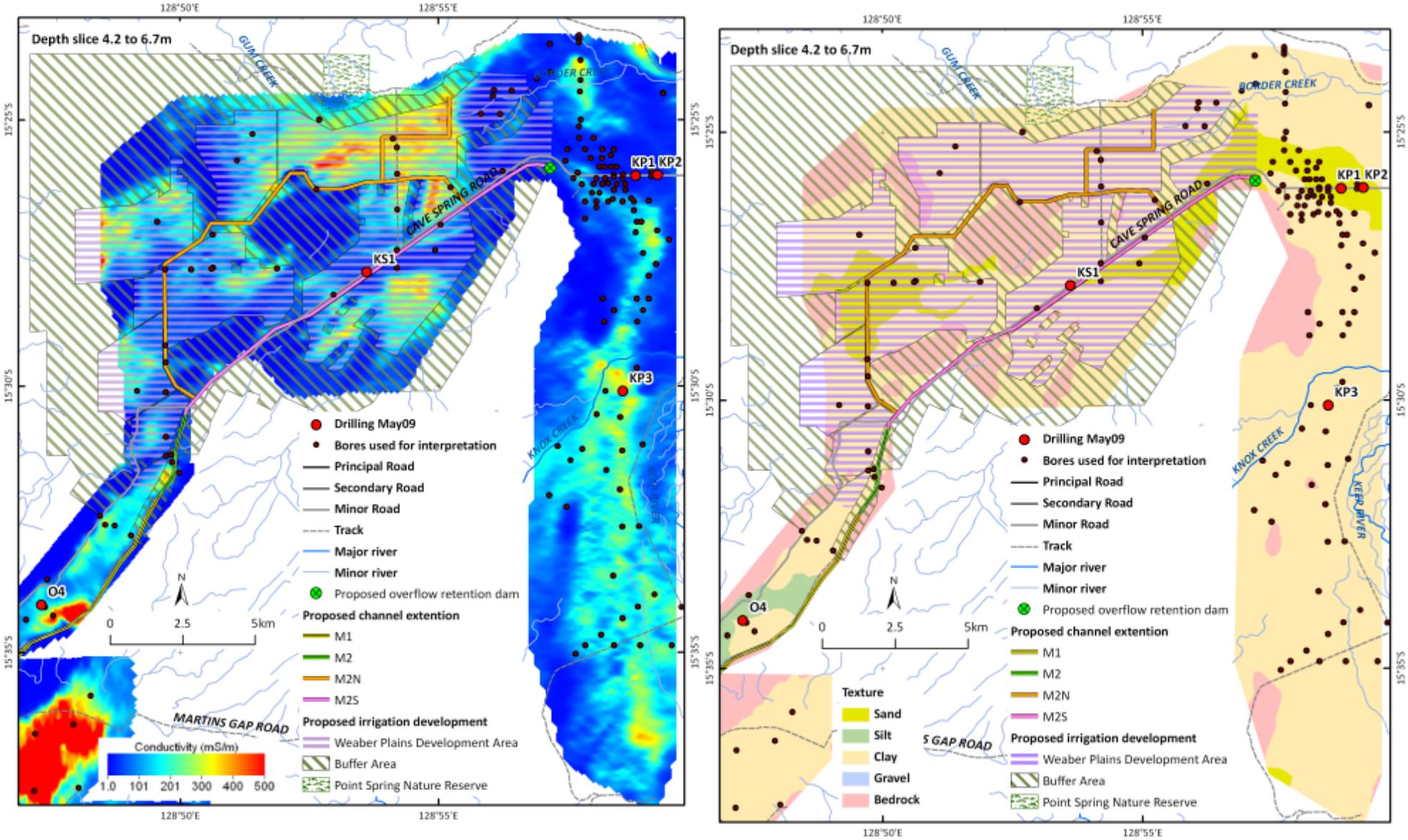

Figure 214: *Weaber, Knox Creek and Keep River Plains. Left: conductivity depth slice 4.2 – 6.7m.* ***Right:*** *interpreted lithology.*

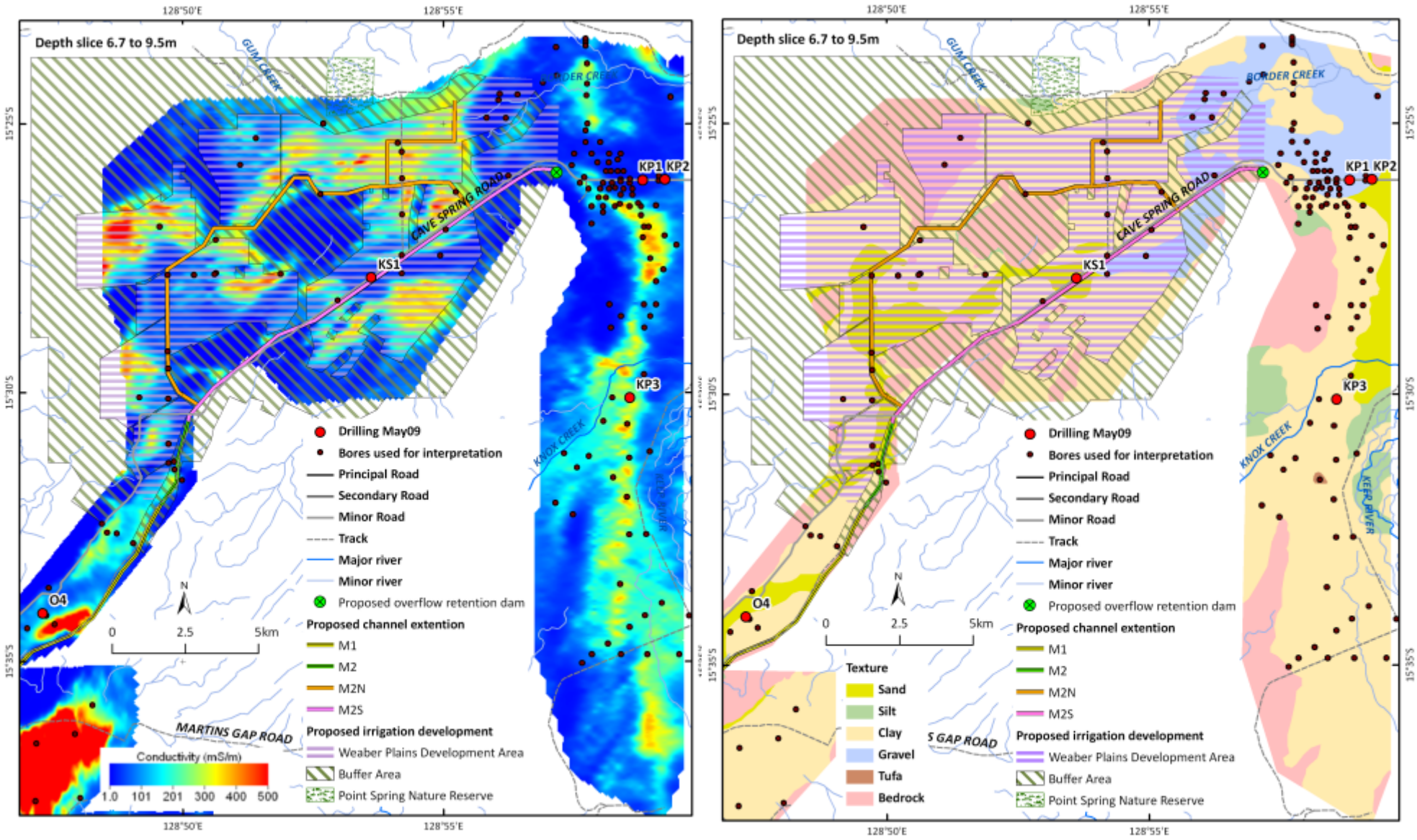

Figure 215: *Weaber, Knox Creek and Keep River Plains. Left: conductivity depth slice 6.7 – 9.5m. Right: interpreted lithology.*

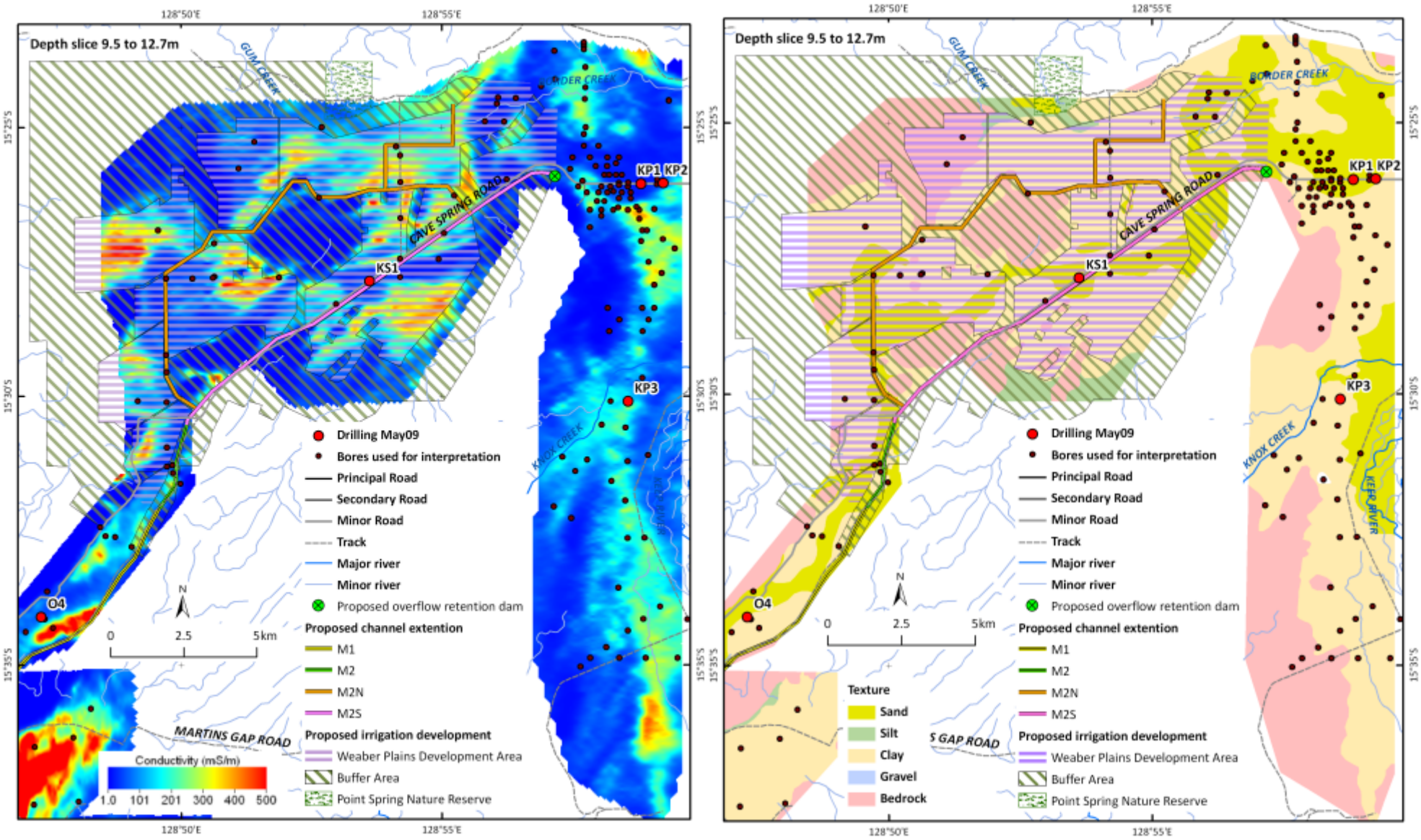

Figure 216: *Weaber, Knox Creek and Keep River Plains. Left: conductivity depth slice 9.5 – 12.7m. Right: interpreted lithology.*

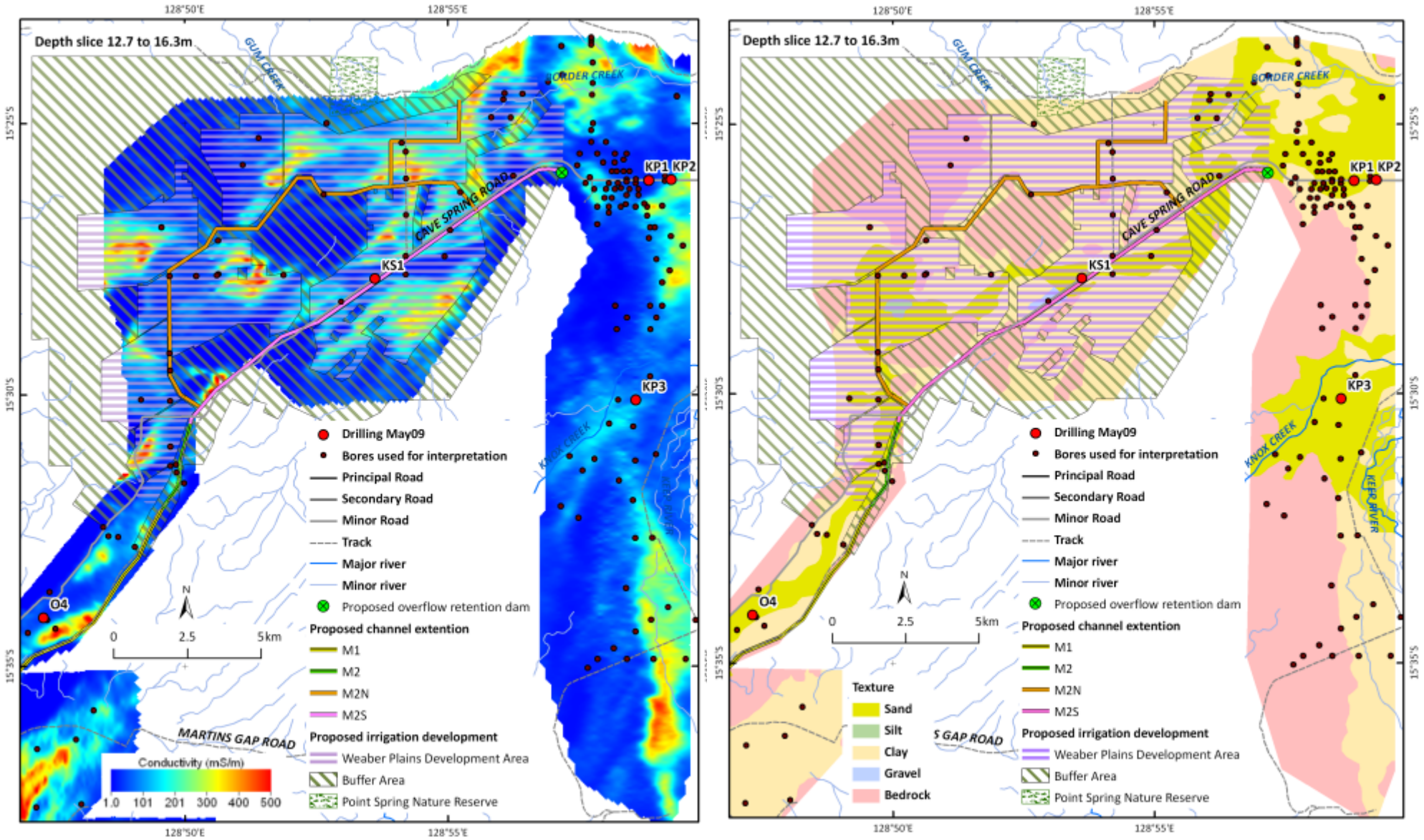

***Figure 217**: Weaber, Knox Creek and Keep River Plains. Left: conductivity depth slice 12.7– 16.3m. Right: interpreted lithology.*

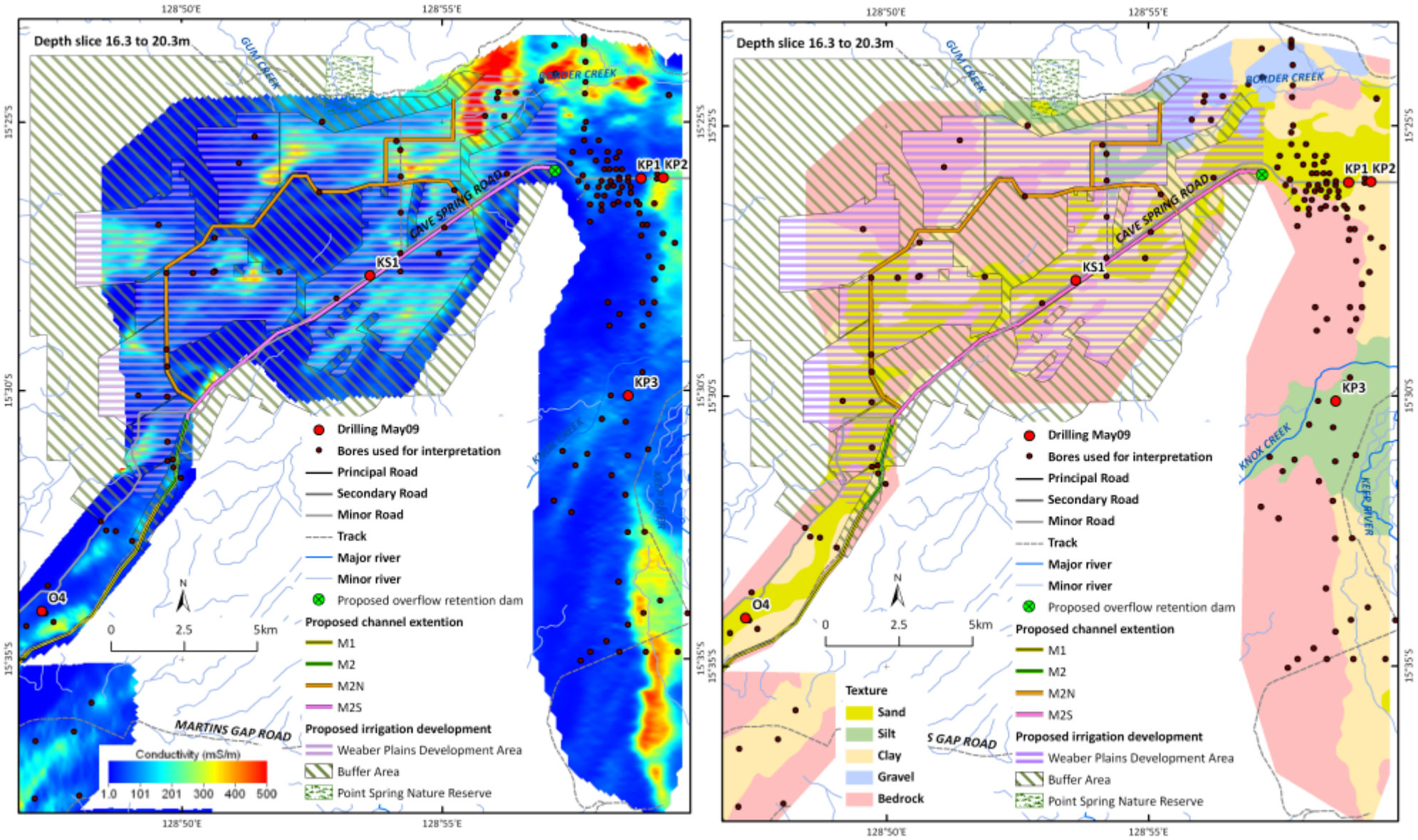

Figure 218: *Weaber, Knox Creek and Keep River Plains. Left: conductivity depth slice 16.3 – 20.3m. Right: interpreted lithology.*

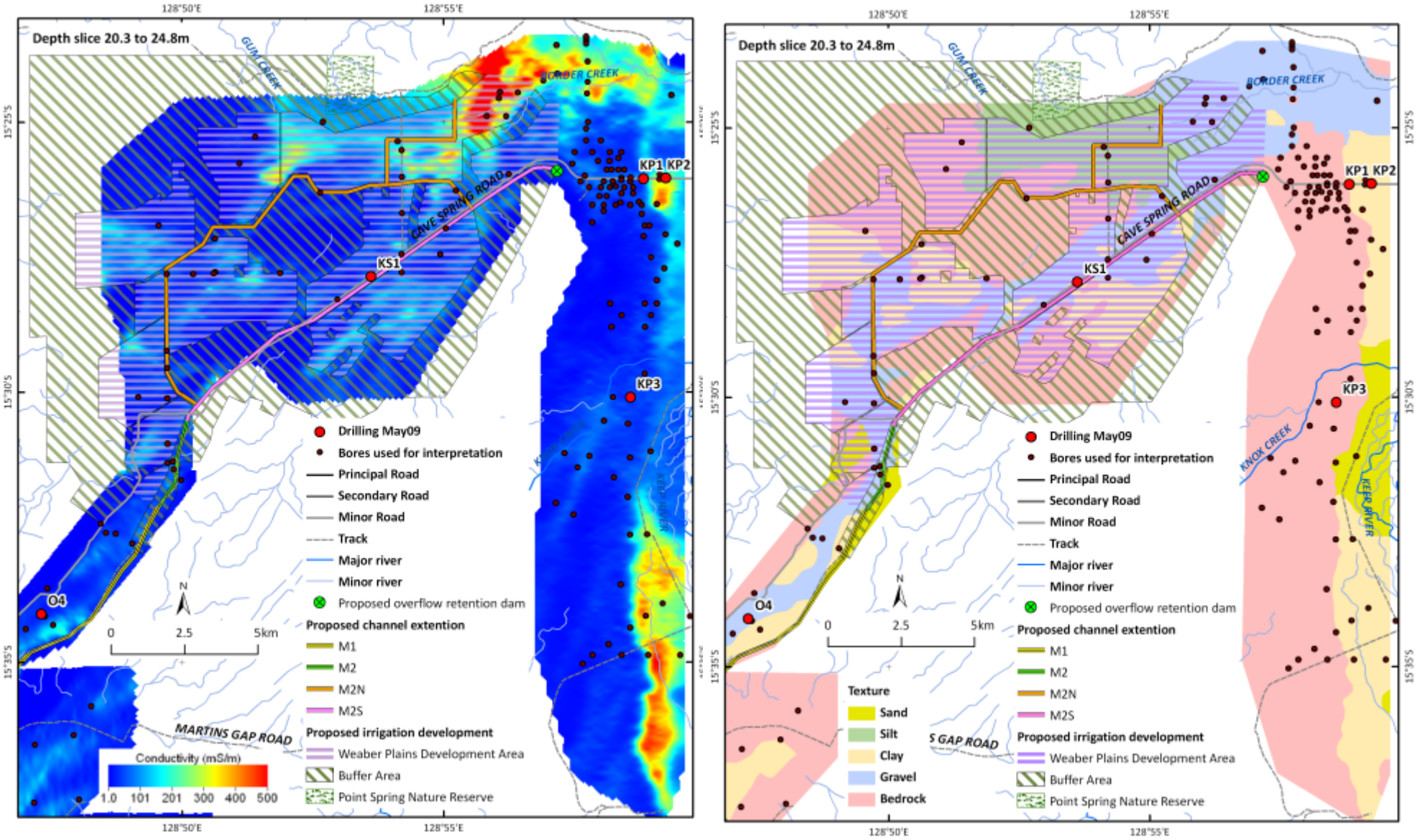

Figure 219: *Weaber, Knox Creek and Keep River Plains. Left: conductivity depth slice 20.3 – 24.8m. Right: interpreted lithology.*

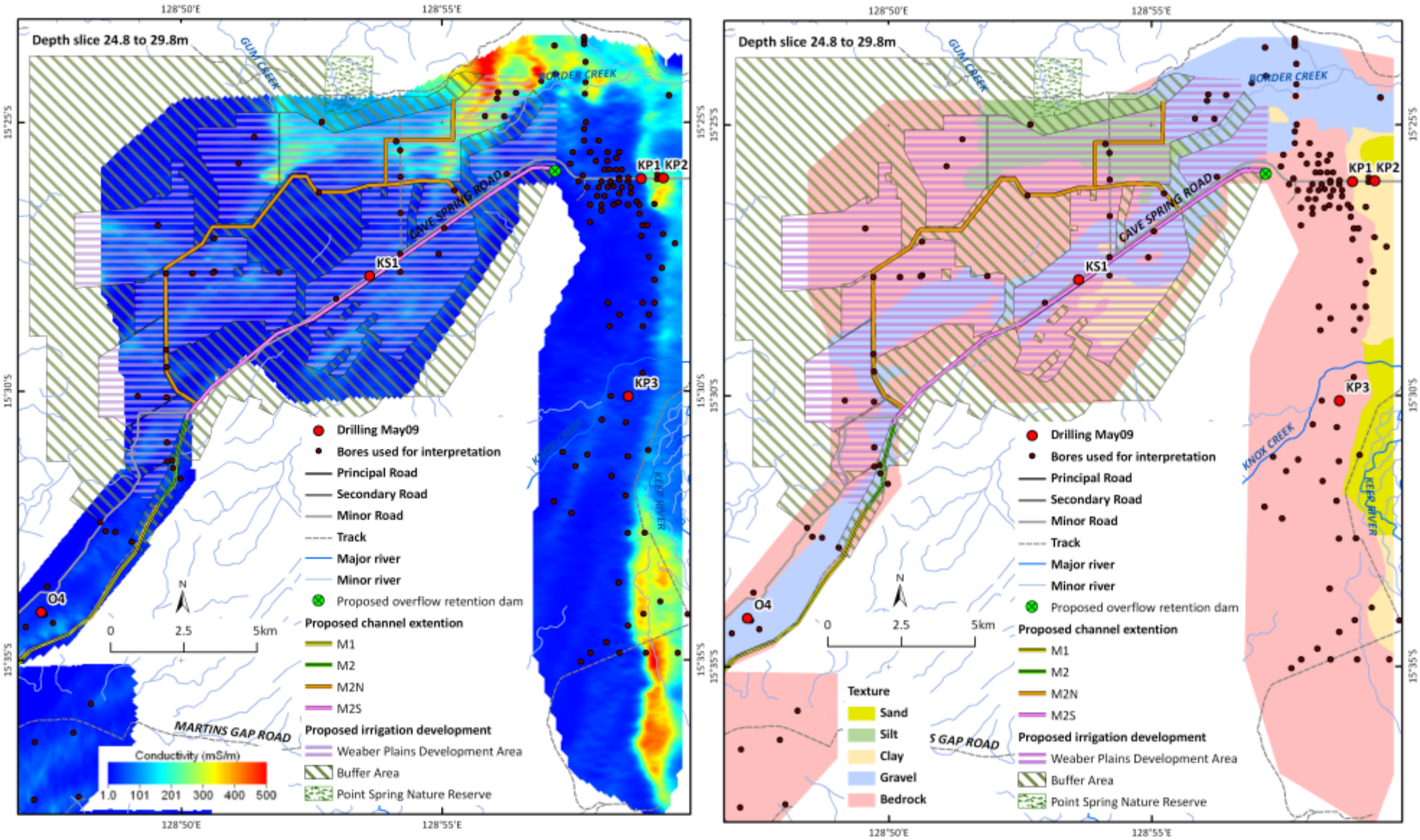

Figure 220: *Weaber, Knox Creek and Keep River Plains. Left: conductivity depth slice 24.8 – 29.8m. Right: interpreted lithology.*

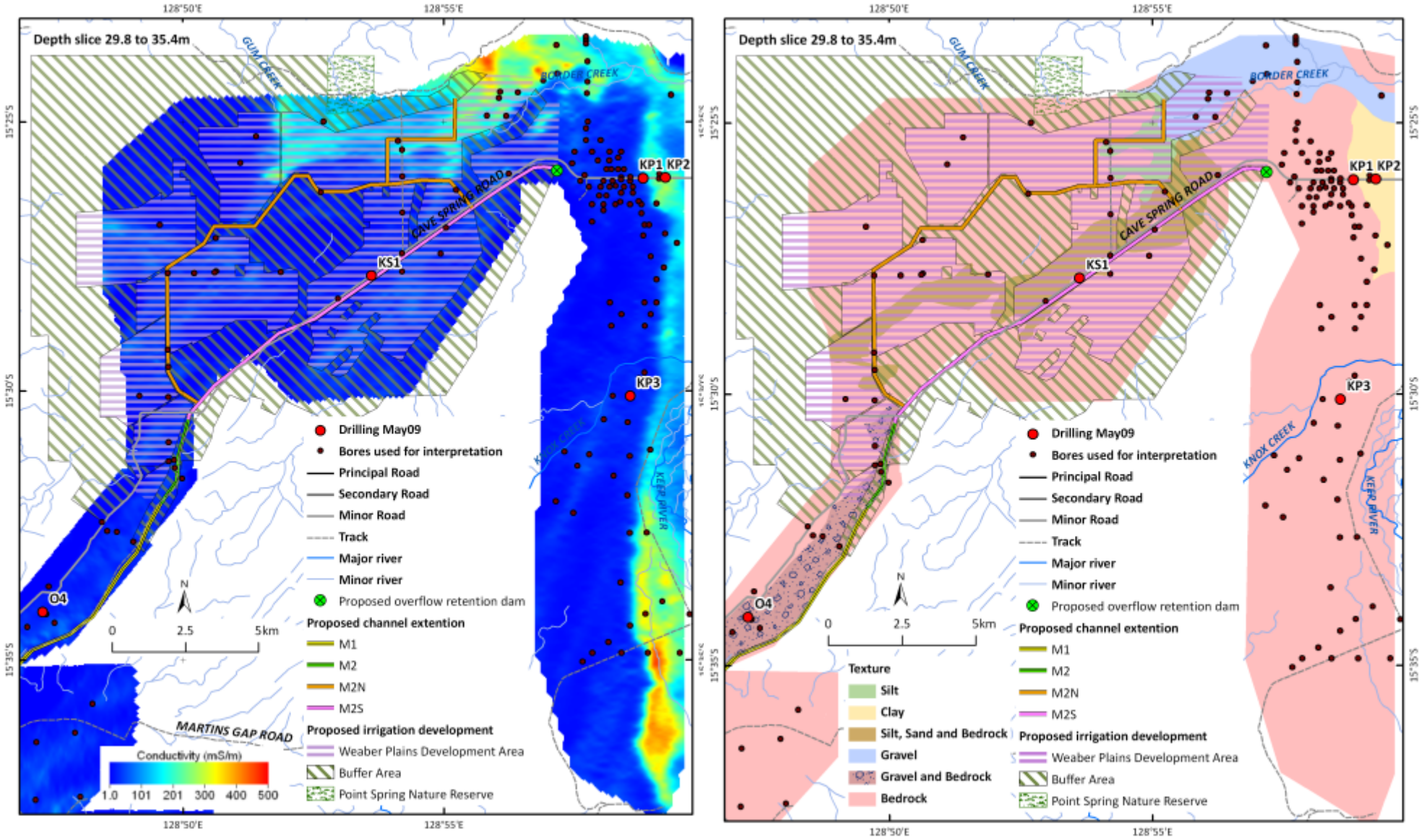

Figure 221: *Weaber, Knox Creek and Keep River Plains. Left: conductivity depth slice 29.8 – 35.4m. Right: interpreted lithology.*

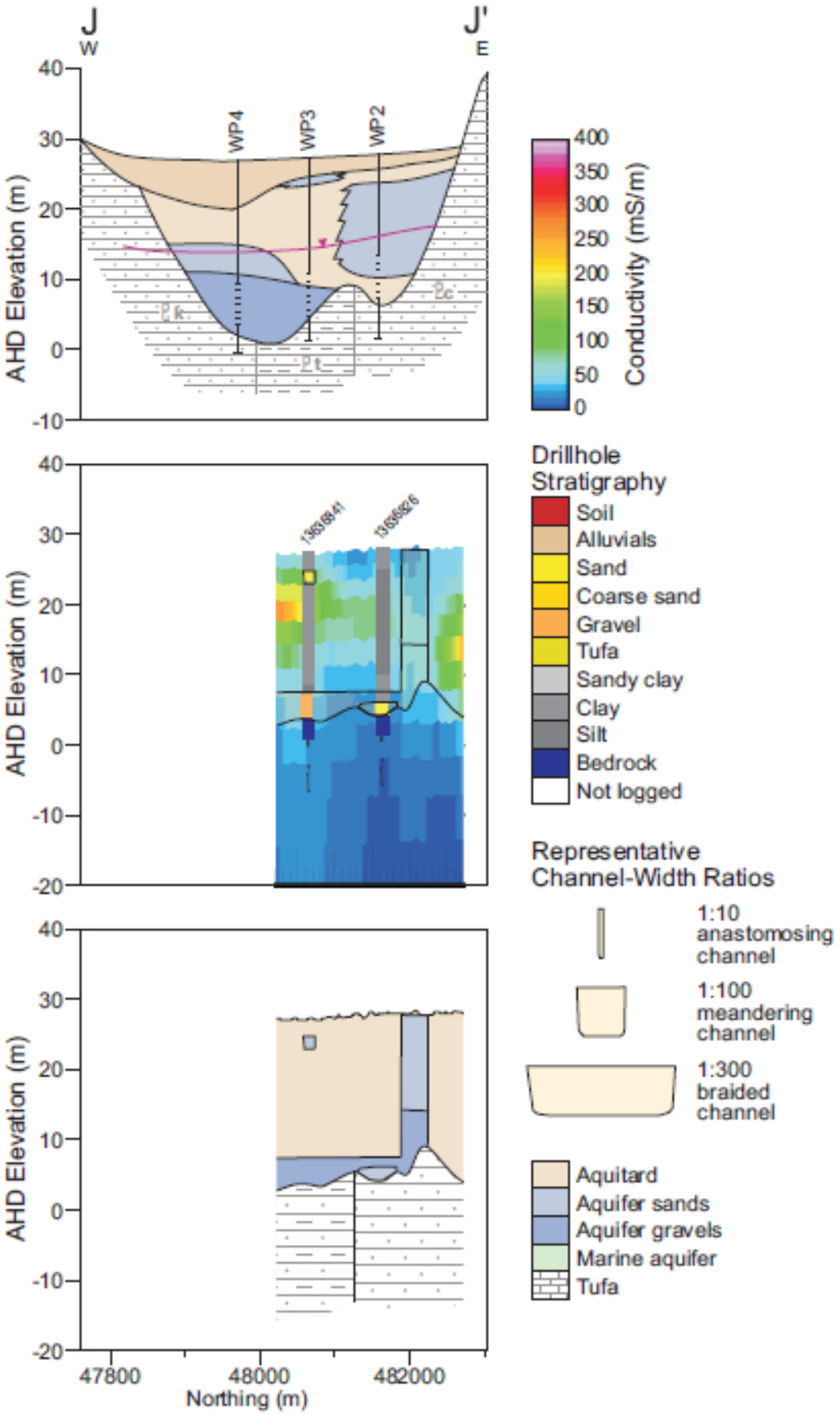

Figure 222: *Northern Cave Springs Gap- Weaber Plain cross-section J-J'. Top panel is cross-section from O'Boy et al., (2001); middle panel is synthetic AEM section showing drillholes colour coded for lithology and with lithology extent interpretation line work displayed; bottom panel is revised lithology interpretation produced in this study.*

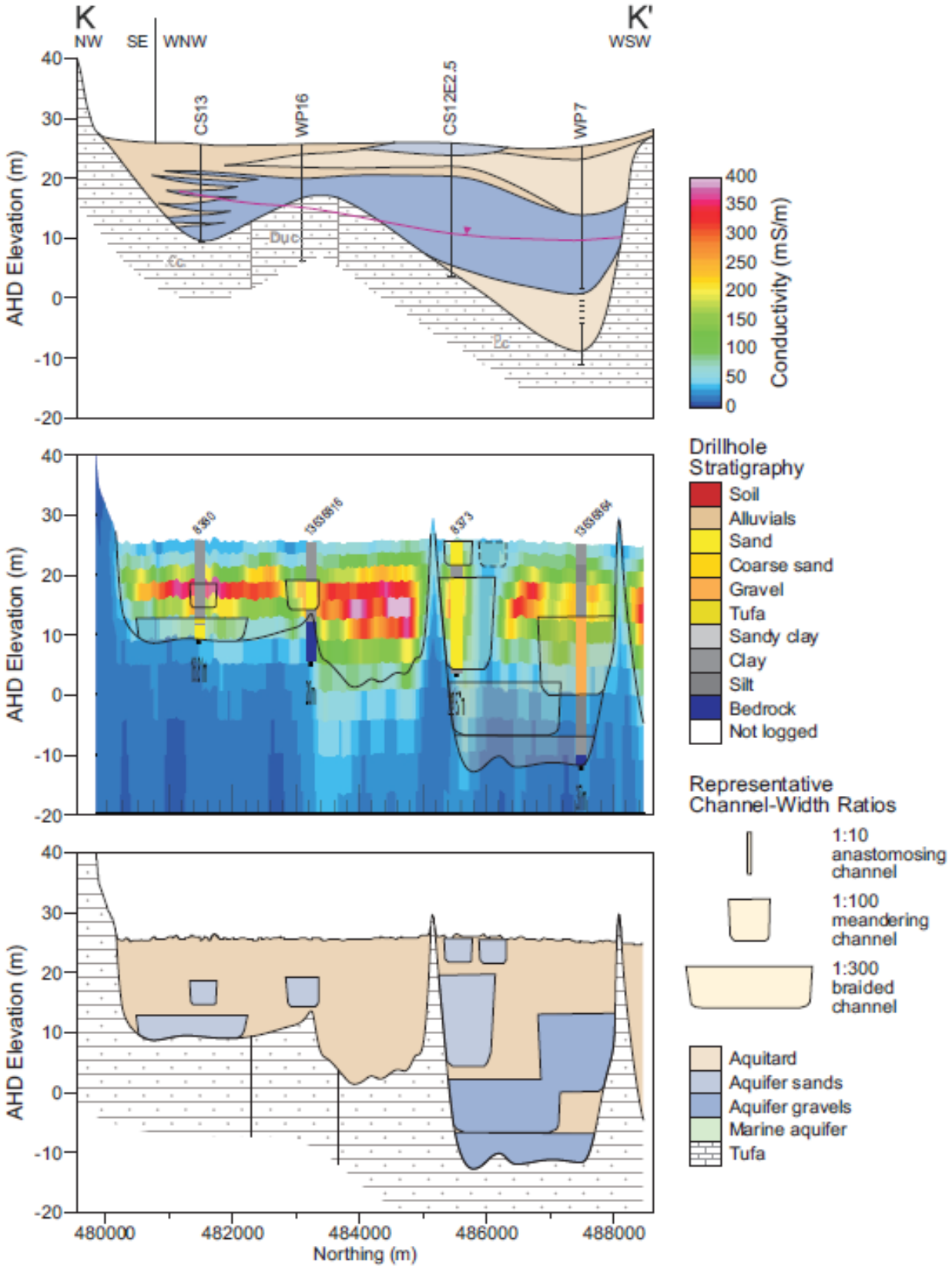

Figure 223: *Western Weaber Plain cross-section K-K'. Top panel is cross-section from O'Boy et al., (2001); middle panel is synthetic AEM section showing drillholes colour coded for lithology and with lithology extent interpretation line work displayed; bottom panel is revised lithology interpretation produced in this study.*

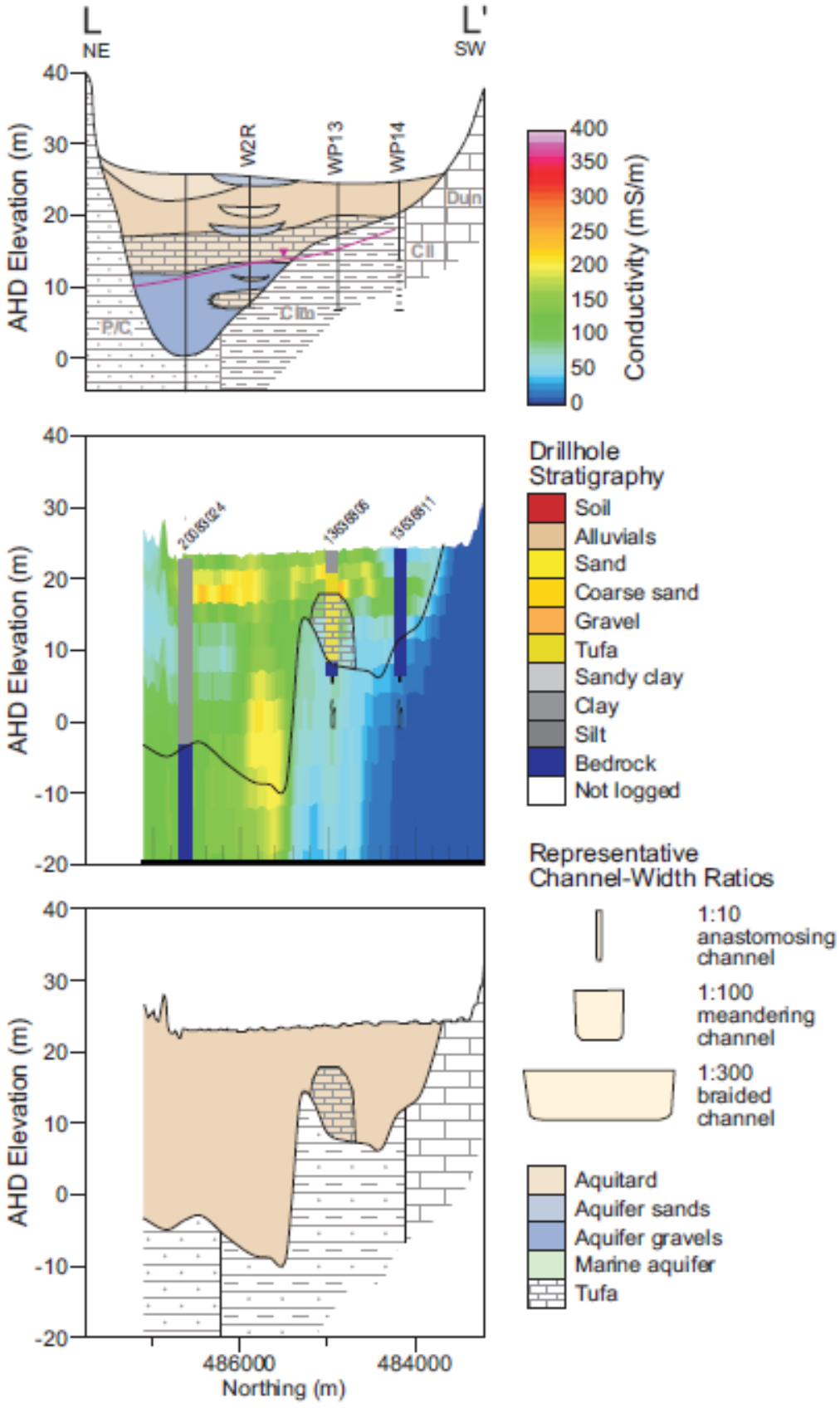

Figure 224: *Northern Weaber Plain cross-section L-L'. Top panel is cross-section from O'Boy et al., (2001); middle panel is synthetic AEM section showing drillholes colour coded for lithology and with lithology extent interpretation line work displayed; bottom panel is revised lithology interpretation produced in this study.*

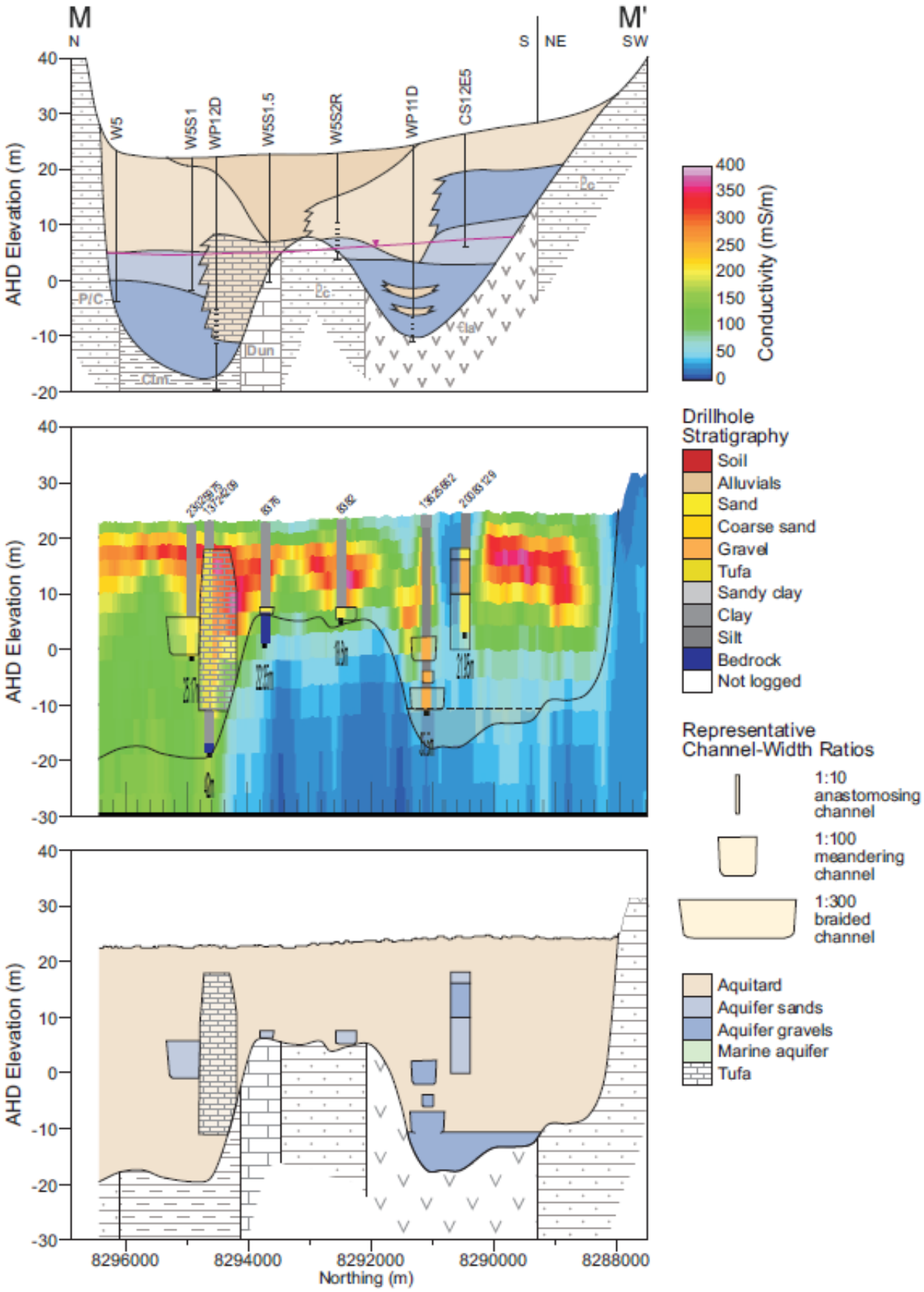

Figure 225: *Central Weaber Plain cross-section M-M'. Top panel is cross-section from O'Boy et al., (2001); middle panel is synthetic AEM section showing drillholes colour coded for lithology and with lithology extent interpretation line work displayed; bottom panel is revised lithology interpretation produced in this study.*

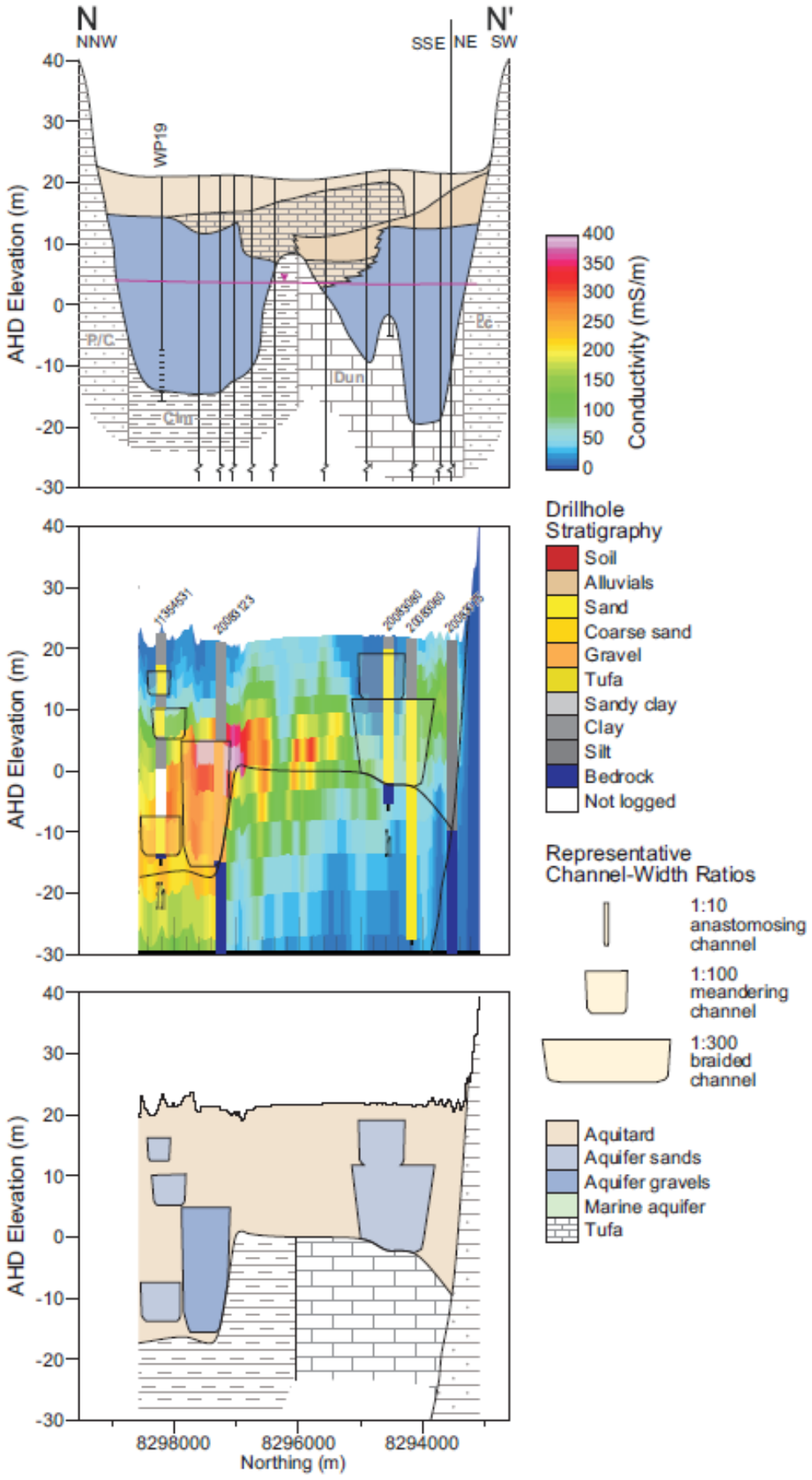

Figure 226: *Eastern Weaber Plain cross-section N-N'. Top panel is cross-section from O'Boy et al., (2001); middle panel is synthetic AEM section showing drillholes colour coded for lithology and with lithology extent interpretation line work displayed; bottom panel is revised lithology interpretation produced in this study.*

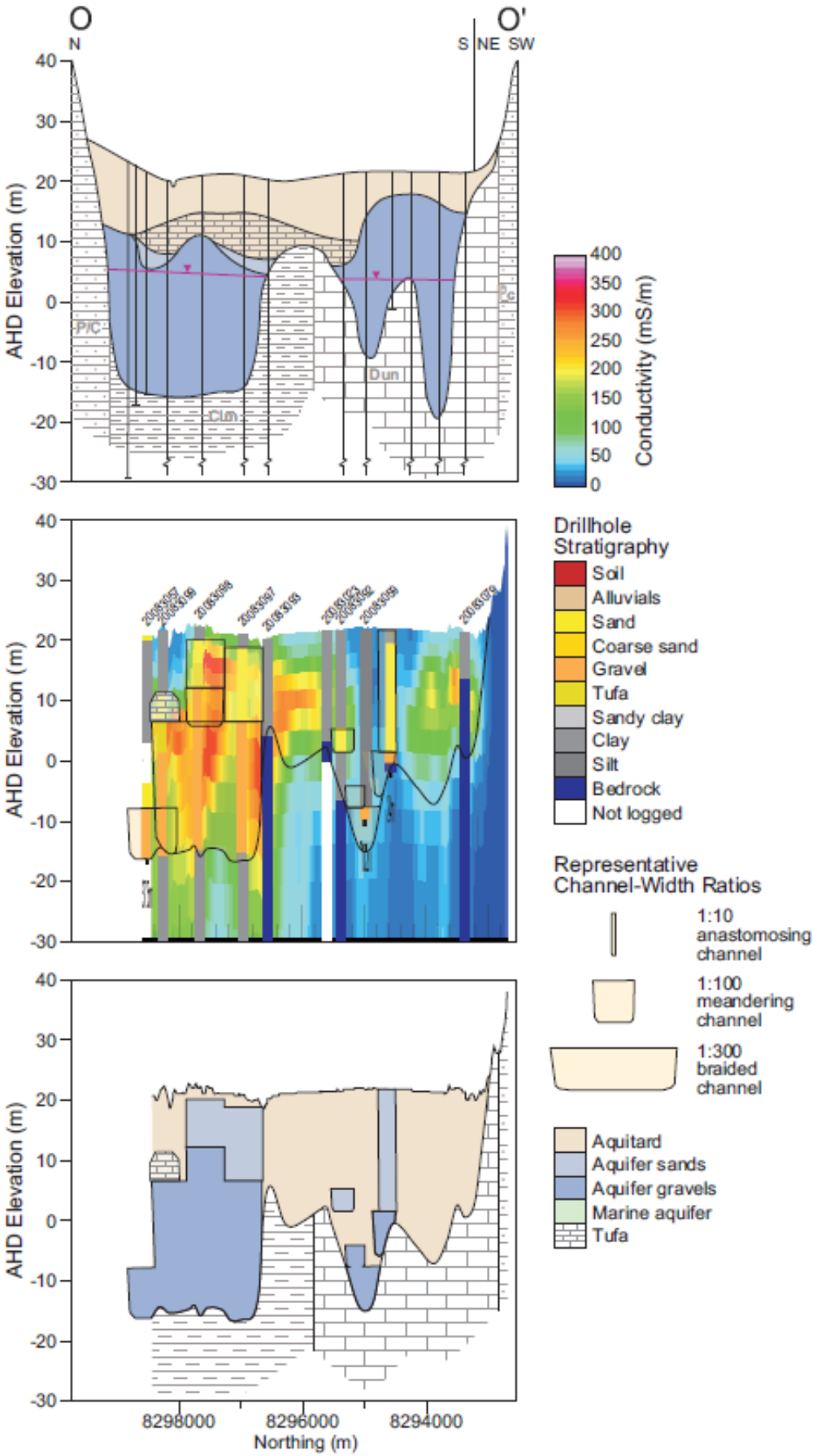

Figure 227: *Eastern Weaber Plain cross-section O-O'. Top panel is cross-section from O'Boy et al., (2001); middle panel is synthetic AEM section showing drillholes colour coded for lithology and with lithology extent interpretation line work displayed; bottom panel is revised lithology interpretation produced in this study.*

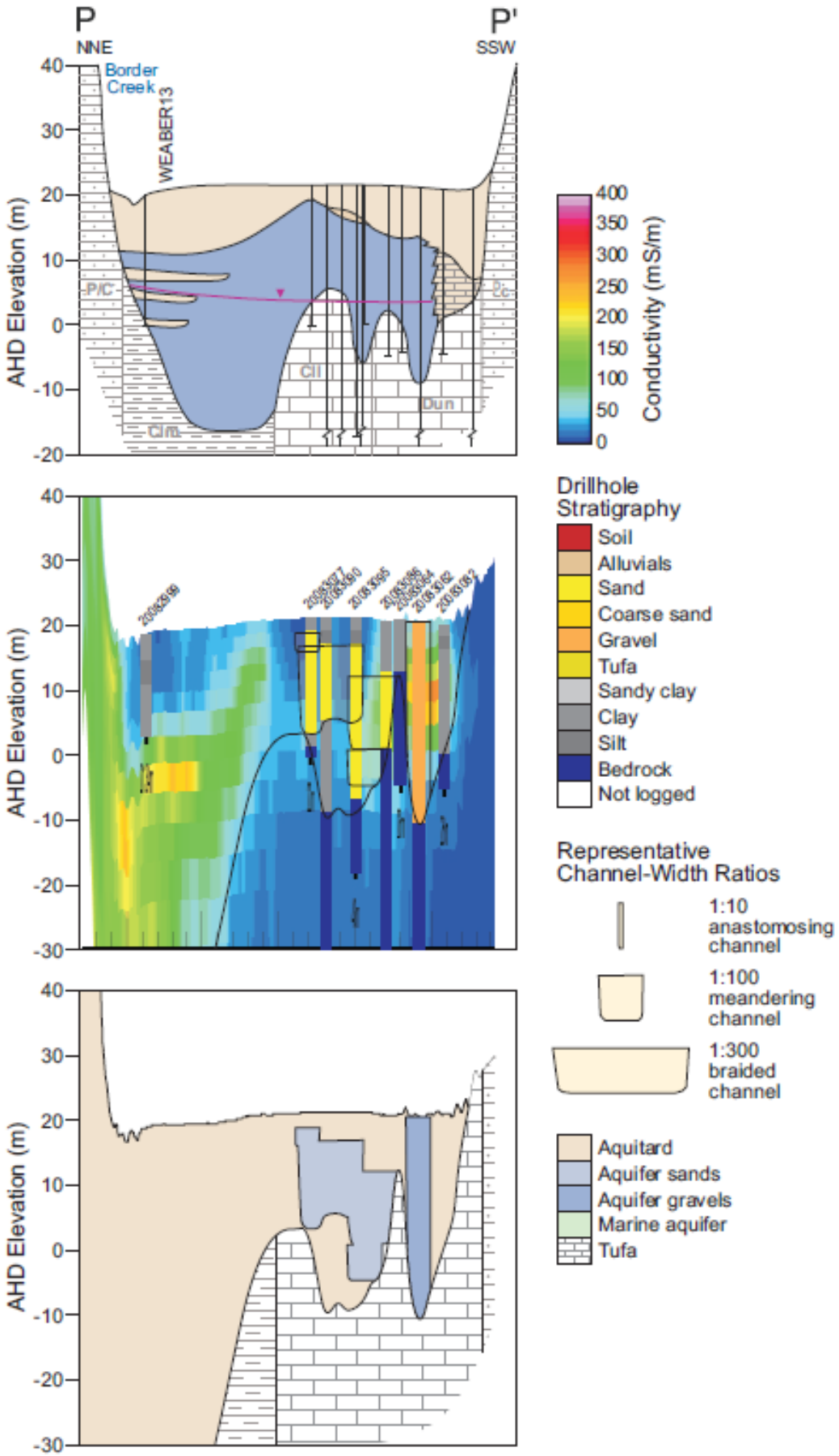

Figure 228: *Eastern Weaber Plain cross-section P-P'. Top panel is cross-section from O'Boy et al., (2001); middle panel is synthetic AEM section showing drillholes colour coded for lithology and with lithology extent interpretation line work displayed; bottom panel is revised lithology interpretation produced in this study.*

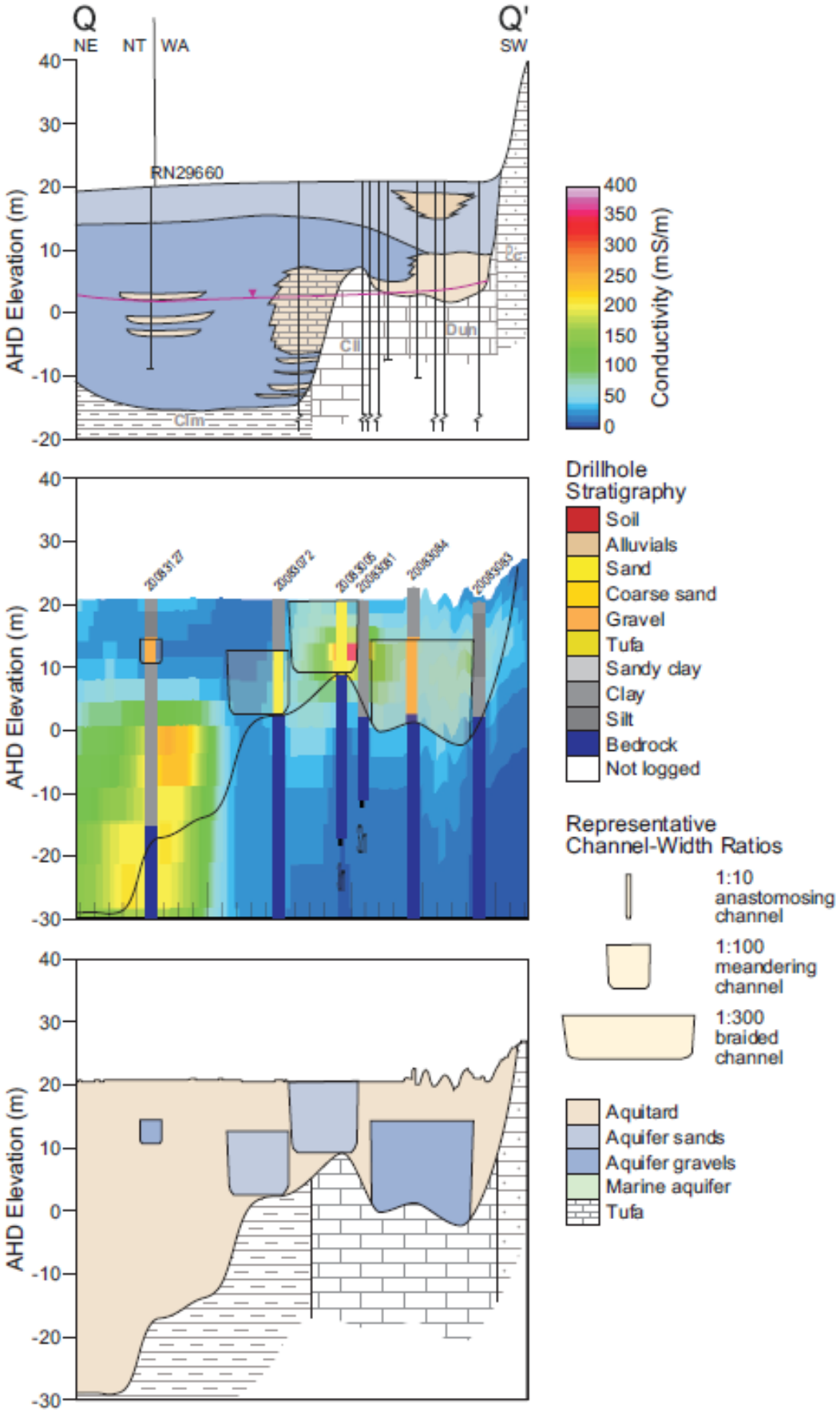

Figure 229: *Eastern Weaber Plain cross-section Q-Q'. Top panel is cross-section from O'Boy et al., (2001); middle panel is synthetic AEM section showing drillholes colour coded for lithology and with lithology extent interpretation line work displayed; bottom panel is revised lithology interpretation produced in this study.*

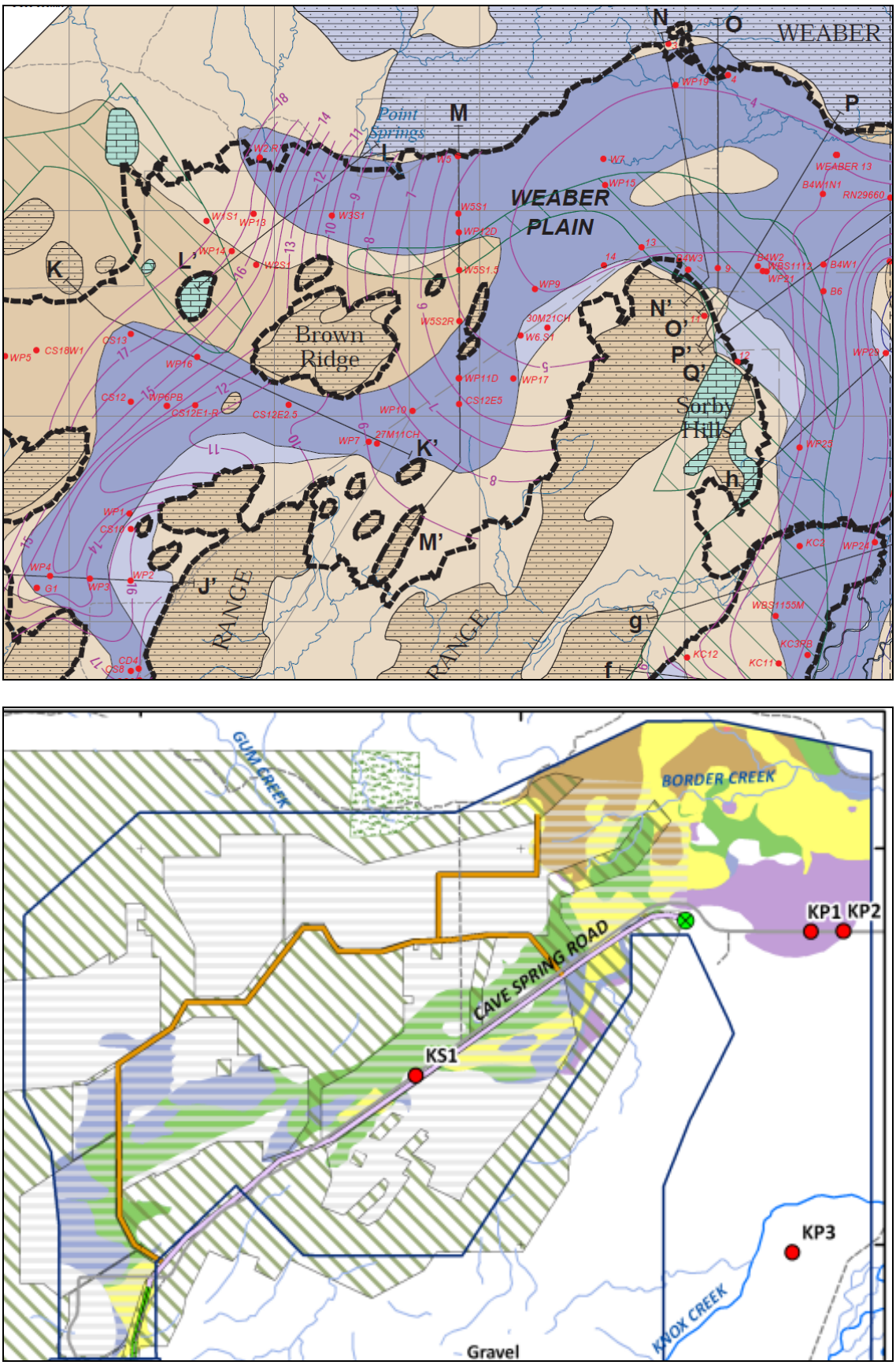

Figure 230: *Comparison of gravel aquifer extent in the Weaber Plain. The upper image is from O'Boy et al., (2001), and the lower image is generated from the AEM data in this study. Overall, the location and extent of the gravel-filled southern palaeochannel and eastern Weaber Plain gravels is similar, with the AEM data denoting a more confined palaeochannel. Overall, the AEM data provide a greater clarity on the 3D thickness of the gravels, while there is also a significant difference in interpretation of gravel extent in the northern Weaber Plain.*

6.5 HYDROSTRATIGRAPHY OF THE KNOX CREEK AND KEEP RIVER (WA) PLAINS

The Knox Creek and Keep River (WA) alluvial deposits are not connected to the palaeo-Ord River system, and overall display a simpler hydrostratigraphy, although there are some similarities. The Knox Creek Succession consists of upward fining gravels, sands, silts and clays and the succession is inferred to have been deposited in an aggrading fluvial plain, similar to the Ord succession.

The location of borehole KP3 is shown in Figure 28. A detailed log of this borehole is presented in Figure 231. The locations and depths of pre-existing holes used in this study for validation of the AEM dataset in this area are shown in Figure 209.

Interpretation of the hydrostratigraphy from the AEM data

The 0-2m conductivity depth slice (Figure 212), and nine conductivity depth slice maps with corresponding maps of interpreted lithology for the Knox Creek and Keep River Plains are shown in Figure 213 to Figure 221. Cross-sections through the Knox Creek and Keep River Plains are shown in Figure 232 to Figure 238. These are synthetic AEM sections (i.e. not sections along original flight lines), and follow the sections originally constructed by O'Boy *et al.,* (2001). For each cross-section, the figures show the original interpretation from O'Boy *et al*., (2001) in the top panel, the new synthetic AEM sections in the centre panel, and the new interpretation in the bottom panel.

Analysis of the conductivity depth slices and cross-sections reveals that the near- surface alluvium in the Weaber Plains is composed almost entirely of clay-rich sediments. Knox Creek succession sediments can be distinguished from those of the Ord Succession in drill core by the presence of indurated bands. The induration takes the form of clay and iron oxide-cemented sandstones, often stained by manganese (Figure 239). The induration suggests that the Knox Creek succession represents deposition over a longer timeframe, even though its surface is continuous with the Ord succession.

The Knox Creek Succession is also characterised by the presence of tufa deposits of carbonate rich clays and silts, and carbonate cemented sands. These are inferred to be from the discharge of carbonate-saturated waters from the limestone karst aquifers along the margins of the Knox Creek Plains. Modern counterparts of these have been reported from creeks and rivers elsewhere in the Kimberley (Wright, 2000). The presence of carbonate bands in many of the cross-sections of O'Boy *et al*. (2001) beneath the Weaber as well as the Knox Creek Plains suggests that a similar succession occurs there as well, except where the Ord River palaeochannel flows through. The Knox Creek succession tends to be poorly sorted gravels cemented with iron and carbonates (Figure 239).

The shallowest depth slice of Knox Creek Plains is characterised entirely by clay-rich materials from which bedrock rises define the western side. A few small hills rise above the alluvium from within the confines of the plains. This architecture continues down to a depth of 6.7m. The 6.7-9.5m conductivity depth slice shows an increase in sand and silt beneath part of the Keep River Plains. Sand and some silt units are evident along the part of the NT border, associated with the course of the Keep River which locally encroaches into WA in this area. Silt as opposed to clay is also associated with the upper reaches of a tributary of Knox Creek which flows from the Pincombe Ranges. Overall, the sand content increases downwards as the sand from the Knox Creek tributary merges with that of the Keep River in the 12.7-16.3m conductivity depth slice.

At a depth of 20.3m the architecture changes significantly. The palaeovalley abruptly narrows and shifts to the east. Sand becomes common along the whole length. Borehole information indicates that the sand also contains gravel lenses. These units are conductive, possibly though the presence of saline water. In this saline groundwater environment, it becomes difficult for the AEM to discriminate between gravel and clay units. Below a depth of 29.9m only bedrock is evident on the WA side of the border.

The gravels at the base of the palaeochannel beneath the Knox Creek Plain are moderately indurated, no shallower gravels are evident in the AEM section above the abrupt widening of the palaeovalley at ~20m depth below surface. As the palaeovalley extends across the border into the NT, where no AEM data exist, we suggest that the Keep River may represent the present expression of the fluvial system that deposited

these gravels. A relatively thin fixed channel connection is predicted to occur between the Keep River and these deeper gravel units.

Comparisons with previous studies

For each of the cross-sections, a comparison between the original cross-sections and the new interpretations, based on the AEM data, has been made. Similarly, comparisons with the original sand and gravel extent maps (O'Boy *et al*., 2001), are also made (Figure 240). Overall, the comparisons are limited because this study was confined to the WA side of the border, whereas the earlier O'Boy *et al*., (2001) study extended on both sides, allowing a better overview of the architecture of the valley fills within their natural limits. However, comparisons were hampered as it was not possible to map the gravel units in this area using AEM. This is because the units are thinner, discontinuous lenses that are often indurated and overprinted. Cross-section comparisons are documented below.

Section b-b'

A reasonable correspondence in the position of the bedrock surface is shown between the AEM data and the original section, even though only the western part of the original section is complemented by the AEM data (Figure 232). The relatively shallow bedrock shelf is clearly visible, as is the contrast between the resistive limestones and the more conductive shale in the bedrock. The contact between the two appears especially conductive, the reasons for this are not known. Less gravel appears present in previous interpretations. A possible explanation for this is that the main part of the valley fill, including the coarser units, lines further to the east under the Keep River, and beyond the limits of the survey.

Section c-c'

A reasonable correspondence is shown once more between the AEM data and the original section regarding the position of the bedrock surface, even though only the western part of the original section is overlapped by the AEM data (Figure 233). The relatively shallow bedrock shelf is still visible, as is the contrast between the resistive limestones and the more conductive shale in the bedrock. The basal units in the alluvium are very conductive, and would appear to comprise both indurated gravel units containing comparatively saline water in the 1000-2500mg/l range as well as clays (Figure 233). The amount of gravel would appear to be less than shown in original sections, although it is hard to discriminate between clays and gravels with AEM in this saline environment. As this the previous section, the main part of the valley fill lies east of the limits of this survey.

Section d-d'

Further reasonable correlation between the original cross-section and the AEM data in the position of the bedrock surface is shown in this section (Figure 234). The relatively shallow bedrock shelf is again present, as is the contrast between the resistive limestones and the more conductive shale in the bedrock. The basal units in the alluvium are very conductive, and would appear to comprise both indurated gravel units containing comparatively saline water in the 1000-2500mg/l range as well as clays (Figure 237). The amount of gravel would appear to be less than shown in original sections, although it is hard to discriminate between clays and gravels with AEM in this saline environment.

Section e-e'

There is a moderate similarity in the position of the bedrock surface between the AEM data and the original section (Figure 235). The bedrock shelf on the western side has a pinnacle in the AEM data corresponds with a DEM feature but is not shown on the original section. There is also a possible doline in the Devonian limestone present, this was drilled by WINSITE bore 20082347. The basal units in the alluvium are very conductive, and would appear to comprise both indurated gravel units containing comparatively saline water in the 1000-2500mg/l range as well as clays (Figure 235). The amount of gravel would appear to be less than shown in original sections, although it is hard to discriminate between clays and gravels with AEM in this saline environment. As with other sections along the Knox Creek Plains, the infilled valley of the Keep River is only partly traversed by the sections.

Section f-f'

There is a moderate correspondence between the two datasets with respect to the position of the bedrock surface (Figure 236). The buried limestone ridge inferred in the original cross-section is less developed and

there is another possible doline, again intersected by a bore, this time WINSITE 20082459. The gravels in the palaeovalley in this section have an extent similar to that predicted.

Section g-g'

There is a good correspondence in the position of the bedrock surface between the AEM data and the original cross-section (Figure 237). The basal gravels appear to be as extensive as predicted. A thicker conductive clay unit appears to form a lens in the fine-grained upper part of the succession.

Section h-h'

A reasonably good correlation with respect to the position of the bedrock surface between the two sets of data is evident (Figure 238). The basal gravels are conductive, and thought to contain saline groundwater. The gravels appear to be capped by highly conductive clay-rich zone. The gravel extent is similar to that in the earlier study, despite only partial profiling across the area.

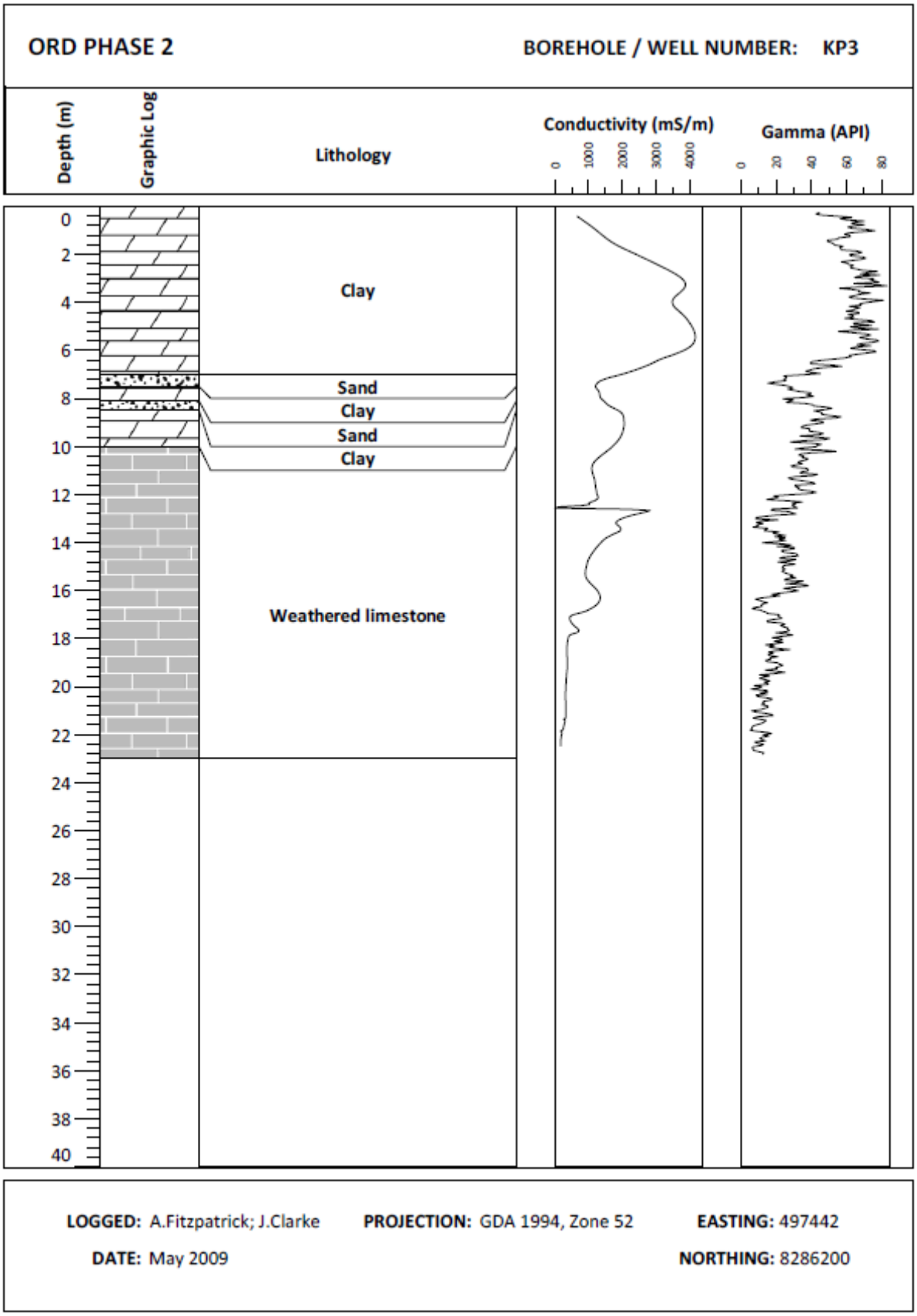

Figure 231: *Ord Phase 2 borehole number KP3. The weathered limestone is tufa..*

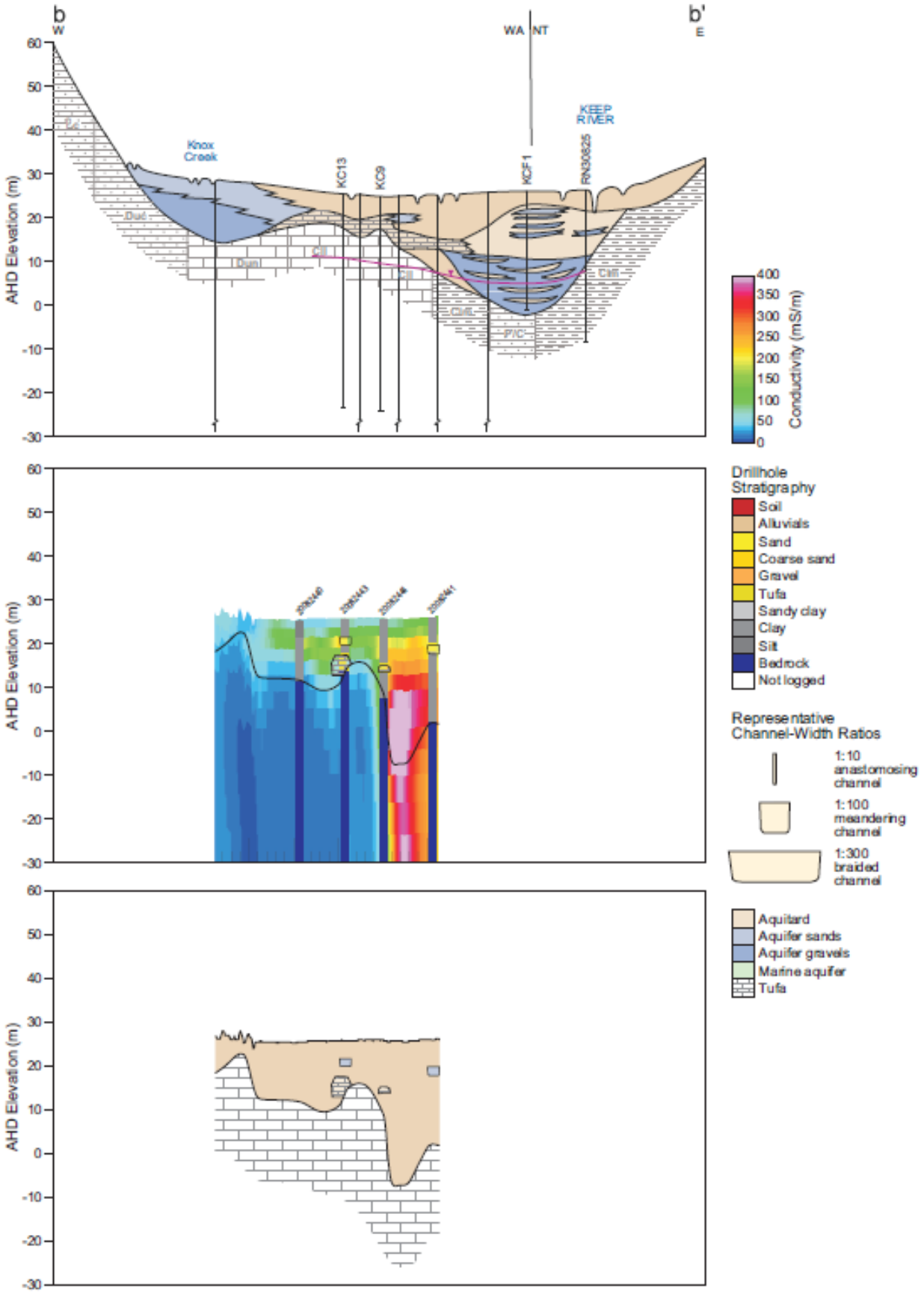

Figure 232: *Keep River Plain cross-section b-b'. Top panel is cross-section from O'Boy et al., (2001); middle panel is synthetic AEM section showing drillholes colour coded for lithology and with lithology extent interpretation line work displayed; bottom panel is revised lithology interpretation produced in this study.*

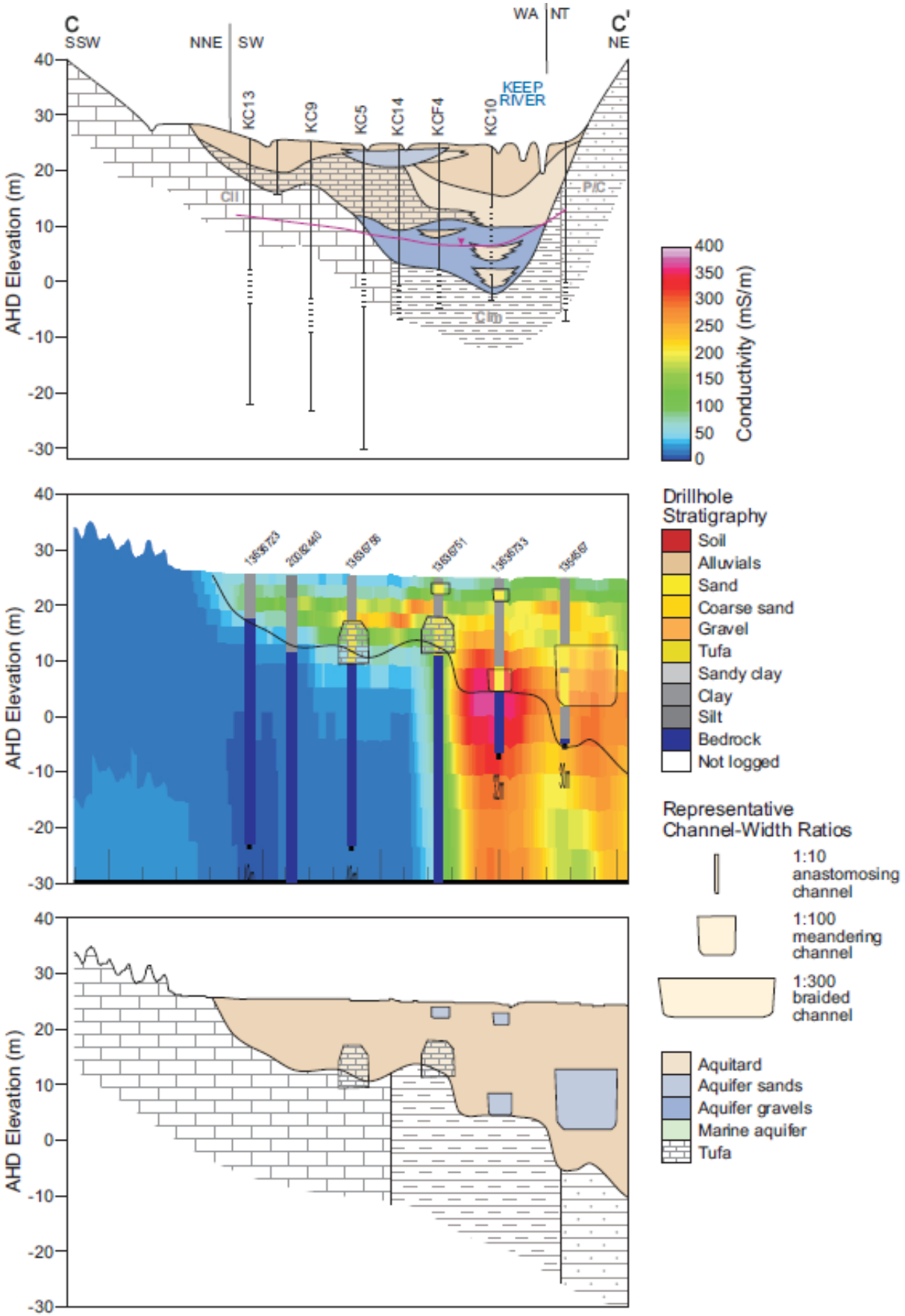

Figure 233: *Keep River Plain cross-section c-c'. Top panel is cross-section from O'Boy et al., (2001); middle panel is synthetic AEM section showing drillholes colour coded for lithology and with lithology extent interpretation line work displayed; bottom panel is revised lithology interpretation produced in this study.*

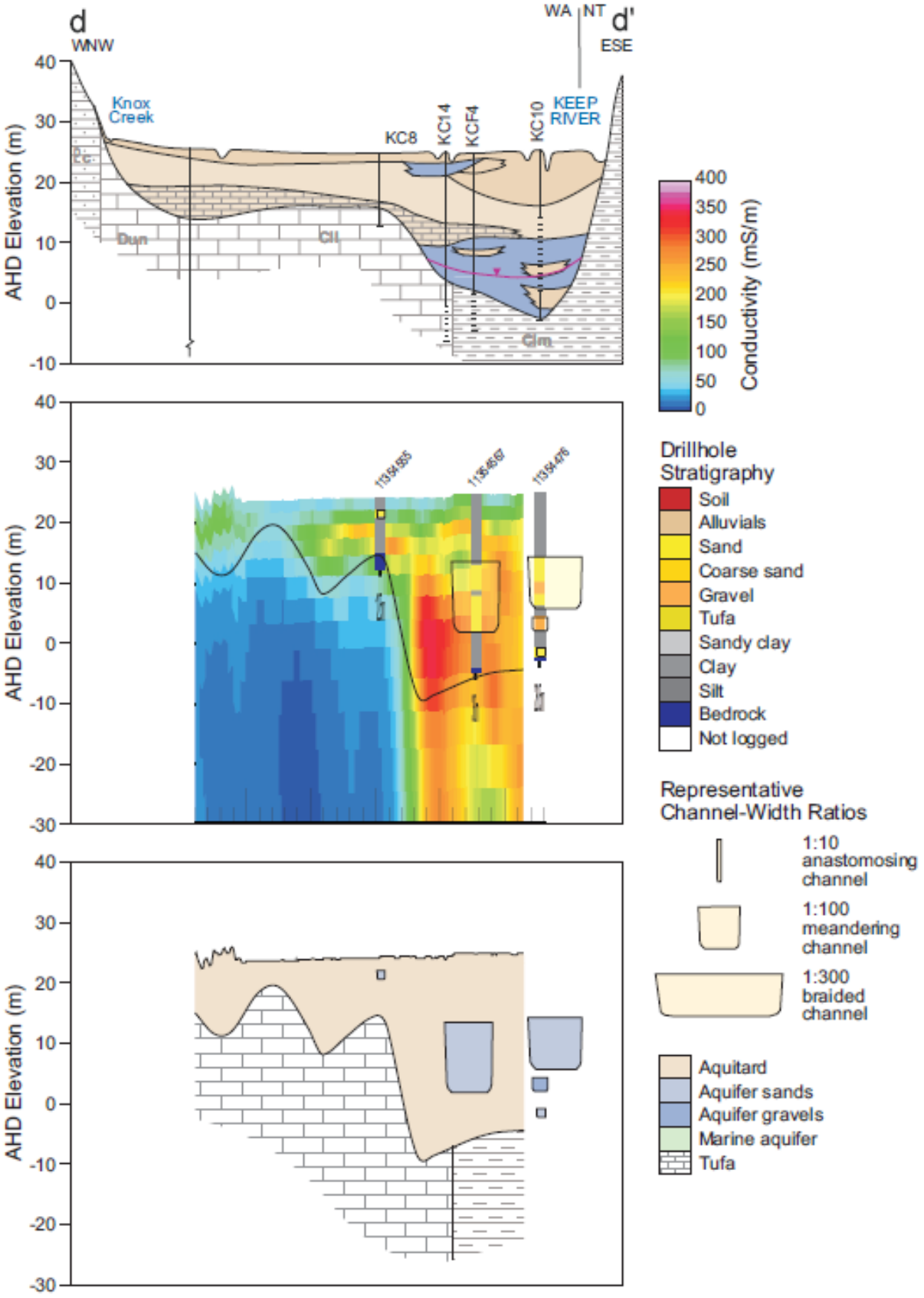

Figure 234: *Keep River Plain cross-section d-d'. Top panel is cross-section from O'Boy et al., (2001); middle panel is synthetic AEM section showing drillholes colour coded for lithology and with lithology extent interpretation line work displayed; bottom panel is revised lithology interpretation produced in this study.*

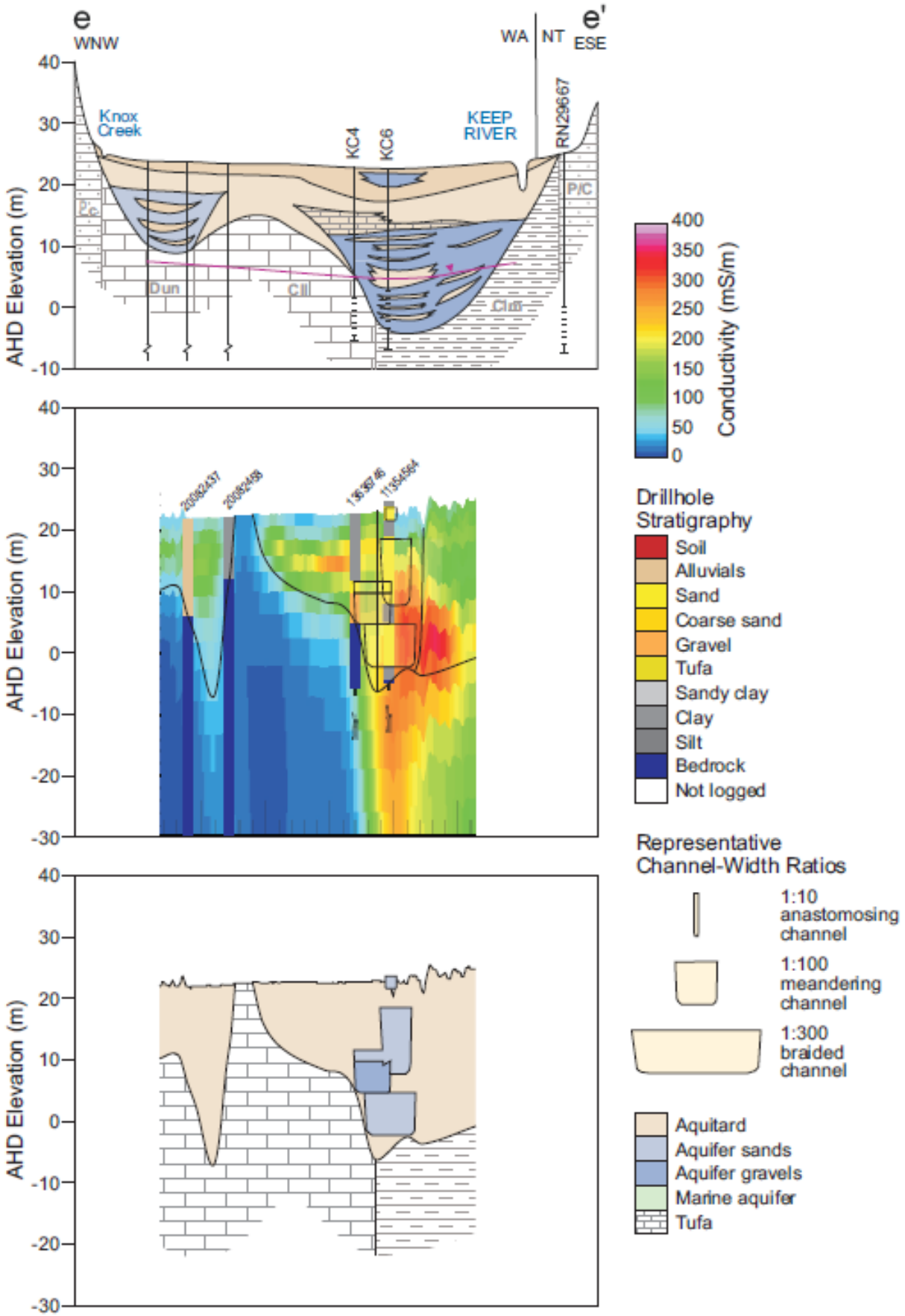

Figure 235: *Keep River Plain cross-section e-e'. Top panel is cross-section from O'Boy et al., (2001); middle panel is synthetic AEM section showing drillholes colour coded for lithology and with lithology extent interpretation line work displayed; bottom panel is revised lithology interpretation produced in this study.*

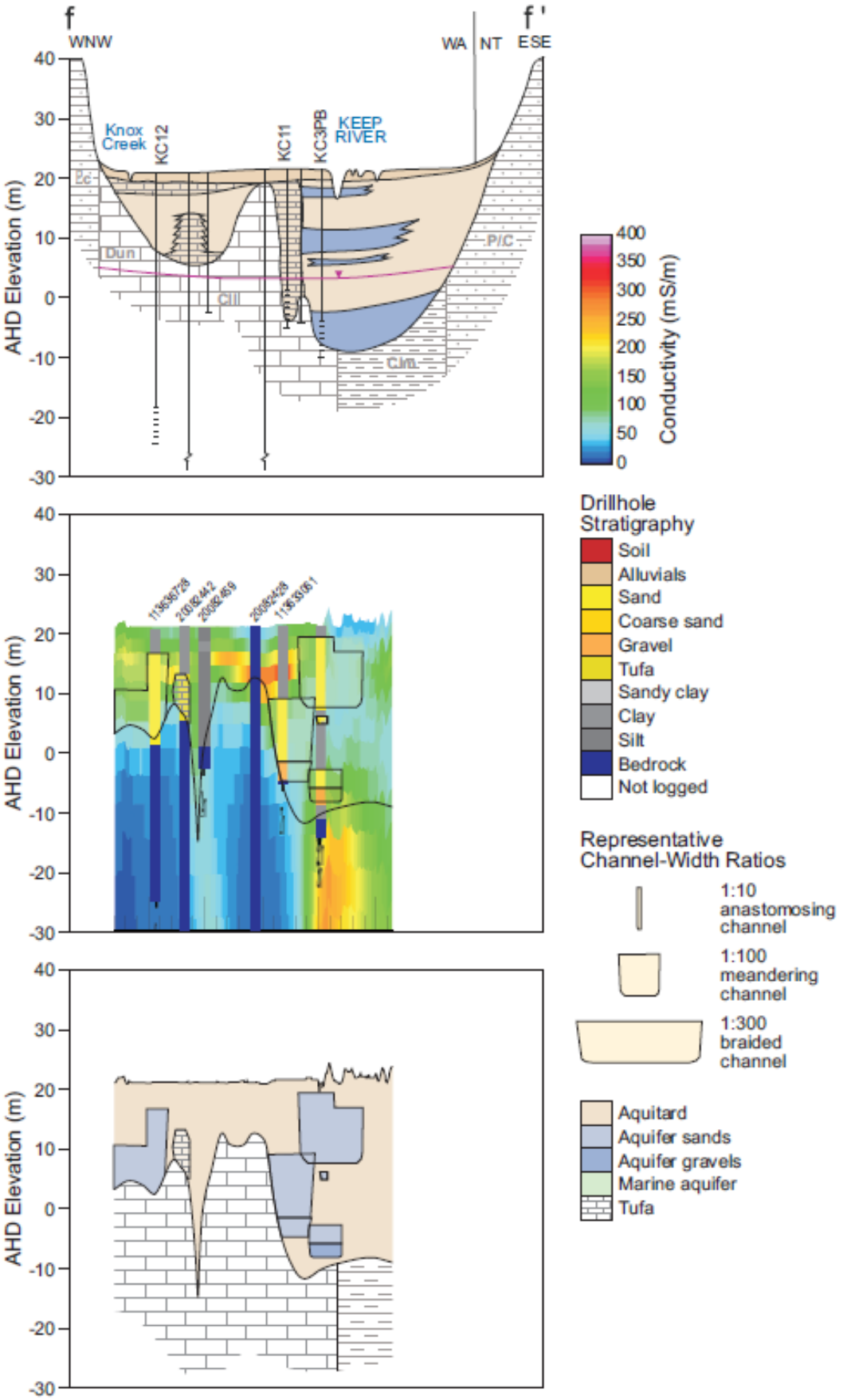

Figure 236: *Keep River Plain cross-section f-f'. Top panel is cross-section from O'Boy et al., (2001); middle panel is synthetic AEM section showing drillholes colour coded for lithology and with lithology extent interpretation line work displayed; bottom panel is revised lithology interpretation produced in this study.*

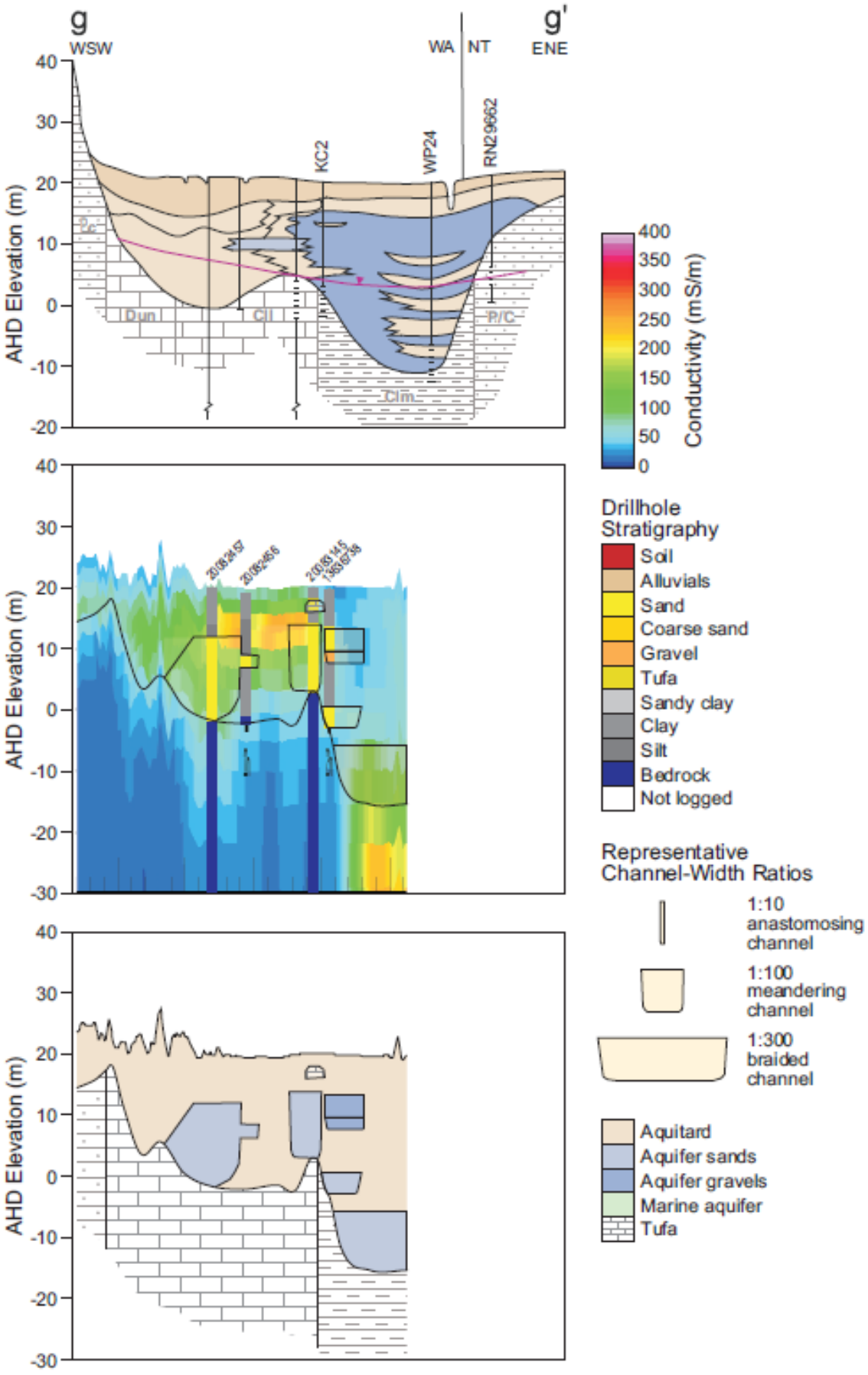

Figure 237: *Keep River –Knox Creek Plain cross-section g-g'. Top panel is cross-section from O'Boy et al., (2001); middle panel is synthetic AEM section showing drillholes colour coded for lithology and with lithology extent interpretation line work displayed; bottom panel is revised lithology interpretation produced in this study.*

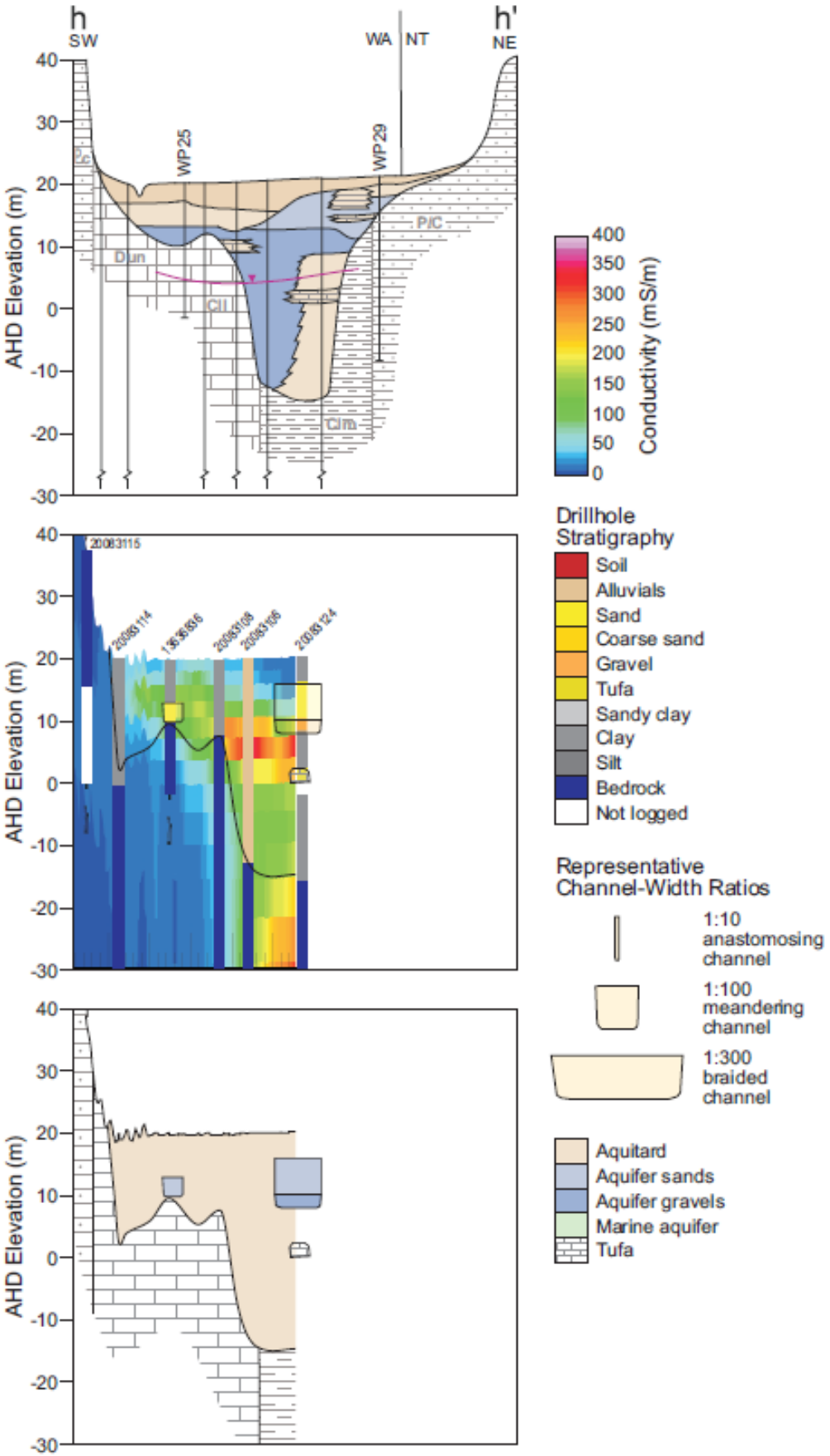

Figure 238: *Keep River –Knox Creek Plain cross-section h-h'. Top panel is cross-section from O'Boy et al., (2001); middle panel is synthetic AEM section showing drillholes colour coded for lithology and with lithology extent interpretation line work displayed; bottom panel is revised lithology interpretation produced in this study.*

Figure 239: *Iron (red-brown) and carbonate (cream)-cemented poorly sorted gravels of Knox Creek succession. Contrast with uncemented gravels of Ord succession in Figure 270.*

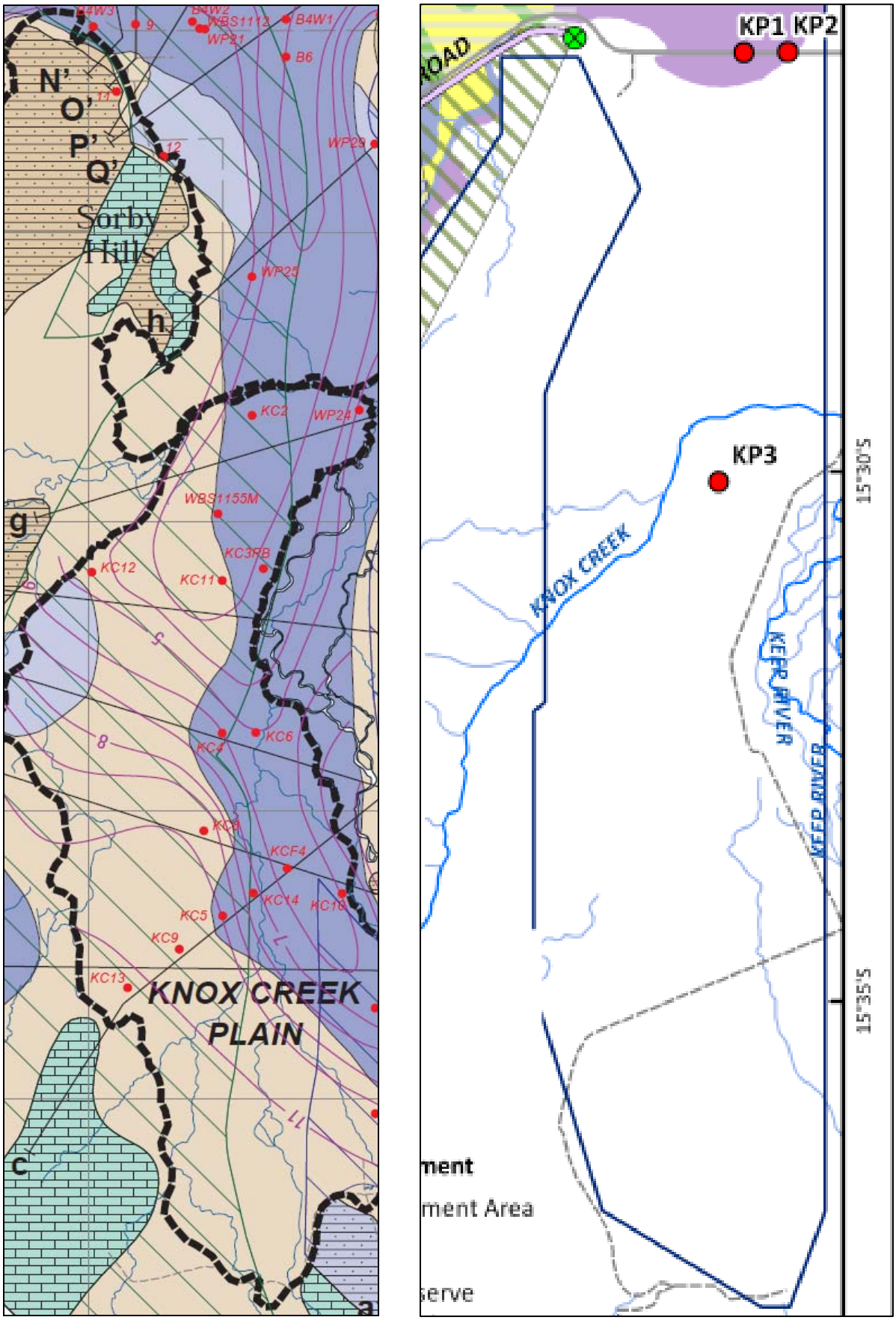

Figure 240: *Comparison of gravel aquifer extent in the Knox Creek and Keep River Plains. The left image is from O'Boy et al., (2001), and the right image is generated from the AEM data in this study. This figure has been included to highlight the fact that it was not possible to map the gravel units in this area using AEM. This is because the units are thinner, discontinuous lenses that are often indurated and overprinted.*

6.6 HYDROSTRATIGRAPHY OF THE PARRY'S LAGOON-MANTINEA PLAIN AND CARLTON HILL AREA

The Parry's Lagoon Succession consists of marine and/or estuarine basal sands that fine rapidly upwards into non-marine fluvial silts and clay. These are capped by mangrove muds and /or lagoonal deposits. This sequence has been incised by the fluvial sediments of the Ord River when it shifted position to its current course, leading to the deposition of fluvial gravels on top of thin marine or marginal marine sediments.

Three new holes (PL 1, 2 and 3) were drilled into the Parry's Lagoon alluvial succession (Figure 28 and Figure 241). Detailed logs of boreholes PL1, PL2 and PL3 are presented in Figure 242 to Figure 244. The locations and depths of pre-existing holes used in this study for validation of the AEM dataset are shown in Figure 241.

Interpretation of the hydrostratigraphy from the AEM data

The 0-2m conductivity depth slice (Figure 245), and nine conductivity depth slice maps with corresponding maps of interpreted lithology for the Knox Creek and Keep River Plains presented in Figure 246 - Figure 261. Cross-sections through the Knox Creek and Keep River Plains are shown in Figure 262 to Figure 267. These are synthetic AEM sections (i.e. not sections along original flight lines), and follow the sections originally constructed by O'Boy *et al.,* (2001). For each cross-section, the figures show the original interpretation from O'Boy *et al*., (2001) in the top panel, the new synthetic AEM sections in the centre panel, and the new interpretation in the bottom panel.

The alluvial succession is dominated by a distinctive pink to yellow, very well sorted, medium quartz sand with minor clay and carbonate that is present in all three holes (Figure 268). Carbonate-cemented burrows and rare marine fossils are present. This sand fines rapidly upwards into upwards into non-marine fluvial silts and clays in PL1 and is overlain along an erosional contact by Ord gravel in PL2.

In PL3 the succession passes upwards into black mud with abundant woody fragments, interpreted as an old mangrove deposit, this in turn is capped by a brackish water lagoon deposit. In all three holes, the marine and estuarine unit corresponds with a highly conductive, seaward dipping sheet visible in the AEM data. The Parry's lagoon succession is interpreted as a transgressive to regressive infill of a large marine embayment that formerly existed in the area. This was incised by the fluvial sediments of the Ord River when it shifted position to its current course, leading to the deposition of fluvial gravels on top of a thin marine or marginal marine succession in PL2.

The shallowest interpreted depth slice in the Mantinea area of the Ord Stage 2 project is characterised by bedrock areas to the south, south-west and north-east, sand and gravel aquifers of the Ord River and small areas of silty to sandy sediments north and south of the river and to the west. These highly conductive sediments contain carbonate and rare shells and are overlain by carbonaceous silts rich in wood in the west. They are interpreted as being the top of a bay filling estuarine to marine succession.

This succession has been incised and then in-filled by the sediments of the modern Ord River. Because of the highly conductive nature of these sediments and of the salt-water wedge entering from the north-west, it is difficult to distinguish different facies within these sediments and aquifers. However, it is possible that House Roof Hill was once completely surrounding by estuarine to marine sediments, indicating that it may once have been an island.

At depths of greater than 6.7m the influence of the coarse river sediments shrinks abruptly, indicating the narrowing of the fluvial valley incised into the marine sediments. Drilling this area, for example PL2, indicates that coarse alluvial sediments do not extend to depths much greater than 9m. On the margins, for example beneath the scroll bars, the alluvial sediments may be much thinner. Below the 9.5-12.7m slice alluvial sediments appear to be absent, except in a few discontinuous locations marking the thalweg. The marine sediments form an almost continuous sheet across the north-western half of the slice. The south-eastern end of the marine sediments show numerous figures, which are interpreted as representing palaeovalley fills.

Below the 16.3-20.3m slice, the extent of the marine sediments also begins to reduce. There is a noticeable contract of the area covered by these sediments to the north-west, leaving behind sinuous linear features that probably represent palaeochannels. The base of these channels fills small palaeovalleys that have been cut into slightly weathered bedrock.

In the deepest interpreted slice, 24.8-29.9m, the marine unit is largely absent except in far northwest. Everywhere else, the slice is dominated by fresh to very slightly weathered bedrock (Figure 268). A strong NW-SE trending structural control is evident in the conductivity data through most of the depth slices (Figure 163 and Figure 164). Further work is required to establish whether some of the control on conductivity in the alluvial sequence represents neotectonics, or groundwater movement above basement faults.

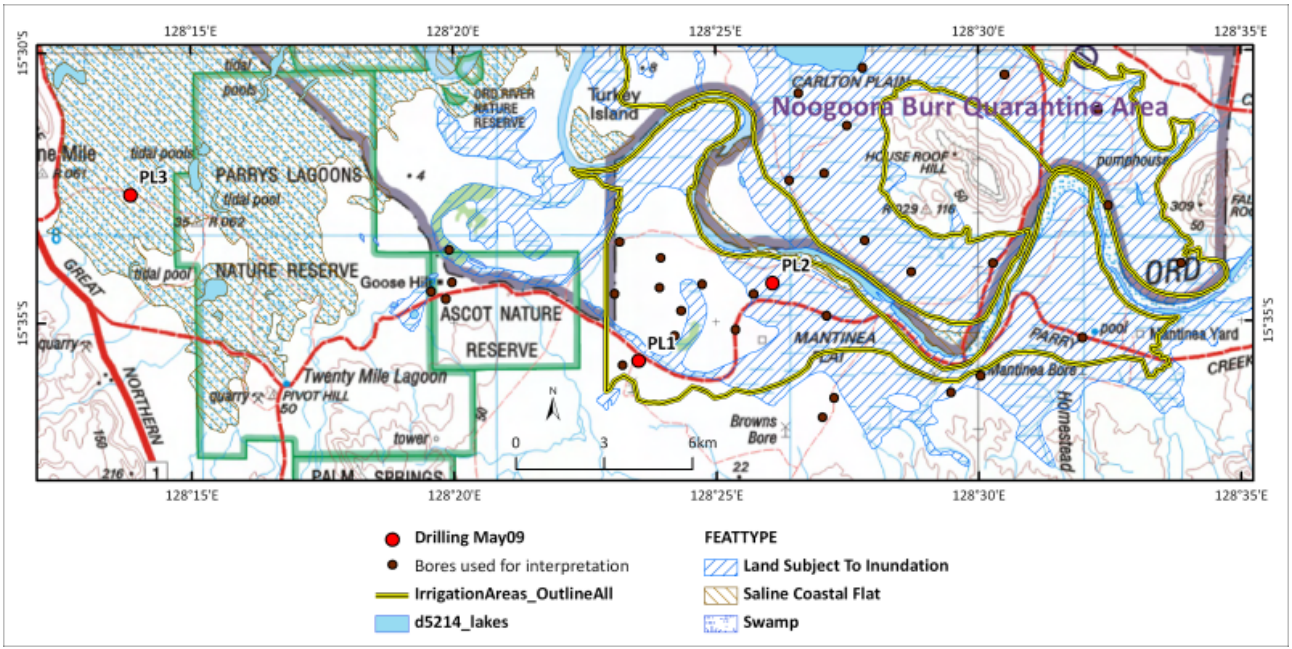

Figure 241: *Drill holes in the Parry's Lagoon- Mantinea Plain- Carlton Hill area.*

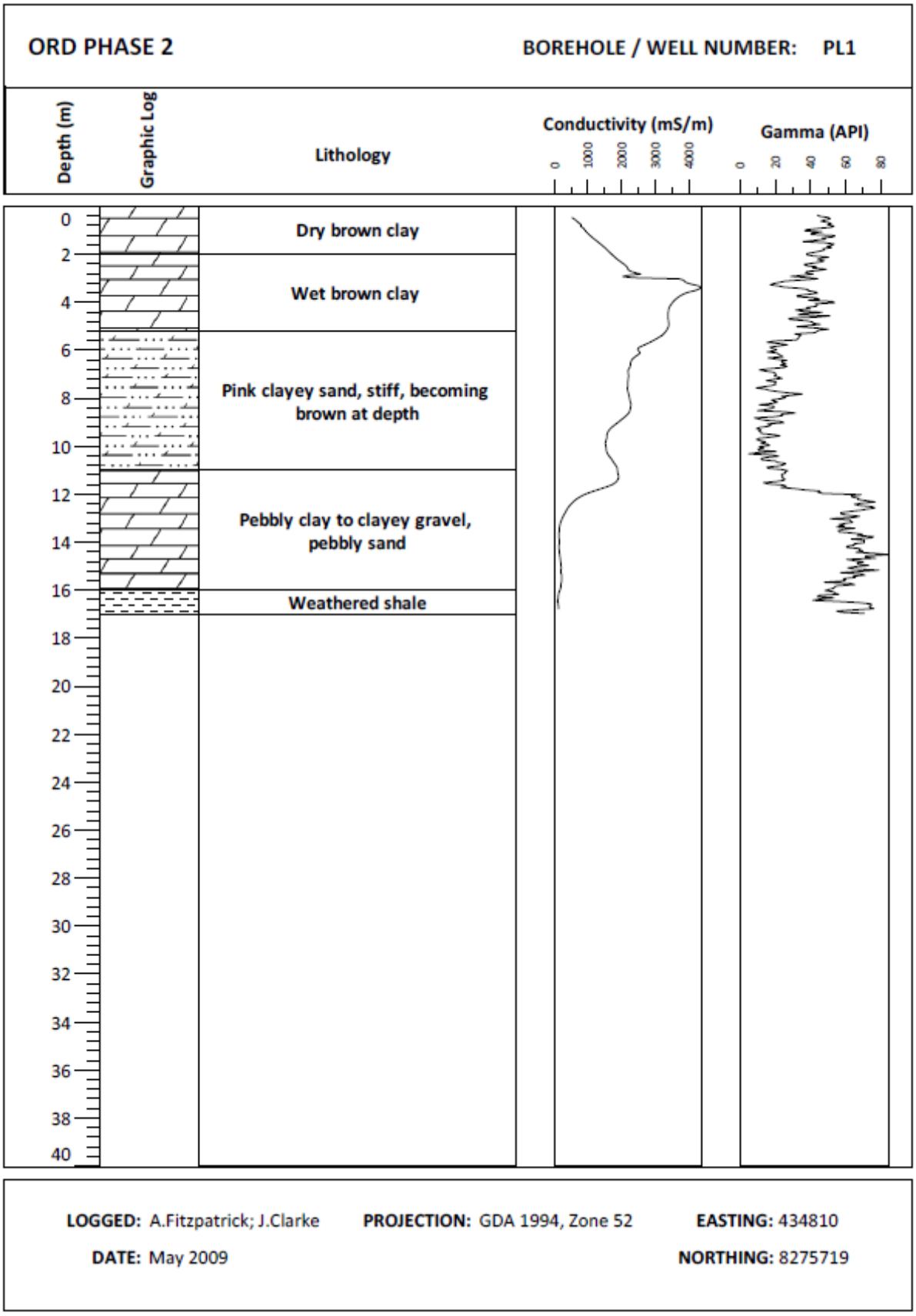

Figure 242: *Ord Phase 2 borehole log PL1.*

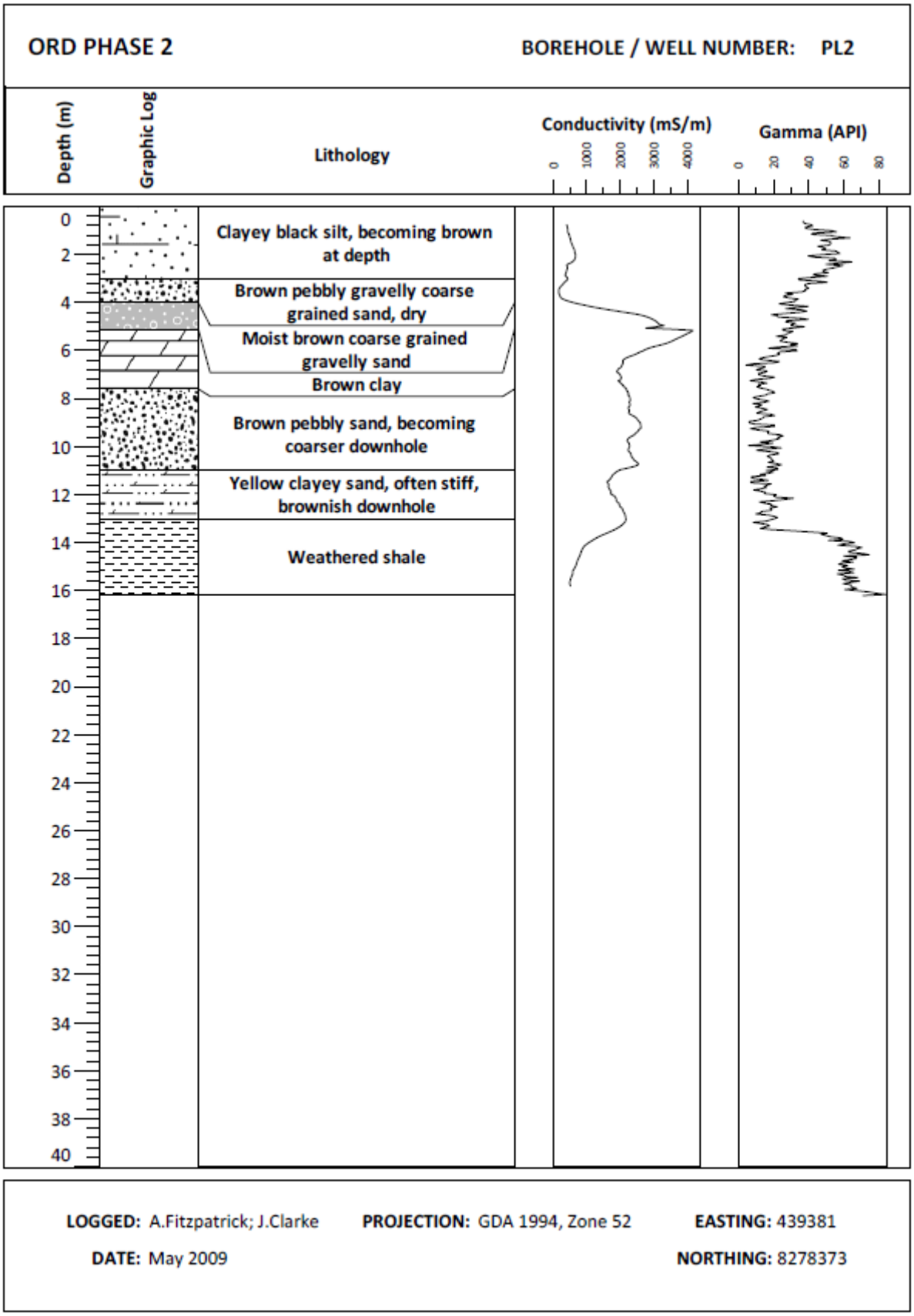

Figure 243: *Ord Phase 2 borehole log PL2.*

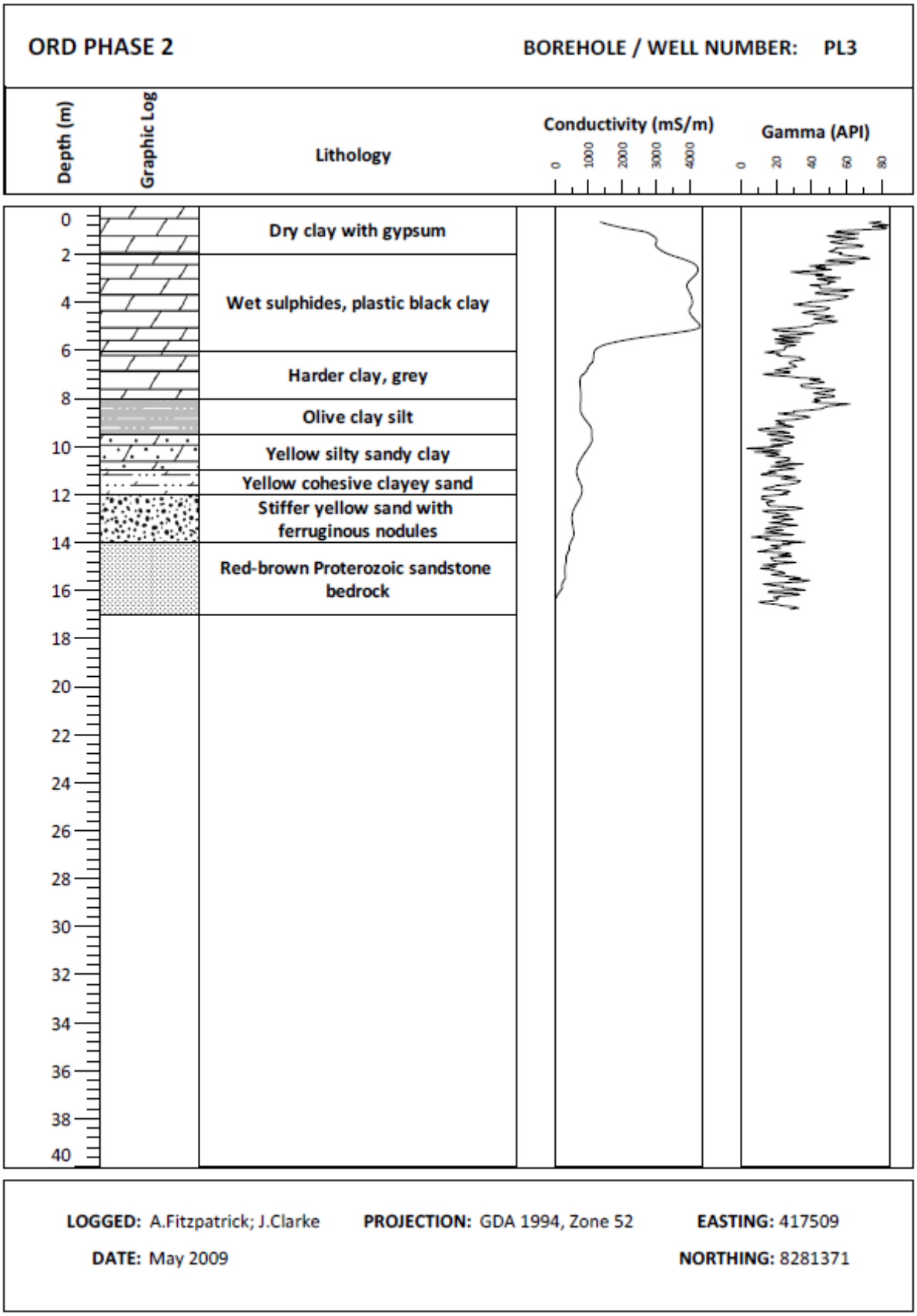

Figure 244: *Ord Phase 2 borehole log PL3.*

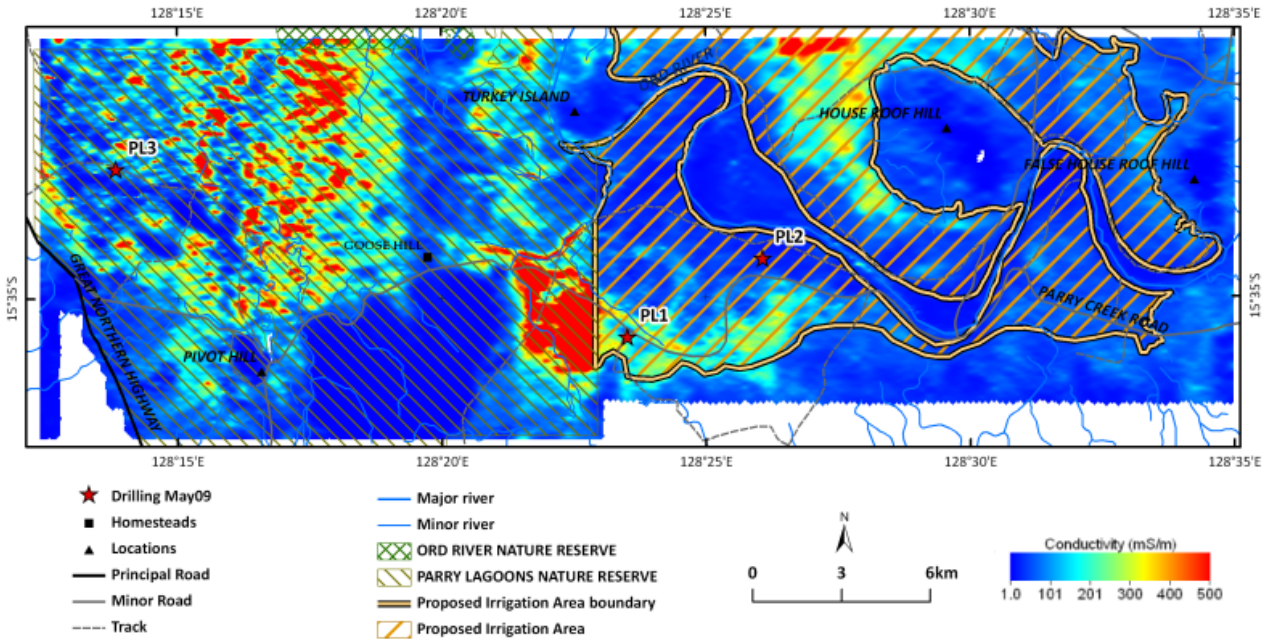

Figure 245: *Parry's Lagoon- Mantinea Plain- Carlton Hill. Conductivity depth slice 0-2m*

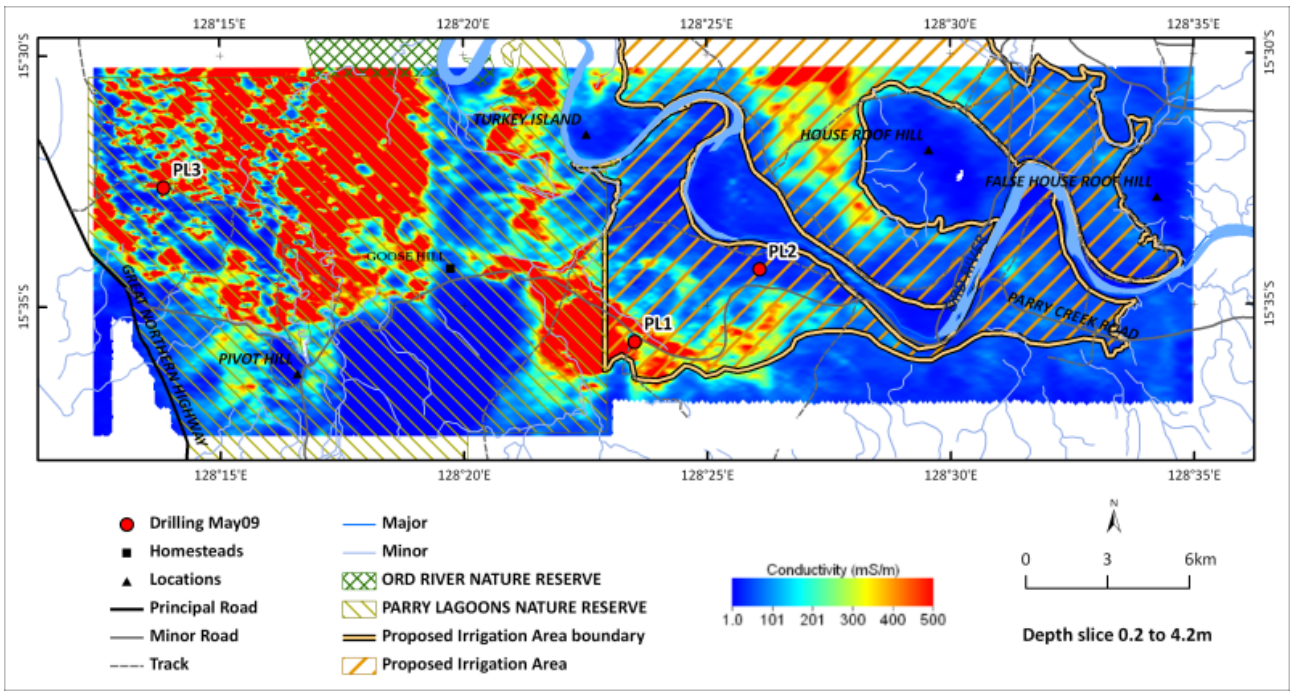

Figure 246: *Parry's Lagoon- Mantinea Plain- Carlton Hill. Conductivity depth slice 2 to 4.2m*

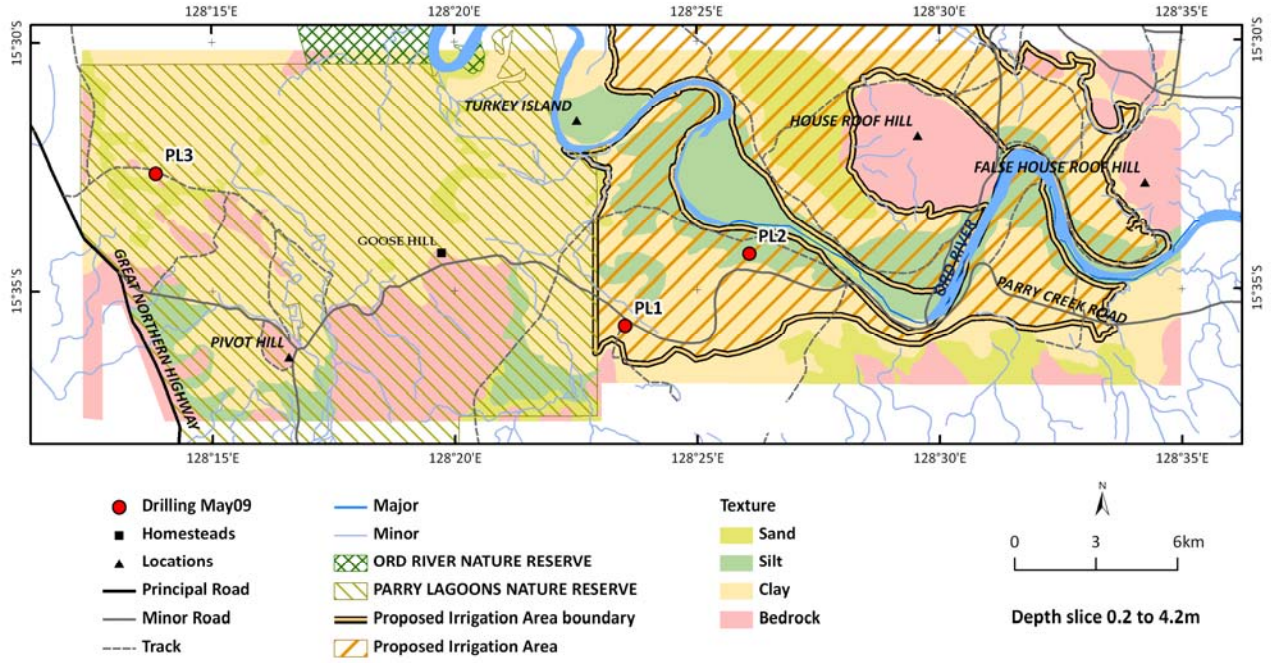

Figure 247: *Parry's Lagoon- Mantinea Plain- Carlton Hill. Lithology interpretation of conductivity depth slice 2 to 4.2m*

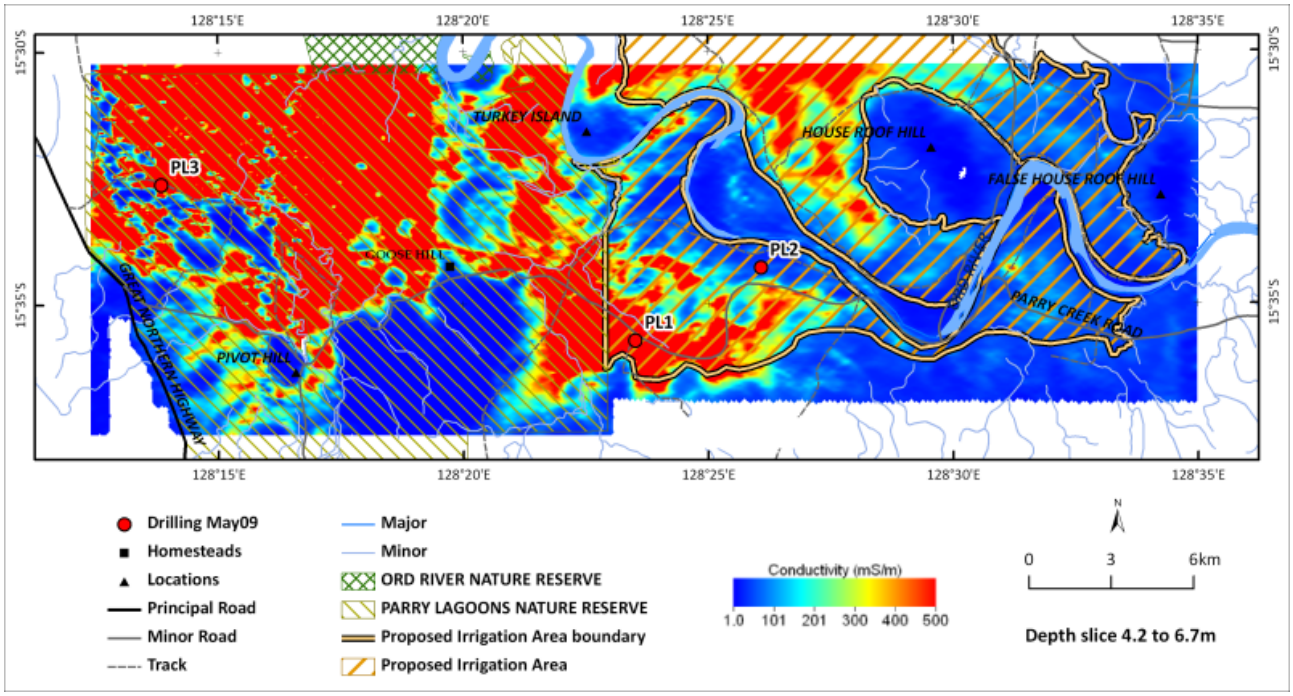

Figure 248: *Parry's Lagoon- Mantinea Plain- Carlton Hill. Conductivity depth slice 4.2 to 6.7m*

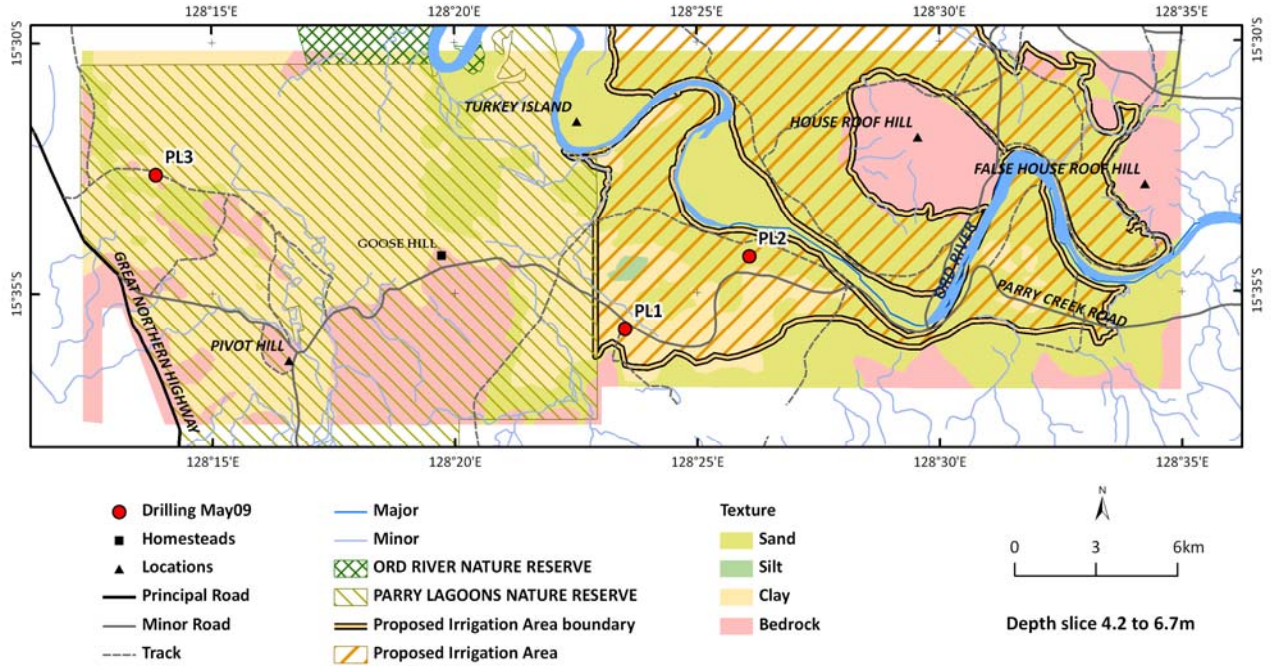

Figure 249: *Parry's Lagoon- Mantinea Plain- Carlton Hill. Lithology interpretation of conductivity depth slice 4.2 to 6.7m*

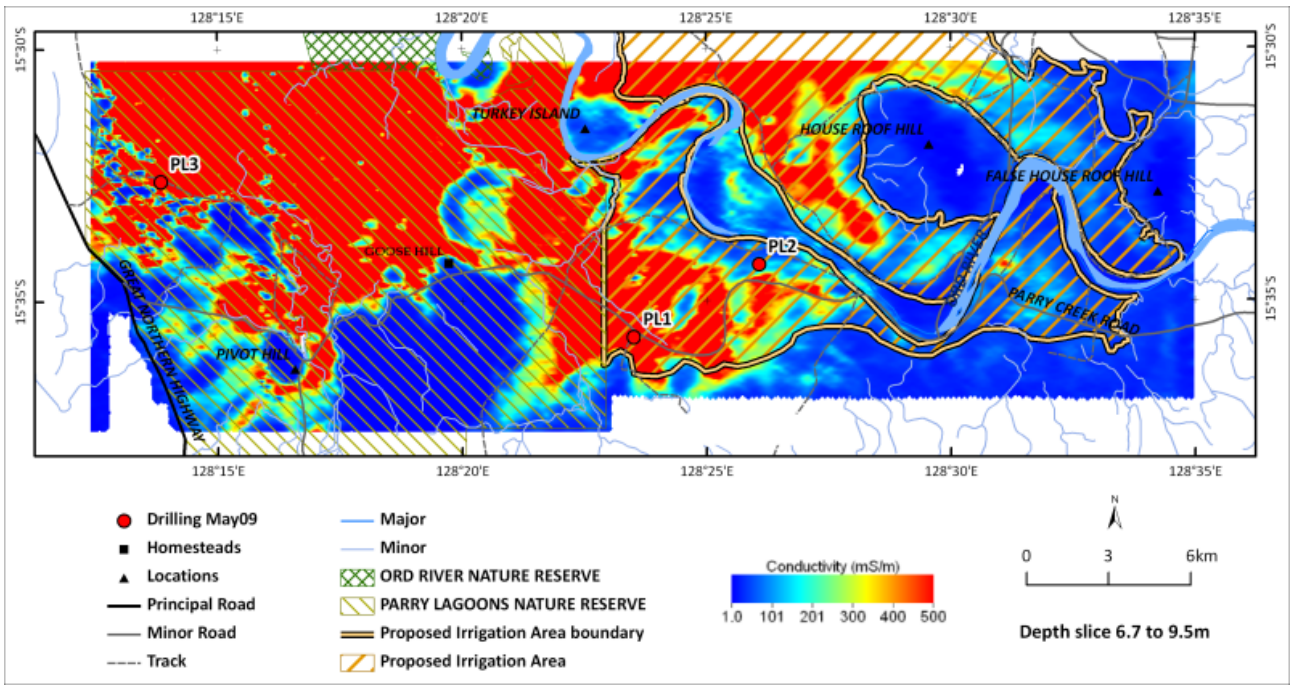

Figure 250: *Parry's Lagoon- Mantinea Plain- Carlton Hill. Conductivity depth slice 6.7 to 9.5m.*

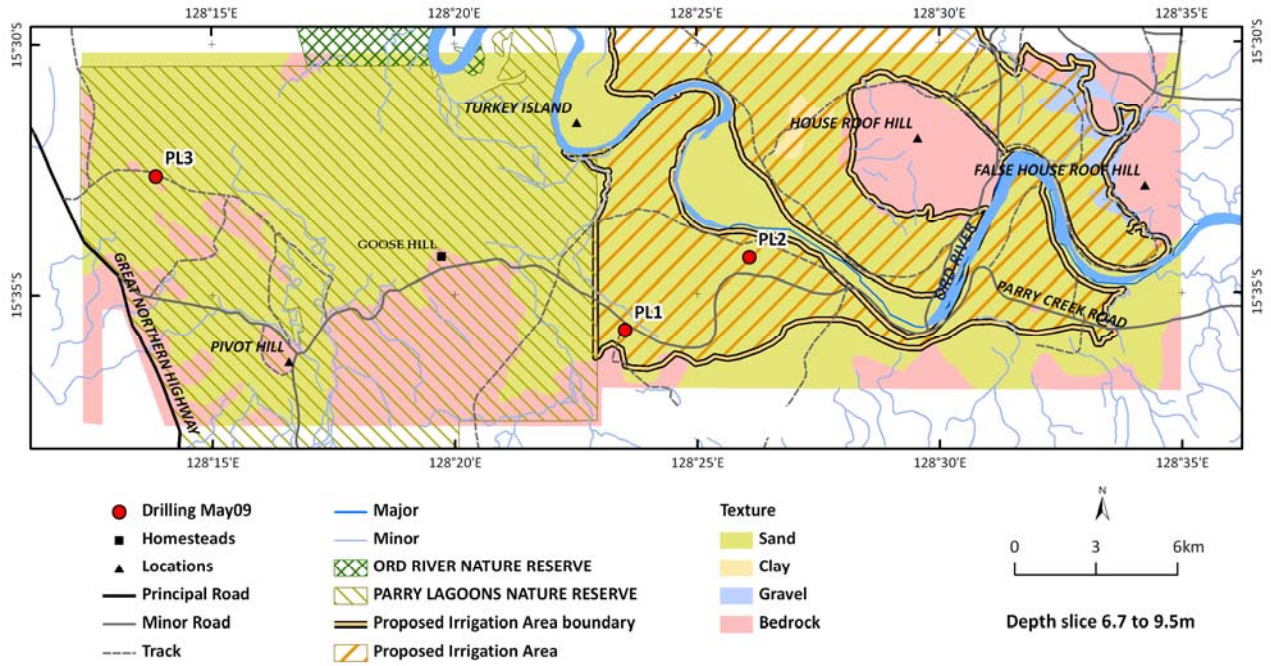

Figure 251: *Parry's Lagoon- Mantinea Plain- Carlton Hill. Lithology interpretation of conductivity depth slice 6.7 to 9.5m.*

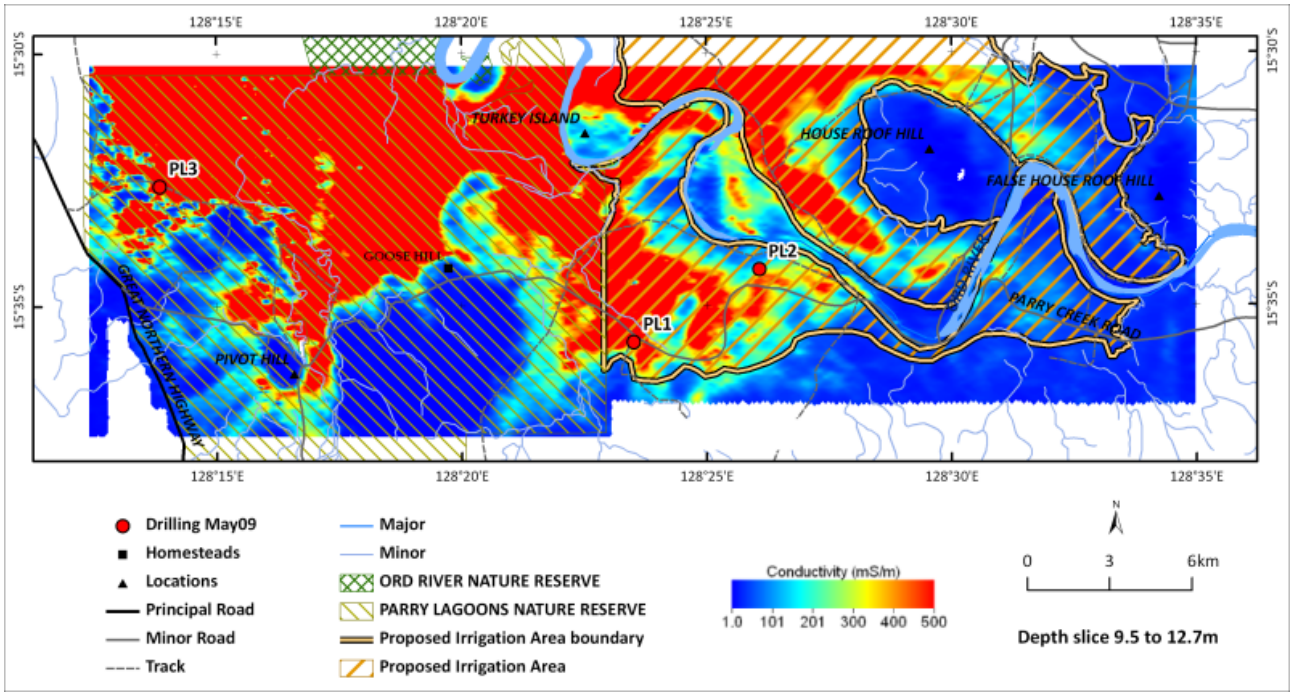

Figure 252: *Parry's Lagoon- Mantinea Plain- Carlton Hill. Conductivity depth slice 9.5 to 12.7m.*

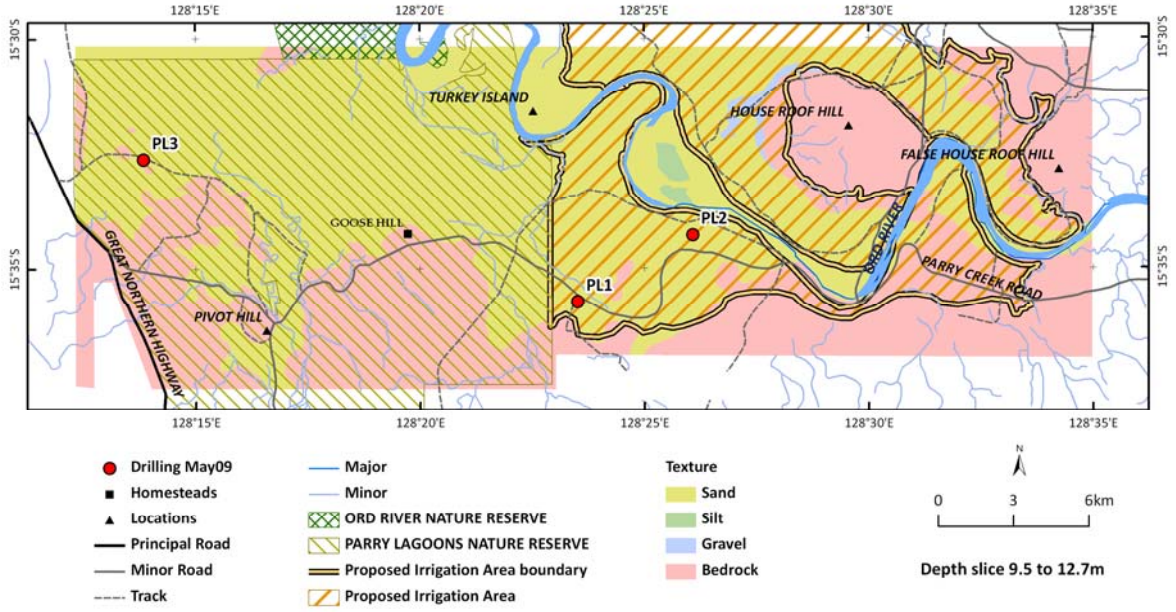

Figure 253: *Parry's Lagoon- Mantinea Plain- Carlton Hill. Lithology interpretation of conductivity depth slice 9.5 to 12.7m.*

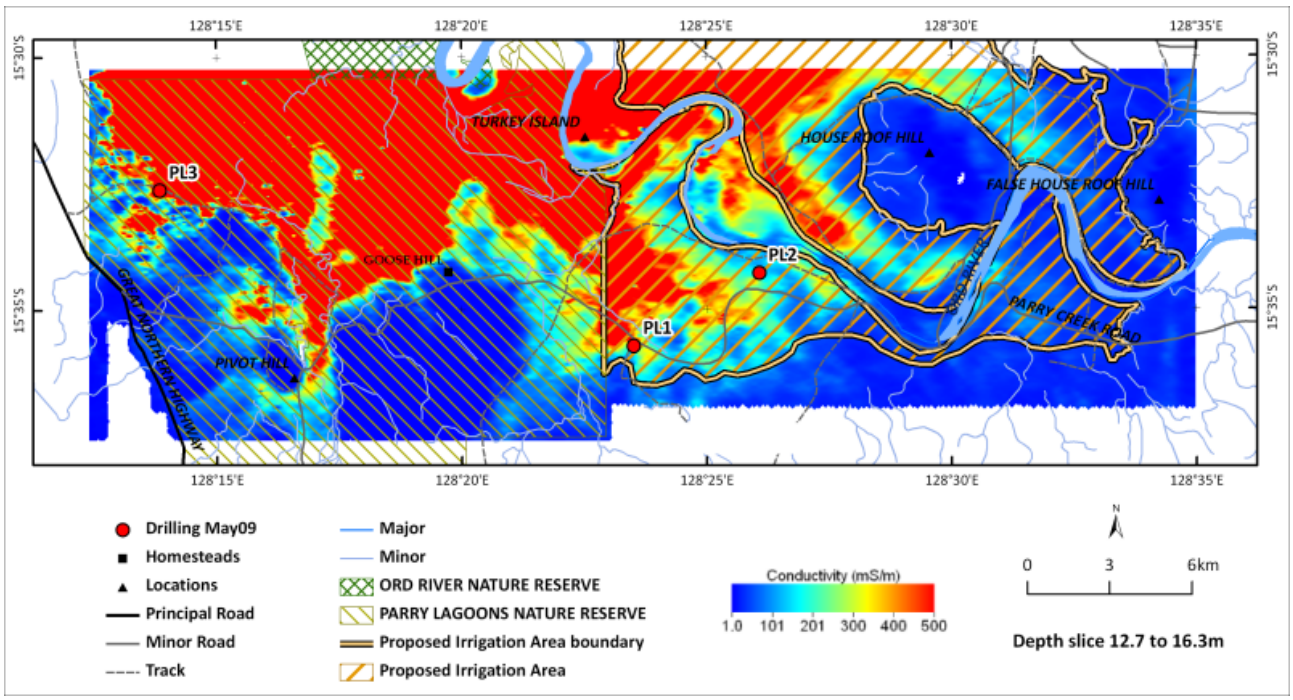

Figure 254: *Parry's Lagoon- Mantinea Plain- Carlton Hill Conductivity depth slice 12.7 to 16.3m*

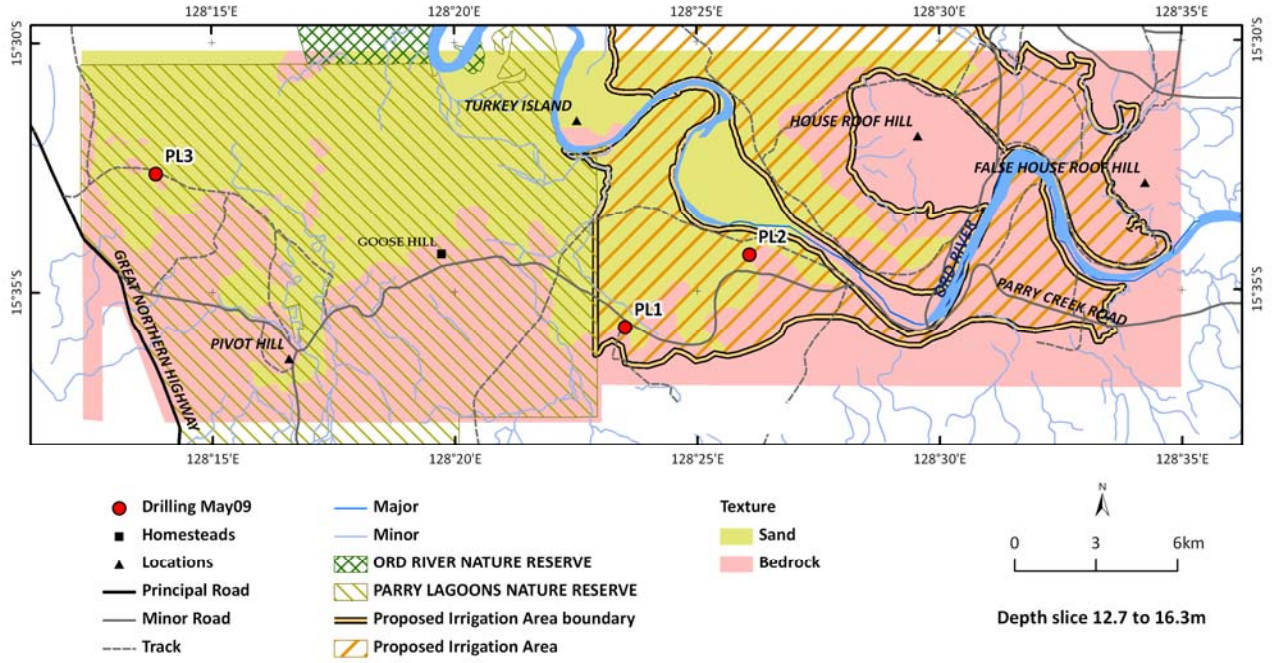

Figure 255: *Parry's Lagoon- Mantinea Plain- Carlton Hill. Lithology interpretation of conductivity depth slice 12.7 to 16.3m.*

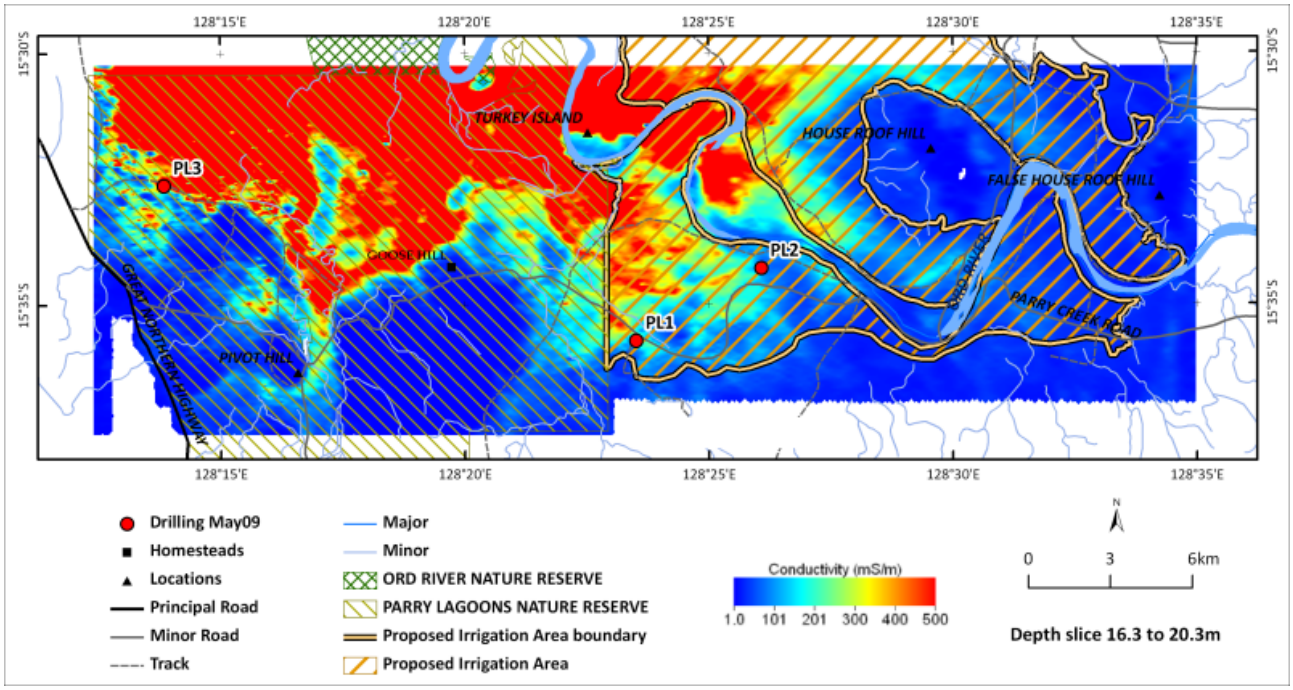

Figure 256. *Parry's Lagoon- Mantinea Plain- Carlton Hill. Conductivity depth slice 16.3 to 20.3m.*

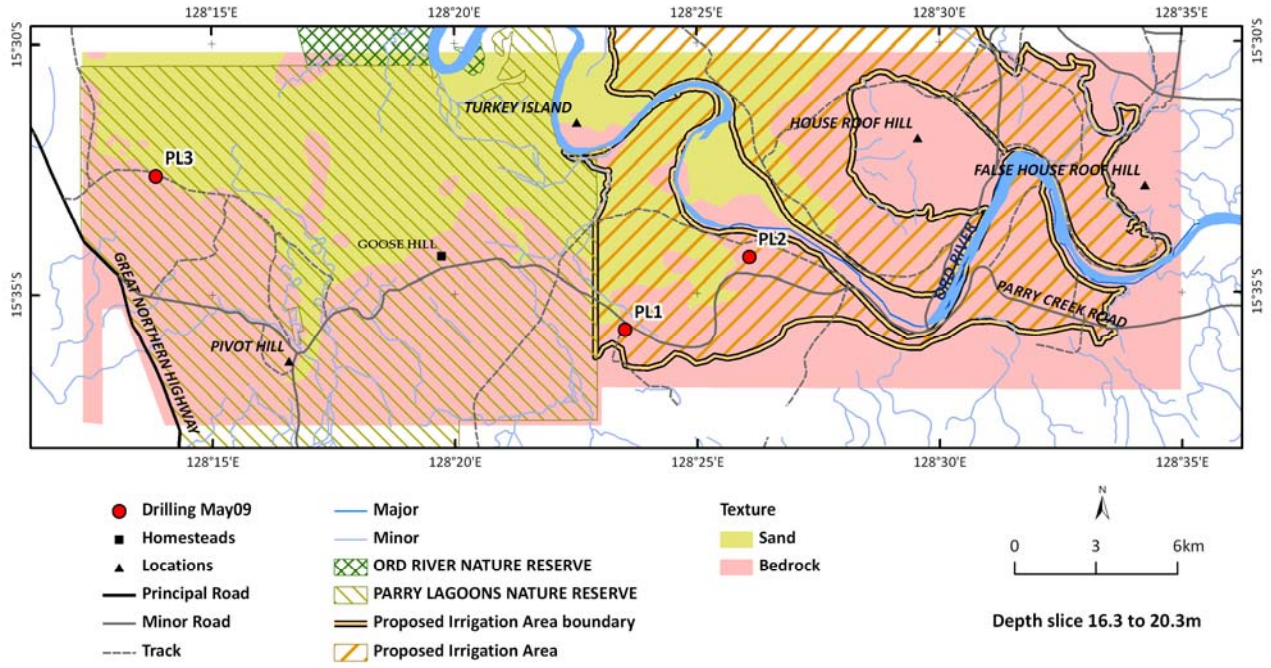

Figure 257: *Parry's Lagoon- Mantinea Plain- Carlton Hill. Lithology interpretation of conductivity depth slice 16.3 to 20.3m.*

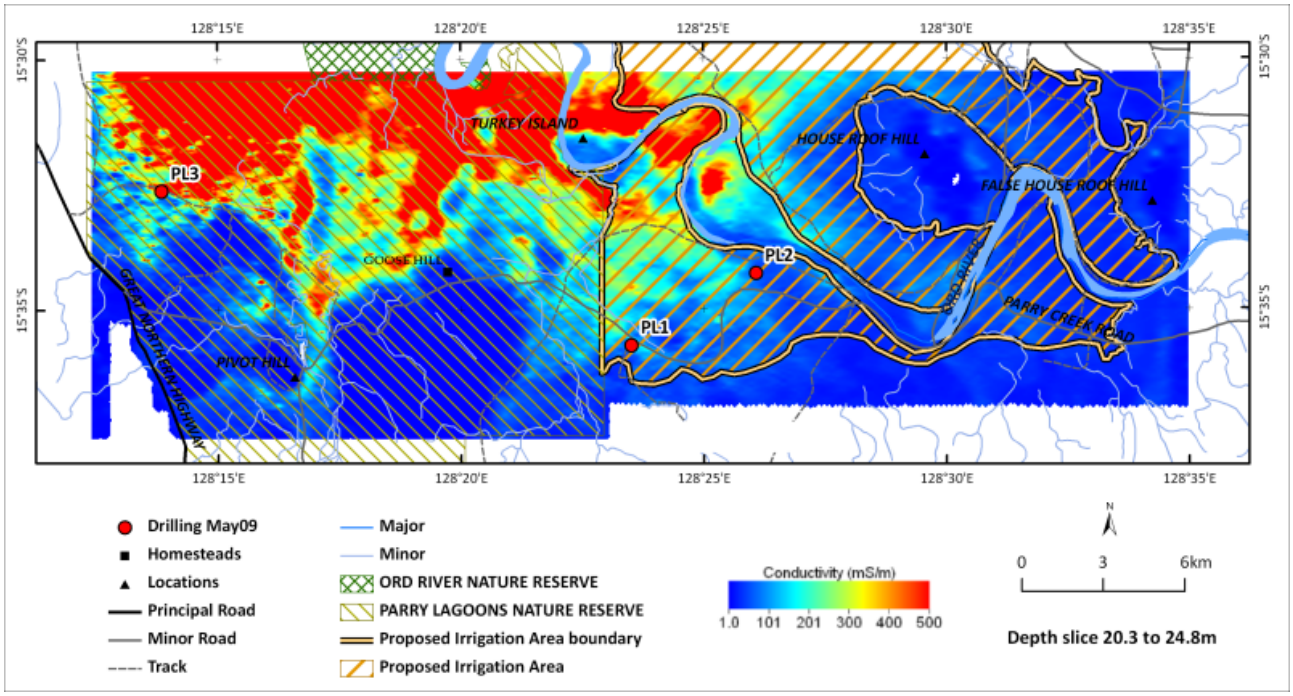

Figure 258: *Parry's Lagoon- Mantinea Plain- Carlton Hill. Conductivity depth slice 20.3 to 24.8m.*

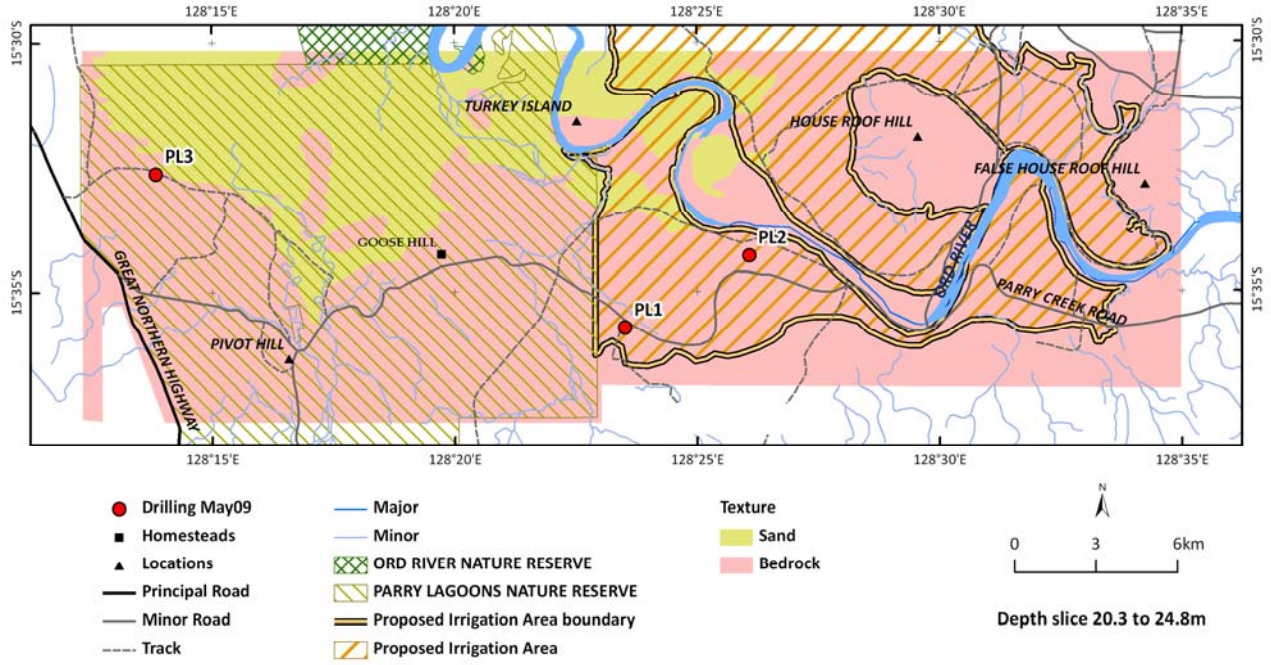

Figure 259: *Parry's Lagoon- Mantinea Plain- Carlton Hill. Lithology interpretation of conductivity depth slice 20.3 to 24.8m. .*

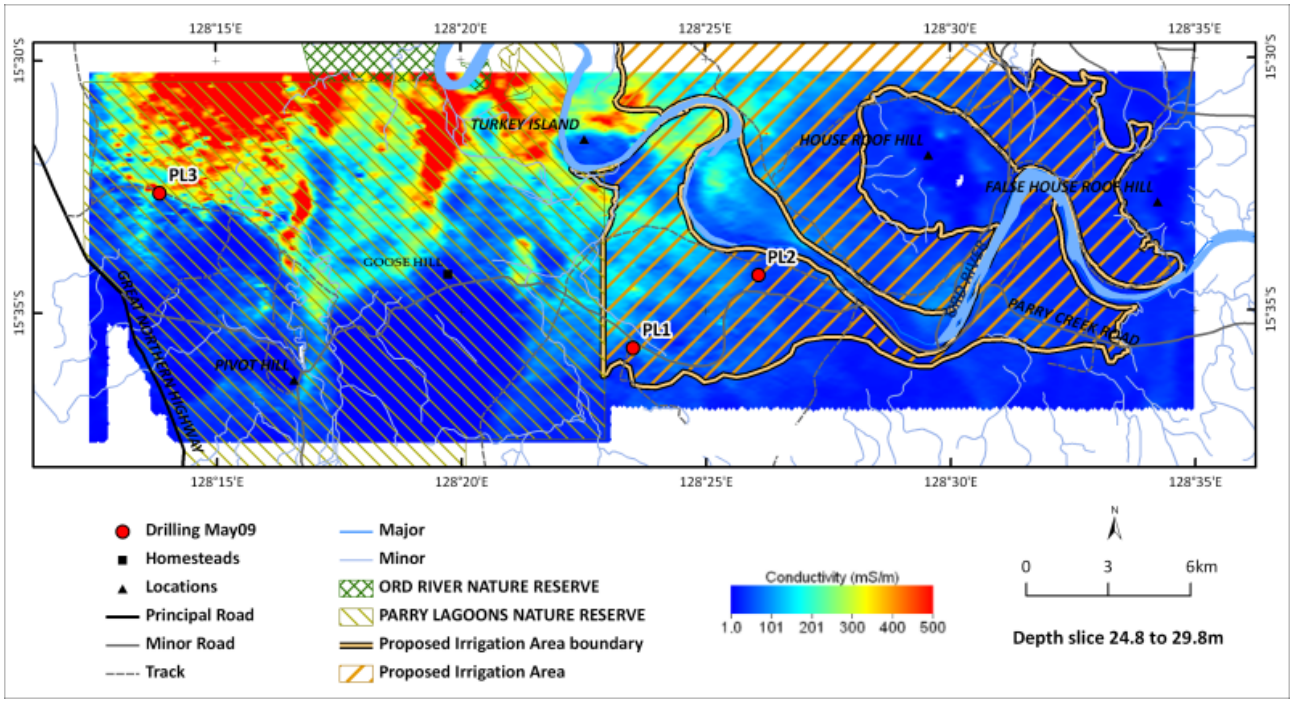

Figure 260: *Parry's Lagoon- Mantinea Plain- Carlton Hill. Conductivity depth slice 24.8 to 29.8m.*

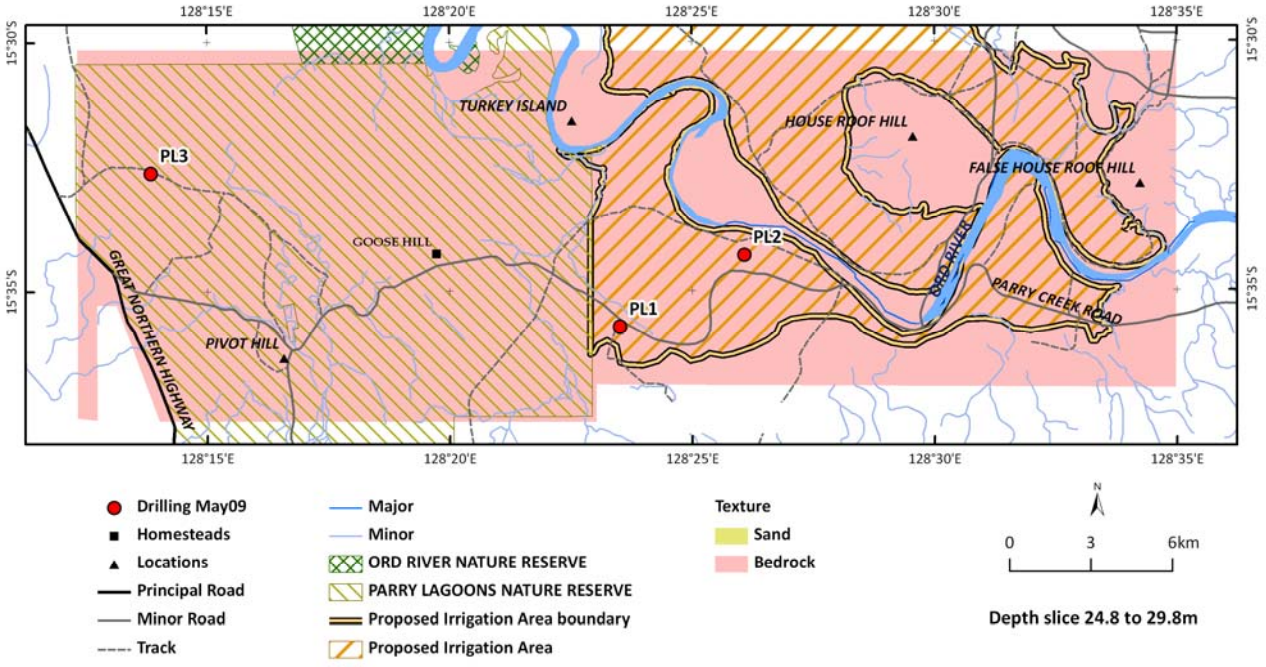

Figure 261: *Parry's Lagoon- Mantinea Plain- Carlton Hill. Lithology interpretation of conductivity depth slice 24.8 to 29.8m.*

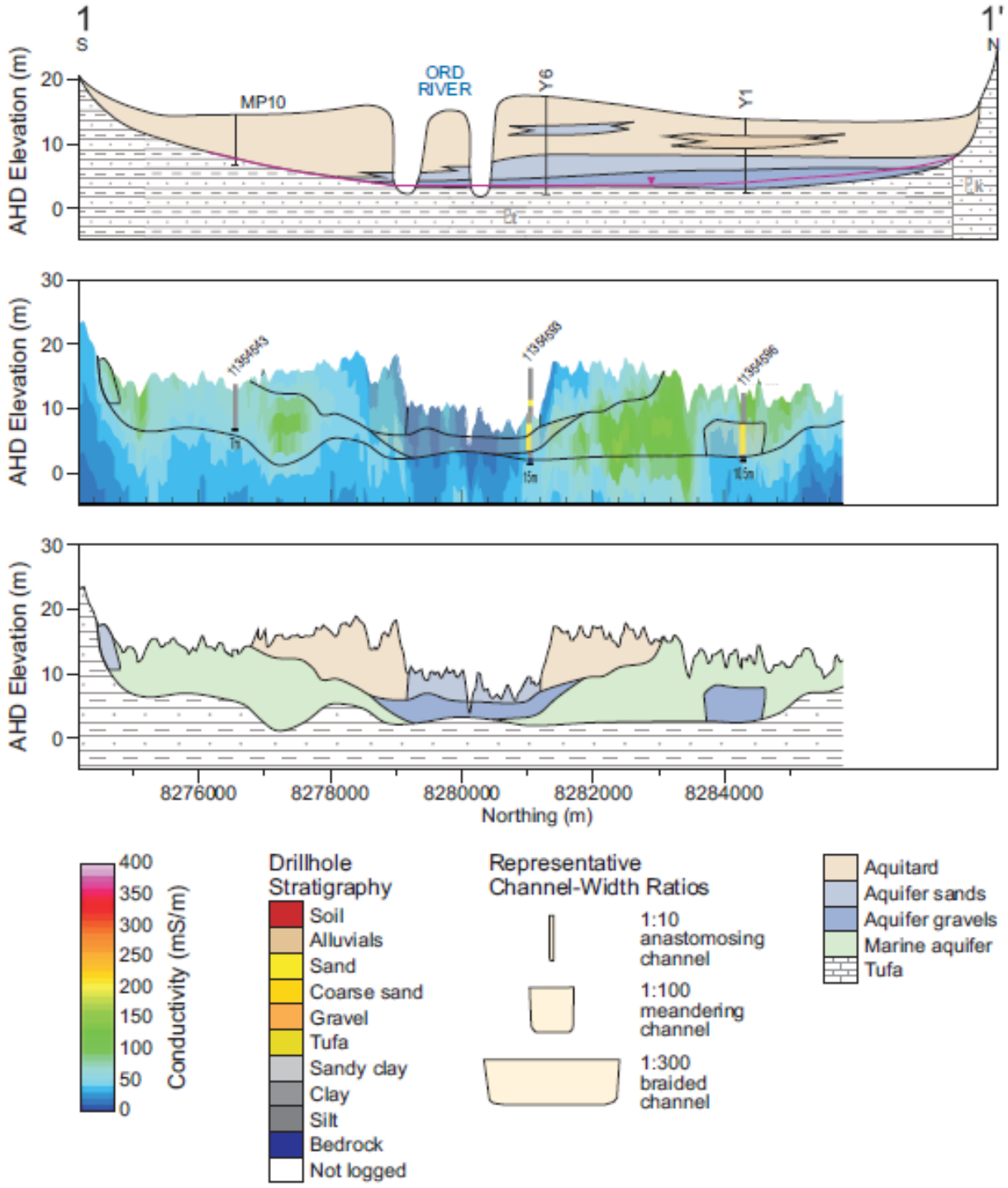

Figure 262: *Parry's Lagoon- Mantinea Plain- Carlton Hill cross section 1-1'. Top panel is cross-section from O'Boy et al., (2001); middle panel is synthetic AEM section showing drillholes colour coded for lithology and with lithology extent interpretation line work displayed; bottom panel is revised lithology interpretation produced in this study.*

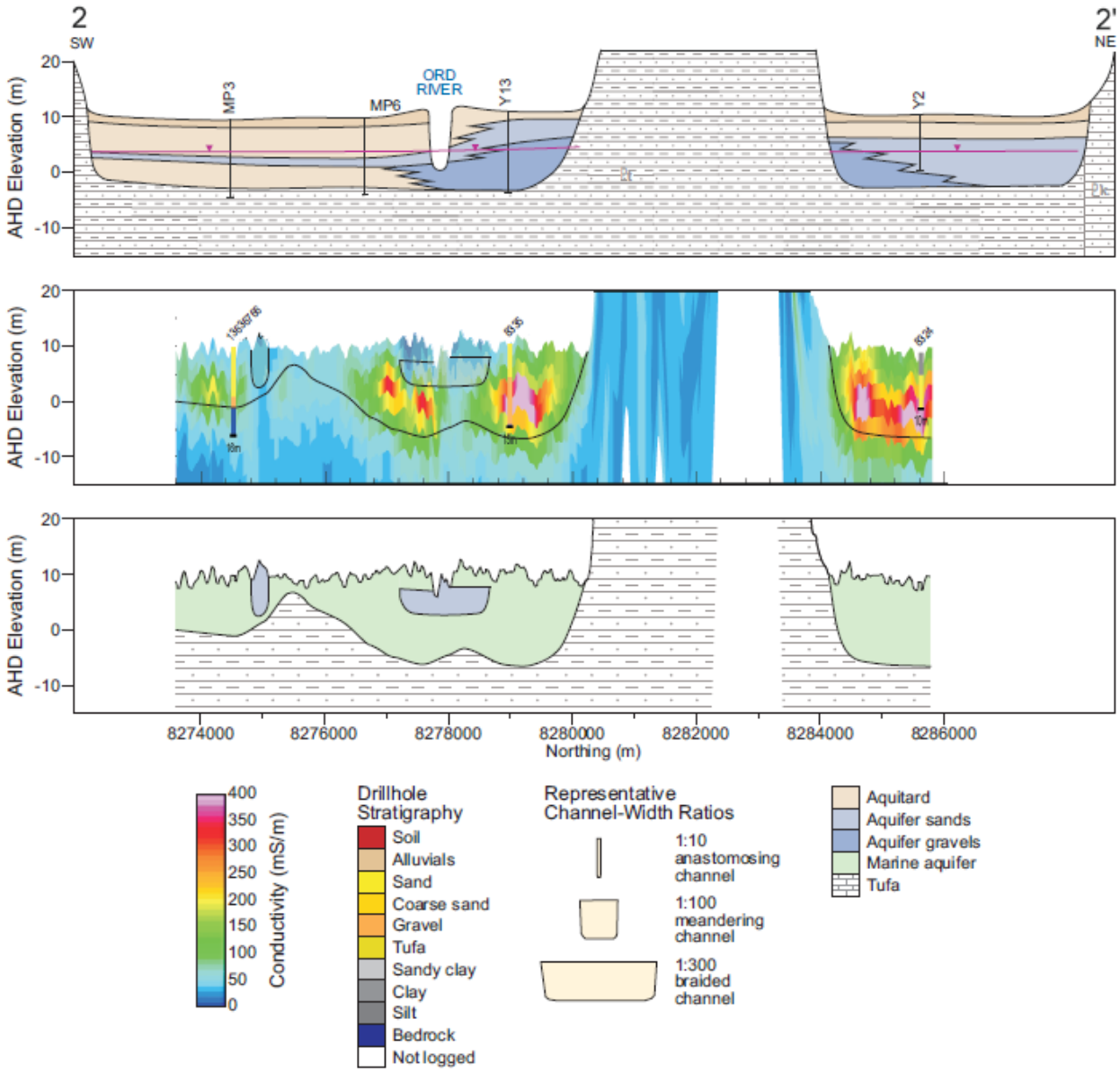

Figure 263: *Parry's Lagoon- Mantinea Plain- Carlton Hill cross section 2-2'. Top panel is cross-section from O'Boy et al., (2001); middle panel is synthetic AEM section showing drillholes colour coded for lithology and with lithology extent interpretation line work displayed; bottom panel is revised lithology interpretation produced in this study.*

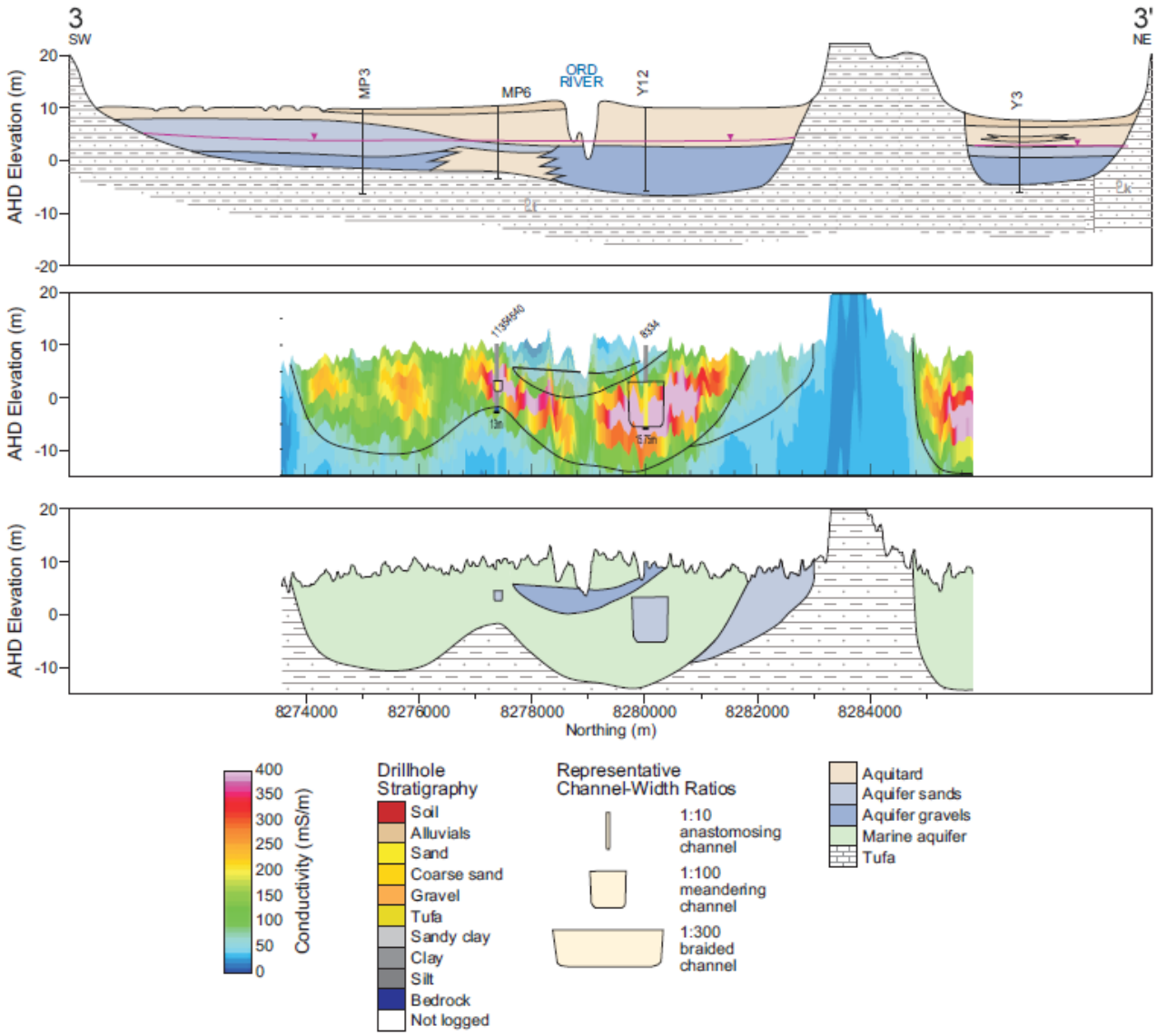

Figure 264: *Parry's Lagoon- Mantinea Plain- Carlton Hill cross section 3-3'. Top panel is cross-section from O'Boy et al., (2001); middle panel is synthetic AEM section showing drillholes colour coded for lithology and with lithology extent interpretation line work displayed; bottom panel is revised lithology interpretation produced in this study.*

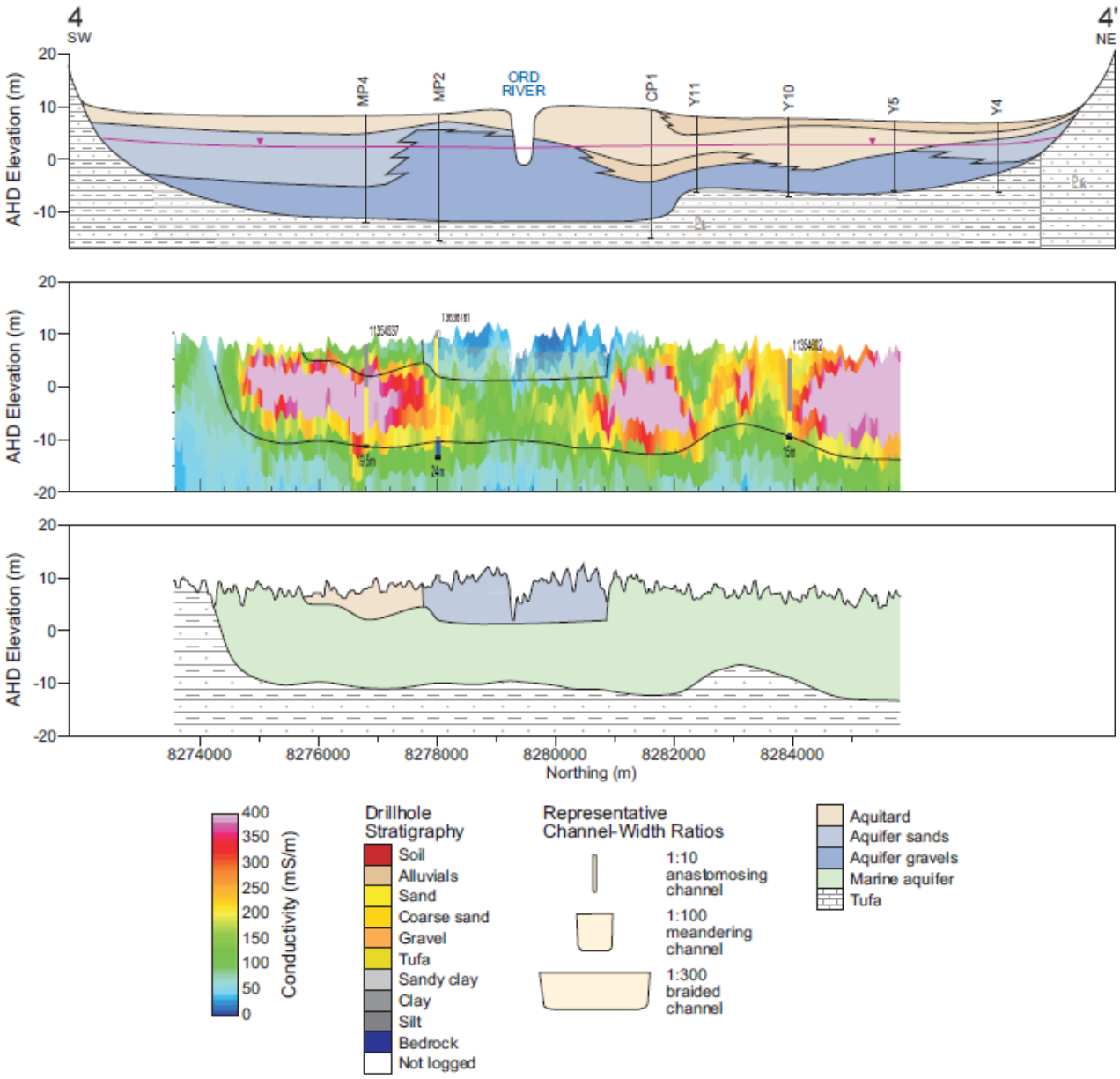

Figure 265: *Parry's Lagoon- Mantinea Plain- Carlton Hill cross section 4-4'. Top panel is cross-section from O'Boy et al., (2001); middle panel is synthetic AEM section showing drillholes colour coded for lithology and with lithology extent interpretation line work displayed; bottom panel is revised lithology interpretation produced in this study.*

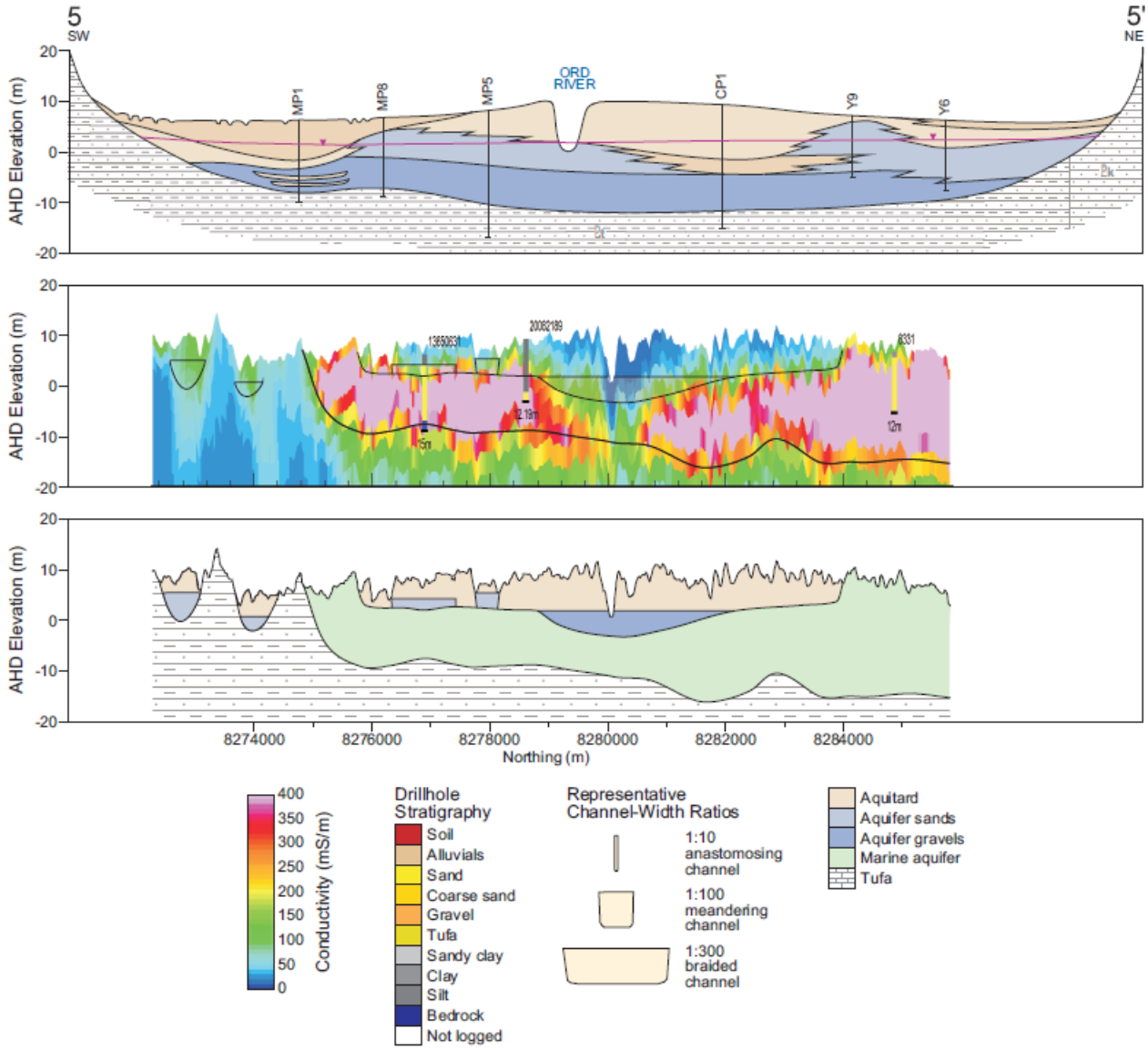

Figure 266: *Parry's Lagoon- Mantinea Plain- Carlton Hill cross section 5-5'. Top panel is cross-section from O'Boy et al., (2001); middle panel is synthetic AEM section showing drillholes colour coded for lithology and with lithology extent interpretation line work displayed; bottom panel is revised lithology interpretation produced in this study.*

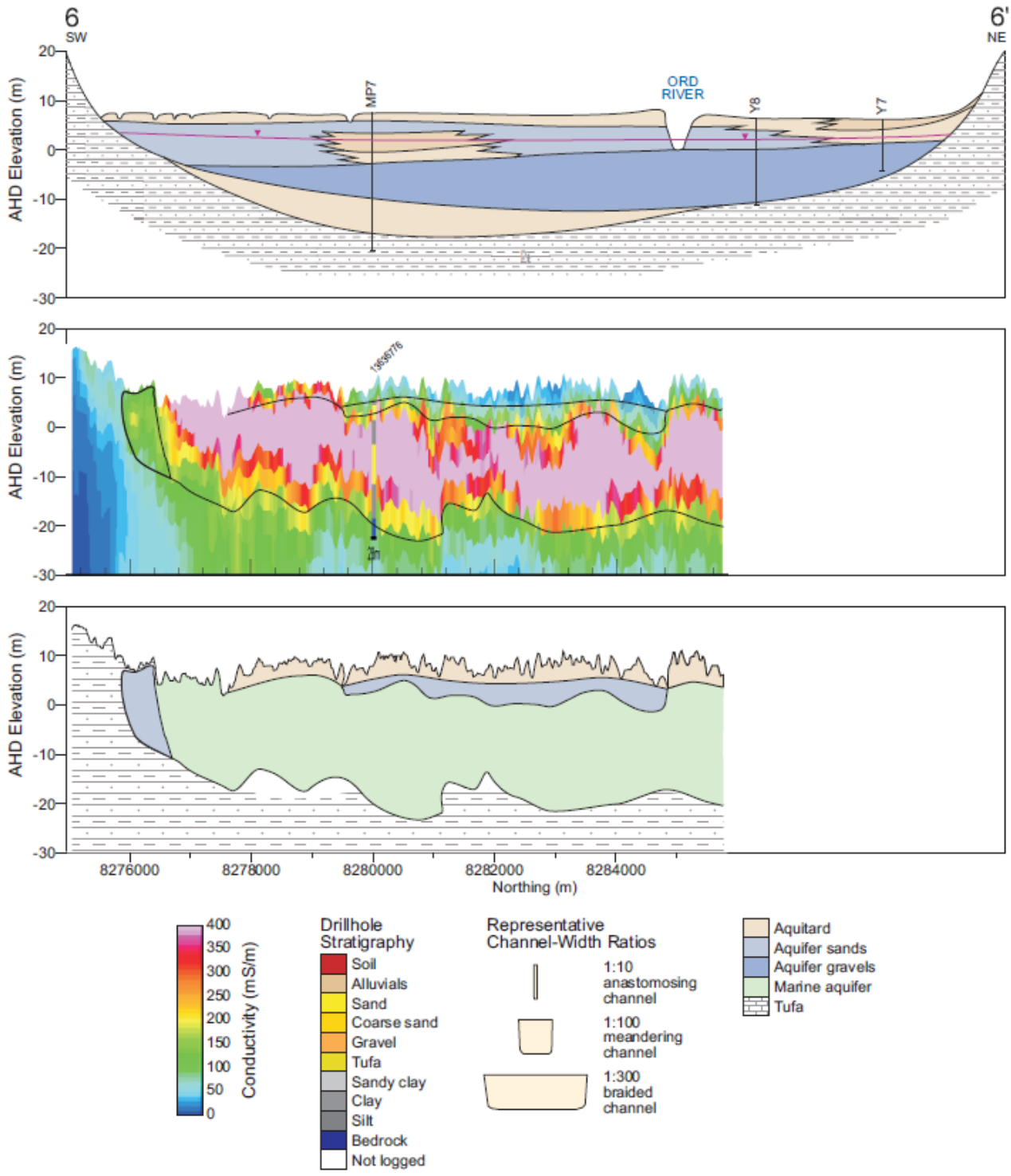

Figure 267: *Parry's Lagoon- Mantinea Plain- Carlton Hill cross section 6-6'. Top panel is cross-section from O'Boy et al., (2001); middle panel is synthetic AEM section showing drillholes colour coded for lithology and with lithology extent interpretation line work displayed; bottom panel is revised lithology interpretation produced in this study.*

Figure 268: *Marginal marine stiff pinkish sands overlying slightly weathered Wyndham Shale bedrock in PL2.*

Comparisons with previous studies

For each of the cross-sections, a comparison between the original cross-sections and the new interpretations, based on the AEM data, has been made. Similarly, comparisons with the original sand and gravel extent maps (O'Boy *et al*., 2001), are also made (Figure 269). It is evident that there is a significant difference in grain size estimates between the two studies, with the present study classifying the main aquifer as sand rather than gravel. The extent and thickness of the aquifers is also less in the present study, which also covers a larger area of the lower Ord floodplain to the west. Cross-section comparisons are documented below.

Section 1-1'

The correspondence between the original cross-section and the AEM data is reasonable concerning the position of the bedrock surface (Figure 262). There are two main differences. The first is the greater degree of irregularity of the bedrock surface. The second is the recognition that much of the valley fill is not alluvial, but marine in origin. Formed by the infilling of a coastal embayment. The Ord alluvium has been incised into this and the surface of the active floodplain is at a slightly lower level. This is the most landward extent of the coastal embayment fill and it is therefore only slightly conductive. A noteworthy feature is the highly resistant zone immediately adjacent to and underlying the Ord River. This is interpreted to be a combination of a flush zone and coarse-grained sediments. The greater width of the resistive zone on the south side corresponds to the presence of scroll bars. The amount of gravel in the original cross-section appears to be correct.

Section 2-2'

There is good correlation in the position of the bedrock surface between the AEM section and the original cross-section (Figure 263). The flush zone of the Ord River is quite narrow in this section and is also symmetrical. This is to be expected given the straight course of the river in this reach. The conductivity highs occur in coarse sediments round the base of House Roof Hill. In sections further to the west, this conductive zone is correlated with marine sediments. We therefore tentatively infer these conductive zones and the eastern most extent of these sediments. If correct, the presence of the sediments both north and south of House Roof Hill indicate that at one stage it may have been and island. The resistive zone immediately beneath the Ord River is attributed either to flushing of the marine sediments, or more likely, that the Ord fluvial sediments have incised completely through the marine sediments to bedrock. There is a small flush zone or coarse channel infill on the southern end of the AEM section. The original cross-section shows gravels as being confined to a coarse apron surrounding House Roof Hill. This is likely to be correct.

Section 3-3'

There is a good comparison between the AEM section and the original cross-section here in connection to the position of the bedrock surface (Figure 264). As in section 2-2', the flush zone of the Ord River is quite narrow and symmetrical. The conductivity highs correlated to the marine sediments encountered in drilling

are more extensive, and crop out on the surface on either side of the river. There occurrence corresponds with what has been mapped as an alluvial plain. This plain is very smooth and contrasts with the well-developed meander plain of the Ord. It is possible that the 'alluvial' plain may instead represent a coastal plain, although this remains to be confirmed. The presence of this marine unit was not detected in the original cross-sections, although marine components to the sediments were described in the original reports by Nixon (1997b) and were encountered in PL1 drilled nearby in the course of this project. The conductivity drops beneath the Ord River, this is interpreted to be due to flushing, and the Ord alluvium appears to have not cut completely though to bedrock. The amount of gravel is probably less than originally described and is likely to be confined to a basal lag to the marine sections and beneath the inset fluvial sediments.

Section 4-4'

Once more the comparison between the AEM section and the original cross-section is good as far as the position of the bedrock surface is concerned (Figure 265). Considerable similarities exist with the previous sections, a mostly flat bedrock surface buried by the sediments, the presence of a conductive sheet interpreted as being a sheet of marine sediments, and a resistive zone along the river. As in section 3-3', the amount of gravel actually present is probably less than shown and is likely to be confined to a basal lag to the marine sediments and as alluvial gravels beneath the inset fluvial sediments. The section here cuts through a series of meanders of the Ord River and the resistive zone is correspondingly much wider than in sections 2-2' and 3-3'. As seen in the sections, there is a flush zone beneath the river and once again, Ord alluvium appears to have not cut completely though to bedrock. The extent of the conductive layer is becoming greater the further west the section is located, supporting its explanation as a marine sediment.

Section 5-5'

The original interpreted cross-section corresponds moderately well with the new data in connection with the position of the bedrock surface (Figure 266). There are a number of differences however. Most of these occur on the southern end of the line, which was originally interpreted as a depositional surface but which the AEM data and the SRTM profile shows to be largely erosional. This is consistent with the geomorphic mapping which identifies this area as being a pediment. The conductive sheet of marine sediments continues to become thicker and more extensive. The Ord alluvium seems to be inset into the marine sediments but, although there is flushing beneath them, they have not cut all the way down to bedrock. This is consistent with the observations in the nearby borehole PL2. The amount of gravel actually present is probably less than originally shown as a number of drill holes (specifically in MP 5, 7, and 8) the gravel is more closely approximate to a coarse sand (Nixon, 1997a) Beneath the inset fluvial sediments there is a thick gravel section, however.

Section 6-6'

There is again a moderate correspondence between the AEM data and the original cross-section in connection with the position of the bedrock surface (Figure 267). The AEM data are dominated by the seaward dipping conductive marine sediments which are clearly pinching out against bedrock at the southern end of the line. The inset nature of the Ord alluvium is clearly shown by the surface resistive zone in the central part of the section and thickening to the north as the section moves closer towards the Ord River across a meander bed. We again infer that the gravel units (Figure 270) are finer grained than shown on the original section. Because the northern limit of the AEM section is terminated at the river the sub-river flush zone is not clearly visible.

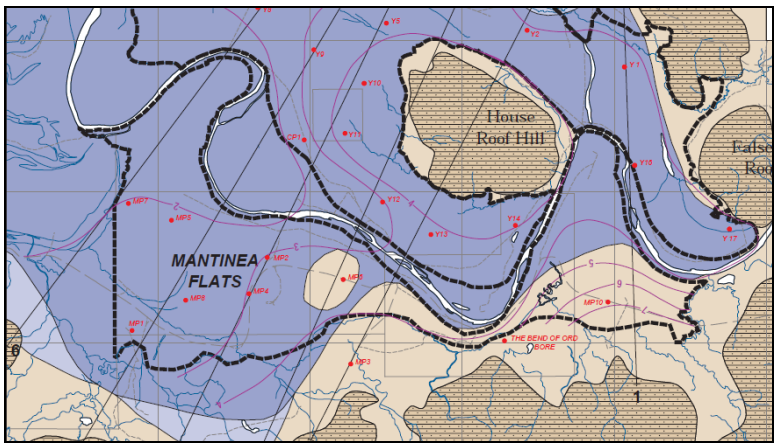

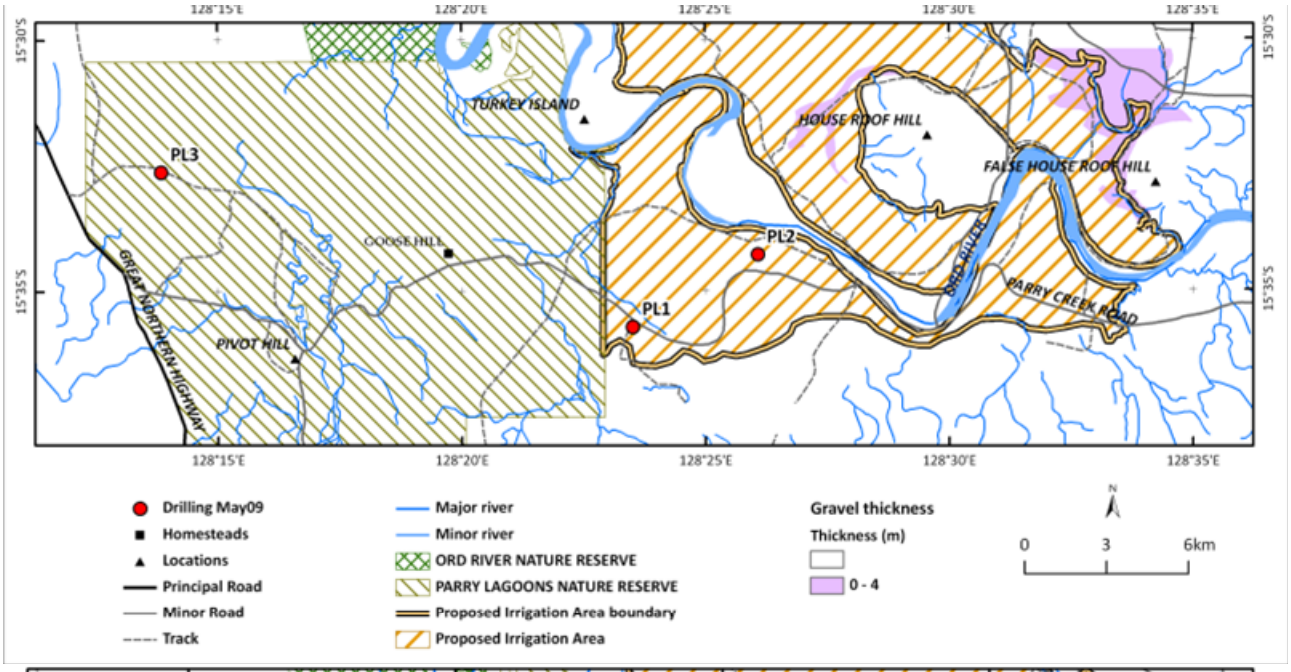

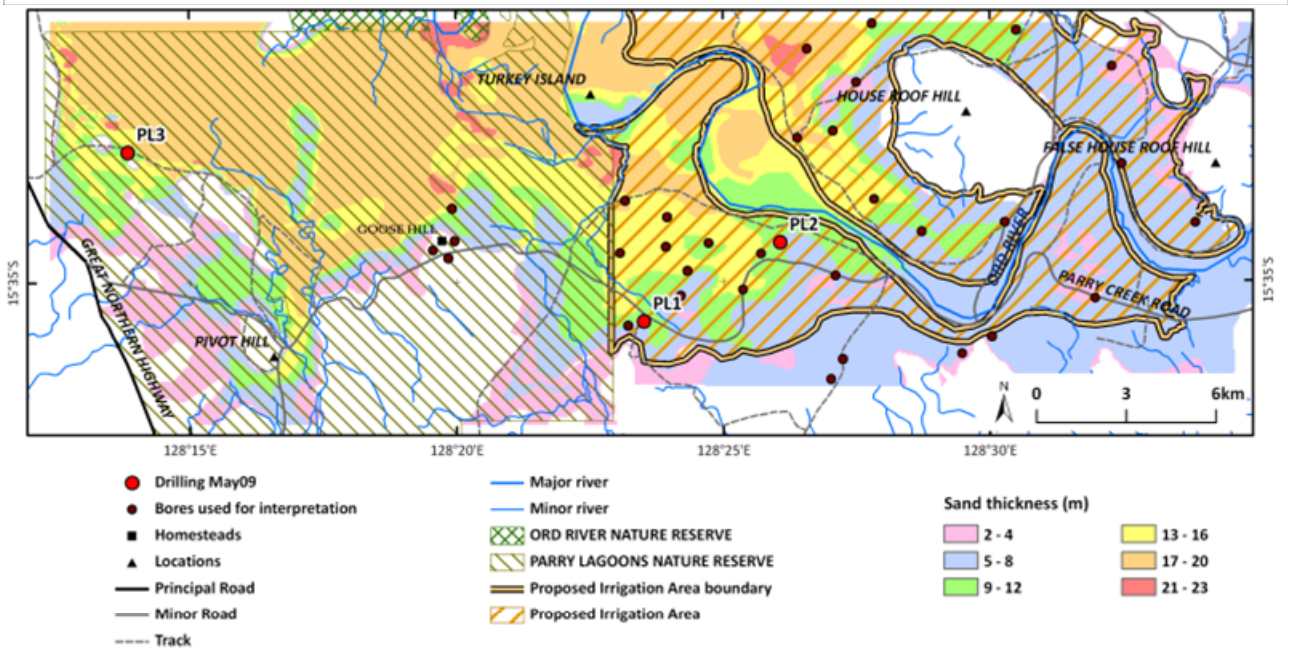

Figure 269: *Comparison of sand and gravel thickness in the Parry's Lagoon-Mantinea Plain- Carlton Hill area. It is evident that there is a significant difference in grain size estimates between the two studies, with the present study classifying the main aquifer as sand rather than gravel. The extent and thickness of the aquifers is also less in the present study, which also covers a larger area of the lower Ord floodplain to the west.*

Figure 270: *Coarse gravels of the Ord Succession in PL2.*

6.7 SUMMARY OF SEDIMENTARY FACIES ARCHITECTURE

Facies architecture suggests that there are three distinct sedimentary successions present. These include marine sediments in the Mantinea and Carton Hill area, indicated by the presence of marine fossils in the subsurface, older palaeovalley and palaeochannel sediments, indicated by induration including carbonates and iron oxides (see cross-sections in O'Boy *et al.,* 2001), and the youngest non-indurated sediments associated with the most recent courses of the Ord River.

The architecture of the flood plain sediments shares common features with other non-marine flood plain systems of northern Australia. One example is the lower reaches of much-studied Magela Creek system, in Kakadu National Park (Nanson *et al*., 1993, where the anastomosing channel and upstream sand-rich, bedrock-confined reaches resembles aspects of the subsurface architecture of the Ord.

Previously, Lawrie *et al.* (2006a, b) related the complex architecture beneath the Ord Stage 1 area to different fluvial depositional systems. Using data from Payenberg & Reilly (2003), Makaske (2001), and Gibling (2006). Lawrie *et al*. (2006a, b) suggested that that the thickness to width ratios of sands and gravel bodies in the subsurface could be used to differentiated the type of channel body that formed them. Braided, meandering and fixed channel (anastomosing) systems are typically 300, 100, and 10 times wider than they are thick, respectively.

On this basis, of the 10 cross-sections of O'Boy *et al*. (2001) re-examined in that report (sections A-A' through to I-I'), all but one showed the basal gravels with thickness to width ratios consistent with deposition in meandering gravel-bed channels. In that report Lawrie *et al.* (2006a) suggested that section F-F' was an exception, with a narrow fixed gravel-bed channel (see Nanson & Young, 1981). With AEM data now available along these sections, we believe that this interpretation is confirmed, with braided gravel-bed river facies making up the base of the section. In addition section F-F' also appears to have a basal gravel unit. Higher in the succession, at the depth where the buried valley widens abruptly at depths of less than 16 m (see previous chapter) the sand and gravel bodies narrow abruptly and consist of isolated palaeochannels surrounded by floodplain silt and clay facies. This again is consistent with what is observed in many valley infill successions (e.g. Nanson & Young 1981). This abrupt reorganisation in architecture greatly limits the potential for lateral groundwater flow at shallower depths except down the l axis of the palaeochannels.

A broadly similar architecture is noted beneath the Knox Creek and Weaber Plains. Gravels are confined to the deepest parts of the palaeovalleys. Once the valleys widen in the subsurface the gravel units narrow and

appear confined, if detected at all, to relatively narrow palaeochannels. The gravels at the base of the palaeochannel beneath the Knox Creek Plain are moderately indurated, no shallower gravels are evident in the AEM section above the abrupt widening of the palaeovalley at ~20 m depth below surface. As the palaeovalley extends across the border into the NT, where no AEM data exist, we suggest that the Keep River may represent the present expression of the fluvial system that deposited these gravels. A relatively thin fixed channel connection is predicted to occur between the Keep River and these deeper gravel units.

The architecture beneath the Weaber Plains appears more complex. The gravels on the northern slide fill local palaeovalleys and are probably well indurated and filled with water that is more saline. In the absence of core samples, we infer that these units are similar to those drilled beneath the Knox Creek Plain. The southern part of the Weaber Plains is underlain by sediments of the Ord palaeochannel system. These sediments consist of relatively narrow gravels at the bottom of the palaeovalley which we infer were deposited in a braided channel system. Once the deepest part of the valley was infilled and the alluvium spilled out across the plain the channel narrowed and became fixed, surrounded by fine-grained floodplain sediments. This reorganisation again occurs at a depth of ~20m below surface.

Comparison between the different river styles exited by the Ord River in its vertical evolution can be compared with those defined by Erskine *et al*. (2005) for northern Australian Rivers.

The initial gravel-rich aggregation of the sediments in the lover part of the valley fill (Ord, Knox Creek and Weaber Plains successions) corresponds to the bedrock-confined rivers (Type 2). One caveat is that the riverbeds were rich in gravels, a feature not seen in both bedrock confined rivers in northern Australia today, but rather only in Type 1 rivers (resistant bedrock rivers). This is because the lower parts of the Ord, Knox Creek and Weaber Plains successions were probably deposited during the early stages of a sea level rise, associated with high-energy stream flows and rapidly rising base levels so that the incised bedrock channels were infilled by aggrading coarse-grained sediments. This is not a situation that exists today and no direct counterpart to these rivers can be found in the present landscape.

The upper part of the Ord, Knox Creek and Weaber Plains successions correspond to the Type 4B and 4C rivers (laterally migrating and laterally stable unconfined rivers, respectively). The Weaber Plains and Ord succession were deposited by fixed channel rivers, as shown by the narrow palaeochannels present in the subsurface. The modern Keep River that deposited the Knox Creek succession is meandering, so the subsurface sediments are likewise interpreted to be the result of laterally migrating unconfined rivers. The exception to this is where the channels cut through a narrow bedrock feature, such as Cave Springs Gap, in these short reaches the rivers would have retained a bedrock-confined character.

The lower Ord River from where deposition resumes west of Tarrara Bar down to the beginning of tidal influence is a Type 4B river, laterally migrating and unconfined.

The recognition of these three successions has a number of implications for the hydrogeology of the project area. These include:

- The hydrogeological architecture is more complex than previously assumed. Not only is there complex depositional architecture to be considered (see Lawrie *et al*., 2006a, b), but there are major internal discontinuities in the sediments in the Stage two area, specially between the young coarse-grained alluvial sediments of the Ord Succession with the fine-grained marine units of Parry's Lagoon Succession in the west (Mantinea and Carlton Plains) and with the more indurated sediments in the east (Weaber and Knox Creek Plains).
- The different successions are likely to have quite different hydrological properties. The sands and gravels of the Ord Succession are the youngest and least indurated overall, and therefore are likely to have the greatest permeability. The sands in the Parry's Succession are much finer grained and better sorted than sands in the Ord and Knox Creek Successions and because of their marine origin are likely to show excellent lateral continuity. However they also have somewhat reduced permeability because of the presence of interstitial and possibly secondary clay and carbonate. The coarse-grained sands and gravels of the Knox Creek Succession, while likely to have a similar architecture to equivalent lithologies of the Ord Succession, will

have reduced permeabilities and numerous permeability barriers because of cementation by carbonate, clays, and iron oxides.

- The highly permeable units of the Ord Succession are likely to be laterally quite confined to the Ord palaeochannel beneath Weaber and Knox Creek Plains, and by extension out beneath the Keep River Plains, and to the meander plain of the modern course of the Ord in the Carlton and Mantinea Plains.
- The highly conductive sheet in the western area is likely to be evolved marine waters trapped in the Parry's Lagoon Succession sediments at the time of their deposition.
- The absence of a buried weathering profile means that there is minimal water or salt storage in the saprolith.

7 Hydrogeochemical Analysis

In this study, pore fluids were extracted from drillcore primarily to assist with calibration, validation and interpretation of the conductivity data derived from the AEM survey. No resources were allocated for a hydrogeochemical study of the groundwater, and the hydrogeochemical data presented in this section is presented largely to provide a baseline dataset for further analysis.

In this study, pore fluids were pressed from 12 cores (Figure 28), drilled to bedrock in the ORIA Stage 1 (Ivanhoe and Packsaddle Plains) and ORIA Stage 2 areas (Weaber, Knox Creek Plains, Mantinea and Parry's Lagoon). Samples were collected from different lithological units through the alluvial sequence, and the pore fluids analysed for EC, major cations, anions, pH and alkalinity (as HCO_3^-).

All the data are contained in the accompanying Appendix volume, and available on the project GIS (Apps *et al.,* 2009). The results show that pore fluid salinities (TDS) vary substantially across the study area, from low (< 200mg/l) to very high (70,000mg/l). The downhole salinity profiles also vary between the sites, with some showing salinity increases with depth, while others show a decrease or remain consistent with depth (Figure 271 a-c). To facilitate the interpretation of these salinity profiles, depths to the standing water level for the drill sites are summarised in Table 33.

Table 33: *Depth from natural surface to standing water level at the drill sites.*

Site	Depth from Natural Surface to Standing Water Level (m)
Ord 1	4.5
Ord 4	1.5
Ord 11	1.8
KP 2	11.5
KP 3	12.0
KS 1	8.8
PL 1	2.6
PL 2	5.6
PL 3	0.6

The salinity of pore fluids obtained from the cores at site Ord11 are low and remain consistent to 15m depth. In comparison, the Ord1 and Ord4 pore fluids are saline and brackish respectively at shallow depths, becoming fresh at 21m and 17m depth respectively (Figure 271a).

In the Keep River area, core salinity of KS1 is brackish at 5m depth and becomes fresh at 13m depth in the saturated zone. The salinity profile of KP3 is saline at shallow depths in the unsaturated zone, and becomes slightly brackish in the saturated zone (> 12m depth). In contrast, the salinity profile of KP2 is low in the unsaturated zone to the watertable, and becomes brackish from about 15m to 30m.

In the Parry's Lagoon area, the salinity profile of PL2 is the relative lowest (brackish) compared to PL1 and PL3, the latter having the highest salinity (55,000 mg/l to > 80,000mg/l). The salinity of PL1 shows a rapid increase from the unsaturated to below the watertable (2.6m depth) and remains consistently around 20,000mg/l from 3m to 11m. A shallow watertable is present at PL3 (0.6m depth) and the salinity at 1.5m is highly saline (~ 71,000 mg/l) and remains consistent to 7m, decreases to ~55,000mg/l between 8m to 12m before increasing to 86,000mg/l at 13m depth.

To aid in the interpretation of the pore fluid chemistry, pH profiles have been graphed for the aforementioned bores (Figure 272, b and c). The pH ranges from circum-neutral to alkaline (i.e. from ~6.5 to 9). In the ORIA, the pH ranges from ~7.5 to 8.5, with no distinct trend with depth, except for Ord11, which remain consistently around 8.2. The pH profile in the Keep River area ranges from 7.5 to ~ 9. The pH generally increases by 0.5 or 1 from the unsaturated to the saturated zones, and fluctuates slightly at depth. At the Parry's Lagoon area, the pH is neutral at shallow depths, and increases to 7.5 and 8 with depth.

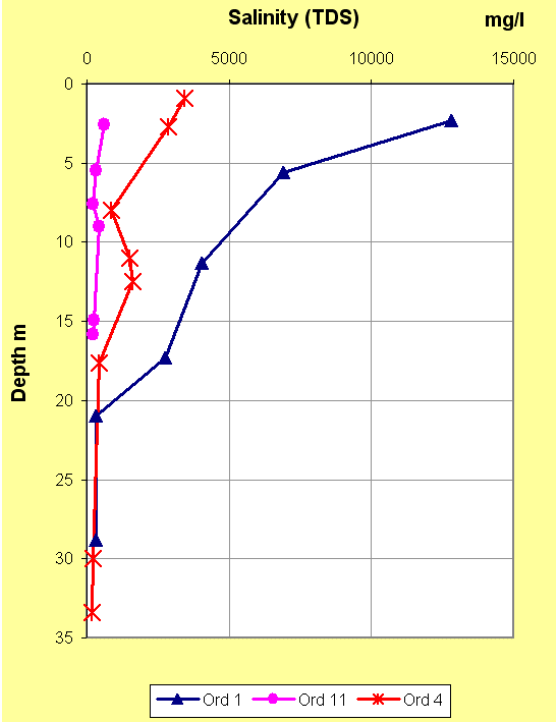

a. Salinity profiles of sedimentary cores in the stage 1 Ord Irrigation area.

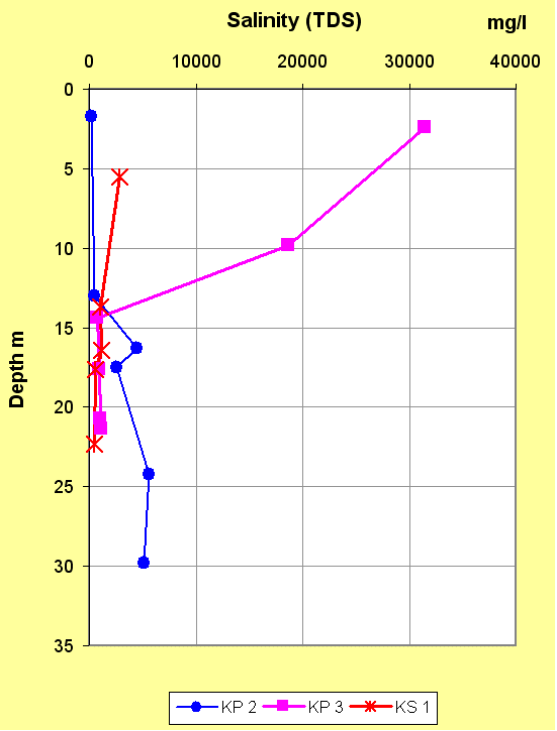

b. Salinity profiles of sedimentary cores in the Keep River area.

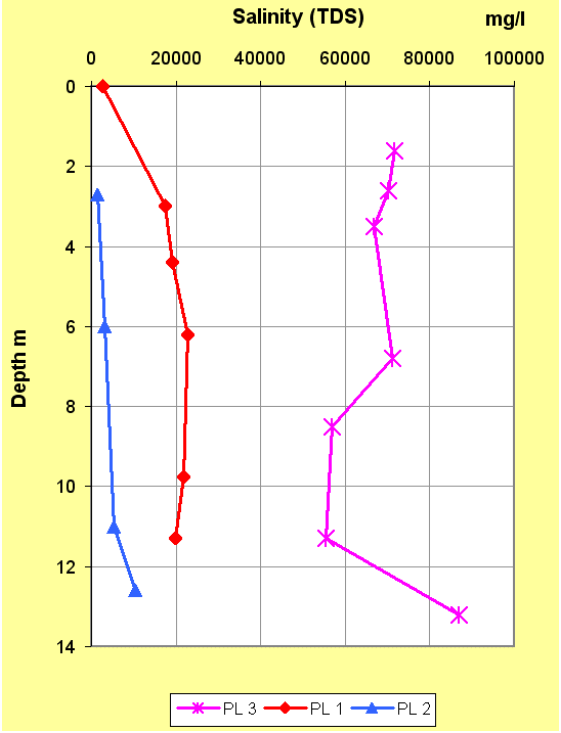

c. Salinity profiles of sedimentary cores in the Parry's Lagoon area.

Figure 271: *Salinity profiles of cores.*

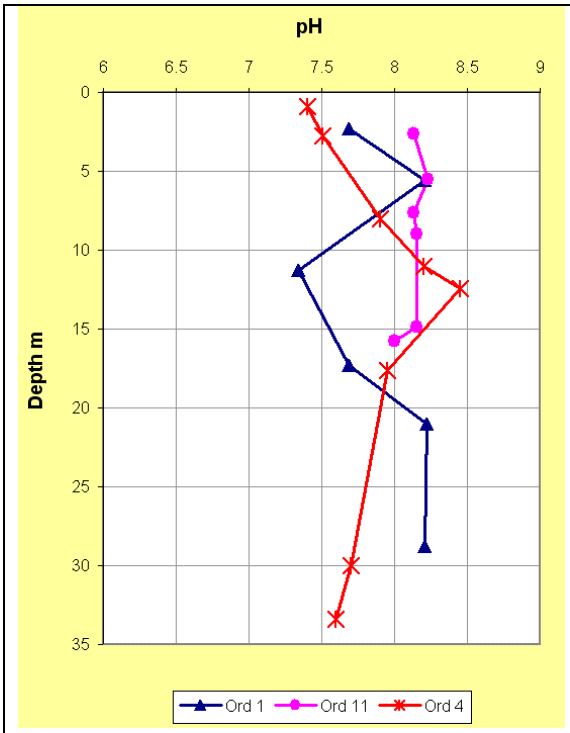

a. pH profiles of sedimentary cores in the stage 1 Ord Irrigation area.

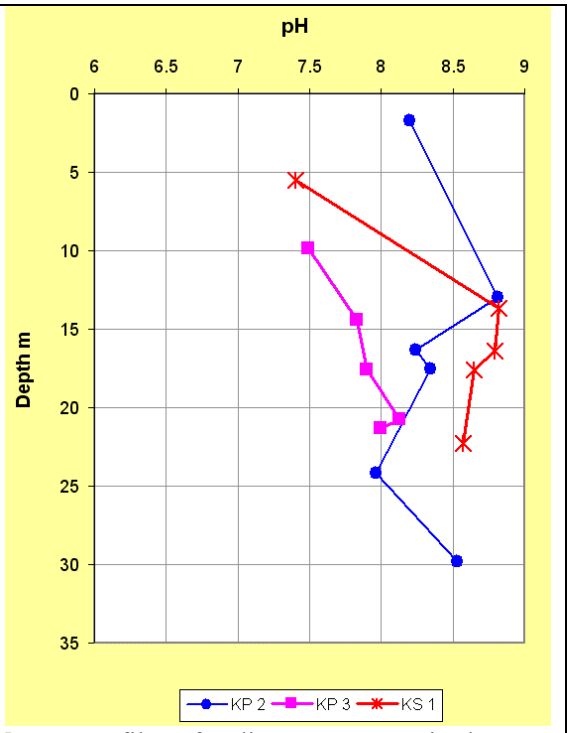

b. pH profiles of sedimentary cores in the Keep River area.

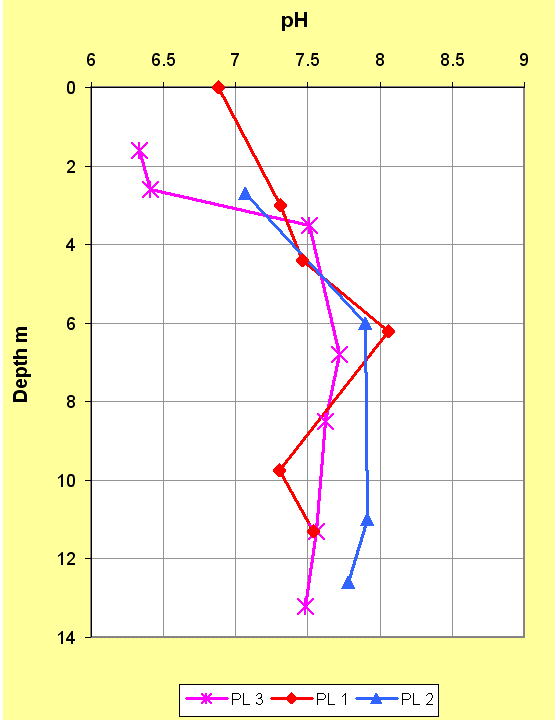

c. pH profiles of sedimentary cores in the Parry's Lagoon area.

Figure 272: *pH profiles from cores.*

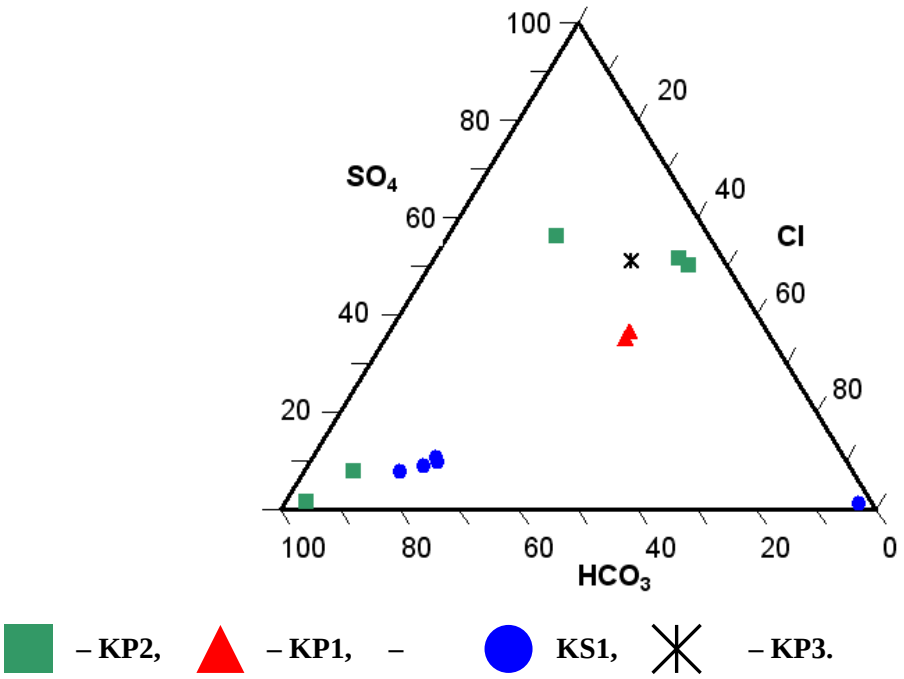

– KP2, **– KP1,** **–** **KS1,** **– KP3.**

Figure 273: *SO_4, Cl, HCO_3 plot from selected bores.*

The hydrogeochemistry of pore fluids from selected bores is shown in Figure 273. The sulphate rich waters are associated with silts and clay at deeper depth. The pH of the Water is alkaline (7.5 to 8.5), so the sulphate is not associated with palaeo-acid sulphate soils, probably due to dissolution of gypsum instead. KS1 and the shallower KP2 have higher bicarbonate ratio (Figure 273).

This pore fluid data can be compared with groundwater sampling and hydrochemical analysis previously undertaken regionally and within the ORIA. Smith & Price (2008) summarised pre-existing knowledge of salinity and groundwater chemistry in the ORIA. They observe that due to its coastal proximity, the ionic composition of rainwater in the irrigation area is likely to reflect the ionic composition of sea salt, which is predominantly (approx. 85 % by mass) sodium chloride (NaCl). In contrast, the surface waters from Lake Argyle, Lake Kununurra and the Ord River are bicarbonate type in anion composition but tend to have no dominant cation type (Figure 274). The enrichment of bicarbonate (HCO_3), sulfate (SO_4), calcium (Ca) and magnesium (Mg) relative to seawater is considered to be the result of geochemical interactions between rainwater and the soil, alluvium and bedrock of the Ord River catchment (Ali *et al*. 2002). In general, surface waters are fresh with small EC values of around 0.3 millisiemens per centimetre (mS/cm) or TDS (Total Dissolved Solids) values of around 180 milligram per litre (mg/l) (Salama *et al*., 2002).

Salama *et al*. (2002) mapped variations in groundwater salinity from fresh (<1,000 µS/cm) to the south near Lake Kununurra to saline (>30,000 µS/cm) to the north. Zones of fresh groundwater were interpreted to reflect recharge from rainfall, the Ord River or leakage from irrigation infrastructure. High groundwater salinities were associated with groundwater flow paths and discharge areas. Smith *et al*. (2007) also inferred irrigation accessions as a recharge mechanism, linking this with bicarbonate type groundwater (Figure 274a). Associated predominance of sodium (Figure 274b) was inferred to be due to dissolution of soil and aquifer minerals.

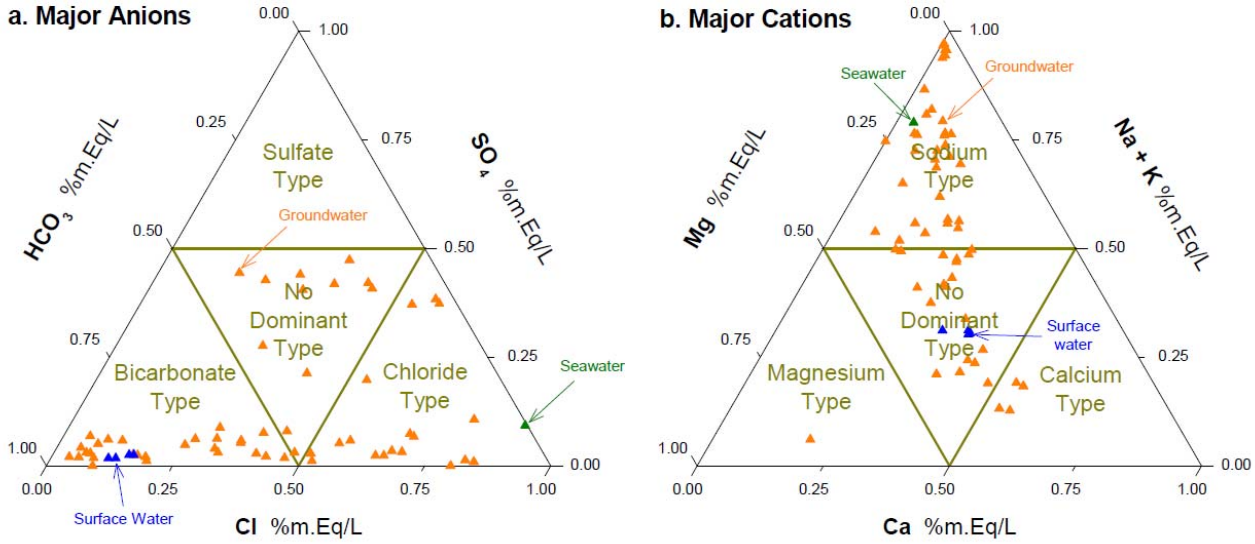

Figure 274: *Surface water and groundwater major ion compositions in the ORIA (Smith et al., 2007).*

Figure 275 plots the pore fluid chemistry on the basis of the ternary diagrams used in the previous studies. In these plots, the pore fluid analyses have been grouped into the key regions that the cored holes are located within. The soil salinity sites that are also plotted refer to 1:5 EC analyses that were undertaken at various locations in the study area. By comparing Figure 274 and Figure 275, the pore fluid chemistry shows similar trends to that seen in the historic groundwater sampling. This includes a dominance of sodium-chloride type pore fluids at Parry's Lagoon, sodium-bicarbonate chemistry in the Weaber South area and indications of sulphate enrichment in the Knox Plain.

The combination of major cations and anions for the pore fluids can be presented as a Durov plot (Figure 276) and a Piper diagram (Figure 277). These show the variability of the hydrochemistry both between and within the various areas of interest. This complexity can relate to mixing of various source waters (such as direct rainfall recharge, irrigation accessions and/or river leakage), combined with differences in aquifer mineralogy and resulting dissolution products. Overall, it looks like the Parry's Lagoon-Mantinea Plain-Carlton Hill pore fluids are Chloride (seawater) type, but Weaber Plain is Na-HCO_3 type. This probably reflects the dominance of seawater intrusion in the former area, and with water-rock interactions and a complex geology beneath the Weaber Plain responsible for the observed pore fluid chemistry. Further analysis of the hydrogeochemistry was outside the scope of this study.

In summary, there are significant differences in pore fluid compositions across the project area. While there is a suggestion of mixing of various source waters evident from distribution patterns within individual boreholes and more generally within areas, further hydrogeochemical study is required to investigate this complexity and the underlying processes.

It is recommended that an integrated approach be taken in terms of:

- The pore fluid analyses from this study be combined with historic groundwater sampling;
- The hydrochemistry of source waters (such as rainfall, irrigation supply and drainage, river and estuarine water) be better characterised, both by analysis of existing water quality data, or by additional data acquisition through specific water sampling programs. This is important to define end-members to assess groundwater chemistry variations on the basis of mixing ratios;
- Incorporating other hydrochemical analyses of groundwater samples such as age dating techniques (e.g. tracers such as chlorofluorocarbons) to obtain a better understanding of groundwater dynamics;
- Installation of time series monitoring of hydrochemistry such as downhole logging of groundwater electrical conductivity or the routine measurement of the stable isotope composition of aggregated monthly rainfall samples. Such monitoring can also provide insights into groundwater dynamics, in particular the understanding of recharge processes.

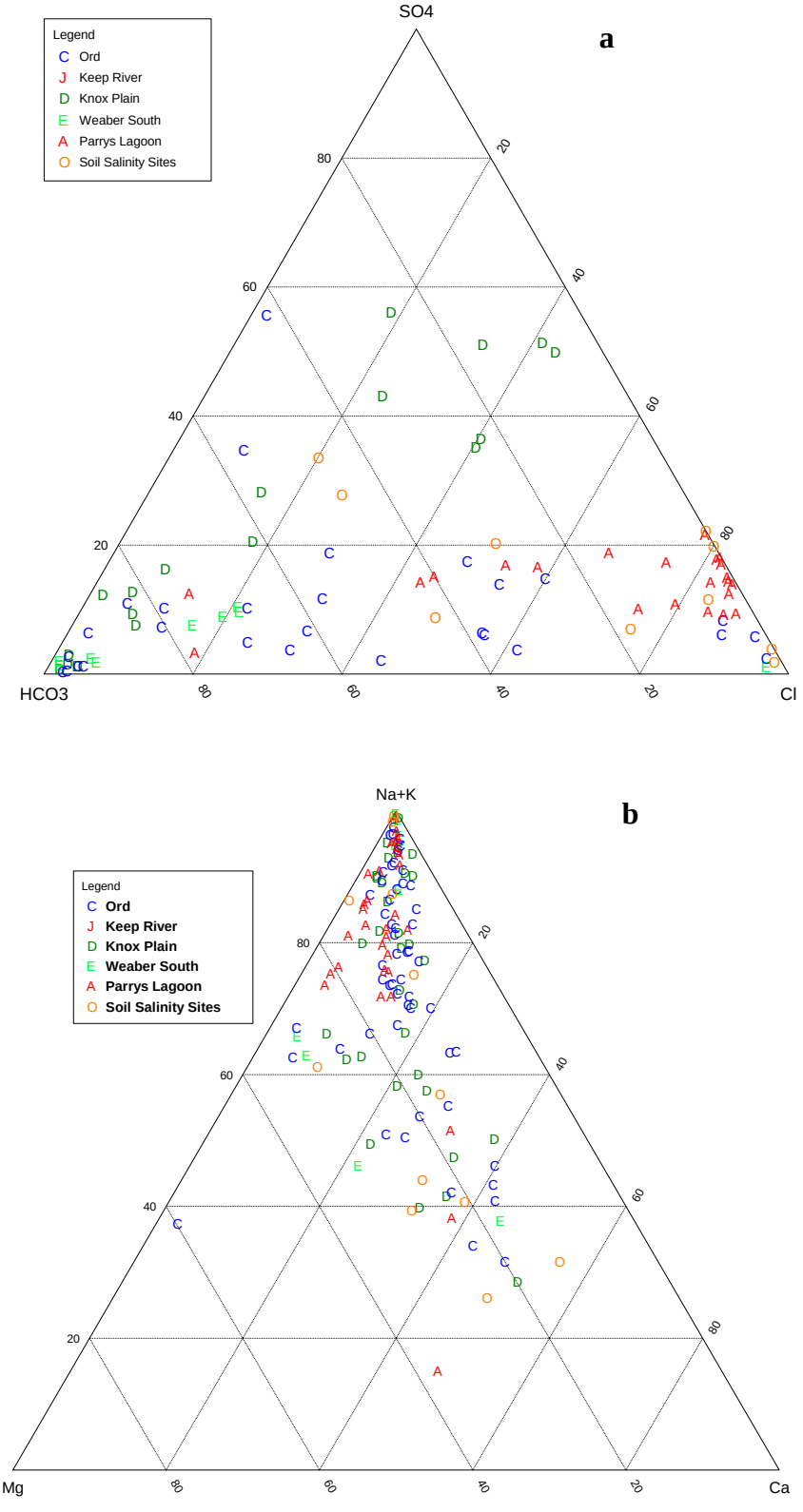

Figure 275: *Ternary diagrams of (a) major anions and (b) major cations for pore fluids from cored geological samples.*

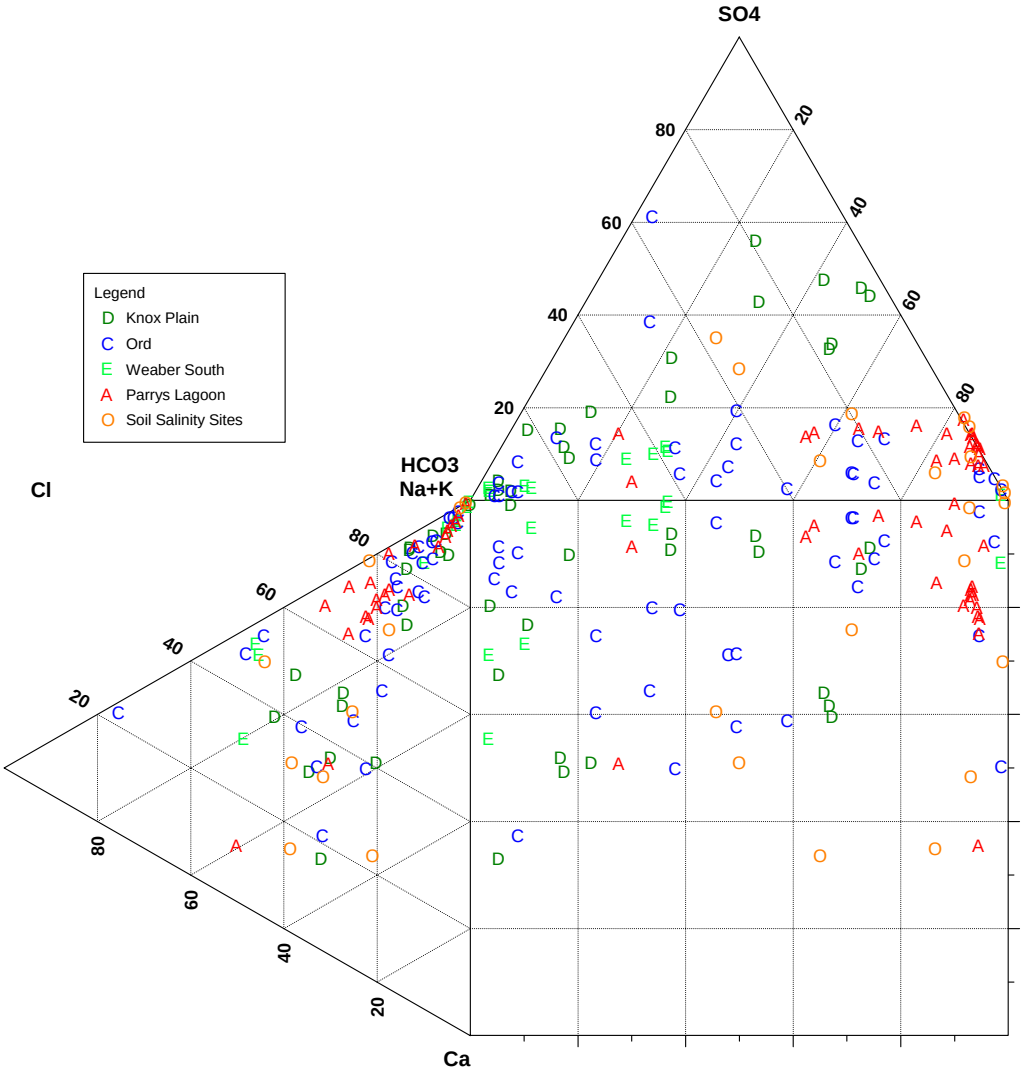

Figure 276: *Durov plot of pore fluid analyses from sedimentary cores.*

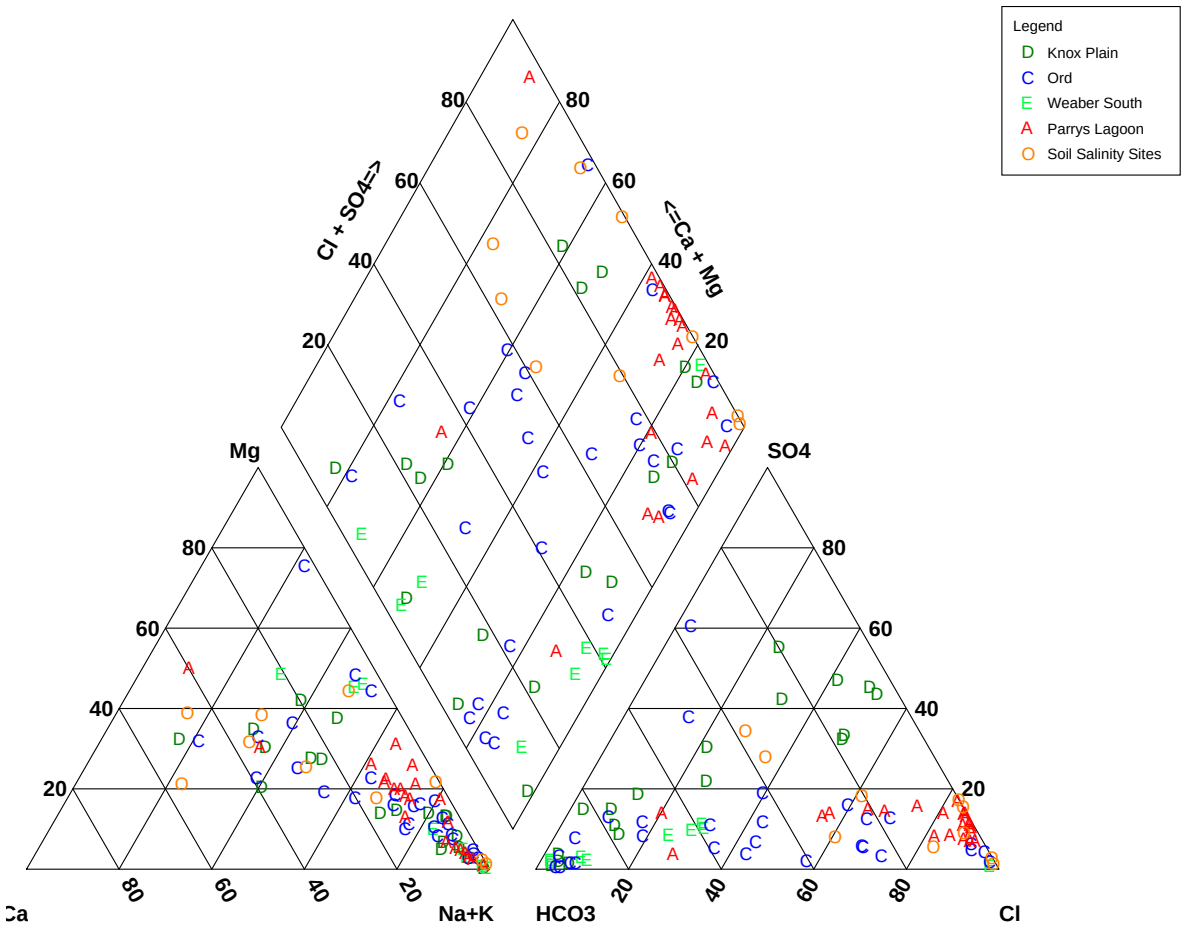

Figure 277: *Piper diagram of pore fluid analyses from sedimentary cores.*

8 Addressing Specific Salinity, Groundwater and Land Management Issues

8.1 PREVIOUS STUDIES AND APPLICATIONS OF AEM FOR SALINITY MAPPING AND MANAGEMENT

A review facilitated by the Australian Academy of Sciences and the Australian Academy of Technological Sciences and Engineering for the Australian Federal Government's Natural Resource Management Ministerial Council in 2005 found that airborne geophysical techniques, combined with ground and borehole control, are important tools in understanding salinity and hydrology at depth at a variety of scales. The review also concluded that the only broadacre, remote sensing technique that can detect and resolve salinity in the sub-surface deeper than the root zone is airborne electromagnetics (Spies & Woodgate, 2005).

A wide range of AEM systems and acquisition platforms are available (Allen, 2005; Spies & Woodgate, 2005), and the technology is now recognised as mature, capable of mapping complex salinity relationships in a variety of landscape settings. AEM systems cover large areas rapidly and generally penetrate to significant depths, often providing important broader contextual information on hydrogeological systems. AEM systems also provide a logistical advantage in being able to acquire data systematically over difficult or inaccessible terrane. Borehole EM technologies provide important constraints on sub-surface salinity distribution and are an essential component in calibration and validation of AEM inversions, ground-EM and in-river EM systems are particularly effective at mapping near-surface salinity with high resolution (Allen, 2005; Spies & Woodgate, 2005).

In Australia, three major national programs have funded AEM projects for salinity mapping and management. These are: 1997-1998 National Airborne Geophysics Project (NAGP; George *et al*., 1998; George & Woodgate, 2002); 2002-2005 South Australian Salinity Mapping and Management Support Program (SMMSP e.g. Walker *et al.*, 2004); and 2005-08 Community Stream Sampling and Salinity Mapping Project (CSS&MP; e.g. Lawrie *et al*., 2008, 2009a; Edwards & McAuley, 2008). Significant advances in all aspects of AEM technology selection, survey design, data processing inversion, data interpretation and integration, and product generation have been witnessed as a consequence of these programs.

The earlier projects utilising AEM technologies were highly variable in their success, and acclaimed for the new knowledge generated rather than their effectiveness in delivering outcomes for salinity management (Green & George, 2002; George & Woodgate, 2002). Moreover, while AEM datasets provide unparalleled insight into regolith architecture and the distribution of salt stores, many earlier surveys had very general exploratory objectives, and had no clearly defined pathways to deliver management outcomes from these data (George *et al*., 2003).

George *et al*. (2003) identified a number of steps required to ensure that airborne geophysical surveys are used appropriately to produce cost-effective salinity management outcomes. Previous failures were attributed to an over-emphasis on technology-led approaches to salinity mapping and management, and a lack of clear problem definition and inadequate prior knowledge or subsequent effort taken to understand the functional elements of each landscape. George *et al*. (2003) also emphasised the need to match the appropriate technology to the salinity management issues to be addressed, and articulated a phased methodology to achieve a successful management outcome using airborne geophysics.

Based largely on the lessons articulated by George *et al.* (2003), AEM surveys have increasingly been designed over the past 6 years to address specific land and water management questions within the context of broader natural resource management strategies (Walker *et al*., 2004). Using this approach, a number of AEM surveys have been shown to be cost-effective in addressing salinity and land management issues (Lawrie *et al.,* 2003a, b, 2008, 2009a, b; Walker *et al.,* 2004; Munday *et al.,* 2007, 2008). Overall, this approach has played a crucial role in demonstrating the relevance of AEM-based information products for salinity, groundwater and broader land and environmental management (Munday *et al*., 2003 a, b; Paine, 2003; Walker *et al*., 2004; Chamberlain & Wilkinson, 2004; Lawrie, 2006b; Cresswell *et al*., 2007; Munday *et al*., 2007, 2008; Lawrie *et al*., 2009a, b). Successful outcomes from these projects have been attributed not

just to advances in science, technology, project design, the calibration and validation of AEM data, and development of customised information products (George *et al*., 2003; Spies & Woodgate, 2005), but also to a high level of consultation between scientists, decision makers and local community groups at all stages in project design, implementation, delivery, knowledge transfer and follow-through (Walker *et al*., 2004).

More specifically, appropriately designed and interpreted AEM-based products have contributed the design of salt interception schemes (Munday *et al*., 2004); the development of saline groundwater disposal options (Munday *et al*., 2008b); and for underpinning strategies to target environmental water flows for sustaining floodplain biodiversity (Walker *et al*., 2004; Munday *et al*., 2006, 2007; Spies & Woodgate, 2005). AEM has also been used to map and predict salinity risk in floodplain environments (Chamberlain & Wilkinson, 2004; Lawrie *et al*., 2008; Munday *et al*., 2008c); map salt water intrusion (Fitterman & Deszcz-Pan, 1998; Munday *et al.,* 2007); and informing irrigation re-zoning and the apportionment of salinity credits (Chamberlain & Wilkinson, 2004; Cresswell *et al*., 2007; Munday *et al*., 2005). Airborne surveys have also been used to map fresh groundwater resources within otherwise salinized landscapes (George *et al*., 1998; Reid *et al*., 2008; Edwards & McAuley *2008*; Lawrie *et al.,* 2009b).

The benefits from AEM surveys are maximised when these technologies are employed within multi-disciplinary, systems-based approaches to the analysis of problems and the development of customised interpretation products (Dent *et al*., 1999; Lawrie *et al*., 2000; Lawrie *et al.,* 2003a, b; Spies & Woodgate, 2005). Systems-based approaches incorporate an understanding of landscape evolution and scale, utilise modern investigative approaches to the conceptualisation of aquifer systems, and incorporates data on water, salinity and vegetation dynamics to provide key constraints on aquifer systems (Lawrie *et al*., 2000, 2008, 2009a).

Over the past 5 years, a staged approach to survey design combined with forward modelling studies have ensured that appropriate AEM technologies are selected to match the target objectives (Green & Munday, 2004; Lawrie, 2006; Munday *et al*., 2007, 2008d; Lawrie *et al*., 2009a, b). In Australian landscape settings AEM-based products are particularly effective at providing high resolution baseline data on the spatial distribution of aquifers and aquitards as well as water quality and salt stores in shallow (<120m) floodplain sediments (Mullen *et al*., 2007; Tan *et al*., 2005; Munday *et al*., 2006, 2007; Lawrie *et al*., 2009a). However, while these datasets and information products address specific gaps in the biophysical knowledge framework, addressing salinity and land management questions usually requires an understanding of underlying biophysical processes and dynamics that often cannot reliably be determined from analysis of spatial patters of conductivity alone (Cresswell *et al*., 2007).

While increasing sophistication of AEM-derived products (e.g. porosity-corrected lithology products, maps of salt load, salt hazard etc; Tan *et al*., 2009) has improved their utility and up-take by land managers, much of the success of AEM surveys in the past 5 years has come from demonstration of relevance through incorporation of AEM-derived products in regional planning and decision support tools and in groundwater modelling frameworks (Chamberlain & Wilkinson, 2004; Walker *et al*., 2004). The high resolution (in 2D and 3D) afforded by AEM datasets enables key elements of the hydrogeological system to be mapped and characterised with greater certainty. This has contributed to improved parameterisation of models, and enables more reliable quantitative assessments to be made of the uncertainties and confidence levels in model predictions. It is the adoption of these multi-disciplinary, multi-scale system approaches that underpin the development of more effective salinity and groundwater management strategies, and enable more targeted salinity management actions (Lawrie, 2008; Lawrie *et al*., 2009a).

To date, a large variety of modelling approaches have incorporated AEM-derived products, reflecting the diversity of land management questions tackled. The approaches vary from GIS-based modelling platforms to fully distributed groundwater flow models. For example, building on the availability of a number of AEM surveys that have been conducted along the River Murray, modelling studies include: the impacts of broad-scale land use planning including land clearing along the River Murray (RCSM: Walker *et al*., 2005; Doble *et al*., 2005, 2008); salt loads in the Murray River (SIMPACT; Wang *et al*., 2005); the links between groundwater processes, evapo-transpiration and vegetation health (WINDS; Munday *et al*., 2008c); leakage from salinity disposal basins (Munday *et al*., 2008), and the potential impacts of flooding and environmental watering in the River Murray Corridor using fully distributed finite difference (MODFLOW) groundwater models (Richardson *et al*., 2007; Yan & Howe, 2008; H. Middlemass, pers. com. 2008).

In particular, new insights into the lateral and vertical connectivity of the aquifer systems are required to assist with groundwater management. Similarly, new insights into distribution of soils, sub-soil clay units, and sand and gravel aquifers in 3D are required to better understand the extent of surface-groundwater interactions, and to identify preferential recharge and infrastructure leakage in the landscape. These are essential to improve the management of surface water, groundwater, salinity, and broader environmental management. To constrain the hydrogeological models it is necessary to better map water quality (salinity), aquifer boundaries, and elements of the sedimentary system, particularly the upper and lower gravels and their connectivity, as groundwater flow is highest through these units. Gaining a better understanding of where the potential increased evaporation and or discharge zones occur would also be desirable. Ultimately, it will be necessary to construct an improved 3D map of the aquifer systems.

The power and long-term value of AEM-based datasets for salinity management lies largely in providing stakeholders with a range of customised information products that help address specific salinity and land management questions (George *et al.,* 2003). This necessitates translating conductivity measurements to estimates of salinity extent, salt hazard and 'loads' and groundwater quality, and requires the differentiation of host lithologies and other hydraulic parameters (such as texture and porosity) acquired through drilling. To address most questions other than those related simply to salinity extent, it is also necessary to relate these map-based products to an understanding of salinity dynamics and processes by carrying out hydrogeochemical studies and incorporating the AEM-derived products within hydrogeological and land use models (Walker *et al.,* 2004; Cresswell *et al*., 2007).

8.2 SPECIFIC SALINITY AND GROUNDWATER MANAGEMENT ISSUES AND QUESTIONS IN THE ORIA

8.2.1 Previous Salinity Investigations

There are very few reported occurrences of primary salinity in soil surveys of the ORIA prior to irrigation in the 1960s. Active primary groundwater-related salinity was unlikely to be present at the commencement of irrigation as water tables were deep, or non-existent within the alluvial aquifers prior to irrigation (O'Boy *et al.*, 2001). The only primary salinity appears to have been localised at the break of slope in the margins of some floodplain environments where discharge of fresh groundwater from adjacent hills today ponds in low-lying areas and evaporates to form small salt scalds.

Importantly, the salinity hazard within the ORIA probably lies not so much in the immediate threat of waterlogging of soils and /or salt visibly scarring the land surface, but in the possible un-seen build up over time of salt in soils and sub-soil root zones (0-2m). Assessment of salinity hazard is made more complex by the lack of any baseline studies or on-going monitoring of sub-soil or soil salinities. Even in the Stage 1 area, the data do not exist, in the public domain at least, to be able to ascertain if salt levels in the sub-soils have increased in the past 10-15 years in areas of shallow water tables. There are however some data to show that groundwater salinities have increased in some Stage 1 areas (Figure 278).

Previous studies have found that at shallow depths (<1m), most of the soils in the ORIA are relatively low in soluble salt. The percentage of salt increases generally with depth, with about half found to be at least slightly saline between 1 and 2m depths (Smith & Price, 2008). At greater depths (>1.8m), up to one third of sub-soil samples across the ORIA Stage 1 and Weaber Plains area are recorded as being at least moderately saline (Burvill, 1991; Smith & Price, 2008). The salt in these sub-soils was either concentrated in the subsoil by evapotranspiration of infiltrated rainwater in areas where leaching of the salt is restricted by very small rates of deep drainage, or reflects evaporation of groundwater in wetter climate periods when palaeo-water tables were higher. Given the relatively rapid rise in water tables observed due to climate changes in the Weaber Plain, the latter explanation cannot be ruled out, although the former explanation is more likely.

In the ORIA, the potential for irrigation-induced soil salinisation, driven by a rise in watertables, was recognised at an early stage in the development. However, the depth of the watertables at the commencement of irrigation was considered to be sufficiently large that evaporation of the groundwater would not take place, with equilibration of water tables expected at significant depths. However, steady rises in the

watertables of 0.3-0.5m per annum began to cause concern in the 1990s (Smith, 2008). Ali & Salama (2003) produced maps of shallow watertable salinity for ORIA Stage 1 (Figure 280). Watertables only stabilised in ~2001, although the levels are still relatively shallow (a considerable portion the Stage 1 area has watertables shallower than 4m; Smith, 2008; Figure 279). Previously, Ali & Salama (2003) produced a map showing shallow groundwater salinities in the ORIA Stage 1 area (Figure 280). In the ORIA Stage 2 areas, the potential for secondary salinity to develop have also been recognised for some time, with moderate to high salt stored in deeper sub-soils (Golders, 1999) and areas where groundwater salinities are higher than in the Stage 1 areas (Kinhill, 1999; O'Boy *et al*., 2001).

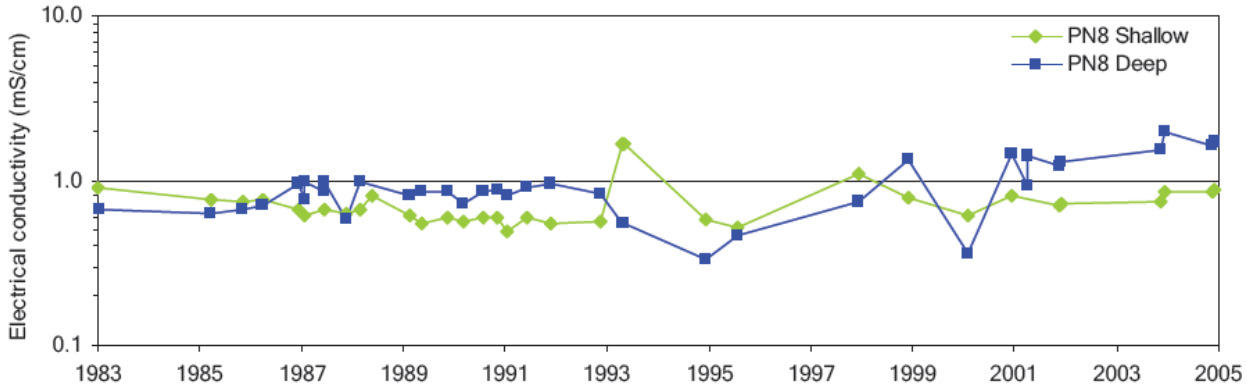

Figure 278: *Electrical conductivity data for deep and shallow monitoring bores at site PN8, Ivanhoe Plain. From CSIRO, 2009.*

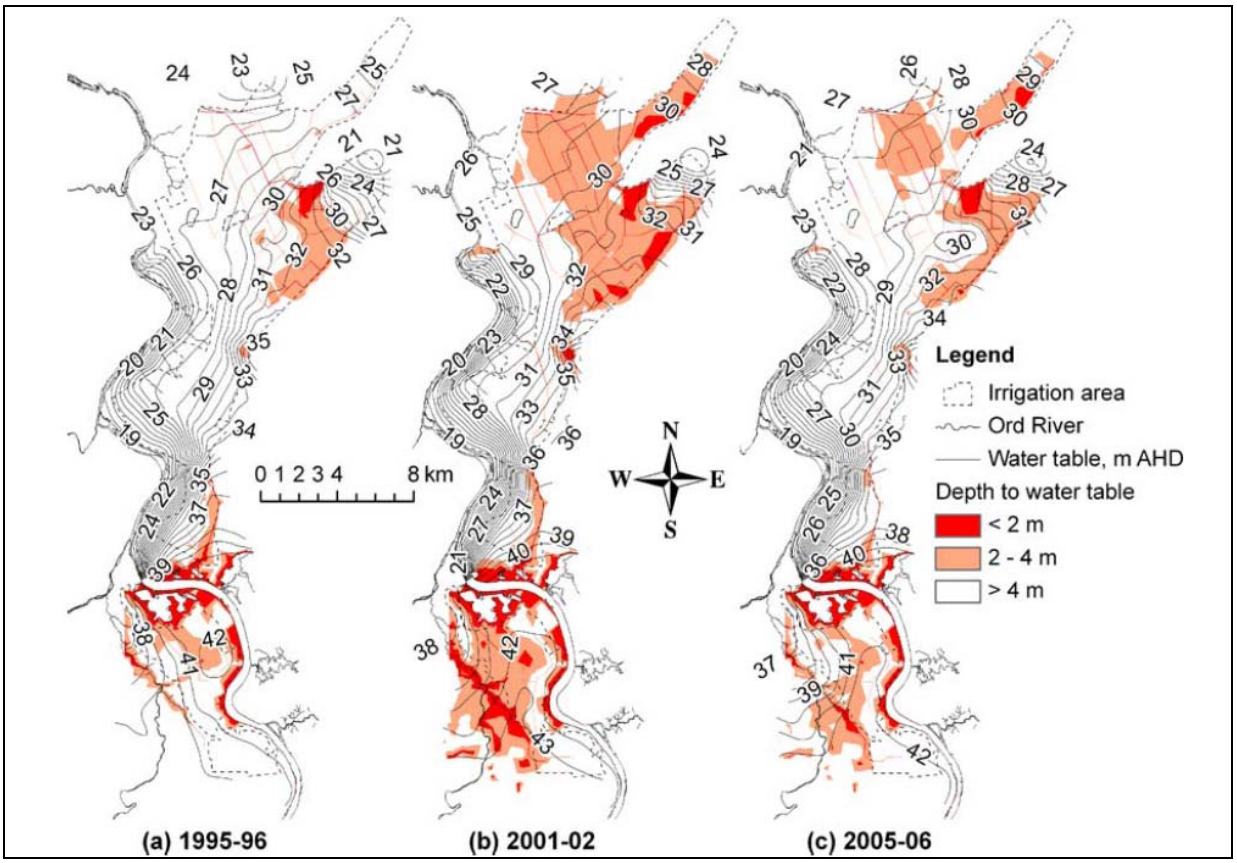

Figure 279: *ORIA Stage 1 depth to water table for 3 periods.*

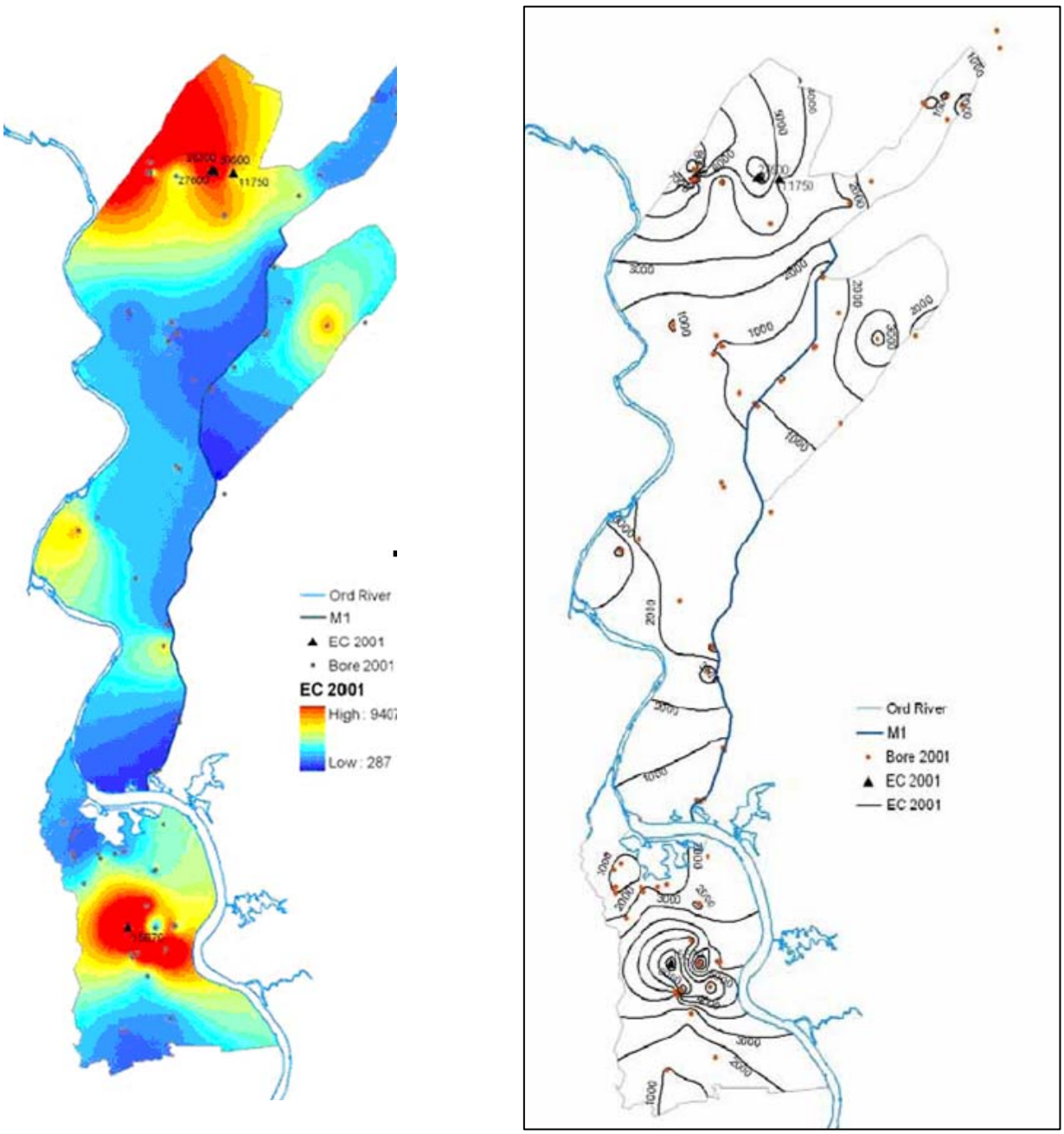

Figure 280: *Shallow water table salinity variation in the ORIA, 2001 (Ali & Salama, 2003). Geophysical investigations in this study were conducted in areas of generally lower salinity (<1000 EC units). EC values in some areas are up to 12,000 EC units.*

8.2.2 Salinity and Groundwater Management Issues and Questions

The Project Steering Committee translated the desired management outcomes, practical management actions and physical attributes into a number of specific priority questions for the AEM Project Interpretation team to focus on. These, a series of high level questions, and the desired management outcomes, are listed in detail in Section 1.3. The principle concerns in the ORIA revolve around salinity and groundwater management and the sustainability of irrigation in the district, as well as the potential impacts on adjacent and/or downstream high value environmental assets.

The Project Steering Committee recognised that the AEM and complementary data could fill key knowledge and data gaps, but that not all of the identified questions could be answered without further investigation and modelling. In particular, it was recognised that additional hydrogeochemical studies would be required to understand the groundwater processes in the ORIA, while hydrodynamic modelling utilising the datasets and knowledge gained in this project would also be required to provide temporal and spatial predictions of

knowledge gained in this project would also be required to provide temporal and spatial predictions of groundwater movements and salinity risk. The Project Steering Committee also prioritised investigations in the Stage 2 Weaber Plain and Stage 1 Ivanhoe Plain areas, with the result that greater attention is paid to addressing a wider range of questions in these areas in the subsequent sections of this report.

8.3 SPECIFIC SALINITY AND GROUNDWATER MANAGEMENT QUESTIONS IN THE ORIA STAGE 1

8.3.1 Ivanhoe Plain, Ord West Band and Cockatoo Sands

Where is salt stored in the landscape (in the saturated and unsaturated zones)?

No surface salt scalds were reported prior to irrigation in the ORIA Stage 1. However, Burvill (1991) reported that approximately one third of all sub-soil samples analysed from the Ivanhoe Plain prior to irrigation were moderately saline (Figure 281). Overall, prior to irrigation it seems that the cracking clays were mostly non-saline to slightly saline, but may have accumulated soluble salt in areas with internal surface drainage, high evapotranspiration and restricted subsurface drainage and leaching (Smith & Price, 2008). Examples include Martin's Swamp and Green's Location. There is also evidence that saline subsoil may also be present beneath the red plain soils in areas bordering the river and creek systems.

Location	Year of Readings	[1]No. of Readings	Salinity Class				
			Non	Slight	Mod.	Very	Extreme
[2]North-west Packsaddle	1993	66	50	2	6	3	5
[3]Packsaddle Infill	1993	28	22	3	3	0	0
[4]M1 Channel	2000	28	22	4	0	1	1
[5]SP1 Channel	2007	5	0	0	2	0	3
[5]Drovers Rd Depression	2007	3	0	0	0	0	3
[6]Oasis Farm soil pit	2005	5	5	0	0	0	0
[6]Innes Farm soil pit	2005	5	5	0	0	0	0
[6]Frank Wise soil pit	2005	5	5	0	0	0	0
[7]Frank Wise	2004	16	14	2	0	0	0
[6]Sugar mill soil pit	2005	5	5	0	0	0	0
[6]Gardner Farm soil pit	2005	5	4	1	0	0	0
[7]Cummings Farm	2004	16	7	4	3	2	0
[7]Cummings Farm	2005	31	31	0	0	0	0
[7]Martin Location	2006	124	100	8	7	9	0

[1]Includes multiple measurement depths at individual sites, [2]Schoknecht 1996a; [3]Schoknecht 1996b; [4]Robinson, C. Department of Agriculture and Food Western Australia, 2006, pers. comm.; [5]Duncan, R. Brolga's Environment, 2007, pers. comm.; [6]Slaven, T. Department of Agriculture and Food Western Australia, 2008, pers. comm., [7]CSIRO data

Figure 281: *Salinity data for soils and sub-soils from the ORIA Stage 1. Data from Smith & Price (2008).*

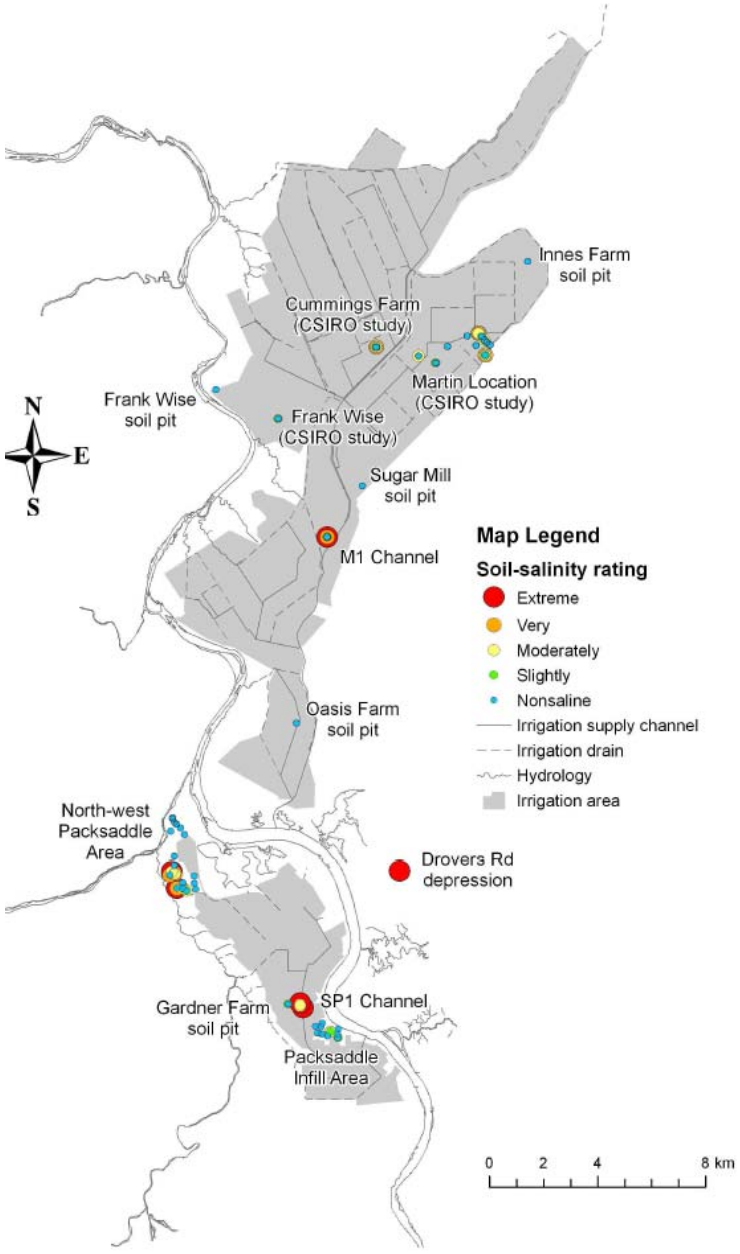

Figure 282: *Surface soil salinity rating for locations in the ORIA Stage 1 and immediately adjacent areas. Map from Smith & Price (2008).*

Previously, no salt store maps have been available for the ORIA Stage 1, and assessment of salinity hazard in this area has relied largely on modelling watertable rise and climatic factors (Ali & Salama, 2003). The new salt store maps, allied with maps of groundwater quality and lithology, assist with groundwater model parameterisation, and should enable more spatially accurate predictions of the salinity hazard to be made. In ORIA Stage 1 and adjacent areas, soils with moderate to extreme salinity values were identified by Smith & Price (2008; Figure 282).

The AEM data, calibrated by pore fluid and textural data from drilling and field sampling, have established that the salt stored in the unsaturated and saturated zones throughout most of the Ivanhoe Plain is between 20 and 130t/ha/m (Figure 283). Depending on how readily these salt stores are mobilised, the levels are high enough to be of concern to irrigated agriculture should the water table rise to within 2m of the ground surface (Ali & Salama, 2003).

Locally, there are smaller areas (1km x 500m) where salt stored in the unsaturated zone is particularly high (>30t/ha/m), and/or salt stored in the saturated zone is high (>60t/ha/m) coincides with areas where the water table is relatively shallow (Figure 283, Figure 284). These areas have a higher potential risk of soil salinisation, and there is anecdotal evidence of poor crop productivity in at least one of these areas. Lower

salt store values are encountered primarily within narrow sand and gravel palaeochannels (e.g. intercepted by drillhole O2, Figure 28), where the total amount of salt stored is low (0-10t/ha/m), but there is a higher risk of the salts being mobilised.

Similarly, the salt store maps, when overlain with plans of water supply and drainage infrastructure, can be used to identify area of higher potential salt mobilisation and salinity risk. For example, there are several locations in the Ivanhoe Plain where the M1 water supply channel and subsidiary water channels transect areas of higher salt store (Figure 283). Leakage from the channels in these areas is likely to pose a higher risk of salt mobilisation and soil salinity developing locally. The salinity risk may be two-fold in these areas: they may be point locations for the mobilisation of salts into drains when the water table is discharging; any they may also be areas of increased salt mobilisation downwards to the water table in the wet season if drains act as points of preferential recharge where they cut down through the upper clay aquitard layers (Smith, 2008; Smith & Price, 2009). In areas of high water table, and where water supply channels are not adequately sealed, there is also the potential in these areas for salt to be mobilised into the water supply infrastructure.

Secondary salinisation along sections of the SP1 and M1 supply channels appears to be a result of persistent leakage of surface water from the channels into the surrounding ground and the formation of local zones of shallow groundwater and moist soil. Leakage of channel water and salt accumulation in the soil occur mainly during irrigation seasons when the channels are full and potential evaporation from the soil is greatest.

Salinisation near Mulligan's Lagoon Road may be a natural discharge point related to groundwater movement from higher landscapes to the east. At this location, there is a change in surface gradient allied to a change from shallow bedrock to thicker alluvial sediments as well as a change of soil type. In this area, the water table has also risen substantially in response to irrigation development and groundwater has been less than two metres below the ground surface for the decade.

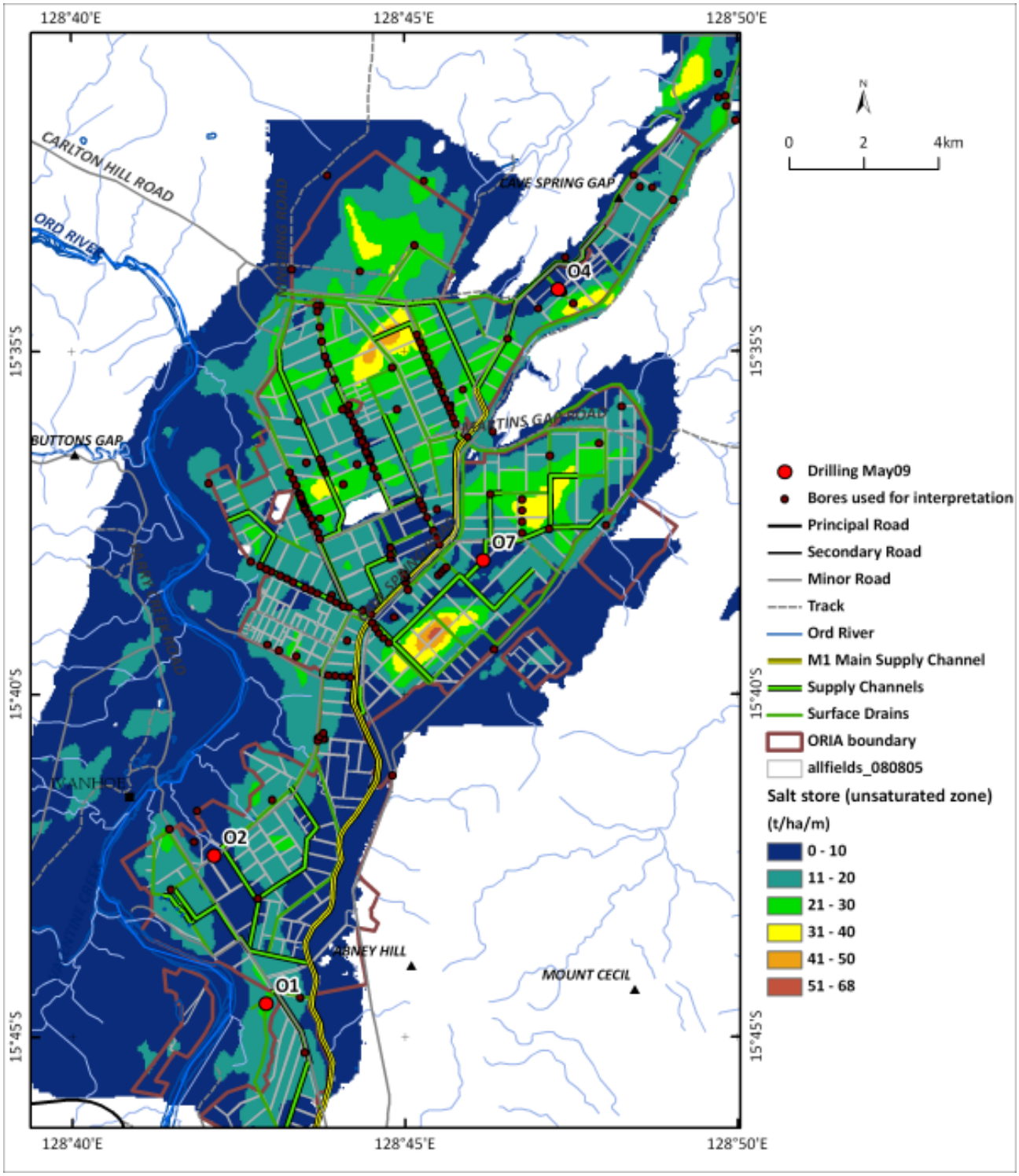

Figure 283: *Salt stored in unsaturated zone in the Ivanhoe Plain and Ord West Bank.*

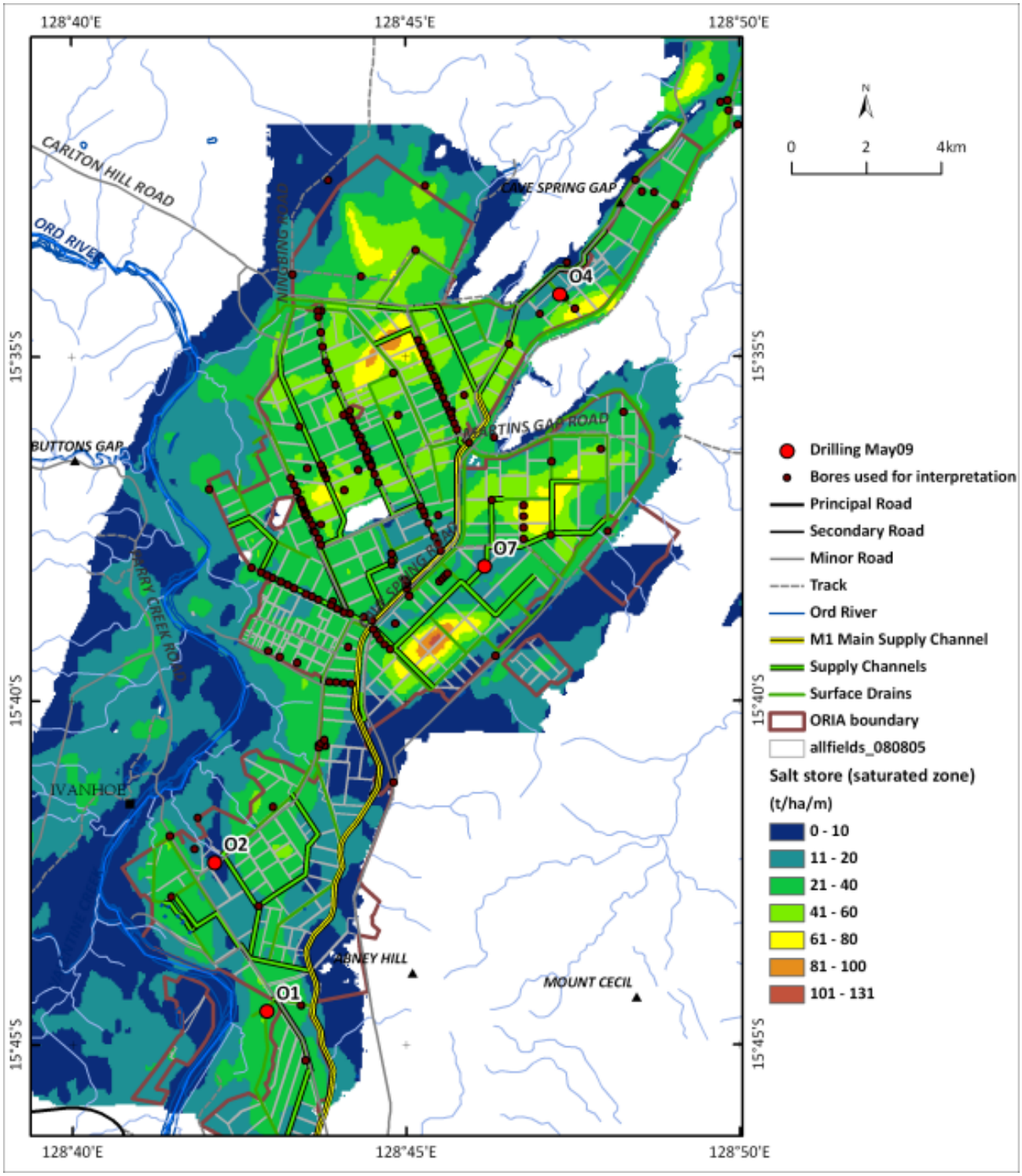

Figure 284: *Salt stored in saturated zone in the Ivanhoe Plain and Ord West Bank.*

What is the distribution of groundwater quality (salinity)?

Previous sampling of groundwater in the ORIA Stage 1 area found salinities greater than 1000 µS/cm over most of the area, with values of over 20,000EC at Greens Location (Ali & Salama, 2003). The latter considered that EC levels between 250 and 750 µS/cm posed a medium salinity risk to irrigated agriculture, with higher values posing a high risk, should the water table rise within a couple of metres of the ground surface.

The new AEM data, calibrated by drilling and field sampling, are generally consistent with the results from previous groundwater sampling. Overall, groundwater salinity is strongly influenced by lithologies, with

higher salinity groundwater generally found in the thickest clay units. The AEM mapping has established that the groundwater quality in the Ivanhoe Plain is quite variable, with values ranging from <500TDS (mg/l; or <800EC) to over 3,000TDS (or >4,800EC; Figure 285). In general, all the palaeochannels have lower values (<1,000TDS, or <1,600EC), with values <500 TDS (<800EC) in the palaeochannel in the south of the area, while the groundwater in the sandy silt and clay lithologies is generally between 1,000 and 4,000TDS (1,600 and 6,300EC respectively).

The AEM based maps of groundwater quality have a much higher spatial resolution than previous maps. This also enables groundwater quality measurements to be linked more directly to specific elements of the hydrostratigraphy, provides targets for groundwater management, and provides the basis for more spatially explicit predictions of salinity hazard. The groundwater quality maps reinforce the need for groundwater management in this area to minimise the salinity risk.

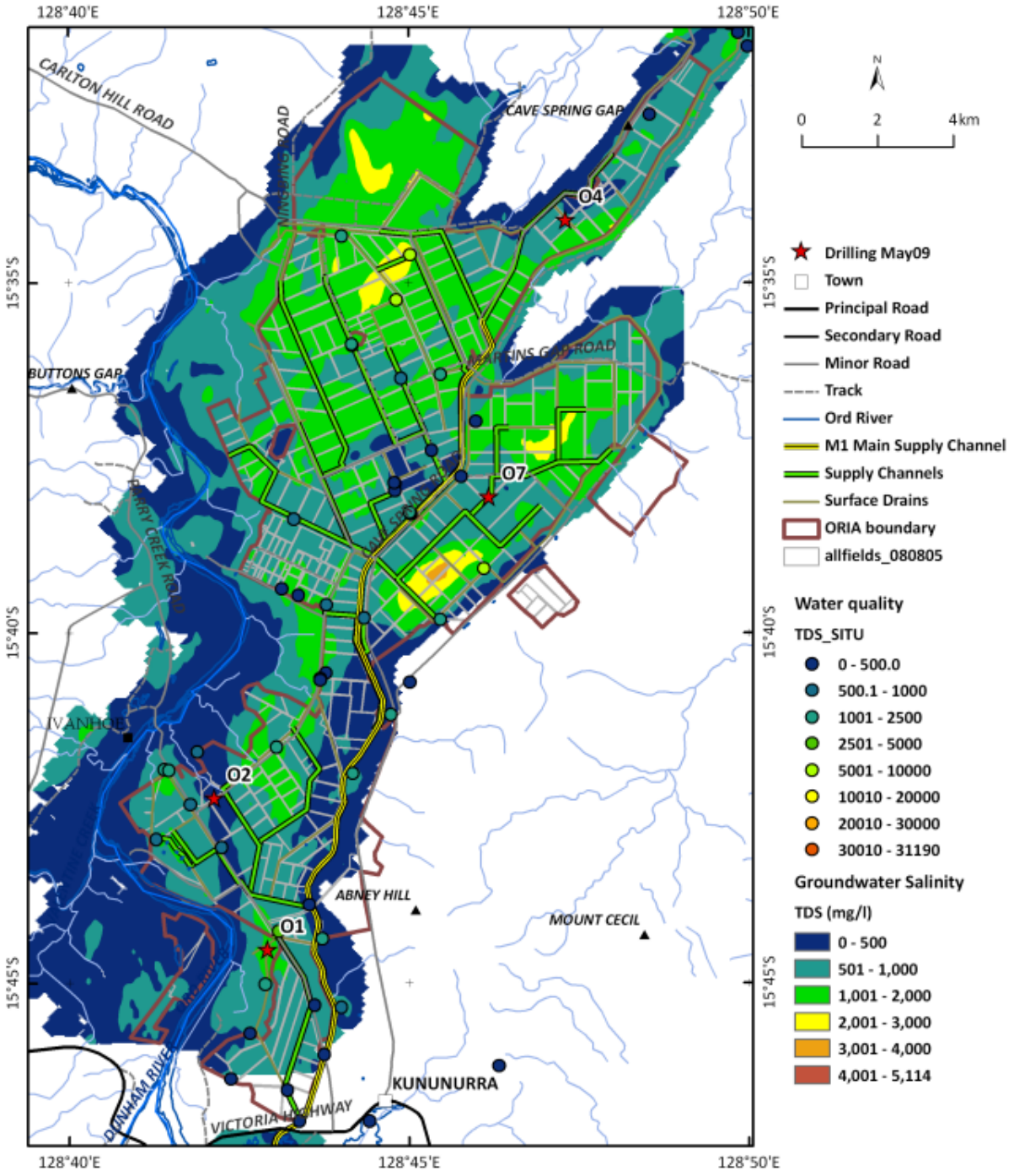

Figure 285: *Map of groundwater quality (salinity) in Ivanhoe Plain and Ord West Bank.*

Where are the areas of highest salinity hazard across the ORIA? Is it possible to identify areas where salt is at higher risk of being mobilised?

New (unsaturated zone) salinity hazard maps for the ORIA Stage 1 area have been produced by integrating the AEM salt store data with borehole data, the water table surface and the LiDAR dataset (Figure 286; Section 4.10). Areas of high salt store with shallow water tables (<2-3m) are deemed to have the highest salinity hazard.

Overall, highly variable salinity hazard across this area, ranging from very low to very high. The northern part of the area has areas of high to very high salinity hazard, as does Cave Springs Gap. Very shallow water tables (<5m) combined with moderately high salt stores in the unsaturated (< 30t/ha/m) and saturated zones (<130t/ha/m). A detailed breakdown of each hazard class for areas within the Ivanhoe Plain and Ord West Bank is shown in Table 34 and Table 35 respectively. The areas of greatest hazard occur in the north and east of the ORIA Stage 1 (Figure 286). In general, these maps show there is a significant salinity hazard in the Ivanhoe Plain area, and reinforces the need to maintain water tables at current or reduced levels. The areas that the figures refer to are shown in Figure 287.

There are also several areas of high to very high hazard that are transacted by water supply and drainage infrastructure that may provide point locations for increased surface-groundwater interaction and point discharge of saline groundwater. The new salinity hazard maps provide a starting point for re-assessing drainage and cropping strategies, monitoring salinity risk and salt export from the area. Further refinements of these maps, including identification of the areas where salt is at higher risk of being mobilised, will be possible when individual data layers are incorporated within appropriate groundwater models.

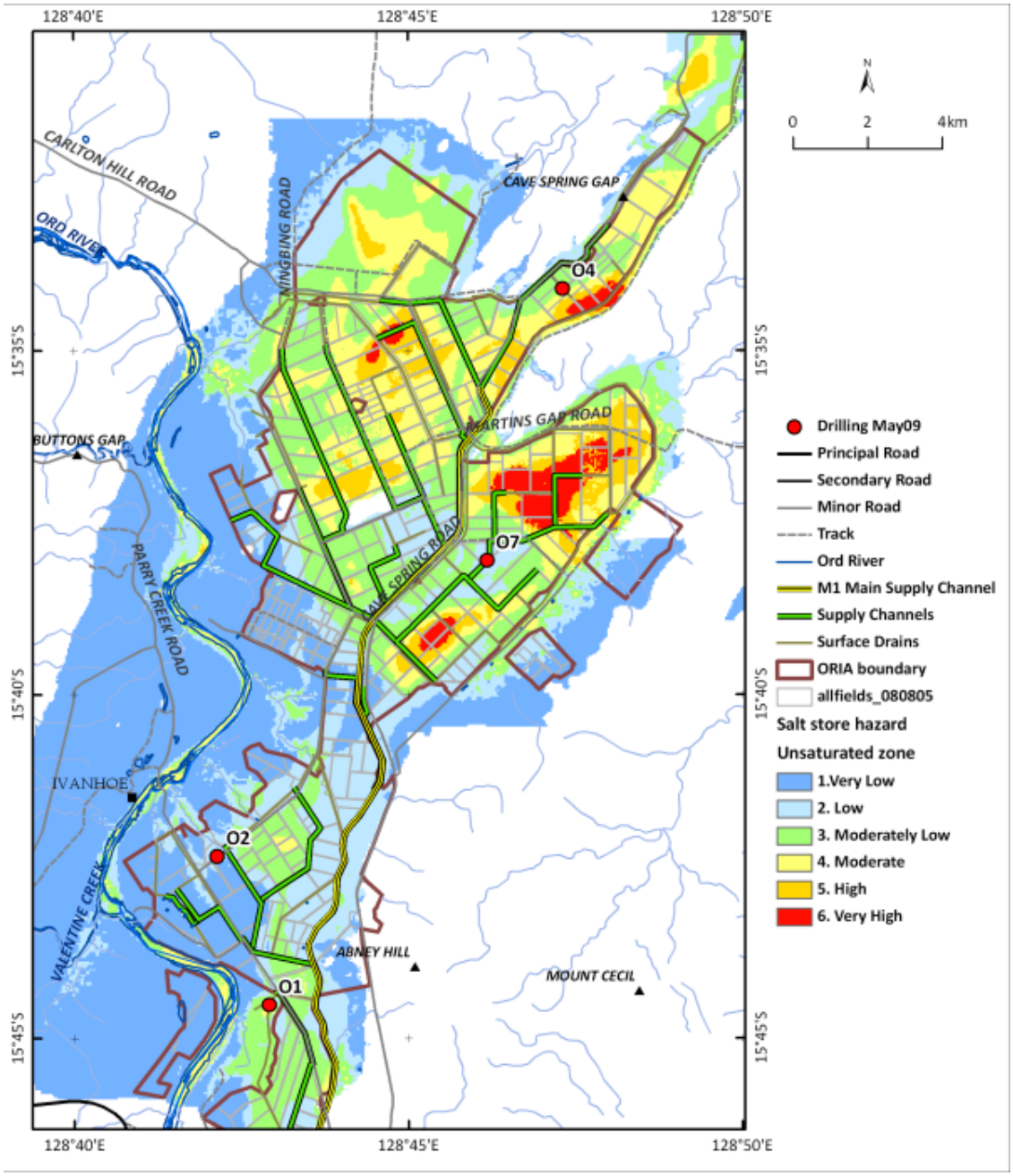

Figure 286: *Salinity hazard (depth to water table and unsaturated salt store) in the Ivanhoe Plain and Ord West Bank.*

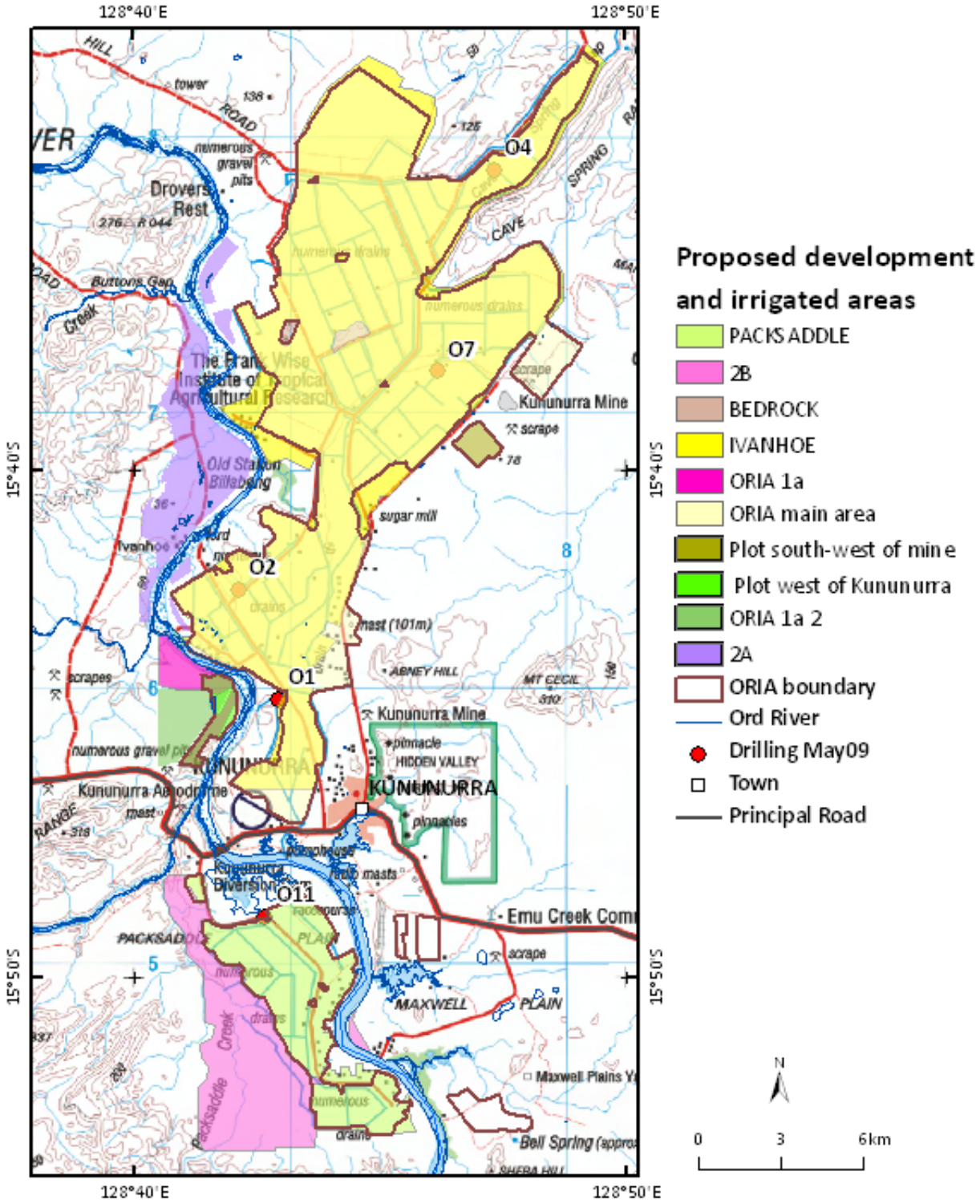

Figure 287: *Areas used in calculations for salinity hazard in ORIA Stage 1 and adjacent Stage 2 areas.*

Table 34: *Predicted salinity hazard (based on AEM-derived unsaturated zone salt store and depth to water table) for individual sub-areas. Note: these figures have been rounded to the nearest whole number.*

Area Name	Hazard Class	Hectares	Percent
ORIA Stage 1 area	1.Very Low	2099	14
	2. Low	3129	21
	3. Moderately Low	4463	30
	4. Moderate	2729	18
	5. High	1156	8
	6. Very High	500	3
	Area not assessed	547	4
ORIA Stage 1 Total		14622	97
Plot SW of mine	1.Very Low	84	1
	2. Low	66	0
	3. Moderately Low	7	0
Plot SW of mine Total		157	1
Plot W of Kununurra	1.Very Low	253	2
Plot W of Kununurra Total		253	2
Grand Total		**15032**	**100**

Table 35: *Table Predicted salinity hazard for the Ord West Bank (based on AEM-derived unsaturated zone salt store and depth to water table) for individual sub-a*reas. *Note: these figures have been rounded to the nearest whole number.*

Area Name	Hazard Class	Hectares	Percent
ORIA 2A	1.Very Low	1831	66
	2. Low	35	1
	3. Moderately Low	10	0
	Area not assessed	4	0
ORIA 2A Total		1879	68
ORIA 1a	1.Very Low	416	15
	2. Low	14	1
	3. Moderately Low	4	0
ORIA 1a Total		434	16
ORIA 1a2	1.Very Low	458	17
ORIA 1a2 Total		458	17
Grand Total		**2772**	**100**

What is the extent (in 3D) of the sand and gravel aquifers, and how are they connected?

New maps of the depth to bedrock (Figure 288), the extent and thickness of gravel (Figure 289) and sand (Figure 290) aquifers have been produced for the ORIA Stage 1. These maps have been compiled by interpreting individual AEM conductivity depth slices and representative conductivity cross-sections using pre-existing drillhole records and data from new drillcore obtained during the project (Section 4.2). These maps illustrate the distribution and extent of the sand and gravel aquifers that comprise the main Ord Palaeovalley. The sand and gravel aquifers are two of the key elements of the hydrostratigraphy, and mapping their extent and thickness will facilitate the construction of improved distributed groundwater models, and enable surface-groundwater interactions and groundwater flow paths to be mapped and understood.

The maps of depth to bedrock confirm the location of the main Ord Palaeovalley that exited through Cave Springs Gap. This feature is incised into bedrock at depths of up to 33m, and at its base is from <2 to 3km in wide (Figure 288 and Figure 203). The palaeochannel is infilled with gravels towards its base, but becomes increasingly sand-filled upwards as the palaeochannel broadens out (Figure 185 - Figure 193). More detailed descriptions of the gravel and sand lithologies, and their extent are provided earlier (Section 5.1). Overall, the AEM has revealed that the gravels are highly variable in thickness (from 5-20m), are more restricted in their spatial extent, and more complex in their lateral and vertical connectivity than previously thought (O'Boy *et al*., 2001; Smith, 2008; Figure 204 - Figure 206). Overall, these new maps will assist greatly with groundwater model parameterisation and enable more reliable quantitative assessments to be made of

groundwater and salinity model predictions. They will also contribute to more robust modelling of land use and groundwater management scenarios.

Trials to test the feasibility of pumping to control the groundwater table were carried out in the Ivanhoe Plain area (Smith *et al*., 2005). They concluded that the palaeochannel aquifer system of the northern Ivanhoe Plain had such large transmissivities and was of such an extent that local pumping to control farm-scale groundwater levels would prove to be ineffective in such areas. The location of the pump tests seems to coincide with one of the major palaeochannels identified in the AEM data.

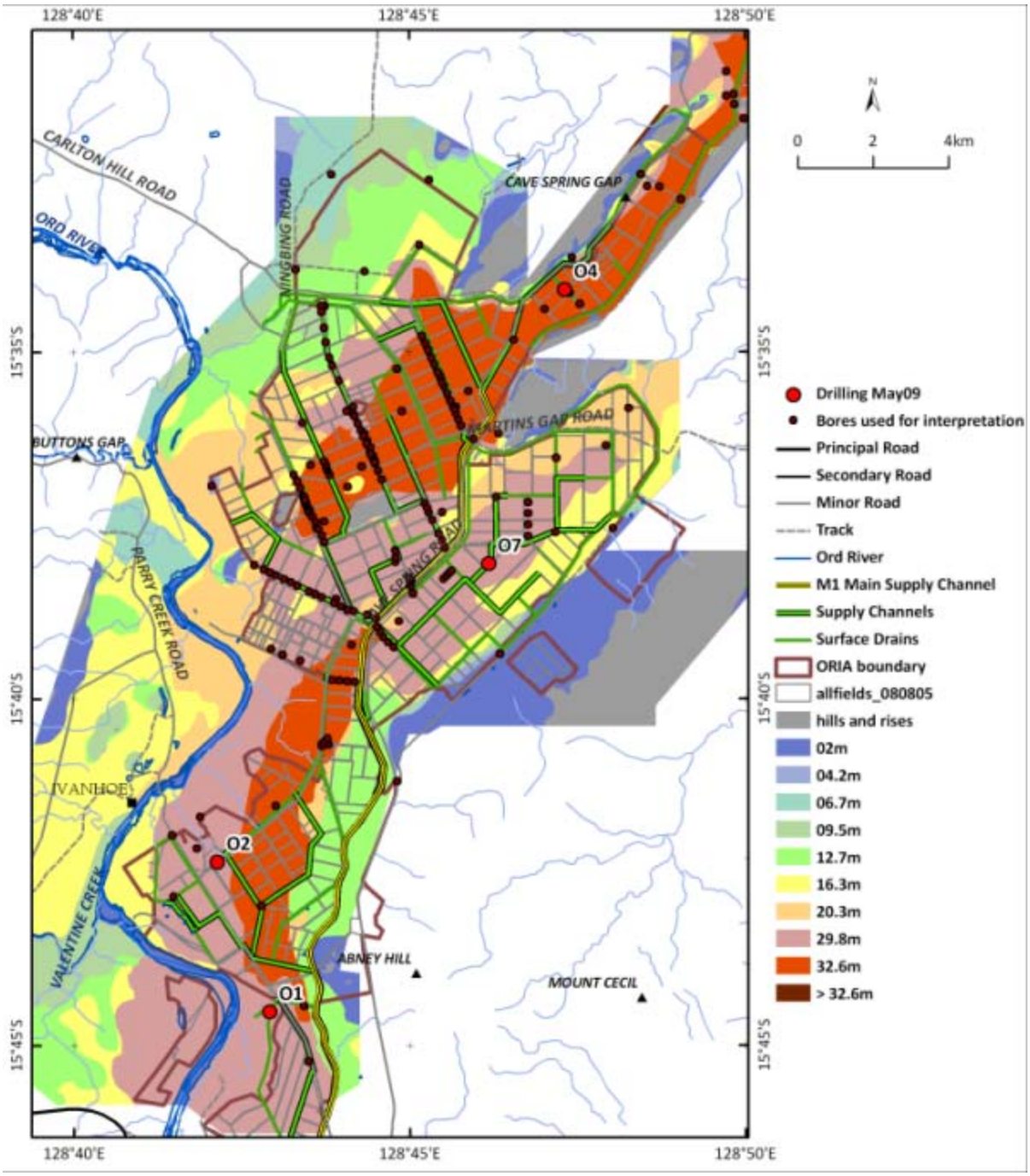

Figure 288: *Depth to bedrock in Ivanhoe Plain and Ord West Bank.*

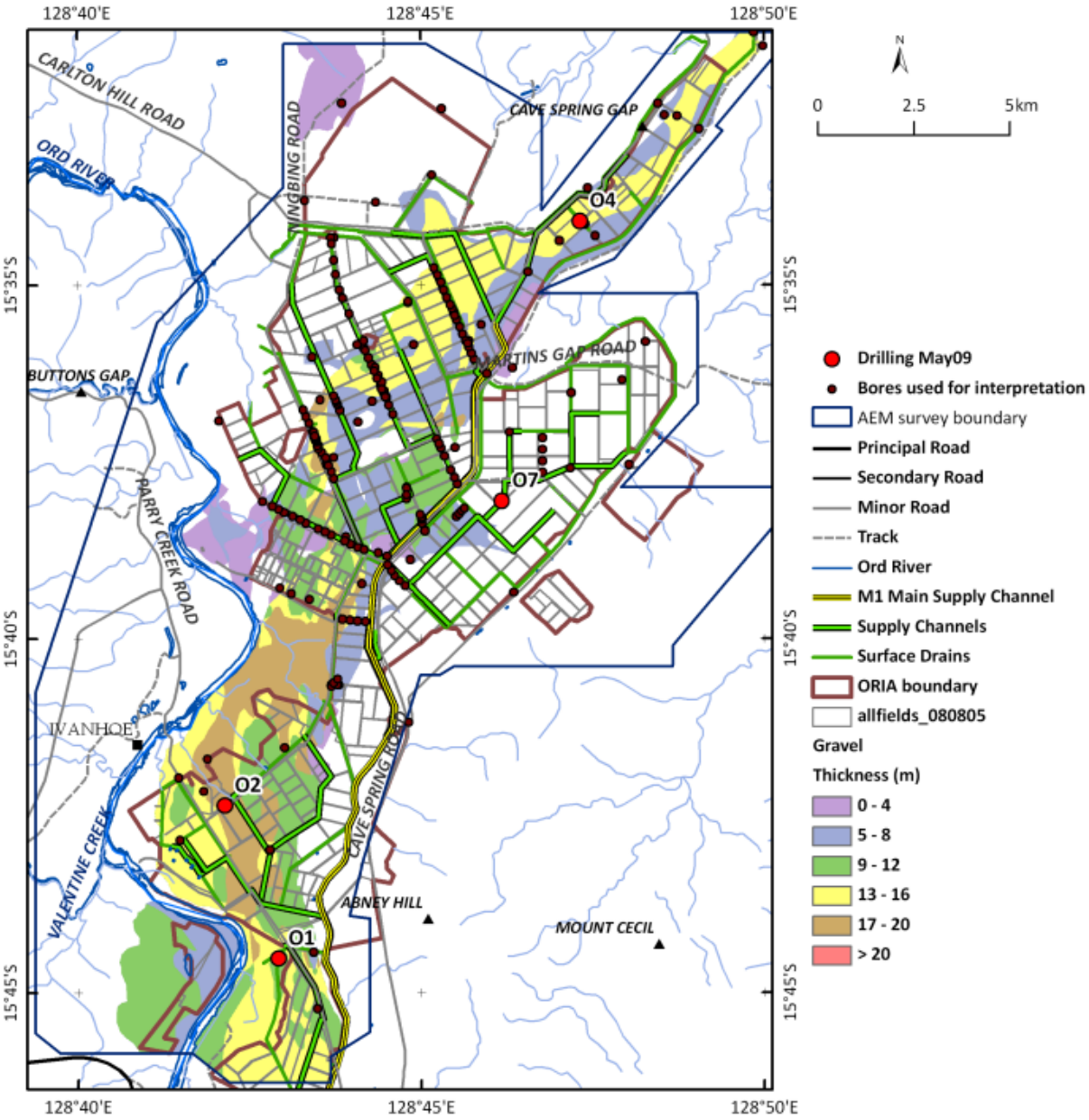

Figure 289: *Thickness of gravel in Ivanhoe Plain and Ord West Bank.*

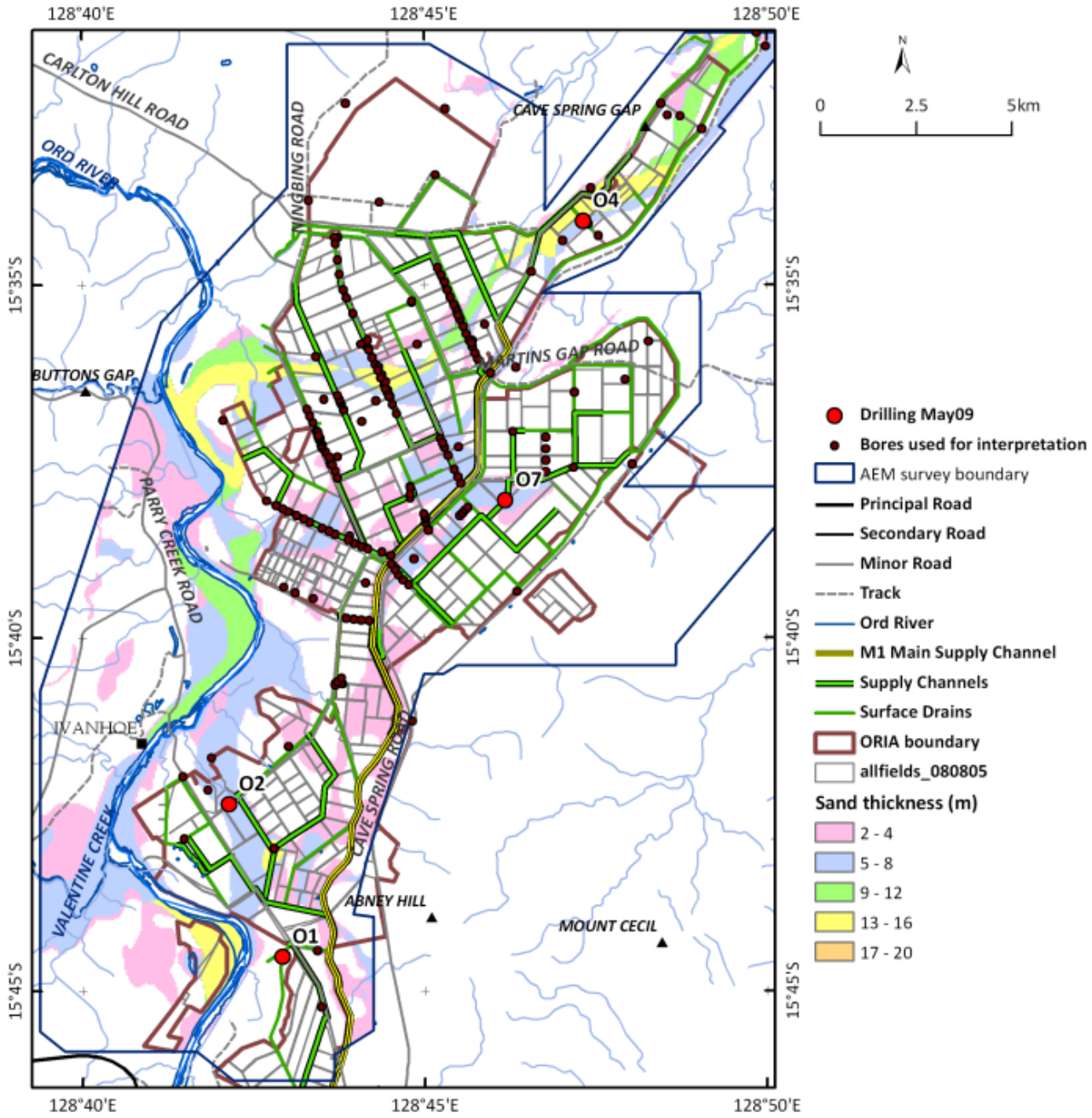

Figure 290: *Thickness of sand in Ivanhoe Plain and Ord West Bank.*

What is the extent and thickness of clays in the sub-surface?

New maps of clay extent and thickness (Figure 291) have been produced for the ORIA Stage 1. These maps have been compiled by interpreting individual AEM conductivity depth slices using pre-existing drillhole records and data from new drillcore obtained during the project (Section 3.3.2). These maps do not incorporate the 0-2m depth slice, as the conductivity measurements in this area are affected significantly by the effects of irrigation.

The maps of clay thickness show that there are significant areas of thick clays (17-28m) in the Ivanhoe Plain. Many of the areas with thicker clays are also areas of high salt store. While it may be more difficult to mobilise salts stored in these thick clay layers, it may be more difficult to lower the water table in these lithologies once they are saturated. Furthermore, the depth of influence of upward flux and transport of salts in the soil layer is higher for a clay-rich soil than a sandy soil, requiring that water tables be kept lower in the clay-rich areas (Ali & Salama, 2003). In an overall fining –up sequence, there are thinner clays (<4 – 8m thick) overlying sand and gravel palaeochannels. These areas of thinner clays may be areas of preferential recharge to the groundwater system. They are also areas of higher potential leakage from water supply and drainage infrastructure.

Mapping the extent and thickness of clays assists with understanding groundwater flow paths, surface-groundwater connectivity including recharge potential, and salinity mobilisation potential. Overall, these maps should also contribute to the development of appropriate salinity mitigation strategies, and assist with refining cropping and drainage strategies.

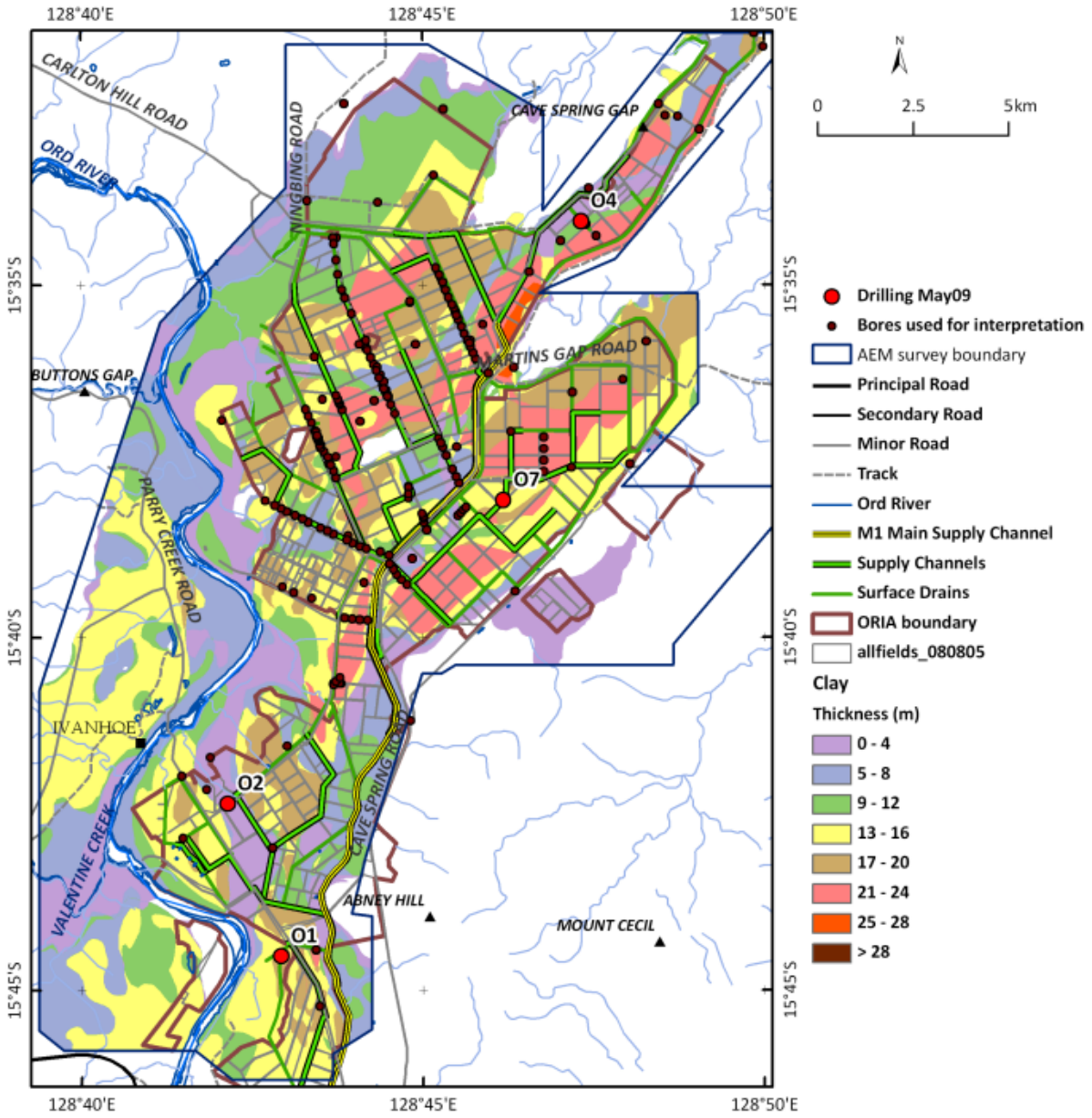

Figure 291: *Thickness of clay in the ORIA.*

What are the spatial and temporal trends in groundwater table movement and salinity?

Extensive work has been undertaken on groundwater table movement in the ORIA Stage 1 over several years (e.g. Smith *et al*., 2005, 2006; Smith, 2008). Because of this, no hydrograph analysis for ORIA Stage 1 was carried out as part of this study. However, a new watertable map was generated to show the depth to groundwater at the time of the AEM survey (Figure 292). This shows that the water table is currently at relatively shallow depths in much of the Ivanhoe Plain.

Previous hydrograph analysis has shown that groundwater has risen 0.3-0.5m per annum since the 1960s, before being stabilised in ~2001 (Smith, 2008). Importantly, water tables peaked in 2001, due in large measure to the success of the existing drains (Smith, 2008; Figure 279). Analysis of groundwater salinity trends shows that there is no observable increase or decrease in groundwater salinities in ORIA Stage 1, despite the increase in water added to the groundwater system (Figure 278). This may be due in part to mobilisation of salt stored in the unsaturated zone by irrigation water and/or rainfall.

As part of the drilling program, samples of pore fluids were collected for hydrogeochemical analysis. While these have the potential to provide some insights into salinity movement and processes, an in-depth study was outside the scope of this study, and only basic major anion and cation chemical analysis was carried out and reported on in this study (Appendix 2).

The AEM dataset provides only a snapshot in time, and cannot provide information on historical trends in salinity or groundwater movement. The AEM data, combined with the new watertable map and drilling data, do however provide a baseline dataset for future studies of salinity dynamics. Moreover, the AEM data have enabled key elements of the hydrogeological system to be mapped. The interpreted data layers for sand and gravel aquifer extent and thickness, clay extent and thickness, salt store and groundwater quality, provide a basis for groundwater model parameterisation, and the analysis of hydrographs within a much-improved hydrogeological framework. These AEM-based interpretation products should also provide the basis for more accurate spatial and temporal predictions of future groundwater table movements and salinity predictions under a range of different groundwater management and cropping strategies.

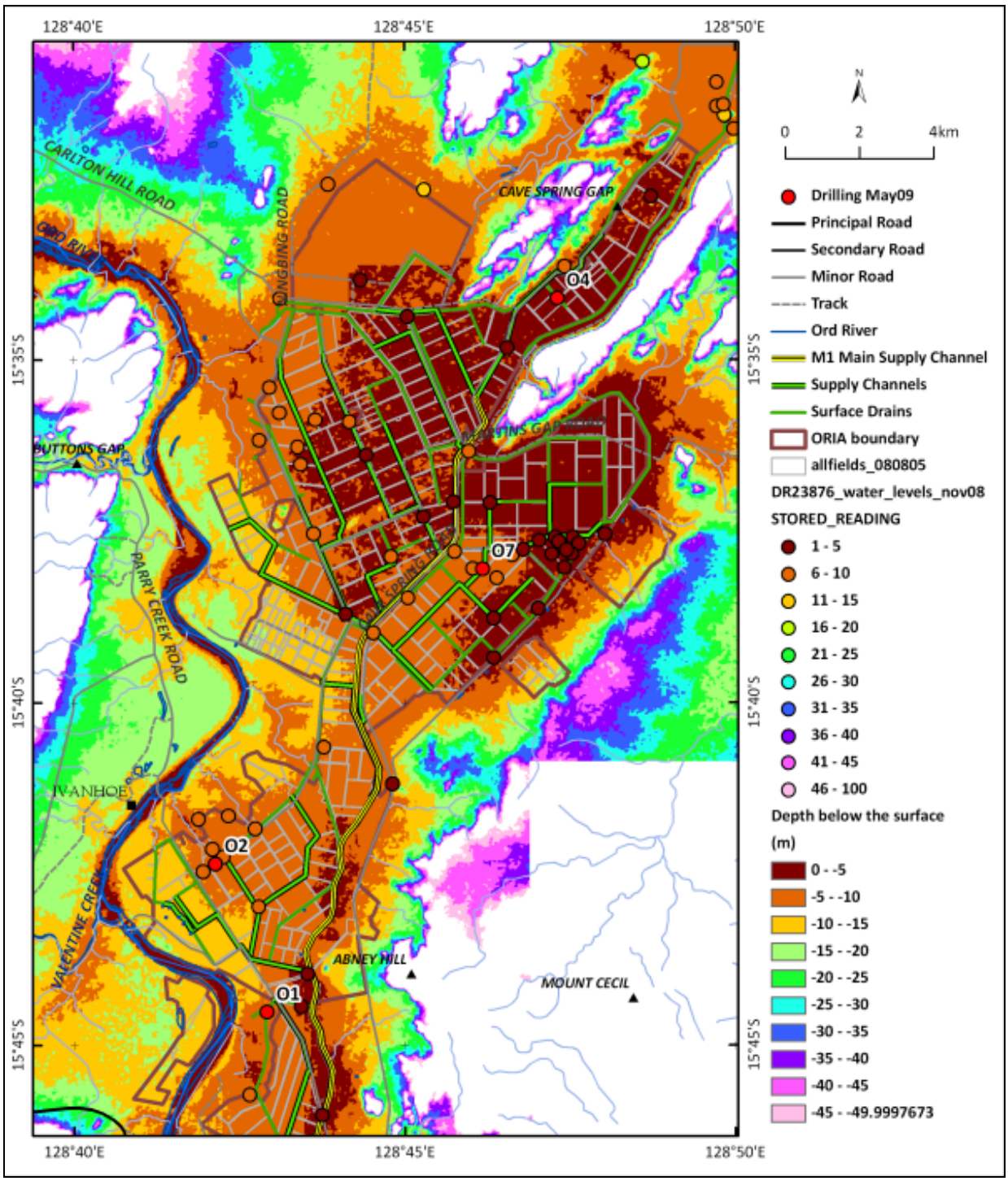

Figure 292: *ORIA Stage 1 water table height.*

What are the drivers of recharge across the ORIA, and where are the high recharge zones?

The rate of groundwater recharge through Cununurra clay prior to agricultural development of the ORIA is thought to have been very small (Banyard, 1983). Recent groundwater modelling (Smith *et al.,* 2006b) also suggested that the pre-irrigation groundwater recharge rate from rainwater was very small to negligible in the ORIA. Analysis in this study of hydrographs in the Weaber and Knox Creek Plains suggests that much higher pre-clearing recharge rates are possible in similar soils, and is dependent on the intensity and magnitude of rainfall events in the wet season.

A map of clay thickness in the 0-2m depth slice shows little variability over the area (Figure 293). However, Smith (2008) found that rapid infiltration and groundwater accession following individual irrigation events

occurs predominantly through the soil macropore system, and that contemporary wet-season accession in the ORIA is equally, if not more, important than dry-season accession (Figure 102).

In the absence of field data measuring recharge rates directly, 4 products have been produced as data layers to provide information relevant to the estimation of recharge rates in the Stage 2 areas. These 4 map products are:

- surface permeability, based on measurements of soil permeability in the top 20cm (Figure 294);
- soil recharge properties for the 0-2m soil layer, using data from soils mapping and field permeability tests (Figure 108);
- total clay thickness, incorporating soil mapping data for the 0-2m depth slice as well as AEM data beneath this (Figure 295);
- clay thickness above the water table (Figure 296). This integrates the previous maps with the water table map, and approximates a map of deep drainage.

These map products are designed primarily as data layers for input into a groundwater model. However, they also enable a qualitative assessment of recharge to the groundwater table to be made. In the surface permeability and soil recharge properties maps, the estimates of recharge rates across all proposed irrigation areas is low. However, these products are based on available soils data only, and the products do not take into considerable macropore bypass flow (Smith, 2008). The hydrograph analysis of bores in the ORIA Stage 1 areas including Ivanhoe Plain, shows that recharge to the groundwater table is significant and relatively fast, suggesting that other products are required to better describe recharge in these floodplain areas.

Figure 295 shows the total clay thickness for Ivanhoe Plain, incorporating the soils layer as well as AEM-derived clay thickness estimates below 2m. When this dataset is overlain on the regional water table map (Figure 296), it suggests that recharge rates to the groundwater table are likely to be highly variable, with more rapid recharge in areas with thinner clay sequences (e.g. over palaeochannels), and slower recharge rates in areas of thick clay above the water table. Low recharge rates are also suggested for large parts of the Knox Creek and Keep River Plains. These products could be used to refine the salt hazard maps in a groundwater model.

However, these products do not explain all the observed variation in the bore hydrographs, and other factors, such as lateral groundwater flow, may be important. For example, there is lateral groundwater flow from the east that is intercepted in the D8 drain (see later in this section), and high runoff areas in bedrock areas immediately adjacent to the floodplains at Cave Springs Gap (Figure 296). Overall, the analysis here suggests that further work is required to understand recharge processes and dynamics in the ORIA.

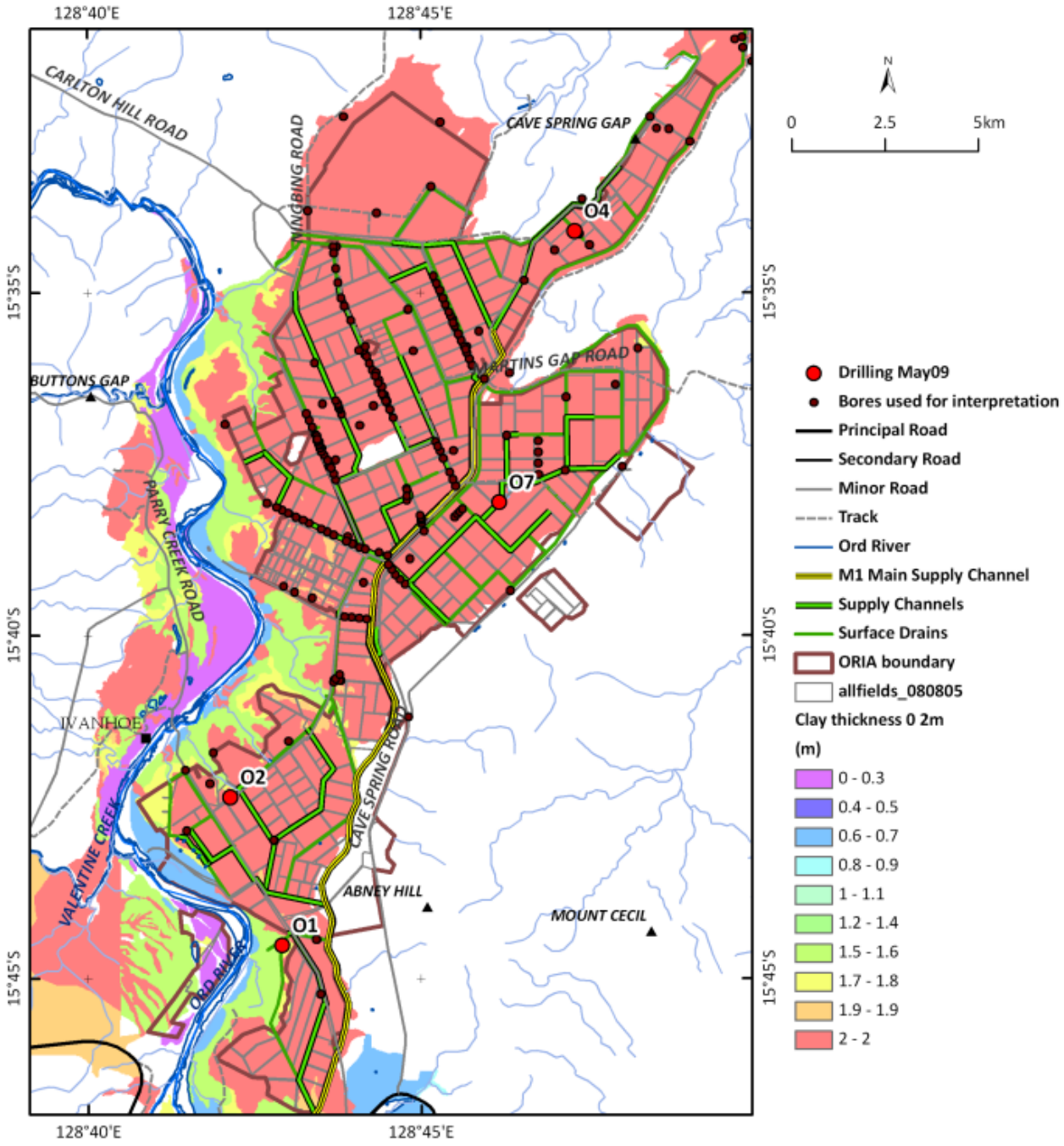

Figure 293: *Map of clay thickness in the 0-2m depth slice, in the Ivanhoe Plain and Ord West Bank.*

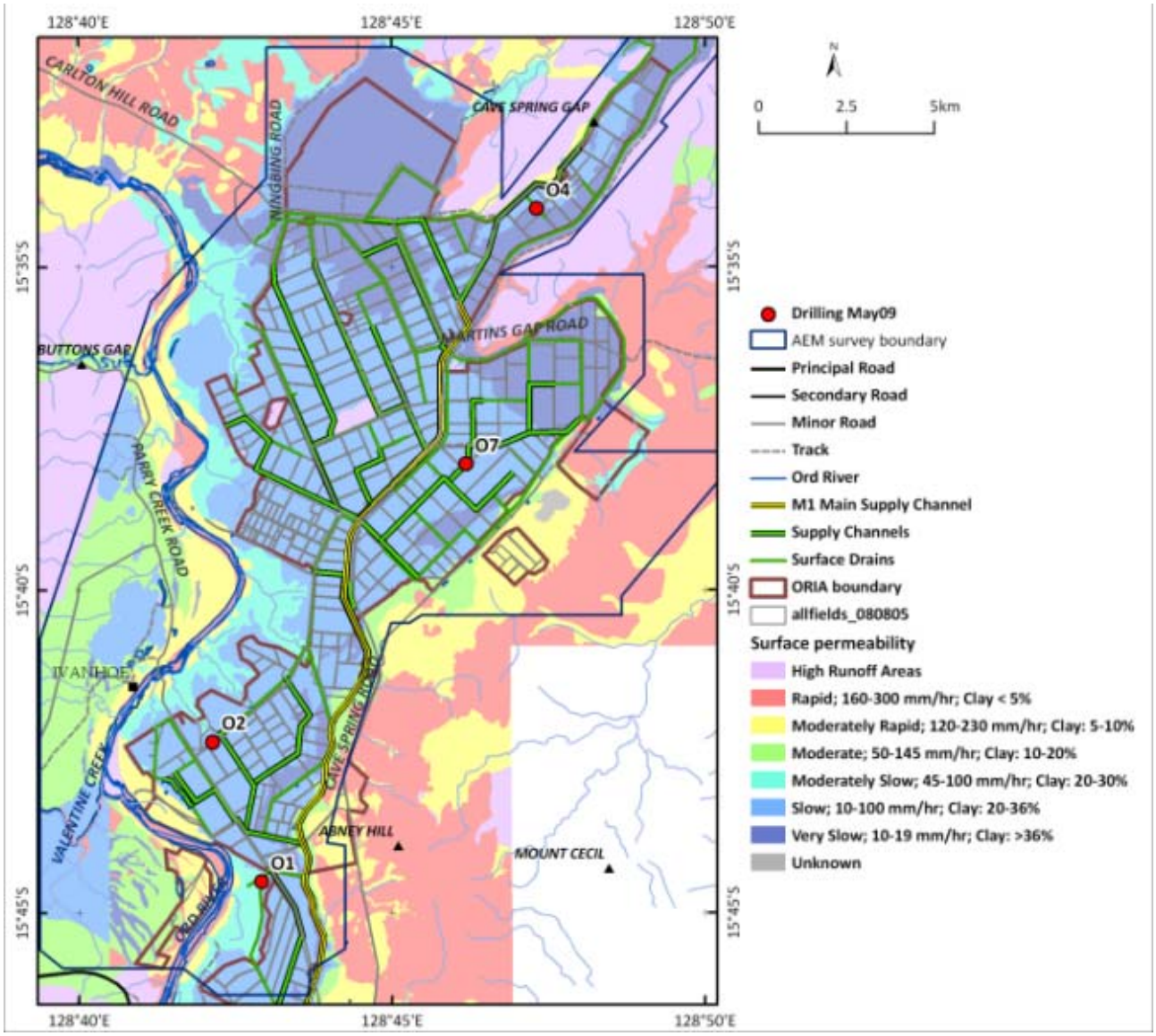

Figure 294: *Ivanhoe Plain and Ord West Bank surface permeability.*

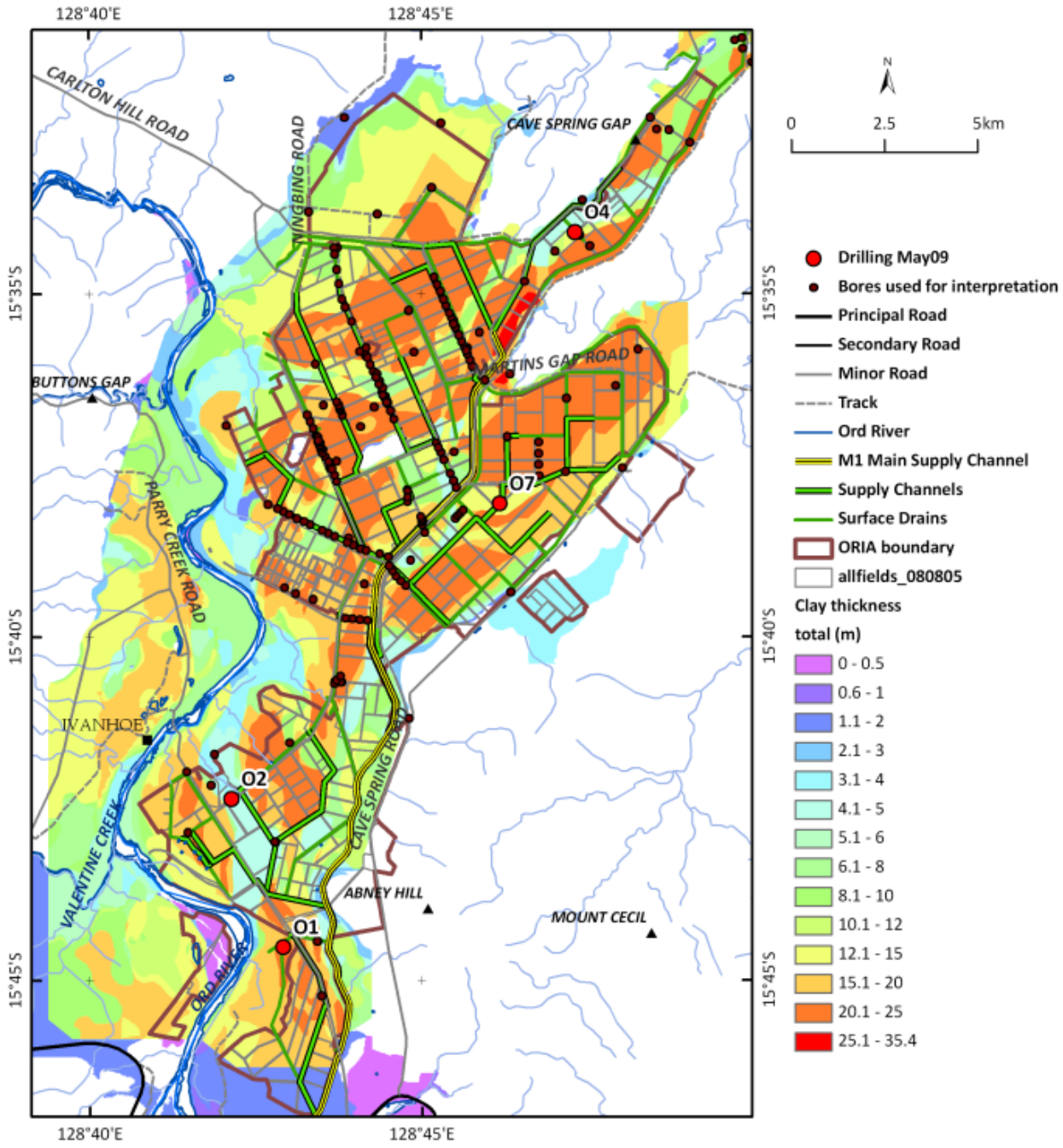

Figure 295: *ORIA Stage 1 Total clay thickness.*

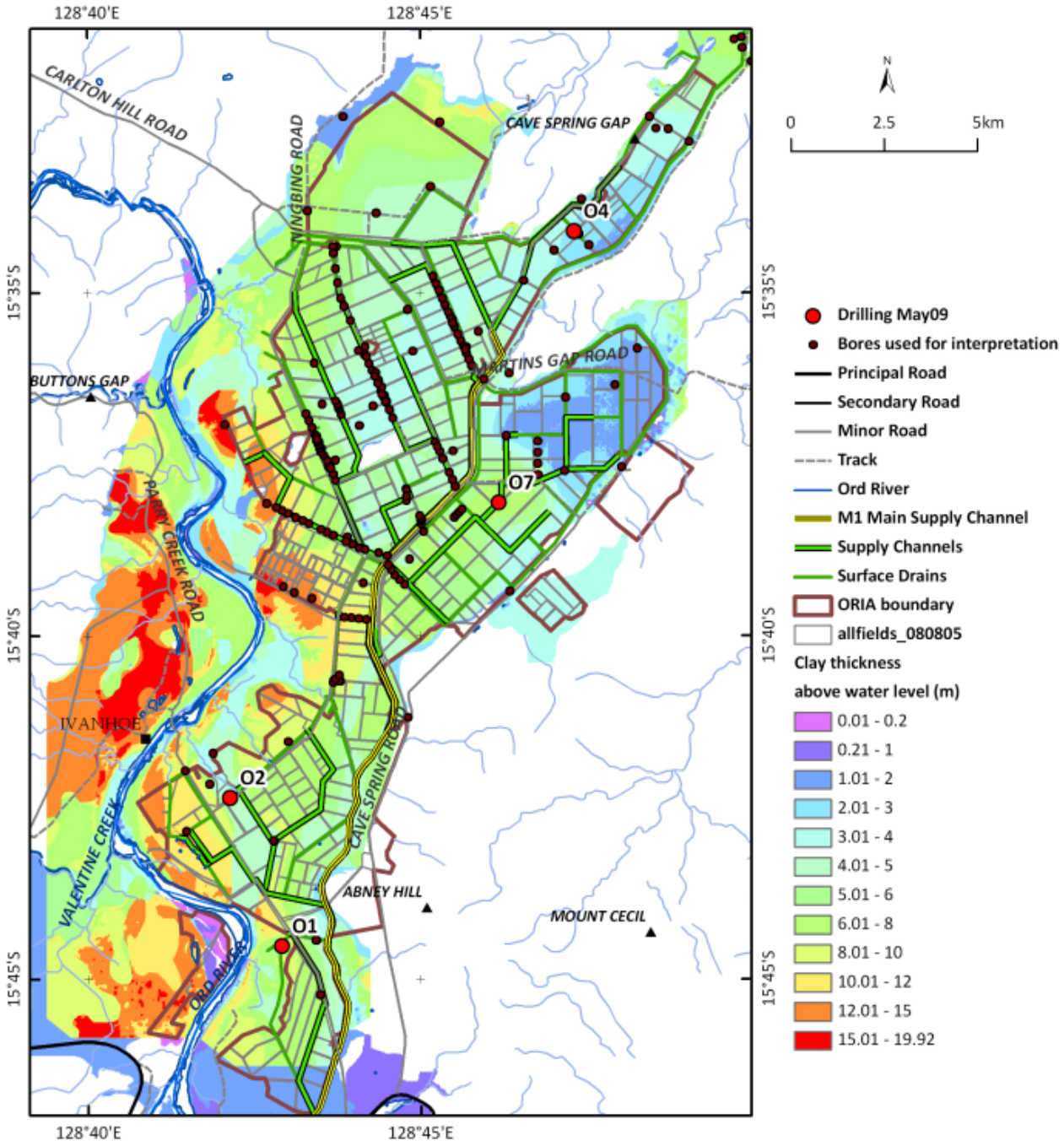

Figure 296: *ORIA Stage 1 clay thickness above the watertable.*

Where does leakage occur from the water supply infrastructure?

Modelling of leakage from the water supply channel network was carried out by Barr *et al*. (2003). They concluded that leakage was greatest from the M1 canal and at Martins and Greens Locations. Leakage was predicted to decrease where the water table had been raised to above the channel bottom. With water tables having stabilised at levels 2-4m below their peaks in much of the area, there is clearly greater potential for greater water leakage. To assess this potential, and to assess the potential for increased near-surface salinity associated with water leakage, focussed investigations were carried out to assess leakage from the M1 supply channel (Lawrie *et al*., 2006a; Smith & Price, 2008).

Prior to AEM data acquisition, leakage from the M1 channel was identified in Block 32 (Figure 297). This block was noted for its poor crop productivity, noted more recently in poor mango crop health (Figure 298). Bare ground was also observed closer to the M1 channel (Figure 297 and Figure 298). Ground geophysics carried out in this block in 2005/6 to provide a baseline dataset for more focussed salinity investigations (Lawrie *et al.,* 2006a; Figure 299). The ground NanoTEM survey noted locally very high electrical

conductivities correlated with the decline in mango crop health, with highly variable shallow conductivity structure, but with localised areas of very high conductivity closer to the M1 channel (Lawrie *et al.,* 2006a; Figure 299).

Ground validation of these higher conductivity zones shows that these correlate with areas of high to extreme salinity (Smith & Price, 2008; Figure 300). A soil pit was dug to a depth of around 3m below ground surface at the end of the 2005–06 wet season at which time the M1 channel had been empty for around three months. The pit did not 'make' water and it was clear that the local watertable elevation was at least 3m below the ground surface. A second pit was dug approximately one month later during the dry season when the M1 channel was full. The soil pit filled with groundwater to a depth of approximately 1.6m below the ground surface, indicating that the local groundwater elevation had risen significantly in response to filling of the channel.

Smith & Price (2008) concluded that salinisation is occurring due to spatially-variable leakage from the channel and the formation of local shallow groundwater areas that are probably seasonal (related to filling of the M1 supply channel). It is noted in this study that leakage and salinity in this area coincide with the location of a shallow palaeochannel (Palaeochannel 3 in Figure 203), parallel to the course of the M1 channel). The silts and sands in the upper part of this palaeochannel may aid leakage from the channel. This particular site is also an area of shallow bedrock that may impede vertical groundwater flow, and result in the pooling and near-surface evaporation of any leakage.

In the present study, a trial survey was conducted along the length of the M1 Canal to ascertain whether the AEM data could be used to identify areas of potential leakage. The average flying height of the transmitter loop along the canal was 21.1m. Results for the survey are presented in Figure 301. This section along the M1 channel is characterised by quite variable conductivities at a local scale. Both resistive and conductive areas occur under the M1 channel itself, while areas of higher electrical conductivities are also evident in both airborne and ground data Figure 299 and Figure 301, Lawrie *et al.,* 2006a).

The AEM section along the M1 supply channel identifies an electrically resistive zone coincident with the leakage point studied by Smith & Price (2008). In Figure 301, this coincides with site A. There are areas of high electrical conductivity immediately adjacent (A and C in Figure 301), that are coincident with areas of salt accumulation in the shallow sub-surface.

In conclusion, the AEM data appear to be showing some areas of potential groundwater leakage from the M1 supply channel, although ground validation of resistive areas is required. It is therefore recommended that further analysis of this dataset be undertaken to identify targets for the digging of pits and /or boreholes to confirm specific potential leakage zones. Some consideration has to be given to the proximity of the basement to the bottom of the canal as the resulting, potentially resistive, response may be confused with an area of leakage.

Similar detailed analysis may also be carried out to investigate potential leakage from other infrastructure assets in the Ivanhoe Plain, and the M2 and M2N channels, but this was beyond the scope of the present study. It is also recommended that synthetic AEM sections be constructed for the M2 and M2N supply channels and proposed drains in the Weaber Plain. This study should incorporate available geotechnical analysis of pits along these routes, as well as further targeted drilling.

Figure 297: *Aerial photograph showing location of seepage from the M1 supply channel, adjacent to areas of bare ground and reduced crop productivity (mangos) that corresponds with areas of locally high watertables (when the supply channel is filled) and high groundwater and sub-soil salinities. Photograph from Smith & Price (2008).*

Figure 298: *Bare (salt scalded) ground and stunted mango trees in an area of saline ground near the M1 supply channel.*

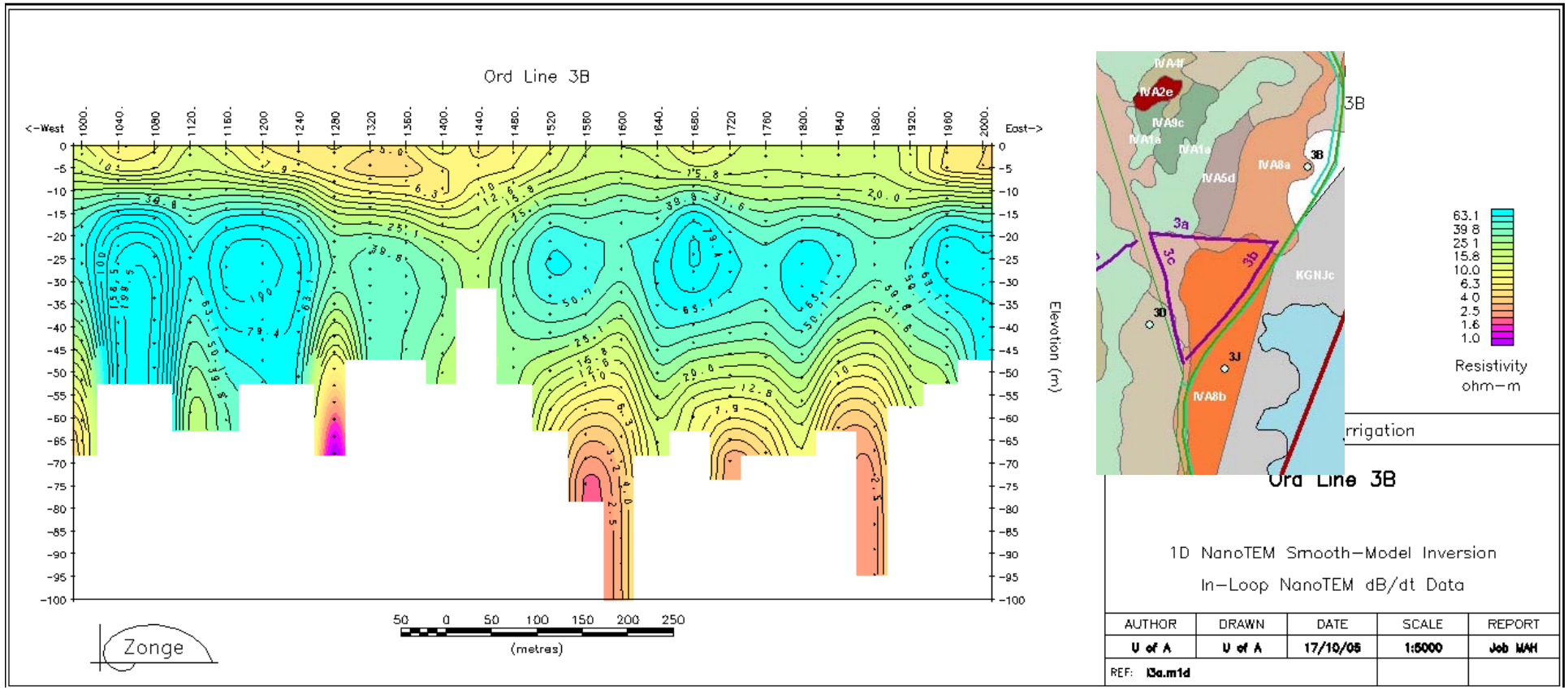

Figure 299: *Ground NanoTEM traverse parallel to the M1 channel. Areas of orange-red in the shallow sub-surface correspond with areas of higher recorded soil and sub-soil salinity values. (see Figure 300).*

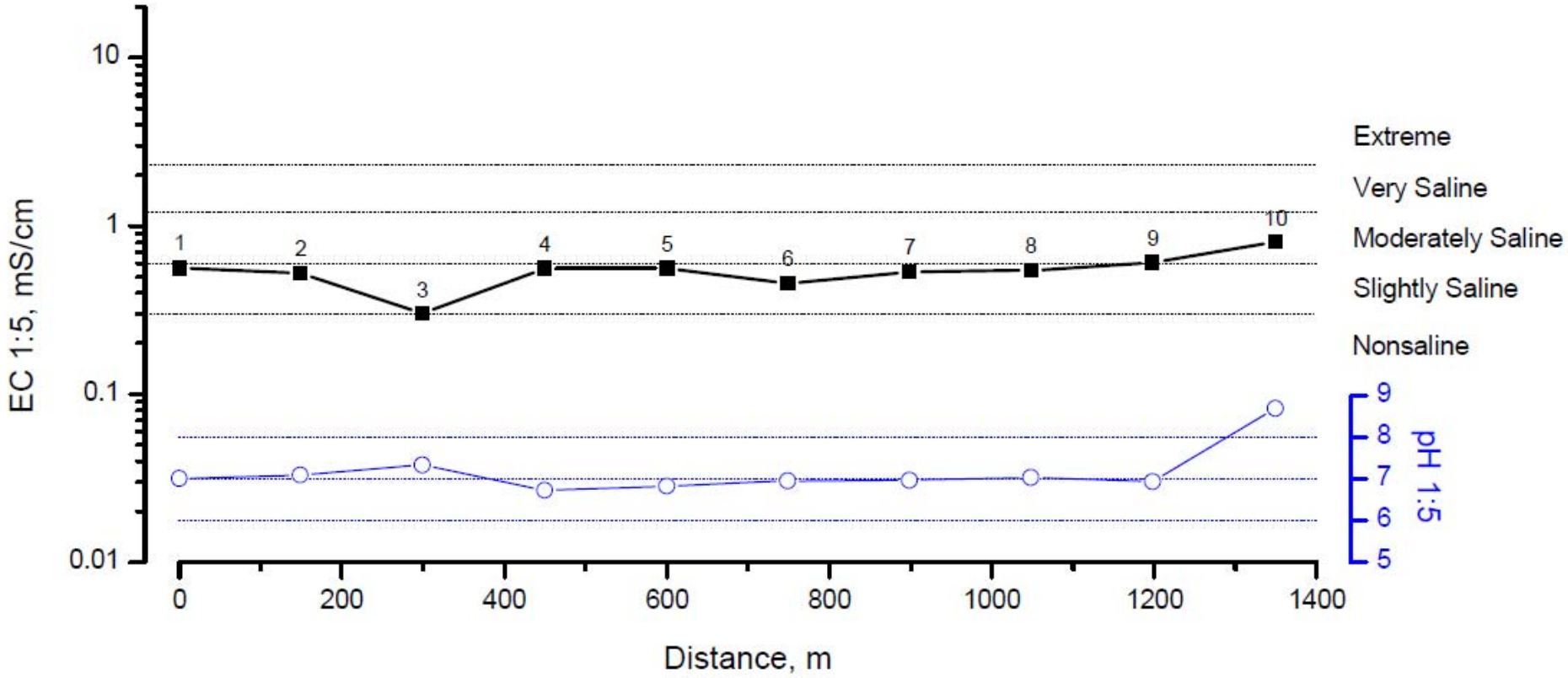

Figure 300: *Groundwater salinity and pH measured in a transect parallel to the M1 Channel (Smith & Price, 2008).*

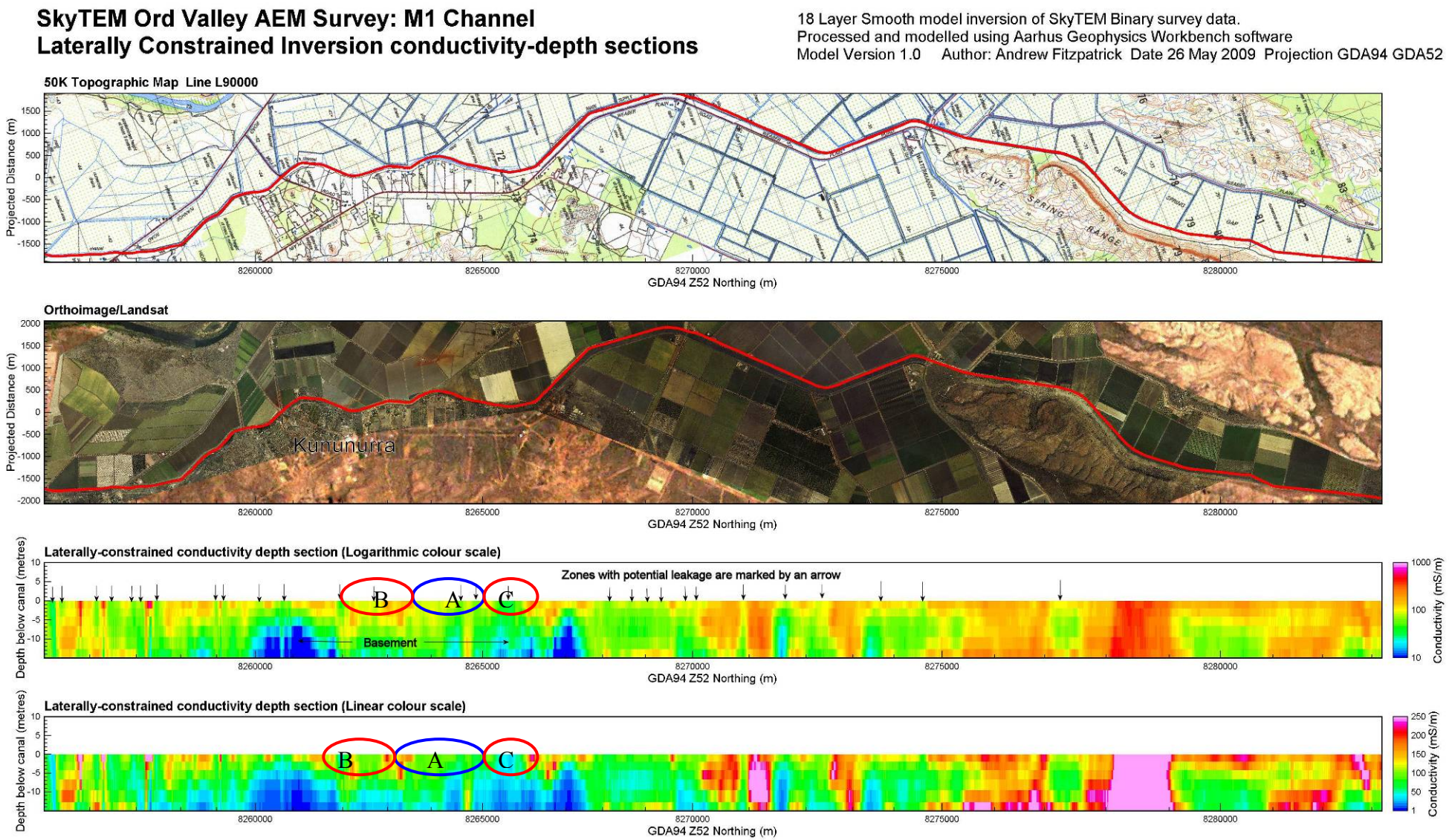

Figure 301: *Map view and corresponding conductivity depth section for the M1 Canal showing interpreted areas where leakage may occur.*

Why is the D4 drain an effective de-watering structure?

The D4 drain (Figure 302) is just one of the drainage structures that have been constructed with the objective of intercepting groundwater and lowering watertables in the northern Ivanhoe Plain (Smith, 2008). Analysis of historic groundwater data allied to the new AEM-based maps shows that the drain transects a wide range of geological materials and variable watertable depths. Parallel to Mulligan's Flat Road, the drain intercepts brackish to saline groundwater that flows through most of the dry season from the higher country to the east. At this location, the drain transects an older internal drainage basin. The drain at this location is intercepting the groundwater flowing from the east.

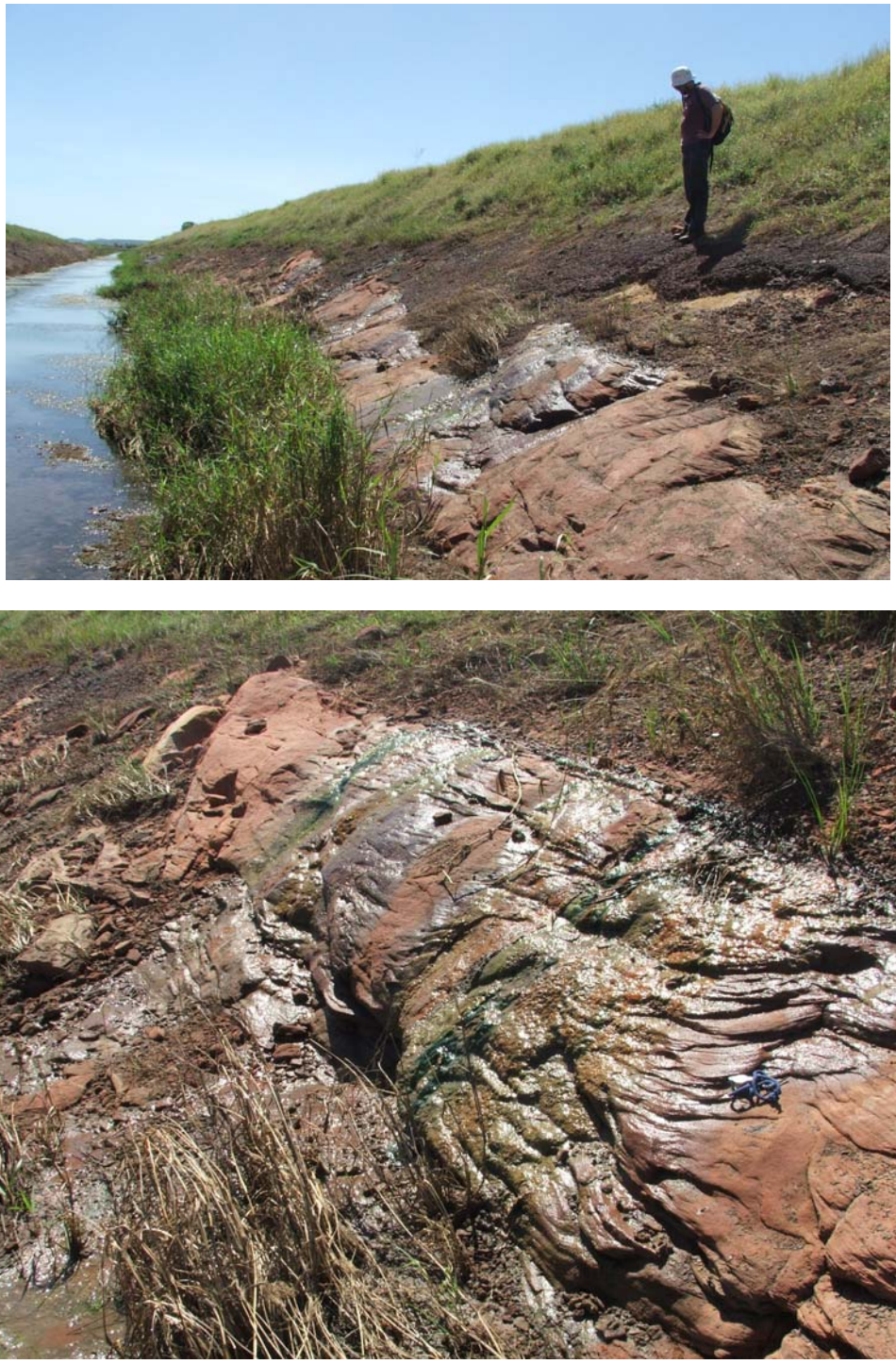

Figure 302: *The D4 drain on the eastern margin of ORIA Stage 1. The top figure shows a perspective view with ferricrete breccias in the upper 2-3m of the surface on the right bank resting on sandstone bedrock. The interface is a zone of continuous groundwater seepage. The lower image shows a close up of seepage at the sandstone-ferricrete interface.*

Further to the north, the D4 drain transects thicker clay soils of Martins Swamp. Watertables are still elevated in some of this area, and other drainage trials suggest the low hydraulic conductivity of soil and sub-soils in these areas minimises the effectiveness of the drains in this area. To the west, the D4 transects less clay-rich silty alluvium, and sandy palaeochannels. The drain appears to work effectively in these coarser textured units.

What is the impact of tree plantations on groundwater levels?

Recent watertable decline beneath a stand of unirrigated Sandalwood and African Mahogany in Martins Location (Figure 303 and Figure 304) has suggested that tree plantations can significantly influence groundwater levels by decreasing local groundwater replenishment and increasing transpiration (Carter *et al*., *in prep*.). In this particular case, watertable drawdown is marked (>5m), but restricted to the immediate area of the plantation (Figure 305).

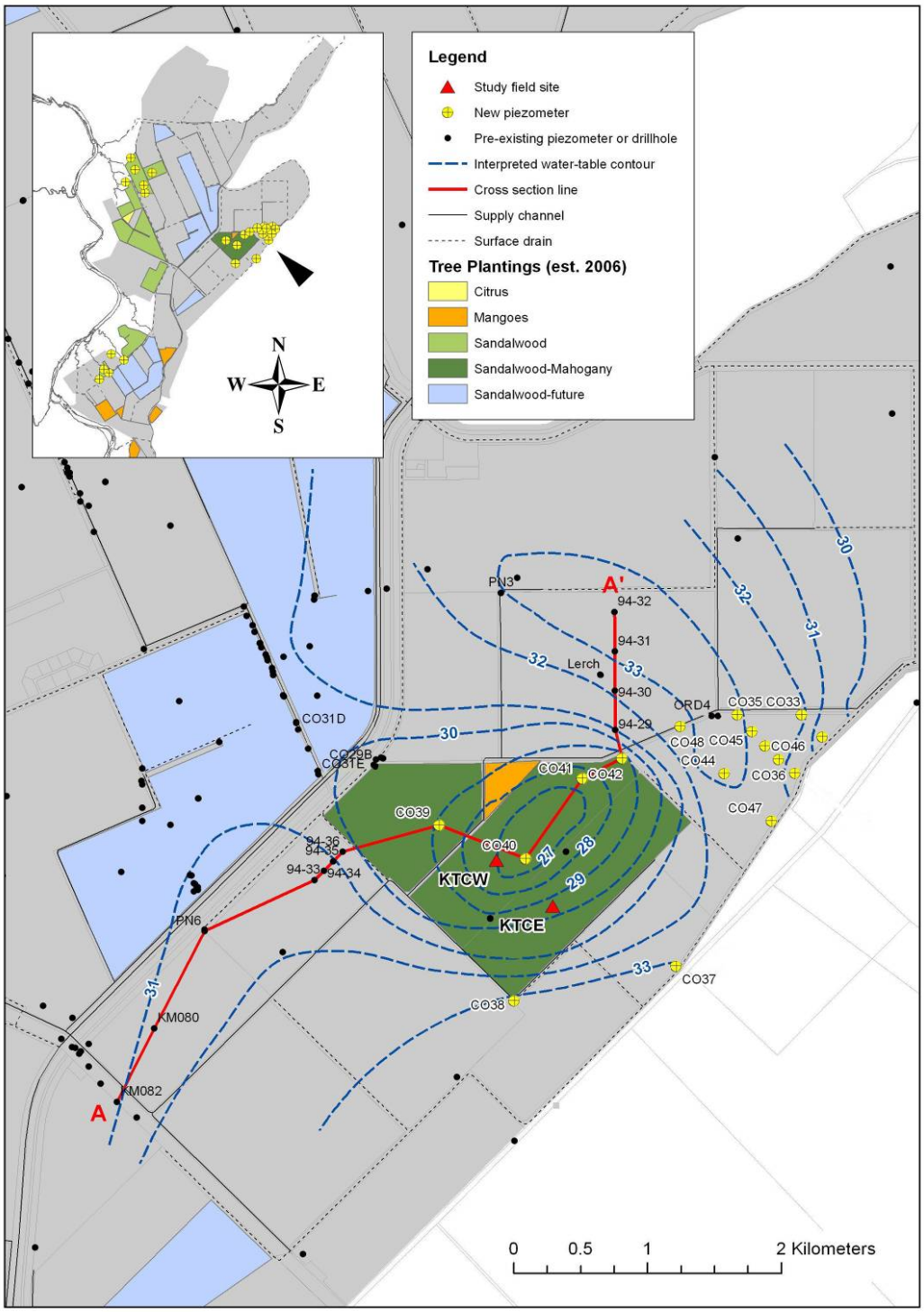

Figure 303: *Location of Mahogany plantation at Martin's Location, in ORIA Stage 1 area. (Figure courtesy of T. Smith, CSIRO).*

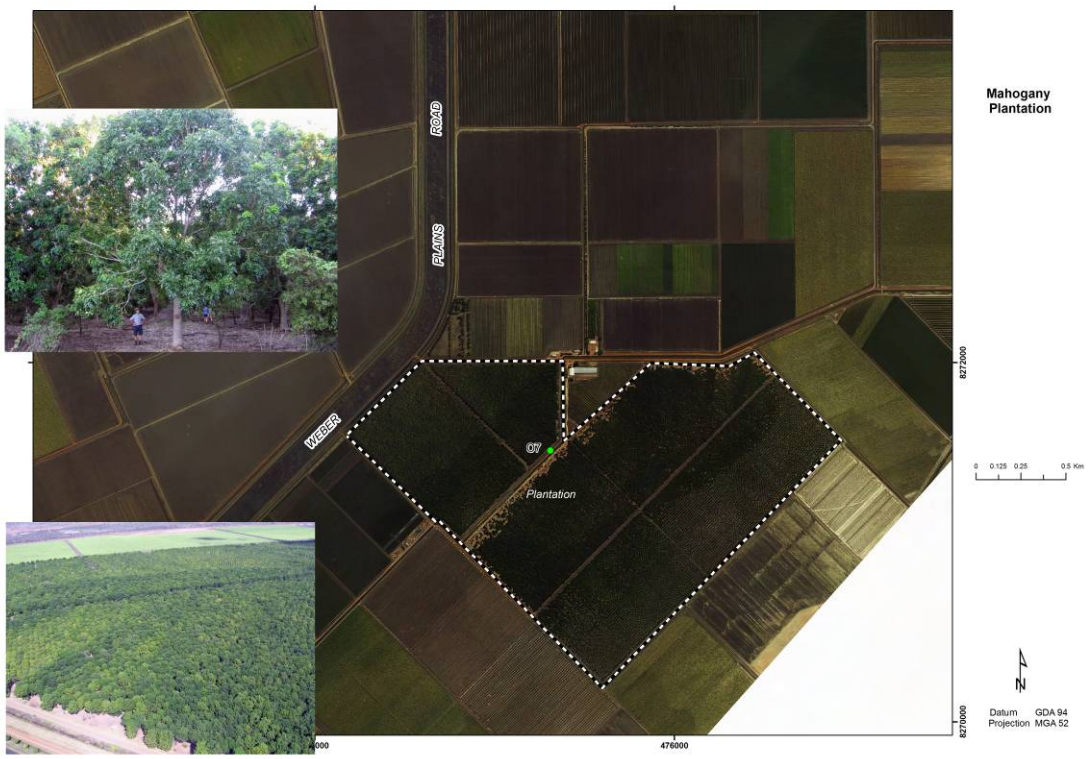

Figure 304: *Oblique (air) and ground photo of the Mahogany plantation with location of bore O7 detailed. Photos courtesy of T. Smith (CSIRO).*

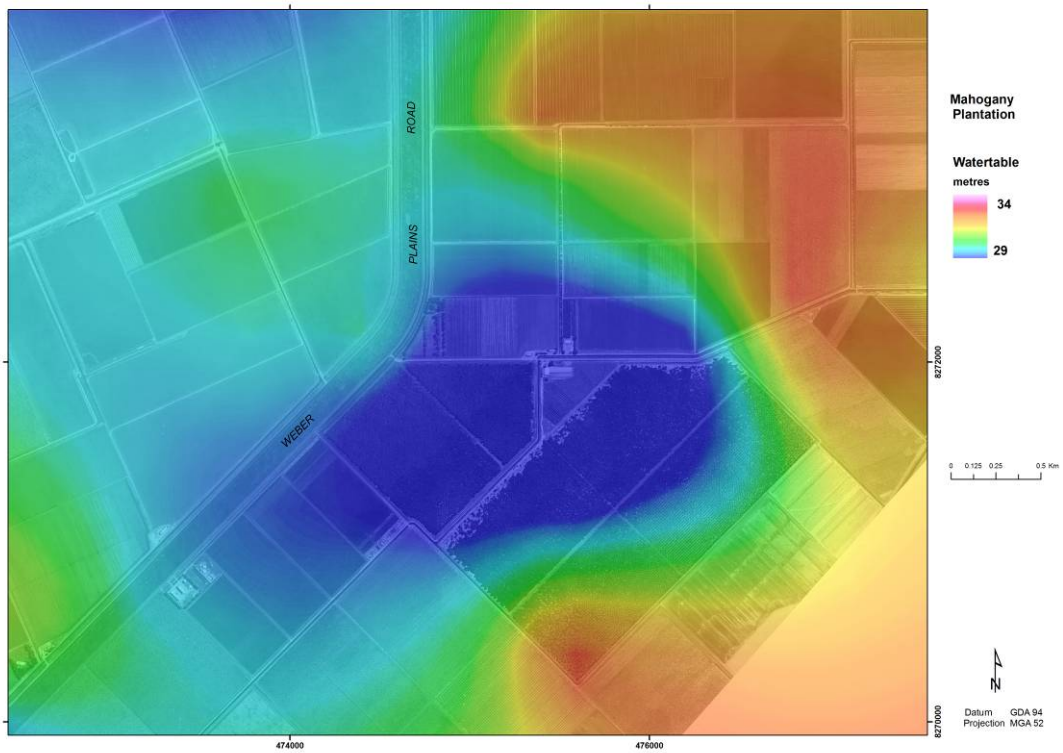

Figure 305: *Grid showing groundwater elevation over the Mahogany plantation at Martins Location.*

The plantation is managed by Kimberley Timber Corporation (KTC) and was planted in 1997 on Cununurra clay, with sandalwood and mahogany (*Khaya senegalensis*) hosts. On average there is a 150 trees per ha stand density with the plantation furrow irrigated 2–3 times per dry season. Irrigation ceased between 2001–06, but when planted the groundwater was around 0-2m below the surface. In 2008, the average depth to

watertable at KTCE was 5-m and 7-m at KTCW (Figure 303). Upon the cessation of irrigation, groundwater levels dropped and the sediments immediately beneath the plantations dried out (T. Smith Pers Comm, 2009). Results from the moisture analysis of core acquired from the sonic bore drilled at O7 in 2009 (Location shown on Figure 304), also indicated relatively low soil moisture levels in the top 10m of the profile (~20%).

Sediments immediately under the plantation are clay rich, with sandy and silty clays encountered at depths of around 5m. A plot of borehole conductivity, and the equivalent airborne vertical conductivity structure for the closest FID for bore 07 is shown in Figure 306. The upper part of the profile is relatively resistive with a low TDS (determined from the analysis of core samples), with higher values observed between 10 and 13m. An analysis of the interval conductivity data derived from the inverted SkyTEM data (Figure 307 - Figure 311), shows a resistive zone developed immediately beneath the plantation, persisting to a depth of >12m. In a conductivity-depth section for section line A-A' (see Figure 303 for traverse location), this resistive zone is clearly apparent (Figure 312).

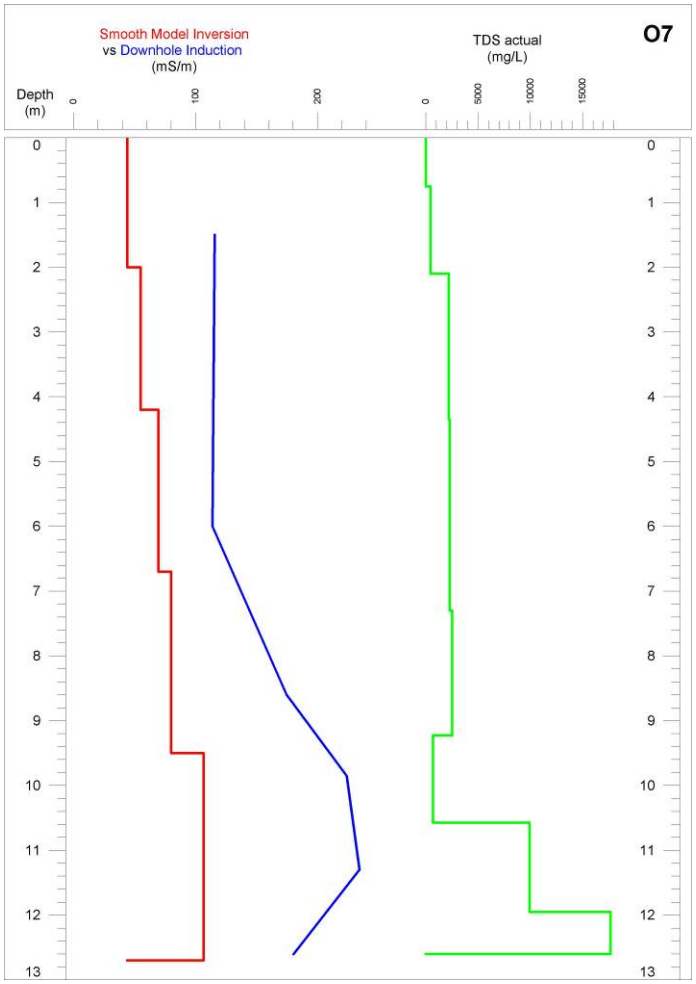

Figure 306: *Plot of borehole conductivity and near coincident inverted SkyTEM data for Hole O7. A plot of TDS measured from pore water samples extracted from core collected at Hole O7 are also shown.*

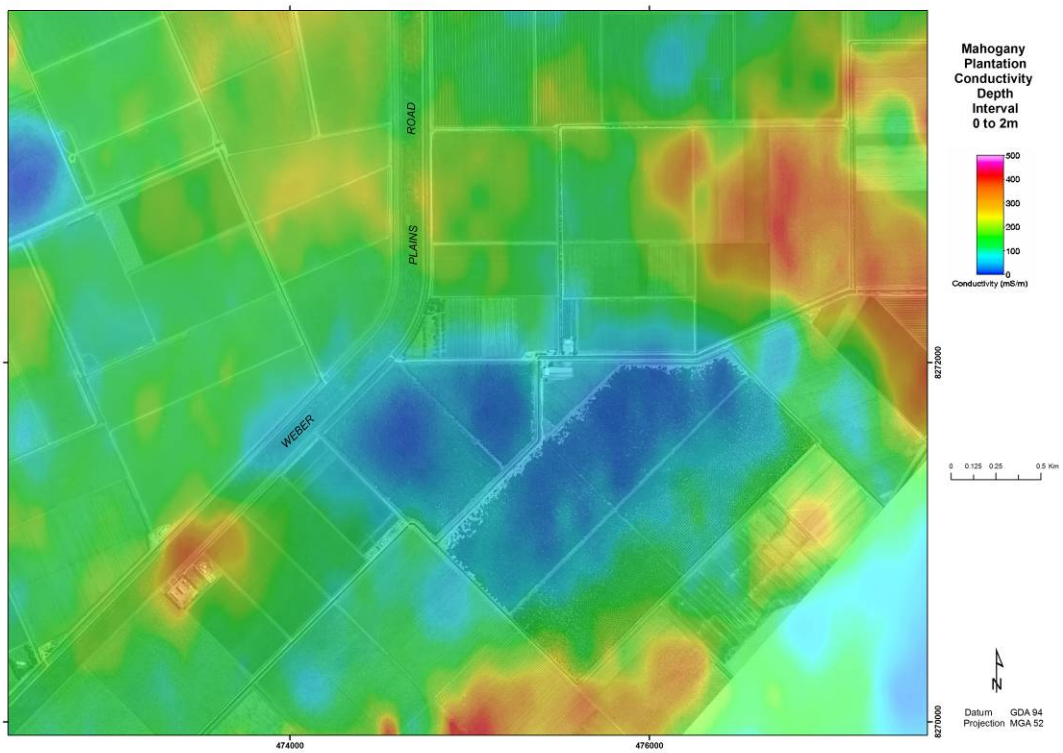

Figure 307: *Pseudocoloured interval conductivity for 0-2m below the ground surface over the Mahogany plantation at Martins Location.*

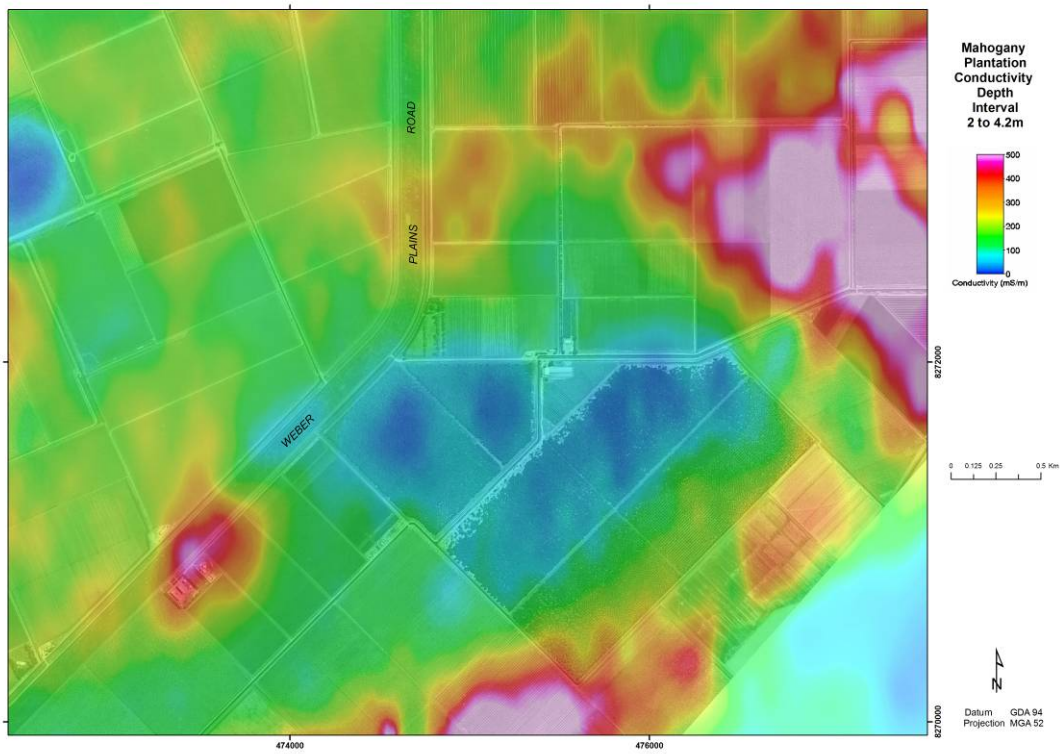

Figure 308: *Pseudocoloured interval conductivity for 2-4.2m below the ground surface over the Mahogany plantation at Martins Location.*

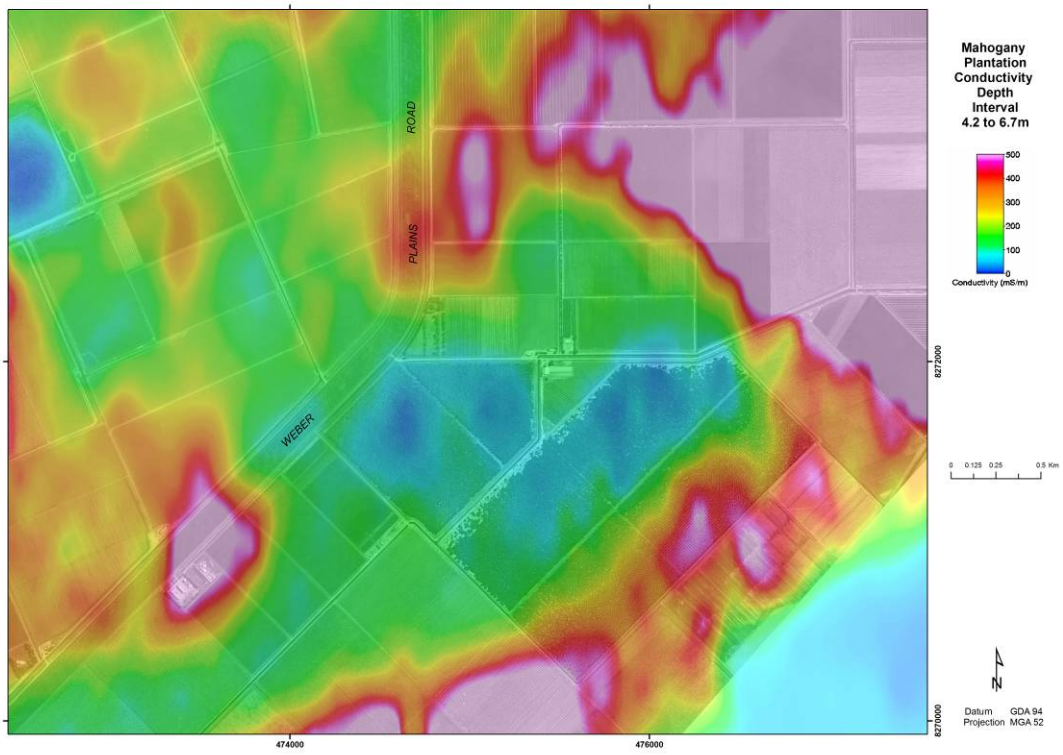

Figure 309: *Pseudocoloured interval conductivity for 4.2-6.7m below the ground surface over the Mahogany plantation at Martins Location.*

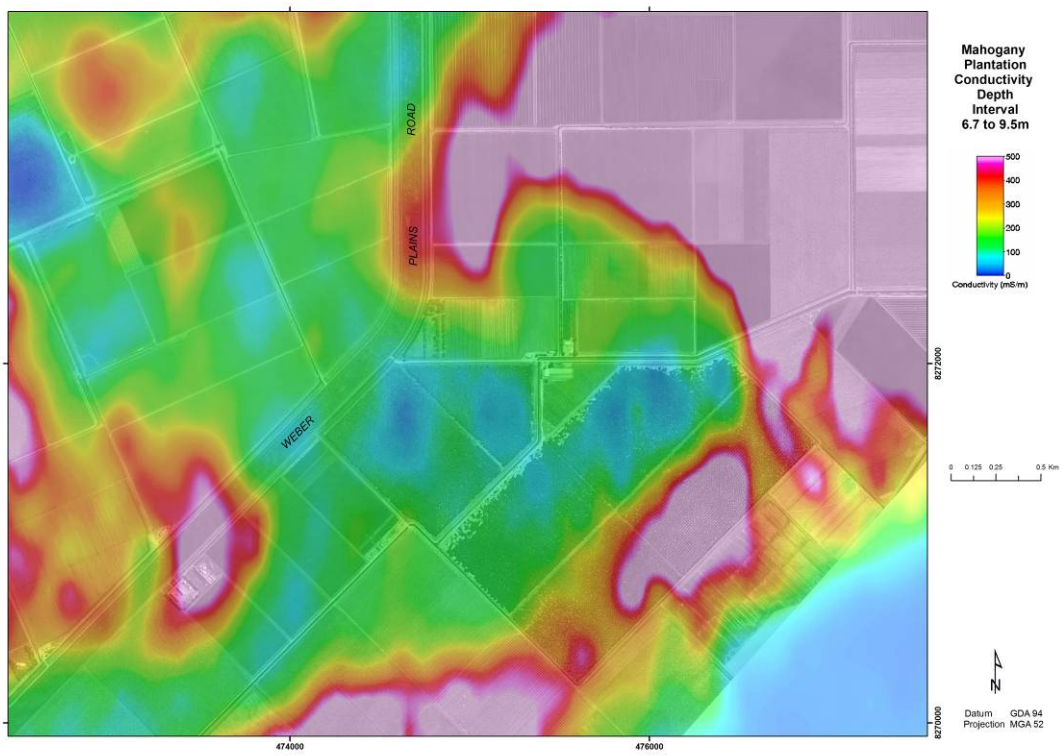

Figure 310: *Pseudocoloured interval conductivity for 6.7-9.5m below the ground surface over the Mahogany plantation at Martins Location.*

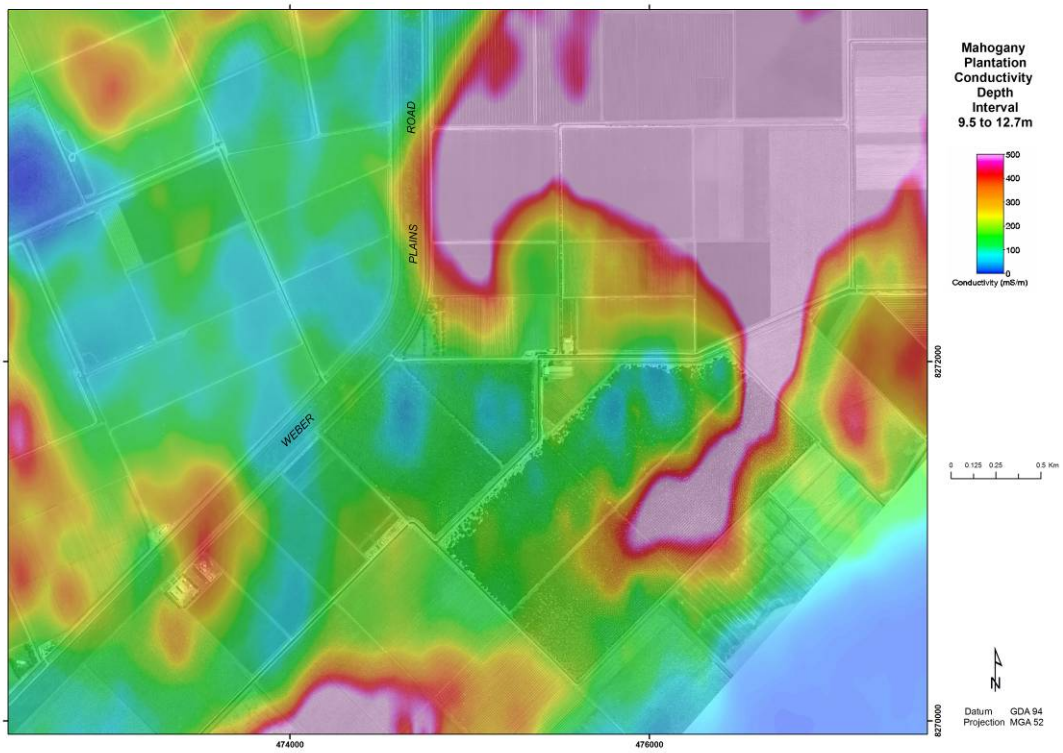

Figure 311: *Pseudocoloured interval conductivity for 9.5-12.7m below the ground surface over the Mahogany plantation at Martins Location.*

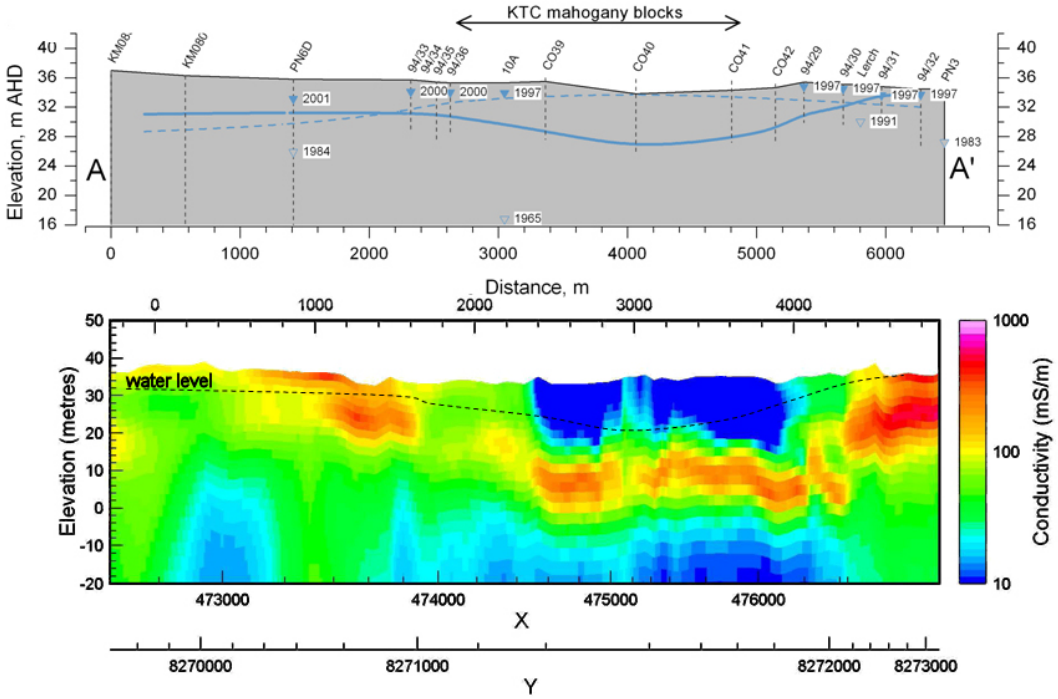

Figure 312: *Conductivity-depth section for traverse A - A' (see Figure 303 for location).*

Beneath the resistive zone, conductivity rises again. The observed ground conductivity structure is attributed to a combination of factors that act together; specifically a low moisture and dissolved salt content in the unsaturated zone, acting to reduce conductivity, with a rise in both in the saturated zone causing an associated rise in conductivity. The close spatial correspondence between the tree plantation and elevated conductivities at depth would tend to rule out simple changes in sediment texture as the primary driver for the observed conductivity patterns.

The observed conductivity structure could be attributed to several processes acting separately or in concert. The first is that the higher conductivities beneath the mahogany stand could be a product of leaching (from irrigation) of salt in the upper profile and its movement and accumulation around the position of the lower groundwater levels. The effect of lowering water levels as the stand developed, the repeated wetting (relating to irrigation and wet season recharge) and leaching of the upper profile may be one mechanism to consider. If these processes are occurring then they would indicate that salt is relatively mobile even in the fine-grained sediments found around Martins location. An alternative process could be that the increased conductivity arises from an accumulation of salt in the capillary fringe resulting from tree water use.

From a salt balance perspective, tree plantations such as found at Martins location may locally keep water tables well below the surface in areas where the aquifer has a relatively low transmissivity, and they may also encourage salt to move down and accumulate beneath the rooting zone. Regardless of the likely cause/process, we believe further investigation of these observations is warranted in light of the findings of a separate study presently being undertaken by Carter *et al.* (in prep) on the interaction between trees and water use in irrigated areas in the Ord Stage 1 region. Whilst this falls outside the scope of the present AEM investigation, it has potentially significant implications for salinity and water table management in the region.

The AEM data for the mahogany plantation also show an interesting (from a soils and plant growth perspective) relationship between tree growth/health and the observed ground conductivity in the near surface (<5m). In Figure 313, there is an observed variability in the canopy cover and tree height across a near surface conductivity transition (dashed line on the air photo) observed in the AEM data, with a deceased cover and tree height noted in plantation trees southeast of that line. Available knowledge for the area suggested that, in the levelling and development of the SE part of the paddock, soils from a deeper in the profile were incorporated into the surface materials prior to planting. Whether these deeper soils were more saline, and therefore responsible for the more conductive response observed in the airborne geophysics, remains to be determined.

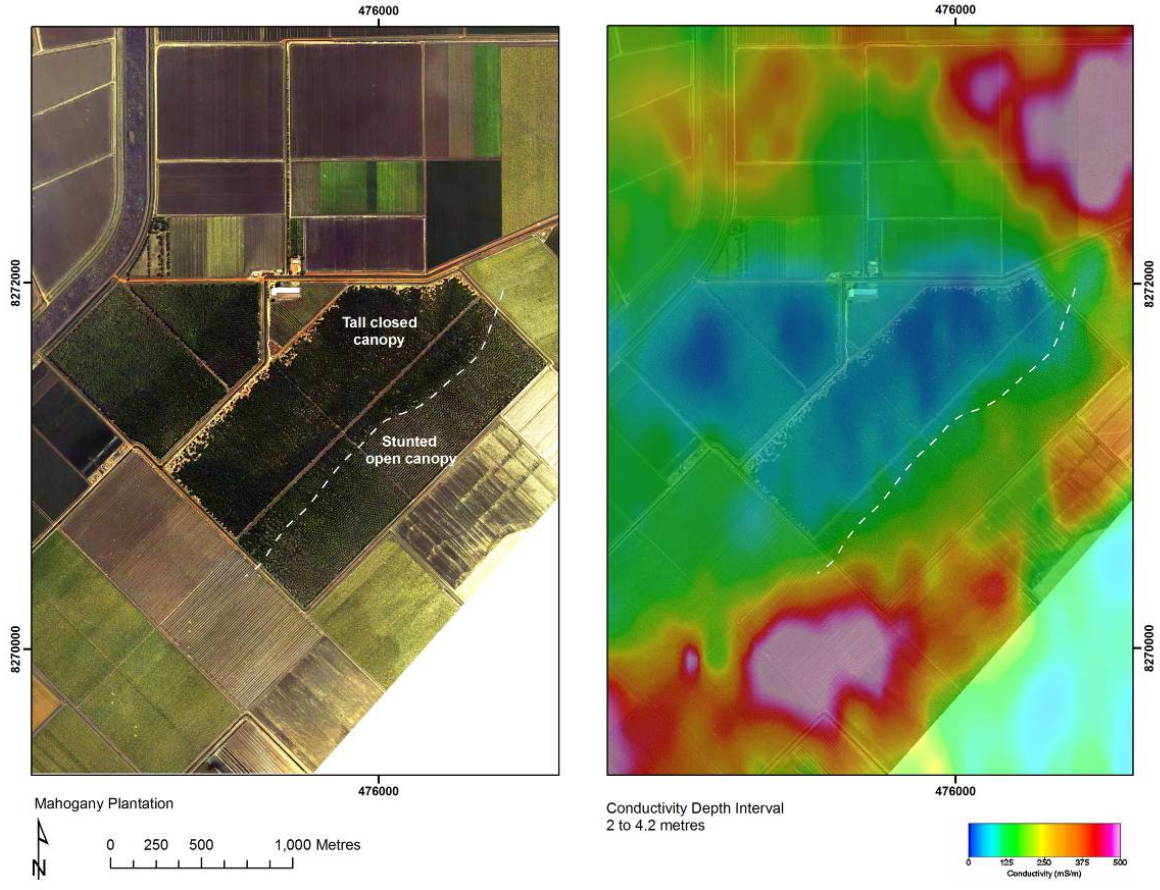

Figure 313: *Correspondence between near surface conductivities observed in the AEM data (right) and variations in tree canopy density and tree height identified as a spatial colour pattern change in the true colour air photo (left).*

In summary, it appears that some tree plantations can significantly influence groundwater levels by decreasing local groundwater replenishment and increasing transpiration. This study also suggests that dissolved salt moves downwards through the profile as groundwater levels drop, indicating it is relatively mobile even in the fine-grained sediments found around Martins location. From a salt balance perspective, tree plantations such as found at Martins location may locally keep water tables well below the surface in areas where the aquifer has a relatively low transmissivity, and they may also encourage salt to move down and accumulate beneath the rooting zone. Plantations may be particularly effective in areas of finer-grained silt and clay lithologies.

How useful are AEM systems in mapping salinity and regolith in areas away from the floodplain (e.g. where much of the development of the Cockatoo systems is proposed)?

The Cockatoo Sands lie largely outside the ORIA development area, but with small tracts to the east of the ORIA Stage 1, and in Ord West Bank. Geomorphic mapping in this study and reconnaissance mapping in previous investigations (Lawrie *et al.,* 2006a) over the Cockatoo Sands area located immediately east of Martins Location in ORIA Stage 1 indicated that the Cockatoo in this area comprises shallow soils (<3m) overlying variably weathered bedrock.

Following a trial survey of two lines and the application of a fast approximate inversion of the SkyTEM data across this area (Figure 314), the near surface interval conductivity data suggested a moderate (~100mS/m) but variable conductivity structure and gave merit to the idea of extending the survey, albeit at a wider line spacing (400m), across the region.

The resulting maps of conductivity from the fully inverted dataset (Figure 184 to Figure 193) show moderate conductivities confined to the near surface layers, particularly in the southern part of the survey area. Investigations in shallow pits have confirmed that sandy soils in this area are generally between 1m and 3m thick, and either overly basement sandstones with a ferricrete cap, or tightly folded and sheared metasediments and metavolcanics. The bedrock in this area is not deeply weathered, except in shear zones.

There is a lack of drilling information in this area, and no new specific ground validation was undertaken at these sites. However, previous investigations noted the presence of high sub-soil salinity levels and moderate to high ground EM responses in areas of mixed soils on the edge of the Cockatoo Sands (Richards, 2002; Lawrie *et al.,* 2006a). Moderately saline groundwater seeps, patches of salinity discharge at surface and salt effervescence at the base of ferricrete zones in the D4 drain have also recorded in these marginal areas (Lawrie *et al.,* 2006a; Smith & Price, 2008). This suggests that the observed higher conductivity responses reflect an accumulation of salts in soils and weathered bedrock at or near surface. The zone of moderate conductivity extends to depth in narrower zones (possibly reflecting saline groundwater in faults or shear zones), and beyond the extent of current irrigation to the east of ORIA Stage 1.

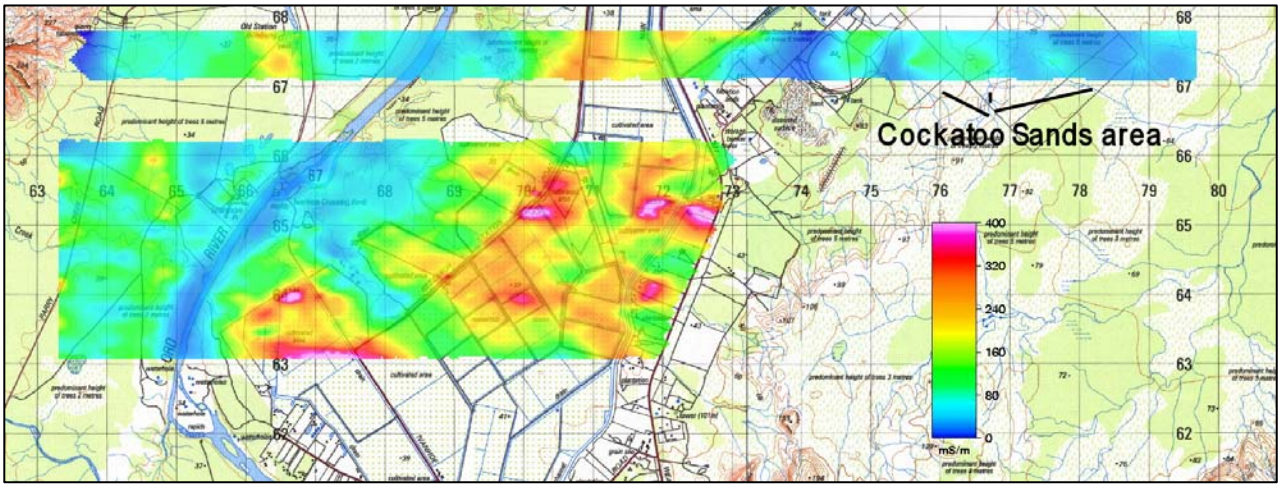

Figure 314: *0-2m interval conductivity from a fast approximate inversion of the SkyTEM data over part of ORIA and the Cockatoo Sands area.*

From this study, and studies elsewhere (Lawrie *et al.,* 2009a), the potential use of AEM technologies in areas of sandy soils of unknown or variable thickness and unknown moisture content, salt store and /or groundwater quality, must be approached with caution. Studies elsewhere have demonstrated that interpreting conductivity responses in dry sandy and /or variably clay-rich soils can be problematic (Lawrie *et al*., 2009a, b). In many instances, it may not be possible to differentiate dry sandy soils containing significant salt content from dry sand with no salt, and to distinguish these from dry clay rich lithologies and/or dry clays containing salts.

A scoping study compiling all available data is recommended to assess the scale of variability, anticipated thickness range, watertable data, and water quality information in areas of the Cockatoo Sands, while soil surveying and geomorphic mapping at appropriate scales is also recommended. Analysis of available satellite imagery may also be of some assistance to identify areas of moisture persistence and vegetation vigour.

If such a scoping study were to conclude that there was sufficient information to suggest that acquisition of EM data is desirable, and would produce useful information, a further evaluation would be required to assess which technology or combination of technologies would be most suited (i.e. ground or airborne) to produce a cost-effective outcome. This evaluation would need to consider the logistics of data acquisition in the area being considered (geography, access etc), and the depth and scale of investigation. Any proposed EM surveys in areas of Cockatoo Sands should perhaps be carried out as soon after the wet season as possible, to maximise the possibility of obtaining conductive responses from profiles with higher soil moisture content.

8.3.2 Packsaddle Plain

Where is salt stored in the landscape (in the saturated and unsaturated zones)?
Evaporation of perennial shallow groundwater along Packsaddle Creek combined with naturally saline subsoil has resulted in very saline to extremely saline surface soil within a distance of around 100m from the creek edge (Smith & Price, 2008). Currently there is no evidence that salinisation has encroached into the adjacent irrigation blocks or is adversely affecting the productivity; however, the extent of salinisation along the creek may increase if the watertable rises further.

Salinisation in low-lying surface depressions east of Lake Kununurra is probably the result of rising groundwater caused by the gradual formation of a subsurface ‘backwater’ (Smith & Price, 2008; Figure 315). Water-table rise throughout the area may be the result of direct leakage of surface water into the sediment bordering the lake and lateral subsurface flow into areas further east, or gradual accumulation of rainfall infiltration that is dammed behind the lake, or a combination of both processes (Smith & Price, 2008).

The hydrogeological conditions east of Lake Kununurra are poorly investigated and the watertable is not monitored. There appears to be no official records of drilling or groundwater elevation measurements either preceding or subsequent to the construction of the Kununurra Diversion Dam. If the ‘backwater’ east of Lake Kununurra is still forming then groundwater will rise higher and the extent and degree of salinisation may increase (Smith & Price, 2008).

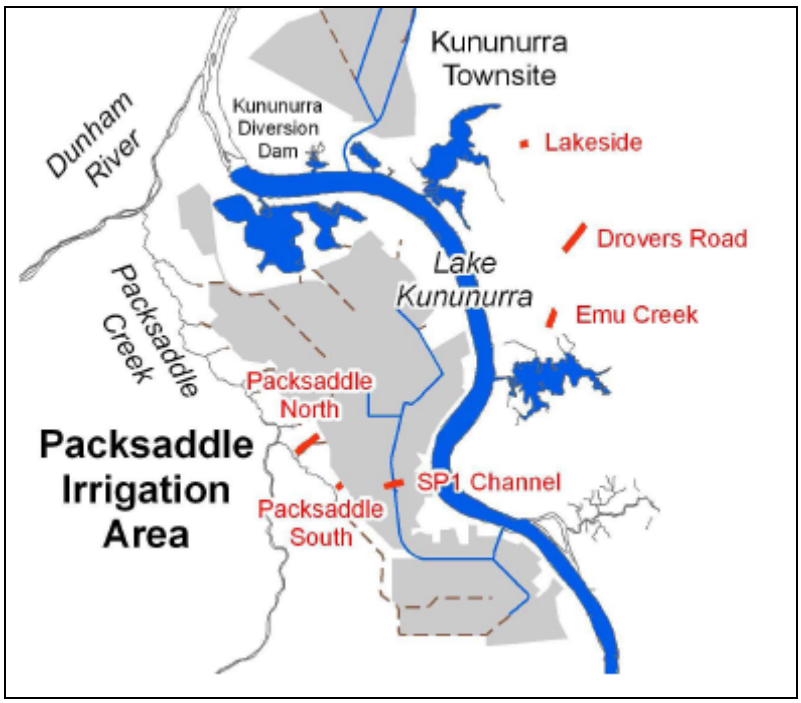

Figure 315: *Salinity occurrences in Packsaddle and in areas adjacent to Lake Kununurra. From Smith & Price (2008).*

In this area, salt scalds are mapped along Packsaddle Creek (Figure 316 to Figure 318). However, previously no salt store maps have been available for Packsaddle Plain, and as with Ivanhoe Plain, assessment of salinity hazard in this area has relied largely on modelling water table rise and climatic factors (e.g. Ali & Salama, 2003).

The AEM data, calibrated by drilling and field sampling, have established that the salt stored in the unsaturated and saturated zones throughout most of the Packsaddle Plain is between 10 and 40t/ha/m (Figure 319 and Figure 320), which is considerably lower than Ivanhoe Plain. However, depending on how readily these salt stores are mobilised, the levels are still sufficiently high to be of some concern to irrigated agriculture should the water table rise to within 2m of the ground surface (Ali & Salama, 2003).

Overall, salt in the unsaturated zone is relatively low (<20t/ha/m), with only a couple of relatively small patches (from a few hundred metres to 1km across) where the salt store in slightly higher (<30t/ha/m). In the saturated zone, the salt stored is slightly higher (11-40t/ha/m). There is a low to moderate potential risk of soil salinisation in this area. Lower salt store values are encountered primarily within narrow sand and gravel palaeochannel in the west and north of the area (Figure 320 and Figure 203), where the total amount of salt stored is low (0-10t/ha/m), but there is a higher risk of the salts being mobilised. The salt store is also lower where the present Ord River has incised through the alluvial fill.

Where the salt store maps are overlain with plans of water supply and drainage infrastructure, small areas of higher potential salt mobilisation and salinity risk are identified, primarily in the centre of the area where the salt store is highest. These correspond with the areas of salt scalding noted earlier. The new salt store maps, allied with maps of groundwater quality and lithology, should assist with groundwater model parameterisation, and should enable more spatially accurate predictions of the salinity hazard to be made for this area.

Figure 316: *Aerial view looking west across Packsaddle Creek, showing permanent water defined by reeds and bare ground. Saline scalds occur along the margin are formed by active saline water seepage.*

Figure 317: *Salt scalding along the margins of a shallow creek feeding in to Packsaddle Creek.*

Figure 318: *Salt effervescence on scalded bare earth close to the banks of Packsaddle Creek.*

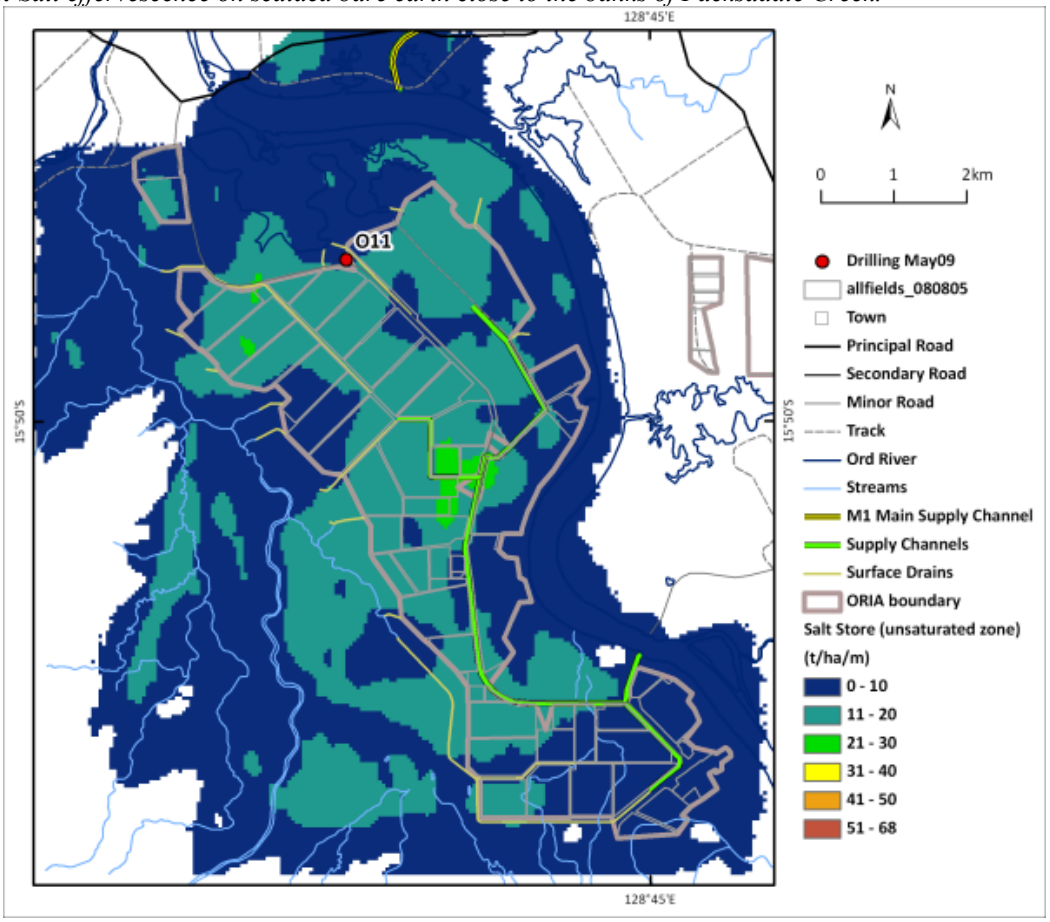

Figure 319: *Packsaddle Plain unsaturated salt store.*

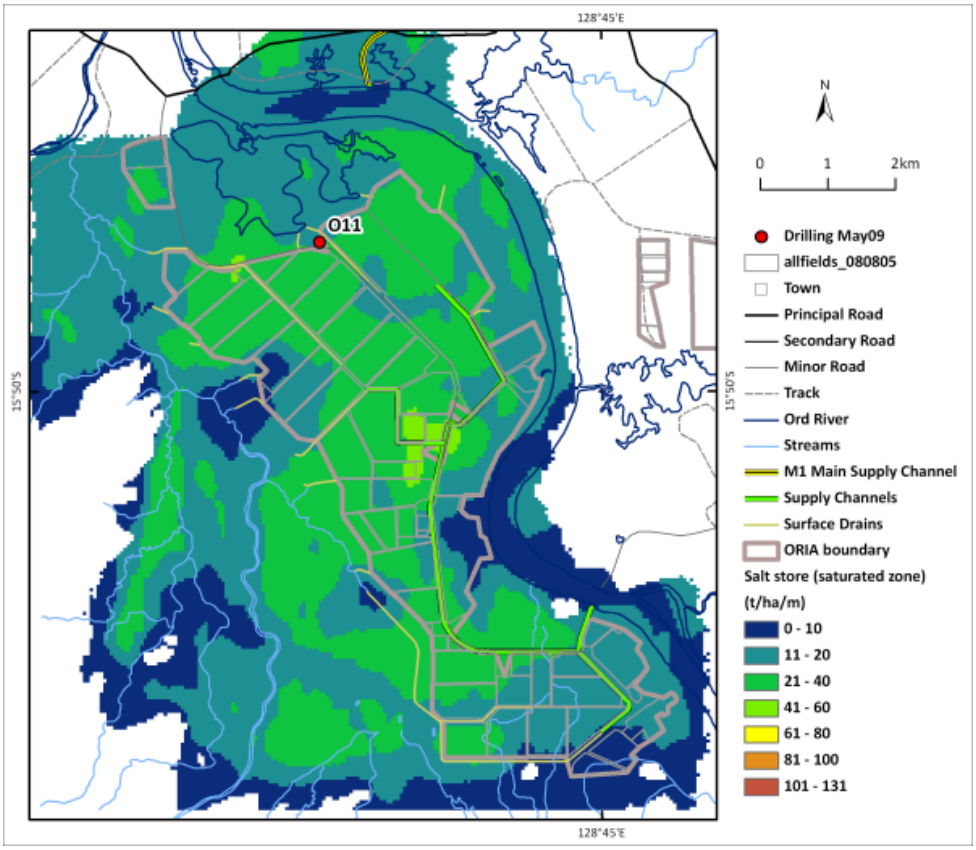

Figure 320: *Packsaddle Plain saturated salt store.*

What is the distribution of groundwater quality (salinity)?

Previous sampling of groundwater in Packsaddle Plain found salinities greater than 750µS/cm over most of the area, with values of over 10,000EC in the centre of the Packsaddle Plain (Ali & Salama, 2003). The latter considered that EC levels between 250 and 750µS/cm posed a medium salinity risk to irrigated agriculture, with higher values posing a high risk, should the water table rise within a couple of metres of the ground surface.

The new AEM-based maps of groundwater quality, calibrated by pore fluid analysis from drilling and field sampling, are generally consistent with the results from previous groundwater sampling programs. Overall, the AEM mapping has established that the groundwater quality in the Packsaddle Plain ranges from 500 – 1,000TDS (mg/l; ~ 800 to 1,600EC) with a few patches between 1,000 and 2,000TDS (or ~ 1,600 to 3,200EC) (Figure 321).

The AEM-based maps of groundwater quality have a much higher spatial resolution than previous maps. This enables groundwater quality measurements to be linked more directly to specific elements of the hydrostratigraphy, provides targets for groundwater management, and provides the basis for more spatially explicit predictions of salinity hazard. The groundwater quality maps reinforce the need for groundwater management in this area to minimise the salinity risk.

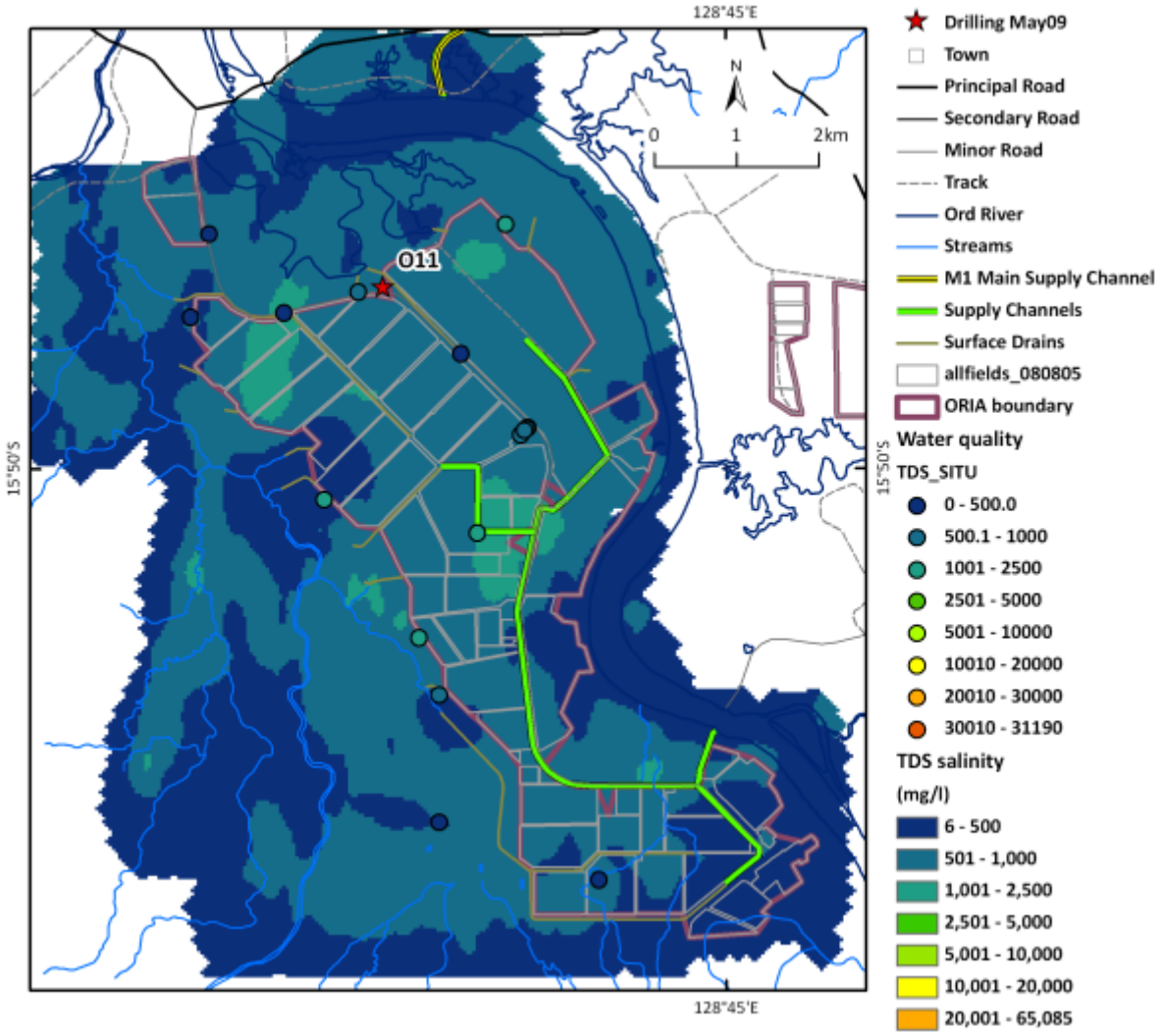

Figure 321: *Packsaddle Plain groundwater salinity*

Salinity hazard

Salama & Pollock (2003) concluded that the factors contributing to the development of secondary salinity in the Packsaddle Plain included shallow groundwater levels that were aggravated by the formation of the Ord River impoundment behind the Diversion Dam, and waterlogging and build up of surface salt deposits associated with surface water discharged from drains. Most of the salinity scalds in the area occur along the banks of Packsaddle Creek which is incised into the plain.

A detailed breakdown of each hazard class for the Ivanhoe Plain and Ord West Bank is shown in Table 36. The areas that the figures refer to are shown in Figure 287. In general, these maps show that the salinity hazard is lower than in the Ivanhoe Plain, but that there are some significant areas of moderate salinity hazard. There is only a relatively small are of high hazard in Packsaddle Plain (Figure 322).

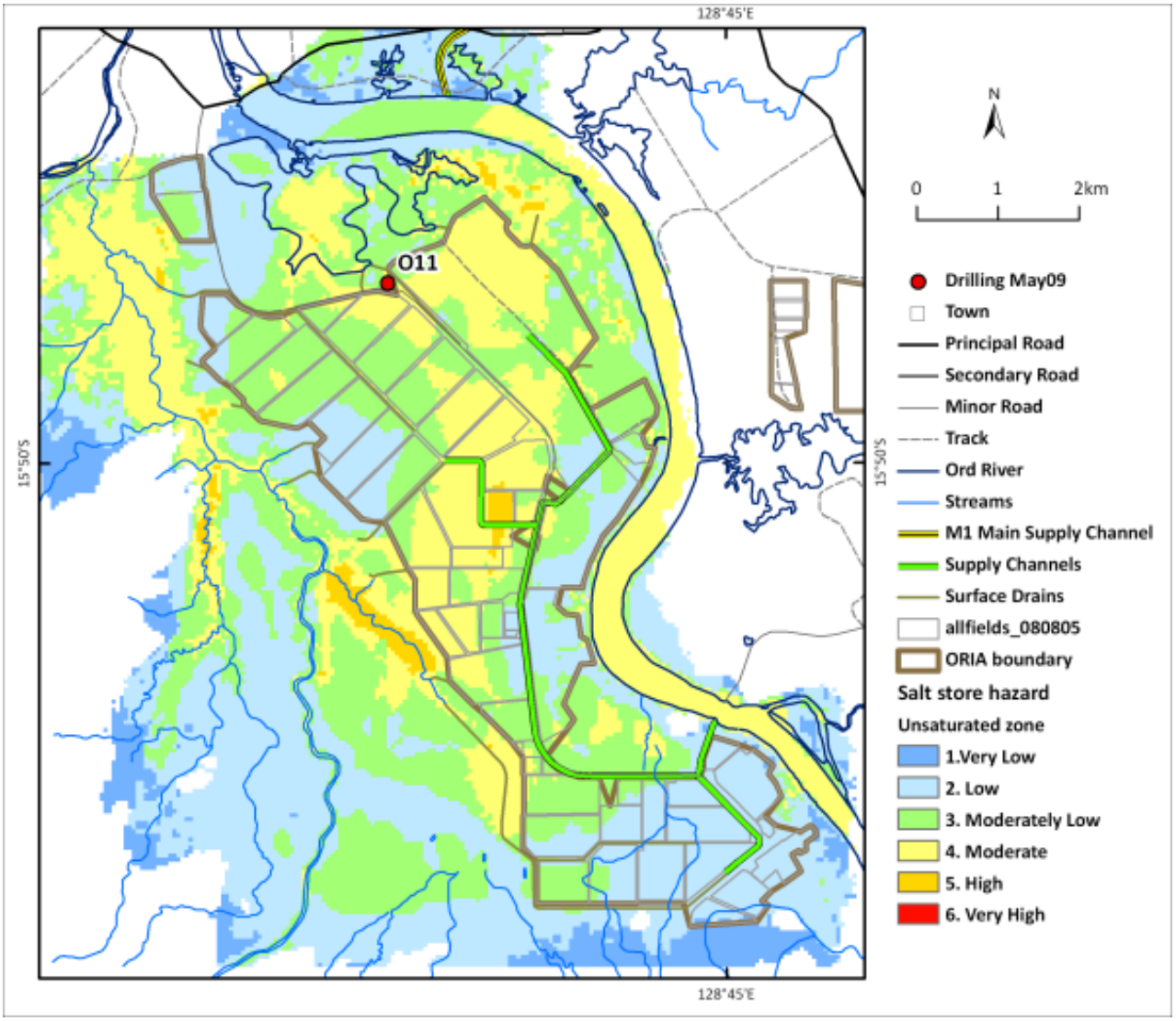

Figure 322: *Packsaddle Plain unsaturated salt store hazard.*

Table 36: *Salt Store Hazard class within proposed Packsaddle irrigation areas. Note: these figures have been rounded to the nearest whole number.*

Area Name	Hazard Class	Hectares	Percent
Packsaddle - 1A	1.Very Low	8	0
	2. Low	880	17
	3. Moderately Low	1029	20
	4. Moderate	685	13
	5. High	20	0
	Area not assessed	28	1
Packsaddle - 1A Total		2649	50
Packsaddle - 2B (proposed extension)	1.Very Low	22	0
	2. Low	1258	24
	3. Moderately Low	738	14
	4. Moderate	200	4
	5. High	67	1
	Area not assessed	330	6
Packsaddle - 2B Total		2613	50
Grand Total		**5263**	**100**

What is the extent and thickness (in 3D) of the sand and gravel aquifers, and how are they connected?
Figure 323 shows the depth to bedrock map for the Packsaddle Plain area. This shows that maximum alluvial fill is deposited in a palaeochannel incised into bedrock in the south and west of the area. The thickness of gravel deposits is shown in Figure 324. The thickness of sands is shown in Figure 244. The distribution of gravels is consistent with deposition in the palaeochannel on the western side of Packsaddle Plain (Figure 203).

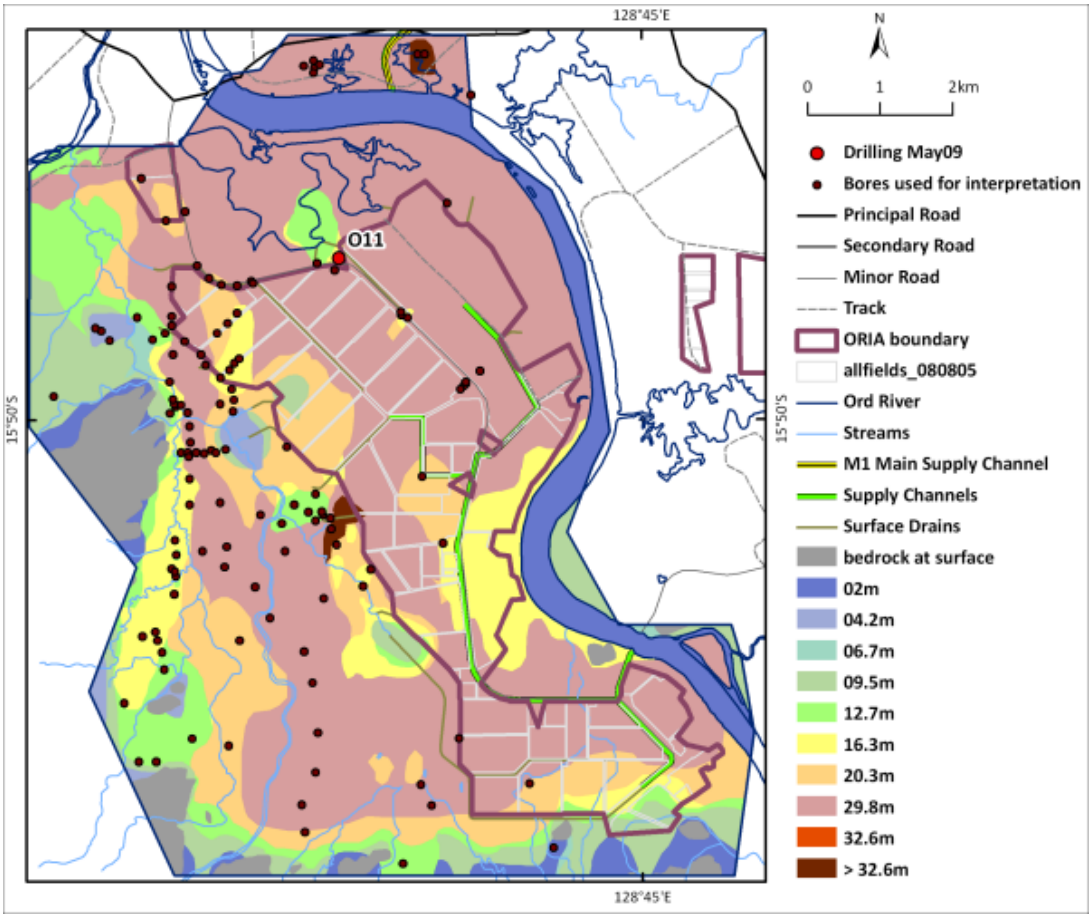

Figure 323: *Packsaddle Plain depth to bedrock map.*

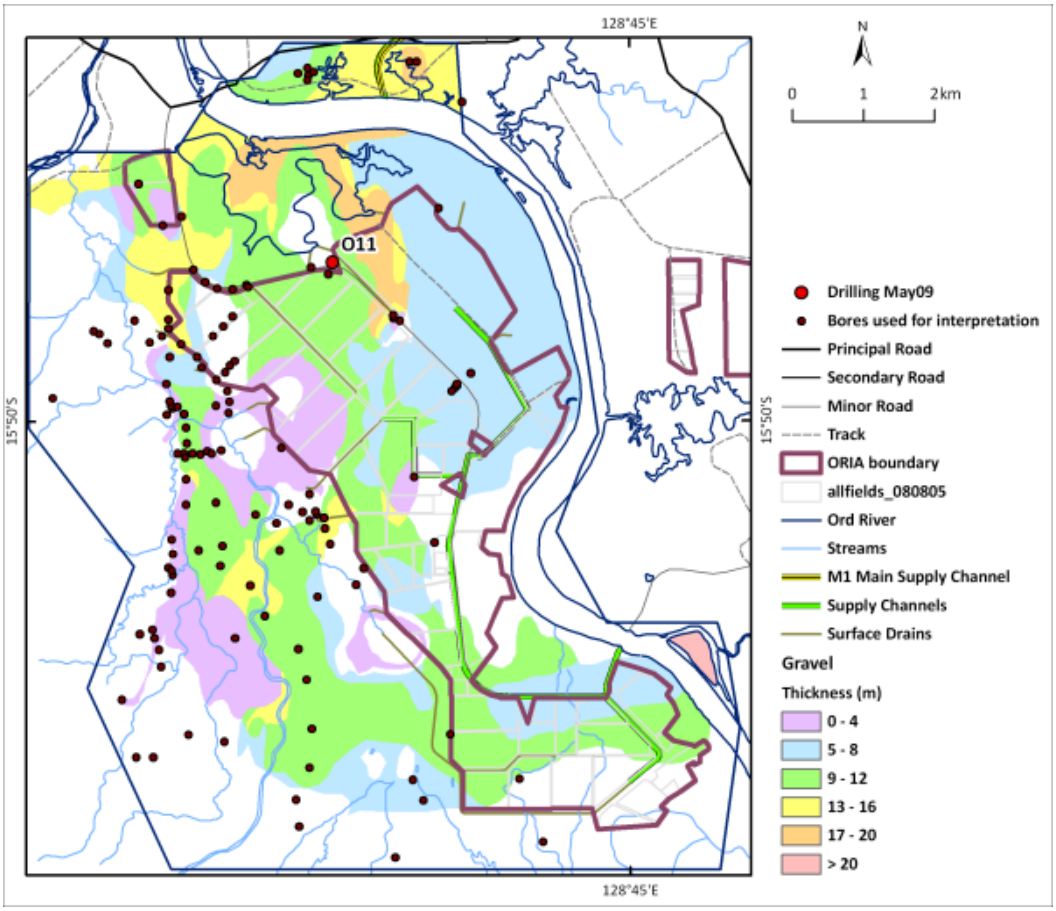

Figure 324: *Packsaddle gravel thickness.*

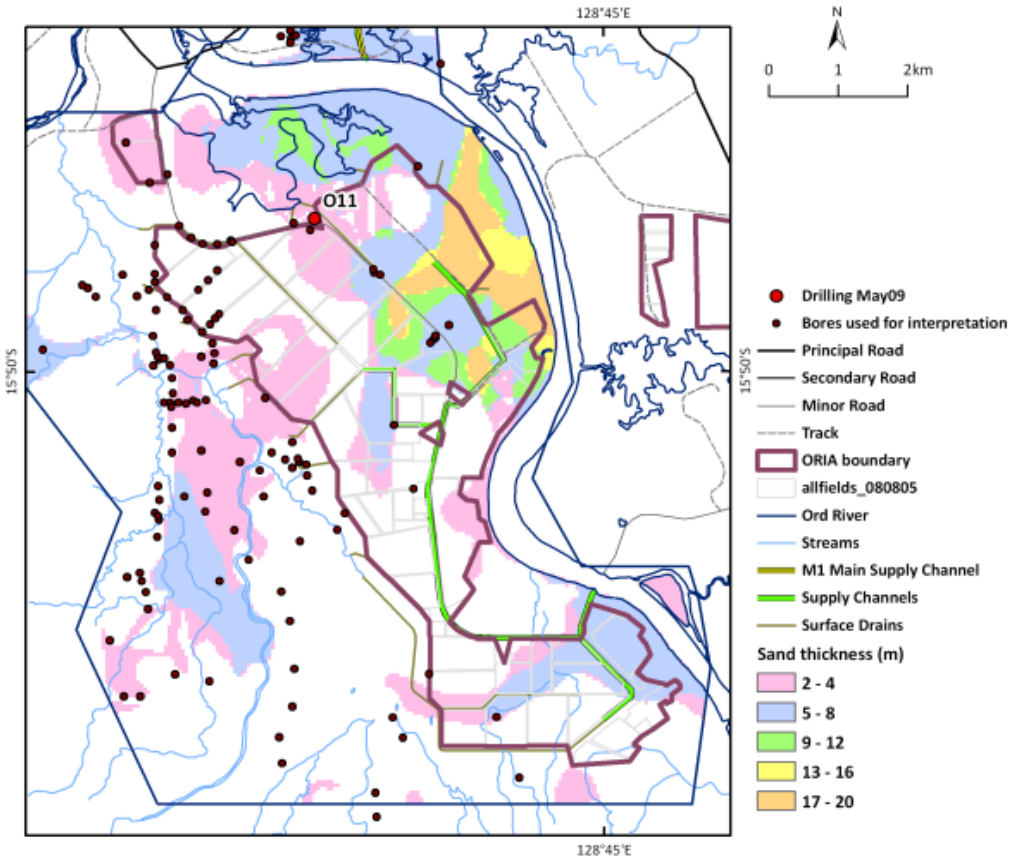

Figure 325: *Packsaddle sand thickness.*

What is the extent and thickness of clays in the sub-surface?

Figure 326 reveals that the thickest clay deposits are also present overlying the palaeochannel deposit in the south and west of the area. Clay thicknesses of up to 20m are observed, in comparison with thicknesses <12m over much of Packsaddle Plain.

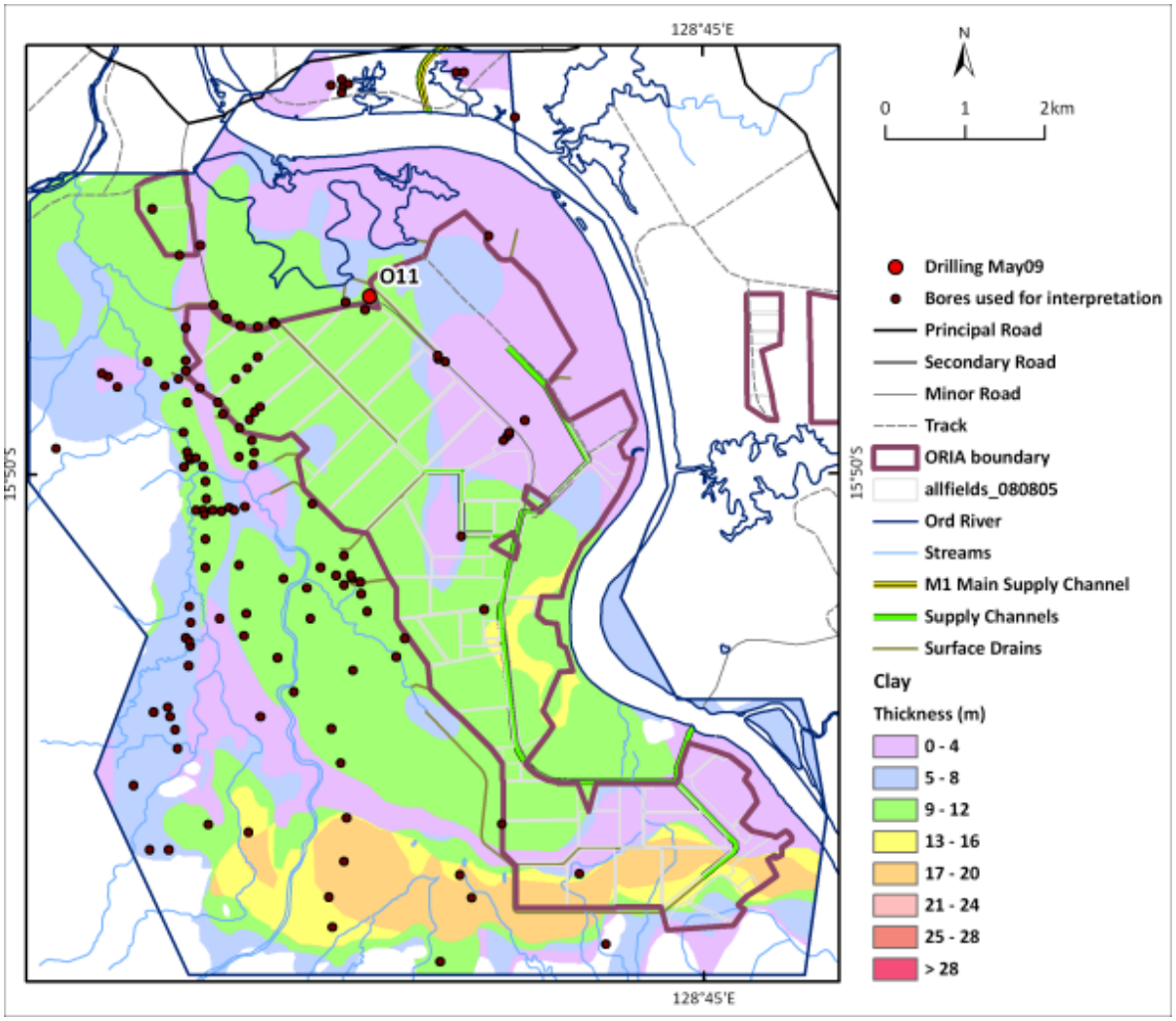

Figure 326: *Packsaddle clay thickness.*

Where are the high recharge zones?

In the absence of field data measuring recharge rates directly, 4 products have been produced as data layers to provide information relevant to the estimation of recharge rates in the Stage 2 areas. These 4 map products are:

- surface permeability, based on measurements of soil permeability in the top 20cm (Figure 327);
- soil recharge properties for the 0-2m soil layer, using data from soils mapping and field permeability tests (Figure 328);
- total clay thickness, incorporating soil mapping data for the 0-2m depth slice as well as AEM data beneath this (Figure 329);
- clay thickness above the water table (Figure 330). This integrates the previous maps with the water table map, and approximates a map of deep drainage.

Soil recharge property maps (Figure B) show areas of moderately rapid recharge to the west of Packsaddle Creek. Overall, however, these maps suggest relatively low recharge rates in the irrigation area (leaving aside macropore bypass mechanisms).

Clay thickness maps show that there are areas of thick clays in an area to the south of Packsaddle Creek, where this trends E-W, and thin clays over the main Ord palaeochannel (Figure 329). Overall, there is a relatively thin layer of clays above the watertable (Figure 330).

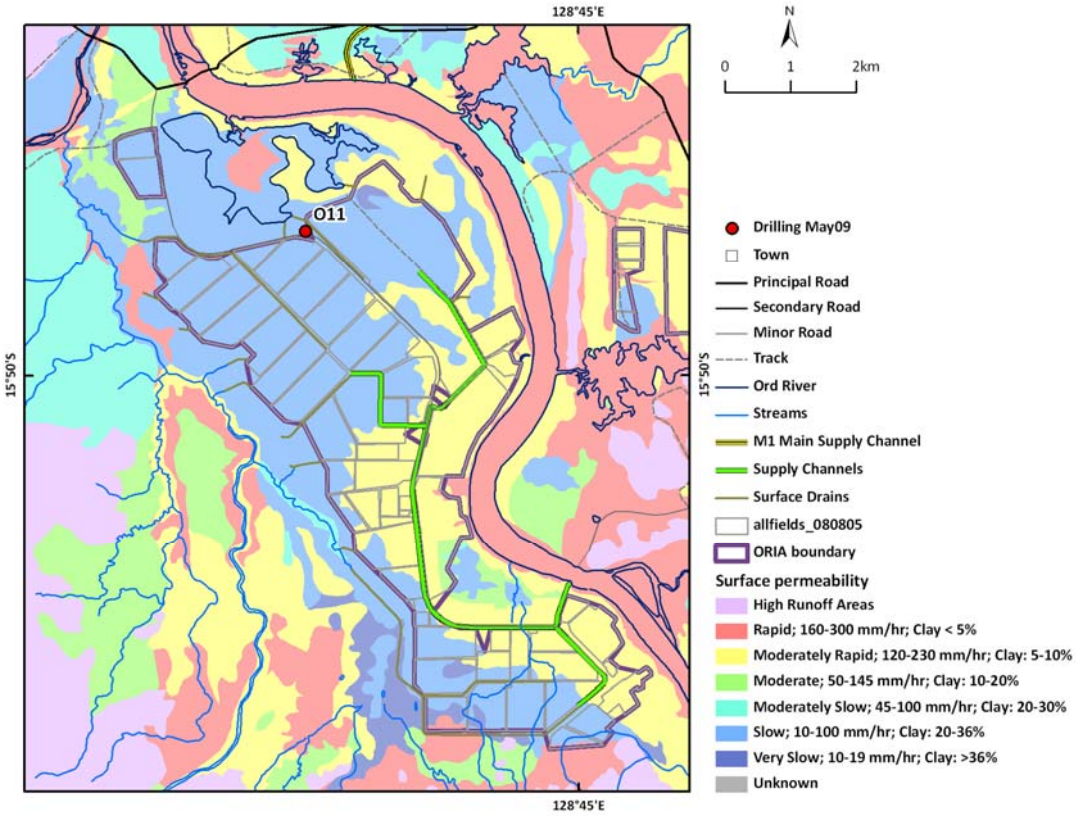

Figure 327: *Packsaddle Plain. Map of surface permeability, based on measurements of soil permeability in the top 20cm .*

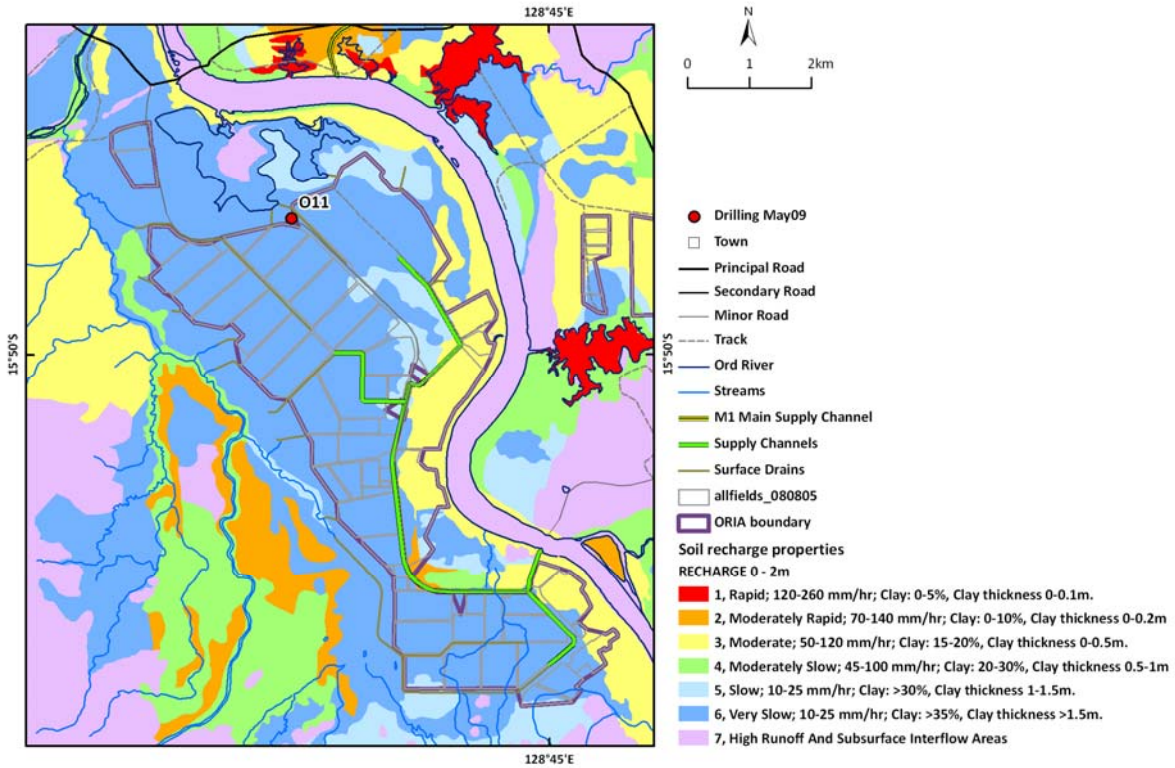

Figure 328: *Packsaddle Plain. Map of soil recharge properties for the 0-2m soil layer, using data from soils mapping and field permeability tests.*

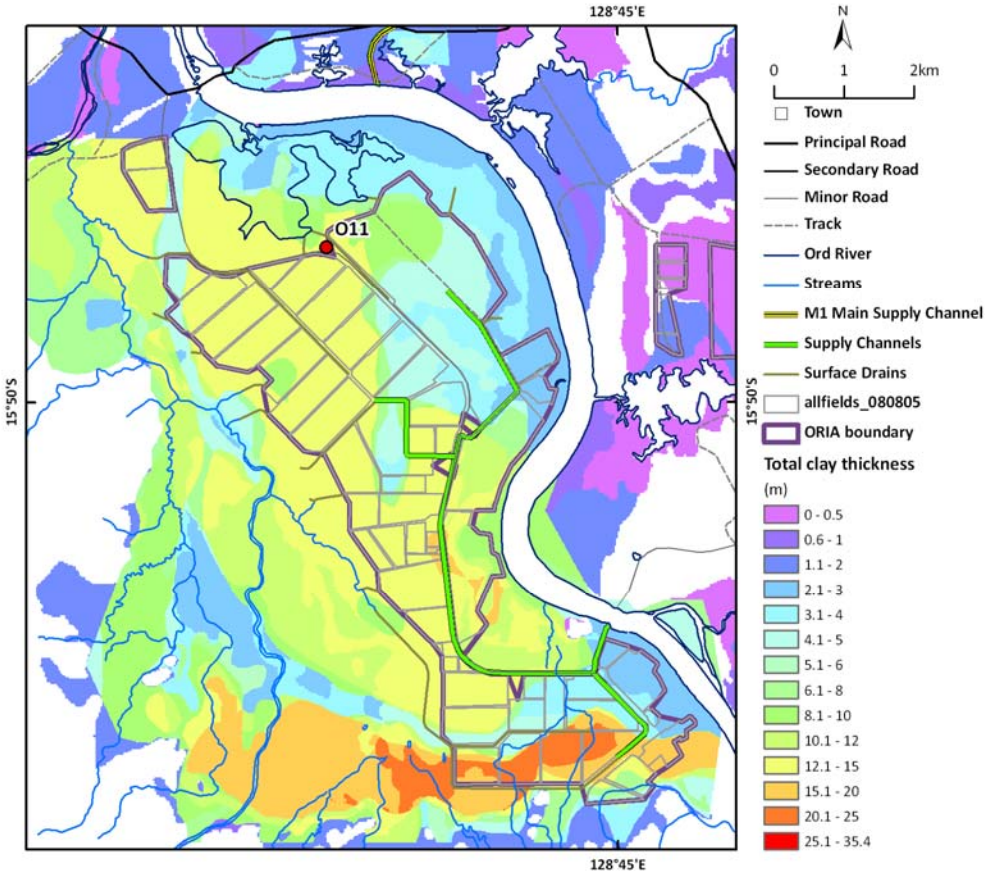

Figure 329: *Packsaddle Plain. Map of total clay thickness, incorporating soil mapping data for the 0-2m depth slice as well as AEM data beneath this layer.*

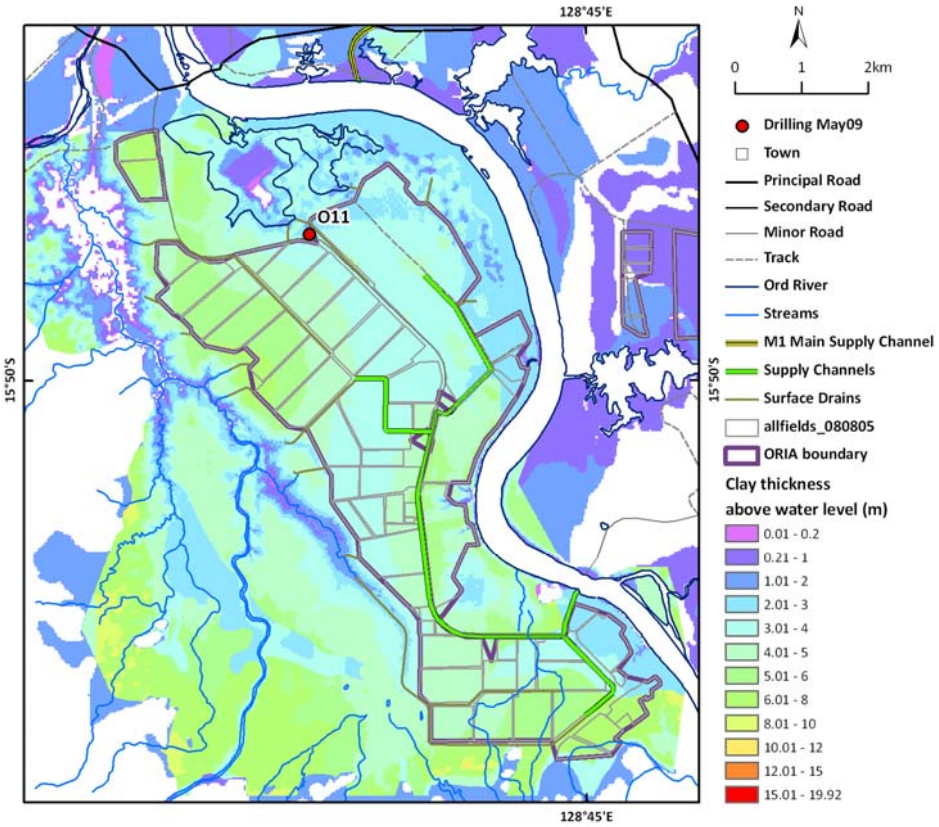

Figure 330: *Packsaddle Plain. Map of clay thickness above the watertable. This integrates the previous maps with the watertable map, and is a surrogate for a map of deep drainage.*

8.4 WEABER, KEEP RIVER AND KNOX CREEK PLAINS

Where is salt stored in the landscape (in the saturated and unsaturated zones)?
Dixon (1977, 1996) investigated the soils on the Weaber Plain as part of the planning for the Ord Stage 2 scheme. Soil salinity values were found to be extremely variable, with soil profiles at 9 sites found to be non-saline within the upper metre but very high salinity values at 5 sties below depths of 0.8–1.4m. At depths varying between 0.8m and 2.8m, the soil salinity varied from moderate to extreme. Dixon (1996) and Smith & Price (2009) considered the amount of soluble salt within these soil profiles could present a severe salinisation hazard if the water table were to rise under irrigation to within several metres of the ground surface. The results from Weaber Plain indicated that primary salinity within the subsoil may be much more extensive there than beneath Ivanhoe and Packsaddle Plains.

Previously, no maps of salt store in either the unsaturated or the saturated zones have been available for the Weaber, Keep River or Knox Creek Plains, and no spatial assessment of salinity hazard. The AEM data, calibrated by pore fluid and textural data from drilling and field sampling, have enabled the salt stored in the Weaber, Keep River or Knox Creek Plains to be mapped and quantified. The salt store in the unsaturated zone across these areas is highly variable spatially, ranging from <10 to 68t/ha/m (Figure 331), while the salt stored in the saturated zone varies from <10t/ha/m to 131t/ha/m (Figure 332). These amounts are similar to those encountered in the Ivanhoe Plain, and generally higher than Packsaddle Plain. However, the spatial extent of salt stores at the higher end of the spectrum (e.g. >40 t/ha/m) is much larger in the Weaber and Knox Creek Plains in particular, in comparison with the ORIA Stage 1. Irregular patches several square km are evident in the data. More than 50% of the area earmarked for irrigation in the Weaber Plain is underlain by high salt stores, particularly in the north and south of the area (Figure 331 and Figure 332). Depending on how readily these salt stores are mobilised, the levels will pose a significant risk to irrigated agriculture should the water table rise to within 2m of the ground surface (Ali & Salama, 2003).

Lower salt store values are encountered primarily within narrow sand and gravel palaeochannels (e.g. intercepted by drillhole KS1, Figure 331, Figure 332), where the total amount of salt stored is low (<10t/ha/m). Analogies in the Murray Basin suggest however that these palaeochannels have the potential to pose a significant salinity risk as they have the potential to act as preferential groundwater flow paths that may carry high salt loads (Lawrie *et al*., 2009a).

There are only a few areas in the proposed Weaber Plain development area where the drainage infrastructure transects areas of high salt store. The M2 and M2S water supply channels largely follow the older southern palaeochannel, which is a zone of low salt store, while the M2N channel transects areas of higher slat store mainly at its eastern end (Figure 331, Figure 332). There would appear to relatively small sections of the water supply infrastructure where there is the potential for increased salt mobilisation downwards to the water table if leakage should occur from the water supply channels.

Given the distribution of relatively high salt stores elsewhere in the Keep River and Knox Creek Plains, similar salinity hazard and risk issues are likely to occur in the areas earmarked for irrigation. Infrastructure planning should utilise the new AEM-based products to minimise the salinity risk to the sustainability of irrigation development in these areas. The new salt store maps, allied with maps of groundwater quality and lithology, provide an initial assessment of the salinity hazard in these areas, and will be of particular assistance in groundwater model parameterisation that will enable spatial and temporal predictions of the salinity risk to be made.

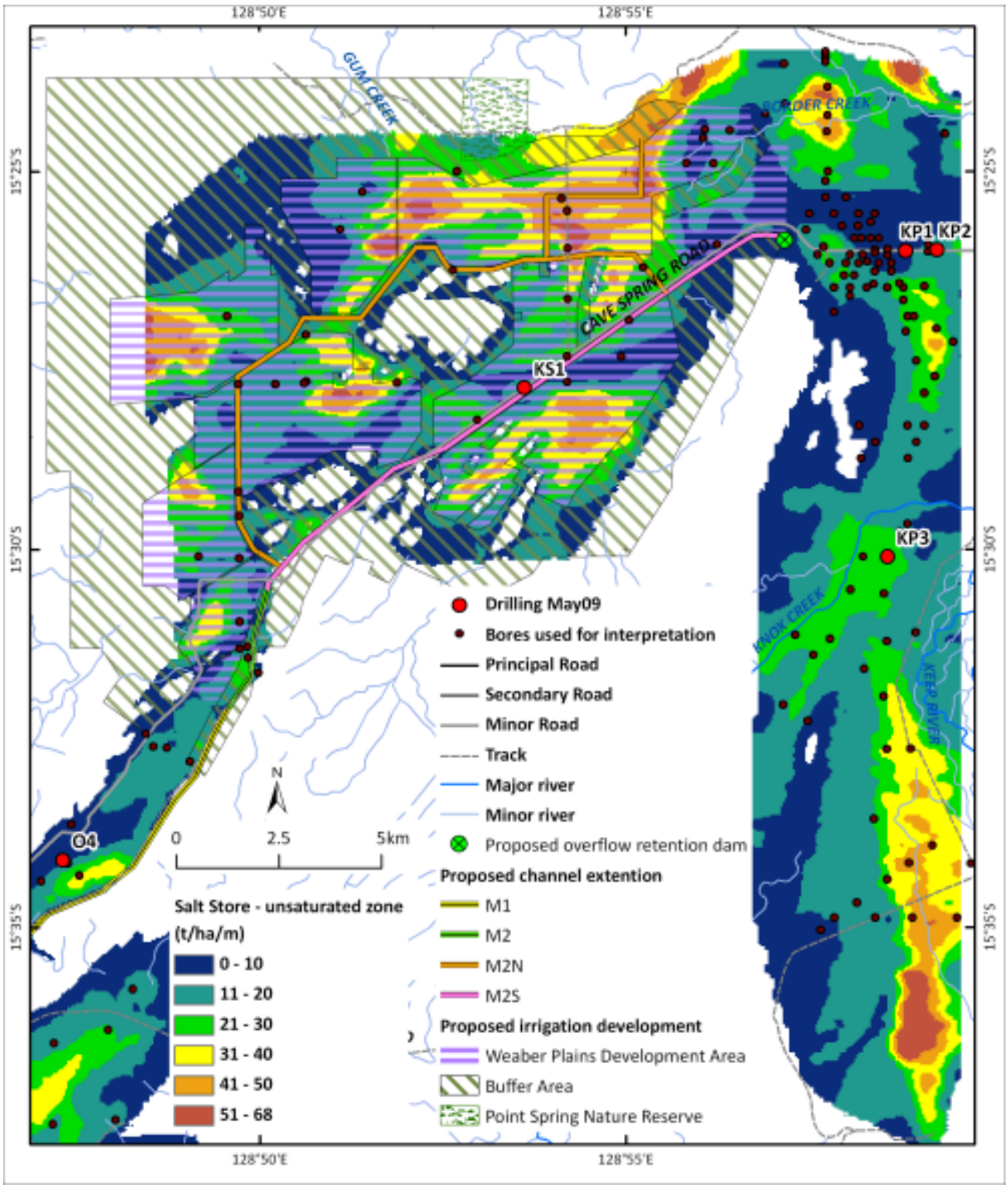

Figure 331: *Weaber, Keep River and Knox Creek Plains unsaturated salt store.*

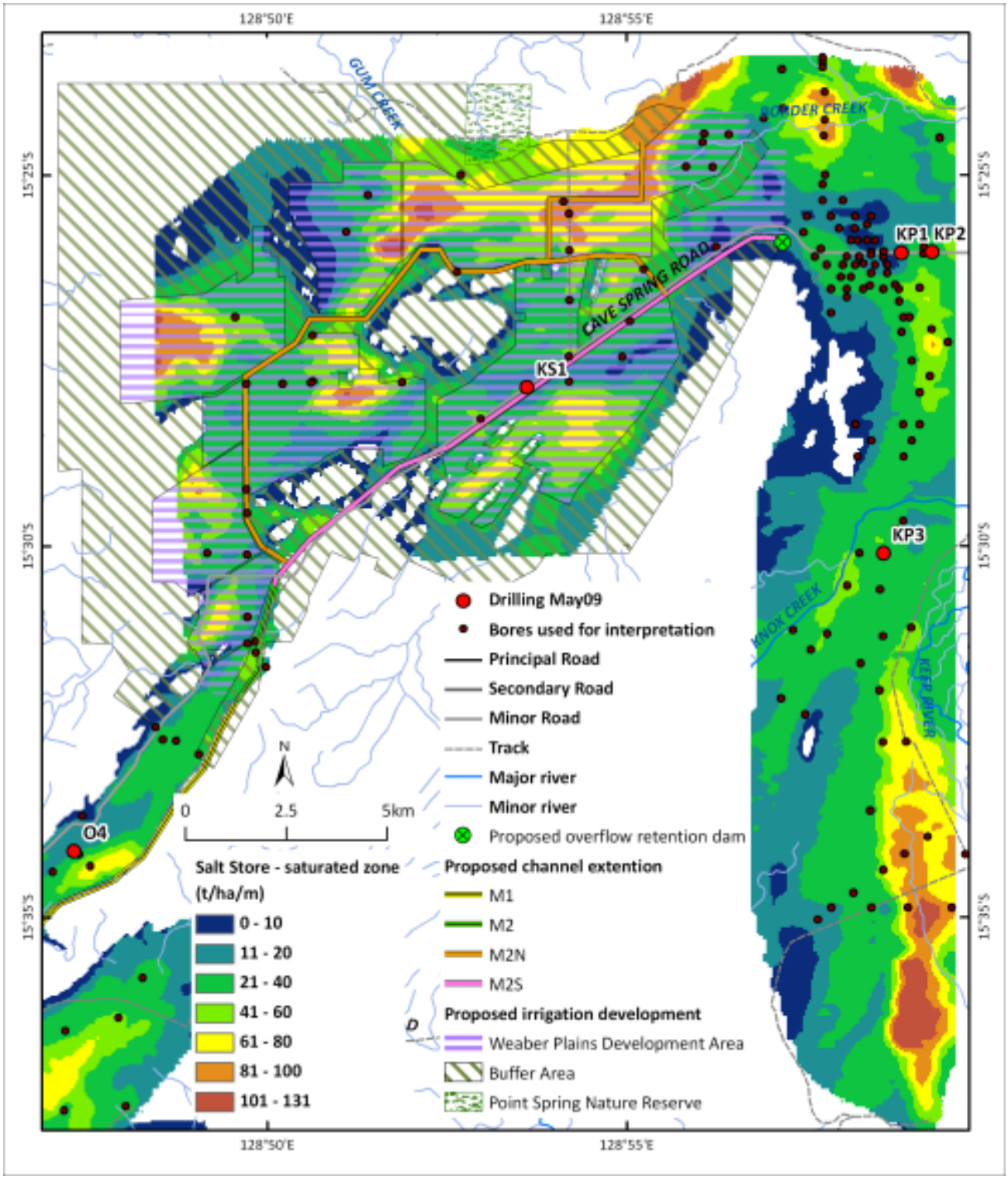

Figure 332: *Weaber, Keep River and Knox Creek Plains saturated salt store.*

What is the distribution of groundwater quality (salinity)?
Previous sampling of groundwater in the Weaber, Keep River and Knox Creek Plains mapped significant areas of high groundwater salinity (>14,000TDS (mg/l; Figure 333) over significant areas of Knox Creek Plain, with smaller areas of high groundwater salinity in the Weaber and Keep river Plains. The previous mapping also identified a background salinity of 1,000 – 3,000TDS over much of the eastern Weaber Plain and the Keep River plain. The latter values would pose a significant risk to many crops grown using irrigated agriculture should the water table rise within a couple of metres of the ground surface, while the values of >14,000TDS would pose an extreme risk to irrigated agriculture.

The new AEM data, calibrated by pore fluids from drilling and field sampling, are generally consistent with the results from previous groundwater sampling. Overall, the AEM mapping has established that the groundwater quality in the Weaber, Keep River and Knox Creek Plains is quite variable, with values ranging from <500TDS (mg/l) to over 5,000TDS (Figure 334). The palaeochannel in the southern Weaber Plain contains relatively low salinity groundwater (<500TDS), however the small palaeochannel in the northern half of the Weaber Plain would appear to contain more saline groundwater, although the palaeochannel is more indurated, and likely to have lower hydraulic conductivities.

The AEM based maps of groundwater quality have a much higher spatial resolution than previous maps. This also enables groundwater quality measurements to be linked more directly to specific elements of the hydrostratigraphy, provides targets for groundwater management, and provides the basis for more spatially explicit predictions of salinity hazard. The relatively high salinities identified in the groundwater quality maps demonstrates the critical importance of groundwater management in this area to minimise the salinity risk.

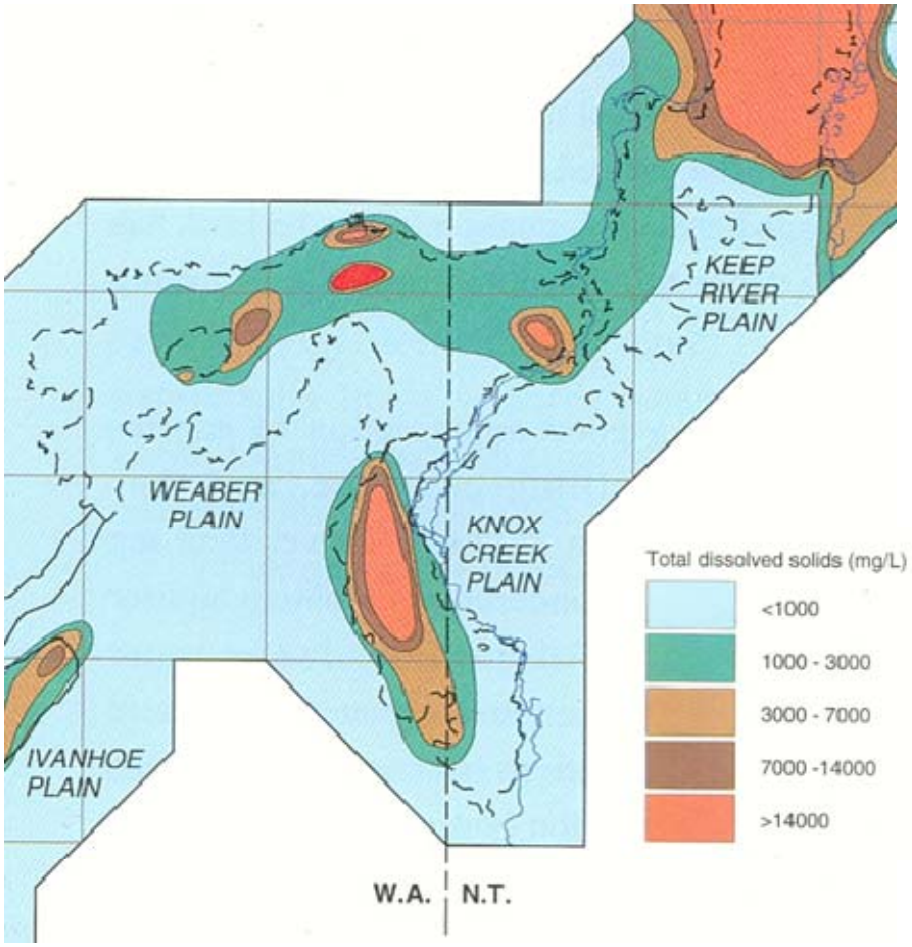

Figure 333: *Weaber, Keep River and Knox Creek Plains groundwater total dissolved salts.*

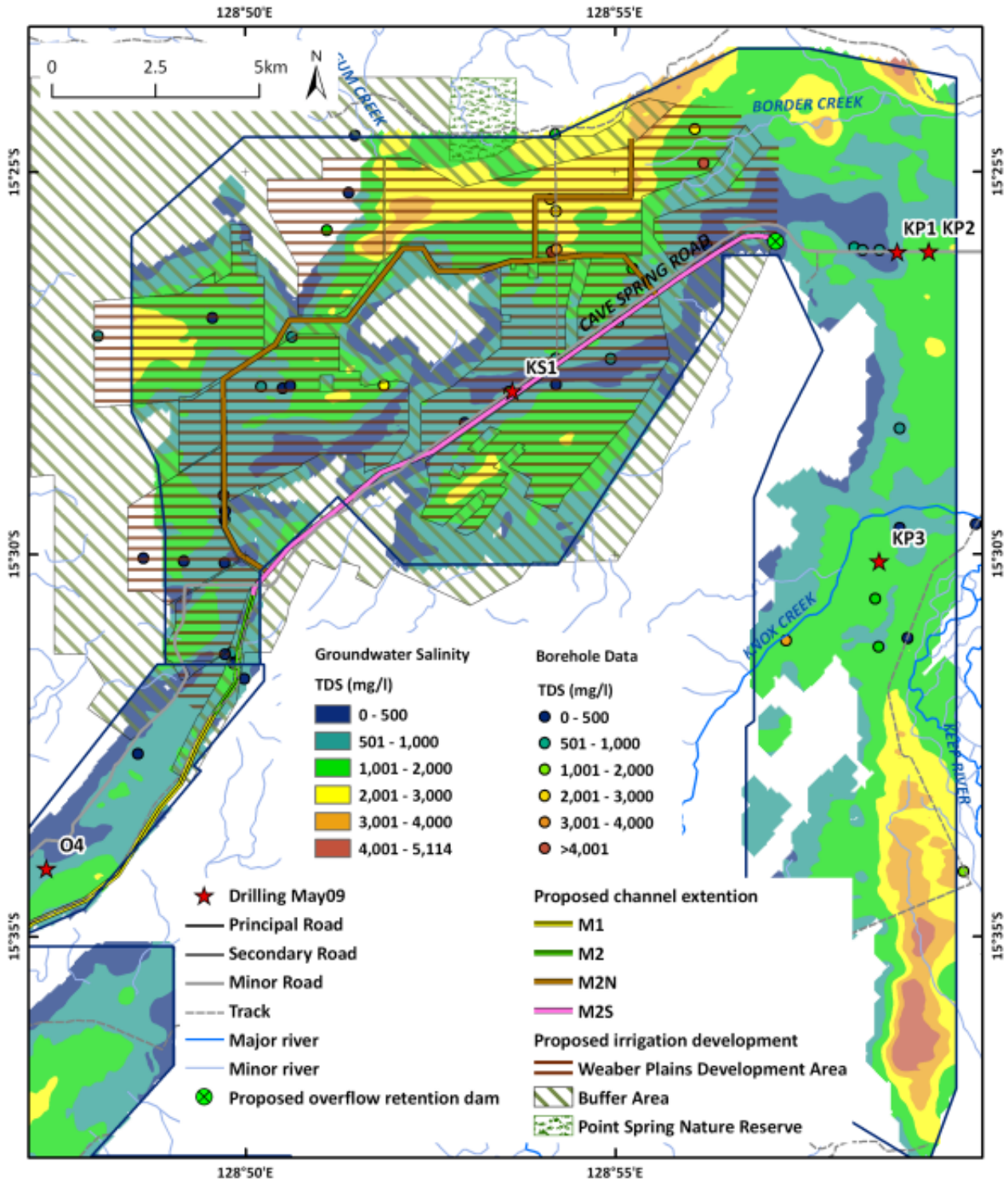

Figure 334: *Weaber, Keep River and Knox Creek Plains groundwater salinity.*

Where are the areas of highest salinity hazard? Is it possible to identify areas where salt is at higher risk of being mobilised?

The areas proposed for development in the Weaber Plain are shown in Figure 335. New (unsaturated zone) salinity hazard maps for the Weaber, Keep River and Knox Creek Plains have been produced by integrating the AEM salt store data with borehole data, the watertable surface and the LiDAR dataset (Figure 336). Areas of high salt store with shallow water tables (<3m) are deemed to have the highest salinity hazard. In general, these maps show there is a very high salinity hazard in the western Weaber Plain where the groundwater table is already very shallow. The areas of high to very high salinity hazard lie largely within the area earmarked for irrigation (Figure 334).

Areas of high salinity hazard also occur elsewhere in the Weaber Plain Stage 2 irrigation area, with the risk only lower due to the greater current depth of the water table in these areas. Over 50% of the area of the Weaber Plain earmarked for Stage 2, irrigation development has a moderate to high salinity hazard (Table 37). This map reinforces the need to maintain water tables at current or reduced levels. A significant area within the Knox Creek Plain also has a moderate to high salinity hazard.

There are only a few areas in the northern Weaber Plain where areas of moderate high salt hazard are transacted by water supply infrastructure (M2N). Elsewhere, it is noted that the proposed overflow retention dam is in an area of very low salt hazard. Further refinements of these maps, including identification of the areas where salt is at higher risk of being mobilised, will be possible when individual data layers are incorporated within appropriate groundwater models.

A second set of maps that use Landsat data to map bare ground and/or salt scalded areas, combined with geomorphic maps, has allowed only a generalised map of surface (soil) salinity potential to be constructed (Figure 123). This map shows the Plain characterised overall as having a low to moderate potential for surface (soil) salinity to develop over the Weaber Plain. However, it was recognised that this approach by itself was not able to identify areas in Stage 2 where the salt store in the sub-soil layers may be high. Importantly, more localised potential surface salinity sites were identified using temporal analysis of Landsat data to map areas of moisture persistence at the surface (Figure 337 to Figure 341). A map showing the areas moisture persisted through most of the dry season was then overlain with the shallow conductivity (0-2m) data (Figure 342). The resulting map is interpreted to show sites with potential sub-soil salinity concentration. In the Weaber Plain, several such sites were mapped in areas where watertables are currently at significant depths below the surface.

An example is in the northern Weaber Plain. The water in the high moisture persistence sites comes primarily from wet season run-off that is localised in internal drainage basins where there is perching and/or low rates of deep drainage. Moisture persistence in this area can also be traced to occurrences fed by groundwater-driven springs, and by overflow from the D8 swamp (in the northern Weaber Plain). In these locations, salt is concentrated in soils and sub-soils by evapotranspiration of infiltrated rainwater and/or spring-derived water. The hydrology of some of these locations will be changed where they are impacted by irrigation development. As these are likely to be sites of high residual salt store in the near surface, they have the potential to become areas of high salt hazard within newly developed irrigation areas. The map showing the persistence of surface soil moisture in areas of high shallow electrical conductivity (in the top 2m; Figure 342), suggests that there are areas of localised high potential for surface (soil) salinity to develop. Ground validation is however required.

Not all areas of high moisture persistence coincide with areas of high shallow conductivity. Areas such as the D8 swamp show high moisture persistence all-year round, yet are interpreted to have low conductivity (sands) rather than saline clay sub-soils. Integrating the AEM data with moisture persistence enables some discrimination of potential surface salinity sites, although more ground validation is required.

The Keep River and Knox Creek Plains have relatively low salinity hazard overall (Table 38; Figure 336), with most of the higher hazard area in south of the Keep River Plain.

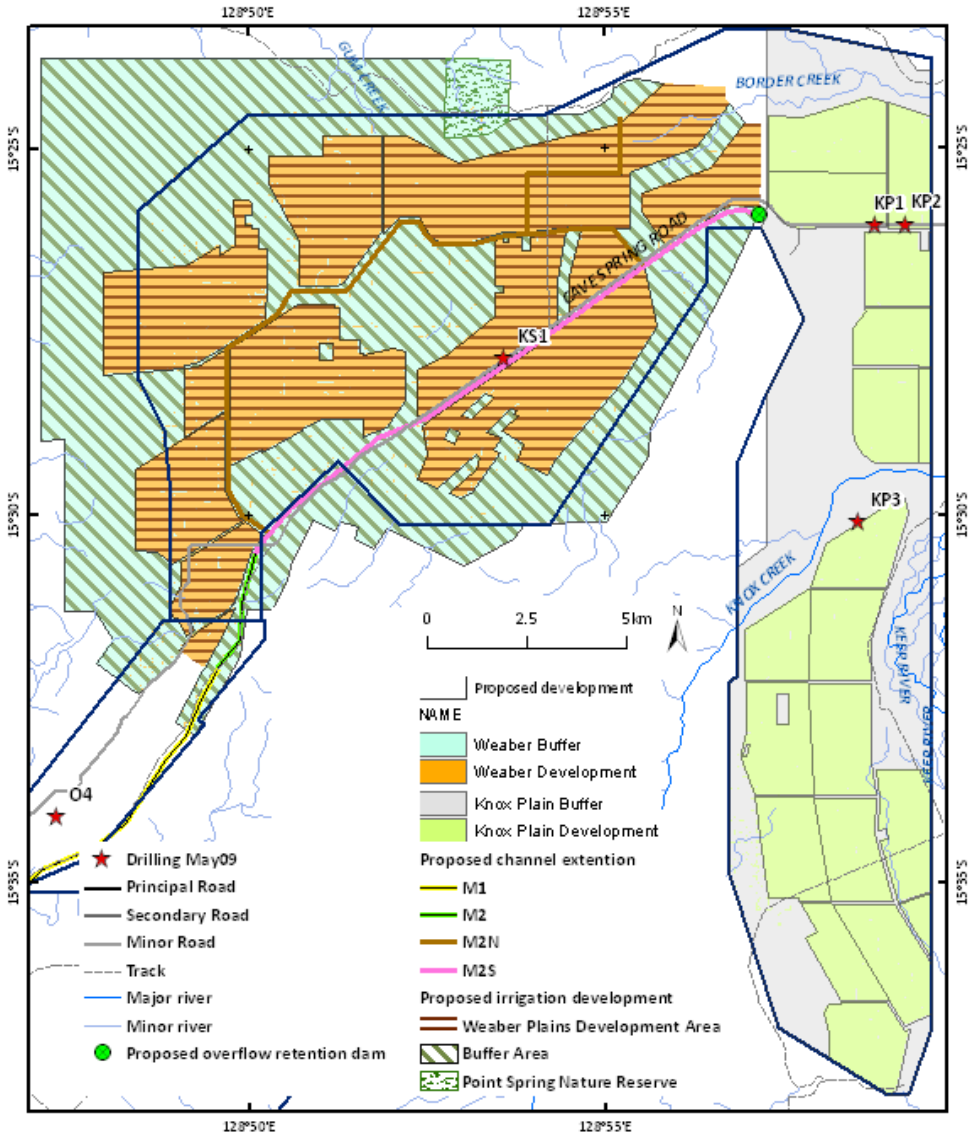

Figure 335: *Areas used in salinity hazard calculations for Weaber, Keep River and Knox Plains.*

Table 37: *Weaber Plain Salinity Hazard area assessment. Note: these figures have been rounded to the nearest whole number.*

Area Name	Hazard Class	Hectares	Percent
Weaber Plain Buffer Zone	1.Very Low	2834	19
	2. Low	817	6
	3. Moderately Low	513	4
	4. Moderate	306	2
	5. High	56	0
	6. Very High	0	0
	Area not assessed	1898	13
Weaber Plain Buffer Zone Total		6423	44
Weaber Plain Development Area	1.Very Low	1988	14
	2. Low	688	5
	3. Moderately Low	1519	10
	4. Moderate	1305	9
	5. High	437	3
	6. Very High	267	2
	Area not assessed	2039	14
Weaber Plain Development Area Total		8242	56
Grand Total		**14665**	**100**

Table 38: *Knox Creek and Keep River Plains Salinity Hazard area assessment. Note: these figures have been rounded to the nearest whole number.*

Area Name	Hazard Class	Hectares	Percent
Keep River (WA) and Knox Creek Plain Buffer Zone	1.Very Low	3193	38
	2. Low	226	3
	3. Moderately Low	10	0
	4. Moderate	124	1
	5. High	29	0
	6. Very High	1	0
	Area not assessed	118	1
Keep River (WA) and Knox Creek Plain Buffer Zone Total		3701	3701
Keep River (WA) and Knox Creek Plain Development Area	1.Very Low	3639	43
	2. Low	483	6
	3. Moderately Low	129	2
	4. Moderate	309	4
	5. High	148	2
Keep River (WA) and Knox Creek Plain Development Area Total		4708	4708
Grand Total		**8409**	**100**

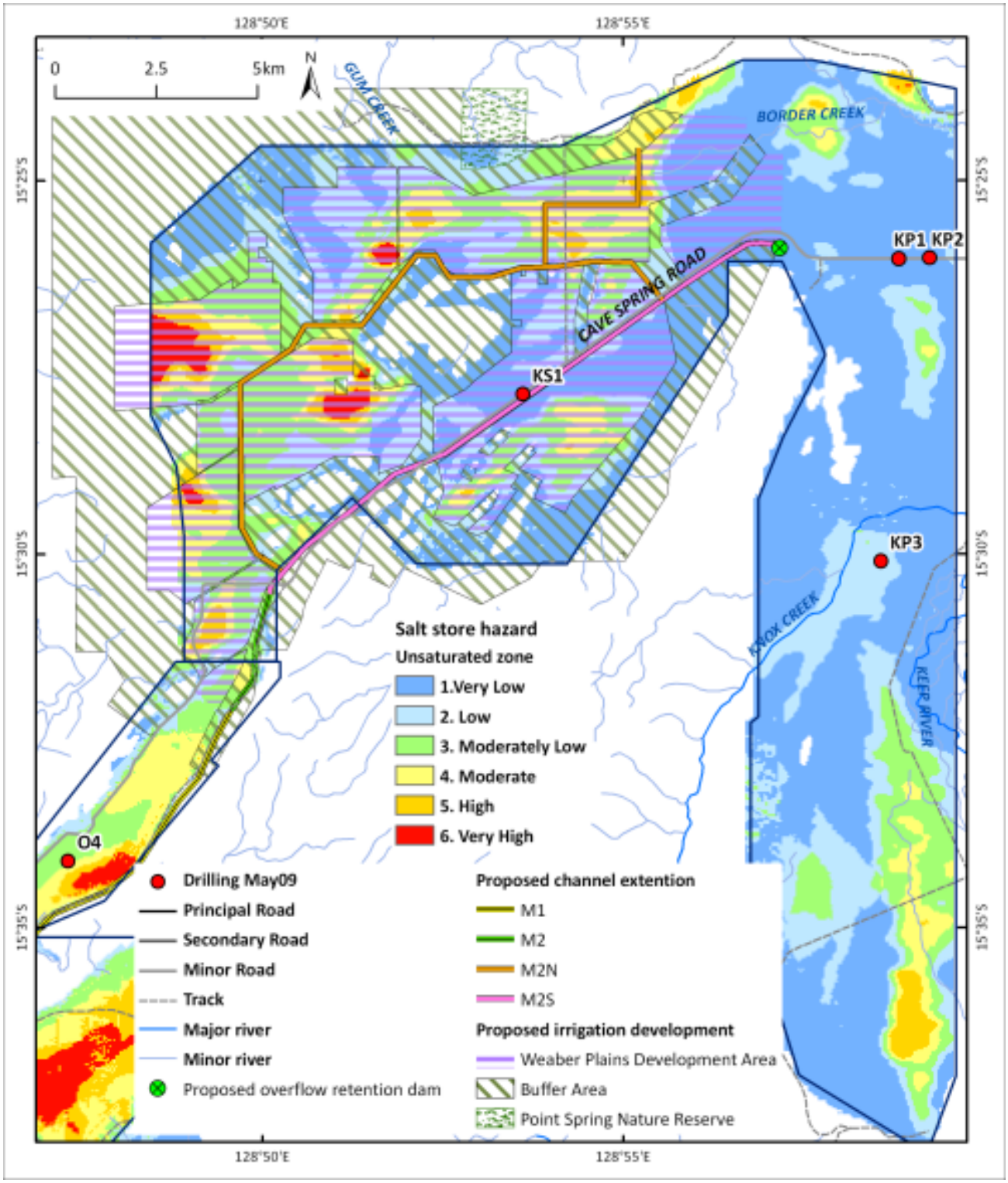

Figure 336: *Weaber, Keep River and Knox Creek Plains salinity hazard (depth to watertable + unsaturated salt store).*

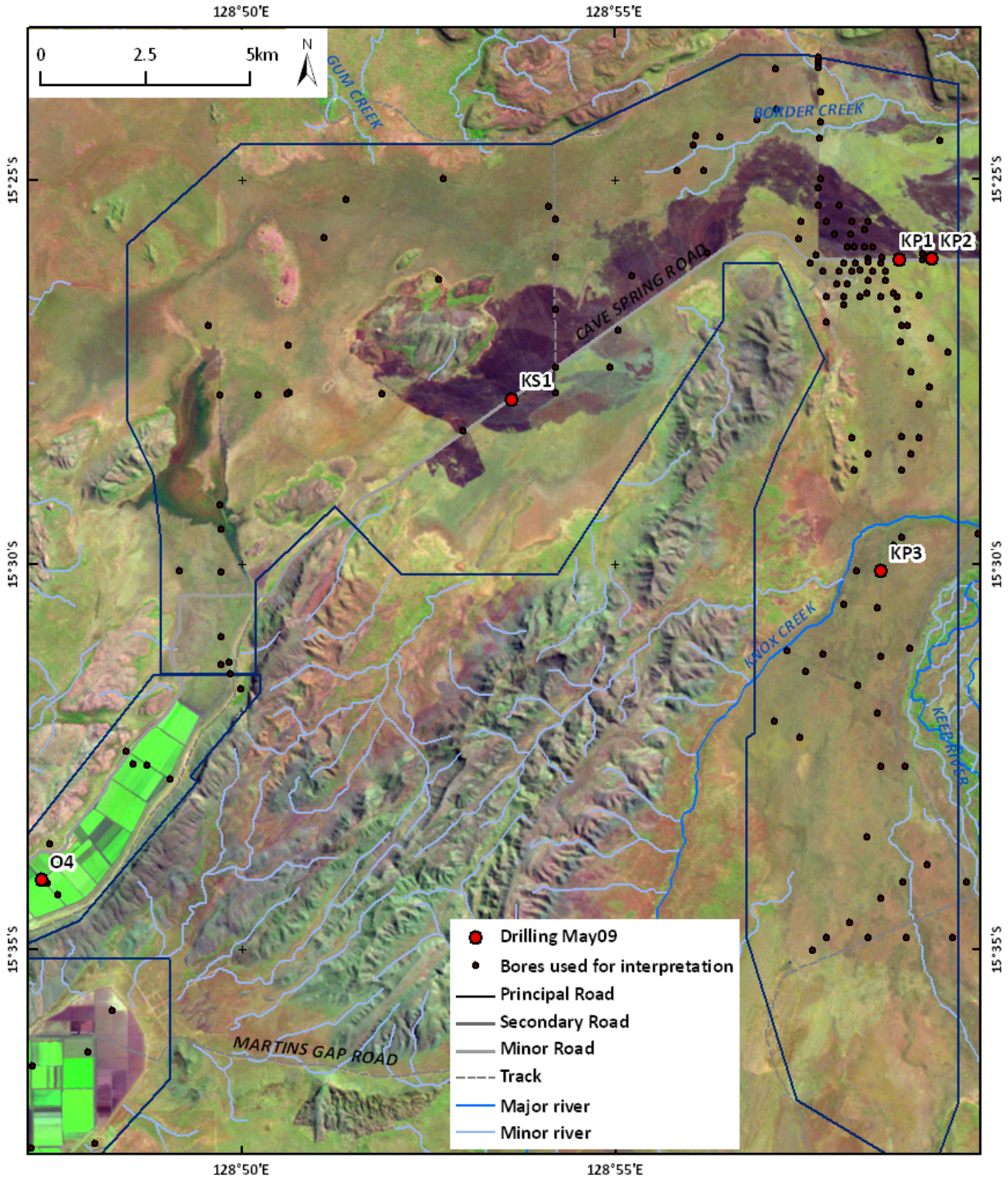

Figure 337: *Map of Weaber, Knox Creek and Keep River Plains showing LANDSAT TM scene from 2nd August 2008.*

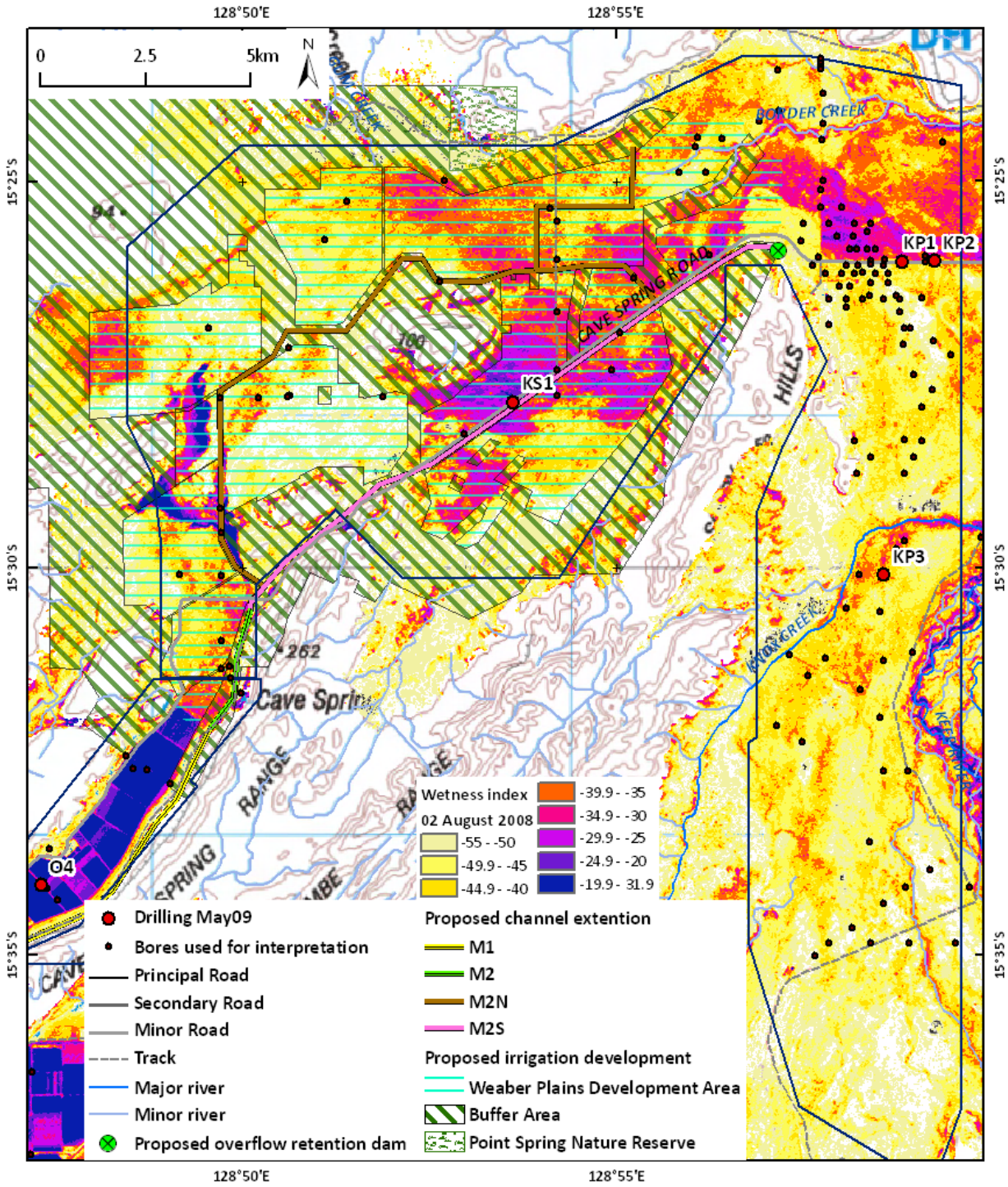

Figure 338: *Map of Weaber, Knox Creek and Keep River Plains showing classified surface wetness index derived from LANDSAT TM scene on 2nd August 2008. The classification highlights variation in soil moisture during one of the driest months.*

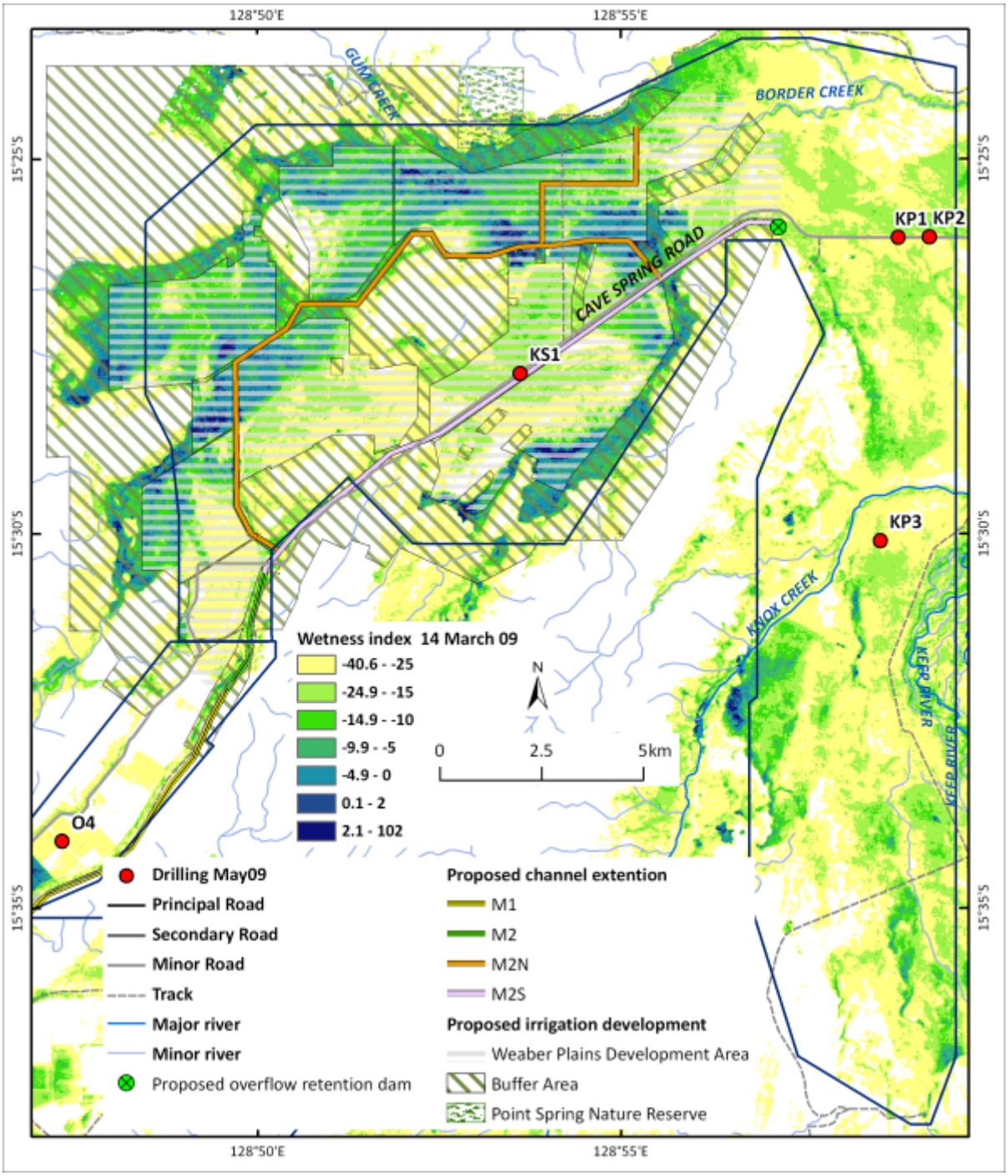

Figure 339: *Map of Weaber, Knox Creek and Keep River Plains showing classified surface wetness index derived from LANDSAT TM scene from 14th March 2009. The classification highlights areas of persistent soil moisture two weeks after a big rain event. Indices > 0 correspond to standing water and lowest position of the landscape; blue-green and light blue colours correspond to low- positioned waterlogged soils with poor drainage. Light yellow areas in contrast represent drier or sandier soils with comparatively better drainage (in vicinity to Border Creek).*

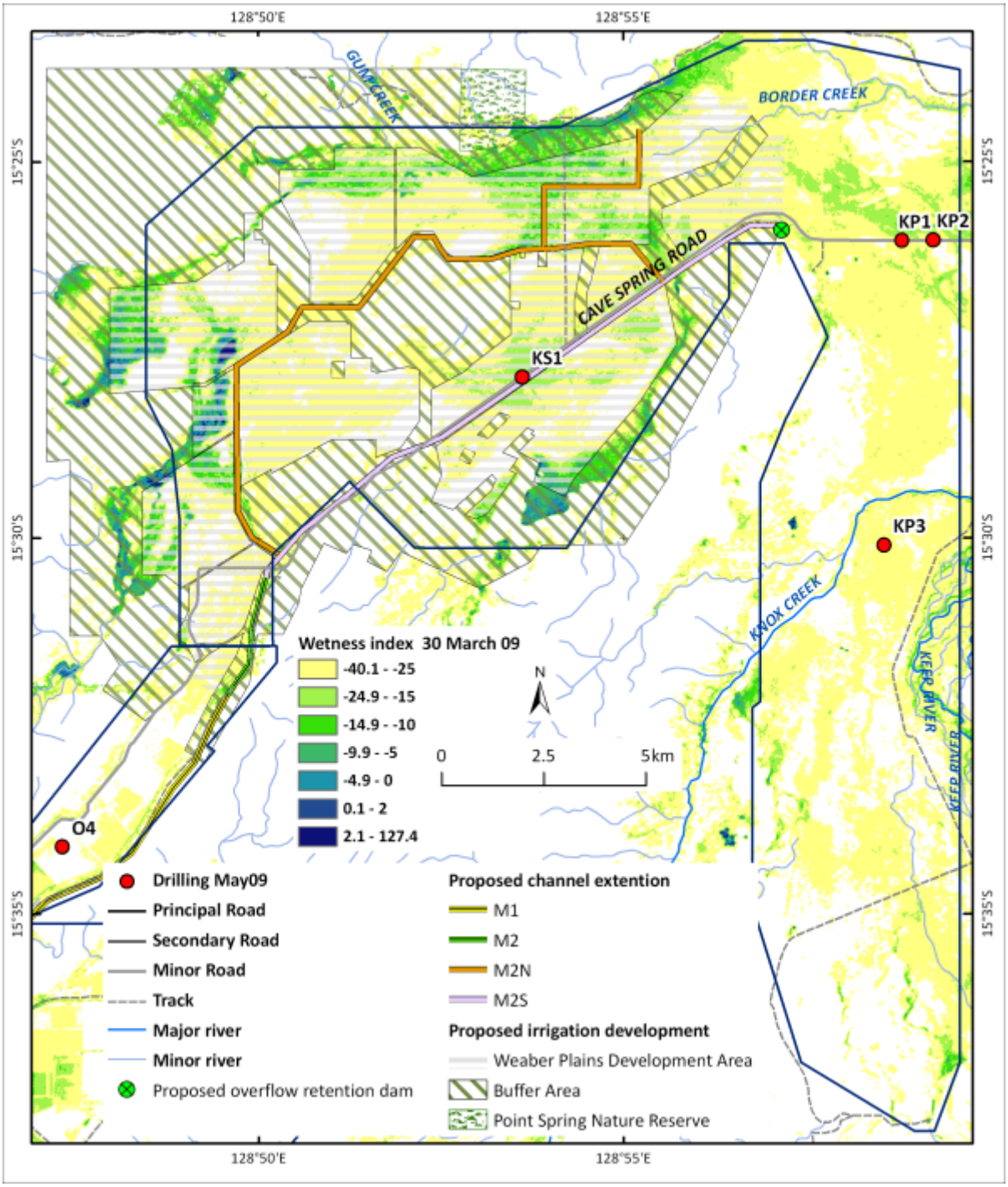

Figure 340: *Map of Weaber, Knox Creek and Keep River Plains showing classified surface wetness index derived from LANDSAT TM scene from 30th March 2009. The classification highlights areas of persistent soil moisture one month after a big rain event. There are few small darker blue areas with standing water; blue-green and light blue coloured areas showing low- positioned waterlogged soils with very poor drainage.*

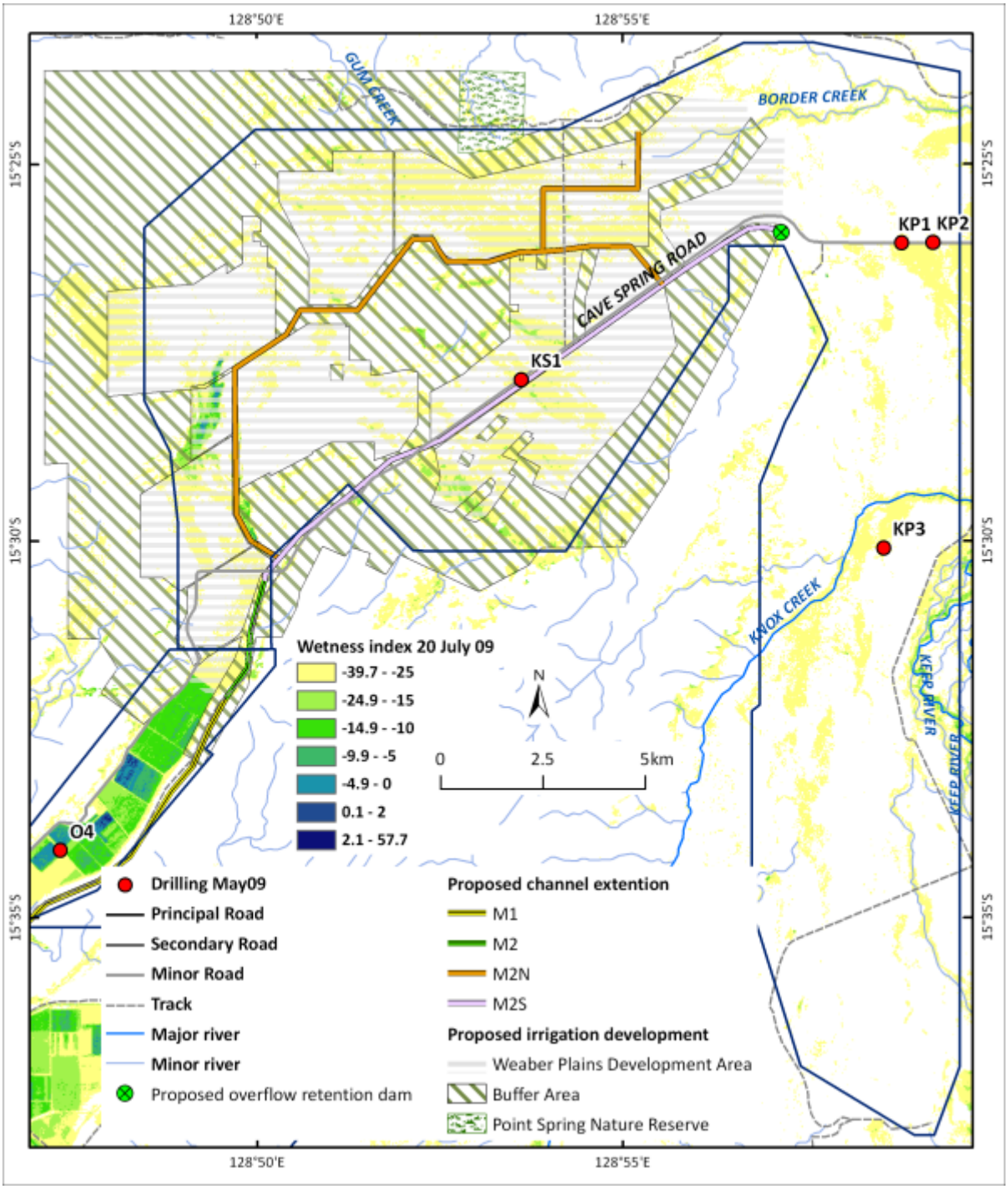

Figure 341: *Map of Weaber, Knox Creek and Keep River Plains showing classified surface wetness index derived from LANDSAT TM scene from 2nd July 2009. The classification highlights areas of persistent soil moisture in the dry season. Very few small green-blue areas located near footslopes.*

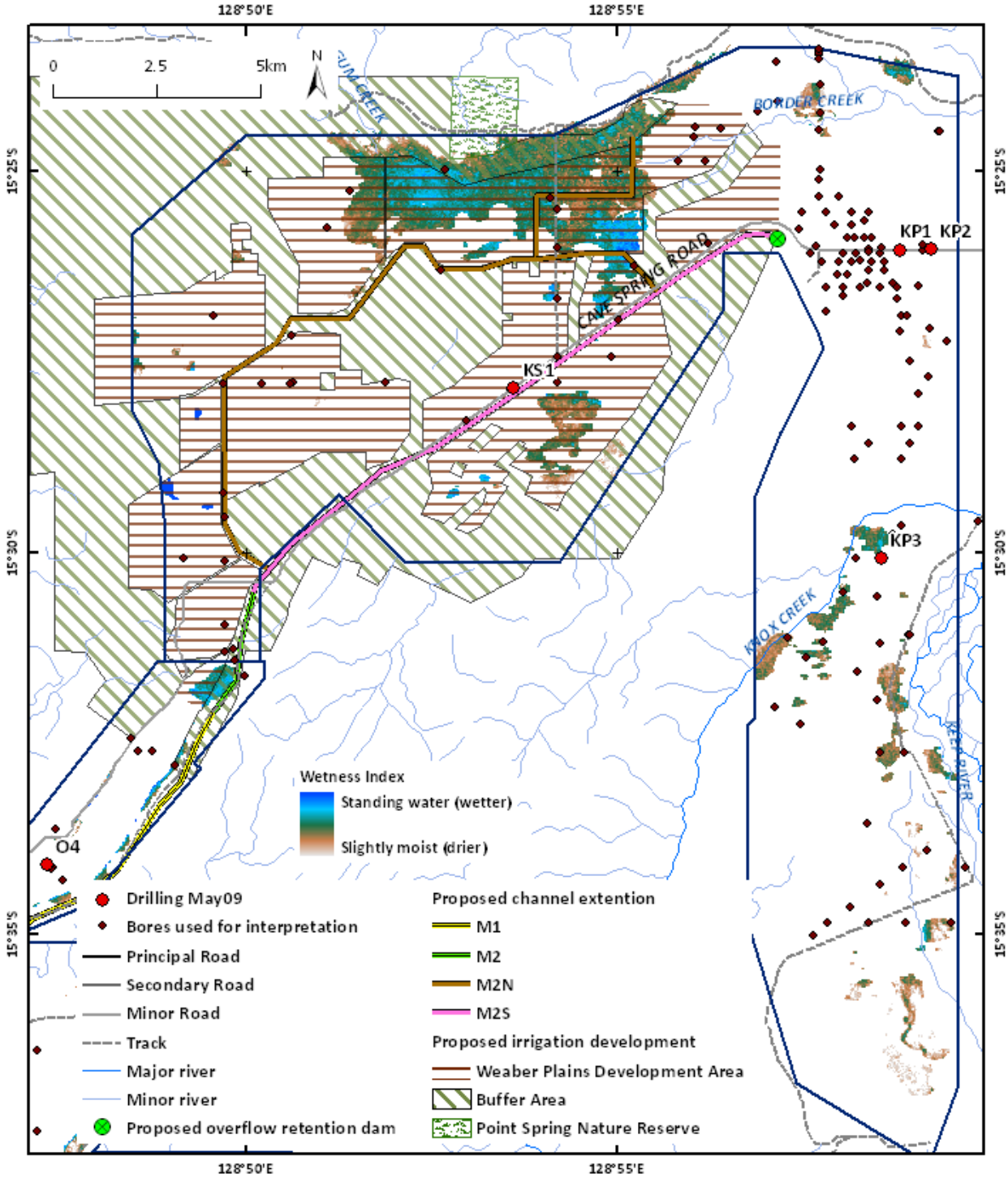

Figure 342: *Map of Weaber, Knox Creek and Keep River Plains showing areas of high surface moisture persistence in areas of high near-surface (0-2m) conductivity*

What is the extent (in 3D) of the sand and gravel aquifers, and how are they connected?

New maps of the depth to bedrock (Figure 343), and the extent and thickness of gravel aquifers (Figure 344) have been produced for the Weaber, Keep River and Knox Creek Plains. Maps of the extent and thickness of the sand aquifers have also been produced (Apps *et al*., 2009). These maps have been compiled by interpreting individual AEM conductivity depth slices and representative conductivity cross-sections using pre-existing drillhole records and data from new drillcore obtained during the project (Section 3.3.2).

The maps of depth to bedrock confirm the location of the main Ord palaeochannel that entered Weaber Plain through Cave Springs Gap, and exited at a point coincident with the present Keep River (Figure 213 - Figure

221; Figure 343). This feature is incised into bedrock at depths of over 32m, with a gentle gradient in the thalweg to the east. At its base the palaeochannel varies from <1 to 2km in width (Figure 343).

The palaeochannel is infilled with gravels towards the base, but becomes increasingly sand-filled upwards as the palaeochannel broadens out (Figure 213 - Figure 221). Maps of gravel and sand thickness are shown in Figure 344 and Figure 345 respectively. More detailed descriptions of the gravel and sand lithologies, and their extent are provided earlier (Section 6.4). In the main southern palaeochannel, gravel thickness is between 9 and 20m, increasing in thickness to the east. Across the Weaber Plain, the AEM has revealed that the gravels are highly variable in thickness (from <5-20m), are more restricted in their spatial extent than previously thought (O'Boy *et al*., 2001).

In the Knox Creek and Keep River Plains, the depth to bedrock is less than in the Weaber Plain, and the valley infill differs, reflecting the differences in sediment source and underlying bedrock geology. The Knox Creek and Keep River Plains appear to contain smaller gravel deposits within a narrower palaeochannel at the base of the sequence. In places, the gravel palaeochannel appears to contain quite saline groundwater, and this makes differentiation of gravels and adjacent silt and clay lithologies difficult in the AEM data. It is not clear from the AEM survey data to what extent the area of high conductivity in the south of the Knox Creek Plain is due to saline groundwater in gravels and/or saline groundwater in clays, as examples of both were encountered in prior drilling. Overall, the Knox Creek-Keep River Plain is a broader, palaeovalley with less complexity in alluvial architecture able to be mapped than in the Weaber Plain. Depth to bedrock is <30m, and the valley infill with finer-grained, silty sands, sands and a much higher percentage of clays than seen in the Stage 1 areas.

The new maps of sand and gravel in these areas will assist greatly with groundwater model parameterisation and enable more reliable quantitative assessments to be made of groundwater and salinity model predictions. They will also contribute to more robust modelling of land use and groundwater management scenarios.

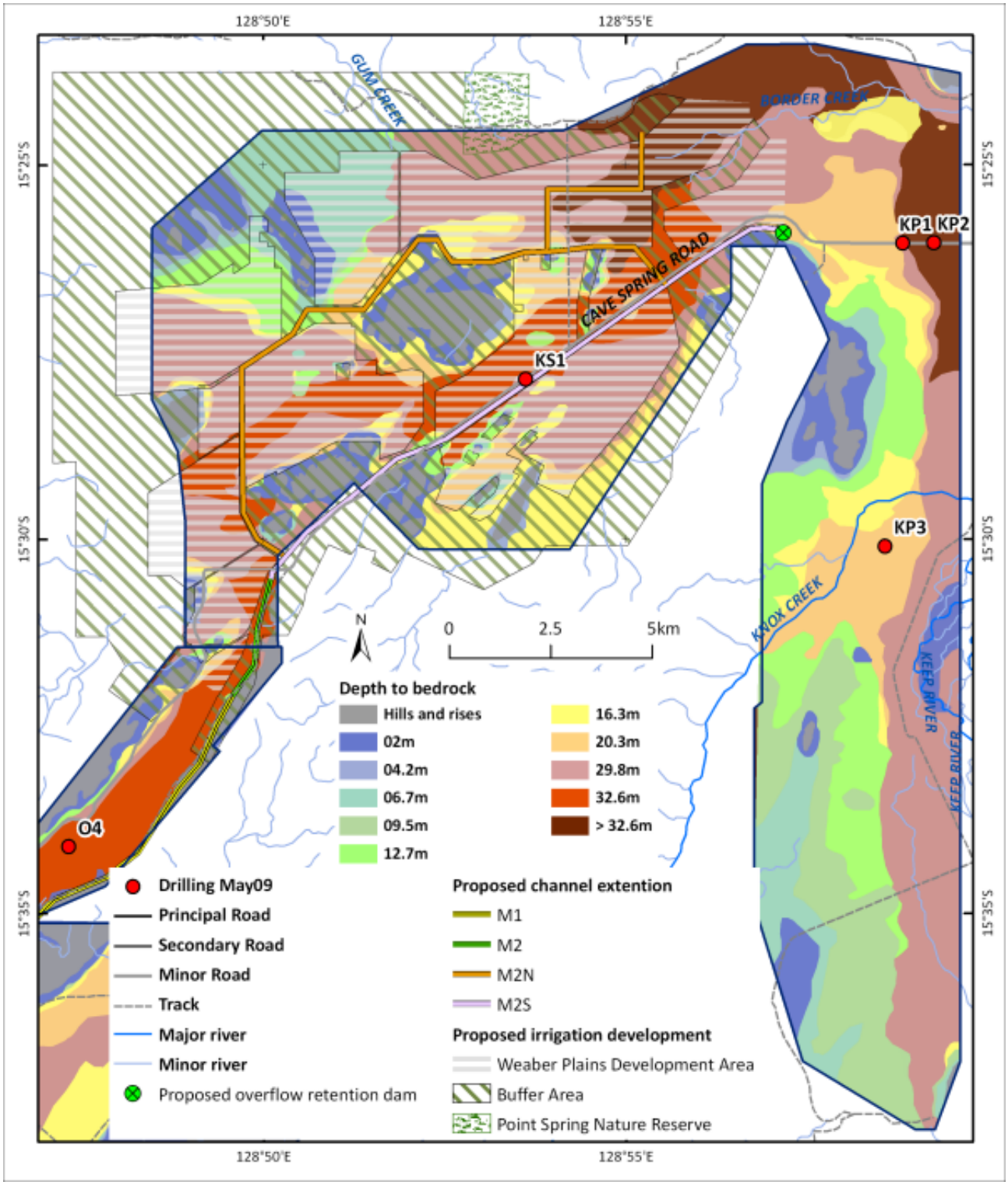

Figure 343: *Weaber, Keep River and Knox Creek Plains depth to bedrock.*

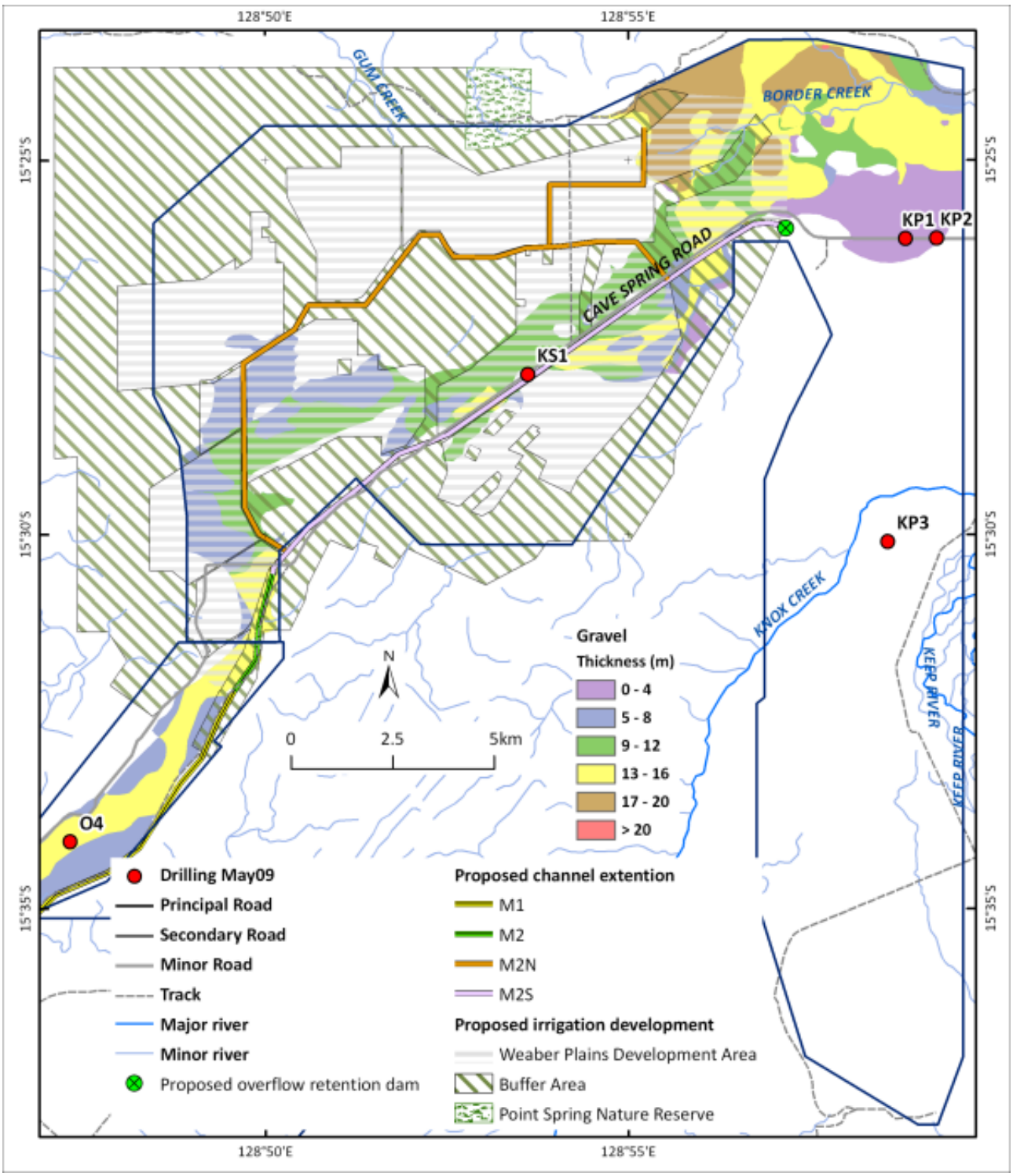

Figure 344: *Weaber, Keep River and Knox Creek Plains gravel thickness.*

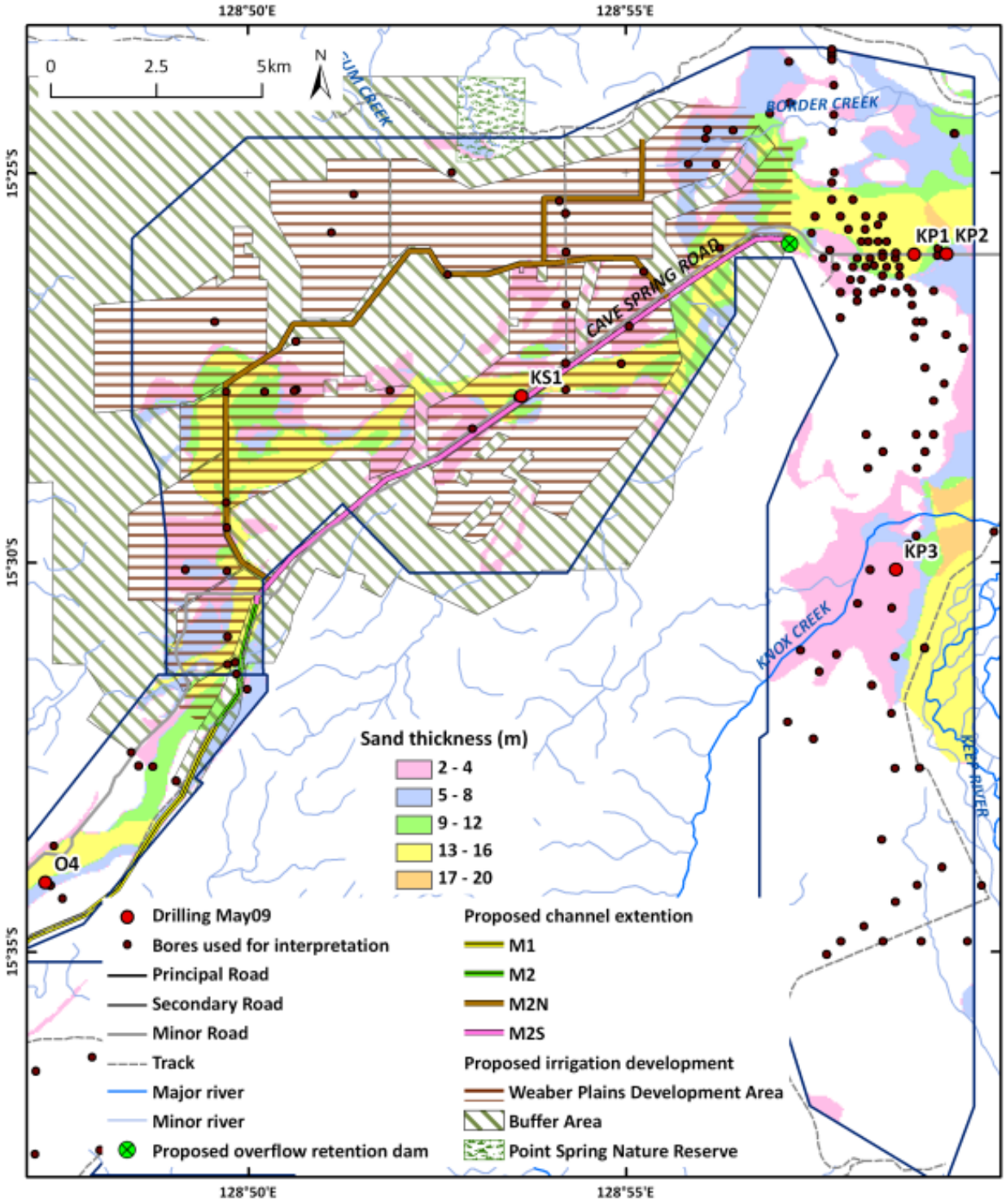

Figure 345: *Weaber, Keep River and Knox Creek Plains sand thickness.*

What is the extent and thickness of clays in the sub-surface?

New maps of clay extent and thickness (Figure 346) have been produced for the Weaber, Keep River and Knox Creek Plains. These maps have been compiled by interpreting individual AEM conductivity depth slices using pre-existing drillhole records and data from new drillcore obtained during the project (Section 3.3.2). These maps do not incorporate the 0-2m depth slice, as the conductivity measurements reflect soil profiles that were mostly dry, and contained little contrast between sand and clay units. Mapping the extent and thickness of clays assists with understanding groundwater flow paths, surface-groundwater connectivity including recharge potential, and salinity mobilisation potential. Overall, these maps should also contribute to the development of appropriate salinity mitigation strategies, and assist with refining cropping and drainage strategies.

In the Weaber Plain, the maps show that clay thickness is highly variable, with relatively thin clays over shallow bedrock pediments, but much thicker clays (up to 28m) thick in areas adjacent to the main palaeochannel. The clay thickness over the main palaeochannel increases from 5-8m in the west to >13m (in general) towards the east (Figure 346). Previously, a thicker section of gravels was interpreted in this location, however on closer examination, it is likely that the gravels only occur as thin (<2m) lenses within clays and silty units. These are likely to be too thin and discontinuous to be mapped in the AEM data. Resolving these features is made more difficult here by the presence of very saline groundwater, which appears to mask lithological signatures.

In the Keep River and Knox Creek Plains, the clay thickness in the valley axis ranges from 25 to >28m in two depocentres (Figure 346). The clay thickness in general thins to the valley margins with a much simpler distribution than observed in the Weaber Plain. This reflects differences in both the sediment source, the route of the palaeo-Ord, and differences in the bedrock geology.

Many of the areas with thicker clays are also areas of high salt store. While it may be more difficult to mobilise salts stored in these thick clay layers, it may be more difficult to lower the water table in these lithologies once they are saturated. Furthermore, the depth of influence of upward flux and transport of salts in the soil layer is higher for a clay-rich soil than a sandy soil, requiring that water tables be kept lower in the clay-rich areas (Ali & Salama, 2003).

In the Weaber Plain Stage 2 irrigation development area, clay thickness is highly variable. Areas of thinner clays may be areas of preferential recharge to the groundwater system. They are also areas of higher potential leakage from water supply and drainage infrastructure. The main M2S and the north-trending arm of the M2N water supply channel both occur in areas of thin clays. The planned course of the M2S channel former overlies an area of thin clays (<4 to <8m) in the west, while the M2N channel overlies thin clays (<4m) over bedrock (Figure 346).

Water table level management is likely to be more difficult in the Weaber Plain area in areas of thick clays, although deep rooting forestry (as demonstrated by the Mahogany stand at Martins Location), may provide a solution. Similar issues may be faced in the Knox Creek and Keep River Plains, where the thicker clay sequences in the valley centres will provide challenges for water table and salinity management.

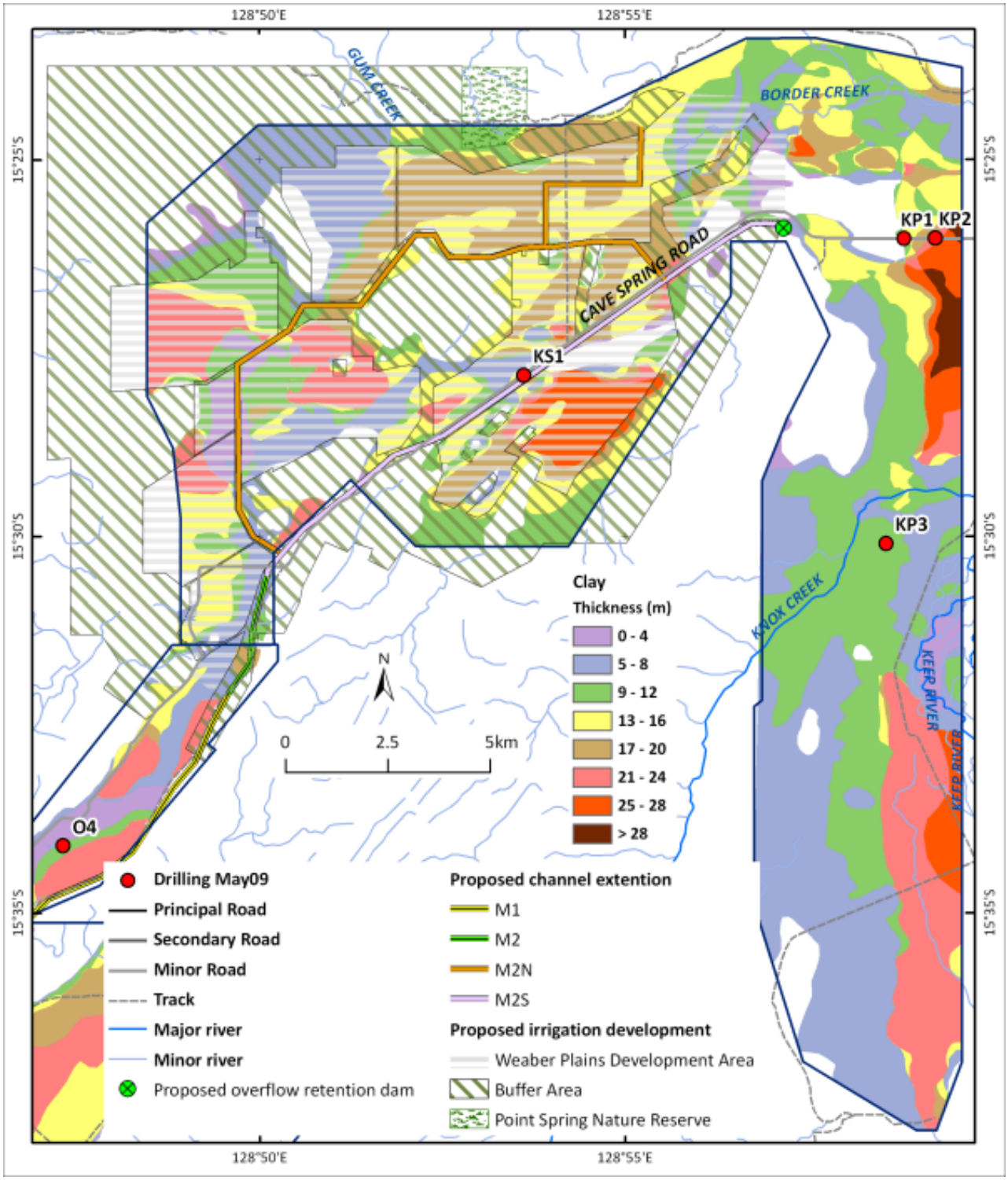

Figure 346: *Weaber, Keep River and Knox Creek Plains clay thickness.*

What are the spatial and temporal trends in groundwater level and salinity?

To analyse the temporal changes in groundwater levels in the Stage 2 areas earmarked for development, trend analysis was undertaken on the historic monitoring of groundwater levels in the Weaber, Keep River and Knox Creek Plains. Table 39 provides an overview of the time series data sourced from the WA Department of Water Hydstra database. Appendix 7 provides more detailed statistics on a bore-by-bore basis. About a third of the 100 monitoring bores used in the assessment had only a single water level measurement recorded in the database. On average, there were 12 readings available for a bore, with the maximum number being 82. Typically, the duration of data collection is about 12 years, and 5 boreholes had water level records spanning over 40 years. The timing of data collection can vary from the 1960's onwards.

Table 39: *Summary of groundwater monitoring in study area.*

Statistic	Value
Number of Monitoring Bores	100
% bores with single reading	32
Average readings/bore	12
Median readings/bore	7
Maximum readings/bore	82
Average monitoring period (years)	11.7
Median monitoring period (years)	12.0
Maximum monitoring period (years)	44

Figure 347 shows a nested bore in cracking soils on Weaber Plain. Figure 348 and Figure 349 map the status of this monitoring record across the study area, in terms of the bore distribution categorised on the basis of total number of readings and the data density (number of readings per year of record), respectively.

Figure 347: *Nested bore in cracking soils on Weaber Plain adjacent to Keep River Road. Richard George (left) and Duncan Palmer (right) for scale.*

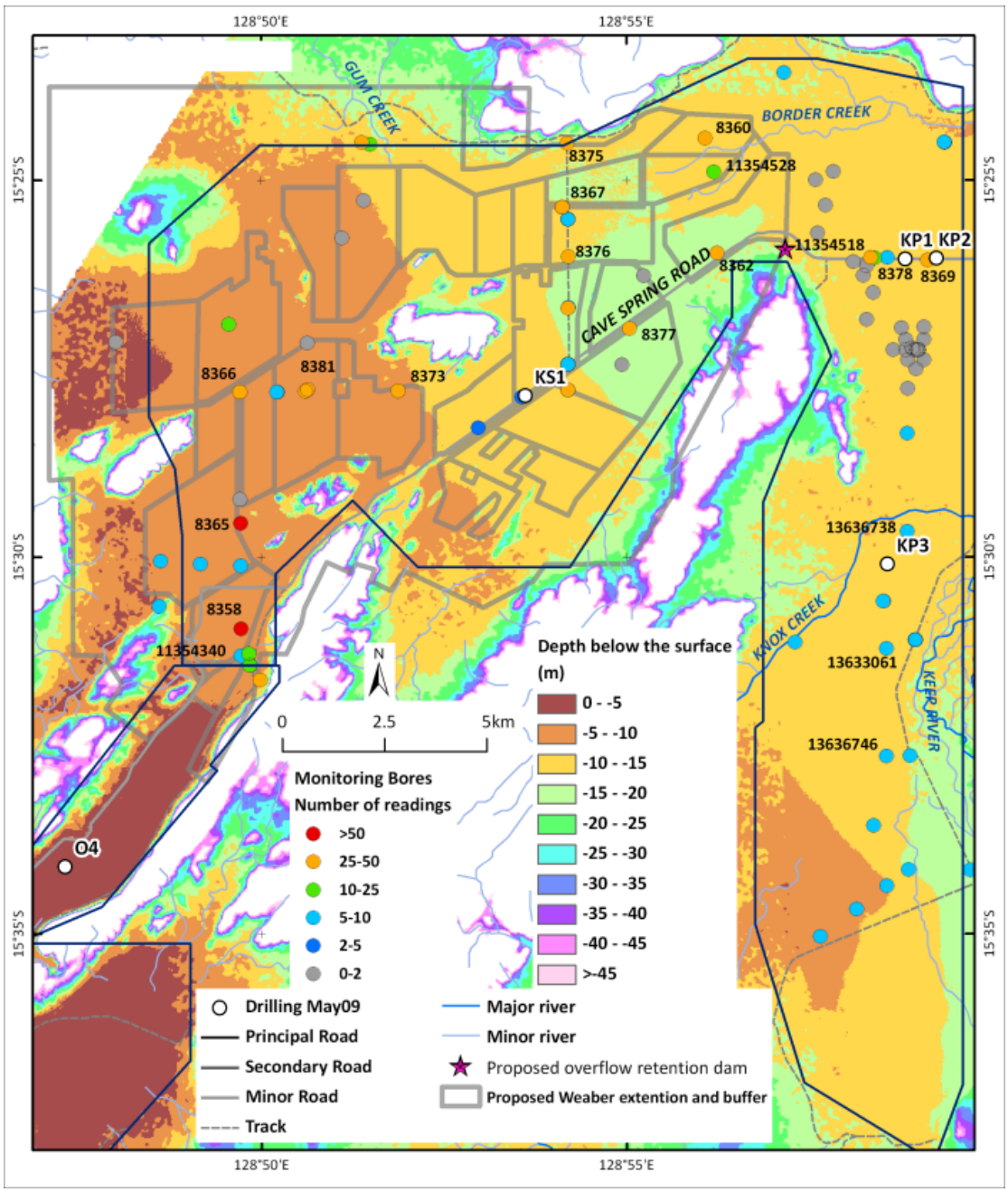

Figure 348: *Map of Weaber, Knox Creek and Keep River Plains showing categorisation of monitoring bores based on total number of readings. The numbered bores on this map are those for which hydrograph records were obtained and 'cleaned up' for this study.*

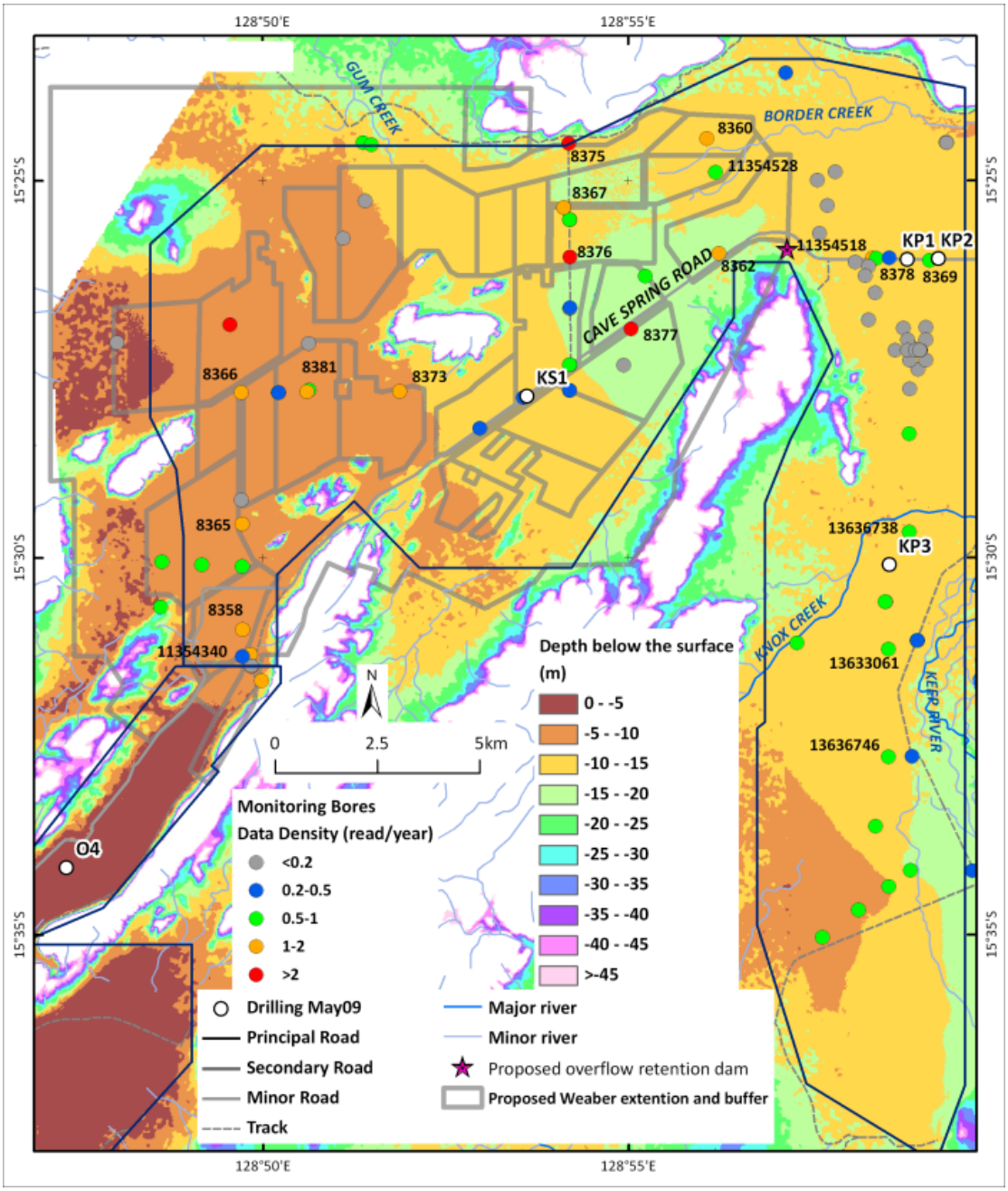

Figure 349: *Map of Weaber, Knox Creek and Keep River Plains showing categorisation of monitoring bores based on data density (number of readings per year of record).*

This categorisation enabled the selection of appropriate bores for the generation of hydrographs, as plotted in Figure 351 to Figure 354. The depth to groundwater level measurements was reduced to groundwater elevations relative to AHD, based on the recorded elevation measurements of the top of casing or ground surface. The residual mass for the Kununurra rainfall data is also plotted in these figures as a reference curve. It should be noted that key piezometers are located in heavily cracking clay soils (Figure 350), with the potential of local macropore bypass flow local to the bores.

Figure 351 contains the key bore hydrographs for the southern half of the Weaber Plain. The monitoring bore with the best data record is Bore 8365 and shows some significant trends over more than four decades (Figure 351c). Initial observed groundwater levels during 1964-1967 are relatively constant, followed by a reasonably consistent watertable rise between 1971 and 1992, in the order of 7cm/year. This is followed by a more rapid groundwater level rise averaging about 57cm/year. Although affected by noisy data and a less extensive data record, other monitoring bores in the area show similar trends. For one bore (ID 113544340),

the post-1992 rapid rise has stabilised to a new groundwater level equilibrium. Table 40 summarises the nature of these two apparent periods of groundwater rise for these bores.

Table 40: *Groundwater level trends in southern Weaber Plain.*

Bore ID	Commencement of Initial Rise	Rate of Initial Rise (cm/yr)	Commencement of Second Rise	Rate of Second Rise (cm/yr)
11355430				75, then stable
8358	1967-1971	22		
8365	1967-1971	7	1992	57
8366	1980-1984	16	1992?	
8381	No Initial Rise		1993	64
8373	No Initial Rise		1993	60

From the early 1990's, the coincidence between the rapid watertable rise and above average rainfall conditions suggests that increased recharge from rainfall is the main driver. The prior, less dramatic, rising trend coincides with rainfall conditions lower than the long-term average. Hence, this would discount a relationship between increased rainfall and recharge for this initial watertable rise. One hypothesis is that this initial rising trend represents the combined effects of sub-surface and surface drainage from the ORIA via Cave Springs Gap, and the D8 drain and D8 swamp. The latter is discussed in more detail later. These inputs would explain the difference in the onset of watertable rise for the monitoring bores (Table 40), with bores to the south near the Gap (8358 and 8365) showing early initiation, whilst bores to the north showed later initiation or no pre-1992 watertable rises at all.

Hydrographs for the key monitoring bores in the northern half of the Weaber Plain are plotted in Figure 351. The data record is more limited, but two broad observations can be made. The first is that the pre-1992 rise evident in the southern half of the Weaber Plain is not apparent in these hydrographs. This may simply reflect being distant from the mechanism and source of the increased recharge, inferred to be irrigation-induced subsurface discharge from Cave Springs Gap. The second observation is that the rapid post-1992 watertable rise is also not apparent (apart from Bore 8375, which requires data checking). Measurements ceased in 1999, so incomplete data is a factor. However, no observed watertable rise during this period may simply indicate that the aquifer is poorly recharged in this particular area.

Figure 353 presents the key borehole hydrographs for the Knox Plain area. The relatively consistent rising trend observed in the southern Weaber Plain during 1967-1992 is also not evident in the Knox Plain. However, some monitoring bores show a more abrupt rising trend during this period. For example, for Bore 8360, static groundwater conditions in the 1970's appear to have been interrupted in 1976 by a rapid watertable rise in the order of 120cm/yr (Figure 353a). This rise is not likely to be linked to enhanced rainfall recharge, as this decade was relatively dry when compared to the long-term average. There is some evidence for limited watertable rise linked to post-1991 wetter conditions, for example Borehole 11354528 (Figure 353b).

The groundwater level monitoring for the Keep River Plain is limited, both in spatial distribution and in duration, having only commenced in the late 1990's. However, post-1992 watertable rises can be observed from this limited dataset (Figure 354). For example, for Bore 13633061, the rate of rise is inferred to be about 54cm/yr. Secondary mechanisms for enhanced recharge, such as irrigation accessions or vegetation clearing, are not the case for this relatively undeveloped part of the catchment. Hence, increased recharge associated with a period of rainfall above the long-term average is considered to be the likely mechanism.

Figure 350: *Piezometer in the western Weaber Plain, located within black soils that have developed an extensive polygonal crack network. Photo courtesy of Richard George.*

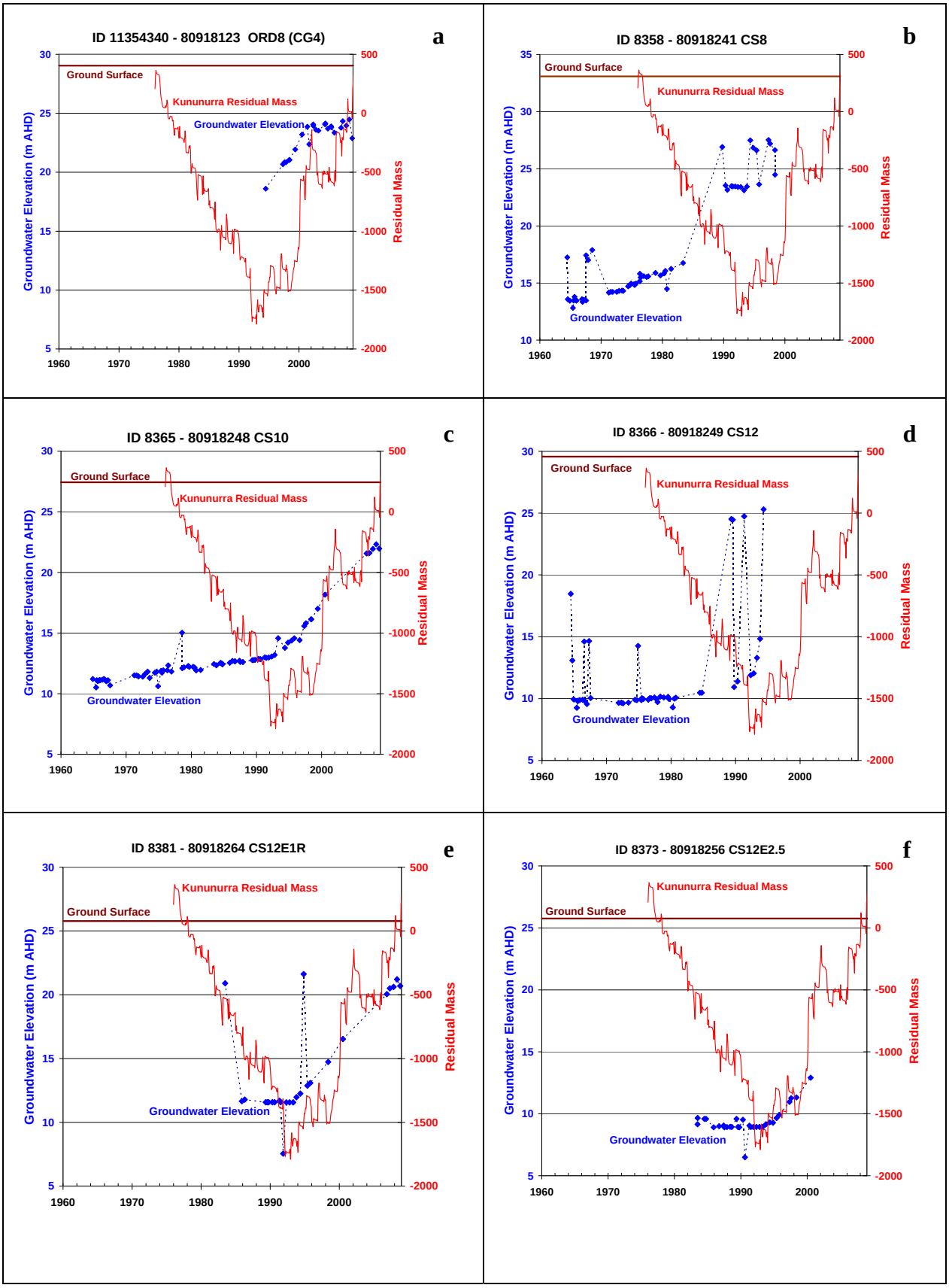

Figure 351: *Selected hydrographs for the southern Weaber Plain.*

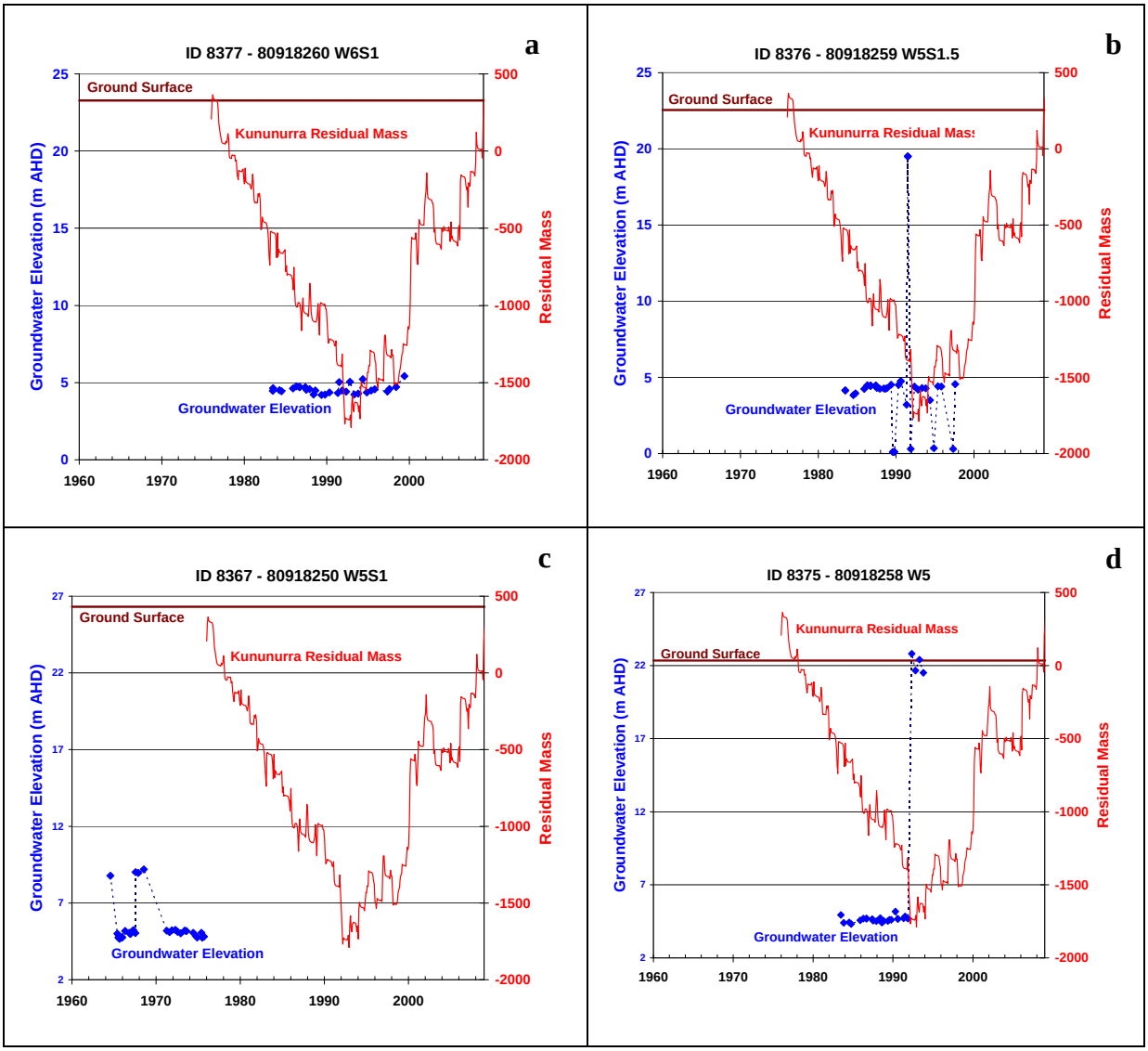

Figure 352: *Selected hydrographs for the northern Weaber Plain.*

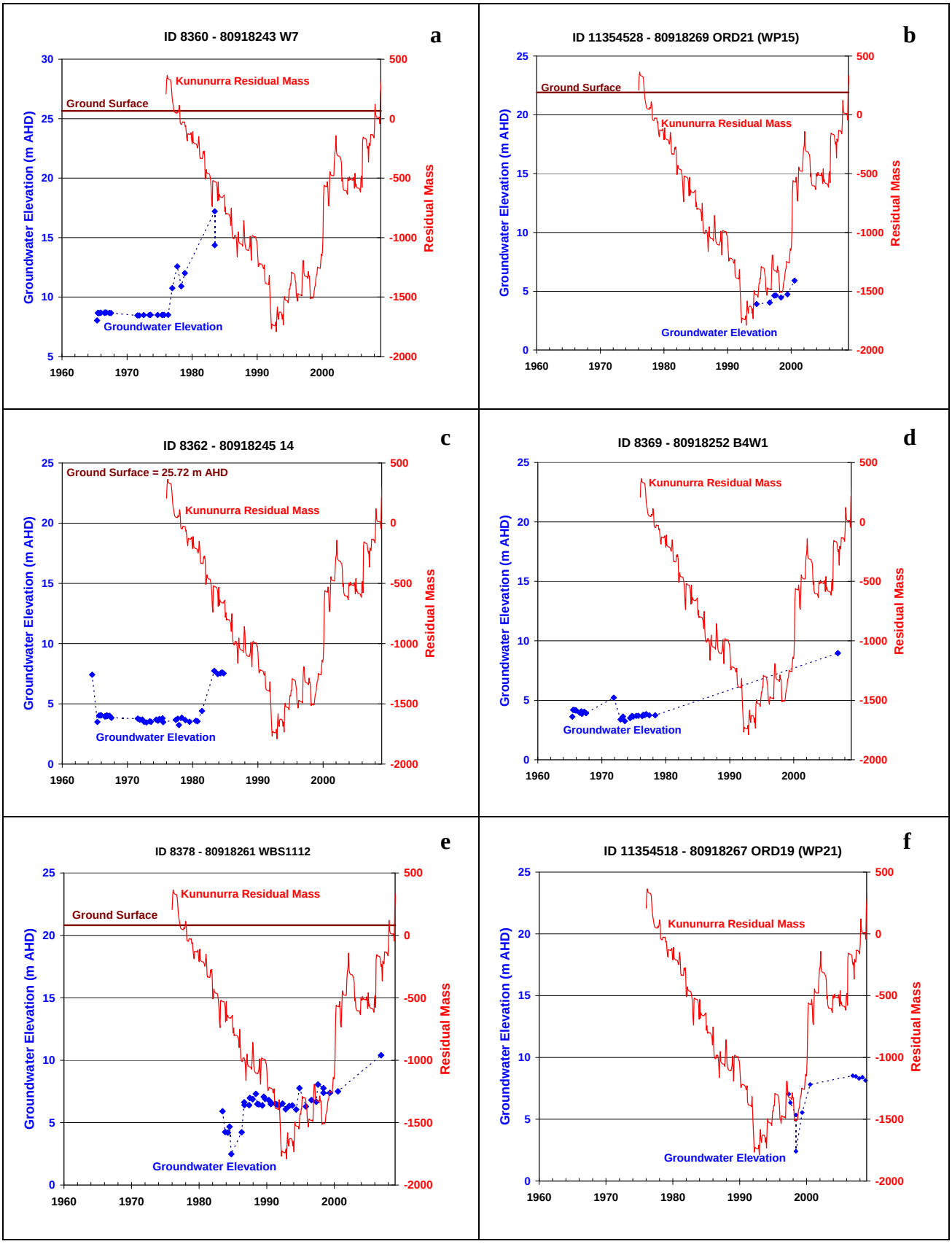

Figure 353: *Selected hydrographs for the Knox Plain.*

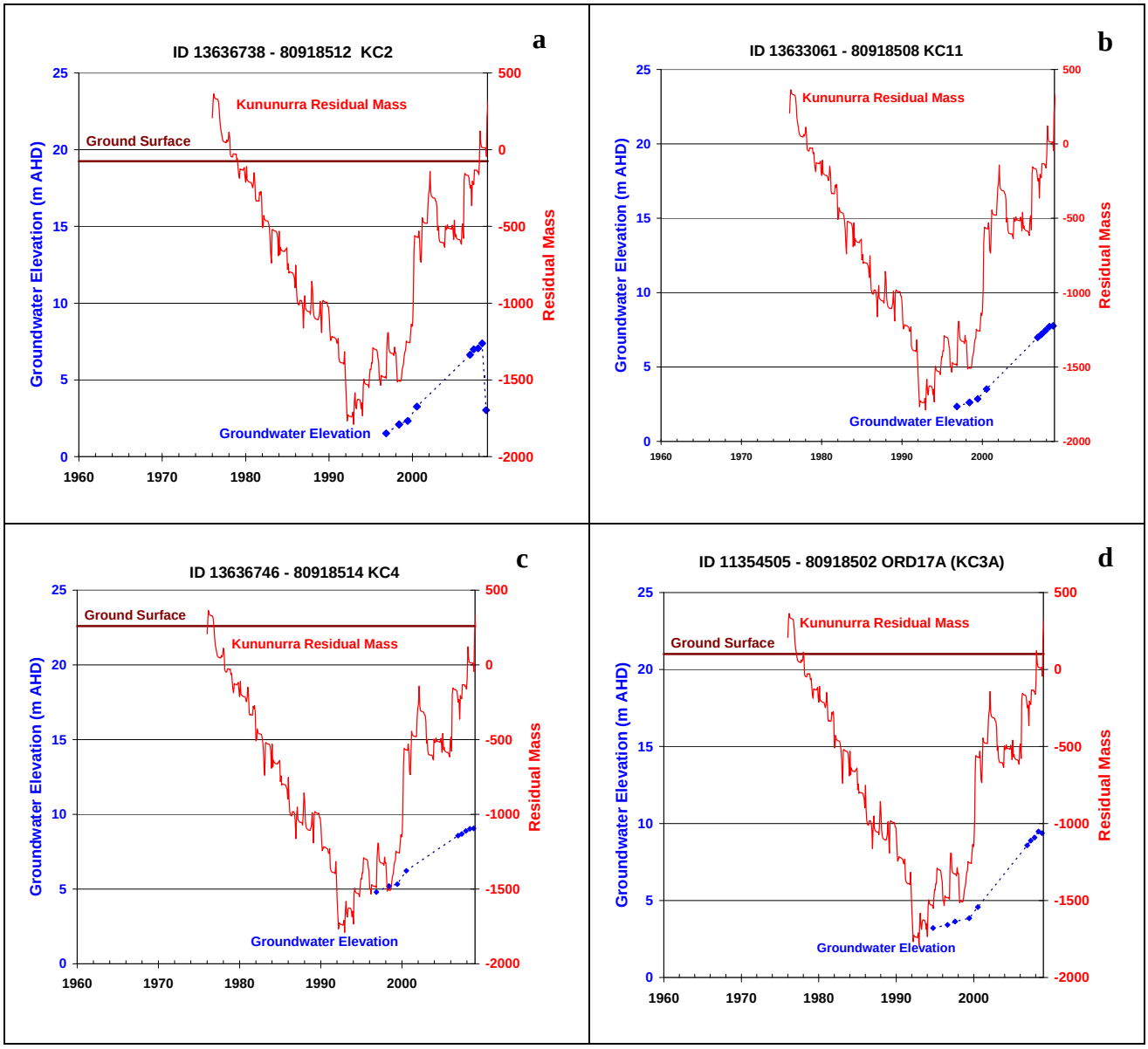

Figure 354: *Selected hydrographs for the Keep River Plain.*

The hydrograph data for the Weaber Pain can be used to understand groundwater recharge dynamics. The watertable fluctuation method (Healy & Cook, 2002) assumes that any rise in groundwater levels in an unconfined aquifer are due to percolating water reaching the watertable. On this basis, the equation used to calculate recharge (R) is:

$$R = S_y * \Delta h$$

Where S_y is specific yield and Δh is the change in the height of the watertable. Recharge is equated to the volume of water stored in the incremental volume of the aquifer defined by the change in height of the watertable. This assumes that other components such as base flow, pumping, inter-aquifer leakage and evapotranspiration are insignificant over the period of time that recharge is occurring.

There are limited Sy data for the ORIA. In the Ivanhoe Plain, screened intervals in the basal sand and gravel aquifer yielded Sy values ranging from 0.02 to 0.05 (O'Boy *et al.,* 2001). However, it was also noted that these values were too low, and likely to reflect the short-term duration of the pump tests. The latter authors also noted that the Sy for unconsolidated fluvial sediments is commonly between 0.05 and 0.2. A test production bore to determine the hydraulic characteristics within the Knox Creek-Keep River Plain sand and

clay alluvium estimated a Sy ranging from 0.05 to 0.15 (O'Boy *et al.,* 2001). Applying this method in the Weaber Plain, and assuming an average watertable rise of 500 mm per year over the past decade, and using a range of S_y values for sands and clays (0.05-0.15), gives a recharge range of 5-75mm/yr over this period. These higher values are not representative, as there are very few areas where there are sands throughout the alluvial sequence. However, values at the higher range may be anticipated coincident with the main Ord palaeochannel, with sands and gravels recorded from the base of the sequence to within a few metres of the surface in the Weaber Plain. The recharge rate in this situation is likely to be governed by the infiltration through the thin sequence of near-surface clays.

However, watertable rise could also include significant lateral accessions, and is likely to include recharge from point sources (such as the D8 swamp), streams and irrigation channels. Smith *et al.* (2006) note that water levels in individual monitoring bores are commonly affected by local responses to local-scale recharge and discharge processes (e.g., local watertable mounds near leaky sections of supply channels and drains). Watertable maps that are produced from a monitoring network with too few bores can contain uncertainty due to unreasonable interpolation of these local watertable responses over large areas. This situation is present in the Ord Stage 1 and reinforces the need to have a sufficient number of monitoring locations to provided dependable estimates of watertable elevation at un-monitored locations. It is not certain whether similar cautions must be taken into account in the Stage 2 area where no irrigation has yet taken place.

In summary, although the historic monitoring record is intermittent, periods of watertable rise have been identified. Relatively rapid watertable rises initiated in the early 1990's can be linked to enhanced recharge associated by relatively wetter conditions, in particular increased frequency of large rainfall events. Evidence for this rising watertable trend can be found in monitoring bores across the entire study area. An earlier, but less dramatic, rising watertable is specifically observed in bores located in the southern half of the Weaber Plain. This is inferred to relate to recharge associated with irrigation drainage via Cave Spring Gap (Figure 355 to Figure 356).

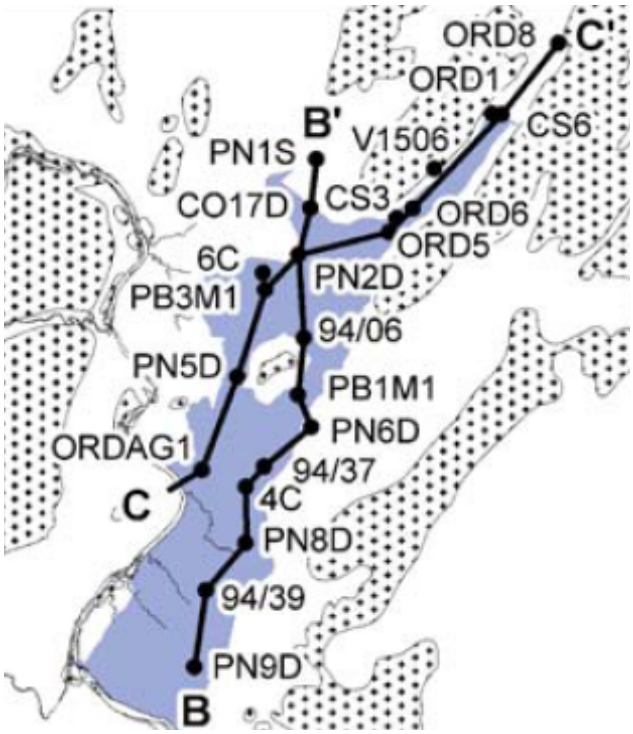

Figure 355: *Map of northern Ivanhoe Plain and Cave Springs Gap showing location of long-section C-C' through sand aquifer in Figure 356.*

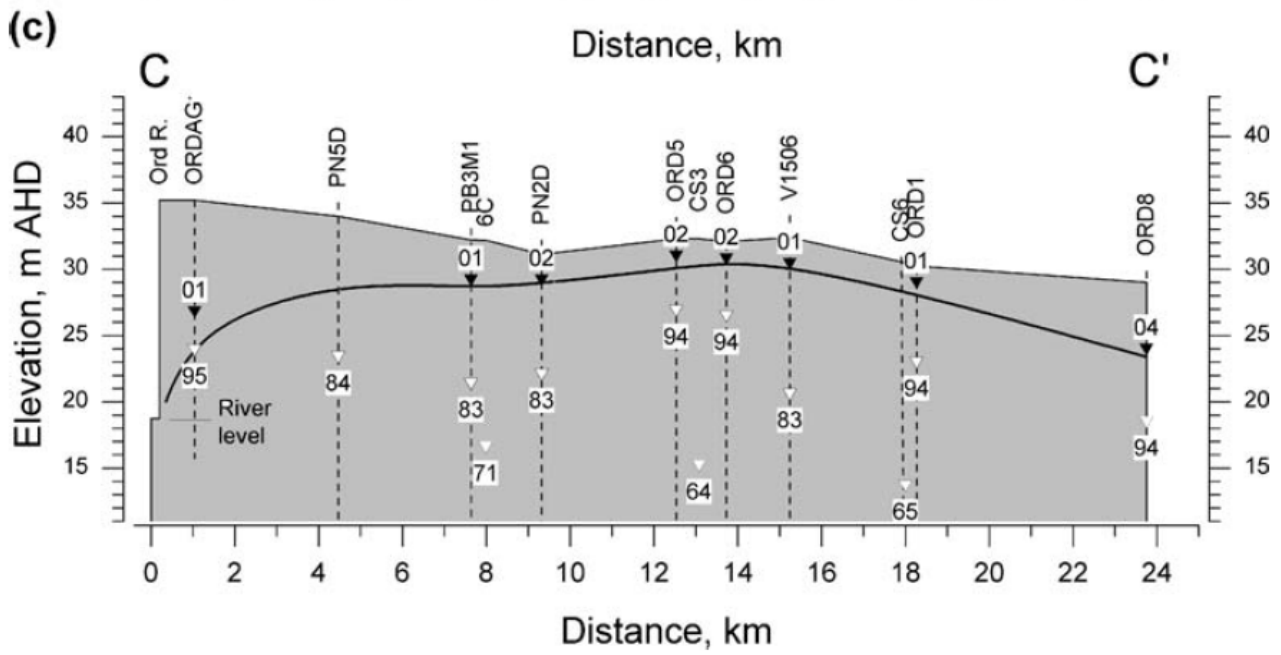

Figure 356: *Long-section through north Ivanhoe Plain and Cave Springs Gap showing watertable depths. Refer to Figure 355 for long-section location.*

This assessment highlights the need for robust baseline monitoring of groundwater conditions in the area. An improved understanding of groundwater dynamics and underlying mechanisms could be achieved by:

(1) The ongoing maintenance and monitoring of bores that already have a long-term data record (such as Bore 8365 in the southern Weaber Plain);

(2) Installation, regular downloading and maintenance of data loggers in key bores, to provide a more detailed time series of groundwater level. The time period between measurements in the existing data record is in the order of months or years. Loggers, calibrated with regular (typically 3-monthly) on-site measurements, would enable the (sub) hourly collection of groundwater level data. This greater frequency is critical for observing groundwater response to rainfall events and to identify seasonal fluctuations. It is currently difficult to distinguish seasonal variability from any underlying longer-term watertable trends;

(3) Collection of supporting data to help interpret recharge mechanisms. This includes groundwater sampling and hydrochemical analysis, such as age dating using isotopes or atmospheric tracers (e.g. CFC). Time series monitoring of both groundwater level and electrical conductivity (salinity) using combined data loggers at specific bores would be also useful for understanding groundwater dynamics.

Where are the high recharge zones?

Tickell *et al*. (2006) established that saline soil water and groundwater beneath the Keep River Plain northeast of Weaber Plain accumulated due to evapotranspiration of infiltrated rainfall in areas where leaching by deep drainage is restricted. In some areas, seasonal swamps are relatively devoid of surface vegetation, and are areas of potential high evapotranspiration (Figure 357). In these earlier studies, mean groundwater recharge in this uncleared floodplain was estimated to be only 0.1mm/yr.

However, hydrograph data in this report (Figure 351 to Figure 354) suggest that pre-clearing recharge rates under similar soils can be much higher, and dependent upon the intensity and duration of rainfall, and total amount of excess rainfall in much of the Weaber and Knox Creek Plains, accession to the groundwater table over the past decade has been up to 600mm per annum (e.g. in the southern Weaber Plain). Earlier, application of the watertable fluctuation method suggested recharge rates of 5-75mm/yr was possible over the past 12-15 years in parts of the Weaber Plain.

Figure 357: *Seasonal swamp, central Weaber Plains, marked by absence of trees*.

Leakage from man-made infrastructure may contribute to some of the recharge observed in the western Weaber Plain. The D8 drain (Figure 358) currently directs about 3Gl/annum water from the ORIA Stage 1 into the Weaber, where it is discharged largely into a permanent artificial wetland termed the D8 swamp (Figure 359 to Figure 360). The D8 swamp is also fed by surface flows from the area to the NE of Greens Location. The volumes of surface water delivered through the D8 drain were likely to have been larger in the past, with a significant reduction (30%) in water due to efficiencies in ORIA Stage 1 over the past 3-5 years. However, it is not clear to what extent these efficiencies flowed through to surface water volumes through the D8 drain due to the need to preserve pressure heads for irrigation in Cave Springs Gap. There is almost certainly a leakage component from the D8 drain itself, as this in places transects the path of the Ord palaeo-channel (Figure 344 to Figure 345).

It is also not established how much of the water stored in the D8 swamp leaks to the groundwater. The soils maps of the area show that the D8 swamp is in an area of Aquitaine soils, and are likely to be up to 2m thick. The 0-2m AEM conductivity depth slice for this area (Figure 361) shows no particularly strong conductivity anomaly at shallow depths associated with the swamp, with the interpretation that the swamp is locally perched on clay soils. However, at greater depths, the conductivity is low in a pattern that appears to be generally coincident with the surface outline of the swamp (Figure 362 to Figure 368). The few bores in this area suggest the presence of sands and basal gravel at depth in this area (Figure 215 to Figure 220). The sand gravels were probably deposited as a bedrock-confined distributary fan and /or arm of the Ord palaeo-channel. The patterning observed in the conductivity depth slices, supported by borehole data, suggests that deposition of sands becoming more restricted in the area of the D8 swamp through time, as the Ord palaeochannel to the south became dominant on its way to the Keep River (Figure 363 to Figure 367). By contrast, the presence of highly conductive anomalies around the northern and eastern ends of the swamp are interpreted as an area of clays with a high salt store marginal to this fan and palaeochannel complex (Figure 363 to Figure 366).

Overall, the shape of the resistive anomaly to depth beneath the swamp would appear to imply potential leakage of fresh water into sands in this fan/palaeochannel. Further drilling is required to confirm the nature of the alluvium in this area, and to help constrain recharge and groundwater models. Significant leakage from the D8 swamp over time has the potential to have contributed significantly to the groundwater mound in this area.

At depth, the northern end of the conductivity anomaly beneath the D8 swamp is coincident with a bedrock pediment (Figure 368). Overall, the palaeo-drainage in the western Weaber Plain appears to have a strong bedrock control (Figure 361 to Figure 368), with the occurrence of shallow bedrock pediments likely to result in lateral groundwater flow at shallow depths in parts of this area.

Overflow in wet years is observed from the D8 swamp to Point Springs and Gum Creek (Figure 359). Development of ephemeral water bodies and swamps in the latter areas appears to be largely due to wet season run-off from the adjacent hills, however overflow from the D8 swamp is also likely to have been a contributor to recharge. The alluvium in this area contains some sandy material likely to assist recharge, while bore hydrographs in this area show rising trends in the 1970s and again in the 1990s (Figure 352).

Figure 358: *The D8 drain near its present termination in the western Weaber Plain. Photograph looking west back towards the hills on the southern margin of Cave Springs Gap.*

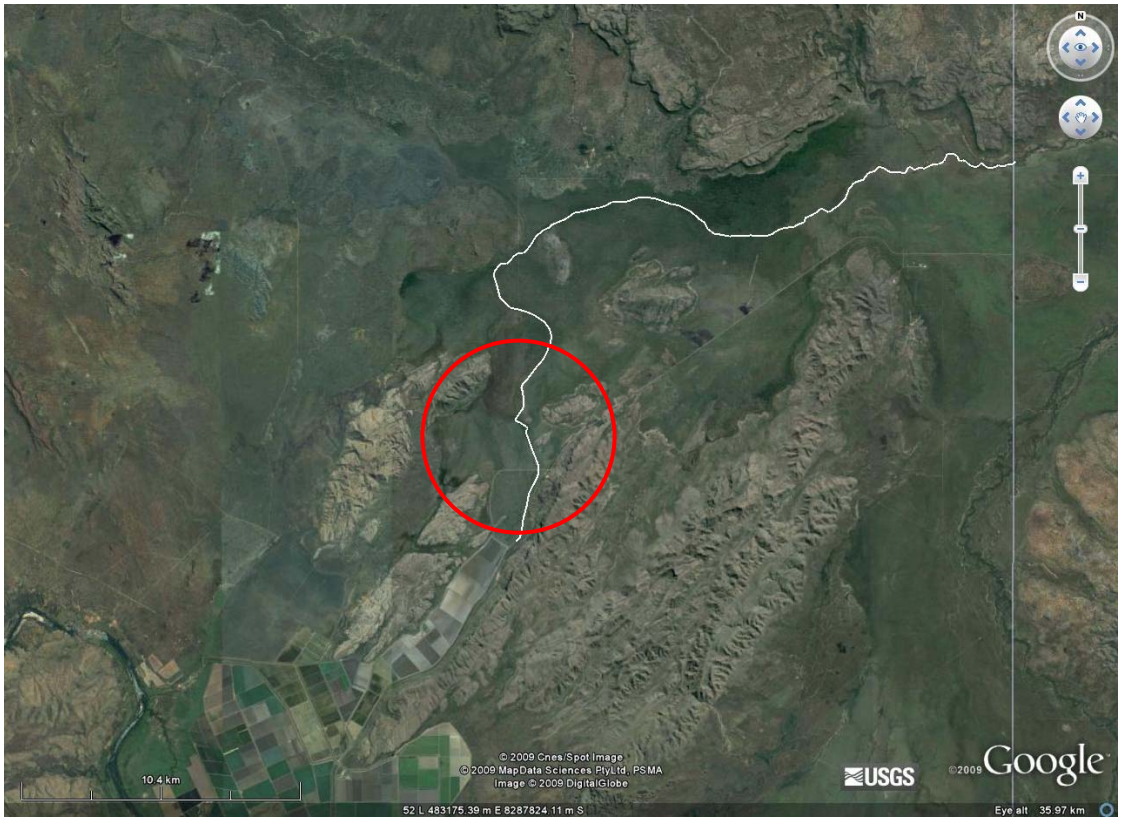

Figure 359: *Google earth image showing the location of the D8 swamp, which is driven by discharge of over 3Gl/yr discharge from the D8 drain. The water body has become a semi-permanent wetland (dark brown area highlighted) formed by the terminus of the M1 supply channel. To the south of the wetland, the M1 channel is denoted by the white line. To the north, the white line denotes the natural drainage line. A blow-up of the wetland area is shown in Figure 142.*

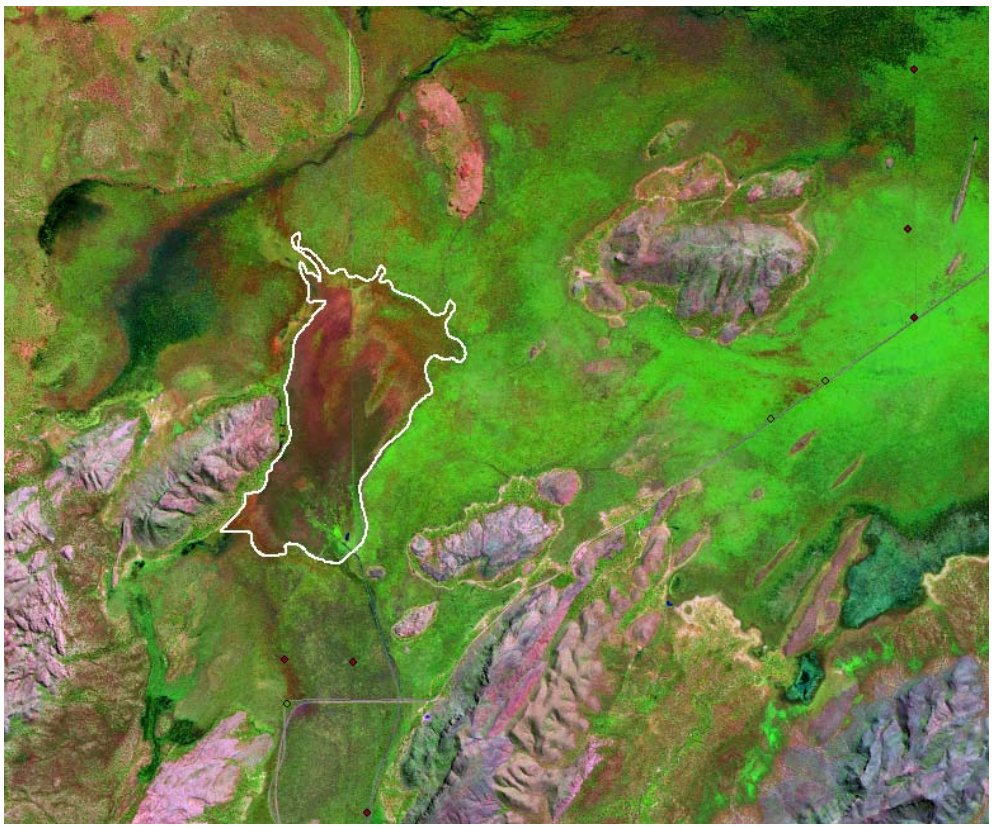

Figure 360: *Spot image from August 2008. This figure shows the location of the D8 swamp (white outline).*

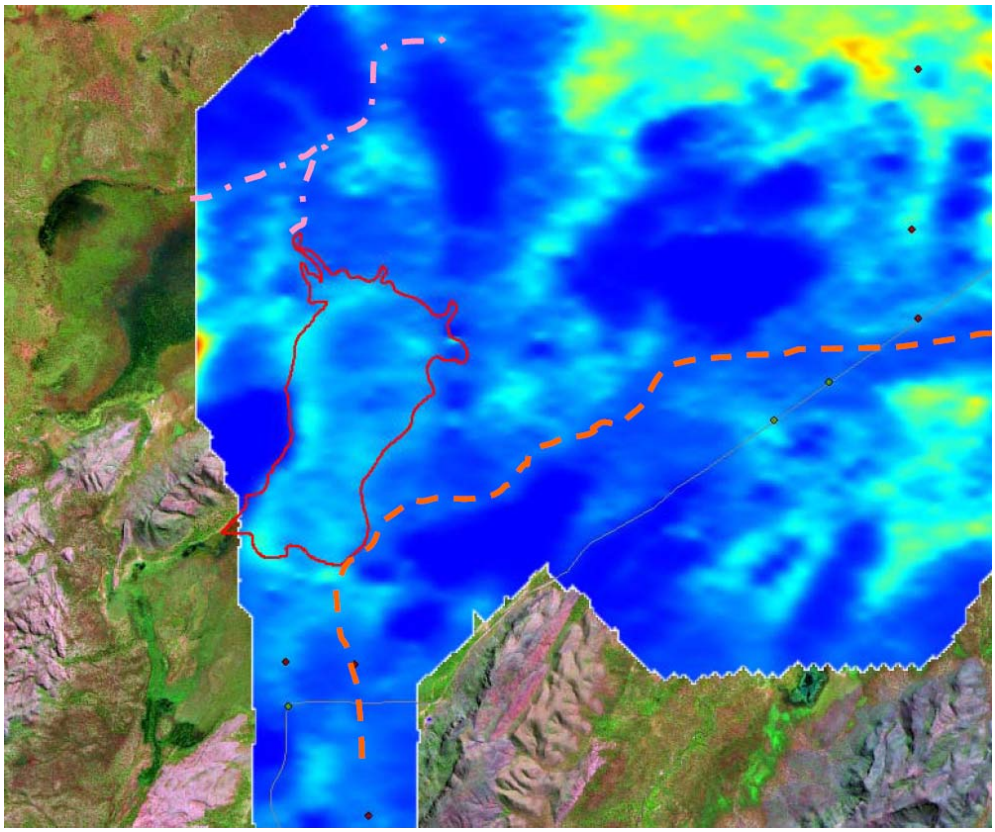

Figure 361: *Conductivity depth slice 0-2m. This figure shows the location of the D8 swamp (red outline), with no really distinctive anomaly associated it. The dark blue areas (resistive) are areas of bedrock. The location of a palaeo-channel (orange dotted line) is just apparent. A shallow resistive anomaly (pink dotted line) is coincident with the overflow from the D8 drain and other local creek drainage.*

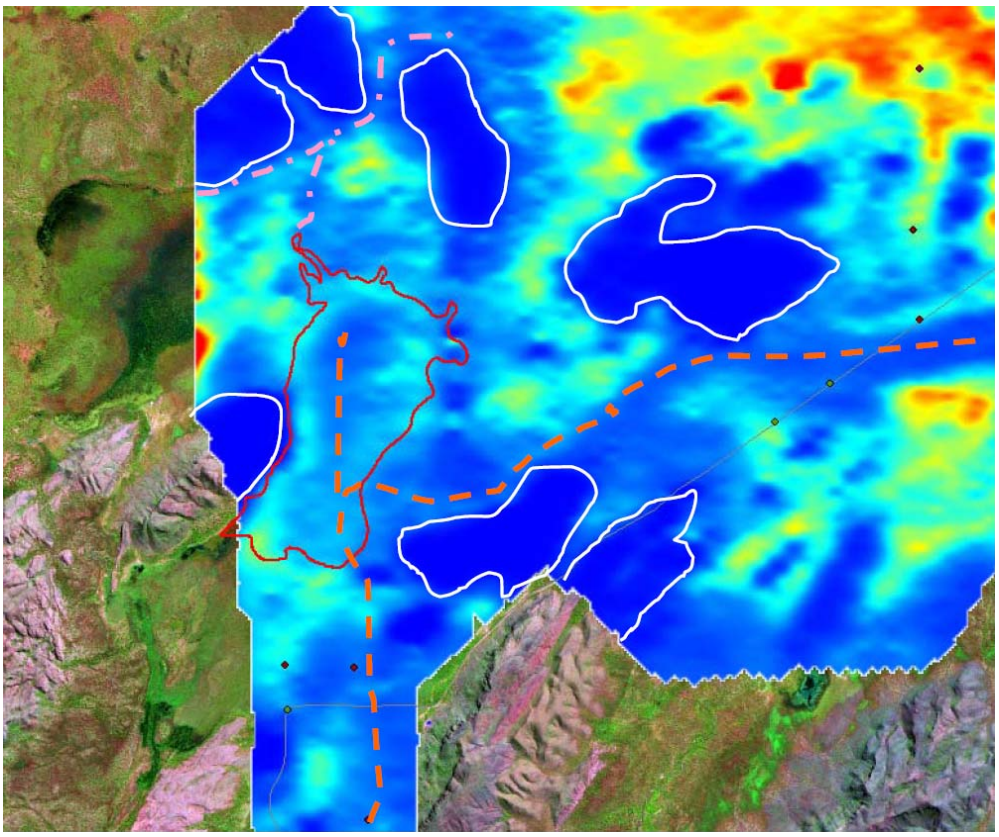

Figure 362: *Conductivity depth slice 2- 4.2m. This figure shows the location of the D8 swamp (red outline). Bedrock (resistive anomalies) is outlined in white. Conductive (saline) clays (yellow-red) are restricted to the NE of the image. Bedrock at depth restricts the location of the Ord palaeochannel (orange dotted line).*

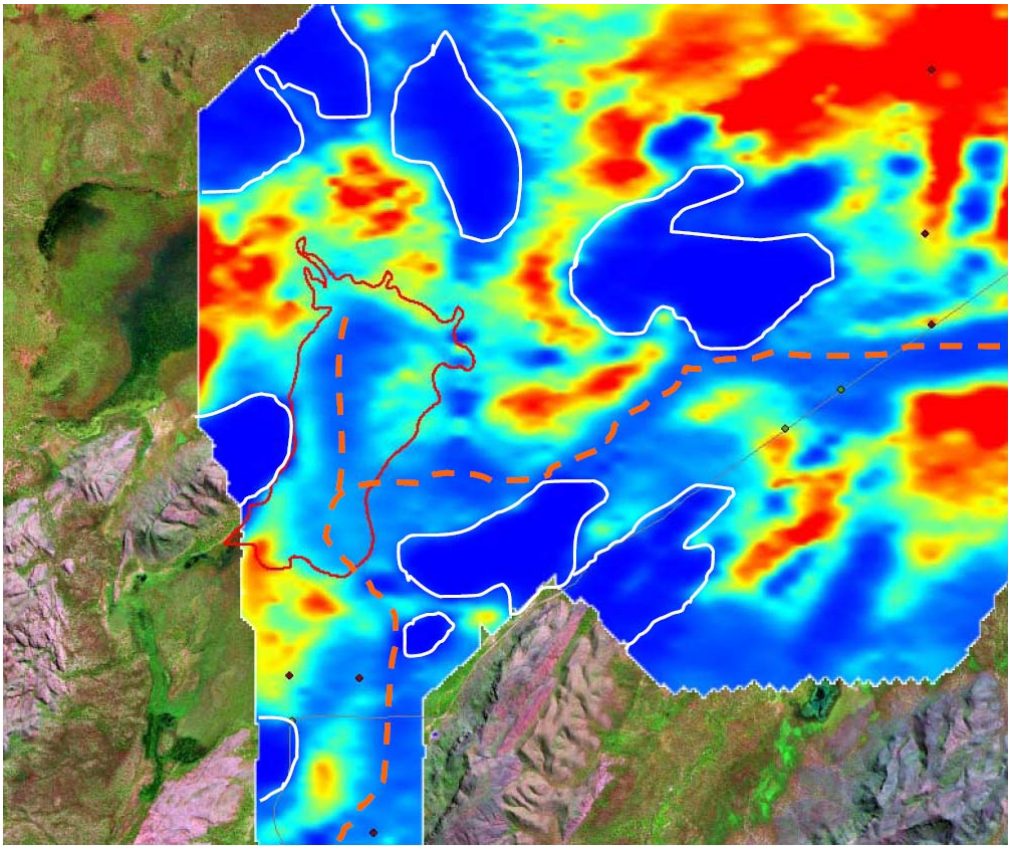

Figure 363: *Conductivity depth slice 4.2- 6.7m. This figure shows the location of the D8 swamp (red outline). Bedrock (resistive anomalies) is outlined in white. Conductive (saline) clays (yellow-red) form irregular areas in areas that were most likely overbank or swamp locations often overlying shallow pediments. Bedrock at depth restricts the location of the Ord palaeochannel (orange dotted line).*

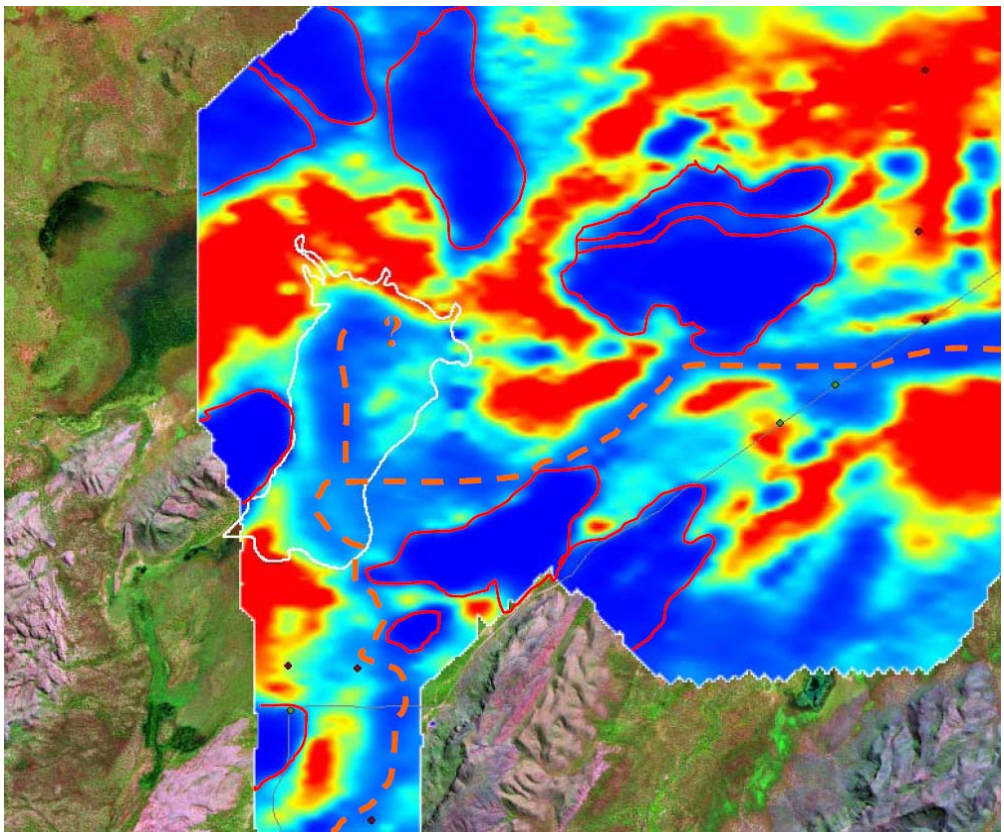

Figure 364: *Conductivity depth slice 6.7-9.5m. This figure shows the location of the D8 swamp (white outline). Bedrock (resistive anomalies) is outlined in red. Conductive (saline) clays (yellow-red) form irregular areas in areas that were most likely overbank or swamp locations often overlying shallow pediments. Bedrock at depth restricts the location of the Ord palaeochannel (orange dotted line).*

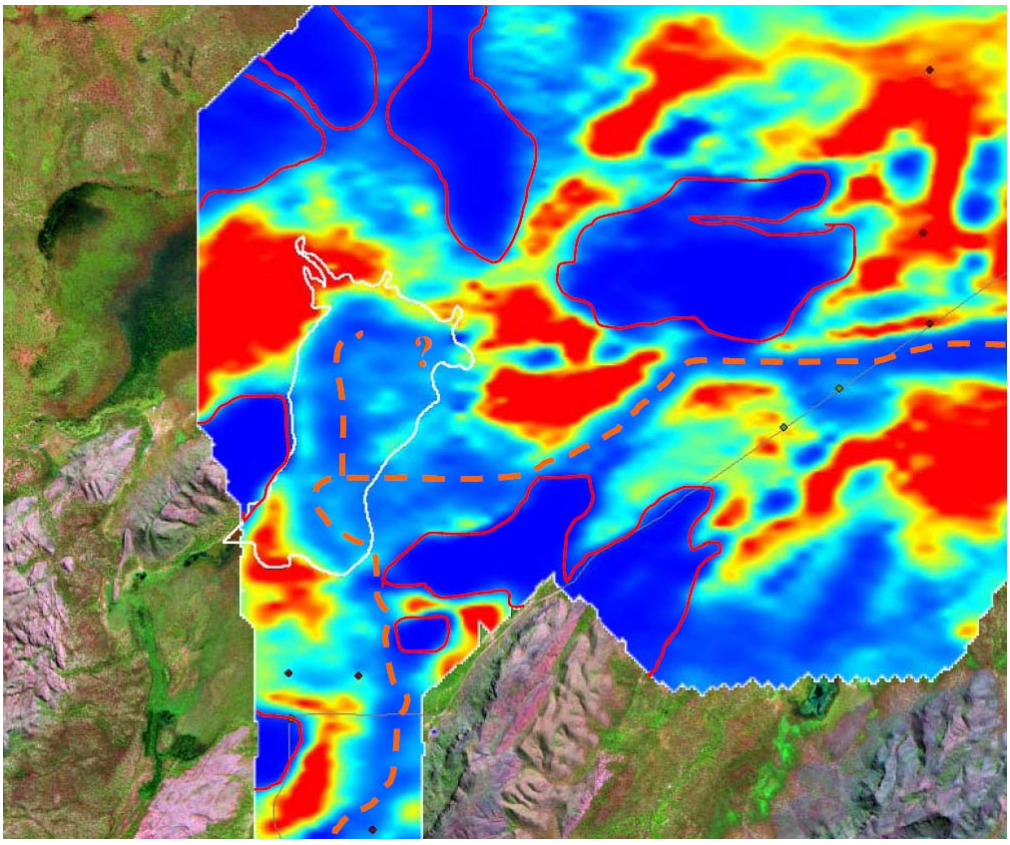

Figure 365: *Conductivity depth slice 9.5-12.7m. This figure shows the location of the D8 swamp (white outline). Bedrock (resistive anomalies) is outlined in red. Conductive (saline) clays (yellow-red) form irregular areas in areas that were most likely overbank or swamp locations. Bedrock at depth restricts the location of the Ord palaeochannel*

(orange dotted line), and may also play a role in the localisation of the resistive anomaly (sands?) containing fresh water) beneath the D8 swamp at depth.

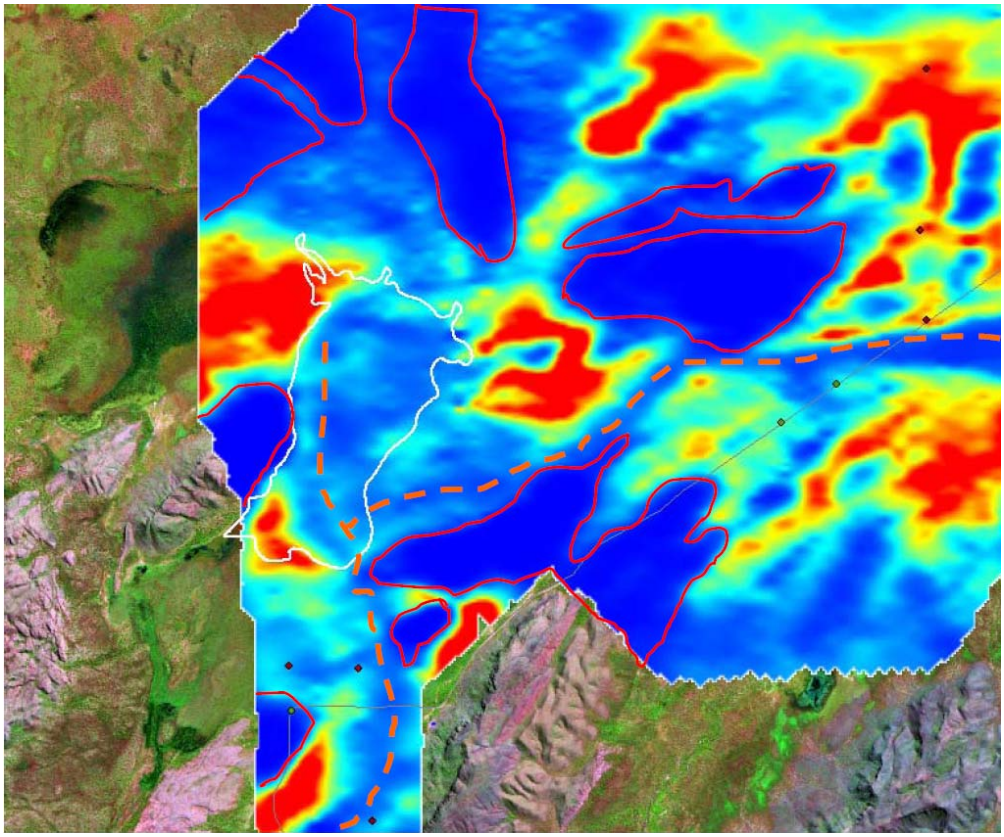

Figure 366: *Conductivity depth slice 12.7-16.3m. This figure shows the location of the D8 swamp (white outline). Bedrock (resistive anomalies) is outlined in red. Conductive (saline) clays (yellow-red) form irregular areas in areas that were most likely overbank or swamp locations. Bedrock at depth restricts the location of the Ord palaeochannel (orange dotted line), and may also play a role in the localisation of the resistive anomaly (sands?) containing fresh water) beneath the D8 swamp at depth.*

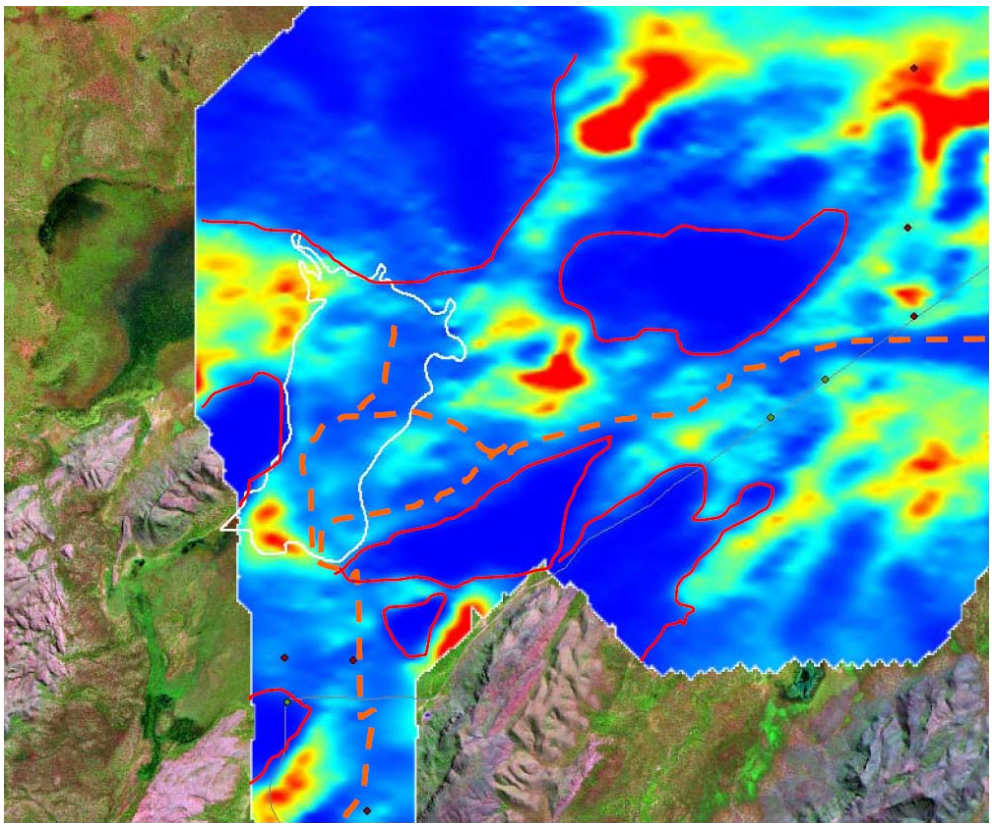

Figure 367: *Conductivity depth slice 16.3-20.3m. This figure shows the location of the D8 swamp (white outline). This figure shows that bedrock (dark blue) appears to restrict the location of the Ord palaeochannel (orange dotted line) at these depths. The conductivity distribution would appear to show a possible second palaeochannel feature beneath the location of the D8 swamp.*

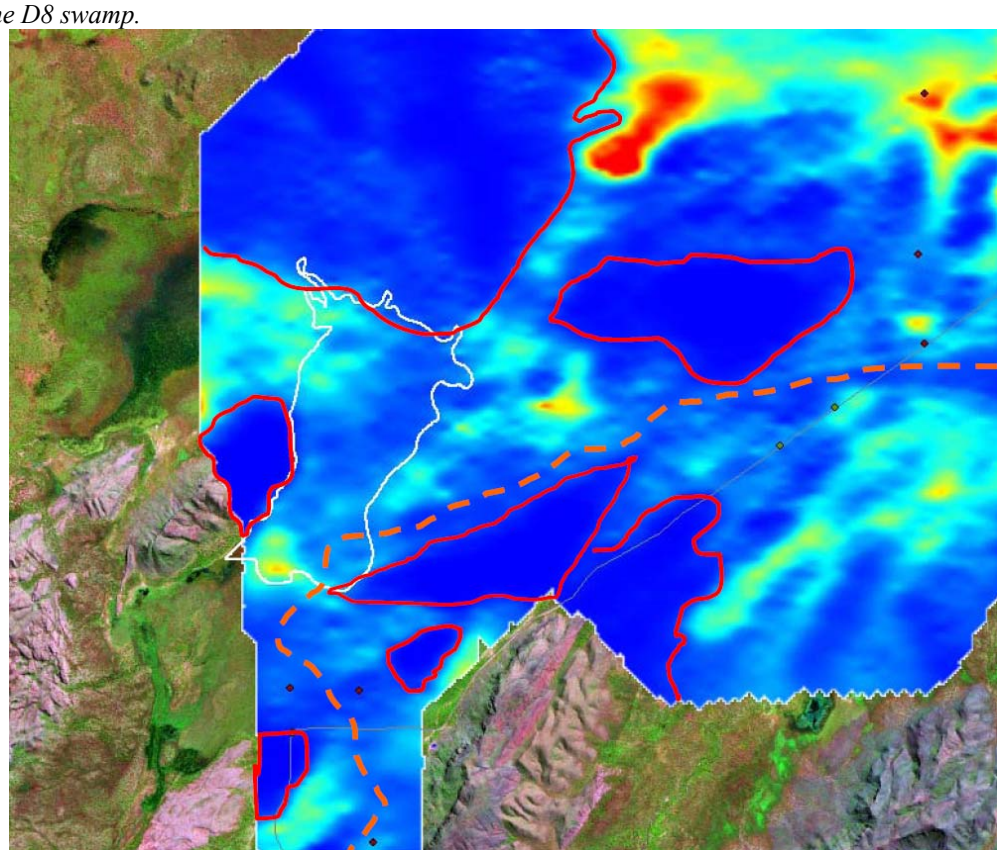

Figure 368: *Conductivity depth slice 20.3-24.8m. This figure shows the location of the D8 swamp (white outline). Bedrock pediments are outlined in red. This figure shows that bedrock at depth restricts the location of the Ord palaeochannel (orange dotted line) at these depths, and may also play a role in the localisation of the resistive anomaly (sands?) containing fresh water) beneath the D8 swamp at depth.*

In the absence of field data measuring recharge rates directly, 4 products have been produced as data layers to provide information relevant to the estimation of recharge rates in the Stage 2 areas. These 4 map products are:

- surface permeability, based on measurements of soil permeability in the top 20cm (Figure 369);
- soil recharge properties for the 0-2m soil layer, using data from soils mapping and field permeability tests (Figure 108);
- total clay thickness, incorporating soil mapping data for the 0-2m depth slice as well as AEM data beneath this (Figure 370);
- clay thickness above the water table (Figure 370). This integrates the previous maps with the water table map, and approximates a map of deep drainage.

These map products are designed primarily as data layers for input into a groundwater model. However, they also enable a qualitative assessment of recharge to the groundwater table to be made. In the surface permeability and soil recharge properties maps, the estimates of recharge rates across all proposed irrigation areas are low. However, these products are based on available soils data only, and the products do not take into considerate macropore bypass flow (Smith, 2008). The hydrograph analysis of bores in these areas shows that recharge to the groundwater table is significant and relatively fast, suggesting that other products are required to describe recharge more adequately in these floodplain areas.

Figure 370 shows the total clay thickness for the Weaber, Keep River and Knox Creek Plains, incorporating the soils layer as well as AEM-derived clay thickness estimates below 2m. This product serves to predict the likely preferential recharge rates and flow paths once water has passed through the upper soil layer macropores. When this dataset is overlain on the regional water table map, it suggests that recharge rates through surface materials are likely to be slower east of drillhole KS1 in the Weaber Plain, where the thickness of clays above the water table increases significantly. Low recharge rates are also suggested for large parts of the Knox Creek and Keep River Plains. On the Weaber Plain, it is common for the existing monitoring bores to be located on heavily cracking clay soils, as shown in Figure 347 to Figure 350.

However, these products do not explain all the observed variation in the bore hydrographs, and other factors, including induration of the northern palaeochannel in the Weaber Plain, may also be factors, as might lateral recharge, which varies across the area.

In general, the thinner clays over the western half of the Weaber Plain (reflecting a shallow water table), and over the southern Ord palaeochannel, indicate these may be areas of higher accession to the groundwater table in the future. These products could be used to refine the salt hazard maps in a groundwater model.

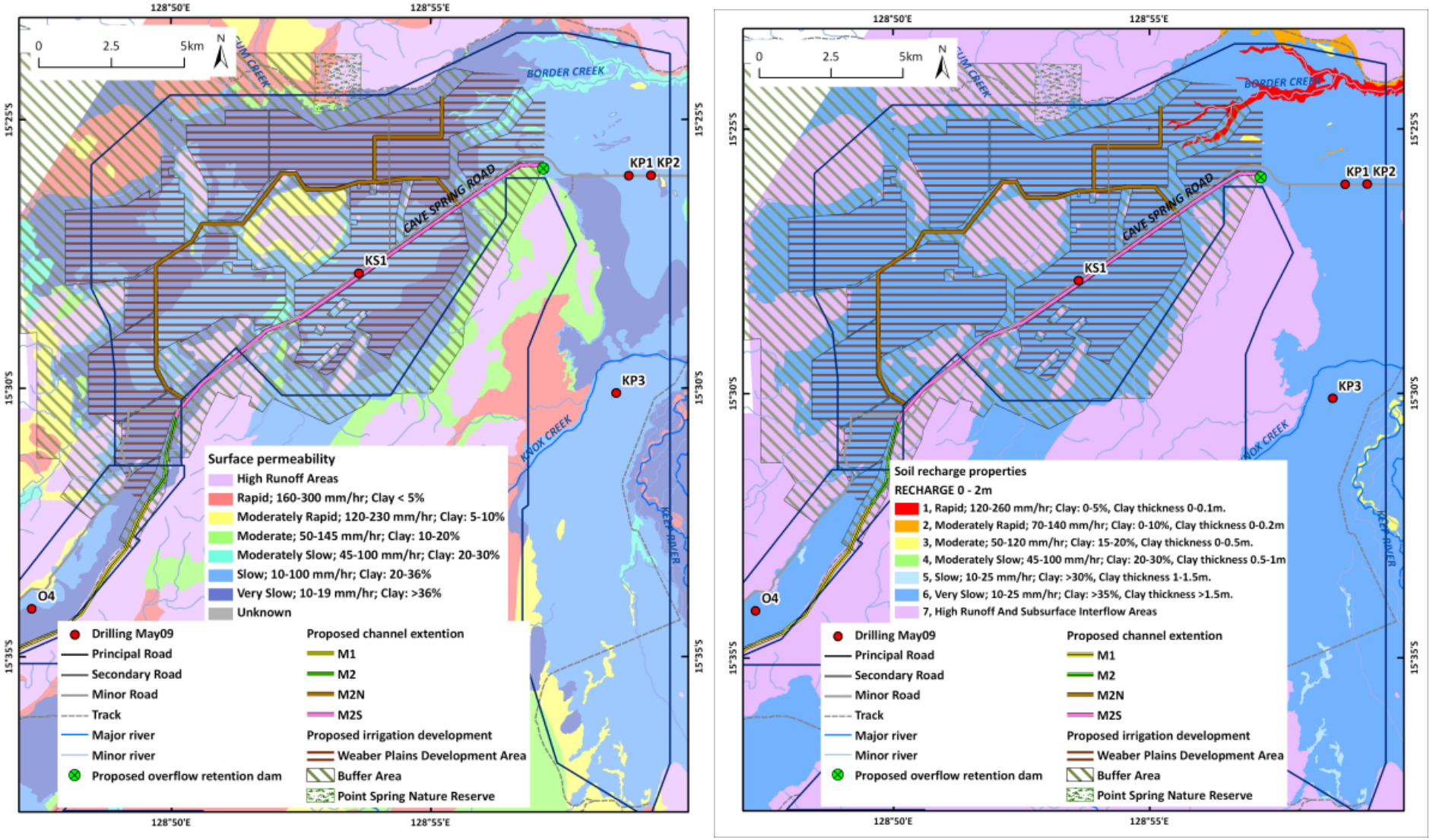

Figure 369: *Weaber, Keep River and Knox Creek Plains. Left: surface permeability. Right: soil recharge properties.*

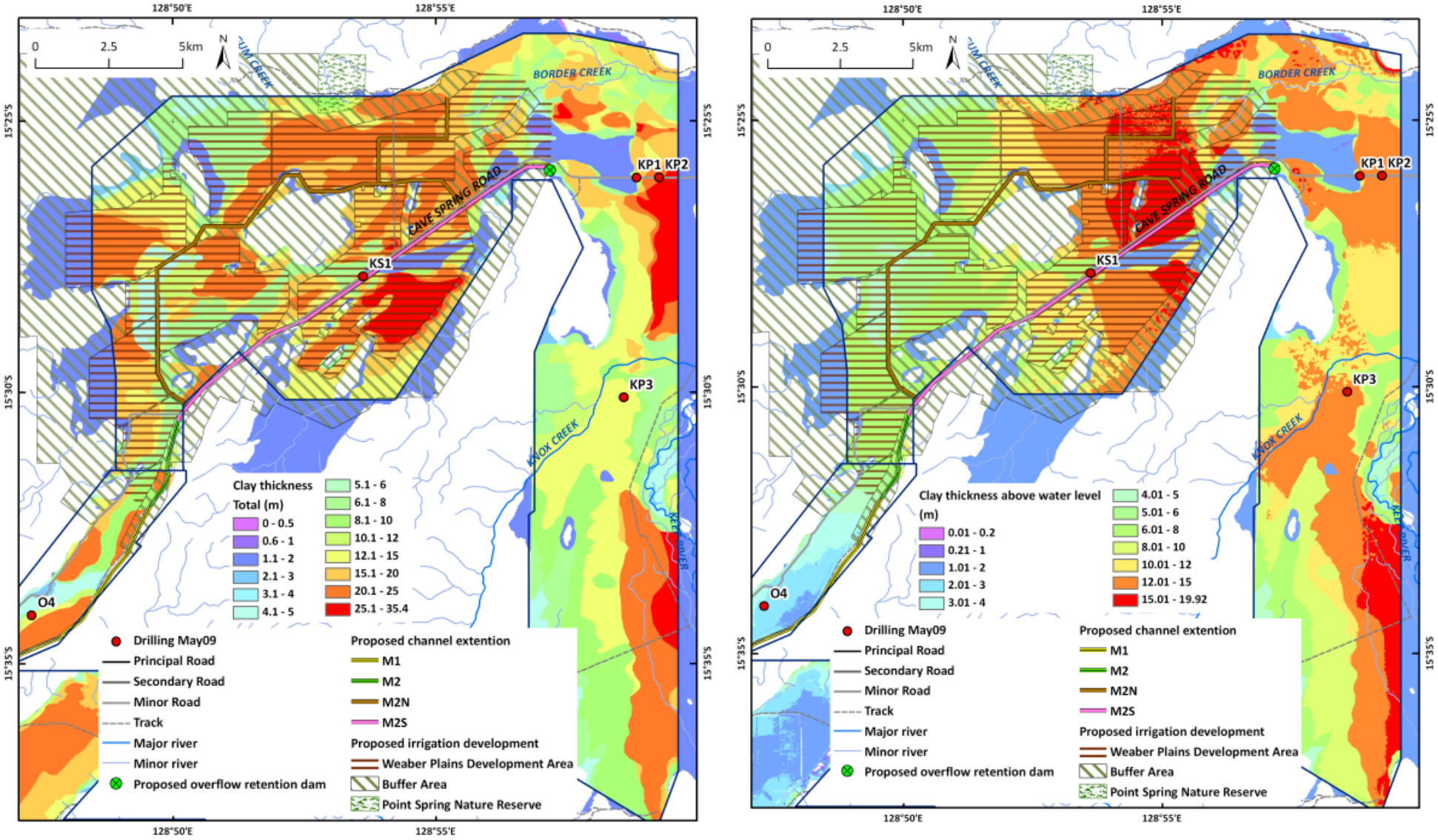

Figure 370: *(A) Map of total clay thickness (left) and (B) clay thickness above the water table (right).*

Where does leakage occur from the water supply infrastructure?
When the lithology maps are overlain with plans of water supply and drainage infrastructure, it is evident that for most of its proposed route, the M2 supply channel roughly follows the older palaeochannel (Figure 213 - Figure 221; Figure 343; Figure 344). Maps show that the channel will be underlain for most of its route by sands and gravels with low salt store can be used to identify area of higher potential salt mobilisation and salinity risk. For example, there are several locations in the Ivanhoe Plain where the M1 water supply channel and subsidiary water channels transect areas of higher salt store (Figure 331, Figure 332). Leakage from the channels in these areas is likely to pose a higher risk of salt mobilisation and soil salinity developing locally. In areas of high water table, and where water supply channels are not adequately sealed, there is also the potential in these areas for salt to be mobilised into the water supply infrastructure.

What is the salinity and waterlogging risk to native and wetlands in the proposed buffer zones around the Stage 2 areas?
Moderate to high vegetation vigour for many of the Stage 2 floodplain areas was observed in NDVI classification of Landsat 5 TM imagery acquired for August 2008 (Figure 83). This is in accordance with anecdotal evidence that there has been increased vegetation growth noted in areas such as the Weaber Plain over the past 12 years in response to increased rainfall (D. Palmer, G. Strickland, pers. comm., 2009). Areas of low vigour tend to occur on thin soils over rocky outcrops and/or on areas of thin soils on sandy colluvial fans.

The unsaturated zone salinity hazard map (Figure 331) shows that in general there is a low salinity hazard in the proposed buffer zones that surround the area earmarked for development in the Weaber Plain. There are a few areas however where there is a moderate salinity hazard however, notably along the course of the M2 channel, in a triangular area between the M2S and M2N water supply channels, as well as along the eastern portion of the northern boundary area (Figure 336). The salt store and groundwater salinities are particularly high in the latter area (Figure 334).

The western boundary area may also have a risk of water logging developing due to the relatively shallow water tables in this area (Figure 348, Figure 349). Along the western boundary, area there are moderate to high salt stores in the proposed development area, however the AEM data only cover part of the adjacent buffer zone, and it is not possible to assess the immediate salinity hazard along some of this boundary.

Where would additional boreholes for validation of the hydrostratigraphy, salinity hazard and the monitoring of future potential salinity risk and groundwater fluctuations, be best sited?
It is anticipated that a number of existing bores will be lost when land clearing and levelling for irrigation development occurs. While the preservation of bores with a long record of observations would be preferred, it is recognised that this might not be practical.

A pragmatic approach has been taken to identify new borehole locations that would assist with validating the hydrostratigraphy and groundwater model, and at the same time provide piezometer sites for the monitoring of future groundwater fluctuations and future potential salinity risk. The AEM conductivity depth slices, lithology maps, salt store, groundwater salinity and salinity hazard maps were used in conjunction with overlays of proposed irrigation infrastructure to identify suitable sites.

Figure 371 shows the locations of proposed bores in the Weaber Plain (only). The locations have been chosen to monitor:
1. fluctuations in pressure heads and water levels within the main Ord palaeochannel and Border Creek,
2. high salinity hazard close to proposed irrigation infrastructure (and possible leakage); and
3. groundwater rise and salinity levels in high hazard areas within the irrigation area where there is potential for lateral groundwater and/or surface flow from surrounding hills.

The Ord palaeochannel is the aquifer unit with the highest hydraulic conductivities in the area, and monitoring bores placed along this can provide invaluable information on pressure heads, water levels and water quality in the gravel-filled palaeochannel. Water levels may rise most quickly in this unit, while there is also some desire to use this for the management of groundwater levels.

Areas of high salinity hazard close to proposed supply channels may have a higher risk of salt mobilisation if leakage results in localised groundwater rises. Similarly, other areas of high hazard should be drilled to monitor possible rises in groundwater tables more broadly.

Most of the bores only need to be drilled to maximum depths of <30m within the alluvium. A network of 15 deeper bores is proposed (Figure 371). A representative number of these would benefit from drilling using the sonic technique to ensure recovery of materials for hydrogeochemical and textural analysis. Hydrogeochemical analysis include age dating should help to assist with understanding groundwater, surface-groundwater and recharge processes Acquisition of pump test data is recommended for the aquifer intervals. The installation of automated loggers is also recommended.

A more localised network of shallow piezometers should be considered in higher risk areas, in the western Weaber Plain where watertables are already reasonably shallow, and in the northern Weaber Plain where run-off from adjacent hills and springs create localised surface inundation and a high salinity hazard (with possible perching of the watertable).

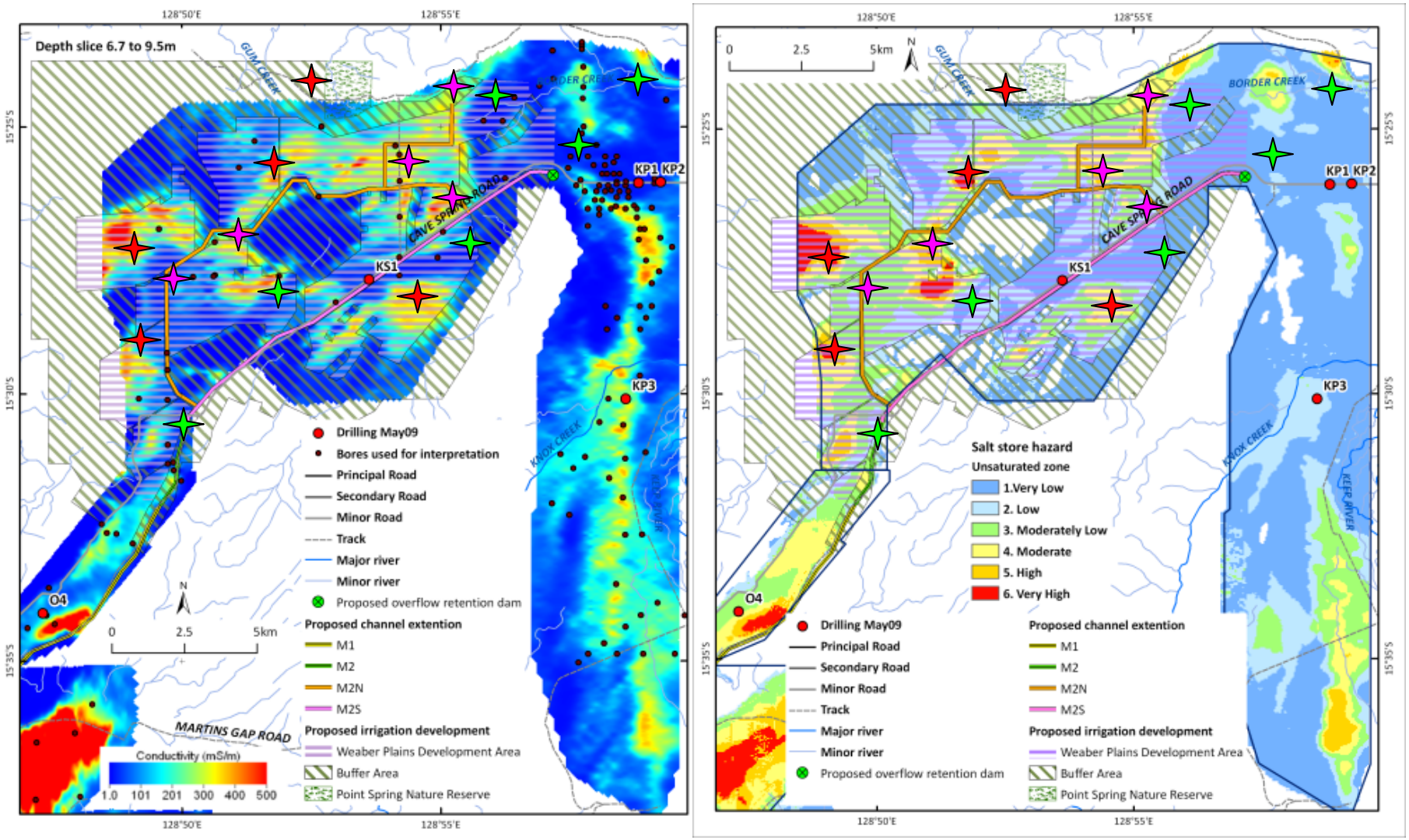

Figure 371: *Proposed piezometer locations. Image on left is AEM conductivity depth slice (6.7-9.5m), image on right is salinity hazard map (unsaturated salt store + depth to water table). The proposed monitoring bores are colour-coded for different purposes: bores located to monitor fluctuations in pressure heads and water levels within the main Ord palaeochannel (and Border Creek) are identified with a green star; bores located to monitor areas of high salinity hazard close to proposed irrigation infrastructure (and possible leakage) are shown with pink stars; bores located to monitor groundwater rise and salinity levels in higher hazard areas within the irrigation area where there is potential for lateral groundwater and/or surface flow from surrounding hills are identified with red stars.*

8.5 MANTINEA PLAIN, CARLTON HILL AND PARRY'S LAGOON

Where is salt stored in the landscape (in the saturated and unsaturated zones)?

There are no prior maps of salt store for either the unsaturated or the saturated zones, or salinity hazard for the Mantinea Plain, Carlton Hill and Parry's Lagoon areas, although prior studies identified highly saline groundwater in the western half of the area (O'Boy *et al.,* 2001). The new AEM-based salt store maps, allied with maps of groundwater quality and lithology, provide an initial assessment of the salinity hazard in these areas, and will be of particular assistance in groundwater model parameterisation. This is required to enable spatial and temporal predictions of the salinity risk to be made.

Figure 372: *Salt scalds at the eastern end of Parry's Lagoon*

Salt scalds are apparent at several locations in the Parry's Lagoon area (Figure 372), with high levels of salt at shallow depths beneath seasonal vegetation including microbial mats (Figure 373). A map of surface salt (Figure 374) shows that there are areas of extremely saline ground in the north-western portion of the area on the Ord floodplain. This is consistent with the proximity to the estuary and tidal influences. Elsewhere in the area, the surface salinity is low to moderate adjacent to the river and near the footslopes of the surrounding hills, and low to moderate in the remainder of the Carlton and Mantinea Plains, as well as in Parry's Lagoon.

The AEM data, calibrated by pore fluid and textural data from drilling and field sampling have enabled the salt stored in the Mantinea Plain, Carlton Hill and Parry's Lagoon area to be mapped and quantified. The salt store in the unsaturated zone across these areas is variable spatially, with a gradient generally to extremely high values in the west. Values for salt stored in the unsaturated zone range from <10t/ha/m near the river in its upper reaches and in the colluvial footslopes, to nearly 500t/ha/m in the Parry's Lagoon area on the lower Ord floodplain in the west (Figure 375). The salt stored in the saturated zone similarly varies from <10t/ha/m along the upper river and footslopes, to 380t/ha/m in the lower Ord Floodplain (Figure 376). These amounts of salt stored are much higher than those encountered anywhere else in the study area, reflecting the general increase in salinity westward.

With regard to the areas earmarked for development, there are significant areas where the amount of salt stored in the unsaturated zone within Carlton Hill, and the western half of the Mantinea development area is >100t/ha/m. Depending on how readily these salt stores are mobilised, the levels will pose a very significant

risk to irrigated agriculture should the water table rise to within 2m of the ground surface (Ali & Salama, 2003). As the water table is already quite shallow (<10m) in these areas, and even shallower in Parry's Lagoon (Figure 389), the risk posed to agriculture by waterlogging of soils and soil salinity is ranked highly in the western half of the proposed Stage 2 development areas. Given the distribution of relatively high salt stores, and shallow water tables, infrastructure planning should utilise the new AEM-based products to minimise the salinity risk to the sustainability of irrigation development in these areas.

Figure 373: *Loose dry microbial mat at Parry's Lagoon near drill pole PL3.*

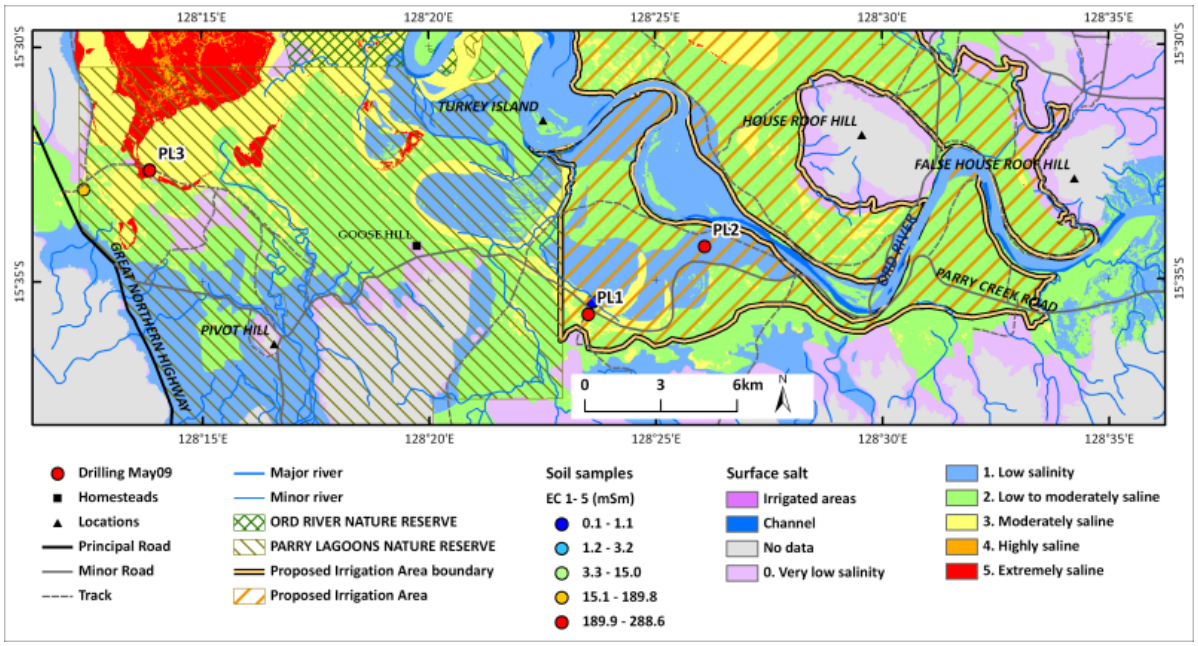

Figure 374: *Parry's Lagoon-Mantinea Plain-Carlton Hill surface salt.*

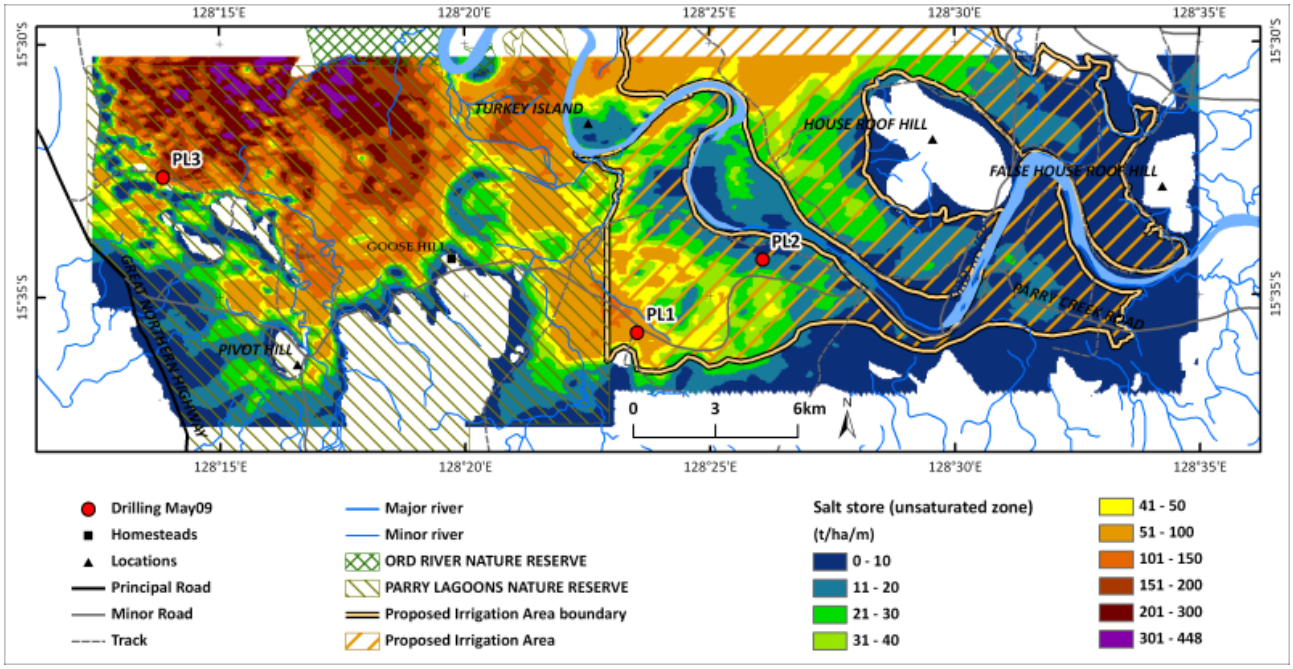

Figure 375: *Parry's Lagoon-Mantinea Plain-Carlton Hill unsaturated salt store.*

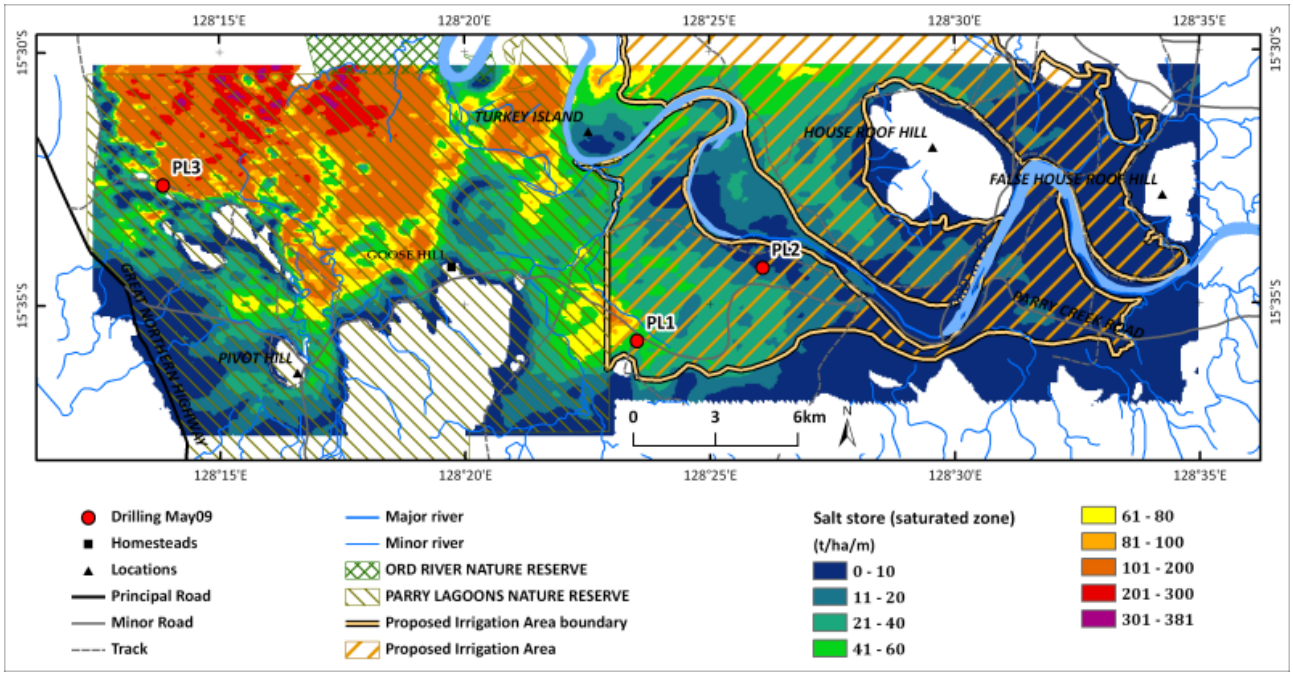

Figure 376: *Parry's Lagoon-Mantinea Plain-Carlton Hill saturated salt store.*

What is the distribution of groundwater quality (salinity)?

Previous sampling of groundwater in the Mantinea Plain, Carlton Hill and Parry's Lagoon area mapped large areas of high groundwater salinity (>14,000TDS (mg/l; Figure 377).The new AEM data, calibrated by pore fluids from drilling and field sampling, are generally consistent with the results from previous groundwater sampling.

The AEM mapping has confirmed that the groundwater quality in the Mantinea Plain, Carlton Hill and Parry's Lagoon increase westwards in a gradient towards the lower Ord Floodplain, with values ranging from <1,000TDS (mg/l) in a 1km zone adjacent to the Ord River, and west of House Roof Hill, as well as in

a narrow zone at the footslopes of the surrounding hills (Figure 377). Groundwater salinities are calculated to increase to over 46,000TDS (mg/l) in the lower Ord Floodplain.

Within the areas earmarked for development in Stage 2, groundwater salinities range from 1,000TDS to over 10,000TDS in the western halves of Mantinea and Carton Hill (Figure 377). The exceptions are the river flush zones (Figure 378 to Figure 380) developed within 1km of the Ord River upstream of Turkey Island. The use of electrical geophysical methods to map gaining and losing sections of rivers relies on their being a significant conductivity contrast between the various components of the hydrogeological system, and presumes that (1) there is a conductivity or resistivity contrast between groundwater leaking from rivers and groundwater stored in the host alluvium, and (2) that the signature of the various groundwater components is not masked by the conductivity of host lithologies. The methodology used to calibrate these flush zones through using porosity-corrected AEM data is outlined in detail in Section 4.9.

River 'flush zones', which are developed where there is loss of river water to the adjacent and/or underlying alluvial sediments, have been mapped elsewhere in Australia (Munday *et al*., 2004). In these examples, it has been possible to map these 'losing' reaches of river system because there is a marked contrast between 'fresh' water leaking from the river system and brackish to saline groundwater stored in adjacent finer grained alluvial sediments (Munday *et al.,* 2004; Lawrie *et al.,* 2009a, b). In this study area, the flush zones around the Ord River are developed asymmetrically, with the broader flush zones occurring on the southern bank. In the 0-5, 5-8 and 8-12m depth slices (Figure 378 - Figure 380), the AEM values are a combination of relatively dry sands in the unsaturated zone and sands saturated with relatively fresh water. The flush zones generally have a central fresher groundwater core, with salinities increasing to the flush zone margins and at depth. The observed gradients are thought to represent mixing zones with more saline groundwater in the alluvial sediments.

In general, groundwater salinities in the flush zones are relatively fresh upstream of House Roof Hill, but brackish to moderately brackish downstream and laterally away from the river. The gradients are thought to be indicative of mixing with more saline groundwater on the margins of the flush zones. The flush zones beneath and immediately adjacent to the river are up to 12m thick (Figure 381). The vegetation vigour map for this area shows that these flush zones are important for maintaining the riparian zones (Figure 83).

Downstream of Turkey Island, 'losing' reaches of the river containing fresh water are very small, and developed to shallower depths, if present at all. Moreover, downstream, it is anticipated that 'losing' reaches of the River will be characterised by more conductive zones where the more brackish to saline conditions of the Estuary are encountered. In the latter scenario, caution has to be exercised to discriminate between saline groundwater in sand aquifers from conductive clays. This commonly requires drilling to validate anomalies (Tan *et al*., 2007). As no drilling data were available downstream of Turkey Island, no attempt was made to distinguish possible saline losing reaches of the River from overbank clays.

With the declines in flooding intensity since river regulation, and an increase in dry season flows, it is likely that the flush zones have changed significantly in the past 40 years, and are unlikely to be recharged as frequently or as extensively as in pre-regulation days. There are insufficient data to ascertain the hydraulic gradients in this area.

In summary, the groundwater salinity values encountered in the western half of the proposed development areas on either bank of the river pose a very significant risk to irrigated agriculture should the water table rise within a couple of metres of the ground surface. The AEM based maps of groundwater quality have a much higher spatial resolution than previous maps. This also enables groundwater quality measurements to be linked more directly to specific elements of the hydrostratigraphy, provides targets for groundwater management, and provides the basis for more spatially explicit predictions of salinity hazard. The relatively high salinities identified in the groundwater quality maps demonstrate the critical importance of groundwater management in this area to minimise the high salinity risk.

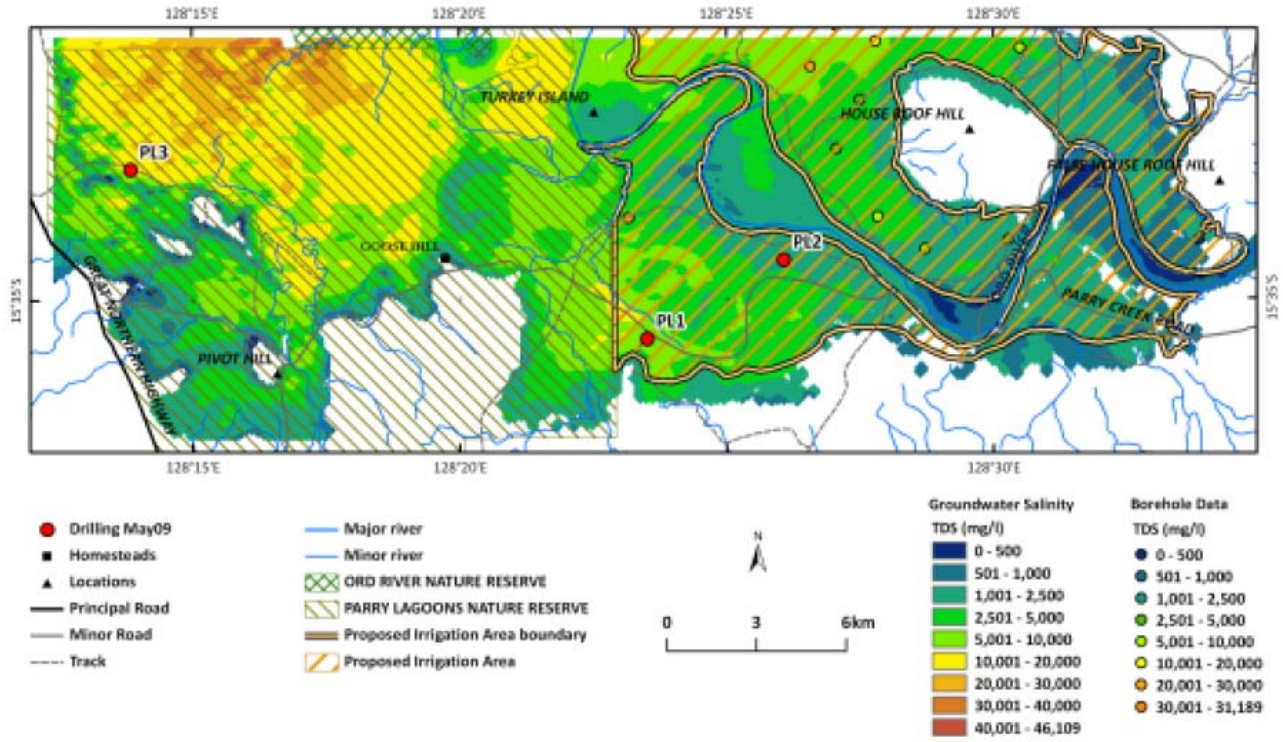

Figure 377: *Parry's Lagoon-Mantinea Plain-Carlton Hill groundwater salinity.*

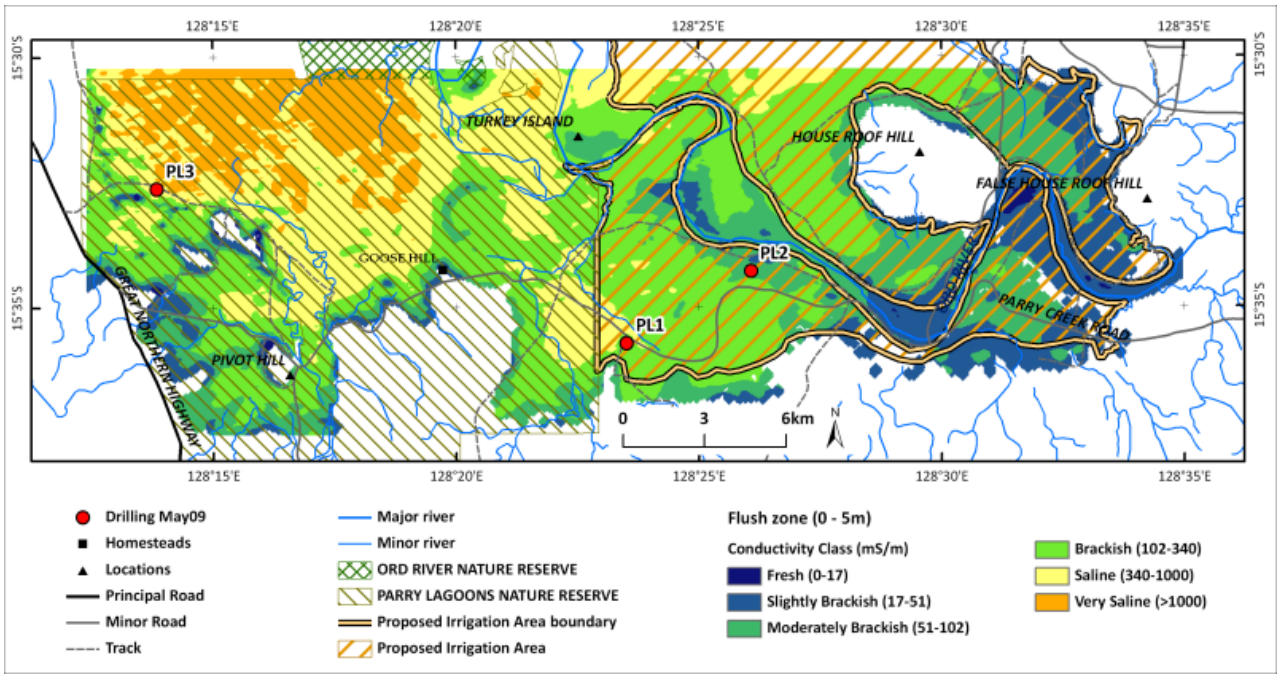

Figure 378: *Parry's Lagoon-Mantinea Plain-Carlton Hill flush zone (0-5m).*

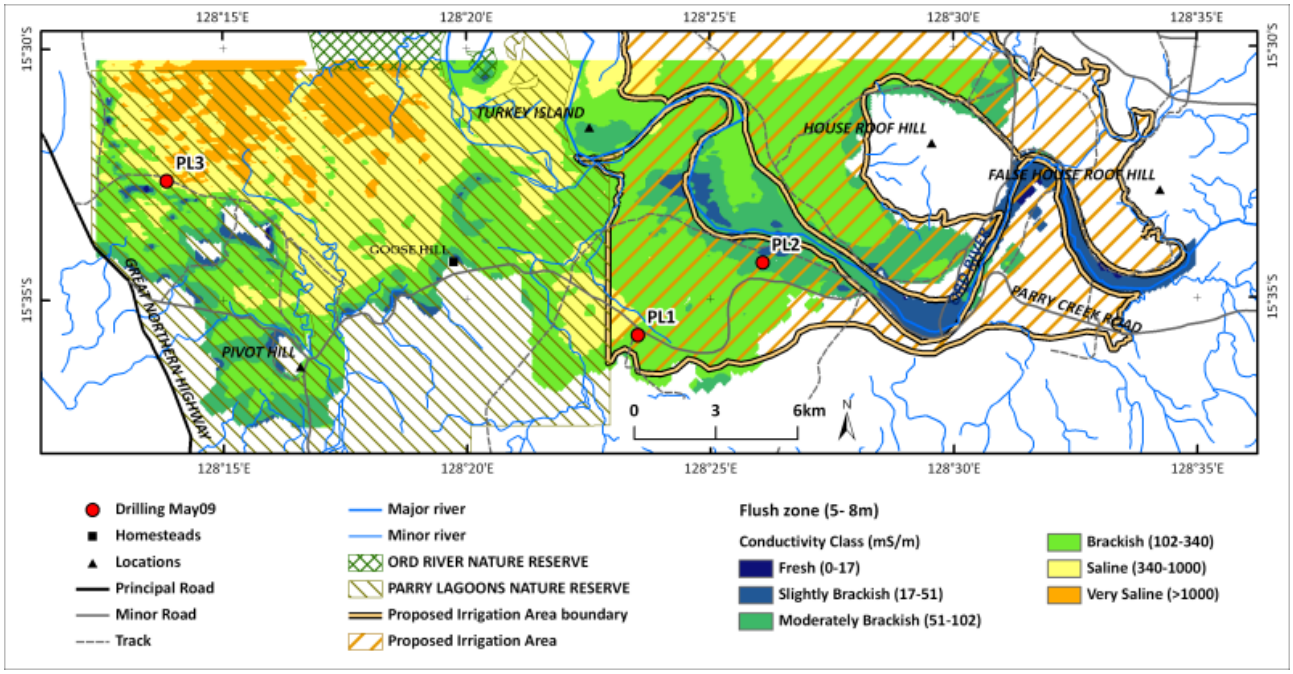

Figure 379: *Parry's Lagoon-Mantinea Plain-Carlton Hill flush zone (5-8 m).*

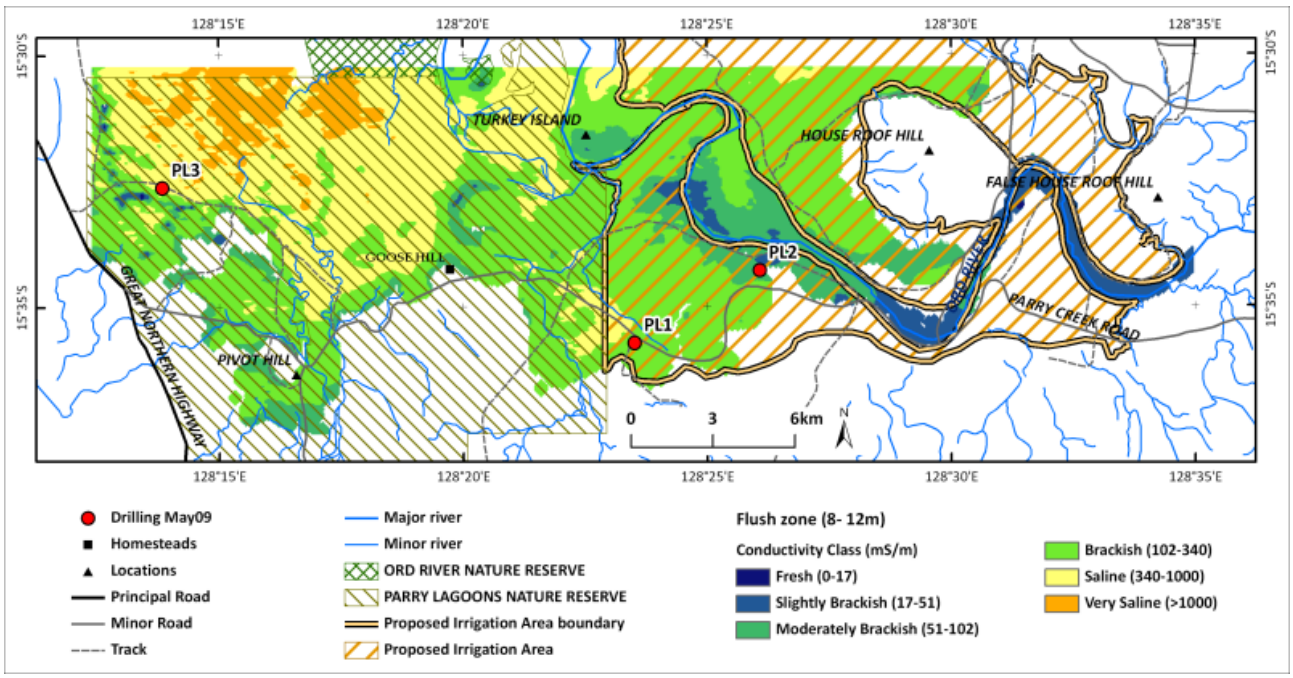

Figure 380: *Parry's Lagoon-Mantinea Plain-Carlton Hill flush zone (8-12m).*

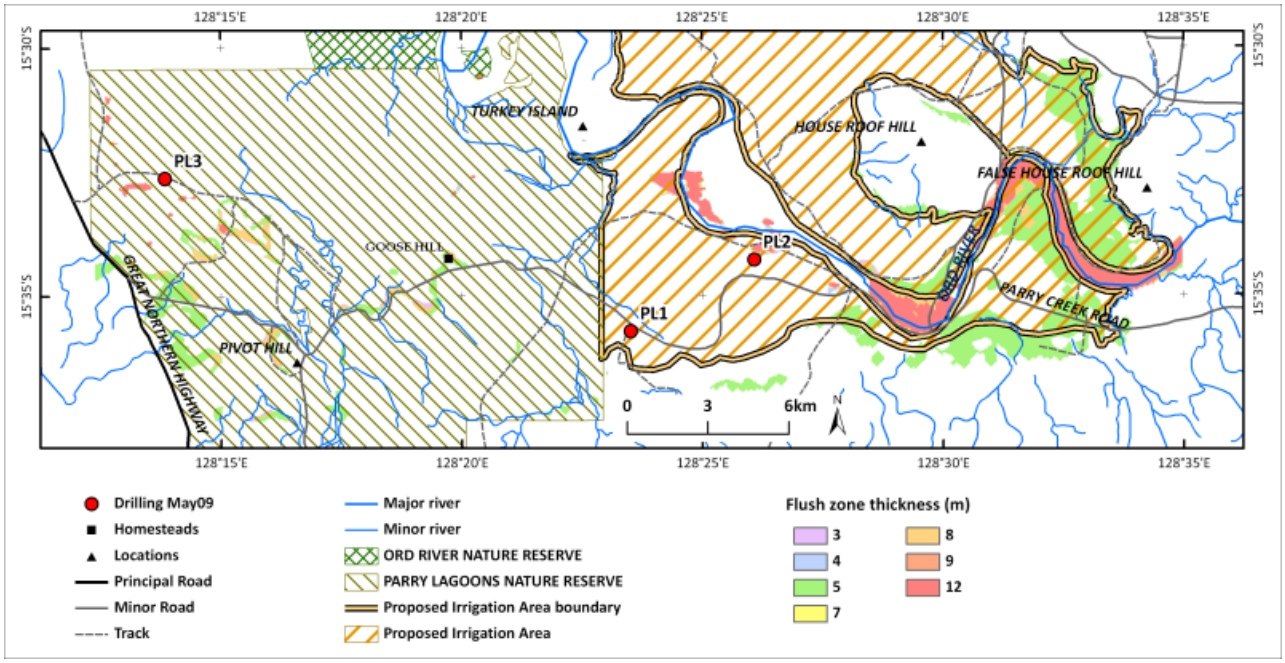

Figure 381: *Parry's Lagoon-Mantinea Plain-Carlton Hill flush zone thickness.*

Where are the areas of highest salinity hazard? Is it possible to identify areas where salt is at higher risk of being mobilised?

New (unsaturated zone) salinity hazard maps for the Mantinea Plain, Carlton Hill and Parry's Lagoon areas have been produced by integrating the AEM salt store data with borehole data, the water table surface and the LiDAR dataset (Section 4.10). Areas of high salt store with shallow water tables (<5m) are deemed to have the highest salinity hazard. In general, these maps show there is an extreme salinity hazard in the western portion of the lower Ord Floodplain at Parry's Lagoon, where the groundwater table is already very shallow (<5m). This area is very close to sea level.

A detailed breakdown of each hazard class is shown in Table 41. The areas that the figures refer to are shown in Figure 383. In general, these maps show that there are areas of extremely high salinity hazard largely within the Parry's Lagoon Ramsar wetland area, encroaching less than 1km into the western portions of areas in Mantinea Plain that are earmarked for irrigation (Figure 382). However, the salinity hazard is ranked as very high from the western boundary of the proposed irrigation areas of both Carlton Hill and Mantinea Plain through to House Roof Hill.

The area to the east of House Roof Hill has a low salt hazard by comparison. In total, over 60% of the Carlton Hill – Mantinea Plain area covered by the AEM survey and earmarked for Stage 2 irrigation development has a salinity hazard ranked as very high or extreme. This map demonstrates that water table management will be of critical importance in this area to minimise the risk of waterlogging and soil salinisation.

Salinity is part of the natural landscape of the lower Ord floodplain, and it is not entirely clear whether the threat of salinity and/or desiccation of the freshwater wetlands have increased since river regulation. The lack of freshwater lenses of any note beneath the billabongs and floodplain show how delicately balanced these wetlands are, and how dependent they are upon surface water inundation in the wet season (Figure 384). The salinity hazard in the Parry's Lagoon area lies in the potential threat to the RAMSAR wetland, and the tourism this supports, rather than irrigation.

Further refinements of these maps, including identification of the areas where salt is at higher risk of being mobilised, will be possible when individual data layers are incorporated within appropriate groundwater models.

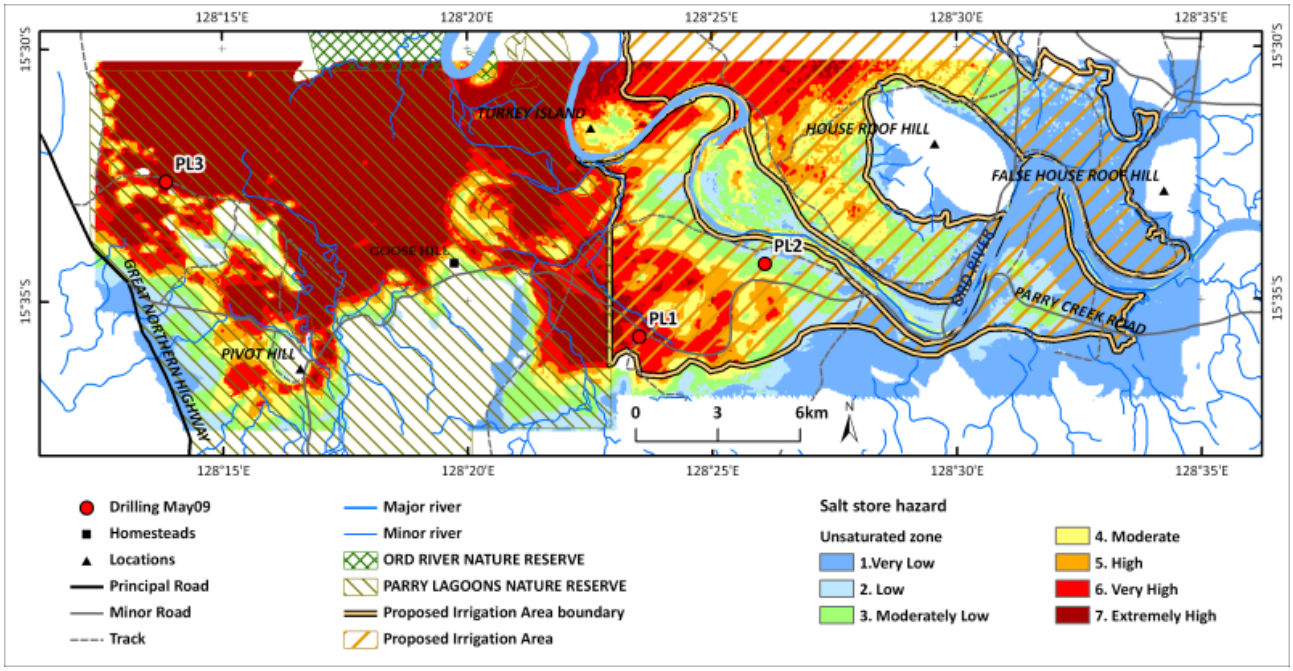

Figure 382: *Parry's Lagoon-Mantinea Plain-Carlton Hill salinity hazard.*

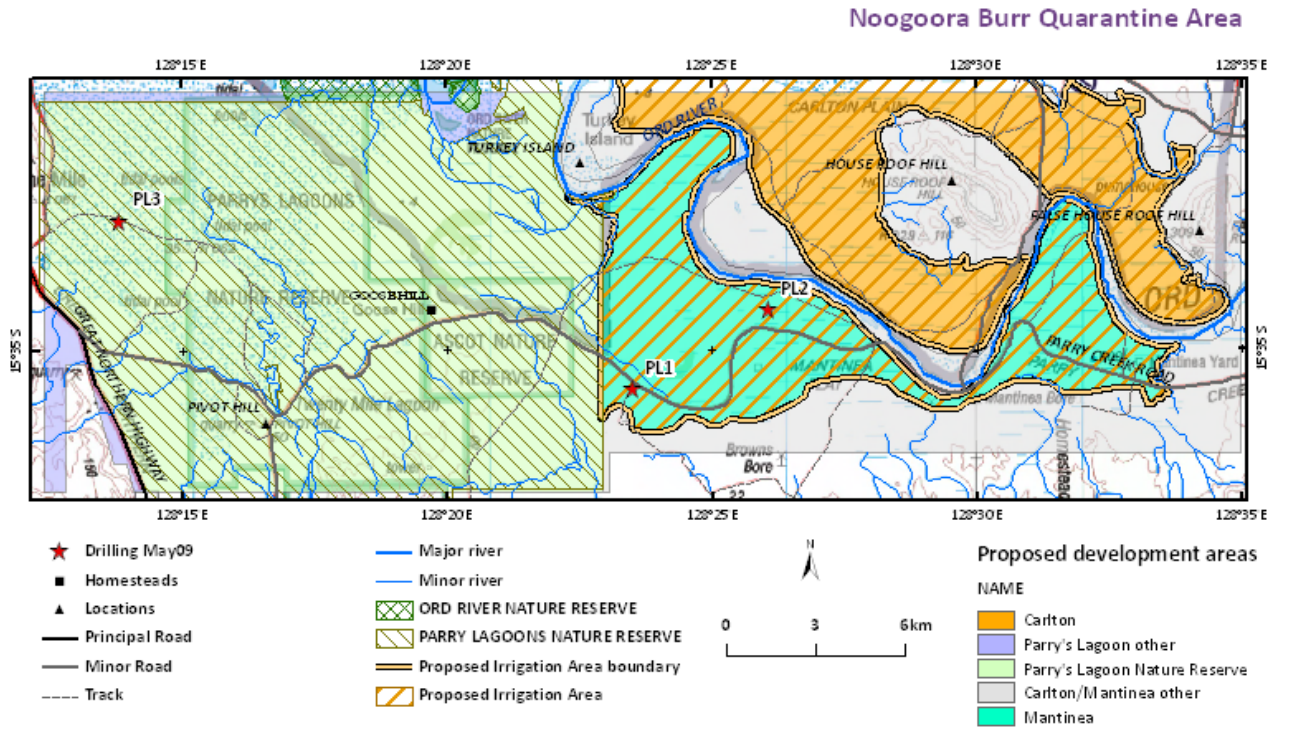

Figure 383: *Parry's Lagoon-Mantinea Plain-Carlton Hill showing proposed development areas and the Parry's Lagoon Nature Reserve.*

Table 41: *Areas used in calculations for Parry's Lagoon, Carlton, and Mantinea. Note: these figures have been rounded to the nearest whole number.*

Area Name	Hazard Class	Hectares	Percent
Carlton Hill Development Area	1-3.Very Low to Moderately Low	412	8
	4. Moderate	119	2
	5. High	67	1
	6. Very High	114	2
	7. Extremely High	13	0
Carlton Development Total		726	14
Mantinea - Carlton other (river riparian zone, hills and southern area)	1-3.Very Low to Moderately Low	1035	20
	4. Moderate	66	1
	5. High	43	1
	6. Very High	35	1
	7. Extremely High	30	1
Mantinea - Carlton other Total		1210	24
Mantinea Development Area	1-3.Very Low to Moderately Low	401	8
	4. Moderate	100	2
	5. High	99	2
	6. Very High	120	2
	7. Extremely High	24	0
Mantinea Development Total		744	15
Parry's Lagoon and Ascot Nature Reserve	1-3.Very Low to Moderately Low	656	13
	4. Moderate	147	3
	5. High	159	3
	6. Very High	282	6
	7. Extremely High	1058	21
Parry's Lagoon Nature Reserve Total		2301.95	2302
Parry's Lagoon and Ascot Nature Reserve - other (mostly SW of main area)	1-3.Very Low to Moderately Low	70	1
	4. Moderate	1	0
	5. High	4	0
	6. Very High	9	0
	7. Extremely High	45	1
Parry's Lagoon other Total		128	3
Grand Total		**5110**	**100**

Figure 384: *View looking NW across Parry's Lagoon showing area of freshwater inundation (May, 2009).*

What is the extent and thickness (in 3D) of the sand and gravel aquifers, and how are they connected?
New maps of the depth to bedrock (Figure 385), and the extent and thickness of gravel and sand aquifers (Figure 386) have been produced for the Mantinea Plain, Carlton Hill and Parry's Lagoon areas. Maps of the extent and thickness of the sand aquifers have also been produced (Figure 387). These maps have been compiled by interpreting individual AEM conductivity depth slices and representative conductivity cross-sections using pre-existing drillhole records and data from new drillcore obtained during the project (Section 4.2).

There is very little gravel deposited in this area, reflecting the relatively recent change in course of the Ord River, and the largely marine /estuarine depositional environment that preceded avulsion of the river to this point. However, the marine sand aquifer is a key element of the hydrostratigraphy in this area, and mapping its extent and thickness will facilitate the construction of improved distributed groundwater models, and enable surface-groundwater interactions and groundwater flow paths to be mapped and understood.

The maps of depth to bedrock confirm the thickening of the depositional succession to the northwest (Figure 385). Depths to bedrock vary from <20m at House Roof Hill to >24m over much of the lower Ord Floodplain west of Turkey Island. More detailed descriptions of the lithologies and their extent are provided earlier (Section 6.6). The new maps of sand extent and thickness in these areas will assist greatly with groundwater model parameterisation and enable more reliable quantitative assessments to be made of groundwater and salinity model predictions. They will also contribute to more robust modelling of land use and groundwater management scenarios.

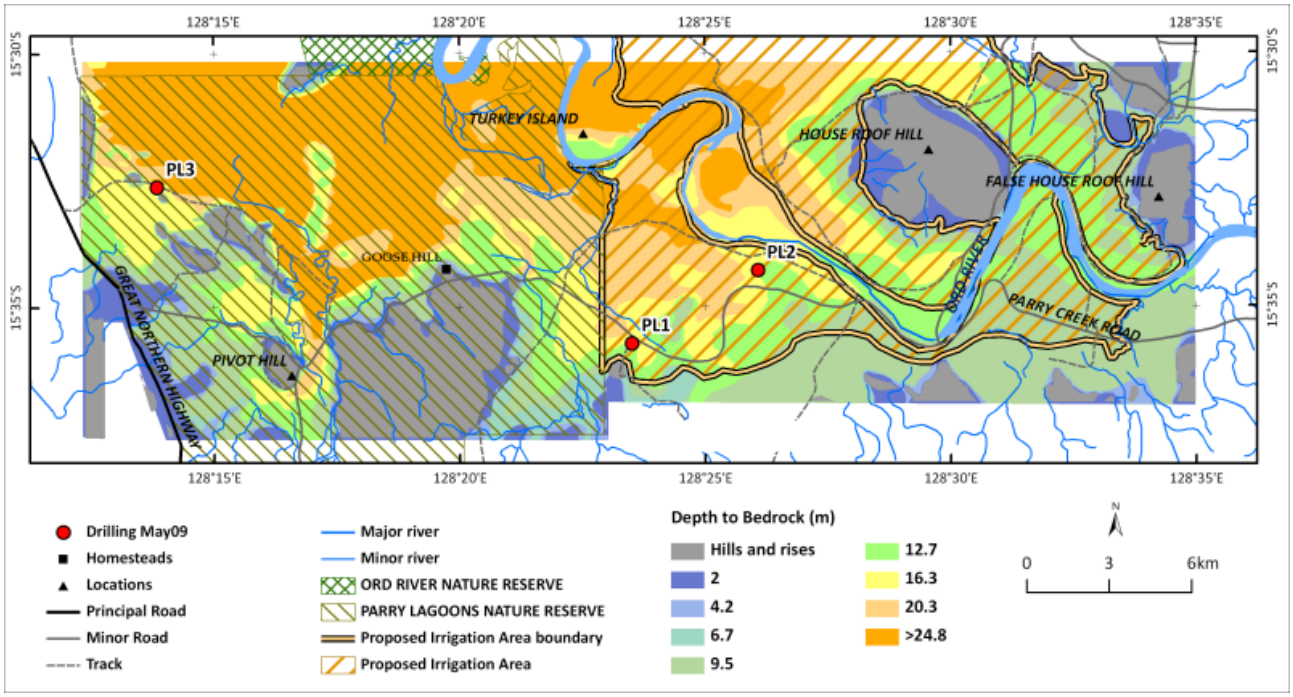

Figure 385: *Parry's Lagoon-Mantinea Plain-Carlton Hill depth to bedrock.*

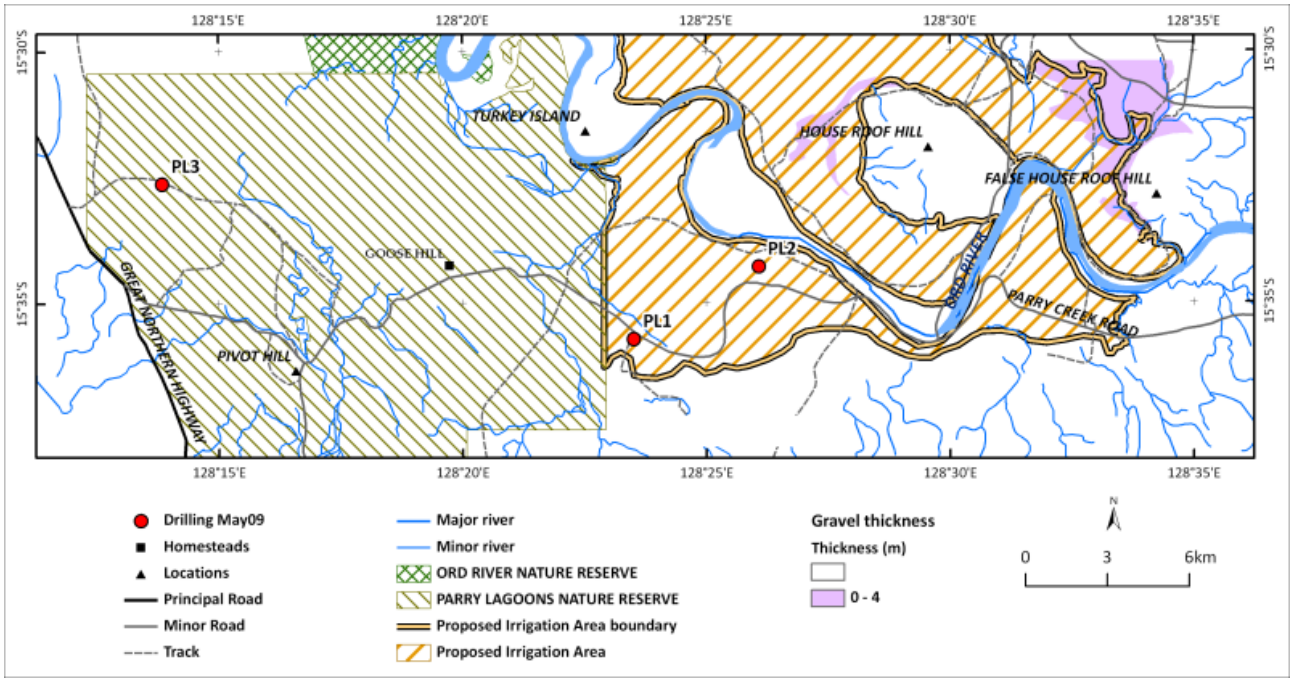

Figure 386: *Parry's Lagoon-Mantinea Plain-Carlton Hill gravel thickness.*

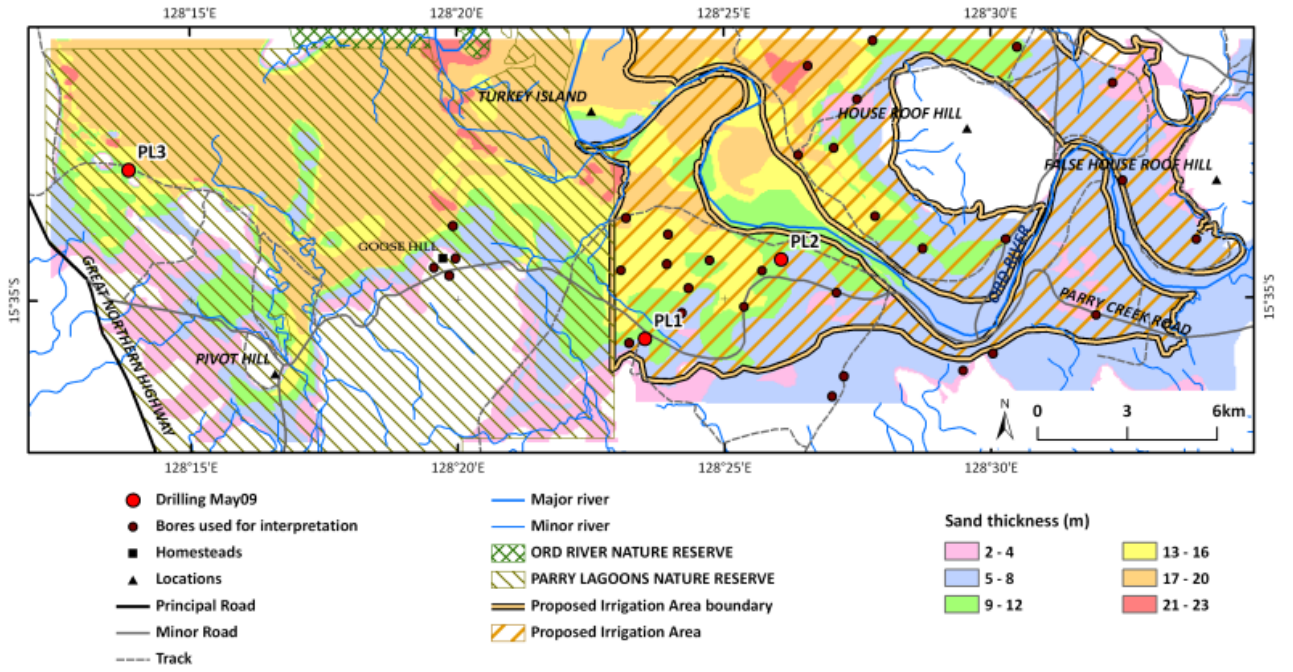

Figure 387: *Parry's Lagoon-Mantinea Plain-Carlton Hill sand thickness.*

What is the extent and thickness of clays in the sub-surface?

New maps of clay extent and thickness (Figure 388) have been produced for the Mantinea Plain, Carlton Hill and Parry's Lagoon areas. These maps have been compiled by interpreting individual AEM conductivity depth slices using pre-existing drillhole records and data from new drillcore obtained during the project (Section 4.2). These maps do not incorporate the 0-2m depth slice, as the conductivity measurements reflect soil profiles that were mostly dry, and contained little contrast between sand and clay units. Mapping the extent and thickness of clays assists with understanding groundwater flow paths, surface-groundwater connectivity including recharge potential, and salinity mobilisation potential. Overall, these maps should also contribute to the development of appropriate salinity mitigation strategies, and assist with refining cropping and drainage strategies.

In the Carlton Hill area, clays are either absent or less than 4m thick. In the Mantinea Plain and Parry's Lagoon areas, there is a greater range, with the thickness of clay generally greater, varying from 4m to >4m (Figure 388). These clays also have a relatively high salt store. However the relatively thin nature of the clays suggests that, once cleared, the potential for accession of excess water from rainfall and/or future irrigation water to the water table is high. When combined with the high salt store and highly saline groundwater, and shallow watertables (Figure 389) managing the salt and water balance in this area will be a particular challenge to the sustainability of irrigation, particularly if reliant upon on-farm management of water. Unlike some of the other Stage 2 areas, the presence of an extensive marine /estuarine sand aquifer may lend itself to groundwater pumping (although the water will be saline).

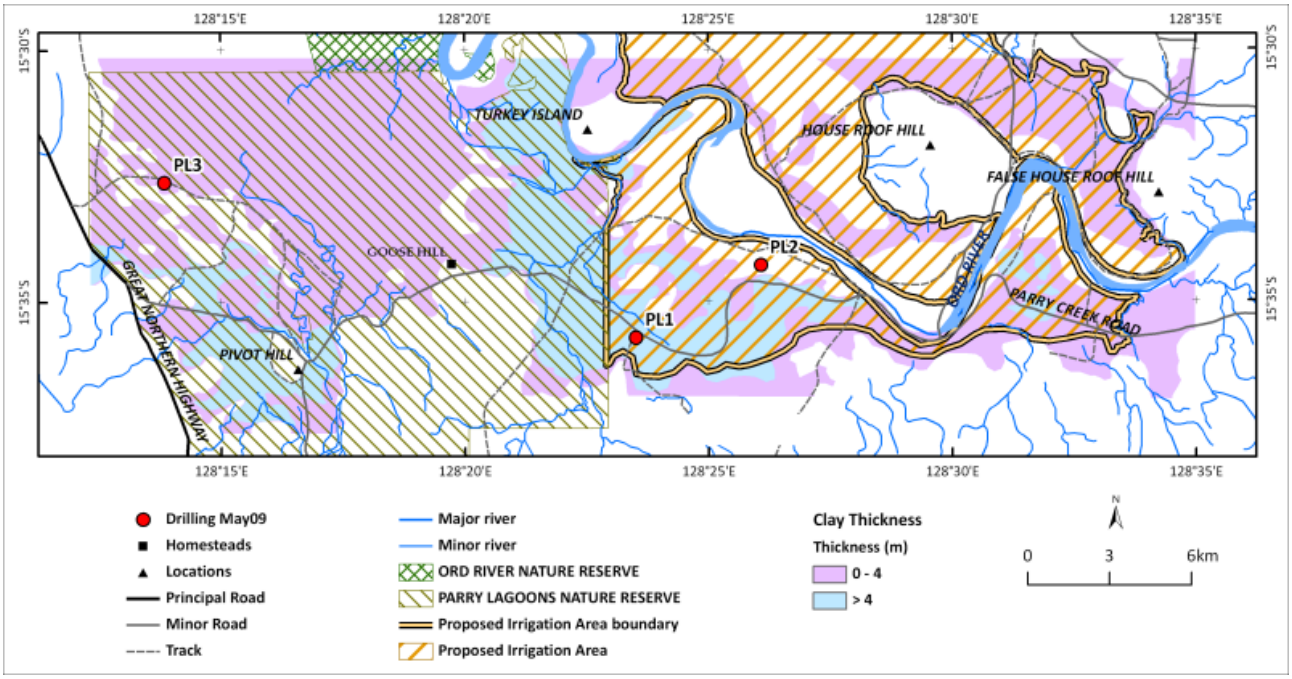

Figure 388: *Parry's Lagoon-Mantinea Plain-Carlton Hill clay thickness.*

What are the spatial and temporal trends in groundwater level and salinity?

There is a paucity of borehole monitoring of water levels and water quality in this area (Figure 389), and no hydrograph analysis was possible. However, a n umber of studies have been carried out to show suggest that there are likely to have been changes in groundwater and groundwater-surface water over time since completion of the Diversion Dam. In particular, it is recorded that the lower Ord Floodplain, including the Parry's Lagoon area, used to flood seasonally. The recharge that is likely to have happened (through thin clays and the sands of the meander belt) with these events no longer occurs, with Parry's Lagoon maintained mainly by seasonal run off from adjacent hills. Whether there were any significant fresh groundwater lenses beneath Parry's Lagoon remains debatable, however it is clear that there is currently no fresh water perching in this area presently.

There has also been a not insignificant shift in the location of the Ord River main channel itself since the Diversion Dam was constructed. The changes were mapped by comparing aerial photographs from the 1948, 1967 with present day imagery. The comparison shows that the main channel in the active meander belt has moved its course by over 2km in places since 1948 (Figure 390 cf Figure 391). Although there is only a small area within the AEM survey area, there is a strong coincidence of the present river flush zones with the older river course, particularly on its north bank (e.g. comparing Figure 390, Figure 391 with Figure 378 - Figure 380).

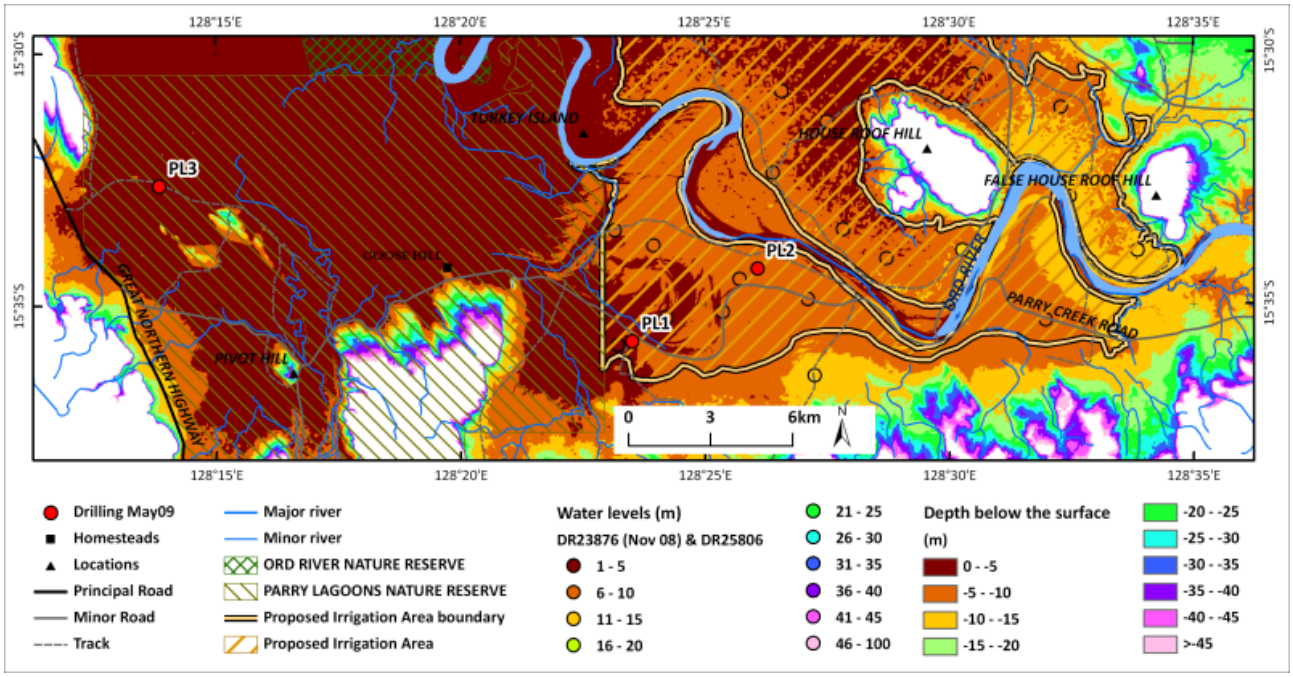

Figure 389: *Parry's Lagoon-Mantinea Plain-Carlton Hill water table depth.*

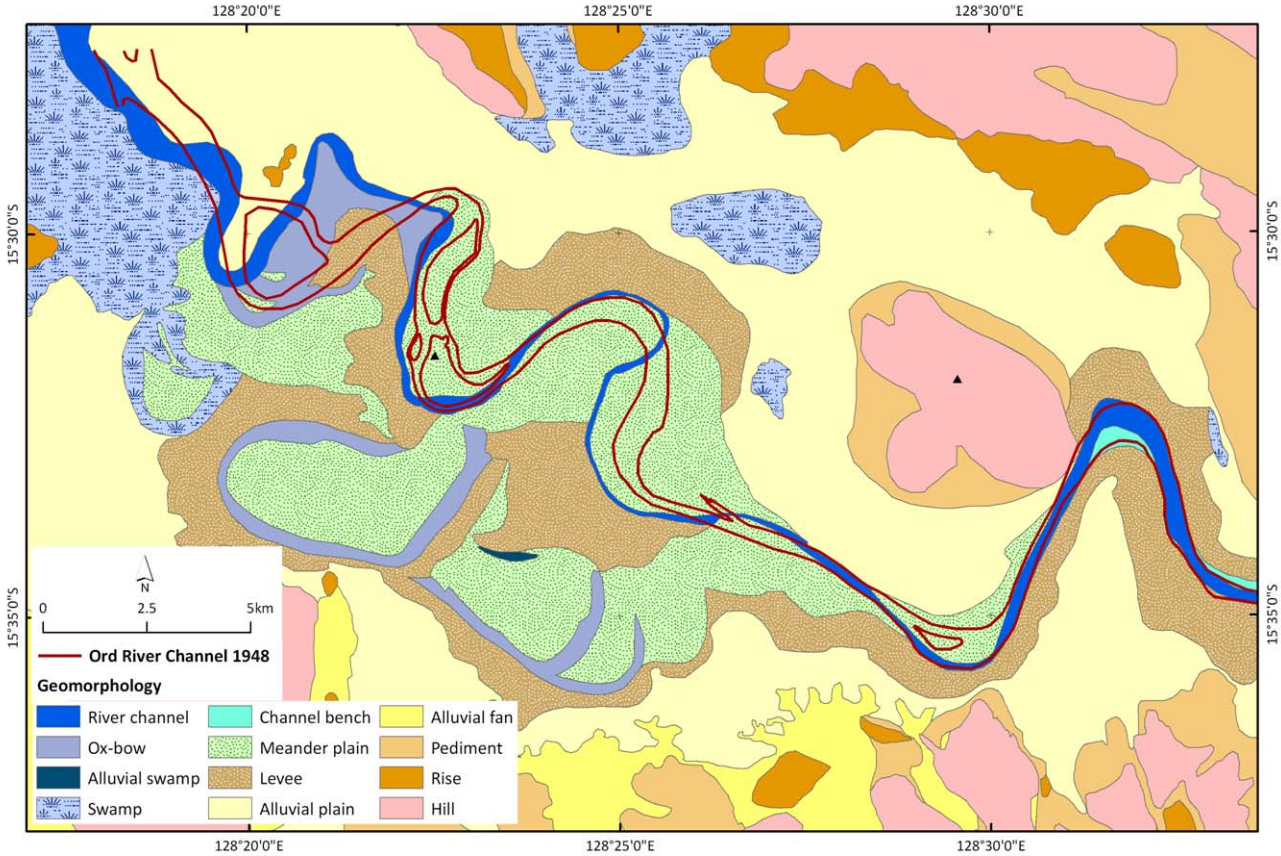

Figure 390: *Parry's Lagoon-Mantinea Plain-Carlton Hill geomorphology and Ord River location 1948.*

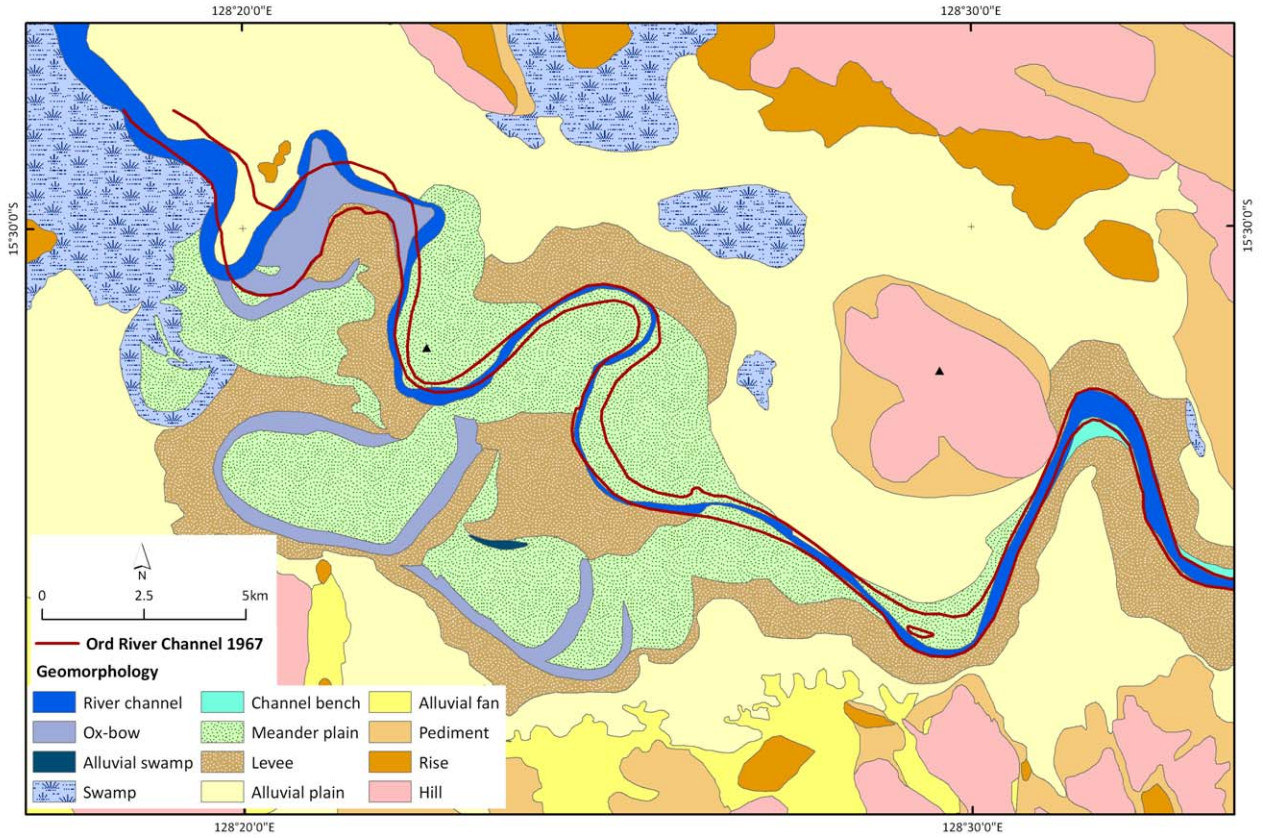

Figure 391: *Parry's Lagoon-Mantinea Plain-Carlton Hill geomorphology and Ord River location 1967.*

Where are the high recharge zones?

In the absence of field data measuring recharge rates directly, 4 products have been produced as data layers to provide information relevant to the estimation of recharge rates in the Stage 2 areas. These 4 map products are:

- surface permeability, based on measurements of soil permeability in the top 20cm (Figure 392);
- soil recharge properties for the 0-2m soil layer, using data from soils mapping and field permeability tests (Figure 393);
- total clay thickness, incorporating soil mapping data for the 0-2m depth slice as well as AEM data beneath this (Figure 394);
- clay thickness above the water table (Figure 395). This integrates the previous maps with the water table map, and approximates a map of deep drainage.

These map products are designed primarily as data layers for input into a groundwater model. However, they also enable a qualitative assessment of recharge to the groundwater table to be made. Figure 395 is perhaps the most useful of these maps as it shows the thickness of clay between the ground and water tables. From this it is evident that there are essentially no clays along the meander belt adjacent to the river, enabling rapid recharge through sands should overbank flooding occur, while in the lower Ord Floodplain, there are only very thin cracking clays overlying the present water table surface, enabling rapid accession to the groundwater table during inundation in the wet season (Figure 384 and Figure 399).

In the proposed irrigation areas, there are very thin (cracking) clays over the water table in Carlton Hill, but much thicker clays (up to 6m) over the water table in the southern half of the Mantinea Plain (Figure 395). These data suggest that it is more likely that recharge to the water table will occur more rapidly in the Carlton Hill area than in the southern half of Mantinea. These products could be used to refine the salt hazard maps in a groundwater model.

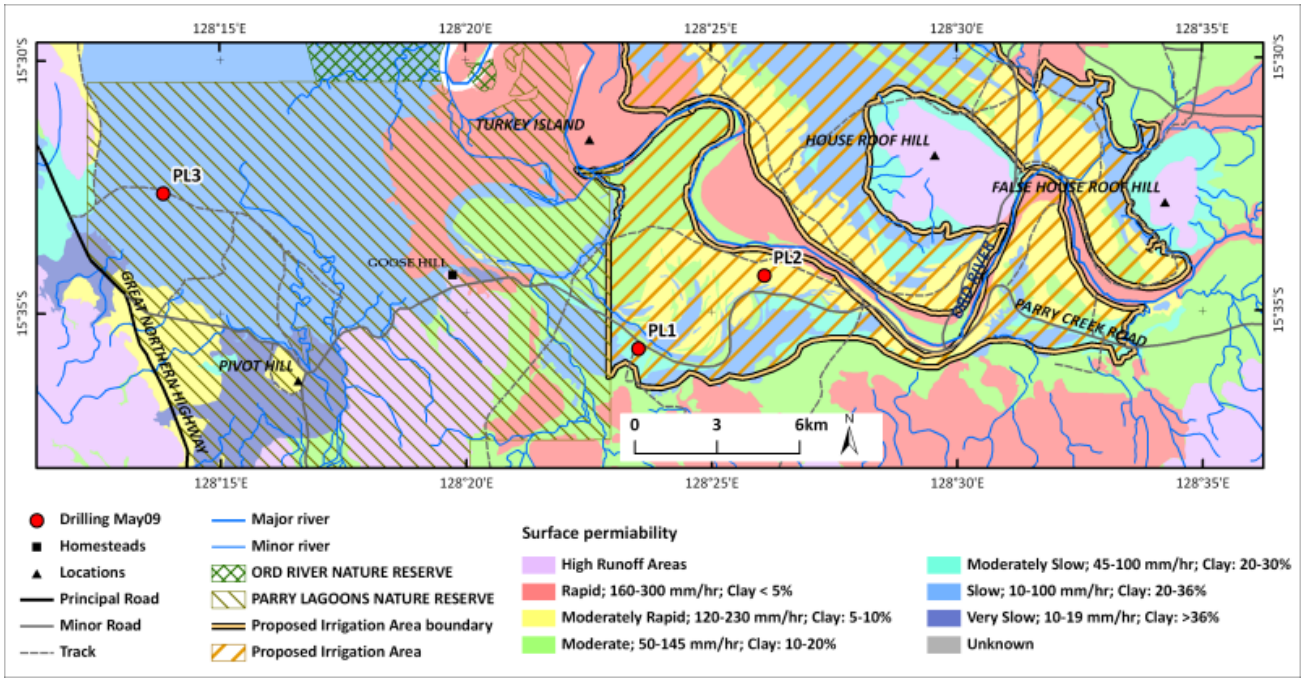

Figure 392: *Parry's Lagoon-Mantinea Plain-Carlton Hill surface permeability.*

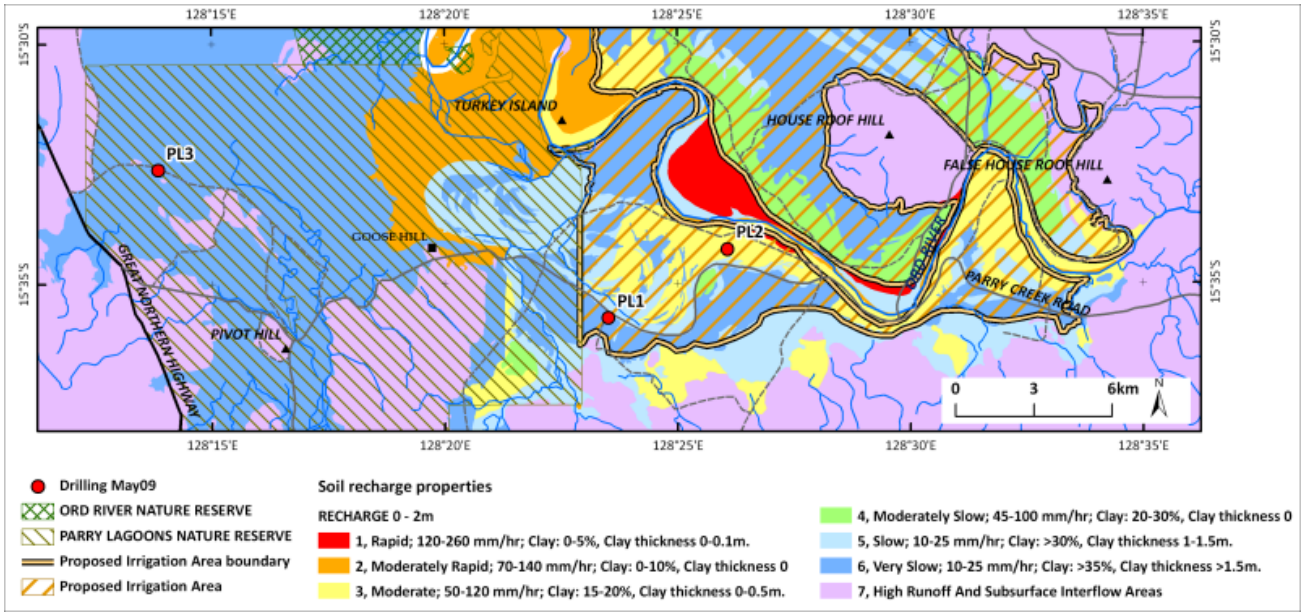

Figure 393: *Parry's Lagoon-Mantinea Plain-Carlton Hill soil recharge properties.*

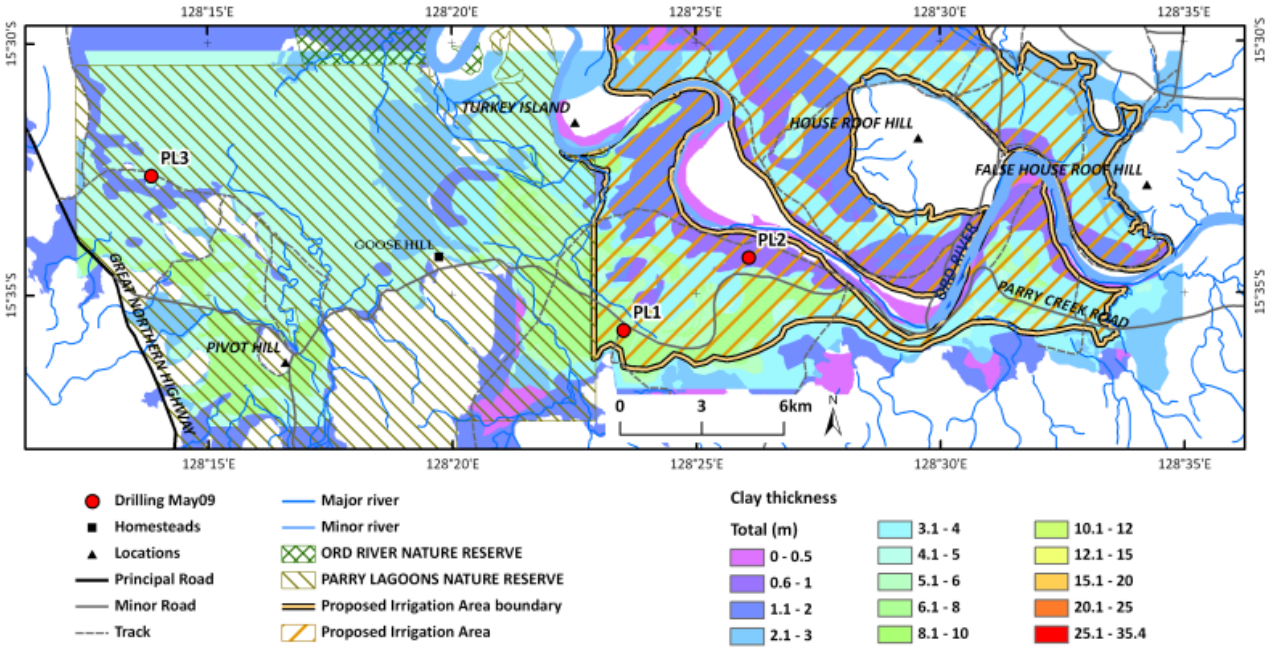

Figure 394: *Parry's Lagoon-Mantinea Plain-Carlton Hill clay thickness.*

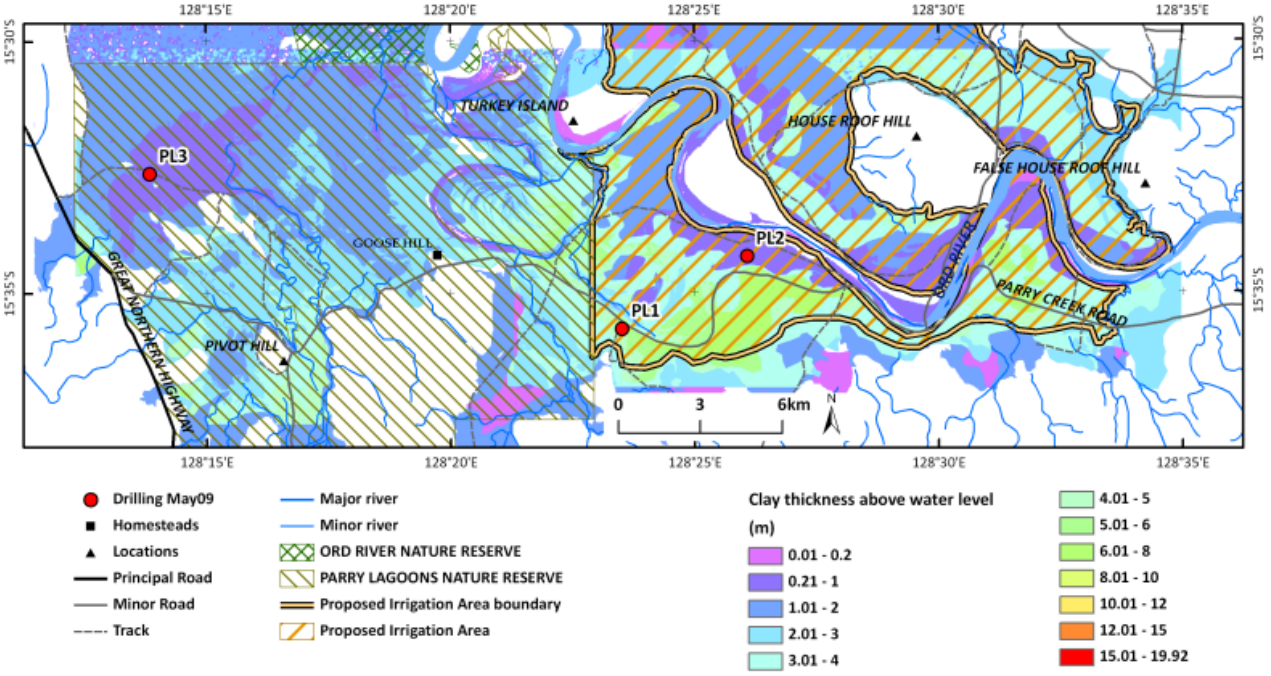

Figure 395: *Parry's Lagoon-Mantinea Plain-Carlton Hill clay thickness above water table.*

What is the nature of surface-groundwater interaction within the Lower Ord Floodplain (Parry's Lagoon)? What is the salinity and waterlogging risk to native vegetation and wetlands in the areas adjacent to the proposed Stage 2 development areas?

Specific questions identified by the Project Steering Committee include:

- What is the extent of flush zones associated with the Ord River?
- Is there evidence of significant fresh groundwater beneath Parry's Lagoon?
- What is the nature of the freshwater-saltwater interface in the Lower Ord Floodplain?

It was shown above that the flush zones associated with the Ord River are quite narrow, and confined to within a 1km discontinuous ribbon near the river. In part, the location of flush zones is related to recent palaeochannel courses. The AEM-based products also show that there is no significant fresh groundwater lense beneath Parry's Lagoon. However, pore fluid data (Figure 116) suggest there is a mixing zone in the

top 6m below the ground surface, although further hydrogeochemical analysis is required to confirm this. In terms of the freshwater-saltwater interface in the lower Ord Floodplain, the AEM data map a gradational zone, with moderately saline groundwater underlying much of the area mapped by the AEM, with a gradient towards more saline groundwater towards the northwest

At the lower Ord River adjacent to the Parry floodplain, under the future climate with future development, climate and hydrological modelling results show moderate changes relative to the future climate with current development, indicating significant additional impact on the hydrological regime as a result of proposed development (CSIRO, 2009). Proposed development appears to have the greatest effect on the low flow regime (CSIRO, 2009). The CSIRO (2009) study also noted that the high flow environmental requirements for regular inundation of riparian zones and deep backwater pools as well as fish passage for the Lower Ord River were met for all the climate and development scenarios.

Flood inundation areas estimated for the March 2000 event (Rogers & Ruprecht, 2000) are shown in Figure 396 to Figure 398. In order to assess what flood heights would be required to reach some of the fresh water lagoons including Marlgu Billabong (Figure 399), the new LiDAR dataset (Figure 400) was used in GIS modelling of a number of inundation scenarios. Scenarios modelled included river flooding and storm surge modelling using an expert GIS approach.

Storm surge modelling has been carried out to a maximum height of 7m (Figure 401). Flood increments of 50cm are displayed by depth slice classification of the DEM (Figure 401). As can be seen from Figure 401, most billabongs, swamps and tidal pools areas in the study area are inundated with a water level rise of approximately 3m. A total of 7m rise would reach the meander loop situated lower of the Mantinea Flats.

River flood modelling, showing extent and corresponding depth were also modelled up to 7m flow heights (Figure 402 and Figure 403). In order to model a river flooding, an input surface has to be levelled along main channel and mender loops. A trend surface of the main channel and low-lying areas was interpolated using elevation points shown in Figure 404. De-trended DEM derived by subtracting a trend surface from original DEM and adjusting elevation at indicated reference point (Figure 405 to Figure 408). Analogously to storm surge model, river flood depth and extents were classified by depth slice ranges of the de-trended DEM with 50cm increment. Flood depth dataset is an ‘inverted’ version of the extent grid.

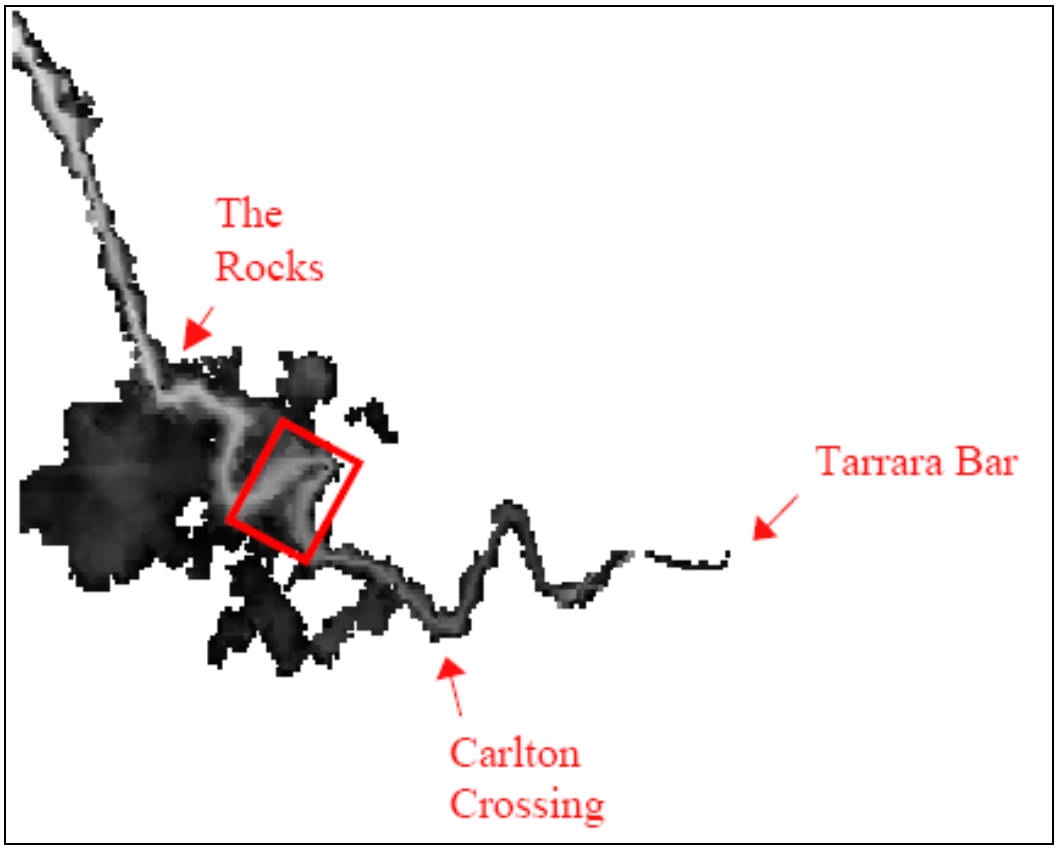

Figure 396: *Map showing location of flood inundation areas (Rogers & Ruprecht, 2000).*

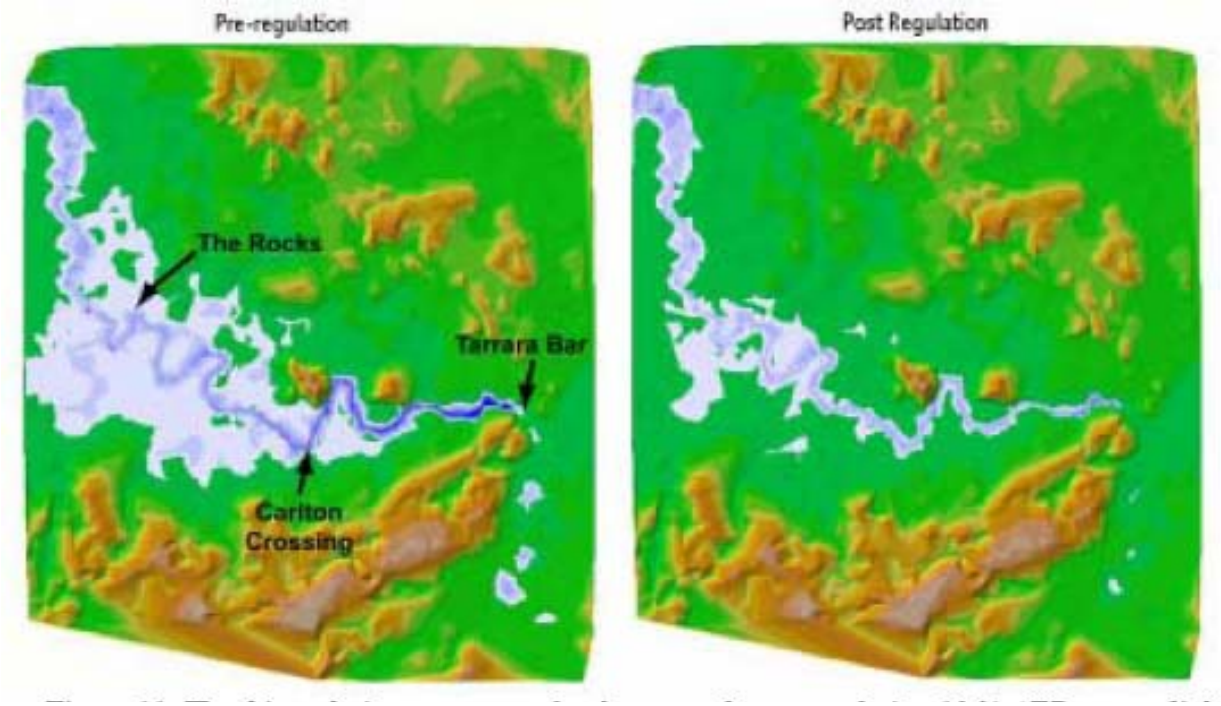

Figure 397: *Flood inundation area maps for the pre- and post-regulation 10%AEP events (grey areas indicate area of inundation).*

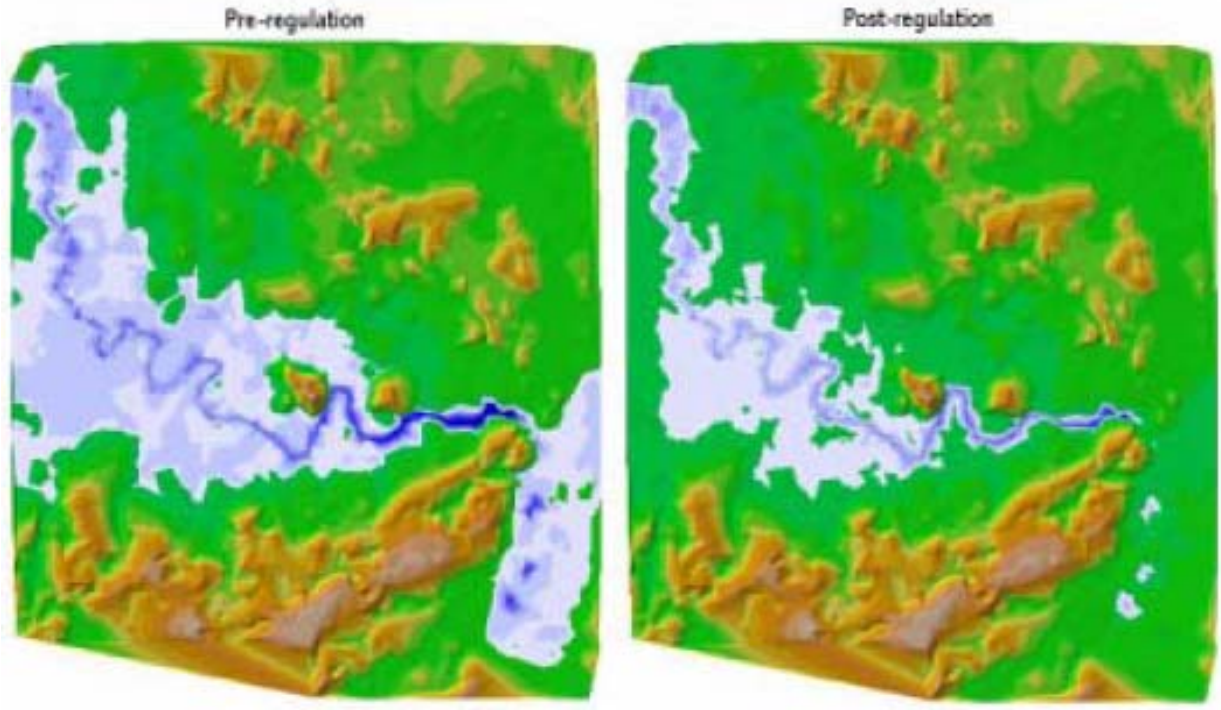

Figure 398: *Flood inundation area maps for the pre- and post-regulation 1%AEP events (grey areas indicate area of inundation).*

In summary, the AEM survey has enabled key elements of the hydrogeological system to be mapped and the map products produced should provide a useful baseline dataset for further studies of surface-groundwater interactions. New LiDAR data also allow for more accurate modelling of potential inundation events.

Figure 399: *View of Marlgu Billabong from the top of Telegraph Hill, near Parry's Lagoon. Semi-permanent fresh water occupies distributary channels from alluvial fans from hills to south, but does not extend vertically for any distance and is invisible in AEM.*

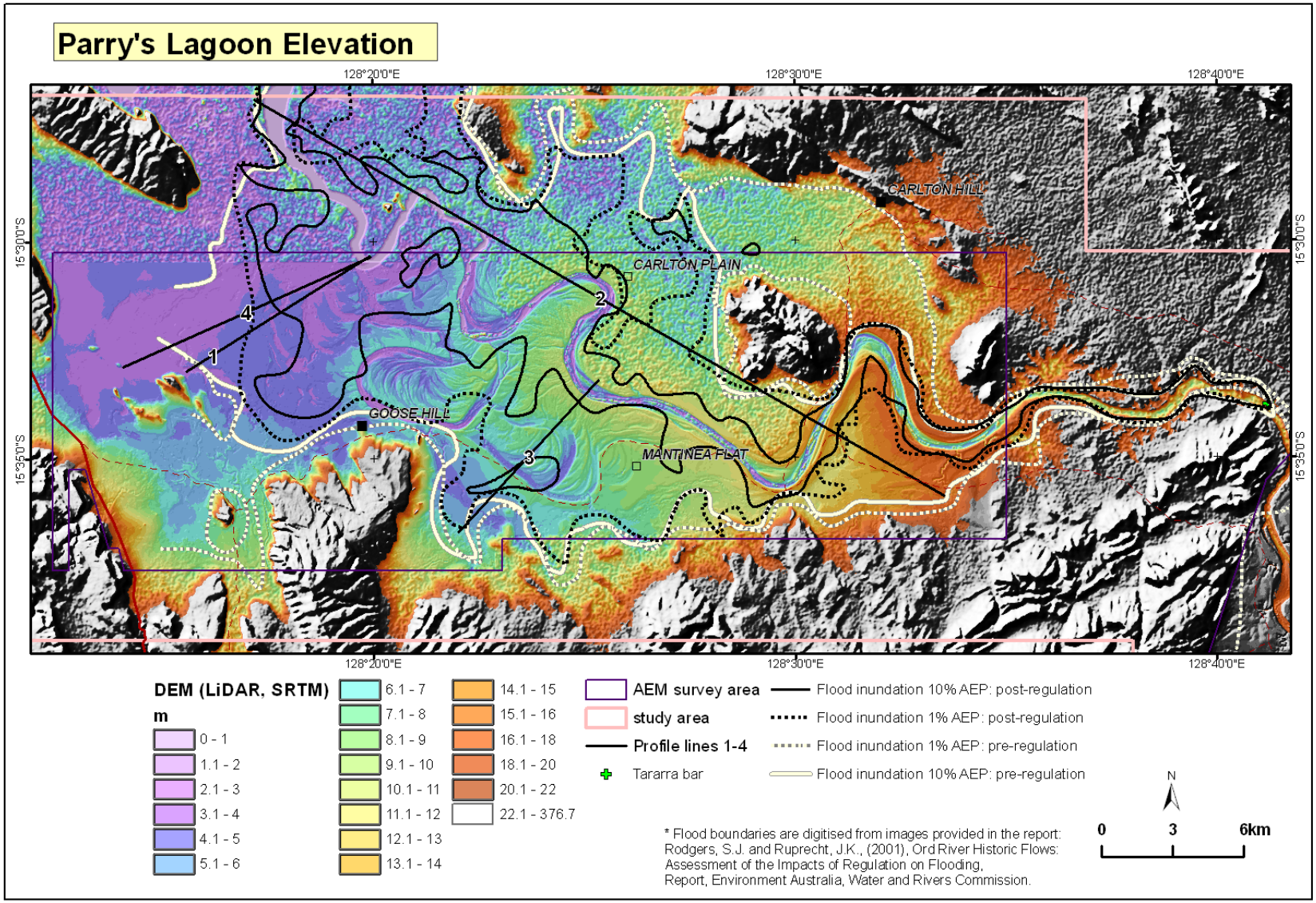

Figure 400: *Digital Elevation Model (DEM) of Parry's Lagoon-Mantinea Plain-Carlton Hill study area showing floodplain elevation ranges respective to Australian Height Datum (AHD).*

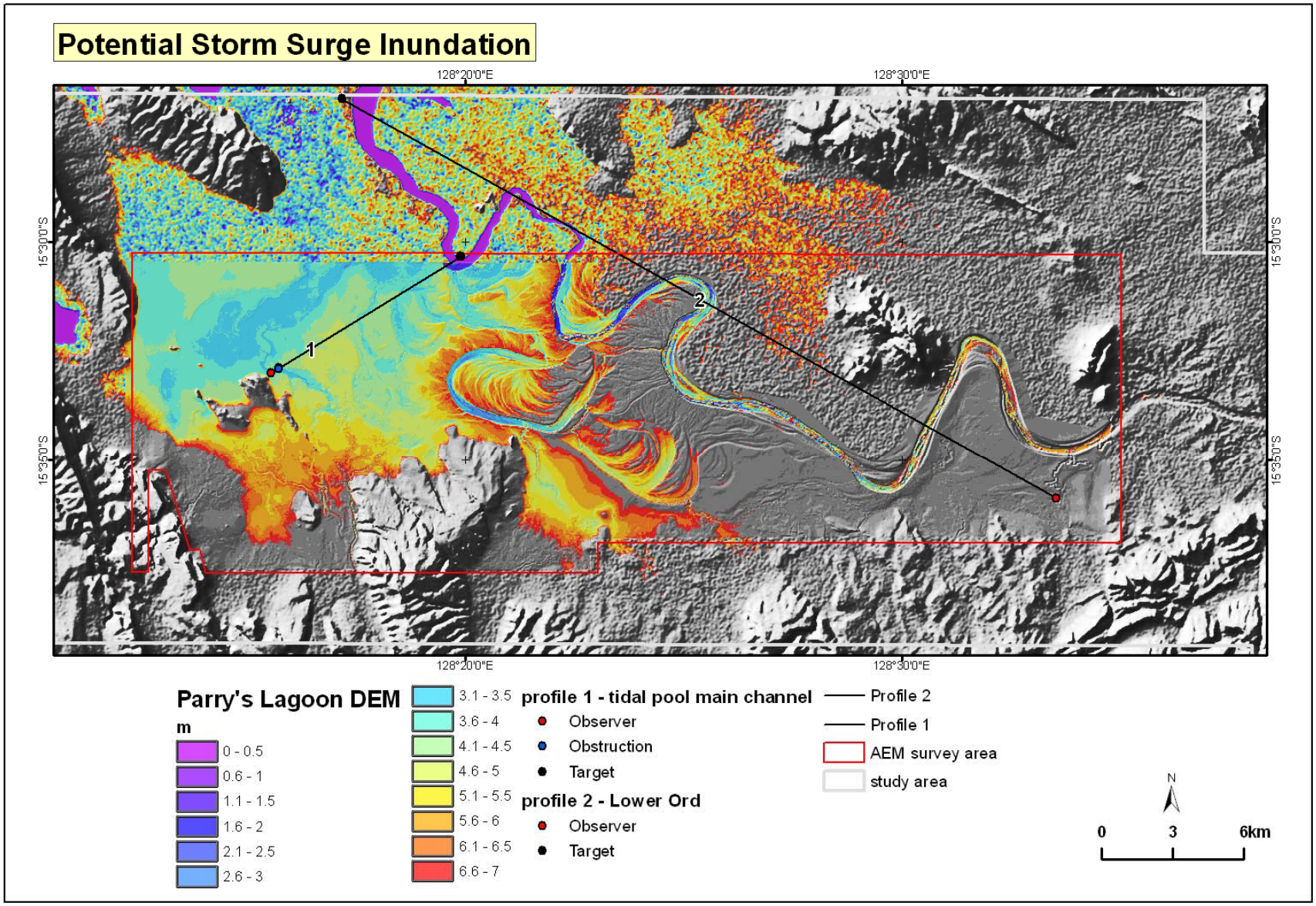

Figure 401: *Modelled potential storm surge showing extents of inundation up to 7m for Parry's Lagoon-Mantinea Plain-Carlton Hill.*

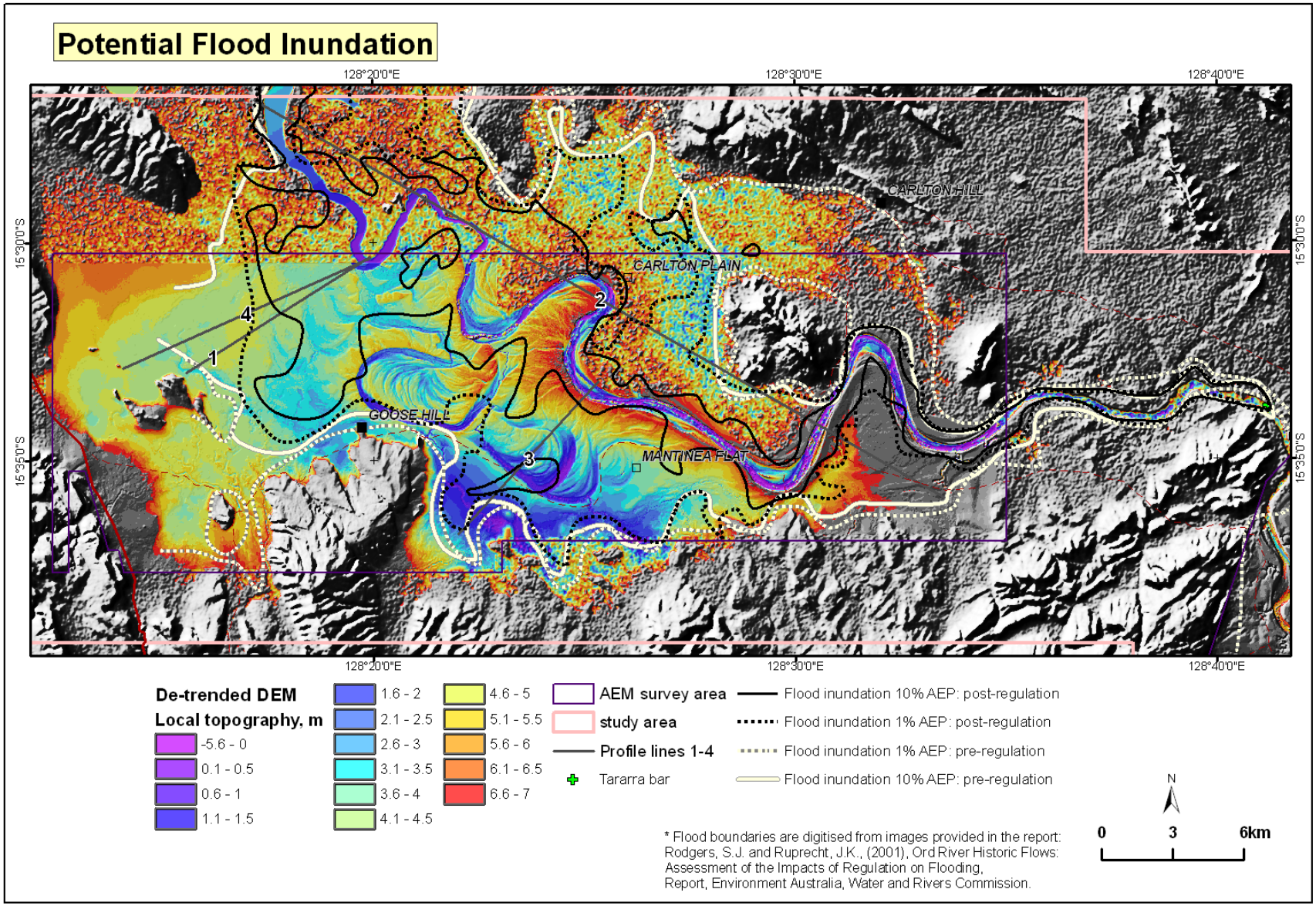

Figure 402: *Modelled potential flood inundation showing elevation ranges respective to the level of the main channel for Parry's Lagoon-Mantinea Plain-Carlton Hill l. Channel tilt of 8m has been removed from DEM.*

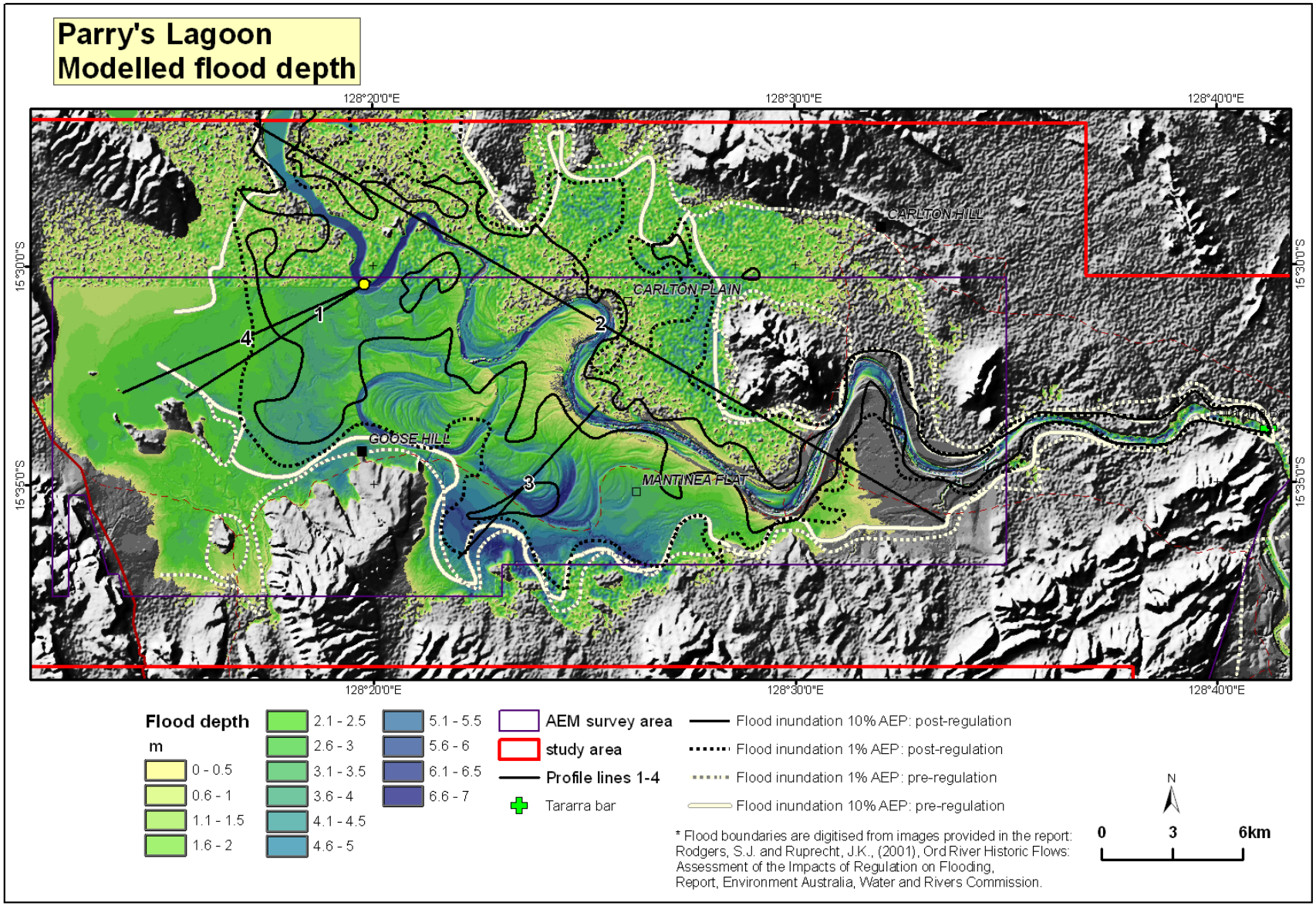

Figure 403: *Flood depth corresponding to the level of modelled potential flood inundation to the extent of 7m for Parry's Lagoon-Mantinea Plain-Carlton Hill. Reference point 0 shown as yellow dot on profile 1.*

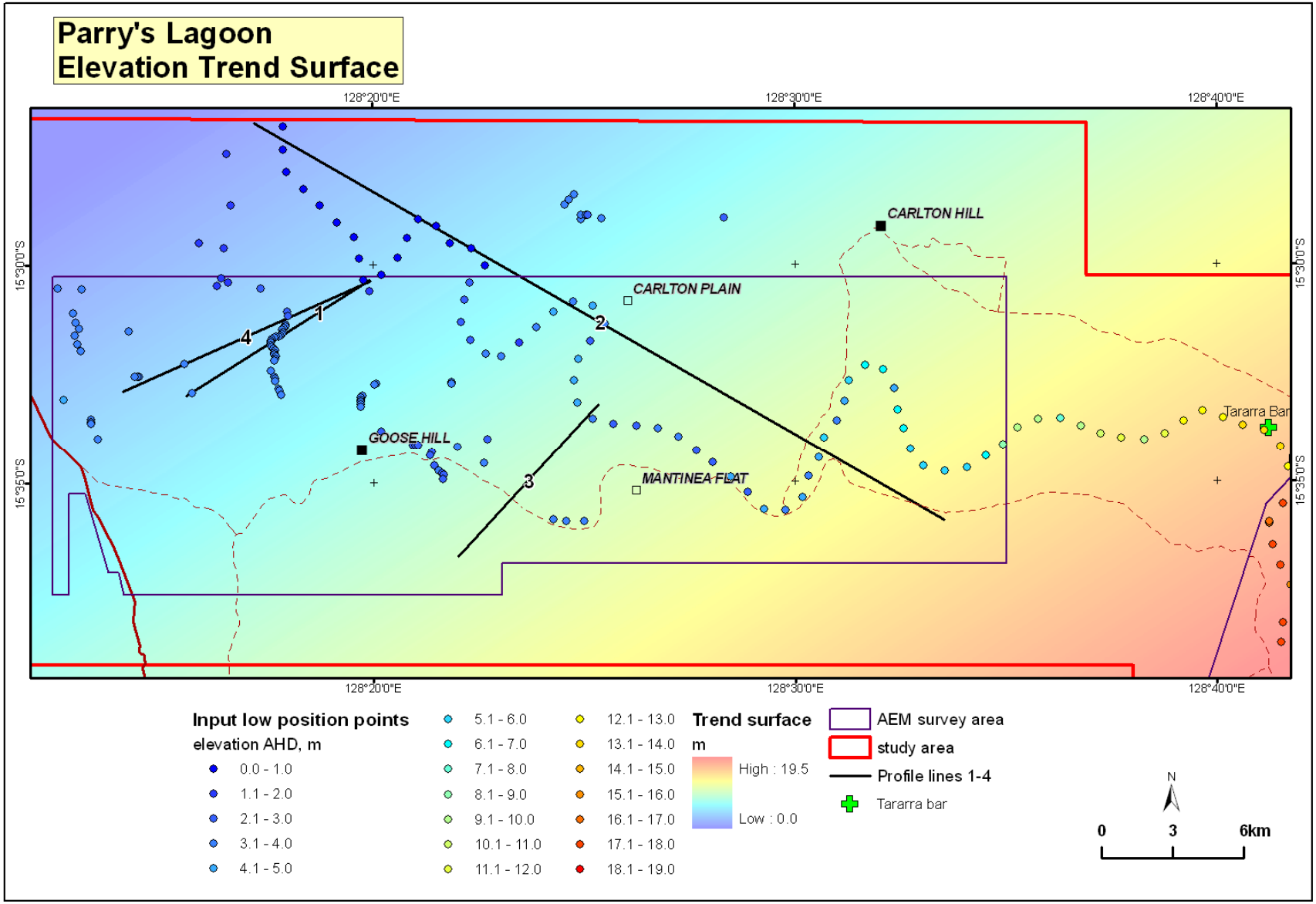

Figure 404: *Interpolated channel elevation trend surface and elevation ranges of the input points along the channel and low-lying areas for Parry's Lagoon-Mantinea Plain-Carlton Hill. Used to remove channel tilt from DEM.*

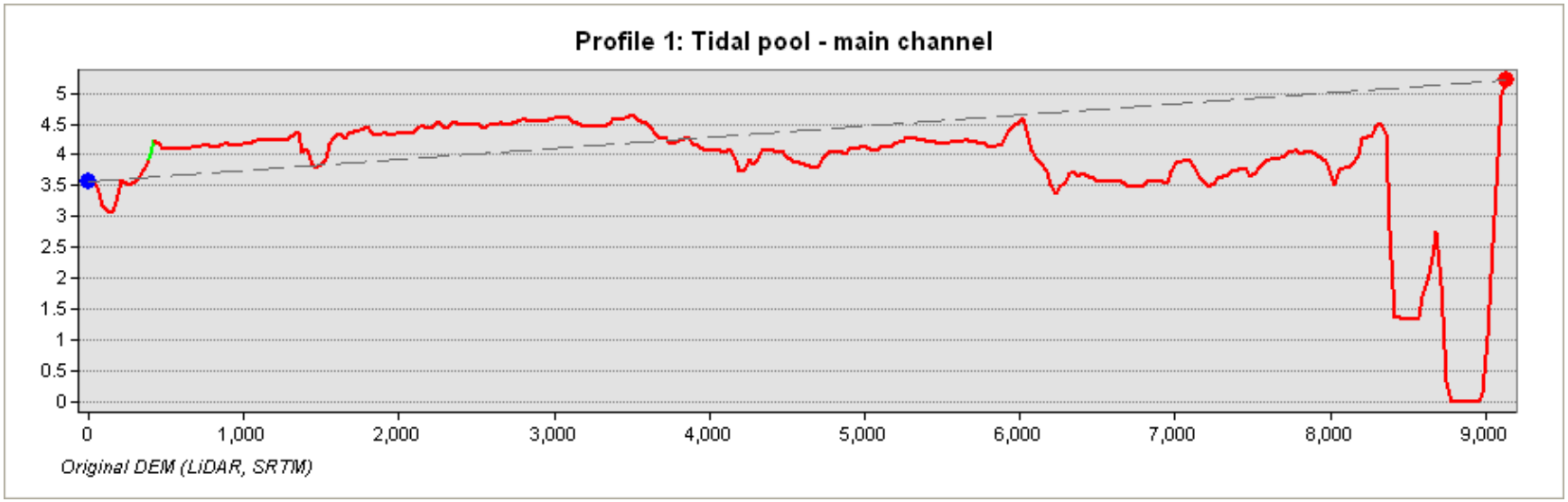

a

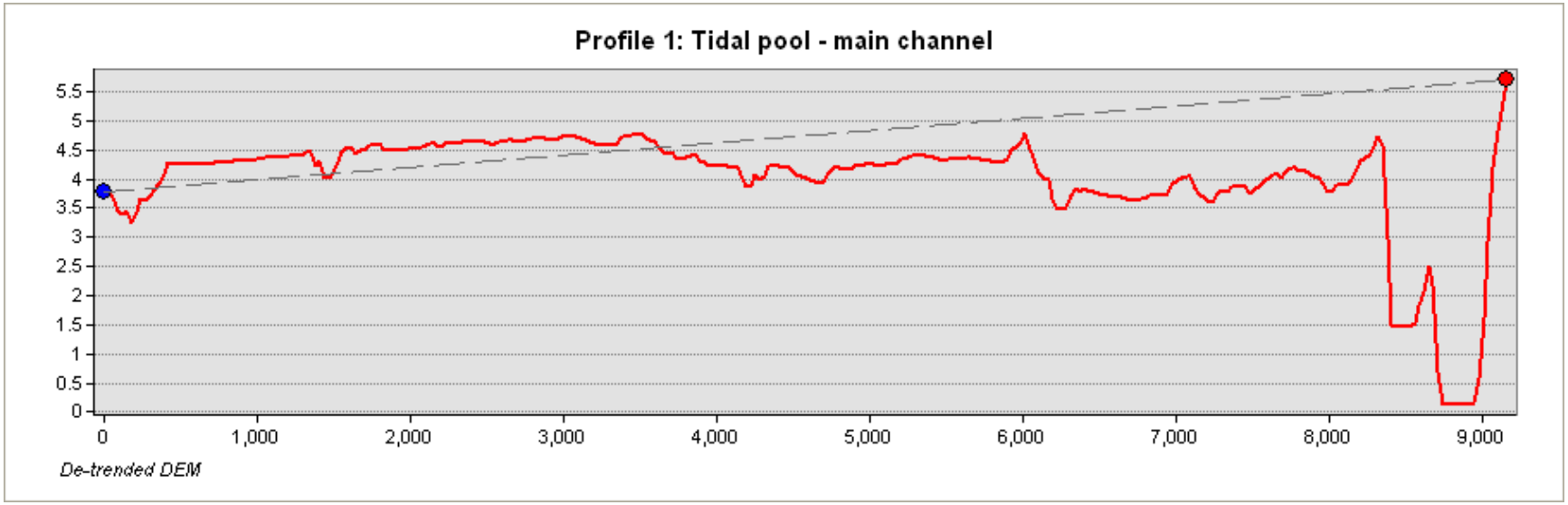

b

Figure 405: *Parry's Lagoon-Mantinea Plain-Carlton Hill. Profile 1 of: a - original DEM from tidal pool to the Ord River channel; b - de-trended DEM from tidal pool to the Ord River channel. Note insignificant elevation differences (~20cm).*

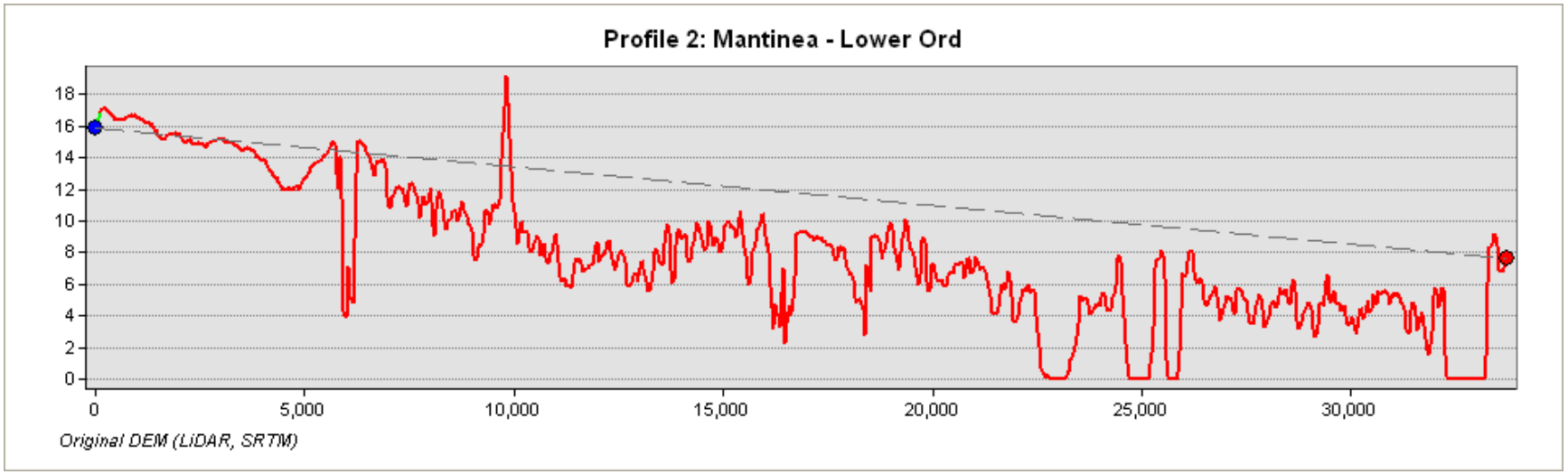

a

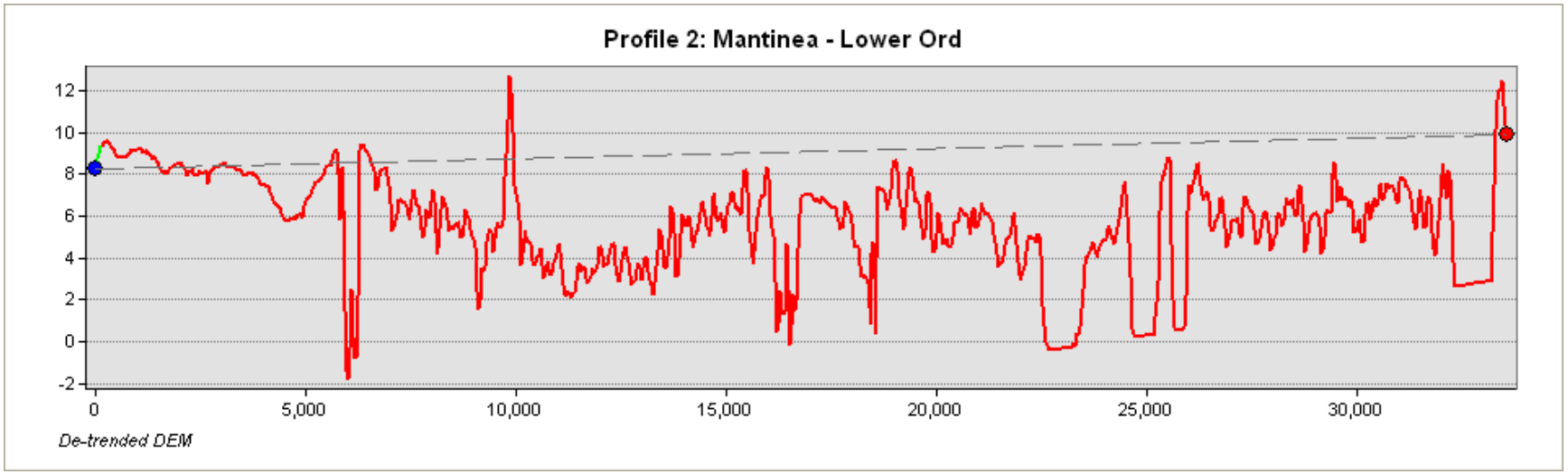

b

Figure 406: *Parry's Lagoon-Mantinea Plain-Carlton Hill. Profile 2 of the: a - of the original DEM from nearby Mantinea yard to the Lower Ord channel; b - de-trended DEM from nearby Mantinea yard to the Lower Ord channel. Note 8m differences in elevation between two DEMs.*

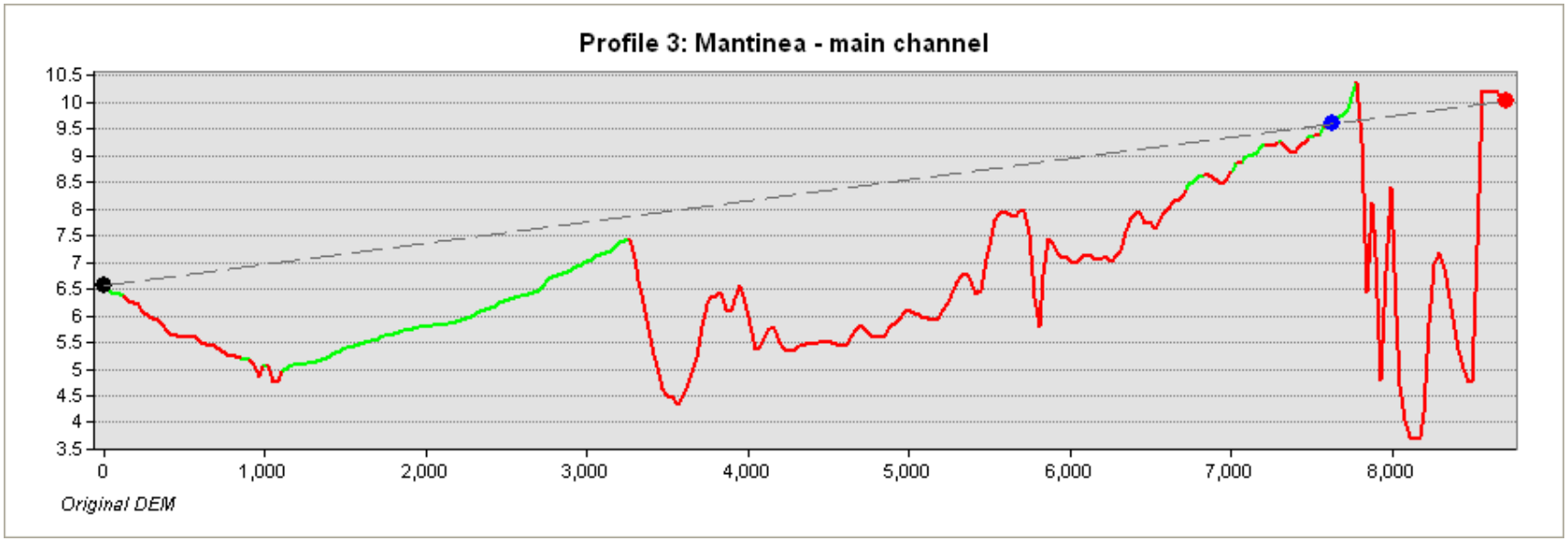

a

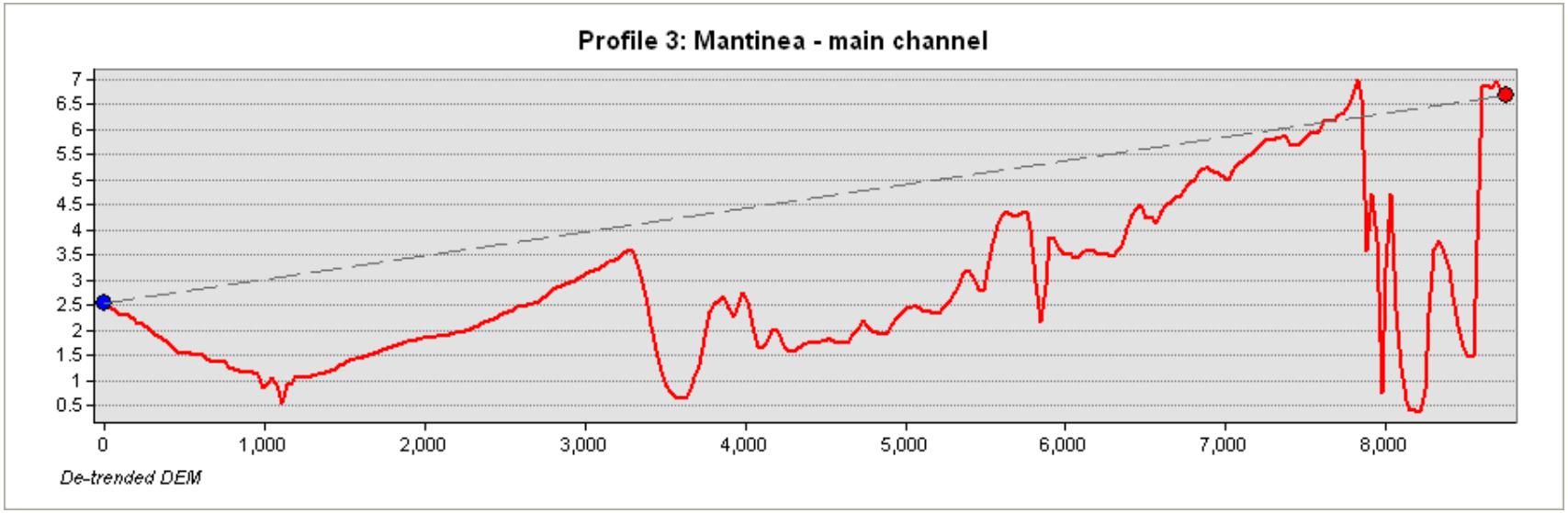

b

Figure 407: *Parry's Lagoon-Mantinea Plain-Carlton Hill. Profile 3 of: a - original DEM across Mantinea meander loop to the Ord channel; b - de-trended DEM across Mantinea meander loop to the Ord channel. Note preserved surface geometry with elevation differences of 4m.*

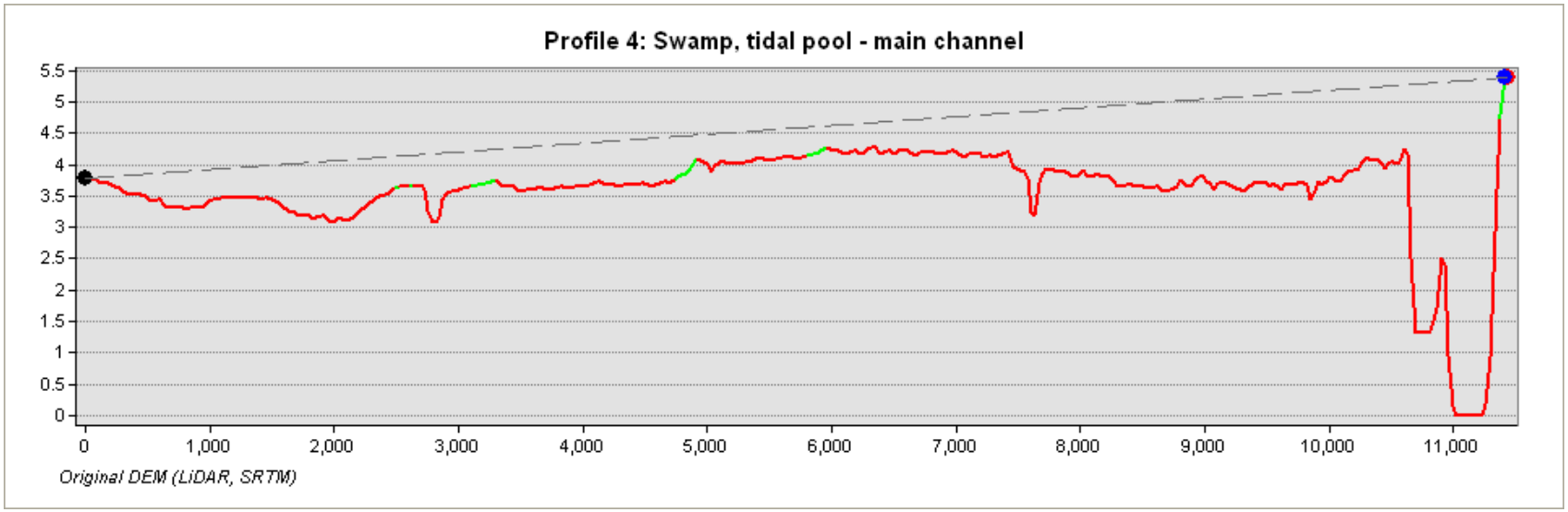

a

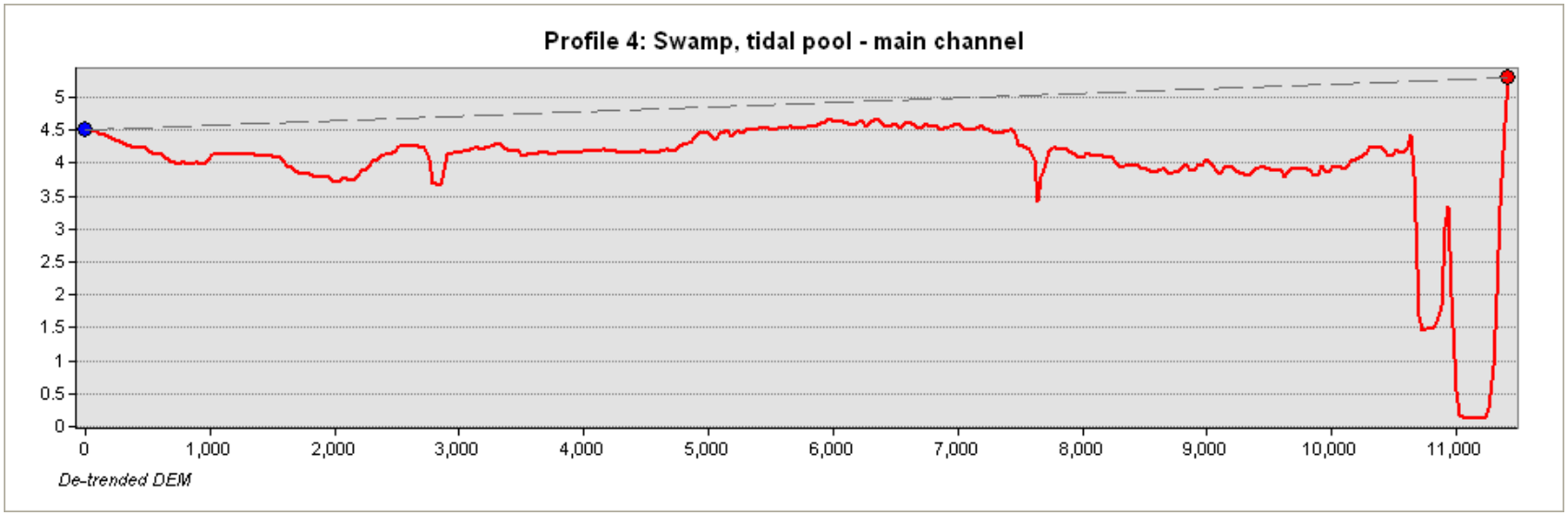

b

Figure 408: *Parry's Lagoon-Mantinea Plain-Carlton Hill. Profile 4 of: a - original DEM across a swamp to the Ord River channel; b - de-trended DEM across a swamp to the Ord River channel. Note elevation differences of ~60cm.*

9 Discussion

This section provides an in-depth discussion of the AEM-based salinity hazard maps produced in this study. This was considered important given the interest in the results of this project across a broad spectrum of the community, and experience elsewhere. It is very easy to 'see red' on conductivity maps and be alarmed. Indeed, crucial to the success in demonstrating the utility of AEM datasets for salinity management has been the development of more evolved information products that help determine whether 'red areas' are a salinity hazard or not. Likewise, extensive knowledge transfer activities have been essential in explaining the power and limitations of these products, and preventing their mis-use.

This section also discusses the vital linkages between the new AEM-derived products and the groundwater and land use modelling that will be required to identify areas at greatest risk from salinisation. Ultimately, it will be the way in which these datasets contribute to improved model parameterisation, and not the stand-alone products themselves, that will underpin the development of sustainable irrigation strategies in the ORIA Stage 2. Understanding the datasets and linkages should therefore be of relevance to existing irrigators and potential investors, those responsible for planning Stage 2 development, and catchment and environmental managers.

Salinity Hazard and Risk Mapping

Salinity is a hazard when it has the potential to be moved to where it can threaten assets such as agriculture, infrastructure, water resources and biodiversity (Spies & Woodgate, 2005). Salinity risk is a measure of the chance that a salt hazard will cause harm to an asset at some time in the future. A ***salinity hazard map*** defines the spatial location (both vertically and horizontally) and concentration of salt load. Salinity hazard maps are normally presented in summary form and do not include whether the salt can or cannot be mobilised (Spies & Woodgate, 2005). ***Salinity risk maps*** should identify the actual class of asset under threat, the timing of the impact of that threat, the level of anticipated impact should it occur, and the geographic location of both the risk and the asset (Spies & Woodgate, 2005).

There is an intimate relationship between the landscape, its geological and climatic history, groundwater processes, soil and alluvium types, and the hazard posed by salt in the landscape. Over the past decade, multi-disciplinary, multi-scale 4D system approaches have been developed to integrate, analyse and interpret the complex hydrogeological, hydrogeophysical and hydrogeochemical datasets required to map salinity within Australia's unique floodplain landscapes (Lawrie *et al*. 2000, 2003a, 2008, and 2009a).

These approaches incorporate an understanding of landscape evolution and scale, utilise modern investigative approaches to the conceptualisation and mapping of aquifer systems and aquitards, and combine state of the art hydrogeochemical and hydrogeophysical techniques to assess hydrogeological processes. The salinity and landscape mapping products generated using systems approaches are particularly useful when used as a starting point for salinity assessment. However, they are more powerful when incorporated into numerical groundwater models that can model temporal changes, and consider many more biophysical parameters including land use practices and infrastructure. Such 4D modelling is essential for predicting hydrodynamic responses and calculating salinity risk in the landscape. Choosing the most appropriate models that are 'fit for purpose' is essential.

It is also essential to recognise however, that despite the improvements in model parameterisation that are possible using sophisticated mapping and modelling technologies and approaches, significant data and knowledge gaps will remain in most areas. In particular, a lack of temporal data and biophysical data at appropriate scales, places limits on model predictions and certainty. 'Expert' knowledge and approaches are required to inform modelling and salinity assessments (Spies & Woodgate, 2005). In other words, there is a certain amount of 'expert interpretation' required in the weighting of different factors, and construction and interpretation of these maps. It is also important to recognise that, as more data and knowledge become available, there is an expectation that these maps will evolve.

Salinity Hazard Maps developed in this project

A number of different approaches were trialled in determining the construction of the salinity hazard maps for the ORIA. The salinity issues facing ORIA Stage 1 and Stage 2 sub-area are arguably quite different in

detail, given significant differences in landscape setting, hydrogeology, and baseline salinity. Moreover, there are important differences in development status, and irrigation planning guidelines. Despite these differences, it was decided to utilise a common approach across all areas for comparative purposes. For the same reasons it was also decided to use the same factor weightings in all areas.

Future salinity and risk mapping and assessments may chose to customise the inputs and weighting of parameters for specific sub-areas. This may be particularly useful in teasing out detail at local scales, and is an approach that should be considered for local groundwater and land use modelling and the development of salinity risk maps.

In this project, two different approaches and products were developed to assess the salinity threat:

- ***Salinity hazard maps***. These combine AEM-derived maps of salt stored in the unsaturated zone with maps of depth to the water table. These data layers are integrated using an informed GIS-based approach that applies variable weighting to these factors. Consequently, the salinity hazard is assessed as high when there are significant quantities of salt stored in the alluvium or soils in areas of shallow groundwater and lowest where there is little or no salt stored in the alluvium and groundwater tables are deep.
- ***Potential surface (soil) salinity maps***. These maps are based on the analysis and classification of Landsat 5 TM data. These are combined with geomorphic maps using an informed GIS-approach, and validated using a combination of pre-existing and new data on soil salinity. They are scaled to reflect the potential for salinity to develop in susceptible soils with stored salts, and are ranked from very low potential to extreme. These maps currently have to be used together with maps of shallow conductivity (0-2m) integrated with moisture persistence (from Landsat) to identify more localised areas of high potential surface (soil) salinity. Further work is required to integrate these products.

Salinity Hazard Maps (sensu stricto)

The 'salinity hazard maps' *sensu stricto* were developed to assess the salinity threat posed by the rise of groundwater to shallow levels, primarily as a consequence of land clearing and irrigation development. The key data layers in this AEM-based suite of maps reflect the key elements of the hydrogeology (watertable depth, salt store in the unsaturated zone and alluvium texture) considered most likely to predict areas of groundwater-driven salinity in soils and sub-soils.

The approach used in this project to produce the salinity hazard maps makes a number of assumptions, specifically:

- The new watertable map is an accurate reflection of the current situation;
- Watertable levels will rise after land clearing and the onset of irrigation;
- Watertable rise is vertical, with no lateral component to flow;
- Watertable rise is a greater hazard where it is already at shallow depths beneath the surface;
- Evapotranspiration of shallow water tables may lead over time to salt accumulation through capillary rise and evapotranspiration, if the watertable rises to within 2-3m of the surface (and either continue to rise and discharge to the surface, or equilibrate at these depths);
- AEM-derived salt store maps accurately quantify the amount of salt stored in the landscape;
- Salt stored in the landscape is available to be mobilised.

In order to understand some of the thinking behind the construction of the salinity hazard maps, and their limitations, these assumptions are discussed in detail below.

Watertable Reliability

Over the past decade, monitoring of watertable levels in ORIA Stage 1 has produced a reasonably dense network of observations, giving a high degree of confidence in watertable levels and fluctuations (Smith *et al.,* 2006; Smith, 2008). The watertable map produced in this study (Figure 85) utilised the data points used in the monitoring program, and additional points where water levels have been measured opportunistically. The resultant maps in the Stage 1 area are assessed to have a high reliability.

However, in the Stage 2 areas, watertable levels have been constructed using less well-monitored sites, and significant gaps remain (spatially and temporally). The watertable map generated in the Stage 2 areas should not be relied upon for local-scale analysis. This is recognised as a data gap and an impediment to more detailed salinity hazard assessments.

Watertable rise

From watertable observations over the past 10 years in particular, it is evident that watertables in the ORIA Stage 1 have now largely equilibrated over much of the Stage 1 area (Smith, 2008). While minor changes (1-2m) due mainly to seasonal fluctuations in rainfall continue to be observed, watertables appear to have stabilised at depths where capillary rise and evapotranspirative concentration of salts in soils are no longer of great concern in much of the ORIA Stage 1 (Smith, 2008). The new maps are therefore probably an over statement of salinity hazard in areas within ORIA Stage 1 where watertables are currently >3-4m below the land surface. This is certainly the case where the drainage infrastructure appears to be effective in stabilising watertables below 3m.

However, the relatively shallow water tables in parts of the northern Ivanhoe and Packsaddle Plain in particular, remain of concern, as the groundwater is sufficiently saline that prolonged evaporation and/or any further and/or seasonal rise could significantly increase the risk of soil salinisation (Smith, 2008). Salinity discharge related to high water tables close to Lake Kununurra would also appear to be an example of the salinity issues that can arise from water tables remaining at shallow depths for prolonged periods of time (Smith & Price, 2008).

The potential for watertables in these areas to rise significantly (to <3m) in the future in the ORIA Stage 1 areas is assessed as low, although this cannot be discounted entirely because of some of the 'wetter' climate model predictions that might produce increased recharge (CSIRO, 2009). In areas where watertables remain <2-3m, and salt stores are high, identification of higher salinity hazard would appear to be a reasonable assumption.

In the Stage 2 areas (such as Weaber plain), previous groundwater models predicted that watertables would rise to shallow levels as a consequence of land clearing and irrigation (SKM, Kinhill, KBR, O'Boy *et al.,* 2001). The information contained in the current study suggests that any new groundwater modelling will most likely confirm the prospect of watertable rise in areas such as Weaber Plain. The new modelling should take into account the new AEM-based products and up-dated watertable and hydrograph data.

The magnitude and rates of rise in the Stage 2 areas is less certain and this will have a bearing on the assessment of salinity hazard. Again, these factors can only be quantified using numerical groundwater modelling. Nevertheless, the factors that weigh on the underlying assumption that watertables will rise to shallow levels as a consequence of land clearing and irrigation in the Stage 2 areas, can be assessed qualitatively, and these are explored below.

Factors that might lead to more rapid watertable rise and equilibration at shallower depths than suggested in previous studies are listed below:

- In the Weaber Plain, it would appear from the evidence presented earlier that watertables have risen significantly in the past 15 years due to increased rainfall, infiltration from the D8 drain and D8 swamp, and lateral groundwater flow from the Stage 1 areas. As a result, aquifer storage is already half full in the western Weaber Plain. These significant rises were not factored in to the previous groundwater models, so it would appear more likely that shallow water tables will occur in the Weaber Plain as a consequence of land clearing and irrigation, if the basic recharge and aquifer storativity assumptions in the previous models hold true;
- Watertables in areas such as Knox Creek Plain and Keep River Plain have also risen in the past 10-15 years, apparently in response to increased rainfall. This also argues for shallower water tables than previously modelled;
- The 3D extent of sand and gravel aquifers throughout the ORIA, including Weaber Plain, is more restricted than previously thought. This suggests that watertable management through

groundwater pumping will be less effective at managing watertables. This places more emphasis on alternative recharge management (cropping and irrigation planning) and drainage strategies.

Factors that serve to argue for watertable equilibrium to occur more slowly, or at greater depths, are listed below:

- The rise in watertable levels in some areas may be slower than initially modelled due to the increase in the proportion of clays mapped using AEM. Clays have higher porosity and lower hydraulic conductivities than sands and gravels.
- Similarly, there is anecdotal evidence that native vegetation systems respond with increased vigour to the increased rainfall, and this is likely to reduce recharge over time. This of course will be a moot point in areas that are cleared for irrigation.
- It is also assumed in the salinity hazard maps that the watertable rise is vertical, with no lateral component to flow. Analysis of hydrograph data and the spatial distribution of the groundwater mound in the western Weaber Plain suggest that the watertables in that area have been effectively migrating eastwards at ~600-800m per annum over the past 10-15 years. The rate at which watertables will rise locally may in effect be dependent upon the location relative to higher recharge zones (natural and infrastructure-related), lateral and vertical hydraulic conductivities, and the occurrence of restrictions laterally as well as vertically.

  Lateral flows are also associated with springs that occur around the margins of the Plains and hill inliers. The occurrence of shallow pediments in areas such as the Weaber Plain is also likely to promote lateral groundwater flow. However, while lateral groundwater flow is almost certain to occur, it is hard to quantify without monitoring data and numerical groundwater modelling, and difficult to predict if there will be a salinity issue lateral to the identified hazard. Ultimately, though, as the drainage basins in the area are effectively semi-confined, watertables will rise throughout the area as areas distally 'catch –up' with areas proximal to areas with higher recharge. Overall, it seems a reasonable assumption that watertable rise and salinity hazard will be largely vertically above the identified salt store.
- Recharge management will clearly be of critical importance in the Stage 2 areas. Irrigation and crop planning to minimise recharge, combined with an appropriate groundwater pumping and drainage system, will be required to reduce recharge, delay watertable rises and manage the watertable to keep it at appropriate depths below the surface. Groundwater and land use modelling will be required to assess how to achieve this. The underlying assumption that watertables will rise as a consequence of land clearing and irrigation would appear realistic, and the potential for watertables to rise to very shallow levels a real possibility without careful management.
- Finally, there is the assumption that watertables can continue to rise without impediment, and that there is a greater hazard where watertables are already at shallow depths beneath the surface. This assumes that there are no further impediments to groundwater rise in areas of shallow watertables. Such impediments may include indurated layers, and examples may include areas of tufa which have been recorded in the northern Weaber Plain in particular.

In the Mantinea Plain and Carlton Hill areas, the potential for watertables to rise after land clearing and irrigation is also likely to be high, particularly in higher rainfall climate scenarios. The assumption of watertable rise is likely to be valid in these areas. However, in the Parry's Lagoon area, and in the westernmost parts of the Mantinea and Carlton Hill areas, gauging the potential for watertables to rise is more complex, as the landscapes are potentially affected by a greater range of hydrogeological processes. For example, the lower Ord floodplain may be subjected to storm surge events, inundation due to flooding of the Ord River, inundation from local run-off, and fluctuations related to seawater intrusion in underlying aquifers. Given the future climate predictions, and the very shallow depths that water tables occur at through these areas, the potential for watertables to rise may be higher in these areas. However, further modelling would be required to assess this properly.

However, on balance, the assumption of rising watertables to shallow levels as a consequence of future clearing and irrigation would appear to be valid for the Weaber Plain, as well as the other Stage 2 areas earmarked for potential development (Knox Creek-Keep River Plains and Mantinea Plain-Carlton Hill). It is likely that recharge control will be a more significant challenge than in the Stage 1 areas, and vital in terms

of managing watertable levels and salinity hazard. Overall, it is predicted that previous model predictions of the rise of watertables to shallow depths in Stage 2 areas such as the Weaber Plain may even have been underestimated. This also suggests that the development of shallow watertables is more likely, with implications for potential salinity hazard. However, this needs to be assessed in new groundwater models.

In addition to the comments above, further refinements to the salinity hazard maps could be made using the AEM-derived lithology maps, particularly maps of clay thickness above the watertable, and the distribution of sand and gravel aquifers (in groundwater models). Watertables will rise more rapidly in areas of sand and gravel than in a clay-rich area. The texture of the alluvium in the unsaturated zone is only considered through incorporation within the salt store maps, and is given a reduced weighting relative to watertable depth.

Evapotranspiration in soils and sub-soils if watertables rise to within 3m of the surface
Previous modelling of the evapotranspiration of shallow water tables in the Ord suggest that salt accumulation will arise through capillary rise and evapotranspiration, if the watertable rises to within 2-3m of the surface (Ali & Salama, 2003). The latter also suggest that the soil will become salinized through repeated cycles of wetting and drying even when the initial groundwater is fresh to brackish.

In the salinity hazard maps produced in this project, the depth to water table has therefore been weighted to have slightly more significance than the amount of salt stored in the landscape, as it is considered that evapo-transpiration will take place readily when the water table is within 2m from surface. Obviously, this will happen more rapidly if the groundwater is already saline. It is noted that the salt store in the saturated zone and groundwater salinity maps closely correlate.

However, the assumptions used in Ali & Salama (2003) remain poorly constrained and require further testing. The fact that shallow watertables in many Stage 1 areas did not result in significant salt scalding is often taken as evidence that the salinity threat is overstated. However, there have been few field demonstrations and no long-term monitoring of soil and sub-soil salinity levels in the Ord, while watertables in many Stage 1 areas remained within 2-3m of the surface for only relatively short periods of time (<5-10 years). There are insufficient data to assess how long watertables need to be maintained at shallow levels for salinity to become a concern.

An early warning may come through declines in crop productivity, although the actual impacts of shallow water tables on salinity levels and crop productivity in the Stage 1 area are not certain by any means. Surface salt discharges have begun to appear in very localised areas on the margins of the Stage 1 area and near leaky infrastructure. This has resulted in minor local losses in crop productivity (e.g. near the M1 supply channel at the mango plantation).

Overall, in the Stage 1 area, the data do not exist, in the public domain at least, to be able to ascertain if salt levels in the sub-soils have increased more generally in the past 10-15 years in areas of shallow water tables. There are only limited data to show that groundwater salinities have increased in the Stage 1 area (Figure 278). However, testament from growers combined with some limited scientific studies suggest there is some evidence of a relationship between high electrical conductivities in the shallow sub-surface and poor crop productivity in ORIA Stage 1. The issue is complicated by other possible causes of poor crop productivity including sodicity, alkalinity and waterlogging (Richards, 2002).

The groundwater in the Stage 2 areas is more saline in general than encountered in the Stage 1 areas. A rise of brackish and/or saline groundwater to shallow depths (<5m) also has the potential to impact on the productivity of more deeply rooting crops. However, the complexity of such predictions is demonstrated by the contrary evidence that mahogany crops may flourish and effectively mobilise salt to greater depths in low permeability materials. The rise of brackish to saline groundwater to shallow levels beneath the Stage 2 irrigation areas also has the potential to adversely impact on adjacent environmental assets through localised development of groundwater mounds and through potential seepage into the drainage network.

In summary, there is considerable uncertainty over the assumption that the rise of groundwater to shallow levels will result in a significant build up of salt in soils and sub-soils. Further investigation and monitoring is required to assess if this component of the salinity hazard assessment is robust. In the absence of other data, the salinity hazard maps have used the available research data and modelling.

Salt store map quantification

A couple of key underlying assumptions have been made in quantifying salt stores using the AEM data. Firstly, there is the fundamental assumption that the AEM inversions accurately reflect the conductivity distribution in each area. The correlations between the AEM inversions and borehole data are excellent overall ($r^2 = 0.84$), however correlations in some sub-areas such as the southern Weaber Plain are not quite as good (r^2~0.6). The reasons for this require further investigation.

Improvements to inversions may be made through the use of borehole data within the inversion process (in specific sub-areas), and by further customising inversions in sub-domains using local geological constraints. Similarly, the assessment of salt store is also based on appropriate attribution of lithology polygons, which is dependent upon the availability of borehole calibration data. In the ORIA, the quality and density of pre-existing data is highly variable, and additional boreholes were required for calibration and validation of the AEM data. Due to limited resources, only 12 new boreholes were drilled, and data gaps remain. The drilling of additional boreholes for monitoring (in areas such as the Weaber Plain) may provide opportunities to improve the salt store assessments by customising the AEM inversions.

Secondly, the methodology used in this project to convert AEM conductivity maps to quantified maps of salt store has been published previously (Tan *et al.,* 2005, Mullen *et al*., 2007; Tan *et al.,* 2008, 2009). The calibration of the AEM maps depends largely on the sample density used to convert the ECa data to salt loads. As there were no pre-existing data, 12 new boreholes were drilled to recover core samples for textural, pore fluid and moisture data. Samples were obtained from representative samples of all the alluvial lithologies, however the distribution of boreholes is not dense, and as with the AEM inversions above, the salt load predictions may be improved with acquisition of additional data in sub-areas.

Overall, the salt store quantification in this component of the hazard mapping and assessment appears to have a reasonable basis.

Salt store mobility

Two key assumptions in the salinity hazard maps are that the mapped salt stores in the unsaturated are available to be mobilised, and that the areas of highest hazard lie in areas classed as having the highest salt hazard values. Previous studies, and laboratory examination of different alluvial and regolith materials suggest that salt stored in thick mud is less readily mobilised as it is held within a low permeability unit. The salt hosted in permeable sand (thin mud) is interpreted as having a higher risk of being mobilised.

However, there is a very close correspondence in most areas between the areas of higher groundwater salinity and high salt store in the unsaturated zone. This is reflected in pore fluid salinities within clay units that have similar salinities to measured groundwater salinities in the same area. The relatively high rates of groundwater rise in both Stage 1 (20+m over 40 years) and in Stage 2 areas such as the western Weaber Plain (6-8m over 12 years), and the close correlation between salt stores, pore fluids and groundwater suggest that there has been significant 'equilibration' between salt stores and groundwater. In other words, use of the unsaturated salt store as a significant component within the salinity hazard maps would appear to be a reasonable predictor of future groundwater salinities, even in fine-textured lithologies. This component of the modelling is assessed as reasonably robust.

However, while the salt concentration in groundwater within sand and gravels may be lower than in adjacent fine-textured units, higher groundwater flows in the former may mean a significant salinity hazard may remain in these lithologies through delivery of higher salt loads despite lower salt concentrations. In this case, the salinity hazard in palaeochannel materials may be underestimated somewhat.

It is also worth noting that there are significant differences in groundwater chemistry through out the ORIA that may affect salinity hazard and risk assessments. For example, the Carlton-Mantinea areas has NaCl & SO_4 waters while the ORIA, Weaber-Knox etc are 'mostly' Na-HCO_3 dominant. Salinity chemistry is not factored into current assessments, and should be examined to help refine products in the future.

Potential surface (soil) salinity maps

It was also seen as important to produce a second product that reflected the potential salinity hazard in areas where salinity (resulting from both surficial and/or groundwater-driven processes) was already identifiable at or very close to the surface. Examples of the latter include groundwater-driven salinity at Packsaddle Creek. Lakeside (Lake Kununurra), and at Parry's Lagoon.

Using the Landsat data to map bare ground and/or salt scalded areas, combined with geomorphic maps, enabled excellent correlations to be obtained between the GIS-modelled predictions of higher salinity and field data. Over 90% of the salt scalds validated by field mapping were identified using this modelling approach. However, it was recognised that this approach by itself was not able to identify areas in Stage 2 where the salt store in the sub-soil layers may be high.

Rather, these maps are more powerful when used in conjunction with maps of shallow conductivity (0-2m) that are integrated with maps of moisture persistence (produced by temporal analysis of Landsat data). The latter identify areas of surface moisture persistence and high conductivity where salts are thought to accumulate at surface (in areas of deeper water tables). Significant areas of moisture persistence, where water and/or high soil moisture levels remain at or near the land surface for much of the dry season, were mapped in areas where watertables are currently at significant depths below the surface.

An example is in the northern Weaber Plain. The water in the latter area comes primarily from wet season run-off that is localised in internal drainage basins where there is perching and/or low rates of deep drainage. Moisture persistence in this area can also be traced to occurrences fed by groundwater-driven springs, and by overflow from the D8 swamp (in the northern Weaber Plain). In these locations, salt is concentrated in soils and sub-soils by evapotranspiration of infiltrated rainwater and/or spring-derived water. The hydrology of some of these locations will be changed where they are impacted by irrigation development. As these are likely to be sites of high residual salt store in the near surface, they have the potential to become areas of high salt hazard within newly developed irrigation areas. It is also likely that a number of areas with high salt stores (and high salinity hazard) within ORIA Stage 1 originated as poorly draining internal basins. These include Greens Location and Martin's Swamp. Future incorporation of the shallow AEM and moisture persistence products in new potential surface (soil) maps is recommended once appropriate validation is undertaken.

Given adequate resources, there are a number of additional ways in which these maps could be improved significantly. For example, integration of the two products and longer term temporal analysis of the Landsat data (back to 1978) could be undertaken to provide a picture of annual and seasonal fluctuations of surface water body and vegetation vigour. This could be used to build an understanding of the links between rainfall and surface moisture. Integration with hydrogeochemical studies could help to determine if any of the shallow salt stores have a (palaeo-) groundwater component, while the products could be improved through additional ground validation. Integration with soils data at appropriate scales would also be extremely valuable, while the use of the soils maps to validate the AEM data which could be used to map sub-soils in the deeper part of the soil profile and top layer in the sub-soils (0-4m).

Overall, the existing potential surface (soil) salinity maps have limited use, but used in conjunction with maps of near-surface conductivity (0-2 or 0-4m), integrated with maps of moisture persistence, may provide valuable baseline data on potential surface and near-surface soil salinity hazard in areas that have yet to be developed.

Summary

The salinity hazard maps generated in this study will help identify areas where salinity could potentially become a threat. Furthermore, both the salinity hazard maps and the new AEM-based maps of groundwater salinity and alluvial materials will provide important additional constraints on numerical groundwater modelling, while integration of these new maps with new knowledge from hydrograph analysis should assist with constraining recharge estimates. These will assist in the development of salinity risk predictions.

However, while the maps of alluvium in particular should provide a useful spatial constraint on recharge and groundwater flow modelling, the lack of pump test data and/or other hydraulic conductivity data for the

different alluvial units will introduce significant uncertainty into model predictions. This can only be overcome with more drilling and acquisition of pump test data. Nevertheless, the new AEM-based products *should* help pinpoint and quantify water and salt balance, and the potential threat of salinisation to crops, infrastructure and the environment.

Overall, the planned regional groundwater modelling of the Weaber Plain is likely to provide only a general idea of salinity risk, and more detailed modelling that couples irrigation planning, land use, and unsaturated and saturated groundwater flow modelling at a local scale may be required for sustainable management of higher risk areas.

Nevertheless, the limitations of the GIS-based salinity hazard maps produced in this report also need to be recognised. A more sophisticated modelling approach might consider other factors including the hydraulic conductivity of the sub-soil alluvium, groundwater flow paths, the influence of shallow bedrock and lateral groundwater flow, and detailed soils maps. Similarly, it has to be recognised that the AEM inversions undertaken for this study were tailored for regional evaluation purposes, and an enhanced dataset with greater 3D spatial resolution could potentially be produced with greater ground validation in smaller sub-areas.

Ultimately, the main benefits of the AEM-based products should lie in the improved parameterisation of groundwater models and salinity risk maps. These are required to underpin development decisions in the ORIA including design of Stage 2 irrigation infrastructure and sustainable cropping strategies.

Higher Level questions from the Project Steering Committee

The Project Steering Committee identified a number of higher-level questions regarding the potential threat that salinity poses to the sustainability of irrigation in the Ord Valley over the longer term. These issues are also discussed briefly below.

Will Ord Stage 1 have a salinity risk in future? If so, where?

The work by Smith (2008), and supported by datasets, products and analysis generated as part of this study, shows that the watertable in most of the ORIA Stage 1 has peaked and/or has declined over much of the present irrigation area. This appears, in large measure, due to the success of the main drains in the area. There have been no significant recorded salinity discharges to date in the ORIA Stage 1, although there is anecdotal evidence that are some areas of reduced crop productivity associated with areas of high electrical conductivity. It is not clear at this time to what extent salinity and/or other soil or sub-soil conditions for these declines in crop productivity, with further work required.

What is the lifetime of ORIA Stage 1 area if salinity is present?

This is an issue that can only be addressed through appropriate modelling, although the datasets and products generated in this project should provide important baseline information. It would appear more than likely that successful watertable management will enable irrigation to be sustainable over the Stage 1 area as a whole. However, it would appear a prudent strategy to carry out some research to assess the linkages between salt store, electrical conductivity and crop production. This should be complemented by a monitoring program of sub-soil and salinity levels to provide baseline data for optimising salinity management and cropping strategies. Such information would almost certainly aid planning for Stage 2.

Will Ord Stage 2 have a salinity risk? If so, where?

This question requires the new products generated in this study to be incorporated in land use and groundwater modelling to assess the salinity risk. As noted before, the precursor salinity levels in the Stage 2 areas are higher than Stage 1. While the salinity hazard maps provide some initial indication of salinity threat, the salinity risk can only be addressed through a program of numerical groundwater modelling that takes into account the new products generated in this study. It is important that the distributed groundwater modelling of saturated zone processes also links to unsaturated zone modelling. A second stage of more detailed modelling may be required to fully integrate infrastructure planning and various cropping strategies.

What is the lifetime of ORIA Stage 2 if salinity is present?

Again, this question can only be addressed through appropriate land use and hydrodynamic modelling. There is considerable experience in farming successfully while managing water balance. It is the hope that the

datasets and products made available through this project will empower land managers and farmers to design sustainable farming systems despite the presence of salinity in the catchment.

What are effective management strategies to mitigate the threat of salinity?
This question lies largely outside the scope of the present study, however a number of new findings provide information that may assist the development of potential strategies. For example, recognition of less extensive aquifers, and the narrowness of the gravel palaeochannel in the Weaber plain will restrict potential groundwater pumping strategies in that area. Similarly, recognition of areas of high salt store and/or higher groundwater salinity should enable irrigation design and water use strategies to be developed that minimise the potential for sub-soil salt accumulation and surface salinity discharge in Stage 2 areas. In areas of very high salt store and extreme salinity hazard, such as parts of Mantinea Plain, groundwater modelling will almost certainly show that this area has a very high risk of salinisation, and salinity mitigation may be extremely difficult if the area is developed for irrigation.

Are the high value environmental assets adjacent to and/or downstream of the irrigation areas at risk of salinity as a consequence of irrigation?
Land use and groundwater modelling is required to fully address this issue. However, the identification of high potential surface salt hazards in the northern Weaber Plain will require infrastructure to be designed to minimise the potential for surface flows of potentially brackish to saline water downstream through Border Creek. Development in western Mantinea is likely to raise already shallow watertables beneath the adjacent Parry's Lagoon area. Groundwater modelling is required to assess the potential impacts of development.

10 Conclusions

This project has produced significant new datasets and knowledge in relation to salinity and groundwater management in the Ord River Irrigation Area (ORIA). The project has acquired new airborne electromagnetic (AEM) and Light Ranging and Detection (LiDAR) datasets, as well as lithological, geophysical and hydrogeochemical data from new drilling.

A suite of map products has been derived using these datasets. These cover the overall project area as well as the 5 individual sub-areas. The latter are: Ivanhoe Plain; Packsaddle Plain; Weaber-Keep River-Knox Creek Plains; and Mantinea Plain-Carlton Hill-Parry's Lagoon. The list of products for each area includes:

- Groundwater levels in the alluvial aquifer at time of AEM survey
- Digital Elevation Model with 0.2cm vertical accuracy from LiDAR
- AEM Conductivity maps of the subsurface and flight line sections
- AEM cross-sections along O'Boy transects
- A 3D AEM model
- Maps of Flush zone extent, water quality and thickness
- Surface groundwater salinity
- Recharge Potential (from 0-2m soil data)
- Predicted Soil Permeability (0-20cm from soil data)
- Predicted Deep Drainage (from AEM map of clay thickness)
- Surface wetness index maps (from Landsat)
- Lithology interpretations of each AEM conductivity depth slice through the alluvial aquifer
- Maps of the extent and thickness of gravels, sands, silts and clays
- Depth to bedrock map
- Salt Store in the unsaturated zone
- Salt Store in the saturated zone
- Salinity Hazard (salt store combined with depth to water table)

The main findings of the study are:

1. The SkyTEM AEM system successfully mapped key hydrogeological elements of the alluvial aquifer over most of the project area. These products will enable better parameterisation of groundwater models and should inform irrigation planning. Key general points to note include:
    - A smooth model 1D layered earth inversion, applied from a regional perspective (i.e. without local constraint), effectively mapped variations in ground conductivity at scales relevant to the regional characterisation of the alluvial aquifer and groundwater system.
    - In general terms, the modelled conductivity structure defined from the SkyTEM smooth model Layered Constrained Inversion (LCI) matches that defined from available bore data exceptionally well, with an adjusted $r^2 = 0.84$ determined. It is therefore reasonable to assume that the modelled ground response from the inverted SkyTEM data provides a good approximation of 'true' ground conductivity as defined by the borehole conductivity tool, and is a reliable base from which to derive a suite of interpretation products.
    - Modelling and associated ground investigations confirmed that the SkyTEM system's depth of investigation was not limited by the thickness or conductivity of the alluvial aquifer and that conductivity variations in the underlying basement were resolved.
    - Overall, the hydrogeological framework documented in earlier investigations (e.g. O'Boy *et al.,* 2001), has been confirmed. However, within the limits of available bore data and the scales of airborne data acquisition, this study has provided greater spatial detail on critical elements of the hydrostratigraphy in the alluvial aquifer. This includes palaeochannel delineation, and the indicative extent and thickness of gravel, sand, silt, clay units in 3D, as well as the mapping in 3D of salt stores and groundwater quality.

- Conductivity signatures for several components of the hydrogeological system are non-unique. Interpretation therefore required the use of borehole and field sampling constraints. While 750 boreholes provided important constraints on the interpretation, the pore fluid and textural data obtained from 12 new cored holes were vital for AEM calibration and the generation of customised interpretation products.
- A ground calibration study of the SkyTEM system conducted at the time of the survey, revealed several small inconsistencies between the modelled and observed responses of the SkyTEM system in operation. Whilst they were judged not to significantly affect the definition of ground conductivity, particularly at depth (>4m), we believe further work on the better definition of near surface (0-2m) conductivities may be warranted if these data are to be used in soil related studies.
- Feedback from individual irrigators is that there is quite a significant correlation between areas of high conductivity mapped using both ground and airborne EM systems in the top few metres of the landscape and reduced crop productivity (for some crops). However, the lack of available soils maps and ancillary supporting data *at appropriate scales* made it impossible to produce a reliable soils map from the AEM data with available project resources. Moreover, it should be noted that in the Stage 2 areas in particular that while the modelled AEM response in the top 2m is good when compared with borehole data, soil profiles in the 0-2m depth slice were very dry over much of the ORIA Stage 2 areas at the time of survey. Further analysis in these areas may not be able to discriminate dry sands and dry clays with a high degree of confidence. The interpretation of the 0-2m depth slice has had to rely on the available (regional) soils data.
- Borehole data were not used to constrain the inversion of the AEM data. Further refinement of the observed ground conductivity in site-specific areas might be obtained through the local constraints. However, it should be noted that these constraints should be representative of ground conditions at the scales observed by the airborne system to be effective. The few examples of a poor correlation between the modelled AEM and borehole responses can be attributed largely to differences in the scale and sampling volume of the AEM versus borehole EM methods. Similarly, the issues of scale preclude the mapping of small-scale features such as the thin gravel lenses within clays (e.g. in southern Knox Creek Plain).
- The SkyTEM AEM system mapped conductivity variations within and beneath relatively thin deposits of the Cockatoo Sands, although it is likely that differentiation of sands with and without high salt content is difficult in the unsaturated zone.

2. ***Salinity hazard*** maps for the ORIA have been produced using an informed GIS-based approach. Salinity is a hazard when it has the potential to be moved to where it can threaten assets such as agriculture, infrastructure, water resources and biodiversity (Spies & Woodgate, 2005). In this study, the salinity hazard maps combine AEM-derived maps of salt stored in the unsaturated zone with maps of depth to the water table. These maps have been designed to predict groundwater-driven salinity hazard. The salinity hazard is assessed as high when there are significant quantities of salt stored in the alluvium or soils in areas of shallow groundwater, and lowest where there is little or no salt stored in the alluvium and groundwater tables are deep. Assumptions are made that water levels will rise after land clearing and the onset of irrigation, and that shallow water tables may lead *over time* to salt accumulation through capillary rise (if within 2-3m of the surface). Prior modelling suggests that relatively modest salinity levels (>750 mg/l TDS) may become a significant salinity hazard to irrigated agriculture through evapotranspiration in the shallow sub-surface.
3. ***Salinity risk*** is a measure of the chance that a salt hazard will cause harm to an asset at some time in the future. The project has also produced a number of other AEM-derived products, including maps of sand, gravel, silt and clay distribution, and groundwater salinity that are designed both as stand-alone products and for input into groundwater models. These can also be used to produce maps of salinity risk of the area. Generation of groundwater models and salinity risk maps should be used to underpin development decisions in the ORIA including design of Stage 2 irrigation infrastructure and sustainable cropping strategies.
4. The interpreted salinity hazard in each of the ORIA sub-areas is summarised below:
    - Mantinea Plain and Carlton Hill: very high salinity hazard in the western half of the areas earmarked for potential irrigation development. High salt stores (>100t/ha/m) in the unsaturated zones, saline groundwater (1,000 to 10,000mg/l TDS) in a shallow sand aquifer, and an

inherently high watertable (<5 to 10m), contribute to this assessment. Recharge potential is higher in Carlton Hill than in Mantinea Plain. The potential for soil waterlogging is also likely to be high in this area.

- The Parry's Lagoon wetland and lower Ord Floodplain have very high salt stores (>500t/ha/m), very shallow water tables (<2m) and extremely high salinity hazard. There are no discernible freshwater lenses beneath the Parry's Lagoon wetlands, although there is some evidence of mixing (of fresh surface water and saline groundwater) in the top 6m. In essence, the wetlands appear to be perched on saline clays and a sand aquifer with very high groundwater salinities (>46,000mg/l TDS). Salinity is a natural part of this landscape, however it remains unclear to what extent the hydrological balance has been altered post-Ord River regulation. The salinity hazard in this area lies not in the threat to irrigation assets, but to the freshwater environmental assets (and tourism assets indirectly) in the lagoons.
- Weaber Plain: the salinity hazard is highly variable across the area earmarked for development, ranging from very high to very low, but with >50% of the area ranked at least moderate. The very high salinity hazard areas occur in the western Weaber Plain where there are areas of high salt store in the unsaturated zone (<68/t/ha/m) and saturated zone (< 131 t/ha/m), high groundwater salinities (< 5,000mg/l TDS), and a very shallow (<5m) groundwater table. The soil waterlogging potential is also likely to be high in this area. Elsewhere in the area earmarked for development, the lower salinity hazard coincides with the palaeochannels, while the flanking clay-rich areas have a moderate to high salinity hazard.
- Knox Creek and Keep River Plains: very low to low salinity hazard in the north of the area, but with a moderate to high salinity hazard in the southern-central area of Knox Creek Plain, coincident with a thick sequence of clays with subsidiary silts and gravels. The southern half of Knox Creek Plain has an area with very high salt stores in the unsaturated zone (30-70t/ha/m) and saturated zones (60- 130t/ha/m), as well as high groundwater salinities (>5,000 mg/l TDS).
- ORIA Stage 1 Ivanhoe Plain: highly variable salinity hazard across this area, ranging from very low to very high. The northern part of the area has areas of high to very high salinity hazard, as does Cave Springs Gap. Very shallow water tables (<5m) combined with moderately high salt stores in the unsaturated (< 30t/ha/m) and saturated zones (<130t/ha/m).
- In ORIA Stage 1 Packsaddle Plain: the salt stored in the unsaturated and saturated zones is between 10 and 40t/ha/m, which is considerably lower than Ivanhoe Plain. There is a low to moderate potential risk of soil salinisation in this area.

5. ***Potential surface (soil) salinity maps*** produced in this study are based on classification of Landsat 5 TM data integrated with geomorphic maps using an informed GIS-approach. They successfully identify most of the known surface salt scalds in the area. However, these maps are more powerful when used in conjunction with maps of shallow conductivity (0-2m) that are integrated with maps of moisture persistence (produced by temporal analysis of Landsat data). The latter identify areas of surface moisture persistence and high conductivity where salts are thought to accumulate at surface (in areas of deeper water tables). Examples include internal drainage basins where there is perching and/or low rates of deep drainage (e.g. northern Weaber Plain). In these locations, salt is likely to be concentrated in soils and sub-soils by evapotranspiration of infiltrated rainwater and/or spring-derived water. Salt concentration in Green's Location and Martin's Swamp in the Stage 1 area may have originated in this way.
6. The AEM survey, validated by drilling data, has been used to map key hydrogeological elements associated with the alluvial aquifer system including those summarised below:
    - In the ORIA Stage 1 area:
        i. The presence and orientation of three discrete palaeochannels, interpreted as elements of the palaeo-Ord drainage system, separated in space and time, have been mapped beneath Ivanhoe and Packsaddle Plains.
        ii. Overall, the amount and extent of gravel present in the Stage 1 areas appears to be significantly less than previously thought, with gravel aquifers present in laterally confined palaeochannel systems. Sand aquifers also appear to be more laterally restricted than previously mapped.
        iii. Buried bedrock ridges and areas of thick clays may retard groundwater flow westward towards the Ord River in the Ivanhoe Plain.

- In the Weaber Plain:
    i. One discrete palaeochannel systems can be mapped. This is the main Ord Palaeochannel that enters Weaber Plain through Caves Springs Gap, and exits though the present Keep River Plain is narrower than previously mapped, and appears to have a very low thalweg gradient (to the NE).
    ii. An older, smaller, discontinuous palaeochannel system occurs in the north of the Weaber Plain. This is heavily weathered, consists of interbedded gravels and clays, and is associated with tufa deposits. This unit does not have a distinct AEM signature. The hydraulic conductivities of the gravels in this palaeochannel are interpreted to be significantly reduced.
    iii. The area of gravel aquifer storage in the Weaber Plain appears to be considerably less than previously considered. Sand aquifers are also more confined, with an abundance of fine-grained silts interpreted to be present higher in the alluvial sequence and laterally connected to the interpreted gravel-rich palaeochannels.
    iv. There are several buried bedrock ridges and shallow pediments that are interpreted to reduce aquifer storage within the alluvium.
- In the Keep River and Knox Creek Plains, a higher percentage of clay is interpreted to be present in the alluvium than previously mapped, with gravels, where present, mainly occurring as thin lenses in silts and clay units. The limited lateral extent and thickness of the coarser textured units prevents their detailed mapping.
- In the Mantinea Plain-Carlton Hill-Parry's Lagoon area, the presence of a marine sand aquifer containing very saline groundwater is confirmed beneath much of the area.

7. In the Weaber, Keep River and Knox Creek Plains, analysis of bore hydrographs has revealed periods of significant watertable rise in areas that have yet to be cleared but are earmarked for irrigation development. A number of important findings have been made:
    - There have been relatively rapid watertable rises across the Weaber, Keep River and Knox Creek Plains (with some local variability). These were initiated in the early 1990's, and water table rises of 10m have been recorded in some bores (southern Weaber Plain near Cave Springs Gap) in this period. This recharge is related to rainfall events. It is notable that this recharge has occurred prior to land clearing, and the recharge rates are much higher than predicted in previous reports.
    - An earlier, but less dramatic rise in the watertable is specifically observed in bores located in the southern half of the Weaber Plain near Cave Springs Gap. This rise of 3-6m, occurred over a 30 year time period, and commenced shortly after irrigation. This is inferred to relate to recharge associated with irrigation drainage via Cave Spring Gap, either as lateral flow through the Ord palaeochannel, and/or through recharge of excess surface waters at the termination of the M1 water supply channel. If the former model is correct, it demonstrates the need to consider groundwater management in the Stage 1 and Stage 2 (Weaber) developments as one management system.
    - The hydrograph responses are contrary to most previous predictions, but are consistent with recent observations about the links between recharge and rainfall in the ORIA Stage 1 areas (Smith, 2008). The hydrograph results point to a need for a fundamental reassessment of the methods of recharge estimation in areas of cracking clay soils in the tropics, where macropore bypass flow may be the key recharge mechanism.

8. The AEM data and complementary drilling and surface mapping datasets have been used to address specific salinity and groundwater management questions identified by the Project Steering Committee. Some potential management implications that can be drawn from their analysis and interpretation in this study, and these are summarised below. It is emphasised that further groundwater modelling is essential to provide enhanced spatial and temporal predictions of groundwater movement and salinity risk as a consequence of irrigation development, landuse and /or climate change:
    - The salinity hazard in many of the Stage 2 areas earmarked for irrigation development is high, with salt stores and groundwater salinity often much higher than in the Stage 1 areas, and pre-clearing water tables quite shallow. Management of deep drainage to control water and salt balance will be essential, and may be particularly challenging in some areas. Cropping strategies

will also have to make allowance for the potential for higher root zone salinities than encountered in the Stage 1 areas.

- In the Weaber-Keep River-Knox Creek Plains, the rapid rise in the groundwater tables over the past decade in response to increased rainfall is of concern, as it demonstrates that the aquifer storage is filling up more rapidly than groundwater flow can drain the system naturally (to the Keep River). This is consistent with the AEM mapping that shows the confined nature of the palaeochannel system, the lack of apparent lateral connectivity across the area, and the low gradient observed at the base of the palaeochannel. Climate modelling suggests this increased rainfall trend is unlikely to reverse in the short to medium term, hence recharge control is likely to be a major factor in determining the sustainability of irrigation in this area (particularly given the need to manage water balance on-farm).
- The pre-1990s rise in the Weaber Plain hydrographs near Cave Springs Gap suggests the probability of groundwater flow between the ORIA Stage 1 area and the Weaber Plain. This is supported by the AEM mapping of the palaeochannel that connects these two areas. Other possible contributions to watertable rise come from leakage from the D8 drain and the D8 swamp. It is suggested that this possible groundwater connection needs to be factored in to any groundwater modelling and management, including potential 'back-flow' to ORIA Stage 1.
- In the ORIA Stage 1 area, recent watertable decline beneath a stand of unirrigated Sandalwood and African Mahogany in Martins Location on Ivanhoe Plain has suggested that tree plantations can significantly influence groundwater levels by decreasing local groundwater replenishment and increasing transpiration. In this study, the AEM data revealed a local resistive anomaly coincident with the plantation. The observed ground conductivity structure is attributed to a combination of factors that act together; specifically a low moisture and dissolved salt content in the unsaturated zone, acting to reduce conductivity, with a rise in both in the saturated zone causing an associated rise in conductivity. These observations suggest that dissolved salt moves downwards through the profile as groundwater levels drop, indicating it is relatively mobile even in the fine-grained sediments found around Martins location. From a salt balance perspective, tree plantations such as found at Martins location may locally keep water tables well below the surface in areas where the aquifer has a relatively low transmissivity, and they may also encourage salt to move down and accumulate beneath the rooting zone. Plantations may be particularly effective in areas of finer-grained silt and clay lithologies.
- The AEM-derived products provide a basis for assessing the potential for leakage from water supply and drainage infrastructure. In the Stage 1 area, there are several locations where irrigation infrastructure transects areas of high potential salinity hazard, as well as areas of higher potential deep drainage. The AEM-based products could be used to target further investigations or remedial actions, and/or reconfigure assets to minimise potential salt mobilisation. It is noted that the M2 supply channel and the proposed irrigation infrastructure in Weaber Plain similarly transects areas of both high salinity hazard and high recharge potential.
- The salinity hazard and lithology maps also have the potential to assist with designing the most appropriate cropping and irrigation strategies in all areas.

The main findings with regard to the broader implications of the project results include:

1. The project has demonstrated the potential for 'calibrated' AEM systems and Fast Approximate Inversion software to shorten project timelines for studies that involve the analysis and interpretation of AEM data. More specifically:
    - Survey acquisition times were reduced through not having to fly as many repeat calibration tests or tie lines.
    - Although data and survey Qa/Qc is required, it necessitated less input from the science team (and the contractors) when compared with previous surveys involving 'uncalibrated' systems employed for similar tasks.
    - AEM data inverted using the FAI/ITEM software were obtained within 24 hrs of data acquisition. The early availability of high quality, approximate models of ground conductivity facilitated the early design of a drilling program, and enabled interpretation to commence immediately.

- The initial multi-layer ITEM inversions had high correlation coefficients (>0.8) when comparing FID points to adjacent borehole induction logs, and the inversions have proven to be very robust.

2. The project has demonstrated the benefits of a phased approach to assessing the methods and technologies to be used as part of a 'hydrogeological systems' approach to salinity and groundwater management.
3. Initially, a borehole-drilling program (with a very limited budget) attempted to take advantage of the availability of an aircore drilling rig in the Ord area. This drilling technique failed to gain adequate returns due to air losses in highly permeable sand and gravel aquifers, and the program was abandoned. Upon receipt of funds for a supplementary drilling program, a sonic drilling rig was commissioned to drill a series of 14 holes. This technique was highly successful, gaining full core recovery through a range of materials including thick clay soils, unconsolidated sands, and coarse-grained gravels containing cobbles. Limited water was used to assist drilling, so pore fluids recovered from core samples were uncontaminated. Drilling was on time, and within budget. The use of the Sonic drilling technique for salinity and groundwater studies was a complete success in this area, and its use in similar studies in a range of geological conditions is commended.
4. The range of products and the analysis detailed in this report should provide a useful basis for planning irrigation development in the ORIA Stage 2 areas, as well as providing an important environmental baseline dataset for environmental assessments and the design of groundwater monitoring programs for Stage 2. Realising the potential and full value of the information contained in this report requires that it be incorporated in future groundwater modelling and planning processes. More broadly, this project has demonstrated the benefits of a phased approach to assessing the methods as part of a 'hydrogeological systems' approach to the management of groundwater and existing and future irrigation developments in Northern Australia.

In conclusion, it is considered that the knowledge and products generated in this study will contribute significantly to future salinity and groundwater management in the ORIA. More specifically, through incorporation in further groundwater and land use modelling and the construction of new salinity risk maps, the products and new knowledge generated will assist with salinity mitigation, improved groundwater management, enhanced water use efficiency, improved crop production (and crop suitability), and protection of environmental assets.

A number of specific recommendations arising form this study are made in the following section.

11 Recommendations

The main recommendations from this study for the ORIA are:

1. A program of groundwater and land use modelling in the Stage 2 areas is recommended to refine salinity hazard and associated risk. This modelling should employ the data and information contained here to assist with an assessment of the likely impacts of land clearing and irrigation (as currently planned) on the groundwater system. The long-term sustainability of the proposed irrigation developments should also be considered in the light of the datasets and products generated from this study. It is recommended that these data and associated model constraints be used to develop strategies which minimise groundwater recharge and to develop sustainable cropping strategies.
2. Groundwater and land use modelling is also recommended to assess the potential consequences of irrigation development on high value environmental assets adjacent to and/or downstream of the Ord Stage 2 areas (Keep and Ord Rivers). In particular:
    - Their potential to affect the perched freshwater lagoons and groundwater dependent ecosystems (GDEs) in the adjacent Ramsar wetlands in Parry's Lagoon requires further study.
    - Modelling is also required to investigate the whether development will affect freshwater flush zones that support riparian vegetation along the Ord River upstream of the estuarine limit in the Stage 2 areas.
    - Given the high potential surface salt hazards in the northern Weaber Plain, there needs to be revised surface flow modelling to assess the potential downstream salinity consequences via modified Border Creek flows.
    - Also, hydrograph data from Smith (2008) combined with the new watertable surface in this study suggest that as the groundwater mound in the Western Weaber Plain rises further, there is the potential for groundwater to flow back towards ORIA Stage 1 (this may already be occurring).
    - New groundwater modelling planned for the Weaber Plain will provide up-dated predictions of watertable levels, and should identify areas at greatest risk of waterlogging and/or salinisation. This needs to be done for a range of climate and land management scenarios. However, it is likely that a second round of more detailed groundwater and land use modelling will be required to determine how irrigation can be operated sustainably. This second stage of modelling will need to assess how best to manage groundwater levels within sub-areas by assessing the recharge under varying cropping and irrigation strategies, in the knowledge that groundwater management control options will be more limited than in the ORIA Stage 1.
3. There remain important knowledge and data gaps in the Stage 2 areas. These may be addressed by implementing:
    a. A targeted program of additional shallow drilling to remove ambiguities in the interpretation of the AEM dataset and parameterise future groundwater models is required within the Stage 2 areas.
    b. A limited hydrogeochemical study to assess the relative contributions of groundwater recharge in the Stage 2 areas, and to understand surface water – groundwater interactions and processes more generally.
    c. A program of soil mapping at an appropriate scale to provide sufficient detail to assist with planning of irrigation infrastructure.
4. Testament from growers combined with some limited scientific studies suggest there is some evidence of a relationship between high electrical conductivities in the shallow sub-surface and poor crop productivity in ORIA Stage 1. The issue is complicated by other possible causes of poor crop productivity including sodicity, alkalinity and waterlogging (Richards, 2002). It is recommended that a focussed study involving the assessment of soils, sub-soils and available EM datasets (ground and airborne) be undertaken to clarify this relationship. The results of such an investigation are required to help understand salinity and groundwater processes, and translate the salinity hazard maps into salinity risk maps that will help identify specific areas of potential damage to crops. These investigations would also assist with determining crop suitability in both ORIA Stage 1 and Stage 2.

5. Knowledge of high precursor shallow salt stores and high potential surface (soil) salinity needs to be taken into account in any irrigation planning.
6. In support of the recommendations of Smith & Price (2008), it is recommended that long-term annual monitoring of soil salinity and groundwater conditions should be established at all locations within the ORIA in Stage 1 where secondary salinisation has been identified and a high salinity hazard and risk is assessed. Similar monitoring should be undertaken to provide baseline data in areas assessed to have high salinity hazard and risk in the Stage 2 areas. The objective of the monitoring should be to measure the degree, extent and trend of soil salinity at each location and across the irrigation area.
7. Hydrograph assessment in the Weaber, Keep River and Knox Creek Plains, highlights the need for robust baseline monitoring of groundwater conditions in the area. An improved understanding of groundwater dynamics and underlying mechanisms could be achieved by:
    - The ongoing maintenance and monitoring of bores that already have a long-term data record (such as Bore 8365 in the southern Weaber Plain).
    - Installation, regular downloading, and maintenance of data loggers in key bores, to provide a more detailed time series of groundwater levels. The time period between measurements in the existing data record is in the order of months or years. Loggers, calibrated with regular (typically 3-monthly) on-site measurements, would enable the (sub) hourly collection of groundwater level data. This greater frequency is critical for observing groundwater response to rainfall events, and to identify seasonal fluctuations in water levels. It is currently difficult to distinguish seasonal variability from any underlying longer-term watertable trends.
    - Collection of supporting data to help interpret recharge mechanisms. This includes groundwater sampling and hydrochemical analysis, such as age dating using isotopes or atmospheric tracers (e.g. CFCs). Time series monitoring of both groundwater level and electrical conductivity (salinity) using combined data loggers at specific bores, and/or the routine measurement of the stable isotope composition of aggregated monthly rainfall samples would be useful for understanding both recharge processes and groundwater dynamics.
    - For monitoring and evaluation purposes, it is recommended that additional shallow piezometers and automated borehole loggers be sited in strategic locations using the AEM data and derived products.
    - It is further recommended that groundwater modelling should incorporate different climate scenarios including the 'average' CSIRO climate model prediction, as well as drier and wetter scenarios using local longer-term records.
8. There remain specific knowledge gaps in our understanding of the hydrogeochemistry and dynamics of groundwater and surface-groundwater interactions across the ORIA. To assist with refining salinity hazard and risk, it is recommended that:
    - Pore fluid analyses from this study should be combined with historic groundwater sampling to better characterise hydrogeochemical domains.
    - Hydrochemistry of source waters (such as rainfall, irrigation supply and drainage, river and estuarine water) be better characterised, both by analysis of existing water quality data, or by additional data acquisition through specific water sampling programs. This is important to define end-members and to assess groundwater chemistry variations on the basis of mixing ratios.
    - Incorporating other hydrochemical analyses of groundwater samples such as age dating techniques (e.g. tracers such as chlorofluorocarbons) should be undertaken to obtain a better understanding of groundwater dynamics and processes.
    - Time series monitoring of hydrochemistry will provide insights into groundwater dynamics, in particular the understanding of recharge processes.
9. It is recommended that further analysis of the AEM data should be undertaken to assist with identifying leakage zones from irrigation infrastructure, and optimising drainage effectiveness in the existing irrigation areas. Specifically it is recommended that:
    - Further analysis should be undertaken of the AEM data along the M1 supply channel to identify potential leakage zones. This would require some ground validation to validate the interpretation.

- Synthetic AEM sections should be constructed for the other supply channels and drains in the existing ORIA Stage 1 area to assist with identifying leakage zones and areas of ineffective drainage. A program of targeted ground validation would be required to validate the interpretation and calibrate the groundwater responses.
- Synthetic AEM sections should be constructed for the M2 and M2N supply channels and proposed drains in the Weaber Plain. This study should incorporate available geotechnical analysis of pits along these routes, as well as further targeted drilling to validate the interpretation and obtain groundwater data, and establish monitoring and evaluation boreholes.

10. From a salinity management and salt balance perspective, tree plantations such as found at Martins location may locally keep water tables well below the surface in areas where the aquifer has a relatively low transmissivity, and they may also encourage salt to move down and accumulate beneath the rooting zone. It is recommended that deep-rooting plantations such as mahogany be considered for water table and salinity management as buffers in areas of finer-grained silt and clay lithologies.
11. The probable connection, through Cave Springs Gap, of the groundwater systems between ORIA Stage 1 and the Weaber Plain suggests that there is a need to consider groundwater management in the Stage 1 and Stage 2 (Weaber) developments as one management system. Groundwater models should certainly consider this connection.
12. It is also recommended that OIC and the relevant State agencies consider an approach to the wider communication of this report's findings and associated data. At present only a limited section of the community and growers have had the chance to look at the data and fewer have been able to take the data away to interpret in their own farms or circumstances. A process to do this should be considered with the OIC, involving both industry, and its representatives, such as the Department of Agriculture and Food, Water and Environment and Conservation.
13. It is recommended that a scoping and technical risk evaluation study be carried out to assess the suitability of AEM methods for mapping salinity hazard and key elements of the hydrostratigraphy in the Keep River Plain in the Northern Territory. Based on the results in this report, an AEM survey may provide valuable information on salinity hazard and environmental baseline conditions, although it is noted that ground conductivities are likely to be much higher in this area, with a higher technical risk likely.

More general recommendations are listed below:

1. It is recommended that integrated hydrogeological assessments be carried out in advance of proposed irrigation development in northern Australia. Integrated assessments should be phased, and include:
    (i) Collation and review of existing information for the purpose of identifying critical knowledge gaps;
    (ii) Scoping and technical risk evaluation to assess the methods and technologies best suited to addressing identified knowledge gaps;
    (iii) Integrated geoscientific studies to enable key elements of the hydrogeological system to be mapped, and groundwater flow and hydrogeochemical processes to be understood;
    (iv) Data synthesis and interpretation using contemporary 'systems' approaches, with an emphasis on delivering products that address specific issues and assist with the improved parameterisation of hydrogeological models;
    (v) Groundwater, surface-groundwater modelling and land use modelling to ascertain the sustainability of proposed developments. Modelling should utilise the best available climate data and modelling scenarios.
2. The acquisition of ground and airborne geophysical data for salinity hazard mapping should only be considered within the context of the broader, integrated, hydrogeological assessment of an area. Technical risk evaluation is required to gauge the merits of employing different geophysical approaches and technologies.
    - Acquisition of AEM data should only proceed after completion of scoping studies to assess the likelihood of success arising from their acquisition.

- Scoping studies are required to identify target aquifers and groundwater systems, and the scale, depth and orientation of target objectives (where possible). This should then be followed by completion of a technology suitability assessment exercise in each area. Technology selection should include forward modelling of system responses, and should follow the best practice procedures developed by the Commonwealth, taking particular note of the ability of AEM system to map key elements of relevant elements of the hydrogeological system.
- AEM data analysis and interpretation should follow a 'hydrogeological systems' approach based on the methodology recommended by the Joint Academies of Science Review of Salinity Mapping Methods in the Australian Landscape Context (Spies & Woodgate, 2005). Based on these recommendations, AEM-based projects need to incorporate a drilling program, complementary ground investigations and hydrogeochemical studies to ensure appropriate survey calibration, validation and interpretation.

3. A similar, phased approach is recommended for the assessment of groundwater resource and Managed Aquifer Recharge opportunities in priority catchments in northern Australia.
4. Future AEM surveys should carefully consider the merits of using calibrated AEM systems and inversion software that can significantly shorten data acquisition and delivery timeframes. These technologies and methods can significantly shorten overall project timeframes and potential costs.
5. The use of sonic drilling technology was an unqualified success in this project with nearly 100% core recovery in wide range of unconsolidated and consolidated geological materials, and delivery of uncontaminated core for hydrogeochemical investigation. The use of this technology in similar studies is strongly commended.
6. Within the context of broader, integrated, hydrogeological assessments, and following on from previous AEM-based studies in the Murray-Darling Basin, it is also recommended that acquisition of AEM data be considered more broadly in Australia to:
    - Assist with the reconfiguration of existing irrigation assets and map potential links to environmental flows.
    - Provide environmental baseline data for proposed and planned future irrigation districts elsewhere in Australia (e.g. in Tasmania).
7. It is recommended that the interpretation of geomorphic and/or sedimentary facies patterns be carried out on conductivity depth slices ***and/or*** on elevation slices (relative to AHD or another datum such as tilted floodplain elevation slices). Selection of the most appropriate datum should be dependent on the objectives of the survey and the nature of the landscape, geology, and questions to be resolved, as well as available resources. We further recommend that this approach be augmented by a line-by-line interpretation of conductivity depth sections linked to borehole lithological information. This issue has arisen as a particular challenge in the application of AEM in defining alluvial aquifer characteristics, and in particular, aquifer bounds, as in areas such as the Ord, they are associated with limited conductivity contrasts that may separate coarser (texturally) alluvial units containing fresh water from underlying bedrock. Both often appear as resistive units, although conductive basement units can also be confused with conductive fine-grained alluvial deposits.
8. In future studies, or in further analysis of the Ord AEM dataset, AEM inversions should be tailored to the particular landscape and/or groundwater system. This may require the use of several different inversions for discrete areas within overall project boundaries. In addition to the commonly employed smooth model layered inversions, blocky, or few-layer inversions may also be of use in particular settings. In particularly difficult situations we advocate that the inversion of individual or groups of soundings be undertaken, trialling a range of starting models, and the use of borehole constraint, rather than employing and applying a common starting model in the inversion of the full dataset. Whilst this adds to the overall cost and time taken in the interpretation, we believe it may significantly increase the accuracy of defined aquifer bounds and characteristics in some settings.
9. A ground calibration procedure undertaken at the time of an AEM survey, whether using ground loops or borehole inductive conductivity measurements, will always be of value in ensuring the accurate definition of ground conductivity, and more particularly will assist in ensuring a consistent system performance within claimed limits. We recommend this be considered as an integral part of any data acquisition and validation activity.

12 References

Aldrick, J.M., Clarke, A.J., Moody, P.W., van Cuylenburg, M.H.R. and Wren, B.A., 1990. Soils of the Ivanhoe Plain, East Kimberley, Western Australia. Western Australian Department of Agriculture Technical Bulletin 82, 74p.

Allen, D., 2005. A Review of Geophysical Equipment applied to Groundwater and Soil Investigation. ANCID/Sustainable Irrigation Travel Fellowship Report. 77p.

Ali, R., Salama, R., Pollock, D., and Bates, L., 2002. Geochemical Interactions between Groundwater and Soil, Groundwater Recycling and Evaporation in the ORIA. CSIRO Land and Water, Perth Technical Report 21/02.

Ali, R. and Salama, R., 2003. Groundwater quality in the Ord River irrigation area, its suitability for irrigation and prediction of salinity and sodicity hazards. CSIRO Land and Water Technical Report 07/03.

Anderson, H.F., Duncan, A.C. and Lynch, S.M., 1993. Geological mapping capabilities of the QUESTEM airborne electromagnetic system for mineral exploration – Mt Isa Inlier, Queensland. Expl. Geoph 24, p. 333-340.

Apps, H.E., Cullen, K., Tan, K.P., Halas, L., Clarke, J.D.A., Lawrie, K.C., Fitzpatrick, A., Munday, T.J., 2009a. Ord Valley AEM Interpretation Project – Project GIS.

Apps, H.E., Cullen, K., Tan, K.P., Halas, L., Clarke, J.D.A., Lawrie, K.C., Fitzpatrick, A., Munday, T.J., 2009b. Ord Valley AEM Interpretation Project - Overview Atlas. 69p.

Apps, H.E., Cullen, K., Tan, K.P., Halas, L., Clarke, J.D.A., Lawrie, K.C., Fitzpatrick, A., Munday, T.J., 2009c. Ord Valley AEM Interpretation Project – ORIA Stage 1 and Ord West Bank Atlas. 66p.

Apps, H.E., Cullen, K., Tan, K.P., Halas, L., Clarke, J.D.A., Lawrie, K.C., Fitzpatrick, A., Munday, T.J., 2009d. Ord Valley AEM Interpretation Project - Mantinea Plain, Carlton Hill & Parry's Lagoon Atlas. 68p.

Apps, H.E., Cullen, K., Tan, K.P., Halas, L., Clarke, J.D.A., Lawrie, K.C., Fitzpatrick, A., Munday, T.J., 2009e. Ord Valley AEM Interpretation Project – Weaber, Knox Creek and Keep River (WA) Atlas. 64p.

Auken, E and Christiansen, A.V., 2004. Layered and laterally constrained 2D inversion of resistivity data. Geophysics, 69, p. 752-761.

Auken, E., Christiansen, A.V., Jacobsen, L. and Sørensen, K.I., 2005. Laterally Constrained 1D-Inversion of 3D TEM Data. SAGEEP 2005, Atlanta, USA, EEGS. Best of EEGS-NS 2004 papers. Proceedings of SAGEEP 2005, Atlanta, EEGS.

Auken, E., Westergaard, J., Christiansen, A.V. and Sorensen, K., 2007. Inversion of SkyTEM data for processing of high resolution hydrogeophysical surveys. Extended Abstract, ASEG 2007, Perth, Western Australia.

Auken, E., Westergaard, J. A., Christiansen, A. V. and Sørensen, K. I., 2007. Processing and inversion of SkyTEM data for high resolution hydrogeophysical surveys. 19th Geophysical Conference and Exhibition, Australian Society of Exploration Geophysicists, Extended Abstracts.

Auken, E., Christiansen, A. V., Westergaard, J. H., Kirkegaard, C., Fopged, N., Viezzoli, A., 2009. An integrated processing scheme for high-resolution airborne electromagnetic surveys, the SkyTEM system. Exploration Geophysics, 40, p. 184-192.

Banyard, R., 1983, Ord River Irrigation Area, Ivanhoe Plain Waterway Infiltration: Public Works Department WA, Water Resources Branch Report. (Unpublished).

Barr, A. D., Pollock, D. W. and Salama, R. B., 2003. Surface water – groundwater interaction modelling: leakage from the Ord River Irrigation Area channel network. CSIRO Land and Water Technical Report 37/03.

Bates, L. E. and Pollock, D. W., 2003. Development of a GIS framework for data integration and management in the Ord River Irrigation Area. CSIRO Land and Water Technical Report 05/03.

Bolton, F., Silvester, S., Price, A., Dawbin, K., & Dodds, R., 2006. Satellite imagery- a tool for farm management in Ord River irrigation Area. In Proceedings, of ANCID Conference, Darwin, 15-17th Oct., 2006. p 54-61.

BOM., 2009. Climate Statistics for the Kimberley Research Station. Bureau of Meterology web site. Address when accessed on 13/9/09 http://www.bom.gov.au/climate/averages/tables/cw_002014.shtml

Brodie, R. and Sambridge, M., 2006. A holistic approach to inversion of frequency domain airborne EM data, Geophysics, 71, No. 6, p. G301-G312.
Burvill, G.H., 1991. Soil surveys and related investigations in the Ord River area, east Kimberley, 1944. Western Australian Department of Agriculture Technical Bulletin 80, 67p.
Carter J, Smith A.J., Silberstein R., Ali, M., Doody, T., Byrne, J., Smart, N., Robinson, C., Palmer, C., Slaven, T., Smith, P. and Palmer, D., (in prep) Interaction between trees and groundwater in the Ord River Irrigation Area. CSIRO: Water for a Healthy Country National Research Flagship.
Chappell, J., 2001. Geomorphology and Holocene geology of coastal and estuarine plains of northern Australia. In Gondwana to greenhouse: Australian environmental geoscience, edited by V.A. Gostin. Special Publication - Geological Society of Australia, Vol.21, p. 303-314.
Chamberlain, T., and Wilkinson, K., 2004 (eds.). Salinity investigations using airborne geophysics in the Lower Balonne area, Southern Queensland. Queensland Department of Natural Resources and Mines, 257p.
Christensen, N.B., 2008. Approximate 1D inversion of the Bookpurnong SkyTEM Data Set. CSIRO Flagship Water for a Healthy Country Report CEM: P2008/1320, 24p.
Christensen, N.B., Reid, J.E., and Halkjaer, M., 2009. Fast, laterally smooth inversion of airborne time-domain electromagnetic data. Near Surface Geophysics, 7, p. 599-612.
Clarke, J., Lawrie, K., Fitzpatrick, A., Apps, H., Lowis, W., Hatch, M., Price, A., Wilkes, P., and Dore, D., 2007. Application of geophysical methods to improve knowledge of groundwater flow and leakage from water supply infrastructure in the Ord and Burdekin irrigation areas. *In* WILKES, P. (Ed.) Geophysics for Irrigators. (Book chapter), CSIRO publishing.
Clarke, J.D.A. and Ringis, J., 2000. Late Quaternary stratigraphy and sedimentology of the inner part of Southwest Joseph Bonaparte Gulf. Australian Journal of Earth Sciences, 47(4), p. 715-732.
Cluett, L., 2005. The role of flooding in morphological changes in the regulated lower Ord River in tropical north-western Australia. River Research and Applications 21(2-3), p. 215-227.
Cobiac, M. D., 2006. Predicting native pasture growth in the Victoria River region of the Northern Territory. University of Adelaide unpublished PhD thesis. Address when accessed http://digital.library.adelaide.edu.au/dspace/bitstream/2440/36784/2/02whole.pdf
Coleman, J.M. and Wright, L.D., 1978. Sedimentation in an arid macrotidal alluvial river system; Ord River, Western Australia. Journal of Geology, 86(5), p. 621-642.
Cresswell R. G., Mullen, I. C., Kingham, R. Kellett, J., Dent, D. L., and Jones, G. L., 2007. Airborne electromagnetics supporting salinity and natural resource management decisions at the field scale in Australia. International Journal of Applied Earth Observation and Geoinformation 9(2), p. 91-102.
CSIRO, 2009. Water in the Ord-Bonaparte region, in CSIRO (Ed). Water in the Timor Sea Drainage Division. A report to the Australian Government from the CSIRO Northern Australia Sustainable Yields Project, CSIRO Water for a Healthy Country Flagship, Australia, p. 183-272.
Cullen, K., Lawrie, K.C., Apps, H.E., Tan, K.P., Halas, L., Clarke, J.D.A., Fitzpatrick, A., Munday, T.J., 2010. Ord Valley AEM Interpretation Project – Appendix Volume. Geoscience Australia Professional Opinion, 2010.
Davis, A.C. & Ley-Cooper, Y., 2010. Can a borehole conductivity log discredit a whole airborne EM survey? ASEG 2010 Conference, Sydney.
Davis, A.C. and Macnae, J.C., 2007a. Quantifying AEM system characteristics using a ground loop: Geophysics, 73(4), p. F179–F188.
Davis, A.C. and Macnae, J.C., 2007b. Measuring AEM waveforms with a ground loop. Geophysics, 73(6), p. F213–F222.
De Vries, J.J. and Simmers, I., 2002. Groundwater recharge: an overview of processes and challenges. Hydrogeology Journal, 10, p. 5-17.
DEWHA, 2008. National Vegetation Information System (NVIS) - WA - Present Native Vegetation (Australian Natural Resources Atlas Data - Stage 1, Version 2) Australian Government Department of the Environment, Water, Heritage and the Arts, address when accessed http://www.environment.gov.au/erin/nvis/index.html
Dixon, J., 1996. Soils of the Weaber Plain East Kimberley, Western Australia: Natural Resources Assessment Group, March 1996, Agriculture Western Australia.
Doble, R., Walker, G., and Simmons, C., 2005. Understanding spatial patterns of discharge in semi-arid regions using a recharge-discharge balance to determine vegetation health. CSIRO Land and Water Technical Report No 13/05. Adelaide: CSIRO. http://www.clw.csiro.au/publications/technical2005/tr13-05.pdf

Doble, R. C., Connor, J., Stenson, M., Elmahdi, A., Jolly, I. D., Miles, M., and Walker, G. R., 2008. Future landscape scenarios in the lower River Murray, south-eastern Australia and their implications for river salinity and floodplain health. Final papers of the 2nd International Salinity Forum, Adelaide, March 30-April 3rd, 2008. http://www.internationalsalinityforum.org/Final%20Papers/doble_E3.pdf

Dudgeon, C.R. & Cox, R.J., 1981. Sorby Hills pumping tests, analysis of results of pumping a-b and I Pods. University of N.S.W., Water Research laboratory Tech. Rept., 81/16 (Unpublished).

Edwards, D. & MacAuley, S., 2008. Airborne Electromagnetic Surveying for answering environmental /land managmetn questions: a case study form the Lower Macquarie Catchment, NSW, Australia. AEM 08, Helsinki, Finland. Ext Abs 08-05, 2p.

Earth Resource Mapping, 2006. Online User Guide, ER Mapper.

Elmore, A.J., Mustard, J.F., Manning, S.J., and Lobell, D.B., 2000. Quantifying vegetation change in semiarid environments: precision and accuracy of spectral mixture analysis and the normalised difference index. Remote Sensing of Environment 73, 87-102.

Erskine, W. D., Saynor, M. J., Erskine, L., Evans, K. G., and Moliere, D. R., 2005. A preliminary typology of Australian tropical rivers and implications for fish community ecology. Marine and Freshwater research 56, p. 253-267.

Fitterman, D.V., and Deszcz-Pan, M., 1998. Helicopter EM mapping of saltwater intrusion in Everglades National Park, Florida: Exploration Geophysics, v. 29, p. 240-243.

Fitzpatrick, A., Munday, T., and Clarke, J., 2007. Determining an appropriate AEM system for informing the hydrogeology of the Ord Irrigation Area, Stage 1 and 2, Western Australia: Interim Report. CSIRO Exploration and Mining Report P2007/867, CSIRO, Perth

Fitzpatrick, A., Munday, T., Cahill, K., Price, A. & Lawrie, K.C., 2008. Atlas of Preliminary data from the Ord Irrigation Area SkyTEM Survey. CSIRO Report No. P2008/2482.

Friend, P.F., 1983. Towards the field classification of alluvial architecture or sequence. *In* Collinson, J. D. and Lewin, J. (Eds). Ancient fluvial systems. International Association of Sedimentology Special Publication 6, 345-354.

George, R.J. and Woodgate, P., 2002. 'Critical factors affecting adoption of airborne geophysics for management of dryland salinity', Exploration Geophysics, vol. 33, pp. 84–89.

George, R.J., Beasley, I., Gordon, D., Heislers, D., Speed, R., Brodie, R., McConnell, C., and Woodgate, P. 1998. Evaluation of airborne geophysics for catchment management. National Report to AFFA on National Airborne Geophysics Project (unpublished).

George, R., Lawrie, K.C. & Woodgate, P., 2003. "Convince me all your bloody data and maps are going to help me manage salinity any better ?" A review of remote sensing methodologies for salinity mapping. *In* Proceedings 9th PURSL (Productive Use of Saline Land) Conference, Yepoon, Qld. 14p.

Gibling, M.R., Nanson, G.C. and Maroulis, J.C. 1998. Anastomosing river sedimentation in the channel country of central Australia. Sedimentology 45, 595-619.

Gibling, M. R., 2006. Width and thickness of fluvial channel bodies and valley hills in the geological record: a literature compilation and classification. Journal of Sedimentary Research 76, p. 731-770.

Gill, E.D., 1973. Geology and geomorphology of the Murray River between Mildura and Renmark, Australia. National Museum, Victoria. Memoirs 34 p1-97

Gippel, C.J. and Blackham, D., 2002. Review of environmental impacts of flow regulation and other water resource developments in the River Murray and Lower Darling River system. Final Report by Fluvial Systems Pty Ltd, Stockton, to Murray-Darling Basin Commission, Canberra, ACT

Golder Associates Pty Ltd., 1999. Factual report on geotechnical investigation Ord River Irrigation Area stage 2, Kununurra. Prepared for Kinhill Engineers Pty Ltd, Victoria Park WA, 342p.

Griffin, T. J. and Grey, K., 1990a. King Leopold and Halls Creek Orogens. In Geology and Mineral Resources of Western Australia. Western Australian Geological Survey Memoir 3, p. 232-255.

Griffin, T. J. and Grey, K., 1990b. Kimberley Basin. In Geology and Mineral resources of Western Australia. Western Australian Geological Survey Memoir 3, p. 293-304.

Grundon, N. J., 2000. The Australian Cashew Industry An Information System RIRDC Publication No 00/15

Gunn, R. H., 1969. Soils of the Kimberley Research Station, Kununurra. CSIRO Division of Land Resources Technical Memorandum 69/21.

Halkjaer, M., Sorensen, K. I., Christensen, N. B., and Auken, E., 2006. SkyTEM – Status and Development. ASEG Preview, 123, p. 29-31.

Halkjaer, M. and Reid, J., 2008. Geoforce-SkyTEM technical description, 13p.

Hallenberg, J.K., 1984. Geophysical logging for mineral and engineering applications. PennWell Books, Tulsa, Oklahoma.
Healey, R.W. & Cook, P.G., 2002. Using groundwater levels to estimate recharge. Hydrogeology Journal, 10(1). 91-109.
Herczeg, A., Dogramaci, S., and Leaney, F., 2001. Origin of dissolved salts in a large, semi-arid groundwater system: Murray Basin, Australia. Marine and Freshwater Research, 52: p. 41-52.
Holben, B., 1986. Characteristics of maximum-value composite images from temporal AVHRr data. International Journal of Remote Sensing, 7, 1417-1434.
Huete, A. R., 1985. Spectral response of a plant canopy with different soil backgrounds. Remote Sensing of Environment, 25, 295-309.
Humphreys, G., Tickell, S., Yin Foo, D., & Jolly, P., 1995. Sub-surface hydrology of the Keep River Plains, Northern Territory Power and water Authority, Water Resources Division (unpub.).
Humphreys G., Foo D.Y., Tickell S., Jolly P., Chin D., 2002. Planning to manage sustainably? Natural resource geophysics as part of resource assessment. *Exploration Geophysics* 33, p. 103–109.
Isbell, R.F., 1996. The Australian Soil Classification CSIRO Publishing, Canberra.
Isbell, R.F., McDonald and Ashton, L.J., 1997. Concepts and Rationale of the Australian Soil Classification ACLEP, CSIRO Land and Water, Canberra.
Jin, S., and S.A. Sader., 2005. Comparison of time-series tasseled cap wetness and the normalized difference moisture index in detecting forest disturbances. Remote Sensing of Environment 94(3): 364-372.
Kaufman, Y. J. & Tanre, D., 1992. Atmospherically resistant vegetation index (ARVI) for EOS-MODIS. IEEE Transactions on Geoscience and Remote Sensing, 30, 261-270.
Kernich, A., Pain, C., Kilgour, P., and Maly, B., 2004. Regolith landforms in the lower Balonne area, southern Queensland, Australia. CRC LEME Open File Report 161, 59 p., CRC LEME Perth.
Kinhill Pty Ltd., 2000. Ord River Irrigation Area Stage 2 proposed development of the M2 area. Draft environmental impact statement. Prepared for Wesfarmers Sugar Company Pty Ltd, Perth WA 6000, 768p.
Lane, R., 2000. Conductive unit parameters: summarising complex conductivity distributions. 70th Meeting, SEG, Calgary, Expanded Abstracts, Volume 1, Section EM 4.2, p. 328-331.
Lane, R., Heislers, D. and McDonald, P., 2001. Filling in the gaps – validation and integration of airborne EM data with surface and subsurface observations for catchment management – an example from Bendigo, Victoria, Australia, Exploration Geophysics, 32, p. 225 – 235
Lane, R., 2002. Ground and airborne electromagnetic methods. *In*: PAPP E. (ed.) Geophysical and Remote Sensing Methods for Regolith Exploration. CRCLEME Open File Report 144, p. 53-79.
Lane, R., Brodie, R., Fitzpatrick, A., 2004. Constrained inversion of AEM data from the Lower Balonne area, Southern Queensland, Australia. CRC LEME Open File Report 163, Cooperative Research Centre for Landscape Environments and Mineral Exploration. [http://leme.anu.edu.au/Pubs/OFR161-162-163-164-166-167/OFR163.pdf]
Lawrie, K. C., Munday, T. J., Dent, D. L., Gibson, D. L., Brodie, R. C., Wilford, J., Reilly, N. S., Chan, R. A. & Baker, P., 2000. A 'Geological Systems' approach to understanding the processes involved in land and water salinisation in areas of complex regolith- the Gilmore Project, central-west NSW. AGSO Research Newsletter, v. 32, p. 13-32, May 2000.
Lawrie, K.C., Gray, M. Fitzpatrick, A., Wilkes, P., Lane, R., Pain C. & Lambert, I., 2003a. Assessing cost-effective salinity mapping strategies using a landscape- based approach for methodology and technology selection. *In* Submission to National Review of Salinity Mapping Methods and Technologies in the Australian Context. CRC LEME Open File Report.
Lawrie, K.C., Gray, M., Fitzpatrick, A., Wilkes P., and Lane, R., 2003b. Reducing the Acquisition Costs of Airborne Electromagnetics Surveys for Salinity and Groundwater Mapping. Preview, October 2003.
Lawrie, K.C., 2006. Land use questions and models of AEM targets report by technical working group chair on proposed River Murray Corridor (South Australian border to Gunbower) Victorian AEM mapping project. CRC LEME Restricted Report 265r. 27p.
Lawrie, K., Clarke, J., Hatch, M., Wilkes, P. and Apps, H., 2006a. Aquifer systems for salinity and water management in the Ord Irrigation Area: a pilot study into the use of geophysics and other geoscience methods. CRC LEME Restricted Report 232R, 73p.
Lawrie, K. C., Clarke, J., Hatch, M., Price, A., and Wilkes, P., 2006b. Improving hydrogeological models of aquifer systems in the Ord Irrigation area: assessing the potential of geophysics and other Geoscience methods. *In* Proceedings of the ANCID Conference, October 2006, Darwin.

Lawrie, K.C., Clarke, J.C. & Tan, K.P., 2007. Geoelectric models for the Ord Valley. CRC LEME Report. 15p. (Unpublished).

Lawrie, K., 2008. To what extent can recent advances in salinity mapping and assessment create new salinity management and policy opportunities? 2nd International Salinity Forum (Plenary Address) Ext. Abs. http://www.internationalsalinityforum.org/Final%20Papers/lawrie_plenary.pdf

Lawrie, K.C., Tan, K.P., Halas, L., Cullen, K., Pain, C.F., Brodie, R.C., Apps, H., Wong, V., Reid, M., Clarke, J.C. & Gibson, D., 2009a. River Murray Corridor (RMC) Salinity Mapping and Interpretation Project: Report on the Barr Creek to Gunbower Island Region. Geoscience Australia Professional Opinion 2009/13, 186 p.

Lawrie, K.C., Brodie, R.S., Gibson, D.L., Ley-Cooper, Y., Davis, A., Magee, J., Cullen, K., Halas, L. & Apps, H., 2009b. Broken Hill Managed Aquifer Recharge Project, Phase 2. Conceptual Managed Aquifer Recharge and Groundwater Resource Targets Identified from Preliminary Analysis of Airborne Electromagnetic Data. Geoscience Australia Professional Opinion 2009. 103p.

Lerner, D.N., 1997. Groundwater recharge (Chapter 4). *In* Saether, O.M. and de Caritat, P. (Eds.), Geochemical processes, weathering and groundwater recharge in catchments, Balkema, Rotterdam, p. 109-150.

Lillesaeter, O., 1982. Spetral reflectance of partly transmitting leaves: Laboratory measurements and mathematical modelling. Remote Sensing of Environment, 12, 247-254.

Littleboy, M., Summerell1, G., Rancic. A., Beecham, R., Emery, K., Stazic, D., Arranz, P., Berhane, D., 2008. Salinity Audit Update: upland areas of the New South Wales Murray-Darling Basin. 2nd Int. Salinity Forum. http://www.internationalsalinityforum.org/Final%20Papers/littleboy_E1.pdf

Liu, G. and Becker, A., 1990. Two-dimensional mapping of sea-ice keels with airborne electromagnetics. Geophysics 55, p. 239-248.

MacAuley, S., 2009. The lower Macquarie AEM survey. DAFF Report. (Unpublished).

Macnae, J.C., 2007. Developments in Broadband Airborne Electromagnetics in the Past Decade. *In* Proceedings of Exploration 07. Fifth Decennial International Conference on Mineral Exploration (Ed Milkereit B). p. 387-398.

Makaske, B., 2001. Anastomosing rivers: a review of their classification, origin, and sedimentary products. Earth Science Reviews 53: p. 149-196.

McDonald, R.C. and Isbell, R.F., 2008. Soil profile. In NCST (Editors). Australian Soil and Land Survey Field Handbook 3rd Edition. The National Committee on Soil and Terrain, Australian Collaborative Land Evaluation Program, Canberra.

McKenzie, N.J. and Cresswell, H.P., 2002. Selecting a method for hydraulic conductivity. In McKenzie, N., Coughlan, K. and Cresswell, H. (Eds) Soil Physical Measurement and Interpretation for Land Evaluation, CSIRO Publishing, Collingwood, 90-107.

McNeill, J.D., 1980. Electromagnetic terrain conductivity measurement at low induction numbers. Geoonics Technical Note TN-6, 15p.

Metternicht, G.I. & Zinck J.A., 2003. Remote sensing of soil salinity: potentials and constraints Remote Sensing of Environment 85 (2003) 1–20 2.

Miall, A.D. 1992. Alluvial deposits. In Walker, R.G. and James, N.P. (Eds). Facies Models: Response to Sea Level Change. Geological Association of Canada, pp. 119-142.

Mory, A. J., 1990a. Bonaparte Basin. *In* Geology and Mineral resources of Western Australia. Western Australian Geological Survey Memoir 3, p. 380-415.

Mory, A. J., 1990b. Ord Basin. *In* Geology and Mineral resources of Western Australia. Western Australian Geological Survey Memoir 3, p. 415-424.

Mory, A. J. and Beere, M., 1988. Geology of the onshore Bonaparte and Ord Basins in Western Australia: Western Australian Geological Survey Bulletin 134.

Mullen, I.C., Wilkinson, K.E., Cresswell, R.G. and Kellett, J., 2007. Three-dimensional mapping of salt store in the Murray-Darling Basin, Australia 2. Calculating landscape salt loads from airborne electromagnetic and laboratory data. International Journal of Applied Earth Observation and Geoinformation 9, p. 103-115.

Mulrennan, M.E. and Woodroffe, C.D., 1998a. Holocene development of the lower Mary River plains, Northern Territory, Australia. The Holocene, 8(5), p. 565-579.

Mulrennan, M.E. and Woodroffe, C.D., 1998b. Saltwater intrusion into the coastal plains of the Lower Mary River, Northern Territory, Australia. Journal of Environmental Management, 54(3), p. 169-188.

Munday, T., Walker, G., Cresswell, R., Wilford, J., Barnett, S. & Cook, P., 2003a. South Australian Salt Mapping and Management Support Project –An example of the considered application of airborne geophysics in natural resource management. 16th ASEG Conference, Adelaide.

Munday, T., Green, A., Brodie, R., Lane, R., Sattel, D., Barnett, S., Cook, P. & Walker, G., 2003b. Developing recharge reduction strategies in the Riverland of South Australia using airborne electromagnetic data – a case study in tailoring airborne geophysics given a particular target and a desired set of outcomes. 16th ASEG Conference, Adelaide.

Munday, T.J. Overton, I. Fitzpatrick, A. Cahill, K. Berens, V. Hatch, M. & Brodie, R. C., 2007. Spatio-temporal monitoring of floodplain environments using electromagnetic methods: a scaled approach to understanding surface water- groundwater interactions on the Chowilla floodplain, S. Australia. *In* 20th SAGEEP, Denver.

Munday, T., Walker, G., and Liddicoat, C., 2004. Application of Airborne Geophysical Techniques to Salinity Issues in the Riverland, South Australia. Report DWLBC 2004/34.

Munday, T., Walker, G., Cresswell, R., Wilford, J., Barnett, S. and Cook, P., 2003b. South Australian Salt Mapping and Management Support Project –An example of the considered application of airborne geophysics in natural resource management. 16th ASEG Conference, Adelaide.

Munday, T.J. Overton, I. Fitzpatrick, A. Cahill, K. Berens, V. Hatch, M. and Brodie, R. C., 2007. Spatio-temporal monitoring of floodplain environments using electromagnetic methods: a scaled approach to understanding surface water- groundwater interactions on the Chowilla floodplain, South Australia. *In* 20th SAGEEP, Denver.

Munday, T., Fitzpatrick, A. and White, J., 2008. Spatial Patterns of Groundwater Induced Salt Accumulation in a Salinising Floodplain and links with the Murray River, South Australia. AGU.

Murray Darling Basin Commission, 1999. The Salinity Audit: A 100 Years Perspective. Murray Darling Basin Ministerial Council, Canberra, Australia.

Nanson, G. C. and Young, R. W., 1981. Overbank deposition and floodplain formation on small coastal streams of NSW. Zeitschrift fur Geomorphologie 25, p. 332-347.

Nanson, G.C., East, T.J., and Roberts, R.G., 1993. Quaternary stratigraphy, geochronology and evolution of the Magela Creek catchment in the monsoon tropics of northern Australia. Sedimentary Geology, 83(3-4), p. 277-302.

Narayan, K. A., Schleeberger, C., Charlesworth, P. B., and Bristow, K. L., 2003. Effects of Groundwater Pumping on Saltwater Intrusion in the Lower Burdekin Delta, North Queensland. In Post, D. A. (ed.) MODSIM 2003 International Congress on Modelling and Simulation. Volume 2, p. 212-217. Modelling and Simulation Society of Australia and New Zealand, July 2003.

National Land & Water Resources Audit, 2001. Australian Dryland Salinity Assessment 2000: Extent, Impacts, Processes, Monitoring and Management options. NLWRA, Canberra.

Newman, G.A., Anderson, W.L. and Hohmann, G.W., 1987. Interpretation of transient electromagnetic soundings over three-dimensional structures for the central-loop configuration: Geophysical Journal of the Royal Astronomical Society, 89, p. 889-914.

Nixon, R. D., 1995. Preliminary results of the Ord River Irrigation Area Stage 1 hydrogeological investigation 1994: Western Australia Geological Survey, Hydrogeology Report No. 1995/2 (unpublished).

Nixon, R. D., 1996. Mantinea Plain hydrogeological investigation preliminary results: Western Australia Geological Survey, Hydrogeology Report No. 24 (unpublished).

Nixon, R. D., 1997a. Ord River Irrigation Area drilling project, bore completion report on the Knox Creek Plain: Western Australia Water and Rivers Commission, Hydrogeology Report No. 65 (unpublished).

Nixon, R. D., 1997b. Ord River Irrigation Area drilling project, bore completion report on the Weaber Plain: Western Australia Water and Rivers Commission, Hydrogeology Report No. 66 (unpublished).

Nixon, R. D., 1997c. Ord River Irrigation Area drilling project, bore completion report on the Carlton Plain: Western Australia Water and Rivers Commission, Hydrogeology Report No. 67 (unpublished).

Nixon, R. D., 1997d. Ord River Irrigation Area drilling project, bore completion report on the Mantinea Plain: Western Australia Water and Rivers Commission, Hydrogeology Report No. 68 (unpublished).

Nixon, R. D., 1997e. Ord River Irrigation Area drilling project, bore completion report on the Packsaddle Plain: Western Australia Water and Rivers Commission, Hydrogeology Report No. 69 (unpublished).

Nixon, R. D., 1997f. Ord River Irrigation Area drilling project, bore completion report on the Ivanhoe Plain: Western Australia Water and Rivers Commission, Hydrogeology Report No. 70 (unpublished).
Nixon, R. D., 1997g. Ord River Irrigation Area drilling project, bore completion report on the Cave Spring Gap: Western Australia Water and Rivers Commission, Hydrogeology Report No. 71 (unpublished).
Nixon, R. D., 1997h. Ord River Irrigation Area miscellaneous data report on the Weaber and Knox Creek Plains: Western Australia Water and Rivers Commission, Hydrogeology Report No. 72 (unpublished).
O'Boy, C.A., Tickell, S.J., Yesertener, C., Commander, D.P., Jolly, P. and Laws, A.T., 2001. Hydrogeology of the Ord River Irrigation area, Western Australia and Northern Territory. Water and Rivers Commission, Hydrolgeological Record Series, Report HG 7, 80p.
Ord Valley Catchment Management Plan, 2000
Ord Valley Catchment Management Plan, 2006
Pain, C. F., Chan, R., Craig, M., Gibson, D., Kilgour, P., and Wilford, J. 2007. RTMAP regolith database field guide and users guide. CRC LEME Open File Report 231, 2nd edition, 92p.
Pain, C.F., Wilford, J.R. and Halas, L. 2009. A Review of Mapping Approaches to Recharge and Discharge Estimation. CSIRO: Water for a Healthy Country National Research Flagship, Geoscience Australia Professional Opinion. In press.
Paine J. G., 2003. Determining salinization extent, identifying salinity sources, and estimating chloride mass using surface, borehole, and airborne electromagnetic induction methods, Water Resour. Res., 39 (3), p. 3-1–3-10
Payenberg, T. H. D. and Reilly, M. R. W., 2003. Core descriptions of ten conventional cores from the St George region, Queensland. CRC LEME Open File Report 166.
Peters, W.S., 2001. Ground electromagnetics: the basics and recent developments. Recent Developments and Future Directions in Geophysics. AIG Bulletin 33, p. 15-32.
Plumb, K. A. and McGovern, J. L., 1968. CAMBRIDGE GULF. WA 1:250,000 geological map series sheet SD52-14, BMR, Canberra.
Pollock, D. W., Salama, R. B., and Viney, N. R., 2003. Water levels and water quality trends in the Ord River Irrigation Area (ORIA) for the period September 2001 – March 2003. CSIRO Land and Water Technical Report 40/03.
Reid, J, Kemp, T., and Eade, R., 2008. SkyTEM Final Report: Ord River SkyTEM Survey. 42pp.
Reid, M., Gill, B., Cheng, X., Fawcett, J., Hekmeijer, P., Clark, R., Hood, A., 2008. Overview of groundwater trends and dryland salinity in Victoria. 2nd Int. Salinity Forum. http://www.internationalsalinityforum.org/Final%20Papers/reid_E1.pdf
Reineck, H.E. and Singh, I.B., 1980. Depositional Sedimentary Environments. Springer-Verlag, Berlin, 549p.
Rhoades, J.D., Raats, P.A.C. and Prather, R.S., 1976. Effects of Liquid-Phase Electrical Conductivity, Water Content, and Surface Conductivity on Bulk Soil Electrical Conductivity. Soil Science Society of America Journal 40, p. 651-665.
Richards, N., 2002. Assessment of the potential value of electromagnetic survey methods for soil permeability investigations, in the Ord River Irrigation Area. Draft Report, WA Dept. of Agriculture. 65p.
Richardson, S. Evans, R., Haworth, D., and Prider, J., 2007. Tri-State Hydrogeological Benchmark Assessment. Resource & Environmental Management Pty Ltd. (Unpublished report).
Ruprecht, J.K., and Rodgers, S.J., 1999. Hydrology of the Ord River. Water and Rivers Commission Report WRT 24.
Rutherford, I.D., 1994. Inherited controls on the form of a large, low energy river: the Murray River, Australia, In Winkley, B.R. and Schumm, S.A. (Eds). The Variability of Large Alluvial Rivers ASCE Press, New York, 177-197.
Salama, R. B. and Pollock, D. W., 2003. Preliminary appraisal of salinity development in the Packsaddle Creek area. CSIRO Land and Water, Technical Report 17/03.
Salama, R., Bekele, E., Pollock, D., Bates, L., Byrne, J., Hick, W., Watson, G. and Bartle, G., 2002. Hydrological response units of the Ord Stage I Irrigation Area and the dynamic filling of the aquifers of the Ivanhoe and Packsaddle Plains. CSIRO Land and Water Technical Report 7/02, 78p.
Salama, R., E. Bekele, L. Bates, Pollock, D. and Gailitis, V., 2002. Hydrochemical and isotopic characteristics of the surface and groundwater of the hydrological zones of the Ord Stage I Irrigation Area. CSIRO Land and Water Technical Report No 8/02.
Sattel, D., 1998. Conductivity information in three dimensions. Expl. Geophys. 29, p. 157-162.

Sattel, D., 2005. Inverting airborne electromagnetic (AEM) data with Zohdy's method: Geophysics, 70 (4), p. G77-G85.
Scanlon, B.R., Healy, R.W. and Cook, P.G., 2002. Choosing appropriate techniques for quantifying groundwater recharge. Hydrogeology Journal 10, p. 18-39.
Scanlon, B.R., Keese, K.E., Flint, A.L., Flint, L.E., Gaye, C.B., Edmunds, W.M. and Simmers, I., 2006. Global synthesis of groundwater recharge in semiarid and arid regions. Hydrological Processes 20, p. 3335-3370.
Scanlon, B.R., Keese, K.E., Flint, A.L., Flint, L.E., Gaye, C.B., Edmunds, W.M. and Simmers, I., 2006. Global synthesis of groundwater recharge in semiarid and arid regions. Hydrological Processes 20, 3335-3370.
Schumm, S.A. and Ethridge, F.G., 1994. Origin, evolution and morphology of fluvial valleys. In Dalrymple, R.W., Boyd, R., and Zaitlin, B.A. (Eds) Incised-valley systems; origin and sedimentary sequences. Special Publication - SEPM 51, 11-27.
Sengpiel, K.P. and Siemon, B., 2000. Advanced inversion methods for airborne electromagnetic exploration. Geophysics, 65, p. 1983-1992.
Shi G., Wenju C., Cowan T., Ribbe J., Rotstayn L. and Dix M., 2008. Variability and trend of North West Australian Rainfall: Observations and coupled climate modelling. Journal of Climate, 21, p. 2938-2959.
Schoknecht, N. and Grose, C., 1996a. Soils of the Knox Creek Plain, East Kimberley, Western Australia and Northern Territory: Agriculture Western Australia, Resource Management Technical Report No. 153.
Schoknecht, N., and Grose, C., 1996b. Soils of the Mantinea Loop Ord river Valley, East Kimberley, Western Australia and Northern Territory, Agriculture Western Australia, Resource Management Technical Report No. 154.
Schoknecht, N., and Grose, C., 1996c. Soils of the Ivanhoe west Bank, East Kimberley, Western Australia and Northern Territory: Agriculture Western Australia, Resource Management Technical Report No. 155.
Schoknecht, N., 1996. Assessment of the suitability for Agriculture of the North-West Packsaddle Area Kununurra: Agriculture Western Australia, Resource Management Technical Report No. 155.
Shephard F.P., 1954. Nomenclature based on sand-silt-clay ratios. Journal of Sedimentary Petrology 24, 151–158.
Smith, A. J., 2008. Rainfall and irrigation controls on groundwater rise and salinity risk in the Ord Irrigation area, northern Australia. Hydrology Journal 16, p. 1159-1175.
Smith, A.J., Pollock, D.W., Salama, R.B. and Palmer, D., 2005. Ivanhoe Plain aquifer pumping trial July 2003 – April 2005: Stage 1 Ord River Irrigation Area, Kununurra, Western Australia. CSIRO Land and Water Technical Report 24/05, 39p.
Smith, A., Pollock, D. and Palmer, D., 2006. Review of groundwater monitoring and reporting in the Ord Stage 1 Irrigation Area, Kununurra, Western Australia. CSIRO Land and Water Science Report 71/06, 37p.
Smith A. J., Pollock, D. W. and Palmer, D., 2006. Groundwater management options to control rising groundwater level and salinity in the Ord Stage 1 Irrigation Area, Western Australia. CSIRO Land and Water Science Report 70/06.
Smith, A.J., Hick, W., Galbraith, R., and Palmer, D., 2006. Ord River Irrigation Area (ORIA) groundwater drainage and discharge evaluation: piezometers installation report. CSIRO Land and Water Science Report 72/06.
Smith, A. J., D. Pollock, Palmer, D. and Price, A., 2007. Ord River Irrigation Area (ORIA) groundwater drainage and discharge evaluation: survey of groundwater quality 2006. CSIRO Land and Water Science Report 44/07.
Smith, A. and Price, A., 2008. Review and Assessment of Soil Salinity in the Ord River Irrigation Area.. CSIRO Land and Water Science Report (Unpublished).
Simpson, H. J., and Herczeg, A. L., 1994. Delivery of marine chloride precipitation and removal by rivers in the Murray-Darling Basin, Australia. Journal of Hydrology 154, 323–50.
Sophocleous, M., 2004. Groundwater Recharge, in Silveira, L., Wohnlich, S. and Usunoff, E.J. (Eds.). Groundwater, in Encyclopedia of Life Support Systems (EOLSS) Developed under the Auspices of the UNESCO, EOLSS Publishers, Oxford, UK, http://www.eolss.net.
Sørensen, K.I. and Auken, E., 2004. SkyTEM - A new high-resolution helicopter transient electromagnetic system. Exploration Geophysics, 35, p. 191-199.

Specht, R.L., 1981. Foliage projective cover and standing biomass. In Gillison, A.N. and Anderson, D.J. (Eds) Vegetation Classification in Australia. pp. 10-21. CSIRO and ANU, Canberra.

Spies B and Woodgate P., (2005). Salinity Mapping Methods in the Australian Context. Land and Water Australia, Department of the Environment and Heritage; and Agriculture Fisheries and Forestry, June 2005. 236p. http://www.nrm.gov.au/publications/salinity-mapping

Stewart, G.A., Perry, R.A., Paterson, S.J., Sleeman, J.R. and Traves, D.M., 1970. Land systems of the Ord - Victoria Area. Land Research Series 28, CSIRO, Melbourne, p. 11-61.

Stoneman, T. C., 1988. Carlton Plains soil survey in the Shire of Wyndham, east Kimberley.

Storey A.W. and Marshall, A., 2008. Lower Ord River Ecological Monitoring Program – Baseline Habitat Mapping. Report by Wetland Research & Management and Andrew Marshall Pty Ltd for Department of Water, July 2008.

Suppiah R. and Hennessy K.J., 1996. Trends in the intensity and frequency of heavy rainfall in tropical Australia and links with the Southern Oscillation. Australian Meteorological Magazine, 45, p. 1-17.

Suppiah R., Collins D. and Della-Marta P. 2001. Observed changes in Australian climate. CSIRO/BoM. http://www.cmar.csiro.au/e-print/open/suppiah_2001a.pdf

Tan, K. P., Apps, H., Halas, L., Gibson, D. & Lawrie, K., 2005. Utilizing Airborne Electromagnetic Data to Model the Subsurface Salt Load. *In* A Catchment, Bland Basin, NSW. In Zerger, A. and Argent, R.M. (eds) MODSIM 2005 International Congress on Modelling and Simulation. Modelling and Simulation Society of Australia and New Zealand, December 2005, pp. 1478-1484 ISBN: 0-9758400-2-9. http://www.mssanz.org.au/modsim05/papers/ascough_1.pdf

Tan, K.P., Halas, L., Apps, H., Gibson, D. and Lawrie, K., 2006. Modelling of salt loads and sedimentary textures from AEM and petro-physical logs (Bland sub-catchment, NSW) for hydrogeological applications. *In* Proceedings: Murray-Darling Basin Groundwater Workshop, Canberra. 18th – 20th August. 7 p.

Tan, K.P., Munday, T.J., Fitzpatrick, A. Lawrie, K. and Gibson, D.L., 2007. Integrating Electromagnetic Data, Petrophysics, Sedimentological/Regolith and Hydrological Information for Salinity Management. Symposium on the Application of Geophysics to Engineering and Environmental Problems (SAGEEP). Seattle, Washington. 11 p.

Tan, K.P., Lawrie, K.C., Halas, L., Pain, C.F., Clarke, J.D.A., Gibson, D., Apps, H., Cullen, K., Brodie, R. and Wong, V., 2009. Methodology for the customised products developed as part of the River Murray Corridor Victorian AEM mapping project. Geoscience Australia, Professional Opinion 2009/12, 75pp.

Thom, B.G., Wright, L.D. and Coleman, J.M., 1975. Mangrove ecology and deltaic-estuarine geomorphology: Cambridge Gulf-Ord River, Western Australia. Journal of Ecology, 63(1), p. 203-233.

Thompson S., Fountain D. and Watts T., 2007. Airborne Geophysics – Evolution and Revolution. *In* Proceedings of Exploration 07: Fifth Decennial International Conference on Mineral Exploration (Ed Milkereit B) p. 19-37.

Tickell, S.J., Cook, P., Sumner, J., Knapton, A. & Jolly, P., 2007. Evaluating the Potential for Irrigation Induced Salinisation of the Keep River Plains. Report WRD13/2007D. 9p.

WA EPA/NT DLPE., 1999. Ord River Irrigation Area Stage 2 (M2 channel supply area), Kununurra: guidelines for an environmental review and management programme (ERMP)/ environmental impact statement (EIS). Western Australian Environmental Protection Authority/Northern Territory Department of Lands, Planning & Environment Joint Environmental Assessment. (WA EPA Assessment Number 1240.

Walker, G.R., Zhang, L., Ellis, T.W., Hatton, T.J. and Petheram, C., 2002. Estimating impacts of changed land use on recharge: a review of modelling and other approaches appropriate for management of dryland salinity. Hydrogeology Journal 10, p. 68-90.

Walker, G., Cresswell, R., Munday, T. and Liddicoat, C., 2004. South Australian Salinity Mapping and Management Support Project: Final Report (Overall Project Summary Report), South Australia. Department of Water, Land and Biodiversity Conservation. Report, DLWBC 2004/39.

Walker, G., Doble, R., Mech, T., Lavis, T., Bluml, M., MacEwan, R., Stenson, M., Wang, E., Jolly, I., Miles, M., McEwan, K., Bryan, B.A., Ward, J., Rassam, D., Connor, J., Smith, C., Munday, T., Nancarrow, B., and Williams, S., (2005). Lower Murray Landscape Futures Phase One Report. Final Year 1 Technical Report prepared for the Centre for NRM, the Victorian NAP Office and CSIRO Water for a Healthy Country. Water for a Healthy Country report. Adelaide: CSIRO. Address when accessed http://www.clw.csiro.au/publications/consultancy/2005/LMLF_Project_Phase_One_Report.pdf

Wang, E., Miles, M., Schultz, T., Cook, P., Maschmedt, D., Munday, T., Leaney, T., Walker, G., and Barnett, S., 2005. Targeting Dryland Areas in the Mallee for Controlling Groundwater Recharge and Salt Load to the Murray River. Report to Client No. #/2005. CSIRO Canberra, ACT, Australia. Address when accessed http://www.clw.csiro.au/publications/consultancy/2005/WfHC_targeting_dryland_areas.pdf

Wolanski, E, Moore, K., Spagnol, S., D'Adamo, N., and Pattiratchi, C., 2001. Coastal, Estuarine, and Shelf Science 53, p. 717-732.

Woodroffe, C.D., Chappell, J., Thom, B.G., and Wallensky, E.,1989. Depositional model of a macrotidal estuary and floodplain, South Alligator River, northern Australia. Sedimentology, 36(5), p. 737-756.

Woodroffe, C.D., Mulrennan, M.E., and Chappell, J., 1993. Estuarine infill and coastal progradation, southern van Diemen Gulf, northern Australia. Sedimentary Geology, 83(3-4), p.257-275.

Wright, J. S., 2001. Tufa accumulations in ephemeral streams: observations from the Kimberley, north-west Australia. Australian Geographer 31(3), p. 333-347.

Wright, L.D., Coleman, J.M., and Thom, B.G., 1973. Processes of channel development in a high-tide-range environment: Cambridge Gulf-Ord River Delta, Western Australia. Journal of Geology, 81(1), p. 15-41.

Yan, W. and Howe, B., 2008. Chowilla Floodplain Groundwater Model. Water Down Under Conference, Adelaide. p 1260-1271.

Young, R.W., 1986. Tower karst in sandstone; Bungle Bungle massif, north-western Australia. Zeitschrift für Geomorphologie 30 (2), p. 189-202.

Zhao, B., Yan, Y., Guo, H. D., He, M., Gu, Y. & Li, B., 2009. Monitoring rapid vegetation succession in estuarine wetland using time series MODIS-based indicators: An application in the Yangtze River Delta area Ecological Indicators, 9, 346-356.

Acknowledgements

The project team would like to thank Ord Irrigation Cooperative, their present CEO Geoff Strickland, Elaine Gardiner (Chair), former CEOs Tony Chafer and Andrew Kelly, and Anna Price (ex-OIC and Brolgas Environment) for their incredible support in seeking the initial funding for this project, managing relations with Peth and Canberra, and maintaining their enthusiasm over the years. Geoff is particularly thanked for his strong support of the project team in the past year, and his patience and understanding of the logistic and organisational challenges brought by a complex inter-disciplinary science project. Anna Price is particularly thanked for her unbounded energy, enthusiasm and coordination skills, and we wish her luck in her next big adventure.

The members of the Ord Valley AEM Interpretation Project Steering Committee are thanked for their wisdom and input over the years, particularly for their work in helping to identify the salinity and groundwater management issues that helped focus the efforts of the team. In particular, Duncan Palmer, Gary Humphries, Tony Smith, Peter Cottrell and Liz Brown are thanked for their words of scientific, technical and practical wisdom, local knowledge, and generous support. Maree, Christine, and Suzy in the OIC office, and the OIC watermen, notably 'Goose', who helped make the interaction with OIC a most pleasant experience over the years. The project was aided significantly by the input from local irrigators, who brought immense local knowledge and practical insights that helped us to frame our products.

Peer review of this report and associated products has been extensive, and we would like to thank all of those stakeholders and reviewers who have taken the time to participate in the workshops and presentations. In particular, we would like to thank Geoff Strickland for coordinating the community and stakeholder workshops held in Kununurra and Perth in August and November 2009, as the feedback received in these workshops has significantly refined the products and messages contained in this report. Special mention goes to Richard George for taking a week out of his busy schedule to participate in the workshops, and collate all the feedback. Richard is also thanked for his exhaustive review of the report, and for ensuring that the products have been utilised in groundwater modelling of the Weaber Plain. Mike Hatch from Adelaide University is thanked for his thorough review of the geophysics sections in the report. The Project Steering Committee is also thanked for constructive comments on map products and the report, while internal reviewers in GA (Jane Coram and Sunderam Baskaran), are thanked for their editing of the final report.

The project leader would like to acknowledge the efforts of all the Ord Valley AEM Interpretation Project team. In particular, I wish to acknowledge the exceptional efforts in short timeframes of the team in GA: Kok Piang Tan, Jon Clarke, Heike Apps, Larysa Halas, Colin Pain and Ross S. Brodie who pulled off one or two miracles to produce some innovative products in a short timeframe, yet again. I also wish to thank Heike Apps and Kristen Cullen who worked tirelessly behind the scenes, with enormous patience, to produce a range of high quality products for the atlas and GIS as well as the majority of the figures for this report. Christian Thun and his team in the GA laboratories are thanked for rapid processing and analysis of the drillcore. And not to forget Tenai Luttrell, who, as always, got us to where we needed to be on time and within budget! Robert Apps is also thanked for his efforts in protracted negotiations with CSIRO, and in ensuring that other contracts were signed in very short timeframes. Finally, I wish to acknowledge the efforts of the late Trish Yates, whose support within GA was essential in ensuring the project could be carried over from CRC LEME.

Glossary

Facies: Sedimentary deposits that have mappable characteristics that can be attributed to specific depositional processes. For example, sand facies that were deposited by rivers as distinct from coastal processes.

Palaeochannel: a buried channel (or more accurately channel fill deposit) that marks the former course of a river, stream or creek. Often incorrectly used as a synonym for *palaeovalley*. However, a *palaeovalley* may contain no or several *palaeochannel* features, and *palaeochannels* need not be associated with palaeovalleys

Palaeovalley: a former surface valley that has been partly to completely infilled by sediments. Often used as a synonym for *palaeochannel*, a palaeovalley strictly speaking may not contain any palaeochannel sediments, if filled by processes other than alluvial, or have several palaeochannels.

Prior Stream: a *palaeochannel* that marks the former course of a stream in the present landscape. May be expressed in the landscape by a low ridge.

"Steer's Head": A term applied to valley cross sections that have narrow lower sections and wide upper sections, resembling the view of a long horn steer seen head-on.

Thalweg: the deepest point of a stream channel.

Aggrade: The vertical piling up of sediment on depositional surfaces such as a floodplain or tidal flat.

Aggradational: The processes and sediments that result when floodplains or tidal flats *aggrade.*

Airborne Electromagnetic (AEM) survey: A geophysical survey method that maps the subsurface conductivity structure of the survey area using a loop mounted on a fixed-wing aircraft or carried beneath a helicopter. Many such systems exist with different performances, allowing the survey to be tailored to the needs of the end users.

Alluvial/alluvium: A sediment deposit formed by the action of rivers.

Alluvial terrace: A deposit of alluvial sediment related to an existing river but found at a higher level in the landscape than that presently being deposited. Alluvial terraces indicate former higher levels of river action

Anabranching: A type of river channel morphology where the channel divides in two for a significant distance.

Anastomosing: A type of river morphology where there are many channels that separate and flow into each other, forming a network.

Architecture: The relationship of different geological units to each other in space. For example *regolith* architecture, sedimentary architecture

Arkose: A *sandstone* containing abundant *feldspar*

Basalt: A dark volcanic rock rich in iron and magnesium, making up the Antrim Plateau and Carson volcanics.

Bedload: The coarse-grained (sand and gravel) faction of the sediment carried by a river along its bed.

Bounding surface: A surface within a sedimentary *succession* that marks the upper or lower limits of a major mappable unit.

Braided: A type of river morphology where there is a wide, sandy river bed composed of many bars and channels.

Cambrian: A period of geological time, between 545 and 490 million years ago, during this period the Antrim Plateau volcanics found in the bed or the Ord River and east and south of Kununurra were erupted.

Carboniferous: A period of geological time, between 359 and 300 million years ago, during this period the rocks that form the Weaber Range and occur beneath the Weaber Plains were deposited.

Cobbles: River-rocks between 64 and 256 mm across.

Conductivity surveys and logging: Measuring the varying electrical conductivity of the earth using surface surveys or profiles down bore holes. Conductivity varies according to the factors such as mineral composition and salt and water content.

Conglomerate: A *sedimentary* deposit formed by the cementing of gravel and cobbles together by minerals precipitated from groundwater.

Devonian: A period of geological time, between 416 and 359 million years ago, during this period the sedimentary rocks to the east of Kununurra were deposited. Lawrie *et al*., 2006. CRC LEME Restricted Report 232R 71

Diagenesis: The changes that occur to a sediments after they are deposited, including cementation and weathering.

DEMs: See *Digital Elevation Models*

Digital Elevation Models (DEMs): Digital representations of the topography of the earth that are important components of *geographic information systems*. DEMs are obatined by a range of systems, including ground surveying, airborne radar and laser surveys, or from satellite radar.

Dissected: A term applied to landscapes which have been extensively eroded by valleys and gullies.

Dolerite: A dark, medium-grained, formerly molten rock, similar in composition to basalt but coarser grained.

Dolostone: A *sedimentary* rock composed largely of the calcium-magnesium carbonate mineral dolomite

Down-hole logging: A method of measuring the geophysical properties of the rocks, soils, or sediments penetrated by a drill hole. A tool that measures properties such as *conductivity* and natural *gamma* radioactivity is lowered down the bore hole, data is recorded during both descent and ascent of the tool. Down-hole logging is a vital technique to calibrate conductivity and surveys and interpret geological logs.

Duricrust: A hard layer formed in the *regolith* by cementation of soil or sediment by minerals of iron, sulphate, silica, or carbonate.

Efflorescence: A surface layer of salts on rock or soil surfaces formed by the evaporation of salty ground or soil water.

Electromagnetic (EM) survey: A geophysical technique that maps the conductivity of the near surface environment using electromatnetic signals generated the survey instrument. Common examples include *NanoTEM*, EM31 and EM39.

Feldspar: A light-coloured mineral containing silicon, aluminium and oxygen and either sodium and calcium or potassium

Ferricrete: An iron-rich *duricrust.*

Ferrihydrite: An iron-hydroxide mineral that precipitates when groundwater rich in dissolved iron is exposed to the atmosphere. Ferrihydrite often forms oil-like shiny filsm on standing or gently flowing water and is an important beginning in the formation of *ferricrete.*

Gamma ray logging: Down-hole *geophysical* logging techniques that maps the gamma radiation released by naturally occurring uranium, thorium and radioactive potassium.

Geophysics: The study of the physical properties of the earth, in particular *magnetic*, *conductivity*, and *radiometric* properties, or variations in the earth's gravity. Geophysical techniques can help understand the subsurface structure of the earth, locate groundwater, and map salinity, as well as having other applications.

Geographical Information Systems (GIS): GIS are systems for creating, storing, analyzing and managing multiple layers of information maps of geology, topography, infrastucture, soils, vegetation, and landuse. GIS systems allow users to create interactive queries to analyze the spatial information.

Goethite: A yellowish-brown iron hydroxide mineral that is common in soils and *regolith*.

Granules: Gravel sediment between 2-4 mm in diameter.

Gravel: All loose, coarse-grained sediments with grains greater than 2 mm in diameter.

Haematite: A reddish-brown iron oxide mineral that is common in soils and *regolith.*

Hydrogeology: The study of geological properties of rocks, soils, and sediments as they relate to groundwater movement and storage.

Indurated: The process of hardening, such as occurs when sediments are turned into rock by various cementing agents, or surface hardening of some exposed rock surfaces that can occur during weathering.

LiDAR: *Li*ght *D*etection *A*nd *R*anging. A means of highly accurate topographic surveying using and aircraft-founded laser scanner to measure the variation in altituide. Also written as LIDAR, Lidar or lidar.

Lithic: A term applied to sand or gravel where the particles are made up of rock fragments.

Incised channel: A river channel, such as that or the Ord River in the Ord Irrigation River, that has cut down below its original flood plain. This usually occurs in response to changes in river flow conditions or geological uplift.

LANDSAT: A polar-orbit satellite launched by NASA to collect *multispectral* images of the Earth surface. Sevn satellites have been launched in the series. Often written as "Landsat".

Magnetic survey: A geophysical survey method that maps the distribution of magnetic materials in the earth. Magnetic surveys can be carried out on the ground or from aircraft.

Meandering: A highly sinuous river channel formed by the river moving in loops of ever increasing amplitude, leaving behind sandy bars on the inside of the loops. The lower reaches of the Ord River is currently characterised by meandering channels.

Metadata: Information about the source and accuracy of information used in a *GIS*

Multispectral imagery: Images acquired by satellites or aircraft that capture more than the three colour bands visible to the human eye. Multispectral images can be manipulated and combined in a *GIS* to emphasise subtle features such as variations in soil composition or vegetation.

NanoTEM survey: An *electromagnetic* ground *geophysical* method widely used to map shallow subsurface conductivity in Australia in support of salinity and groundwater investigations.

Optically Stimulated Luminescence Dating: Optically Stimulated Luminescence (OSL) dating is a method that can be used to determine the length of time since a sediment was buried.

ORIA: *O*rd River *I*rrigation Area.

Orthophoto/orthoimage: An Orthophoto is an aerial photograph or series of phtographs that has been geometrically corrected ("orthorectified") so that the scale is uniform, adjusting for topographic reliefhttp://en.wikipedia.org/wiki/Orthophoto - cite_note-0#cite_note-0, lens distortion, and camera tilt.. Hence the photo has the same lack of distortion as a map. Orthoimage is the term used for a digital orthophoto.

Overbank flow: Flow formed when a river overtops its banks and flows out across the floodplain.

Palaeochannels: Former river channels that are recognised in the surface (from aerial or satellite images) or subsurface (typically in *AEM* surveys or drilling).

Palaeosol: A buried soil profile representing a former land surface.

Palaeovalley: Ancient valley filling sediments including (but not restricted to) those of *palaeochannels*. Typically palaeovalley sediments are not associated with currently active processes.

Palaeozoic: A geological era that encompasses the time between 545 and 251 million years. The Palaeozoic includes the *Cambrian*, *Devonian* and *Carboniferous* periods within it.

Pediment: A gently-sloping apron of exposed or shallowly buried bedrock surrounding hills and rises.

Pedogenic: Processes or features pertaining to soil formation

Progradation: The seaward movement of the coastal zone caused by infilling of coastal environments by sediments derived from the land after a *transgression.*

Proterozoic: A geological era that encompasses the time between 2500 and 545 million years. The rocks to the west of Kununurra are almost exclusively Proterozoic in age.

Quartz: A very common mineral composed of silicon dioxide that commonly occurs in river sands and as the main mineral in sandstones.

Quartzite: A *sandstone* composed largely of quartz that has been recrystallised by exposure to geological heat and pressure.

Radiometrics: The collection of information of the distribution of naturally occurring uranium, thorium and radioactive potassium from their emitted gamma radiation, usually from an aircraft. Radiometric data is normally plotted as three colour images with a different colour for each element. Radiometric data typically reviewed as part of a *GIS* and is very useful in the mapping of soil types and *salinity* outbreaks and is able to see through vegetation and crops to a large extent.

Regolith: Everything between fresh rock and fresh air, including *weathered* rocks, soils, shallow ground water and sediments.

Relict: A term applied to landscape features that are no longer being actively formed. For example, the floodplain of the Ord River is regarded as relict because, prior to dam construction, it was not being inundated during seasonal floods.

Salinity: Areas where salt is being deposited in the near surface environment. Salinity is a natural phenomenon but can be increased through use land use practices involving inappropriate types of soil management, vegetation clearing, cropping, and irrigation.

Sandstone: A *sedimentary* rock composed of sand-sized particles.

Sedimentary: Pertaining to deposition of sediments and sedimentary process, for example a sedimentary rock is a rock once composed of sediments such as sand, gravel, silt, etc.

Shale: A *sedimentary* rock composed of clay particles

Silcrete: *Duricrust* formed by the precipitation of *silica* in the *regolith*

Silica: Term applied to fine-grained *quartz* cements in sediments and soils.

Silicification: the process by which silica is deposited.

Siltstone: A *sedimentary* rock composed of silt-sized particles

Sinuous/sinuosity: A measure of the degree to which a river channel winds its way through the landscape. Highly sinuous streams have many, strongly curved bends, low sinuosity channels are relatively straight.

SkyTEM: An *AEM* system used to survey the Ord Stage 1 and 2 areas in this study.

Sodicity: A measure of the degree to which sodium is accumulating in a soil, typically though not exclusively a consequence of soil salinity.

Succession: Term applied to a series of sedimentary deposits

Stratigraphy: The study of how different layers of sediments can be related to each other.

SRTM: *Digital Elevation Model* data collected during the 2000 STS-99 *S*huttle *R*adar *T*opography *M*ission by the Space Shuttle Endeavour. SRTM data is widely available and 3 arc second (~90 M) on a restricted basis at 1 arc second (~30 m) horizontal resolutions.

Transgression: A long-term rise in relative sea level causing flooding of the coastal zone, for example, after the end of the last ice age.

Transgressive: Pertaining to processes or sediments resulting from a *Transgression.*

Transmissivity: A measure of the ability of groundwater to pass through soil, sediment or rock.

Tufa: Tufa is a deposit of calcium carbonate in springs and riverbeds. Where present, tufas can cement existing river sediments as well as forming constructs of nearly pure carbonate. They are a common feature of many Australian rivers, especially those of the tropics and arid zone.

Unconformity: A *bounding surface* where the rocks below rest at a different angle to those above, for example where alluvial gravels rest of bedrock.

Varnish: Thin, reflective paint like coating on *weathered* rock surfaces, typically, red, reddish-brown, brown, or black in colour, composed of oxides and hydroxides of iron and manganese, typical of seasonally to permanently dry weathering environments.

Weathered/weathering: The physical and chemical changes a rock undergoes when it is exposed to the atmosphere and shallow groundwater.

XRD: X-ray diffraction. An analytical method used to determine the mineralogy of soil, sediment, and rock samples.